SHOUT
SHARE
IT

MUS
489D

HARVARD UNIVERSITY

Library of the
Museum of
Comparative Zoology

US ISSN 0027-4100

Bulletin OF THE
Museum of
Comparative
Zoology

A Review of the North American Fossil Amiid Fishes

JOHN R. BORESKE, JR.

HARVARD UNIVERSITY
CAMBRIDGE, MASSACHUSETTS, U.S.A.

VOLUME 146, NUMBER 1
18 JANUARY 1974

PUBLICATIONS ISSUED
OR DISTRIBUTED BY THE
MUSEUM OF COMPARATIVE ZOOLOGY
HARVARD UNIVERSITY

BULLETIN 1863–
BREVIORA 1952–
MEMOIRS 1864–1938
JOHNSONIA, Department of Mollusks, 1941–
OCCASIONAL PAPERS ON MOLLUSKS, 1945–

Other Publications.

Bigelow, H. B., and W. C. Schroeder, 1953. Fishes of the Gulf of Maine. Reprint.

Brues, C. T., A. L. Melander, and F. M. Carpenter, 1954. Classification of Insects.

Creighton, W. S., 1950. The Ants of North America. Reprint.

Lyman, C. P., and A. R. Dawe (eds.), 1960. Symposium on Natural Mammalian Hibernation.

Peters' Check-list of Birds of the World, vols. 2–7, 9, 10, 12–15.

Sprinkle, J., 1973. Morphology and Evolution of Blastozoan Echinoderms.

Turner, R. D., 1966. A Survey and Illustrated Catalogue of the Teredinidae (Mollusca: Bivalvia).

Whittington, H. B., and W. D. I. Rolfe (eds.), 1963. Phylogeny and Evolution of Crustacea.

Proceedings of the New England Zoological Club 1899–1948. (Complete sets only.)

Publications of the Boston Society of Natural History.

Authors preparing manuscripts for the *Bulletin of the Museum of Comparative Zoology* or *Breviora* should send for the current Information and Instruction Sheet, available from Editor, Publications Office, Museum of Comparative Zoology, Harvard University, Cambridge, Massachusetts 02138, U.S.A.

© The President and Fellows of Harvard College 1974

A REVIEW OF THE NORTH AMERICAN FOSSIL AMIID FISHES

JOHN R. BORESKE, JR.[1]

CONTENTS

Abstract 1
Introduction 2
Acknowledgments 2
Abbreviations 3
Amia calva 3
Nomenclature 3
Ecology 4
Geographic Distribution 4
Pleistocene Occurrences 4
Diagnosis 5
Morphometrics 5
Methods 6
General Proportions and Growth 8
Comparisons with Fossil Forms 10
Discussion 17
Meristics 18
Supravertebral Scale Rows 18
Branchiostegal Rays 20
Fin Rays 20
Vertebral Elements 25
Vertebral Column of *Amia calva* 28
Vertebral Features 28
Vertebral Dimensions 33
Valid North American Fossil Genera and Species 37
Amia fragosa 37
Amia uintaensis 47
Amia cf. *uintaensis* 64
Amia scutata 66
Amia cf. *scutata* 70
Amia cf. *calva* 72
Amiidae *incertae sedis* 72
Specimens Removed from the Amiidae 74
Summary and Conclusions 75
Literature Cited 81
Plates 84

ABSTRACT. North American amiid fishes range from Cretaceous (Albian) to Recent. Amiids are common fossils in Late Cretaceous and Tertiary freshwater deposits and apparently occupied a habitat much like that of the Recent species *Amia calva*. Morphometric, meristic, and cranial characters of articulated specimens from the Fort Union Formation (Paleocene), Green River Formation (Eocene), Florissant Formation (Oligocene), Pawnee Creek Formation (Miocene), and a Recent *A. calva* sample from Wisconsin have been used here in an attempt to revise the taxonomy and evolutionary history of the group.

Whereas seven genera and twenty-three species of fossil amiids have been described on the basis of disarticulated, often isolated elements, only three taxa have been described from complete or partially complete material. *Amia fragosa* (Late Cretaceous to Middle Eocene), *A. uintaensis* (Paleocene to Early Oligocene), *A. scutata* (Early to Middle Oligocene), and *A. calva* (Middle Pliocene to Recent) are here considered the only valid taxa. Amiid remains are first known in the North American fossil record from the Early Cretaceous (Albian) Paluxy Formation of Texas. This disarticulated material shows resemblances both to *Amia* and to the Late Mesozoic European genera *Urocles* and *Amiopsis*. *Paramiatus gurleyi* (Romer and Fryxell, 1928) from the Green River Formation of Wyoming is a synonym of *A. fragosa*. The differences between *Amia* and the large Early Cenozoic form *Protamia* are insufficient for recognition of *Protamia* as a genus distinct from *Amia*. The Eocene and Oligocene forms *Protamia media, Pappichthys medius, P. plicatus, P. sclerops, P. laevis, P. symphysis, P. corsonii, Amia whiteavesiana,* and *A. macrospondyla* are synonyms of *A. uintaensis;* they were based on undiagnostic cranial and vertebral characters. Morphometric and meristic similarities indicate that little evidence exists for maintaining separate Oligocene species *Amia scutata* and *A. dictyocephala*. *Amia exilis* is a synonym of *Amia scutata;* it was based on undiagnostic vertebral characters. *A. scutata* is morphometrically distinguishable from *A. calva* only on the basis of a slightly larger head/stan-

[1] Museum of Comparative Zoology, Harvard University, Cambridge, Massachusetts 02138

dard-length ratio. The Eocene taxa *Amia depressus, A. newberrianus, A. gracilis,* and *Hypamia elegans* are *nomina dubia.*

Comparison of the fossil forms with the Recent *Amia calva* suggests the following taxonomic and possible phylogenetic relationships: (1) *Amia fragosa* survived until the Middle or Late Eocene, with no phylogenetic affinities with the modern form; (2) *Amia uintaensis* appears to be closer than *Amia fragosa* to the ancestry of *Amia calva,* which evolved through an intermediate form such as *Amia scutata;* (3) establishment of the Recent species *Amia calva* had begun at least by the beginning of the Pliocene; and (4) there are similarities in the Paleocene and Eocene amiid fossil record of North America and Europe.

INTRODUCTION

Amia is a genus of freshwater fishes that includes one of two extant representatives of the holostean level of organization. It includes a number of species of which only *Amia calva* exists today; other forms of *Amia* are found in the fossil record, and extend from the Late Cretaceous to approximately the Middle Pliocene. This study is an attempt to determine the taxonomic and phylogenetic relationships among the various species of *Amia.* It is established on osteology as well as on morphometric and meristic data from both Recent and fossil forms. This data is used to compare the available features of the fossil forms with Recent *Amia calva* and to determine the validity of previous descriptions based on various osteological, morphometric, or meristic character-states.

Until recently, a major difficulty in interpreting the taxonomy of fossil amiids has been the paucity of articulated specimens. Five genera and twenty-one species of fossil forms have been described from disarticulated, often isolated, elements (Table 19); only two taxa have been described from articulated specimens: *Paramiatus gurleyi* (Romer and Fryxell, 1928) and *Amia scutata* (Osborn *et al.,* 1875). Recent works by Estes (1964) and Estes and Berberian (1969), based on disarticulated elements from the Late Cretaceous Lance and Hell Creek formations, are the only published studies of *Amia fragosa,* although O'Brien (1969) completed an M.A. thesis on the osteology of *A. fragosa,* describing articulated specimens from the Late Cretaceous Edmonton Formation of Alberta.

Much more articulated material is now available and provides more detailed information on the cranial and postcranial anatomy of amiids. These specimens have been useful in this revision of the taxonomy as well as in the determination of possible relationships to European and Asian forms.

In an attempt to understand the evolution and interrelationships of the fossil and Recent amiids, a growth-series study has been made on a Recent *A. calva* sample from Wisconsin, and is compared morphometrically and meristically with the fossil forms. A great number of fossil specimens, including the holotypes and paratypes of all North American amiid species, have been examined. Several European taxa have been studied at the British Museum (Natural History), London; Muséum National d'Histoire Naturelle, Paris; and the Institut Royal des Sciences de Belgique, Brussels.

ACKNOWLEDGMENTS

I am especially grateful to Professor Richard Estes (University of California at San Diego) for his advice and criticism in the preparation of this manuscript. Cecile Janot-Poplin and Sylvie Wenz (Muséum National d'Histoire Naturelle, Paris), and Karel Liem (Museum of Comparative Zoology) read the manuscript and offered criticisms that substantially improved the text.

Additional thanks are due to Donald Baird (Princeton University), Henry Booke and Barry Cameron (Boston University), William J. Hlavin (Cleveland Museum of Natural History), Farish A. Jenkins, Jr. (Museum of Comparative Zoology), Charles Meehan (Chamberlayne College), Robert R. Miller (University of Michigan), David Parris (New Jersey State Museum), Colin Patterson (British Museum of Natural History), Clayton Ray (National Museum of Natural History), Bobb Schaeffer (American Museum of Natural History), Hans-Peter Schultze (Geologisch-Paleon-

tologisches Institut der Georg-August-Universität, Göttingen), Keith Thomson (Yale University), and Rainer Zangerl (Field Museum of Natural History) for their helpful suggestions. I am also grateful to Leslie Whone for preparation of tables, and to Siri Falck-Pedersen Boreske, Laszlo Meszoly, and Charles Chamberlain for illustrations.

This study was supported by grants from Sigma Xi, Marsh Fund, and the Albion Foundation.

ABBREVIATIONS

AMNH—American Museum of Natural History, New York, New York.
ANSP—Academy of Natural Sciences of Philadelphia, Philadelphia, Pennsylvania.
BMNH—British Museum (Natural History), London, England.
CM—Carnegie Museum, Pittsburgh, Pennsylvania.
F:AM—Frick-American Museum Collection, New York, New York.
FHKSM—Fort Hays Kansas State Museum, Hays, Kansas.
FMNH—Field Museum of Natural History, Chicago, Illinois.
FSM—Florida State Museum, Gainesville, Florida.
MCZ—Museum of Comparative Zoology, Harvard University, Cambridge, Massachusetts.
MNHN—Muséum National d'Histoire Naturelle, Paris, France.
NMC—National Museum of Canada, Ottawa, Canada.
PU—Museum of Natural History, Princeton University, Princeton, New Jersey.
ROM—Royal Ontario Museum, Toronto, Canada.
SMUSMP—Shuler Museum of Paleontology, Southern Methodist University, Dallas, Texas.
UA—University of Alberta Museum, Edmonton, Canada.
UCMP—Museum of Paleontology, University of California, Berkeley, California.
UMM—West Texas Museum, University of Texas, El Paso, Texas.
UMMP—University of Michigan Museum of Paleontology, Ann Arbor, Michigan.
UMMZ—University of Michigan Museum of Zoology, Ann Arbor, Michigan.
USNM—National Museum of Natural History, Washington, D.C.
YPM—Peabody Museum of Natural History, Yale University, New Haven, Connecticut.

AMIA CALVA LINNAEUS, 1766

Amia calva is the only extant species of the family Amiidae. It is a predaceous fish that exclusively inhabits fresh waters of the eastern United States. Except for the gar, *Lepisosteus*, *Amia calva* is the only other living representative of the holostean fishes. Its common name, "bowfin," refers to the long dorsal fin that arches in a bow over most of the length of the fish's back. *Amia calva* has previously been known as the dogfish, marshfish, mudfish, grindle, or lawyer.

The osteology of *Amia calva* has been extensively described and discussed by Schufeldt (1885), Bridge (1877), Allis (1889, 1897), and Goodrich (1930). The following discussion is limited only to the nomenclatural problems, ecology, geographic distribution, and character-states of *Amia calva* that are relevant to study of the fossil forms.

Nomenclature

Jordan and Evermann (1896) noted that although Linnaeus (1766) had applied the binomial name *Amia calva* to the genus, Gronow (1763) had earlier used *Amia* as a nonbinomial name for fishes presently classified as *Apogon* Lacépède. They further suggested that should Gronow's earlier application of the name be given precedence and transferred to *Apogon*, then *Amiatus* Rafinesque (1815) should replace *Amia* Linnaeus. Jordon (1906) stated that this transfer of names was a necessary compliance with the rules of nomenclature, but later (1919), although citing Opinion 20

(1910) of the International Commission on Zoological Nomenclature which favored Gronow's priority, Jordan found the transfer of names inconvenient, for most authors had rejected Gronow's names as pre-Linnaean. In 1925, Jordan recommended to the Commission that certain names of Gronow supported by Opinion 20 be rejected in favor of the more accepted Linnaean terminology. The Commission's Opinion 89 (1925) resolved (among others) the nomenclatural problem of *Amia,* by concurring with Jordan's recommendation that ". . . *Amia* Gronow be set aside in favor of *Amia* Linnaeus, even if other names of Gronow are allowed." Rafinesque's name *Amiatus* is then a junior synonym of *Amia* Linnaeus.

Some later workers seem to have been unaware of Opinion 89. Thus Hussakof (1932) accepted the validity of the transfer of the name *Amia* Gronow to the percoid teleost *Apogon.* Romer and Fryxell (1928) named their fossil amiid from the Eocene Green River Formation *Paramiatus* instead of *Paramia,* and Whitley (1954) changed the name of Lehman's (1951) fossil amiid from the Eocene of Spitzbergen from *Pseudamia* to *Pseudamiatus.* The latter is invalid as *Pseudamia* was a valid name in itself and *Pseudamiatus* is its junior synonym regardless of the *Amia-Amiatus* controversy.

Ecology

Aside from notes regarding breeding, diet, and zoogeographical occurrences, little has been written in the past 50 years about the ecology of *Amia calva.* Dean (1898) and Reighard (1903) have made the only extensive published investigations of the habits and habitat of the fish. A thorough study of the biology of *A. calva* throughout its range is long overdue.

Geographic Distribution

The distributional map of *Amia calva* (Fig. 1) is based on information drawn from Hubbs and Lagler (1967), and Blair *et al.* (1968), and from examinations of unpublished records at the Ohio State University Museum of Zoology, Museum of Comparative Zoology, and the University of Michigan Museum of Zoology. The distribution limit is a flexible boundary allowing for seasonal occurrences and other natural variations. The known northern limit of *A. calva* extends from the Mississippi drainage system in Minnesota south of Duluth, eastward through Lake Nipissing and the Ottawa River to the St. Lawrence-Champlain basin (encompassing Quebec as far north as Quebec City, and Vermont). *A. calva* is distributed throughout the Great Lakes region, but is not found in the Lake Superior drainage basin, except in its outlet, the St. Mary's River. Southward, it has been recorded from the Hudson River to western Connecticut (recorded as the result of introduction; Hubbs and Lagler, 1967); Harrisburg, Pennsylvania, to the Susquehanna River; and along the Atlantic slope to the Carolinas and Florida. Westward, *A. calva* occurs along the Gulf Coast to southern Texas as far south as Brownsville, and northward, through eastern Texas, southeastern Oklahoma, northwestern Arkansas, eastern Missouri, and approximately 50 miles west of the Mississippi River to Brainard, Minnesota.

Pleistocene Occurrences

Amia calva has been reported from only three Pleistocene localities: (1) Chicago, Illinois, (2) Vero Beach, Florida, and (3) Itchtucknee River deposits, Columbia County, Florida (MCZ 9524, 9529, 9542). Hay (1911: 552) reported "Professor Frank Baker (Chicago Academy of Science) has shown me a considerable part of the skeleton and scales of a bowfin which he found in the Pleistocene clay near Chicago." A thorough search of the Chicago Academy of Science collections failed to produce this specimen. Hay (1917, 1923) listed *Amia calva* among the fossil vertebrate remains found in the Pleistocene sands at Vero Beach, Florida. Swift (1968), in his review of fossil fishes of Florida, figured Hay's *Amia* specimens (left dentary and a gular plate; FSM collections) and concluded that

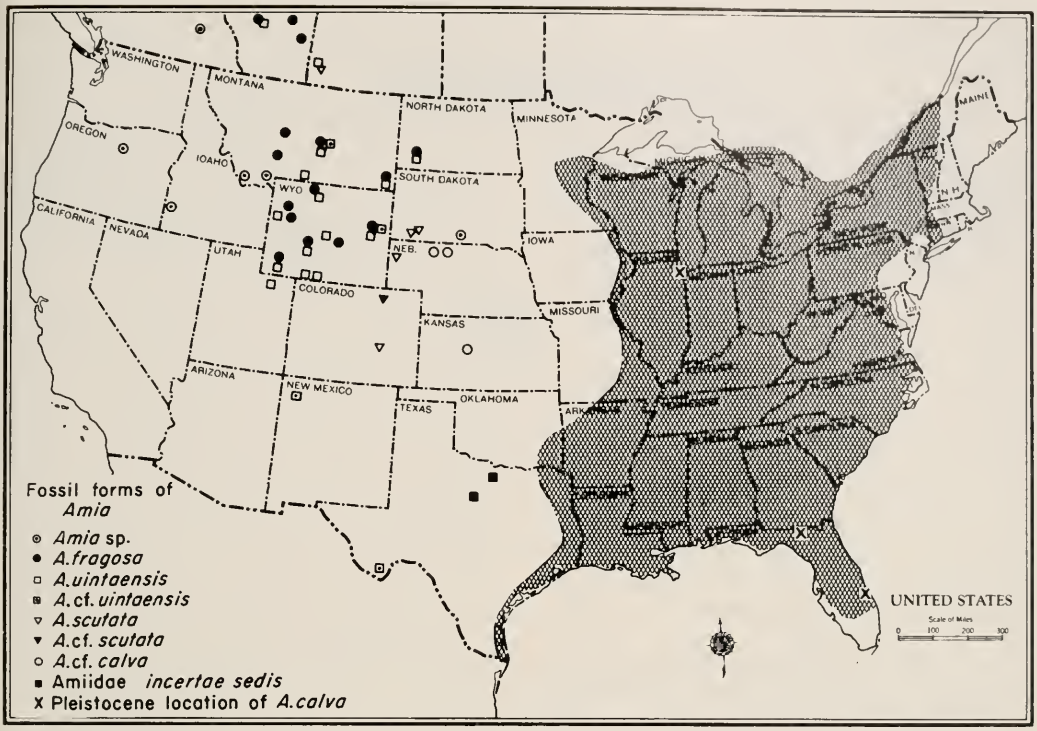

Fig. 1. Distribution of *Amia calva*. Fossil occurrences of *Amia* spp. are represented by symbols explained in the legend.

A. calva was probably very common in the Pleistocene fresh waters of the United States. The paucity of Pleistocene material does not necessarily mean the fish was not common in the Pleistocene, but does indicate that *Amia* remains have not been extensively collected or identified in existing museum Pleistocene collections.

Diagnosis

Vertebral meristics similar to *A. scutata*, but head/standard-length proportion (0.271 mean) is smaller than in the fossil forms. Extrascapular strap-shaped and relatively wide at midline, as in *A. scutata*, but posterior edge is curved so that it is proximally convex, then concave toward the distal corner, which results in a posterolateral projection. Pterotic borders frontal posteriorly rather than laterally; anterior end is as wide as posterior end. Orbital excavation is shallower than in other species, with a mean depth-to-length ratio of 0.100. Infraorbital 4 is smaller than infraorbital 5, less robust than in fossil *Amia*. Preoperculum as wide dorsally as ventrally. Symphyseal incurving of dentary relatively less than in *A. fragosa*, but greater than in *A. scutata* and *A. uintaensis;* little or no overlapping of dorsal coronoid articulation surface on ventral surface of ramus; deep Meckelian groove. Ventroposterior process of cleithrum less sculptured than in other species of *Amia*. Vomerine teeth sharp, conical, numbering between 15–27, more anteriorly placed than in *A. uintaensis* or *A. fragosa*. Bones less ossified than in fossil *Amia*. Greatest known standard-length 650 mm.

MORPHOMETRICS

Comparison of morphometric and meristic data of Recent and fossil *Amia* has facilitated an evaluation of the taxonomy as well as clarified anatomical trends. Many

generic or specific character-states for *Amia "dictyocephala," Amia scutata, "Paramiatus gurleyi,"* and *Amia fragosa* have been previously established on osteological data based primarily on gross anatomical proportions (head/standard-length ratio and positions of insertion of pelvic and anal fins/standard-length ratios) and skull proportions (parietal/frontal and operculum width/length ratios). Meristic character-states have also been used for *A. "dictyocephala"* and *A. scutata.*

Although an age-growth analysis on *Amia calva* was done by Cartier and Magnin (1967), no morphometric investigation of a growth-series of Recent *A. calva* has yet been completed or used for comparison with fossil forms. Estes and Berberian (1969: 10) suggest that knowledge of the growth-series of *A. calva* would be of considerable importance in tracing the ancestry of the modern species.

Hammett and Hammett (1939) made a morphometric study of the Recent *Lepisosteus platyrhincus,* taking length dimensions of a sample of live fish from Florida. Since *Lepisosteus,* like *Amia,* is one of the two extant holosteans, their analysis is potentially useful in providing information on the ancient species. However, they did not actually compare the live material or data with any fossil material.

According to Imbrie (1956), Simpson *et al.* (1960), and Gould (1966), growth studies offer excellent means with which to clarify evolutionary and taxonomic problems in the fossil record. An interesting model utilizing morphometric data for synonymy of fossil forms was made by Thomson and Hahn (1968) on the growth-series patterns of Devonian rhipidistian fishes, in which they showed that *Thursius clappi* was actually a juvenile form of *Eusthenopteron foordi.* In studying fossil material, as Thomson and Hahn (1968: 201) indicate, there is a problem in determining the age, sexual maturity, and environmental regime of the animal. Also, of course, it is necessary to have sufficient fossil material with which to erect an adequate growth-series.

This present analysis is undertaken (1) to determine whether skull and axial skeletal proportions of amiids are isometric or allometric with increasing size, (2) to establish the variation in meristic characters of Recent *A. calva,* and (3) to compare morphometrics and meristics of Recent *A. calva* with those of the fossil forms. This study utilizes a small sample of 18 Recent *A. calva* specimens from the St. Croix River, Wisconsin. Measurements were taken from a growth series that includes the size range of most of the articulated fossil forms. The largest *A. calva* specimen, from St. Joseph County, Michigan (UMMZ 197683), was analyzed to see whether the large specimen would agree with the anatomical proportions and meristic characters of the Wisconsin specimens. Three smaller specimens from Pewaukee, Wisconsin (MCZ 8970), were also included. The fossil sample contains six complete and ten partially complete amiid specimens ranging in age from Late Cretaceous to Late Miocene which, although morphometrically similar in varying degree, are too few to warrant conclusions in themselves.

Methods

Measurements chosen for this study (Fig. 2) are those of Hubbs and Lagler (1967: 20). In fossil forms, because of the lack of preservation of internal soft anatomy as well as the impossibility of determining their interbreeding potential, these particular measurements necessarily assume an increased taxonomic significance, since they often provide the only viable parameters with which to designate genera and species. Measurements taken on *A. calva* are limited to those also represented in the fossil specimens. Each of the *A. calva* measured was X-rayed, except for three small specimens, which were cleared and stained. The range of error for all measurements taken on Recent and fossil material is ± 0.04 mm. The range of error for the ratios is ± 0.08 mm;

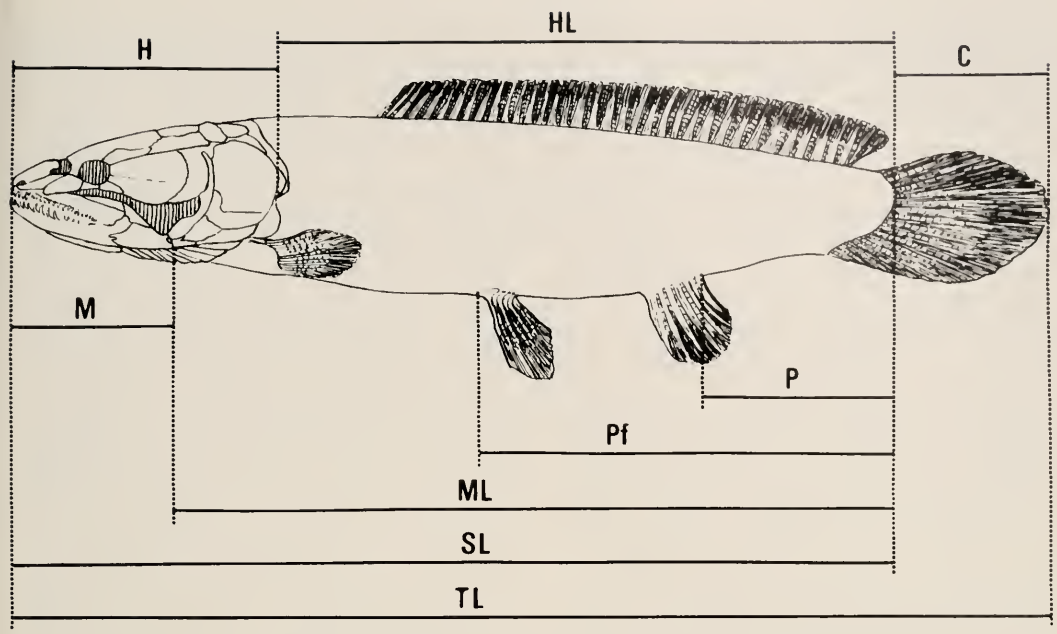

Fig. 2. Index to the measurements used, superimposed upon an outline drawing of *Amia*.

Key for body measurements:

TL = Total-Length
SL = Standard-Length
H = Head-Length
C = Caudal-Length
Pf = Insertion of Pelvic Fin
P = Insertion of Anal Fin
HL = Standard-Length minus Head-Length
ML = Standard-Length minus Mandible-Length

Key for abbreviations of cranial elements used in morphometric study:

M = Mandible
G = Gular
I^5 = Infraorbital 5
F = Frontal
Par = Parietal
O = Operculum

Table 1. Length dimensions of 22 specimens of *Amia calva* L.: 21 from Wisconsin (MCZ 8970*), 1 from Michigan (UMMZ 197683)**
Measurements in mm

Specimen Code	Class Range Total Length	No.	TL	SL	ML	H	HL	Pf	P	C
1*	80.0	1	80.0	70.5	57.0	22.0	48.5	32.5	12.5	10.5
2*	95.0–105.0	2	100.0	85.0	70.0	25.0	60.0	39.5	16.0	15.0
3	207.0–212.0	6	210.0	175.0	145.0	50.5	124.5	80.9	35.0	35.0
4	227.9–232.0	4	230.0	193.0	161.0	54.6	138.4	88.5	35.5	36.0
5	241.0	1	241.0	199.0	165.9	56.8	142.2	93.5	38.0	42.0
6	291.0	1	291.0	237.0	197.0	64.0	173.0	115.0	52.5	54.0
7	310.0	1	310.0	248.0	207.0	68.5	179.5	112.0	46.0	62.0
8	339.0	1	339.0	274.0	230.0	73.0	202.0	125.0	51.0	64.0
9	385.0	1	385.0	313.0	259.0	82.0	231.0	142.0	52.0	72.0
10	433.0	1	433.0	349.0	293.0	91.0	258.0	170.0	71.0	84.0
11	475.0	1	475.0	399.0	335.0	103.0	296.0	181.0	82.0	76.0
12	507.0	1	507.0	423.0	359.5	109.0	317.0	192.0	93.0	81.0
13**	756.0	1	756.0	648.0	545.3	164.0	480.0	299.0	138.0	102.0

See Figure 2 for abbreviations.

this margin of error is graphically inconsequential in this study. Specimens of *A. calva* whose total length was between 207 mm and 507 mm were selected because this range of *A. calva* would provide the best information for comparison with the fossil species. Twenty-two specimens of *A. calva* were measured (Table 1). Eighteen of these are from the St. Croix River, Wisconsin. These 18 specimens of *A. calva* fall into ten categories arranged here by approximately 20–30-mm class range increments in total-length. Although these categories represent arbitrary rather than biological growth stages, they provide sufficient information on the morphologic size changes of *A. calva.* Three smaller specimens (MCZ 8970, also from Wisconsin) with a size range of 80–105 mm total length (TL) were included to determine whether they would follow the predicted allometric effect on the growth-series line, since, as Thomson and Hahn (1968: 205) note, it is a common feature for the early stages of juvenile animals to have heads proportionately larger than the bodies. Hay (1895) notes that an 80-mm *A. calva* is beyond the embryonic stage and is an early juvenile with most of its bones at least partially ossified. The 80-mm specimen has a proportionately larger head to standard-length ratio than the other members of the growth-series (Table 3). Although this ratio decreases slightly with increasing size, the head/standard-length ratio of 0.312 for the 80-mm specimen does not deviate far from the growth-series line (Figs. 3–4).

The largest specimen (UMMZ 197683) was used as a size limit for the other end of the growth-series continuum. It may be assumed that this fish had already reached the size or point of maturity at which fish normally begin to decrease their rate of growth. This specimen still retains the morphological proportions of the smaller specimens (Figs. 3–4) and, like them, falls remarkably close to the constant relative size-growth lines of the various proportions. Although from Michigan, this specimen does not appear to deviate from the growth-series line established by the Wisconsin specimens of *A. calva.* The Michigan specimen of *A. calva,* since it agrees with the growth-series continuum established by the Wisconsin specimens, is helpful in extending comparison to the larger fossil amiids: "*Paramiatus gurleyi*" (FMNH 2201), *Amia fragosa* (MCZ 5341), and *Amia uintaensis* (PU 13865), which are outside the size range of the Wisconsin sample.

General Proportions and Growth

Allometric growth, according to Gould (1966: 595), describes geometrically progressive change in shape or proportions with size, and is generally represented by a curvilinear line or, in certain cases, by a straight line in which the Y-intercept is significantly different from 0.

For the *Amia calva* growth series discussed here, the ordered pairs corresponding to the proportions in each series have been plotted on a graph, as well as the straight line corresponding to the equation $y = a + bx$ (of the best fit computed ac-

Table 2. Length dimensions of 6 articulated fossil amiids
Measurements in mm

	TL	SL	ML	H	HL	Pf	P	C
A. scutata PU 10172	est404.0	339.0	276.5	106.0	233.0	159.0	73.0	est65.0
A. scutata UMMP V-57431	—	388.0	313.8	121.0	267.0	183.0	83.0	—
A. kehreri BMNH P33480	249.0	191.0	160.8	59.2	131.8	89.0	38.5	58.0
"*Paramiatus gurleyi*" FMNH 2201	702.0	510.0	430.0	157.0	353.0	est265.0	78.0	192.0
A. fragosa MCZ 5341	575.0	455.0	383.0	142.0	313.0	210.0	75.0	115.0
A. uintaensis PU 13865	848.0	664.0	—	214.0	450.0	288.0	116.0	160.0

See Figure 2 for abbreviations.

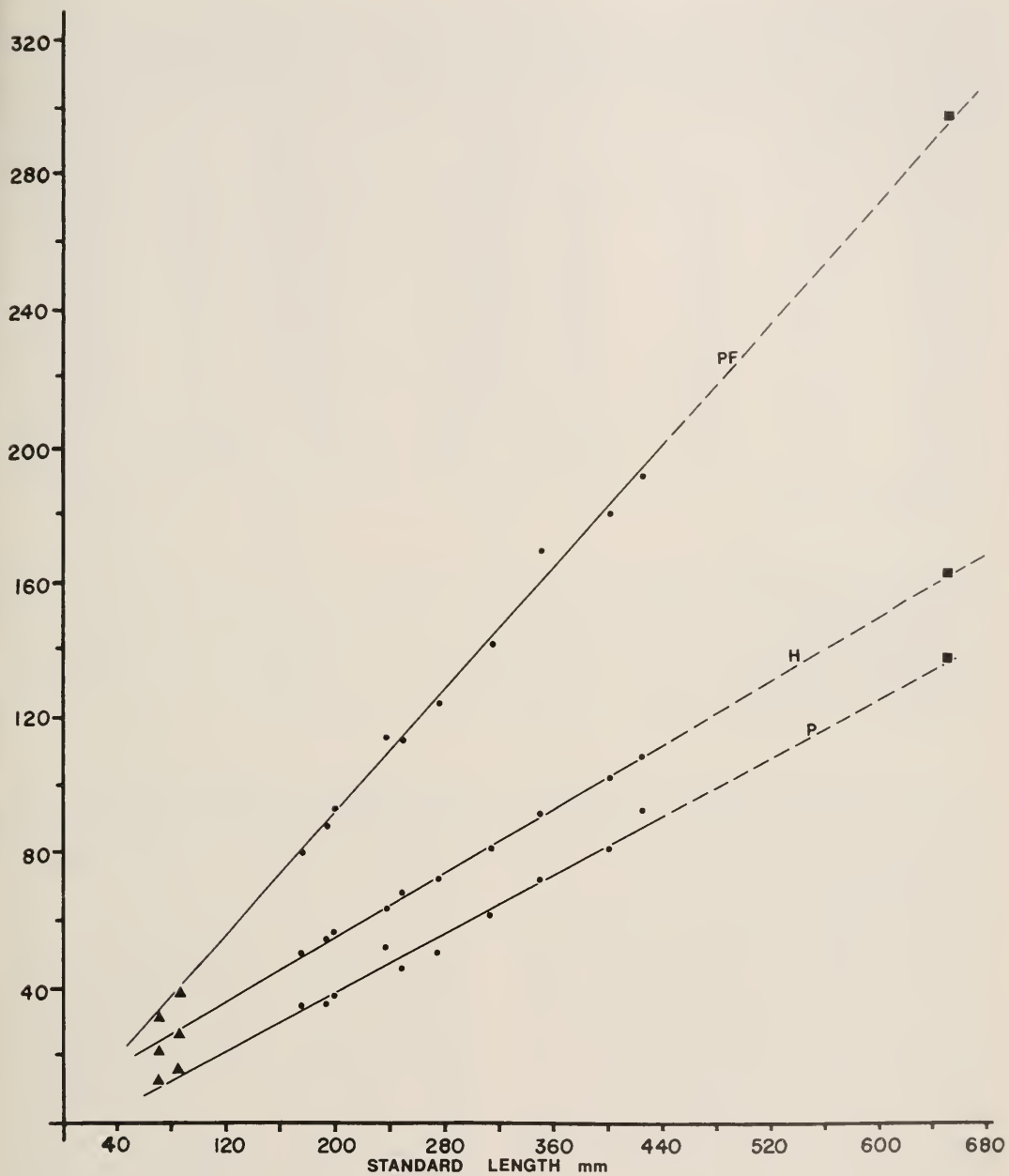

Fig. 3. Relative growth-lines of head-length (H), pelvic fin insertion (Pf), and anal fin insertion (P) plotted orithmetically against standard-length, for 18 specimens of Recent *Amia calva* (▲ = MCZ 8970 and ■ = UMMZ 197683 are included for comparison).

cording to the method of least squares); the results of these calculations appear in Figures 3–4. Practically all the ratios in Figure 3 fall onto straight lines, each of which nearly passes through the origin of the graph. The coefficient of correlation is almost equal to 1.0 in each case, an indication that the computed straight line provides

Table 3. Comparison of length proportions in 22 specimens of *Amia calva* with fossil amiids

Specimen Code	H/SL	Pf/SL	P/SL
1	0.312	0.461	0.177
2	0.294	0.464	0.188
3	0.289	0.462	0.200
4	0.283	0.459	0.184
5	0.285	0.470	0.191
6	0.270	0.485	0.222
7	0.276	0.452	0.185
8	0.266	0.456	0.186
9	0.262	0.455	0.198
10	0.261	0.487	0.203
11	0.258	0.454	0.206
12	0.258	0.454	0.220
13	0.259	0.461	0.213
	0.258–0.289* mean = (0.271)*	0.452–0.487* mean = (0.463)*	0.184–0.222* mean = (0.199)*
Oligocene			
A. scutata PU 10172	0.313	0.469	0.215
A. scutata UMMP V-57431	0.312	0.472	0.214
Eocene			
A. kehreri BMNH P33480	0.310	0.466	0.201
"Paramiatus gurleyi" FMNH 2201	0.308	est0.520	0.153
A. fragosa MCZ 5341	0.312	0.462	0.165
A. uintaensis PU 13865	0.322	0.434	0.175

* Range and mean exclude Specimen Codes 1 & 2 (MCZ 8970) and 13 (UMMZ 197683).

a very good fit for the ratio series, and that the relative growth of these three dimensions is essentially isometric rather than allometric. The Wisconsin specimens (including the 80–105-mm specimens) and the larger Michigan specimen all fall close to the line calculated for each of the three ratios (Fig. 3). The proportions of head-length/standard-length, insertion of pelvic fins/standard-length, and insertion of anal fins/standard-length are shown in Table 3. The head/standard-length ratio shows a slight decrease with increasing size, but this ratio series nonetheless has a very high coefficient of correlation for the strength of the linear relationship (Fig. 4).

The lengths of the mandible, parietal, frontal, and operculum in Recent *A. calva* appear in Table 4, and the proportional ratios in Table 6. The relative growth rate of each of these proportions is constant with X and Y-intercepts of the straight line close to the origin. The coefficient of correlation for the variables in each of the proportions is 0.997, 0.975, and 0.997, respectively (Fig. 5). Combined, these two factors indicate constant and therefore isometric relative size-growth of the compared skull element.

Comparisons with Fossil Forms

Six articulated fossil specimens were available for measurement and calculation of head/standard-length and positions of insertion of pelvic and anal fins/standard-length (Tables 2–3). The measurements taken from the fossil forms are as exact as conditions allow, although it must be stressed that varying degrees of crushing and distortion have occurred in fossilization, and evaluation of the morphometrics should be qualified with this in mind.

Head/standard-length ratios (Fig. 4). The fossil forms all show a slightly greater head/standard-length ratio than does the Recent species (Table 3; Fig. 4). *A. uintaensis* (PU 13865) is the largest of

Table 4. Length dimensions of Mandible (M), Gular (G), Frontal (F), Parietal (Par), Infraorbital 5(I^5), and Operculum (O) in 22 specimens of *A. calva*
Measurements in mm

Specimen Code	M	G	F	Par	I^5	Operculum Dors.-Vent. (OL)	Operculum Ant.-Post. (OD)
1°	13.5	8.0	10.0	5.0	5.0	8.1	7.5
2°	14.9	9.4	11.4	6.1	5.8	9.0	8.4
3	30.0	19.0	18.0	9.7	12.0	14.0	12.9
4	32.0	21.0	20.0	9.9	13.5	15.0	14.2
5	33.5	20.5	19.0	10.0	14.2	16.0	14.9
6	39.0	26.0	25.0	11.0	17.0	16.9	16.5
7	42.0	28.0	25.5	11.5	18.0	18.1	17.5
8	45.0	27.0	26.2	13.5	21.0	19.8	18.5
9	53.0	31.0	31.0	14.7	22.5	22.8	21.8
10	56.0	32.5	32.2	17.0	26.5	22.6	22.5
11	63.0	39.0	38.4	18.5	30.5	28.1	27.8
12	66.5	42.5	39.0	19.5	31.5	27.8	28.5
13°°	102.7	—	60.7	30.0	—	—	—

° MCZ 8970.
°° UMMZ 197683.

all the fossil specimens, but nonetheless has a greater head/standard-length ratio than any of the others. The head of this form is so much more elongated than the head in *A. fragosa* (MCZ 5341), *A. kehreri* (BMNH P33480), and *"Paramiatus gurleyi"* (FMNH 2201) that it offsets the fact that its vertebral column includes approximately 20 more vertebrae than do these three forms (Table 9). Thus, although *A. uintaensis*

Table 5. Length dimensions of Head (H), Mandible (M), Gular (G), Frontal (F), Parietal (Par), Infraorbital 5(I^5), and Operculum (O) in fossil amiids
Measurements in mm

	H	M	G	F	Par	I^5	Operculum Dors.-Vent. (OL)	Operculum Ant.-Post. (OD)
A. cf. *scutata* UCMP 38222	—	65.2	—	46.0	23.0	35.0	—	—
A. scutata PU 10172	106.0	62.5	31.2	35.0	16.0	—	29.0	28.0
A. scutata UMMP V-57431	121.0	74.2	—	44.3	20.0	—	29.1	27.9°°
A. "dictyocephala" AMNH 2802	111.5	68.0	—	38.0	17.0	29.1	32.0	30.0
A. kehreri BMNH P33480	59.2	30.2	—	20.0	8.4	15.3	20.5	19.0
"Paramiatus gurleyi" FMNH 2201	157.0	80.0	—	58.0	23.6	25.0	40.0	37.0
A. fragosa MCZ 5341	142.0	72.0	68.7	56.0	22.8	—	39.0	36.2
A. fragosa MCZ 9264	80.0	40.0	—	26.0	10.5	18.5	—	—
A. uintaensis PU 13865	214.0	—	—	88.0	34.0	—	55.0	51.0
"Protamia" mongoliensis AMNH 6372	—	—	81.0	—	—	—	54.0	52.0
A. uintaensis PU 16236	315.0°°	220.0	158.0	160.0	60.0	—	—	95.0
A. fragosa MCZ 9291	—	—	—	—	—	—	27.0	25.0
A. fragosa AMNH 9315	—	—	—	—	—	—	29.0°°	27.0
A. fragosa UA 5450°	—	—	—	26.0	10.0	—	—	—
A. fragosa UA 5458°	—	—	—	30.0	12.0	—	—	—
A. fragosa UA 5480°	—	—	—	—	—	20.0	26.0	24.0

° Data from O'Brien (1969).
°° Est.

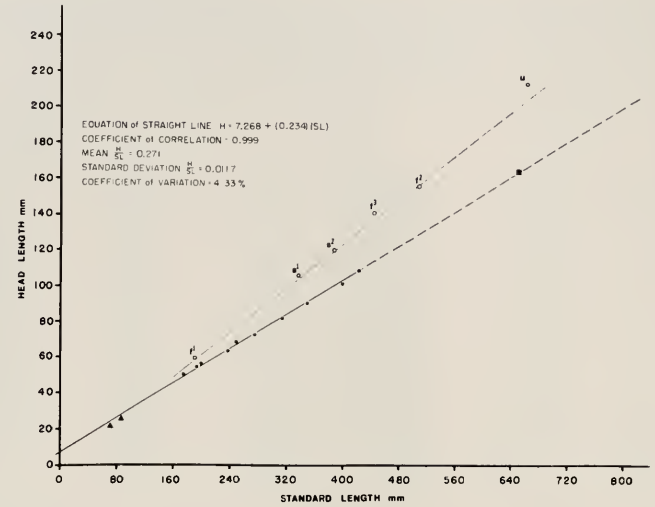
EQUATION of STRAIGHT LINE H = 7.268 + (0.234)(SL)
COEFFICIENT of CORRELATION = 0.999
MEAN H/SL = 0.271
STANDARD DEVIATION H/SL = 0.0117
COEFFICIENT of VARIATION = 4.33 %
HEAD LENGTH mm
STANDARD LENGTH mm
0
20
40
60
80
100
120
140
160
180
200
220
240
0
80
160
240
320
400
480
560
640
720
800

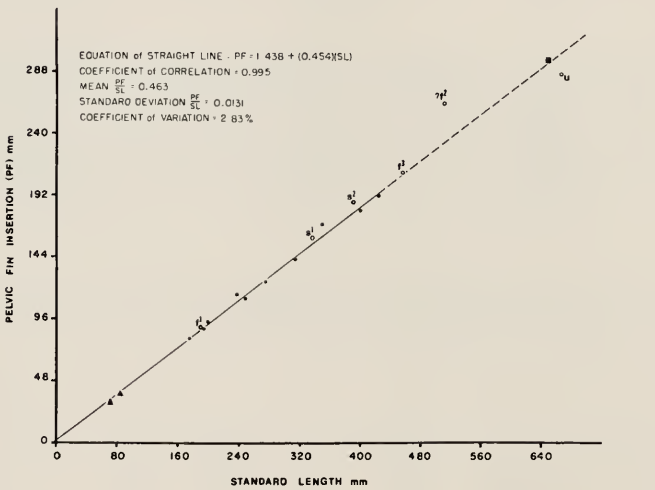
EQUATION of STRAIGHT LINE : PF = 1.438 + (0.454)(SL)
COEFFICIENT of CORRELATION = 0.995
MEAN PF/SL = 0.463
STANDARD DEVIATION PF/SL = 0.0131
COEFFICIENT of VARIATION = 2.83%
PELVIC FIN INSERTION (PF) mm
STANDARD LENGTH mm
0
48
96
144
192
240
288
0
80
160
240
320
400
480
560
640

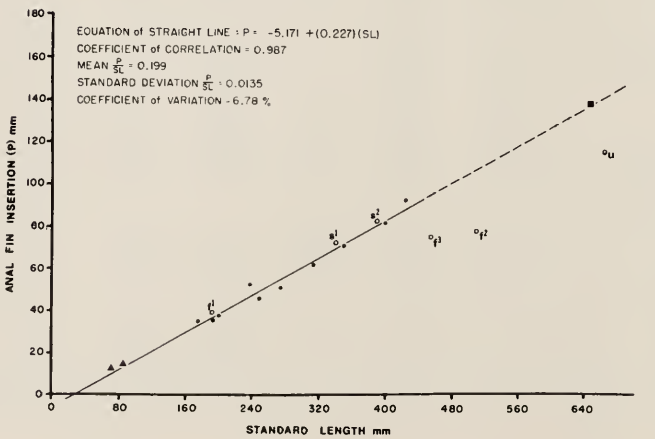
EQUATION of STRAIGHT LINE : P = -5.171 + (0.227)(SL)
COEFFICIENT of CORRELATION = 0.987
MEAN P/SL = 0.199
STANDARD DEVIATION P/SL = 0.0135
COEFFICIENT of VARIATION = 6.78 %
ANAL FIN INSERTION (P) mm
STANDARD LENGTH mm
0
20
40
60
80
100
120
140
160
180
0
80
160
240
320
400
480
560
640

has significantly more vertebrae than these other forms, this feature is not reflected in a comparison of head/standard-length ratios (Table 3). This is also true, to a lesser extent, in both *A. scutata* specimens (PU 10172, UMMP V-57431) from the Oligocene Florissant Formation; these specimens fall into the head/standard-length range of the three fore-mentioned forms, but like *A. uintaensis*, possess vertebral columns having nearly the same number of centra as those in *A. calva*. Thus in themselves the head/standard-length ratios are of little help in comparing the fossil forms, but when coupled with the corresponding lengths of the vertebral column (based on number of centra) they are informative. *A. uintaensis* (PU 13865) and *A. scutata* (PU 10172, UMMP V-57431) have relatively elongated heads; *A. kehreri* (BMNH P33480), *A. fragosa* (MCZ 5341), and "*Paramiatus gurleyi*" (FMNH 2201) have relatively shorter heads, since the head/standard-length ratio is less than might otherwise be expected considering the smaller total-number of centra (only two-thirds the number of centra of *A. uintaensis*, *A. scutata*, and *A. calva*). A tentative growth-line (also calculated by the best-fit method) was included for *A. fragosa* on the basis of three specimens (Fig. 4). In comparison with the growth-line of the Recent species (0.271 mean), it reflects the larger head/standard-length ratio of *A. fragosa* (0.310 mean). The growth-line computed for *A. fragosa* is linear and falls near the origin, indicating that increase in head size/standard-length was isometric, as in *A. calva*.

Fin relationships. In the smaller fossil forms, the ratio of the point of insertion of the pelvic fin/standard-length shows little deviation from the modern species (Table 3; Fig. 4) except for two Eocene specimens, "*Paramiatus gurleyi*" (FMNH 2201) and *A. uintaensis* (PU 13865), which fall outside of the range on either side of the size-growth line. The greater ratio for "*Paramiatus gurleyi*," however, is probably the result of distortion in its preservation. The length of the pelvic fin insertion/standard-length does not appear to be a satisfactory taxonomic index, distinguishing neither the fossil forms from one another nor the fossil forms from the Recent *A. calva*.

"*Paramiatus gurleyi*" (FMNH 2201), *A. uintaensis* (PU 13865), and *A. fragosa* (MCZ 5341) have a relatively shorter dimension between the anal fin and the end of the vertebral column than do *A. calva*, *A. scutata*, and *A. kehreri* (Fig. 31). Any attempt to interpret the fossil data for this ratio is complicated by the fact that considerable overlap with the Recent species occurs. Both long-bodied (*A. scutata*) and short-bodied (*A. kehreri*) forms fall within the range of *A. calva*, while other long-bodied (*A. uintaensis*) and short-bodied (*A. fragosa*, including "*Paramiatus gurleyi*") forms fall below the range of the Recent species (Table 3). Although the ratio of anal fin/standard-length may possibly be useful in distinguishing *A. fragosa* (including "*Paramiatus gurleyi*") from *A. calva*, *A. scutata*, and *A. kehreri*, it is not useful in distinguishing either of the two fossil forms from one another or from *A. calva*. The smaller dimension indicated by the low ratios (0.153, 0.165) of *A. fragosa* is doubtless a reflection of its shorter axial column. The relatively small (0.175) ratio for *A. uintaensis* is probably in part the result of its longer head, which increases its standard-length in relation to the other forms; at any rate, the difference between the *A. uintaensis* ratio and the range for Recent *A. calva* is not very significant.

Mandible/head ratios. A comparison of

Fig. 4. Relative growth-lines (broken-solid lines) of head-length, pelvic fin insertion, and anal fin insertion plotted arithmetically against standard-length for Recent *Amia calva* (▲ = MCZ 8970 and ■ = UMMZ 197683 are included for comparison) with compared fossil forms: f^1 = *A. fragosa (A. kehreri)* BMNH P33480; f^2 = *A. fragosa (Paramiatus gurleyi)* FMNH 2201; f^3 = *A. fragosa* MCZ 5341; s^1 = *A. scutata* PU 10172; s^2 = *A. scutata* UMMP V-57431; *u* = *A. uintaensis* PU 13865. The broken-dotted line is the "best fit" line for available specimens of *A. fragosa*.

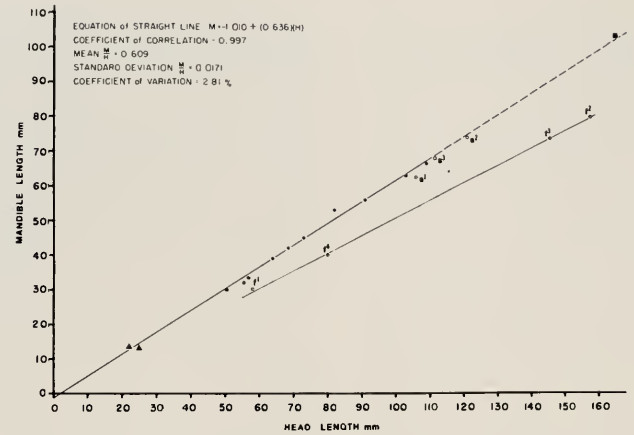
EQUATION of STRAIGHT LINE M = -1.010 + (0.636)(H)
COEFFICIENT of CORRELATION = 0.997
MEAN M/H = 0.609
STANDARD DEVIATION M/H = 0.0171
COEFFICIENT of VARIATION = 2.81 %
MANDIBLE LENGTH mm
HEAD LENGTH mm

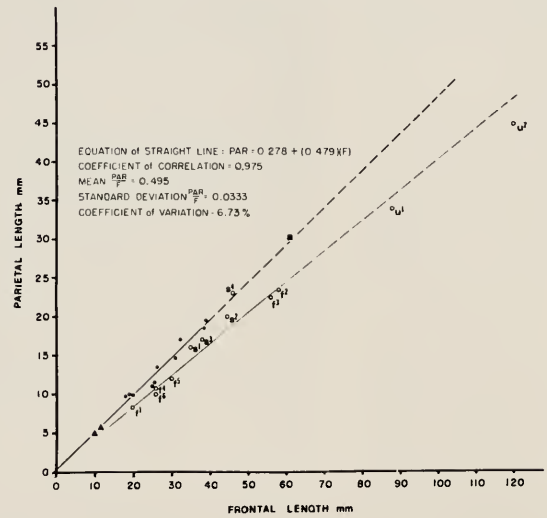
EQUATION of STRAIGHT LINE : PAR = 0.278 + (0.479)(F)
COEFFICIENT of CORRELATION = 0.975
MEAN PAR/F = 0.495
STANDARD DEVIATION PAR/F = 0.0333
COEFFICIENT of VARIATION = 6.73 %
PARIETAL LENGTH mm
FRONTAL LENGTH mm

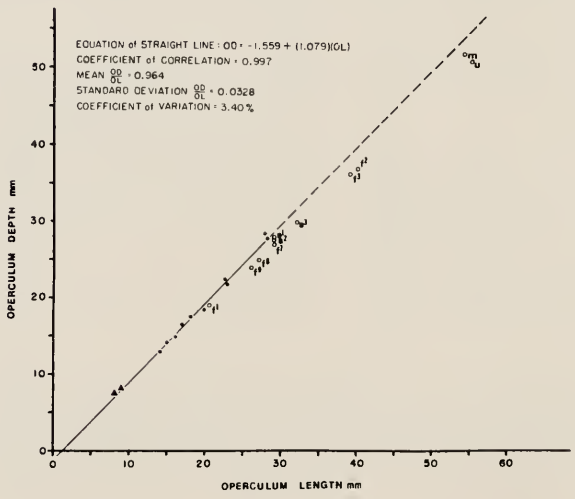
EQUATION of STRAIGHT LINE : OD = -1.559 + (1.079)(OL)
COEFFICIENT of CORRELATION = 0.997
MEAN OD/OL = 0.964
STANDARD DEVIATION OD/OL = 0.0328
COEFFICIENT of VARIATION = 3.40 %
OPERCULUM DEPTH mm
OPERCULUM LENGTH mm

Table 6. Cranial proportions in 22 specimens of *A. calva*

Specimen Code	M/H	Par/F	OD/OL
1	0.614	0.500	0.926
2	0.596	0.535	0.933
3	0.594	0.539	0.921
4	0.586	0.495	0.947
5	0.590	0.526	0.931
6	0.609	0.440	0.976
7	0.613	0.451	0.967
8	0.616	0.515	0.934
9	0.646	0.474	0.956
10	0.615	0.528	0.996
11	0.611	0.482	0.989
12	0.610	0.500	1.025
13	0.626	0.497	—
	0.586–0.646° mean = (0.609)°	0.440–0.539° mean = (0.495)°	0.921–1.025° mean = (0.964)°

° Range and mean exclude Specimen Codes 1 & 2 (MCZ 8970) and 13 (UMMZ 197683).

the mandible/head ratios of Recent *A. calva* with those of the fossil forms (Table 7; Fig. 5) indicates that the *A. scutata* and *A. "dictyocephala"* (AMNH 2802) ratios are very close to those of *A. calva*. The *A. fragosa* specimens (including *"Paramiatus gurleyi"* FMNH 2201 and *A. kehreri* BMNH P33480) have a mean mandible/head ratio of 0.507, which, when compared to the *A. calva* mean ratio of 0.609, indicates a relatively smaller mandible to head size (Table 7). Unfortunately, *A. uintaensis* (PU 13865) cannot be used in this comparison, since the mandibles are buried in matrix. A reconstruction of a disarticulated *A. uintaensis* (PU 16236) specimen from the Late Paleocene has been made, and its ratio is approximately 0.693. Thus mandible/head proportions may be valid for distinguishing specimens of *A. fragosa* and *A. uintaensis* from one another as well as from *A. calva* and *A. scutata*. This ratio, however, cannot be used as a valid criterion for distinguishing *A. scutata* from *A. calva*. The 0.693 mandible/head ratio of *A. uintaensis* indicates that this form has the largest mouth gape of the four valid species. A tentative growth-line for the mandible/head-length proportion of *A. fragosa*, established on four specimens, shows that its jaw is 16 percent smaller than that of *A. calva*, and in this respect confirms Romer and Fryxell's (1928) reconstruction of *"Paramiatus gurleyi."*

Parietal/frontal ratios. Only articulated frontals and parietals were measured for this study. The frontal-length was taken from the anteriormost extent of the dermal sculpture to the median point between the most anterior and posterior extents of the frontal-parietal suture; the parietals were also measured by their midline anteroposterior length. The parietal/frontal ratio of the fossil forms as compared with that of the Recent *A. calva* indicates that, in varying degree, the fossil species have relatively shorter parietals and longer frontals (Table 7; Fig. 5). The largest specimen of *A. uintaensis* (PU 16236) is mostly disarticulated, but fortunately the skull table is intact. It has the smallest parietal/frontal ratio of all the fossil species, 0.375. The Eocene *A. uintaensis* specimen (PU 13865) has a slightly larger ratio of 0.386, which is nearly equal to the Edmonton *A. fragosa* (UA 5450). All the other available *A. fragosa* specimens, including *"Paramiatus gurleyi"* (FMNH 2201), have slightly larger ratios and are quite consistent, ranging only

Fig. 5. Relative growth-lines (broken-solid lines) of mandible-length plotted arithmetically against head-length, parietal-length plotted arithmetically against frontal-length, and operculum-depth (anteroposteriorly) plotted arithmetically against operculum-length (dorsoventrally) for Recent *Amia calva* (▲ = MCZ 8970 and ■ = UMMZ 197683 are included for comparison when element measurements are available) with compared fossil forms: f^1 = *Amia fragosa (A. kehreri)* BMNH P33480; f^2 = *A. fragosa (Paramiatus gurleyi)* FMNH 2201; f^3 = *A. fragosa* MCZ 5341; f^4 = *A. fragosa* MCZ 9264; f^5 = *A. fragosa* UA 5458; f^6 = *A. fragosa* UA 5450; f^7 = *A. fragosa* AMNH 9315; f^8 = *A. fragosa* MCZ 9291; f^9 = *A. fragosa* UA 5480; s^1 = *A. scutata* PU 10172; s^2 = *A. scutata* UMMP V-57431; s^3 = *A. scutata (A. dictyocephala)* AMNH 2802; s^4 = *A.* cf. *scutata* UC 38222; u^1 = *A. uintaensis* PU 13865; u^2 = *A. uintaensis* PU 16236; m = *A. mongoliensis* AMNH 6372. The broken-dotted line is the "best fit" line for available specimens of *Amia fragosa*.

Table 7. Comparison of cranial proportions of recent and fossil amiids

	M/H	Par/F	OD/OL
Recent			
A. calva (18) (Wisc.)	0.586–0.646 mean = (0.609)	0.440–0.539 mean = (0.495)	0.921–1.025 mean = (0.964)
Miocene			
A. cf. *scutata* UCMP 38222	—	0.500	—
Oligocene			
A. scutata PU 10172	0.590	0.457	0.965
A. scutata UMMP V-57431	0.613	0.451	0.959
A. "dictyocephala" AMMH 2802	0.610	0.447	0.937
Eocene			
A. kehreri BMNH P33480	0.510	0.420	0.927
"Paramiatus gurleyi" FMNH 2201	0.509	0.407°	0.925
A. fragosa MCZ 5341	0.507	0.408	0.928
A. fragosa MCZ 9264	0.500	0.404	—
A. uintaensis PU 13865	—	0.386	0.927
"Pappichthys" mongoliensis AMNH 6372	—	—	0.963
Paleocene			
A. uintaensis PU 16236	0.693°	0.375	—
Cretaceous			
A. fragosa MCZ 9291	—	—	0.926
A. fragosa AMNH 9315	—	—	0.931°
A. fragosa UA 5450	—	0.385	—
A. fragosa UA 5458	—	0.400	—
A. fragosa UA 5480	—	—	0.923

° Est.

between 0.400–0.408. One of the specific character-states that Estes and Berberian (1969: 6) list for *A. fragosa* is a frontal-length of approximately 2.8 times the length of the parietals, which would give a ratio of 0.357. This figure is smaller than that of the known articulated forms, including the specimens from the Edmonton and Willwood formations. Although they may have placed too much emphasis on this specific character-state, Estes (1964), Janot (1967), and Estes and Berberian (1969) are justified in distinguishing *A. fragosa* from *A. calva* on this basis since the ratio of the fossil form is smaller than that of the Recent *A. calva*, whose parietal/frontal proportions have a mean ratio of 0.495, the frontals being approximately twice the length of the parietals. A tentative growth-line for parietal/frontal proportions, established on six specimens of *A. fragosa*, including *"Paramiatus gurleyi"* (FMNH 2201) and *A. kehreri* (BMNH P33480), illustrates this difference between the fossil form and the Recent species (Fig. 5). *A. kehreri* displays slightly larger parietals, with a ratio of 0.420, but considering the geographic and temporal differences from the other *A. fragosa* specimens, it is remarkably close in this feature to its North American relatives. The parietal/frontal proportions of the specimens of *A. "dictyocephala"* and *A. scutata* fall near the lower end of the 0.440–0.539 range of *A. calva*, and the Miocene specimen of *Amia* (UCMP 38222), with its ratio of 0.500, is very near the mean for *A. calva*. There is thus a definite trend from the Cretaceous to the Miocene (and Recent) toward an increase in parietal/frontal ratio. The *A. uintaensis* and *A. fragosa* specimens have parietal/frontal ratios smaller than those of *A. calva*, while

the *A. "dictyocephala"* and *A. scutata* specimens are close to *A. calva* in this proportion. There is, however, enough intraspecific variation of parietal/frontal ratios in the fossil species to cause an interspecific overlap of the various forms, so that it is impossible to determine any definitive limits between the consecutive fossil species and *A. calva.*

Operculum-depth/operculum-length ratios. Although the fossil forms have a slightly narrower operculum-depth relative to their operculum-length, they all fall within the operculum ratio range of 0.921–1.025 for *A. calva* (Fig. 5). Table 6 indicates that with increasing size in *A. calva* there may be a trend from a narrower to a slightly broader operculum. Romer and Fryxell (1928: 521) describe the operculum of *"Paramiatus gurleyi"* as being greater dorsoventrally than anteroposteriorly. Although Cretaceous and Eocene specimens of *A. fragosa* have operculum ratios (0.923–0.963) lower than the mean (0.964) for *A. calva,* they still fall within the range (0.921–1.025) of the Recent form. Thus the variation of operculum shape within *A. calva* contradicts Hussakof's (1932) supposition that the operculum in *"Pappichthys" mongoliensis* (with a ratio of 0.963) is proportionately narrower than that of *A. calva,* as well as Estes and Berberian's (1969) diagnosis that *A. fragosa* has a relatively shorter operculum-length as compared with height than *A. calva.* Janot (1967) was also cautious in assigning taxonomic importance to the operculum proportions because of the great variability within the Recent species. The operculum width/length ratios in the fossil specimens show little taxonomic significance, although, as Estes and Berberian (1969: 7) note, there does appear to have been a slight temporal trend toward a broader operculum.

Discussion

The six relative growth proportions (Figs. 4–5) that were plotted for the *A. calva* growth-series remained constant and therefore isometric. This may be explained by the fact that these ratios are derived from external rather than internal dimensions, and, as Gould (1966) points out, it is usually the internal elements that must increase at an allometric rate in order to maintain the external surface area, whose dimensions may be increasing at an isometric rate (see meristic study). It may be assumed that the relative growth for these six proportions also maintained an isometric rate in the fossil forms, since their ratios invariably fall near the growth-lines for the Wisconsin *A. calva* sample (Figs. 4–5). However, this assumption would have to be confirmed with an actual growth-series of the fossil forms.

The comparison of Recent with fossil forms has also made it possible to determine the taxonomic value of the skull/body and skull proportions. The morphometric comparison of the fossil forms with Recent *A. calva* suggests the following taxonomic and phylogenetic trends:

1. All the fossil forms have slightly longer heads relative to their standard-length than does the Recent species (Fig. 31). Unless the differences in vertebral meristies are also considered, however, the morphometric data for this feature are not useful in comparing the various fossil forms. *A. uintaensis* and, to a lesser extent, *A. scutata* have relatively longer heads with a vertebral column of approximately 85 centra. *A. fragosa,* on the other hand, is a short-bodied form (approximately 65 centra) with a short head. *A. calva* has a relatively long vertebral column (81–90 centra) with a shorter head than the other long-bodied forms (*A. uintaensis* and *A. scutata*).
2. Pelvic fin insertion has no taxonomic significance.
3. Anal fin insertion may have minor taxonomic significance for the North American specimens of *A. fragosa* which are relatively shorter in this dimension than in the other species. There is too much morphological overlap between

the species, however, to make this a useful criterion.

4. *A. uintaensis* has a relatively longer mandible/head ratio (0.693) than any of the other species of *Amia,* while *A. fragosa* has a smaller ratio (0.507 mean). The mandible/head ratio of *A. scutata* (0.604 mean) is close to that of *A. calva* (0.609 mean).
5. There is a trend from the Late Cretaceous to Late Miocene in the lengthening of the parietals in relation to the frontals. Although it is possible to discern groups that fall into categories of smaller and larger ratios (Table 7), interspecific morphological overlap makes it difficult to separate any one of the fossil species from the others on this criterion.
6. All the fossil forms have operculum depth/width proportions that fall into the lower limits of the *A. calva* range (0.921–1.025). These ratios show a slight temporal trend towards increasing width, but, while this is perceptible, it is insufficient to indicate taxonomic significance.

These trends suggest possible phylogenetic relationships between the various amiid species. The morphometric similarities indicate that little evidence exists for maintaining *A. scutata* and *A. "dictyocephala"* as separate species. The Oligocene *A. scutata* is distinguishable quantitatively from *A. calva* only on the basis of a larger head/standard-length ratio, and in this feature it is intermediate between *A. calva* and *A. uintaensis.* The morphometric evidence indicates similarities between *A. fragosa* (Cretaceous-Eocene), *"Paramiatus gurleyi"* (Eocene), and *A. kehreri* (Eocene). Head/standard-length ratio is approximately the same among these three forms; insertion of anal and pelvic fins/standard-length ratios shows only minor differences. Mandible/head size and parietal/frontal ratios are almost identical. Of all the species, *A. uintaensis* is the most morphometrically distinct. It has a relatively greater mandible/head ratio and a smaller parietal/frontal ratio than *A. fragosa* (Table 7). Even though it possesses approximately the same total number of centra as *A. calva* and *A. scutata* (Table 9), it still has a greater head/standard-length ratio than the two latter species. Temporally, there are minor trends in *Amia* towards lengthening of the parietals in relation to the frontals, and increasing operculum width to depth.

MERISTICS

Meristic elements have been used in species diagnoses of various fossil amiids by Cope (1875), Osborn *et al.* (1878), Romer and Fryxell (1928), and Estes (1964). A meristic study of both Recent and fossil species of *Amia* was undertaken to determine the relative value of such diagnoses in the taxonomy of the amiids. A comparison of the number of supravertebral scale rows, the number of branchiostegal rays, and the number of pectoral, pelvic, anal, dorsal, and caudal fin rays comprises the first part of the study, while comparative vertebral meristics comprise the second part.

Supravertebral Scale Rows

Cope (1875) differentiated *A. scutata* from *A. calva* and *A. "dictyocephala"* on the basis of *A. scutata's* (USNM 5374) having seven and a half longitudinal rows of large scales above the vertebral column. Cope (1875) described *A. "dictyocephala"* (USNM 3992) as bearing ten to twelve rows of scales above the vertebral column. A count of the scale rows between dorsal fin distal pterygiophores and the vertebral column in 20 Recent *A. calva* (Table 8) gave a range of seven to nine supravertebral scale rows. Although the number of scale rows will vary with the region of the trunk anatomy from which the count might be taken, Cope did not designate the point at which he made his scale row count. Also, his specimen was so poorly preserved that his count may have been affected by distortion of the scales. The only way that a valid comparison of all the forms could be made was

Table 8. Comparison of meristic elements in recent and fossil North American amiids

	Supra-vertebral Scale Rows	Branchi-ostegal Rays	Pectoral-Fin Lepido-trichia	Pelvic-Fin Lepido-trichia	Anal-Fin Lepido-trichia	Dorsal-Fin Lepido-trichia	Caudal-Fin Lepido-trichia
Amia calva (20) Recent	7–9 7.5 av.	10–13 11.4 av.	16–19 16.8 av.	7–8 7.2 av.	8–11 10.5 av.	45–49 48.0 av.	23–27 25.7 av.
A. scutata YPM 6243° USNM 4087° PU 10172°	7	11	—	7	9	47°°	—
A. scutata USNM 5374	7.5	—	—	—	9	—	—
A. scutata YPM 6241	8	—	—	—	9	—	23
A. scutata UMMP V-57431	7	11	17	7	9	46°°	—
A. "dictyocephala" USNM 3992	7.8	—	—	7	9	48°°	—
A. "dictyocephala" AMNH 2802	—	11	—	—	—	—	—
A. "dictyocephala" AMNH 2670	9°°	—	—	—	—	47°°	—
A. uintaensis PU 13865	7	—	16	9	9°°	—	23
A. uintaensis AMNH 785	9°°	—	—	7	10	—	24
A. fragosa MCZ 5341	8	12	18	7	8	45	19–20
"Paramiatus gurleyi" FMNH 2201	7–8	12	17	8	8	44–45°°	19
A. fragosa UA 5506	—	10	—	—	—	—	—
A. fragosa UA 5425	—	—	—	—	—	—	19

° All one specimen.
°° Est.

to take the supravertebral scale row count of both the USNM 3992 specimen and the other fossil and Recent amiid specimens at the same point. In this case, I took all counts on a vertical line at the level of the posterior pterygiophore of the anal fin. I counted the number of scale rows in specimens of *A. fragosa*, *A. uintaensis*, and *"Paramiatus gurleyi"* in addition to those of Cope's types of *A. scutata* (USNM 5374) and *A. "dictyocephala"* (USNM 3992), as well as referred specimens of *A. scutata;* I then compared them with the supravertebral scale row range in *A. calva*. The supravertebral scale rows of fossil *Amia* (Table 8) appear to fall within the supravertebral scale row range of Recent *A. calva*. Although Cope had described *A. "dictyocephala"* (on the basis of USNM 3992) as having 10–12 scale rows, I believe his count is too high. The supravertebral scale rows in this and other fossil forms are difficult to observe for several reasons. Amiid scales are aligned diagonally to the vertebral column rather than in parallel, making it often difficult, particularly in fossil material, to determine to which diagonal column the overlapping scale rows belong. Also, the scales on the USNM 3992 specimen are broken into many parts, and Cope may therefore have been counting partial scales as whole ones. I believe that I obtained a more reasonable estimate of the supravertebral scale row count in this specimen in the following manner: I measured the average of the anteroventral

width of complete scales from the abdominal region (in which the scales are the same size as in other places in the mid-body region) and then divided that amount into the distance between the midpoint of the vertebral column and the dorsal fin distal pterygiophore. In this case, the quotient was 7.8, which is comparable with the counts of approximately 7–9 in the other Oligocene specimens and in *A. calva* (Table 8). No taxonomic significance can thus be applied to the number of scale rows above the vertebral column since counts in Recent and fossil *Amia* fall within a relatively narrow range.

Branchiostegal Rays

The number of branchiostegal rays was included in the species diagnosis for *A. "dictyocephala"* (AMNH 2802), in which Cope (1875) counted 12 rays. Osborn *et al.* (1878) observed 13 branchiostegal rays in *A. scutata* (PU 10172) and Romer and Fryxell (1928) figured 12 such rays for *"Paramiatus gurleyi"* (FMNH 2201). O'Brien (1969) counted 10 rays in *A. fragosa* (UA 5506) from the Edmonton Formation. On the basis of disarticulated material from the Late Cretaceous Lance Formation, Estes (1964) estimated that *A. fragosa* would bear 14 branchiostegal rays, like the Late Jurassic *Sinamia zdanskyi* described from China by Stensiö (1935; see Liu *et al.*, 1963 for range and distribution). In the Recent *A. calva* sample (Table 8), the number of branchiostegal rays ranges from 10 to 13; the range among the few known examples of fossil forms is from 10 to 13, an indication that the number of branchiostegal rays has remained constant.

Fin Rays

Because of confusing duplication of terminology used for fin description in the literature, I will use that of Lagler *et al.* (1962) for the appendicular skeleton unless I indicate otherwise.

All fin ray counts on Recent *A. calva* were obtained from X-rays of 20 specimens from Wisconsin and Michigan. The counts taken from fossil forms are as accurate as conditions allow, although a number of the specimens are incomplete or show only traces of the actual fin. The results of this study must therefore be considered with this in mind. I obtained these counts from as close as possible to the internal fin supports rather than to the segmented and bifurcated distal lepidotrichia. There is a one-to-one correspondence between the number of lepidotrichia and the number of pterygiophores in the anal and dorsal fins; however, this is not the case in the pectoral, pelvic, and caudal fins, which have more lepidotrichia than fin supports (Fig. 31).

Pectoral fin. The number of pectoral fin lepidotrichia has not been previously noted in any of the original species descriptions of fossil *Amia*. There are four specimens in which it is possible to make a pectoral fin ray count (Table 8). *A. scutata* (1), *A. uintaensis* (1), and *A. fragosa* (2) specimens bear 16 to 18 pectoral lepidotrichia, a number which is approximately the average for 20 specimens of Recent *A. calva* which displayed from 16 to 19 pectoral fin rays (Table 8). O'Brien's (1969) analysis of *A. fragosa* (Edmonton Formation) does not include any quantitative comparison of its pectoral fins with those of *A. calva*. He does, however, observe that the pectoral fins are qualitatively similar in the two species. The pectoral fins of *A. fragosa, A. scutata,* and *A. uintaensis* thus do not vary meristically from those of *A. calva*. Lehman (1951: 8), in his description of *Pseudamia heintzi* from the Eocene of Spitzbergen, notes that the pectoral fin has 13 complete nonbifurcating lepidotrichia in the visible portion of the fossil. This count is different from that of both Recent and fossil North American amiids, but as Lehman's plate 3 indicates, this difference may be caused by matrix that overlies the ventral portion of the pectoral fin, possibly covering additional lepidotrichia.

Pelvic fin. The number of lepidotrichia of the pelvic fin was part of Cope's (1875) species diagnosis for *A. "dictyocephala"* (USNM 3992) and that of Osborn *et al.*

(1878) for *A. scutata* (PU 10172). I counted the lepidotrichia of these specimens as well as those of one additional Oligocene specimen and compared them with my sample of *A. calva*, which showed between seven and eight pelvic lepidotrichia (Table 8). Although Osborn *et al.* (1878) counted ten pelvic lepidotrichia, my recount of their *A. scutata* specimen (PU 10172) showed only seven (Plate 4). The bifurcation of the fin rays might have been inadvertently included in their original count. The holotype of *A. "dictyocephala"* (USNM 3992) (Fig. 27) showed seven rather than the six lepidotrichia that Cope (1875) had diagnosed. A specimen of *A. scutata* (UMMP V-57431) (Fig. 27A) also has seven lepidotrichia; both of these are within the range of Recent *A. calva*. Of the remaining fossil forms, *A. fragosa* and *"Paramiatus gurleyi"* have eight, and *A. uintaensis* nine, *A. uintaensis* being the only fossil form not to fall within the range of Recent *A. calva*. This difference is insufficient to demonstrate any taxonomic value, however, at least until more *A. uintaensis* specimens are known.

Anal fin. Anal fin lepidotrichia have been included in the diagnoses of *A. "dictyocephala"* and *A. scutata* (Cope, 1875), and also in the description of *A. scutata* (Osborn *et al.*, 1878). Each of the original counts of nine anal rays for each specimen concurs with my recount and also falls within the range of eight to eleven for Recent *A. calva* (Table 8). *A. fragosa, "Paramiatus gurleyi,"* and *A. uintaensis* also fall within the range of *A. calva*.

Dorsal fin. Although the number of lepidotrichia in the dorsal fin has been mentioned by several authors in their diagnoses of fossil amiids, it is one of the more difficult meristic counts to obtain, since a complete dorsal region of the fossil is required. Cope's type of *A. "dictyocephala"* (USNM 3992) lacks a complete dorsal fin, so he counted only the 32 dorsal lepidotrichia between the beginning of the dorsal fin and the posterior lepidotrichia of the anal fin (Cope, 1875). Osborn *et al.* (1878) reported 53 dorsal lepidotrichia for *A. scutata* (PU 10172), but this must have been an estimate, since the posterior portion of the dorsal fin as well as the entire caudal fin is missing (Plate 4C). As the two *A. scutata* specimens with complete dorsal fins (AMNH 2670, UMMP V-57431) have, respectively, 47 and 46 dorsal lepidotrichia (Table 8), it seems that the count of Osborn *et al.* (1878) was high and that the PU 10172 specimen would probably have corresponded with the other Oligocene specimens.

Romer and Fryxell's (1928) diagnosis for *"Paramiatus gurleyi"* includes a dorsal fin ray count of 45, which they note as being slightly fewer than the count for *A. calva*. O'Brien's (1969) discussion of Edmonton Formation *A. fragosa* does not include any counts of dorsal lepidotrichia, although he does note that the relative length of the entire dorsal fin in *A. fragosa* is similar to that of *A. calva*. In the *A. calva* specimens I studied, the dorsal fin rays ranged between 45 and 49, the average approximately 48. Romer and Fryxell's diagnosis of *"Paramiatus gurleyi"* as having slightly fewer dorsal lepidotrichia than *A. calva* is correct, but this and all the related fossil forms fall within the lower range of *A. calva* (Table 8). The number of dorsal fin rays appears to have little taxonomic value.

It is interesting that the complete *Amia fragosa* (MCZ 5341), *"Paramiatus gurleyi"* (FMNH 2201), and *A. kehreri* (BMNH P33480) specimens have dorsal fins of nearly the same length and contain the same number of lepidotrichia as *A. calva*, despite the fact that, on the basis of the number of vertebrae, these species have a much shorter body (Table 9). This contributes to a proportional difference in the body forms of these species, since the dorsal fin in *A. fragosa* (including *"Paramiatus gurleyi"*) terminates much closer to the caudal fin than in *A. calva* (Plate 1; Fig. 31). However, as Shufeldt (1885) and Hay (1895) implied, it is very doubtful that the dorsal fin was fused into a continuous structure with the caudal fin in some ancestral

amiid. The Late Mesozoic European forms of *Urocles* and *Amiopsis* have a much abbreviated dorsal fin that terminates more anteriorly than does that of the species of *Amia.* For *Amiopsis dolloi,* an Early Cretaceous (Wealden) amiid from Bernissart, Belgium, Traquair (1911) figured 17 dorsal fin supports, while Lange (1968) establishes a specific range of 17–25 for the Eu-European Upper Jurassic *Urocles.* The basis of Shufeldt's (1885: 85–86) model for a primitive amiid with a continuous dorsal-caudal fin was the presence in Recent *Amia calva* specimens of what Shufeldt called a "series of delicate little bones that continue the interspinous bones of the dorsal fin as far as the caudal fin." These five bones he considered to be the continuation of the dorsal interneural spines; Hay (1895), in his discussion of *Amia calva,* refers to them as "epural interspinous bones." These small bones can also be seen in several of the fossil amiids I have studied, especially *A. scutata* (YPM 6241), *A. fragosa* (UA 5425), and *A. uintaensis* (AMNH 785) (Fig. 8). From these fossil forms, however, it is difficult to determine whether the origin of these bones is from the dorsal or caudal neural spines. An examination of the caudal fin of *Urocles lepidotus* (Fig. 6; also Nybelin, 1963: 506, fig. 17), which is known to have an abbreviated, more anteriorly located dorsal fin, shows that these epural bones are associated with the caudal fin, which supports the upper caudal lepidotrichia in much the same manner as the hypurals in the ventral tail region. A further indication that these epural interspinous bones are not vestigial dorsal spine supports is found in Traquair's (1911) plate 7 of *Amiopsis dolloi* and his plate 8 of *Amiopsis lata* (both species from the Cretaceous [Wealden] of Belgium); these plates show the bones to be clearly associated with the caudal lepidotrichia (Fig. 7).

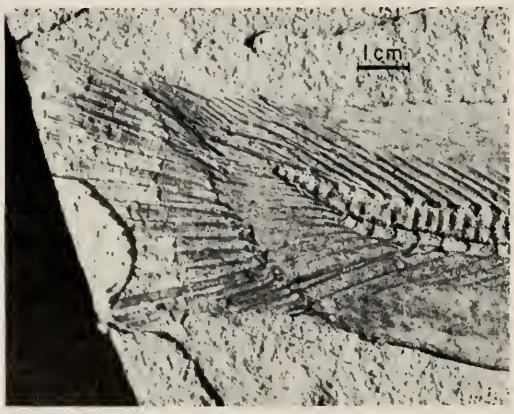

Fig. 6. *Urocles lepidotus* MCZ 8300, caudal fin.

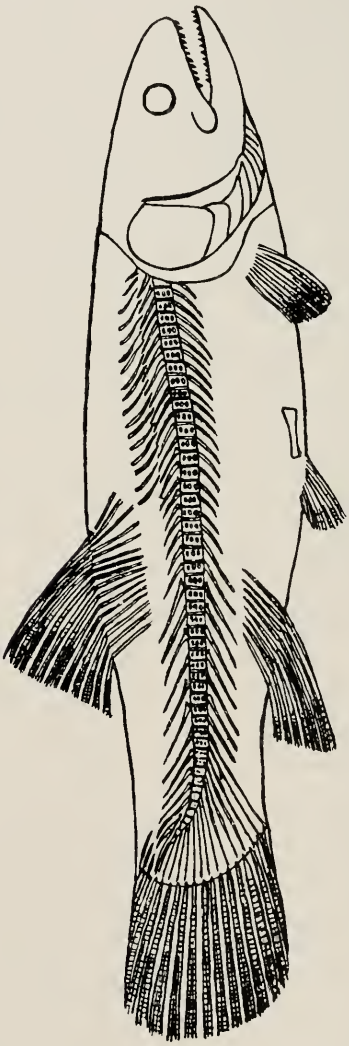

Fig. 7. Restorotion of *Amiopsis dolloi,* scales omitted Early Cretaceous (Wealden), Bernissart, Belgium (after Traquair, 1911).

There are no intermediate interspinous bones between these bones in the caudal region and those of the much more anteriorly situated dorsal spine. The fin of a 648-mm SL Recent *Amia calva* (Fig. 10) does, however, confirm that Shufeldt (1885) was correct in stating that the epurals are continuations of the interneural spines. Figure 10 shows three free interspinous epurals, with a fourth that is either being fused onto a neural spine or is actually a single greatly elongated neural spine. As only two of these epurals are attached to lepidotrichia, there is not a one-to-one correspondence between the two elements, as in the hypurals in the main caudal region.

Caudal fin. With the exception of Romer and Fryxell's (1928) diagnosis of "*Paramiatus gurleyi*," none of the original descriptions of fossil *Amia* include counts of the caudal fin rays. Although Romer and Fryxell observed 20 caudal lepidotrichia, a recount shows only 19 (Fig. 8E). Other fossil forms that also show 19 caudal fin rays are *A. fragosa* (UA 5425) from the Edmonton Formation, *A. fragosa* (MCZ 5341) from the Green River Formation, and *A. kehreri* from Messel (Andreae, 1895, plate 1, fig. 23). Another specimen of *A. kehreri* from Messel (BMNH P33480) has 18 lepidotrichia (Plate 2). Traquair's (1911) plate 7 of three specimens of *Amiopsis dolloi* shows between 15 and 17 caudal lepidotrichia, while *Urocles* spp. have a range between 12–18 caudal lepidotrichia (Lange, 1968). The only Oligocene specimen with a complete caudal fin (YPM 6241) has 23 caudal lepidotrichia; the Eocene specimens of *Amia uintaensis* show 23 to 24. Although my sample of *Amia calva* displays caudal fins with a range of 23 to 27 lepidotrichia, the number of these caudal fin rays is skewed toward the higher limit of the range (Fig. 9). There is thus a considerable difference between the number of lepidotrichia in *Amia fragosa* and the majority of the *A. calva* specimens. *A. scutata* is, however, within the range of the Recent species, but occupies the lower limits of the range.

Thus, of all the meristic elements so far considered, it appears that the greatest disparity between the fossil forms and the Recent *A. calva* is in the number of caudal fin rays. The number of caudal fin rays therefore appears to have taxonomic importance and may have some functional as well as morphological correspondence to the two different amiid body types.

As discussed in the preceding section on dorsal fins, there are two attachment bases for the caudal lepidotrichia: epural interspinous bones and the hypurals. The epurals are usually attached to only two or three of the caudal fin rays, while the remainder of the lepidotrichia are supported by the hypurals. Nybelin (*in* 1963: 488) defines hypurals as "those haemal elements located to the rear of the emergence of the caudal artery from the haemal canal" (trans. Lund, 1967: 210) (Fig. 10B). Lund (1967: 210) agrees instead with Whitehouse (1910: 592), who defines hypurals as "any hypaxial elements that support caudal fin rays" (Fig. 10A). Lund states that the sole function of a hypural is to support a caudal fin ray and therefore the first hypural would be "the first haemal spine in rearward progression to support a caudal fin ray and the first ural centrum is the centrum supporting the first hypural element." Lund's definition is more practical for paleontological use. Since there is an intermediate joint (Figs. 8, 10), the majority of the hypurals are not attached directly to the urals. However, as Shufeldt (1885) and Hay (1895) observed, the posteriormost seven to nine hypurals are ankylosed to the corresponding vertebrae (Fig. 10C). This same co-ossified condition of the last hypurals is also evident in the fossil forms, so that the number of these fused hypurals has remained constant throughout the evolutionary history of *Amia*. Also, as Figure 10 shows, the seven or eight anteriormost hypurals of Recent *A. calva* have a one-to-two correspondence with the ventral lepidotrichia. In most of the available fossil amiid specimens, the ventral caudal portion is poorly preserved, so that it is difficult to

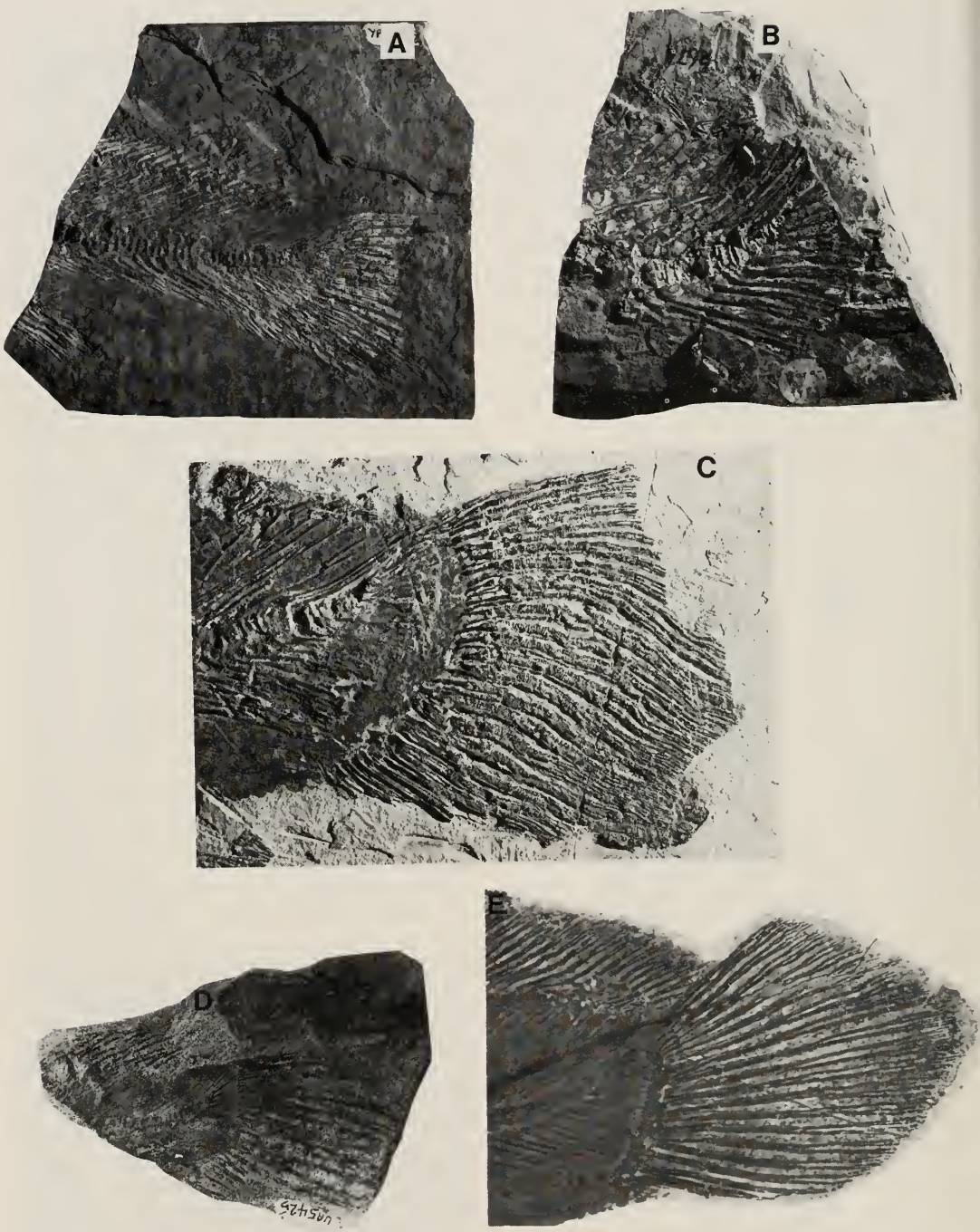

Fig. 8. Caudal regions: A, *Amia scutata* YPM 6241; B, *A. scutata* AMNH 2671; C, *A. uintaensis* AMNH 785; D, *A. fragosa* UA 5425; and E, *A. fragosa* FMNH 2201.

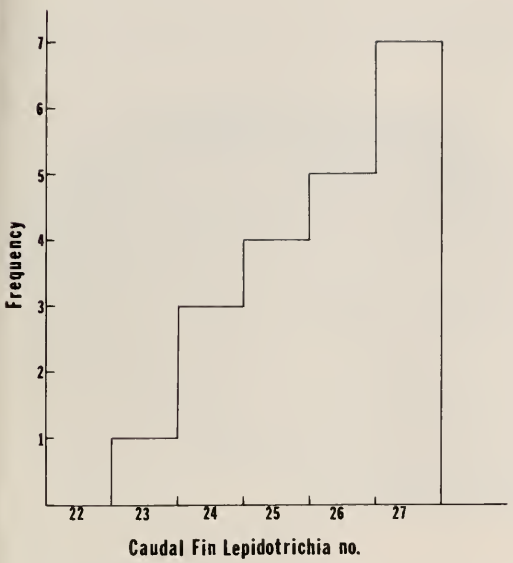

Fig. 9. Number of caudal lepidotrichia in 20 specimens of Recent *Amia calva*.

arrive at an accurate count of the total number of hypurals or to verify whether this one-to-two relationship exists in all the amiid fossil forms. The only available fossil form in which this one-to-two hypural-lepidotrichia correspondence in the ventral caudal region can clearly be seen is in *A. scutata* (YPM 6241; Fig. 8).

Vertebral Elements

Two regions of the vertebral column, the trunk and the caudal regions, are defined by their relationships to the ribs, neural arches, and haemal arches. The trunk region consists of monospondylous vertebrae that possess paired basapophyses having gradually changing angles, dorsal neural facets, and ventral aortal facets. The number of trunk vertebrae in my sample of *Amia calva* varies from 36 to 38. The caudal region consists of three types of vertebrae, listed from anterior to posterior: regular monospondylous centra bearing neural and haemal arches, diplospondylous centra bearing neither neural nor haemal arches (neural and haemal facets still present), and ural centra. Since the neural and haemal facets are still present in the diplospondylous centra, there is no way to differentiate the latter from the monospondylous type in a disarticulated state. In my sample of *A. calva*, the number of regular caudal monospondylous centra (24–26) fluctuates by two centra, that of the diplospondylous caudal centra (14–17) by three (Table 9).

The posterior caudal region of *A. calva* consists of two types of urals: centra with hypurals attached by a layer of cartilage (free urals), and centra that are fused directly onto the hypurals, often lacking the neural arches (fused urals). When disarticulated, the fused urals can often be distinguished from the free urals, since part of the hypural usually remains fused to the ural, extending the posterior articular surface downward. The nonfused (free) urals cannot be distinguished in a disarticulated state from the monospondylous or diplospondylous caudal centra. The number of urals with fused hypurals is readily counted, since they are distinguishable from the remainder of the vertebrae. In order to identify a free ural, it is necessary to observe the relationship between the ural and its corresponding hypural and lepidotrichia. It is often difficult to make this distinction between free and fused urals, since the caudal region is seldom complete in articulated fossil forms. In *A. calva* the number of urals with ankylosed hypurals ranges between seven and nine. There are approximately seven principal urals fused to hypurals, followed by one or two small additional urals that do not articulate with the preceding vertebrae but lie dorsal to the upturned portion of the vertebral column. Because it is difficult to discern these urals in smaller specimens of *A. calva*, the count may be slightly biased, and a comparison of the fossil forms with the range established for *A. calva* must be made with this consideration in mind.

I counted the number of centra between the anterior dorsal fin pterygiophore and the posterior anal fin pterygiophore, since Cope (1875) used the number of central elements between these points as a specific character for *A. "dictyocephala"* (USNM

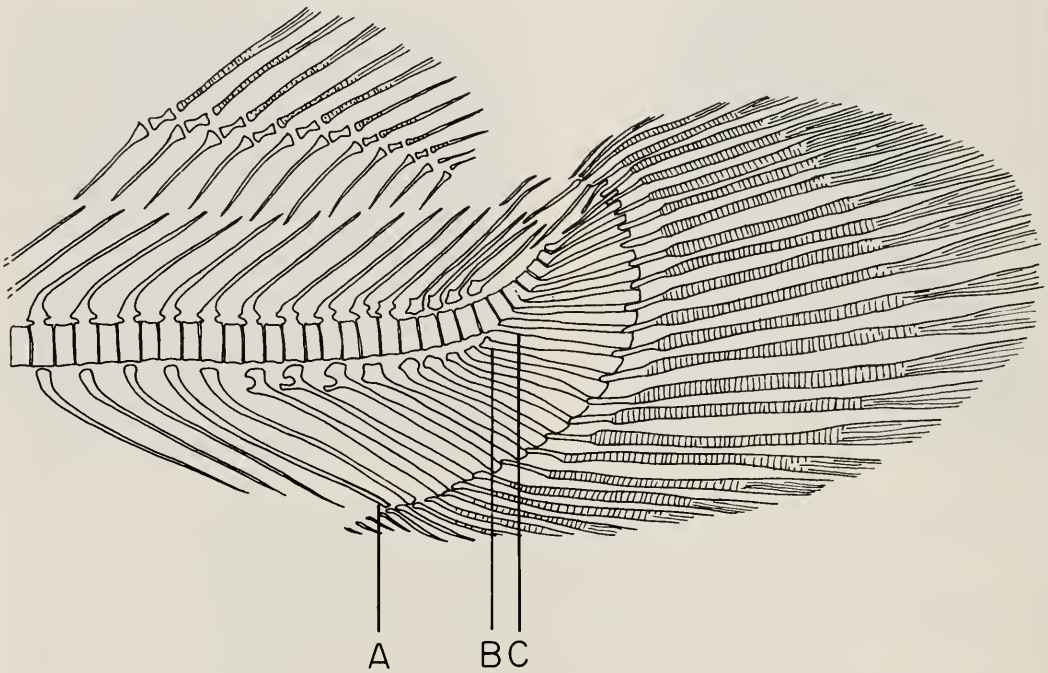

Fig. 10. *Amia calva* (648 mm SL) caudal: A, Whitehouse (1910) and Lund's (1967) definition of first ural; B, Nybelin's (1963) definition of first ural; C, first fused ural.

3992). The range for the number of centra in this region of Recent *A. calva* is 33 to 37.

There is considerable variation in total number of centra (*i.e.*, segments) in Recent *A. calva* (81–90), which may pose a problem in comparing specific vertebrae. Thus in two *A. calva*, for example, the eightieth vertebral segment of one individual might not correspond to the same position in the vertebral column or even type of centrum as the eightieth segment of the second individual. This should be considered in any comparisons of several *A. calva* individuals, as well as in comparisons of the fossil forms, which share this variation in vertebral segments (Table 9). Also, fusion of vertebral elements may occur in Recent *A. calva*. In some specimens, as many as five centra were found fused together at points throughout the vertebral column; this condition was present to a lesser degree or absent in other specimens (Tables 10–12). These fused centra also occur in the fossil forms, as in *A. uintaensis* (YPM 6244). The actual number of such fused centra can often be established only by counting external features such as basapophyses, neural facets, aortal facets, or haemal facets.

Romer and Fryxell's (1928) study of "*Paramiatus gurleyi*" is the only published description of a complete articulated fossil amiid. They distinguished this form from the Recent species by the supposed presence of a deeper body, and also noted that the number of centra was considerably less than in *A. calva*. The vertebral column is completely preserved, so that it is possible to obtain an accurate count of the vertebrae (Plate 1B). "*Paramiatus gurleyi*" has 67 vertebral segments in contrast to the mean of 86 in *A. calva* (Table 9). Osborn *et al.* (1878) described *A. scutata* (PU 10172) on the basis of a specimen lacking a caudal fin (Plate 4). Since the specimen is otherwise complete, they were able to estimate that their specimen had 82 vertebral segments.

Cope (1875) described *A. "dictyoce-*

Table 9. Comparison of vertebral characters in recent and fossil amiids

	Total Number of Centra°°	Number of Trunk Centra	Number of Mono-spondylous Caudal Centra	Number of Diplo-spondylous Caudal Centra	Number of Ural Centra with Fused Hypurals	Number of Centra between Anterior Dorsal-Fin Pterygiophore and Posterior Anal-Fin Pterygiophore°
Recent						
Amia calva (20) Wis. & Mich.	81–90 mean = 85.8	36–38 mean = 37.3	24–26 mean = 25.2	14–17 mean = 16.2	7–9 mean = 8.3	33–37 mean = 35.5
Oligocene						
A. scutata PU 10172	83°°°	36	25	15	7°°°	35
A. scutata UMMP V-57431	81°°°	36	24°°°	15°°°	7°°°	37
A. "dictyocephala" USNM 3992°	—	—	—	—	—	35
Eocene						
"Paramiatus gurleyi" FMNH 2201°	67	26	19	16	6	26
Amia uintaensis PU 13865	85	31	26	21	7	36
Amia uintaensis AMNH 785	—	—	25	20	7	—
A. fragosa MCZ 5341	65	25	18	15	7	25
A. kehreri BMNH P33480	62°°°	24	16	16	6°°°	24

° = types.
°° = including diplospondylous units (as one).
°°° Est.

phala" from a specimen (USNM 3992) in which only the mid-body region was preserved. He felt that the number of vertebrae between the anterior dorsal fin pterygiophore and the posterior anal fin pterygiophore had taxonomic significance. A comparison of this specimen with Recent *A. calva* showed that the vertebral count of this region is essentially the same in both species. This character is therefore not useful in distinguishing this species from the Recent form or in characterizing it as a specific taxon. The specimens of *A. scutata* are within the range of *A. calva* in total number of vertebrae as well as in the number of vertebrae in the various categories (Table 9). Based on the similarity of number of vertebrae in *A. scutata* to that of *A. calva,* it appears that the amiid vertebral column has not changed meristically from Oligocene to Recent.

Additional data from five undescribed fossil amiid specimens with relatively complete axial skeletons has been of considerable help in estimating vertebral counts of the fossil forms. A complete specimen of *A. uintaensis* from the Green River Formation (PU 13865) has a complete axial skeleton (Plate 3). Interestingly, the total number of centra (85) does not differ from that of *A. scutata* or *A. calva* (Table 9). The only variation is in the number of trunk centra and the number of diplospondylous caudal centra. There are fewer trunk centra in this specimen of *A. uintaensis* (31) than in *A. scutata,* which has a mean of 36, or in *A. calva,* whose trunk centra are a mean of 37. A partially com-

plete *A. uintaensis* specimen (AMNH 785), also from the Green River Formation, shows almost the same number of diplospondylous caudal centra as PU 13865 (20–21 respectively). The lesser number of trunk centra in both specimens of *A. uintaensis* is thus offset by a greater number of diplospondylous caudal centra. In comparing the vertebral column of *A. uintaensis* with that of *A. calva, A. scutata,* and *A. fragosa,* it appears that although *A. uintaensis* shares the same total number of vertebral segments with *A. scutata* and *A. calva,* it does not conform to their proportional division of the column into trunk and caudal regions. *A. uintaensis* has a trunk/total-number vertebral ratio of 0.365, while *A. fragosa* has a ratio of 0.300 as compared to the *A. calva* ratio of 0.440. Three complete specimens referred to here as *A. fragosa* (*"Paramiatus gurleyi"* FMNH 2022, *A. kehreri* BMNH P33480, and *A. fragosa* MCZ 5341) have vertebral columns that differ proportionately and meristically from *A. calva, A. scutata,* and *A. uintaensis. A. fragosa* has significantly fewer centra than the other fossil forms, with approximately 12 fewer trunk vertebrae and 8 fewer monospondylous caudal centra. It has approximately the same number of diplospondylous caudal centra as *A. calva* and *A. scutata,* with the number of fused hypurals also essentially the same (Table 9). Thus *A. fragosa* and *A. uintaensis* are meristically distinct from one another and also from *A. scutata* and *A. calva,* suggesting that these two earlier forms can be taxonomically separated on vertebral meristic characters.

VERTEBRAL COLUMN OF *AMIA CALVA*

The existing taxonomy of many North American fossil amiids is based primarily on vertebral characters. Many of the species of *"Protamia,"* and the genus itself as described by Leidy (1873a) from the Bridger Formation, have been established solely on height/width proportions and length (thickness), shape of the neural and aortal facets, and various foramina of isolated vertebrae. Fossil species of *Amia* from the Bridger and Cypress Hills formations have also been defined on character-states of isolated vertebrae. In order to analyze this usage, variation in vertebral character-states of *A. calva* has been studied.

The axial skeleton of Recent *Amia calva* is relatively well known. It is one of the few modern forms that have diplospondylous vertebral centra posteriorly, a condition that, according to Schaeffer (1967), functionally increases the flexibility of the posterior part of the body. Shufeldt (1885) was one of the first to describe the vertebrae of *Amia,* and Hay's (1895) well-known work on the vertebral column of *Amia* provides a relatively complete and informative description of the axial skeleton, as well as one of the first discussions of intracolumnar variation of the centra. Hay observed some gradual changes in centrum proportions, and in the position of the neural and aortal facets.

Vertebral Features

Dorsal and ventral facets, basapophyses, foramina, and ridges on the centra have been used as diagnostic characters in the taxonomy of fossil amiids. There are three types of paired facets on the vertebrae: dorsal neural facets for the neural arches, ventral aortal facets for the aortal supports, and haemal facets for the haemal arches.

Neural facets. The neural facets are shallow depressions under the neural arch bases, which in life are filled with cartilage. Cartilage is present between the centrum and its associated neural arch. Some specimens of *A. calva* have much deeper facets, with a small ossified ridge built up on the borders. These neural facets occur in pairs on the dorsal surface of both trunk and caudal vertebrae, and between the two facets lies a groove that partially receives the spinal cord.

According to Hay (1895: 7–9), there is a marked anteroposterior change in the position of the neural facets. He contended that at the anteriormost end of the vertebral column the neural arch bases occur between two vertebrae and rest equally on

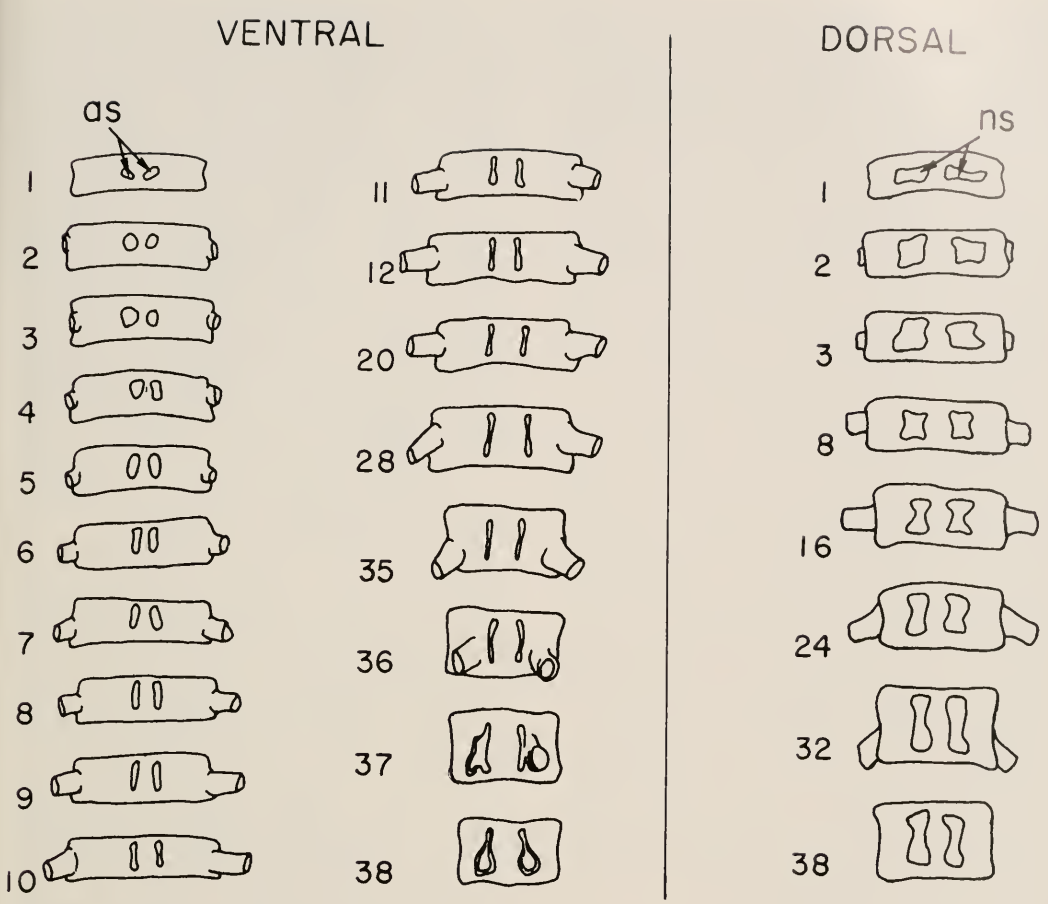

Fig. 11. Configuration of aortal facets (as) and neural facets (ns) on trunk and anterior caudal vertebrae of *Amia calva* (339 mm SL).

both; going posteriorly these bases shift gradually backward. He also observed that there is a change in the spacing of the neural arches; they are close together in the anterior trunk region and more widely spaced posteriorly. Hay is correct in regard to the change in spacing of the neural arches, but he is not altogether correct in his description of the change in position of these arches in relation to the centra. An examination of the Wisconsin *A. calva* sample showed that, after the first few anteriormost centra and corresponding neural arches, the middle of the neural arches is situated at the juncture between the centra. This placement continues along the axial column until the first diplospondylous vertebra occurs. At this point, the next five to seven neural arches are found aligned to the middle of each of the corresponding centra, after which the arches appear to move forward slightly and correspond irregularly to the vertebral bodies.

The configuration of the neural facets themselves varies in the trunk region of the vertebral column of *A. calva*. The neural arches in the anterior trunk region are thicker and wider than those in the more posterior trunk region which have become more flattened and elongated. The shape of the neural facets reflects this trend (Fig. 11). After the first two centra, the facets assume an hourglass shape, being narrower in the middle and broader at each end.

This can be related to the fact that the neural arches are situated at the juncture of two centra so that each neural facet supports the anterior and posterior halves of two different neural arches, whose bases are narrow at the extremity and thick in the center. Although the neural facets in any given specimen of *A. calva* conform to this general trend, the individual configuration of the facets varies slightly. Given this variation in shape of the neural facets, it is useless to attempt characterization of the vertebral column of any amiid species based on configuration of neural facets.

Aortal and haemal facets. On the ventral side of the trunk vertebrae are two thin cartilaginous projections that are located on either side of the dorsal aortal supports. When the skeleton is dried, these projections leave marked depressions, which, like the neural facets, vary gradually from the first anterior vertebra to the last few trunk vertebrae; at this point the aortal facets coalesce with the basapophyses (Fig. 11). The point where these two elements are completely merged marks the termination of the trunk centra, and the next centrum is that of the first caudal vertebra. These structures, which were derived anteriorly from the basapophyses and aortal facets, here become the haemal facets.

The first pair of aortal facets is very small and ovoid. The next few centra bear aortal facets that, as Hay (1895) also observed, are circular. The following aortal facets become successively elongated, until, with the tenth or twelfth vertebra, these facets have evolved into a long pair of slits, usually narrower at the midpoint. Posteriorly, these slitlike aortal facets remain basically the same shape until, at the end of the dorsal trunk region, they merge with the basapophyses to form haemal facets. Hay (1895: 54–57) states that the cartilaginous aortal supports penetrate deeply into the centra of younger individuals, while in older specimens they rest superficially on the centra. The aortal facets are deeper and more distinct than the neural facets.

Beginning with approximately the tenth or twelfth vertebra, the slit-shaped aortal facets are vertically situated on either side of an indentation that contains the aorta (Fig. 11). The first four centra have thicker and shorter supports with relatively little or no space between them. The aorta lies ventrally under the basioccipital, which bears aortal supports whose facets are of the same shape as the first four centra (Estes and Berberian, 1969, fig. 2B for *A. fragosa*). The aortal facets of the first eight vertebrae are different from all other trunk vertebrae, whose shape, as mentioned above, is basically an elongated slit. These aortal supports are thus helpful in distinguishing the first eight or so vertebrae from the remainder of the trunk centra in disarticulated specimens (Fig. 11).

Haemal facets. The haemal facets, which contain a cartilaginous layer between the centrum and the haemal arches, are nearly rectangular-shaped pairs that do not vary along the caudal portion of the vertebral column until the first fused urals. The furrow or indentation that lies between the aortal facets in the trunk centra continues in the caudal region between the paired haemal facets, although it gradually decreases in width and depth. Unlike the neural facets, the haemal facets are outlined by an ossified border, which can be helpful in distinguishing dorsal from ventral surfaces in disarticulated caudal vertebrae.

Since the ossified walls are tilted 20 degrees posteriorly to accommodate the haemal arches, which articulate with the cartilaginous layer diagonally rather than laterally, those borders are also useful in determining the anteroposterior orientation of the centrum.

Basapophyses. Amia trunk centra are distinguished from the caudal vertebrae by their having prominent paired processes, which have been called transverse processes, parapophyses, or diapophyses. I follow the terminology of Bolk *et al.* (1936), wherein they designate these structures, which are the processes for pleural ribs, as basapophyses ("basalstümpfe"). The first centrum often lacks these basapophyses

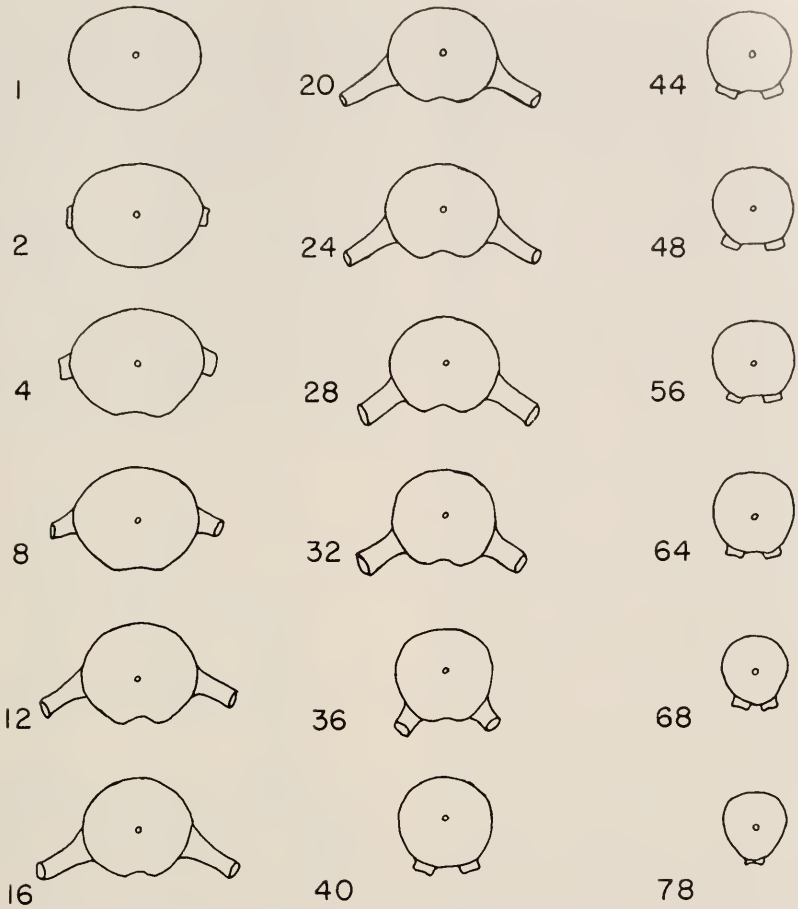

Fig. 12. Shape of selected trunk and caudal vertebrae in *Amia calva* (339 mm SL).

(Tables 10–12), which are always present on the succeeding centra and progressively become longer until approximately the twelfth (Fig. 12). The basapophyses are approximately the same length between the twelfth and the thirty-second centra, from which point they begin to diminish gradually in length until the last trunk centrum, where they coalesce with the aortal facets. The lengths of the basapophyses were not individually measured; this data would be of little practical use in a comparison of Recent and fossil material since these relatively fragile structures are rarely preserved intact in fossils. The distal end of each basapophysis is attached to a pleural rib by means of cartilage. The proximal ends of the basapophyses are ankylosed to the ventral half of the vertebral body. These paired processes are solid cylinders (hollow at the tips) that are slightly flattened dorsoventrally. Each pair of basapophyses may not always be of equal length or diameter, but they are extremely regular in position. They form two continuous and symmetrical lines that gradually come closer together until the last trunk centrum, where they are separated only by aortal supports.

An important aspect of the basapophyses in *A. calva* is the angle between each individual pair which gradually decreases posteriorly. Since the angle between the basapophyses is generally still available in

fossil forms, even in those with broken basapophyses, it is used here as a basis of comparison between the Recent and fossil forms. Since the angles steadily decrease posteriorly along the vertebral column (Figs. 12, 14), they are also useful in orienting disarticulated centra to approximate position along the column. Although there is individual variation in these angles (Tables 10–12), they are nevertheless consistent enough to help in determining the general position in the column of any single trunk centrum. The range of angles extends from approximately 180 degrees anteriorly to 45 degrees posteriorly. Since the three *A. calva* specimens studied were of varying sizes (193 mm SL, 382 mm SL, and 423 mm SL), it would appear that there is no significant change in the angles with increasing size or age of the fish (Fig. 14). Although this transition is not perfectly linear, the angles are always decreasing posteriorly, and at least in the specimens I measured, there was never an instance of an angle's measurement being greater than that of the preceding centrum. The angle decrease occurs at a fairly constant rate until approximately the thirtieth trunk vertebra, at which point the rate of decrease of the angles is much accelerated (Fig. 14). The angle of the basapophyses is thus a reliable parameter in identifying the general position of isolated trunk centra.

Foramina, bone ridges, and first centrum. The trunk centra of *A. calva* have lateral foramina that, although lacking the uniformity of the neural and aortal facets, occur in irregular, distinct paired linear patterns. The foramina of the trunk and caudal vertebrae transmit numerous small blood vessels.

On the lateral surfaces perpendicular to the anterior and posterior articular surfaces of the individual centra are prominent bone ridges. These bone ridges add support to the arch anlagen, and also help unify the anlagen into a sturdy, functional vertebral body (Schaeffer, 1967). Externally, these bone ridges are not as regular as they are internally, although they still lie anteroposteriorly in the lateral and ventral regions and extend vertically along the basapophyses. They are also quite prominent in the notochordal furrow. Such bone ridges are not a unique feature of *A. calva*, and are common in teleosts.

The centra in *A. calva* are amphicoelous. The first four to six centra differ from all corresponding centra by having the anterior articular surface more convex than concave. The first centrum in nearly all specimens observed lacked basapophyses, and should therefore be considered a minor taxonomic character since first centra do occasionally occur with very small basapophyses. The

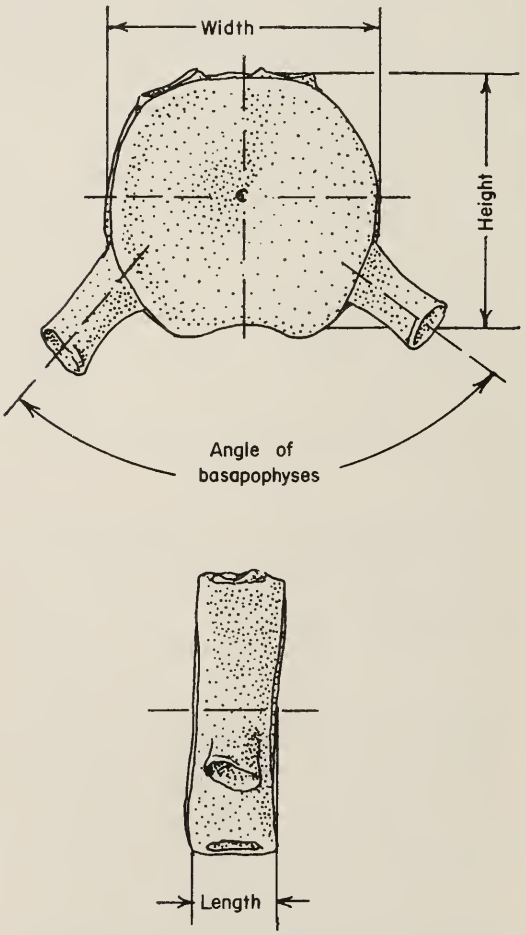

Fig. 13. Index to the measurements used, superimposed upon an outline drawing of an *Amia calva* vertebra.

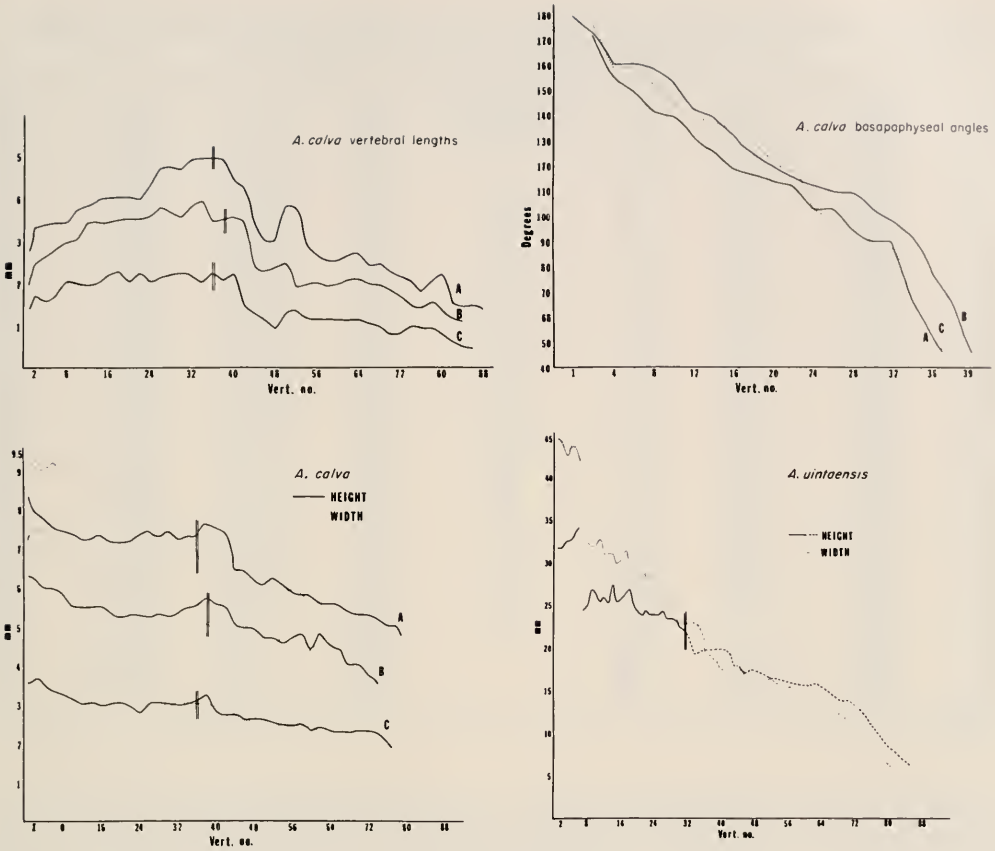

Fig. 14. Intracolumnar variation in the angle of basapophyses, length, height, and width of vertebrae in Recent *Amia calva* (A = 423 mm SL; B = 382 mm SL; C = 193 mm SL). Intracolumnar variation in height and width of trunk and caudal vertebrae in *A. uintaensis*. Vertebral column model based on first six centra from PU 10101 and fifty-nine centra from CM 25362; missing caudal centra have been interpolated and inferred based on PU 13865. The first anterior centra (PU 10101) were larger specimens and thus the anterior region of the trunk vertebral column model is "out-of-phase." Vertical lines = last trunk centrum.

ovoid shape of the aortal facets is a constant feature of all first four to six centra observed.

Vertebral Dimensions

A superficial but often-used character for diagnosing fossil amiid species has been the shape of the centrum. Descriptions for *Amia whiteavesiana, A. macrospondyla, A. exilis, A. elegans, A. depressus, A. newberrianus, Protamia symphysis, P. media, P. gracilis, P. uintaensis, P. plicatus, P. corsonii,* and *P. laevis* include centrum measurements for height, width, and length (thickness), as well as qualitative descriptions of the form and proportions of the centrum. Because isolated amiid vertebrae have often been the only anatomical material found in the fossil record, the original diagnoses were obviously limited in that a great deal of emphasis was placed on the vertebral centrum. In considering a single centrum shape as diagnostic for an amiid species, early authors implicitly assumed the vertebral column to be static, with no physical change or variation among the centra other than regional. Many new species were therefore described solely on variation in shape from other known amiid types.

Table 10. Intracolumnar variation in height, width, length, and angle of basapophyses of vertebrae in recent *Amia calva* (193 mm SL)

Vert. Cent.	Height (mm)	Width (mm)	Length (mm)	Angle of Basapophyses (Degrees)	Vert. Cent.	Height (mm)	Width (mm)	Length (mm)
1	3.55	4.35	1.40		44	2.75	2.75	1.35
2	3.65	4.20	1.70	176	46	2.60	2.65	1.15
4	3.70	4.25	1.65	159	48	2.65	2.65	.90
6	3.40	4.15	1.70	159	50	2.55	2.60	1.30
8	3.25	3.90	2.05	153	52	2.50	2.45	1.35
10	3.15	3.65	2.00	145	54	2.50	2.50	1.20
12	3.00	3.65	1.90	140	56	2.45	2.45	1.15
14	3.05	3.60	2.00	138	58	2.50	2.45	1.20
16	2.95	3.55	2.20	134	60	2.30	2.40	1.15
18	3.00	3.55	2.30	130	62	2.40	2.30	1.15
20	3.05	3.40	2.10	122	64	2.30	2.20	1.15
22	2.90	3.65	2.25	118	66	2.30	2.05	1.10
24	2.75	3.25	2.10	103	68	2.25	2.15	1.00
26	3.00	3.50	2.15	99	70	2.30	2.15	.80
28	3.05	3.35	2.20	93	72	2.30	2.10	.85
30	3.00	2.90	2.25	91	74	2.25	2.05	1.00
32	2.95	3.05	2.15	90	76	2.05	1.90	.90
34	3.00	3.00	2.05	74	77	1.87	1.75	.90
36	3.10	3.08	2.25	63	80		1.65	.80°
37	3.15	3.00	2.15	44	82		1.50	.68
38	3.25	3.00	2.10		84		1.25	.53
40	2.80	2.90	2.25		86		.80	.50
42	2.75	2.90	1.50					

° Fused.

Table 11. Intracolumnar variation in height, width, length, and angle of basapophyses of vertebrae in recent *Amia calva* (382 mm SL)

Vert. Cent.	Height (mm)	Width (mm)	Length (mm)	Angle of Basapophyses (Degrees)	Vert. Cent.	Height (mm)	Width (mm)	Length (mm)
1	6.30	7.21	1.90	180	42	5.50	5.05	3.50
2	6.25	7.41	2.45	173	44	5.15	4.65	2.40
4	6.00	7.50	2.50	161	46	5.00	4.80	2.35
6	5.95	7.25	2.85	161	48	4.90	4.60	2.37
8	5.82	7.10	2.95	159	50	4.70	4.45	2.50
10	5.56	6.90	3.05	154	52	4.70	4.45	1.90
12	5.50	6.65	3.45	143	54	4.65	4.55	2.00
14	5.50	6.25	3.45	140	56	4.70	4.45	2.10
16	5.50	6.25	3.45	133	58	4.80	4.10	1.90°
18	5.35	6.30	3.50	125	60	4.40	4.45	2.00
20	5.25	6.25	3.55	120	62	4.80	4.45	2.12°
22	5.30	6.25	3.55	116	64	4.50	4.10	2.12°
24	5.30	6.25	3.65	113	66	4.40	3.85	2.00
26	5.20	6.20	3.85	110	68	4.00	3.75	2.00
28	5.35	6.15	3.70	110	70	4.05	3.70	1.87
30	5.25	6.00	3.60	105	72	3.75	3.50	1.75
32	5.35	5.80	3.85	100	74	3.50	3.35	1.50
34	5.45	5.50	3.90	92	76	3.20	3.15	1.47
36	5.50	5.15	3.50	78	78		2.65	1.65
38	5.75	5.10	3.55	66	80		2.00	1.40
39	5.70	5.07	3.60	46	82		1.95	1.20
40	5.65	5.05	3.65		84		1.80	1.12

° Fused.

Table 12. Intracolumnar variation in height, width, length, and angle of basapophyses of vertebrae in recent *Amia calva* (423 mm SL)

Vert. Cent.	Height (mm)	Width (mm)	Length (mm)	Angle of Basapophyses (Degrees)	Vert. Cent.	Height (mm)	Width (mm)	Length (mm)
1	8.25	9.25	2.80		44	6.45	6.40	3.45
2	8.00	9.15	3.35	172	46	6.40	6.21	3.05
4	7.80	9.05	3.40	156	48	6.20	6.00	3.05
6	7.55	9.20	3.45	150	50	6.10	5.85	3.85
8	7.45	8.80	3.45	142	52	6.25	5.85	3.80
10	7.40	8.80	3.75	140	54	6.10	5.85	2.95
12	7.25	8.75	3.85	132	56	5.95	5.90	2.70
14	7.25	8.75	4.00	126	58	5.80	5.85	2.65
16	7.35	8.70	4.05	119	60	5.80	5.65	2.60
18	7.15	8.50	4.15	117	62	5.65	5.70	2.80
20	7.15	8.50	4.10	114	64	5.60	5.30	2.70
22	7.15	8.40	4.00	112	66	5.55	5.20	2.45
24	7.35	8.35	4.37	103	68	5.50	5.05	2.50
26	7.45	8.30	4.75	103	70	5.30	4.95	2.35
28	7.30	8.20	4.75	95	72	5.30	4.90	2.20
30	7.47	8.10	4.70	90	74	5.20	4.80	2.10
32	7.25	7.95	4.95	90	76	5.05	4.65	1.85
34	7.35	7.45	5.00	67	78	5.00	4.50	2.10°
36	7.35	6.90	5.00	52	80	4.75	4.45	2.25
37	7.50	6.70	4.95	46	82		4.15	1.55
38	7.65	6.50	4.90		84		3.25	1.50
40	7.60	6.50	4.50		86		2.50	1.50
42	7.40	6.20	4.35		88		2.00	1.45

° Fused.

One of the detailed studies on intracolumnar vertebral variation is Hoffstetter and Gasc's (1969) work on the vertebral column of snakes. Measuring individual centra in sequence, they plotted this variation; similar graphs are used here (Fig. 14). Three specimens of *A. calva* (193 mm SL, 382 mm SL, and 423 mm SL) were dissected and the individual vertebral dimensions measured to determine vertebral variation.

Length. Centrum length (thickness) was measured anteroposteriorly at the midline, above the basapophyses (Fig. 13). It was necessary to establish such a control for this measurement because of the variation in thickness within each centrum. In the trunk region, the centra are thickest ventrally at the neural and dorsal facets. The caudal vertebrae follow a similar pattern, being slightly thicker ventrally and dorsally, and thinner laterally. Every second centrum was measured for length (Tables 10–12). There is a distinct intracolumnar variation for this measurement, although the difference in length between consecutive vertebrae is usually small. There is also a general, if somewhat irregular, pattern in centrum length in *A. calva* (Fig. 14). The first two or three vertebrae of each *A. calva* specimen are relatively thin. These are followed by centra that gradually increase in length until approximately the last trunk centrum at the midbody. At this point there is a general trend again towards thinner vertebrae, although this pattern is erratic, particularly between the fiftieth and the fifty-fourth centra, where the thickness is suddenly increased and then decreases. This sudden change here in vertebral thickness occurs directly above the midline of the anal fin. The shortest vertebrae are the fused urals.

Height. Centrum height was taken dorsoventrally at the midline, between the aortal and neural facets (Fig. 13). Every second centrum was measured up to the fused urals, in which an accurate measure-

Table 13. Intracolumnar variation in height, width, length, and angle of basapophyses of vertebrae in *Amia uintaensis* CM 25362

Vert. Cent.	Height (mm)	Width (mm)	Length (mm)	Angle of Basapophyses (Degrees)	Vert. Cent.	Height (mm)	Width (mm)	Length (mm)
7	24.5	32.8	9.8	179	37	19.5	19.5	7.5
8	25.0	32.5	9.8	178	38	19.8	18.8	7.0
9	26.8	32.0	9.5	177	39	19.8	18.5	6.9
10	26.5	32.1	9.5	176	40	20.0	17.5	6.5
11	25.5	32.8	9.0	174	41	—	—	6.5
12	26.0	31.0	9.1	172	42	19.5	18.0	6.5
13	25.4	31.1	9.5	164	43	18.5	17.5	6.0
14	27.5	31.0	9.5	160	44	18.5	17.5	6.2
15	25.5	30.0	10.0	156.5	45	17.5	17.5	6.0
16	26.0	30.5	9.8	154	46	17.2	16.0	6.0
17	26.5	31.5	9.5	153	47	17.0	16.0	6.0
18	27.0	30.5	9.8	149	48	16.5	16.0	5.5
19	25.1	29.5	9.5	143	49	16.5	—	6.0
20	24.5	29.5	9.5	132	50	16.2	15.5	5.5
21	24.0	30.0	9.5	122	51	16.0	15.0	5.8
22	24.5	28.2	9.0	117	52	16.0	15.5	5.0
23	24.0	29.0	9.5	110	53	15.5	14.0	5.5
24	24.0	28.5	9.0	102	54	15.2	14.5	5.2
25	24.0	26.5	8.5	102	55	15.5	13.2	6.0
26	24.5	27.0	10.0	97	56	15.0	12.2	5.5
27	23.5	25.0	11.0	90	57	14.5	12.0	6.5
28	23.5	25.0	11.0	83	58	14.5	12.5	5.5
29	23.2	25.0	12.0	80	59	14.0	11.5	5.2
30	23.0	22.5	11.0	62	60	14.0	—	5.0
31	25.0	22.5	11.0	46	61	13.5	11.5	5.0
32	—	—	11.0		62	13.5	10.5	4.5
33	—	—	10.0		63	—	—	4.5
34	23.0	19.5	9.5		64	12.0	9.0	4.5
35	22.5	—	9.5		65	8.5	7.0	4.2
36	21.0	20.0	7.5					

ment would be obscured by the fusion of the hypurals. This series of measurements shows a basic pattern that is similar for each of the individuals studied, although there is less intracolumnar variation in the height than in the length measurements (Tables 10–12). The greatest height generally occurs at the anteriormost region of the column, then decreases slightly until the midtrunk region (Fig. 14). At this point the height gradually increases until it peaks at the end of the trunk region and the beginning of the caudal section, after which it decreases again toward the caudal region (Fig. 14).

Width. The width measurements were taken perpendicular to the height measurements, at the widest section of the centrum (Fig. 13). This dimension has a greater linear slope than the length and height dimensions (Fig. 14), which follow a more bell-shaped curve. There is a greater variation within the vertebral column for width dimensions (Fig. 14), as comparison of the height and width slopes reveals. The greatest intracolumnar width is always at the anteriormost portion of the trunk region, after which this dimension gradually decreases. There appear to be two areas where the rate of decrease is greater, these being at the terminus of the trunk region and at the first fused ural.

Height/width ratio. The centrum height/width ratio has been a commonly used diagnostic character in amiid taxonomy. Hay (1895: 7) correctly noted that the trunk vertebrae are somewhat broader than high (Fig. 14), and at the terminus of the trunk

region the centra are nearly circular. The proportions tend to be reversed in the caudal region, however, with the height generally exceeding the width, although to a lesser degree than the proportional difference in the trunk region. The basic trend in shape through the vertebral column is thus a marked horizontally elliptical centrum approaching a progressively circular one, which then again becomes slightly vertically elliptical. Thus there is quite a variation in the centrum shape throughout the axial column, so that no one shape or ratio of dimensions could reasonably be considered diagnostic for all the centra of the vertebral column.

VALID NORTH AMERICAN FOSSIL GENERA AND SPECIES

Amia fragosa (Jordan, 1927)

Kindleia fragosa Jordan, 1927: 145.
Stylomyleodon lacus Russell, 1928a: 103.
Paramiatus gurleyi Romer and Fryxell, 1928: 519.

Holotype. NMC 8533e, anterior portion of right dentary.

Paratypes. NMC 8534a–d, f–n. (a), left operculum fragment; (b), cranial fragment; (c), anterior portion of left dentary; (d), anterior portion of right dentary; (f–g), coronoid with two styliform teeth preserved; (h–i), vomer without teeth preserved; (j), styliform tooth fragment; (k–l), posterior portion of right dentary; (m), left maxilla; (n), anterior portion of right dentary.

Type locality and horizon. Rumsey, Alberta. East half of section 31, T 34 S, R 21 W, Rumsey Quadrangle, Alberta; Edmonton Formation.

Age range. Campanian (Late Cretaceous) to Bridgerian (Middle Eocene).

Hypodigm. Cretaceous. Oldman Formation, Alberta: AMNH 5934, palatal fragments with styliform teeth; AMNH 5935, operculum and dentary. "Mesaverde" Formation, Wyoming: AMNH 5932, dentary and numerous coronoid teeth; AMNH 5933, vertebrae. Judith River Formation, Montana: AMNH 10109, left vomer bearing styliform teeth; AMNH 10110, dentary fragments, vertebrae, and skull elements. Edmonton Formation, Alberta: ROM 3064, coronoid teeth; ROM 3065, dentaries, vertebrae, and cranial fragments; UA 5398–5507, articulated and disarticulated specimens (see O'Brien, 1969 for identifications). Lance Formation, Wyoming: AMNH 9316, pterotic; AMNH 9315, operculum; CM 25363, dentaries; PU 17013, dentaries; UCMP 54013–54015, 54017, 54019, 54021–54030, 54035–54038, 54040–54056, 54059–54069, 54070–54120, 54141–54167, 54174–54180, 54188–54198, 54260, 54262, disarticulated elements (see Estes, 1964 for identifications). Hell Creek Formation, Montana: PU 17016, 17048, dentaries; PU 17014, coronoid teeth; PU 20554, dentary and vertebrae; MCZ 9286–9293, 9390–9432, 9559, disarticulated elements (see Estes and Berberian, 1969 for identifications).

Paleocene. Fort Union Formation, Wyoming: PU 17115, coronoid teeth; PU 17126, coronoid teeth and vertebrae; PU 17117, dentary and maxilla; PU 21525, portion of cranial roof with associated dentaries; PU 20523, dentary and coronoid teeth; PU 21174, vertebrae. Paskapoo Formation, Alberta: UA 131, dentary, numerous tooth plates, and vertebrae. Tongue River Formation, Montana: PU 20577, vertebrae, premaxillary fragment, and coronoid teeth; PU 20578, basioccipital and vertebrae; PU 17068, vertebra and dentary fragment. Melville Formation, Montana: AMNH 2635, cranial elements and associated dentaries. Tullock Formation, Montana: PU 17069, vomers.

Eocene. Willwood Formation, Wyoming: MCZ 9264, nearly complete skull; PU 18780, tooth plate; PU 21175, dentary fragment and coronoid teeth; PU 16756, dentary and cranial fragments; PU 17649, anterior portion of skull; PU 21173, skull fragments and vertebrae; PU 13261–13262, cranial fragments and coronoid teeth. Golden Valley Formation, North Dakota: PU 18567, coronoid teeth and vertebrae. Wasatch Formation, Wyoming: PU 13260, tooth plates; PU 13259, cranial fragments and dentaries. Bridger Formation Wyo-

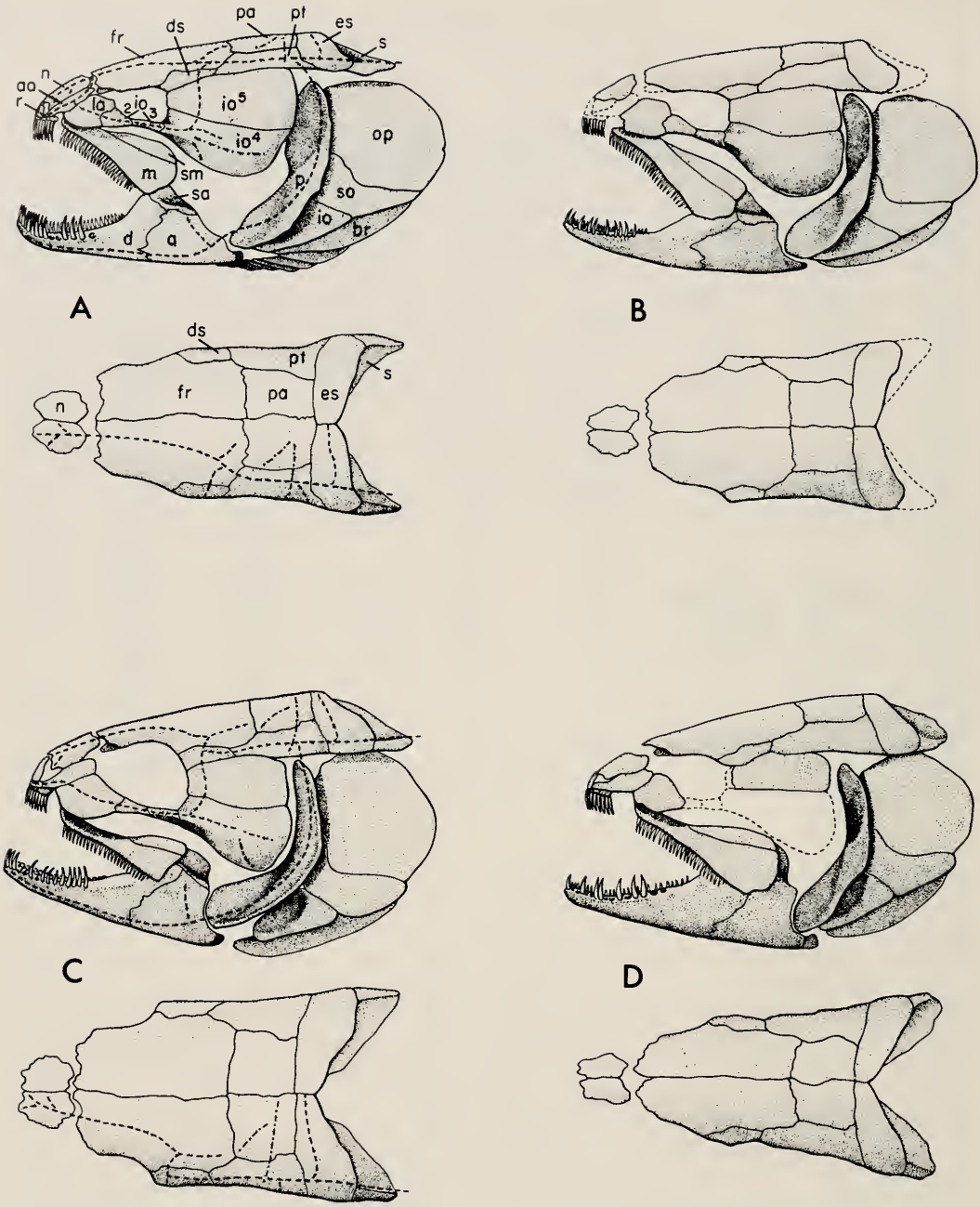

Fig. 15. A, *Amia calva*, Recent, Wisconsin; above, lateral, and below, dorsal views of skull. B, *Amia scutata*, Early and Middle Oligocene; above, lateral, and below, dorsal views of skull (sensory canal system and pit-lines are not known since skull elements are in articulation). C, *Amia fragosa*, Late Cretaceous to Middle Eocene; above, lateral, and below, dorsal views of skull (sensory canal system and pit-lines after Estes, 1964). D, *Amia uintaensis*, Paleocene to Early Oligocene; above, lateral, and below, dorsal views of skull (sensory canal system is only known in the mandible, operculum, nasal, lacrimal, antorbital, extrascapular, and suprascapular, all of which conform with those of *A. calva*).

Abbreviations: a, angular; ao, antorbital; br, branchiostegal rays; d, dentary; ds, dermosphenotic; es, extrascapular; fr, frontal; io, interoperculum; io^2 io^3 io^4 io^5, infraorbital series (suborbitals & postorbitals); la, lacrimal; m, maxilla; n, nasal; op, operculum; p, preoperculum; pa, parietal; pt, pterotic; r, rostral (ethmoid); s, suprascapular; sa, surangular; sm, supramaxilla; so, suboperculum. Dotted lines indicate the sensory canal system; dashed lines indicate pit-lines.

ming: YPM 6245, vomer and cranial fragments; YPM 6246, vertebrae; YPM 6247, dentary; YPM 6248, vertebra and cranial fragments; YPM 6254, vertebrae, basioccipital, vomer; YPM 6261, left operculum; ANSP 5630, vertebra. Green River Formation, Wyoming: MCZ 5341, FMNH 2201, complete specimens.

Known distribution. North Dakota, Wyoming, Montana, and Alberta.

Revised diagnosis. Vertebral column with significantly fewer total centra (65 mean) than the other species, with approximately twelve fewer trunk vertebrae (25 mean) and eight fewer monospondylous caudal centra (17 mean). Distance between anal fin insertion and the end of the vertebral column relatively short, with dorsal fin terminating close to caudal fin. Caudal lepidotrichia 19–20 rather than 23–27. Ascending processes of parasphenoid perpendicular to the main anteroposterior parasphenoid axis; more posterior placement of parasphenoid tooth-patch. Parietals squared in outline. Marginal teeth simple pointed cones, palatal teeth usually stout styliform crushers. Supraorbital sensory canal not entering parietal. Excavation of orbital notch in frontal relatively larger. Dentary with additional horizontal shelf of coronoid articulation surface adjacent to lingual border of alveolar ridge; coronoid articulation surface extensive, overlapping ventral half of ramus; dentary with pronounced arch rather than gradual curve in ventral outline. Greatest known standard-length 510 mm.

Introduction

Jordan (1927) described *Kindleia fragosa* as a new genus of cichlid fish from the Late Cretaceous Edmonton Formation of Alberta. This tentative placement of *Kindleia* within the Cichlidae was largely the result of his misinterpreting the splenial tooth plates for fused lower pharyngeal bones (Estes, 1964). One month later, Russell (1928a) independently published a description of *Stylomyleodon lacus*, a new fossil amiid from the Late Paleocene Paskapoo Formation of Alberta, and referred other specimens from the Edmonton Formation of Alberta to the same species. His description also included a dentary and palatal teeth modified for crushing. His relegation of the genus to the Amiidae was based on a correct interpretation of the "splenial" (=coronoid) tooth plates (Estes, 1964). He suggested a relationship of *Stylomyleodon* to *Platacodon nanus* (at that time erroneously considered an amiid; see Estes, 1964) with the essential difference being hemispherical rather than flattened tooth crowns.

Jordan later (1928) noted the similarity of the two genera *Kindleia* and *Stylomyleodon* and asserted the prior claim of his name *Kindleia*. Although he made no comment on Russell's attributing *Stylomyleodon* to the Amiidae, he rejected Russell's comparison of that genus with *Platacodon* on the basis of Marsh's earlier conviction that the latter was mammalian. In reply to Jordan, Russell (1928b) defended the validity of his genus on the supposition that its dentary was distinct from that of *Kindleia*, although he did agree on the similarity of teeth and jaw fragments of the two genera. Russell (1929) further attempted to validate *Stylomyleodon* as a genus by comparing his type with new specimens collected by Princeton University. This new material confirmed his association of the maxilla-dentary and palatine-coronoid dentitions, and also substantiated his interpretation of *Stylomyleodon* as an amiid in which the coronoid teeth were specialized for crushing. He also admitted that there was insufficient *Platacodon* material to determine any conclusive similarities with *Stylomyleodon*, but, referring to Hatcher's (1900, 1901) work, did insist that *Platacodon* was a fish. Simpson (1937) reported finding additional specimens of *Stylomyleodon* Russell in the Fort Union Formation at Crazy Mountain Field sites of Montana.

Estes (1964), from his studies of amiid material from the Lance Formation of Wyoming, observed that whereas the type dentary referred by Russell to *Stylomyleo-*

don was the posterior portion of an amiid dentary, Jordon's type was the anterior portion. From this fact he confirmed the synonymy of *Stylomyleodon* with the genus *Kindleia,* at that time believing that it was generically separated from *Amia.* Janot (1967) agreed with Estes on the synonymy of *Stylomyleodon* with *Kindleia,* but did not find sufficient cause to distinguish *Kindleia* generically from *Amia.* Russell (1967) continued to leave the nomenclatural problem of *Stylomyleodon-Kindleia* unsettled. Estes and Berberian (1969) studied material from the Late Cretaceous Hell Creek Formation of Montana and confirmed Janot's proposition that *Kindleia* is a synonym of *Amia.* They also suggested the possibility of synonymy of *A. fragosa* with *A. kehreri* (Middle Eocene, Germany), *A. russelli* (Late Paleocene, France), *A. munieri* (Early Oligocene, France), and *Paramiatus gurleyi* (Early Eocene, Wyoming), but postponed formal synonymy of *A. fragosa* with the prior name *A. kehreri* (Andreae, 1892), pending more detailed study of Early and Middle Cenozoic specimens from Europe. Estes and Berberian (1969: 10) concluded that the minor variations that separated *A. fragosa* and its related forms in Europe from *A. calva* are "superficial and essentially primitive," and indicated that the group might be close to the ancestry of the Recent species *A. calva.*

A nearly complete skull from the Eocene Willwood Formation of Wyoming (Fig. 16), two axial skeletons from the Eocene Green River Formation of Wyoming (Plate 1), and a sample of disarticulated elements from the Late Cretaceous, Paleocene, and Early Eocene have yielded more information on the osteology of *Amia fragosa.* Estes (1964), O'Brien (1969), and Estes and Berberian (1969) have studied this species in detail, and I therefore discuss these specimens only as they modify conclusions reached by those studies.

Fossil Record

In addition to the stratigraphic list given by Estes and Berberian (1969: 14, table 1) of major freshwater deposits carrying *A. fragosa,* three new localities are recorded here: the Late Paleocene Silver Coulee local fauna of the Fort Union Formation, Wyoming, and the Early Eocene Willwood and Wind River formations, Wyoming. The major deposits in which remains of *A. fragosa* have been found are summarized in Table 18. Estes and Berberian (1969: 10) state that the stratigraphic range of *A. fragosa* extends from the Late Cretaceous through at least Middle Eocene time in North America. The earliest deposit in which remains of *A. fragosa* have been found is the Late Cretaceous (Campanian) Oldman Formation of Alberta, and the latest deposit is the Middle Eocene (Bridgerian) Bridger Formation of Wyoming.

Cavender (1968: 128), however, describes *Amia* scales from the Late Eocene (Duchesnean) Clarno Formation of Oregon. Although these small scales (approximately 2 mm in length) are not as robust as those of *A. fragosa,* they are more ossified than *A. scutata* and *A. calva* scales. These scales, along with the scales from the Horsefly River Beds of British Columbia (UMMP collections) cannot at present be identified as to species. They are best referable to *Amia* sp., since no identifiable *A. fragosa* elements have been found later than Bridgerian and no specific character-states for scales of *Amia* have yet been determined.

Description

Neurocranium. Estes (1964: 29) stated that the greater length of the basioccipital and the presence of a second pair of aortal supports in *Amia calva* indicated that the basioccipital posterior to the spinal (intervertebral) arterial foramina included only one fused vertebra in *Amia fragosa* instead of the two found in *A. calva.* O'Brien (1969: 42) observed a similar condition in two complete *A. fragosa* specimens from the Edmonton Formation of Alberta. Estes and Berberian (1969: 2–3) found nine basioccipitals with one fused vertebra and eleven with two fused vertebrae from the

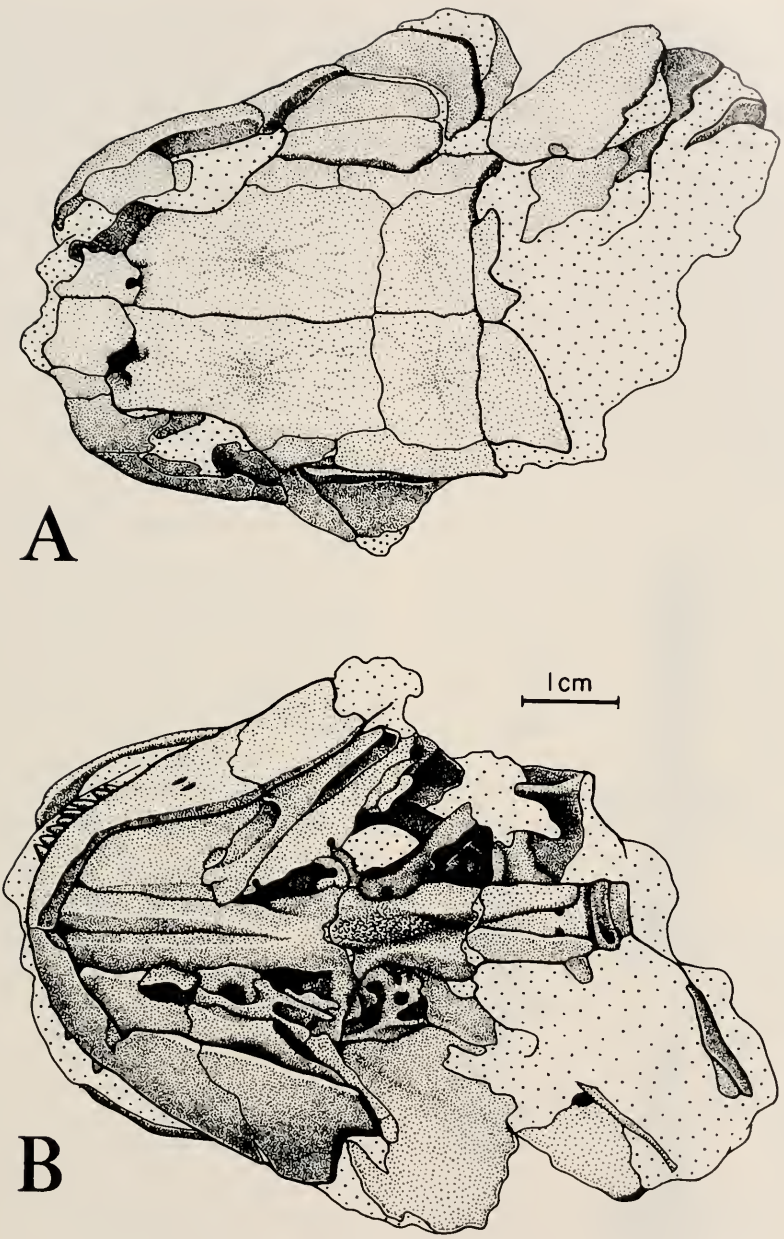

Fig. 16. *Amia fragosa* MCZ 9264, Early Eocene, Willwood Formation, Wyoming; A, dorsal; B, ventral.

Hell Creek Formation of Montana and interpreted this as a variation in *A. fragosa* not observed in the Lance sample. Janot (1967) noted that basioccipitals of the European Late Paleocene *Amia* sp. also showed this variation. Estes and Berberian (1969: 2) suggested that a weak tendency for fusion of vertebrae could be correlated with increasing size, and that such variation might possibly exist in the Recent species as well. Fifty Recent *A. calva* skeletons examined, with a size range of 100–480

mm SL, have the first two vertebrae fused to the basioccipital. Three articulated and twenty-two disarticulated Eocene and Oligocene *Amia uintaensis* basioccipitals all have two vertebrae fused to the basioccipital. Unfortunately, in specimens of *A. fragosa* (MCZ 9264, PU 13261) having a visible parasphenoid, the basioccipital regions are poorly preserved. There is a possibility that the Lance sample by chance contained only specimens with one fused vertebra since there are only six specimens known. Until more specimens of *A. fragosa* and *A. uintaensis* with intact basioccipitals become available, it is difficult to discuss this point further.

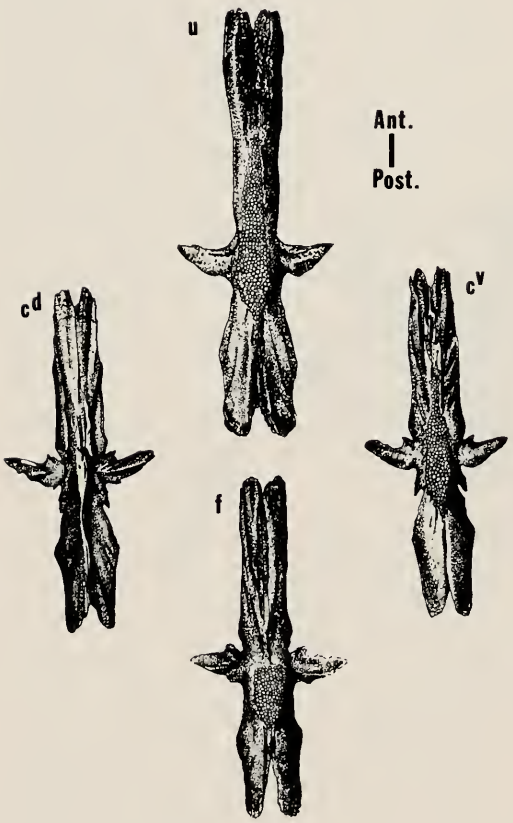

Fig. 17. Comparison of parasphenoids of *Amia* spp.: c, *Amia calva*, Recent, after Janot, 1967 (c^d = dorsal, c^v = ventral); f, *A. fragosa* (ventral); u, *A. uintaensis* (ventral).

The length of the *A. fragosa* parasphenoid posterior to the ascending processes is 10 percent shorter and slightly wider than in *A. calva,* with the ascending processes more posterior than in the Recent species (Fig. 17). The proportion of the length posterior to the processes to the length anterior to these processes (0.780) is not as small as in *A. uintaensis* (0.704) or as great as in *A. calva* (0.900), and, on the basis of this small sample, *A fragosa* is intermediate among the three species for this character. The region posterior to the processes also appears more convex than in *A. calva,* but not as convex as in *A. uintaensis.* The ascending processes are almost perpendicular to the main anteroposterior axis of the parasphenoid. Those of *A. fragosa* form an approximately 85-degree angle with the parasphenoid axis, while the ascending processes of both *A. calva* and *A. uintaensis* form approximately 70–75-degree angles. The mid-ventral surface of the parasphenoid bears small, sharp, conical teeth. This tooth-bearing surface of *A. fragosa* terminates anteriorly toward the middle of the ascending processes, whereas in *A. calva* this region narrows to a point and extends to the posterior end of the vomers (Fig. 17). In *A. uintaensis,* this region also extends to the vomers, but covers a wider surface area in the anterior region than in *A. calva.* Nearly all the tooth-bearing surface of *A. fragosa* lies in the posterior half of the parasphenoid, while in *A. calva* this surface is centered between the posterior and anterior areas; in *A. uintaensis* two-thirds of this surface lie in the anterior region of the parasphenoid. The entire tooth-bearing surface of *A. fragosa* is wider than that of *A. calva,* since the anterior half of the tooth-bearing surface tapers anteriorly in *A. calva,* while in *A. fragosa* the anterior portion maintains a more constant width. The basic outline of the tooth-bearing surface in *A. fragosa* is subrectangular; that of *A. calva* is more tear-drop shaped, with the anterior apex widened and extended to the vomers. The two posterior parasphenoid flanges are

more splayed in *A. fragosa* than in *A. calva* or *A. uintaensis,* and overlie three-fourths of the basioccipital length. As Estes (1964: 29) notes, there is a relatively greater dorsoventral parasphenoid thickness in *A. fragosa* than in *A. calva.* The parasphenoid of *A. uintaensis* is proportionately more massive than that of *A. fragosa;* this massiveness, however, is probably a function of its greater size.

In *A. fragosa,* as in *A. uintaensis,* the extrascapular is tear-drop shaped, being narrow at the midline and expanded distally, while in *A. calva* and *A. scutata,* it is more strap-shaped and longer at the midline. The proximal anterior corner is squared off, as in *A. scutata* and *A. calva.* The anterior edge is distally concave at the pterotic-extrascapular suture, and the posterior edge is convex, particularly toward the distal end, which is straight rather than curved as in the other species of *Amia. A. fragosa* and *A. uintaensis* lack the posterolateral projection displayed in *A. calva.*

The suprascapular resembles that of *A. calva,* except that the distal edge is relatively straight, rather than incurved. The posterior border is also straight, while in *A. calva* there is generally a slight concavity in the middle of this edge; in *A. uintaensis* this border is convex.

The pterotic extends further anteriorly than in *A. calva,* but not to the extent that it does in *A. uintaensis* or *A. scutata.* The dermosphenotic-pterotic suture is directed posterolaterally in *A. fragosa* and anterolaterally in *A. uintaensis, A. scutata,* and *A. calva.* As in *A. uintaensis* and *A. scutata,* this bone in *A. fragosa* is narrower anteriorly than posteriorly, whereas in *A. calva* the widths of these ends are relatively equal.

The dermosphenotic in *A. fragosa* is about the same relative size as in the other species of *Amia.* The anterior angle that forms the posterior border of the orbit is slightly more pronounced than in *A. scutata* and *A. uintaensis,* and considerably more so than in *A. calva* (Fig. 28).

The parietal in *A. fragosa* is characteristically square, whereas in *A. calva, A. scutata,* and *A. uintaensis* it is longer than wide. The length of the parietal relative to that of the frontal is less than in *A. calva* and *A. scutata* and about the same as in *A. uintaensis.* The characteristic deep excavation in the frontal for the orbit is displayed in all available specimens of *A. fragosa.* This led Estes (1964: 36) to postulate the presence of supraorbital bones, but the articulated specimens figured by O'Brien (1969) show that this was not the case. As Figure 28 shows, the ratio of orbital depth to length is greater in *A. fragosa* than in the other *Amia* species. As noted in the preceding section on the cranial morphometrics of the Recent *A. calva,* it is difficult to assign a specific character-state of parietal/frontal proportions to any of the individual fossil *Amia* species because of the similarity in parietal/frontal proportions (Table 7). It is apparent, however, that the frontals of the earlier species *A. fragosa* and *A. uintaensis* are longer relative to parietal-length than in the mid-Tertiary *A. scutata* or Recent *A. calva.* This feature is useful in comparing *A. fragosa* with these two species, but ineffective in distinguishing it from *A. uintaensis.*

As Estes and Berberian (1969) noted, the nasal displays a bifurcation of the anterior border that is lacking in *A. calva.* The bifurcation is also present in *A. uintaensis,* and the bone has approximately the same outline and size relative to head size as the other forms. All available specimens of *A. fragosa* show that the nasals lie much closer to the frontals than in *A. calva, A. scutata,* or *A. uintaensis.* Although Estes (1964) states that the lacrimal conforms closely with that of *A. calva,* his restoration lacks the small posterior notch in *A. fragosa* which accommodates the anterior process of infraorbital 2. The lacrimal in *A. fragosa* is evenly tapered at the posterior end, and is anteroposteriorly longer than in other *Amia.* It is also more dorsoventrally convex than in *A. scutata* and *A. calva.*

As in *A. scutata,* infraorbital 4 in *A.*

fragosa is much more dorsoventrally expanded than in *A. calva,* with the anteroposterior length extending almost to the anterior edge of the preoperculum. Infraorbital 4 of *A. fragosa* and *A. scutata* is more concave at the dorsal edge, and much more convex ventrally. The pit-line marks extend further ventrad than is indicated in the reconstruction by Estes (1964).

Branchiocranium. In *A. fragosa,* the supramaxilla is relatively shorter than in *A. uintaensis, A. scutata,* and *A. calva,* with a greater curve in the maxillo-supramaxillary suture. The dorsoposterior corner in *A. fragosa* tends to be angular, as in *A. scutata,* whereas in *A. calva* and *A. uintaensis* it is more rounded. The supramaxilla is deeper and more truncated at the anterior end than in other species of *Amia.*

There is a dorsal shelf adjacent to the lingual border of the alveolar ridge which widens the anterodorsal surface of the dentary (Fig. 18). This shelf is lacking in *A. calva* and *A. uintaensis,* in which the coronoid articulation surface slopes directly downward from the alveolar ridge. This region of the lingual dentary surface underlying the coronoids extends more ventrad at the symphyseal edge than in *A. calva,* and distinctly overlaps the ventral part of the ramus. There is no such overlapping in *A. calva;* the dorsal and ventral halves of this region separate to form Meckel's groove. The anterodorsal section of the dentary in *A. uintaensis* overlaps the ventral half, but not to the extent that it does in *A. fragosa,* and as the coronoid articulation surface is thicker, this thickened area of bone forms the dorsal wall of Meckel's groove as in *A. calva* (Fig. 18). As Estes (1964: 36) noted, the coronoid teeth are styliform and extend almost to the ventral border of the ramus at the anterior end; in contrast, the coronoid teeth of *A. calva, A. scutata,* and *A. uintaensis* are pointed and the coronoids do not extend as far ventrally as in *A. fragosa.* The anterior half of the dentary length is more curved than in *A. calva, A. scutata,* and *A. uintaensis* (Fig. 18). This is displayed in the MCZ 9264 specimen (Fig. 16), in which this curve approximates a 120-degree angle at the midpoint of the alveolar ridge. The outline of the dentary differs from that of *A. calva* and *A. uintaensis* in that the anterior end maintains an almost constant width up to the sharp curve at the midpoint of the alveolar ridge, at which point it widens noticeably. When the outline and curvature of the anterior end of the dentary of *A. fragosa* are compared with those of other species, the resulting difference appears to be correlated with *A. fragosa's* relatively smaller mandible/head ratio (Table 7), smaller mouth gape, and its wider cranial roof (Fig. 15).

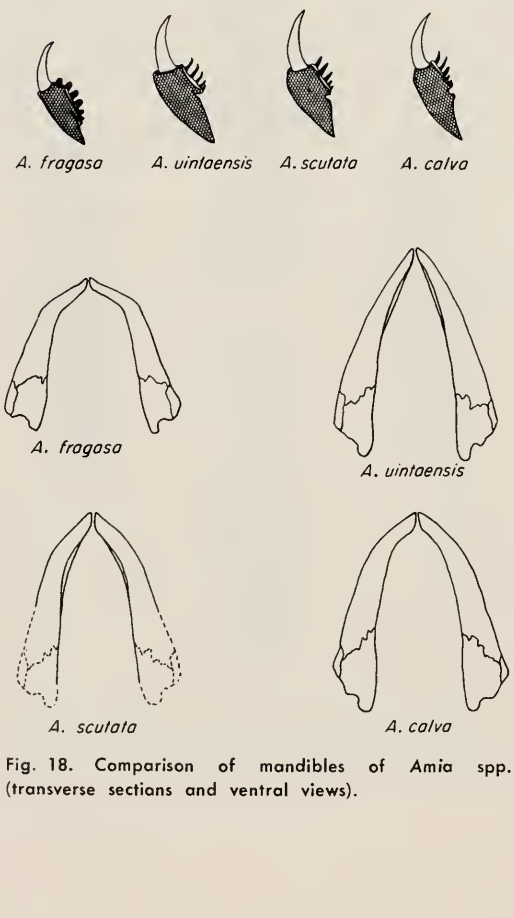

Fig. 18. Comparison of mandibles of *Amia* spp. (transverse sections and ventral views).

Post-cranial Skeleton. On the basis of specimens having only the lateral surface of the vertebral column exposed, it was concluded that centra of *A. fragosa* are indistinguishable from those of *A. scutata* and *A. calva.* Small disarticulated vertebrae are also basically similar in morphology, there-

fore it is impossible to differentiate *A. fragosa, A. scutata*, and *A. calva*. The mid-trunk vertebrae of *A. fragosa, A. scutata*, and *A. calva* differ from *A. uintaensis* mid-trunk vertebrae, which are generally larger, and subtriangular rather than ovoid. *A. fragosa* does, however, have a vertebral column that differs proportionately and meristically from that of other species (Fig. 31). It has a significantly smaller total number of centra than the other species, with approximately 12 fewer trunk vertebrae and 8 fewer monospondylous caudal centra. It has the same number of diplospondylous caudal centra as *A. calva* and *A. scutata;* the number of fused hypurals is also generally the same (Table 9). The low number of total vertebrae in *A. fragosa* is reflected by its shorter, deeper-bodied shape. The distance between the anal fin insertion and the end of the vertebral column is relatively shorter than in the other species. The dorsal fin also terminates closer to the caudal fin than in any of the other species of *Amia* (Plate 1; Estes and Berberian, 1969: 10). *A. fragosa* has fewer caudal lepidotrichia (19–20) than the other species of *Amia* (23–27). The head/standard-length ratio of *A. fragosa* is greater than that of *A. calva,* but is not significantly different from that of *A. uintaensis* or *A. scutata* (Table 3). The latter case is true despite the greater number of vertebral centra in *A. uintaensis* and *A. scutata;* this disparity may be explained largely by the fact that the *A. fragosa* skull itself is relatively shorter than that of the other two forms, particularly *A. uintaensis,* which has a greater head/standard-length ratio than *A. fragosa.* Thus head/standard-length does not significantly reflect the length of the vertebral column, but may be used as a character with this qualification in mind. The known total-length of *A. fragosa* falls within the range of *A. calva* and below that of *A. uintaensis* (Tables 1–2).

Discussion

Marsh (1871: 105) described *Amia newberrianus* and *Amia depressus* on the basis of disarticulated vertebrae and cranial elements from the Bridger Formation of Wyoming. His main criteria for distinguishing these forms from *A. calva* and from each other were that the chordal foramen of *A. newberrianus* was "considerably above the center in the dorsal vertebrae," and that *A. depressus* possessed broader vertebrae than *A. newberrianus* and lacked the median groove on the lower surface of the centra. The vertebrae indicated that both species were approximately the size of *A. calva.* Osborn *et al.* (1878: 102) noted that since Marsh gave no measurements, "the reference to *Amia depressus* cannot be certain." Marsh further noted that these specimens belonged to the Yale College Museum, but the specimens now seem to have been lost. Marsh had apparently assumed that the characteristics of one vertebra represented those of the entire vertebral column and was unaware of intracolumnar variation in height/width proportions, aortal facet morphology, and position of chordal foramen in the vertebral column of *Amia.* I infer from Marsh's report that the type specimen of *A. depressus* is probably a first to third trunk vertebra, since the aortal grooves are lacking (Fig. 11) and vertebral width exceeds height (Fig. 14). Using the position of chordal foramen as a character distinguishing *A. newberrianus* is undiagnostic since the position of the chordal foramen changes in relation to the relative position of the vertebra along the column (Fig. 12). Therefore, on the basis of Marsh's undiagnostic characters and the similarity in size and morphology of the vertebrae to those of *A. fragosa* and *A. calva*, I consider both *A. depressus* and *A. newberrianus* as *nomina dubia.*

Leidy (1873a: 98) described *Amia gracilis* from a single trunk vertebra, also from the Bridger Formation of Wyoming. He noted that the centrum has two "oblong fossae" (aortal facets) instead of the characteristic pair of ventral ridges found in *Amia calva.* The size of the centrum indicated to Leidy that *A. gracilis* was a smaller species than *A. calva* (Leidy, 1873b). The vertebra

(ANSP 5360) corresponds approximately to the twelfth trunk vertebra in *Amia,* since the aortal facets are oblong and unridged (Fig. 11). Although *A. gracilis* is small, it falls well within the size range of *A. fragosa* and *A. calva,* and is considered as a *nomen dubium.*

Estes and Berberian (1969: 10) suggested the possibility of synonymy of *Paramiatus gurleyi* (Plate 1) and *Amia fragosa* with the European *Amia kehreri* (Plate 2) on the basis of the close proximity of dorsal and caudal fins for the former and similarity of skull elements and teeth for the latter. It was shown in the previous section that *Paramiatus gurleyi* conforms not only to *A. kehreri,* but also to North American specimens of *A. fragosa* on the basis of body morphometrics and meristics. Cranial morphometrics were also shown to be similar. In addition, an X-ray (FMNH X2201) of the *Paramiatus gurleyi* skull reveals infraorbitals 4 and 5 to be longer than Romer and Fryxell (1928) and Estes (1964) had noted. The two infraorbitals extend posteriorly to the anterior edge of the preoperculum as they do in *A. fragosa* (UA 5398) from the Late Cretaceous Edmonton Formation of Alberta. The X-ray has also revealed a displaced left vomer with 26 styliform teeth which has been rotated through the skull roof and covered with matrix. All other cranial elements conform morphologically with other Cretaceous and Eocene specimens of *A. fragosa.* These additional similarities of *Paramiatus gurleyi* and *A. fragosa* confirm the synonymy of these two species which was suggested by Estes and Berberian (1969: 10), and I therefore include *Paramiatus gurleyi* in the synonymy of *Amia fragosa.*

Comments on Related European Forms

Amia kehreri was described by Andreae (1892, 1895) from a caudal region, infraorbital 4, disarticulated trunk vertebrae, and a left operculum from Middle Eocene (Lutetian) deposits at Messel bei Darmstadt (specimens at the University of Heidelberg, Andreae Collection). On the basis of specimens from the same deposit (BMNH P33480, Plate 2; P33488), it conforms morphometrically with *A. fragosa* in head/standard-length, pectoral fin insertion/standard-length, mandible/head-length, and operculum-length/operculum-depth (Tables 3, 7). The distance between the anal fin and the end of the vertebral column exceeds that of the North American *A. fragosa* specimens, but is less than in *A. scutata* or *A. calva.* The parietal/frontal ratio is also greater than in *A. fragosa,* but smaller than in *A. scutata* or *A. calva.* Meristics of vertebral elements as well as the cranial characters discussed by Estes and Berberian (1969) also conform with those of *A. fragosa.* I agree with Estes and Berberian (1969: 10) that only differences in temporal and geographical factors appear to distinguish *Amia kehreri* from *A. fragosa;* any osteological dissimilarities are of minor significance.

The Middle Eocene European Geiseltal deposits contain numerous amiid fossils; according to Estes and Berberian (1969) some showed resemblances to *A. kehreri.* This material is currently being described by Anna Jerzmánska, Uniwersytet Wrocławski, Wrocław, Poland.

Another related form is *Amia valenciennesi* from the Eocene of Puy-de-Dôme, France. Agassiz (1843) described the form from one complete specimen and an anterior region of another (BMNH P446, 27736). Piton (1940) reviewed these specimens along with new material collected at the same locality. *A. valenciennesi* also resembles *A. kehreri* in its vertebral number of 68 centra, close approximation of dorsal and caudal fins, and an infraorbital 4 larger than infraorbital 5; these similarities indicate that synonymy with *A. kehreri* is in order. The name *A. valenciennesi* precedes *A. kehreri,* and thus has priority.

Estes and Berberian (1969: 7) showed that *Amia russelli* Janot (1966, 1967) from the Late Paleocene of France resembles *A. fragosa* in (1) square parietals, (2) similar

parietal/frontal ratio, (3) large orbital excavation in frontal, and (4) similar operculum height/width ratio. Thus *A. russelli* conforms with many of the most distinct characters of *A. kehreri* and *A. valenciennesi*, and should be considered a synonym of the latter.

Estes (1964) re-evaluated Dechaseaux's (1937) redescription of the Early Oligocene *Amia munieri* from France and noted similarities with *A. fragosa* which included (1) styliform vomerine teeth, (2) branchiostegal rays rounded distally, (3) larger infraorbital 4 than infraorbital 5, and (4) similar parietal/frontal proportions. The principal difference between the forms is the small excavation for orbits in *A. munieri*. Since Dechaseaux's and Estes' studies, the specimen (MNHN R4632, skull and associated cranial and postcranial elements) is being further prepared to display the cranial roof and palate more extensively. The frontal lacks a prominent excavation for the orbits as Estes (1964: 40) has noted, and in this feature *A. munieri* resembles *A. scutata* and *A. calva*. *A. munieri* is a very important form because it represents the only complete amiid specimen known from the Early Oligocene, and, as noted, it displays intermediate morphology of the cranial features among the species of *Amia*. *A. munieri* occurs very late in time in relation to the last known occurrence of *A. fragosa* in North America, and because there are no complete specimens known from this age, it represents a stage of evolution among the amiids that is not found in North America.

Lehman (1951) described *Pseudamia heintzi* (Tromsø Museum Naturhistorisk collections, Tromsø, Norway) from a fairly complete articulated specimen and two skulls from probable Eocene deposits in Spitzbergen. He differentiated this form from *Amia* on the basis of (1) *Sinamia*-like metapterygoid and (2) presence of a concave notch on the dorsoposterior border of the operculum. Estes (1964) noted that Lehman was incorrect in his interpretation of the nature of the metapterygoid and operculum, and therefore suggested that *Pseudamia* might be placed in the genus *Amia*. From the examination of Lehman's plates, it appears that this form resembles *A. fragosa* in its deep-bodied shape and low parietal/frontal ratio (approximately 0.410), and that it may be synonymous with *A. valenciennesi* and *A. kehreri*. Further preparation would possibly be helpful in uncovering palatal teeth, whose morphology would aid in a more definitive description. Although the exact age of the Eocene deposit in which the specimen occurred is uncertain, this Spitzbergen locality, if Early Eocene, lies on the possible migration route of amiids (and other vertebrates) between North America and Europe.

Amia uintaensis (Leidy, 1873)

Protamia uintaensis Leidy, 1873a: 98.
Protamia media Leidy, 1873a: 98.
Pappichthys plicatus Cope, 1873: 635.
Pappichthys sclerops Cope, 1873: 635.
Pappichthys laevis Cope, 1873: 636.
Pappichthys symphysis Cope, 1873: 636.
Pappichthys corsonii Cope, 1873: 636.
Pappichthys medius Cope, 1884: pl. 4.
Amia whiteavesiana Cope, 1891: 2.
Amia macrospondyla Cope, 1891: 2.

Holotype. ANSP 5558, anterior trunk vertebra.

Paratypes. ANSP 8044, first anterior trunk vertebra; ANSP 3151, three posterior trunk vertebrae; ANSP 5622, basioccipital.

Type locality and horizon. Henry's Fork. North half of section 5, T 12 N, R 111 W, Sweetwater County, Wyoming; Bridger Formation.

Age range. Torrejonian (Middle Paleocene) to Chadronian (Early Oligocene).

Hypodigm. Paleocene. Fort Union Formation, Wyoming and Montana: PU 17117, maxillary; PU 17068, vertebrae and dentaries; PU 16236, disarticulated skull and trunk vertebrae; CM 25364, dentary; PU 17064, trunk vertebrae. Tongue River Formation, Montana: PU 20578, basioccipital and vertebrae. Paskapoo Formation, Alberta: ROM 4653, vertebrae.

Eocene. Willwood Formation, Wyoming: PU 21173, basioccipitals; PU 17227, basioccipital and trunk vertebrae; PU 17649,

portion of cranium; PU 18760, skull fragments, dentary, and vertebrae. Wasatch Formation, Wyoming: AMNH 4635, dentary and maxilla. Golden Valley Formation, North Dakota: PU 18568, basioccipital. Green River Formation, Wyoming: USNM 18147, skull fragments and vertebrae; AMNH 785, complete caudal region; PU 13865, nearly complete specimen; MCZ 12916, disarticulated skull and associated vertebrae. Wind River Formation, Wyoming: AMNH 2437, dentary and skull fragments. Bridger Formation, Wyoming: CM 25362, portion of cranium and vertebral column; AMNH 4631, portion of cranium with dentaries, gular, and basioccipital; USNM 170976, maxilla; YPM 6238–6240, 6242, 6244, 6250–6253, 6257–6258, vertebrae and basioccipitals; USNM 170973, 5450, 3962, 3963, 3966, PU 20523, 10101, ANSP 2337–2339, vertebrae; USNM 2181, ANSP 5632, trunk vertebrae; USNM 3959, trunk and caudal vertebrae; ANSP 5580, mid-trunk vertebra; AMNH 2539, anterior portion of a left dentary, two premaxillae, right quadrate, left epihyal, anterior portion of an ectopterygoid, three trunk vertebrae, and numerous fragments of angular; USNM 3965, left dentary; USNM 3968, anterior dentary fragment; AMNH 2570, pre-maxillary fragment, fragments of angular, left quadrate fragment, trunk vertebra fragment, and a caudal vertebra; USNM 3960, PU 10099, 10110, vertebrae and a ural centrum; USNM 5476, basioccipital; USNM 3961, left dentary fragment. Washakie Formation, Wyoming: FMNH 27465, 4509, vertebrae. Uinta Formation, Utah: CM 2382, maxillary fragment.

Oligocene. Cypress Hills Formation, Saskatchewan: NMC 6197, trunk vertebra; NMC 6198, caudal vertebra.

Known distribution. Montana, Wyoming, Utah, North Dakota, Alberta, and Saskatchewan.

Revised diagnosis. Vertebral column with approximately 20 more vertebral segments in total number (85) than *A. fragosa,* and five fewer trunk centra (31) and five more diplospondylous caudal vertebrae (21) than in the other long-bodied forms, *A. scutata* and *A. calva.* Mid-trunk vertebrae subtriangular rather than ovoid. Palatal teeth sharp, greatly curved inwardly. Between 40–45 vomerine teeth as compared with 15–17 in *A. fragosa, A. scutata,* and *A. calva.* Hyomandibular more deeply notched between opercular process and extensor (dorsal) surface than in other species; opercular process relatively larger. Angle between alveolar ridge and exterior surface of the dentary forms a more acute angle than in the other species. Mandibular ramus less curved than in other species, so that angle between symphyseal ends of dentaries is relatively narrow. Greater mandible/head ratio (0.693) and head/standard-length ratio (0.322) than any of the other forms: *A. uintaensis* has a head relatively longer and a mouth gape relatively wider than do other species. Most specimens are significantly larger than the other species, with a relatively greater degree of ossification of all bones. Greatest known standard-length 800 mm.

Introduction

Leidy (1873a) reported numerous disarticulated vertebrae of a fossil fish related to *Amia* from the Bridger Formation of Wyoming. He distinguished a new genus *Protamia* from *Amia* by its "two oval fossae" (aortal facets) on the ventral surface of the centrum, and by large vertebrae characteristically with a much greater width to height proportion. *Hypamia,* another new genus from the same locality which Leidy also related to *Amia,* was characterized by also being larger than *A. calva,* and by vertebrae whose sides converged into a "medium prominence excavated into a pair of oval fossae" deeper than those of *Protamia.* Later (1873b), Leidy published a more complete and illustrated account of the various species of the new genera *Protamia* and *Hypamia.* In the same year Cope (1873) described a new amiid genus, also from the Bridger Formation, which he named *Pappichthys.* He distinguished this new genus from *Amia* by the "presence of

only one series of teeth, instead of several, on the bones about the mouth." Osborn *et al.* (1878) reported other finds of *Pappichthys* from the Bridger Formation which seemed to fit Cope's description. Cope (1884) further discussed his new genus, and rejected Leidy's prior nomenclature and description.

Newton (1899) discussed this nomenclatural controversy and asserted the validity of Leidy's genus *Protamia*, since Cope's later diagnosis was no more effective in characterizing the new genus than Leidy's prior one. Newton believed that Cope's description of *Pappichthys* as having only a single row of marginal teeth was taxonomically undiagnostic, since this condition would also include *A. calva*. Romer and Fryxell (1928) accepted Leidy's earlier description and genus as diagnostic, and referred *Pappichthys* to *Protamia*. They also mentioned *Hypamia* but found little to distinguish it from *Amia*.

Hussakof (1932) continued to use Cope's name, however, and reported large specimens of *Pappichthys* from the Eocene of Mongolia. He also noted Cope's error in diagnosing the tooth characteristics of the genus, since *Pappichthys* (*Protamia*) has several rows of small teeth on the "splenial bone." In comparison with *Amia* he noted "points of difference in nearly every bone available for comparison," and concluded that *Pappichthys* was a valid genus, "not merely a group of large-sized extinct species of *Amiatus*."

Estes (1964), like Romer and Fryxell (1928), referred *Pappichthys* to *Protamia*, and reported several vertebrae and a maxillary fragment from the Cretaceous Lance Formation of Wyoming. He interpreted the increase in breadth over thickness of the vertebrae as a possible "function of increased size," a condition that would also allow for the comparatively more massive nature of the maxillary fragment. He also considered the retention of this genus as arbitrary until enough materials were available. Janot (1967) did not consider this single distinguishing characteristic of the vertebrae as sufficient foundation for the erection of a new genus, and therefore suggested referring *Protamia* to *Amia*. Estes *et al.* (1969) concurred with Janot in synonymizing *Protamia* with *Amia*. The present study confirms this synonymy; Leidy's species (1873a) has priority and the valid name of this fish is thus the oldest specific name, *Amia uintaensis*.

Revision of all forms referred now or in the past to *Protamia* is much needed, for these large amiids were diagnosed on characters of isolated vertebrae and skull fragments. This study gives more useful diagnostic characters that provide a basis on which the taxonomy of this group can be established.

Fossil Record

The major deposits carrying remains of *Amia uintaensis* (Table 18) range in age from Middle Paleocene to Early Oligocene. Middle Paleocene specimens occur in the Fort Union, Tongue River, and Paskapoo formations and consist mostly of isolated and broken centra, and dentary and maxillary fragments. A nearly complete skull (PU 16236) with associated trunk and caudal centra from the Bear Creek local fauna of Montana (Fort Union Formation) is the only articulated specimen from the Late Paleocene. The Eocene material includes one complete articulated specimen (PU 13865), one complete caudal region (AMNH 785), and a disarticulated skull (MCZ 12916) from the Green River Formation. PU 13865 (Plate 3) has the axial skeleton intact in matrix, with a dislocated fifth centrum that is the only one available for three-dimensional measurements. This is also the only specimen in which a complete vertebral count can be taken. AMNH 785 provides excellent meristic information for the caudal region (Fig. 8C). CM 25362, from the Bridger Formation, consists of a left palatal and opercular series and an almost complete, disarticulated vertebral column that permitted the taking of a series of centrum measurements. Other skull fragments and vertebrae occur in many deposits

throughout the Eocene (Table 18). The latest occurrence of *A. uintaensis* is represented by two isolated centra from the Cypress Hills Formation (Oligocene, Chadronian).

Description

Neurocranium. Posterior to the spinal arterial foramina the basioccipital includes two fused vertebrae. As the basioccipitals display great variation in the morphology of the articular surface, it is difficult to characterize this form on the basis of this feature. However, the articular surface is generally kidney-shaped, with dorsal indentations between the neural facets, and ventrally there is an indentation distal to the aortal facets. In *A. fragosa* and *A. calva* the basioccipital has ovoid articular surfaces with no dorsal indentations between the neural facets (Estes, 1964: 29, fig. 15). In lateral view the distal articular surface of the *A. uintaensis* basioccipital is not perpendicular to the parasphenoid flanges; the dorsal half of this surface is more anteriorly directed than the ventral half.

The parasphenoid is longer relative to its width than it is in either *A. calva* or *A. fragosa,* primarily in the region anterior to the ascending processes. At the point nearest the ascending processes, it lacks the pronounced convexity and the accompanying anterior lateral notches found in *A. calva* and *A. fragosa.* The ascending processes are slightly less anteriorly oriented in ventral view than in *A. calva,* but more so than in *A. fragosa* (Fig. 17). The region posterior to the ascending processes is relatively shorter than in *A. fragosa* or *A. calva;* it is also more massive and more ventrally convex than in the other two forms. The posterior parasphenoid flanges resemble those of *A. calva* more than *A. fragosa* in outline as well as juxtaposition; those of *A. fragosa* are more laterally splayed than in *A. uintaensis* or *A. calva.* The tooth-bearing surface differs considerably from that of *A. fragosa* and somewhat from *A. calva* in outline and extent. As in *A. calva,* this surface extends anteriorly to the vomers, but its width is much greater and more constant than in *A. calva,* which is narrowly tapered anteriorly. Posteriorly, this surface extends further than in *A. calva,* but not as far as in *A. fragosa.* Approximately two-thirds of the tooth-bearing surface lies anterior to the ascending processes, while in *A. calva* this area is anteroposteriorly centered, and in *A. fragosa* it is nearly all posterior. The tooth-bearing surface covers a greater portion of the ventral surface of the parasphenoid than in *A. fragosa* or *A. calva;* its basic outline is diamond-shaped, with the anterior apex widened and extended to the vomers, while that of *A. fragosa* is subrectangular and that of *A. calva* is tear-drop shaped with the apex sharply protracted anteriorly.

In *A. uintaensis* the distal edge of the suprascapular is convex as in *A. calva,* while in *A. fragosa* this edge is almost a straight line. The posterior border is more rounded distally than in *A. calva* and is convex rather than concave.

In having the extrascapular rounded at the distal border, *A. uintaensis* is the same as *A. calva* and *A. scutata,* but differs from both of them in that the posterior border is not concave, and from *A. calva* alone in lacking the distal posterior process. The anterior border is relatively straight, unlike the condition in *A. calva* and *A. scutata,* in which the lateral distal ends of the anterior borders are directly posteriad. As in *A. fragosa* the midline is shorter than in *A. scutata* and *A. calva.*

As in *A. scutata* and in *A. fragosa* the pterotic is narrower at the anterior than posterior border, while in *A. calva* and, to an extent, in *A. scutata* the ends are subequal. As in *A. fragosa* they extend farther anteriorly and adjoin the frontals posterolaterally. The dermosphenotic-pterotic suture is anterolaterally directed, as in *A. scutata,* but not as pronounced as in *A. calva.* The anterolateral edge of the pterotic is indented and forms, with the dermosphenotic, an additional concavity in the outline of the cranial roof. Aside from this

anterior indentation, the lateral borders are relatively straight, as compared with the smoothly concave exterior sides of the pterotics in *A. scutata, A. calva,* and *A. fragosa.* The posterior border forms a smooth line, as in *A. fragosa,* and lacks the small lappet that *A. scutata* and *A. calva* display.

The dermosphenotic is similar to that of *A. calva* in relative size and outline, although it does not jut as deeply into the frontals. Its anterior border is rounded, as in *A. calva,* rather than sharply angular, as in *A. fragosa.* The posterior half of the outer lateral border is indented to form a concavity with the anterior tip of the pterotics. The parietal in *A. uintaensis* is elongated anteriorly, as in *A. calva* and *A. scutata,* while that of *A. fragosa* is relatively square. The orbital excavation in the lateral sides of the frontal is shallow as in *A. calva* and *A. scutata,* while that of *A. fragosa* is characteristically deep (Fig. 28). The sensory canal cannot be determined. The frontals are more elongated relative to parietal length than in *A. calva* and *A. scutata;* the parietal/frontal ratio is only slightly smaller than that of *A. fragosa* (Table 7). The distal lateral border tapers anteromedially, and the anterior ends are relatively pointed anteriorly, forming a deep notch on the midline suture.

There is a slight bifurcation of the anterior border of the nasal as in *A. fragosa.* The nasal bones are relatively narrower than in *A. fragosa* or *A. calva,* but are otherwise similar in shape and relative size. They are fairly well separated from the frontals, as in *A. calva* and *A. scutata,* rather than abutting them as in *A. fragosa.*

The lacrimal in *A. uintaensis* resembles that of *A. fragosa* in general morphology, although it lacks the posterior notch for the anterior end of infraorbital 2 which is present in the other species of *Amia.* The lacrimal, like that in *A. fragosa,* is relatively longer and more tapered posteriorly than in *A. scutata* and *A. calva.* It is more dorsally convex than in the other forms, but only slightly more so than in *A. fragosa.*

The infraorbital 5 in *A. uintaensis* is similar to that in *A. fragosa* and *A. scutata,* being less robust posteriorly than in *A. calva.* As in the other forms, it is narrower anteriorly than posteriorly. The ventral border is relatively straight, while that of the other forms is posteriorly convex. Infraorbitals 2, 3, and 4 have not been identified.

The vomerine tooth patch in *A. uintaensis,* as in *A. fragosa,* extends more posteriorly than in *A. calva* (Fig. 19). The vomerine teeth are sharp and greatly curved posteriorly; they exceed those of *A. fragosa* and *A. calva* in number, each vomer bearing between 40–50 teeth, as compared to half that number in *A. fragosa* and *A. calva.* The rostral and antorbital are identical to that of the other species.

Branchiocranium. The suture between the anterior and posterior dermopalatine cannot be discerned. In *A. uintaensis* the dermopalatine has about twice the number of teeth as in *A. calva,* and the tooth patch extends more distad. The teeth are sharply pointed, as are the vomerine teeth.

The hyomandibular is more deeply excavated between the opercular process and the extensor (dorsal) surface, and the opercular process is more massive and extends further ventrad, forming a larger articulation surface, as compared with the other species of *Amia.* The articular surface of the quadrate is more robust than in other species of *Amia* and displays three cristae ventrally rather than dorsally as in *A. calva* and *A. robusta* (Janot, 1967: 144). The ceratohyal resembles that of *A. calva* and *A. fragosa* with the exception of its being thicker at the neck of the proximal end. The metapterygoid in *A. uintaensis* conforms very closely to that of *A. calva* in outline and in the position of the anterior

Fig. 19. Comparison of vomers of A, *Amia calva;* B, *A. uintaensis;* and C, *A. fragosa.*

basal process and the posterolateral otic process.

The maxilla in *A. uintaensis* is more robust and relatively longer, and its posterior border is dorsoventrally wider than in the other forms, particularly *A. fragosa.* As in *A. calva* the small supramaxillary notch occurs more anteriorly than in *A. fragosa.* The dorsoposterior border is rounded, as in *A. calva* and *A. scutata,* rather than sharply angular, as in *A. fragosa.* Anteriorly the maxilla is deeper and more thickly ossified than in the other forms, but this may be a function of greater size. The supramaxilla resembles that of *A. calva* in general morphology, being elongated and narrowly tapered anteriorly, with a smoothly rounded posterior end conforming to the curve of the maxilla. The maxillo-supramaxillary suture is straight as in *A. calva.* The premaxilla is identical to that of the other species.

The dentary of *A. uintaensis* is similar to that of *A. calva* and *A. scutata* in lacking the dorsal shelf of the anterior lingual border of the alveolar ridge which occurs in *A. fragosa.* The coronoids articulate more or less vertically on the alveolar ridge, as in *A. scutata* and *A. calva.* The anterodorsal region of the dentary slightly overlaps the ventral half, but not to the extent that it does in *A. fragosa; A. uintaensis* seems to be intermediate between *A. fragosa* and *A. calva* in this feature, the latter having no such ventral overlapping at the symphyseal edge. The coronoid articulation surface of the *A. uintaensis* dentary is thicker than in *A. fragosa* and *A. calva,* but only slightly more so than in *A. scutata.* At the termination of this surface, this thickened area of bone forms the dorsal wall of the Meckelian groove, as in *A. calva.* The ventral wall of this groove is less well defined than in *A. calva,* with *A. scutata* being intermediate. The anterior half of the dentary length in *A. uintaensis* is evenly tapered to the symphyseal edge; it is elongated and lacks the sharp curve present in *A. fragosa* at the midpoint of the alveolar ridge (Fig. 18). There is only a trace of such a curve in the dentaries of *A. calva* and *A. scutata* which are also more elongated and evenly tapered than in *A. fragosa,* although not to the extent that they are in *A. uintaensis.* Anteriorly, the bone is also relatively thicker than in *A. fragosa* and *A. calva; A. scutata* also displays this greater ossification at the anterior end of the dentary. Posteriorly, the dentary is very similar to that of *A. calva.* The coronoid teeth are sharp and conelike, extending to the midpoint of the lingual surface, as in *A. calva.* As Janot (1967) shows for *A. robusta,* the alveolar ridge is more horizontal in *A. uintaensis* and forms a more acute angle with the exterior surface of the dentary than it does in *A. fragosa* or *A. calva; A. scutata* is intermediate between *A. uintaensis* and *A. calva* in this feature (Fig. 18). In *A. uintaensis* the first coronoid (symphyseal) overlies only the dorsal half of the anterior articular surface of the dentary, as in *A. calva* and *A. scutata.* The teeth are more sharply pointed than in any of the other forms (Fig. 18). The second coronoid is fragmentary, but appears to resemble that of *A. calva* with the exception of its having more sharply pointed teeth. The prearticular specimens available are fragmentary, but the lingual surface possesses blunt-conical teeth similar to those in *A. calva* and *A. fragosa.* Dorsally, however, these teeth are as sharply pointed as the coronoid teeth. The angular is slightly longer and higher than that of *A. calva.* The posterior border is more vertical, with the articular notch less pronounced. It is more heavily ossified than in *A. calva,* but this may be a function of size. The surangular in *A. uintaensis* is basically similar to that of *A. calva,* although it is situated more dorsally and is more rounded at the dorsal edge.

The gular is longer than that of *A. calva* and *A. fragosa* (Fig. 20). It is also slightly narrower at the posterior end than the anterior end, while the reverse is generally true in *A. calva.* Otherwise, the gular strongly resembles that of *A. calva.* Despite a few minor dissimilarities, the preoperculum resembles that of *A. calva.* There is a

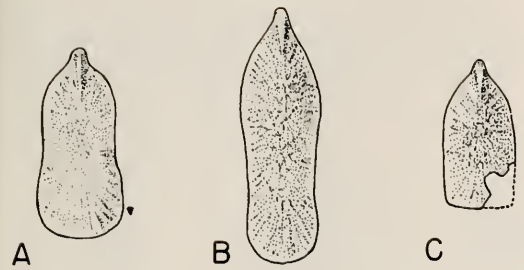

Fig. 20. Comparison of gulars of A, *Amia calva;* B, *A. uintaensis;* and C, *A. fragosa.*

slightly more pronounced concavity in the ventroposterior border than is exhibited in *A. calva;* this concavity is altogether lacking in *A. fragosa.* The line of curvature is about the same as in *A. calva;* in *A. fragosa* the preopercuhim is more deeply curved. The dorsal half is not quite as wide as the ventral half, while in *A. calva* both ends are fairly equal. In *A. fragosa,* however, the dorsal half is much narrower and more tapered than the ventral half, which is relatively wider and bulbous. The operculum in *A. uintaensis* is similar to that of *A. calva* and *A. scutata* in operculum-depth/operculum-length (Table 7). The subopercuhim conforms in general morphology with that of *A. calva,* although it is slightly more robust, particularly in the posterior region. The corners tend to be angular, as in *A. scutata* and *A. calva,* rather than rounded, as in *A. fragosa.* The interopercuhim is similar to that of *A. calva,* although more robust. The anterodorsal border is more convex than in *A. calva,* and is more deeply impressed into the preopercuhim. The anteroventral border is narrowly tapered as in *A. calva,* rather than smoothly rounded as in *A. fragosa.* The first branchiostegal ray conforms to that of the other species. Although the lack of articulated material makes any count of the rays difficult, in MCZ 12916 there are 12 disarticulated branchiostegal rays on the right side of the cranial roof. As in *A. fragosa* the distal ends of the rays are consistently rounded, rather than squared as in *A. calva.*

Post-cranial skeleton. The supracleithrum in *A. uintaensis* resembles that of *A. calva* and *A. fragosa,* excepting the dorsal articulation surface, which is rectilinear rather than pointed as in *A. calva.* The distal lateral border in the Paleocene specimens lacks the notch that occurs in *A. calva,* but this notch is present in the Eocene specimens. The metacleithrum in *A. uintaensis* is more elongated than in *A. calva* and *A. fragosa.* The dorsal end is narrower than in *A. calva,* and the ventral end is squared off. The cleithrum in *A. uintaensis* is largely similar to that of the other *Amia* species, but is more massive at the proximal end than in *A. calva,* and the dermal sculpture covers a greater area than in *A. calva,* extending to the distal border as in *A. fragosa* and *A. scutata* (Fig. 21). The mid-distal border is smoothly convex and lacks the notch ventral to the metacleithrum which is present in *A. calva.*

The preceding study of the vertebral skeleton of *A. calva* revealed changes in height/width proportions, position of chordal foramen, configuration of neural and aortal facets, and in the basapophyseal angles and length of basapophyses which may be used here to discern similar trends in *A. uintaensis* centra, for the fossil vertebrae display the same features characteristic of the Recent species even in disarticulated state.

CM 25362 from the Bridger Formation is the only specimen that has a relatively complete, disarticulated, undistorted verte-

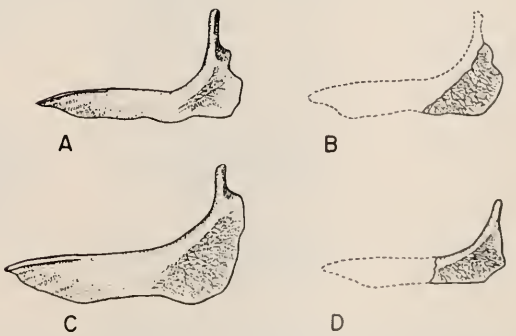

Fig. 21. Comparison of cleithra of A, *Amia calva;* B, *A. scutata;* C, *A. uintaensis;* and D, *A. fragosa.*

bral column; as the centra are separable this specimen is useful in comparisons with isolated vertebrae. There are 59 centra present: 25 trunk centra and 34 caudal centra, including two fused urals. Many of the preserved caudal centra are only fragments. Since the articulated specimen (PU 13865) has 85 vertebrae (see Table 9 for regional numbers) it may be assumed that about 25 vertebrae are missing from CM 25362. When comparing vertebrae from different regions of the column in the two specimens, it appears that CM 25362 lacks approximately six trunk and approximately twenty caudal centra. The first anterior trunk centrum present in the CM 25362 series possesses aortal facet configurations similar to those of the seventh vertebra of the articulated specimen (PU 13865). An articulated but separable series of six uncrushed anterior trunk vertebrae (PU 10101), also from the Bridger Formation, aids in the reconstruction of the anterior region of the *A. uintaensis* vertebral column (Figs. 22–25). The basapophyseal angles of these six PU 10101 vertebrae do not vary from 180 degrees. The first six anterior trunk vertebrae from a partly disarticulated vertebral column from the Paleocene specimen (PU 16236) resemble the six PU 10101 centra in length and shape of aortal facets, even though PU 16236 is a smaller individual. The height/width ratio of these latter centra is difficult to determine, however, since the specimen underwent postdepositional crushing. The nearly complete vertebral series of the CM 25362 specimen has been used for the construction of the remaining trunk and caudal region in the model of the *A. uintaensis* vertebral column. The trunk centra of CM 25362 have been arranged according to basapophyseal angles that decrease from 180 to 46 degrees, as in *A. calva.* Decreasing size was used to arrange the caudal vertebrae.

Although *A. uintaensis* occurs much ear-

Table 14. Angle of basapophyses, length, height, and width of vertebrae of *Amia uintaensis* compared with type specimens of synonymized taxa as illustrated in figure 22

Relative Vertebral Number	Specimen	Angle of Basapophyses (Degrees)	Length (mm)	Height (mm)	Width (mm)
1	*A. uintaensis* PU 10101	—	8.0	32.0	45.0
	A. uintaensis PU 16236		6.0	31.0	44.0
	P. uintaensis ANSP 8044		8.0	32.0	46.0
	P. sp. USNM 170973		5.5	19.0	29.0
2	*A. uintaensis* PU 10101	180°	8.0	32.0	44.5
	A. uintaensis PU 16236		8.5	28.5	39.0
	A. whiteavesiana NMC 6197		8.5	29.0	40.0
	P. sp. FMNH P27465		9.0	28.0	36.0
3	*A. uintaensis* PU 10101	180°	10.0	33.0	43.0
	A. uintaensis PU 16236		8.0	30.0	41.5
	P. sp. USNM 3966		8.5	21.5	29.0
	P. medius USNM 3959		8.5	22.0	30.0
4	*A. uintaensis* PU 10101	180°	10.0	33.0	44.0
	A. uintaensis PU 16236		7.5	33.0	40.8
5	*A. uintaensis* PU 10101	180°	11.0	33.5	44.0
	A. uintaensis PU 16236		9.5	31.5	39.0
	A. uintaensis PU 13865		4.5	16.5	21.5
6	*A. uintaensis* PU 10101	180°	11.0	34.0	42.5
	A. uintaensis PU 16236		9.0	33.5	34.0
	P. uintaensis ANSP 5558		10.5	32.5	40.0

lier in time than *A. calva* and *A. scutata*, it has approximately the same total number of centra (85), and like them is a longer-bodied form than its contemporary, *A. fragosa*, which has a mean of 65 centra. The vertebral column of *A. uintaensis* does,

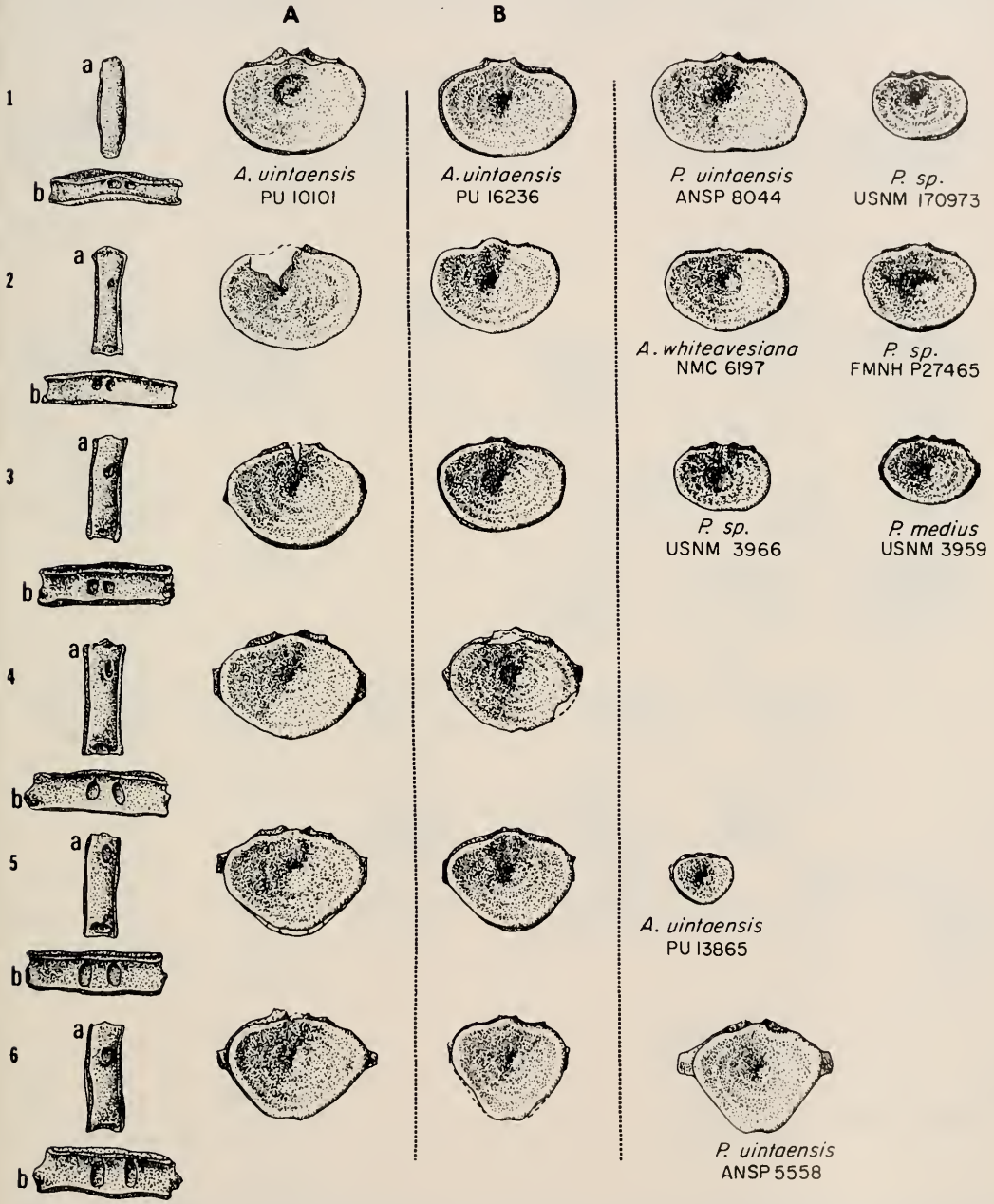

Fig. 22. First anterior trunk vertebrae (A,B) of *Amia uintaensis* compared with type specimens of synonymized taxa (refer to Table 14 for data).

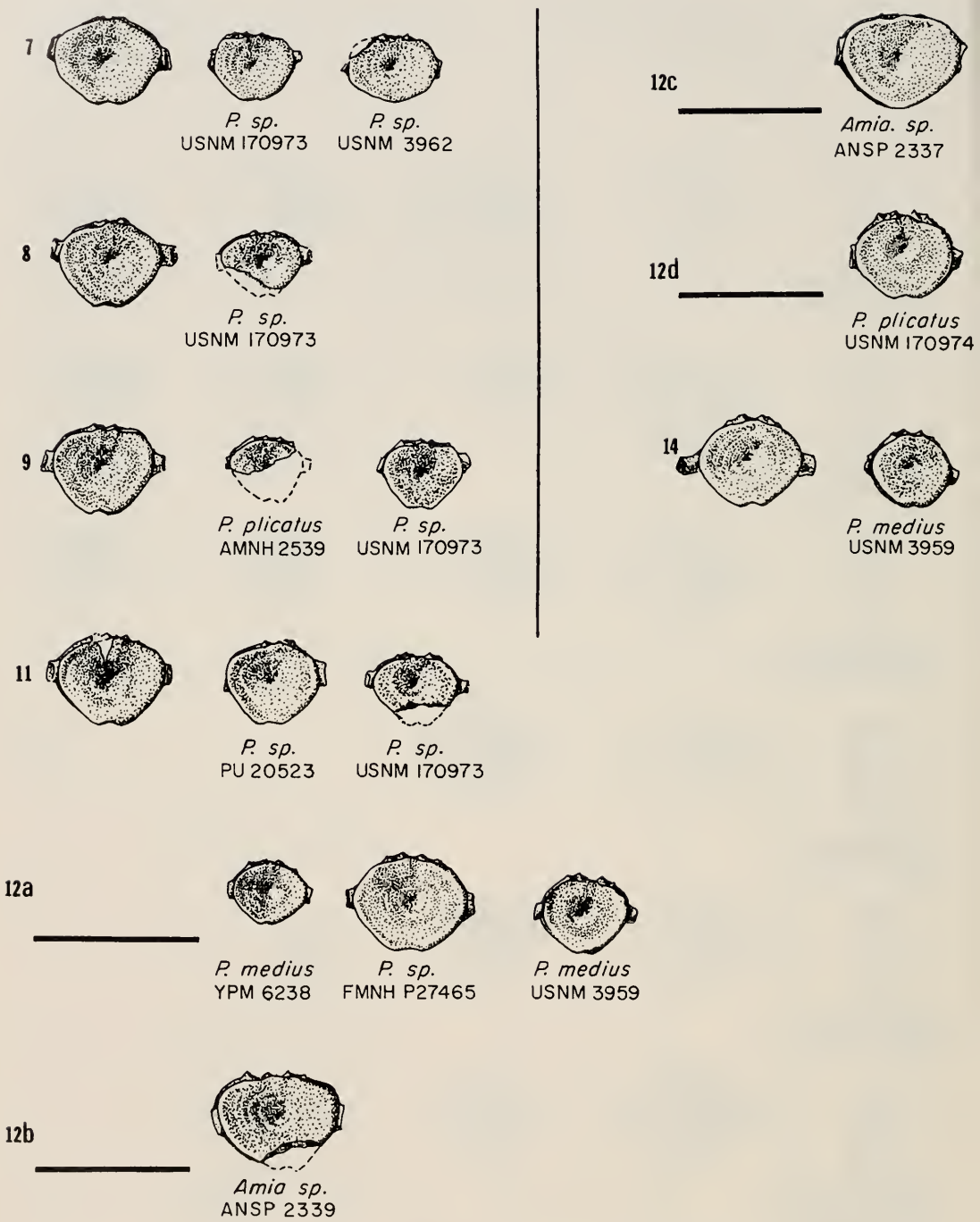

Fig. 23. Seventh through fourteenth mid-trunk vertebrae of *Amia uintaensis* compared with type specimens of synonymized taxa (refer to Table 15 for data).

however, differ meristically from that of *A. calva* and *A. scutata* in number of vertebrae in the various regions. There are 31 trunk centra in *A. uintaensis* (PU 13865), as opposed to 37 (mean) in *A. calva* and 36 (mean) in *A. scutata*. The number of diplospondylous vertebrae is 20–21, as compared with 14–17 in *A. calva* and 15 in *A. scutata*. This variation from *A. calva* and *A. scutata* in the organization of the verte-

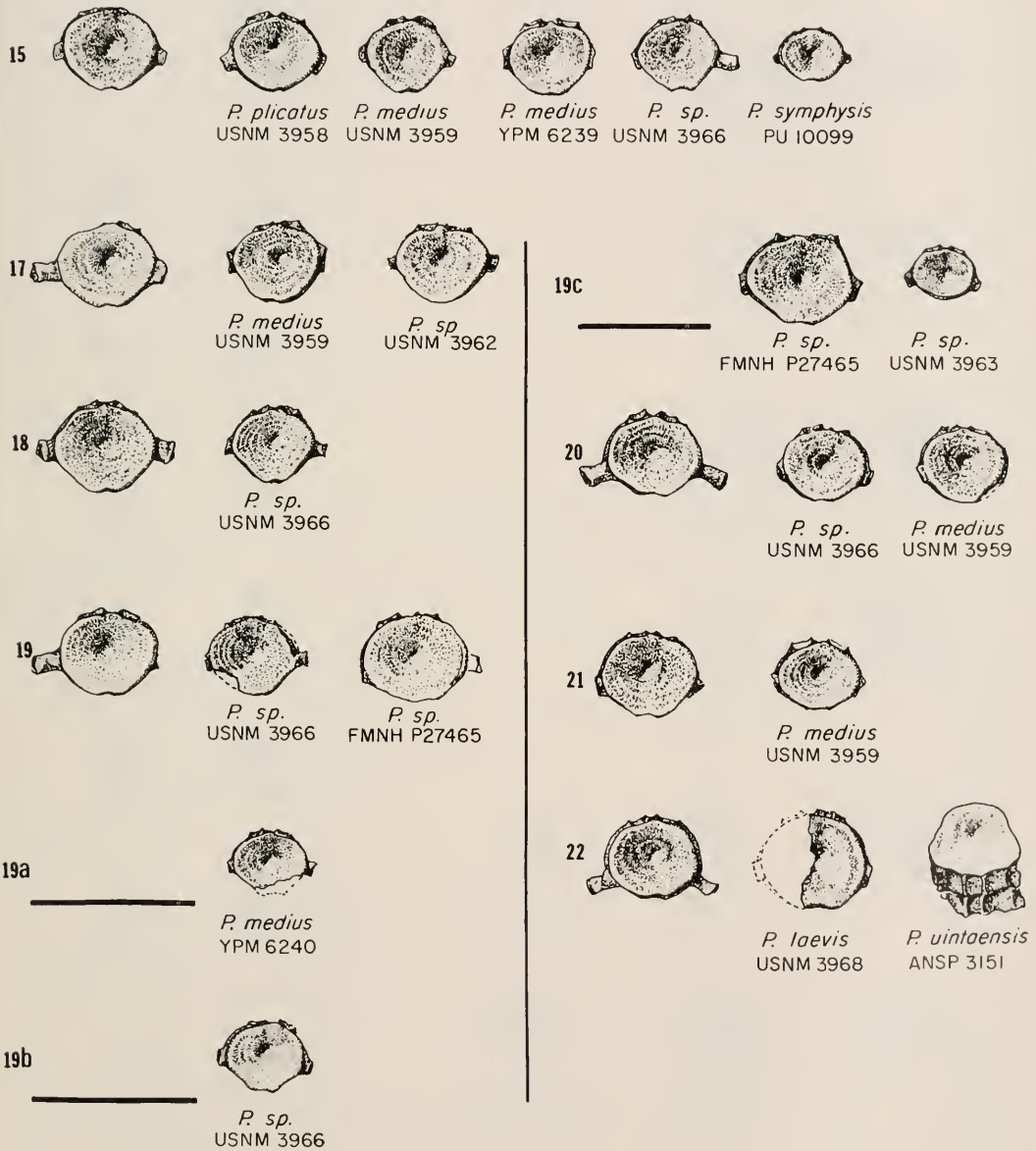

Fig. 24. Fifteenth through twenty-second posterior trunk vertebroe of *Amia uintaensis* compared with type specimens of synonymized toxa (refer to Table 16 for data).

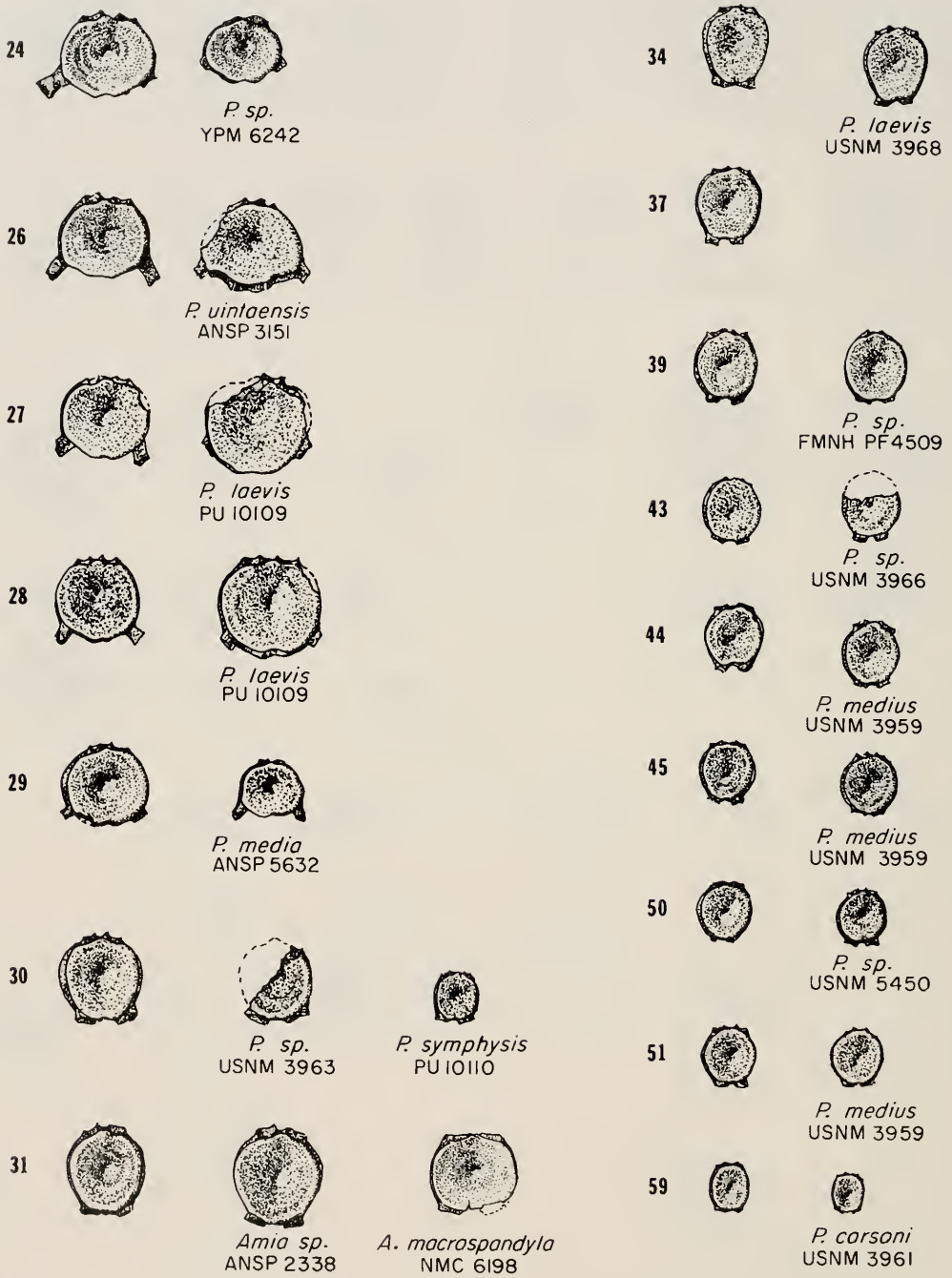

Fig. 25. Posterior trunk and caudal vertebrae of *Amia uintaensis* compared with type specimens of synonymized taxa (refer ta Table 17 for data).

Table 15. Angle of basapophyses, length, height, and width of vertebrae of *Amia uintacusis* compared with type specimens of synonymized taxa as illustrated in figure 23

Relative Vertebral Number	Specimen	Angle of Basapophyses (Degrees)	Length (mm)	Height (mm)	Width (mm)
7	*P. sp.* USNM 170973	179°	8.5	19.5	25.5
	P. sp. USNM 3962		7.0	20.0	28.0
8	*P. sp.* USNM 170973	178°	8.5	19.5°	26.0
9	*P. plicatus* AMNH 2539	177°	6.0°	18.0°	24.0
	P. sp. USNM 170973		8.0	21.0	25.5
11	*P. sp.* PU 20523	174°	7.5	25.0	30.0
	P. sp. USNM 170973		7.5	22.0°	25.0
12a	*P. medius* YPM 6238	171°	6.0	19.0	24.0
	P. sp. FMNH P27465		11.0	30.0	35.0
	P. medius USNM 3959		9.0	22.0	28.0
12b	*Amia sp.* ANSP 2339	167°	10.0	29.0°	40.0
12c	*Amia sp.* ANSP 2337	166°	10.0	29.0	38.5
12d	*P. plicatus* USNM 170974	163°	8.0	24.0	30.0
14	*P. medius* USNM 3959	160°	7.5	19.0	23.0

° Est.

Table 16. Angle of basapophyses, length, height, and width of vertebrae of *Amia uintacusis* compared with type specimens of synonymized taxa as illustrated in figure 24

Relative Vertebral Number	Specimen	Angle of Basapophyses (Degrees)	Length (mm)	Height (mm)	Width (mm)
15	*P. plicatus* USNM 3958	156°	8.5	22.5	25.0
	P. medius USNM 3959		8.5	23.0	27.0
	P. medius YPM 6239		8.5	22.0	24.5
	P. sp. USNM 3966		8.5	21.0	25.5
	P. symphysis PU 10099		5.5	15.5	20.0
17	*P. medius* USNM 3959	153°	9.0	24.0	29.0
	P. sp. USNM 3962		9.0	23.0	28.0
18	*P. sp.* USNM 3966	149°	9.0	21.0	25.5
19	*P. sp.* USNM 3966	143°	8.5	23.0	27.8
	P. sp. FMNH P27465		11.0	28.0	33.0
19a	*P. medius* YPM 6240	139°	7.0	19.0	23.0
19b	*P. sp.* USNM 3966	138°	—	—	—
19c	*P. sp.* FMNH P27465	136°	11.0	25.0	35.0
	P. sp. USNM 3963		7.0	16.5	20.0
20	*P. sp.* USNM 3966	132°	9.0	21.0	27.0
	P. medius USNM 3959		9.0	22.0	26.0
21	*P. medius* USNM 3959	122°	9.5	22.0	27.0
22	*P. laevis* USNM 3968	117°	10.0	26.0	30.0
	P. uintacusis ANSP 3151		12.0	28.0	29.0

Table 17. Angle of basapophyses, length, height, and width of vertebrae of *Amia uintaensis* compared with type specimens of synonymized taxa as illustrated in figure 25

Relative Vertebral Number	Specimen	Angle of Basapophyses (Degrees)	Length (mm)	Height (mm)	Width (mm)
24	*P. sp.* YPM 6242	102°	9.0	17.0	22.0
26	*P. uintaensis* ANSP 3151	97°	10.0	23.0	28.0
27	*P. laevis* PU 10109	90°	13.0	29.0	33.0
28	*P. laevis* PU 10109	83°	14.0	28.0	30.0
29	*P. media* ANSP 5632	80°	8.0	16.0	18.0
30	*P. sp.* USNM 3963	62°	11.0	—	—
	P. symphysis PU 10110		6.0	14.0	13.5
31	*Amia sp.* ANSP 2338	46°	13.0	26.0	23.0
	A. macrospondyla NMC 6198		12.0	25.0	22.0
34	*P. laevis* USNM 3968		6.5	22.0	18.0
39	*P. sp.* FMNH PF 4509		7.0	19.0	18.0
43	*P. sp.* USNM 3966		7.0	19.0	18.0
44	*P. medius* USNM 3959		6.0	16.0	18.0
45	*P. medius* USNM 3959		5.5	17.5	18.0
50	*P. sp.* USNM 5450		7.0	15.0	13.5
51	*P. medius* USNM 3959		5.0	17.0	11.0
59	*P. corsonii* USNM 3961		4.0	11.0	10.0

bral column into regions and types of vertebrae appears to be a useful taxonomic character of *A. uintaensis.*

The neural, aortal, and haemal facets do not appear to vary much from those of *A. calva.* The first six ventral aortal facets show basically the same pattern for both species (Figs. 11, 22). The angle of basapophyses in *A. uintaensis* differs from that of *A. calva* in two ways. The first six vertebrae all have basapophyseal angles of 180 degrees, and it is not until the seventh vertebra that these angles gradually begin to decrease. Because of this more posterior beginning in the decrease of the angles and because there are fewer trunk vertebrae, the rate of decrease of the basapophyseal angle is greater. These angles range from 180 degrees anteriorly to approximately 45 degrees posteriorly, about the same as the range for *A. calva.*

The intracolumnar variation in centrum shape seen in the vertebral column of Recent *A. calva* also occurs in *A. uintaensis* (Fig. 14). In some respects the latter shares certain characteristics with *A. calva.* The first centrum is broad and thin, and usually lacks basapophyses (Fig. 22). However, centra between the fourth and twentieth vertebrae begin to acquire an almost subtriangular outline, as opposed to the subelliptical form of the *A. calva* trunk centra (Fig. 12). The subtriangular shape may be a function of greater size of the centra.

The chordal foramen is open in all known vertebrae of *A. uintaensis* from the Paleocene, Eocene, and Oligocene, but is often filled with detritus during fossilization. Estes (1964: 42) observed that Cretaceous specimens as well as the Late Paleocene specimen (PU 16236) had the chordal foramen smoothly closed with bone. A re-

examination of PU 16236 reveals that the chordal foramen is actually filled with fine sediment rather than bone, so that the character of the closed foramen can only be applied to the Cretaceous specimens. Chordal foramen position in all specimens shows slight intracolumnar variation along the trunk as in *A. calva,* although occurring more dorsally. In the caudal region there is virtually no difference between the two forms.

Leidy characterized "*Protamia*" *uintaensis* on the basis of five centra and one basioccipital. His height/width proportions were described in relation to those in an undiagnostic intracolumnar standardization of the centra of the *A. calva* vertebral column. My measurements of the anterior trunk centra reveal that the holotype ANSP 5558 has a width 1.3 times the height, and paratype ANSP 8044 has a width 1.6 times the height. Other paratype centra are posterior trunk centra with width/height ratios of approximately 1:1. Romer and Fryxell (1928: 521) described a displaced posterior trunk centrum as having a height of 10 mm and a width of 12.5 mm, about the same as in ANSP 5558. Estes (1964: 43), in his discussion of the height/width proportions of *A. uintaensis* centra, misinterpreted Leidy's (1873a, 1873b) diagnosis of "*Protamia*" *uintaensis* and Romer and Fryxell's (1928) diagnosis of "*Paramiatus gurleyi,*" indicating that vertebrae of the former were three times as wide as deep, those of the latter two times. Estes was correct, however, in his assumption that there is intracolumnar variation in height/width ratios.

The general pattern of intracolumnar variation in the *A. uintaensis* vertebral column is quite similar to that of *A. calva;* there is the same trend from horizontally elliptical centra to circular or vertically elliptical centra (Fig. 14). Thus the earlier diagnoses of *A. uintaensis* using height/width ratios that attributed the proportions of the anteriormost trunk vertebrae to the entire column are undiagnostic.

On the basis of isolated centra and skull material, the most commonly used character in differentiating *A. uintaensis* from *A. calva* has been the former's greater size. However, the articulated specimen (PU 13865), which is the smallest known *A. uintaensis,* is only 146 mm longer than *A. fragosa* (FMNH 2201) and 16 mm longer than the largest *A. calva* known to me (UMMZ 197683). Estes (1964) suggested that the widening of the *A. uintaensis* vertebrae might be a function of its greater size; Gould's (1966) statement that internal elements generally increase at allometric rates to provide sufficient surface area to maintain the external surface area offers a partial explanation as to why the large *A. uintaensis* vertebrae have greater width in proportion to height than they do in smaller amiid vertebrae.

Discussion

Two species of *Protamia,* one species of *Hypamia,* six species of *Pappichthys,* and three species of *Amia* have been described on vertebral characters from isolated centra and disarticulated cranial elements (Table 19). With the exception of *Amia whiteavesiana, A. selwyniana,* and *A. macrospondyla* from the Oligocene Cypress Hills Formation of Alberta, all these taxa are based on material from the Bridger Basin, Bridger Formation, of Wyoming. Each of these 12 taxa will be re-evaluated in the following discussion. Of the twelve species and four genera, "*Protamia*" *uintaensis* (Leidy, 1873a) is the oldest name. Leidy's type specimens are all trunk vertebrae. The holotype ANSP 5558 (Fig. 22) is approximately the sixth anterior vertebra and displays the characteristic subtriangular outline of other specimens. The paratypes include trunk vertebrae (ANSP 8044, 3151), and a large basioccipital (ANSP 5622). The holotype vertebrae and the basioccipital are considered diagnostic for *Amia uintaensis,* on the basis of their possessing the characteristic subtriangular vertebral outline, and a kidney-shaped articular surface of the basioccipital.

Leidy (1873a) described *Protamia media* from two large trunk centra from the

Bridger Formation of Wyoming. His main criterion for distinguishing this form from *A. calva* and from the other species of "*Protamia*" was that the vertebrae were twice the size of *A. calva* vertebrae and "somewhat smaller than *Protamia uintaensis*" (Leidy, 1873b). The holotype USNM 2181 appears to be from the anterior trunk region (approximately the seventh or eighth centrum, as suggested by its proportions and configurations of aortal facets). The basapophyseal angle is approximately 178–180 degrees. The paratype ANSP 5632 is from the posterior trunk region, with an 80-degree basapophyseal angle, which is approximately equivalent to the twenty-ninth centrum in *A. uintaensis* (Table 17; Fig. 25). Cope (1884, plate 4, figs. 7–20) figured "*Pappichthys medius*" on the basis of 14 disarticulated centra from the same locality (USNM 3959). Eight of these are from the trunk region and correspond to centra within the anterior to mid-trunk region of *A. uintaensis* (Tables 15–16; Figs. 23–24). The remaining six centra correspond to centra in the caudal region (Tables 16–17; Figs. 24–25). Cope gave no description, but in figuring these specimens he allocated to them his own genus, emending Leidy's (1873a) prior nomenclature. Both Leidy and Cope had apparently assumed that the characteristics of one or a few vertebrae represented those of the entire column. Both species fall well within the size range of *A. uintaensis* (Tables 14–17), and are here considered synonyms of the latter.

Leidy (1873a) described *Hypamia elegans* from one small trunk vertebra. He characterized this form as possessing a centrum that was characteristically "short in proportion with its breadth, and it presents sutural impressions for a contiguous pair of neural arches" (Leidy, 1873b). ANSP 5580 appears to be from the mid-trunk region, comparable to approximately the nineteenth centrum as suggested by its proportions and configuration of aortal facets. The basapophyseal angle is 138–139 degrees. These character-states and the small size are not unique, occurring as the do in all the other species of *Amia; Hypamia elegans* is therefore a *nomen dubium.*

Cope (1873) described *Pappichthys plicatus* from the anterior portion of a large left dentary (AMNH 2539). Other type material included two premaxillae, a right quadrate, a left epihyal, an anterior portion of an ectopterygoid, three trunk vertebrae, and numerous fragments of angulars. He characterized this form primarily on the basis of dermal sculpture of the "cranial fragments being roughly grooved." The angular in *A. uintaensis* is generally marked by more pronounced dermal sculpture than the other mandible elements. His diagnosis of the vertebrae (USNM 3958) is based on proportions and morphology of neural and aortal facets, both of which correspond to various trunk vertebrae in *A. uintaensis* (Tables 15–16; Figs. 23–24). The description of the remaining elements conforms with other elements of *A. uintaensis. Pappichthys plicatus* is therefore a synonym of the latter.

Cope (1873) described *Pappichthys sclerops* from a large left dentary. He characterized this form as possessing a dentary "more compressed and deeper" than that in *A. calva* and other species of "*Pappichthys.*" The dentary (USNM 3965) in all respects greatly resembles all dentaries that have been referred to *A. uintaensis,* and I regard *Pappichthys sclerops* as a synonym of the latter.

Cope (1873) described *Pappichthys laevis* from a large anterior dentary fragment (USNM 3968). Other type materials include a premaxillary fragment, fragments of angulars (AMNH 2570), a left quadrate fragment, a trunk vertebra fragment, and a caudal vertebra. Although Cope distinguished this taxon from other species of *Pappichthys* on vertebral proportions, variances in dermal sculpture, dentary alveolar count, and obliqueness of alveolar face, these character-states occur in *A. uintaensis. Pappichthys laevis* is therefore a synonym of the latter.

Cope (1873) described *Pappichthys symphysis* from two large fragments of trunk vertebrae and a ural (USNM 3960). His diagnosis rests primarily on configuration of neural facets and basapophyseal length. Osborn *et al.* (1878: 104) later reported two caudal vertebrae as cotypes (PU 10099, 10110). Cope (1873) described *Pappichthys corsonii* from 12 centra (USNM 5475–5476), a basioccipital (USNM 5476), and a left dentary fragment (USNM 3961). He distinguished this form from *Pappichthys symphysis* on different neural facet morphology, basapophyseal length, and height/width proportions. Merrill (1907: 14) cites "*Pappichthys symphysis* = *Pappichthys corsonii*" without further discussion. The centra of both forms conform to centra in the vertebral column of *A. uintaensis* (Table 17; Fig. 25) and the characters assigned to the dentary and basioccipital of *Pappichthys corsonii* are also found in *A. uintaensis;* thus both *P. symphysis* and *P. corsonii* are synonyms of *A. uintaensis.*

From the Early Oligocene Cypress Hills Formation, Saskatchewan, Cope (1891) described *Amia whiteavesiana* from an anterior vertebra (NMC 6197), and *Amia macrospondyla* from a caudal vertebra (NMC 6198). Both these forms were founded on variations of vertebral characters (height/width proportions, lack of basapophyses, and chordal foramen position) that are also represented in the vertebral column of *A. uintaensis.* The type centrum of *A. whiteavesiana* corresponds approximately to the second anterior vertebra in *A. uintaensis* (Table 14; Fig. 22), that of the type centrum of *A. macrospondyla* with the thirty-first centrum in *A. uintaensis* (Table 17; Fig. 25). Prior to the appearance of Cope's (1891) publication, Ami (1891), in his review of the Cypress Hill fauna, mistakenly listed *A. whiteavesiana* under the name *A. selwyniana. A. macrospondyla* and *A. whiteavesiana* are here considered synonyms of *A. uintaensis; A. selwyniana* is a *nomen nudum.*

Comments on European and Asian Forms

Janot (1967) described a large amiid, *Amia robusta,* from the Late Paleocene of France, on the basis of disarticulated material. She distinguished this form from *A. calva* and *A. russelli* on the angle of the ventral border of the dentary face, and on morphology of the parasphenoid tooth-bearing surface in addition to other minor morphological differences. Many of the diagnostic elements or associations on which *A. uintaensis* is based, such as coronoid and vomerine teeth, regional vertebral counts and dorsal cranial elements, are missing in her material. The elements that she does figure, however, closely resemble the comparative bones in *A. uintaensis.* Similarities include rounded distal ends of branchiostegal rays (also in *A. fragosa*), subtriangular morphology of trunk vertebrae, extensive surface of parasphenoid tooth-patch, and shallow orbital notch in frontal (also in *A. scutata* and *A. calva*). These marked similarities suggest that *A. robusta* is a synonym of *A. uintaensis.* Current work on the relationship of the North American and European continents in the Early Cenozoic (McKenna, 1972) indicates that they were connected until the Early Eocene and that there is great similarity between the Paleocene and Early Eocene mammalian taxa at that time. There is thus no zoogeographic problem inherent in synonymizing these two species.

Hussakof (1932) described *Pappichthys mongoliensis* from disarticulated elements from the Late Eocene Ulan Shireh beds of the Shara Murun region, Inner Mongolia (collected by the American Museum Central Asiatic Expeditions.) At the time of Hussakof's description, this collection (AMNH 6372) represented the most extensive material of "*Pappichthys.*" The collection includes numerous dentaries, maxillae, three gulars, three opercula, three cleithra, an hyomandibular, a supracleithrum, a vomer, and trunk and caudal vertebrae.

Hussakof distinguished this form from *A. calva* by the length of the dentaries and the morphology of the operculum, and from species of "*Pappichthys*" and "*Protamia*" on the basis of comparison of vertebral size. A comparison of the Mongolian material with *A. uintaensis* shows some dissimilarities, but there is still a closer affinity between this form and *A. uintaensis* than with the other species of *Amia.* The vomer bears numerous sharp vomerine teeth; the hyomandibular is deeply arched, and the lingual face of the dentaries conforms to that of *A. uintaensis.* The dentary, however, is quite elongated anteriorly, the supracleithrum is narrower, and the dorsal border of the operculum is short and ascends at a 30-degree angle rather than being horizontal as in *A. uintaensis* (and in other *Amia* species). The extrascapular is narrow and tapered to a point rather than flattened medially. Thus, although *Pappichthys mongoliensis* is similar to *A. uintaensis* in many features and is clearly related to it, it also differs in some respects. It undoubtedly belongs to the genus *Amia,* and retention of all the Mongolian specimens in *Amia mongoliensis* seems the most practical alternative at this time. The Mongolian higher vertebrate taxa indicate that the Turgai Straits at least partially isolated Mongolia from Europe during at least part of the Cretaceous, Paleocene, and Eocene, and that probably little exchange took place until the Late Eocene (Szalay and McKenna, 1971: 280–281). It may be possible that *A. mongoliensis* evolved from *A. uintaensis* during this migration.

Amia cf. *uintaensis*

Hypodigm. Cretaceous. Lance Formation, Wyoming: CM 256, YPM 6311, trunk vertebrae; UCMP 56276, two fragments of a single vertebra; UCMP 56277, one complete vertebra, one vertebral fragment, one left maxillary fragment. Hell Creek Formation, Montana: AMNH 6385, trunk vertebra; MCZ 9334, dentary tooth tips. Aguja Formation, Texas: UMM collections, maxillary fragment. Ojo Alamo Formation, New Mexico: USNM collections, trunk vertebra.

Discussion

Cretaceous specimens of large amiids occur in both Lance and Hell Creek formations and consist mostly of isolated and broken centra, and teeth that have been identified primarily on the basis of size. The characteristic subtriangular outline of the trunk vertebrae is even more pronounced in these Cretaceous specimens, wherein the lateral centrum walls between the basapophyses and the aortal facets are concave (Fig. 26). The chordal foramen is, as Estes (1964: 42) noted, closed with bone, as are one-third of the vertebrae referred to *A. fragosa* from the Lance Formation. However, Estes observed lateral concavities between the neural facets and basapophyses in a large vertebral centrum (AMNH 6385) from the Hell Creek Formation (mistakenly cited by him as AMNH 6835 from the Oldman Formation of Alberta). Estes apparently confused neural with aortal facets and thus figured the vertebra upside down. Correct orientation of the centrum (Fig. 26) shows concavities between the basapophyses and the aortal facets. Thus, Estes was incorrect in concluding that *A. fragosa, A. calva,* and the Eocene specimens of *A. uintaensis* "also seem to lack the concavity between the 'basapophysis' and neural arch present in the large Cretaceous specimens." Two other specimens from the Lance Formation (YPM 6311, CM 256; Fig. 26) also show the prominent concavities between the basapophyses and aortal, rather than neural, facets. In addition to the vertebrae, Estes described a maxillary fragment as being larger and more robust than that of *A. fragosa,* although "characteristically amiid in tooth implantation and general shape." A more complete maxillary fragment (UMM collections) from the Aguja Formation (Big Bend National Park, Brewster County, Texas) conforms with Estes' (1964) description.

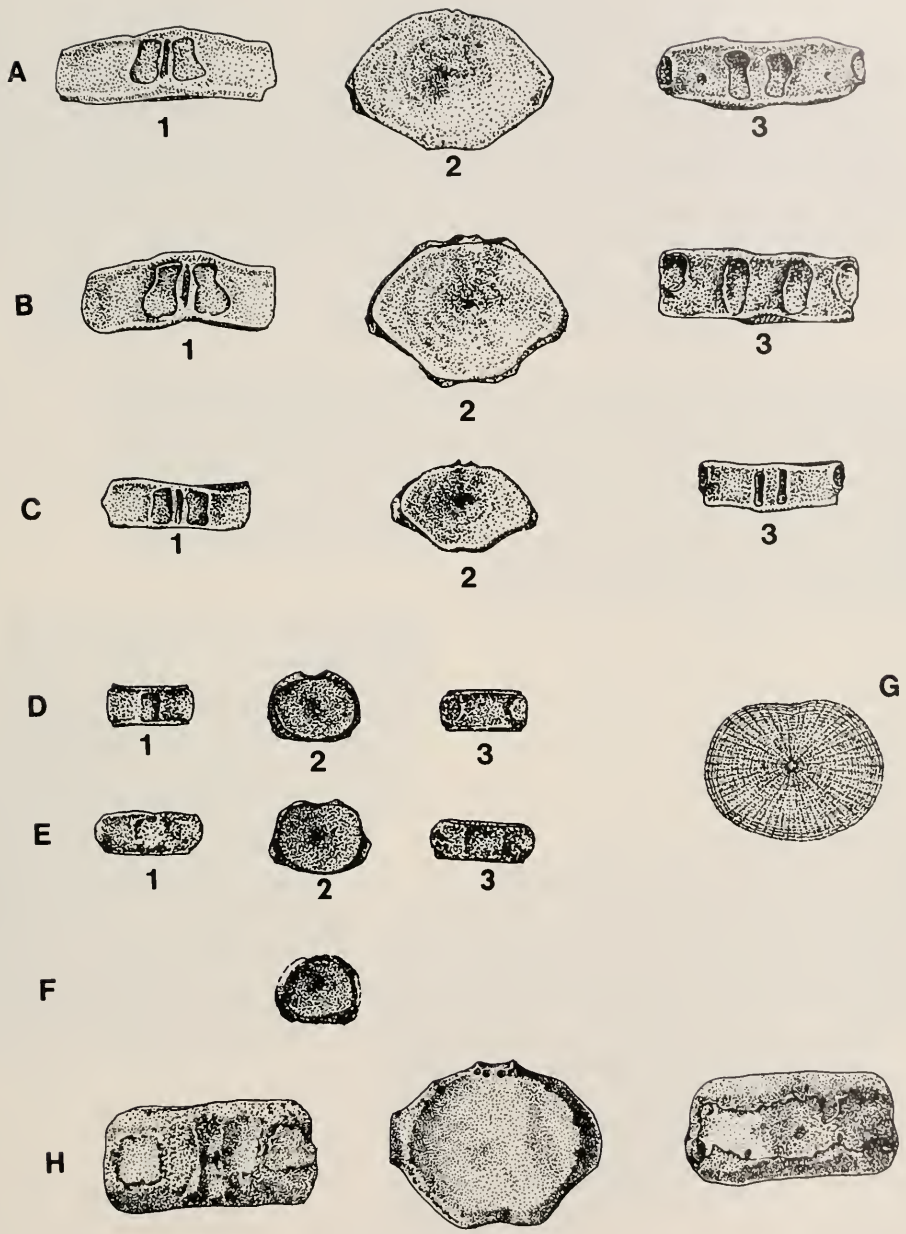

Fig. 26. Comparison of different Cretaceous vertebrae. *Amia* cf. *uintaensis:* A, anterior trunk vertebra, CM 256, Lance Formation, Wyoming; B, posterior trunk vertebra, AMNH 6385, Hell Creek Formation, Montana; C, mid-trunk vertebra, YPM 6311, Lance Formation, Wyoming. Chondrichthyes: D, E, G (thin section), trunk vertebrae, FHKSCM 13024–9, Black Creek Formation, North Carolina; F, trunk vertebra, MCZ 12879, Peedee Formation, North Carolina. Cetacean: H, caudal vertebra, FHKSCM 13025, Calvert Formation?, North Carolina.
1 = dorsal, 2 = articular surface, 3 = ventral

Only three new centra and a maxillary fragment have been identified since Estes' (1964) study. The vertebrae, as noted above, differ in certain minor respects from the Paleocene and Eocene specimens. Whether or not this material actually represents *A. uintaensis* or an earlier stage of evolution can only be determined when more complete Cretaceous material is available.

Amia scutata Cope, 1875

Amia dictycephala Cope, 1875: 3.
Amia exilis Lambe, 1908: 12.

Holotype. USNM 5374, incomplete specimen lacking the head and body anterior to the middle of the dorsal fin; anal and part of dorsal and caudal fins well preserved.

Type locality and horizon. Florissant, Colorado. East half of section 2, T 13 S, R 71 W, Teller County, Colorado; Florrisant Formation.

Age Range. Chadronian (Early Oligocene) to Orellan (Middle Oligocene).

Hypodigm. Oligocene. Cypress Hills Formation, Saskatchewan: NMC 6200, 6205, vertebrae; NMC 6201, basioccipital. Chadron Formation, South Dakota: PU 17172, left dentary with posterior coronoid bearing teeth, and a trunk vertebra. Lower Brule Formation, South Dakota and Nebraska: FMNH PF4508, PF4509, CM 3814, vertebrae; FMNH PF4506, right vomer bearing teeth. Florissant Formation, Colorado: PU 10172, nearly complete specimen (counterpart = YPM 6243, anterior half; USNM 4087, caudal half); YPM 6241, complete caudal region (with counterpart); UMMP V-57431, nearly complete specimen; USNM 3992, partial specimen, lacking skull and tail; AMNH 2802, nearly complete skull; AMNH 2670, partial specimen, lacking skull and caudal region; AMNH 2671, caudal region.

Known distribution. South Dakota, Nebraska, Colorado, and Saskatchewan.

Revised diagnosis. Vertebral meristics similar to those of *A. calva,* but head/standard-length proportion is intermediate between that of *A. uintaensis* and *A. calva.* Extrascapular thicker at distal end than in *A. calva,* with concave posterior border. Pterotic more similar to that of *A. uintaensis* than of *A. calva;* anterior portion narrow and extended laterally to the frontal. Orbital excavations more marked than in *A. calva,* but not as deep as in *A. uintaensis* or *A. fragosa.* Preoperculum resembles that of *A. uintaensis* more than that of *A. calva,* being narrower dorsally than ventrally. Symphyseal incurving of the dentary less than in *A. calva,* but greater than in *A. uintaensis.* Ventroposterior process of cleithrum heavily sculptured as in *A. fragosa* and *A. uintaensis.* Infraorbital 4 larger than infraorbital 5 as in *A. fragosa* and *A. uintaensis.* Ossification of cranial bones extensive as in other fossil species, greater than in *A. calva.* Greatest known standard-length 390 mm.

Introduction

Cope's (1875: 3) description of *Amia scutata* is based on a specimen lacking the head and body anterior to the middle of the dorsal fin, from the Middle Oligocene Florissant Formation near Florissant, Colorado. He distinguished this form from *Amia dictyocephala* (found in the same deposit; Cope, 1875) and *Amia calva* by its larger scales "of which only seven and a half longitudinal rows are visible above the vertebral column." Cope described *A. dictyocephala* from two partially complete specimens lacking skulls and caudal fins (USNM 3992, AMNH 2670), two complete caudal regions (AMNH 2671, USNM 4087), and a nearly complete skull (AMNH 2802); Osborn *et al.* (1878) later described another specimen of *A. scutata* from the same deposit. This specimen was more complete, consisting of an axial skeleton and a crushed skull. They believed *A. scutata* to be a valid form, differing from *A. calva* in having a proportionately larger head.

Comparison of known specimens of *A. scutata* revealed that the counterparts to the specimen described by Osborn *et al.* (PU 10172) were separated and sold to two

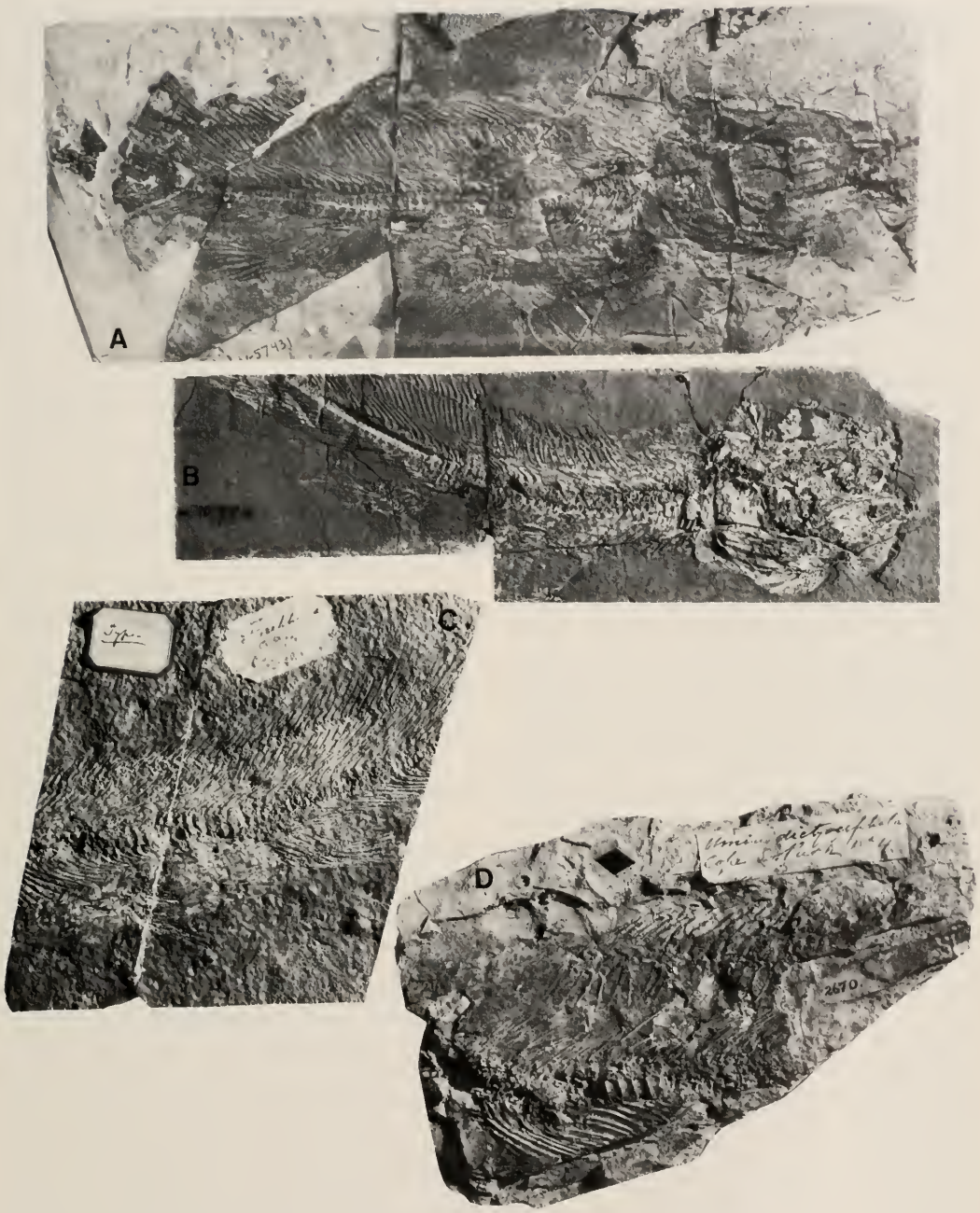

Fig. 27. A, *Amia scutata* UMMP V-57431; B, *A. scutata* PU 10172; C, *A. "dictyocephala"* USNM 3392; D, *A. "dictyocephala"* AMNH 2670.

different museums. The caudal portion of the counterpart was found in the National Museum of Natural History (USNM 4087) and is one of the paratypes used by Cope (1875) in his description of *A. dictyocephala*. The anterior region was found

unlabeled at the Yale Peabody Museum (YPM 6243; Plate 4).[1]

In 1967 another nearly complete specimen was discovered from the same deposit (Fig. 27A) and Cavender (1970: 42) reported the specimen *A. dictyocephala* as differing from *A. calva* in having a larger infraorbital 4, in the sculpture of cleithrum, and "by its proportionately larger head and orbit, and somewhat shorter body."

Fossil Record

Other than the Florissant Formation, the only deposits from which elements of *A. scutata* can be identified are the Cypress Hills Formation of Saskatchewan, Chadron Formation of South Dakota, and the Lower Brule Formation of South Dakota and Nebraska. Becker (1961: 38) reported amiid scales (UMMP collections) from the Late Oligocene Passamari Formation and Middle Oligocene Grant Horse Prairie Shale of Montana (Becker, 1962). Since no specific characters for scales of *Amia* have yet been determined, it is best to allocate this material to *Amia* sp. Skinner *et al.* (1968: 415) has reported *Amia* sp. vertebrae (F:AM 42947) from the Early Miocene Turtle Butte Formation of South Dakota. Only two specimens were found; since the vertebrae of *A. scutata* and *A. calva* are morphologically and meristically similar, Skinner *et al.'s* identification is the only possible one at this time. The stratigraphic range of *A. scutata* is therefore limited to the Early and Middle Oligocene.

Description

Neurocranium. The basioccipital (PU 10172, NMC 6201) is similar to that of *A. calva.* The only available parasphenoid (PU 10172) is poorly preserved, but closely resembles that of *A. calva* in length and position of ascending processes.

The extrascapular in *A. scutata* differs slightly from that of *A. calva* in that the distal end is relatively thicker and the posterior lappet is less pronounced; also, the posterior border is more convex (Fig. 15). As in *A. calva,* however, the proximal anterior corner is squared off, and the medial suture is relatively long. The pterotic in *A. scutata* resembles that of *A. uintaensis* more than that of *A. calva* in general morphology, since the anterior half is narrower than the posterior half; in the Recent species the ends are nearly symmetrical. The anterior border extends further laterally than in *A. calva,* and, as in *A. uintaensis,* adjoins the distal lateral side of the frontal, rather than the posterior border as in *A. calva.* The dermosphenotic, parietal, frontal, and nasal of *A. scutata* conform to these bones in *A. calva.* The parietal/frontal ratio is marginally within the lower limit of the range of *A. calva* (Table 7). The orbital excavation in the

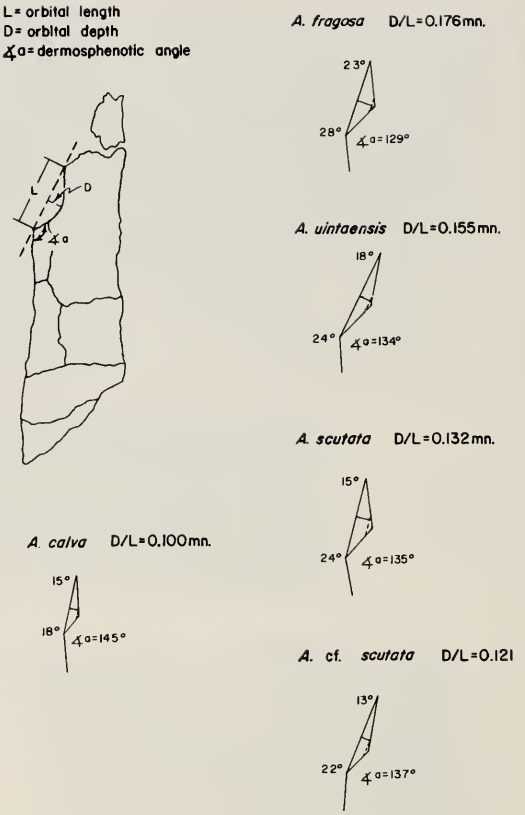

Fig. 28. Orbital dimensions of *Amia* spp.

[1] The counterparts (USNM 4087, YPM 6243) to PU 10172 have been subsequently acquired by the Museum of Natural History, Princeton University.

frontal (Fig. 28) is greater than in *A. calva* but less than in *A. fragosa* or *A. uintaensis*. Suprascapulars, antorbitals, and rostrals are not preserved.

The lacrimal is similar to that of *A. calva*, bearing a posterior notch for the reception of infraorbital 2, but in *A. scutata* the lacrimal is more robust. Infraorbital 2 and infraorbital 3 are similar to these bones in *A. calva*. Infraorbital 4 is more massive posteriorly than in *A. calva;* it exceeds infraorbital 5 in dorsoventral length, and the posterodorsal corner, which in *A. calva* is markedly acute is, in *A. scutata*, more squared off. This bone more closely resembles that of *A. fragosa;* it is not available for comparison in *A. uintaensis*. Infraorbital 5 is less massive posteriorly than in *A. calva;* in this feature it resembles that of *A. fragosa*. It is also, as in *A. fragosa* and *A. uintaensis*, deeper anteriorly than in *A. calva*.

Branchiocranium. The supramaxilla in *A. scutata* is elongated and tapered to a point anteriorly, with a relatively straight ventral border as in *A. calva*. It is slightly longer and more robust posteriorly, the posterodorsal border being higher and less obliquely curved than in *A. calva*, *A. uintaensis*, and *A. fragosa*. The premaxilla resembles that of *A. calva*. The maxilla is wider posteriorly and more ossified anteriorly than that of *A. calva*, but otherwise agrees with the bone in the Recent species.

Dermopalatine, autopalatine, entopterygoid, ectopterygoid, metapterygoid, and vomer are not preserved. However, conical vomerine teeth are displayed on PU 10172, and resemble those of *A. calva* rather than those of *A. fragosa* or *A. uintaensis*. The relative number of teeth and their extent on the vomer cannot be discerned.

As in *A. calva* and *A. uintaensis*, the dentary in *A. scutata* lacks the dorsal shelf adjacent to the lingual border of the alveolar ridge seen in *A. fragosa* (Fig. 18). The bone is very thick, especially toward the mid-lingual surface, where the dorsal and ventral halves meet to form the Meckelian groove. As in *A. uintaensis* the upper wall of this groove is primarily formed by the thickness of bone in dorsal half of the lingual surface; the ventral half is barely overlain by the dorsal half. The first coronoid does not extend past the Meckelian groove, and bears sharp conical teeth, as in *A. calva* (Fig. 18). The anterior half of the dentary is more incurved than in *A. uintaensis*, but not to the extent that it is in *A. calva*. The anterior width of the dentary also resembles that of *A. calva* and *A. uintaensis* in that it is evenly tapered almost to the symphyseal edge. The angular and surangular are similar to comparable bones in *A. calva*, except that they, like the dentary, are more extensively ossified. The mandible/head-length ratio in *A. scutata* is well within this ratio range for *A. calva* (Table 7). The prearticular is not preserved.

The preoperculum is similar to that of *A. uintaensis*, being narrower dorsally than ventrally, rather than having both halves relatively equal in width, as in *A. calva*. The operculum resembles that of *A. calva* in morphology and operculum-depth/operculum-length (Table 7). The subopercular and interoperculum resemble those of *A. calva* in general morphology, but the suture between them is longer anteroposteriorly. The branchiostegal rays are squared off distally, as in *A. calva*.

Post-cranial skeleton. The supracleithrum and metacleithrum are not preserved. The only part of the cleithrum available for study is the ventroposterior process in UMMP V-57431 which in *A. calva* is the only area of this bone that is visible externally. This region of the cleithrum in *A. scutata* is heavily sculptured (Fig. 21), and as in *A. uintaensis* and *A. fragosa*, this dermal ornamentation extends to the edge of the bone. In *A. calva*, this dermal structure is limited to the center and dorsal region of this part of the cleithrum.

The vertebral column of *A. scutata* resembles that of *A. calva* both in number of centra (Table 9) and in general morphology of the centra. The head/standard-length proportion (0.312) is greater than in *A. calva* (0.271), but less than in *A. uintaen-*

sis (0.322). The insertion of pectoral fin/standard-length and insertion of anal fin/standard-length ratios are both within the ranges of *A. calva,* although the latter proportion for *A. scutata* is somewhat greater than the mean for *A. calva* (Fig. 31).

Discussion

In the same paper as his description of *Amia scutata,* Cope (1875: 3) described *Amia dictyocephala,* also from the Florissant Formation. *A. dictyocephala* was distinguished from *A. scutata* by having 10 to 12 supravertebral scale rows, and 35 vertebrae between the anterior dorsal fin pterygiophore and the posterior anal fin pterygiophore (USNM 3992 AMNH 2670). He further characterized this form from a skull (AMNH 2802) that "possesses twelve branchiostegal rays, and a relatively smaller orbit than in *Amia calva.*" A re-examination of these specimens in the previous section on meristics showed that Cope's supravertebral scale row count was in error, and there is no perceptible difference in this feature between Recent and fossil *Amia* species (Table 8). In *A. calva,* the range for the number of centra between the insertion of the dorsal fin and the terminus of the base of the anal fin is 33–37. In the type specimen of *A. dictyocephala* (USNM 3992) the number of centra is 35, and the mean number in specimens of *A. scutata* is 36; there is clearly no way that this feature can be used to distinguish *A. dictyocephala* from *A. scutata* and *A. calva.* Cope, on the basis of AMNH 2802, thought that an orbit in *A. dictyocephala* was smaller than one in *A. calva,* but the small size was due largely to the constriction of the orbit that resulted from crushing of the dermosphenotic and upward displacement of infraorbital 5. The characters that Cope used to differentiate *A. dictyocephala* from *A. scutata* are undiagnostic, and my studies of the specimens show no morphological or meristic difference; *A. dictyocephala* is here considered to be a synonym of *A. scutata.*

Lambe (1908: 12–13) described *Amia exilis* from a single basioccipital (NMC 6201) and two mid-trunk vertebrae (NMC 6200, 6205) from the Early Oligocene Cypress Hills Formation of Saskatchewan. The temporal occurrence of these elements is equivalent to that of *A. scutata.* Lambe's description of the basioccipital conforms to that of *A. scutata* in being more extensively ossified than in *A. calva.* His diagnosis of the two centra is founded on height/width proportions, chordal foramen position, basapophyseal angle, and configuration of neural facets. Because *A. scutata* resembles *A. calva* in vertebral morphology, the characters that Lambe uses to distinguish *A. exilis* are undiagnostic; I therefore consider *A. exilis* as a synonym of *A. scutata.*

Amia cf. *scutata*

Hypodigm. Miocene. Pawnee Creek Formation, Colorado: UCMP 38222, nearly complete cranial roof, infraorbitals 4 and 5, nearly complete anterior portion of palate, two branchiostegal rays, maxillae, and right dentary.

Description

The general morphology of the cranial roof resembles both *A. scutata* and *A. calva* in parietal/frontal ratio (Table 7), rectangular parietals, and shape of dermosphenotic and nasal (Fig. 29). The extrascapular more closely resembles that of *A. scutata* in its greater width and less pronounced distal posterior lappets. The pterotic also resembles that in *A. scutata* in its being narrower anteriorly than posteriorly, and in bordering the frontal laterally rather than posteriorly. The size and depth of the orbital excavation is intermediate between that of *A. scutata* and *A. calva* (Fig. 28). The maxilla is similar to that of *A. calva,* being less robust posteriorly than that of *A. scutata.* The branchiostegal rays are squared off distally, as are those of both *A. calva* and *A. scutata.* Infraorbital 4, although posteroventrally incomplete, is clearly closer to that of *A. scutata* than *A. calva* in being relatively larger than infraorbital 5, and in the posterodorsal corner being squared off rather than acute as in *A. calva.* Infraorbital 5 resembles that

of *A. scutata* in size relative to infraorbital 4, the anterior end being narrower than in *A. scutata;* this feature contributes to lessening the relative width of the orbit. The dentary resembles that of *A. scutata* in being wider anteriorly than in *A. calva;* the dorsal lingual surface only slightly overlaps the ventral lingual surface as in *A. scutata* (Fig. 18); Meckel's groove is thus similar to that of *A. scutata.* There is no available palate in *A. scutata* for comparison. The number of vomerine teeth is 18 and 21, which is bracketed by the range for *A. calva* (Estes and Berberian, 1969: 5). As Estes (1964) noted for this specimen, these teeth are sharper and more incurved externally than internally; this disparity is more distinct in this form than in the extant species. The hyomandibular, entopterygoid, ectopterygoid, dermopalatine, and premaxilla are poorly preserved, but appear to resemble these bones in *A. calva.*

Discussion

Estes (1964: 36) and Estes and Tihen (1964: 454) referred to this specimen as *Amia* sp. (and in error gave the source as White River Formation). The specimen resembles *A. scutata* in some elements, *A. calva* in others, and is intermediate in several character-states, notably bone thickness and size of orbits. It does, however, appear to show a stronger resemblance to *A. scutata* than to *A. calva,* particularly in

Fig. 29. *Amia* cf. *scutata* UC 38222, Late Miocene, Pawnee Creek Formation, Colorado.

the morphology of the extrascapular, pterotic, dentary, and infraorbitals 4 and 5, and I have thus compared it with the fossil species. Since this is a form that is both morphologically and temporally intermediate between *A. scutata* and *A. calva*, it is difficult to determine whether or not this specimen actually represents *A. scutata* or a later stage of evolution leading to *A. calva*, but it is at least of interest in documenting the slow phyletic development toward *A. calva* in mid-Cenozoic time.

Amia cf. *calva*

Hypodigm. Pliocene. Lower Valentine Formation, Nebraska: UCMP 65851, anterior portion of left dentary and a trunk vertebra; UMMP 52187, right nasal, ectopterygoid fragment, unidentified cranial fragments; UMMP 42185, right dentary fragment. Ogallala Formation, Kansas: UMMP 55574–55578, three right and two left dentary fragments; UMMP 55579, incomplete right cleithrum; UMMP 55583, a right extrascapular; UMMP 55580, a right maxilla; UMMP 55585, a left premaxilla; UMMP 55586, several scales.

Discussion

Smith (1962), and Estes and Tihen (1964) described as *Amia sp.* a nasal and dentary, and cranial fragments from the Lower Valentine Formation, Nebraska. Wilson (1968) described as *Amia calva* denatry fragments, a premaxilla, a maxilla, an extrascapular, an incomplete cleithrum, and several scales from the Ogallala Formation, Kansas. This Early Pliocene material resembles *A. calva* more closely than does the Miocene *A.* cf. *scutata* specimen noted above; the elements are very lightly ossified as in the Recent species. The cleithrum is distinctly *A. calva*-like in its lack of distal marginal dermal sculpture. The dentary fragments are also thinly ossified as in *A. calva,* but are slightly wider relative to the dentary in the Recent species, as in the Miocene form. Temporally, this Pliocene material is later than the Miocene form and earlier than *A. calva;* morphologically, however, the available elements conform with *A. calva.*

Amiidae *incertae sedis*

Hypodigm. Cretaceous. Paluxy Formation, Texas: SMUSMP 62270, dentary fragments, premaxillary fragment, vertebrae, maxillary fragments, and an unidentified palatal bone bearing teeth; FMNH 7050, basioccipital; FMNH 7051, mid-trunk vertebra; FMNH 7052, anterior trunk vertebra fragment; FMNH 7053–7054, anterior trunk vertebrae; FMNH 7055, caudal vertebra; FMNH 7056, small vertebrae; FMNH 7049, unidentified palatal bone bearing teeth.

Description

The dentaries are fragmentary (Fig. 30); the only diagnostic features available for comparison with other amiid forms are related to the anterior region of the dentary. The surfaces pits on the exterior side of the dentary are relatively larger and deeper than in any species of *Amia.* The dentaries lack the dorsal shelf adjacent to the lingual side of the alveolar ridge seen in *A. fragosa.* The coronoid articulation surface descends directly from the alveolar ridge, as in a *Urocles* dentary from the Late Jurassic (Purbeck) of England (BMNH 48236). The lingual surface above the Meckelian groove is relatively short, even more so than in *Amia uintaensis,* and the groove itself is quite wide, more so than in BMNH 48236. The anterior portions of the dentaries are relatively straight, rather than incurved as in *Amia fragosa,* and are evenly tapered to the symphyseal edge. The dentary and premaxilla teeth are broken, but in dorsal view the interior surfaces of the broken teeth are very even, lacking the serrated outline seen in other species of *Amia.* Only the anterior portion of the premaxilla is present; it bears nine alveoli, conforming in this respect with all *Amia* species. The premaxilla, although incomplete, displays the anterior (ventral) edge of the large foramen that is characteristic of *Amia.* Only part of the anterior maxilla is present in the specimens available, and since the more diagnostic aspects

occur posteriorly, it is difficult to determine any affinities with particular species; the anterior portions that are available generally conform with those of *Amia*. The specific bones to which the palatal fragments belong cannot be identified. The smaller fragment (SMUSMP 62270) bears pillar-shaped teeth with nipple-like tips, as in the tooth-bearing palatal bones in species of *Amia*. Posterior to the spinal arterial foramina the basioccipital includes one fused vertebra. As in *Amia fragosa* and

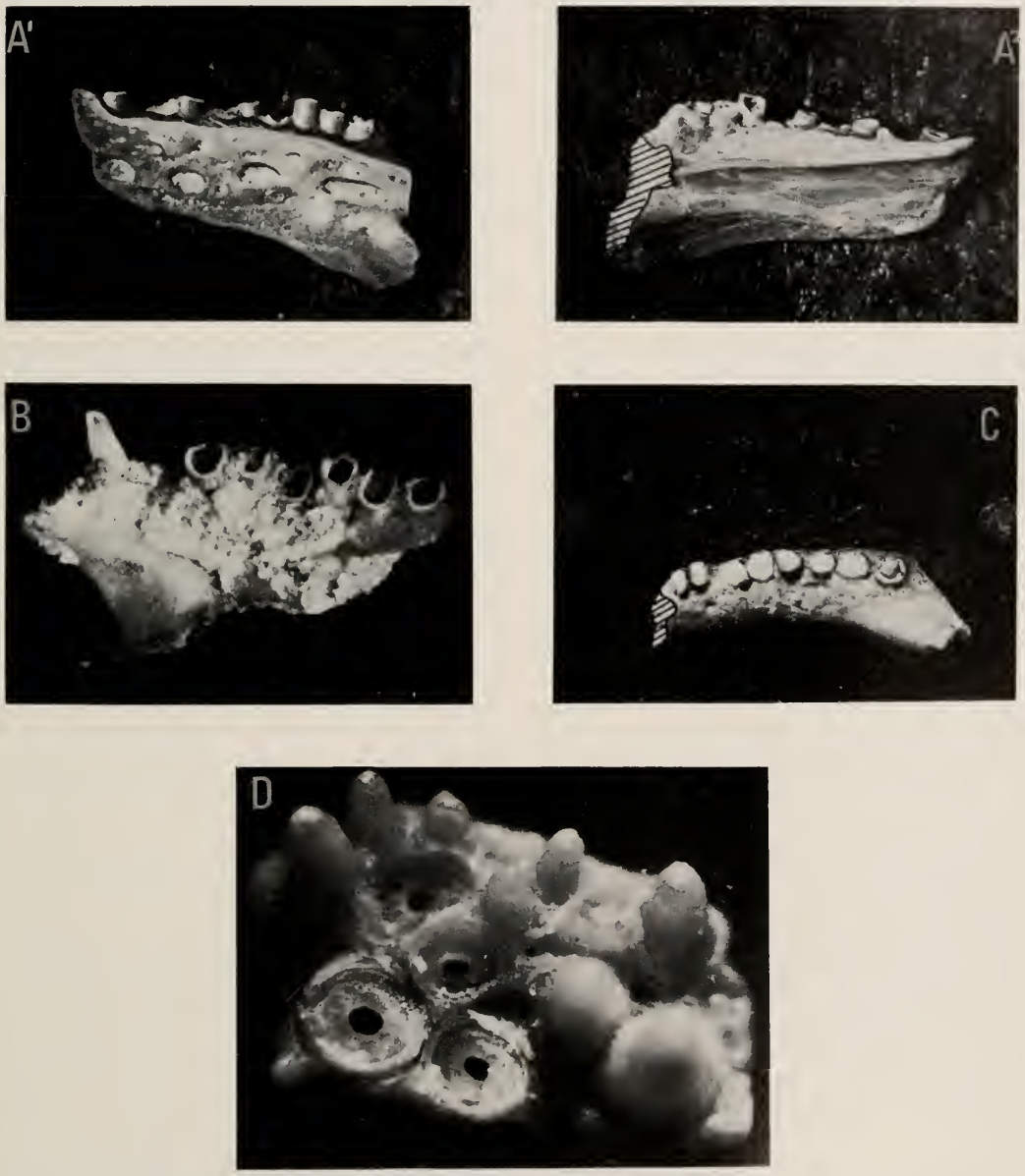

Fig. 30. Amiidae *incertae sedis*, Early Cretaceous, Paluxy Formation, Texas: A^1–A^2, anterior portion of left dentary; B, premaxillary fragment; C, anterior portion of right maxilla; D, unidentified palatal fragment. ×0.15

Amia calva, the basioccipital has an ovoid articular surface with no dorsal indentations between the neural facets. The large vertebrae are thickly ossified, as in the Cretaceous specimens of *Amia* cf. *uintaensis.* The chordal foramina are closed and the only available large mid-trunk centrum displays the pronounced triangular outline characteristic of *Amia uintaensis.* None of the large vertebrae display the characteristic *Amia* aortal facets; they do, however, possess neural facets, and the mid-trunk centra bear basapophyses. The small vertebrae are also thickly ossified and the chordal foramina of the trunk vertebrae are closed. As Traquair (1911: 39) noted for *Amiopsis dolloi,* the lateral sides of the vertebrae are marked by a number of variable excavations, or "oval fossae" (Fig. 7). These smaller mid-trunk vertebrae, unlike the large ones, display both aortal and neural facets, as well as basapophyses and lateral oval fossae.

Discussion

Thurmond (1969: 88) reported "various fragments of an undetermined amiid" from the Paluxy Formation of Texas, which is the earliest known occurrence of amiids in North America. He further noted that amiid material occurred both in freshwater and marine zones and that a further description of this material would be the subject of a later study. He was uncertain as to whether the amiids occurring in the marine zones were actually marine or were freshwater forms secondarily deposited in the marine areas. None of the material can be referred to *Amia* since it displays characteristics of *Amia uintaensis, Amia fragosa, Urocles,* and *Amiopsis,* as noted in the above description. The vertebrae suggest the possibility of more than one form: the large vertebrae are subtriangular and resemble *Amia uintaensis* in morphology, with the exception of the lack of aortal facets on the trunk vertebrae. The small vertebrae are *Amia fragosa*-like in morphology; they possess aortal facets, but also display lateral oval fossae characteristic of *Amiopsis.* In reviewing the European Jurassic and Cretaceous *Urocles,* Lange (1968) found little morphological justification to warrant continued generic distinction between *Urocles* and species described by Woodward (1916) as belonging to *Amiopsis* from the Purbeck Beds near Weymouth, Dorset. Lack of knowledge of the skull of *Amiopsis* makes it impossible to compare cranial elements with those of other amiids; the singular postcranial feature characterizing *Amiopsis* is the lateral oval fossae of the vertebrae. Although Lange suggests that both *Amiopsis* and *Amia* evolved independently from different *Urocles* species-groups, it is premature to attempt to do more than indicate morphological similarities or dissimilarities since the phylogenetic relationship of *Amiopsis* with *Urocles* or *Amia* cannot be clearly defined until a much-needed review of the taxon has been completed, and until more *Amiopsis* material is made available for study.

The Paluxy material shows resemblances to two early *Amia* species, *Amia uintaensis* and *Amia fragosa,* as well as to the Late Mesozoic European amiids, *Urocles* and *Amiopsis.* Whether the Paluxy material represents one or more forms intermediate between *Amia* and *Urocles* (or *Amiopsis*) or whether it belongs to some other group of amiids that became extinct before the end of the Cretaceous cannot be determined, since taxonomic evaluation of this material is limited by the lack of articulated specimens.

SPECIMENS REMOVED FROM THE AMIIDAE

Miller (1968: 468–470, pl. 1, figs. 1, 3, 7–9) questionably identified as *Protamia* sp. one large (FHKSCM 13025) and three small centra (FHKSCM 13024–9) recovered from a channel sandstone cut into the Upper Cretaceous Black Creek Formation, Phoebus Landing, North Carolina. Since all known *Amia* are freshwater forms and since these centra were associated with various marine vertebrates, Miller (1968: 467) concluded that the channel sandstone con-

tained a mixed fauna, "the channel sandstone formed in an estuarine or tidal environment."

My studies indicate that these specimens are not amiid. The smaller vertebrae are horizontally ovoid. *A. uintaensis* trunk centra have concavities between the basapophyses and aortal facets (Fig. 26, A–C). A thin section (Fig. 26, G) through the articular surface of one of the North Carolina specimens (FHKSCM 13924–9) has a radial structure resembling that of *Squatina* and other sharks (Hasse, 1882, tables 17–18). All layers are laminated parallel to the exterior surface and are crossed by various perpendicular vascular foramina. Their articular surfaces are slightly concave, while those of *Amia* are markedly so. Each of the small vertebrae bear horizontal basapophyses as in Recent *Squalus*, and are best referred to the elasmobranchs.

The large vertebra is a cetacean caudal (Fig. 26, H), possibly belonging to the Cetotheriidae (Clayton Ray, 1971, personal communication). The centrum is ovoid, with very slightly concave articular surfaces, and lacks a chordal foramen, as well as ventral facets. The dorsal facets for the accommodation of metapophyses are well defined. Since this centrum is from a marine mammal, it is more probably from the Miocene (Calvert Formation?) than from the Cretaceous Black Creek Formation.

Eastman (1899) described *Amiopsis dartoni* from a partial opercular series, pectoral fin, and associated cycloid scales from the Late Jurassic marine Sundance Formation, South Dakota. Eastman felt that the many "stout ribs" associated with the pectoral fin suggested a well-ossified *Amia*-like vertebral column and the semicircular operculum conformed with that of *A. calva*. Since the scales are covered superficially with ganoine and appear elliptical, Eastman placed this form among the Amiidae. He allocated the generic name, *Amiopsis*, on a temporal basis. According to Bobb Schaeffer, (1971, personal communication) the holotype (USNM 4792) and the paratypes (MCZ 9696, USNM 4793) are to be tentatively referred to the Leptolepidae on the basis of morphology of opercular series and pectoral fin lepidotrichia. Schaeffer is currently studying the Late Jurassic North American fishes and is including a more extensive discussion of this material in his review.

SUMMARY AND CONCLUSIONS

This survey of the osteology, morphometrics, and meristics of the North American fossil amiids indicates that the extant and fossil forms fall into four groups worthy of specific status: (1) *Amia fragosa*, (2) *A. uintaensis*, (3) *A. scutata*, and (4) *A. calva*. All these forms, excepting *A. fragosa*, have somewhat elongated bodies (approximately 85 centra) and sharp, conical coronoid and palatal teeth. Although the coronoid and palatal teeth of *A. uintaensis* are more sharply curved inwardly, the teeth are closer in morphology to those of *A. scutata* and *A. calva* than to the styliform teeth of *A. fragosa*. *A. uintaensis*, *A. fragosa*, and *A. scutata* all have a larger infraorbital 4 than infraorbital 5, greater degree of ossification of cranial elements, deeper orbital notch in the frontal, greater head/standard-length, and generally larger parietal/frontal ratio. These character-states clearly set the fossil species of *Amia* apart from the Recent *A. calva*.

Articulated specimens have yielded more information on the osteology of *A. fragosa*. *A. fragosa* is a short-bodied form (approximately 65 centra) with a smaller number of caudal lepidotrichia than in the other species of *Amia*, styliform palatal and coronoid teeth, deeper orbital excavation in the frontals, square parietals, and a short box-like skull having relatively short mandibles that occupy about half the head-length. The styliform crushing palatal teeth of *A. fragosa* suggest a durophagous habit, rather than the more predaceous habit indicated by the sharp palatal teeth of *A. uintaensis*, *A. scutata*, and *A. calva*. Although it is known that *A. calva* includes molluscs and crustaceans in its diet, perhaps *A. fragosa* was more exclusively adapted for shell crushing than the Recent species.

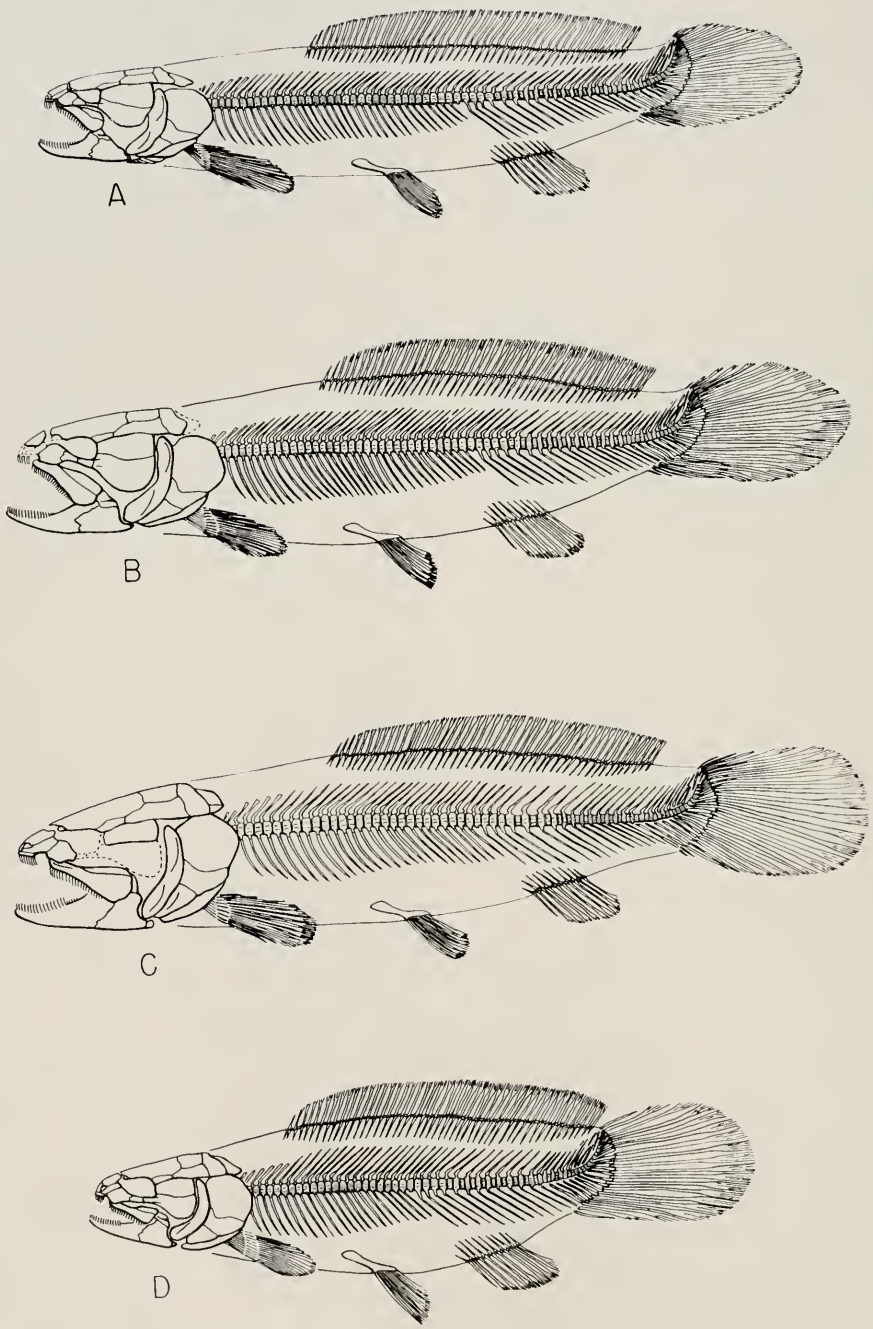

Fig. 31. Skull and body structure of A, *Amia calva;* B, *A. scutata;* C, *A. vintaensis;* and D, *A. fragosa.*

			Amia calva	*Amia* cf. *calva*	*Amia* cf. *scurata*	*Amia scurata*	*Amia uintaensis*	*Amia* cf. *uintaensis*	*Amia fragosa*	Amiidae *incertae sedis*	*Amia* sp.
PLEISTOCENE	POST-BLANCAN		X								
	BLANCAN										
PLIOCENE	HEMPHILLIAN	FOSSIL LAKE BEDS (IDAHO FM.)		X							
	CLARENDONIAN	WAKEENEY l.f. (OGALLALA FM.)		X							
		LOWER VALENTINE FM.		X							
MIOCENE	BARSTOVIAN	EUBANKS l.f. (PAWNEE CREEK FM.)			X						
	HEMINGFORDIAN										
	ARIKAREEAN	TURTLE BUTTE FM.									X
OLIGOCENE	WHITNEYAN	RUBY PAPER SHALE (PASSAMARI FM.)									X
	ORELLAN	GRANT HORSE PRAIRIE SHALE									X
		FLORISSANT FM.				X					
		ORELLA MEMBER (BRULE FM.)				X					
	CHADRONIAN	CHADRON FM.				X					
		CYPRESS HILLS FM.				X	X				
EOCENE	DUCHESNEAN	CLARNO FM.									X
		HORSEFLY RIVER BEDS									X
	UINTAN	UINTA FM.					X				
		WASHAKIE FM.					X				
	BRIDGERIAN	BRIDGER FM.					X		X		
	WASATCHIAN	WIND RIVER FM.					X				
		FOSSIL LAKE BEDS (GREEN RIVER FM.)					X		X		
		GOLDEN VALLEY FM.					X		X		
		WASATCH FM.					X		X		
		GRAYBULL BEDS (WILLWOOD FM.)					X		X		
PALEOCENE	CLARKFORKIAN	BEAR CREEK l.f. (FORT UNION FM.)					X				
		SILVER COULEE l.f. (FORT UNION FM.)							X		
	TIFFANIAN	MELVILLE FM.							X		
		SAUNDERS CREEK l.f. (PASKAPOO FM.)					X		X		
		CEDAR POINT QUARRY l.f. (FORT UNION FM.)							X		
	TORREJONIAN	MEDICINE ROCKS l.f. (TONGUE RIVER FM.)					X		X		
		ROCK BENCH l.f. (FORT UNION FM.)							X		
	PUERCAN	TULLOCK FM.							X		
		MANTUA l.f. (FORT UNION FM.)							?X	X	
CRETACEOUS	MAASTRICHTIAN	HELL CREEK FM.							X	X	
		LANCE FM.							X	X	
		OJO ALAMO FM.							X		
		AGUJA FM.							X		
		EDMONTON FM.								X	
	CAMPANIAN	JUDITH RIVER FM.								X	
		"MESAVERDE" FM.								X	
		OLDMAN FM.								X	
	ALBIAN	BUTLER FARM l.f. (PALUXY FM.)									X

TABLE 18. MAJOR DEPOSITS CONTAINING REMAINS OF *Amia* IN THE WESTERN INTERIOR OF THE UNITED STATES AND CANADA

Seven genera and twenty-three amiid species (Table 19) have been described in the literature. Estes (1964) synonymized *Stylomyleodon lacus* with *Kindleia fragosa,* and Estes and Berberian (1969) referred the genus *Kindleia* to *Amia,* thereby confirming the suggestion of Janot (1969). *Paramiatus gurleyi* (Romer and Fryxell, 1928) is unquestionably a synonym of *A. fragosa.* Regardless of possible synonymy with European taxa, the stratigraphic range of *A. fragosa* is remarkably long, extending as it does from the Late Cretaceous through the Middle Eocene. Although *A. fragosa* is better known than the other fossil species, and was extensively described by Estes (1964), O'Brien (1969), and Estes and Berberian (1969), its phylogenetic relationship to them and to *A. calva* could not be understood without comparative information on both the other fossil forms and *A. calva* (Fig. 32).

A. newberrianus and *A. depressus* (Marsh, 1871), and *A. gracilis* (Leidy, 1873a), described from undiagnostic vertebral characters, are considered here as *nomina dubia.*

A. uintaensis is a form having a relatively greater body-length than the other species of *Amia.* It has approximately the same total number of vertebrae as *A. calva* and *A. scutata,* but the arrangement of the column varies meristically from them. Its head is more elongated than that of the other forms, with the jaws occupying over two-thirds of the head-length. The vomerine teeth are sharp (as are the palatal and coronoid teeth), as they are in *A. scutata* and *A. calva,* but are more than twice as numerous as in these later forms. The present study confirms the opinions of Romer and Fryxell (1928), Estes (1964), and Estes and Berberian (1969) that the differences between *Amia* and *Protamia, Hypamia,* and *Pappichthys* are insufficient for the recognition of any of the latter as genera distinct from *Amia. Hypamia elegans* (Leidy, 1873a) is considered a *nomen dubium,* being based on vertebral characters that cannot be distinguished from those of the other species. *Protamia media* (Leidy, 1873a), *Pappichthys symphysis, P. corsonii, P. medius, P. plicatus, P. sclerops, P. laevis* (all described by Cope, 1873), as well as *Amia macrospondyla* and *A. whiteavesiana* (Cope, 1891), are all considered here as synonyms of *A. uintaensis;* they were based on undiagnostic vertebral characters and morphology of the skull elements. Material of large amiids from the Late Cretaceous Lance and Hell Creek formations is referred to *A.* cf. *uintaensis,* since the material differs only in minor respects from the Paleocene and Eocene specimens. It cannot be determined whether this material represents actual populations of *A. uintaensis* or an earlier stage of its evolution. The stratigraphic range of *A. uintaensis* extends from the Paleocene to the Early Oligocene.

A. scutata, an Early to Middle Oligocene long-bodied form, shares cranial characters with both *A. uintaensis* and *A. calva.* Although it has closer morphometric and meristic affinities to the Recent form, it is structually and temporally intermediate between *A. uintaensis* and *A. calva;* it resembles the more primitive *A. uintaensis* in the morphology of Meckel's groove and coronoid articulation surface of the dentary, greater ossification, and in having an elongated skull with a greater head/standard-length than in *A. calva. A. dictyocephala* (Cope, 1875) is considered a synonym of *A. scutata;* it was based on undiagnostic meristic characters. In the evolutionary continuum, *A. scutata* appears to be an intermediate stage between *A. uintaensis* and *A. calva* (Fig. 32). A more direct line of evolution exists between *A. scutata* and *A. calva;* this is supported by Miocene and Pliocene amiid material that displays cranial elements closely transitional between the two species. Thus the Recent species of *A. calva* had begun at least by the beginning of the Pliocene, and *A. calva* was apparently distinct from *A. scutata* by that time. It appears that *A. fragosa* represents an amiid population that survived until the Middle or Late Eocene and had no phylogenetic affinities with the modern form beyond this time.

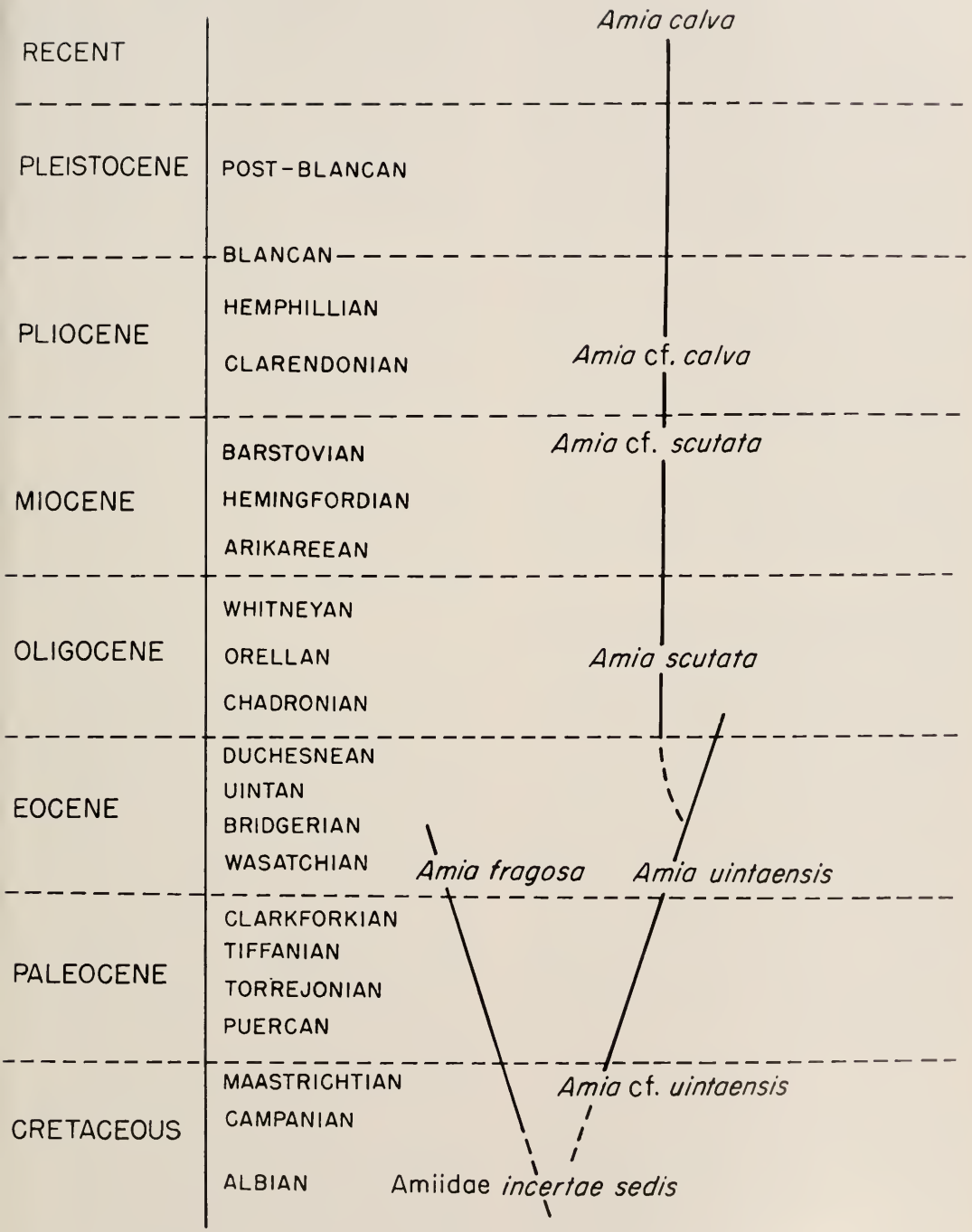

Fig. 32. Suggested phylogenetic relationships within the genus *Amia*.

In the North American fossil record, fossil remains unquestionably those of the family Amiidae first occur in the Lower Cretaceous (Albian) sediments of Texas. However, none of the material can be referred to any known species of *Amia;* it displays character-states resembling those of *Amia uintaensis* and *Amia fragosa,* as well as the European *Urocles.* Some of the vertebrae resemble those of *Amiopsis.* The Paluxy material may represent either one or more forms transitional between *Amia* and the Late Mesozoic European *Urocles* (or *Amiopsis*), or an as yet undescribed line. The body-length of *Amia fragosa* appears to be a primitive feature derived from the earlier amiids *Urocles, Sinamia, Ikechaoamia,* and *Amiopsis.* Despite their different vertebral columns, *Amia fragosa* and *A. uintaensis* show similar morphology of the cranial elements, but the nature of the probable common origin of these forms is still uncertain in the absence of a more complete fossil record.

Remains of amiids referable to or close to *Amia fragosa* and *A. uintaensis* have been described from the Paleocene, Eocene, and Oligocene of Europe, and the Eocene of Asia. Additional but still not definitive evidence supports Estes' (1964) and Estes and Berberian's (1969) suggested synonymy of *A. russelli* (Late Paleocene, France), *A. kehreri* (Middle Eocene, Germany), and *A. munieri* (Early Oligocene, France) with *A. fragosa. Pseudamia heintzi* (Eocene, Spitzbergen) and *A. valenciennesi* (Eocene, France) are also possible synonyms of *A. fragosa. A. valenciennesi* is the oldest name and would take precedence over *A. fragosa.* Cranial similarities confirm the synonymy of *A. robusta* (Late Paleocene, France) with *A. uintaensis.*

European and North American fossil *Amia* occurred in freshwater deposits and apparently occupied a habitat much like that of the Recent species. According to Westoll (1965: 19–20) the distribution of freshwater vertebrates is a useful indication of "direct continental communication," since "... descendents of a common stock on different modern continents must have used essentially a terrestial route." The present study further amplifies similarities in the Paleocene and Early Eocene amiid fossil record of North America and Europe. This distribution of amiids adds to the similarity of assemblages of Paleocene and Early Eocene lower vertebrates (Estes *et al.,* 1967) and mammals (McKenna, 1972) on the two continents. The occurrence of *Pseudamia heintzi* in the Eocene deposits of Spitzbergen may be additional evidence for the existence of the De Geer migration route (bridging Europe, Spitzbergen, and North America during the Paleocene and until the close of Sparnacian time), especially if suggested relationship to *A. fragosa* could be demonstrated. The Asian form *A. mongoliensis* resembles *A. uintaensis* in minor respects but is sufficiently distinct in itself to be maintained as a separate species.

Table 19. Amiid genera and species of various authors discussed in text in relation to the revised taxonomy

Amia calva	*Amia calva*
Kindleia fragosa *Stylomyleodon lacus* *Amia fragosa* *Paramiatus gurleyi*	*Amia fragosa*
Amia scutata *Amia dictyocephala* *Amia exilis*	*Amia scutata*
Protamia uintaensis *Protamia media* *Pappichthys medius* *Pappichthys plicatus* *Pappichthys sclerops* *Pappichthys laevis* *Pappichthys symphysis* *Pappichthys corsonii* *Amia whiteavesiana* *Amia macrospondyla*	*Amia uintaensis*
Amia depressus *Amia newberrianus* *Amia gracilis* *Hypamia elegans*	*nomina dubia*
Amia selwyniana	*nomen nudum*

LITERATURE CITED

Agassiz, L. 1843. Recherches sur les poissons fossiles. Neuchâtel, tomes 1–5, atlases 1–5.

Allis, E. 1889. The anatomy and development of the lateral line system of *Amia calva*. J. Morphol., 2: 1–540.

———. 1897. The cranial muscles and cranial and first spinal nerves in *Amia calva*. J. Morphol., 12(3): 1–814.

Ami, H. 1891. On some extinct Vertebrata from the Miocene rocks of the north-west Territories of Canada recently described by Professor Cope. Science, 18: 53.

Andreae, A. 1892. Vorläufige Mitteilung über die Ganoiden (*Lepidosteus* und *Amia*) des Mainzer Beckens. Verh. Nat. med. Ver. Heidelberg (N.F.), 5: 7–15.

———. 1895. Beiträge zur Kenntniss der fossilen Fische des Mainzer Beckens. Abh. Senck. naturf. Ges., 18: 351–365.

Becker, H. 1961. Oligocene plants from the Upper Ruby River Basin, southwestern Montana. Mem. Geol. Soc. Amer., 82: 1–127.

———. 1962. Two new species of *Mahonia* from the Grant-Horse Prairie Basin in southwestern Montana. Bull. Torrey Bot. Club, 89: 114–117.

Blair, W., A. Blair, P. Brodkorb, F. Cagle, and G. Moore. 1968. Vertebrates of the United States. New York: McGraw-Hill Press, 450 pp.

Bolk, L., E. Göppert, E. Kallius, and W. Lubosch. 1936. Handbuch der vergleichenden Anatomie der Wirbeltiere 4. Berlin: Urban und Schwarzenberg, 1116 pp.

Boreske, J. 1972. Taxonomy and taphonomy of the North American fossil amiid fishes. (Abstr.) Bull. Geol. Soc. Amer., 4(1): 3–4.

Bridge, T. 1877. The cranial osteology of *Amia calva*. J. Anat. Phys., 11: 605–622.

Cartier, D., and É. Magnin. 1967. La croissance en longueur et en poids des *Amia calva* L. de la région de Montréal. Canad. J. Zool., 45: 797–804.

Cavender, T. 1968. Freshwater fish remains from the Clarno Formation Ochoco Mountains of north-central Oregon. Ore Bin, 30 (7): 125–141.

———. 1970. A new find of *Amia dictyocephala* Cope from the Middle Tertiary Florissant Lake Beds of western North America. Abst. paper given at 50th Annual Meeting, Amer. Soc. Ichth. Herp.: 42.

Cope, E. 1873. On the extinct Vertebrata of the Eocene of Wyoming, observed by the expedition of 1872, with notes on the geology. Ann. Rept. U.S. Geol. Surv. Terr. (1st series), No. 6: 545–649.

———. 1875. On the fishes of the Tertiary shales of South Park. Bull. U.S. Geol. Surv. Terr. (2nd series), No. 1: 3–5.

———. 1884. The Vertebrata of the Tertiary Formations of the West. Rept. U.S. Geol. Surv. Terr. (Hayden), 3: 745–746.

———. 1891. On Vertebrata from the Tertiary and Cretaceous rocks of the northwest Territory. Book 1. The species from the Oligocene or Lower Miocene of Cypress Hills. Contrib. Geol. Surv. Canad. Paleo., 1: 2–4.

Dean, B. 1898. On the dogfish (*Amia calva*), its habits and breeding. Rept. Comm. Fisheries, Game, and Forests New York, No. 4: 1–10.

Dechaseaux, C. 1937. Le genre *Amia*, son histoire paléontologique. Ann. Paléont., 26: 3–16.

Eastman, C. 1899. Jurassic fishes from the Black Hills of South Dakota. Bull. Geol. Soc. Amer., 10: 397–407.

Estes, R. 1964. Fossil vertebrates from the Late Cretaceous Lance Formation, eastern Wyoming. Univ. Calif. Publ. Geol. Sci., 49: 1–180.

———, and P. Berberian. 1969. *Amia* (= *Kindleia*) *fragosa* (Jordan), a Cretaceous amiid fish, with notes on related European forms. Breviora, Mus. Comp. Zool., No. 329: 1–14.

———, ———, and C. Meszoely. 1969. Lower vertebrates from the Late Cretaceous Hell Creek Formation, McCone County, Montana. Breviora, Mus. Comp. Zool., No. 337: 1–33.

———, M. Hecht, and R. Hoffstetter. 1967. Paleocene amphibians from Cernay, France. Amer. Mus. Novitates, No. 2295: 1–25.

———, and J. Tihen. 1964. Lower vertebrates from the Valentine Formation of Nebraska. Amer. Midl. Nat., 72(2): 453–472.

Goodrich, E. 1930. Studies on the Structure and Development of Vertebrates. London: Macmillan Co. Ltd., xxx + 837 pp.

Gould, S. 1966. Allometry and size in ontogeny and phylogeny. Biol. Reviews, 41: 587–640.

Hammett, F., and R. Hammett. 1939. Proportional length growth of gar (*Lepisosteus platyrhincus* DeKay). Growth, 3(2): 197–209.

Hasse, C. 1882. Das natürliche System der Elasmobranchier. Jena: Verlag von Gustav Fischer, pp. 77–284.

Hatcher, J. 1900. The Carnegie Museum paleontological expeditions of 1900. Science, 12 (306): 718–720.

———. 1901. Some new and little known fossil vertebrates. Ann. Carnegie Mus. Pittsburgh, No. 1: 128–129.

Hay, O. 1895. On the structure and develop-

ment of the vertebral column of *Amia*. Publ. Field Columb. Mus. Zool., 1(1): 1–54.

———. 1911. The Pleistocene of Indiana. Ann. Rept. Geol. Nat. Res. Indiana, **36**: 552.

———. 1917. Vertebrata mostly from stratum No. 3, at Vero, Florida; together with descriptions of new species. Rept. Geol. Surv. Florida, **9**: 43–68.

———. 1923. The Pleistocene of North America and its vertebrated animals from the states east of the Mississippi River and from the Canadian Provinces east of longitude 95 degrees. Bull. Carnegie Inst., **322**: 336–382.

Hoffstetter, R., and J. Gasc. 1969. Vertebrae and ribs of modern reptiles. *In* Biology of the Reptilia. New York: Academic Press, xvi + 468 pp.

Hubbs, C., and K. Lagler 1967. Fishes of the Great Lakes Region. Ann Arbor: University of Michigan Press, viii + 289 pp.

Hussakof, L. 1932. The fossil fishes collected by the Central Asiatic Expeditions. Amer. Mus. Novitates, No. 553: 1–16.

Imbrie, J. 1956. Biometrical methods in the study of invertebrate fossils. Bull. Amer. Mus. Nat. Hist., **108**: 217–252.

Janot, C. 1966. *Amia russelli* nov. sp., nouvel Amiidé (Poisson holostéen) du Thanétien de Berru, près de Reims. C. R. Soc. Géol. France, **1966**(3): 142.

———. 1967. A propos des amiidés actuels et fossiles. Colloq. Intern. C. N. R. S., **163**: 139–153.

Jordan, D. 1906. The fishes of Samoa. Bull. Bureau Fisheries, **25**: 237.

———. 1919. The genera of fishes. Publ. Leland Stanford Junior University, **1919**: 259.

———. 1925. Opinion 89. *In* Opinions rendered by the International Commission on Zoological Nomenclature. Smithsonian Misc. Coll., **73**(3): 27–29.

———. 1927. *Kindleia,* a new genus of cichlid fishes from the Upper Cretaceous of Alberta. Canad. Field Nat., **41**: 145–147.

———. 1928. Note on *Kindleia* and *Stylomyleodon* (fossil fish from Cretaceous deposits of Alberta). Canad. Field Nat., **42**: 47.

———, and B. Evermann. 1896. The fishes of North and Middle America. Bull. U.S. Nat. Mus., **47**: 112–113.

Lagler, K., J. Bardach, and R. Miller. 1962. Ichthyology. New York: John Wiley and Sons, Inc., vii + 523 pp.

Lambe, L. 1904. Progress in vertebrate paleontology in Canada. Trans. Roy. Soc. Canada, No. 2: 27–43.

———. 1908. The Vertebrata of the Oligocene of the Cypress Hills, Saskatchewan. Contrib. Paleo. Canada, 3(4): 12–13.

Lange, S. 1968. Zur Morphologie und Taxonomie der Fischgattung *Urocles* aus Jura und Kreide Europas. Palaeontographica, Abt. A, **131**: 1–78.

Lehman, J. 1951. Un nouvel Amiidé de l'Eocène du Spitzberg, *Pseudamia heintzi.* Tromsø Mus. Årshefter, **70**: 1–11.

Leidy, J. 1873a. Notice of remains of fishes in the Bridger Tertiary Formation of Wyoming. Proc. Acad. Nat. Sci. Philadelphia, **1873**: 97–99.

———. 1873b. Contributions to the extinct vertebrate fauna of the western territories. Rept. U.S. Geol. Surv. Terr. (Hayden), **1**: 185–189.

Liu, T-S., H-T Liu, and T-T Su. 1963. The discovery of *Sinamia zdanskyi* from the Ordos Region and its stratigraphical significance. Vert. Palasiatica, 7(1): 1–30.

Lund, R. 1967. An analysis of the propulsive mechanisms of fishes, with reference to some fossil actinopterygians. Ann. Carnegie Mus., **39**(15): 195–218.

Marsh, O. 1871. Communication on some new reptiles and fishes from the Cretaceous and Tertiary. Proc. Acad. Nat. Sci. Philadelphia, **1871**: 103–105.

McKenna, M. 1972. Was Europe connected directly to North America prior to the Middle Eocene? *In* Evolutionary Biology, Vol. 6. New York: Appleton-Century-Crofts, pp. 179–189.

Merrill, G. 1907. Catalogue of the figured specimens of fossils, minerals, and ores in the Department of Geology, United States National Museum. Bull. U.S. Nat. Mus., **53**: 6–15.

Miller, H. 1968. Additions to the Upper Cretaceous vertebrate fauna of Phoebus Landing, North Carolina. J. Elisha Mitchell Sci. Soc., **84**: 467–471.

Newton, E. 1899. On the remains of *Amia,* from the Oligocene strata in the Isle of Wight. Quart. J. Geol. Soc. London, **4**: 1–10.

Nybelin, O. 1963. Zur Morphologie und Terminologie des Schwanzskelettes der Actinopterygier. Arkiv. Zool., **15**(35): 485–516.

O'Brien, D. 1969. Osteology of *Kindleia fragosa* Jordan (Holostei: Amiidae) from the Edmonton Formation (Maestrichtian) of Alberta. M.A. Thesis, University of Alberta: vi + 118 pp.

Osborn, H., W. Scott, and F. Speir. 1878. Paleontological report of the Princeton scientific expedition of 1877. Contrib. Mus. Geol. Arch. Princeton, No. 1: 102–104.

Piton, L. 1940. Paléontologie du gisement Eocène de Menat (Puy-de-Dôme, flore et faune). Mem. Soc. Sci. Nancy, **56**: 1–303 pp.

Reighard, J. 1903. The natural history of *Amia*

calva Linnaeus. Mark Anniversary Volume (art. 4): 57–109.

Romer, A., and F. Fryxell. 1928. *Paramiatus gurleyi,* a new deep-bodied amiid fish from the Eocene of Wyoming. Amer. J. Sci., **16** (96): 519–527.

Russell, L. 1928a. A new fossil fish from the Paskapoo Beds of Alberta. Amer. J. Sci., **15** (86): 103–107.

———. 1928b. The genera *Kindleia* and *Stylomyleodon.* Amer. J. Sci., **15**(87): 264.

———. 1929. The validity of the genus *Stylomyleodon.* Amer. J. Sci., **17**(100): 369–371.

———. 1967. Paleontology of the Swan Hills area, north-central Alberta. Roy. Ontario Mus. Contrib., No. 71: 1–31.

Schaeffer, B. 1967. Osteichthyan vertebrae. J. Linn. Soc. (Zool.), No. **47**: 185–195.

Shufeldt, R. 1885. The osteology of *Amia calva.* Washington: Government Printing Office, 93 pp.

Simpson, G. 1937. The Fort Union of the Crazy Mountain Field, Montana, and its mammalian faunas. Bull. U.S. Nat. Mus., **169**: x + 287 pp.

———, A. Roe, and R. Lewontin. 1960. Quantitative Zoology. New York: Harcourt, Brace, and Co., iv + 440 pp.

Skinner, M., S. Skinner, and R. Gooris. 1968. Cenozoic rocks and faunas of Turtle Butte, south-central South Dakota. Bull. Amer. Mus. Nat. Hist., **138**: 381–436.

Smith, C. 1962. Some Pliocene fishes from Kansas, Oklahoma, and Nebraska. Copeia, **1962**(3): 505–520.

Stensiö, E. 1935. *Sinamia zdanskyi,* a new amiid from the Lower Cretaceous of Shantung, China. Paleont. Sinica, ser. C, No. 3: 1–48.

Swift, C. 1968. Fossil bony fishes from Florida. Plaster Jacket, No. 7: 2–11.

Szalay, F., and M. McKenna. 1971. Beginning of the age of mammals in Asia: the Late Paleocene Gashato fauna, Mongolia. Bull. Amer. Mus. Nat. Hist., **144**: 270–317.

Thomson, K., and K. Hahn. 1968. Growth and form in fossil rhipidistian fishes (Crossopterygii). J. Zool., **156**: 199–223.

Thurmond, J. 1969. Lower vertebrates and paleontology of the Trinity Group. Ph.D. Thesis, Southern Methodist University (Libr. Congr. No. 70-19259). 136 pp. Univ. micro. Ann Arbor, Mich. (diss. abstr. 31: 2156).

Traquair, R. 1911. Les poissons wealdiens de Bernissart. Mém. Mus. Roy. Hist. Nat. Belg., **6**: 1–65.

Westoll, T. 1965. Geological evidence bearing upon continental drift. Symposium on Continental Drift. Royal Soc. London, **1965**: 12–25.

Whitehouse, R. 1910. The caudal fin of the Teleostomi. Proc. Zool. Soc. London, **1910**: 590–627.

Whitley, G. 1954. More new fish names and records. Aust. Zool., **12**: 57.

Wilson, R. 1968. Systematics and faunal analysis of a Lower Pliocene vertebrate assemblage from Trego County, Kansas. Contrib. Mus. Paleo. Univ. Mich., **22**(7): 75–126.

Woodward, A. 1916. The fossil fishes of the English Wealden and Purbeck formations. Palaeontogr. Soc. London, Pt. 1, **1915**: 1–48.

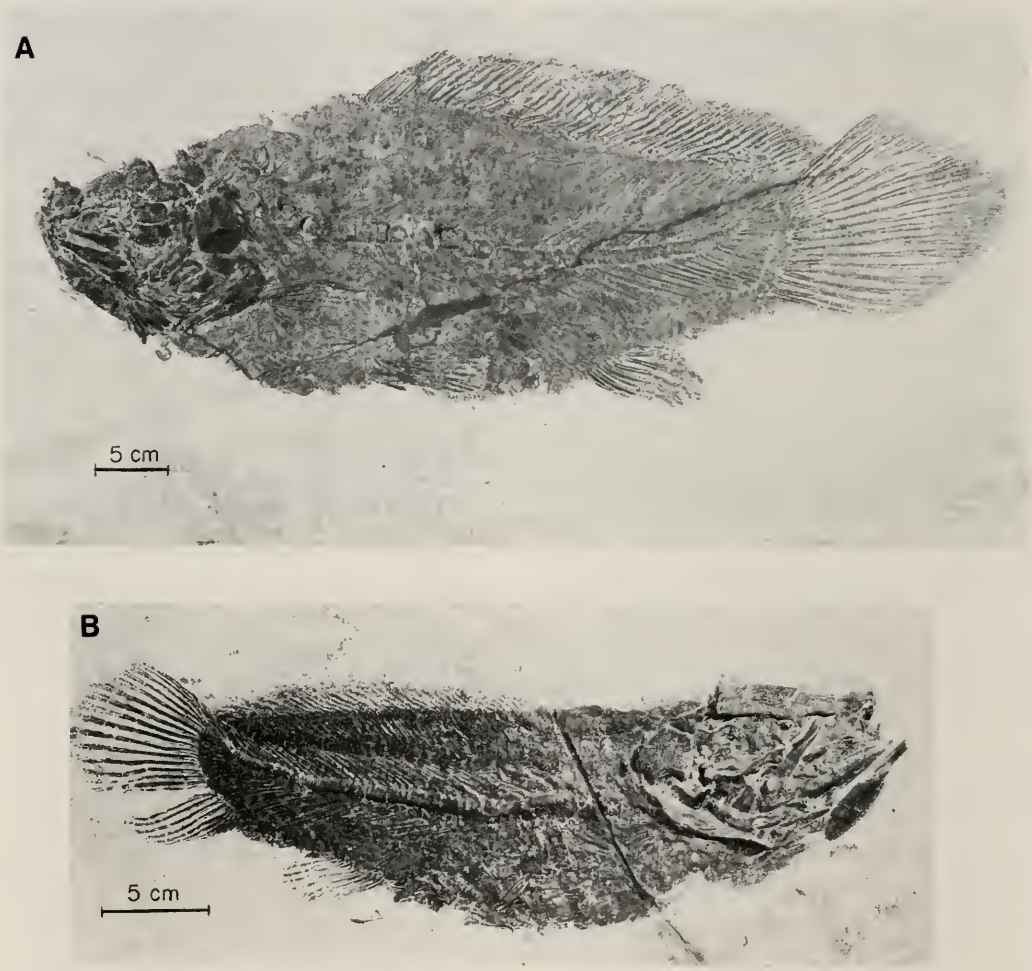

Plate 1. A, "*Paramiatus gurleyi*" FMNH 2201, Early Eocene, Green River Formation, Wyoming; B, *Amia fragosa* MCZ 5347, Early Eocene, Green River Formation, Wyoming.

Plate 2. *Amia kehreri* BMNH P33480, collected by Walter Kühne in 1951 from Middle Eocene deposits at Messel bei Darmstadt.

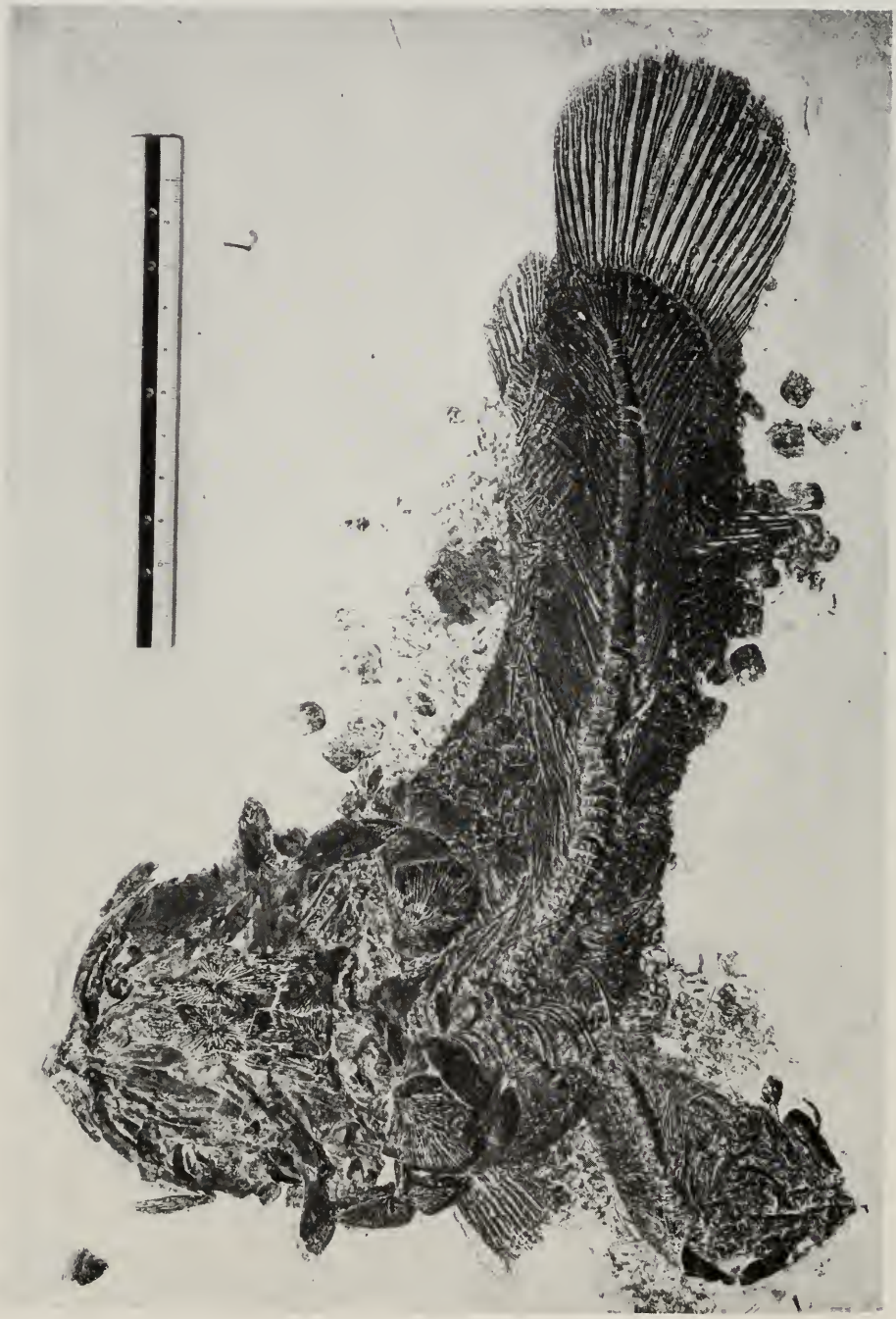

Plate 3. *Amia uintaensis* PU 13865, Early Eocene, Green River Formation, Wyoming.

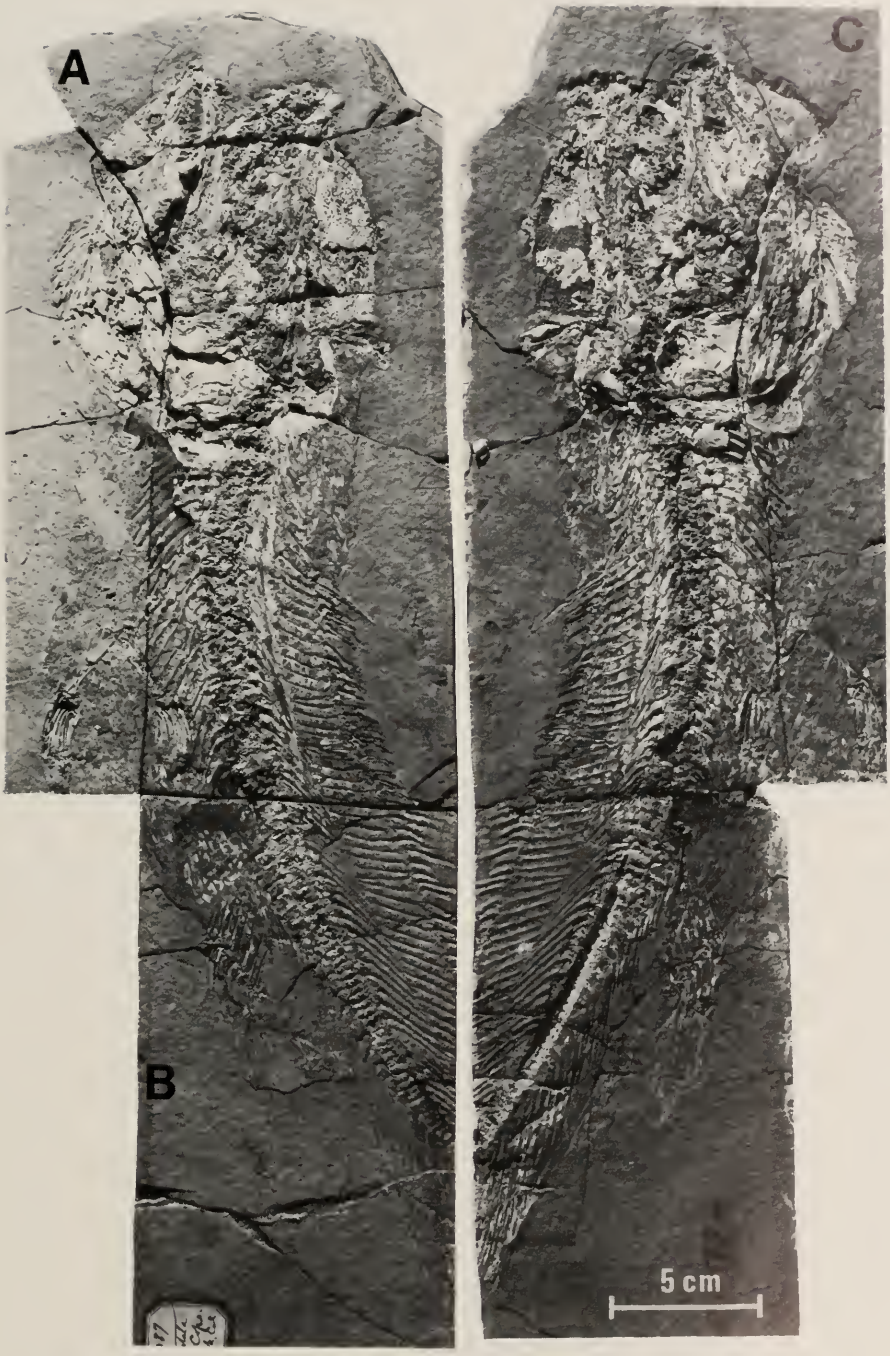

Plate 4. *Amia scutata*, Middle Oligocene, Florissant Formation, Colorado: A, counterpart YPM 6243; B, counterpart USNM 4087; C, PU 10172.

US ISSN 0027-4100

Bulletin OF THE
Museum of
Comparative
Zoology

An Analysis of Variation in the Hispaniolan Giant Anole, *Anolis ricordi* Duméril and Bibron

ALBERT SCHWARTZ

HARVARD UNIVERSITY
CAMBRIDGE, MASSACHUSETTS, U.S.A.

VOLUME 146, NUMBER 2
19 APRIL 1974

PUBLICATIONS ISSUED
OR DISTRIBUTED BY THE
MUSEUM OF COMPARATIVE ZOOLOGY
HARVARD UNIVERSITY

BULLETIN 1863–
BREVIORA 1952–
MEMOIRS 1864–1938
JOHNSONIA, Department of Mollusks, 1941–
OCCASIONAL PAPERS ON MOLLUSKS, 1945–

Other Publications.

Bigelow, H. B., and W. C. Schroeder, 1953. Fishes of the Gulf of Maine. Reprint.

Brues, C. T., A. L. Melander, and F. M. Carpenter, 1954. Classification of Insects.

Creighton, W. S., 1950. The Ants of North America. Reprint.

Lyman, C. P., and A. R. Dawe (eds.), 1960. Symposium on Natural Mammalian Hibernation.

Peters' Check-list of Birds of the World, vols. 2–7, 9, 10, 12–15.

Sprinkle, J., 1973. Morphology and Evolution of Blastozoan Echinoderms.

Turner, R. D., 1966. A Survey and Illustrated Catalogue of the Teredinidae (Mollusca: Bivalvia).

Whittington, H. B., and W. D. I. Rolfe (eds.), 1963. Phylogeny and Evolution of Crustacea.

Proceedings of the New England Zoological Club 1899–1948. (Complete sets only.)

Publications of the Boston Society of Natural History.

Authors preparing manuscripts for the *Bulletin of the Museum of Comparative Zoology* or *Breviora* should send for the current Information and Instruction Sheet, available from Editor, Publications Office, Museum of Comparative Zoology, Harvard University, Cambridge, Massachusetts 02138, U.S.A.

© The President and Fellows of Harvard College 1974

AN ANALYSIS OF VARIATION IN THE HISPANIOLAN GIANT ANOLE, *ANOLIS RICORDI* DUMÉRIL AND BIBRON

ALBERT SCHWARTZ[1]

Abstract. The nominal Hispaniolan species of giant anole, *Anolis ricordi*, is considered to be in actuality composed of three distinct allopatric species: *A. ricordi*, *A. barahonae*, and *A. baleatus*. Subspecies of all three species are described, but only *A. baleatus* is well represented in collections. A theoretical history of this species complex upon Hispaniola is presented.

The Hispaniolan giant anole, *Anolis ricordi* Duméril and Bibron, 1837, has been known to science for more than a century; yet only in the last 35 years has it become evident that this species is not homogeneous in its characteristics throughout Haiti and the República Dominicana. The species was first named (as *Anolis ricordii*) from Santo Domingo, as the entire island was known at that historical period, but specimens seem to have been rare in collections thereafter. Schmidt (1921: 10) reported four *A. ricordi* from two Dominican localities. Cochran (1941: 133) listed 24 specimens (all but one of which were in the National Museum of Natural History) from 11 localities. Mertens (1939: 68–70) studied 17 specimens in European collections and was the first to recognize that there were two readily distinguishable populations that he considered subspecies: *A. r. ricordi* in Haiti, and *A. r. baleatus* Cope in the República Dominicana. Williams (1962) reviewed the species in more detail and examined 90 specimens. For this suite of anoles, he described *A. r. barahonae* from the Sierra de Baoruco in the southwestern República Dominicana. Still later, Williams (1965) studied an additional 80 specimens and named *A. r. leberi* from Camp Perrin on the extreme distal portion of the Haitian Tiburon Peninsula. Thus, with increasing quantities of material from more diverse localities, our knowledge of the distribution and variation in this species has increased accordingly.

A great many problems remain, however, when one deals in detail with the variation in *A. ricordi*. Williams (1962, 1965) pointed out that records of the species were of such a scattered nature (especially on the Tiburon Peninsula but also elsewhere on the island) that intergrades between several of the subspecies remained unknown and also that there were no specimens available from large areas between named populations. Williams and Rand (1969), in their excellent summary of the geographic differentiation in all species of Hispaniolan anoles, pointed out (p. 15) that *Anolis ricordi* was composed of "several described subspecies, some of which are sharply enough distinct to raise the question of possible species status." This is most especially true of the taxa *ricordi*, *baleatus*, and *barahonae*, all of which are extremely well characterized by both pigmental and structural details, but all of which occupy areas (extensive in the cases of *ricordi* and *baleatus*) without known intergradation between them or without close geographic approximation. Thus, the closest ap-

[1] Miami-Dade Community College, Miami, Florida 33167.

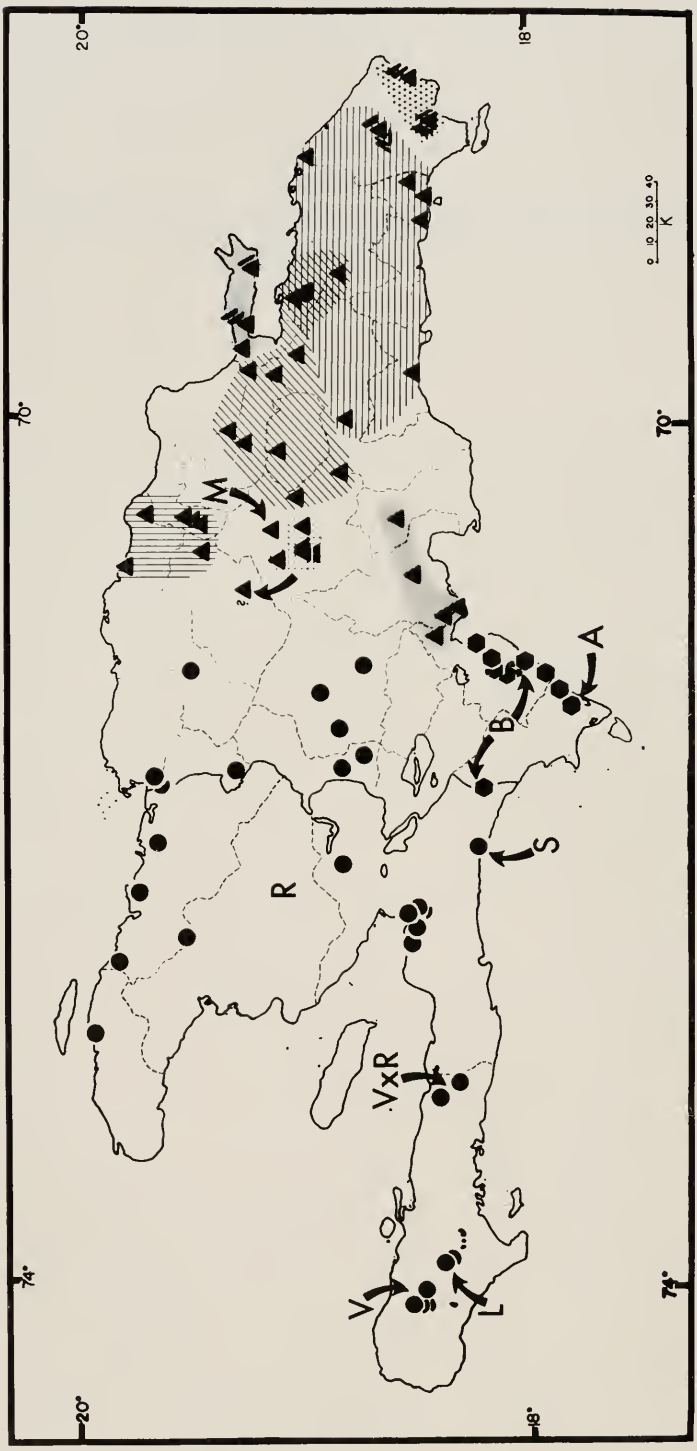

Figure 1. Map of Hispaniola, showing the known distributions of the Hispaniolan giant anoles, as follows. *Anolis ricordi*—solid circles; *Anolis barahonae*—solid hexagons; *Anolis baleatus*—solid triangles. All solid circles other than those marked individually are *A. r. ricordi* = R; V = *A. r. viculus*; L = *A. r. leberi*; S = *A. r. subsolanus*; V × R = intergrades between *A. r. viculus* and *A. r. ricordi*. B = *A. b. barahonae*; A = *A. b. albocellatus*. Subspecies of *A. baleatus*: *baleatus*—broad vertical lines; *caeruleolatus*—broad diagonal lines; *samanae*—fine stippling; *multistruppus* = M; *sublimis*—moderate stippling; *scelestus*—broad horizontal lines; *litorisilva*—coarse stippling; *fraudator*—fine diagonal lines. Overlap of symbols represents area of intergradation. Questioned locality is specimen from Los Montones which may be *A. b. sublimis*.

proaches of the ranges of *ricordi* and *baleatus* (Copey and Peña, both in the República Dominicana) are separated by some 115 kilometers airline. The subspecies *barahonae* and *ricordi* (Sierra de Baoruco and associated eastern coastal areas in the República Dominicana, and Saltrou in Haiti) are known from localities separated by about 115 kilometers, and *barahonae* and *baleatus* by a gap of about 115 kilometers (between the Sierra de Baoruco and near Villa Altagracia, both in the República Dominicana).

Schwartz and Garrido (1972) recently showed that the Cuban giant anole, *Anolis equestris* Merrem, is, in fact, a complex of five species; they also suggested (p. 71) that, as Williams and Rand had pointed out, there was a good possibility that the Hispaniolan *Anolis ricordi* in time might likewise be shown to be a complex of species. It is the purpose of the present paper to discuss the variation in *A. ricordi,* based upon the examination of 403 specimens from a broad selection of geographic localities throughout Hispaniola. Despite my having studied far more material than any previous investigator, there still remain many problems that cry out for solution. As Schwartz and Garrido also pointed out in their analysis of *Anolis equestris,* the present paper in no way should be considered as the final word on *A. ricordi;* rather it is an attempt to comment in detail upon the known variation and distribution of this species in Hispaniola which may serve as a stepping stone for further work upon the species.

Between 1962 and 1971, I and my associates collected extensively in both Haiti and the República Dominicana. Latterly, between 1968 and 1971, my work in Hispaniola has been under the sponsorship of two National Science Foundation grants, GB-7977 and B-023603. Specimens of *Anolis ricordi* collected in 1962–63 were available to Williams and were reported upon by him (1965); in fact, the long series of *A. ricordi* from Camp Perrin, Haiti, secured for me by native collectors in 1962, was the material upon which *A. r. leberi* was based. Our unique experience at Camp Perrin—namely, of many *A. ricordi* received from local Haitians—showed that the species may not be necessarily rare. However, as in *A. equestris* in Cuba, the cryptic greens of *A. ricordi* render the species virtually invisible during the day except to all but the most experienced observer. In 1963, Richard Thomas discovered that *A. ricordi* might be secured at night, since individuals sleep quite exposed in a variety of arboreal situations and are very conspicuous. Thus, with the knowledge that the *agrama* (as the species is known in Haitian Creole) or the *saltacocote* (as the species is known in Dominican Spanish) might be common and thus easily secured by native collectors, and that individuals might be readily secured at night while they slept, I had as one of my objectives to secure as many *A. ricordi* as possible in order to clarify the status of the named subspecies and in an attempt to narrow the geographic gaps that seemed to exist between *ricordi, baleatus,* and *barahonae.* As more material accumulated, we were successful in the latter attempt, but the range of variation in newly acquired material showed that the situation was more complex than was supposed. In addition to specimens in the Albert Schwartz Field Series (ASFS), collected by myself and field assistants, I have examined material in the American Museum of Natural History (AMNH), the Museum of Comparative Zoology (MCZ), and the National Museum of Natural History (USNM). For the loans of specimens I am grateful to Richard G. Zweifel, George W. Foley, Ernest E. Williams, and George R. Zug. In all of these collections there are other specimens that I have deliberately not elected to study, since many of them are from localities that are now well represented by more recently collected lizards or that have poor locality data. Specimens in the collection of the Museum of Comparative Zoology have been collected under NSF grant B-019801X and previous grants to Dr. Williams. Most of the re-

cently taken ASFS *A. ricordi* have detailed descriptions of color and pattern in life, but, as in all such endeavors that span several years, it is unfortunate that *all* details of color and pattern have not been consistently recorded as time has passed. Likewise, there are no color or pattern data on most old specimens; thus, I feel less secure in dealing with these older specimens or those collected by others than myself and parties than I am with those in the ASFS which are carefully documented. However, specimens from other localities must in some way be dealt with, and I have done so as carefully as possible, considering details of geography and what is known about specimens of *A. ricordi* from adjacent localities.

I wish to acknowledge with enthusiasm the efforts on my behalf in the field of the following men, without whose efforts the quantity of *A. ricordi* presently available to me would be far less: Jeffrey R. Buffett, Carl Butterfield, James R. Dennis, Danny C. Fowler, Ronald F. Klinikowski, David C. Leber, James A. Rodgers, Jr., Bruce R. Sheplan, and Richard Thomas. C. Rhea Warren has given me a specimen of *A. ricordi* from northern Haiti. My notes on coloration and pattern of *A. ricordi* have been greatly supplemented during the present study by the color portraits executed in the field by D. C. Leber; one of these has been reproduced in black-and-white in Williams (1965), but the reproduction hardly does justice to the detailed beauty of all the originals. I have been able to examine the holotype of *Eupristis baleatus* Cope through the courtesy of Alice G. C. Grandison and A. F. Stimpson of the British Museum (Natural History). Holotypes and paratypes have been designated or deposited in the above collections and in the Carnegie Museum (CM).

THE PROBLEM

Mertens (1939) was the first to point out that Haitian and Dominican *A. ricordi* differed from each other in one notable character—the height of the dorsal crest scales. His figure 41 shows this character extremely clearly: in nominate *ricordi* from Haiti, the nuchal crest scales are low and inconspicuous, whereas in Dominican *baleatus* the nuchal crest scales are long and attenuate. In addition, Mertens (1939: 69) characterized *ricordi* as having 9 to 12 scales between the eyes; males of this subspecies have one or more sharply defined black blotches on the sides of the nape, the occipital area flecked with black, and often have black longitudinal stripes on the flanks. On the other hand, *baleatus* has from 6 to 8 scales between the eyes, and males are without any black head, nape, or lateral markings. Williams (1962) compared these two taxa with *barahonae* in regard to four characters: height and relative length of nuchal and dorsal crest scales, number of snout scales at the level of the second canthal scale, and body pattern. Later, when he described *A. r. leberi,* Williams (1965) employed these same characters to differentiate that subspecies.

The differences in these characters between the four recognized subspecies are unequivocal: one can differentiate at a glance between such distinctive animals as *leberi* and *barahonae* or between *ricordi* and *baleatus,* without recourse to microscopic examination. The whole aspects of all four taxa are quite distinctive, whether one is dealing with living or long-preserved animals. What has been equivocal is the relationships of these four taxa, since, as I pointed out previously, they have been known from rather isolated groups of localities, widely separated from each other. In only one case (*leberi-ricordi*) have specimens been regarded as intergradient between two subspecies: these intergrades are from a geographically plausible locality that itself is widely removed from the two "parent" populations.

As material has gradually accumulated, it has become increasingly obvious that the situation is even more complex than has been previously recognized. For example, in 1971, I had occasion to compare long series of living examples from the Península

de Samaná and the adjacent "mainland" at Caño Abajo, and I was at once struck with the differences between these two samples, both of which have been regarded as *baleatus*. In this case, the differences are not particularly subtle but they do involve differences in coloration and pattern which often are evanescent after preservation. The same statement may be made about *A. ricordi* from the region near La Vega and those from the Cordillera Septentrional. In 1971 I had occasion to collect specimens from both these regions on two successive days and thus was able to compare freshly collected material directly. Again, the differences are ones of pattern and color, but they are so striking that it is misleading to consider both these populations as being identical genetically. I could multiply the above examples but to no purpose; it is obvious, when one sees living *A. ricordi* in the field, that there are several populations presently assigned to *baleatus* which are quite distinctive.

On the basis of specimens collected by Richard Thomas and myself in 1963, Williams (1965) reported *A. r. ricordi* for the first time from the northwestern República Dominicana in the region near Pepillo Salcedo and Copey in Monte Cristi Province. He noted, however, that, "Despite the new collections one embarrassment remains. No certain intergrades between the two strikingly different forms *ricordii* and *baleatus* are yet known. . . . However, the area in which intergrades may occur is being narrowed: on the north coast of the Dominican Republic between Monte Cristi and Santiago and in the center of Hispaniola between Mirebalais (MCZ 68479, 69404) and Santiago. This still leaves a very wide area of ignorance." Since the above was written, I have secured specimens of the nominate subspecies in four other regions: at Restauración, Dajabón Province, along the Dominico-Haitian border and about 40 kilometers airline south of the Monte Cristi localities; on the southern slopes of the Cordillera Central near Juan de Herrera in San Juan Province; and throughout the Sierra de Neiba between Hondo Valle and Vallejuelo in La Estrelleta and San Juan provinces. These latter two regions (the southern slopes of the Cordillera Central and the Sierra de Neiba) are separated by the rather xeric Valle de San Juan. Elsewhere to the east and north, the Cordillera Central harbors *A. ricordi* with long nuchal crest scales and without black nape and head markings in males (*i.e.*, = *baleatus*), as at San José de Ocoa, La Vega, and the interior uplands near El Río, and near Los Montones on the Río Bao. The fourth locality is perhaps the most significant; there is one subadult male from Santiago Rodríguez Province near Los Quemados which is clearly a *ricordi*. Of the *baleatus* localities, this one is closest to Los Montones, a distance of 50 kilometers airline. Thus the gap between *ricordi* and *baleatus* in northern República Dominicana has been more than halved, and there still is no genetic influence of one subspecies upon the other.

To the south, specimens of *A. ricordi* from the Sierra Martín García, and Azua and Peravia provinces likewise narrow the gap there between *baleatus* and *ricordi* on one hand and between *baleatus* and *barahonae* on the other. In the former case, the distance between *ricordi* and *baleatus* (Vallejuelo and Sierra Martín García) is about 60 kilometers airline, without character dilution. In the instance of *barahonae* and *baleatus*, only 20 kilometers separate known localities (Barahona and Sierra Martín García) for these two taxa: however, the actual kilometrage is deceiving, since, lying between these localities, is the Valle de Neiba and the Bahía de Barahona. Although this eastern extreme of the Valle de Neiba is rather mesic and supports (or did support) large trees in many areas that would presumably be suitable for *A. ricordi*, the break between these two populations is sharp despite presumably suitable ecology. I have little doubt that *A. ricordi* occurs in this intervening region, and the interaction of *barahonae* and *baleatus* therein will be most interesting to ascertain.

Even more intriguing is the fact that the

Sierra Martín García is an extreme eastern isolate of the Sierra de Neiba, which is elsewhere occupied by *A. r. ricordi.* This small range, which reaches an elevation of 1350 meters, is completely surrounded by extremely arid desert or low rolling xeric hills, as well as by the Bahía de Barahona on its southwestern edges. The herpetofauna of the Sierra Martín García is just becoming known, and it supports a remarkable fauna, including an endemic species of *Diploglossus* (Thomas, 1971) and a new species of *Sphaerodactylus,* as well as other unexpected novelties. Nevertheless, *A. ricordi* seems to have reached this range from the northeast (*i.e.,* the southern slopes of the Cordillera Central), since I regard the Martín García lizards as identical to those from Azua and Peravia provinces.

Finally, the geographic relationship of *barahonae* and *ricordi* has been to some extent clarified. *A. r. barahonae* has been known only from the eastern uplands of the Sierra de Baoruco and from three southern lowland localities (Enriquillo, half-way between Enriquillo and Oviedo, and Oviedo). Each of the latter localities is represented by a single specimen. The Enriquillo and Enriquillo-Oviedo specimens are quite obviously *barahonae,* but, as Williams (1965: 4) noted, the specimen from close to Oviedo is quite different in style of pattern and color from typical *barahonae.* To the west, in Haiti, there has been but a single specimen from Saltrou which Williams (1965: 2) considered *A. r. ricordi* and which "narrows the geographic gap between *ricordii ricordii* and *r. barahonae;* however, it does nothing to narrow the character gap." Two additional facts are important. First, in 1971, we secured a pair of *A. ricordi* from along the Dominico-Haitian border north of Pedernales; these individuals, although differing somewhat from typical *barahonae* and strongly from the single Oviedo specimen, in no way show any tendencies toward *A. r. ricordi.* They are clearly related to *barahonae,* a rather surprising fact since they are much closer (35 kilometers) to Saltrou than they are to any *barahonae* locality (65 kilometers at Enriquillo). Secondly, Williams has recently received a fine series of *A. ricordi* from Source Carroyé near Thiotte; these lizards are quite obviously *not A. r. ricordi* but are closer in many ways to the far-western *A. r. leberi.* Thus the situation along the southern Haitian coast between Saltrou and the eastern coast of the República Dominicana at Oviedo and its environs remains a true puzzle. It seems likely that *A. r. ricordi* does not cross the high Massif de la Selle, except possibly by some circuitous route, and that *A. r. barahonae* occurs up to the Dominico-Haitian border, to within 11 kilometers of a station (Source Carroyé) where another taxon occurs, without character dilution.

Interpretations of all these facts are seriously hampered by the lack of specimens of *A. ricordi* from throughout the Haitian Tiburon Peninsula. Material from the peninsula may be divided into four basic lots: a short series from the region about Castillon on the northern slopes of the Massif de la Hotte near the tip of the peninsula; a very long series of specimens from Camp Perrin on the low southern slopes of the Massif de la Hotte (the type series of *A. r. leberi*); a short series from midway along the peninsula at Miragoâne-Paillant; and a moderate number of specimens from near the base of the peninsula in the region of Morne Decayette-Pétionville-Port-au-Prince. The lack of material from such well-collected areas as Jérémie on the northwestern coast or Jacmel and Les Cayes on the southern coast is extremely puzzling—we simply know nothing about lowland *A. ricordi* throughout much of the Tiburon Peninsula, except for the above scattered records and the southern coast at Saltrou near the Dominican border (and the latter locality is not even on the peninsula proper).

To summarize the data from elsewhere in Haiti and the República Dominicana, there is a huge distributional hole in central Haiti, with but two specimens (*ricordi*) from Mirebalais, widely separated

from southern *ricordi* at and near Port-au-Prince, and then a group of scattered localities along the northern littoral of Haiti from Port-de-Paix in the west to Terrier Rouge in the east, and one specimen from Marmelade in the interior Chaine de Marmelade. All these Haitian specimens have low nuchal crest scales, and males variably possess some black nape and side markings, but there are differences between specimens from the various sections which presently defy analysis, since the material is too meagre and from too scattered localities.

The República Dominicana fares far better as far as detailed coverage is concerned. Aside from the material previously noted as assigned to *ricordi* or *barahonae*, there are now good series available from the eastern half of the country, and, although there are certain gaps even within this region, they are not so appalling as are those in Haiti. *A. ricordi* is rarer (or perhaps less easily encountered) in arid regions, and thus the most striking gaps in the western half of the República Dominicana are those involving arid regions on the one hand or high mountain masses on the other. The latter situation, especially if the slopes are pine-clad, does not appear suitable for *A. ricordi*, and the species may be truly absent from the uplands above 4000 feet (1220 meters), the highest elevation from which the species is known. In arid regions, *A. ricordi* appears to be restricted to riverine woods and forests; in such situations, the species may not be uncommon, but it may require diligence to secure even one specimen from a particular region.

The detailed discussion above should give the reader a background of both the history and present knowledge of the distribution of *A. ricordi* against which the following accounts can be most logically followed. One further point is of interest. *A. ricordi* is unknown by specimens from any of the large Hispaniolan satellite islands. In some cases (Isla Beata) the species is not expected for a variety of reasons, but in others (Ile de la Gonâve, Ile de la Tortue, Ile-à-Vache) there seems no logical reason for the absence of *A. ricordi*, discounting the vagaries of overseas transport. The species does occur on Isla Saona, but remains uncollected there. Fowler and Sheplan saw a sleeping *A. ricordi* on the northern coast of Isla Saona in December 1971, but, after it had been shot, it was lost in the undergrowth. The occurrence of *A. ricordi* on any Hispaniolan satellite is noteworthy, and it will be most interesting to determine the status of the Isla Saona population.

METHODOLOGY

The series of 403 *A. ricordi* was divided into 14 samples on the basis of geography, as follows: *República Dominicana:* 1) Península de Samaná (54 specimens); 2) northeastern República Dominicana, from Duarte and eastern La Vega provinces east to the *haitises* region in northeastern San Cristóbal Province (37); 3) extreme eastern Hispaniola, Punta Cana-Juanillo, Boca de Yuma, La Altagracia Province (16); 4) southeastern República Dominicana from Higüey and Las Lisas, La Altagracia Province, west to Santo Domingo and Yamasá, San Cristóbal Province (61); 5) lowlands at the northern base of the Cordillera Central at Guaïguí, La Vega Province (21); 6) Cordillera Central at and above elevations of 2000 feet (18); 7) Cordillera Septentrional and north (15); 8) Sierra Martín García and Peravia and Azua provinces (6); 9) Sierra de Baoruco and associated east coast of the Península de Barahona (33); 10) Oviedo, Pedernales Province (1); *Haiti:* 11) Saltrou and vicinity, Dépt. de l'Ouest (15); 12) region about Port-au-Prince, Mirebalais, northern Haitian littoral, Chaine de Marmelade, and (in the República Dominicana) region about Pepillo Salcedo, Copey, Los Quemados, Restauración, and the southern slopes of the Cordillera Central and the Sierra de Neiba (50); 13) Camp Perrin and Marceline, Dépt. du Sud (54); and 14) vicinity of Castillon, Dépt. du Sud (6). This division into 14 regional

samples was completed after preliminary examination of the material, scale counts and detailed review of field notes on coloration and pattern were all made. In addition, two other small lots (eight specimens from the vicinity of Miragoâne, Dépt. du Sud, Haiti, and seven specimens from El Seibo Province, República Dominicana) were examined separately; in both cases, these short series indicate intergradient tendencies between pairs of the 14 major samples noted above, and they were not included with the latter.

The following data were taken on each specimen:

1) Snout–vent length, in millimeters.

2) Number of snout scales across snout at level of the second canthal scale, reckoned from the anterior corner of the orbit.

3) Number of vertical rows of loreal scales.

4) Minimum number of scales between supraorbital semicircles.

5) Number of scales between the interparietal scale and the supraorbital semicircles on each side, this datum written as a fraction (*i.e.*, 5/5 = five scales in this position on each side).

6) Number of scale rows between the subocular scales and the supralabial scales.

7) Number of vertical rows of dorsal scales in a distance equal to that from the tip of the snout to the anterior bony wall of the orbit, this distance measured by vernier calipers, laid off on the back about three rows below the median dorsal crest scales, and the number of scales counted under a binocular dissecting microscope.

8) Number of horizontal rows of dorsal scales in the snout–eye distance, the scales counted at midbody. This count was not taken in most juveniles or on those specimens that were shrunken or poorly preserved since, under the latter circumstances, some smaller ventrolateral or ventral scales will be included.

9) Number of transverse rows of ventral scales in the snout–eye distance.

10) Number of lamellae on phalanges II and III of the fourth toe.

11) Height of the nuchal crest scales, categorized as very high, high, moderate, or low.

12) Height of dorsal crest scales, categorized as high, moderate, or low.

13) Dorsal coloration and pattern of males and females, separately.

14) Ventral coloration of males and females, separately.

15) Color of dewlap, in males and females, separately.

16) Color and pattern of chin and throat in males and females, separately.

17) Color and pattern of upper surface of head in males and females, separately.

18) Color of eyeskin.

19) Color and pattern of upper surfaces of hindlimbs.

20) Color and pattern of juveniles and subadults.

The above characteristics are variously useful as far as delimiting the nameworthy populations of *A. ricordi.* Detailed comments on these characteristics are made below, with especial attention to pitfalls in their reliability and usage.

1) The snout–vent length of mature individuals of both sexes is remarkably uniform throughout the entire series. Males are easily distinguished from females at any age by the presence of one (occasionally two) pairs of enlarged postanal scales. Many ASFS specimens have the hemipenes extruded. Males in general reach a larger snout–vent length than females; the largest male (ASFS V29284) has a snout–vent length of 180 and is from sample (4), whereas the largest female (ASFS V31397) has a snout–vent length of 151 and is from sample (12). The mean difference in snout–vent lengths between the two sexes is about 10 mm in almost all samples with the exception of maximally sized individuals in both sexes in sample (2) where the difference is 3 mm, sample (3) where the difference is 27 mm, sample (4) where the

difference is 32 mm, and sample (7) where both sexes are of the same size. Whether these exceptions to the 10-mm generalization are meaningful is debatable. At least samples (2) and (4) include long series of specimens, and even samples (3) and (7) include more than ten individuals. Adults of the two sexes are readily distinguished morphologically, since males have a high tail "fin" that is supported by the bony extensions of the neural spines; this feature is lacking in females, although they may have a much reduced caudal crest in the form of a low ridge. The terminal half of the tails of many males is crestless; I at first considered that this was due to breakage with subsequent regeneration without regeneration of the tail "fin." Many specimens have this condition, however, without any obvious change in basic caudal scale shape and arrangement, and this is the normal condition in the tails of males. Often the uncrested portion of the tail is quite differently colored or patterned than the remainder of the tail; such cases are due to regeneration.

2) The number of snout scales at the level of the second canthal has been employed as a characteristic to separate the recognized subspecies. Williams (1962, 1965) recorded the following variation in the four subspecies: *ricordi*, 7–9; *baleatus*, 2–5; *barahonae*, 4–6; and *leberi*, 4–6 (3–6 on map, fig. 2, 1965: 7). It should be recalled that Williams himself pointed out that this count *alone* would not distinguish all these taxa from each other. Certainly overlap between *baleatus* and *ricordi* is nonexistent, and between *baleatus* on one hand, and *barahonae* or *leberi* on the other hand, the overlap is small. Counts on 403 specimens made by myself do not extend the parameters of snout scales at all: within the entire lot of specimens, these scales vary from 2 to 9, just as in Williams's data. However, the variation within populations may be much greater than Williams anticipated. For instance, in sample (13), the counts vary between 2 and 7, and in series (12) between 4 and 8. Most samples have three or four categories of number of snout scales. I am in no way implying that this is an invalid or poor character for differentiation of populations of *A. ricordi*, however; it is, rather, an extremely useful one but requires amplification and interpretation.

If we examine only those samples (1–8) which are assigned to *baleatus*, the amount of variation in snout-scales is 2–5, exactly that assigned to this taxon by Williams. However, within the broad area covered by *baleatus*, there are strong modalities of snout-scales. In samples (1), (4), (5), and (6), the mode is 2 scales, whereas in samples (2), (7) and (8), the mode is 4. Only one sample, (3), has bimodes of 2 and 4 scales. In *barahonae* (9) the range is 2–5 (mode 4). In those samples which are associated with nominate *ricordii* (samples 11 and 12), *leberi* (sample 13) and adjacent Castillon material (sample 14), the range is 2–9, thereby showing complete overlap in range of this count with that of both *baleatus* and *barahonae*. In fact, in *leberi* (13) alone, the range of snout scales (2–7) almost embraces that for all other samples and thus the entire species. Modalities in this complex of samples are 5 (sample 11), 7 (sample 12), 4 (sample 13) and 6 (sample 14). Sample (7) is nominate *ricordi*.

3) The number of vertical rows of loreal scales ranges from 5 to 10. The greatest variability is in samples (1), (2), (7), and (12), where the row counts in each case are 5–9, 6–10, 5–9, and 6–10. Most samples have four categories of number of loreal rows. The modes vary as follows: 5 (sample 11), 6 (samples 8, 9, 13), 7 (samples 1, 3, 4, 5, 6, 7, 12, and 14), and 8 (sample 2).

4) The minimal number of scales between the supraorbital semicircles varies between 1 and 5; no specimen has the semicircles in contact. Modes in general are very strong, and the usual mode is 3 scales (samples 1–7; sample 8 has a bimode of 2 and 3 scales); these are all samples that

are assigned to *baleatus.* A mode of 3 scales occurs also in samples (11) and (13), and of 4 in samples (12) and (14).

5) The number of scales between the interparietal scale and the supraorbital semicircles varies between 3/3 and 7/7. Modes (which in some cases are quite strong and in others less so) are: 4/4 (samples 1, 5, 6, 8, 9, 11, 13, 14) and 5/5 (samples 2, 4, 7, 12). Sample (3) is peculiar in having the mode 4/5 (six of 16 lizards), with adjacent counts of 4/4 (four lizards) and 5/5 (five lizards). There is high variability in this count; it can be assessed in another fashion, namely, the frequency with which any scale count (*i.e.*, 4, 5, 6, etc.) occurs within the sample, regardless of its pairing with another count on the other side of the head. With the use of this technique, the frequency of involvement of 4 scales in the interparietal-semicircle contact varies between 43 percent (sample 1) and 67 percent (sample 8), and of 5 scales between 52 percent (sample 2) and 64 percent (sample 7). Of the entire lot of specimens, there is only one occurrence of 7/7 in this position (sample 12) but many occurrences of 3/3 (samples 1, 5, 6, 9, 11, 12, 13, a total of 12 incidences).

6) The number of scale rows between the subocular scales and the supralabials is fairly constantly 1, and this is a strong mode or the exclusive category in all samples except sample (13). In this lot (which is the type series, with a few new specimens, of *leberi*), 48 percent of the lizards have the suboculars and supralabials in contact. Elsewhere, contact is absent in samples (7) and (11). The frequency of contact varies in all other samples between 3 percent (sample 9) and 17 percent (samples 6, 8, and 14). These three samples are widely separated geographically and the frequency in none of them even approaches the very high incidence of contact in sample (13). However, it is noteworthy that samples (13) and (14) are adjacent geographically.

7), 8), 9) In reference to all counts involving laying out the snout–orbit distance on the body, I can do no better than once more to reiterate the cautions previously expressed (Schwartz, 1964; Garrido and Schwartz, 1968; Schwartz and Garrido, 1972) in reference to *Anolis equestris* and members of the genus *Chamaeleolis.* For these standard-distance counts, old and poorly preserved, limp, curled, uninjected, or otherwise distorted specimens are much less useful and reliable than properly preserved, injected, and positioned lizards. Luckily, by far the largest quantity of *A. ricordi* under study are well preserved. However, I have abandoned counts of horizontal dorsals on young juveniles, even well-preserved ones, or on any adults whose condition precluded taking these counts meaningfully. The juvenile situation is peculiar in that invariably, despite the relatively shorter snout of young specimens, laying out this distance to count horizontal rows involved including several rows of extremely lateral and ventral scales, which are smaller than true dorsals and which thus tend to increase the horizontal counts. I have taken vertical dorsals and ventrals on juveniles, however, and they do not skew the data. Of the three standard-distance counts, those of vertical dorsals and ventrals are much more reliable than are those of horizontal dorsals.

Vertical dorsal scale rows vary between 12 and 26, with the low count in sample (4) and the high count in sample (12). Means range from 15.4 (sample 4) to 21.1 (sample 12). These two represent, respectively, lots assignable to *baleatus* and *ricordi, sensu lato.* No generalizations of mean number of vertical dorsals in reference to samples and geography can be made, since the range in samples now associated with *baleatus* varies between 15.4 and 19.2, with *ricordi* 17.3 and 21.1, *barahonae* 17.2, and *leberi* 16.5 and 16.7. Comparisons and significance of vertical dorsal scale counts are shown in Table I.

Number of horizontal dorsal rows ranges from 13 (sample 1) to 34 (sample 7). Means vary between 17.1 (sample 11) to 24.6 (sample 12). The latter sample is that

Table I. Comparison of number of vertical dorsal scales in populations of giant Hispaniolan anoles

Taxon	N	M (± 2 standard error of mean)	*leberi*	*subsolanus*	*barahonae*	*samanae*	*caeruleolatus*	*litorisilva*	*scelestus*	*multistruppus*	*sublimis*	*baleatus*
ricordi	50	21.1 ± .57	+	+	+	+	+	+	+	+	+	+
leberi	54	16.5 ± .46		−	−	−	−	−	+	+	+	−
subsolanus	15	17.3 ± .96			−	−	−	−	+	−	+	−
barahonae	33	17.2 ± .67				−	−	−	+	−	+	−
samanae	54	16.6 ± .46					−	−	+	+	+	−
caeruleolatus	37	17.1 ± .72						−	+	+	+	−
litorisilva	16	15.9 ± .75							−	+	+	+
scelestus	60	15.4 ± .45								+	+	+
multistruppus	20	18.6 ± 1.06									−	−
sublimis	18	19.2 ± .70										−
baleatus	15	17.5 ± 1.16										

A. r. viculus, A. b. albocellatus, and *A. b. fraudator* are not included. A "+" in the table indicates that the two subspecies involved differ significantly (non-overlap of two standard errors of mean); a "−" indicates no statistical difference. Note that the mean of *A. r. ricordi* differs significantly from the means of all other taxa; that of *scelestus* differs significantly from those of all other taxa except *litorisilva;* and that of *sublimis* differs significantly from those of all other taxa except *multistruppus* and *baleatus.*

of nominate *ricordi,* the former a peripheral isolate of *baleatus.*

Number of transverse rows of ventral scales varies between 15 (samples 1 and 13) and 34 (sample 7). Means range from 20.2 (sample 13) to 25.1 (sample 6); sample (13) is *leberi.*

10) The number of lamellae on phalanges II and III of the fourth toe varies between 27 and 39. The variation in any population is so great that this count is meaningless as far as differentiation between any populations of *A. ricordi.*

11), 12) Williams (1962, 1965) described the relative heights and lengths of both the nuchal and dorsal body crest scales. Certainly the differences between *baleatus* and *ricordi,* for instance, are so very obvious on casual examination that one has no difficulty in ascertaining the taxon involved. Williams also pointed out (1962: 4–5) that in some specimens there is "sometimes a regular alternation of relatively high triangular single scales and pairs of much lower, more quadrangular scales," with the result, on some specimens, of double crest scale rows on the neck; the net effect of this condition is a rather indiscriminate grouping or elongate patch of multiple nuchal crest scales. Although this condition occurs erratically, it seems to be most predominant in specimens from the Tiburon Peninsula, but it occurs elsewhere in nominate *ricordi* and even occasionally in specimens assigned now to *baleatus.* Such a "hypertrophied" nuchal crest condition does not completely fit any logical geographical pattern nor is it totally consistent within any sample, although there are tendencies toward it as noted above. In any event, it does not obscure the height of the nuchal crest scales.

In my own analysis, I have used a slightly different method in recording height of crest scales. Nuchal scales were recorded for each specimen as very high, high, moderate, or low. Such a verbal quantification is not totally satisfactory, since the investigator's impressions may change as the study progresses. To avoid this pitfall, I re-examined many specimens that had been studied earlier in the work and reconfirmed my own early impressions with my later ones. Body crest scales were recorded as high, moderate, and low.

In nuchal crest scales, very high scales are those which are very elongate, attenuate, almost spinelike (but of course flexible,

not stiff), with the base much shorter than the height of the scale. High scales are those which are shorter and less attenuate than very high scales, but whose height is still much greater than the base. Moderate scales are lower and not attenuate, although they may be pointed, with the height and base about equal in length. Low scales are lower than long. The same categories and interpretations apply to body crest scales, although no lizard has the body crest scales so high as the nuchal scales.

Several other points are pertinent. I have not used this datum from juvenile and subadult lizards (all lizards below 100 mm snout–vent length) since it is obvious that, regardless of the taxon or sample, all young *A. ricordi* have low nuchal and dorsal crest scales, which, as the lizard matures, become increasingly more specialized until the adult condition is reached at about 110 mm snout–vent length. Thus young *ricordi* and young *baleatus,* two taxa that are remarkably distinct in this feature as adults, are identical in crest development.

Secondly, it might be assumed that (especially) nuchal crest scales might be better developed in adult males than in adult females; this excessive development might reasonably be assumed or construed as a sexually dimorphic character, with hyperdevelopment in males. Such does not seem to be the case, and many female *baleatus,* for instance, have very high nuchal crest scales, as high as those of males. In fact, comparisons of males and females of individual samples show that, within each sample, there is remarkable consistency between frequencies of the very high, high, and moderate categories in both sexes.

Thirdly, as one might expect, there is a sequence of crest scale heights in the nuchal-body series. If the nuchal scales are very high, the body scales are high; if the nuchal scales are moderate, the body scales are low, etc. In no case have I recorded a transition from very high nuchal crest scales to moderate body scales, for example. There is thus a definite correlation between height of nuchal scales and those of the body crest.

13)–19) The color and pattern details of *Anolis ricordi* throughout its range need not be gone into in detail at this point. It is now sufficient to acknowledge that these lizards show metachrosis varying from shades of green and green-gray to brown. The pattern elements, however, are quite stable, although the hues involved in the pattern itself may change with changing base colors. There is little evidence to indicate that a lizard which is, for instance, blotched in one color phase will become crossbanded in another. Thus, despite changes in hues and even in base colors, patterns remain constant. It is of interest to note that greens seem to be the colors that predominate in the wild. The few *A. ricordi* that I have seen during the day have always been green. The many lizards that I have seen and collected at night were almost always green, and usually at their maximum of pattern expression while they slept. It is this nocturnal assumption of the green phase coloration that renders these lizards so very conspicuous at night while they sleep on exposed branches, vines, or among the arboreal greenery. Even in those populations (Boca de Yuma, Sierra de Baoruco) in which the greens involved are not bright, the lizards are still quite obvious at night. It is only rarely that one encounters a brown *A. ricordi* at night. I have notes on only one instance of this condition, a subadult lizard from the Cordillera Septentrional.

15) The dewlap coloration in *A. ricordi* is variable. In some populations, males have a pale yellow to gray dewlap, whereas in others the males have dewlaps that are peach or vivid orange. It should be noted that both sexes in *A. ricordi* have dewlaps and that the general hue of the female dewlap is like that of the males, except that basally it is usually streaked with browns, dark grays, or charcoal, and the ground color is less bright than that of males. In some regions, the female dewlap is quite differently colored than that of males.

20) Juveniles and subadults present several problems that are presently insoluble. I suspect that much will be revealed once

we know the repertory of pattern and color in young individuals, but these data are not available now. Although there are many young specimens at hand, they are inconsistent within populations or even small samples. The juvenile color is normally some shade of green (or browns under stress), most often with two to four pale (cream, whitish, pale gray) crossbands. Many small specimens are a uniform green without any dorsal markings. In other juveniles, the dorsum has many conspicuous crossbands with two shades of greens (or browns), separated by prominent bands of pale greens (yellow-green, pea-green), to give a very tigroid lizard; this condition persists into the adults of one population, as does the more simply banded juvenile pattern noted above in other populations. The juveniles usually have dark gray to charcoal dewlaps, regardless of their sexes, and often there are charcoal or white markings on the neck or above the forelimb insertion or somewhere anteriorly. These variants are discussed under each subspecies below, and there is no need to go into the details here. However, I do wish to point out that juvenile patterns are more variable than are those of adults, and that I do not know how to interpret this situation.

SYSTEMATIC ACCOUNTS

Anolis ricordi Duméril and Bibron

Anolis ricordii Duméril and Bibron, 1837. Erp. gén., 4: 167.

Type locality. St.-Domingue; holotype, Muséum National d'Histoire Naturelle 1272.

Definition. A giant species of Hispaniolan *Anolis* characterized by the combination of moderate size (males to 160 mm, females to 151 mm snout–vent length), snout scales at level of second canthal scales variable, between 2 and 9 (modally 4, 5, 6, or 7 by population) but usually 4 to 9 (97 percent), vertical loreal rows 5 to 10 (modes by population 5, 6, and 7), scales between supraorbital semicircles 2 to 5 (modes 3 or 4 by population), interparietal scale separated from supraorbital semicircles modally by 4 or 5 scales, vertical dorsal scales generally small (14 to 26 in standard-distance), ventral scales relatively large (15 to 32 in standard-distance), nuchal crest scales in both sexes moderate to low, never very high or high, body crest scales usually low, subocular scales usually not in contact with supralabials but one population is remarkably exceptional in this character; dorsal body coloration and pattern some shade of green, in some geographic regions flecked irregularly with paler and darker green to give a beadwork effect; male body pattern either of irregular black to dark brown blotches on the neck, occipital region of the head, and on sides (often delimiting two pale longitudinal bands) or with three longitudinal dark brown stripes on each side or with dark saddles and a bluish green flank stripe or with a powdery pale blue-green lateral stripe; females usually without dark dorsal or lateral markings although in some areas females have a darker brown reticulum, three pale gray to yellow narrow crossbands, longitudinal black lines, or two purple flank stripes; dewlap in males variable, from yellowish gray to peach, bright orange, or deep yellow, in females from peach to deep yellow or dull orange or even inky brown or inky blue-black, chin and throat dull yellow, yellow-green, or pale blue-green in males, eyeskin dark (charcoal, dark brown) to light (pale blue) in males, charcoal to pale green in females, and usually with a prominent pale subocular semicircle clearly delineated.

Distribution. The Tiburon Peninsula in Haiti, east to the vicinity of Saltrou, Dépt. de l'Ouest, thence north to the northern Haitian coast from Port-de-Paix east to Terrier Rouge and thence into the Republica Dominicana east as far as the vicinity of Los Quemados, Santiago Rodríguez Province, south to Restauración, Dajabón Province; also extending from Haiti onto the southwestern slopes of the Cordillera Central in San Juan Province and in the Sierra de Neiba in La Estrelleta and San Juan provinces; altitudinal distribution from sea level to elevations of about 4000 feet (1220 meters) south of Castillon, Dépt. du Sud,

Haiti, and to 3500 feet (1068 meters) west of Marmelade in the Chaine de Marmelade, Dépt. de l'Artibonite, and 3400 feet (1037 meters) south of Elías Piña in the Sierra de Neiba, La Estrelleta Province, República Dominicana.

Anolis ricordi ricordi Duméril and Bibron

Type locality. "St.-Dominguc"; here restricted to the vicinity of Port-au-Prince, Dépt. de l'Ouest, Haiti.

Definition. A subspecies of *A. ricordi* characterized by the combination of modally 7 snout scales between second canthal scales, 7 vertical rows of loreal scales, 4 scales between the supraorbital semicircles, 5/5 scales between the interparietal and the supraorbital semicircles, high number of vertical dorsal scales (17–26; mean 21.1), high number of ventral scales (19–32; mean 24.7), nuchal crest scales moderate (rarely) to low (usually), body crest scales moderate (rarely) to low (usually), subocular scales usually in contact with supralabial scales; males usually with some black lateral markings on the neck and thoracic region, and on the occipital region of the head, but at times these markings are absent (see discussion below), females green and without definite black lateral markings but at times reticulate with brown, the reticulum delimiting a pair of clear green lateral stripes or with three pale gray to green vertical narrow bars; dewlap variable, in males from peach or pale peach to gray or yellowish gray, and in females from peach to blue-gray or inky blue or inky black (see discussion beyond).

Distribution. Northern Haiti from Port-de-Paix east to Terrier Rouge and into the República Dominicana as far east as the vicinity of Los Quemados, Santiago Rodríguez Province, and as far south as Restauración, Dajabón Province, south in Haiti to the Port-au-Prince region (Morne Decayette, Diquini, Pétionville), as well as east into the República Dominicana in the Sierra de Neiba and the southwestern slopes of the Cordillera Central in La Estrelleta and San Juan provinces.

Discussion. I have little doubt that the extensive range that I here ascribe to nominate *A. ricordi* is incorrect. There are several very obvious differences in coloration and pattern between northern and southern specimens of *A. r. ricordi;* thus the definition of the subspecies, in order to include all pattern variants, is necessarily cumbersome. The problem is presently unresolvable since, other than the series from near Port-au-Prince and the specimens from northern Haiti, there are huge areas in Haiti whence specimens remain unknown. A detailed discussion of the chromatic and pattern features in the various segments of *A. r. ricordi* is given below.

The series of 50 specimens assigned to the nominate subspecies shows the following variation. The largest male (ASFS V31395) has a snout–vent length of 160, the largest female (ASFS V31397) 151; both are from 4.1 mi. NW Juan de Herrera, San Juan Province, República Dominicana. Snout scales at level of second canthals vary between 4 and 8; the mode is 7 (22 specimens). The vertical loreal rows vary between 6 and 10, with a mode of 7 (20 specimens). There are between 3 and 5 scales between the supraorbital semicircles (mode 4). There are modally 5 scales between the interparietal and the semicircles; 5 scales are involved in 53 percent of the combinations; actual counts are 3/3 (1), 4/4 (10), 4/5 (8), 5/5 (17), 5/6 (9), 6/6 (2), 7/7 (1), and 5/7 (1). Vertical dorsals range between 17 and 26 (mean 21.1), horizontal dorsals between 19 and 30 (24.6), and ventrals between 19 and 32 (24.7). Of 28 adult males, six have moderate nuchal crest scales and 22 have these scales low; of 11 females, all have the nuchal crest scales low. Body crest scales are moderate in two males and low in 26, and 11 females have the body crest scales low. The suboculars are separated from the supralabials in 45 of 49 instances, and contact between these scales occurs in four lizards (8 percent).

The southern specimens from the Port-au-Prince region and including two from

Mirebalais, consist of ten adult males, three adult females, and two juvenile females (MCZ 60013–14). The latter two specimens (with snout–vent lengths of 89 and 92 mm) can be easily dismissed in that they are presently patternless green. Color notes in life on one southern male (ASFS V9024) state that in the green phase, the lizard had the dorsum a mixture of pale green, brown, and yellow, with green the predominant color, the net effect being one of beadwork. The upper surface of the head was a mixture of pinkish and yellow scales, the mental region and adjacent upper labials were dull yellow, and the venter pale green. The dewlap was peach with the dewlap scales yellow. All males (with the exception of MCZ 69404, which is an albino) have some black to dark brown occipital blotching, usually extending onto the neck and thence onto the area above the forelimb insertion. The extent of the dark anterior markings is variable, but they are present in all males and quite vivid in freshly taken specimens. A pale subocular crescent is present, often extending posteriorly to form a pale preauricular blotch, bounded above by a large dark temporal blotch that may form an occipital chevron by joining its mate on the other side. Southern females were recorded in life as pale to bright green without any dark pattern, with a moderately well-defined pale subocular crescent that may expand into a pale preauricular blotch; the venters were yellow-green. In one female, the dewlap was reported as blue-gray with yellow-green streaks. The hindlimbs are not prominently banded. Neither sex has the throat marked with any blotching or dotting, although the females have the throat somewhat clouded with dull dark green.

The series for the Sierra de Neiba and the Cordillera Central consists of six males, four females, and eight juveniles and subadults. The males were described in life as being dark green with pale green crossbands, or pale green with four paler green crossbands, or patternless green. The upper surface of the head was creamy tan. Black blotches occur in this series of males also, but the occiput lacks clearly defined black areas, and the black on the body is much more extensive than it is in all southern males, the extreme condition being that shown by ASFS V31395, which has extensive black blotching over two-thirds of the back and sides. The pale subocular crescent is very obscure, but there is a prominent pale preauricular spot in most males. The females from this region are plain green, without dark markings, and there is a prominent pale supralabial blotch in the area which in males is occupied by the pale preauricular blotch. Dewlaps in males and females were invariably recorded as peach, and both sexes had charcoal eyeskins. As in southern specimens, the chins and throats are pale green and without any definite markings, except that the throats of females are suffused with darker green. The eight juveniles and subadults range in snout–vent length from 68 mm to 92 mm. The two smallest specimens, a male and a female, were rich pea-green in life with four, narrow, cream transverse crossbars, and the smaller had in addition black streaking in the green areas and a black postauricular smudge. The ventral color was rich pea-green and the dewlap skin was blue-black. All juveniles and subadults with snout–vent lengths of between 76 and 92 were bright emerald-green dorsally and without any dorsal dark or pale markings; one female juvenile (snout–vent length 78) had a lateral black nuchal spot followed by a bright yellow preaxillary bar, as well as a bright yellow subocular mark. The dewlap was recorded as black in a juvenile female with a snout–vent length of 89. Of the subadults, the most peculiar is a male (ASFS V31323) with a snout–vent length of 90 which shows, as preserved, a vague series of vertical lateral pale and dark areas, but as yet no black blotching typical of adult males.

The northern specimens are six males and one female from Haiti, five males and two females from the República Dominicana, and one Haitian subadult and two Domin-

ican subadult and juvenile lizards. Haitian males are not only quite different from northern Dominican males, but they are also strikingly different from central and southern males. In the Haitian males, the dorsum is gray-green with yellow-green flecking, or a beadwork mixture of dark and light green scales. The upper surface of the head is dark with light flecking, and in one male the head was recorded as dark brown with the centers of the scales pale purple. No male has any occipital dark blotching, and any body blotching, if it is at all present, is extremely restricted and maximally expressed as small black areas above the forelimb insertion (MCZ 66147). The pale subocular crescent is obscure, but there is a pale postlabial line leading to the auricular opening. Northern Dominican males, on the other hand, are brightly colored and have extensive black neck and side markings; in two males these latter extend far posteriorly on the body and tend to delimit two lateral stripes on each side. The upper surfaces of the head are not mottled but are pale uniform tan. In life, the pale subocular crescent is bold and pale blue to white, and it may extend to the auricular opening. In Haitian males, the dewlap is grayish to yellowish peach (pl. 12C5; all color designations from Maerz and Paul, 1950), pale gray-green (about pl. 19B2), or yellowish gray (about pl. 20B1). In northern Dominican males, the dewlap is pale peach to pale yellow or grayish yellow, and the dewlap may be speckled with brown basally.

The single Haitian female is presently unmarked green, with faint scattered cream flecking. The larger of the two Dominican females was pale green above with a darker brown reticulum outlining a pair of green lateral stripes on each side. There was a postauricular brown smudge, followed by a pale blue axillary smudge. The temples were yellow-green, the lores pale blue and brown, the eyeskin pale green, and there was a pale blue subocular crescent that extended into a preauricular pale blotch. The top of the head was marbled pale tan and dark brown, and the venter was the same color as the dorsum. The other Dominican female was green without any dorsal markings.

The Haitian subadult (MCZ 66148) is a female with a snout–vent length of 106. It is speckled with pale scales on a dark ground like Haitian males. The smaller of the two Dominican males (ASFS V18008) has a snout–vent length of 75 and was bright yellow-green above with two cream crossbands and a yellow subocular crescent. The second Dominican male (ASFS V32160) has a snout–vent length of 103 mm, and, like Dominican adult males, has extensive black blotching on the head, neck, and almost the entire dorsum. The ground color was pale green, and the dewlap was dark brown.

To summarize all the above data, it is obvious that I have included several populations in *A. r. ricordi* which differ rather strikingly among themselves. Southern Haitian males are marked with black on the occiput, neck, and anterior sides, and central Dominican and northern Dominican specimens increase this tendency to show even more extensive black lateral markings. On the other hand, northern Haitian males as a group show very little or no black markings and are basically green-flecked green lizards. Northern Dominican males are much more colorful than specimens from elsewhere, and much more contrastingly marked. On the other hand, all females are fairly similar, with the exception of the remarkably colored and patterned female from the northern República Dominicana. I suspect that it will ultimately be shown that there are at least two more nameworthy populations included in *A. r. ricordi* as here defined by me: a northern Haitian subspecies, a northern and central Dominican population, as well as the southern Haitian one. But the specimens at this time are from such disjunct localities and are so limited in number that I am unwilling to make the suggested nomenclatural additions.

Remarks. *A. r. ricordi* occurs in a wide

variety of situations but is of course always associated with trees. Its altitudinal range is from sea level at many localities to elevations of 3500 feet (1068 meters) in the Chaine de Marmelade in northern Haiti and 3400 feet (1037 meters) in the Sierra de Neiba. Almost all specimens taken by myself and parties were secured sleeping at night. Williams (1965: 2–3) noted that in the Monte Cristi region these lizards sleep in viny tangles, especially where there are dense "mats" or "curtains" of vines under a canopy. Such a situation is ideal in the xeric forests in the Monte Cristi area. At Las Matas de Farfán, the lizards were easily secured at night in a high-canopied *cafetal*, sleeping on limbs, branches, or on vines, either vertical or horizontal. A specimen from Morne Calvaire near Pétionville was seen during the late morning on a mango tree in an open pasture, about 4 feet (1.2 meters) above the base. Thomas commented in his field notes upon a specimen from Le Borgne which was observed 8 feet (2.4 meters) above the ground on the trunk of a tree; this male led the pursuers a merry chase through a series of three trees and finally sought refuge in dense grass on the ground, where it was caught! The male from Terrier Rouge was collected with a slingshot while it rested head-down on the main branch of a large tree 15 feet (4.6 meters) above the ground. South of Las Matas de Farfán I secured a juvenile sleeping on a horizontal vine in a tree-fern thicket adjacent to a mountain brook. The association of *A. r. ricordi* with rivers or lakes is certainly fortuitous; the greatest concentrations of these lizards occur in such obviously mesic situations only because there is often gallery forest restricted, or limited by man, to streamsides. However, such a situation is not a guarantee of securing specimens. In our effort to narrow the previously existing gap between *ricordi* and *baleatus* in the northwestern República Dominicana, we questioned natives concerning the occurrence of *saltacocotes* in the region along the gallery-forested Río Yaque del Norte, which here passes through cactus desert. We were assured that the lizards indeed occurred there, and we were fortunate in finding a superb area of gallery forest in the steep-sided valley of the Río Guarabo, west of Los Quemados. The Guarabo is a southern affluent of the Yaque, and we had no doubt that these splendid hardwoods harbored *A. ricordi*. But it was not until our fifth nocturnal visit that a single subadult was secured, despite the attentions of four collectors. The woods here present a perfect aspect for *A. ricordi* —dense and large trees connected and interlaced with vines and lianas, all quite rich and mesic; still, our experience indicates that, at least at the time of our visit, *A. ricordi* was distinctly uncommon or difficult to see in what elsewhere surely would have been a typically simple area for collection of these lizards. In this instance, demands for at least one specimen from this region forced persistence which ultimately yielded the requisite animal. Such may well be the case in many otherwise xeric regions, where *A. ricordi* is restricted to (and perhaps is rare in) more mesic riverine hardwood stands.

Specimens examined. HAITI: *Dépt. de l'Ouest*, Source Leclerc, Morne Decayette (MCZ 65729–31); Diquini (MCZ 8619, USNM 118902, USNM 123347, USNM 123988); Port-au-Prince (AMNH 49501); Pétionville (MCZ 60013–14); Morne Calvaire, 1 mi. (1.6 km) SW Pétionville, 2300 feet (702 meters) (ASFS X1711, ASFS V8514, ASFS V9024); Mirebalais (MCZ 69404); Lancironelle, nr. Mirebalais (not mapped) (MCZ 68479); *Dépt. de l'Artibonite*, 8–9 km W Marmelade, 3500 feet (1068 meters) (ASFS V9925); *Dépt. du Nord Ouest*, Port-de-Paix (MCZ 63338); *Dépt. du Nord*, 3 mi. (4.8 km) SW Le Borgne (ASFS V10005); 2 mi. (3.2 km) SW Cap-Haïtien (ASFS V10766); Ti Guinin, nr. Cap-Haïtien (not mapped) (MCZ 66147–49); 8 mi. (12.8 km) E Terrier Rouge (ASFS V10169). REPÚBLICA DOMINICANA: *Monte Cristi Province*, 1 km W Copey (ASFS V1269, ASFS V1411–12, ASFS V1470); Laguna de Salodillo, 7

km E Pepillo Salcedo (ASFS V1413); *Dajabón Province,* Restauración (ASFS V18006–08); *Santiago Rodríguez Province,* 1.8 mi. (2.9 km) W Los Quemados, 500 feet (153 meters) (ASFS V32160); *La Estrelleta Province,* 6.7 mi. (10.7 km) E Hondo Valle, 2500 feet (763 meters) (ASFS V31428); 11.0 mi. (17.6 km) S Elías Piña, 3400 feet (1037 meters) (ASFS V31509); *San Juan Province,* 4.9 mi. (7.8 km) NW Vallejuelo, 2400 feet (732 meters) (ASFS V31305); 6.1 mi. (9.8 km) S Las Matas de Farfán, 1800 feet (549 meters) (ASFS V14562, ASFS V31469, ASFS V31319–26); 4.1 mi. (6.6 km) NW Juan de Herrera, 1600 feet (488 meters) (ASFS V31395–99).

Anolis ricordi leberi Williams

Anolis ricordii leberi Williams, 1965. Breviora, Mus. Comp. Zool., No. 232: 4.

Type locality. Camp Perrin, Département du Sud, Haiti; holotype, MCZ 80935.

Definition. A subspecies of *A. ricordi* characterized by the combination of modally 4 snout scales between second canthals, 6 vertical rows of loreal scales, 3 scales between the supraorbital semicircles, 4/4 scales between the interparietal and the supraorbital semicircles, low number of vertical dorsal scales (14–21; mean 16.5), low number of ventral scales (15–28; mean 20.2), nuchal crest scales usually moderate, rarely low in males, usually low, occasionally moderate in females, subocular scales in contact with supralabials in almost 50 percent of the specimens; males either pale yellow-green with four dark saddles and a bluish green flank stripe, or with about three longitudinal dark brown lateral stripes, or simply dark brown, females bright green (much brighter than males), with longitudinal black lines indicated and at times a greenish tan middorsal wash; dewlap bright orange or orange with an anterior brown wash in males, and dull orange, at times suffused or marbled with brown, in females.

Distribution. Known only from the vicinity of the type locality and Marceline, on the southern slopes of the Massif de la Hotte, between elevations of 1000 and 1220 feet (305 and 372 meters), Dépt. du Sud, Haiti.

Discussion. In contrast to the situation in *A. r. ricordi, A. r. leberi* is known from a long series of specimens all from the same general area, at elevations between 1000 feet and 1220 feet (305 and 372 meters). Williams (1965: 6) assigned a single juvenile (MCZ 38277) from Tardieu, near Pic Macaya, Dépt. du Sud, Haiti, to *leberi* with some reservation. This locality is northwest of Camp Perrin-Marceline, is on the northern slopes of the Massif de la Hotte, and is much closer to the known distribution of the next subspecies to be described below.

The series of 54 *A. r. leberi* shows the following variation. The largest male (ASFS X3034) has a snout–vent length of 147, the largest female (AMNH 98723) 153; both are from Camp Perrin. Snout scales at level of the second canthal are extremely variable, and range between 2 and 7; the mode is 4 (23 specimens). The vertical loreal rows vary between 5 and 8, with a mode of 6 (26 specimens). There are between 1 and 4 scales between the supraorbital semicircles (mode 3). There are modally 4 scales between the interparietal and the semicircles; 4 scales are involved in 64 percent of the combinations; actual counts are 3/3 (3), 3/4 (7), 4/4 (25), 4/5 (10), 5/5 (2), 5/6 (2), 6/6 (1), 3/5 (1), and 5/7 (1). Vertical dorsals range between 14 and 21 (mean 16.5), horizontal dorsals between 15 and 24 (18.0), and ventrals between 15 and 28 (20.2). Of 39 adult males, 30 have the nuchal crest scales moderate and nine have them low; of 13 females, five have the nuchal scales moderate and eight have them low. Body crest scales are moderate in 12 males and low in 27 males, whereas only one female has the dorsal crest scales moderate and 12 have them low. The subocular are separated from the supralabials by 1 row of scales in 28 specimens and are in contact with the supralabials in 26 specimens. *A. r. leberi* is the only population

that has such a high incidence (48 percent) of subocular-supralabial contact.

Males show three basic patterns: 1) dorsal ground color pale yellow-green with four dark brown saddles and a bluish green flank stripe that is complete; 2) about three longitudinal dark brown stripes, the central one being the most prominent and complete; 3) and a uniform dark velvety brown. In the two lighter phases, the eyeskin is pale blue, chin and throats are dull yellow-green, and the subocular crescent is pale blue and very conspicuous. The dewlaps in males are orange (brighter than any Maerz and Paul designation) or orange with an anterior brown wash. Females are bright green dorsally (much brighter than males) with longitudinal black lines indicated. There is a greenish tan wash on the upper surface of the head, and there may be a greenish tan middorsal zone on the body. The dewlap in females is dull orange, often suffused or marbled with brown, and the eyeskin is green, paler than that of the dorsum. In males, the venter is pale green and may be washed with brown even in the green phase, and in females the venter is pale yellow-green, paler than the bright green of the dorsum.

In general aspect, male *A. r. leberi* are lineate dorsally and laterally, the bold dark longitudinal lines usually interrupted by four irregular pale vertical crossbands, which are in turn bordered with darker pigment. Although my field notes indicate that there are about three longitudinal dark stripes in males, these three stripes are the result of modification of two stripes, of which the more dorsal is the broader. In many specimens, this upper flank stripe maintains its integrity, but in many others the upper stripe is hollowed centrally, resulting in three narrow dark stripes, rather than two stripes, of which the upper is very broad and the lower is narrow. Although females show some longitudinal striping, it is much less conspicuous than in males. Male throats are immaculate, whereas female throats are suffused with dark green.

There are three juveniles and subadults from the type locality. The smallest (MCZ 83982) is a female with a snout–vent length of 52. The body is longitudinally streaked, but there are as yet no definite longitudinal lines. The subadults (MCZ 80949–50, a male with a snout–vent length of 105, and a female with a snout–vent length of 93) both show indications of the longitudinal stripes that are characteristic of adults, but the stripes are better defined in the subadult male than in the female. The two adult males and two adult females from Marceline agree in all pattern details with the topotypical series; Marceline and Camp Perrin are separated by about 4.5 kilometers airline.

Comparisons. Although both *A. r. ricordi* and *A. r. leberi* have several features in common, namely, the moderate to low nuchal and body crests, the presence of some sort of black body markings, and a prominent pale subocular crescent, these two subspecies are eminently distinct. They differ in: modal number of second canthal snout scales (*ricordi* 7, *leberi* 4), modal number of loreal rows (*ricordi* 7, *leberi* 6), modal number of scales between the interparietal and supraocular semicircles (*ricordi* 5/5, *leberi* 4/4), higher means of vertical dorsal scales and ventrals (21.1, 24.7 in *ricordi,* 16.5, 20.2 in *leberi,* respectively) and the very high incidence of contact between the subocular scales and the supralabials in *leberi* versus the rarity of this condition in *ricordi.* In addition, the dewlap in male *ricordi* is most often some shade of peach (although the variation in dewlap shades and colors in *ricordi* is readily acknowledged), whereas in male *leberi* the dewlap is orange or orange with a brown anterior wash. A ready hallmark between the two subspecies is the presence of a pale preauricular blotch in *ricordi,* a condition always absent in both sexes of *leberi,* with the result that instead of the pale subocular crescent's being incorporated into a postlabial line or preauricular blotch as it often is in *ricordi,* it is a bold and contrasting pattern element.

Remarks. All Camp Perrin specimens of

A. r. leberi were collected by natives and thus I have no precise knowledge of the habitat nor habits of this subspecies. Camp Perrin lies in the lower southern foothills of the high Massif de la Hotte, at about 1000 feet (305 meters), and the area in general is very mesic and presumably was once well forested, although now it supports *cafeières* with a high-canopy hardwood shade cover. Williams (1962: 10) cited field notes by A. S. Rand and J. D. Lazell, Jr., on *A. r. leberi* at Camp Perrin and Marceline; both accounts involve trees associated with coffee plantings.

Specimens examined. HAITI: *Dépt. du Sud,* Camp Perrin (ASFS X3033–35, ASFS X3038–39, ASFS X3041–42, ASFS X3182, AMNH 93713–36, MCZ 80935–37, MCZ 80939–42, MCZ 80944–53, MCZ 83982); Marceline (MCZ 121115); Marceline area, *ca.* 1000 feet (305 meters) (MCZ 122269, MCZ 121779–80).

Anolis ricordi viculus new subspecies

Holotype. USNM 193974, an adult male, from Castillon, 2500 feet (763 meters), Département du Sud, Haiti, taken by native collector on 25–26 June 1971. Original number ASFS V25059.

Paratypes. ASFS V25058, same data as holotype; ASFS V25060, same locality and collector as holotype, 27 June 1971; ASFS V24801, *ca.* 2 km (airline) S Castillon, 3500–4000 feet (1068–1220 meters), Dépt. du Sud, Haiti, R. Thomas, 24 June 1971; ASFS V9335, *ca.* 5 km (airline) SE Marché Leon, 2200 feet (671 meters), Dépt. du Sud, Haiti, native collector, 15 March 1966; MCZ 119035, Castillon, Dépt. du Sud, Haiti, T. P. Webster, A. R. Kiester, and native collectors, 31 August 1969.

Definition. A subspecies of *A. ricordi* characterized by the combination of modally 6 snout scales between the second canthals, 7 vertical rows of loreal scales, 4 scales between the supraorbital semicircles, 4/4 scales between the interparietal and the supraorbital semicircles, low number of vertical dorsal scales (15–19; mean 16.7), moderate number of ventral scales (19–24; mean 21.8), nuchal crest scales usually moderate but occasionally low in both sexes, dorsal body crest scales low in both sexes, subocular scales almost always separated by one row of scales from supralabial scales; males bright green dorsally with powdery pale blue-green lateral stripes, throat pale green and unmarked, venter pale green with pinkish and yellowish suffusions, females dark olive-green to bright green with two purple to powdery blue-gray flank stripes edged with dark brown, lower sides spotted bright green, yellow-green, or bright green with four bright yellow-green crossbands edged with black, throat pale green; dewlap deep yellow to orange in males, dull orange (almost brown) to deep yellow with orange streaking and bluish edge in females.

Distribution. Known only from the vicinity of Castillon on the northern slopes of the Massif de la Hotte at elevations between 2200 and 4000 feet (671 and 1220 meters) on the Tiburon Peninsula in Haiti; probably the subspecies occurring at Tardieu near Pic Macaya (see discussion).

Description of holotype. An adult male with a snout–vent length of 143 and a tail length of 165 (regenerated); snout scales at level of second canthals 6, 7 vertical rows of loreal scales, 3 scales between supraorbital semicircles, 6/5 scales between interparietal and supraorbital semicircles, vertical dorsals 15, horizontal dorsals 22, ventrals 20, one row of scales between suboculars and supralabials, fourth toe lamellae on phalanges II and III 31, nuchal crest scales moderate, body crest scales low; in life, bright green above with a pair of lateral stripes on each flank powdery pale blue-green, the same color also on the face; throat and neck pale blue-green; venter pale green with pinkish and yellowish suffusions; dewlap deep yellow, almost orange.

Variation. The series of three males and three females shows the following variation. The largest male (ASFS V25058) has a snout–vent length of 148, the largest female (ASFS V25060) 141; both are from

Castillon. Snout scales at level of the second canthal range between 5 and 9; the mode is 6 (four specimens). The vertical loreal rows are 6 or 7, with a mode of 7 (five specimens). There are between 3 and 5 scales between the supraorbital semicircles (mode 4). There are modally 4 scales between the interparietal and the supraorbital semicircles; 4 scales are involved in 58 percent of the combinations; actual counts are 4/4 (3), 4/5 (1), 5/5 (1), and 5/6 (1). Vertical dorsals range between 15 and 19 (mean 16.7), horizontal dorsals between 17 and 27 (20.0), and ventrals between 19 and 24 (21.8). Of three males, two have the nuchal crest scales moderate and one has them low; the same situation applies to the three females. All specimens have the body crest scales low. The suboculars are usually separated from the supralabials by one row of scales and are in contact with the supralabials in one individual (17 percent).

Thomas's field notes on three males show the variation in dorsal coloration and pattern. The dorsum was bright green with the flank stripes powdery pale blue-green, this color occurring also on the face. The throat and neck were also pale blue-green and the venter was pale greenish with pink and yellow suffusions. One male (ASFS V9335) also had a white shoulder patch, but other pattern details on this individual were lacking since the specimen was badly damaged. The dewlap in the males was recorded as deep yellow (almost orange) and orange (Pl. 11L6). One female was green to dark olive-green dorsally with two purple flank stripes, edged with dark brown, which were powdery blue-gray anteriorly. The lower sides were spotted and suffused with bright green or yellow-green. The venter was pale green with a pinkish wash in the pectoral region. The second female was marked in quite a different fashion, and the specimen still maintains the pattern after preservation. The dorsum was bright green with four bright yellow-green transverse body bands with black edges; in this specimen longitudinal stripes were also present but only in the nuchal region, and the venter, including the throat, was pale green. In both females, the dewlaps were recorded as "very dull orange" and "deep yellow, almost brown, anteriorly, with orangish longitudinal striae, each edged with dark gray-green, between striae pale gray-green and most basal striae greenish; edge of dewlap grayish (faintly blue)."

Comparisons. *A. r. viculus* is so very different from *A. r. ricordi* in both color and pattern that detailed comparisons are hardly necessary. The black occipital, nuchal, and anterior body blotches of male *ricordi* are absent in male *viculus*, and the longitudinally striped pattern in both sexes of *viculus* does not occur in *ricordi*. The two subspecies differ also in scale counts, as follows: modal number of snout scales at second canthals (*ricordi* 7, *viculus* 6), scales between interparietal and supraorbital semicircles (*ricordi* 5/5, *viculus* 4/4), and much lower means of vertical dorsal and ventral scales (21.1, 24.7 in *ricordi*, 16.7, 21.8 in *viculus*, respectively). The two taxa are similar in number of loreal rows, number of scales between the semicircles, and in relative frequency of contact between the subocular and supralabial scales.

In every way, *viculus* is much closer to *leberi* than to *ricordi*. The basic pattern elements are comparable in these two subspecies, since both are lineate; however, the longitudinal flank stripes in *leberi* are dark, whereas in *viculus* they are light; the single banded female *viculus* is quite different in general aspect from banded *leberi*. As far as scale counts are concerned, the two subspecies differ in the following manner: modal number of snout scales at second canthals (*leberi* 4, *viculus* 6), number of vertical loreal rows (*leberi* 6, *viculus* 7), and scales between supraorbital semicircles (*leberi* 3, *viculus* 4). In mean number of vertical dorsals and ventrals, the two subspecies are very similar, and both have the 4/4 condition as the mode for the interparietal-semicircle relationship.

Discussion. Williams (1962: 7–8) con-

sidered the four specimens then available from the central portion of the Tiburon Peninsula as intergrades between *ricordi* and *leberi.* A few more specimens have accumulated since that time; now there are one adult male, one juvenile male, and six adult females from this central region, as follows: HAITI: *Dépt. du Sud,* Pemel, nr. Miragoâne (not mapped) (MCZ 66015–16), Paillant, 1800 feet (549 meters) (ASFS V26535–37); Fond des Nègres (ASFS V26254, USNM 72631, USNM 72633). As preserved, the adult male shows fairly obvious longitudinal streaking of gray and dull green, a few scattered dark flecks or small blotches above the forelimb insertion, and a prominent subocular pale crescent. The adult male is an almost ideal representation of extreme intergradation between *viculus* and *ricordi,* with both pale longitudinal stripes and scattered remnants of the typical *ricordi* extensive body blotching. Three recently collected females in life were green with longitudinal stripes, which were delimited by absence of black flecking that occurs elsewhere on the green ground. In the brown phase, these longitudinal stripes had a reddish wash. In all females, the pale subocular crescent is obvious and bold, and in one female (MCZ 66016) there is an additional preauricular pale area that resembles the condition in nominate *ricordi.* I have no color data on the male dewlaps, but that of one female (ASFS V26535) was dull yellow distally and pale blue, smudged with charcoal, basally; the dewlap scales were yellow-green. The juvenile male (snout–vent length 79) in life had a pattern of longitudinal dorsolateral stripes and dorsal crossbands, with a pale yellow subocular crescent. I interpret these lizards as intergradient between *ricordi* and *viculus.* The central Tiburon localities, however, are far removed from the known localities of *viculus* (110 km) on one hand and of *ricordi* (70 km) on the other. Williams (1965: 7) regarded the Fond des Nègres and Pemel specimens as *ricordi* × *leberi* intergrades, and they could indeed be so interpreted. Since, however, *leberi* occurs on the southern slopes of the Massif de la Hotte, and *viculus* on the northern slopes of that range, and since all intergradient specimens are from the northeastern regions of the extreme eastern portion of the Massif de la Hotte, it seems much more likely that these central Tiburon specimens are intergradient between *ricordi* and *viculus* on geographic grounds. They do not disagree with my concepts of how intergrades between these two subspecies probably should appear.[1]

[1] Since the above comments on the intergradient specimens were written, Williams has secured a series of 28 lizards (MCZ 132302–29) from St. Croix, 1 mi. (1.6 km) from Paillant, Dépt. du Sud, Haiti, from this same general region. There are no color data on the specimens. The measurements (in mm) and scale counts of these lizards, combined with those from the eight previously available specimens, follow. Largest male (MCZ 132325) 155, largest female (ASFS V26535) 148. Snout scales at second canthals 4–9 (mode 6); loreal rows 4–8 (mode 6). Modally 4/4 scales between the interparietal and the supraorbital semicircles; other counts: 3/3 (2), 3/4 (2), 4/5 (4), 5/5 (11), 5/6 (1), 3/5 (1); 4 scales are involved with 50 percent of the combinations. Vertical dorsals range between 14 and 21 (mean 17.0), horizontal dorsals between 15 and 24 (18.3), and ventrals between 16 and 31 (21.4). Of the males, four have the nuchal crest scales moderate and 15 have them low; of the females, one has the nuchal crest scales moderate and 15 have them low. Body scales are low in all adult specimens. The suboculars are modally separated from the supralabials by one row of scales and are in contact with the supralabials in seven lizards (19 percent).

In scale counts, the entire series is much closer to *viculus* than to *ricordi;* however, in some characteristics, the series is closer to *leberi* or to the subspecies yet to be described from extreme southeastern Haiti. In fact, comparison of the scale counts shows that there is little resemblance between the modes and means between these geographically intermediate specimens and nominate *ricordi,* and as a whole they seem much more closely allied to one of the other Tiburon subspecies.

The males in the St. Croix series are variable in pattern but none shows any clear-cut dark blotching, typical of *A. r. ricordi.* Some males are more or less unicolor (medium brown as preserved), whereas others have longitudinal stripes, alternating light and dark, with usually one broad

There remains one other specimen from the distal portion of the Tiburon Peninsula; this is a juvenile male (MCZ 38277) with a snout–vent length of 78, from Tardieu, near Pic Macaya, collected by P. J. Darlington. It is presently dull brown, but there are clear indications of black-edged dorsal crossbands that closely resemble the condition in one of the female paratypes of *viculus*. Tardieu is presently unlocatable on modern maps, but Darlington has indicated to Williams that this place lies just to the north of Pic Macaya, and thus rather close to Castillon. Since there are no juvenile *viculus*, I have no concepts of their appearance; on geographic grounds, however, I have little doubt that the Tardieu male is representative of *viculus* rather than of *leberi*.

Remarks. It may seem remarkable that there should be two distinctive subspecies of *A. ricordi* in such close geographical proximity; Castillon and Marceline are separated by only 29 kilometers airline, and if the Tardieu specimen is *viculus*, then the distance between the localities for the two subspecies is even shorter. However, between Castillon and Marceline lies the high ridge of the La Hotte, including the culminating peak of that range, Pic Macaya, with an elevation of 7698 feet (2347 meters). Such high and rugged country is probably ecologically unsuitable for *A. ricordi*, and the northern and southern populations associated with the La Hotte have differentiated because of isolation caused by the intervening massif.

The known altitudinal range of *A. r. viculus* is between 2200 and 4000 feet (671 and 1220 meters). The Castillon area, according to Richard Thomas, is generally mesic but much of the original forest has been cut. Still, enough trees and ravine woods remain to offer haven for such a tolerant and adaptable species as *A. ricordi*. One female from south of Castillon was taken by Thomas on the trunk of a large tree about 5 feet (1.5 meters) above the ground; all other ASFS specimens were secured by natives.

The name *viculus is* from the Latin for "hamlet" or "small village" in allusion to Castillon, the type locality.

Anolis ricordi subsolanus new subspecies

Holotype. MCZ 130270, an adult male, from Source Carroyé, near Saltrou, Département de l'Ouest, Haiti, one of a series collected by George Whiteman in March 1972.

Paratypes. MCZ 130264–69, MCZ 130271–77, same data as holotype; MCZ 69405, nr. Saltrou, Dépt. de l'Ouest, G. Whiteman, summer 1962.

Definition. A subspecies of *A. ricordi*

---

dark stripe along the upper sides and most prominent. One male has extensive dark brown body markings, vertically oriented and alternating with paler tannish areas to give a more-or-less vertically barred appearance. The pale subocular crescent is very obvious in all males, and there is no indication of a pale preauricular area.

The females are undistinguished. Most are more or less solid green with some scattered paler green scales to give a beadwork effect dorsally, but there are also indications in some specimens of longitudinal paler areas to give a somewhat longitudinally lined appearance. As in the males, the subocular pale crescent is obvious, and there may be a weakly differentiated pale preauricular area.

This newly collected series of *A. ricordi* is puzzling. The entire lot is so like, in general aspect, specimens of *leberi* and *viculus* (and the yet-to-be-named subspecies in southwestern Haiti) and shows so little tendency toward *A. r. ricordi* that it is difficult to interpret them as intergradient between *ricordi* and *viculus*. The adult male (MCZ 66015) noted above in the body of the text is from "Pemel, near Miragoâne," a site that is unlocatable on modern maps. Pemel may be "near Miragoâne" in only the very broadest sense. Specimens that are *known* to have been taken in the Miragoâne-Paillant area show little evidence of intergradation between *viculus* and *ricordi*, and are much closer to the former subspecies.

Everything considered, I strongly suspect that with additional collecting on the central Tiburon Peninsula it is probable that two taxa will be found to occur here in sympatry and without wide areas of intergradation, or that *ricordi*-styled anoles occur close to (but do not intergrade with) *leberi*-styled anoles. The evidence at the moment is far from unequivocal that *ricordi* and *viculus* intergrade in this area. Only much additional collecting along the Tiburon Peninsula will reveal the actuality of the relationships of *A. ricordi* with its southeastern relatives.

characterized by the combination of modally 5 snout scales between second canthals, 5 vertical rows of loreal scales, 3 scales between the supraorbital semicircles, 4/4 scales between the interparietal and the supraorbital semicircles, moderate number of vertical dorsal scales (16–21; mean 17.3), moderate number of ventral scales (18–27; mean 21.0), nuchal crest scales rarely moderate, usually low in males, low in females, subocular scales always separated from supralabials scales by one row of scales; males vaguely lineate dorsally with two broad lateral grayish flank stripes, or with three paler (green in life?) crossbands; females like males, or heavily blotched with black laterally and on the occiput, the black lateral markings in the areas that are elsewhere occupied by the gray lateral flank stripes; a pale subocular crescent present and prominent but no pale preauricular blotch; dewlap color unknown.

Distribution. Known only from the region about Saltrou, in extreme southeastern Haiti, but see discussion below.

Description of holotype. An adult male with a snout–vent length of 144 mm and a tail length of 209 mm (regenerated); snout scales at level of second canthals 4, 6 vertical rows of loreal scales, 3 scales between supraorbital semicircles, 3/4 scales between the interparietal and the supraorbital semicircles, vertical dorsals 18, horizontal dorsals 17, ventrals 19, one row of scales between suboculars and supralabials, fourth toe lamellae on phalanges II and III 33, nuchal crest scales low, body crest scales low; as preserved, dorsum dull dark brown with three prominent blue-green crossbands, more or less confluent middorsally, and outlined in dark brown to black; top of head brown, paler than sides; throat greenish, dewlap dull gray; belly dark gray, underside of hindlimbs green; tail brown.

Variation. The holotype and paratypic series are composed of 10 males and five females. The largest male (MCZ 130274) has a snout–vent length of 152, the largest female (MCZ 69405) 150; the male is a topotype, the female is from near Saltrou. Snout scales at level of the second canthals range between 4 and 7; the mode is 5 (six specimens). The vertical loreal rows vary between 5 and 7, with a mode of 5 (eight specimens). There are between 2 and 4 scales between the supraorbital semicircles (mode 3). There are modally 4 scales between the interparietal and the supraorbital semicircles; 4 scales are involved in 58 percent of the combination; actual counts are 3/3 (1), 3/4 (3), 4/4 (4), 4/5 (3), 5/5 (2), and 5/6 (2). Vertical dorsals range between 16 and 21 (mean 17.3), horizontal dorsals between 14 and 23 (17.1), and ventrals between 18 and 27 (21.0). Of 10 males, two have the nuchal crest scales moderate and eight have these scales low; all five females have the nuchal crest scales low. All specimens have the body crest scales low. In all specimens the subocular scales are separated from the supralabials by one row of scales.

I have no color notes in life nor have I seen live specimens of *A. r. subsolanus.* Consequently, my comments on pattern in this subspecies are based solely upon preserved material. In the series of males and females, each sex shows two basic patterns. The more common is a pair of longitudinal flank stripes, the upper being broader, usually dull grayish in contrast to a greenish ground color. In two specimens (one male and one female; MCZ 130267 and MCZ 69405) these stripes are very prominent and black; although they no longer have their integrity in the female, they are still very obvious. In addition, in the female there is black pigment in the occipital region. A pale subocular crescent is present in all specimens and is usually very conspicuous. In two specimens (the holotypic male and a female—MCZ 130266) the dorsal pattern consists of three transverse crossbands that are green, more or less fused middorsally, and outlined with black or dark brown. Many females show the lat-

eral flank stripes much less clearly than do the males, but usually the stripes are at least indicated.

Comparisons. In general aspect, *subsolanus* much more closely resembles far western *leberi* and *viculus* than geographically closer *ricordi.* The latter subspecies, however, occurs on the northern side of the Massif de la Selle, whereas the localities for *subsolanus* are to the south of that range. Since I do not know the coloration in life of *subsolanus,* I am unable to compare its pigmentation with that of the other subspecies. The presence of both longitudinally striped and transversely barred specimens in *subsolanus* suggests its affinity with *leberi* and *viculus. A. r. subsolanus* differs from *A. r. ricordi* in that the latter has (in its southern populations) dark anterior markings on the occiput and above the forelimb insertions, whereas these markings are absent in *subsolanus.* Additionally, southern *ricordi* are patternless green, whereas *subsolanus* females are longitudinally lined and may have heavy dark anterior markings (somewhat like male *A. r. ricordi*). At the time of Williams's review of *A. ricordi* (1965: 2), there was but a single *A. ricordi* from the Saltrou region; by chance, this specimen (MCZ 69405) is the heavily marked female upon which I commented above. Although Williams (*loc. cit.*) considered it a male, it lacks enlarged postanal scales and a tail "fin," and it is a female. Since female *A. r. ricordi* lack dark anterior markings, this female is really quite different from females of the northern subspecies.

From the western subspecies *leberi* and *viculus, subsolanus* differs meristically in the following ways. From *leberi, subsolanus* differs in having 5 versus 4 snout scales at the second canthal, 5 versus 6 vertical loreal rows, higher means in vertical dorsal scales and ventral scales, and also lacks specimens that have the suboculars in contact with the supralabials (*leberi* has 48 percent of the specimens with this condition). From *viculus, subsolanus* differs in having 5 versus 6 snout scales at second canthal, 5 versus 7 vertical loreal rows, 3 versus 4 scales between the supraorbital semicircles, and higher means of vertical dorsal scales and ventral scales. In addition to the pattern differences noted above which differentiate *subsolanus* from nominate *ricordi, subsolanus* has 5 versus 7 snout scales at the second canthals, 5 versus 7 vertical loreal rows, 3 versus 4 scales between the supraorbital semicircles, 4/4 versus 5/5 scales between the interparietal and the supraorbital semicircles, and lower means in vertical dorsal scales and ventral scales.

Remarks. I am once more hampered in my interpretation of *subsolanus* by the large distributional gap between its two stations and any other stations for *A. ricordi* to the west. The absence of specimens from the southern coast, from such well-known areas as Jacmel and Aquin, is truly puzzling. The nearest locality to *subsolanus* along the Tiburon Peninsula is Fond des Nègres (*ricordi* × *viculus*), some 120 kilometers to the west. Still further, the area known to be occupied by *A. r. leberi* lies some 205 kilometers to the west, near the peninsula's tip. Known stations for *A. r. ricordi* are very much closer (40 kilometers) but lie to the north of the Massif de la Selle. Closer even than any of these is *barahonae; barahonae* and *subsolanus* are known in this region for localities separated by about 11 kilometers (see comments below), but there is no evidence of intergradation between these two taxa.

It is perhaps pertinent that *leberi, viculus,* and *subsolanus* all seem closer in most characteristics to each other than they do to nominate *ricordi.* If it were not for the specimens that I interpret as intergradient between *ricordi* and *viculus* in the Miragoâne-Paillant-Fond des Nègres region, I would be very tempted to consider these three taxa as a species distinct from *A. ricordi.* Much additional material from along the Tiburon Peninsula will perhaps show that my interpretation is wrong.

The name *subsolanus* is from the Latin for "eastern," in allusion to the occurrence of this subspecies in southeastern Haiti. The precise areas where *subsolanus* occurs are a matter of question. I am unable to locate Source Carroyé on any modern map. Williams advised me that Source Carroyé is very near Thiotte (according to the collector, "Source Carroyé is located northeast direction and about ½ mile from the main road after you leave the place of the 'marché'," that market being at Thiotte). The elevation of Thiotte is about 900 meters. The lone specimen from "near Saltrou" also poses the problem of just how "near" this specimen was taken to Saltrou itself. Any information on details of localities or elevations of this and other specimens taken along the Dominico-Haitian border are mandatory. The distance between the Thiotte locality for *subsolanus* and the Pedernales specimens of *barahonae* is about 11 kilometers. It is especially pertinent that *barahonae* is not known, along the Dominico-Haitian border, from the lowlands (where, incidentally, *Anolis coelestinus* is called *saltacocote* by the natives), but that *barahonae* occurs here as an inhabitant of mesic riverine woods at an elevation of 600 feet (183 meters).

Anolis barahonae Williams

Anolis ricordii barahonae Williams, 1962. Breviora, Mus. Comp. Zool., No. 155: 8.

Type locality. Polo, Valle de Polo, Barahona Province, República Dominicana; holotype, MCZ 43819.

Definition. A giant species of Hispaniolan *Anolis* characterized by the combination of moderate size (males to 158 mm, females to 148 mm snout–vent length), snout scales at level of second canthal scales 2 to 5 (mode 4), vertical loreal rows 2 to 5 (mode 6), scales between supraorbital semicircles 1 to 4 (mode 2), interparietal scale separated from supraorbital semicircles modally by 4 scales, vertical dorsal scales generally small (15 to 34 in standard-distance), ventral scales relatively small (17 to 29 in standard-distance), nuchal crest scales in both sexes rarely high, usually moderate to low, dorsal body crest scales rarely moderate, usually low, subocular scales rarely in contact with supralabial scales; dorsal body coloration basically lichenate gray-green, grays, to browns and black, giving a blotched effect that also occurs in even the smallest juveniles, and rarely (only in juveniles) with any indication of transverse crossbars, or solid brown to grayish with faintly bluish white dark-edged ocelli; dewlap pale yellow to peach in males, pale yellow to pale peach in females; pale subocular crescent absent in adults but indicated in juveniles by a pale subocular spot.

Distribution. The Sierra de Baoruco and associated lowlands on the Península de Barahona, República Dominicana, including (probably) the semi-xeric forests of the lowlands south of the Sierra de Baoruco and southern Haiti; altitudinal distribution from sea level to 2600 feet (793 meters) northeast of Las Auyamas, Barahona Province.

Anolis barahonae barahonae Williams

Type locality. Polo, Valle de Polo, Barahona Province, República Dominicana.

Definition. A subspecies of *A. barahonae* characterized by the combination of modally 4 snout scales between second canthal scales, 4 vertical rows of loreal scales, 2 scales between the supraorbital semicircles, 4/4 scales between the interparietal and the supraorbital semicircles, relatively low number of vertical dorsal scales (15–23; mean 17.2), high number of ventral scales (17–29; mean 22.1), nuchal crest scales moderate to low, body crest scales rarely moderate, usually low, subocular scales usually separated from supralabial scales by one row of scales, both sexes and juveniles patterned with varying shades of gray-green, grays, browns and black, giving a lichenate blotched effect; juveniles with vague indications of three transverse gray bands but that pattern only very rarely even indicated in adults; dewlap pale yellow to pale peach in both sexes, the

female dewlap suffused with gray basally; pale subocular crescent absent in adults but indicated by a clear white subocular spot in juveniles and subadults.

Discussion. *A. b. barahonae* has a relatively circumscribed range in the Sierra de Baoruco in the southeastern República Dominicana. Until our 1971 collections, the taxon had been known only from the eastern portion of that massif, but two specimens taken 13.0 mi. (20.8 km) N of Pedernales along the Dominico-Haitian border are unquestionably *A. barahonae.* These individuals differ slightly from more eastern specimens of *A. b. barahonae* in coloration, but they are so close to the nominate subspecies that for the moment I have no hesitancy in regarding them as that taxon.

The series of 33 specimens of *A. b. barahonae* shows the following variation. The largest males (ASFS V29722, MCZ 125504) have snout–vent lengths of 158, the largest female (AMNH 50256) 148; the males are from north of Pedernales and near Polo, and the female is from Barahona. Snout scales at level of second canthals vary between 2 and 5; the mode is 4 (18 specimens). The vertical loreal rows vary between 5 and 8, with a mode of 6 (11 specimens). There are between 1 and 4 scales between the supraorbital semicircles (mode 2). There are modally 4 scales between the interparietal and the supraorbital semicircles; 4 scales are involved with 58 percent of the combinations; actual counts are 3/3 (3), 3/4 (6), 4/4 (13), 4/5 (3), and 5/5 (5). Vertical dorsals range between 15 and 23 (mean 17.2), horizontal dorsals between 15 and 24 (18.2), and ventrals between 17 and 19 (22.1). Of 16 males, seven have the nuchal crest scales moderate and nine have these scales low; of 10 females, three have these scales moderate and seven have them low. Body crest scales are moderate in one male and low in 15, whereas all 10 females have the body crest scales low. The subocular scales are separated from the supralabial scales in 32 of 33 specimens (3 percent).

Exclusive of the male and female from north of Pedernales, eastern specimens of *A. b. barahonae* are lichenate or blotched with gray-green, grays, browns, and black in a random pattern, although occasional individuals show remnants of the slightly more obviously banded condition of the juveniles. No specimen has been recorded in the field as being bright green, and in general the tones of green in *barahonae* are dull and grayish. Some specimens (especially ASFS V30921, a male) were recorded as being gray, heavily blotched with black, and thus without any green tints whatsoever. The dewlap color in males varies between pale peach and peach, and in females between pale peach and yellow.

The Pedernales specimens were recorded in life as being dark brown to gray dorsally, obscurely banded with tannish. The heads were tan above, the eyeskin pale gray, and the female had the upper surfaces of all limbs banded green and dark brown. The most noteworthy difference between these western specimens and those from the eastern uplands of the Sierra de Baoruco and its associated lowlands is that the dewlaps in both sexes were pale yellow, that of the female suffused with gray basally.

Available juveniles and subadults vary in length between 62 and 95. The juveniles are colored and patterned essentially like the adults, except that three pale grayish crossbands are vaguely indicated in most specimens. These bands are quite indistinct and much obscured by the lichenate *barahonae* pattern. Some juveniles were recorded as being banded and mottled pale gray, dull pea-green, and black, with a black nuchal patch and a white nuchal crescent on each side, whereas others were recorded as crossbanded gray and dusky, with some greenish on the lips, and the tails banded gray and dusky to cream.

Remarks. Specimens secured by myself and parties have all been taken in wooded situations, between elevations of 600 feet and 2600 feet (183 and 793 meters). Riverine woods and the large shade trees in the upland *cafetales* of the Sierra de Baoruco offer optimum habitat for the species. Both

adults and juveniles were secured sleeping at night; in general, the juveniles sleep lower on shrubs and low trees, whereas adults sleep higher (up to 15 feet—4.6 meters) on limbs, branches, and woody vines. At night, despite the absence of bright greens in the coloration, the lizards are quite obvious because their pale grayish hues contrast to the adjacent greenery. All ages of *A. b. barahonae* sleep exposed, as do other Hispaniolan giant anoles. The pair from 13.0 mi. N Pedernales were secured in rich riverine woods at an elevation of 600 feet (183 meters); this is purely a gallery forest situation, since in this region the open slopes are clad in *Acacia* forest or dry scrubby woodlands, whereas rivers and creeks support much more luxuriant arboreal growth.

Almost all localities for *A. b. barahonae* are in the highlands. However, the lizard presumably occurs in coastal forested regions as well. There are specimens from the city of Barahona (which is coastal) and from halfway between Enriquillo and Oviedo, which is presumed to be coastal or nearly so. A third specimen from Enriquillo likewise is presumably from a coastal locality. However, in each of these cases, it is possible that the lizards were secured in the adjacent Sierra de Baoruco; this mountain range comes abruptly to the coast between Barahona and Enriquillo, and it would be a simple matter to label specimens from non-coastal localities as having come from coastal populated areas. Although negative evidence at best, we have never ourselves secured *A. barahonae* along this coastal region, and residents of Barahona responded negatively when approached to collect this lizard for us.

A. b. barahonae is known from a locality (13.0 mi. N Pedernales) that is only (presumably) 11 kilometers from a locality (Thiotte) where *A. r. subsolanus* occurs. There are no other localities where these two species approach each other, although, since the northern slopes of the Sierra de Baoruco are confluent with the northern slopes of the Massif de la Selle and its affiliates, it is not unlikely that somewhere along these northern reaches *A. barahonae* comes into contact with *A. r. ricordi.* There is no obvious reason for *A. b. barahonae* to be promptly replaced by *A. r. subsolanus* at the Dominico-Haitian border; the political boundary on these southern slopes is the Río Pedernales, a small stream that surely offers no obstacle for these arboreal lizards. It follows that *A. b. barahonae* must occur in southeastern Haiti. Thus, as previously noted, the accuracy of the *subsolanus* localities is more than academic. It is possible that in southeastern Haiti, *A. barahonae* is a more lowland lizard and *A. ricordi* (*subsolanus*) occurs on the higher and better forested slopes of the Massif de la Selle—the division may thus be altitudinal as well as ecological. The precise relationships between these two species remain to be determined; only further detailed collecting in extreme southeastern Haiti will reveal the siutation there. As far as distinguishing *A. r. subsolanus* from *A. b. barahonae,* there is no problem, since the styles of pattern (and presumably coloration) are so very different as to preclude confusion. If intergradation between *subsolanus* and *barahonae* occurs (and since I here regard *barahonae* as a species distinct from *ricordi,* I am obviously convinced that it does not), then it must take place very quickly, in a distance of some 11 kilometers, since *subsolanus* and the Pedernales *barahonae* are completely different and typical of their own populations, without any indication of intergradation between them.

Specimens examined. REPÚBLICA DOMINICANA: *Barahona Province,* Barahona (AMNH 50255–56); 14 km SW Barahona, 1200 feet (366 meters) (ASFS V23460–63, ASFS V30263–70); Valle de Polo (MCZ 56141, AMNH 51235–37, AMNH 51240, AMNH 51036); nr. Polo (MCZ 125504–06); Las Auyamas (ASFS V30921); 8 km NE Las Auyamas, 2600 feet (793 meters) (ASFS X9676); Hermann's finca, nr. Paraíso (AMNH 51231–33); Enriquillo (AMNH 51241); *Pedernales Province,* half-

way between Enriquillo and Oviedo (AMNH 51230); 13.0 mi. (20.8 km) N Pedernales, 600 feet (183 meters) (ASFS V29722–23); locality unknown (AMNH 51229).

Anolis barahonae albocellatus new subspecies

Holotype. MCZ 125611, an adult male, from 13.1 mi. (21.0 km) SW Enriquillo, Pedernales Province, República Dominicana, taken by Richard Thomas on 10 December 1964. Original number ASFS V4422.

Definition. A subspecies of *A. barahonae* characterized by the combination of 4 snout scales between second canthal scales, 7 vertical rows of loreal scales, 3 scales between the supraorbital semicircles, 4/4 scales between the interparietal and the supraorbital semicircles, apparently relatively high number of vertical dorsal scales (19), high number of ventral scales (26), nuchal crest scales high, body crest scales low, subocular scales separated from supralabial scales by one row of scales, male (females unknown) dorsal ground color nonlichenate brown to grayish with white (faintly bluish) randomly placed dark-edged ocelli, head light brown above, dewlap pale yellow with a pink margin, and a pale subocular spot.

Distribution. Known only from the type locality, but presumably distributed through the semi-arid forests of the Península de Barahona south of the Sierra de Baoruco (see discussion).

Description of holotype. An adult male with a snout–vent length of 150 and a tail length of 265; snout scales at level of second canthal 4, 7 vertical rows of loreal scales, 3 scales between interparietal and supraorbital semicircles, vertical dorsals 19, horizontal dorsals 23, ventrals 23, one row of scales between suboculars and supralabials, fourth toe lamellae on phalanges II and III 34, nuchal crest scales high, body crest scales low; in life, dorsum brown to grayish, not lichenate, with randomly scattered white (faintly bluish) dark-edged ocelli involving from 1 to 4 scales; venter white with gray mottling or stippling; dewlap pale yellow with pink along its outer margin; upper surface of head light brown, with large pale subcircular areas anterior to the ear opening, and a conspicuous pale blotch below the eye; soles of hands and feet conspicuously pale yellow.

Comparisons. No mensural nor meristic characters separate *albocellatus* from *barahonae*. On the other hand, the distinctive coloration, pattern, and dewlap color of *albocellatus* are very different from those of *barahonae*, and the presence of high nuchal crest scales likewise differentiates *albocellatus* from the moderate to low scales in *barahonae*. More detailed comparisons are impossible, but certainly *albocellatus* is quite distinctive when compared with *barahonae*.

Discussion. It may seem foolhardy to name a subspecies of *A. barahonae* from a single specimen whose locality is only 11 kilometers from a presumed locality for *A. b. barahonae* (half way between Enriquillo and Oviedo). The holotype of *A. b. albocellatus* is that lizard about which Williams (1965: 4) commented, saying it "is typical in squamation but peculiar in having very distinct small *light* spots on the flanks. . . . . It will be recalled that it was a specimen from Enriquillo (AMNH 51241) that caused some hesitation when *barahonae* was first described. In AMNH 51241 the pattern was thought to be obscure banding; the present specimen clearly shows spots tending to be vertically aligned—a condition which is easily transformed into vertical banding. It is possible that the *ricordii* populations in the vicinity of Enriquillo consistently show a distinctive pattern though characteristically *barahonae* in squamation."

The specimen (AMNH 51230) from halfway between Enriquillo and Oviedo is a young male with a snout–vent length of 121. Since this lizard presumably came from the lowlands of the Península de Barahona, it might logically be expected to be *albocellatus*. However, the lizard is now

drab patternless brown, and there are no indications that it was ever spotted. Presumably *albocellatus* and *barahonae* intergrade between Enriquillo (which lies at the extreme southeastern corner of the Sierra de Baoruco) and Oviedo (which lies well down on the Península de Barahona).

Several facts have prompted my naming this lonely specimen. First, I have examined the Enriquillo specimen noted by Williams, and, although it shows some indication of vertical crossbars, they are not any more conspicuous than those in some more recently taken *A. b. barahonae* from the Baoruco highlands (Williams examined only 17 *barahonae* at the time of its original description; I have studied almost twice this number). Secondly, the xeric to semi-arid region south of the Sierra de Baoruco has come to be known as an area of local differentiation at the subspecific level for a variety of reptiles; this alone is no reason for naming *albocellatus,* of course. Thirdly, although since 1964 when the holotype was collected both I and others have spent considerable time on the Península de Barahona and in the vicinity of Oviedo, we have never seen or secured another *A. barahonae* in this region. In September 1966, the very severe hurricane Inez passed directly across the Península. What had once been high-canopied semi-arid forest (as at Oviedo) has been either totally destroyed or been reduced (by 1969) to a landscape of bare snags with some leafy growth just now beginning to appear but at a much lower canopy-level than previously. The changes between the Oviedo area in 1964 and 1969 are so massive that, upon my first visit there after Inez, I was unable to orient myself in reference to our older collecting localities! Certainly this entire region has suffered greatly, and, with the destruction of trees, it seems reasonable to assume that *A. barahonae* has suffered equally. The population may never have been high, since such semi-arid woods are not at all optimal habitat for any of the Hispaniolan giant anoles, and the destruction of the habitat must surely have affected *A. b. albocellatus* adversely. Since persistent visits to this area have yielded no new material, and since the lizard may presently be very rare, I have decided upon the present course rather than wait in hope for someone to secure a second (or more) lizard.

Remarks. The Península de Barahona has been shown to have distinctive subspecies (or even species) of a variety of reptiles. Species that have described endemic subspecies south of the Sierra de Baoruco include: *Sphaerodactylus difficilis* Barbour, *Leiocephalus barahonensis* Schmidt, *Ameiva chrysolaema* Cope, *Ameiva lineolata* Duméril and Bibron, *Amphisbaena gonavensis* Gans and Alexander, and *Dromicus parvifrons* Jan. Endemic Península de Barahona species are: *Anolis longitibialis* Noble, *Typhlops syntherus* Thomas, *Leptotyphlops pyrites* Thomas, and *Uromacer wetmorei* Cochran. Only one amphibian, *Eleutherodactylus alcoae* Schwartz, is restricted to the Península. To the former list can now be added *Anolis barahonae.* The eastern half of the Península, although xeric, was originally clothed in dry forest, much of it upon a series of limestone terraces, the highest point of which is the Loma Gran Sabana, having an elevation of 1082 meters in the north and descending to Cerro Caballo, and Loma de Chendo, having elevations of 322 and 233 meters, respectively, to the south. West of this ridge, the land descends abruptly to *Acacia-cactus* desert to the east of Cabo Rojo, and this habitat continues to the Dominico-Haitian border at Pedernales. Presumably, *A. b. albocellatus* occurs throughout the eastern half of the Península in the formerly high-canopied forests of the limestone terraces.

The holotype was secured by Richard Thomas during the day in a viny tangle in semi-xeric woods near Oviedo; the lizard was in an edge situation, since beyond the dense vine tangle the woods thinned to more scrubby and cleared areas.

The name *albocellatus* is from the Latin

"albus" for "white" and "ocellus" for "eye," in allusion to the white spots that are typical of the holotype.

Anolis baleatus Cope

Eupristis baleatus Cope, 1864, Proc. Acad. Nat. Sci. Philadelphia, p. 168.

Type locality. Santo Domingo; holotype, British Museum (Natural History) 1946.8.29.22.

Definition. A giant species of Hispaniolan *Anolis* characterized by the combination of large size (males to 180 mm, females to 148 mm snout–vent length), snout scales at level of second canthal scales 2 to 5 (modally 2 or 4, by population) but usually 2 or 3 (75 percent), vertical loreal rows 5 to 10 (modes by population 6, 7 or 8), scales between supraorbital semicircles 1 to 4 (modally 3), interparietal scales separated from supraorbital semicircles modally by 4 or 5 scales, vertical dorsal scales generally small (12 to 24 in standard-distance), ventral scales relatively small (15 to 34 in standard-distance), nuchal crest scales in both sexes very high to high, rarely moderate, never low, body crest scales usually high to moderate, rarely low, subocular scales usually not in contact with supralabial scales; dorsal body coloration and pattern usually some shade of green, varying from dull greenish brown to bright emerald green, either conspicuously crossbanded with few (3 or 4) to very many crossbands, in the latter condition the lizards appearing tigroid, or, on the other hand, without crossbanding but blotched, never striped or with dark occipital, nuchal, or lateral dark markings, dewlap in males from pale yellow to vivid orange, in females from brownish or very pale yellow to orange or gray, often suffused with grayish or brownish, or nearly white, chin and throat yellowish, green, or orange, often with a dark dotted or mottled or reticulate pattern, and pale subocular crescent absent in adults.

Distribution. The eastern two-thirds of the República Dominicana, from Puerto Plata, Santiago, and La Vega provinces south to San Cristóbal Province and the Distrito Nacional, and east to La Altagracia Province; also in and near the Sierra Martín García and the southern slopes of the Cordillera Central and the Sierra de Ocoa in Azua and Peravia provinces; occurs on Isla Saona but unrepresented by specimens from that satellite island.

Anolis baleatus baleatus Cope

Type locality. "Santo Domingo"; here restricted to the vicinity of Puerto Plata, Puerto Plata Province, República Dominicana (see rationale for this restriction below).

Definition. A subspecies of *A. baleatus* characterized by the combination of modally 4 snout scales between second canthal scales, 7 vertical rows of loreal scales, 3 scales between the supraorbital semicircles, moderate number of vertical dorsal scales (14–21; mean 17.5), high number of ventral scales (19–34; mean 23.8), nuchal crest scales very high (usually) to high or moderate (rarely), body crest scales high (rarely) to moderate (usually), subocular scales always in contact with supralabial scales, males from pale green or rich bluish green to brown dorsally, with three bright yellow to darker green or greenish brown irregular crossbands, lower sides usually bright yellow, females apparently with the same body patterns and hues as the males (see below), throat in males bright yellow to bright orange, rarely mottled with brown, dewlap in males always vivid to brilliant orange, and the upper surfaces of hindlimbs bluish green, conspicuously barred with bright yellow.

Distribution. Known from the Cordillera Septentrional and the northern coastal plain of the República Dominicana, from Puerto Plata, Espaillat, and Santiago provinces, but probably occurring elsewhere in this range and to the north of it; specimens from Los Bracitos, Duarte Province, should also be included (on geographical grounds) with *A. b. baleatus*, since Los Bracitos lies

in the eastern extremity of the Cordillera Septentrional, but the specimens are old and greatly discolored and I have not considered them as pertaining to the nominate subspecies.

Discussion. Eupristis baleatus Cope was named from a single specimen from "Santo Domingo." I have examined the holotype, collected by A. Sallé, in the British Museum (Natural History). Considering its length of time in preservative, it is in excellent condition and shows a striking pattern of three bold pale body crossbands on a darker dorsal ground color, contrastingly banded hindlimbs and tail, and immaculate throat. The specimen is a female, and, unfortunately, I have only two adult females from the range ascribed above to *A. b. baleatus;* both are without color data in life. At least one of them (MCZ 57717) resembles the pattern of the *baleatus* holotype to a striking degree.

Through the courtesy of Ernest E. Williams, I have a copy of a map prepared by William J. Clench which shows the localities where A. Sallé is known to have collected. Considering the era of his travels (the mid-1800's), Sallé traveled widely throughout the República Dominicana, from (in the north) Puerto Plata, Pontón, Santiago, Moca, La Vega and Cotuí, east to Higüey, Cabo Engaño and San Rafael del Yuma, in the eastern interior to Hato Mayor and El Seibo, along the southern coast from Santo Domingo to San Cristóbal, Baní, Azua, Barreras, and Barahona, and into the Valle de San Juan to the city of San Juan. He also ascended the southern slopes of the Cordillera Central near San José de Ocoa. Although much of Sallé's Dominican travels was in territory of *A. baleatus,* he was also in the ranges of *A. ricordi* and *A. barahonae.* The holotype, as Williams (1962: 2, footnote 1) pointed out, has elongate nuchal crest scales, and there is no doubt that the name *baleatus* is applicable to some population that possesses this character. Since Sallé traveled within the range of the northern population of *A. bealeatus,* I have restricted the type locality of the name to the vicinity of a major city that is presumed to lie within the area to which I ascribe this boldly crossbanded subspecies.

The series of 15 *A. b. baleatus* shows the following variation. The largest males (ASFS V33558, ASFS V18123) have snout–vent lengths of 148, and the largest female (MCZ 128380) has the same dimension. These three lizards are all from the Cordillera Septentrional north of Puesto Grande. Snout scales at level of the second canthal vary between 2 and 4; the mode is 4 (eight specimens). The vertical loreal rows vary between 5 and 9, with a mode of 7 (six specimens). There are 3 scales between the supraorbital semicircles in all specimens. There are modally 5 scales between the interparietal and the semicircles; 5 scales are involved in 63 percent of the combination; actual counts are 4/4 (1), 4/5 (4), 5/5 (7), 5/6 (1), 6/6 (1), and 5/7 (1). Vertical dorsals range between 14 and 21 (mean 17.5), horizontal dorsals between 16 and 26 (19.7), and ventrals between 19 and 34 (mean 23.8). Of nine adult males, six have the nuchal crest scales very high, two have these scales high, and one has them moderate. Of three females, the nuchal crest scales are very high in two and high in one. The body crest scales are high in one male and moderate in eight males; in three females, the body crest scales are high in one and moderate in two. All specimens have the subocular scales in contact with the supralabial scales.

Males are usually conspicuously crossbanded. Specimens have been recorded as pale green with three irregular darker green crossbands, brown with three faint green-brown crossbands, or rich bluish green with three bright yellow crossbands. The lower sides are bright yellow (which grades into a grayish venter), and this color also occurs on the throat, which varies from yellowish to bright yellow or orange, occasionally mottled with brown. The dewlap is brightly colored; it has been recorded as "vivid orange," "bright vivid orange," "brilliant yellow-orange," and "very bright

orange." The upper surface of the head is reddish brown and the hindlimbs are green to bluish green, barred with bright yellow. In general, male *A. b. baleatus* are vividly patterned and colored lizards. I have collected no females myself and thus have no notes on this sex from life; however, one recently (1971) collected female (MCZ 128380) still is dark green with several thin vertical pale crossband remnants on the sides and back, and another female (MCZ 57717) is contrastingly patterned in dark and pale green, the latter occurring as vertical crossbands.

The series includes three subadults, with snout–vent lengths between 73 and 83. One of these (ASFS V33559; snout–vent length 80) was medium brown dorsally with a black postocular streak and an orrange dewlap that was streaked with black basally. None of the subadults as preserved shows any crossbanding or other pattern elements. It is interesting that the only Hispaniolan giant anole taken at night sleeping in the brown phase is the above mentioned subadult.

Remarks. All ASFS specimens collected by myself and parties were secured at night while the lizards were sleeping. Typical situations are in gallery forest and *cafetales* along mountain streams in the Cordillera Septentrional. Favored sleeping sites for these lizards in the region are pendant and semi-pendant woody vines; Fowler reported that one adult male secured by him at night was not asleep and was slowly ascending a tree trunk as Fowler approached. It is possible that this lizard had been disturbed by the bright light from Fowler's flashlight or by unfamiliar movements and noises, since I doubt that any of the Hispaniolan giant anoles are normally active at night. However, all these lizards waken quickly when disturbed and unless promptly secured, gradually wander away into the greenery and are lost to view. One of the juveniles was secured only 6 feet (1.8 meters) above the ground, whereas one of the adults was shot from a tree limb 35 feet (10.7 meters) above a mountain stream. The specimen from near Sosúa was taken in dense hardwoods on a limestone substrate.

The altitudinal distribution of *A. b. baleatus* is from 1400 to 2200 feet (427 to 671 meters), but the taxon occurs much lower than this, since the specimen from near Sosúa was in limestone hills near sea level.

Specimens examined. REPÚBLICA DOMINICANA: *Espaillat Province,* 2 km N Puesto Grande, 1400 to 2200 feet (427 to 671 meters) (ASFS V18048, ASFS V33557–59); 5 km N Puesto Grande (MCZ 128380); 11 km N Puesto Grande, 2100 feet (641 meters) (ASFS V18123, ASFS V18292): *Puerto Plata Province,* 11 km SE Sosúa (ASFS V1717); *Santiago Province,* Pena (MCZ 57713, MCZ 57715–19); no locality other than Santo Domingo—British Museum (Natural History) 1946.9.28.22—holotype of *Eupristis baleatus.*

Anolis baleatus multistruppus new subspecies

Holotype. USNM 193975, an adult male, from Guaigüí, 3 mi. (4.8 km) S La Vega, La Vega Province, 300 feet (92 meters), República Dominicana, one of a series taken by Danny C. Fowler, Albert Schwartz, and Bruce R. Sheplan on 9 November 1971. Original number ASFS V33680.

Paratypes. ASFS V33681–86, MCZ 125612–15, CM 54107–12, same data as holotype; ASFS V18547–50, same locality as holotype, J. R. Dennis, J. A. Rodgers, Jr., and A. Schwartz, 27 July 1969.

Definition. A subspecies of *A. baleatus* characterized by the combination of modally 2 snout scales between second canthal scales, 7 vertical rows of loreal scales, 3 scales between the supraorbital semicircles, 4/4 scales between the interparietal and the supraorbital semicircles, high number of vertical dorsal scales (14–24; mean 18.6), moderate number of ventral scales (18–29; mean 22.3), nuchal crest scales very high to high (usually) to moderate (rarely), body crest scales high (rarely) to moderate (usually), subocular scales almost al-

ways separated from supralabial scales by one row of scales, both sexes as adults retaining the complex juvenile pattern of many fine dark green, green, and yellow vertical bars, occasionally (in females) bright pea green with three pale green crossbars more prominent than any other dorsal pattern elements, throat green to yellow green, dewlap in males very pale yellow to very pale peach, suffused basally with pale gray, in females very pale yellow to pale yellow, strongly suffused with pale gray to entirely pale gray.

Distribution. Known only from the type locality but presumed to occur on the northern and probably eastern lower faces of the Cordillera Central in proper habitats; possibly extending as far west on the northern face of this range as the Río Bao near Los Montones (see discussion below).

Description of holotype. An adult male with a snout–vent length of 146 and a tail length (broken) of 97; snout scales at level of second canthals 2, 9 vertical rows of loreal scales, 3 scales between the supraorbital semicircles, 4/4 scales between the interparietal and the supraorbital semicircles, vertical dorsals 21, horizontal dorsals 25, ventrals 29, one row of scales between the suboculars and supralabials, fourth toe lamellae on phalanges II and III 30, nuchal crest scales high, body crest scales moderate; in life, dorsal body pattern of many fine green, dark green, and yellow crossbands, upper surface of head grayish tan in contrast to the brighter dorsal colors, chin and throat very pale yellow or yellow-green with no clearly delineated darker green markings, and dewlap very pale yellow, much suffused basally with gray.

Variation. The series of 21 *A. b. multistruppus* is composed of eight males and 13 females. The largest male has a snout–vent length of 146 and is the holotype. The largest female (ASFS V33684) has a snout–vent length of 136 and is a topotype. Snout scales at the level of the second canthals range between 2 and 5; the mode is 2 (15 specimens). The vertical loreal rows vary between 6 and 9, with a mode of 7 (nine specimens). There are 2 or 3 scales between the supraorbital semicircles (mode 3). There are modally 4 scales between the interparietal and the supraorbital semicircles; 4 scales are involved in 58 percent of the combinations; actual counts are 3/3 (1), 3/4 (2), 4/4 (8), 4/5 (5), 5/5 (3), and 5/6 (1). Vertical dorsals range between 14 and 24 (mean 18.6), horizontal dorsals between 17 and 25 (20.6), and ventrals between 18 and 29 (22.3). All three adult males have the nuchal crest scales high, and of ten females, three have these scales very high, five have them high, and two have them moderate. All three males have the body crest scales moderate, whereas two females have the body crest scales high, eight have them moderate, and one has them low. In all but one specimen (5 percent), the suboculars are separated from the supralabials by 1 scale.

Adults of both sexes retain the juvenile multibanded pattern of dark greens, medium greens, and yellow. One adult female was recorded as bright pea-green with three pale green crossbands, which are remnants of the hollowed yellow centers of the five or six dark brown to dark green crossbands. In general, the total aspect of adults and juveniles is of a contrastingly tigroid lizard, the stripes varying shades of greens, yellows, and (in the dark phase) browns. The upper surface of the head is grayish tan in males and tannish green in females, and the throat is unmarked green to yellow-green. One of the most striking features of *A. b. multistruppus* is the faded dewlap coloration. In males, the colors vary between very pale yellow and very pale peach, basally suffused with pale gray. In females, the dewlap is even more drab, with pale yellow the basic color, but the gray suffusion may be so extensive as to limit the yellow pigment to the dewlap edge or to cause the dewlap to be pale gray.

The type series includes seven juveniles and subadults, with snout–vent lengths be-

tween 47 and 99. These present a uniform aspect of multiple dorsal bands as described above, and even the largest of the subadults clearly shows this condition. In life, a small juvenile (snout–vent length 53) was recorded as pale gray with a yellow-green head and about four reversed chevrons between the neck and the hindlimbs, these chevrons being the pale hollowed remnants of the darker crossbands, which, in this individual, are obscure. The small lizard also had a black postocular line and a charcoal postangular smudge. The juvenile and subadult dewlaps are pale flesh to very pale yellow, somewhat suffused basally with light to very dark gray.

Comparisons. Meristically, *multistruppus* differs from nominate *baleatus* in having 2 (rather than 4) snout scales at the level of the second canthals, 4/4 (rather than 5/5) scales between the interparietal and the supraorbital semicircles, and in having slightly less ventrals (means 22.3 and 23.8). There is also a strong tendency for both sexes of *baleatus* to have very high nuchal crest scales, whereas these scales are more often only high in *multistruppus*. It is in color and pattern that these two subspecies differ most strikingly. In the introduction to the present paper I commented on my having collected specimens from the Cordillera Septentrional and Guaigüí on two succeeding days, and on the color and pattern differences being at once very apparent. The bright orange throat and dewlap of *baleatus* contrast quite obviously with the pale yellow to gray dewlaps in *multistruppus*. The body patterns of the two subspecies likewise are quite different, with the finely and multibanded *multistruppus* in contrast to the irregularly banded dorsum with only three bands in *baleatus*.

Discussion. A. b. multistruppus is known with certainty from only a single locality, which lies at the foot of the Cordillera Central at an elevation of 300 feet (92 meters). The locality is unique in that it represents an extensive stand of original lowland forest in this region, hardwood forest which abuts upon the lower pine-clad slopes of the mountains. This locality, Guaigüí, is separated from the known range of *A. b. baleatus* by the Valle de Cibao, which here is a moderately arid and broad valley presently very much under cultivation. I have seen no specimens from this intervening valley but surely the lizards occur there, despite the cultivation.

One other specimen requires mention. This is a subadult male (ASFS V33856) with a snout–vent length of 55, from 3.4 mi. (5.4 km) SE Los Montones, Río Bao, 1600 feet (488 meters). This locality is on the northern slopes of the Cordillera Central, some 45 kilometers to the west of Guaigüí, but separated from Guaigüí by intervening, moderately high spurs of the Cordillera Central. The specimen was secured by a local boy in an area of high-canopied forest along the Río Bao. A visit by ourselves to this area at night yielded no *A. baleatus*, despite exceptionally fine conditions. The lizard in life was all green except for a white preaxillary bar, and the dewlap was dull brownish. This specimen in no way resembles comparably sized juvenile *multistruppus*, in either color or pattern. Its status remains uncertain.

To the east, *multistruppus* must come in close contact or intergrade with the subspecies that occurs throughout the northeastern portion of the República Dominicana; details of this contact will be discussed under the account of the latter subspecies. Likewise, to the south, *multistruppus* may come into contact with the subspecies in the high Cordillera Central; details of this association will be discussed under the description of the Central subspecies.

Remarks. All specimens of *A. b. multistruppus* were collected on two occasions, while the lizards slept at night. Young individuals were taken from generally low situations on shrubs and the lower branches of trees, whereas adults were observed sleeping in the higher canopy; the total range of heights was between 5 feet

and 25 feet (1.5 and 7.6 meters). The Río Camú flows through the Guaigüí woods, and many individuals were taken from tree limbs that overhang the river.

The name *multistruppus* is from the Latin "multus" for "many" and "struppus" for "thong, strap," in allusion to the many dorsal crossbands in this subspecies.

Anolis baleatus sublimis new subspecies

Holotype. CM 54104, an adult male, from 0.3 mi. (0.5 km) E El Río, 3800 feet (1159 meters), La Vega Province, República Dominicana, taken by Richard Thomas on 26 June 1963. Original number ASFS X8114.

Paratypes. ASFS X8558, 4 km SW El Río, 4000 feet (1220 meters), La Vega Province, República Dominicana, R. F. Klinikowski, 2 July 1963; USNM 62104–05, El Río, La Vega Province, República Dominicana, W. L. Abbott, 19 May 1919; AMNH 41294, El Río, La Vega Province, República Dominicana, G. K. Noble, 31 August 1922; ASFS V18594, La Palma, 14 km E El Río, 3500 feet (1068 meters), República Dominicana, J. A. Rodgers, Jr., 30 July 1969; MCZ 107019–21, La Palma, 14 km E El Río, 3500 feet (1068 meters), La Vega Province, República Dominicana, native collectors for E. E. Williams and A. S. Rand, 25–31 July 1968; MCZ 128397, La Palma, 14 km E El Río, 3500 feet (1068 meters), La Vega Province, República Dominicana, T. P. Webster and R. B. Huey, 6 July 1971; ASFS V18363–69, 8 km W Jarabacoa, 2000 feet (610 meters), La Vega Province, República Dominicana, J. A. Rodgers, Jr., 19 July 1969.

Definition. A subspecies of *A. baleatus* characterized by the combination of modally 2 snout scales between second canthal scales, 7 vertical rows of loreal scales, 3 scales between the supraorbital semicircles, 4/4 scales between the interparietal and the supraorbital semicircles, high number of vertical dorsal scales (17–21; mean 19.2), high number of ventral scales (19–32; mean 25.1), nuchal crest scales very high (usually) to high (rarely), body crest scales always high, subocular scales almost always separated from supralabial scales by one row of scales, both sexes either marbled or blotched with varying shades of greens or browns, or dark brown banded with dull cream, never with many fine crossbars, venter in males pale green, flecked with darker green, and male dewlaps pale yellow-orange to orange, gray basally and marbled green anteriorly, female dewlaps irregularly yellow-orange with brown spotting.

Distribution. The uplands of the Dominican Cordillera Central at elevations between 2000 and 4000 feet, in the area between El Río, La Palma, and Jarabacoa.

Description of holotype. An adult male with a snout–vent length of 143 and a tail length of 167 (regenerated); snout scales at level of second canthals 3, 7 vertical rows of loreal scales, 2 scales between the supraorbital semicircles, 4/4 scales between the interparietal and the supraorbital semicircles, vertical dorsals 20, horizontal dorsals 21, ventrals 29, one row of scales between the suboculars and supralabials, fourth toe lamellae on phalanges II and III 31, nuchal crest scales and dorsal body crest scales high; in life, dorsum dark brown banded with dull cream, this pattern extending onto the tail, eyeskin grayish with a pale yellow eyering, venter pale green, flecked with darker green, chin and throat concolor with and patterned like venter, dewlap pale yellow-orange, grayish basally and marbled with green anteriorly.

Variation. The series of 18 *sublimis* is composed of nine males and nine females. The largest male (USNM 62104) has a snout–vent length of 150, the largest female (MCZ 107021) 141; the male is from El Río, the female from La Palma. Snout scales at the level of the second canthals range between 2 and 5; the mode is 2 (10 specimens). The vertical loreal rows vary between 6 and 9, with a mode of 7 (eight specimens). There are 2 to 4 scales between the supraorbital semicircles (mode 3). There are modally 4 scales

between the interparietal and the supraorbital semicircles; 4 scales are involved in 65 percent of the combination; the actual counts are 3/3 (1), 3/4 (1), 4/4 (10), 4/5 (1), 5/5 (3), and 5/6 (1). Vertical dorsals range between 17 and 21 (mean 19.2), horizontal dorsals between 17 and 24 (20.4), and ventrals between 19 and 32 (25.1). Of the six adult males, three have the nuchal crest scales very high and three have them high, whereas all five adult females have these scales very high. All adults of both sexes have the dorsal body crest scales high. Three lizards (17 percent) have the subocular scales in contact with the supralabials.

In the green phase, adults of both sexes are irregularly marbled or blotched with varying shades of green or browns, whereas in the brown phase, the body is dark brown with three cream crossbands. In males the venter and the chin and throat are pale green, flecked or mottled with darker green, the flecking or mottling variably expressed in the series. The dewlap in males is pale yellow-orange to orange, gray basally and often with marbled green markings anteriorly, these markings being a continuation of the dark green throat markings. In females, the dewlap is irregularly mottled with yellow-orange and has some brown spotting. As preserved, the series is remarkably uniform in showing vague pale-and-dark marblings or mottlings, and no adult shows any indication of crossbands.

The series of paratypes includes six juveniles and subadults, with snout–vent lengths between 49 and 94. The three smallest of these (49–70) are presently patternless, as is also a specimen with a snout–vent length of 73. Two other subadults (snout–vent lengths 75 and 94) show vague indications of mottled dorsum with (in the larger) three slightly paler dorsal crossbands. The larger of these two specimens was recorded in life as dark green dorsally with pale green crossbands, and the interbars are mottled or marbled with greens. The smallest juvenile noted above was bright yellow-green in life and had the venter slightly paler yellow-green; the concealed surfaces of the thighs were lead-gray, bordered above by buffy. The absence of pale crossbars in very young specimens of *sublimis* is noteworthy

Comparisons. There are no meristic counts that separate *sublimis* from adjacent *multistruppus;* the means of ventral scales in the two subspecies differ slightly, however (22.3 in *sublimis*, 25.1 in *multistruppus*). There is also a tendency for *sublimis* to have more consistently very high to high nuchal crest scales. The two subspecies differ abundantly in body pattern, however, with *multistruppus* having many fine dorsal crossbands and *sublimis* having basically a blotched dorsal pattern with three bars present in some instances. The juveniles of these two subspecies are equally as distinct as the adults are in dorsal body pattern. The dewlaps are brighter in male *sublimis* than in male *multistruppus,* the latter tending toward pale yellow and yellow-grays, whereas in the former the dewlaps are yellow-orange to orange, although there is a gray basal suffusion. The ventral and throat flecking or mottling in *sublimis* differs from the unmarked condition in *multistruppus.*

A. b. sublimis differs from *A. b. baleatus* in having 2 (rather than 4) snout scales at the level of the second canthals, 4/4 (rather than 5/5) scales between the interparietal and supraorbital semicircles, higher means of vertical dorsal scales (19.2 versus 17.5) and ventrals (25.1 versus 23.8). Both subspecies have very high to high nuchal crest scales. In color, *baleatus* is much the brighter, with an immaculate bright yellow to orange throat and bright yellow to orange dewlap in males, whereas the dewlaps in *sublimis* are as bright as those in *baleatus* but have a gray basal wash. The patterned throat and venter in *sublimis* differ from the immaculate throat in *baleatus.* The dorsal patterns of these two subspecies likewise are quite different, that of *baleatus* regularly consisting of

three pale crossbands, whereas that of *sublimis* is mottled or blotched.

Discussion. A. b. sublimis is closest geographically to *multistruppus;* the two subspecies are known from localities separated by only 20 kilometers airline (Guaigüí and 8 km W Jarabacoa), but minimally by a 1700-foot (519 meters) difference in elevation and by extensive stands of pine forest, a habitat which no Hispaniolan giant anole occupies. All specimens of *sublimis* were collected in montane gallery forest along streams, and the subspecies appears to be restricted to this sort of situation. Rand and Williams (1969: 9) noted that they collected one juvenile about 10 feet (3 meters) up on a small branch of a forest tree at La Palma, and that two adults were brought to them by natives from a large tree in a nearby agricultural area. *A. b. sublimis* is thus not known to come into contact with *multistruppus* on the northern slopes of the Cordillera Central nor with the yet-to-be-described subspecies to the east in the Dominican lowlands. Likewise, it should be recalled that the southwestern slopes of this range are occupied by *A. r. ricordi;* the nearest localities for *ricordi* and *sublimis* (Juan de Herrera; south of El Río) are separated by about 70 kilometers airline, but this intervening area is composed of the rugged and very high massif of the Cordillera Central whose upper elevations are covered by pine. It seems unlikely that *ricordi* and *sublimis* come into contact directly across the Cordillera.

The juvenile (ASFS 33856) from near Los Montones upon which I commented in the discussion of *A. b. multistruppus* may be correctly assigned to *sublimis,* since the habitat and elevation for that specimen is much more like that for *sublimis* than *multistruppus.* In color and lack of pattern it agrees quite well with small *sublimis,* but until adults have been collected in the Los Montones region (which lies some 30 kilometers to the northwest of Jarabacoa, the closest *sublimis* locality) I am reluctant to extend the known range of *sublimis* into that area. It is this Los Montones *A. baleatus* which is closest geographically (50 kilometers) to an *A. ricordi* locality (Los Quemados) in the northwestern portion of the República Dominicana.

Remarks. All ASFS *A. b. sublimis* were taken at night while asleep. All situations, as noted above, were stream-associated hardwood forest and *cafetales,* and the lizards slept on vines and branches in their customary fashion. The restriction of *sublimis* to riverine gallery forest is doubtless artificial, since it is only along rivers and streams in this area that any of the original montane hardwood forests still remain. In one case (west of Jarabacoa) the stream was extremely steep, whereas in others the streams were level. The altitudinal distribution (to which the name *sublimis* refers) is high. Only *A. r. viculus* reaches as high an elevation in the Massif de la Hotte in southwestern Haiti.

Anolis baleatus caeruleolatus new subspecies

Holotype. USNM 193976, an adult male, from 1.0 mi. (1.6 km) S Caño Abajo, María Trinidad Sánchez Province, República Dominicana, one of a series collected by native collectors on 28 November 1971. Original number ASFS V34486.

Paratypes. CM 54119–26, MCZ 125628–33, ASFS V34502–13, same data as holotype; AMNH 6017, Villa Riva, Duarte Province, República Dominicana, C. R. Halter, May–July 1915.

Associated specimens. REPÚBLICA DOMINICANA: *Duarte Province,* Los Bracitos (AMNH 41465–66); *ca.* 4 km NE Pontón (Río Cuaba) (ASFS V2987); *Sánchez Ramírez Province,* 1 km SE La Mata (ASFS V33650–51); *La Vega Province,* 12.8 km NW Bonao, 1200 feet (366 meters) (ASFS V4317); 71 km NW Santo Domingo (= near La Cumbre) (MCZ 128369); *San Cristóbal Province,* 5.0 mi. (8.0 km) NE Gonzalo, 1000 feet (305 meters) (ASFS V29420–21).

Definition. A subspecies of *A. baleatus* characterized by the combination of mod-

ally 4 scales between second canthal scales, 8 vertical rows of loreal scales, 3 scales between the supraorbital semicircles, 5/5 scales between the interparietal and the supraorbital semicircles, moderate number of vertical dorsal scales (14–22; mean 17.1), moderate number of ventral scales (15–32; mean 22.4), nuchal crest scales very high to high (usually) to moderate or even low (rarely) in both sexes, body crest scales extremely variable, modally moderate in both sexes, but with some occurrences of high and many occurrences of low body crest scales, subocular scales almost always separated from supralabial scales by one row of scales, both sexes some shade of green (usually dark) with four pale green crossbars and with bright sky-blue blotches along the junction of the green dorsal color and the paler venter (less prominent in females than in males), dewlap in males pale yellow to orange, in females pale yellow to orange but with much dark brown to grayish streaking or smudging, throat in males deep yellow-orange and immaculate or with very faint greenish dots, in females yellow-green to bright yellow, always with some darker green dots, rarely marbled with dark green, but never streaked with that color.

Distribution. Northeastern República Dominicana, from Duarte, Sánchez Ramírez, La Vega, and northern and eastern San Cristóbal provinces, to the base of the Península de Samaná (Caño Abajo); intergrades with the subspecies to the south and east in the region of El Seibo Province.

Description of holotype. An adult male with a snout–vent length of 137 and a tail length of 250; snout scales between second canthals 4, 7 vertical rows of loreal scales, 3 scales between the supraorbital semicircles, 6/6 scales between the interparietal and supraorbital semicircles, vertical dorsals 16, horizontal dorsals 23, ventrals 26, one row of scales between the suboculars and supralabials, fourth toe lamellae on phalanges II and III 30, nuchal crest scales very high, body crest scales moderate; in life, dorsum dark green with four pale green crossbars, the dark green color blending quickly at the junction of the dorsal and ventral color into a series of diagonally directed sky-blue areas that give a ragged appearance to the junction of the dorsal and ventral colors; dorsal crossbands continue onto the tail; casque gray-green, eyeskin pale pea-green; dewlap pale yellow-orange, chin slightly deeper yellow-orange, throat yellow-orange, immaculate except for some vague pale greenish smudges posterolaterally.

Variation. The series of *A. b. caeruleolatus* consists of 20 males and 17 females. The largest male (ASFS V34505) has a snout–vent length of 148, the largest female (AMNH 6017) 145. The male is from the type locality, the female from Villa Riva. Snout scales at the level of the second canthals range between 2 and 5; the mode is 4 (14 specimens). The vertical loreal rows vary between 6 and 10; the mode is 8 (15 specimens). There are 2 or 3 scales between the supraorbital semicircles (mode 3). There are modally 5 scales between the interparietal and the supraorbital semicircles; 5 scales are involved in 52 percent of the combinations; actual counts are 4/4 (3), 4/5 (6), 5/5 (10), 5/6 (7), 6/6 (4), 6/7 (1), 4/6 (1), and 5/7 (1). Vertical dorsals range between 14 and 22 (mean 17.1), horizontal dorsals between 15 and 25 (19.9), and ventrals between 15 and 32 (22.4). Of 16 adult males, four have the nuchal crest scales very high, 11 have them high, and one has them moderate. Of 17 adult females, four have the nuchal crest scales very high, ten have them high, and three have them moderate. In the adult males, the body crest scales are high in six males, moderate in eight, and low in two, whereas in the adult females, these scales are high in five, moderate in six, and low in six. All but two lizards (6 percent) have the suboculars separated by one row of scales from the supralabials.

In a series of 12 adult male topotypes, the dorsal ground color was recorded as some shade of green (usually dark green)

with four pale pea-green crossbands. The dorsal green color blends quickly ventrolaterally into a series of irregular sky-blue patches or blotches that mark the border between the dorsal green and the pale yellow to cream venter. These sky-blue patches are often prominently extended onto the lateral margins of the venter as a series of diagonal, posteriorly directed areas, which, upon preservation, are still prominent features of the lower sides. The upper surface of the head was gray-green to brown, the eyeskin pale pea-green. The dorsal banded pattern of dark and light green continues onto the tail. The dewlap is pale yellow-orange, yellow, or orange, and the chin is slightly deeper yellow-orange, concolor with the throat, which is either immaculate (usually) or with very faint greenish dots or smudges. Eleven female topotypes were colored and patterned dorsally like the males, with the pattern extending onto the tail, but there is only a vague indication of the ventrolateral sky-blue pigmentation. The necks of females were often streaked with dark and pale greens. The chin and throat were yellow to yellow-green, regularly with some darker green dots, blotches, or occasionally marbled with dark green. The female dewlap was yellow to pale orange, streaked with dark brown or grayish.

Two females from the *haitises* region near Gonzalo were deep to emerald green in life with yellow dewlaps having varying amounts of brown streaking or smudging; the limbs were contrastingly banded dark and pale green. The throats were bright yellow to bright green, with scattered deeper green spots in each case. In a pair from La Mata, the dorsa were bright green, somewhat marbled with yellow and yellow-green, the upper surfaces of the heads were pale fawn, the eyeskin pale grayish green, and the dewlaps orange in both sexes.

The series of *A. b. caeruleolatus* includes four juveniles and subadults with snout–vent lengths from 60 to 91; the largest of these is a topotype that was colored and patterned like adults except that the sky-blue lower edges to the dorsal color were absent and the dewlap was streaked brown and gray basally. The chin and throat were immaculate pale green. There are no color data on the other juveniles, and none of them presently shows any pattern.

Comparisons. A. b. caeruleolatus differs from all previously described subspecies in having the sky-blue patching along the lower sides. In having four dorsal pale green body bands, *caeruleolatus* differs strikingly from *multistruppus* with its multiple banding; in addition, the dewlap of *multistruppus* is pale and often grayish, in contrast to the generally brighter dewlaps of *caeruleolatus.* From nominate *baleatus, caeruleolatus* differs in having the throat yellow to yellow-green rather than bright yellow to orange, and female *caeruleolatus* have the throat with dark green markings. From high upland *sublimis, caeruleolatus* differs in having the sky-blue blotches ventrolaterally and in lacking ventral markings, and whereas *caeruleolatus* has comparably pigmented dewlaps, those in *sublimis* are generally paler and often suffused at least basally with gray. The dorsal patterns of both *sublimis and caeruleolatus* are comparable, since both are crossbanded.

As far as meristic counts are concerned, *caeruleolatus* differs from the named subspecies in the following ways. Compared with *baleatus, caeruleolatus* has modally 8 (rather than 7) vertical loreal rows, and a lower mean number of ventral scales (22.4 versus 23.8). There is also a strong tendency for adult *caeruleolatus* to have moderate to low body crest scales, whereas in *baleatus* the tendency is toward high to moderate body crest scales. Compared with *multistruppus, caeruleolatus* has modally 4 (rather than 2) snout scales at the level of the second canthals, 8 rather than 7 vertical rows of loreals, 5/5 rather than 4/4 scales between the interparietal and the supraorbital semicircles, and a lower mean of vertical dorsal scales (17.1 versus 18.6). With regard to body crest scales,

these two subspecies show the same situation as *caeruleolatus* and *baleatus*. Compared with *sublimis*, *caeruleolatus* has 4 (rather than 2) snout scales at the level of the second canthals, 8 (rather than 7) vertical rows of loreals, 5/5 (rather than 4/4) scales between the interparietal and the supraorbital semicircles, and lower means of both vertical dorsals (17.1 versus 19.2) and ventrals (22.4 versus 25.1). *A. b. sublimis* has not been recorded as having the dorsal body crest scales other than high, in contrast to the strong tendency in *caeruleolatus* of having these scales moderate to low.

Discussion. *A. b. caeruleolatus* centers in the extremely mesic eastern portion of the Valle de Cibao in that area that has the most rainfall in the República Dominicana. I have already commented on the specimens from Los Bracitos, Duarte Province; these specimens are old and patternless and are from a locality in the Cordillera Septentrional which is, farther west, occupied by *A. b. baleatus;* I include them with *caeruleolatus* provisionally. The specimen from Pontón, Duarte Province, is a juvenile (ASFS V2987; snout–vent 60) and is presently patternless; no color data are available. It too I only provisionally regard as *caeruleolatus*. The two specimens from La Vega Province (ASFS V4317, MCZ 128379) are also without color data in life, and the former is a patternless juvenile (snout–vent 69). Specimens from these last two localities also require verification as to subspecific status.

A. b. caeruleolatus presumably intergrades with four subspecies: *baleatus*, *multistruppus*, the subspecies on the Península de Samaná, and subspecies to the southeast. Only in the last case are specimens that I interpret as intergradient known, and they will be discussed under the description of the southeastern subspecies. No intergrades are known between the Samaná subspecies, *baleatus*, or *multistruppus*. Distance between *caeruleolatus* and the nearest localities for these subspecies are: Samaná subspecies—13 kilometers (Caño Abajo and 5 km NW Sánchez); *baleatus*—50 kilometers (Los Bracitos and Pena); *multistruppus*—12 kilometers (12.8 km NW Bonao and Guaigüí). Of these presumed areas of contact, that between *caeruleolatus* and the Samaná subspecies is not unexpected; the area between the two known localities is very open and relatively barren and devoid of trees and appears always to have been so. There are fine high swamp-forests in the western part of this intervening region, and it is possible that intergrades between these two distinctive subspecies will be encountered in these forests. Most puzzling is the absence of intergradation between *caeruleolatus* and *multistruppus*. The specimen from northwest of Bonao is a juvenile, but it does not show the characteristic multiple crossbands of both young and adult *multistruppus*. It may be that *multistruppus* occupies only the foothills of the Cordillera Central and that the zone of intergradation between *multistruppus* and *caeruleolatus* is very abrupt.

Remarks. *A. b. caeruleolatus* is known from sea level to an elevation of 1000 feet (305 meters) in the *haitises* region near Gonzalo and 1200 feet (366 meters) northwest of Bonao. Specimens were secured primarily from native collectors; the long series of topotypes is due to the industry of the inhabitants of Caño Abajo. The Caño Abajo area is one of *cafetales* and *cacaotales* with high canopied shade-trees, and the lizards apparently are extremely abundant in this optimal habitat. The pair of lizards from La Mata were secured by me while they were copulating on the side of a large shade-tree in a *cafetal* about 4 feet (1.2 meters) above the ground at 1225 hours. The two females from Gonzalo were taken during the day on large trees adjacent to a small spring in the *haitises;* the surrounding area was under heavy cultivation, but the doline slopes were covered locally with undisturbed forest.

The name *caeruleolatus* is from the Latin "caeruleus" for "blue" and "latus"

for "side," in allusion to the sky-blue lower sides of this subspecies.

Anolis baleatus samanae new subspecies

Holotype. CM 54105, an adult male, from 7.6 mi. (12.2 km) NE Sánchez, 1000 feet (305 meters), Samaná Province, República Dominicana, one of a series collected by native collectors on 28 November 1971. Original number ASFS V34474 .

Paratypes. ASFS V34475–79, same data as holotype; USNM 193990–92, same locality as holotype, native collectors, 27 November 1971; MCZ 125634, 5.0 mi. (8.0 km) NW Sánchez Province, República Dominicana, J. Aria, 27 November 1971; ASFS V34495–96, 5.0 mi. (8.0 km) NW Sánchez, Samaná Province, República Dominicana, J. Aria, 28 November 1971; CM 54127–30, 5.0 mi. (8.0 km) NW Sánchez, Samaná Province, República Dominicana, J. Aria, 30 November 1971; MCZ 125635–39, USNM 193993–4001, 5.0 mi. (8.0 km) NW Sánchez, Samaná Province, República Dominicana, J. Aria, 1 December 1971; ASFS V34514, ASFS V34836–38, Las Terrenas, Samaná Province, República Dominicana, native collector, 28 November 1971; ASFS V1904, 6 km E Sánchez, Samaná Province, República Dominicana, R. Thomas, 30 October 1963; AMNH 28651, Samaná, Samaná Province, República Dominicana, J. King, August 1924; AMNH 39817–23, AMNH 42285, Laguna, Samaná Province, República Dominicana, W. G. Hassler, October–December 1929; USNM 61928, Cayo Hondo, Samaná Province, República Dominicana, W. L. Abbott, February 1919.

Definition. A subspecies of *A. baleatus* characterized by the combination of modally 2 snout scales at level of second canthal scales, 7 vertical rows of loreal scales, 3 scales between the interorbital semicircles, 4/4 scales between the interparietal and the supraorbital semicircles, moderate number of vertical dorsal scales (13–20; mean 16.6), moderate number of ventral scales (16–29; mean 22.1), nuchal crest scales very high to high (usually) to moderate or low (rarely) in both sexes, body crest scales high to moderate but often low in both sexes, subocular scales almost always separated from supralabial scales by one (rarely 2) row of scales; dorsum in both sexes in life blotched dark green, greenish, dull gray-green, brown, or blackish, dewlaps in males dull yellow to pale yellowish orange, in females very pale yellow to pale yellowish orange, streaked with blackish or brown basally, and chin and throat in males cream to yellowish or yellow-orange, mottled with black or gray, in females pale green to greenish yellow with dark green to brown streaking or even reticulate.

Distribution. The Península de Samaná in the northeastern República Dominicana, and apparently islets in the Bahía de Samaná.

Description of holotype. An adult male with a snout–vent length of 145 and a tail length of 222 (regenerated); snout scales between second canthals 3, 6 vertical rows of loreal scales, 3 scales between the supraorbital semicircles, 4/4 scales between the interparietal and the supraorbital semicircles, vertical dorsals 18, horizontal dorsals 19, ventrals 21, one row of scales between the suboculars and supralabials, fourth toe lamellae on phalanges II and III 30, nuchal crest scales very high, body crest scales high; in life, dorsum mottled dull greens and gray-brown with whitish (almost cream but suffused with pale gray); upper surface of head mixed dark brown and gray, venter dull greenish, dewlap orange, chin and throat creamy to yellowish, not marked with green.

Variation. The series of 54 *A. b. samanae* consists of 32 males and 22 females. The largest male (AMNH 39807) has a snout–vent length of 157; the largest females (CM 54130, USNM 193994) have snout–vent lengths of 145. The male is from Laguna, the females from 5.0 mi. NW Sánchez. Snout scales at the level of the second canthals range between 2 and 5; the mode is 2 (24 specimens). The vertical loreal rows vary between 5 and 9; the

mode is 7 (25 specimens). There are 2 or 3 scales between the supraorbital semicircles (mode 3). There are modally 4 scales between the interparietal and the supraorbital semicircles; 4 scales are involved in 43 percent of the combinations: actual counts are 3/3 (2), 3/4 (3), 4/4 (17), 4/5 (8), 5/5 (13), 5/6 (5), 6/6 (1), 6/7 (2), 4/6 (1), and 3/5 (1). Vertical dorsals range between 13 and 20 (mean 16.6), horizontal dorsals between 13 and 27 (19.3), and ventrals 16–29 (22.1). Of 30 adult males, 14 have the nuchal crest scales very high, 15 have them high, and one has them moderate; in 20 adult females, nine have the nuchal crest scales very high, nine have them high, one has them moderate, and one has them low. Body crest scales in males are high in three lizards, moderate in 16, and low in ten; in females, 11 have these scales moderate and ten have them low. The suboculars are separated from the supralabials by one row of scales in all but four specimens (7 percent), which have them in contact, and one specimen (2 percent), which has 2 rows of scales in this position.

A. b. samanae is basically a blotched lizard, and no adults show any indication of crossbanding. The body is irregularly blotched with blackish, dark green, dull green, gray-brown, and occasionally there are sky-blue areas along the ventrolateral margin of the dorsal coloration in males, but these areas are not so prominent as in *caeruleolatus*. Regardless of the dorsal shades, the upper surface of the head is mixed dark brown and shades of gray in both sexes. The hindlimbs are finely barred with pale and dark green. The venter is dull greenish in both sexes. The dewlap in males varies from dull yellow or pale yellowish orange to orange, and the chin and throat are yellowish, cream, or yellow-orange, mottled with black or gray. In females, the dewlaps are very pale yellow, pale yellow-orange, or grayish orange, at times streaked with blackish or brown basally, and the chin and throat ground color is pale green, marbled, streaked, or even reticulate with dark green to (rarely) brown.

There are one juvenile (AMNH 28651; snout–vent length 40) and two subadult (snout–vent lengths 92 and 97) *A. b. samanae*. The subadults are old and discolored but their patterns seem not to differ from those of full adults. The juvenile on the other hand, has four bold pale crossbars on the dorsum, the pattern continuing onto the tail. This young individual has the umbilicus still present and is presumably near hatchling size.

Comparisons. Since *samanae* and *caeruleolatus* are adjacent geographically, the most pertinent comparisons are between them. Examples of these two populations, as noted in the introduction to the present paper, were available to me simultaneously and I was struck with their differences in life. *A. b. samanae* is a blotched lizard whereas *caeruleolatus* is a crossbanded one; the latter subspecies also typically has sky-blue ventrolateral blotches, a feature absent (or occasionally poorly expressed) in male *samanae*. Male dewlap colors are similar in both subspecies, although female dewlap colors in *samanae* seem somewhat paler than those of *caeruleolatus*. The chin and throat markings of the two subspecies are quite distinct; in male *caeruleolatus*, the throat is deep yellow to yellow-orange, at best with very faint grayish dots or smudges, whereas in male *samanae* the throat is yellowish or cream to yellow-orange, mottled with black or gray. In female *caeruleolatus*, the throat is yellow to yellow-green, always with some dark green dots, blotching, or marbling, whereas in *samanae* females, the throat is pale green, greenish yellow, or yellow-green, with dark green to brown streaking or reticulum.

The only subspecies thus far described which is blotched like *samanae* is the Cordillera Central *sublimis*, although *caeruleolatus* may show a marbled dorsum in some areas. No pigmental or pattern differences separate *samanae* and *sublimis*, since in both dorsal coloration and color of

the dewlap the major color involved is green. However, the throat in male *sublimis* is pale green, whereas in *samanae* it is cream to yellow-orange. Certainly *multistruppus* and *samanae* are easily distinguished in the field by their very different dorsal patterns, for example, and *baleatus,* with its very, very bright chin and throat, both of which are immaculate, is quite distinctive from *samanae.*

In meristic data, *samanae* differs from *caeruleolatus* in having 2 (rather than 4) snout scales, 7 (rather than 8) vertical rows of loreals, and 4/4 (rather than 5/5) scales between the interparietal and the supraorbital semicircles. From *multistruppus, samanae* differs in having a lower mean of vertical dorsal scales (16.6 versus 18.6), and the same difference occurs between *samanae* and *sublimis* (16.6 versus 19.2) and in ventrals (22.1 versus 25.1). From *baleatus, samanae* differs in having 2 (rather than 4) snout scales, 4/4 (rather than 5/5) scales between the interparietal and the supraorbital semicircles, and lower means in both vertical dorsals (16.6 versus 17.5) and ventrals (22.1 versus 23.8). The nuchal crest scales in *samanae* are more consistently very high to high than they are in any of the other subspecies of *A. baleatus.*

Discussion. As pointed out in the discussion of *A. b. caeruleolatus,* there are no intergrades known between that subspecies and *samanae.* The isthmus of the Península de Samaná is much cleared and locally even barren, but there are large western swampy areas that support magnificent hardwood forests toward the landward side. These forests may well support intermediates between *samanae* and *caeruleolatus,* or, because of their proximity to the mainland, they may be inhabited by *caeruleolatus.* Specimens from 5.0 mi. NW Sánchez, that locality for *samanae* which is closest to a known locality for *caeruleolatus* (18 kilometers), show no tendencies toward the crossbanded condition of *caeruleolatus.*

A. b. samanae is the only Hispaniolan giant anole known by specimens from any off-shore island or islet. The specimen from Cayo Hondo, taken by W. L. Abbott, constitutes this record, although I am unable to locate this islet. I assume it is one of the archipelago within the Bahía de Samaná.

Remarks. All but one *A. b. samanae* secured by myself and parties were native-collected. The exception is a lizard taken by Richard Thomas, one of two seen on a small tree and in a vine tangle in a steep limestone ravine east of Sánchez. The area of the type locality is in the uplands of the Sierra de Samaná on the road between Sánchez and Las Terrenas. Thus newly constructed road passes through superb mesic high-canopied forest, and much of the area is not yet seriously disturbed. Obviously from the number of lizards secured by natives in this region, *A. b. samanae* is common. The range is not high, with a maximum elevation of 1673 feet (510 meters) in Monte Las Cañitas; this mountain lies between Sánchez and Las Terrenas. Specimens from Las Terrenas itself were secured by natives from near-coastal mesic *cafetales* and *cacaotales,* and lizards from northwest of Sánchez were in similar situations.

Only three other reptiles (*Diploglossus sternurus alloeides* Schwartz, *Leiocephalus personatus pyrrholaemus* Schwartz, and *Dromicus parvifrons niger* Dunn) are known to have differentiated at the subspecific level on the Península de Samaná. *Sphaerodactylus clenchi* Shreve and *Sphaerodactylus samanensis* Cochran both occur there and have as yet unnamed populations, one of which in each case is limited to the peninsula. It is also of interest to note that in *Anolis distichus* Cope, the Samaná population is identical to the population on the southern shores of the Bahía de Samaná (*ignigularis* Mertens), but that the range of this subspecies is interrupted at the head of the Bahía de Samaná by *A. d. dominicensis* Reinhardt and Lütken (see Schwartz, 1968: 280–81, for details).

Anolis baleatus litorisilva new subspecies

Holotype. USNM 193977, an adult male, from 1.2 km SSW Punta Cana, La Altagracia Province, República Dominicana, one of a series collected by Danny C. Fowler and Bruce R. Sheplan, on 24 November 1971. Original number ASFS V35095.

Paratypes. ASFS V35096–100, same data as holotype; CM 54113–14, MCZ 125616–17, 5.5 km SSW Punta Cana, La Altagracia Province, República Dominicana, D. C. Fowler, 27 November 1971; ASFS V29090, Juanillo, La Altagracia Province, República Dominicana, native collector, 24 July 1971; ASFS V961–62, 0.5 mi. NW Boca de Yuma, La Altagracia Province, República Dominicana, R. F. Klinikowski, R. Thomas, 2 September 1963; ASFS V1136, 2.5 km NW Boca de Yuma, La Altagracia Province, República Dominicana, native collector, 4 September 1963; ASFS V17573, 4 km NW Boca de Yuma, La Altagracia Province, República Dominicana, A. Schwartz, 13 June 1969; ASFS V17616, 2 km NW Boca de Yuma, La Altagracia Province, República Dominicana, J. B. Strong, 15 June 1969.

Definition. A subspecies of *A. baleatus* characterized by the combination of 2 or 4 scales at level of the second canthal scales, 7 vertical rows of loreal scales, 3 scales between the interorbital semicircles, 4/5 scales between the interparietal and the supraorbital semicircles, low number of vertical dorsals (13–19; mean 15.9), low number of ventral scales (18–26; mean 21.3), nuchal crest scales always very high to high in both sexes, body crest scales high (rarely) to moderate or low, subocular scales usually separated from supralabial scales by one row of scales; dorsum in life varying from light blue-brown to light greenish brown in males, dull brown to olive-brown in females, blotched with creamy to gray, dewlap in males bright orange, brownish in females, and chin and throat (including lips) bright orange in males, pale yellow-green in females.

Distribution. Extreme eastern República Dominicana in La Altagracia Province, from Punta Cana to the vicinity of Boca de Yuma.

Description of holotype. An adult male with a snout–vent length of 136 and a tail length of 183 (regenerated); snout scales between second canthals 2; 6 vertical rows of loreal scales, 3 scales between the supraorbital semicircles, 5/5 scales between the interparietal and the supraorbital semicircles, vertical dorsals 15, horizontal dorsals 16, ventrals 25, subocular scales in contact with the supralabial scales, fourth toe lamellae on phalanges II and III 31, nuchal crest scales very high, dorsal body crest scales high; in life, dorsum blotched light blue-brown and light green-brown; venter pale gray-green; chin, lips, and dewlap bright orange.

Variation. The series of 16 *A. b. litorisilva* is composed of six males and ten females. The largest male (MCZ 125616) has a snout–vent length of 158, the largest female (ASFS V961) 131. The male is from 5.5 km SSW Punta Cana, the female from 0.5 mi. NW Boca de Yuma. Snout scales at the level of the second canthals range between 2 and 5; there are two modes, 2 and 4, each with five individuals. The vertical loreal rows vary between 6 and 9; the mode is 7 (nine specimens). There are 2 to 4 scales between the supraorbital semicircles (mode 3). There are modally 4/5 scales between the interparietal and the supraorbital semicircles; 5 scales are involved with 59 percent of the combinations; actual counts are 4/4 (4), 4/5 (6), 5/5 (5), and 5/6 (1). Vertical dorsals range between 13 and 19 (mean 15.9), horizontal dorsals between 14 and 22 (18.5), and ventrals between 18 and 26 (21.3). Of four adult males, three have the nuchal crest scales very high and one has them high; of five adult females, two have these scales very high and three have them high. In the males, the body crest scales are high in one and moderate in three, and in the females, these scales are

moderate in two and low in three. The suboculars are separated from the supralabials by one row of scales in all but one specimen (6 percent).

A. b. litorisilva is essentially a blotched lizard whose colors do not include bright or even medium greens. The color notes on the holotype apply equally well to the other adult males—the dorsum is blotched with bluish browns and light greenish browns, without any clear greens, and the blotching is often more pronounced on the head than on the body. In females, the dorsum is dull brown to olive-brown with only occasional slight remnants of a lighter green pattern on the head; the blotching in the female involves creamy to gray pigmentation. The venter is pale gray-green or whitish green in males, pale greenish gray in females. The dewlap in all adult males was recorded as bright orange, and brownish in females. In males, the chin (including the lips) is bright orange, and pale yellow-green in females. The upper surface of the head in males is blotched like the body and is dark chocolate in females. In females, the upper surfaces of the hindlimbs were recorded as olive-brown, blotched with cream to gray like the dorsum.

The series of *A. b. litorisilva* contains seven juveniles and subadults (snout–vent lengths 45 to 88). The smallest juvenile (ASFS V17573, female) was bright green in life with four pale buffy crossbands and dark green shadow-bars between the crossbands; the tail was ringed cream and dark gray, and the venter was pale green. The dewlap was yellow-green and gray. A slightly larger female (ASFS V17616) with a snout–vent length of 57 was yellow-green dorsally and without bands, the head was brown; the eyeskin was green, and the venter yellow-green. The tail was banded black and yellow-green, and the dewlap was mainly brown with the scale rows yellow-green. A still larger female (ASFS V1136) with a snout–vent length of 67 was green, faintly crossbarred with grayish green, and there were charcoal smudges on the neck. Two male subadults with snout–vent lengths of 71 and 83 (ASFS V35099–100) from the type locality were recorded by Fowler as follows: "One with a strong vertical banding pattern alternating brown-green and white-gray, which extends from tip of tail to the head where it becomes slightly more diffuse; on the other, the dorsal ground color is dull brown with remnants of banding pattern only around head; the ventral ground color of the first is gray-green with brown mottling, the second is dull gray-brown; in both juveniles, the dewlap is orange-green and the chin and lips are green." The largest subadult (ASFS V29090) was patternless green above, and the dewlap was orange with charcoal stripes; the specimen is a female.

Comparisons. Because of its blotched (rather than crossbanded) pattern, *litorisilva* requires comparison with *samanae* and *sublimis*. The general effect of the dorsa of all three subspecies is quite similar, but *samanae* and *sublimis* are much the brighter lizards, with greens predominant in the dorsal pigmentation. On the other hand, *litorisilva* is a much more drab lizard, without clear greens in the adults, the tendency being toward more sombre hues, primarily shades of browns. From all other described subspecies, *litorisilva* differs in being blotched rather than crossbanded and also in having much less gaudy dorsal colors. In meristic counts, *litorisilva* differs from the remaining subspecies in the following ways. From *caeruleolatus, litorisilva* differs in having 7 (rather than 8) vertical loreal rows, and lower means of vertical dorsals (15.9 versus 17.1) and ventrals (21.3 versus 22.4). From *multistruppus, litorisilva* differs in lower means of vertical dorsals (15.9 versus 18.6) and ventrals (21.3 and 22.3). From *sublimis, litorisilva* differs in having lower means of vertical dorsals (15.9 versus 19.2) and ventrals (21.3 versus 25.1). From *baleatus, litorisilva* differs in having lower means of vertical dorsals (15.9 versus 17.5) and ventrals (21.3 versus 23.8). Meaningful comparisons of *litorisilva* with

other subspecies in counts of snout scales, and scales between the interparietal and the supraorbital semicircles, are impossible since *litorisilva* has a bimodal condition in the former (and the bimodes are 2 and 4, those counts which occur singly as the mode in the other subspecies) and has a mode of 4/5 in the latter (whereas all other species have either 4/4 or 5/5). Considering the fairly large series of *litorisilva* (16 specimens), these two "abnormal" conditions are puzzling. At least in the case of 4/5 counts, the absence of 3/3 or 3/4 counts in *litorisilva* suggests that this subspecies tends toward a 5/5 count.

Discussion. *A. b. litorisilva* appears to be the extreme eastern isolate of the more widespread *A. baleatus* stock. It occupies semi-arid forests on and near the coast (as at Juanillo and Punta Cana) and on the limestone ridge behind Boca de Yuma. Both situations are far more xeric than is customary for *A. baleatus*, and the faded nongreen coloration of the adults is doubtless a response to the dry and open to dense forest conditions of this region. Nevertheless, individuals are quite conspicuous at night as they sleep exposed. *A. b. litorisilva* presumably comes into contact with the subspecies to the north and west (named below) but intergrades are presently unknown; in the vicinity of Higüey (the closest locality for the adjacent subspecies) the lizards are more brightly colored and crossbanded and quite unlike *litorisilva*.

Remarks. All but one specimen of *litorisilva* were collected by myself and parties. Individuals were found sleeping in primarily coastal forest (to which the name, from "litus" for "shore" and "silva" for "forest," refers in Latin) at elevations from 4 to 15 feet (1.2 to 4.6 meters) above the ground. Generally, juveniles sleep closer to the ground and in more dense situations than adults. One juvenile was taken from a roadside *Acacia*, a most unusual situation (since *Acacia* is a distinct xerophyte) for any giant anole. Several adults were taken in dense viny tangles, sleeping on the woody vines; the advantage of this situation was made quite obvious when I attempted to catch a large adult at night by hand. The light from my flashlight wakened the lizard almost immediately, and although I was extremely careful not to jar any of the vines, this was a vain endeavor. At the first jostling, the lizard jumped to the ground and escaped in the dry leaf litter and understory.

Anolis baleatus scelestus new subspecies

Holotype. CM 54106, an adult male, from 5.1 mi. (8.2 km) E Santo Domingo (from Río Ozama), Distrito Nacional, República Dominicana, one of three collected by David C. Leber and Richard Thomas on 18 June 1964. Original number ASFS V2460.

Paratypes. ASFS V2461–62, same data as holotype; MCZ 125618–27, 8.4 mi. (13.4 km) NE La Romana, 100 feet (31 meters), La Romana Province, República Dominicana, B. R. Sheplan, 22 November 1971; CM 54115–18, USNM 193981–89, 8.4 mi. (13.4 km) NE La Romana, 100 feet (31 meters), La Romana Province, República Dominicana, D. C. Fowler, A. Schwartz, 17 July 1971; MCZ 16321, La Romana, La Romana Province, República Dominicana, E. Leider, 1922; ASFS V29284–300, 0.2 mi. (0.3 km) N Otra Banda, 350 feet (107 meters), La Altagracia Province, República Dominicana, D. C. Fowler, A. Schwartz, 26 July 1971; ASFS V21699–700, 1 km NE Higüey, La Altagracia Province, República Dominicana, J. R. Dennis, R. Thomas, 16 August 1969; USNM 193979–80, 0.7 mi. (1.1 km) W Higüey, La Altagracia Province, República Dominicana, R. Thomas, 29 August 1963; ASFS V1038, 1 mi. (1.6 km) W Higüey, La Altagracia Province, República Dominicana, R. Thomas, 3 September 1963; ASFS V28757, 15.5 mi. (24.8 km) E San Pedro de Macorís, Río Cumayasa, La Romana Province, D. C. Fowler, 12 July 1971; ASFS V28910–16, 15.5 mi. (24.8 km) E San Pedro de Macorís, Río Cumayasa, San Pedro de Macorís Province, República Dominicana, D. C. Fowler, A.

Schwartz, 16 July 1971; ASFS V28847, 15.5 mi. (24.8 km) E San Pedro de Macorís, La Romana Province, República Dominicana, A. Schwartz, 15 July 1971.

Associated specimens. REPÚBLICA DOMINICANA: *La Altagracia Province,* 1 km SE Las Lisas (ASFS V17434-35); *San Cristóbal Province,* 8 km N Yamasá, 200 feet (61 meters) (ASFS V28656).

Definition. A subspecies of *A. baleatus* characterized by the combination of modally 2 scales at level of the second canthal scales, 7 vertical rows of loreal scales, 3 scales between the supraorbital semicircles, 5/5 scales between the interparietal and the supraorbital semicircles, low number of vertical dorsals (12–20; mean 15.4), low number of ventral scales (17–28; mean 21.1), nuchal and body crest scales always very high to high in both sexes, subocular scales usually separated from supralabial scales by one (occasionally two) row of scales; dorsum in both sexes either green with three pastel green crossbands or dark green flecked with light green, cream with some greenish to brownish green smudges, dewlap in males deep yellow to deep orange, streaked or smudged with dark brown to charcoal, and throat in females dark green marbled with yellow and pale green (males unrecorded).

Distribution. Southeastern República Dominicana, from the Sierra de Yamasá and the vicinity of Santo Domingo in the west, east to the region about Higüey and Las Lisas in La Altagracia Province.

Description of holotype. An adult male with a snout–vent length of 152 and a tail length of 267; snout scales between second canthals 4; 8 vertical rows of loreal scales, 2 scales between the supraorbital semicircles, 4/5 scales between interparietal and supraorbital semicircles, vertical dorsals 16, horizontal dorsals 16, ventrals 22, subocular scales separated from supralabial scales by one row of scales, fourth toe lamellae on phalanges II and III 34, nuchal crest scales high, body crest scales moderate; in life, dorsum olive-green with six pastel green crossbands, tail and venter light green; dewlap dark yellow.

Variation. The series of 61 *A. b. scelestus* consists of 27 males and 34 females; a large number of the specimens are juveniles and subadults. The largest male (ASFS V29284) has a snout–vent length of 180, the largest female (ASFS V29286) 147; both are from near Otra Banda. Snout scales at the level of the second canthals range between 2 and 4; the mode is 2 (32 specimens). The vertical loreal rows vary between 5 and 8, with a mode of 7 (25 specimens). There are 1 to 4 scales between the supraorbital semicircles (mode 3). There are modally 5/5 scales between the interparietal and the supraorbital semicircles; 5 scales are involved in 49 percent of the combinations; actual counts are 3/4 (2), 4/4 (14), 4/5 (14), 5/5 (17), 5/6 (11), 6/6 (1) and 4/6 (1). Vertical dorsals range between 12 and 20 (mean 15.4), horizontal dorsals between 15 and 25 (18.8), and ventrals between 17 and 28 (21.1). Of 11 adult males, nine have the nuchal crest scales very high and two have them high. Of 16 adult females, nine have these scales very high and seven have them high. Body crest scales in males are high in two lizards, moderate in eight, and low in three; in females, the body crest scales are high in two, moderate in eight, and low in six. Fifty-three specimens have the suboculars separated from the supralabials by one row of scales, whereas in four lizards (7 percent) these scales are in contact, and in two lizards (3 percent) they are separated by two rows of scales.

In general, both sexes of *A. b. scelestus* show a pattern of about six or seven fine crossbands that are often obscured by dorsal blotching. Colors are shades of greens, with brighter green the base color and the blotching tending toward darker shades. The crossbands are lighter pastel shades of green, and in some lizards the dorsal ground color is olivaceous. Another variant, which is somewhat more prevalent in females, is an olive green to dark green

dorsum, flecked with pale green. Two females from near Higüey showed still another style of body pattern and color, with the dorsal ground color cream with some dark green to brownish green smudges, and the neck with alternating pale blue and charcoal markings, the pale blue markings persisting onto the cheeks. In males the upper surface of the head is brown, and in females it is mixed brown and green, with the snout and supraocular scales deep green in some lizards. In females, the chin and throat are dark green, marbled with yellow and pale green. The dewlap is rather variable; in males it has been recorded as dark yellow or deep yellow to orange or dark orange, whereas in females the dewlap varies from yellow to dark orange with dark brown, olivaceous, or charcoal streaking, marbling, or smudging. Although there are no color notes in life, in the preserved lizards the eyeskin is regularly pale gray, and I presume that in life the eyeskin is set off from the rest of the head color in some pigmental fashion. Many specimens of both sexes have the lower sides tigroid with "stripes" extending conspicuously onto the lateral sides of the abdomen.

There are 34 juvenile and subadult *A. b. scelestus,* with snout–vent lengths between 46 (USNM 193989) and 94 (ASFS V21699–700). Three juveniles (snout–vent lengths 46–61) have umbilici still present. This entire suite of young lizards shows a remarkable diversity in dorsal pattern. Even small specimens may be either unicolor green (usually with a vertical nuchal white crescent and a white subocular spot), green with three or four yellow body bands, or there may be many more bands resulting from the interposition of pale body bands between the primary pale body bands. One specimen (ASFS V29296; snout–vent length 70, male) has both pale body bands and interstitial pale blotching, whereas another lizard (MCZ 125621; snout–vent length 86, female) already shows the adult pattern of several fine pale crossbands on a green ground. The largest subadults, however, (ASFS V21699–700; snout–vent lengths 94, male and female) are both presently unicolor and show no indications of the adult body banding. That a single juvenile may demonstrate a pattern change is shown by the following notes on ASFS V28757, a female with a snout–vent length of 54: "Alive, emerald green with about four pale yellow crossbands on body; dead—seven narrow brown body bands which are hollowed, and the dorsal ground color now pale yellow-green." The dewlap in young males is orange, in young females from dull yellow streaked with charcoal to charcoal.

Comparisons. In color and pattern, *A. b. scelestus* differs from all other subspecies. No other named population has six or seven narrow dorsal crossbands; even *multistruppus* is much more conspicuously banded than *scelestus* and lacks any sort of dorsal blotching. *A. b. scelestus* is known to intergrade with more northern *caeruleolatus* and is presumed to meet *litorisilva.* In each case, there is no difficulty distinguishing the adjacent forms chromatically. *A. b. caeruleolatus* typically has (in males) sky-blue blotches along the junction of the dorsal and ventral colors, and is prominently crossbanded with three dorsal crossbands. *A. b. litorisilva* is a blotched lizard, the dorsal colors much more drab than those of *scelestus,* tending toward browns and brownish greens. Perhaps *scelestus* most closely resembles *multistruppus,* but, although both are banded, the bands in *multistruppus* are much finer and much more numerous than the six or seven pale dorsal crossbars in *scelestus.*

A. b. scelestus, with modally 2 snout scales, differs from *caeruleolatus,* which has 4 snout scales. In having 7 vertical loreal rows, *scelestus* differs from *caeruleolatus,* which has 8 rows. In having 5/5 scales between the interparietal and supraorbital semicircles, *scelestus* differs from *samanae, multistruppus,* and *sublimis,* all of which have 4/4. *A. b. scelestus* has the lowest

mean of vertical dorsals (15.4) of all named subspecies, being most closely approached by *litorisilva* (15.9). *A. b. scelestus* males are larger than those of any other subspecies (180 in *scelestus,* 158 in *litorisilva,* which is second largest) and in fact this subspecies exceeds all other Hispaniolan giant anoles in size, being most closely approached by male *A. r. ricordi,* which reach a snout–vent length of 160.

Discussion. I am uncertain that all specimens included in *scelestus* should be so associated. This is especially true of the specimen from near Yamasá (ASFS V28656); this is a juvenile male and its taxonomic status remains somewhat in doubt, since it is young. It is also possible that specimens from Santo Domingo likewise are not identical with more eastern lizards, although the two samples agree fairly well.

A. b. scelestus and *A. b. caeruleolatus* intergrade in the region of El Seibo Province; I have examined the following material from El Seibo which I consider intergradient: 3.5 mi. (5.6 km) S Sabana de la Mar (ASFS X7877); 2.1 mi. (3.4 km) N El Valle (ASFS X7861–62); 3 km N El Valle (ASFS V3157–58); 10.5 km N Hato Mayor (ASFS V35329–30). This series consists of three juveniles and four young adults (with snout–vent lengths between 112 and 127). The single adult male (ASFS X7877) was tannish gray in life with darker brown blotches, a pale green venter, and an orange dewlap. Two adult females (ASFS X7861–62) were pale pea-green with vertical gray bars, the upper surface of the head grayish tan, venter green, and dewlap grayish orange. The lower jaw and throat were green mottled with darker green. In general this series seems closer to *caeruleolatus* than to *scelestus,* but the male lacks sky-blue ventrolateral markings. On the other hand, the vertical gray bars, recorded for the female, resemble the pattern of *scelestus* rather than that of female *caeruleolatus.* It seems likely that *caeruleolatus* and *scelestus* intergrade in this region.

Remarks. Almost all ASFS *scelestus* were secured while the lizards were asleep at night. Typical situations are lowland *cacaotales* and *cafetales* with their high canopied shade-trees, along lowland streams (as at Otra Banda and Yamasá), and in woods associated with limestone cliffs (east of Santo Domingo). The long series from the Río Cumayasa is from the high riverine woods along that stream; remarkably, we secured only juveniles and subadults at this locality, despite three nocturnal visits. One juvenile from this locality was taken on the exposed branch of an *Acacia* tree along an open road. Perhaps the most remarkable place whence *A. b. scelestus* has been taken is the locality northeast of La Romana. This place is a deep and well-wooded ravine through which flows a clear stream; however, the ravine is completely surrounded on all sides by cane fields, and the ravine woods are completely isolated at the ravine rim from other such ecologies, if they even still exist in this area. *A. b. scelestus* was exceptionally abundant in this particular and very restricted strip of riverine gallery forest. Elevations above ground recorded for sleeping *scelestus* range from 2 to 20 feet (0.6 to 6.1 meters), with juveniles usually sleeping much lower than adults. The altitudinal distribution of *A. b. scelestus* is in general low, with recorded elevations from sea level to 200 feet. It is likely that this subspecies also occurs in the uplands of the Cordillera Oriental, but as yet there are no specimens from areas within that rather low-lying but mesic and well-forested massif.

The name *scelestus* is from the Latin for "unlucky, wretched," in allusion to the difficulties involved with collecting this subspecies at the La Romana ravine noted above.

The transition between *scelestus* and *litorisilva* must be very abrupt; the two subspecies are known from localities separated by only 28 kilometers. The habitats of the two subspecies are quite different, with *scelestus* inhabiting very mesic situations

and *litorisilva* xeric coastal woods. Interestingly, this same eastern region of the República Dominicana is also an area of abrupt changes in subspecies of *Anolis distichus*, where the subspecies *ignigularis* Mertens and *properus* Schwartz have ranges which coincide rather closely with those of *scelestus* and *litorisilva* (see Schwartz, 1968: 275, map). The question of intergradation between *scelestus* and the southwestern subspecies next to be named will be discussed under that taxon.

Perhaps more so than any other subspecies, *scelestus* seems to show a very spotty distribution. Two instances are worthy of mention. There are excellent extensive coastal forests at Cabo Caucedo south of the Aeropuerto Internacional de las Américas on the southern Dominican coast. Repeated diurnal and nocturnal visits to these splendid woods yielded no *A. baleatus*, despite what seems to be more than adequate habitat. A second locality, east of Boca Chica along the same coast, likewise supports extensive fine stands of lowland hardwood forests, and there also, despite many diurnal and nocturnal visits, we have never encountered *A. baleatus*. It is possible that these two instances of fairly dry coastal woods are not suitable for *scelestus* (whereas they surely would be for *litorisilva*) and that *scelestus* simply does not occur there.

Anolis baleatus fraudator new subspecies

Holotype. USNM 193978, an adult female, from 4 km W, 6 km N Azua, Azua Province, República Dominicana, one of two taken by Richard Thomas, on 23 July 1969. Original number V21384.

Paratypes. ASFS V21385, same data as holotype; ASFS V21433, Barreras, Azua Province, República Dominicana, native collector, 25 July 1969; ASFS V723, 1.1 mi. (1.8 km) S San José de Ocoa, 1400 feet (427 meters), Peravia Province, República Dominicana, R. F. Klinikowski, 24 August 1958; ASFS V21203, Sierra Martín García, about 3000 feet (915 meters), above Barreras, Azua Province, República Dominicana, R. Thomas, 20 July 1969; ASFS V31207, Sierra Martín García, above Barreras, between 2000 and 2800 feet (610 and 854 meters), west slope, Mt. Busú, Barahona Province, República Dominicana, B. R. Sheplan, 15–17 September 1971.[1]

Definition. A subspecies of *A. baleatus* characterized by the combination of modally 4 scales at level of the second canthal scales, 6 vertical rows of loreal scales, 2 or 3 scales between the supraorbital semicircles, 4/4 scales between the interparietal and the supraorbital semicircles, high number of vertical dorsal scales (17–21; mean 18.8), low number of ventral scales (18–26; mean 20.7), nuchal scales high, body crest scales moderate in only adult female, subocular scales usually separated from supralabial scales by one row of scales; dorsum (in female) mottled pale and darker gray, with three irregular white crossbands, and blotched with yellow-green, top of snout and lores straw, labials dull yellow, and dewlap nearly white with a yellowish or cream wash.

Distribution. The Sierra Martín García in Barahona and Azua provinces, and along the southern slopes of the Cordillera Central and the Sierra de Ocoa in Azua and Peravia provinces.

Description of holotype. An adult female with a snout–vent length of 133 and tail length of 244; snout scales between second canthals 4; 6 vertical rows of loreal scales, 2 scales between supraorbital semi-

[1] Since the present manuscript was completed, a juvenile female (MCZ 132301) with a snout–vent length of 57 mm, was secured by E. E. Williams and J. Roughgarden at a locality south of La Horma, Peravia Province, on 19 July 1972. This lizard is to be considered a paratype. It has 3 snout scales at the level of the second canthals, 6 loreal rows, 3 scales between the supraorbital semicircles, 5/5 scales between the interparietal and the semicircles, 16 vertical rows of dorsal scales and 20 rows of ventral scales, and 1 scale between the suboculars and the supralabials. Both nuchal and body crest scales are low. As preserved, the lizard is dull greenish with indications of dark dorsal crossbars, and it lacks any pale dorsal markings.

circles, 4/3 scales between the interparietal and the supraorbital semicircles, vertical dorsals 17, horizontal dorsals 24, ventrals 21, subocular scales separated from supralabial scales by one row of scales, fourth toe lamellae on phalanges II and III 33, nuchal crest scales high, body crest scales moderate; in life, dorsum mottled pale and dark gray, blotched with yellow-green and with three irregular white crossbands, labials dull yellow, top of snout and lores straw, and dewlap nearly white with a yellowish or cream wash.

Variation. The only adult is the holotype; the remainder of the paratypic series is composed of juveniles and subadults with snout–vent lengths between 74 and 96 (three males, two females). Snout scales at the level of the second canthals range between 2 and 4; the mode is 4 (four specimens). The vertical loreal rows vary between 5 and 7, with a mode of 6 (three specimens). There are 2 or 3 scales between the supraorbital semicircles; both categories have the same frequency. There are modally 4/4 scales between the interparietal and the supraorbital semicircles; 4 scales are involved in 67 percent of the combinations; actual counts are 3/4 (2), 4/4 (3), and 5/6 (1). Vertical dorsals range between 17 and 21 (mean 18.8), horizontal dorsals between 20 and 24 (21.4), and ventrals between 18 and 26 (20.7). The only adult specimen (a female) has the nuchal crest scales high and the dorsal body crest scales moderate. Five specimens have the suboculars separated from the supralabials by one row of scales and one lizard has these scales in contact (17 percent).

The details of the color and pattern of the only adult, the female holotype, have already been given. The juveniles and subadults show the same general pattern configuration as does the adult. The smallest juvenile (snout–vent length 72), a female topotype, was gray with yellowish mottling and a pattern of three irregular crossbands, a faint white scapular stripe, and black postauricular and postorbital spots. The dewlap was charcoal with white scales. The next largest individual (snout–vent length 74), a male, had the dorsum pale green with irregular transverse barring; the upper surfaces of the limbs were pale green and gray-green, and the tail was banded pale green and gray-green. The venter was whitish. The dewlap was very dark yellowish with an orange wash posteriorly. A slightly larger male (snout–vent length 85) was pale green, much marbled and shaded with tan to gray and with some faint evidence of transverse crossbands; the chin and throat were gray-green, and the dewlap pale grayish orange. A female from the Sierra Martín García (snout–vent length 88) was green and brown dorsally and without pale markings; the dewlap was marbled with charcoal. Finally, the largest subadult (snout–vent length 76), a male, had the dewlap dirty yellow with orange streaking. In the case of *fraudator,* the very pale (almost white) adult female dewlap appears to be preceded ontogenetically by brighter and more typically *A. baleatus* hues.

Comparisons. No other subspecies of *A. baleatus* approaches the pale colors of *fraudator,* nor does any other subspecies have such a pale dewlap. Although *fraudator* combines the blotching and transverse crossbands in the same fashion as does *scelestus, fraudator* is in all ways a paler lizard. Comparisons in details of color and pattern with all other subspecies of *A. baleatus* are unnecessary. *A. b. fraudator* differs from *samanae, scelestus, multistruppus,* and *sublimis* in having 4 rather than 2 snout scales at the second canthals, and only *fraudator* has a mode of 6 vertical rows of loreals (7 or 8 in all other subspecies). In having 4/4 scales between the interparietal and the supraorbital semicircles, *fraudator* differs from *caeruleolatus, scelestus,* and *baleatus,* all of which have 5/5. Although *fraudator* has a high mean (18.8) of vertical dorsals, in which it is exceeded only by *sublimis* (mean 19.2), *fraudator* has the lowest mean (20.7) of

ventrals of all subspecies, being approached most closely by *scelestus* (21.1).

Discussion. Apparently *A. b. fraudator* is a pale subspecies that is restricted to favored situations in the xeric regions associated with the Llanos de Azua along the southern slopes of the Cordillera Central and the Sierra de Ocoa, a southern affiliate of the former range. The subspecies apparently also occurs in the Sierra Martín García, an eastern isolate of the Sierra de Neiba (which, it will be recalled, is elsewhere occupied by *A. r. ricordi*) and surrounded by extreme desert. The specimen from Barreras, which lies at the foot of the Sierra Martín García, is interesting in that it seems a most unlikely locality for any giant anole; however, I assume that the specimen, which was native-collected, was taken either in nearby *Cocos* groves or on the lower wooded slopes of the range itself. Two specimens from the higher elevations of the Martín García are from dense woods, and the specimen from San José de Ocoa was taken from a large tree at the edge of a pasture. The type locality is semi-xeric woods with vine tangles and mango trees in an otherwise cultivated but xeric region. Probably *A. b. fraudator* is widely distributed in suitable situations through much of this region, but the lizard appears to be rare; Buffett and I collected in semi-mesic riverine woods at a locality 4 km W and 17 km N Azua at an elevation of about 500 feet (153 meters), both during the day and at night, without seeing any giant anoles. Natives just south of San José de Ocoa at an elevation of 1400 feet (427 meters) did not secure specimens for us in semi-mesic woodlands. Since the altitudinal distribution of *fraudator* extends from sea level to about 3000 feet (915 meters) in the Sierra Martín García, the elevations of the above-mentioned localities are within the known altitudinal range of the subspecies, and indeed our San José de Ocoa locality was quite close to where Klinikowski secured one of the paratypes.

Remarks. The name *fraudator* is from the Latin for "deceiver" in reference to the resemblances between this subspecies and *A. barahonae.* In fact, my decision to regard *fraudator* as a subspecies of *baleatus* rather than *barahonae* is based more upon the juveniles than the adults of *fraudator;* this is not exclusively due to the fact that there are more juveniles of *fraudator* than adults but rather that the patterns shown by juvenile *fraudator* are more typically those of *A. baleatus* than of *A. barahonae. A. b. barahonae* and *A. b. fraudator* are alike in modal numbers of scales at the level of the second canthals (4), vertical loreal rows (6), and scales between the interparietal and the supraorbital semicircles (4/4), and they do not differ strikingly in means of body scales (17.2, 18.8 in vertical dorsals; 18.2, 21.4 in horizontal dorsals; 22.1, 20.7 in ventrals). In these means, *barahonae* is lower in dorsal body counts, but higher in ventral counts. The moderate nuchal crest scales of *fraudator* occur also in *barahonae,* but most female *barahonae* have these scales low. No female *barahonae* has moderate dorsal body crest scales as does the female *fraudator,* whereas moderate body crest scales occur in females of most subspecies of *A. baleatus* (only female *sublimis* lack them). Taking all evidence into consideration, I have elected to consider *fraudator* a subspecies of *A. baleatus,* but its resemblances to *A. barahonae* are acknowledged. The distance separating these two species in this area is only 20 kilometers (see introduction), and it is not unlikely that *A. barahonae* has been derived from *fraudator* across the strait that is now the Valle de Neiba (see discussion). On the other hand, *A. b. fraudator* is removed by some 60 kilometers from the nearest *A. ricordi* locality in the nearby Sierra de Neiba. There is no question that *fraudator* is not correctly associated nomenclatorially with *A. ricordi.*

The apparent geographic isolation of *fraudator* in relation to other subspecies of *A. baleatus* is probably artificial. The nearest records for other subspecies are: *caeruleolatus*—38 kilometers (San José de Ocoa and La Cumbre); *scelestus*—55 kilo-

meters (San José de Ocoa and Yamasá); and *sublimis*—50 kilometers (San José de Ocoa and south of El Río). There are suitable habitats for giant anoles between *caeruleolatus, scelestus,* and *fraudator,* but specimens are lacking. The intervening high Cordillera Central between the ranges of *sublimis* and *fraudator* probably acts as a barrier to prevent contact between these two subspecies.

DISCUSSION

My decision to consider *Anolis ricordi* as three species rather than one has some precedent in the Schwartz and Garrido (1972) treatment of the Cuban *Anolis equestris,* wherein that species was divided into five species. However, the two situations, although comparable, are far from identical. In the *A. equestris* complex, there are at least a few incidences of sympatry between members of the species-complex which give clues to the facts of the situation; there are strong differences in size of dorsal scales; there are some strong differences between details of pattern and coloration of the axillary stripe and the dewlap which likewise suggest that we are there dealing with more than one species. But on the other hand, the Hispaniolan giant anoles show absolute differences in the nuchal and body crest scales and differences in the pattern of the body itself, as well as modal differences in scutellar details. In addition, there are no cases as yet known in Hispaniola of sympatry between the three entities that I regard as full species. The gaps between them are narrow, however, and I feel strongly that it is merely a matter of getting into the intermediate areas and, once there, being fortunate enough to encounter giant anoles.

It should be obvious from my systematic treatment that I am convinced that we are dealing in Hispaniola with three distinct species—*ricordi, barahonae,* and *baleatus.* Surely the differences between *ricordi* and *baleatus* are such that, when taken in sum, one has no doubts that he is involved with two very different animals. The differences here are much greater, for instance, than between *Anolis distichus* Cope and *Anolis brevirostris* Bocourt, two species that were long confused and that resemble each other morphologically to a very great degree. Yet once one learns what the characters are for separating them, he experiences little difficulty in dealing with both populations or individuals, either allo- or sympatric, of these two species. The differences in life, as far as pattern and color are concerned, are not particularly subtle, and the details of scutellation are not dichotomous, but the modal differences are so well correlated with the pigmental and pattern traits that we now recognize these two species with assurance.

An even more obvious parallel is *Anolis carolinensis* Voigt and *Anolis allisoni* Barbour in Cuba. These two species of green anoles, long confused as *A. porcatus* Gray (or *A. c. porcatus*), were shown by Ruibal and Williams (1961) to be a sibling pair, fairly allopatric but both widely distributed throughout much of Cuba, and to differ structurally by the condition of the postauricular area. The presence (*allisoni*) or absence (*carolinensis*) of a deep and elongate postauricular groove in these two species is correlated with very striking differences in adult pattern and coloration and other details of scutellation.

The same situation, that of two species masquerading under a single name, can also be demonstrated in *Anolis alutaceus* Cope and *Anolis clivicola* Barbour and Shreve (Schwartz and Garrido, 1971), and the two species recently confused under *Anolis spectrum* Peters; both these situations pertain to Cuban species. Sr. Garrido also advises me that he has much evidence to indicate that *Anolis cyanopleurus cupeyalensis* Peters is in fact a sympatric sibling, rather than a subspecies, of *A. cyanopleurus* Cope.

I could cite other examples in Antillean iguanids (*Leiocephalus*) and anguids (*Diploglossus*) which demonstrate quite clearly the above trend. As more material

from more diverse localities becomes available, and as this material is subjected to re-evaluation with differing and more modern philosophies, our impressions of relationships among Antillean anolines have been modified or changed. A major factor in such revisions has invariably been a great quantity of new material from areas that had previously been unsampled, coupled with pigmental, ecological, and ethological data from the living specimens. A second general line of evidence, equal to or possibly surpassing morphological and distributional data in importance, is karyotypic and electrophoretic information. One or both of these areas of investigation are increasing our knowledge of the complexities within such a genus as *Anolis*. When these two areas of research—morphological and biochemical—can be brought to bear simultaneously upon a single species or species complex, the results may be even more meaningful than either is alone. As yet this has not been done in any of the Antillean giant anoles, so that my conclusions, based upon morphology and distribution, remain to be verified by other evidence. Yet I feel as secure as any systematist can be when he is dealing with data that are incomplete.

As pointed out in the introduction to the present paper, the taxa *ricordi*, *baleatus*, *barahonae*, and *leberi* are, on inspection, unequivocally distinct. But the degree or level of differentiation of these four taxa seems to be two-fold. On one hand (*ricordi* and *baleatus*), the two populations are easily separable on the basis of a structural feature (the nuchal crest scales), a character that is strongly correlated with obvious pigmental and pattern traits. On the other hand, the differences between *barahonae* or *leberi* and *ricordi* are primarily ones of pigmentation and pattern, with morphological differences much less trenchant than between *ricordi* and *baleatus*. At the outset such a dichotomy suggests that it might be more proper to consider "*A. ricordi*" as a complex of full species than as one species with four (or more) subspecies. Apparently Williams and Rand (1969) had the same inclinations, since they indicated that the differences between some of the then-named populations of *A. ricordi* were such as to suggest that there might be more than one species involved.

Once the above assumption has been made—namely, that *A. ricordi* is composed of more than one species—then the problem first becomes one of differentiating and delimiting the component species. There is no difficulty here in separating *A. ricordi* and *A. baleatus* on the basis of crest scales. None of the populations of *A. baleatus* has the moderate (rarely) to low (usually) nuchal crest scales of *A. r. ricordi*. In addition, the narrow geographical gaps that exist between *A. ricordi* and *A. baleatus* also suggest that these two taxa may be either allopatric or may meet and occur sympatrically without intergradation.

The status of the Tiburon populations that I associate nomenclatorially with *A. ricordi* and that of *A. barahonae* as a distinct species are less clear than the *ricordi-baleatus* relationship. First, the named populations *leberi*, *viculus*, and *subsolanus* have in common a suite of pattern and color features that ally them more closely to each other than to *A. r. ricordi*. The only evidence for this relationship is the occurrence of presumed *viculus* × *ricordi* intergrades in the Miragoâne-Paillant region. Were it not for these specimens, I would be strongly tempted to consider the three Tiburon taxa as comprising a separate species. Any interpretation of the relationships of the Tiburon taxa suffers from paucity of material from a variety of localities.

The situation with *A. barahonae* is in some ways puzzling. Although there is no question that it is distinct from *A. ricordi*, its relationships to *A. baleatus* are much less certain. This uncertainty is caused by *A. b. fraudator*, that population assigned to *A. baleatus* which is closest geographically to *A. barahonae*. It is particularly unfortunate that *fraudator* is known from only

one adult and several juvenile and subadult specimens, since adult males (primarily) would be most instructive in comparing *fraudator* with *barahonae*. On the other hand, the closeness of *fraudator* and *barahonae* in characteristics may be rather a reflection of the ancestry of *A. barahonae*—namely, that it is a south island (*sensu* Williams, 1961) invader from the north, and that the parent population has been *fraudator* rather than any other subspecies of *A. baleatus* or *A. ricordi* from the west.

It might be more proper either to consider *A. barahonae* as conspecific with *A. baleatus* (the two taxa linked through *fraudator*), or to consider *fraudator* a subspecies of *A. barahonae;* either interpretation has merit. The course that I have taken seems satisfactory at the moment but surely is subject to reinterpretation with the acquisition of more material from this critical geographic area.

The history of the Hispaniolan giant anoles appears to be correlated with the two palaeo-islands that have been fused at the level of the Cul de Sac-Valle de Neiba plain with lowering Pleistocene sea levels. I suggest the following history for the complex; the reader should keep in mind that such a history is based upon taxonomic premises that are inductive, and the cautions and uncertainties that I expressed above have special application here.

Distributional evidence suggests that the giant Hispaniolan anole stock was originally restricted to the north island (north of the Cul de Sac-Valle de Neiba plain). In this region, two distinctive species arose, *ricordi* in the west and *baleatus* in the east. There apparently has been local differentiation on the north island at a subspecific level in both these species, but that in *ricordi* remains unanalyzed because of too few specimens. On the other hand, differentiation in *A. baleatus* is now fairly well known and documented. This species occurs east of the Cordillera Central and on the southern slopes of that range and in the Sierra Martín García. There have been local population differentiations in response to the various ecologies within the area occupied, with two major integumental trends (coloration and pattern) and details of scutellation of the head and body (although the latter is not so clear as the former).

There seem to have been two subsequent invasions of the south island. To the west, a (presumably) early invasion of the *A. ricordi* stock crossed what is now the Cul de Sac Plain into the Port-au-Prince area. It is pertinent that many north island species have made this same crossing and have extended their ranges but little further. These species with more restricted ranges have been handicapped either by competition with already established species, improper ecological situations, or relatively recent arrival. *A. ricordi* seems to have been an early arrival, without local competitors, and with abundant proper ecology (mesic forests). The species has thus expanded its range after the original crossing to cover the entire Tiburon Peninsula, having somewhere succeeded in crossing the mountainous spine of the Massif de la Hotte-Massif de la Selle. Local differentiation along the Tiburon in response to lack of genetic contact across the interior mountains has also taken place. Further speculations on details of the history of *A. ricordi* on the Tiburon Peninsula are pointless, since the specimens upon which any generalisations may be made do not as yet exist in collections.

A second invasion to the east occurred presumably at a later date, after the establishment of *A. ricordi* on the Tiburon Peninsula. This latter invasion resulted in the differentiation of *A. barahonae* (from a *fraudator* or pre-*fraudator* stock on the southern portion of the north island) in the Sierra de Baoruco and its subsequent expansion onto the southern portion of the Península de Barahona and east along the southern slopes of the Sierra de Baoruco. With the previous establishment of *A. ricordi* to the west (as at Thiotte), the western movement of *A. barahonae* was

halted by the presence of the related species. I have no doubt that both *A. ricordi* and *A. barahonae* will be found to be closely allopatric or sympatric in extreme southeastern Haiti between the Dominico-Haitian border and Saltrou, and also that these two species meet and interact along the northern slopes of the Sierra de Baoruco and the Morne des Enfants Perdus.

One other distributional detail requires comment. The occurrence of *A. r. ricordi* in the main mass of the Sierra de Neiba on the northern side of the Valle de Neiba and of *A. b. fraudator* in the Sierra Martín García, an extreme eastern isolate of the Sierra de Neiba, has already been noted. The Martín García seems to have been long isolated from not only the Sierra de Neiba but also from all other Hispaniolan mountain masses; it is ideally a montane island in a sea of desert. It seems likely that this range was unoccupied by giant anoles of either species (*A. ricordi* or *A. baleatus*), despite the fact that the range forms a portion of the Neiba uplift. Invasion of the Martín García was possible from either the northwest (*ricordi*) or the northeast (*baleatus*). Of the two species, *A. baleatus* was the more vagile and reached the Sierra Martín García from the relatively more mesic southern slopes of the Cordillera Central before *A. ricordi* reached it across the deserts and xeric hills between the Sierra de Neiba and the Martín García. This upland population in turn was responsible for the invasion of the Sierra de Baoruco across the better forested and more mesic eastern end of the Valle de Neiba.

Wetmore and Swales (1931: 235) reported the finding of recent *Anolis ricordi* skeletal material in Barn Owl (*Tyto alba*) pellets from L'Acul, Dépt. du Sud, Haiti, on the Tiburon Peninsula, and Hecht (1951: 23) noted the abundant remains of the species from deposits in "Deep Cave," near St. Michel de l'Atalaye, Dépt. de l'Artibonite, Haiti. Etheridge (1965: 101) reported *A. ricordi* remains from recent owl pellets near the mouth of a cave near Boca de Yuma, La Altagracia Province, República Dominicana. Etheridge (*op. cit.*: 87–88) also noted pre-Columbian giant anole remains from a cave at Cerro de San Francisco near Pedro Santana, La Estrelleta Province, República Dominicana. From the suite of about 80 cranial elements and eight pelves, Etheridge extrapolated that the maximally sized individuals in the cave deposits had a snout–vent length of 190–192 mm, some 30 mm larger than any living *A. ricordi* recorded (159 mm, *fide* Etheridge, *op. cit.*: 88). The maximally sized Hispaniolan giant anole recorded in the present paper reaches a length of 180 mm (male *A. b. scelestus* from Otra Banda, La Altagracia Province, República Dominicana). The difference between this modern living lizard and the maximally sized pre-Columbian lizards is not so great as Etheridge's data suggest. Intriguingly, the Cerro de San Francisco area lies within the known range of *A. r. ricordi*, and the largest specimens of this subspecies (male with a snout–vent length of 160 mm, female 151 mm) are from the southern slopes of the Cordillera Central, very close to the Cerro de San Francisco area. Although there seems to have been some change in maximum size in Hispaniolan giant anoles with the passage of time, these changes have not been of the magnitude that previous data suggested.

LITERATURE CITED

Cochran, D. M. 1941. The herpetology of Hispaniola. Bull. U.S. Natl. Mus., **177**: 398, 120 figs., 12 pls.

Cope, E. D. 1864. Contributions to the herpetology of tropical America. Proc. Acad. Nat. Sci. Philadelphia, pp. 166–181.

Duméril, A. M. C., and G. Bibron. 1837. Erpétologie générale ou histoire naturelle complete des reptiles, vol. 4. 571 pp., 14 pls.

Etheridge, R. E. 1965. Fossil lizards from the Dominican Republic. Quart. Jour. Florida Acad. Sci., **28**(1): 83–195, 3 figs.

Garrido, O. H., and A. Schwartz. 1968. Cuban lizards of the genus *Chamaeleolis*. Quart. Jour. Florida Acad. Sci., **30**(3): 197–220, 2 figs.

Hecht, M. K. 1951. Fossil lizards of the West

Indian genus *Aristelliger* (Gekkonidae). Amer. Mus. Novitates, No. 1538: 1–33, 8 figs.

Maerz, A., and M. R. Paul. 1950. A Dictionary of Color. New York: McGraw-Hill Book Co., pp. vii + 1–23, 137–108, 56 pls.

Mertens, R. 1939. Herpetologische Ergebnisse einer Reise nach der Insel Hispaniola, Westindien. Abh. senckenberg. naturf. Ges., **449**: 1–84, 10 pls.

Rand, A. S., and E. E. Williams. 1969. The anoles of La Palma; aspects of their ecological relationships. Breviora, Mus. Comp. Zool., No. 327: 1–18, 1 fig.

Ruibal, R., and E. E. Williams. 1961. Two sympatric Cuban anoles of the *carolinensis* group. Bull. Mus. Comp. Zool., **125**(7): 183–208, 11 figs.

Schmidt, K. P. 1921. Notes on the herpetology of Santo Domingo. Bull. Amer. Mus. Nat. Hist., **44**(11): 7–20, 12 figs.

Schwartz, A. 1964. *Anolis equestris* in Oriente Province, Cuba. Bull. Mus. Comp. Zool., **131**(12): 407–428, 7 figs.

———. 1968. Geographic variation in *Anolis distichus* Cope (Lacertilia, Iguanidae) in the Bahama Islands and Hispaniola. Bull. Mus. Comp. Zool., **137**(2): 255–309, 4 figs., 2 pls.

———, and O. H. Garrido. 1971. The status of *Anolis alutaceus clivicolus* Barbour and Shreve. Caribbean Jour. Sci., **11**(1–2): 11–15.

———, and ———. 1972. The lizards of the *Anolis equestris* complex in Cuba. Stud. Fauna Curaçao and Caribbean Is., **39**(134): 1–86, 8 figs.

Thomas, R. 1971. A new species of *Diploglossus* (Sauria: Anguidae) from Hispaniola. Occ. Papers Mus. Zool., Louisiana State Univ., 40: 1–9, 4 figs.

Wetmore, A., and B. H. Swales. 1931. The birds of Haiti and the Dominican Republic. Bull. U.S. Natl. Mus., **155**: 1–483, 2 figs., 26 pls.

Williams, E. E. 1961. The evolution and relationships of the *Anolis semilineatus* group. Breviora, Mus. Comp. Zool., No. 138: 1–8, 1 pl.

———. 1962. Notes on Hispaniolan herpetology. 6. The giant anoles. Breviora, Mus. Comp. Zool., No. 155: 1–15, 1 fig.

———. 1965. Hispaniolan giant anoles (Sauria, Iguanidae): new data and a new subspecies. Breviora, Mus. Comp. Zool., No. 232: 1–7, 2 figs.

———, and A. S. Rand. 1969. Anolis insolitus, a new dwarf anole of zoogeographic importance from the mountains of the Dominican Republic. Breviora, Mus. Comp. Zool., No. 326: 1–21, 6 figs.

US ISSN 0027-4100

Bulletin OF THE
Museum of
Comparative
Zoology

A Revision of the Cardinalfish Genus *Epigonus* (Perciformes, Apogonidae), with Descriptions of Two New Species

GARRY F. MAYER

HARVARD UNIVERSITY
CAMBRIDGE, MASSACHUSETTS, U.S.A.

VOLUME 146, NUMBER 3
19 SEPTEMBER 1974

PUBLICATIONS ISSUED
OR DISTRIBUTED BY THE
MUSEUM OF COMPARATIVE ZOOLOGY
HARVARD UNIVERSITY

Breviora 1952–
Bulletin 1863–
Memoirs 1864–1938
Johnsonia, Department of Mollusks, 1941–
Occasional Papers on Mollusks, 1945–

SPECIAL PUBLICATIONS.

1. Whittington, H. B., and E. D. I. Rolfe (eds.), 1963. Phylogeny and Evolution of Crustacea. 192 pp.
2. Turner, R. D., 1966. A Survey and Illustrated Catalogue of the Teredinidae (Mollusca: Bivalvia). 265 pp.
3. Sprinkle, J., 1973. Morphology and Evolution of Blastozoan Echinoderms. 284 pp.
4. Eaton, R. J. E., 1974. A Flora of Concord. 211 pp.

Other Publications.

Bigelow, H. B., and W. C. Schroeder, 1953. Fishes of the Gulf of Maine. Reprint.

Brues, C. T., A. L. Melander, and F. M. Carpenter, 1954. Classification of Insects.

Creighton, W. S., 1950. The Ants of North America. Reprint.

Lyman, C. P., and A. R. Dawe (eds.), 1960. Symposium on Natural Mammalian Hibernation.

Peters' Check-list of Birds of the World, vols. 2–7, 9, 10, 12–15.

Proceedings of the New England Zoological Club 1899–1948. (Complete sets only.)

Publications of the Boston Society of Natural History.

Price list and catalog of MCZ publications may be obtained from Publications Office, Museum of Comparative Zoology, Harvard University, Cambridge, Massachusetts, 02138, U.S.A.

© The President and Fellows of Harvard College 1974.

A REVISION OF THE CARDINALFISH GENUS *EPIGONUS* (PERCIFORMES, APOGONIDAE), WITH DESCRIPTIONS OF TWO NEW SPECIES[1]

GARRY F. MAYER[2]

TABLE OF CONTENTS

Abstract 147
Introduction 147
Methods 148
Systematics 150
Genus *Epigonus* Rafinesque 151
Diagnosis 151
Description 151
Key to the Species of *Epigonus* 152
Epigonus telescopus 152
Epigonus macrops 159
Epigonus pandionis 163
Epigonus fragilis 169
Epigonus occidentalis 170
Epigonus denticulatus 175
Epigonus oligolepis 179
Epigonus trewavasae 183
Epigonus pectinifer 186
Epigonus robustus 189
Epigonus lenimen 193
Epigonus crassicaudus 197
Species *Incertae Sedis* 199
Microichthys coccoi 199
Acknowledgments 199
Literature Cited 200
Appendix 203

ABSTRACT. A study of the deep-sea Apogonidae results in a revision of the genus *Epigonus* Rafinesque. Twelve species are recognized, including two new forms—*E. oligolepis* and *E. pectinifer*. *E. fragilis* (Jordan and Jordan) is resurrected and redescribed on the basis of new material, and *Hynnodus atherinoides* Gilbert and *H. megalops* Smith and Radcliffe are synonymized with *E. occidentalis* Goode and Bean.

Species descriptions include discussions of distribution, geographic variation, ontogenetic change, and taxonomic problems. An investigation of the types of *E. lenimen* (Whitley) reveals that the holotype and paratypes are not conspecific. Instead, the paratypes are members of *E. denticulatus* Dieuzeide. A key to the species of *Epigonus* is provided at the beginning of the paper.

INTRODUCTION

Selected species of *Epigonus* have been harvested by man for at least two hundred fifty years. Vaillant (1888: 25) remarked that *E. telescopus* was recognized in ancient times, and Risso (1810: 303) reported that this species was prized for its firm, delicious-tasting meat, although it was rarely taken. The presence of common names for *E. telescopus* in vocabularies of western Mediterranean and North Atlantic fishing communities (Döderlein, 1889) provides additional evidence of man's long-term awareness of the species. *E. telescopus* is still occasionally sold in the markets of southwestern Europe.

Two other species of *Epigonus* are captured by commercial fishermen. *E. denticulatus* is edible (Dieuzeide et al., 1953: 218) and is taken in the Mediterranean. Until recently this form was mistaken for the young of *E. telescopus*. *E. crassicaudus* is caught by Chilean fishermen. Like *E.*

[1] This paper is based on a portion of a thesis presented to Harvard University in partial fulfillment of the requirements for the Ph.D. in Biology.

[2] Department of Marine Science, University of South Florida, St. Petersburg, Florida 33701 and Museum of Comparative Zoology, Harvard University, Cambridge, Massachusetts 02138.

telescopus, it is not taken in sufficient numbers to support a separate fishery but is captured by fishermen trawling for more abundant deepwater organisms.

Although African *Epigonus* are not presently exploited, tropical eastern Atlantic stocks may represent future sources of protein for mankind. Surveys sponsored by the Organisation of African Unity and the U.S. Agency for International Development revealed these fishes are "of possible potential importance (not necessarily by present marketing standards) [Williams, 1968: 79]." The same may be true for Caribbean and Gulf of Mexico *Epigonus*; however, complete data have not been compiled for the latter areas.

A major hindrance to the evaluation of deep-sea cardinalfish stocks has been taxonomic confusion. The systematic history of *Epigonus* began in 1810 with Risso's description of *Pomatomus telescopus* and Rafinesque's account of its synonym *Epigonus macrophthalmus*. During the following seventy-one years, work on the genus was primarily limited to re-descriptions of *E. telescopus* and discussions of its biology (*e.g.*, Cuvier, 1828; Valenciennes, 1830; Capello, 1868; Moreau, 1881).

The surge in oceanographic exploration during the last quarter of the nineteenth and beginning of the twentieth centuries rapidly increased the number of nominal *Epigonus*-like species. Among the forms described between 1881 and 1920 were *Apogon pandionis* Goode and Bean, 1881; *E. occidentalis* Goode and Bean, 1896; *Hynnodus atherinoides* Gilbert, 1905; *Oxyodon macrops* Brauer, 1906; and *Hynnodus megalops* Smith and Radcliffe, 1912. In the following decade, three new species and two new genera appeared in the literature.

Much of the confusion associated with the taxonomy of *Epigonus* stems from material described prior to 1930. Early taxa were based on small samples. Because many nations participated in oceanographic research, specimens were deposited in scattered institutions and descriptions appeared in diverse publications. Consequently, it was difficult for workers to obtain either comparative material or a broad overview of the group's systematics. These shortcomings were aggravated by inaccurate, under-illustrated descriptions based on ill-considered characters. It was common, for example, to use dentition patterns to define generic boundaries, yet tooth arrangements are difficult to observe, easily damaged, and subject to ontogenetic and geographic variation. As a result, an inordinately large number of *Epigonus*-like forms was recognized by the end of the 1920's.

Although generic taxonomy was streamlined by Fowler and Bean in 1930 and Matsubara in 1936, species-level taxonomy became increasingly complex. New forms were described in 1935, 1950, 1954, and 1959. In addition, misidentifications of *Epigonus* were published in several widely circulated works on regional faunas (*e.g.*, Smith, 1949b and 1961; Gosline and Brock, 1960).

The aim of the present study is to clarify the species-level systematics of the *Epigonus*-like fishes. Data from traditional characters are evaluated and augmented by information from characters not previously examined for this group. A special effort is made to discuss features such as dentition patterns that caused taxonomic confusion in the past. The ecology, functional anatomy, zoogeography, and evolution of *Epigonus* will be discussed in future works on the genus.

METHODS

Measurements were made to the nearest tenth of a millimeter by the use of Helios needlepoint dial calipers; characters larger than 190 mm were measured with a meter rule or GPM Anthropometer. Measurements routinely taken include:

Standard length (SL)—from tip of snout to base of caudal fin.

Head length (HL)—from tip of snout to tip of opercular spine.
Body depth—between dorsal and ventral surfaces of body at level of pelvic fin base.
Head height—from quadratomandibular joint vertically to bony rim above eye.
Eye diameter—between anterior and posterior margins of orbit as defined by first and sixth suborbitals.
Snout length—from tip of snout to anterior margin of orbit.
Interorbital width—shortest distance between bony rims above eyes.
Maxillary length—from tip of snout to posterior margin of maxilla.
Lower jaw length—from tip of mandible to quadratomandibular joint.
Caudal peduncle depth—shortest distance between dorsal and ventral surfaces of caudal peduncle.
Caudal peduncle length—from posteriormost anal fin ray to caudal fin base.
First spine length (first spine of first dorsal fin, D_1I; first spine of second dorsal fin, D_2I; second spine of anal fin, AII; pelvic fin spine, P_2I)—from base to tip of spine along anterior edge.

Counts were made under a dissecting microscope with the use of dissecting needles or insect pins. A Fibre-Lite High Intensity Illuminator proved invaluable for examinations of oral, branchial, and visceral structures. Gill raker and branchiostegal counts were made on the left side of specimens; remaining counts and measurements were made on the right side whenever possible. Counts made include: fin spines (indicated by Roman numerals), fin rays (indicated by Arabic numerals), branchiostegal rays, rakers on first gill arch, lateral line scales, pyloric caeca, vertebrae (precaudal + caudal, including hypural fan), pleural and epipleural ribs, and basal pterygiophores between neural spines 9 and 10.

Osteological data were obtained from radiographs taken at the Woods Hole Oceanographic Institution, the Museum of Comparative Zoology, and the Harvard University School of Public Health. Holotypes of *Oxyodon macrops* and *Scepterias lenimen* were radiographed at the Zoologisches Museum der Humboldt Universität and Australian Museum, respectively. More comprehensive osteological studies were based on cleared and stained specimens prepared by trypsin digestion (Taylor, 1967). Osteological terminology follows that presented by Gosline (1961) and Mead and Bradbury (1963). Suborbital bones are numbered from 1 to 8 beginning with the rostralmost element (lacrimal).

Statistical data were analyzed with the use of the Harvard Computation Laboratory's IBM 360/65 digital computer. Standard techniques described by Mayr (1969: 189–193) and Simpson et al. (1960: 65–68, 83–88) were employed for analyzing meristic data. Morphometric characters were examined with the aid of regression techniques specified by Simpson et al. (1960: 215–233, 238) and Bailey (1959: 91–99).

Before undertaking regression analyses, morphometric data were plotted against SL. Graphs were drawn according to a BMD 05D plotting routine (Dixon, 1967: 71) and served as visual tests for linearity of scatter. Only characters exhibiting linear scatters were analyzed by regression techniques. As a second precaution against nonlinearity, subadult specimens (< 40 mm SL) were excluded from statistical samples.

Data from several morphometric characters are presented both as ratios (*i.e.*, percent of SL or HL) and as regression parameters. The former are intended only as identification aids. As Royce (1957: 17) points out, heterogenic growth makes the use of ratios in fish taxonomy inefficient and may lead to erroneous conclusions.

Collection and institution names are abbreviated as follows in this paper:

ABE —Collection of Dr. T. Abe, Tokyo
AM —Australian Museum, Sydney

BMNH —British Museum (Natural History), London
BPBM —Bernice P. Bishop Museum, Honolulu
CM —Carnegie Museum; collections presently housed in FMNH, Chicago
DM —Dominion Museum, Wellington
EBM —Estación de Biologia Marina, Universidad de Chile, Viña del Mar
FMNH —Field Museum of Natural History, Chicago
IRSN —Institut Royal des Sciences Naturelles de Belgique, Brussels
ISH —Institut für Seefischerei, Hamburg
LACM —Los Angeles County Museum of Natural History, Los Angeles
MCZ —Museum of Camparative Zoology, Harvard University, Cambridge
MNHN —Muséum National d'Histoire Naturelle, Paris
MZF —Museo Zoologico di Firenze, Florence
RUSI —J.L.B. Smith Institute of Ichthyology, Rhodes University, Grahamstown
SAM —South African Museum, Cape Town
SMF —Natur-Museum Senckenberg, Frankfurt am Main
SU —Stanford University; collections presently housed in the California Academy of Sciences, San Francisco
TABL —Tropical Atlantic Biological Laboratory, Miami
UMML —Rosenstiel School of Marine and Atmospheric Science, University of Miami, Miami
USNM —National Museum of Natural History, Washington, D.C.
UZM —Universitetets Zoologiske Museum, Copenhagen
ZMB —Zoologisches Museum der Humboldt Universität, Berlin

Descriptions are based on material listed by Mayer (1972: Appendix II). Additional data were obtained from examinations of the seventeen specimens listed below. All seventeen fishes were radiographed.

E. robustus: ISH 1132/66, 3 specimens, 121.1–142.5 mm, WALTHER HERWIG Sta. 237/66, 36°00′S, 52°58′W, 800 m. ISH 189/71, 9 specimens, 147.0–198.0 mm, WALTHER HERWIG Sta. 121/71, 37°44′S, 54°43′W, 800 m. ISH 269/71, 1 specimen, 147.5 mm, WALTHER HERWIG Sta. 340/71, 38°50′S, 54°25′W, 1000 m. ISH 430/71, 1 specimen, 124.1 mm, WALTHER HERWIG Sta. 348/71, 38°20′S, 54°33′W, 997–1040 m.

E. fragilis: LACM 32668–6, 1 specimen, 72.5 mm, 2 mi. off Haleiwa, Oahu, Hawaii, 65 fms. SU 32262, 2 specimens, 90.0–93.9 mm, Honolulu, Hawaii.

Distributions were determined from material examined and from published accounts. Because of the confusion in *Epigonus* taxonomy, published data were used only if species identifications could be verified from included descriptions, illustrations, etc. Data from specimens of doubtful identity were not considered. A complete list of station data taken from the literature is provided by Mayer (1972: Appendix II).

No attempt has been made to provide exhaustive synonymies for *Epigonus* species. References are cited only if they (1) are taxonomically or zoogeographically important; (2) provide outstanding descriptions, illustrations, or synonymies; or (3) represent verifiable misidentifications. Nontaxonomic accounts have been omitted, as have references to cruise summaries and faunal lists.

SYSTEMATICS

Statistical data are presented in tables accompanying species descriptions; meristic

characters with low variability are reported in the text as value, followed in parentheses by number of specimens exhibiting that value. Meristic and mensural data from holotypes of new species are presented in the Appendix.

Genus *Epigonus* Rafinesque, 1810

Epigonus Rafinesque, 1810: 64. (Type species: *Epigonus macrophthalmus* Rafinesque, 1810 by monotypy. A synonym of *Pomatomus telescopus* Risso, 1810.)

Telescops Bleeker, 1876: 261. (Type species: *Pomatomus telescopium* [sic!] Risso, 1810 by original designation. *Pomatomus* deemed inapplicable.)

Pomatomichthys Giglioli, 1880: 20. (Type species: *Pomatomichthys constanciae* Giglioli, 1880 by monotypy. A synonym of *Pomatomus telescopus* Risso, 1810.)

Hynnodus Gilbert, 1905: 217. (Type species: *Hynnodus atherinoides* Gilbert, 1905 by monotypy. A synonym of *Epigonus occidentalis* Goode and Bean, 1896.)

Oxyodon Brauer, 1906: 287. (Type species: *Oxyodon macrops* Brauer, 1906 by monotypy.)

Xystramia Jordan, 1917: 46. (Type species: *Glossamia pandionis* Goode and Bean, 1881 by original designation. *Glossamia* deemed inapplicable.)

Scepterias Jordan and Jordan, 1922: 44. (Type species: *Scepterias fragilis* Jordan and Jordan, 1922 by monotypy.)

Parahynnodus Barnard, 1927: 525. (Type species: *Parahynnodus robustus* Barnard, 1927 by monotypy.)

Diagnosis. *Epigonus* is distinguished from other lower perciform genera by a mosaic of characters including 8 suborbital bones, all lacking subocular shelves; large, thin-walled swimbladders with posterodorsal ovals; VII or VIII first dorsal fin spines; I,9 or I,10 second dorsal fin elements; II,9 anal fin elements; 15–23 pectoral fin rays; and 17–35 gill rakers. No member of the genus exhibits fang-like conical teeth, such as are found in *Cheilodipterus*, or anteriorly projecting teeth, such as are found in *Rosenblattia*.

Description. Body elongate, fusiform; dorsal and ventral profiles slightly convex, similar. Mouth oblique, terminal; upper jaw protrusile; maxilla excluded from gape, sheathed by lacrimal anteriorly, free posteriorly; supramaxilla absent. Eye large, round or oval. Nostrils paired, rounded or slit-like, two on each side of head.

Premaxillae, mandibles, vomer, and palatines edentulous or bearing conical teeth; tongue and endopterygoids rarely dentigerous; ectopterygoids edentulous. Gill rakers moderate to long, 17–35; branchiostegal rays 7 (3 + 4); pseudobranchiae present.

Opercular spine either weak, flattened and poorly ossified, or pungent and bony; spine ventral to one or more horny or membranous spinelets. Preopercle with double edge; angle frequently produced.

Dorsal fins VII–I,9, VII–I,10, or VIII–I,10, separated by distinct interdorsal space; rudimentary subcutaneous eighth spine present in seven-spined forms. Anal fin II,9; pectoral fins 15–23; pelvic fins I,5; caudal fin forked, 9 + 8 principal rays, upper- and lowermost rays unbranched.

Scales large, deciduous, ctenoid. Lateral line complete, extending parallel to dorsal profile on dorsolateral surface of trunk, descending to midline on posterior portion of caudal peduncle, continuing on tail; lateral line scales 33–51; canal simple, broadening into deltoid or Y-shaped tube at rear edge of scale. Scale pockets covering most of body including occiput, soft dorsal, anal, and caudal fins; scales absent from snout; no axillary scale at base of P_2I spine.

Suborbitals 8, all lacking subocular shelves. Vertebrae 25; basapophyses on vertebrae 3 or 4. Predorsals 3, first and second interdigitating between neural spines 2 and 3, third located behind neural spine 3. Caudal skeleton with 2 autogenous haemal spines, 6 hypurals (hypural 1 = parhypural *sensu* Monod, 1968), 3 epurals, 2 (rarely 1) pairs of uroneurals. Actinosts 4, 3½ borne by scapula.

Swimbladder large, thin-walled, lacking anterior or posterior projections to cranium and neural arches; diaphragm absent; oval posterodorsal; retia mirabilia well developed. Stomach U- or Y-shaped; pyloric

caeca 5–34, may be modified into luminescent organs; intestines simple, folded into three segments. Specimens dioecious; no evidence of hermaphroditism or oral brooding.

Habitat: Engybenthic; continental slope between approximately 200 and 1200 meters.

Key to Species of *Epigonus*

1a Opercular spine weak, poorly ossified, or absent (opercular spine refers to the ventralmost reinforced projection from the posterodorsal edge of the opercle) 2
b Opercular spine pungent, bony 7
2a Lateral line scales 46–51; tongue edentulous or bearing scattered tooth patches 3
b Lateral line scales 33–36; tongue covered with tooth patches (Fig. 1A) ..... *E. oligolepis*
3a Gill rakers 23–34; premaxillary teeth short, conical or villiform, not visible when mouth closed 4
b Gill rakers 17–21; premaxillary teeth elongate, thin, inwardly recurved, visible when mouth closed ..... *E. macrops*
4a Pyloric caeca 7–14; first dorsal fin VII, rarely VIII; vertebral count 10 + 15; specimens not exceeding 220 mm SL 5
b Pyloric caeca 21–34; first dorsal fin VIII, rarely VII (D_1VIII often small or rudimentary); vertebral count 11 + 14; specimens to 550 mm SL ..... *E. telescopus*
5a Body long, shallow; depth 15.8–23.6% SL; peduncle length 25.4–32.2% SL; caudal peduncle ring absent 6
b Body short, deep; depth 22.4–29.6% SL; peduncle length 22.0–26.3% SL; caudal peduncle ring present on specimens shorter than 110–120 mm SL (Fig. 1B) ..... *E. pandionis*
6a Gill rakers 28–34; pyloric caeca 10–14; head length 31.2–38.6% SL; 2 pterygiophores between neural spines 9 and 10, rarely 1 ..... *E. denticulatus*
b Gill rakers 25–26, pyloric caeca 7–8; head length 30.0–34.0% SL; 1 pterygiophore between neural spines 9 and 10 ..... *E. fragilis*
7a Body moderate to deep, 20.0–32.0% SL; dorsal fins VII–I,9, rarely VII–I,10; gill rakers 26–35 8
b Body shallow, 14.0–19.5% SL; dorsal fins VII–I,10, rarely VII–I,9; gill rakers 22–27 ..... *E. occidentalis*
8a Gill rakers of lower arch simple, awl-shaped 9
b Gill rakers of lower arch pectinate (Fig. 1C) ..... *E. pectinifer*
9a Tongue edentulous 10
b Tongue covered with tooth patches ..... *E. trewavasae*
10a Head length 28.0–36.6% SL; head height 14.7–18.8% SL; gill filaments moderate or short 11
b Head length 36.8–41.9% SL; head height 18.9–21.1% SL; gill filaments long ..... *E. crassicaudus*
11a Fin spines long, D_2I 14.8–18.7% SL, AII 13.0–20.8% SL; interorbital width 8.7–10.2% SL; eyes large, 40.0–51.1% HL ..... *E. lenimen*
b Fin spines moderate, D_2I 10.0–12.6% SL, AII 9.2–13.3% SL; interorbital width 6.5–8.2% SL; eyes moderate to small, 37.4–42.2% HL ..... *E. robustus*

Epigonus telescopus (Risso, 1810)
Figure 2

Pomatomus telescopus Risso, 1810: 301, plate IX, fig. 31 (original description; Nice; holotype examined, MNHN B862); Lowe, 1841: 173; Capello, 1868: 160; Moreau, 1881: 386, fig. 125; Vaillant (in part), 1888: 376.

Epigonus macrophthalmus Rafinesque, 1810: 64 (original description; no type locality; holotype lost).

Pomatomus telescopium Cuvier, 1828: 171 (incorrect emendation of *Pomatomus telescopus* Risso, 1810); Valenciennes, 1830: 495; Valenciennes, 1837–1844: 6, plate I; Günther, 1859: 250; Cocco, 1885: 85; Holt and Calderwood, 1895: 405, plate LXII.

Pomatomus cuvieri Cocco, 1829: 143 (original description; seas of Messina; holotype not examined).

Pomatomus cuvierii Valenciennes, 1830: 501 (incorrect emendation of *Pomatomus cuvieri* Cocco, 1829).

?*Pomatomichthys constanciae* Giglioli, 1880: 20 (original description; Straits of Messina; holotype not examined, MZF 3089); Goode and Bean, 1896: 234.

Epigonus telescopus Goode and Bean, 1896: 232; Cligny, 1903: 9; Barnard, 1927: 523; Gall, 1931: 1, fig. 1; Fowler, 1936: 736, fig. 326; Smith, 1949b: 206, fig. 474.

Scepterias lenimen, Whitley (in part) (not Whitley, 1935), 1968: 56.

Diagnosis. E. telescopus is the largest species of the genus, growing to over 550 mm SL. Specimens are characterized by 21–34 pyloric caeca and eight first dorsal

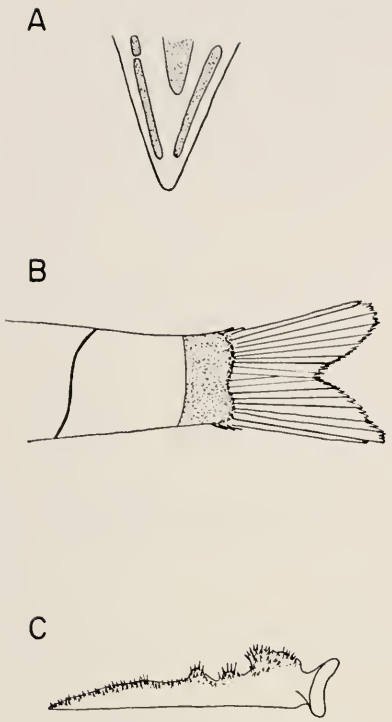

Figure 1. A. Tongue of *E. oligolepis*. Stippled areas indicate tooth patches; shape and size of tooth patches may vary among specimens. B. Caudal peduncle of young *E. pandionis* showing anterior ring and posterior band. C. Gill raker of *E. pectinifer* showing nub-like processes.

fin spines. The opercular spine is blunt and poorly ossified and distinguishes the species from *E. occidentalis*, *E. trewavasae*, *E. pectinifer*, *E. robustus*, *E. lenimen*, and *E. crassicaudus*, which have pungent opercular spines. Unlike remaining congeners, *E. telescopus* possesses 11 + 14 vertebrae.

Description. Meristic data presented in Table 1; regression data for morphometric traits presented in Table 2.

Body thickset, shortened; anterodorsal profile slightly convex, rising most steeply from tip of snout to interorbital region; body moderate to deep, 21.2–26.3% SL; caudal peduncle short, 19.0–26.5% SL.

Head moderate to deep, height 13.3–17.2% SL; length 30.5–37.9% SL; snout blunt; angle of gape moderate to large; lower jaw equalling or protruding slightly beyond upper jaw. Maxilla rarely exceeding ⅓–¾ eye length, posterior margin of maxilla broad, posteriormost point near ventral surface of bone; maxillae of large specimens scaled. Eye round, 49.5–58.9% HL; circumorbital tissues scaled, scale pockets particularly apparent in large specimens; anterodorsal rim of orbit projecting into profile in small forms, reaching profile in larger forms; interorbital width 9.0–10.9% SL.

Dentition variable with age (see Ontogenetic change); premaxillae, mandibles, vomer, and palatines dentigerous; tongue edentulous.

Opercle bearing short, poorly ossified spine ventral to 1–8 membranous or poorly ossified spinelets; spine and spinelets separated by shallow gap; spinelets occasionally obscured by underlying membranes. Preopercle variable with age; angle rounded, slightly produced in specimens shorter than

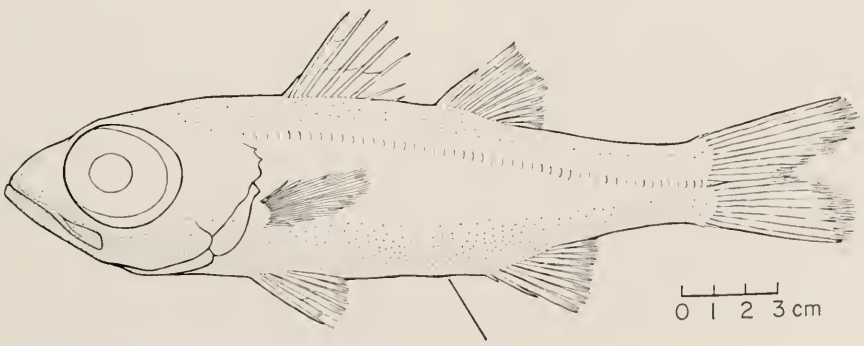

Figure 2. *Epigonus telescopus*, 220.0 mm SL, ISH 70/63.

Table 1. *Epigonus telescopus* meristic data. $\bar{X}$ = mean; SD = standard deviation; n = number of specimens.

	$\bar{X}$	Range	SD	n
Pectoral fin rays	20.85	19–23	0.71	54
Gill rakers	24.40	23–26	0.85	52
Lateral line scales	48.14	46–50	1.09	50
Pyloric caeca	25.25	21–34	3.59	16

200 mm SL, broadly produced in larger forms; minute serrations on angle and ventral surface of bone, rarely along posterior surface dorsal to angle; striations radiating from inner edge of angle. Interopercles and subopercles without striations, occasionally bearing minute serrations on posteroventral surfaces. Gill rakers simple, awl-like.

First dorsal fin VII (7), VIII (46), eighth spine small or rudimentary, lacking membranous connection to preceding spines; second dorsal fin I,9 (1), I,10 (52), I,11 (1); anal fin II,9 (56); D_1I long, 3.5–6.3% SL; D_2I, AII short, 5.3–9.5%, 5.7–10.6% SL respectively; P_2I moderate, 6.5–11.9% SL.

Vertebrae 11 + 14 (18); epipleural ribs

Table 2. *Epigonus telescopus* regression data. b = regression coefficient ± 95% confidence interval; a = Y intercept; n = number of specimens. All regressions on SL.

	b	a	n
HL	0.35 ± 0.01	1.60	50
Body depth	0.25 ± 0.01	−2.43	48
Head height	0.19 ± 0.00	0.45	45
Eye diameter	0.13 ± 0.01	6.57	44
Snout length	0.10 ± 0.00	−2.19	49
Interorbital width	0.10 ± 0.00	−0.32	52
Maxillary length	0.16 ± 0.00	0.00	48
Lower jaw length	0.19 ± 0.00	−0.61	50
Caudal peduncle depth	NONLINEAR		
Caudal peduncle length	0.21 ± 0.01	3.35	51
D_2I	0.06 ± 0.02	3.89	11
AII	0.06 ± 0.01	4.18	31
P_2I	NONLINEAR		

Table 3. Ontogenetic changes in the dentition of *E. telescopus*.

A. PREMAXILLARY DENTITION			
	‹200 mm SL	200-400 mm SL	› 400 mm SL
Extent	1/2-2/3 of ventral surface	2/3-7/8 of ventral surface	2/3-7/8 of ventral surface
Pattern	1 row	1-2 irregular rows tapering to 1 row	Multiple irregular rows
B. MANDIBULAR DENTITION			
	‹150 mm SL	150-250 mm SL	› 250 mm SL
Extent	Entire coronoid surface	Entire coronoid surface	Entire coronoid surface
Pattern	1 row	2-3 irregular rows tapering to 1-2 rows	3, 4, or 5 irregular rows
C. VOMERINE DENTITION			
	‹ 175 mm SL		› 175 mm SL
Extent	Center of vomer		Entire face of vomer
Pattern	Scattered teeth in few irregular rows		Numerous teeth in multiple irregular rows
D. PALATINE DENTITION			
	‹ 150 mm SL		› 150 mm SL
Extent	Length of ventral surface		Length of ventral surface
Pattern	1-2 irregular rows tapering to 1 row		2-5 irregular rows tapering to 1 row

7 (11), 8 (2), inserting on vertebrae 1–7 or 1–8 respectively; pleural ribs 9 (17), inserting on vertebrae 3–11.

Large specimens black or brown-violet, iridescent in life (Risso, 1810; Steindachner, 1891; Dons, 1938). Color in alcohol variable with mode of collection and preservation; skin often abraded, revealing underlying white-orange tissue; scale pockets mottled with black or brown, melanophores more densely packed near caudal edges; pigment darker in larger fish; skin oily, cutaneous fat deposits adding rust-colored tint; opercular area black. Guanine deposits occasionally occurring on opercular, thoracic, and abdominal regions; iris black with silver highlights; branchial membranes black; mouth darkening with age (see Ontogenetic change).

Description based on 54 specimens 68.1–553 mm SL.

Ontogenetic change. Several marked ontogenetic changes occur in *E. telescopus*, the most noticeable involving dentition patterns. Tooth-bearing bones of young specimens exhibit relatively prominent conical teeth. Teeth become more numerous with growth but appear smaller and form weak conical or villiform bands. As Table 3 illustrates, older specimens have more complex tooth patches with larger numbers of tooth rows.

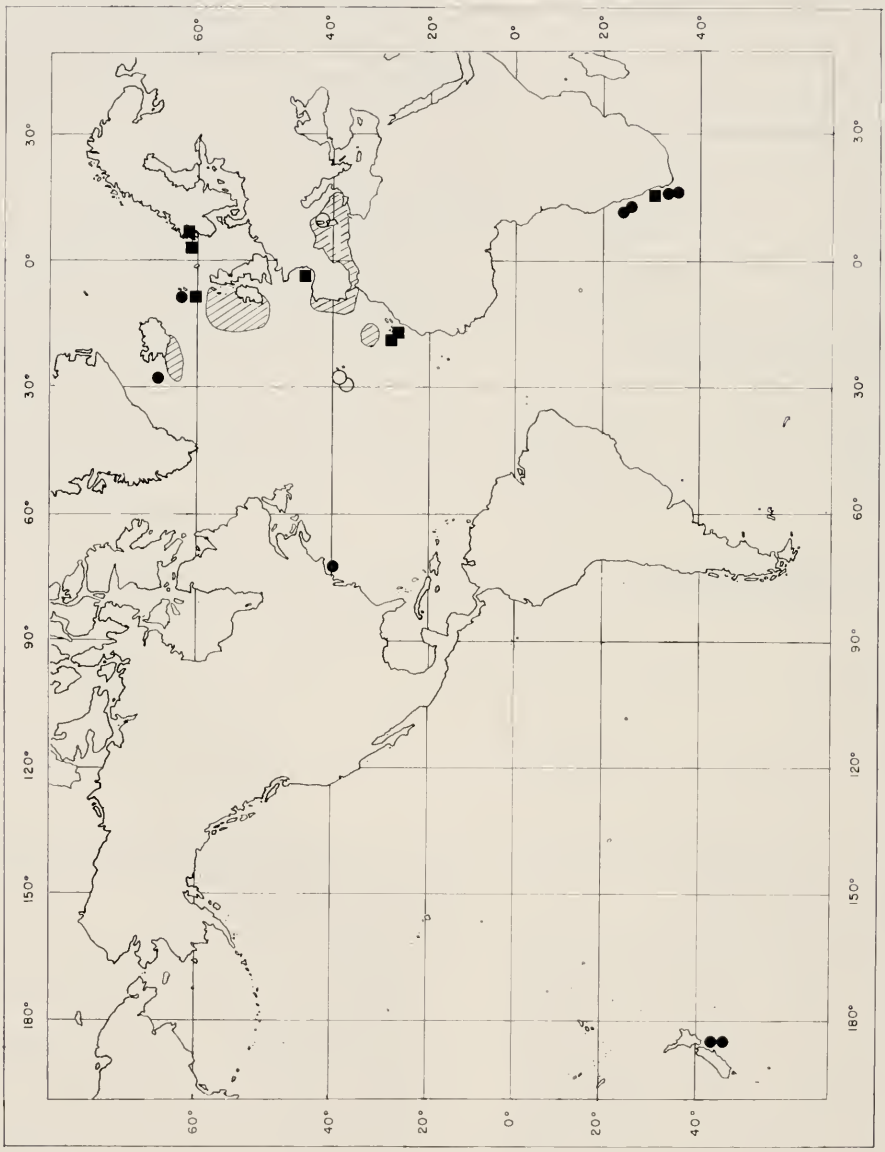

Figure 3. Distribution of *E. telescopus*. ● individual haul of demersal adults; ■ report of adults from the literature; ○ report of pelagic juveniles from the literature; cross-hatching indicates areas where *E. telescopus* are frequently taken.

A second change involves oral pigmentation. Young individuals have white or pale yellow mouths; melanin is present only in the vicinity of the pharynx. By the time specimens reach 175–225 mm SL, black pigment extends anteriorly to cover the entire tongue. Shortly thereafter, the palate becomes totally blackened, and by 300 mm SL, the entire mouth is dark.

The above changes are associated with alterations in intestinal length. Measurements of fourteen specimens ranging from 90.7–553 mm SL indicate that intestinal length increases from 66–73% SL in small specimens (90.7–128.5 mm) to 98–108% SL in moderate-sized individuals (220–250 mm). Thereafter, intestines grow more slowly, reaching 110–115% SL in the largest specimens. The coincidence of rapid intestinal growth, dentition changes, and development of oral pigment suggests that *E. telescopus* modifies its feeding habits with growth.

Distribution. E. telescopus has an antitropical distribution in the Atlantic, occurring from Iceland to the Canary Islands and reappearing along the western coast of South Africa (Fig. 3). Specimens have also been taken in the Subtropical Convergence region east of New Zealand. The species is well known in the western Mediterranean and has been captured once off the eastern coast of North America. A single specimen is known from shallow water off Norway (Dons, 1938).

Adults are taken by bottom trawl or longline and are most abundant from 300 to 800 meters; however, specimens have been captured from water as shallow as 75 to 80 meters to as deep as 1000 to 1200 meters. Koefoed (1952) reports four pelagic juveniles from the Azores; Bertolini (1933) mentions the presence of juveniles in the Tyrrhenian Sea.

Earlier workers reported the range of *E. telescopus* to include St. Helena (Valenciennes, 1837–1844; Günther, 1868; Bauchot and Blanc, 1961), tropical west Africa (Osorio, 1898; Poll, 1954; Bauchot and Blanc, 1961), and the Indian Ocean (Steindachner, 1907; Fowler, 1935). These accounts are based on misidentified or tenuously identified material. The specimens described by Günther, Poll, and Bauchot and Blanc are *E. pandionis*, while that examined by Fowler is *Scombrops*-like. Valenciennes' identification is based on an unpublished description and figure by a St. Helena resident and must be regarded with suspicion. Reports by Steindachner and Osorio could not be evaluated, because neither includes a description or figure of the material studied.

Geographic variation. The scarcity of material from South Africa and New Zealand makes it difficult to judge the degree to which Northern and Southern Hemisphere populations of *E. telescopus* have diverged. Comparisons of dorsal and pectoral fins, pleural and epipleural ribs, lateral line scale counts, gill rakers, and pyloric caeca reveal no subspecific differences (coefficients of difference $\leqslant 0.44$). Morphometric characters, on the other hand, exhibit greater variability. Of eight traits successfully analyzed, three are significantly different at both the 95%, 98%, and 99% levels of confidence (Table 4). These differences suggest that northern and southern populations represent geminate subspecies; however, additional material must be collected, especially from the Southern Hemisphere, before definitive statements can be made on intraspecific variability.

Taxonomic notes. Pomatomichthys constanciae Giglioli, 1880 is provisionally considered a junior synonym of *E. telescopus* on the basis of work by Tortonese and Queirolo (1970). These authors re-examined and, for the first time, figured the holotype of *P. constanciae*. The latter species is known only from the type specimen. The original description (Giglioli, 1880) is incomplete; no adequate redescription has ever been published.

Data from the papers mentioned above indicate a similarity between *P. constanciae*

TABLE 4. COMPARISON OF REGRESSION COEFFICIENTS FROM NORTHERN AND SOUTHERN HEMISPHERE POPULATIONS OF *E. TELESCOPUS*. DATA EVALUATED AT THE 95%, 98%, AND 99% LEVELS OF CONFIDENCE. DF = DEGREES OF FREEDOM; Nb = REGRESSION COEFFICIENTS OF NORTHERN HEMISPHERE SPECIMENS; Sb = REGRESSION COEFFICIENTS OF SOUTHERN HEMISPHERE SPECIMENS; SD = SIGNIFICANT DIFFERENCE BETWEEN TABULAR AND CALCULATED VALUES OF t; t = CALCULATED VALUES OF t.

					Significance		
	Nb	Sb	DF	t	95	98	99
HL	0.35	0.36	46	1.54	—	—	—
Body depth	0.25	0.24	44	0.82	—	—	—
Head height	0.20	0.18	41	3.88	SD	SD	SD
Eye diameter	0.13	0.12	40	1.75	—	—	—
Snout length	0.09	0.10	45	3.19	SD	SD	SD
Interorbital width	0.10	0.10	48	1.05	—	—	—
Maxillary length	0.15	0.16	12	0.16	—	—	—
Lower jaw length	0.19	0.19	14	0.71	—	—	—
Caudal peduncle depth	NONLINEAR						
Caudal peduncle length	0.21	0.22	47	0.58	—	—	—
D_2 I	INSUFFICIENT DATA						
A II	0.06	0.04	23	3.80	SD	SD	SD
P_2 I	NONLINEAR						

TABLE 5. COMPARISON OF DORSAL AND PECTORAL FIN COUNTS FROM *E. TELESCOPUS*, *P. CONSTANCIAE*, AND *E. TREWAVASAE*. DATA FOR *P. CONSTANCIAE* FROM GIGLIOLI (1880) AND TORTONESE AND QUEIROLO (1970); REMAINING DATA FROM PRESENT STUDY.

	E. telescopus	P. constanciae	E. trewavasae
First dorsal fin	VIII, rarely VII	VII	VII
Second dorsal fin	I, 10, rarely I, 9	I, 9	I, 9. rarely I, 10
Pectoral fin	19 - 23	18	16 - 18

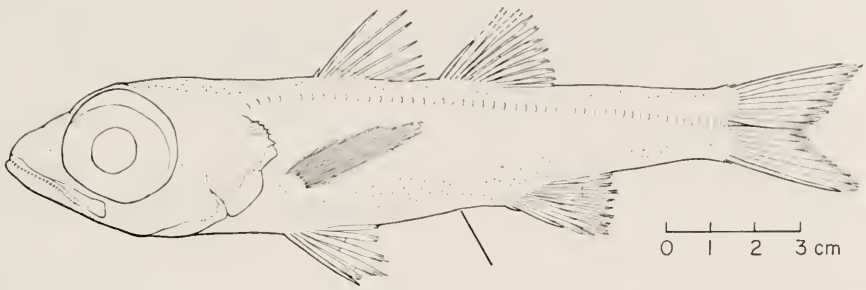

Figure 4. *Epigonus macrops*, 154.6 mm SL, USNM 207679.

and *E. telescopus* but also suggest an affinity between *P. constanciae* and *E. trewavasae* Poll, 1954. As is shown in Table 5, dorsal and pectoral fin counts fall within the range of *E. trewavasae* rather than *E. telescopus*. Tortonese and Queirolo's figure similarly shows the holotype to possess a sharp opercular spine, short D_1I, and long P_2I—all characteristics of *E. trewavasae*. Mensural data fail to differentiate *P. constanciae* from either species. Unlike *E. trewavasae* but like *E. telescopus*, the holotype lacks lingual teeth (Giglioli, 1880).

In view of the uncertainty surrounding *P. constanciae*, a closer study of this form must be undertaken. The problem is all the more pressing, because *E. trewavasae* is recorded from the Mediterranean for the first time in this paper.

Common names. Comprehensive lists of common names for *E. telescopus* are provided by Döderlein (1889), Nobre (1935), and Bini (1968). Three names not recorded in these works are "Mejluza"—Gran Canaria (Steindachner, 1891), "Devil-fish"—North Sea area (Ehrenbaum, 1928), and "Big-eyed cardinal fish"—New Zealand (Anonymous, 1961).

Epigonus macrops (Brauer, 1906)
Figure 4

Oxydon macrops Brauer, 1906: 288, fig. 172 (original description; Indian Ocean, land-locked sea on west coast of Sumatra, VALDIVIA Sta. 186, 03°21′01″S, 101°11′05″E, 903 m; syntype examined, ZMB 17678); Weber and de Beaufort, 1929: 351, fig. 81; Norman, 1939: 60.

Diagnosis. *E. macrops* may be distinguished from all congeners by its low gill raker counts (17–21). It is further characterized by eight fully developed first dorsal fin spines and eight pyloric caeca, one of which may function as a luminescent organ.

Description. Meristic values presented in Table 6; regression data for morphometric traits presented in Table 7.

Body elongate; anterodorsal profile rising steeply to occipital area; thereafter, weakly convex, almost horizontal to first dorsal fin; body depth 19.7–24.1% SL; caudal peduncle length 22.0–26.7% SL.

Head length 34.1–38.5% SL; head height 17.2–21.9% SL; snout blunt; angle of gape large; lower jaw protruding beyond upper jaw. Maxilla rarely exceeding ⅓–⅔ eye length; posterior margin of maxilla broad, bearing posteriormost point at ventral surface of bone. Eye round to oval, 39.7–48.3% HL; anterodorsal rim of orbit projecting strongly into dorsal profile; interorbital region wide, 9.5–11.7% SL.

Teeth conical, frequently recurved. Premaxillary and mandibular teeth prominent, needle-like, arranged in single row along length of jaws; mandibular teeth occasionally forming double row near symphysis; vomerine teeth few, moderate, arranged in 2–4 irregular rows or in a triangular or diamond-shaped patch; palatines bearing 2–6 teeth, arranged in single row covering anterior half or second quarter of bone; tongue edentulous.

Opercular spine short, weak, bony, ven-

Table 6. *Epigonus macrops* meristic data. $\overline{X}$ = mean; SD = standard deviation; n = number of specimens.

	$\overline{X}$	Range	SD	n
Pectoral fin rays	18.87	18–19	0.35	30
Gill rakers	18.63	17–21	0.87	32
Lateral line scales	48.61	46–50	0.83	28
Pyloric caeca	8.00	8	0.00	15

tral to 3–10 spinelets; spine and spinelets separated by shallow, occasionally narrow gap. Preopercular angle weakly produced, rounded, serrate; serrations occasionally extending to posterior and ventral surfaces of bone, rarely absent; striations radiating from inner edge of angle. Subopercle and interopercle generally serrated, occasionally striated. Gill rakers short, awl-like.

First dorsal fin VII (1), VIII (29); second dorsal fin I,9 (1), I,10 (31); anal fin II,9 (30), II,10 (1). D_1I, D_2I, AII short, equalling 1.2–2.9%, 5.3–7.7%, 5.9–9.9% SL respectively; P_2I moderate, 11.7–14.1% SL.

Vertebrae 10 + 15 (25); epipleural ribs 6 (23), inserting on vertebrae 1–6; pleural ribs 8 (24), inserting on vertebrae 3–10.

Table 7. *Epigonus macrops* regression data. b = regression coefficient ± 95% confidence interval; a = Y intercept; n = number of specimens. All regressions on SL.

	b	a	n
HL	0.35 ± 0.02	1.48	26
Body depth	0.22 ± 0.02	0.51	31
Head height	0.18 ± 0.02	1.74	19
Eye diameter	0.14 ± 0.02	3.41	29
Snout length	0.08 ± 0.01	−0.18	22
Interorbital width	0.11 ± 0.01	0.36	30
Maxillary length	0.14 ± 0.01	1.31	22
Lower jaw length	0.18 ± 0.01	1.18	31
Caudal peduncle depth	0.12 ± 0.01	−1.53	29
Caudal peduncle length	0.24 ± 0.02	0.70	30
D_2I	0.02 ± 0.02	7.05	13
AII	0.04 ± 0.01	4.73	22
P_2I	0.13 ± 0.02	0.49	16

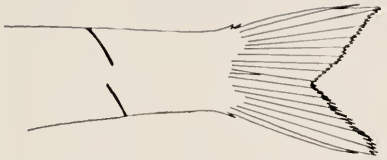

Figure 5. Caudal peduncle of young *E. macrops* bearing anterodorsally canted ring.

Specimens probably black in life. Color in alcohol variable with preservation; scale pockets covered with black melanophores near posterior edges; skin frequently abraded, revealing pink-yellow musculature; opercular bones transparent, colored black by underlying branchial membranes; iris black; mouth black in adults. Young bearing anterodorsally canted caudal peduncle ring (see Ontogenetic change). First pyloric caecum modified into luminescent organ (see Remarks).

Description based on 32 specimens 77.8–206.0 mm SL.

Ontogenetic change. The transition from juvenile to adult in *E. macrops* is marked by changes in pigmentation and body shape. Pelagic juveniles 15–37.9 mm SL and young demersal forms 77.8–79.8 mm SL bear a thin, black, anterodorsally tilted ring circling the center portion of the caudal peduncle (Fig. 5). Specimens larger than 90 mm SL lack this marking. Melanophores forming the rings are deeply embedded in the peduncle musculature and cannot be obliterated by abrading the surface of the fish.

Adult *E. macrops* are characterized by black oral and branchial membranes. Although these areas are colorless or poorly pigmented in specimens smaller than 40 mm SL, the former surfaces darken and the latter become covered with brown melanophores by the time fish reach 80 mm SL.

Juvenile *E. macrops* appear longer and shallower than adults. Ratio-on-size diagrams for interorbital width (*i.e.*, interorbital width/SL vs. SL) indicate allometric growth takes place in small specimens. Similar statements are probably true for head height, eye length, and caudal peduncle measurements but could not be tested because of damage to juvenile specimens.

Distribution. E. macrops adults are taken exclusively by bottom trawls between 550 and 1100 meters in the Indian Ocean, Gulf of Mexico, Caribbean Sea, and Western Atlantic. Specimens are most abundant between 640 and 920 meters. Pelagic juveniles are known from the Caribbean at depths of 120 to 550 meters (Fig. 6).

Geographic variation. No investigation made because of inadequate Indian Ocean samples.

Taxonomic notes. Brauer's description of *Oxyodon macrops* (1906) is based on two syntypes from the eastern Indian Ocean (172 and 212 mm total length). Of these, only the larger is in the Zoologisches Museum der Humboldt Universität; the smaller has been lost. The misplaced type may have been deposited in the Zoologisches Institut der Universität Leipzig and may reappear when portions of this collection, presently stored in Berlin, are sorted and catalogued (Karrer, personal communication).

Remarks. Specimens of *E. macrops* bear eight pyloric caeca; one of these appears modified into a bioluminescent organ. The luminescent caecum arises from the midventral surface of the pylorus just before the duodenum and main body of pyloric appendages (Fig. 7). It extends ventrally until it reaches the floor of the abdominal cavity, bends anteriorly and inserts into a pouch formed by the black peritoneal lining of the body cavity. At the posterior edge of the pelvic girdle, the caecal pouch lies over a thin, translucent portion of the body wall which may function as a bioluminescent window. Externally the bioluminescent window is covered by a single large scale. The caecal pouch is lined with silver or silver-gray pigment. Guanine deposits appear most concentrated anterodorsally.

Although there is no direct evidence to

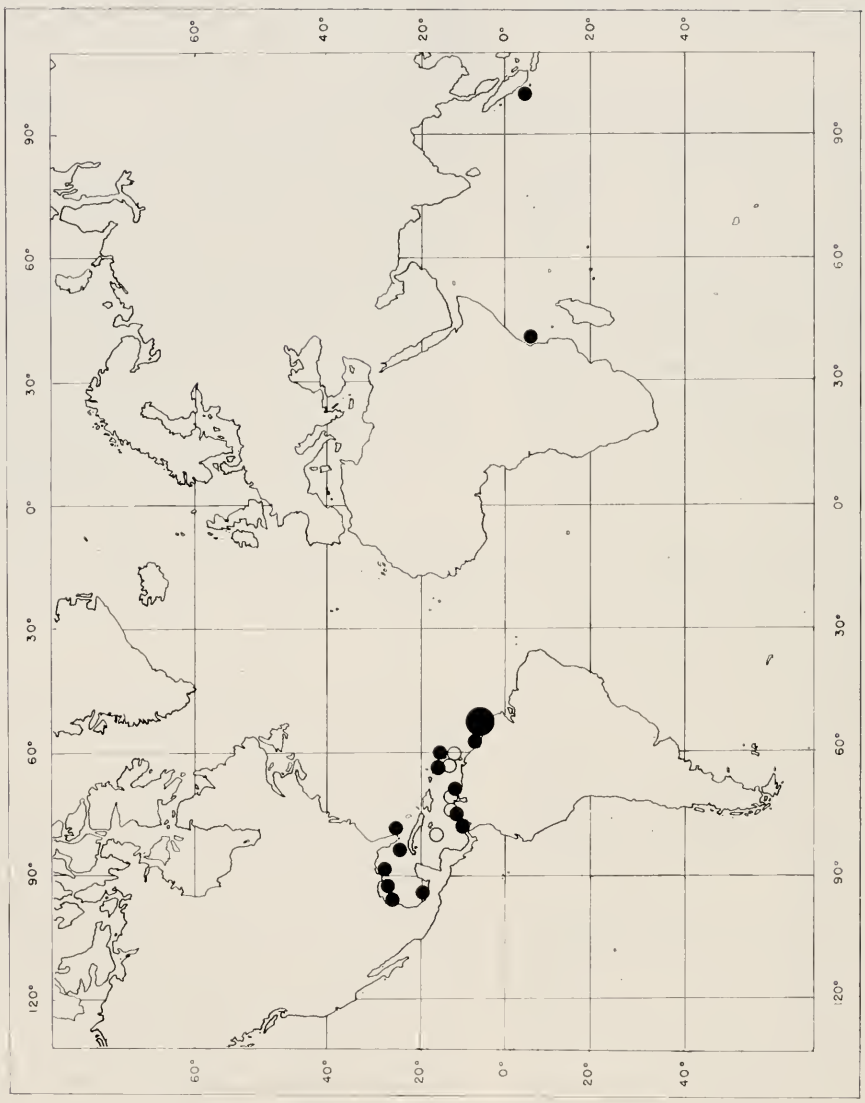

Figure 6. Distribution of *E. macrops*. ● individual haul of demersal adults; ⬤ five or more hauls of demersal adults; ○ individual haul of pelagic juveniles.

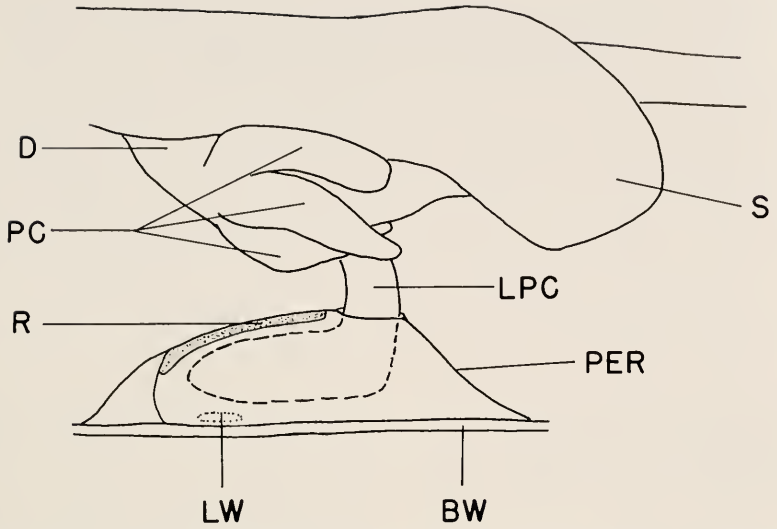

Figure 7. Luminescent organ of *E. macrops*. BW, body wall; D, duodenum; LPC, luminescent pyloric caecum; LW, luminescent window; PC, nonluminescent pyloric caeca; PER, peritoneum; R, reflector; S, stomach.

support the claim that *E. macrops* is luminescent, the modifications described above are similar to those found in several luminescent perciforms. *Pempheris klunzingeri* and *Parapriacanthus ransonneti* (Pempheridae) have luminescent organs embedded in the thoracic ventral musculature formed from, or directly associated with, the first pair of pyloric caeca (Haneda et al., 1966). Luminescent shallow-water apogonids such as *Apogon ellioti* and *Siphamia majimai* also have luminescent organs associated with the alimentary canal. In both of the latter forms, anal and/or thoracic organs are connected by duct to the intestine. As in *E. macrops*, tissue above the luminescent structures may serve as a reflector (Iwai, 1959; Haneda et al., 1966).

Common names. None.

Epigonus pandionis (Goode and Bean, 1881)
Figure 8

Apogon pandionis Goode and Bean, 1881: 160 (original description; off entrance to Chesapeake Bay; holotype examined, USNM 26228); Jordan and Gilbert, 1882: 564.

Figure 8. *Epigonus pandionis*, 141.7 mm SL, TABL uncatalogued.

Table 8. *Epigonus pandionis* meristic data. $\bar{X}$ = mean; SD = standard deviation; n = number of specimens.

	$\bar{X}$	Range	SD	n
Pectoral fin rays	17.81	17–19	0.57	97
Gill rakers	27.84	26–30	0.88	101
Lateral line scales	47.63	46–49	0.66	81
Pyloric caeca	10.81	10–13	0.74	72

Glossamia pandionis Goode and Bean, 1896: 231.
Xystramia pandionis Jordan, 1917: 46.
Epigonus telescopus, Poll (not Risso, 1810), 1954: 89, fig. 26; Bauchot and Blanc (in part), 1961: 70.

Diagnosis. *E. pandionis* is the most robust species of the genus. Specimens shorter than 110–125 mm SL are distinguished by a posterodorsally canted ring circling the caudal peduncle.

E. pandionis differs from *E. macrops* and *E. telescopus* by bearing VII (rarely VIII) spines in the first dorsal fin and 10–13 pyloric caeca. It is unlike *E. oligolepis* because it has 46–49 lateral line scales and may be distinguished from *E. trewavasae*, *E. pectinifer*, *E. robustus*, *E. lenimen*, *E. crassicaudus*, and *E. occidentalis* because it lacks a pungent, bony opercular spine. *E. pandionis* most closely resembles *E. fragilis* and *E. denticulatus* but is differentiated by its short caudal peduncle (22.0–26.3% SL) and deep body (22.4–29.6% SL). It further differs from *E. denticulatus* by exhibiting gill raker counts of 26–30 and a single basal pterygiophore between neural spines 9 and 10.

Description. Meristic values presented in Table 8; regression data for morphometric traits presented in Table 9.

Body shortened, robust; anterodorsal profile convex, particularly between occiput and first dorsal fin; body deep, 22.4–29.6% SL; caudal peduncle short, broad, length 22.0–26.3% SL.

Head length 33.0–39.0% SL; head height 19.0–22.2% SL; snout blunt; angle of gape large; upper jaw subequal to lower jaw. Maxilla reaching ⅖–½ eye length; posterior margin broad, posteriormost point at ventral edge of bone. Eye round or slightly oval, 37.4–48.7% HL; anterodorsal rim of orbit projecting into profile in smaller specimens, reaching profile in larger forms; interorbital region wide, 9.2–11.5% SL.

Dentition variable with age (see Ontogenetic change); premaxillae, mandibles, vomer, and palatines dentigerous, bearing conical, occasionally recurved teeth; tongue edentulous.

Opercular spine short, horny, ventral to 2–5 (usually 3–4) poorly ossified spinelets; spine separated from spinelets by gap; spinelets occasionally obscured by underlying membranes. Preopercular angle broad, rounded, moderately produced; striations radiating from inner ridge to edges of angle; serrations along posterior and ventral surfaces of bone. Subopercle and interopercle bearing scattered serrations. Gill rakers awl-like.

First dorsal fin VII (95), VIII (5); second dorsal fin I,9 (2), I,10 (97), I,11 (1), II,10 (1); anal fin II,8 (2), II,9 (96), II,10 (1); D_1I long, 3.6–8.1% SL; D_2I, AII, P_2I short, equalling 5.0–8.6%, 5.0–8.7%, 8.9–12.7% SL respectively.

Vertebrae 10 + 15 (36); epipleural ribs 6 (25), 7 (1), inserting on vertebrae 1–6 and 1–7 respectively; pleural ribs 8 (36), inserting on vertebrae 3–10.

Table 9. *Epigonus pandionis* regression data. b = regression coefficient ± 95% confidence interval; a = Y intercept; n = number of specimens. All regressions on SL.

	b	a	n
HL	0.36 ± 0.01	0.04	77
Body depth	0.29 ± 0.01	−2.64	75
Head height	0.21 ± 0.01	−0.30	67
Eye diameter	0.16 ± 0.01	−0.15	80
Snout length	0.08 ± 0.00	0.05	73
Interorbital width	0.11 ± 0.00	0.33	74
Maxillary length	0.17 ± 0.01	−0.35	74
Lower jaw length	0.19 ± 0.00	−0.01	78
Caudal peduncle depth	0.12 ± 0.00	−0.61	80
Caudal peduncle length	0.24 ± 0.01	0.54	81
D_2 I	0.05 ± 0.01	1.69	46
AII	0.05 ± 0.01	2.11	56
P_2 I	0.10 ± 0.01	0.71	75

Pigmentation variable with age (see Ontogenetic change); scale pockets mottled with black; fin membranes black; opercular region of adults black-slate gray; mouth primarily light; iris black. Specimens frequently abraded, underlying tissue pale yellow-rust brown; guanine deposits rare, if present occurring on opercular complex, isthmus, thorax, or abdomen; silvered forms generally from old collections.

Descriptions based on 104 specimens 45.7–194.0 mm SL.

Ontogenetic change. Maturation in *E. pandionis* is accompanied by changes in pigmentation and dentition. The most striking transformation involves caudal peduncle markings. Specimens smaller than 85 mm SL bear a thin, black, posterodorsally sloped ring circling the central portion of the caudal peduncle. Melanophores forming the ring are deeply embedded in peduncle musculature and are not easily abraded. A broader, more superficial band of pigment circles the caudal peduncle at the base of the caudal fin (Fig. 1B). As specimens grow beyond 85 mm, the rings become fainter and begin to disappear. Fish larger than 110 mm SL may completely lack peduncle markings, and by 125 mm SL, rings are absent from virtually all specimens. Since *E. pandionis* becomes sexually mature at approximately 110 mm SL, altered markings may reflect changes in habit or behavior associated with reproductive individuals.

Gill rakers and branchial membranes are converted from pale yellow to black. Specimens smaller than 55 mm SL bear scattered black melanophores on gill rakers but lack opercular pigmentation. By 60 mm SL rakers have become totally dark, and traces of melanin have appeared on membranes lining the opercle. Pigment becomes denser with growth and spreads ventrally. By 100 mm SL the opercle is completely lined with dark tissue. Since

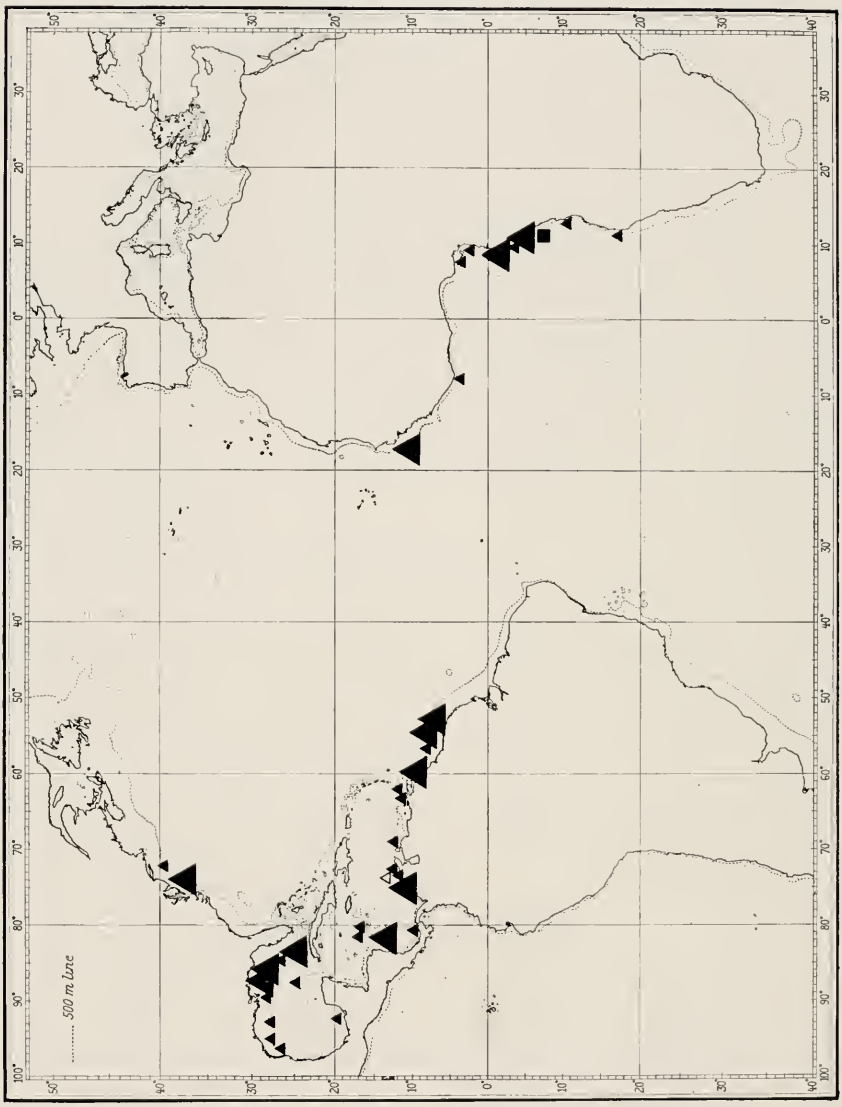

Figure 9. Distribution of *E. pandionis*. ▲ individual haul of demersal adults; ▲ three or more hauls of demersal adults; △ individual haul of pelagic juveniles; ■ report of adults from the literature.

opercular bones are translucent, the process appears outwardly as a darkening of the opercle.

Ontogenetic changes in dentition involve the production of increasingly complex tooth patches. Specimens smaller than 80 mm SL bear single rows of teeth on the premaxillae and palatines. Mandibular teeth are arranged in patterns analogous to those found on the premaxillae or in double rows that taper to a single row posteriorly. Vomerine teeth occur in 1–2 chevron-shaped clumps. As growth takes place, teeth are added to all dentigerous surfaces. Large specimens (>130 mm SL) have as many as 3–4 tooth rows on palatines and anterior segments of dentaries and premaxillae. Vomerine teeth may become sufficiently numerous to cover the entire face of the bone.

Distribution. E. pandionis is amphi-Atlantic, occurring primarily in the Caribbean, Gulf of Mexico, and Gulf of Guinea (Fig. 9). The species has been taken as far north as New Jersey and as far south as French Guiana in the western Atlantic. It occurs between Portuguese Guinea and Angola in the eastern Atlantic. Adults are captured exclusively by bottom trawls between 210 and 600 meters. American forms are most numerous from 300 to 500 meters, while African populations are most abundant between 260 and 450 meters. A single pelagic juvenile (35.5 mm SL, MCZ 48839) was taken at 275 to 300 meters in the Caribbean.

Geographic variation. Statistical analyses provide conflicting assessments of the similarity of African and American populations. Meristic characters reveal little variability. Coefficients of difference calculated for standard counts are always less than or equal to 0.49—far below conventional levels of subspecies recognition. Mensural data, on the other hand, suggest there are considerable differences between the populations. Of thirteen traits analyzed, seven separate eastern and western populations at the 95% level of confidence, five separate them at the 98% level, and two separate them at the 99% level (Table 10).

A closer examination of the characters exhibiting significant differences reveals that regression coefficients of American *E. pandionis* are always greater than those of African forms. Since regression coefficients are a measure of relative growth, observed intraspecific variation may reflect environmental factors.

Water temperature is a major parameter determining growth rates in fishes. If other factors are controlled, rates of growth increase proportionally with temperature (Brown, 1957: 391). With this in mind, it is interesting that temperatures are generally higher and superficial warm-water layers thicker in the western tropical Atlantic (Ekman, 1953). At 300 meters Gulf of Mexico and Caribbean temperatures vary from 10 to 18° C while west African temperatures range between 9 and 11° C. At 500 meters the difference is slightly less pronounced—8–13° C as opposed to 6–8° C (from temperature profiles in Fuglister, 1960; Wüst, 1964; and Nowlin and McLellan, 1967). One would therefore expect western Atlantic *E. pandionus* to grow more rapidly and exhibit larger regression coefficients than eastern Atlantic forms. In view of these findings, the two morphs are not considered to represent separate subspecies.

Remarks. See *E. trewavasae*: Remarks for discussion of *E. pandionis sensu* Lozano (1934), Navarro et al. (1943), and Maurin (1968).

Specimens of doubtful identity. Five specimens were examined that resembled *E. pandionis* but could not, with certainty, be placed in the species. Four were taken in the Atlantic, the fifth in the Gulf of Oman (see Mayer, 1972: Appendix II for complete data). These fishes were not considered when preparing the description of *E. pandionis*, nor were they used in morphometric, meristic, or distribution analyses.

The Atlantic specimens include three

Table 10. Comparison of regression coefficients from eastern and western Atlantic populations of *E. pandionis*. Data evaluated at the 95%, 98%, and 99% levels of confidence. DF = degrees of freedom; Eb = regression coefficients of eastern Atlantic specimens; SD = significant difference between tabular and calculated values of t; t= calculated values of t; Wb = regression coefficients of western Atlantic specimens.

					Significance		
	Wb	Eb	DF	t	95	98	99
HL	0.36	0.37	60	0.97	—	—	—
Body depth	0.29	0.29	71	0.31	—	—	—
Head height	0.22	0.20	63	2.41	SD	SD	—
Eye diameter	0.17	0.15	76	2.14	SD	—	—
Snout length	0.09	0.08	69	3.00	SD	SD	SD
Interorbital width	0.11	0.11	70	2.13	SD	—	—
Maxillary length	0.18	0.16	70	3.35	SD	SD	SD
Lower jaw length	0.20	0.18	74	2.63	SD	SD	SD
Caudal peduncle depth	0.13	0.12	76	2.39	SD	SD	—
Caudal peduncle length	0.23	0.24	77	1.16	—	—	—
D_2 I	0.05	0.06	32	1.83	—	—	—
A II	0.05	0.05	52	0.91	—	—	—
P_2 I	0.10	0.10	71	0.83	—	—	—

fishes from St. Helena. The most recently collected (UZM P45148) was incorrectly identified as *E. telescopus* by Bauchot and Blanc (1961). The two older forms (BMNH 1868.3.11.14/15) are probably the fish discussed by Günther (1868). The remaining specimen (USNM 207703) was taken in the Caribbean.

The four Atlantic individuals are basically similar to *E. pandionis* but exhibit shallower heads (17.4–19.8% SL), narrower interorbital regions (8.6–9.4% SL), fewer pyloric caeca (8–9), and fewer gill rakers (25–27). In these respects they resemble *E. fragilis*. Little is known about the habits of the variants; station data are available for only the Caribbean form, which was taken at relatively shallow depths. Exact determination of the variants' status must await the capture of additional material.

The Indian Ocean form (BMNH 1889.4.15.24) is distinguished from *E. pandionis* by its shallow body (22.5% SL), narrow interorbital region (8.3% SL), dentigerous glossohyal, numerous weak opercular spinelets, and elongate gill filaments. The last trait suggests the fish may have inhabited an oxygen minimum layer. As with the Atlantic variants, additional material must be collected before the status of the form can be determined.

Common names. None.

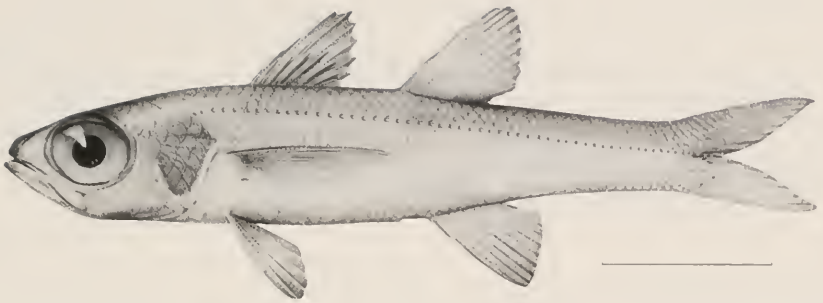

Figure 10. *Epigonus fragilis*, HOLOTYPE, 89.1 mm SL, CM 3900/FMNH 55204 (from Jordan and Jordan, 1922).

Epigonus fragilis (Jordan and Jordan, 1922) Figure 10

Scepterias fragilis Jordan and Jordan, 1922: 45, plate II, fig. 2 (original description; Honolulu market; holotype examined, CM 3900/FMNH 55204).

?*Hynnodus fragilis* Pietschmann, 1930: 13.

Diagnosis. *E. fragilis* most closely resembles *E. pandionis* but may be distinguished by its shallow body (18.8–21.1% SL) and short, shallow head (length 31.7–34.0% SL, height 16.0–17.4% SL). Unlike *E. pandionis*, *E. fragilis* lacks peduncle rings on specimens smaller than 100–120 mm SL.

In the past *E. fragilis* has been confused with *Hynnodus atherinoides*, a junior synonym of *E. occidentalis*. *E. fragilis* may be distinguished on the basis of body depth (see above), pectoral fin counts (16–17), and the absence of a pungent, bony opercular spine. Weak opercular armor, together with second dorsal fin counts of I,10 differentiate *E. fragilis* from *E. trewavasae*, *E. pectinifer*, *E. robustus*, *E. lenimen*, and *E. crassicaudus*. Gill raker counts of 25–26 separate *E. fragilis* from all remaining congeners except *E. telescopus*. *E. fragilis* may be distinguished from the latter by the presence of 7–8 pyloric caeca.

Description. *E. fragilis* is known from only five specimens. Of these, the holotype is of little descriptive value. The specimen is severely dehydrated and has become discolored, brittle, and shrunken. The following account is based primarily on two recently captured specimens of *E. fragilis* (LACM 32668-6 and USNM 207704) and two forms collected by D. S. Jordan in 1921 (SU 23246). The latter are mentioned in the original description of *E. fragilis* but are not designated as types.

All meristic and mensural data are presented in the text. Detailed statistical analyses were not undertaken because of small sample size.

Body elongate; anterodorsal profile convex, rising without interruption from tip of snout to first dorsal fin. Body depth 18.8–21.1% SL; caudal peduncle length 25.4–26.9% SL.

Head short, 31.7–34.0% SL; head height 16.0–17.4% SL; snout blunt, 7.2–7.9% SL; angle of gape moderate; jaws equal. Maxilla reaching ½ eye length; posteriormost point of maxilla at ventral edge of bone. Eye round, 38.1–41.5% HL; anterodorsal rim of orbit reaching profile; interorbital width 8.8–9.4% SL.

Dentition variable with age. Teeth conical; premaxillary teeth in irregular double rows anteriorly, tapering to single row posteriorly, occupying anterior ½–¾ of bone. Mandibular dentition more prominent than that of premaxilla; teeth recurved, occupying from ¾ to entire length of dentary, arranged in single or double rows near symphysis and single row posteriorly. Vomerine teeth recurved, arranged in oval or diamond-shaped patch, covering entire face of bone in adults. Palatine teeth

Figure 11. *Epigonus occidentalis*, 152.7 mm SL, MCZ 48840.

medially recurved, arranged in single–triple rows anteriorly, tapering to single row posteriorly; tongue edentulous.

Opercular spine weak, ventral to 7–9 small serrae; angle of preopercle produced, rounded, ornamented with striations and weak serrations; subopercle and interopercle unornamented. Gill rakers 25 (3), 26 (1), simple, awl-like. Pyloric caeca 7(1), 8 (2).

First dorsal fin VII (4), VIII (1); second dorsal fin I,10 (5); anal fin II,9 (5); pectoral fin 16 (1), 17 (3); D_1I moderate to long, 5.9–8.9% SL; D_2I short, 6.9% SL; P_2I long, 10.1–10.2% SL; AII broken.

Vertebrae 10 + 15 (4); epipleural ribs not visible on radiographs; pleural ribs 8 (4), inserting on vertebrae 3–10. Pored lateral line scales 49 (2).

Color in alcohol yellow-brown; fin membranes dark; iris silver-black; mouth light; branchial membranes light, darkening with age.

Distribution. E. fragilis is endemic to the Hawaiian Islands (Fig. 12). The species is demersal and has been taken between 120 and 125 meters.

Taxonomic notes. Six years after *E. fragilis* was described, Fowler (1928) synonymized the species with a second Hawaiian apogonid, *Hynnodus atherinoides* Gilbert, 1905. The synonymy achieved moderate acceptance and appeared in several publications (*e.g.*, Matsubara, 1936; Tinker, 1944; Gosline and Brock, 1960). Fowler's conclusions were based on a 33-mm specimen (BPBM 3914) obtained by the Tanager Expedition. The specimen is in extremely poor condition. All coloration has been lost, most of the muscle tissue has decomposed, and much of the skeleton has become decalcified. Although it is impossible to identify the fish because of its condition, the following traits suggest it is neither *E. fragilis* nor *H. atherinoides*: dorsal fin elements—VIII–I,8; anal fin elements—II,6; vertebrae—11 + 14. These data differ from Fowler's report of VI–I,8 dorsal elements, no anal spines, and 7 anal rays.

As was discussed in the diagnosis, *E. fragilis* is distinct from *H. atherinoides*. Fowler's synonymy appears to have been based on inaccurate data taken from an incorrectly identified fish.

Common names. None.

Epigonus occidentalis Goode and Bean, 1896
Figure 11

Epigonus occidentalis Goode and Bean, 1896: 233, plate LXVI, fig. 236 (original description; Steamer BLAKE, off Barbados, 237 fms.; holotype examined, MCZ 28032).

Hynnodus atherinoides Gilbert, 1905: 618, plate 79 (original description; ALBATROSS Sta. 3867, Pailolo Channel, Hawaii, 284–290 fms.; holotype examined, USNM 51601); Jordan and Jordan, 1922: 44; Fowler and Bean, 1930: 121.

Hynnodus megalops Smith and Radcliffe, 1912 (*in* Radcliffe, 1912): 445, plate 38, fig. 3 (original description; ALBATROSS Sta. 5388, 12°51′30″N, 123°26′15″E, between Burias and Luzon, Philippines, 226 fms.; holotype examined, USNM 70255).

Table 11. *Epigonus occidentalis* meristic data. $\overline{X}$ = mean; SD = standard deviation; n = number of specimens.

	$\overline{X}$	Range	SD	n
Pectoral fin rays	20.21	19–21	0.59	56
Gill rakers	24.68	22–27	1.08	60
Lateral line scales	48.15	46–51	0.97	46
Pyloric caeca	9.27	8–13	1.05	45

Table 12. *Epigonus occidentalis* regression data. b = regression coefficient ± 95% confidence interval; a = Y intercept; n = number of specimens. All regressions on SL.

	b	a	n
HL	0.34 ± 0.02	0.72	48
Body depth	0.19 ± 0.02	−1.72	48
Head height	0.15 ± 0.01	0.53	49
Eye diameter	0.16 ± 0.01	0.66	49
Snout length	0.08 ± 0.00	0.06	49
Interorbital width	0.08 ± 0.01	0.83	39
Maxillary length	0.13 ± 0.01	0.88	51
Lower jaw length	0.15 ± 0.01	1.26	51
Caudal peduncle depth	0.10 ± 0.01	−0.90	54
Caudal peduncle length	0.23 ± 0.01	1.50	53
D_2 I	0.05 ± 0.00	1.42	34
AII	0.05 ± 0.01	2.18	42
P_2 I	0.09 ± 0.01	0.67	47

Diagnosis. *E. occidentalis* is distinguished from all other congeners by the combination of shallow body depth (14.1–19.5% SL), reduced gill raker counts (22–27), and the presence of a pungent, bony opercular spine. It is frequently confused with *E. denticulatus*.

Description. Meristic values presented in Table 11; regression data for morphometric traits presented in Table 12.

Body elongate, cigar-shaped; anterodorsal profile weakly convex, flattened, rising gradually from tip of snout to interorbital region, leveling off toward occipital region, and rising gradually to base of first dorsal fin. Body depth 14.1–19.5% SL, body

width subequal to or greater than body depth; caudal peduncle narrow, length 22.4–28.1% SL.

Head length 30.5–37.9% SL; head height 13.3–17.2% SL; angle of gape moderate to small; lower jaw equalling or protruding slightly beyond upper jaw. Maxilla reaching ¼–⅔ eye length; posterior margin of maxilla moderate to narrow, posteriormost point at ventral edge of bone. Eye long, oval, 40.6–52.3% HL; anterodorsal rim of orbit reaching or projecting into dorsal profile; interorbital region narrow, 5.6–8.5% SL.

Teeth conical; premaxillary and mandibular teeth frequently recurved, arranged in simple single row or single row widening to double or triple rows near symphysis; teeth covering ⅔ to entire length of premaxilla and ¾ to entire length of dentary; vomerine teeth arranged in 1–4 irregular rows; palatines rarely edentulous, teeth 1–10, arranged in single row, covering anterior ¼–½ of bone; tongue edentulous.

Opercular spine pungent, bony, ventral to 1–3 poorly ossified spinelets; spine separated from spinelets by shallow indentation. Preopercular angle produced, rounded or pointed, bearing serrations and striations; subopercle serrate, occasionally striate; interopercle variable, frequently serrate. Gill rakers short, awl-like.

First dorsal fin VII (59); second dorsal fin I,10 (59); anal fin II,8 (1), II,9 (59); D_1I, D_2I, AII, P_2I short, equalling 1.1–4.2%, 4.8–7.8%, 4.8–9.2%, and 8.0–11.3% SL respectively.

Vertebrae 10 + 15 (35); epipleural ribs 6 (19), 7 (5), inserting on vertebrae 1–6 or 1–7 respectively; pleural ribs 7 (31), 8 (1), inserting on vertebrae 2–9 or 3–9.

Color in alcohol variable with preservation; skin frequently removed by trawling; underlying tissue pale yellow, yellow-pink, occasionally marked with rust brown; scale pockets and fin membranes black; opercular area black-slate gray, occasionally tinged with silver; lower jaw, branchiostegal membranes, and thoracic and abdominal regions occasionally silvered; guanine most prevalent on specimens from old collections. Mouth color variable with age (see Ontogenetic change); iris and branchial region dark.

Description based on 62 specimens 58.2–178.9 mm SL.

Ontogenetic change. The most striking age-related change in *E. occidentalis* is the development of oral pigmentation. As in *E. telescopus* and *E. macrops*, immature forms bear pigmentless or slightly pigmented mouths, while adults have blackened oral membranes. Pigmentation first appears in specimens 80–110 mm SL. Melanophores develop just anterior to the pharynx and spread rostrally, covering a third of the roof and floor of the mouth and half of the tongue by the time specimens reach 115–130 mm SL. By 150 mm SL the tongue is completely black, and by 175–180 mm the entire mouth is dark. Branchial membranes undergo an analogous transformation before specimens reach 58 mm SL.

A faint black ring circling the middle of the caudal peduncle was observed on three small *E. occidentalis* (< 65 mm SL). Similar markings were absent from larger individuals. The rings are reminiscent of markings observed on young *E. macrops* and *E. pandionis* and probably represent a juvenile feature that is lost with growth.

Distribution. E. occidentalis has been taken in the Caribbean, Gulf of Mexico, and western tropical Atlantic. It is also known from the Philippine and Hawaiian Islands (Fig. 12). The species is caught by bottom trawls between 360 and 735 meters. Adults are most abundant in the Caribbean from 500 to 550 meters.

Geographic variation. E. occidentalis, as here defined, includes two nominal species —*Hynnodus atherinoides* Gilbert, 1905 and *H. megalops* Smith and Radcliffe, 1912. The former originally represented a Hawaiian endemic; the latter represented a Philippine form. In 1930 Fowler and Bean synonymized the Pacific morphs. In the

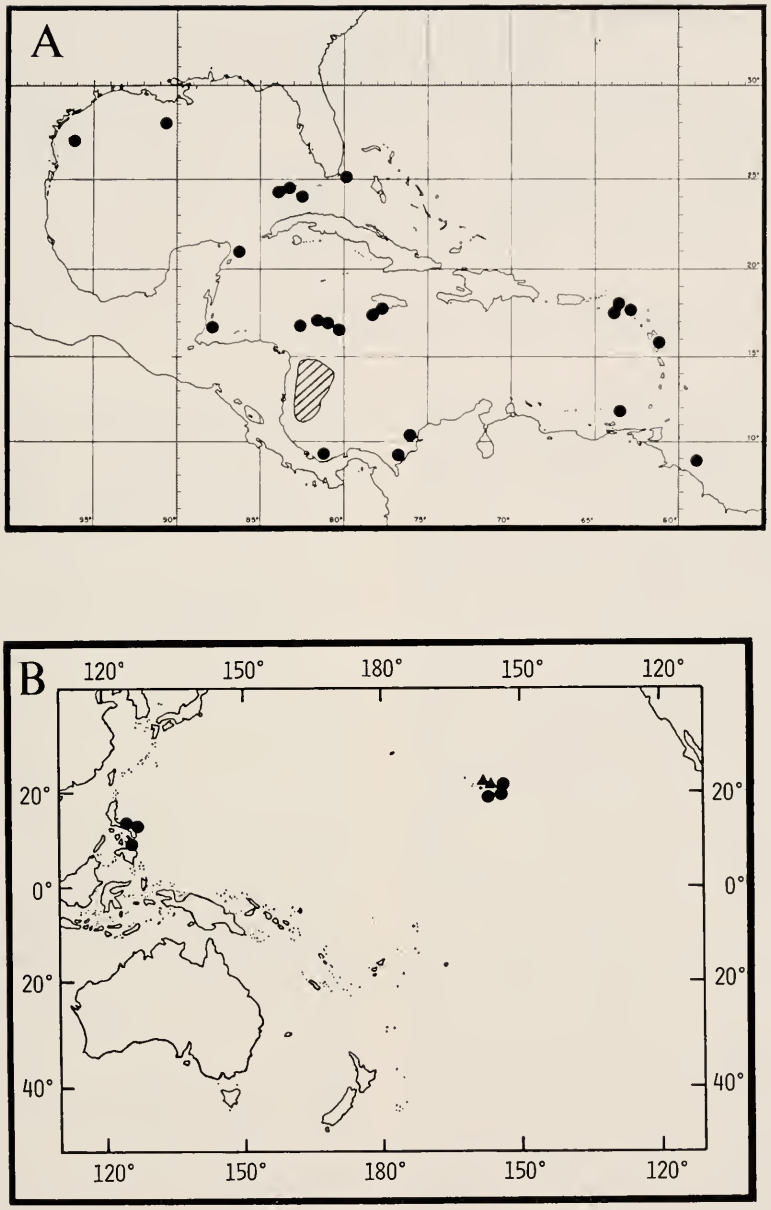

Figure 12. Distribution of *E. tragilis* and *E. occidentalis*. Map A shows localities in the Caribbean and Gulf of Mexico. Map B shows localities in the western Pacific. ▲ *E. tragilis*, individual haul of demersal adults; ● *E. occidentalis*, individual haul of demersal adults; cross-hatching indicates areas where *E. occidentalis* are frequently taken.

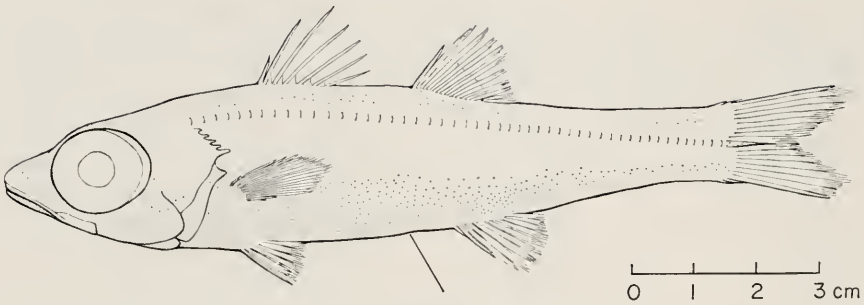

Figure 13. *Epigonus denticulatus*, 115.1 mm SL, UMML 12463.

authors' opinions, characters separating the two forms were "simply minor discrepancies of portraiture and should never have been credited as specific distinctions [p. 122]."

Although descriptions and illustrations of *H. atherinoides* and *H. megalops* suggest a link with *E. occidentalis*, detailed comparisons of the three forms were never made. To a large extent this was the result of inadequate sampling. Until the initiation of the OREGON cruises in 1950, few *E. occidentalis* were available for study. Pacific forms are still poorly represented; only seven specimens have been collected. Reports of additional material by Fowler (1928), Matsubara (1936), Smith (1949a,b, 1961), Kamohara (1952), and Moreland (1957) are based on misidentifications.

Comparisons of *E. occidentalis* and the *H. atherinoides–H. megalops* complex provide no evidence to support their status as separate species. Analyses of head length, body depth, head height, eye diameter, snout length, interorbital and maxillary widths, caudal peduncle length and depth, and AII and P_2I lengths reveal no significant differences between the populations at either the 95%, 98%, or 99% levels of confidence. Meristic data also show considerable overlap for most characters; however, the coefficients of difference for pyloric caeca and gill raker counts are above conventional levels of subspecies recognition (1.68 and 1.99, respectively). In addition, Atlantic and Pacific populations may be distinguished by minor qualitative characters such as:

(1) short, rounded preopercular angles in Atlantic forms; longer, pointed angles in Pacific specimens;
(2) fusion of uroneurals 1 and 2 in Atlantic forms (based on 3 alizarin preparations); separate occurrence in Pacific forms (based on 1 alizarin preparation).

On the basis of the above information, Atlantic and Pacific forms are placed in the same species but considered members of separate subspecies. Formal description of the subspecies must await the capture of additional Pacific specimens.

Remarks. A single unripe female *E. occidentalis* (USNM 197353, 172.1 mm SL) was found carrying small egg masses in the anterior portion of its mouth (anterior to the tongue and vomer). The masses contained 125 oval eggs 0.40–0.55 mm in diameter. The presence of eggs in the mouth of an *Epigonus* is of interest, because several shallow-water apogonids exhibit oral brooding. No such activity has ever been reported for deep-sea forms.

Although it is difficult to say with certainty, the *E. occidentalis* eggs are probably not incubating clutches, but rather non-apogonid ova ingested during trawling. Unlike the egg masses of typical oral brooding apogonids, those found in *E. occidentalis* are broken, disrupted, and contain very few eggs. An 84.9-mm specimen of *Cheilodipterus affinis* was reported in-

Table 13. *Epigonus denticulatus* meristic data. $\bar{X}$ = mean; SD = standard deviation; n = number of specimens.

	$\bar{X}$	Range	SD	n
Pectoral fin rays	19.09	18–20	0.56	54
Gill rakers	30.98	28–34	1.10	58
Lateral line scales	48.12	46–49	0.76	43
Pyloric caeca	11.83	10–14	0.85	42

cubating 21,000 eggs 0.35–0.4 mm in diameter (Smith et al., 1971: 8–9). The ova fully occupied the oral and branchial chambers and extensively distended the head. These conditions were not observed in *E. occidentalis*.

It is possible that the eggs represent the remnants of a larger mass that was spit out and partially reingested. However, were this the case, one might expect to find eggs in the stomach (Sakomoto, 1930) or gill rakers. No eggs were found in either region.

Finally, Breder and Rosen (1966) state that eggs of oral brooding apogonids are held together by fibers attaching to one pole. The eggs of *E. occidentalis* are loosely embedded in an open matrix of fibers. Grape-like egg clusters characteristic of *Apogon semilineatus* (Ebina, 1931: 20) were not observed.

Common names. None.

Epigonus denticulatus Dieuzeide, 1950
Figure 13

Pomatomus telescopus, Vaillant (in part) (not Risso, 1810), 1888: 376.

Scepterias lenimen, Whitley (in part) (not Whitley, 1935), 1935: 230; Whitley (in part), 1940: 420.

Epigonus atherinoides, Matsubara (not Gilbert, 1905), 1936: 120, fig. 1A; Smith, 1961: 378, fig. 3; Kamohara, 1952: 37, fig. 31.

Hymnodus atherinoides, Smith (not Gilbert, 1905), 1949a: 101; Smith, 1949b: 210, fig. 495A.

Epigonus denticulatus Dieuzeide, 1950: 89, figs. 1–2 (original description; Algerian Coast at 200–500 m; holotype not examined); Tortonese, 1952: 72, 1 fig.; Dieuzeide et al., 1953: 216, 2 figs.; Tortonese and Queirolo, 1970: 33, fig. 6.

Diagnosis. *E. denticulatus* lacks a fully ossified opercular spine, bearing instead 3–7 membranous projections. This feature distinguishes it from *E. occidentalis*, *E. trewavasae*, *E. pectinifer*, *E. robustus*, *E. lenimen*, and *E. crassicaudus*, which have pungent, bony opercular spines. *E. denticulatus* is differentiated from *E. telescopus*, *E. macrops*, and *E. fragilis* by the presence of 10–14 pyloric caeca and 28–34 gill rakers. It differs from *E. oligolepis* by bearing 46–51 lateral line scales. *E. denticulatus* closely resembles *E. pandionis* but may be distinguished on the basis of the former's shallow body (15.8–23.6% SL), long caudal peduncle (25.9–32.2% SL), and short D_1I (2.4–3.7% SL).

Description. Meristic values presented in Table 13; regression data for morphometric traits presented in Table 14.

Body fusiform, slightly compressed; anterodorsal profile rising gradually above snout, becoming steeper and slightly convex over eyes, thereafter rising gradually to first dorsal fin; body moderate to shallow, depth 15.8–23.6% SL; caudal peduncle narrow, length 25.9–32.2% SL.

Head moderate to short, 31.2–38.6% SL; head height 16.0–19.8% SL; snout short, blunt; angle of gape moderate to large; lower jaw protruding slightly beyond upper jaw. Maxilla reaching ⅓–½ eye length,

Table 14. *Epigonus denticulatus* regression data. b = regression coefficient ± 95% confidence interval; a = Y intercept; n = number of specimens. All regressions on SL.

	b	a	n
HL	0.32 ± 0.01	2.88	57
Body depth	0.25 ± 0.01	-4.09	54
Head height	0.16 ± 0.01	0.86	56
Eye diameter	0.14 ± 0.01	1.39	58
Snout length	0.07 ± 0.00	0.33	56
Interorbital width	0.09 ± 0.00	0.37	55
Maxillary length	0.14 ± 0.01	1.37	56
Lower jaw length	0.15 ± 0.01	1.61	57
Caudal peduncle depth	0.11 ± 0.01	-0.78	57
Caudal peduncle length	0.28 ± 0.01	0.61	57
D_2I	0.05 ± 0.01	2.24	36
A II	0.06 ± 0.01	1.43	40
P_2I	0.08 ± 0.01	0.92	41

posteriormost point near ventral surface of bone. Eye round or slightly oval, 40.3–48.0% HL; anterodorsal rim of orbit reaching dorsal profile, projecting into profile in smaller specimens; interorbital width 8.2–10.4% SL.

Teeth small, conical, occasionally recurved; premaxilla bearing single row of teeth along anterior ⅓–¾ (usually ½) of bone. Mandibular teeth arranged along length of dentary in irregular single row, occasionally double near symphysis; larger specimens with 3–4 rows near symphysis. Vomerine teeth variable, arranged in 1–4 irregular rows. Palatine dentition occupying length of bone, arranged in simple single row or double row tapering to single row posteriorly; large specimens bearing 3–4 rows of teeth anteriorly. Tongue generally edentulous, rarely bearing isolated tooth patches on glossohyal or edges of tongue.

Opercle lacking bony spine, bearing instead 3–7 (usually 5–6) jagged, membranous projections; projections often obscured by underlying tissues. Peropercular angle produced, broadly rounded, striations radiating from inner edge, angle occasionally serrate; subopercle and interopercle occasionally serrate. Gill rakers simple, awl-like.

First dorsal fin VII (53); second dorsal fin I,9 (1), I,10 (56), 10 (1); anal fin II,8 (1), II,9 (57). D_1I moderate, 2.4–3.7% SL; D_2I, AII, P_2I short, 5.2–8.0%, 6.0–8.2%, 7.9–10.0% SL respectively.

Vertebrae 10 + 15 (44); epipleural ribs 6 (32), 7 (1), inserting on vertebrae 1–6 or 1–7 respectively; pleural ribs 8 (44), inserting on vertebrae 3–10.

Color in alcohol variable with preservation; skin frequently removed by trawling, underlying tissue pink-brown or yellow; scale pockets mottled with numerous brown-black melanophores, dorsal surfaces of body and head more heavily pigmented.

Guanine deposits frequently occurring on gill cover, ventral surface of mandible, isthmus, thoracic region, and abdomen to anus; iris black; mouth light; branchial region dark.

Description based on 58 specimens 57.0–187.5 mm SL.

Ontogenetic change. Two young specimens of *E. denticulatus* (29.2 mm SL, MCZ 48846, and 49.7 mm SL, MCZ 48847) were examined in the course of this investigation. These specimens were taken by midwater trawls made in the central North Atlantic and Gulf of Mexico and reveal that the life cycle of *E. denticulatus* includes a pelagic juvenile stage.

The pelagic young resemble adults in most respects. For example, the juveniles bear diagnostic gill raker counts and opercular ornamentation. However, slight changes in body shape are associated with growth. The 29.2 mm specimen has a more shallow body, shorter head, narrower interorbital region, and smaller eyes than demersal adults. Similar trends are present but less apparent in the larger juvenile.

Juvenile dentition patterns are basically like those of adults but involve fewer and relatively larger recurved teeth. Oral and branchial regions are light in young specimens. The latter areas darken with age.

Distribution. E. denticulatus is the only cosmopolitan species in the genus (Fig. 14). Specimens have been taken from the southwest coast of Japan, the Gulf of Mexico, and the Caribbean. In addition, the species occurs continuously from the western Mediterranean, south along the western coast of Africa to the tip of the continent. It reappears south of the Great Australian Bight and southeast of New Zealand.

Adults are generally taken by bottom trawls between 300 and 600 meters, although specimens have been captured from as shallow as 200 meters and as deep as 830 meters. Pelagic juveniles have been taken by IKMT between 130 to 145 meters and 350 to 425 meters.

Geographic variation. E. denticulatus may be divided into North Atlantic, Southern Hemisphere, and Japanese populations. North Atlantic forms include material from the Mediterranean, northeast Atlantic, Caribbean, and Gulf of Mexico. Southern Hemisphere populations contain specimens from the southeast Atlantic, Australia, and New Zealand.

Statistical analyses reveal surprisingly little divergence between North Atlantic and Southern Hemisphere specimens. Coefficients of difference for standard meristic characters are far below accepted levels for subspecies recognition (all are $\leqslant 0.53$), and regression coefficients for mensural data are virtually identical. Only maxillary lengths differ significantly at the 95% level of confidence. It is clear from the data that North Atlantic and Southern Hemisphere *E. denticulatus* do not represent separate subspecies.

Detailed analyses of the Japanese population could not be undertaken because of inadequate sampling. Only one specimen was available from the area. On the basis of this fish, the Japanese population appears closely allied to the rest of the species. With the exception of eye diameter, standard counts and measurements made on the Japanese morph fall within the 95% and 99% confidence intervals of remaining *E. denticulatus*. Eye diameter falls outside the 95% confidence interval but within the 99% confidence interval.

The similarity of *E. denticulatus* populations, despite the wide range of the species, suggests (1) there may be considerable gene flow between populations, (2) the present distribution may have been achieved only recently, or (3) evolution is occurring very slowly. Discovery of a pelagic juvenile in the mid-North Atlantic gives credence to the first hypothesis and provides a mechanism for the dispersal of a species with demersal adults such as *E. denticulatus*.

Common names. "Castagnera brüna" in Monaco (Bini, 1968).

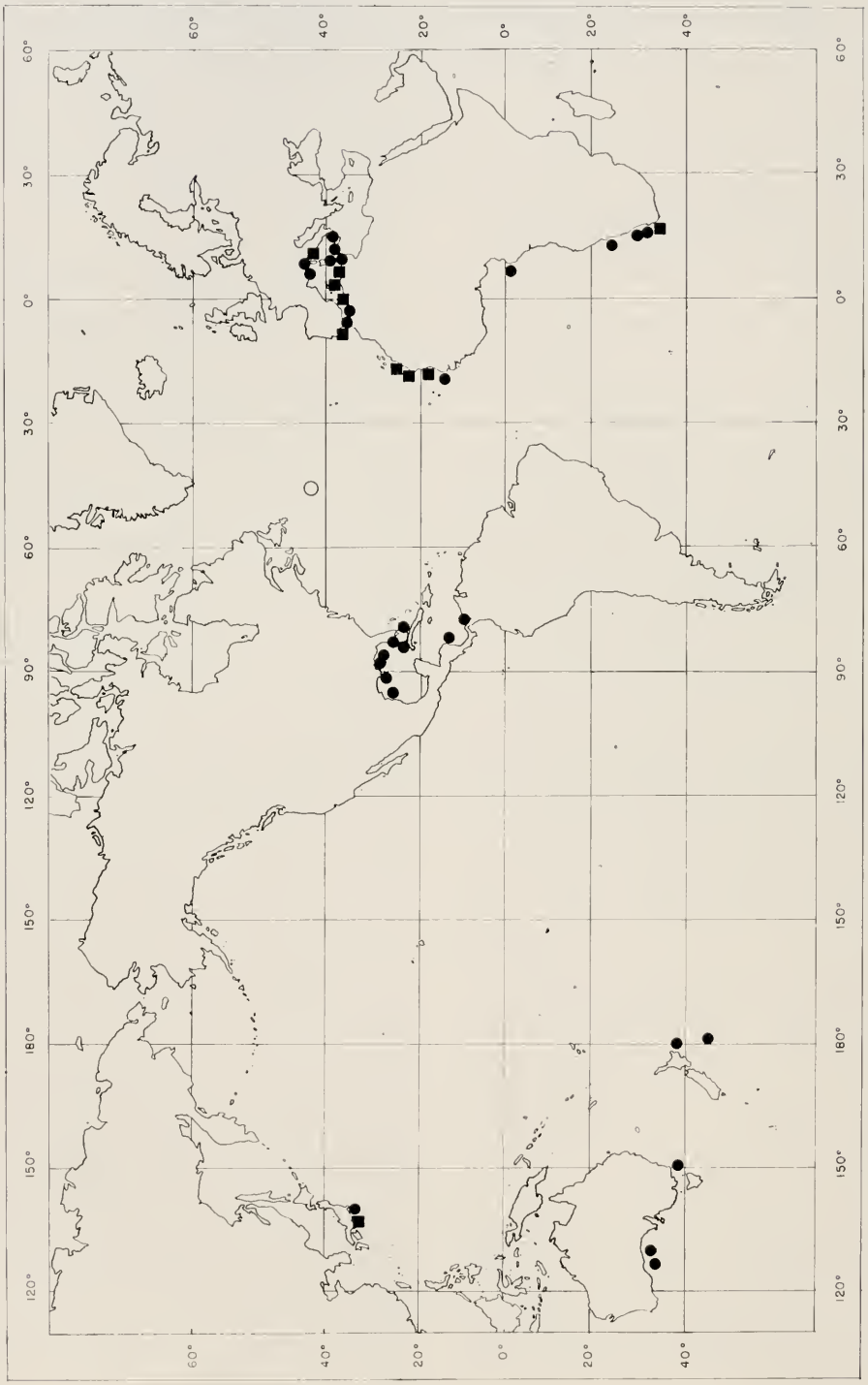

Figure 14. Distribution of *E. denticulatus*. ● individual haul of demersal adults; ○ individual haul of pelagic forms; ■ report from the literature.

Epigonus oligolepis sp. nov.
Figure 15

Holotype: One specimen, 90.8 mm SL, taken from the Straits of Florida by M/V COMBAT, Sta. 436: 21 July 1957, 1319 to 1530 hrs.; 24°13′N, 81°42′W; 300 fms., 40′ flat trawl. USNM 207718.

Paratypes: One specimen, 126.7 mm SL, M/V OREGON, Sta. 4731: 27 February 1964; 27°35′N, 92°32′W; 250–300 fms.; 40′ flat trawl. MCZ 48848.

Three specimens, 52.7–72.7 mm SL, Steamer ALBATROSS, Sta. 2643: 9 April 1886; 25°25′00″N, 79°55′15″W; 211 fms. USNM 109430.

Three specimens, 53.7–84.2 mm SL, M/V OREGON, Sta. 5043: 26 September 1964; 12°01′N, 61°53.5′W; 210–250 fms.; 40′ shrimp trawl. USNM 207719.

One specimen (cleared and stained), 62.0 mm SL, locality data identical with those of preceding lot. USNM 207720.

One specimen, 117.1 mm SL, M/V OREGON, Sta. 3741: 26 August 1962; 29°10′N, 88°01.5′ W; 300–340 fms.; 100′ flat trawl. USNM 207721.

Diagnosis. E. oligolepis is distinguished from all congeners by lateral line scale counts of 33–36 and the presence of lingual and endopterygoid teeth.

Description. Meristic values presented in Table 15; regression data for morphometric traits presented in Table 16.

Body elongate, moderately compressed; anterodorsal profile rising gradually from tip of snout to interorbital region, rising more steeply and becoming slightly convex to occiput, thereafter rising gradually to base of first dorsal fin; body depth 19.8–24.5% SL; caudal peduncle length 23.9–27.2% SL.

Head moderate to long, 34.4–43.0% SL; head height 16.6–18.8% SL; snout pointed; angle of gape moderate; lower jaw protruding beyond upper jaw. Maxilla reaching ⅖–½ eye length; posterior margin of maxilla rounded, posteriormost point between midline and ventral margin of bone. Eye round to slightly oval, 40.1–43.7% HL; anterodorsal rim of orbit reaching or projecting into dorsal profile; interorbital width 8.5–9.6% SL.

Teeth small, conical; premaxilla edentulous or bearing few teeth on anterior ⅓–⅖ of bone; mandibular teeth arranged in single or double row anteriorly, single row posteriorly; teeth covering anterior half of bone and occasionally extending along length of dentary. Vomer covered with irregular tooth patches, teeth extending posteriorly along midline of palate; palatine teeth arranged in single or multiple rows anteriorly, single row posteriorly, covering from half to entire length of bone; endopterygoid dentigerous; auxiliary tooth patches occurring between vomer, palatines, and endopterygoids; tongue dentigerous, bearing lateral and glossohyal tooth patches (Fig. 1A).

Opercular spine weak, poorly ossified, ventral to 2–6 membranous spinelets; spine and spinelets separated by moderate gap; spinelets occasionally obscured by underlying membranes. Preopercular angle rectangular or slightly produced; preopercle, subopercle and interopercle unserrated. Gill rakers simple, awl-like.

First dorsal fin VII (10); second dorsal fin I,10 (10); anal fin II,8 (1), II,9 (9). Fin spines moderate; D_1I 2.7–4.0% SL; D_2I 10.9–12.1% SL; AII 10.3–12.2% SL; P_2I 11.0–13.6% SL.

Vertebrae 10 + 15 (10), epipleural ribs 7 (4), 8 (1), inserting on vertebrae 1–7 or 1–8 respectively; pleural ribs 7 (10), inserting on vertebrae 3–9.

Color in alcohol variable with preservation; specimens frequently abraded revealing underlying pale yellow or pink-purple tissue. Recently collected specimens bear scale pockets mottled with numerous melanophores; dorsal surfaces of head and trunk more heavily pigmented; iris black. Specimens from old collections devoid of melanin, bearing silver on opercular region, isthmus, thoracic region, and abdomen to anus; iris silver. Mouth light, dotted with brown or black melanophores; branchial region light in small specimens, darkening with age.

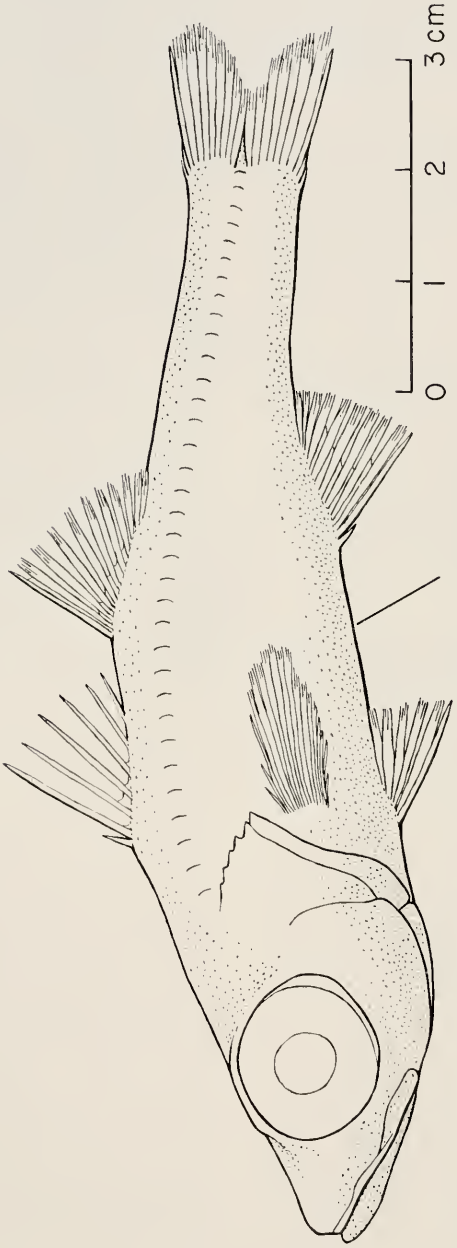

Figure 15. *Epigonus oligolepis*, HOLOTYPE, 90.8 mm SL, USNM 207718.

Table 15. *Epigonus oligolepis* meristic data. $\overline{X}$ = mean; SD = standard deviation; n = number of specimens.

	$\overline{X}$	Range	SD	n
Pectoral fin rays	17.20	16–18	0.79	10
Gill rakers	30.50	29–31	0.71	10
Lateral line scales	34.70	33–36	1.06	10
Pyloric caeca	8.83	8–10	0.75	6

Table 16. *Epigonus oligolepis* regression data. b = regression coefficient ± 95% confidence interval; a = Y intercept; n = number of specimens. All regressions on SL.

	b	a	n
HL	0.36 ± 0.11	0.88	7
Body depth	0.26 ± 0.02	−2.45	10
Head height	0.21 ± 0.06	−2.56	5
Eye diameter	0.15 ± 0.03	0.48	9
Snout length	0.08 ± 0.03	0.97	5
Interorbital width	0.10 ± 0.01	−0.51	9
Maxillary length	0.18 ± 0.02	−0.92	6
Lower jaw length	0.17 ± 0.02	1.45	10
Caudal peduncle depth	0.11 ± 0.02	−1.20	10
Caudal peduncle length	0.26 ± 0.04	0.58	9
D_2 I	0.13 ± 0.01	−1.07	6
AII	0.12 ± 0.02	−0.33	10
P_2 I	0.12 ± 0.03	0.13	9

Description based on 10 specimens 53.7–126.7 mm SL.

Ontogenetic change. Two juvenile *E. oligolepis* (32.0–32.2 mm SL, USNM 207722) were taken by bottom trawls from the Gulf of Mexico. These specimens exhibit many traits characteristic of adult forms but differ in head shape, meristics, and dentition. Unlike adults, young *E. oligolepis* have smaller eyes (38.2–39.4% HL) and wider interorbital regions (10.4% SL). Dorsal fin and gill raker counts are reduced to VI–I,10 and 26 respectively. Premaxillary, mandibular, and lingual tooth patterns are similar to those of mature individuals, but dentition associated with

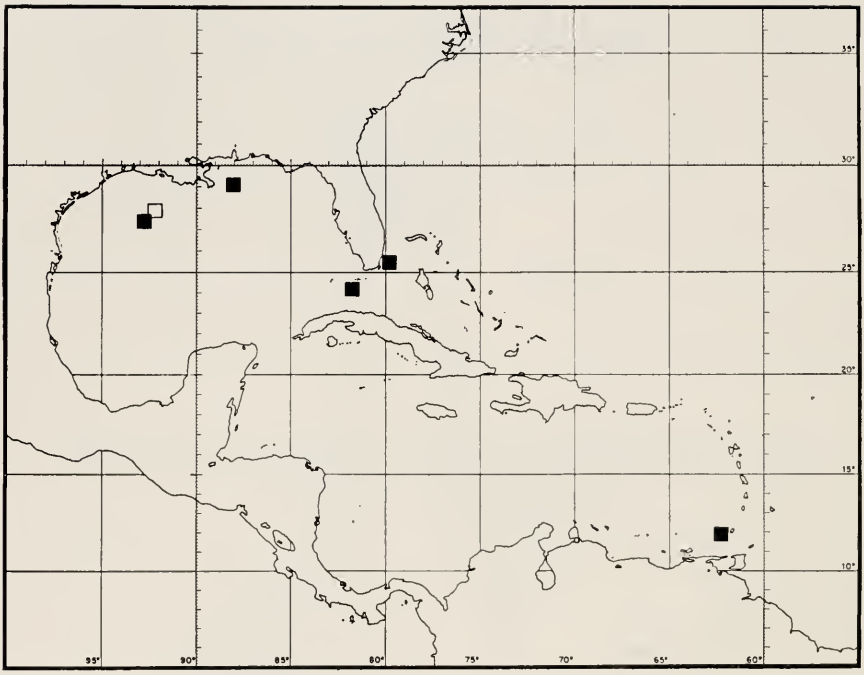

Figure 16. Distribution of *E. oligolepis*. ■ individual haul of demersal adults; □ individual haul of demersal juveniles.

the roof of the mouth is strongly reduced. Vomers and palatines are edentulous or bear 1–4 teeth; auxiliary tooth patches have not developed. Endopterygoid teeth are present but few in number, relatively long, and medially recurved.

Distribution. E. oligolepis is endemic to the Gulf of Mexico-Caribbean region (Fig. 16). Specimens have been taken by bottom trawls between 380 and 660 meters.

Remarks. The type specimens of *E. oligolepis* exhibit two seemingly disparate color patterns. One lot, taken in 1886 by the ALBATROSS, is devoid of melanin but bears extensive guanine deposits. Remaining fish, all more recently collected, bear no silver but are dotted with numerous melanophores. These differences are artifacts of preservation.

Specimens collected by early workers were generally placed directly into ethanol, while material obtained today is fixed in 10 percent formalin (Hubbs and Lagler, 1958: 16–17). When ethanol is used as a fixative, it leaches out melanins but does not affect guanine deposits. Specimens become pale, but silver pigment is retained. Formalin has the opposite effect; it blackens melanophores but destroys guanine crystals. The appearance of preserved specimens is thus dependent on fixative composition, concentration, and immersion time. An alcohol-formalin mixture containing one tablespoon of full strength formalin per two gallons of 65–75 percent ethanol might be used instead of conventional fixatives to preserve both guanine and melanin deposits (Myers, personal communication).

Etymology. Oligolepis (Greek), few scales, from *oligos*, few, and *lepis*, scale; a noun in apposition, refers to the reduced number of lateral line scales characterizing the species.

Common names. None.

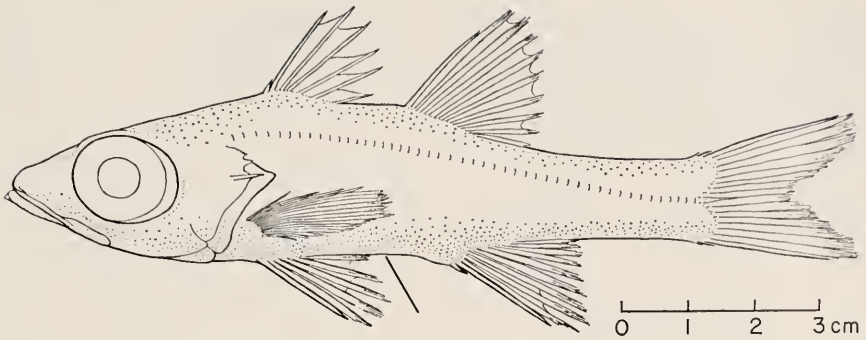

Figure 17. *Epigonus trewavasae*, 98.6 mm SL, USNM 207723.

Epigonus trewavasae Poll, 1954
Figure 17

Glossamia pandionis, Lozano (not Goode and Bean, 1881), 1934: 89; Navarro, 1942: 202; Navarro et al., 1943: 136, plate XXII, fig. A.

Epigonus trewavasae Poll, 1954: 91, fig. 27 (original description; NOORDENDE III Sta. 52, 06°08′S, 11°30′E, 280–290 m; holotype examined, IRSN 209).

Epigonus pandionis, Maurin (not Goode and Bean, 1881), 1968: 69, fig. 36.

Diagnosis. *E. trewavasae* is most likely to be confused with *E. robustus*, *E. lenimen*, *E. crassicaudus*, and *E. pectinifer*. It is distinguished from the first three species by vertebral counts of 10 + 15 and the presence of glossohyal and lateral lingual teeth. The fourth form, *E. pectinifer*, bears only glossohyal teeth or a totally edentulous tongue. *E. trewavasae* may be further differentiated from *E. pectinifer* on the basis of the former's 30–35 awl-like gill rakers and long, pungent D_2I and AII (12.7–16.5% SL, 13.8–16.8% SL respectively). *E. trewavasae* is unlike remaining congeners because it bears a pungent, bony opercular spine, second dorsal fin counts of I,9, and pectoral fin counts of 16–18.

Description. Meristic values presented in Table 17; regression data for morphometric traits presented in Table 18.

Body elongate; anterodorsal profile flat, rising without interruption from snout to base of first dorsal fin; body moderate to deep, 23.1–27.0% SL; caudal peduncle length 24.3–27.5% SL.

Head length 33.7–38.1% SL; head height 16.6–18.7% SL; snout pointed; angle of gape small to moderate; lower jaw protruding beyond upper jaw, bearing two nubs on anterior surface of mandible. Maxilla reaching slightly less than ½ eye length; posterior margin of maxilla narrow, rounded, or bearing posteriormost point near midline of bone; short, pungent mustache-like process projecting from posteroventral surface of maxillary head. Eye round, slightly oval in younger specimens, 41.1–49.1% HL; anterodorsal rim of orbit reaching profile; interorbital width 8.8–10.8% SL.

Dentition variable with age (see Ontogenetic change); teeth conical, small, frequently microscopic, present on premaxillae, mandibles, and vomer; palatines occasionally edentulous; tongue bearing lateral and glossohyal tooth patches.

Opercular spine pungent, bony, surmounted by 2–3 horny spinelets; spine and spinelets separated by large gap; spinelets often obscured by underlying opercular membranes. Preopercular angle narrowly produced, unserrated or bearing serrations on angle and ventral surface of bone; interopercle and subopercle unserrated or weakly serrated. Gill rakers simple, awl-like.

First dorsal fin VII (14); second dorsal fin I,9 (13), I,10 (1); anal fin II,9 (14); D_1I moderate, 2.4–3.2% SL; D_2I, AII, P_2I,

TABLE 17. *EPIGONUS TREWAVASAE* MERISTIC DATA. $\overline{X}$ = MEAN; SD = STANDARD DEVIATION; n = NUMBER OF SPECIMENS.

	$\overline{X}$	Range	SD	n
Pectoral fin rays	17.54	16–18	0.66	13
Gill rakers	33.15	30–35	1.46	13
Lateral line scales	47.69	47–49	0.75	13
Pyloric caeca	7.00	6– 8	0.60	12

TABLE 18. *EPIGONUS TREWAVASAE* REGRESSION DATA. b = REGRESSION COEFFICIENT ± 95% CONFIDENCE INTERVAL; a = Y INTERCEPT; n = NUMBER OF SPECIMENS. ALL REGRESSIONS ON SL.

	b	a	n
HL	0.38 ± 0.03	−2.03	13
Body depth	0.29 ± 0.02	−4.43	12
Head height	0.19 ± 0.01	−1.26	12
Eye diameter	0.17 ± 0.02	−0.49	13
Snout length	0.07 ± 0.02	1.19	13
Interorbital width	0.09 ± 0.01	1.41	13
Maxillary length	0.15 ± 0.02	0.69	13
Lower jaw length	0.16 ± 0.01	0.39	13
Caudal peduncle depth	0.13 ± 0.01	−1.79	13
Caudal peduncle length	0.26 ± 0.02	−0.08	13
D_2 I	0.15 ± 0.03	−0.32	12
AII	0.18 ± 0.03	−0.65	11
P_2 I	0.14 ± 0.01	0.36	13

long, pungent, 12.7–16.5%, 13.8–16.8%, 13.8–16.2% SL respectively.

Vertebrae 10 + 15 (12); epipleural ribs 6 (9), 7 (2), inserting on vertebrae 1–6 or 1–7 respectively; pleural ribs 7 (8), 8 (4), inserting on vertebrae 3–9 or 3–10 respectively.

Color variable with preservation; specimens abraded, revealing underlying yellow to yellow-pink tissue; fin membranes dark; scale pockets covered with dense brown or black melanophores; dorsal surface of trunk more heavily pigmented than ventral; opercles brown, black, or slate gray; guanine deposits occurring occasionally on opercular region and from isthmus to bases of paired fins; iris black with silver highlights; mouth light; branchial re-

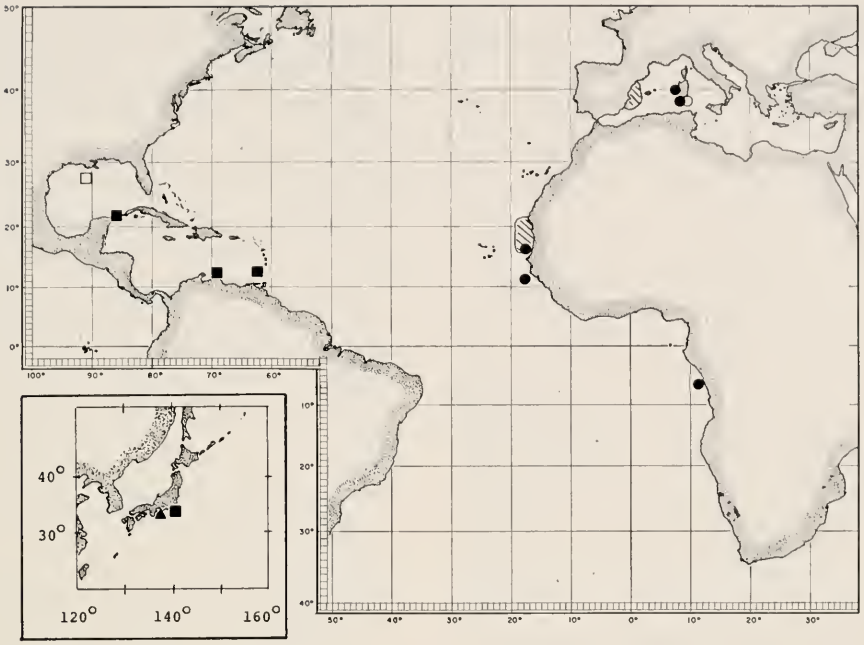

Figure 18. Distributions of *E. trewavasae* and *E. pectinifer*. Large map shows localities in the Atlantic; insert shows localities off Japan. *E. trewavasae:* ● individual haul of adults; ○ individual haul of juveniles; cross-hatching indicates areas of capture cited in the literature. *E. pectinifer:* ■ individual haul of adults; □ individual haul of juveniles; ▲ report from the literature.

gion light in small specimens, becoming black with age.

Description based on 13 specimens 70.9–153.9 mm SL.

Ontogenetic change. The most striking ontogenetic changes in *E. trewavasae* are associated with the development of adult tooth patterns. Large specimens bear irregular double or triple rows of premaxillary and mandibular teeth that taper to a single row posteriorly. Vomers are covered with minute conical teeth, while palatines are either edentulous or bear single to double rows of teeth.

Dentition patterns are simple in small specimens but become more complex as teeth are added during growth. A 29.8-mm juvenile lacks both premaxillary and mandibular teeth. By 70–75 mm SL teeth are present in single rows on the jaws, and by 145 mm SL adult tooth patterns prevail. As premaxillary tooth patches widen, they extend posteriorly and eventually cover the first half of the bone. Analogous expansion occurs in vomerine tooth patches.

Distribution. E. trewavasae is known from equatorial west Africa, northwest Africa, and the western Mediterranean (Fig. 18). It has been taken by bottom trawls between 200 and 600 meters.

Geographic variation. Statistical comparisons of African and Mediterranean *E. trewavasae* were not made because of small sample size. As additional material is collected, the following intraspecific differences should be examined:

(1) vomerine and palatine teeth more strongly developed in Mediterranean forms;
(2) chin nubs more strongly developed in African forms;
(3) preopercular serrations more strongly developed in Mediterranean forms.

Although the significance of these features

is unknown, they suggest that African and Mediterranean forms may represent separate subspecies.

Taxonomic notes. Pomatomichthys constanciae Giglioli, 1880 may be a synonym of *E. trewavasae* Poll, 1954. See *E. telescopus*: Taxonomic notes, for a discussion of this possibility.

Remarks. Dieuzeide (1950: 104–105) reported that specimens designated as *Glossamia pandionis* by Lozano (1934) and Navarro et al. (1943) were actually misidentified *E. denticulatus*. This is incorrect. Lozano's report is based on a single specimen (131 mm total length) taken from the Catillian coast. Among the characters cited for this fish are dorsal fin counts of VII–I,9, pectoral counts of 16, and an AII subequal to the eye diameter (p. 89). All of these are characters diagnostic of *E. trewavasae*. *E. denticulatus* bears 10 rays in the second dorsal fin, 18–20 pectoral rays, and an AII equalling half the eye diameter.

Navarro et al.'s specimens also appear to be *E. trewavasae*. Although no description is provided, the account includes a photograph (plate XXII, fig. A) that shows the fish have deep bodies, pungent opercular spines, and long D_2I, AII, and P_2I's. All of these features are characteristic of *E. trewavasae*.

More recently, Maurin (1968) mistook *E. trewavasae* for *E. pandionis*. Proportional measurements of body depth, head height, AII, and P_2I made on Maurin's figure 36 (p. 69) fall within ranges characteristic of *E. trewavasae*; however, published gill raker counts of 28–30 (p. 70) are lower than expected.

Common names. None.

Epigonus pectinifer sp. nov.
Figure 19

Holotype: A 114.3-mm SL specimen taken from the Caribbean west of Grenada by M/V OREGON, Sta. 5043: 26 September 1964, 12°01′N, 61°53.5′W, 210–250 fms., 40′ shrimp trawl. USNM 207725.

Paratypes: One specimen, 97.4 mm SL, 16 September 1964, Suruga Bay, commercial trawl. ABE 64–2085.

One specimen, 100.6 mm SL, 14–31 October 1964, Suruga Bay, commercial trawl. ABE 64–2245.

One specimen, 99.8 mm SL, 14–31 October 1964, Suruga Bay, commercial trawl. ABE 64–2248.

Two specimens, 95.2–117.1 mm SL, station data identical with those of holotype. MCZ 48850.

One specimen (cleared and stained), 108.1 mm SL, station data identical with those of holotype. MCZ 48851.

One specimen, 94.8 mm SL, R/V PILLSBURY, Sta. P–582: 23 May 1967; 21°10′N, 86°18′W; 250–155 fms.; 10′ otter trawl. UMML 30378.

One specimen, 111.2 mm SL, M/V OREGON, Sta. 4405: 27 September 1963; 11°53′N, 69°28′W; 215 fms.; 40′ flat trawl. USNM 207726.

Ten specimens, 101.8–120.6 mm SL, station data identical with those of holotype. USNM 207727.

Nine specimens 81.5–118.9 mm SL, station data identical with those of holotype. USNM 207728.

Two specimens (cleared and stained), 94.8–98 mm SL, station data identical with those of holotype. USNM 207729.

Epigonus robustus, Matsubara (not Barnard, 1927), 1936: 121, fig. 1B; Kamohara, 1952: 37.

Diagnosis. E. pectinifer is characterized by comb-like gill rakers on the lower half of the first gill arch. This feature, together with glossohyal dentition (present in most specimens) and vertebral counts of 10 + 15, differentiate *E. pectinifer* from *E. robustus*, *E. lenimen*, and *E. crassicaudus*. *E. pectinifer* most closely resembles *E. trewavasae* but is distinguished by less extensive lingual dentition, fewer gill rakers (26–30), and shorter D_2I and AII (11.2–12.7% SL and 11.9–14.0% SL respectively). *E. pectinifer* may be separated from remaining congeners by its pungent, bony opercular spine, second dorsal fin counts of I,9, and pectoral fin counts of 15–18.

Description. Meristic values presented in Table 19; regression data for morphometric traits presented in Table 20.

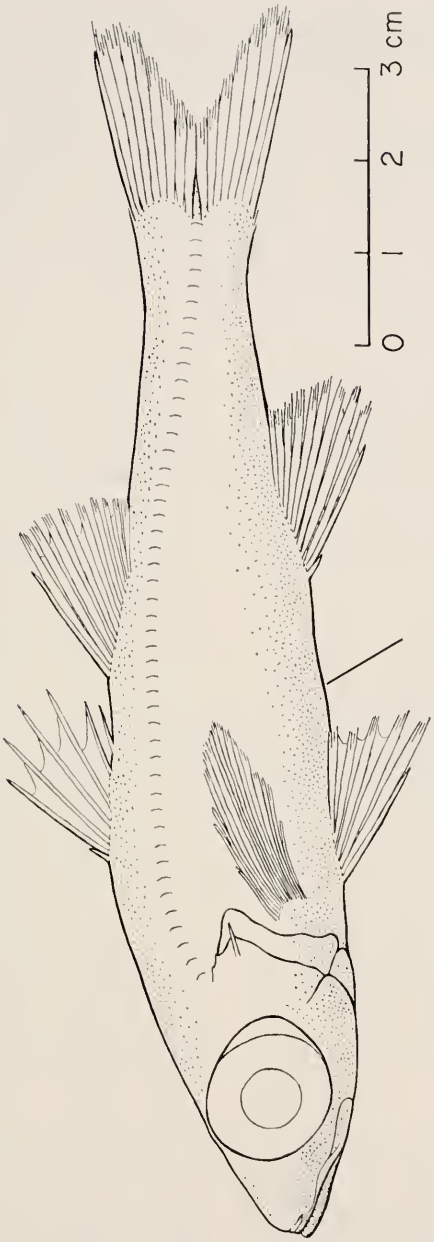

Figure 19. *Epigonus pectiniter*, PARATYPE, 111.4 mm SL, USNM 207727.

Table 19. *Epigonus pectinifer* meristic data. $\overline{X}$ = mean; SD = standard deviation; n = number of specimens.

	$\overline{X}$	Range	SD	n
Pectoral fin rays	16.03	15–18	0.57	29
Gill rakers	27.59	26–30	0.98	29
Lateral line scales	48.14	47–49	0.58	29
Pyloric caeca	6.10	5–7	0.41	29

Table 20. *Epigonus pectinifer* regression data. b = regression coefficient ± 95% confidence interval; a = Y intercept; n = number of specimens. All regressions on SL.

	b	a	n
HL	0.35 ± 0.05	−2.21	27
Body depth	0.28 ± 0.03	−4.95	28
Head height	0.18 ± 0.03	−2.83	19
Eye diameter	0.17 ± 0.03	−3.18	28
Snout length	0.09 ± 0.03	0.03	26
Interorbital width	0.10 ± 0.03	−1.84	28
Maxillary length	0.17 ± 0.04	−2.10	26
Lower jaw length	0.15 ± 0.03	0.55	28
Caudal peduncle depth	0.84 ± 0.03	1.88	28
Caudal peduncle length	0.27 ± 0.04	−0.22	28
D_2 I	0.11 ± 0.02	0.62	24
A II	0.12 ± 0.02	0.32	24
P_2 I	0.11 ± 0.02	1.30	28

Body elongate; anterodorsal profile flat or slightly convex, rising without interruption from snout to base of first dorsal fin; body depth 21.1–24.6% SL; caudal peduncle narrow, length 25.1–28.7% SL.

Head short to moderate, 31.3–35.7% SL, shallow, 14.2–16.9% SL; snout wide, pointed; angle of gape small; lower jaw protruding slightly beyond upper jaw; nubs at anterior end of mandible paired, barely discernible, or absent. Maxilla reaching ⅛–½ eye length, posterior margin narrow, rounded, or bearing posteriormost point near midline of bone; short, pungent, mustache-like process projecting from posteroventral surface of maxillary head. Eye round or slightly oval, 38.7–45.4% HL; anterodorsal rim of orbit not

reaching profile; interorbital width 7.7–9.4% SL.

Teeth small, conical; premaxilla edentulous or bearing teeth anteriorly; when present, teeth 1–15, arranged in single row. Mandibular teeth covering all or part of dentary, arranged in single row. Vomerine teeth strong, arranged in tightly packed oval patch. Palatines edentulous or bearing teeth anteriorly; when present, teeth 1–6, arranged in single row; tongue with glossohyal teeth, rarely edentulous.

Opercular spine pungent, bony, ventral to 2–3 horny spinelets; spine and spinelets separated by large gap; spinelets occasionally obscured by underlying membranes. Preopercular angle narrowly produced, serrated; subopercle and interopercle unserrated or weakly serrated. Gill rakers pectinate, bearing nub-like projections proximally along mesial surfaces (Fig. 1C); pectinate structure variable in extent, most prominent on ventral portions of gill arch.

First dorsal fin VII (28); second dorsal fin I,9 (29); anal fin II,9 (29); D_1I short, 1.6–2.8% SL; D_2I moderate, 11.2–12.7% SL; AII, P_2I, 11.9–14.0% SL.

Vertebrae 10 + 15 (29); epipleural ribs 6 (17), 7 (13), inserting on vertebrae 1–6 or 1–7 respectively; pleural ribs 8 (29), inserting on vertebrae 3–10.

Color in alcohol brown-black; fin membranes black; scale pockets covered with densely packed melanophores; skin often abraded, revealing underlying yellow-pink tissue; iris black; branchial region white to dark gray; mouth light.

Description based on 30 specimens 81.5–120.6 mm SL.

Ontogenetic change. A 33.8-mm *E. pectinifer* was taken by bottom trawl in the Gulf of Mexico (USNM 207731). The specimen appears similar to adults and provides little evidence of ontogenetic change. The major difference is the presence of six rather than seven first dorsal fin spines.

Distribution. E. pectinifer is known from the Caribbean Sea, Gulf of Mexico, and eastern coast of Japan (Fig. 18). Specimens were taken between 280 and 550 meters.

Geographic variation. Definitive comparisons of Japanese and American *E. pectinifer* were not undertaken, because only three oriental specimens were available for study. The latter forms were, however, individually compared with American fish. The analyses revealed virtually no differences between the populations aside from a slight tendency toward broader caudal peduncles and shorter maxillae and mandibles by the Japanese specimens.

Remarks. A teratological specimen of *E. pectinifer* was taken from the Yucatan Channel (109 mm SL, UMML 30379). The fish was captured at depths characteristic of *E. pectinifer* and bears diagnostic traits such as 27 gill rakers (many are pectinate), VII + I dorsal fin spines, 16 pectoral fin rays, and 10 + 15 vertebrae. The tongue is edentulous. Unlike the condition in typical forms, opercles are not fully ossified and lack spines and spinelets. Similarly, the lateral line is incomplete on the right side and bears only 43 pored scales on the left. Other differences include enlarged teeth and chin nubs, 10 rather than 9 dorsal rays, and 8 rather than 5–7 pyloric caeca.

The aberrant specimen was not considered in preparing the species description.

Etymology. Pectinifer (Latin), comb-bearer, from *pecten*, comb, and *ferare*, to bear; a noun in apposition, refers to the comb-like gill rakers characterizing this species.

Common names. None.

Epigonus robustus (Barnard, 1927)
Figure 20

Epigonus macrops Gilchrist and von Bonde, 1924: 14, plate I, fig. 3 (original description; S.S. PICKLE Sta. 344, 30°12′00″S, 14°25′00″E, 510 fms.; Sta. 347, 31°58′00″S, 16°00′00″E, 670 fms.; syntype examined, RUSI 669; name suppressed, junior homonym of *Oxyodon macrops* Brauer, 1906); Barnard, 1927: 523; Smith, 1961: 377, fig. 2.

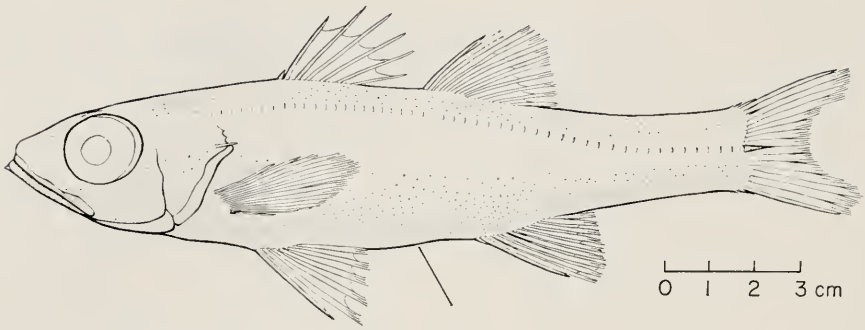

Figure 20. *Epigonus robustus*, 154.6 mm SL, LACM 11449-7.

Parahynnodus robustus Barnard, 1927: 525, plate XXII, fig. 4 (original description; off Cape Point, 460 fms.; holotype in poor condition, not examined, SAM 13080).
Hynnodus robustus Smith, 1949b: 210, fig. 495.

Diagnosis. *E. robustus* strongly resembles *E. pectinifer*, *E. trewavasae*, and *E. lenimen*. It may be distinguished from the former two species by the absence of lingual teeth. In addition, unlike *E. pectinifer*, it has awl-like gill rakers. *E. robustus* differs from *E. lenimen* by having a narrow interorbital region (6.5–8.2% SL), short D_2I (10.0–12.6% SL) and short AII (9.2–13.3% SL). *E. robustus* may be distinguished from *E. crassicaudus* by the former's short head (28.0–34.0% SL) and shallow body (20.3–24.6% SL). It differs from remaining congeners by bearing a pungent, bony opercular spine, vertebral count of 11 + 14, and nine rays in the second dorsal fin.

Description. Meristic values presented in Table 21; regression data for morphometric traits presented in Table 22.

Body elongate, moderately compressed; anterodorsal profile weakly convex, rising without interruption from tip of snout to base of first dorsal fin; body depth 20.3–24.6% SL; caudal peduncle moderate to long, 25.3–30.7% SL.

Head short, shallow, length 28.0–34.0% SL, height 14.8–16.3% SL; snout short, pointed; angle of gape moderate to large; lower jaw protruding beyond upper jaw, bearing two nubs of variable prominence on anterior surface of mandible. Maxilla reaching ⅓–½ eye length; posterior margin of maxilla narrow, rounded or bearing posteriormost point near midline of bone; small, weak mustache-like process projecting from posteroventral surface of maxillary head. Eye round to oval, small, 37.4–42.4% HL; anterodorsal rim of orbit not reaching dorsal profile; interorbital region narrow, 6.5–8.2% SL.

Teeth small, conical; premaxilla edentulous or bearing single row of teeth on anterior half of bone; mandibular dentition covering all or part of dentary, arranged in double row anteriorly, tapering to single row posteriorly; vomer bearing 1–6 irregular rows of teeth; palatines edentulous or bearing teeth on anterior half of bone; tongue edentulous.

Opercular spine pungent, bony, ventral to 2–3 membranous or horny spinelets; spine separated from spinelets by wide gap; spinelets often obscured by underlying membranes. Preopercular angle not produced, serrations on posterior and/or ventral surfaces of bone rarely absent; subopercle and interopercle serrated. Gill rakers simple, awl-like.

First dorsal fin VI (1), VII (27), VIII (1); second dorsal fin I, 9 (28), II, 8 (1); anal fin II, 9 (29). D_1I short, 1.4–2.5% SL; D_2I, AII, P_2I moderate to long, 10.0–12.6%, 9.2–13.3%, 11.7–15.3% SL respectively.

Vertebrae 11 + 14 (29); epipleural ribs

Table 21. *Epigonus robustus* meristic data. $\overline{X}$ = mean; SD = standard deviation; n = number of specimens.

	$\overline{X}$	Range	SD	n
Pectoral fin rays	16.79	16–18	0.55	29
Gill rakers	31.68	30–33	0.93	29
Lateral line scales	48.76	47–50	0.91	29
Pyloric caeca	6.36	5– 8	0.78	28

Table 22. *Epigonus robustus* regression data. b = regression coefficient ± 95% confidence interval; a = Y intercept; n = number of specimens. All regressions on SL.

	b	a	n
HL	0.28 ± 0.02	5.35	28
Body depth	0.28 ± 0.02	−7.80	28
Head height	0.17 ± 0.02	−1.65	20
Eye diameter	0.11 ± 0.01	2.44	28
Snout length	0.06 ± 0.02	1.80	23
Interorbital width	0.09 ± 0.01	−1.97	28
Maxillary length	0.12 ± 0.01	2.14	24
Lower jaw length	0.14 ± 0.01	1.27	27
Caudal peduncle depth	0.13 ± 0.01	−1.69	28
Caudal peduncle length	0.25 ± 0.02	5.32	28
D_2 I	0.08 ± 0.02	5.49	21
A II	0.07 ± 0.02	8.18	15
P_2 I	0.09 ± 0.02	6.74	24

6 (2), 7 (8), inserting on vertebrae 1–6 or 1–7 respectively; pleural ribs 9 (29), inserting on vertebrae 3–11.

Color variable with preservation, pale yellow to rust brown; scale pockets outlined by small black or brown melanophores; opercular region tinged with black; iris black; mouth light, mottled with brown or black melanophores; branchial region black. Body very oily; body cavity filled with rust brown fat globules; viscera and swimbladder often completely enveloped in fat.

Description based on 29 specimens 121.1–198.0 mm SL.

Distribution. Most specimens of *E. ro-*

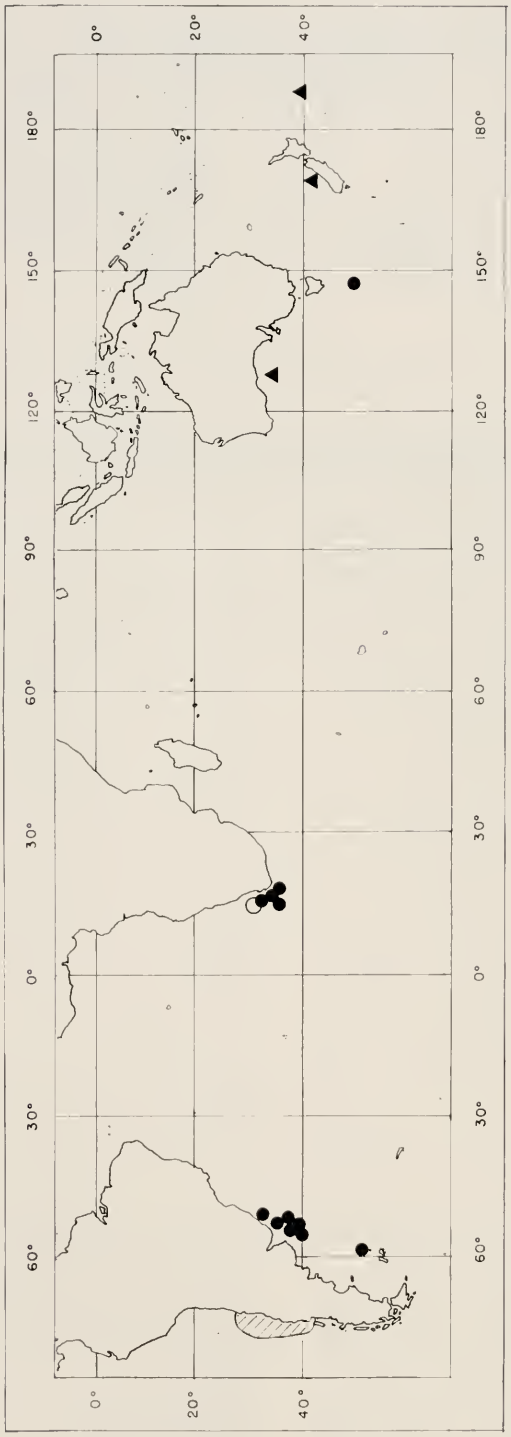

Figure 21. Distributions of *E. robustus*, *E. lenimen*, and *E. crassicaudus*. ● individual haul of *E. robustus* adults; ○ individual haul of *E. robustus* juveniles; ▲ individual haul of *E. lenimen*; cross-hatching indicates range of *E. crassicaudus*.

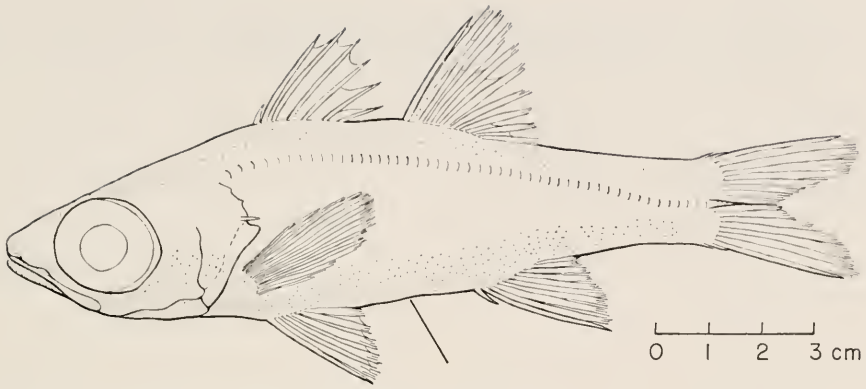

Figure 22. *Epigonus lenimen*, 139.0 mm SL, UZM P45165.

bustus have been taken by bottom trawls between 800 and 1225 meters off southeastern South America, South Africa, and Australia (see Fig. 21). One specimen (ISH 430/71) was taken by a deep pelagic trawl.

Geographic variation. No investigation was undertaken because insufficient material was available from South Africa and Australia.

Taxonomic notes. Epigonus macrops Gilchrist and von Bonde, 1924 was described from two syntypes; the larger was 198 mm (SL?). These specimens, together with many others collected by the Fisheries and Marine Biological Survey, were lost while being transferred to the South African Museum. A portion of the material was subsequently rediscovered at Rhodes University, Grahamstown. From the contents Smith (1961: 378) described a specimen that he believed to be "Gilchrist and von Bonde's type of *macrops* from 600 fathoms off St. Helena Bay." This fish was re-examined during the present study.

Smith's specimen measures 162.2 mm SL and thus cannot be the larger syntype; however, it conforms to the descriptions and proportions supplied by Gilchrist and von Bonde and probably represents the smaller type for which no length was published.

An unusual aspect of the syntypes is that the locations at which they were captured will never be precisely known. The specimens were taken at different stations. Although these are recorded in both the original description of *E. macrops* and in the 1921 report of the Fisheries and Marine Biological Survey (Gilchrist, 1922), neither account specifies which data are associated with which syntype.

Common names. None.

Epigonus lenimen (Whitley, 1935)
Figure 22

Scepterias lenimen Whitley (in part), 1935: 230 (original description; Great Australian Bight: south from Eucla, 350–450 fms.; holotype examined, AM E3368); Whitley, 1940: 420, fig. 33; Whitley (in part), 1968: 56.
Epigonus lenimen Scott, 1962: 191, 1 fig.

Diagnosis. E. lenimen is distinguished from *E. robustus* and *E. crassicaudus* by its broad interorbital region (8.7–10.2% SL), long D_2I (14.9–18.7% SL), and large eyes (40.0–51.1% HL). It is further differentiated from *E. crassicaudus* by shorter head lengths (32.7–36.6% SL) and shallower head heights (16.2–18.8% SL). *E. lenimen* lacks lingual teeth but has 11 + 14 vertebrae and thus may be distinguished from *E. trewavasae* and *E. pectinifer*. Unlike remaining congeners, *E. lenimen* bears a pungent, bony opercular spine, nine second dorsal fin rays, and 16–18 pectoral fin rays.

Table 23. *Epigonus lenimen* meristic data. $\overline{X}$ = mean; SD = standard deviation; n = number of specimens.

	$\overline{X}$	Range	SD	n
Pectoral fin rays	16.96	16–18	0.58	28
Gill rakers	30.29	28–34	1.27	24
Lateral line scales	48.12	47–50	0.91	26
Pyloric caeca	7.33	7–9	0.56	24

Table 24. *Epigonus lenimen* regression data. b = regression coefficient ± 95% confidence interval; a = Y intercept; n = number of specimens. All regressions on SL.

	b	a	n
HL	0.35 ± 0.01	−0.12	29
Body depth	0.28 ± 0.02	−3.32	27
Head height	0.19 ± 0.01	−1.08	27
Eye diameter	0.18 ± 0.01	−1.60	27
Snout length	0.08 ± 0.01	0.31	27
Interorbital width	0.10 ± 0.01	−0.59	26
Maxillary length	0.16 ± 0.01	0.08	27
Lower jaw length	0.16 ± 0.01	0.55	28
Caudal peduncle depth	0.11 ± 0.01	−0.14	28
Caudal peduncle length	0.24 ± 0.02	2.26	26
D_2 I	0.17 ± 0.02	−0.79	18
A II	0.21 ± 0.02	−2.36	22
P_2 I	0.19 ± 0.01	−2.13	28

Description. Meristic values presented in Table 23; regression data for morphometric traits presented in Table 24.

Body elongate; anterodorsal profile flat or weakly concave, rising without interruption to first dorsal fin, more steeply inclined behind occiput in large specimens; body moderate to deep, 21.5–27.5% SL; caudal peduncle moderate to long, 23.6–29.3% SL. Head length 32.7–36.6% SL; head height 16.2–18.8% SL; snout moderately pointed; angle of gape moderate, variable with age; lower jaw protruding slightly or not at all; no prominent nubs on anterior surface of mandible. Maxilla reaching ⅓–½ eye length; posterior margin

Table 25. Comparison of *E. lenimen* paratypes with specimens of *E. lenimen* and *E. denticulatus*. Paratype meristics reported as value, followed in parentheses by number of specimens exhibiting that value. Ratios are expressed as percentages.

	E. lenimen	E. lenimen paratypes	E. denticulatus
Dorsal fin rays	8 — 9	9(1), 10(11)	10
Pectoral fin rays	16 — 18	19(6), 20(6)	18 — 20
Vertebrae	11 + 14	10 + 15	10 + 15
Pyloric caeca	7 — 9	10(1), 11(3) 12(7)	10 — 14
BH/SL	21.5 — 27.5	18.4 — 21.7	15.8 — 23.6
D_2 I/SL	14.9 — 18.7	6.0 — 7.6	5.3 — 8.0
A II/SL	13.0 — 20.8	6.2 — 7.1	6.0 — 8.2
P_2 I/SL	12.5 — 18.7	8.5 — 9.9	7.9 — 10.0

of maxilla narrow, rounded, or bearing posteriormost point near midline of bone; weak mustache-like process projecting from posteroventral surface of maxillary head, process occasionally absent. Eye large, oval, 40.0–51.1% HL; anterodorsal rim of orbit reaching dorsal profile; interorbital width 8.7–10.2% SL.

Teeth small, conical; premaxilla edentulous or bearing single row of teeth occupying anterior half of bone. Mandible edentulous or bearing single row of teeth occupying up to ¾ of dentary; tooth row occasionally double near symphysis. Vomer edentulous or bearing up to seventeen teeth arranged in diamond-shaped patch or in 1–3 irregular rows; palatines edentulous or bearing 1–2 teeth anteriorly; tongue edentulous.

Opercular spine pungent, bony, ventral to 1–5 (usually 2) membranous or horny spinelets; spine and spinelets separated by wide gap; spinelets frequently obscured by underlying membranes. Preopercular angle narrowly produced, occasionally serrated; subopercle and interopercle unserrated or weakly serrated. Gill rakers simple, awl-like.

First dorsal fin VII (29); second dorsal fin I,8 (1), I,9 (28); anal fin II,8 (2), II,9 (26); D_1I moderate, 2.0–4.1% SL; D_2I, AII long, 14.9–18.7%, 13.0–20.8% SL respectively; P_2I moderate to long, 12.3–18.7% SL.

Vertebrae 11 + 14 (29); epipleural ribs 6 (6), 7 (12), 8 (2), inserting on vertebrae 1–6, 1–7, or 1–8 respectively; pleural ribs 9 (28), inserting on vertebrae 3–11.

Color in alcohol variable; skin often abraded, revealing underlying pale pink-yellow tissue; fin membranes and scale pockets mottled with numerous black melanophores; head, opercular region, and fin bases deep rust brown. Guanine deposits variable, occurring on ventral portions of opercular region, isthmus, pectoral and pelvic fin bases, and abdomen to anus; silver chromatophores on dorsal, anal, pectoral, or pelvic fin rays; iris black with silver highlights; mouth light, dotted with melanophores; branchial region light in small specimens, blackening with age.

Description based on 32 specimens 40.0–147.8 mm SL.

Distribution. E. lenimen is known from three localities (Fig. 21). The holotype

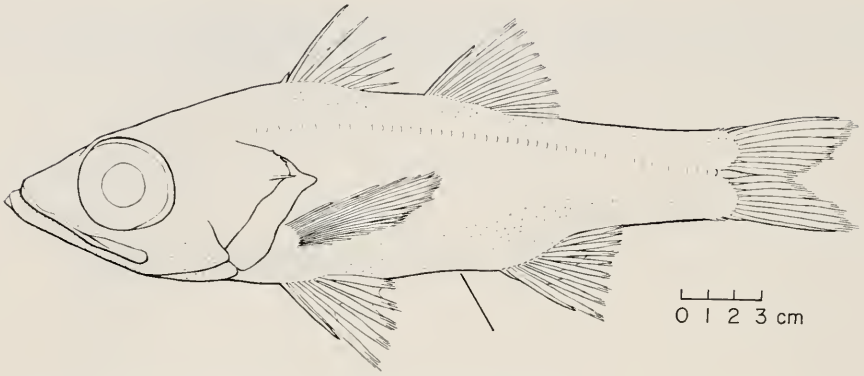

Figure 23. *Epigonus crassicaudus*, 259.0 mm SL, MCZ 48855.

was taken south of Australia between 622 and 823 meters. Remaining specimens were taken off New Zealand between 530 and 660 meters.

Taxonomic notes. Although G. P. Whitley was the first to describe *E. lenimen* (1935), inaccuracies in his papers have produced several problems. The most serious involve the type series and type locality of the species.

The original description of *E. lenimen* designates a holotype and nine paratypes. A figure of the new form was not included but was published in a subsequent paper (Whitley, 1940: fig. 33). Both the description and the illustration were based exclusively on the holotype. Whitley realized that the paratypes were different from the holotype but considered them to be poorly preserved specimens (Whitley, 1935: 320).

A re-examination of the type series reveals that the paratypes are not conspecific with the holotype. They are, instead, members of *E. denticulatus*. As is shown in Table 25, counts and measurements from the paratypes always fall within ranges characteristics of *E. denticulatus*. Pectoral fin counts, vertebral number, pyloric caecum counts, and fin spine lengths are particularly noteworthy in this respect. The paratypes further resemble *E. denticulatus* by bearing dentigerous palatines and weak opercular armor. *E. lenimen*, on the other hand, is characterized by edentulous palatines and pungent opercular spines.

Confusion over the type locality stems from Whitley's 1940 paper. The locality is cited as "from 190–320 fathoms, S.W. from Eucla, Great Australian Bight [p. 420]." This contradicts the data presented in the original description: "Great Australian Bight; south from Eucla, 350 to 450 fathoms [p. 231]." The 1940 citation is extremely similar to station data listed for paratypes AM E3581–3582 in 1935 ("Great Australian Bight; SW from Eucla, 190–320 fathoms. 126° 45½′E long. [p. 231]"). In the absence of other information, it must be concluded that erroneous locality data were inserted in the 1940 publication through an editorial oversight.

The most recent taxonomic questions arise from Whitley's check list of New Zealand fishes (1968). This work includes two incorrect citations in the synonymy of *E. lenimen*. The first is based on a fish taken off the Chatham Islands and tentatively identified as *Hynnodus atherinoides* (Moreland, 1957). This specimen was later re-identified as *Grahamichthys radiatus* (Moreland, personal communication). The second misidentified specimen is a "Big-eyed Cardinal Fish" captured off Cape Palliser, New Zealand (Anonymous, 1961). This fish is actually a specimen of *E. telescopus* and is presently in the collec-

tions of the Dominion Museum (DM 3072, examined).

Common names. None.

Epigonus crassicaudus de Buen, 1959
Figure 23

Epigonus crassicaudus de Buen, 1959: 196 (original description; preabysmal zone off Valparaiso, Chile; holotype not examined, EBM 10.183).

Diagnosis. E. crassicaudus is strongly compressed. It reaches 260–270 mm SL and is the second largest species in the genus. *E. crassicaudus* may be distinguished from *E. trewavasae*, *E. pectinifer*, *E. robustus*, and *E. lenimen* by its deep head (18.9–21.2% SL) and deep body (24.3–32.0% SL). It differs from remaining congeners by bearing 9 rays in the second dorsal fin and 6–7 pyloric caeca.

Description. Meristic values presented in Table 26; regression data for morphometric traits presented in Table 27.

Body elongate, compressed; anterodorsal profile rising from tip of snout to occiput, becoming moderately convex from occiput to base of first dorsal fin. Body deep, 24.3–32.0% SL; caudal peduncle broad, moderate to short, 21.6–26.4% SL.

Head long, deep, postorbital portion greatly expanded, length 36.8–41.9% SL; height 18.9–21.2% SL; snout moderately pointed in small specimens, blunt in adults; angle of gape moderate to small; mandible long, strongly protuberant, young bearing two weak nubs on anterior surface of lower jaw. Maxilla reaching ⅓–½ eye length; posterior margin of maxilla broad, rounded or bearing posteriormost point between midline and ventral surface of bone. Eye round, small, 34.2–39.6% HL; surrounded by numerous small scale pockets; anterodorsal rim of orbit reaching dorsal profile; interorbital region narrow, 6.2–8.5% SL.

Teeth small, conical, occasionally villiform, larger in small specimens; premaxillary teeth arranged in irregular single or double rows tapering to single row posteriorly and covering from ⅓ to entire length of bone; mandibular teeth arranged in multiple rows, tapering to single row posteriorly, covering from ½ to entire length of dentary; vomer edentulous or bearing up to six irregular rows of minute teeth; palatines edentulous or bearing 1–3 teeth anteriorly; tongue edentulous.

Opercular spine pungent, bony, ventral to 3–5 flat, horny spinelets; spine separated from spinelets by narrow gap; spinelets often obscured by underlying membranes. Preopercular angle slightly produced, posterior and/or ventral surfaces serrated; subopercles and interopercles serrated. Gill rakers awl-like, short; gill filaments long.

First dorsal fin VII (22); second dorsal fin I,9 (20), I,10 (2); anal fin II,8 (1), II,9 (21); D_1I 2.0–3.6% SL; D_2I 9.8–13.2% SL; AII 10.3–14.0% SL; P_2I 13.0–15.5% SL.

Vertebrae 11 + 14 (25); epipleural ribs 6 (2), 7 (16), inserting on vertebrae 1–6 or 1–7 respectively; pleural ribs 9 (25), inserting on vertebrae 3–11.

Color in alcohol variable with preservation; skin frequently abraded, exposing underlying pink tissue and orange-rust fat deposits; skin extremely oily; fin membranes black; scale pockets mottled with numerous black melanophores; dorsal portion of body darker than ventral; forehead, snout, anterior half of mandible, and circumorbital area heavily invested with black pigment; opercles black or slate gray. Guanine deposits occasionally on opercles, isthmus, pectoral and pelvic fin bases, and abdomen to anal fin; iris variable—black, silver, or black with silver highlights; mouth and branchial region light, darkening with age.

Description based on 27 specimens 80.3–262.5 mm SL.

Ontogenetic change. Two juvenile *E. crassicaudus* (12.2 mm SL, MCZ 48857, and 21.7 mm SL, MCZ 48858) were taken off the Chilean coast by midwater trawl. Although these forms bear characteristics diagnostic of the species, they differ con-

TABLE 26. *EPIGONUS CRASSICAUDUS* MERISTIC DATA. $\overline{X}$ = MEAN; SD = STANDARD DEVIATION; n = NUMBER OF SPECIMENS.

	$\overline{X}$	Range	SD	n
Pectoral fin rays	18.05	17–19	0.58	22
Gill rakers	32.27	31–34	0.70	22
Lateral line scales	47.86	46–49	0.85	21
Pyloric caeca	6.87	6– 7	0.35	15

TABLE 27. *EPIGONUS CRASSICAUDUS* REGRESSION DATA. b = REGRESSION COEFFICIENT ± 95% CONFIDENCE INTERVAL; a = Y INTERCEPT; n = NUMBER OF SPECIMENS. ALL REGRESSIONS ON SL.

	b	a	n
HL	0.39 ± 0.02	0.47	20
Body depth	0.30 ± 0.04	−3.75	21
Head height	0.21 ± 0.02	−1.62	18
Eye diameter	0.14 ± 0.01	0.74	21
Snout length	0.08 ± 0.01	0.08	19
Interorbital width	NONLINEAR		
Maxillary length	0.17 ± 0.01	−0.49	20
Lower jaw length	0.20 ± 0.01	−1.17	22
Caudal peduncle depth	0.12 ± 0.01	−0.65	20
Caudal peduncle length	0.22 ± 0.03	4.32	20
D_2 I	0.10 ± 0.02	3.34	12
A II	0.11 ± 0.02	2.63	17
P_2 I	0.14 ± 0.01	0.05	16

siderably in appearance and habit from adults.

Most striking is the juvenile pigment pattern. Pelagic specimens are basically pale yellow with large, brown patches covering most of the caudal peduncle. Caudal peduncle rings, like those found on *E. pandionis* young, are absent, although myotomes are outlined by thin brown bands. Brown pigment extends anteriorly as a band from the caudal peduncle to the frontal region of the head. A poorly defined black stripe extends across the snout to the anterior rim of the orbit. In general, juvenile *E. crassicaudus* resemble *E. telescopus* young figured by Koefoed (1952: plate IIA).

The midwater capture of *E. crassicaudus*

juveniles suggests that the life cycle of the species includes a pelagic stage. Unfortunately, the data available are not sufficient to determine the duration of this stage.

Distribution. E. crassicaudus is endemic to the waters off central Chile (Fig. 21). Adults have been captured by bottom trawls made between 200 and 400 meters; juveniles were taken by midwater trawls fishing from 200 to 270 meters.

Common names. None.

Species *Incertae Sedis*

Microichthys coccoi Rüppell, 1852: 1 (original description; "Mare siculum"; holotype not examined, SMF 1069).

The original description of *M. coccoi* provides only a superficial account of the holotype. Subsequent papers either paraphrase Rüppell's work (*e.g.*, Canestrini, 1860; Döderlein, 1889) or are based on material not compared to the holotype (*i.e.*, Facciola, 1900; Caporaicco, 1926; Gonzales, 1946). It is questionable whether the latter specimens are conspecific with the holotype.

Most recent revisers (*e.g.*, Schultz, 1940; Norman, 1957) have synonymized *Microichthys* with *Apogon*; however, the data are inconclusive and also suggest an affinity with *Epigonus* (Fraser, 1972: 5). A reexamination of the holotype must be undertaken to clarify the status of *M. coccoi*.

A second species of *Microichthys*—*M. sanzoi* Spartà, 1950—does not appear to be an *Epigonus* on the basis of vertebral and dorsal fin counts. The only known specimen of this species has been lost (Tortonese, personal communication).

ACKNOWLEDGMENTS

This work would not have been possible without the assistance and support of numerous people. I wish to thank the following scientists and institutions for material used in this study: J. R. Paxton and D. Hoese, Australian Museum; A. W. Wheeler and G. Palmer, British Museum (Natural History); J. Randall, Bernice P. Bishop Museum; W. Eschmeyer, California Academy of Sciences; E. Bertelsen, Carlsbergfondets; J. Moreland, Dominion Museum; L. P. Woods, Field Museum of Natural History; P. Struhsaker, National Marine Fisheries Service, Honolulu; R. Raymond, Instituto de Fomento Pesquero; X. Missonne, Institut Royal des Sciences Naturelles de Belgique; G. Krefft, Institut für Seefischerei; M. M. Smith, J. L. B. Smith Institute of Ichthyology; I. Nakamura, Kyoto University; R. J. Lavenberg, Los Angeles County Museum of Natural History; M. Bauchot, Muséum National d'Histoire Naturelle; M. Poll, Musée Royal de l'Afrique Centrale; E. A. Lachner and T. H. Fraser, National Museum of Natural History; M.-L. Penrith, South African Museum; George R. Miller, Tropical Atlantic Biological Laboratory; R. S. Gaille, Texas Parks and Wildlife Department; M. Leible, Universidad Catolica de Chile; C. R. Robins, University of Miami; J. Nielsen, Universitetets Zoologiske Museum; B. Nafpaktitis, University of Southern California; T. Abe, University of Tokyo; R. Backus and J. Craddock, Woods Hole Oceanographic Institution; and C. Karrer, Zoologisches Museum, Berlin. W. Klausewitz of the Natur-Museum Senckenberg provided invaluable information on the holotype of *Microichthys coccoi*, and E. Tortonese of the Museo Civico di Storia Naturale, Genoa, answered numerous questions about problematical forms such as *Pomatomichthys constanciae* and *Microichthys sanzoi*.

I am greatly indebted to Ernst Mayr, Giles W. Mead and Karel F. Liem for their guidance, criticism, and support of my work. I am also grateful to Richard L. Haedrich for reading the manuscript and assisting in the planning of this research. Special thanks are extended to G. S. Myers for assistance with taxonomic problems.

I wish to thank the staffs of the Fish Department, Museum of Comparative Zoology, and Department of Natural Sci-

ences, Boston University, for their useful comments and practical help. Karen Greenleaf and Pat Allen typed the final draft of this manuscript.

Illustrations of eleven of the twelve species of *Epigonus* were prepared by L. Laszlo Meszoly. Jordan and Jordan's illustration of *E. fragilis* (Fig. 10) was made available through the courtesy of the Carnegie Museum.

Finally, a hearty *vielen Dank* to my wife for her patience, encouragement, and editorial assistance.

Support for this work was provided by NSF Graduate Fellowships during 1966 to 1971 and a grant from Harvard University's Committee on Evolutionary Biology (GB 7346).

LITERATURE CITED

Anonymous. 1961. Caught only 3 times before. Wellington Evening Post.

Bailey, N. T. 1959. Statistical Methods in Biology. New York: John Wiley and Sons, Inc. 200 pp.

Barnard, K. H. 1927. A monograph of the marine fishes of South Africa, Part II. Ann. South African Mus., **12**(2): 419–1065.

Bauchot, M. L., and M. Blanc. 1961. Poissons marins de l'Est Atlantique Tropical, II. Percoidei (Téléostéens Perciformes) 1ère partie. Atlantide Rep. No. 6: 65–100.

Bertolini, F. 1933. Apogonidae. Fauna e flora del Golfo di Napoli. Uova, larve e stadi giovanili di Teleostei. Pubbl. Staz. Zool. Napoli, **38**: 306–309.

Bini, G. 1968. Atlante dei Pesci delle Coste Italiane, Vol. IV. Roma: Mondo Sommerso Editrice. 163 pp.

Bleeker, P. 1876. Systema Percarum revisum. Pars I et II. Arch. Néerl. Sci., **11**: 274–340.

Brauer, A. 1906. Die Tiefsee-Fische. I. Systematischer Teil. Wiss. Ergeb. Deut. Tiefsee-Exped. "Valdivia," 1898–1899, **15**: 1–420.

Breder, C. M., and D. E. Rosen. 1966. Modes of Reproduction in Fishes. Garden City, N. Y.: Natural History Press. 941 pp.

Brown, M. E. 1957. Experimental studies on growth. *In* The Physiology of Fishes, Vol. 1, M. E. Brown (ed.). New York: Academic Press, Inc., pp. 361–400.

Buen, F. de. 1959. Notas preliminares sobre la fauna marina preabismal de Chile, con descripción de una familia de rayas, dos géneros y siete especies nuevos. Bol. Mus. Nac. Hist. Natur., **27**(3): 171–201.

Canestrini, J. 1860. Zur Systematik der Percoiden. Verh. Zool. Bot. Ver. Wien, **10**: 291–314.

Capello, F. de B. 1868. Peixes novos de Portugal e da Africa occidental e caractéres distinctivos d'outras especies já conhecidas. J. Sci. Math. Phys. Natur. Acad. Real Sci. Lisboa, **1**(2): 154–169.

Caporaicco, L. di. 1926. Il cranio de "Microichthys coccoi" Rüpp. Monit. Zool. Ital., **37**(6): 127–132.

Cligny, A. 1903. Poissons des Côtes d'Espagne et de Portugal (Océan Atlantique). Première partie. Boulogne. 30 pp.

Cocco, A. 1829. Su di alcuni nuovi pesci de' mari di Messina. Giorn. Sci. Lett. Art. Sicil., **7**(77): 138–147.

———. 1885. Indice Ittiologico del Mare di Messina. Nat. Sicil., **4**(4): 85–88.

Cuvier, G. 1828. Des pomatomes. *In* Histoire Naturelle des Poissons, Tome Second, G. Cuvier and A. Valenciennes. Paris: F. G. Levrault, pp. 169–174.

Dieuzeide, R. 1950. Sur un *Epigonus* nouveau de la Méditerranée (*Epigonus denticulatus*, nov. sp.). Bull. Sta. Aquic. Pêche Castiglione, N.S., No. 2: 89–105.

———, M. Novella, and J. Roland. 1953. Catalogue des poissons des Côtes algériennes. II. Ostéoptérygiens. Bull. Sta. Aquic. Pêche Castiglione, N.S., No. 5: 1–258.

Dixon, W. J. (ed.). 1967. BMD Biomedical Computer Programs. Univ. Calif. Publ. Automatic Computation No. 2. Berkeley: Univ. Calif. Press. 600 pp.

Döderlein, P. 1889. Manuale Ittiologico del Mediterraneo. Fascicolo IV. Palermo: Giornali di Sicilia. 188 pp.

Dons, C. 1938. Notes on fishes III. *Epigonus telescopus* (Risso), new to Norway. Det Kgl. Nor. Vidensk. Selsk. Forh., **11**(35): 141–142.

Ebina, K. 1931. Buccal incubation in the two sexes of a percoid fish, *Apogon semilineatus* T. & S. J. Imp. Fish. Inst. Tokyo, **27**(1): 19–21.

Ehrenbaum, E. 1928. Rare fishes in the North Sea. Nature (London), **121**(3053): 709.

Ekman, S. 1953. Zoogeography of the Sea. London: Sidgwick and Jackson, Ltd. 417 pp.

Facciola, L. 1900. Sul *Microichthys coccoi* Rüpp. Monit. Zool. Ital., **11**(5): 188–194.

Fowler, H. W. 1928. The fishes of Oceania. Mem. Bernice P. Bishop Mus., **10**: 1–540.

———. 1935. South African fishes received from Mr. H. W. Bell-Marley in 1935. Proc. Acad. Nat. Sci. Philadelphia, **87**: 361–408.

———. 1936. The marine fishes of West Africa

based on the collection of the American Museum Congo Expedition, 1909–1915. Bull. Amer. Mus. Nat. Hist., **70**(2): 607–1493.

———, and B. A. Bean. 1930. The fishes of the families Amiidae, Chandidae, Duleidae, and Serranidae obtained by the United States Bureau of Fisheries Steamer "Albatross" in 1907 to 1910, chiefly in the Philippine Islands and adjacent seas. Bull. U.S. Nat. Mus., **10**(100): 1–334.

Fraser, T. H. 1972. Comparative osteology of the shallow water cardinal fishes [Perciformes: Apogonidae] with reference to the systematics and evolution of the family. Ichthyol. Bull. J. L. B. Smith Inst. Ichthyol., Rhodes Univ., No. 34: 1–105.

Fuglister, F. C. 1960. Atlantic Ocean atlas of temperature and salinity profiles and data from the International Geophysical Year of 1957–1958. Woods Hole Oceanogr. Inst. Atlas Ser., 1: 1–209.

Gall, J. le. 1931. *Epigonus telescopus* Risso 1810. *In* Faune Ichthyologique. Copenhagen, Conseil Permanent International pour l' Exploration de la Mer, 2 pp.

Giglioli, E. H. 1880. Elenco dei Mammiferi, degli Uccelli e dei Rettili Ittiofagi Appartenenti alla Fauna Italica e Catalogo degli Anfibi e dei Pesci Italiani. Firenze: Stamperia Reale. 85 pp.

Gilbert, C. H. 1905. The deep-sea fishes of the Hawaiian Islands. *In* The Aquatic Resources of the Hawaiian Islands. II, D. S. Jordan and B. W. Evermann (eds.). Bull. U. S. Fish. Comm., **23**: 575–716.

Gilchrist, J. D. F. 1922. Report No. 2 for the year 1921. Fish. Mar. Biol. Surv. South Africa, Rep. No. 2: 1–84.

———, and C. von Bonde. 1924. Deep-sea fishes procured by the S. S. "Pickle" (Part II). Fish. Mar. Biol. Surv. South Africa, Rep. No. 3, Spec. Rep. VII: 1–24.

Gonzales, T. 1946. Contributo alla conoscenza dello sviluppo post-embrionale in *Microichthys coccoi*, Rüppell. Boll. Pesca Piscicolt. Idrobiol., Ser. 22, **1**(1): 39–46.

Goode, G. B., and T. H. Bean. 1881. Description of a new species of fish, *Apogon pandionis*, from deep water off the mouth of Chesapeake Bay. Proc. U. S. Nat. Mus., **4**: 160–161.

———, and ———. 1896. Oceanic Ichthyology. Washington, D. C.: Smithsonian Institution. 553 pp.

Gosline, W. A. 1961. The perciform caudal skeleton. Copeia, **1961**(3): 265–270.

———, and V. E. Brock. 1960. Handbook of Hawaiian Fishes. Honolulu: Univ. Hawaii Press. 372 pp.

Günther, A. 1859. Catalogue of the Fishes in the British Museum, Vol. I. London. 524 pp.

———. 1868. Report on a collection of fishes made at St. Helena by J. C. Melliss, Esq. Proc. Zool. Soc. London, pp. 225–228.

Haneda, Y., F. H. Johnson, and O. Shimomura. 1966. The origin of luciferin in the luminous ducts of *Parapriacanthus ransonneti*, *Pempheris klunzingeri*, and *Apogon ellioti*. *In* Bioluminescence in Progress, F. H. Johnson and Y. Haneda (eds.). Princeton: Princeton Univ. Press, pp. 533–545.

Holt, E. W., and W. L. Calderwood. 1895. Survey of fishing grounds, west coast of Ireland, 1890–1891. Report on the rarer fishes. Scient. Trans. R. Dublin Soc., Ser. 2, **5**: 361–524.

Hubbs, C. L., and K. F. Lagler. 1958. Fishes of the Great Lakes Region. Ann Arbor: Univ. Michigan Press. 213 pp.

Iwai, T. 1959. Notes on the luminous organ of the apogonid fish, *Siphamia majimai*. Ann. Mag. Natur. Hist., Ser. 13, **2**(21): 545–550.

Jordan, D. S. 1917. Notes on *Glossamia* and related genera of cardinal fishes. Copeia, No. 44: 46–47.

———, and C. H. Gilbert. 1882. Synopsis of the fishes of North America. Bull. U. S. Nat. Mus., **16**: 1–1018.

———, and E. K. Jordan. 1922. A list of the fishes of Hawaii, with notes and descriptions of new species. Mem. Carnegie Mus., **10**(1): 1–92.

Kamohara, T. 1952. Revised descriptions of the offshore bottom-fishes of Prov. Tosa, Shikoku, Japan. Rep. Kôchi Univ. Nat. Sci., No. 3: 1–22.

Koefoed, E. 1952. Zeomorphi, Percomorphi, Plectognathi. Rep. Sci. Res. Michael Sars N. Atl. Deep-Sea Exped. 1910, **4**, Pt. 2(2): 1–26.

Lowe, R. T. 1841. A synopsis of the fishes of Madeira; with principal synonyms, Portuguese names, and characters of the new genera and species. Trans. Zool. Soc. London, **2**(14): 173–200.

Lozano, L. 1934. Algunos peces pelágicos o de profundidad procedentes del Mediterráneo occidental. Bol. Soc. Españ. Hist. Natur., **34**: 85–92.

Matsubara, K. 1936. Biometry of two species of Japanese cardinal-fishes, with special reference to their taxonomy. J. Imp. Fish. Inst. Tokyo, **31**: 119–130.

Maurin, C. 1968. Écologie ichthyologiques des fonds Chalutables atlantiques (de la baie ibéro-marocaine à la Mauritanie) et de la Mediterranée occidentale. Thèses presentées à la Faculté des Sciences de l'Université de Nancy. No. d'Ordre: A. O. 2 182. 145 pp.

Mayer, G. F. 1972. Systematics, functional anatomy, and ecology of the cardinalfish genus *Epigonus* (Apogonidae). Ph. D. Thesis, Harvard University. 190 pp.

Mayr, E. 1969. Principles of Systematic Zoology. New York: McGraw-Hill, Inc. 428 pp.

Mead, G. W., and M. G. Bradbury. 1963. Names of bones. *In* Fishes of the Western North Atlantic, H. B. Bigelow and W. C. Schroeder (eds.). Mem. Sears Found. Mar. Res., **1**(3): 20–23.

Monod, T. 1968. Le complexe urophore des poissons téléostéens. Mém. Inst. Fondam. Afr. Noire, No. 81. 705 pp.

Moreau, E. 1881. Histoire Naturelle des Poissons de la France. Vol. II. Paris: G. Masson. 572 pp.

Moreland, J. 1957. Appendix 6: Report on the fishes. New Zealand Dep. Sci. Ind. Res. Bull., **122**: 34.

Navarro, F. de P. 1942. Nota preliminar sobre los peces de la costa de Africa, desde el Cabo Bojador à la Bahia de Tanit (Resultados de una compaña industrial de pesca d'arrastre). Bol. Real Soc. Españ. Hist. Natur., **40**(5–6): 189–214.

———, F. Lozano, J. M. Novaz, E. Otero, and J. Sáinz Pardo. 1943. La pesca d' arrastre en los fondos del Cabo Blanco y del Banco Arguín (Africa Sahariana). Trab. Inst. Españ. Oceanogr. Número 18. 225 pp.

Nobre, A. 1935. Descrição dos Peixes de Portugal. Vertebrados (mamiferos, reptis e peixes). I. Fauna Marinha de Portugal. Pôrto. 574 pp.

Norman, J. R. 1939. Fishes. Sci. Rep. John Murray Exped., **7**(1): 1–116.

———. 1957. A Draft Synopsis of the Orders, Families and Genera of Recent Fish and Fish-like Vertebrates. London: British Museum (Natural History). 649 pp.

Nowlin, W. D., jr., and H. J. McLellan. 1967. A characterization of the Gulf of Mexico waters in winter. J. Mar. Res., **25**(1): 29–59.

Osorio, B. 1898. Da distribuição geographica dos peixes e crustaceos colhidos nas possessões Portuguezos d'Afrique occidental e existentes no Museu Nacional de Lisboa. J. Sci. Math. Phys. Natur. Acad. Real Sci. Lisboa, Ser. 2, **5**: 185–202.

Pietschmann, V. 1930. Remarks on Pacific fishes. Bull. Bernice P. Bishop Mus., **73**: 1–24.

Poll, M. 1954. Poissons IV. Télcostéens acanthoptérygiens (première partie). Résultats scientifiques. Expédition Océanographique Belge dans les Eaux Côtières Africaines de l'Atlantique Sud (1948–1949), **4**(3A): 1–390.

Radcliffe, L. 1912. Descriptions of fifteen new fishes of the family Cheilodipteridae, from the Philippine Islands and contiguous waters. Proc. U. S. Nat. Mus., **41**(1868): 431–446.

Rafinesque, C. S. 1810. Indice d' Ittiologia Siciliana; Ossia, Catalogo Metodico dei Nomi Latini Italiani, e Siciliani dei Pesci, che si Rinvengono in Sicilia: Disposti Secondo un Metodo Naturale e Seguito da un Appendice che Contiene la Descrizione di Alcuni Nuovi Pesci Siciliani. Messina: Presso Giovanni del Nobolo. 70 pp.

Risso, A. 1810. Ichthyologie de Nice ou Histoire naturelle des poissons du départment des Alpes Maritimes. Paris: Chez F. Schoell. 388 pp.

Royce, W. R. 1957. Statistical comparison of morphological data. *In* Contributions to the Study of Subpopulations of Fishes, J. C. Marr (coordinator). U. S. Fish. Wildl. Serv. Spec. Sci. Rep. Fish., No. 208: 7–28.

Rüppell, W. 1852. Verzeichniss der in dem Museum der Senckenbergischen naturforschenden Gesellschaft aufgestellten Sammlungen. Vierte Abteilung. Fische und deren Skelette. Frankfurt-a.M.: J. D. Sauerländer. 40 pp.

Sakamoto, K. 1930. Buccal incubation in the percoid fish, *Apogon lineatus* T. & S. J. Imp. Fish. Inst. Tokyo, **26**(1): 9–10.

Schultz, L. P. 1940. Two new genera and three new species of cheilodipterid fishes, with notes on the other genera of the family. Proc. U. S. Nat. Mus., **88**(3085): 403–423.

Scott, T. D. 1962. The Marine and Fresh Water Fishes of South Australia. Adelaide: South Australian Branch of the British Science Guild. 338 pp.

Simpson, G. G., A. Roe, and R. C. Lewontin. 1960. Quantitative Zoology. New York: Harcourt, Brace and World, Inc. 440 pp.

Smith, C. L., E. H. Atz, and J. C. Tyler. 1971. Aspects of oral brooding in the cardinalfish *Cheilodipterus affinis* Poey (Apogonidae). Amer. Mus. Novitates, No. 2456: 1–11.

Smith, J. L. B. 1949a. Forty-two fishes new to South Africa, with notes on others. Ann. Mag. Natur. Hist., Ser. 12, **2**: 97–111.

———. 1949b. The Sea Fishes of Southern Africa. South Africa: Central News Agency, Ltd. 550 pp.

———. 1961. Fishes of the family Apogonidae of the western Indian Ocean and the Red Sea. Ichthyol. Bull. Rhodes Univ., No. 22: 373–418.

Spartà, A. 1950. Su di una nuova specie di *Microichthys*: *M. sanzoi* (n. sp.). Boll. Pesca, Piscicolt. Idrobiol., Ser. 26, **5**(2): 202–206.

Steindachner, F. 1891. Ichthyologische Beiträge (XV). Über einige seltene und neue Fischarten aus dem canarischen Archipel. Sitzber. Akad. Wiss. Wien, **100**(1): 343–374.

———. 1907. Fische aus Südarabien und Sokótra. Denkschr. Akad. Wiss. Wien, **71**: 123–168.

Taylor, W. R. 1967. An enzymatic method of clearing and staining small vertebrates. Proc. U.S. Nat. Mus., **122**(3596): 1–17.

Tinker, S. W. 1944. Hawaiian Fishes. Honolulu: Tongg Publishing Company. 404 pp.

Tortonese, E. 1952. Un percoide marino e batifilo nuovo per l'ittiofauna italiana (*Epigonus denticulatus* Dienz.). Boll. Pesca Piscicolt. Idrobiol. Ser. 28, **7**(1): 72–74.

———, and L. C. Queirolo. 1970. Contributo allo studio dell 'ittiofauna del Mar Ligure orientale. Ann. Mus. Civ. St. Natur. Genova, **78**: 21–46.

Vaillant, L. 1888. Poissons. Expéditions Scientifiques du Travailleur et du Talisman pendant les Années 1880, 1881, 1882, 1883. Paris: G. Masson. 406 pp.

Valenciennes, A. 1830. Additions et corrections aux tomes II, III, IV, et V. *In* Historie Naturelle des Poissons, Tome Sixieme, G. Cuvier and A. Valenciennes. Paris: F. G. Levrault, pp. 495–559.

———. 1837–1844. Ichthyologie des îles Canaries, ou Histoire naturelle des poissons raportés par M. M. Webb et Berthelot. *In* Histoire Naturelle des Îles Canaries, P. B. Webb and S. Berthelot (eds.). Vol. 2, Pt. 2. Paris, pp. 1–109. [pp. 1–8 published Dec. 1842; plate 1 published May 1837.]

Weber, M., and L. F. de Beaufort. 1929. The Fishes of the Indo-Australian Archipelago. V. Anacanthini, Allotriognathi, Heterosomata, Berycomorphi, Percomorphi: Families Kuhliidae, Apogonidae, Plesiopidae, Pseudoplesiopidae, Priacanthidae, Centropomidae. Leiden: E. J. Brill, Ltd. 458 pp.

Whitley, G. P. 1935. Studies in ichthyology. No. 9. Rec. Aust. Mus. Sydney, **19**(4): 215–250.

———. 1940. Illustrations of some Australian fishes. Aust. Zool., **9**(4): 397–428.

———. 1968. A check-list of the fishes recorded from the New Zealand region. Aust. Zool., **15**(1): 1–102.

Williams, F. 1968. Report on the Guinean Trawling Survey, Vol. I. General Report. OAU Scientific, Technical and Research Commission, Publication 99. 828 pp.

Wüst, G. 1964. Stratification and Circulation in the Antillean-Caribbean Basins. New York: Columbia Univ. Press. 201 pp.

APPENDIX

The following chart lists all meristic and morphometric data for the holotypes of *E. oligolepis* sp. nov. and *E. pectinifer* sp. nov. Measurements are given in millimeters.

	E. oligolepis USNM 207718	*E. pectinifer* USNM 207725
MERISTIC DATA		
Dorsal fin	VII-I, 10	VII-I, 9
Anal fin	II, 9	II, 9
Pectoral fin	18	15
Pelvic fin	I, 5	I, 5
Lateral line scales	34	47
Gill rakers	31	27
Pyloric caeca	10	6
Vertebrae	10 + 15	10 + 15
Pleural ribs	7	8
Epipleural ribs	7	6
MORPHOMETRIC DATA		
SL	90.8	114.3
HL	33.2	40.5
Body depth	21.2	28.1
Head height	17.1	18.8
Eye diameter	14.5	16.1
Snout length	7.8	10.9
Interorbital width	8.4	10.0
Maxillary length	15.6	18.2
Lower jaw length	16.3	18.5
Caudal peduncle depth	8.9	11.7
Caudal peduncle length	23.6	32.1
D_2 l	10.9	13.7
A ll	11.1	13.7
P_2 l	12.3	14.4

US ISSN 0027-4100

Bulletin OF THE
Museum of
Comparative
Zoology

The Spider Family Anyphaenidae in America North of Mexico

NORMAN PLATNICK

HARVARD UNIVERSITY
CAMBRIDGE, MASSACHUSETTS, U.S.A.

VOLUME 146, NUMBER 4
19 SEPTEMBER 1974

PUBLICATIONS ISSUED
OR DISTRIBUTED BY THE
MUSEUM OF COMPARATIVE ZOOLOGY
HARVARD UNIVERSITY

Breviora 1952–
Bulletin 1863–
Memoirs 1864–1938
Johnsonia, Department of Mollusks, 1941–
Occasional Papers on Mollusks, 1945–

SPECIAL PUBLICATIONS.

1. Whittington, H. B., and E. D. I. Rolfe (eds.), 1963. Phylogeny and Evolution of Crustacea. 192 pp.
2. Turner, R. D., 1966. A Survey and Illustrated Catalogue of the Teredinidae (Mollusca: Bivalvia). 265 pp.
3. Sprinkle, J., 1973. Morphology and Evolution of Blastozoan Echinoderms. 284 pp.
4. Eaton, R. J. E., 1974. A Flora of Concord. 211 pp.

Other Publications.

Bigelow, H. B., and W. C. Schroeder, 1953. Fishes of the Gulf of Maine. Reprint.

Brues, C. T., A. L. Melander, and F. M. Carpenter, 1954. Classification of Insects.

Creighton, W. S., 1950. The Ants of North America. Reprint.

Lyman, C. P., and A. R. Dawe (eds.), 1960. Symposium on Natural Mammalian Hibernation.

Peters' Check-list of Birds of the World, vols. 2–7, 9, 10, 12–15.

Proceedings of the New England Zoological Club 1899–1948. (Complete sets only.)

Publications of the Boston Society of Natural History.

Price list and catalog of MCZ publications may be obtained from Publications Office, Museum of Comparative Zoology, Harvard University, Cambridge, Massachusetts, 02138, U.S.A.

© The President and Fellows of Harvard College 1974.

THE SPIDER FAMILY ANYPHAENIDAE IN AMERICA NORTH OF MEXICO[1]

NORMAN PLATNICK[2]

Abstract. Evidence from the tracheal system, claw tufts and courtship behavior is used to justify the family status of Anyphaenidae. Suggested relationships between Anyphaenidae and Clubionidae, Amaurobiidae and Argyronetidae are disclaimed. The family Amaurobioididae is newly synonymized with Anyphaenidae. Generic problems within the family are discussed. The thirty-six species occurring north of Mexico are described, their diagnostic characters pointed out and illustrated, their distributions mapped, notes on their habits given, and keys to genera, species groups and species provided. The genera *Anyphaenella* and *Cragus* are newly synonymized with *Wulfila*. Thirteen species are described as new: *Anyphaena alachua*, *A. arbida*, *A. autumna*, *A. catalina*, *A. cochise*, *A. gertschi*, *A. gibboides*, *A. hespar*, *A. lacka*, *A. rita*, *Aysha aruuda*, *Wulfila bryantae* and *W. wunda*. Nineteen new synonymies are recognized.

INTRODUCTION

This study had three objectives: to determine whether or not the anyphaenids should be treated as a distinct family; to examine the relationships between the anyphaenids and the other groups of spiders with which they have been associated in the past; and to reclassify the species occurring north of Mexico on generic and specific levels.

The anyphaenids are a diverse group with perhaps five hundred species. Thirty-six species are known to occur in America north of Mexico and are included here. About 375 species have been described from the Neotropic region, as well as around ten from the Palearctic and five from the Oriental. The South American species show the widest spectrum of body forms; they range from 2–25 mm in length and are often intricately colored or have peculiarly elongate chelicerae or legs.

As in most spiders, little is known of the ecology or behavior of anyphaenids. They are wandering hunters. In the eastern United States, where long-legged species predominate, they are most often collected by sweeping foliage in fields and meadows, and seem to be primarily nocturnal. However, in the western United States, where most species have shorter legs, they are usually found in forests by sifting through litter and turning logs and stones. They feed on various groups of insects, and though they have been observed to prey heavily on such Lepidoptera as the fall webworm, *Hyphantria cunea* (Warren et al., 1967), they are probably not very selective. In captivity they will consume *Drosophila* eagerly. Their principal enemies in nature are the mud-dauber wasps of the family Sphecidae, as evidenced from the hundreds of individuals, particularly

[1] This study was presented to the Department of Biology at Harvard University in partial fulfillment of the requirements for the degree of Doctor of Philosophy.

[2] Present address: Department of Entomology, The American Museum of Natural History, Central Park West at 79th Street, New York, New York 10024.

of the diurnally active genus *Aysha*, that are frequently collected from wasp nests. Krombein (1967) cites especially the wasp genus *Trypargilum* in this respect. Like most nearctic spiders, males and females usually mature in early spring, with males living through early summer and females living through the summer. In some southern species, however, both sexes are found mature year-round. Also, some species in the *Anyphaena celer* group are mature throughout the winter. Anyphaenids make little use of silk, other than in building retreats under leaves or stones and of course in building egg sacs, which are usually round, made of soft white silk, not leathery or papery, and contain between 50 and 150 eggs.

The North American species are 2–9 mm long; the largest species belong to the genus *Aysha*, the smallest to *Wulfila*. There are always eight eyes in two rows; the median eyes are usually closer to the laterals than to each other; unlike many gnaphosids, the eyes are always round, and unlike many clubionids, the anterior median eyes are usually smaller than the others. Other than the genitalia, the main structural differences between males and females are the sternal and coxal modifications (pointed spurs, rounded knobs, or clumps of short thick setae) found on males in some groups.

In many species groups it would be impossible to distinguish the species without using genitalic characters. The palpus (Text-fig. 3) usually has a large median apophysis (the shape of which is often species-specific), a small conductor and a conspicuous embolus. Besides the retrolateral tibial apophysis (almost always of great diagnostic value) a ventral tibial apophysis (some *Aysha*) or a retrolateral patellar apophysis (some *Teudis*) may be present. The female epigyna and internal genitalia are extremely diverse and difficult to characterize. The two epigynal openings are located posteriorly and are extremely difficult to see unless a portion of the male embolus has been left behind after mating. Many species have an additional anterior median epigynal opening into which the retrolateral tibial apophysis or median apophysis fits during mating. The genitalia of anyphaenids, particularly of the South American species, are more complex than those of clubionids and gnaphosids. Among the clubionids, only *Chiracanthium* has genitalia that seem in any way close to those of anyphaenids.

For the area treated here, only three important papers have been published on anyphaenids. Bryant (1931) summarized the very sparse data then available on the group in the United States, while Chickering (1937, 1940) described many of the species occurring in Panama and the Canal Zone, a number of which also occur in the United States.

ACKNOWLEDGEMENTS

I would like to thank first Herbert W. Levi for his painstaking and patient help with all aspects of this project. Willis Gertsch contributed much of his knowledge of the group as well as the drawings, done by the late Wilson Ivie, of the genus *Oxysoma*.

This investigation was supported in part by Public Health Service Research Grant AI–01944 from the National Institutes of Allergy and Infectious Diseases, H. W. Levi, principal investigator; by Grant GB–36161 from the National Science Foundation, H. W. Levi, principal investigator; and by Grant GB–19922 from the National Science Foundation, R. C. Rollins, principal investigator. The Department of Biology, Harvard University, by means of Summer Research Grants in Evolutionary Biology in 1971 and 1972 and a Richmond Fellowship in 1973, afforded me much of the time and field work necessary to complete this work. Miss Suzanne Barbier of Radcliffe College assisted greatly with the examination of tracheal systems and her work is deeply appreciated.

Finally, the following people loaned

specimens from their private collections or from their cited institutions: Paul H. Arnaud, Jr. (California Academy of Sciences), Joseph A. Beatty, Jr., James E. Carico, John A. L. Cooke (American Museum of Natural History), Charles D. Dondale (Canadian National Collections), R. R. Forster (Otago Museum), Willis J. Gertsch (American Museum of Natural History), Al Jung, B. J. Kaston, Robin Leech, William B. Peck, Vince Roth, Richard J. Sauer (Michigan State University), William A. Shear, Bea Vogel, H. K. Wallace, Fred R. Wanless (British Museum, Natural History), and Howard V. Weems (Florida State Collection of Arthropods).

THE FAMILY STATUS OF ANYPHAENIDAE

Simon considered the anyphaenids to be a subfamily of the large family Clubionidae and used as the key character for distinguishing the anyphaenids the advanced placement of the tracheal spiracle. Later authors, notably Petrunkevitch and Bristowe, thought this character so significant that they gave the anyphaenids family status, though still believing the group to be closely related to the Clubionidae. The comparatively recent discovery that in some families closely related, congeneric species sometimes have very different respiratory systems (see Levi, 1967) has led most arachnologists to denigrate the importance of respiratory structures as macrotaxonomic characters. Thus most modern arachnological works still treat the anyphaenids as a subfamily of Clubionidae. A notable exception, however, is Lehtinen (1967), who maintains (correctly, I believe) that the classical family Clubionidae is a highly polyphyletic assemblage of unrelated two-clawed spiders that lack any noticeable modifications of the body. Lehtinen splits the clubionids into several families, largely but not strictly along the lines of the old subfamily divisions, and accords the anyphaenids full status as a family. Forster (1970) agrees with this assessment of the anyphaenids.

To check on the validity of this classification, a variety of clubionid genera were examined and compared with anyphaenids, with the result that the anyphaenids are here considered a distinct family, for two major reasons. One is the classical reason —the tracheal system. Examination of the tracheae of males and females of the clubionids *Clubiona obesa* Hentz, *Chiracanthium mildei* L. Koch, *Trachelas tranquillus* (Hentz), *Castianeira cingulata* (C. L. Koch), *Agroeca pratensis* Emerton, *Phrurotimpus alarius* (Hentz), and the anyphaenids *Anyphaena celer* (Hentz), *Anyphaena pectorosa* L. Koch, *Anyphaena californica* (Banks) and *Aysha gracilis* (Hentz) disclosed three major differences between anyphaenid and clubionid tracheae (see Methods for the technique used). First, anyphaenid tracheae extend through the pedicel of the spider into the cephalothorax and legs, while those of clubionids are restricted to the abdomen (see Figs. 47 and 50). Associated with this is the externally observable advanced placement of the tracheal spiracle in anyphaenids. Second, the tracheae are relatively much larger in anyphaenids. In all the clubionids examined, even the main tracheal tubes are very thin and narrow; anyphaenid tracheae are three to four times as wide. Third, none of the clubionid species examined showed any sexual dimorphism in the tracheal system, whereas male anyphaenids have considerably larger tracheae than do the females. The size of the tracheae may be correlated with the high activity levels of anyphaenids: my collecting experience indicates that they can run extremely rapidly when disturbed.

The larger size of the tracheae in males may be associated with the increased respiration necessary for the extra activity required to locate, court and copulate with a female. Anyphaenid courtship is extremely active; films of the courtship of *Anyphaena accentuata* show that the abdo-

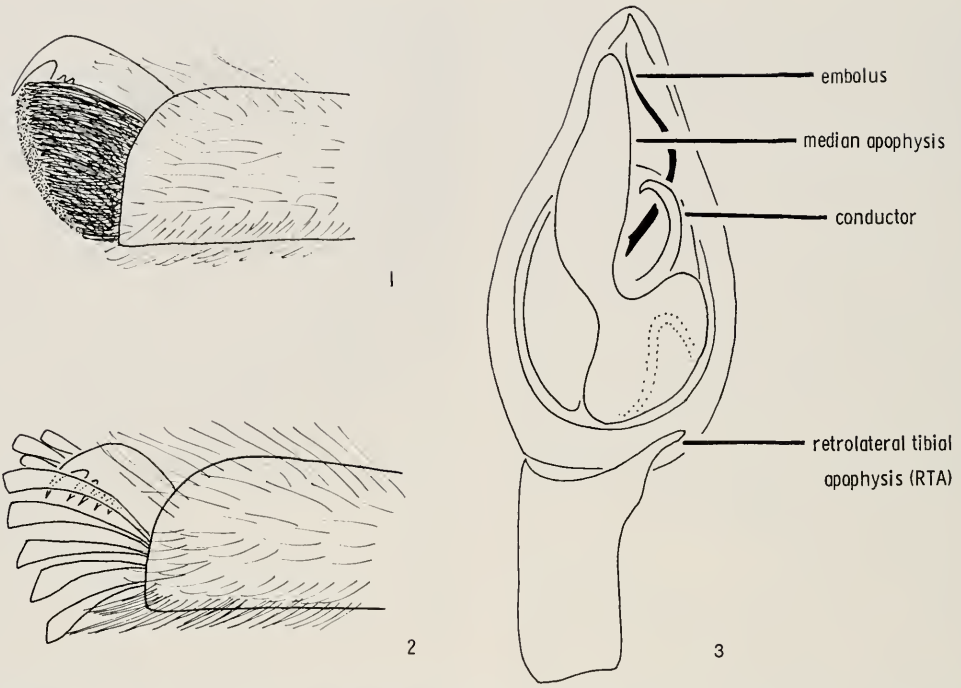

Text-Figures 1–3. Claw tuft of *Clubiona obesa* Hentz, lateral view, diagrammatic. 2. Claw tuft of *Aysha gracilis* (Hentz), lateral view, diagrammatic. 3. Generalized palpal structure of *Anyphaena*.

men of the male is vibrated up and down so rapidly that only a blur is visible (Thompson, G. H., and E. R. Skinner, *Courtship in Spiders*, Oxford Scientific Films). Although the mating behavior of very few species in either group has been studied in detail, the vast difference between anyphaenid courtship and the rather sluggish courtship behavior of *Clubiona* and related genera would seem to provide additional evidence for separating the two groups (Platnick, 1971).

Evidence that is probably just as important as the tracheae for considering Anyphaenidae a distinct group is provided by the claw tufts. Clubionids have claw tufts that are composed of numerous straight simple setae densely clumped together (Text-fig. 1). Anyphaenid claw tufts, however, are composed of two rows of large, lamelliform setae that are greatly expanded at their distal ends (Text-fig. 2). All the anyphaenids examined have these peculiar, easily recognizable claw tufts, but so far as known, no clubionids do, though some phruroliths have superficially similar claw tufts.

For these reasons, Anyphaenidae is here considered a distinct family not very closely related to any of the groups currently included in the Clubionidae.

RELATIONSHIPS OF THE FAMILY ANYPHAENIDAE

In addition to the clubionids, the anyphaenids have been associated with three other families of spiders: Amaurobiidae, Argyronetidae and Amaurobioididae. Lehtinen (1967) placed the anyphaenids in his branch Amaurobiides and stated that they are probably derived from Amaurobiidae: Macrobuninae and therefore lack ecribellate, two-clawed relatives. Forster (1970) agreed with the placement of Anyphaenidae in Amaurobiides (and specifi-

cally included the family in his superfamily Dictynoidea) but cited the families Argyronetidae and Amaurobioididae as close relatives. Representatives of all three families were examined to determine the degree of their relationship, if any, to the Anyphaenidae.

Lehtinen gave no evidence for his statement that the anyphaenids are probably derivatives of Amaurobiidae: Macrobuninae, presumably because there seems to be none. An examination of specimens of one genus in this subfamily, *Arctobius* Lehtinen, indicates that it would be difficult to find araneomorph spiders less likely to have given rise to the anyphaenids. The species of *Arctobius* are cribellate, three-clawed spiders that lack claw tufts and possess an unelaborated tracheal system. Further, the genitalia show no similarities to those of anyphaenids.

Likewise, Forster gave no evidence for associating the family Argyronetidae with the anyphaenids; his decision to do so was based, I believe, on the similarities in the tracheal systems of the two groups. The elaboration of the tracheal system in *Argyroneta*, however, is probably associated with their invasion of an aquatic habitat and the resultant demands on the respiratory system. All the other characters, including the three claws, lack of claw tufts and the characteristic pattern of trichobothria distribution, indicate that *Argyroneta* is, as it is usually regarded, a close relative (if not actually a member) of the family Agelenidae.

The family Amaurobioididae was created by Hickman (1949) for the single genus *Amaurobioides* O. P.-Cambridge, which has at various times been included in the families Drassidae (= Gnaphosidae), Ctenidae, Clubionidae and Miturgidae. The genus is known from New Zealand, Tasmania, southern Chile and South Africa. The spiders live in rock crevices in the tidal zone, where they build tubular silk retreats and are regularly submerged at high tide (Lamoral, 1968).

Specimens of this rare genus provided by R. R. Forster revealed not only a typically anyphaenid-like tracheal system, but also the lamelliform claw tufts so characteristic of anyphaenids. Further, the genitalia are close to those of the anyphaenid genus *Oxysoma*, and the body form is similar to that of several species of anyphaenids known from Chile, Peru, and Argentina. For these reasons, the family Amaurobioididae is newly synonymized with Anyphaenidae in the taxonomic section of this paper.

Thus the problem of the correct macrotaxonomic placement of Anyphaenidae has been clarified but not solved by this study of the groups with which the family has been associated in the past. Future work should start with an examination of the family Miturgidae (as construed by Lehtinen).

Although it was necessary to limit the scope of the detailed revision to the manageable number of species occurring north of Mexico, all available specimens from other areas were examined to gain an overview of the family. Preliminary impressions indicate that the family probably originated in the southern half of South America with subsequent radiations northward. As indicated by the ability of *Amaurobioides* to withstand prolonged submersion, it is likely that early anyphaenids were able to survive hydrochore dispersal by rafting, etc., across considerable expanses of water.

GENERIC PROBLEMS IN THE ANYPHAENIDAE

The generic taxonomy of anyphaenids is currently chaotic. Every author who has worked with the group, including Petrunkevitch (1930), Bryant (1931) and Chickering (1937), has expressed frustration at the confusion and ambiguity in the use of many of the most common generic names. One of the principal causes of this confusion is the interesting evolutionary pattern encountered time and again within

this family: species tend to occur in groups that are remarkably homogeneous in genitalic structure but quite distinct from other such groups. Often many of the species in these groups are sympatric, are found in a rather limited area and are clearly the result of radiation within that area. An excellent example of this is the occurrence of nine closely related species of the *Anyphaena celer* species group in the mountains of southeastern Arizona. It is tempting to consider each of these groups a genus, as unambiguous key characters are then available to distinguish genera. Such an approach would at least double the number of genera found in the United States, and, if applied to the Central and South American fauna, would necessitate the creation of a vast number of new genera. If, instead, characters referring to the general body form are used, a more workable classification in terms of both number and size of genera results. Unfortunately, this makes the unambiguous definition of genera much more difficult and makes keys to genera awkward and cumbersome. With either approach, however, reliable genera composed of monophyletic groups of species can be established.

The second approach to anyphaenid classification has been taken by the majority of former authors, and is continued in this work. Thus the European genus *Anyphaena* is used for the bulk of the anyphaenids occurring in the United States, even though only one of our species, *Anyphaena aperta*, is actually a close relative of the European *Anyphaena accentuata*, type species of the genus. Nonetheless, all the species here included in *Anyphaena* share a basic body form. The neotropical genus *Wulfila* is used for all the pale, long-legged species, even though they are genitalically quite diverse; the other genera used here are similarly construed. Although this system is not wholly satisfactory, it seems decidedly better than creating a host of new generic names that are likely to fall into synonymy when a detailed generic revision of the group as a whole can be carried out.

METHODS

Tracheae were examined by dissecting away the dorsal cuticle of the abdomen and boiling the spider in ten percent sodium hydroxide for ten minutes. By this method, all the soft structures in the abdomen are digested away, leaving the tracheae intact.

Types of the new species are being deposited in the American Museum of Natural History, New York City, and the Museum of Comparative Zoology, Harvard University. Type depositories are abbreviated as follows: AMNH—American Museum of Natural History, BMNH—British Museum, Natural History, MCZ—Museum of Comparative Zoology.

Measurements and drawings were made with a standard ocular grid. Measurements of gross morphological features are accurate to $\pm$ 0.04 mm; measurements of ocular features are accurate to $\pm$ 0.01 mm. Rather than selecting a small number of measurements and providing means and standard deviations for these on the basis of a small series of specimens, one male and one female of each species were measured in detail. As only one of the species included here shows any significant variation in size, this procedure was deemed more informative. Actual measurements are given rather than ratios since in many cases (e.g., *Anyphaena catalina* and *A. arbida*) closely related species differ significantly in size but not in their relative proportions. Most of the measurements taken are self-explanatory, though a few need further comment. Cephalic width refers to the width of the carapace at a point just behind the posterior median eyes, and thus provides an indication of the degree to which the carapace is narrowed in front.

The difficult problem of accurately describing the eye relationships has been

solved by providing a set of measurements from which it is possible to reconstruct, using graph paper, the exact eye arrangement. Diameters are given using the conventional abbreviations (AME = anterior median eye, ALE = anterior lateral eye, PME = posterior median eye, PLE = posterior lateral eye). The length of each eye row is measured from the lateral edge of one lateral eye to the lateral edge of the other lateral eye. Curvature of the eye rows is described as viewed frontally, not dorsally. This was accomplished by positioning the spider in sand, a technique found most useful for making all the measurements. The dimensions of the median ocular quadrangle (MOQ) are given, as well as the distances between each of the eyes. The latter measurements extend between the edges of the lenses of the eyes under consideration (not just between the dark circles surrounding each eye).

The relative length and thickness of each leg is indicated by the tibial length index—the tibial width divided by the tibial length, with the result multiplied by 100 to obtain a whole number. All tibial measurements were taken from a dorsal view and refer to the maximum lengths and widths. The lower the tibial index, the longer and thinner the leg; conversely, the higher the index, the shorter and thicker the leg. In practice the index varies from around 3 to 35.

Ventral spination of the leg segments is indicated by the standard formula in which the number of spines on the proximal, median and distal thirds of the leg segment are given. Only ventral spines, not lateral ones, are included, and any even number in the formula may be taken to represent a pair of spines. Unless the last number is followed by an asterisk, the last pair of spines is terminally located. Thus, for example, the formula 2–2–2* indicates that the segment bears three pairs of ventral spines, the last pair of which is not terminally located. The term "spine" is used in its conventional arachnological sense and refers to the movable macrosetae found on the legs. Similarly, the term "clypeus" is used to refer to the area between the anterior eye row and the anterior edge of the carapace and not to the small sclerite folded under the carapace. Since neither usage of the term reflects certain knowledge of homology with the insect clypeus, the old and established usage should be maintained.

Scale lines for the drawings always equal 0.1 mm. Each scale line applies to all consecutively numbered drawings until a new scale line appears. Exceptions are noted in the captions.

TAXONOMY

Anyphaenidae

Anyphaenidae Bertkau, 1878, Arch. Naturg., 44: 358, 379. Type genus *Anyphaena* Sundevall, 1833.

Amaurobioididae Hickman, 1949, Pap. Proc. Roy. Soc. Tasmania, 1948: 31. Type genus *Amaurobioides* O.P.-Cambridge, 1883. NEW SYNONYMY.

Diagnosis. The combination of the advanced tracheal spiracle and the lamelliform claw tufts will serve to distinguish the anyphaenids from all other families.

Description. Chelicerae diaxial, not fused together at base. Labium free. Without cribellum or calamistrum. With one pair of book lungs and a tracheal spiracle located considerably anterior to the spinnerets, most often midway between spinnerets and epigastric furrow, sometimes closer to one or the other. Eight eyes in two rows. Six spinnerets, anterior spinnerets approximate, colulus represented only by hairs, anal tubercle unmodified. Legs prograde, metatarsi and tarsi I and II scopulate, tarsi with two toothed claws and claw tufts composed of lamelliform setae.

Key to Genera
in America north of Mexico

1a. Tracheal spiracle much closer to epigastric furrow than to spinnerets ..... *Aysha*

1b. Tracheal spiracle roughly midway between epigastric furrow and spinnerets 2
2a. Legs very long and thin. Leg I greatly elongated, tibial index (width/length × 100) usually 5 or less ..... *Wulfila*
2b. Legs normal, tibial index of leg I usually 8 or more 3
3a. Chelicerae with 2 retromarginal teeth ..... *Oxysoma*
3b. Chelicerae with 4–9 retromarginal denticles 4
4a. Carapace usually with two dark paramedian longitudinal bands; chelicerae not produced forward; femora not much darker than other leg segments ..... *Anyphaena*
4b. Carapace without dark paramedian longitudinal bands; either chelicerae produced forward or femora much darker than other leg segments ..... *Teudis*

Anyphaena Sundevall

Anyphaena Sundevall, 1833, Conspectus Arachn., 28. Type species by monotypy *Aranea accentuata* Walckenaer, 1802.

Diagnosis. The combination of the following characters will serve to distinguish the genus in America north of Mexico: tracheal spiracle roughly midway between epigastric furrow and spinnerets, leg I not greatly elongated, chelicerae with 4–9 retromarginal denticles and not produced forward, femora not much darker than other leg segments. The carapace usually has two dark paramedian longitudinal bands. The genus is used here in a very broad sense; this prevents simple diagnosis, and makes detailed descriptions of each species group more meaningful than a description of the whole genus.

Uncertain names. Types of the following species were unavailable and are too poorly described to permit identification: *Clubiona agrestis* Hentz, 1847, type destroyed; *Clubiona fallens* Hentz, 1847, type destroyed; *Clubiona sublurida* Hentz, 1847, type destroyed; *Anyphaena argentata* Becker, 1879, type lost; and *Anyphaena striata* Becker, 1879, type lost. The three Hentz *Clubiona* species were transferred to *Anyphaena* by Marx (1890), but there is little justification for this in the vague descriptions. All the above names are regarded as *nomina dubia.*

Species groups. Although there seem to be several species groups of *Anyphaena* in the Neotropic region, only four occur north of Mexico. The *celer* group is the largest; it has representatives at least as far south as Panama and probably contains over thirty species. The *pectorosa* and *pacifica* groups are closely related and occur commonly in Mexico as well as the United States; it is difficult to place females in one group or the other unless the male is also known; they probably contain together at least twenty species. The *accentuata* group is predominantly Palearctic and probably contains at least five species.

Key to Species Groups

1a. Metatarsi I and II with one pair of ventral spines ..... *accentuata* group
1b. Metatarsi I and II with two pairs of ventral spines 2
2a. Retrolateral tibial apophysis of males bifid, with ventral prong elongated (Figs. 18–20, 25–32). Epigynum of females with a hood (Figs. 21, 23, 33, 36, 37, 39–42) ..... *celer* group
2b. Retrolateral tibial apophysis of males not bifid or elongated (Figs. 55–58, 69–71). Epigynum without a hood (Figs. 66, 67, 72, 74, 77, 79) 3
3a. Eastern United States. Coxae III and IV of males with pointed spurs (Figs. 59–62). Female epigyna on broad sclerotized plates (Figs. 74, 77, 79); internal genitalia lacking long ducts (Figs. 75, 78, 80) ..... *pectorosa* group
3b. Western United States. Coxae III and IV of males without pointed spurs, though rounded knobs may be present. Female epigyna not on broad sclerotized plates (Figs. 66, 67, 72); internal genitalia with long, sometimes coiling, ducts (Figs. 68, 73, 76) ..... *pacifica* group

Anyphaena celer Group

Diagnosis. Males of the *celer* group may be recognized by their retrolateral tibial apophysis, which is usually bifid with an elongated ventral prong (Figs. 18, 20, 26). Females have a characteristic epigynum consisting of a hood, two sidepieces and a midpiece (Figs. 9, 33), though the mid-

piece is reduced in *A. crebrispina* and *A. dixiana* (Figs. 21, 23).

Description. Total length 3–7 mm, with males of most species between 3.3–4.6 mm, females of most species between 4.1–5.9 mm. Carapace longer than wide, narrowed in front to less than half its maximum width. Clypeus height greater than anterior median eye diameter. Posterior median, posterior lateral and anterior lateral eyes subequal in size, larger than anterior medians. Procurved posterior eye row longer than recurved anterior row. Median ocular quadrangle longer than wide in front, wider than long in back. Anterior median eyes separated by their diameter, by their radius from anterior laterals. Posterior medians separated by their diameter, slightly closer to posterior laterals than to each other. Anterior laterals separated by their radius from posterior laterals. Sternum longer than wide, unmodified. Chelicerae with 4–5 promarginal teeth and 6–9 retromarginal denticles. Abdomen longer than wide, tracheal spiracle midway between epigastric furrow and base of spinnerets. Leg formula 1423. Metatarsi I and II with two pairs of ventral spines. Males often with femur III thickened distally, set with stiff short setae ventrally; tibia III ventral spines thickened, cone-like; coxae set with clumps of stiff short setae. Palpus with an elongated median apophysis, retrolateral tegular apophysis, conspicuous curving embolus and conductor. Retrolateral tibial apophysis bifid, with dorsal prong reduced in some species. Epigynum with hood, two sidepieces and midpiece; two simple spermathecae.

Variation. None of the species in this group show any significant individual or geographic intraspecific variation in structure, size or coloration.

Key to Species

1a. Dorsal and ventral prongs of retrolateral tibial apophysis (RTA) roughly equal in length (Figs. 18, 19); epigynal hood wide, more than four times the minimum width of epigynal sidepiece (Figs. 9, 11); eastern U.S. 2

1b. Ventral prong of retrolateral tibial apophysis (RTA) much longer than dorsal prong (as in Figs. 26, 27); epigynal hood narrow, less than four times the minimum width of epigynal sidepiece (as in Figs. 33, 36); western U.S. 3

2a. Dorsal prong of RTA broad, with a translucent ridge (Fig. 18); epigynal hood a thick oval, sidepieces straight (Fig. 9) ..... *celer*

2b. Dorsal prong of RTA narrow, without a translucent ridge (Fig. 19); epigynal hood a thin oval, sidepieces rounded (Fig. 11) ..... *maculata*

3a. Base of RTA expanded into a broad triangle (Fig. 20); retrolateral tegular apophysis prolonged medially (Fig. 3); epigynal sidepieces more than three times the width of epigynal hood (Fig. 21) ..... *crebrispina*

3b. Base of RTA not expanded; retrolateral tegular apophysis not prolonged medially; epigynal sidepieces less than three times the width of epigynal hood 4

4a. Dorsal prong of RTA bearing a sharp spur (Fig. 25); epigynal midpiece greatly reduced, sidepieces widely separated posteriorly (Fig. 23) ..... *dixiana*

4b. Dorsal prong of RTA without a spur; epigynal midpiece conspicuous, sidepieces approximate posteriorly 5

5a. Males 6

5b. Females 14

6a. Dorsal prong of RTA with two triangular processes separated by a concave notch (Fig. 26) ..... *judicata*

6b. Dorsal prong of RTA without triangular processes 7

7a. Dorsal prong of RTA with a long recurved hook (Fig. 29) ..... *autumna*

7b. Dorsal prong of RTA without a long recurved hook 8

8a. Dorsal prong of RTA with a basal hook (Figs. 31, 38) 9

8b. Dorsal prong of RTA without a basal hook 10

9a. Conductor and retrolateral tegular apophysis recurved (Fig. 15) ..... *catalina*

9b. Conductor and retrolateral tegular apophysis not recurved (Fig. 17) ..... *arbida*

10a. Dorsal prong of RTA a sharply pointed spike (Fig. 32) ..... *hespar*

10b. Dorsal prong of RTA not a sharply pointed spike 11

11a. Embolus with a conspicuous enlargement (Figs. 7, 13) 12

11b. Embolus without a conspicuous enlargement (Figs. 21, 33) 13

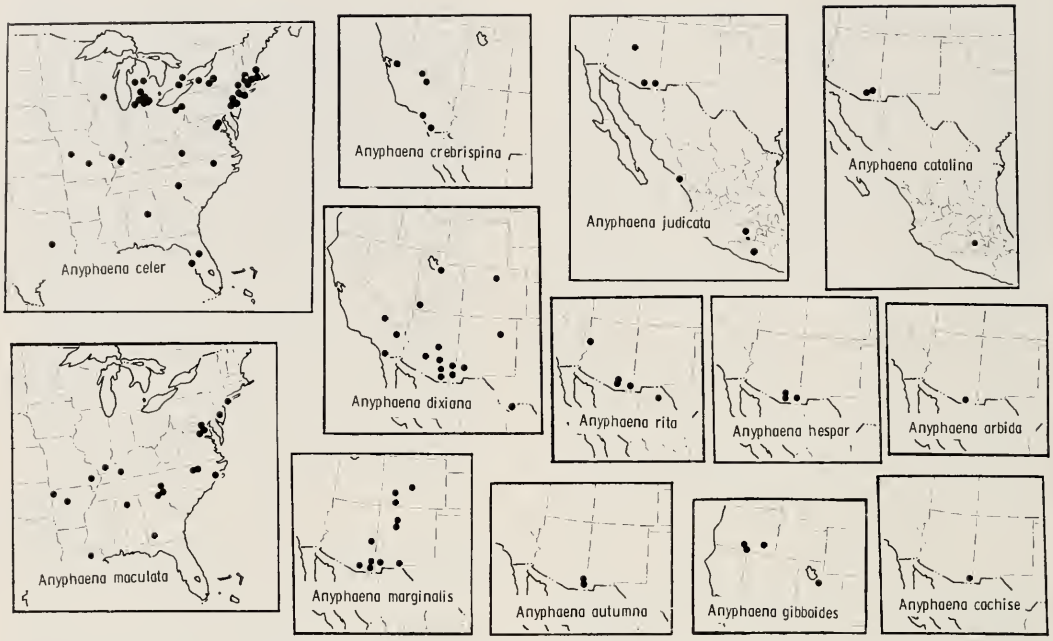

Map 1. Distributions of *Anyphaena arbida*, *A. autumna*, *A. catalina*, *A. celer*, *A. cochise*, *A. crebrispina*, *A. dixiana*, *A. gibboides*, *A. hespar*, *A. judicata*, *A. maculata*, *A. marginalis* and *A. rita*.

12a. Dorsal prong of RTA more than half the length of ventral prong (Fig. 35) ..... *cochise*

12b. Dorsal prong of RTA less than half the length of ventral prong (Fig. 28) ..... *rita*

13a. Median apophysis sharply pointed; conductor short, bent (Fig. 14); Oregon and Utah ..... *gibboides*

13b. Median apophysis rounded; conductor long, straight (Fig. 6); Arizona and New Mexico ..... *marginalis*

14a. Epigynal hood wider than long; midpiece not wider than hood, without constrictions; sidepieces very wide (Fig. 40); Oregon and Utah ..... *gibboides*

14b. Epigynal hood as long as wide *or* midpiece wider than hood *or* sidepieces narrow; Arizona and New Mexico 15

15a. Epigynal midpiece a very broad triangle (Fig. 37) ..... *rita*

15b. Epigynal midpiece otherwise 16

16a. Spermathecae much further apart posteriorly than anteriorly (Fig. 49) ..... *hespar*

16b. Spermathecae as far apart anteriorly as posteriorly 17

17a. Epigynal hood much wider than long (Fig. 39) ..... *autumna*

17b. Epigynal hood as long as wide 18

18a. Epigynal midpiece less than twice the length of epigynal hood (Fig. 41) ..... *catalina*

18b. Epigynal midpiece more than twice the length of epigynal hood 19

19a. Epigynal midpiece a short triangle (Fig. 33) ..... *judicata*

19b. Epigynal midpiece an elongate triangle (Fig. 36) ..... *marginalis*

Anyphaena celer (Hentz)
Map 1; Figures 1, 9, 10, 18

Clubiona celer Hentz, 1847, J. Boston Soc. Natur. Hist., 5: 452, pl. 23, fig. 20 (♀). Male holotype, female allotype from Alabama and North Carolina in the Boston Soc. Natur. Hist. (Boston Museum of Science), destroyed by beetles.

Anyphaena incerta Keyserling, 1887, Verh. zool. bot. Ges. Wien, 37: 452, pl. 6, fig. 22 (♀). Female holotype from Cambridge, Massachusetts, in MCZ, examined. Emerton, 1890, Trans. Connecticut Acad. Sci., 8: 186, pl. 6, figs. 2–2d, ♂, ♀.

Anyphaena celer, Simon, 1897, Hist. Natur. Araign., 2: 96. Bryant, 1931, Psyche, 38: 111, pl. 6, fig. 9, pl. 8, figs. 25, 28, ♂, ♀. Chickering, 1939, Pap. Michigan Acad. Sci., 24: 51, figs.

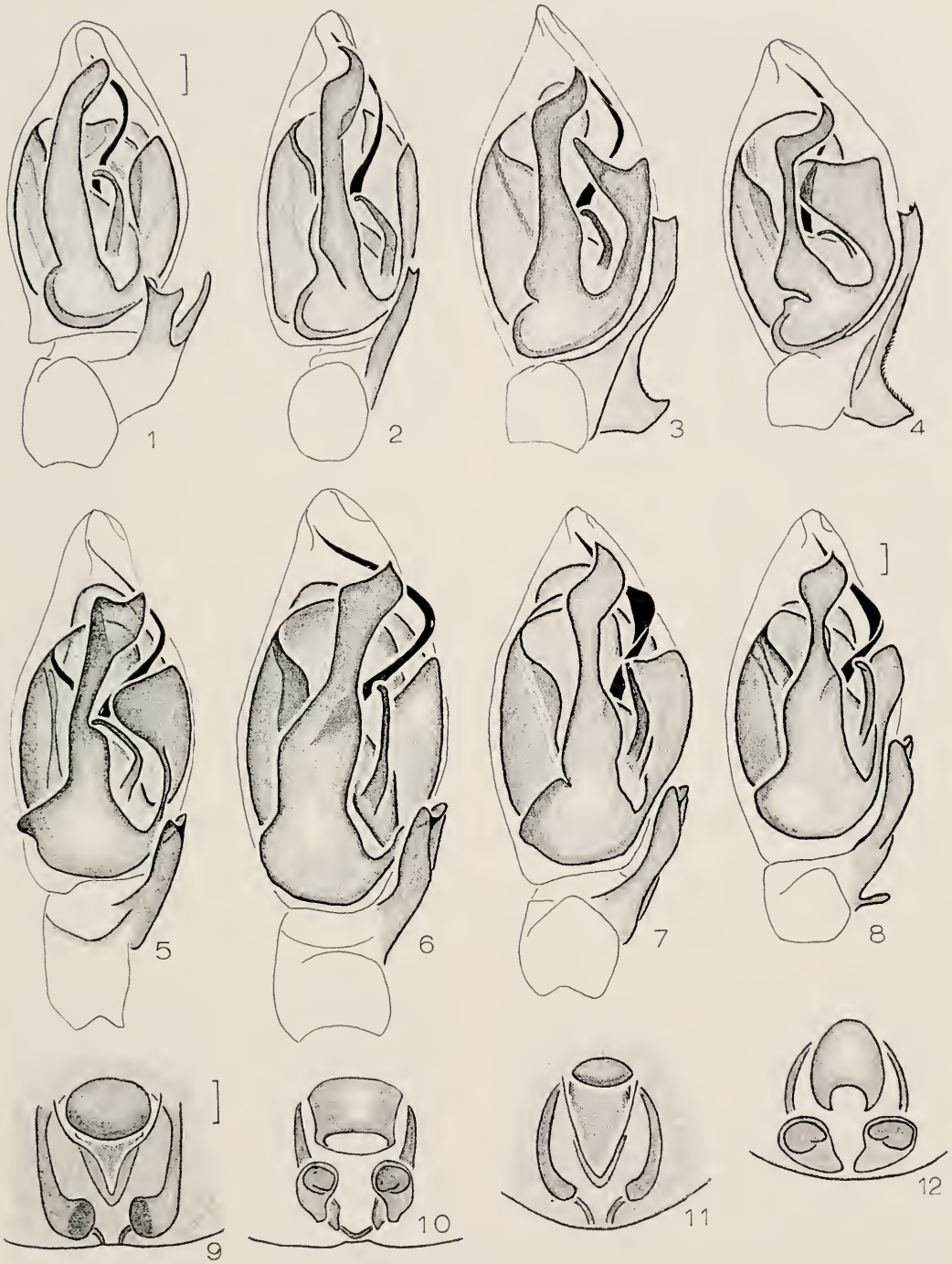

Plate 1

Figures 1–8. Left palpi, ventral view. Figures 9, 11. Epigyna, ventral view. Figures 10, 12. Internal genitalia, dorsal view. 1, 9, 10. *Anyphaena celer* (Hentz). 2, 11, 12. *Anyphaena maculata* (Banks). 3. *Anyphaena crebrispina* Chamberlin. 4. *Anyphaena dixiana* (Chamberlin and Woodbury). 5. *Anyphaena judicata* O. P.-Cambridge. 6. *Anyphaena marginalis* (Banks). 7. *Anyphaena rita* new species. 8. *Anyphaena autumna* new species.

1–4, ♂, ♀. Comstock, 1940, Spider Book, rev. ed., p. 577, figs. 634–635, ♂, ♀. Kaston, 1948, Bull. Connecticut Geol. Natur. Hist. Surv., 70: 407, figs. 1471–1476, ♂, ♀. Roewer, 1954, Katalog der Araneae, 2:528. Bonnet, 1955, Bibliographia Araneorum, 2: 343.

Gayenna celer, Comstock, 1912, Spider Book, p. 563, figs. 634–635, ♂, ♀.

Diagnosis. *Anyphaena celer* is most closely related to *A. maculata*. Males of both species have dorsal and ventral RTA prongs roughly equal in length, but *A. celer* males may be distinguished by the translucent ridge on their dorsal prong (Fig. 18). Females may be separated by the straight epigynal sidepieces and widely oval epigynal hood of *A. celer* (Fig. 9).

Male (Jackson Co., Illinois). Total length 4.54 mm. Carapace 2.12 mm long, 1.58 mm wide, cephalic width 0.83 mm, clypeus height 0.07 mm, pale yellow with thin dark broken border and two dark paramedian longitudinal bands. Eyes: diameters (mm): AME 0.06, ALE 0.12, PME 0.11, PLE 0.12; anterior eye row 0.44 mm long, slightly recurved; posterior eye row 0.60 mm long, procurved; MOQ length 0.24 mm, front width 0.19 mm, back width 0.31 mm; eye interdistances (mm): AME–AME 0.06, AME–ALE 0.03, PME–PME 0.10, PME–PLE 0.10, ALE–PLE 0.05.

Sternum 1.06 mm long, 0.94 mm wide, pale yellow with dark markings opposite coxae, translucent border and darkened extensions to coxae. Chelicerae 0.79 mm long with 4 promarginal teeth and 8 retromarginal denticles, pale yellow with boss outlined in gray. Labium and endites pale yellow, darkest proximally; endites not invaginated.

Abdomen 2.30 mm long, 1.62 mm wide, pale white with transverse rows of dark markings; venter with scattered dark markings. Epigastric furrow 0.85 mm from tracheal spiracle, spiracle 0.88 mm from base of spinnerets.

Legs pale yellow with scattered dark markings. Tibial lengths (mm) and indices: I 1.98, 12; II 1.82, 14; III 1.17, 21; IV 1.73, 16. Ventral spination: tibiae I–IV 2–2–2; metatarsi I, II 2–2–0, III 2–0–2, IV 2–2–2. Femur III thickened distally with clump of short thick setae ventrally. Tibia III ventral spines 1, 2 on retrolateral side thickened, cone-like. Coxae III, IV prolateral ventral surface with clump of short thick setae.

Palpus as in Figures 1, 18.

Female (Wayne Co., Ohio). Coloration as in male. Total length 5.87 mm. Carapace 2.07 mm long, 1.39 mm wide, cephalic width 0.86 mm, clypeus height 0.05 mm. Eyes: diameters (mm): AME 0.05, ALE 0.10, PME 0.10, PLE 0.10; anterior eye row 0.42 mm long, recurved; posterior eye row 0.58 mm long, procurved; MOQ length 0.30 mm, front width 0.19 mm, back width 0.32 mm; eye interdistances (mm): AME–AME 0.07, AME–ALE 0.05, PME–PME 0.12, PME–PLE 0.07, ALE–PLE 0.08.

Sternum 0.99 mm long, 0.88 mm wide. Chelicerae 0.76 mm long with teeth as in male.

Abdomen 4.10 mm long, 2.13 mm wide. Epigastric furrow 1.57 mm from tracheal spiracle, spiracle 1.37 mm from base of spinnerets.

Legs unmodified. Tibial lengths (mm) and indices: I 1.58, 15; II 1.42, 16; III 1.01, 24; IV 1.60, 15. Ventral spination: tibiae I, II 2–2–2, III, IV 1–1–2; metatarsi I, II 2–2–0, III 2–0–2, IV 2–2–2.

Epigynum as in Figure 9, internal genitalia as in Figure 10.

Natural history. Mature males have been taken every month except June, mature females year-round. Specimens have been taken in houses, deciduous forests, on leaves, flowers, treesides, in pitfalls and footprints in snow.

Distribution. Eastern United States from southern New England west to Wisconsin, south to Florida and Texas (Map 1).

Anyphaena maculata (Banks)
Map 1; Figures 2, 11, 12, 19

Gayenna maculata Banks, 1896, Trans. Amer. Ent. Soc., 23: 64. Male holotype from Washington, D.C., in MCZ, examined. Bishop and

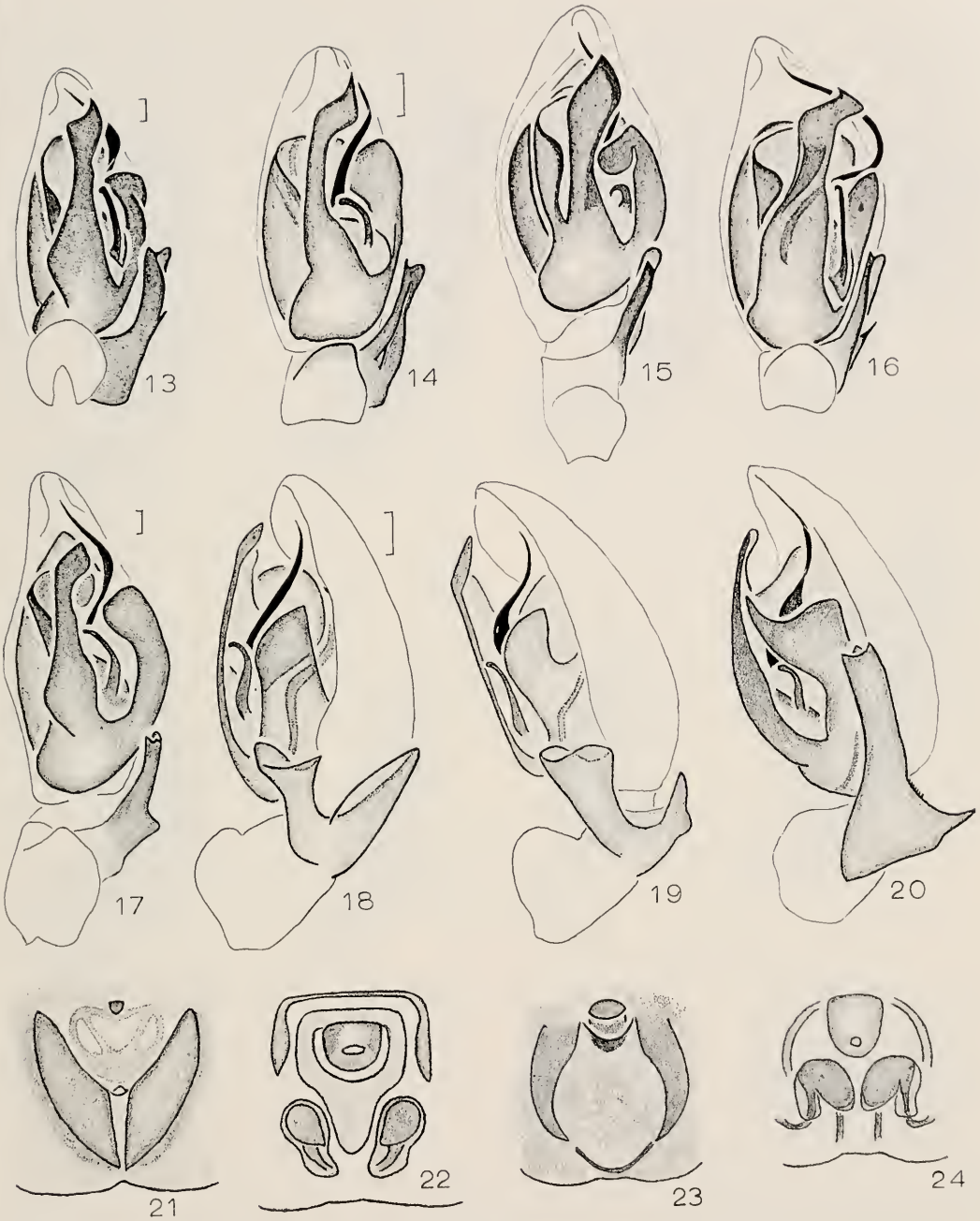

Plate 2

Figures 13–17. Left palpi, ventral view. Figures 18–20. Left palpi, retrolateral view. Figures 21, 23. Epigyna, ventral view. Figures 22, 24. Internal genitalia, dorsal view. 13. *Anyphaena cochise* new species. 14. *Anyphaena gibboides* new species. 15. *Anyphaena catalina* new species. 16. *Anyphaena hespar* new species. 17. *Anyphaena arbida* new species. 18. *Anyphaena celer* (Hentz). 19. *Anyphaena maculata* (Banks). 20, 21, 22. *Anyphaena crebrispina* Chamberlin. 23, 24. *Anyphaena dixiana* (Chamberlin and Woodbury).

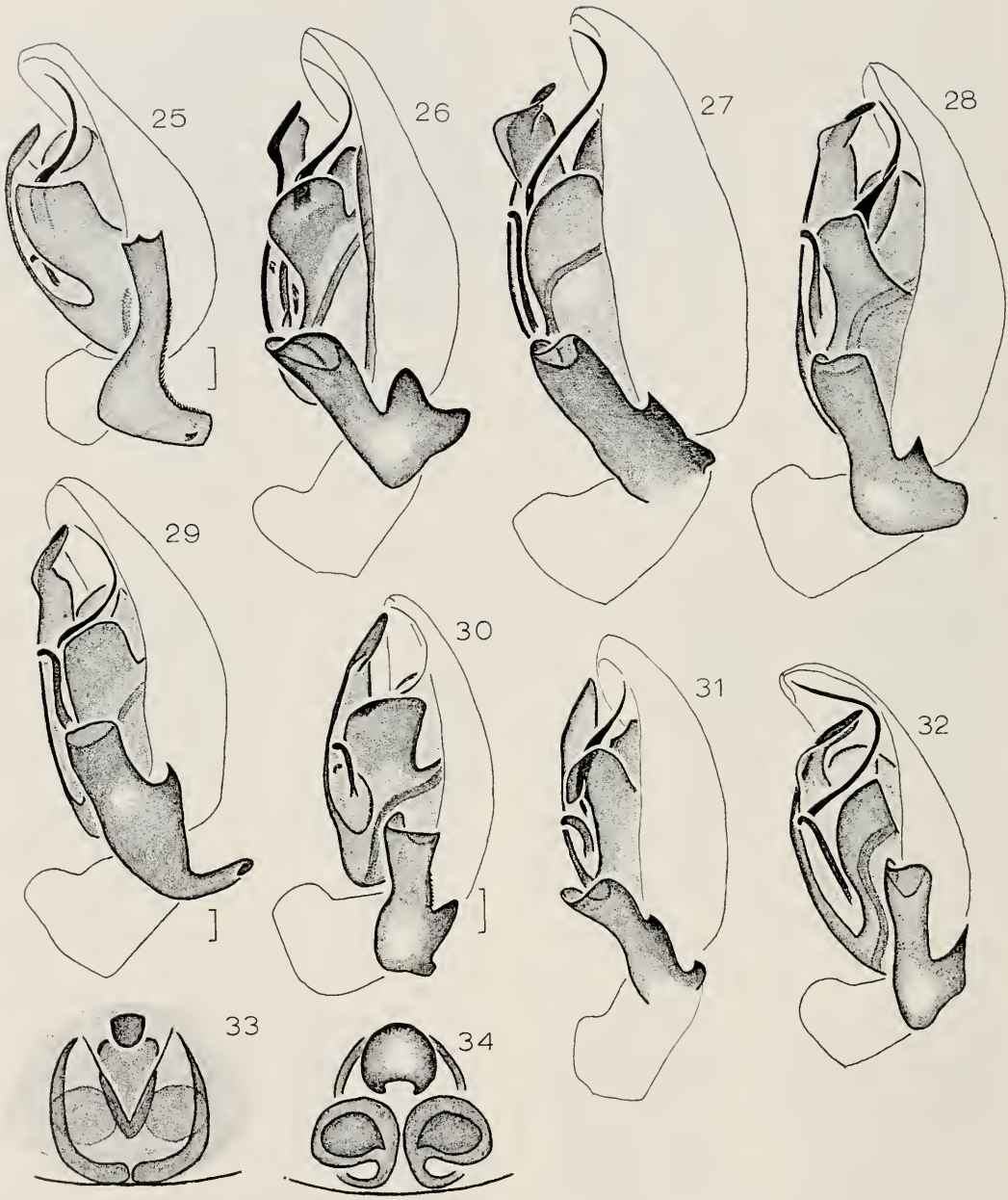

Plate 3

Figures 25–32. Left palpi, retrolateral view. Figure 33. Epigynum, ventral view. Figure 34. Internal genitalia, dorsal view. 25. *Anyphaena dixiana* (Chamberlin and Woodbury). 26, 33, 34. *Anyphaena judicata* O. P.-Cambridge. 27. *Anyphaena marginalis* (Banks). 28. *Anyphaena rita* new species. 29. *Anyphaena autumna* new species. 30. *Anyphaena gibboides* new species. 31. *Anyphaena catalina* new species. 32. *Anyphaena hespar* new species.

Crosby, 1926, J. Elisha Mitchell Sci. Soc., 41: 189, pl. 24, figs. 37, 38, ♂, ♀.

Anyphaena maculata, Simon, 1897, Hist. Natur. Araign., 2: 96. Bryant, 1931, Psyche, 38: 111, pl. 6, fig. 8, pl. 8, fig. 31, ♂, ♀. Kaston, 1948, Bull. Connecticut Geol. Natur. Hist. Surv., 70: 409, figs. 1457–1458, ♂, ♀. Roewer, 1954, Katalog der Araneae, 2: 529. Bonnet, 1955, Bibliographia Araneorum, 2: 345.

Diagnosis. *Anyphaena maculata* is most closely related to *A. celer*. Males may be distinguished by the short dorsal prong of the RTA, which lacks a translucent ridge (Figure 19); females by their rounded epigynal sidepieces and narrowly oval epigynal hood (Figure 11).

Male (Durham Co., North Carolina). Coloration as in *Anyphaena celer*. Total length 3.74 mm. Carapace 2.09 mm long, 1.54 mm wide, cephalic width 0.77 mm, clypeus height 0.08 mm. Eyes: diameters (mm): AME 0.07, ALE 0.11, PME 0.10, PLE 0.10; anterior eye row 0.44 mm long, recurved; posterior eye row 0.58 mm long, procurved; MOQ length 0.23 mm, front width 0.20 mm, back width 0.31 mm; eye interdistances (mm): AME–AME 0.05, AME–ALE 0.03, PME–PME 0.10, PME–PLE 0.10, ALE–PLE 0.04.

Sternum 1.08 mm long, 0.79 mm wide. Chelicerae 0.63 mm long with 4 promarginal teeth and 8 retromarginal denticles.

Abdomen 2.02 mm long, 1.08 mm wide. Epigastric furrow 0.31 mm from tracheal spiracle, spiracle 0.41 mm from base of spinnerets.

Tibial lengths (mm) and indices: I 2.00, 11; II 1.75, 13; III 1.12, 24; IV 1.82, 15. Ventral spination: tibiae I, II 2–2–2*, III, IV 2–2–2; metatarsi I 2–1–0, II 2–2–0, III 2–0–2, IV 2–2–2. Modifications of third leg as in *A. celer*.

Palpus as in Figures 2, 19.

Female (Pope Co., Illinois). Coloration as in male of *A. celer*.

Total length 4.68 mm. Carapace 2.07 mm long, 1.60 mm wide, cephalic width 0.97 mm, clypeus height 0.08 mm. Eyes: diameters (mm): AME 0.08, ALE 0.10, PME 0.10, PLE 0.11; anterior eye row 0.48 mm long, recurved; posterior eye row 0.63 mm long, procurved; MOQ length 0.30 mm, front width 0.22 mm, back width 0.33 mm; eye interdistances (mm): AME–AME 0.07, AME–ALE 0.04, PME–PME 0.14, PME–PLE 0.11, ALE–PLE 0.05.

Sternum 1.15 mm long and 0.95 mm wide. Chelicerae 0.71 mm long with teeth as in male.

Abdomen 3.02 mm long, 2.11 mm wide. Epigastric furrow 0.85 mm from tracheal spiracle, spiracle 0.90 mm from base of spinnerets.

Legs unmodified. Tibial lengths (mm) and indices: I 1.42, 18; II 1.48, 18; III 0.99, 25; IV 1.58, 16. Ventral spination: tibiae I, II 2–2–2*, III 1–1–2, IV 2–1–2; metatarsi I, II 2–2–0, III 2–0–2, IV 2–2–2.

Epigynum as in Figure 11, internal genitalia as in Figure 12.

Natural history. Mature males have been taken from late September through early February, mature females from mid-October through mid-April. Specimens have been taken from Spanish moss, by sweeping in bottomland pine and hardwood forests, by sifting leaves and by Malaise trap.

Distribution. Mid-eastern states from Long Island south to North Carolina, west to southern Illinois, eastern Missouri and northern Alabama (Map 1).

Anyphaena crebrispina Chamberlin

Map 1; Figures 3, 20, 21, 22

Anyphaena crebrispina Chamberlin, 1919, Pomona Coll. J. Ent. Zool., 12: 10, pl. 4, fig. 4 (♂). Male holotype from Claremont, California, in MCZ, examined. Bryant, 1931, Psyche, 38: 113, pl. 6, fig. 11, ♂. Roewer, 1954, Katalog der Araneae, 2: 528. Bonnet, 1955, Bibliographia Araneorum, 2: 343.

Anyphaena zina Chamberlin, 1919, Pomona Coll. J. Ent. Zool., 12:11, pl. 4, fig. 5 (♀). Female holotype from Claremont, California, in MCZ, examined. Roewer, 1954, Katalog der Araneae, 2: 530. Bonnet, 1955, Bibliographia Araneorum, 2: 349. NEW SYNONYMY.

Diagnosis. *Anyphaena crebrispina* is the most aberrant member of the *celer* group, but is most closely related to *A. dixiana*.

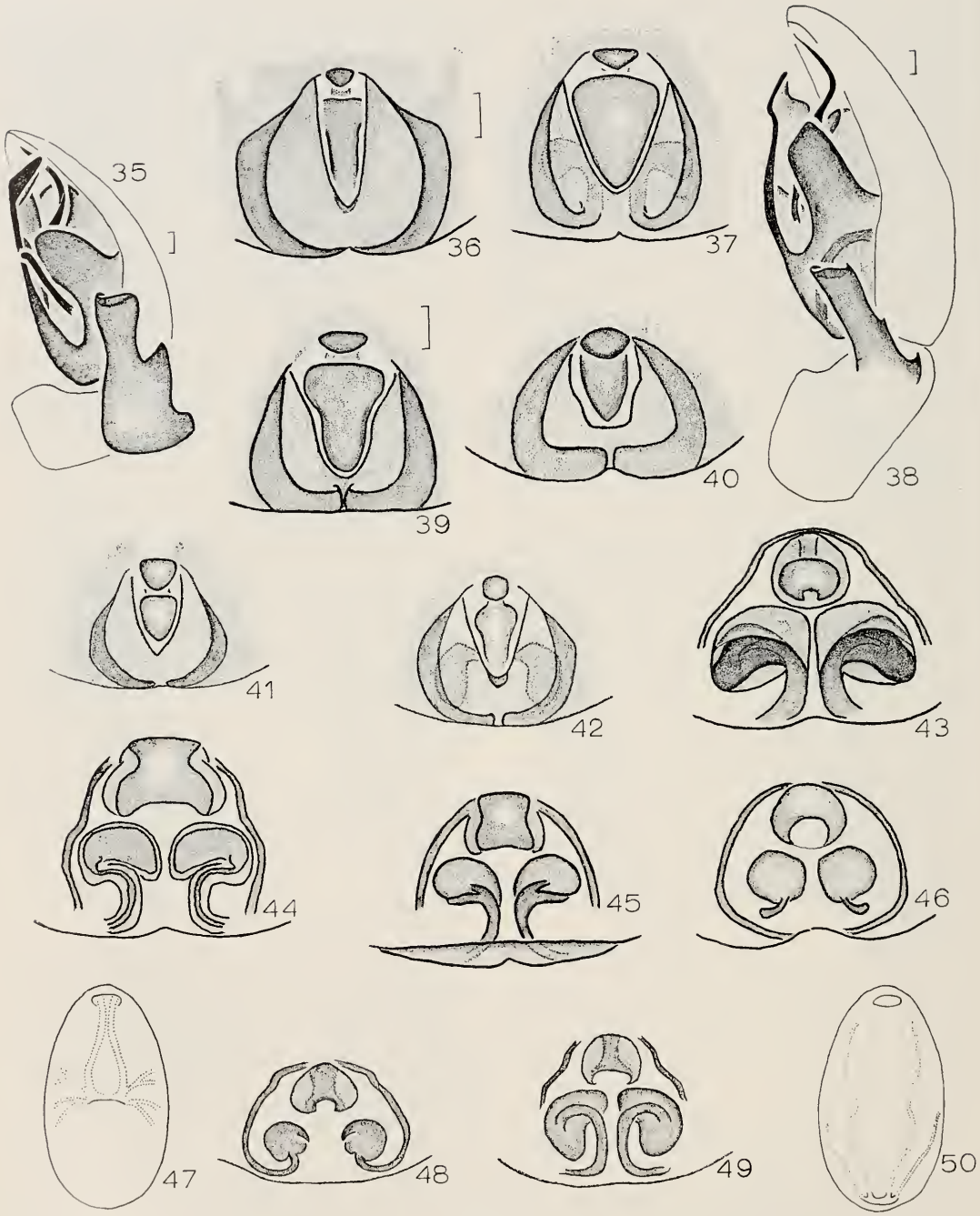

Plate 4

Figures 35, 38. Left palpi, retrolateral view. Figures 36, 37, 39–42. Epigyna, ventral view. Figures 43–46, 48, 49. Internal genitalia, dorsal view. Figure 47. Anyphaenid tracheae, diagrammatic. Figure 50. Clubionid tracheae, diagrammatic. 35. *Anyphaena cochise* new species. 36, 43. *Anyphaena marginalis* (Banks). 37, 44. *Anyphaena rita* new species. 38. *Anyphaena arbida* new species. 39, 45. *Anyphaena autumna* new species. 40, 46. *Anyphaena gibboides* new species. 41, 48. *Anyphaena catalina* new species. 42, 49. *Anyphaena hespar* new species.

Males of *A. crebrispina* may be readily distinguished by the greatly expanded base of the RTA (Fig. 20). If this species were known solely from the female, it would be impossible to place it in the *celer* group: the epigynum, with its greatly expanded sidepieces and its lack of an externally visible midpiece, is totally unlike that of any other species in this group (Fig. 21).

Male (Los Angeles Co., California). Coloration as in *Anyphaena celer*. Total length 4.61 mm. Carapace 2.00 mm long, 1.57 mm wide, cephalic width 0.74 mm, clypeus height 0.10 mm. Eyes: diameters (mm): AME 0.07, ALE 0.10, PME 0.10, PLE 0.10; anterior eye row 0.43 mm long, recurved; posterior eye row 0.56 mm long, procurved; MOQ length 0.25 mm, front width 0.18 mm, back width 0.29 mm; eye interdistances (mm): AME–AME 0.04, AME–ALE 0.02, PME–PME 0.09, PME–PLE 0.09, ALE–PLE 0.04.

Sternum 1.10 mm long, 0.88 mm wide. Chelicerae 0.55 mm long with 5 promarginal teeth and 8 retromarginal denticles.

Abdomen 2.65 mm long, 1.58 mm wide. Epigastric furrow 0.79 mm from tracheal spiracle, spiracle 0.68 mm from base of spinnerets.

Tibial lengths (mm) and indices: I 1.69, 13; II 1.51, 15; III 1.06, 22; IV 1.69, 14. Ventral spination: tibiae I 2–2–2*, II 1–2–2*, III 1–2–2, IV 2–2–2; metatarsi I, II 2–2–0, III 2–0–2, IV 2–2–2. Modifications of third leg as in *A. celer*.

Palpus as in Figures 3, 20.

Female (Los Angeles Co., California). Coloration as in male of *A. celer*. Total length 4.39 mm. Carapace 1.85 mm long, 1.37 mm wide, cephalic width 0.77 mm, clypeus height 0.08 mm. Eyes: diameters (mm): AME 0.07, ALE 0.09, PME 0.09, PLE 0.09; anterior eye row 0.41 mm long, recurved; posterior eye row 0.56 mm long, procurved; MOQ length 0.23 mm, front width 0.18 mm, back width 0.28 mm; eye interdistances (mm): AME–AME 0.04, AME–ALE 0.02, PME–PME 0.10, PME–PLE 0.08, ALE–PLE 0.04.

Sternum 1.08 mm long, 0.86 mm wide. Chelicerae 0.64 mm long with 4 promarginal teeth and 9 retromarginal denticles.

Abdomen 2.99 mm long, 1.98 mm wide. Epigastric furrow 0.95 mm from tracheal spiracle, spiracle 0.90 mm from base of spinnerets.

Legs unmodified. Tibial lengths (mm) and indices: I 1.39, 15; II 1.31, 16; III 0.75, 28; IV 1.44, 14. Ventral spination: tibiae I 2–2–2*, II 1–2–0, III 1–1–0, IV 1–1–2; metatarsi as in male.

Epigynum as in Figure 21, internal genitalia as in Figure 22.

Natural history. Mature males have been taken in November, mature females from early December through late April. Specimens have been taken by Berlese funnel sampling of grape bark.

Distribution. Central and southern California (Map 1).

Anyphaena dixiana (Chamberlin and Woodbury), new combination

Map 1; Figures 4, 23, 24, 25

Gayenna dixiana Chamberlin and Woodbury, 1929, Proc. Biol. Soc. Washington, 42: 138, pl. 1, fig. 3 (♀). Female holotype from St. George, Utah, in AMNH, examined. Roewer, 1954, Katalog der Araneae, 2: 540 (*G. dixima* [sic]). Bonnet, 1957, Bibliographia Araneorum, 2: 1977.

Anyphaena coloradensis Bryant, 1931, Psyche, 38: 112, pl. 6, figs. 9, 10, pl. 7, figs. 30, 33 (♂, ♀). Male holotype, female allotype from Boulder, Colorado, in MCZ, examined. Roewer, 1954, Katalog der Araneae, 2: 528. Bonnet, 1955, Bibliographia Araneorum, 2: 343. NEW SYNONYMY.

Diagnosis. This distinctive species is closest to *Anyphaena crebrispina*, but may be quickly recognized by the spur borne on the dorsal prong of the RTA of males (Fig. 25) and the greatly reduced epigynal midpiece of females (Fig. 23).

Male (Cochise Co., Arizona). Coloration as in *Anyphaena celer* except that posterior spinnerets have dorsal surface sharply divided into dark brown lateral and pale orange median halves.

Total length 3.85 mm. Carapace 1.67

mm long, 1.44 mm wide, cephalic width 0.65 mm, clypeus height 0.07 mm. Eyes: diameters (mm): AME 0.06, ALE 0.09, PME 0.09, PLE 0.10; anterior eye row 0.39 mm long, recurved; posterior eye row 0.51 mm long, procurved; MOQ length 0.25 mm, front width 0.16 mm, back width 0.26 mm; eye interdistances (mm): AME–AME 0.04, AME–ALE 0.03, PME–PME 0.08, PME–PLE 0.08, ALE–PLE 0.05.

Sternum 0.96 mm long, 0.76 mm wide. Chelicerae 0.53 mm long with 4 promarginal teeth and 6 retromarginal denticles. Endites slightly invaginated at middle.

Abdomen 2.56 mm long, 1.49 mm wide. Epigastric furrow 0.76 mm from tracheal spiracle, spiracle 0.76 mm from base of spinnerets.

Tibial lengths (mm) and indices: I 1.69, 11; II 1.37, 14; III 0.81, 28; IV 1.44, 16. Ventral spination: tibiae I, II 2–2–2*, III, IV 1–2–2; metatarsi I, II 2–2–0, III 2–0–2, IV 2–2–2. Modifications of third leg as in *A. celer*.

Palpus as in Figures 4, 25.

Female (Cochise Co., Arizona). Coloration as in male. Total length 4.14 mm. Carapace 2.03 mm long, 1.57 mm wide, cephalic width 0.86 mm, clypeus height 0.09 mm. Eyes: diameters (mm): AME 0.05, ALE 0.08, PME 0.09, PLE 0.10; anterior eye row 0.43 mm long, recurved; posterior eye row 0.60 mm long, procurved; MOQ length 0.26 mm, front width 0.20 mm, back width 0.32 mm; eye interdistances (mm): AME–AME 0.09, AME–ALE 0.05, PME–PME 0.15, PME–PLE 0.09, ALE–PLE 0.07.

Sternum 1.15 mm long, 0.86 mm wide. Chelicerae 0.71 mm long with 5 promarginal teeth and 8 retromarginal denticles.

Abdomen 2.50 mm long, 1.69 mm wide. Epigastric furrow 0.60 mm from tracheal spiracle, spiracle 0.67 mm from base of spinnerets.

Legs unmodified. Tibial lengths (mm) and indices: I 1.46, 16; II 1.33, 17; III 0.94, 24; IV 1.49, 17. Ventral spination as in male.

Epigynum as in Figure 23, internal genitalia as in Figure 24.

Natural history. Mature males have been taken from mid-August through mid-May, mature females from late September through late April. Specimens have been taken from 5400 to 9000 feet (1650–2750 m), in yellow pine/oak and montane forests, in alfalfa, under dead agave and frequently in houses.

Distribution. Northcentral Colorado south to western Texas, west to southern California (Map 1).

Anyphaena judicata O. P.-Cambridge
Map 1; Figures 5, 26, 33, 34

Anyphaena judicata O. P.-Cambridge, 1896, Biologia Centrali Americana, Aran., 1: 203, pl. 26, fig. 4 (♂). Male holotype from Omiltemi, Guerrero, Mexico, in BMNH, examined. F. O. P.-Cambridge, 1900, Biologia Centrali Americana, Aran., 2: 96, pl. 7, fig. 9, ♂. Roewer, 1954, Katalog der Araneae, 2: 525. Bonnet, 1955, Bibliographia Araneorum, 2: 345.

Diagnosis. Anyphaena judicata is most closely related to an unnamed Mexican species (or group of species) and has no close relatives among the species occurring north of Mexico. Males may be easily recognized by the distinctive form of the dorsal prong of the RTA (Fig. 26). The female epigynum is closest to that of *A. marginalis*, but the midpiece is proportionately shorter and wider and the sidepieces are narrower and diminish in width anteriorly smoothly, without the sharp decrease in width shown by *A. marginalis* (Fig. 33).

Male (Cochise Co., Arizona). Coloration as in *Anyphaena celer*, except that posterior spinnerets have entire dorsal surface dark brown.

Total length 3.46 mm. Carapace 1.76 mm long, 1.44 mm wide, cephalic width 0.68 mm, clypeus height 0.09 mm. Eyes: diameters (mm): AME 0.06, ALE 0.10, PME 0.09, PLE 0.10; anterior eye row 0.40 mm long, recurved; posterior eye row 0.52 mm long, procurved; MOQ length 0.26 mm, front width 0.17 mm, back width

0.28 mm; eye interdistances (mm): AME–AME 0.05, AME–ALE 0.03, PME–PME 0.11, PME–PLE 0.06, ALE–PLE 0.04.

Sternum 0.95 mm long, 0.68 mm wide. Chelicerae 0.56 mm long with 4 promarginal teeth and 7 retromarginal denticles.

Abdomen 1.80 mm long, 1.15 mm wide. Epigastric furrow 0.61 mm from tracheal spiracle, spiracle 0.63 mm from base of spinnerets.

Tibial lengths (mm) and indices: I 2.25, 6; II 1.93, 8; III 1.01, 21; IV 1.66, 11. Ventral spination: tibiae I 4–2–2*, II 3–2–2*, III 1–2–0, IV 1–1–2; metatarsi I, II, 2–2–0, III 2–0–2; IV 1–2–2. Femur III unmodified. Tibia III ventral spine 1 on retrolateral side missing, ventral spine 2 thickened, cone-like. Coxae I, II and III (but not IV) with a small number of short, thick setae. Coxae III with a tubercule.

Palpus as in Figures 5, 26.

Female (Cochise Co., Arizona). Coloration as in male.

Total length 4.72 mm. Carapace 1.76 mm long, 1.37 mm wide, cephalic width 0.81 mm, clypeus height 0.06 mm. Eyes: diameters (mm): AME 0.07, ALE 0.10, PME 0.10, PLE 0.10; anterior eye row 0.44 mm long, recurved; posterior eye row 0.60 mm long, procurved; MOQ length 0.29 mm, front width 0.21 mm, back width 0.32 mm; eye interdistances (mm): AME–AME 0.07, AME–ALE 0.03, PME–PME 0.13, PME–PLE 0.09, ALE–PLE 0.05.

Sternum 0.97 mm long, 0.77 mm wide. Chelicerae 0.58 mm long with teeth as in male.

Abdomen 3.13 mm long, 2.09 mm wide. Epigastric furrow 1.21 mm from tracheal spiracle, spiracle 1.31 mm from base of spinnerets.

Legs unmodified. Tibial lengths (mm) and indices: I 1.69, 11; II 1.31, 14; III 0.88, 23; IV 1.66, 12. Ventral spination as in male.

Epigynum as in Figure 33, internal genitalia as in Figure 34.

Natural history. Mature males have been taken from mid-June through mid-August, mature females from late March to November, most in July and August. Specimens have been taken from 5100 to 8000 feet (1550–2450 m), by sweeping and under rocks.

Distribution. Arizona south to Guerrero, Mexico (Map 1).

Anyphaena marginalis (Banks), new combination
Map 1; Figures 6, 27, 36, 43

Gayenna marginalis Banks, 1901, Proc. Acad. Natur. Sci. Philadelphia, 53: 574, pl. 23, fig. 22 (♀). Female holotype from Beulah, San Miguel Co., New Mexico, was probably deposited in the MCZ along with the other types from this paper but was not found by Bryant when the MCZ types were cataloged; lost, presumed destroyed. Roewer, 1954, Katalog der Araneae, 2: 540. Bonnet, 1957, Bibliographia Araneorum, 2: 1978.

Diagnosis. Anyphaena marginalis is most closely related to *A. hespar*, both species having a simple embolus and elongated conductor. Males of *A. marginalis* (Fig. 27), however, do not have the spine-like dorsal prong of the RTA of *A. hespar*, and females of *A. marginalis* (Fig. 36) do not have the conspicuous bulge in the epigynal midpiece which characterizes *A. hespar* females.

Male (Graham Co., Arizona). Coloration as in *Anyphaena celer*.

Total length 3.78 mm. Carapace 1.98 mm long, 1.60 mm wide, cephalic width 0.72 mm, clypeus height 0.09 mm. Eyes: diameters (mm): AME 0.06, ALE 0.10, PME 0.08, PLE 0.10; anterior eye row 0.40 mm long, straight; posterior eye row 0.55 mm long, procurved; MOQ length 0.20 mm, front width 0.17 mm, back width 0.28 mm; eye interdistances (mm): AME–AME 0.05, AME–ALE 0.02, PME–PME 0.11, PME–PLE 0.08, ALE–PLE 0.04.

Sternum 1.13 mm long, 0.81 mm wide. Chelicerae 0.54 mm long with 5 promarginal teeth and 6 retromarginal denticles.

Abdomen 2.00 mm long, 1.33 mm wide. Epigastric furrow 0.52 mm from tracheal

spiracle, spiracle 0.59 mm from base of spinnerets.

Tibial lengths (mm) and indices: I 1.67, 13; II 1.35, 16; III 1.03, 26; IV 1.62, 14. Ventral spination: tibiae I 4–2–2*, II 2–2–2*, III, IV 1–2–2; metatarsi I, II 2–2–0, III 2–0–2, IV 2–2–2. Femur III unmodified. Tibia III ventral spine 1 on retrolateral side missing. Coxae unmodified.

Palpus as in Figures 6, 27.

Female (Graham Co., Arizona). Coloration as in male of *A. celer*.

Total length 4.26 mm. Carapace 2.11 mm long, 1.55 mm wide, cephalic width 0.86 mm, clypeus height 0.08 mm. Eyes: diameters (mm): AME 0.07, ALE 0.10, PME 0.11, PLE 0.10; anterior eye row 0.44 mm long, straight; posterior eye row 0.64 mm long, procurved; MOQ length 0.30 mm, front width 0.19 mm, back width 0.33 mm; eye interdistances (mm): AME–AME 0.05, AME–ALE 0.03, PME–PME 0.12, PME–PLE 0.09, ALE–PLE 0.06.

Sternum 1.05 mm long, 0.80 mm wide. Chelicerae 0.65 mm long with 4 promarginal teeth and 8 retromarginal denticles.

Abdomen 2.52 mm long, 1.53 mm wide. Epigastric furrow 0.67 mm from tracheal spiracle, spiracle 0.68 mm from base of spinnerets.

Legs unmodified. Tibial lengths (mm) and indices: I 1.44, 18; II 1.21, 21; III 0.99, 25; IV 1.60, 17. Ventral spination as in male except tibia III 1–1–2.

Epigynum as in Figure 36, internal genitalia as in Figure 43.

Natural history. Mature males have been taken from late August through late May, mature females in all months except January and October. Specimens have been taken from 6000 to 9300 feet (1850–2850 m), in yellow pine/oak forests and under rocks. I found this species in great abundance by sorting pine litter at Rustler's Park in the Chiricahua Mountains of southeastern Arizona in August 1972.

Distribution. Arizona, New Mexico and Colorado (Map 1).

Anyphaena hespar new species
Map 1; Figures 16, 32, 42, 49

Types. Male holotype, female paratype from Bear Canyon, Santa Catalina Mountains, Pima Co., Arizona, 8 December 1968 (Karl Stephan), deposited in AMNH. Male and female paratypes from Pima Co., Arizona, deposited in MCZ. The specific name is an arbitrary combination of letters.

Diagnosis. Anyphaena hespar is most closely related to *A. marginalis*. Males of the former may be distinguished by the spine-like dorsal prong of their RTA (Fig. 32), females by the conspicuous bulge in their epigynal midpiece (Fig. 42).

Male (Pima Co., Arizona). Coloration as in *Anyphaena celer*.

Total length 3.13 mm. Carapace 1.62 mm long, 1.31 mm wide, cephalic width 0.59 mm, clypeus height 0.08 mm. Eyes: diameters (mm): AME 0.05, ALE 0.08, PME 0.08, PLE 0.08; anterior eye row 0.33 mm long, straight; posterior eye row 0.45 mm long, procurved; MOQ length 0.19 mm, front width 0.14 mm, back width 0.24 mm; eye interdistances (mm): AME–AME 0.05, AME–ALE 0.03, PME–PME 0.08, PME–PLE 0.07, ALE–PLE 0.04.

Sternum 0.95 mm long, 0.79 mm wide. Chelicerae 0.39 mm long with 4 promarginal teeth and 8 retromarginal denticles.

Abdomen 1.80 mm long, 1.10 mm wide. Epigastric furrow 0.56 mm from tracheal spiracle, spiracle 0.56 mm from base of spinnerets.

Tibial lengths (mm) and indices: I 1.31, 17; II 1.08, 21; III 0.81, 28; IV 1.39, 18. Ventral spination: tibiae I 4–2–2*, II 3–2–2*, III 1–2–2, IV 2–2–2; metatarsi I, II 2–2–0, III 2–0–2, IV 2–2–2. Femur III unmodified. Tibia III ventral spine 1 on retrolateral side missing, spine 2 thickened, cone-like. Coxae unmodified.

Palpus as in Figures 16, 32.

Female (Pima Co., Arizona). Coloration as in male of *A. celer*.

Total length 3.06 mm. Carapace 1.55 mm long, 1.26 mm wide, cephalic width 0.67 mm, clypeus height 0.06 mm. Eyes:

diameters (mm): AME 0.05, ALE 0.08, PME 0.08, PLE 0.08; anterior eye row 0.33 mm long, straight; posterior eye row 0.49 mm long, procurved; MOQ length 0.20 mm, front width 0.14 mm, back width 0.26 mm; eye interdistances (mm): AME–AME 0.05, AME–ALE 0.03, PME–PME 0.10, PME–PLE 0.07, ALE–PLE 0.04.

Sternum 1.04 mm long, 0.70 mm wide. Chelicerae 0.47 mm long with teeth as in male.

Abdomen 1.85 mm long, 1.08 mm wide. Epigastric furrow 0.49 mm from tracheal spiracle; spiracle 0.41 mm from base of spinnerets.

Legs unmodified. Tibial lengths (mm) and indices: I 1.13, 20; II 0.92, 25; III 0.72, 33; IV 1.26, 18. Ventral spination: tibiae I, II 4–2–2*, III 1–1–2, IV 1–2–2; metatarsi as in male.

Epigynum as in Figure 42, internal genitalia as in Figure 49.

Natural history. Mature males and females have been taken from late October through early April. Specimens have been taken from leaf litter and under rocks.

Distribution. Southeastern Arizona (Map 1).

Anyphaena rita new species
Map 1; Figures 7, 28, 37, 44

Types. Male holotype, female paratype from Bear Canyon, Santa Catalina Mountains, Pima Co., Arizona, 8 December 1968 (Karl Stephan), deposited in AMNH. Male and female paratypes from Pima Co., Arizona, deposited in MCZ. The specific name is a noun in apposition derived from the Santa Rita Mountains, where the species is abundant.

Diagnosis. Anyphaena rita is most closely related to *A. cochise*, both species having a conspicuously enlarged region of the embolus and a slightly recurved tip of the median apophysis. Males of *A. rita* (Fig. 28) may be distinguished by their smaller size and by the differences in the dorsal prong of the RTA. Females of *A. cochise* are unknown, but the epigynum of *A. rita*, with its extremely broad midpiece, is quite distinctive (Fig. 37).

Male (Pima Co., Arizona). Coloration as in *Anyphaena celer*.

Total length 4.10 mm. Carapace 1.94 mm long, 1.60 mm wide, cephalic width 0.67 mm, clypeus height 0.07 mm. Eyes: diameters (mm): AME 0.05, ALE 0.08, PME 0.09, PLE 0.09; anterior eye row 0.36 mm long, recurved; posterior eye row 0.53 mm long, procurved; MOQ length 0.22 mm, front width 0.15 mm, back width 0.27 mm; eye interdistances (mm): AME–AME 0.05, AME–ALE 0.03, PME–PME 0.09, PME–PLE 0.09, ALE–PLE 0.05.

Sternum 1.13 mm long, 0.77 mm wide. Chelicerae 0.50 mm long with 4 promarginal teeth and 8 retromarginal denticles.

Abdomen 2.30 mm long, 1.26 mm wide. Epigastric furrow 0.67 mm from tracheal spiracle, spiracle 0.65 mm from base of spinnerets.

Tibial lengths (mm) and indices: I 1.55, 14; II 1.39, 16; III 0.97, 23; IV 1.62, 14. Ventral spination: tibiae I 4–2–2*, II 3–2–2*, III, IV 2–2–2; metatarsi I, II 2–2–0, III 2–0–2, IV 2–2–2. Femur III unmodified. Tibia III ventral spines not thickened. Coxae III and IV with only a few short thick setae.

Palpus as in Figures 7, 28.

Female (Pima Co., Arizona). Coloration as in male of *A. celer*.

Total length 5.04 mm. Carapace 2.05 mm long, 1.53 mm wide, cephalic width 1.03 mm, clypeus height 0.09 mm. Eyes: diameters (mm): AME 0.05, ALE 0.10, PME 0.10, PLE 0.11; anterior eye row 0.41 mm long, recurved; posterior eye row 0.58 mm long, procurved; MOQ length 0.32 mm, front width 0.18 mm, back width 0.29 mm; eye interdistances (mm): AME–AME 0.07, AME–ALE 0.03, PME–PME 0.09, PME–PLE 0.10, ALE–PLE 0.08.

Sternum 1.13 mm long, 0.81 mm wide. Chelicerae 0.67 mm long with teeth as in male.

Abdomen 2.75 mm long, 1.94 mm wide. Epigastric furrow 1.06 mm from tracheal

spiracle, spiracle 0.95 mm from base of spinnerets.

Legs unmodified. Tibial lengths (mm) and indices: I 1.48, 15; II 1.26, 18; III 1.03, 21; IV 1.58, 17. Ventral spination as in male except tibiae III, IV 1–2–2, metatarsi IV 2–1–2.

Epigynum as in Figure 37, internal genitalia as in Figure 44.

Natural history. Mature males have been taken from mid-October through late March, mature females from early June through early February. Specimens have been taken from 4000 to 6800 feet. (1200–2075 m), in oak/grassland and under rocks.

Distribution. Arizona to Chihuahua, Mexico (Map 1).

Anyphaena cochise new species
Map 1; Figures 13, 35

Types. Male holotype from Rustlers Park, 8600 ft. (2625 m), Chiricahua Mountains, Cochise Co., Arizona, 9 September 1950 (W. J. Gertsch), deposited in AMNH. Male paratype from Cochise Co., Arizona, deposited in MCZ. The specific name is a noun in apposition and refers to the type locality.

Diagnosis. Anyphaena cochise is most closely related to *A. rita*, but the dorsal prong of the RTA is relatively longer in *A. cochise* (Fig. 35). Females of this species are unknown.

Male (Cochise Co., Arizona). Coloration as in *Anyphaena celer.*

Total length 5.44 mm. Carapace 2.52 mm long, 2.09 mm wide, cephalic width 0.88 mm, clypeus height 0.14 mm. Eyes: diameters (mm): AME 0.09, ALE 0.13, PME 0.13, PLE 0.13; anterior eye row 0.53 mm long, straight; posterior eye row 0.75 mm long, procurved; MOQ length 0.30 mm, front width 0.23 mm, back width 0.40 mm; eye interdistances (mm): AME–AME 0.05, AME–ALE 0.04, PME–PME 0.14, PME–PLE 0.11, ALE–PLE 0.06.

Sternum 1.44 mm long, 1.08 mm wide. Chelicerae 0.75 mm long with 4 promarginal teeth and 7 retromarginal denticles.

Abdomen 3.38 mm long, 1.94 mm wide. Epigastric furrow 0.92 mm from tracheal spiracle, spiracle 1.03 mm from base of spinnerets.

Tibial lengths (mm) and indices: I 2.32, 12; II 2.05, 13; III 1.39, 20; IV 2.14, 14. Ventral spination: tibiae I 4–2–2*, II 2–2–2*, III 1–2–2, IV 2–2–2; metatarsi I, II 2–2–0, III 2–0–2, IV 2–2–2. Femur III unmodified. Tibia III ventral spine 1 on retrolateral side thickened slightly. All coxae with a few scattered short thick setae.

Palpus as in Figures 13, 35.

Female. Unknown.

Natural history. Mature males have been taken in early September at 8600 feet (2625 m).

Distribution. Known only from the type locality (Map 1).

Anyphaena autumna new species
Map 1; Figures 8, 29, 39, 45

Types. Male holotype, female paratype from Rustler Camp, Chiricahua Mountains, Cochise Co., Arizona, 9 September 1950 (W. J. Gertsch), deposited in AMNH. Male and female paratypes from Cochise and Graham Co., Arizona, deposited in MCZ. The specific name refers to the season of collection.

Diagnosis. Anyphaena autumna is unlikely to be confused with any other species. The long recurved hook on the RTA and the peculiar form of the tip of the median apophysis are unlike any other species (Figs. 8, 29). The epigynum is closest to that of *A. gibboides*, but the midpiece has a characteristic constriction near its midpoint (Fig. 39).

Male (Cochise Co., Arizona). Coloration as in *Anyphaena celer*, though the paramedian bands on the carapace are darker and wider than in that species.

Total length 5.51 mm. Carapace 2.50 mm long, 1.98 mm wide, cephalic width 1.03 mm, clypeus height 0.12 mm. Eyes:

diameters (mm): AME 0.09, ALE 0.12, PME 0.12, PLE 0.13; anterior eye row 0.55 mm long, recurved; posterior eye row 0.75 mm long, procurved; MOQ length 0.30 mm, front width 0.26 mm, back width 0.38 mm; eye interdistances (mm): AME–AME 0.08, AME–ALE 0.05, PME–PME 0.15, PME–PLE 0.11, ALE–PLE 0.06.

Sternum 1.46 mm long, 1.08 mm wide. Chelicerae 0.79 mm long with 4 promarginal teeth and 9 retromarginal denticles.

Abdomen 3.20 mm long, 2.16 mm wide. Epigastric furrow 1.04 mm from tracheal spiracle, spiracle 1.06 mm from base of spinnerets.

Tibial lengths (mm) and indices: I 2.16, 13; II 1.93, 15; III 1.39, 22; IV 2.16, 14. Ventral spination: tibiae I 2–2–2, II, III, IV 1–2–2; metatarsi I, II 2–2–0, III 2–0–2, IV 2–2–2. Third legs unmodified.

Palpus as in Figures 8, 29.

Female (Cochise Co., Arizona). Coloration as in male.

Total length 6.41 mm. Carapace 2.34 mm long, 1.87 mm wide, cephalic width 1.12 mm, clypeus height 0.12 mm. Eyes: diameters (mm): AME 0.10, ALE 0.13, PME 0.13, PLE 0.13; anterior eye row 0.59 mm long, recurved; posterior eye row 0.70 mm long, procurved; MOQ length 0.33 mm, front width 0.27 mm, back width 0.42 mm; eye interdistances (mm): AME–AME 0.06, AME–ALE 0.03, PME–PME 0.17, PME–PLE 0.12, ALE–PLE 0.07.

Sternum 1.42 mm long, 1.08 mm wide. Chelicerae 0.99 mm long with 4 promarginal teeth and 8 retromarginal denticles.

Abdomen 3.96 mm long, 2.63 mm wide. Epigastric furrow 1.33 mm from tracheal spiracle, spiracle 1.33 mm from base of spinnerets.

Legs unmodified. Tibial lengths (mm) and indices: I 1.75, 16; II 1.60, 18; III 1.10, 25; IV 1.89, 15. Ventral spination: tibiae I 4–4–2, II 2–4–2, III 1–1–2, IV 1–2–2; metatarsi as in male.

Epigynum as in Figure 39, internal genitalia as in Figure 45.

Natural history. Mature males and females have been taken in August and September. Specimens have been taken at 8200 feet (2500 m). I collected a few immature males (which matured in the laboratory) of this species in pine litter in the Chiricahua Mountains, Arizona, where mature *A. marginalis* were extremely abundant.

Distribution. Southeastern Arizona (Map 1).

Anyphaena gibboides new species
Map 1; Figures 14, 30, 40, 46

Types. Male holotype, female paratype from City Creek Canyon, Salt Lake Co., Utah, 22 May 1943 (Wilton Ivie), deposited in AMNH. Male and female paratypes from Lake Co., Oregon, deposited in MCZ. The specific name is an arbitrary combination of letters.

Diagnosis. Anyphaena gibboides is a distinctive species. Males have a sharply pointed median apophysis and serrate RTA which will separate them from the other known species (Figs. 14, 30). The epigynum is closest to that of *A. autumna*, but lacks the constriction of the midpiece found in that species (Fig. 40).

Male (Salt Lake Co., Utah). Coloration as in *Anyphaena celer.*

Total length 3.31 mm. Carapace 1.60 mm long, 1.28 mm wide, cephalic width 0.54 mm, clypeus height 0.07 mm. Eyes: diameters (mm): AME 0.05, ALE 0.08, PME 0.08, PLE 0.08; anterior eye row 0.34 mm long, straight; posterior eye row 0.48 mm long, procurved; MOQ length 0.23 mm, front width 0.15 mm, back width 0.24 mm; eye interdistances (mm): AME–AME 0.05, AME–ALE 0.08, PME–PME 0.08, PME–PLE 0.07, ALE–PLE 0.05.

Sternum 0.85 mm long, 0.72 mm wide. Chelicerae 0.49 mm long with 4 promarginal teeth and 8 retromarginal denticles.

Abdomen 1.94 mm long, 1.24 mm wide. Epigastric furrow 0.58 mm from tracheal spiracle, spiracle 0.59 mm from base of spinnerets.

Tibial lengths (mm) and indices: I 1.33, 17; II 1.24, 19; III 0.99, 23; IV 1.47, 16. Ventral spination: tibiae I 2–2–0, II 1–2–0, III 2–2–0, IV 2–2–2; metatarsi I, II 2–2–0, III 2–1–2, IV 2–2–2. Modifications of third leg as in *A. celer* save that all coxae have clumps of short thick setae.

Palpus as in Figures 14, 30.

Female (Salt Lake Co., Utah). Coloration as in male of *A. celer*.

Total length 3.74 mm. Carapace 1.75 mm long, 1.35 mm wide, cephalic width 0.83 mm, clypeus height 0.09 mm. Eyes: diameters (mm): AME 0.06, ALE 0.09, PME 0.08, PLE 0.08; anterior eye row 0.41 mm long, recurved; posterior eye row 0.57 mm long, procurved; MOQ length 0.24 mm, front width 0.18 mm, back width 0.28 mm; eye interdistances (mm): AME–AME 0.06, AME–ALE 0.03, PME–PME 0.12, PME–PLE 0.09, ALE–PLE 0.06.

Sternum 1.19 mm long, 0.83 mm wide. Chelicerae 0.62 mm long with 4 promarginal teeth and 6 retromarginal denticles.

Abdomen 2.36 mm long, 1.39 mm wide. Epigastric furrow 0.72 mm from tracheal spiracle, spiracle 0.70 mm from base of spinnerets.

Legs unmodified. Tibial lengths (mm) and indices: I 1.39, 18; II 1.24, 20; III 0.75, 27; IV 1.39, 18. Ventral spination: tibiae I 2–2–0, II, III 1–2–0, IV 1–2–2; metatarsi I, II 2–2–0, III 2–0–2, IV 2–2–2.

Epigynum as in Figure 40, internal genitalia as in Figure 46.

Natural history. Mature males and females have been taken in late May and June. Habitat data is lacking.

Distribution. Northern Utah west to southeastern Oregon (Map 1).

Anyphaena catalina new species
Map 1; Figures 15, 31, 41, 48

Types. Male holotype, female paratype from Mt. Lemon, Santa Catalina Mountains, Pima Co., Arizona, 13 July 1916 (F. E. Lutz), deposited in AMNH. Male and female paratypes from Pima Co., Arizona, and México, Mexico, deposited in MCZ. The specific name is a noun in apposition and refers to the type locality.

Diagnosis. Anyphaena catalina is most closely related to *A. arbida*, though males of *A. catalina* may be readily distinguished by their recurved retrolateral tegular apophyses (Figs. 15, 31). Females of *A. arbida* are unknown; those of *A. catalina* may be recognized by the epigynal hood being roughly equal in size to the epigynal midpiece (Fig. 41).

Male (Pima Co., Arizona). Coloration as in *Anyphena celer*.

Total length 3.53 mm. Carapace 1.78 mm long, 1.42 mm wide, cephalic width 0.72 mm, clypeus height 0.09 mm. Eyes: diameters (mm): AME 0.05, ALE 0.09, PME 0.08, PLE 0.09; anterior eye row 0.40 mm long, recurved; posterior eye row 0.51 mm long, procurved; MOQ length 0.21 mm, front width 0.17 mm, back width 0.26 mm; eye interdistances (mm): AME–AME 0.07, AME–ALE 0.04, PME–PME 0.09, PME–PLE 0.08, ALE–PLE 0.04.

Sternum 0.90 mm long, 0.70 mm wide. Chelicerae 0.56 mm long with 4 promarginal teeth and 6 retromarginal denticles.

Abdomen 1.85 mm long, 0.90 mm wide. Epigastric furrow 0.61 mm from tracheal spiracle, spiracle 0.65 mm from base of spinnerets.

Tibial lengths (mm) and indices: I 2.07, 8; II 1.94, 9; III 1.08, 23; IV 1.80, 10. Ventral spination: tibiae I 4–2–2*, II 2–2–2*, III, IV 2–2–2; metatarsi I, II 2–2–0, III 2–0–2, IV 2–2–2. Modifications of third leg as in *A. celer* save that femur III lacks short thick setae and all coxae bear clumps of them.

Palpus as in Figures 15, 31.

Female (Pima Co., Arizona). Coloration as in male of *A. celer*.

Total length 4.57 mm. Carapace 1.84 mm long, 1.42 mm wide, cephalic width 0.94 mm, clypeus height 0.09 mm. Eyes: diameters (mm): AME 0.07, ALE 0.09, PME 0.09, PLE 0.09; anterior eye row 0.47 mm long, recurved; posterior eye row

0.63 mm long, procurved; MOQ length 0.26 mm, front width 0.22 mm, back width 0.33 mm; eye interdistances (mm): AME–AME 0.08, AME–ALE 0.04, PME–PME 0.15, PME–PLE 0.11, ALE–PLE 0.07.

Sternum 1.01 mm long, 0.85 mm wide. Chelicerae 0.68 mm long with 4 promarginal teeth and 8 retromarginal denticles.

Abdomen 2.74 mm long, 1.85 mm wide. Epigastric furrow 0.86 mm from tracheal spiracle, spiracle 0.94 mm from base of spinnerets.

Legs unmodified. Tibial lengths (mm) and indices: I 1.51, 14; II 1.33, 17; III 0.94, 23; IV 1.48, 16. Ventral spination: tibiae I, II 2–2–2*, III 1–2–2, IV 2–2–2; metatarsi as in male.

Epigynum as in Figure 41, internal genitalia as in Figure 48.

Natural history. Mature males and females have been taken in July and August. Specimens have been taken at 7500 feet (2300 m) in yellow pine/oak and douglas fir/white fir forests.

Distribution. Southeastern Arizona south to central Mexico (Map 1).

Anyphaena arbida new species
Map 1; Figures 17, 38

Types. Male holotype from Carr Canyon, Huachuca Mountains, Cochise Co., Arizona, 26 August 1950 (M. A. Cazier), deposited in AMNH. Male paratype from Cochise Co., Arizona, deposited in MCZ. The specific name is an arbitrary combination of letters.

Diagnosis. Anyphaena arbida is most closely related to *A. catalina*. Males of the former (Figs. 17, 38) lack the recurved retrolateral tegular apophysis of *A. catalina;* females of *A. arbida* are unknown.

Male (Cochise Co., Arizona). Coloration as in *Anyphaena celer*, except that posterior spinnerets are as in *A. dixiana*.

Total length 6.95 mm. Carapace 3.28 mm long, 2.41 mm wide, cephalic width 1.22 mm, clypeus height 0.14 mm. Eyes: diameter (mm): AME 0.11, ALE 0.13, PME 0.13, PLE 0.15; anterior eye row 0.64 mm long, recurved; posterior eye row 0.89 mm long, procurved; MOQ length 0.43 mm, front width 0.31 mm, back width 0.44 mm; eye interdistances (mm): AME–AME 0.09, AME–ALE 0.04, PME–PME 0.18, PME–PLE 0.14, ALE–PLE 0.09.

Sternum 1.62 mm long, 1.33 mm wide. Chelicerae 1.30 mm long with 4 promarginal teeth and 8 retromarginal denticles.

Abdomen 3.71 mm long, 2.16 mm wide. Epigastric furrow 1.08 mm from tracheal spiracle, spiracle 1.12 mm from base of spinnerets. Spinnerets surrounded by a clump of unusually long setae.

Tibial lengths (mm) and indices: I 6.88, 5; II 3.35, 10; III 2.20, 16; IV 3.35, 10. Ventral spination: tibiae I 4–2–2*, II 3–2–2*, III, IV 2–2–0; metatarsi I, II 2–2–0, III, IV 2–2–2. Third legs unmodified.

Palpus as in Figures 17, 38.

Female. Unknown.

Natural history. Mature males have been collected in August. Habitat data is lacking.

Distribution. Cochise Co., Arizona (Map 1).

Anyphaena pectorosa Group

Diagnosis. The *pectorosa* group is closely related to the *pacifica* group, but males may be distinguished by the spurs on their coxae (Figs. 59–62). Females have the epigynum on a characteristic sclerotized plate (Figs. 74, 77, 79) and simple spermathecae (Figs. 75, 78, 80).

Description. Total length 4.5–6.5 mm. Carapace longer than wide, narrowed in front to less than half its maximum width in males, to slightly more than half its maximum width in females. Clypeus height more than 1.5 times the diameter of an anterior median eye. Posterior median, posterior lateral and anterior lateral eyes subequal in size, almost twice the diameter of anterior medians. Procurved posterior eye row longer than slightly recurved anterior row. Median ocular quadrangle almost

twice as wide in back as in front. Anterior median eyes separated by slightly less than their diameter, slightly closer to anterior laterals than to each other. Posterior medians separated by slightly more than their diameter, slightly closer to posterior laterals. Anterior laterals separated by their radius from posterior laterals. Sternum longer than wide, with a low hirsute knob behind its middle in some males. Chelicerae with 4 promarginal teeth and 7–9 retromarginal denticles. Abdomen longer than wide, tracheal spiracle midway between epigastric furrow and base of spinnerets. Leg formula 1423. Metatarsi I and II with two pairs of ventral spines. Males with coxae II bearing round knobs, coxae III and IV bearing spurs. Palpus with an elongated median apophysis, enlarged conductor and inconspicuous embolus. Retrolateral tibial apophysis short. Epigynum on a sclerotized plate, without a hood. Two simple spermathecae.

Variation. The species in this group show little intraspecific variation, individual or geographical, in size, structure or coloration.

Key to Species

1a. Coxae III of males with posterior spur bifid (Figs. 59, 61, 62); sternum of males with a low hirsute knob behind middle; sclerotized epigynal plate wider posteriorly than anteriorly (Figs. 74, 79) 2

1b. Coxae III of males with posterior spur not bifid (Fig. 60); sternum of males without a low hirsute knob behind middle; sclerotized epigynal plate wider anteriorly than posteriorly (Fig. 77) ..... *fraterna*

2a. Distal tip of palpal median apophysis bent sharply towards cymbium (Figs. 55, 58); sclerotized epigynal plate with pronounced posterolateral corners (Fig. 74) 3

2b. Distal tip of palpal median apophysis not bent sharply towards cymbium (Fig. 57); sclerotized epigynal plate without pronounced posterolateral corners (Fig. 79) ..... *alachua*

3a. Distal tip of palpal median apophysis meeting the recessed, dorsal branch of the apophysis (Fig. 55); sclerotized epigynal plate with pronounced posterolateral corners (Fig. 74) ..... *pectorosa*

3b. Distal tip of palpal median apophysis not meeting the recessed, dorsal branch of the apophysis (Fig. 58); females unknown ..... *lacka*

Anyphaena pectorosa L. Koch
Map 2; Figures 51, 55, 59, 74, 75

Anyphaena pectorosa L. Koch, 1866, Arachn. Fam. Drass., 198, pl. 8, figs. 131, 132 (♂). Male holotype from Baltimore, Maryland, in BMNH, examined. Bryant, 1931, Psyche, 38: 110, pl. 6, fig. 5, ♂. Chickering, 1939, Pap. Michigan Acad. Sci., 24: 51, figs. 5–8, ♂, ♀. Comstock, 1940, Spider Book, rev. ed., p. 577, fig. 636, ♀. Kaston, 1948, Bull. Connecticut Geol. Natur. Hist. Surv., 70: 408, figs. 1453, 1477–1480, ♂, ♀. Roewer, 1954, Katalog der Araneae, 2: 529. Bonnet, 1955, Bibliographia Araneorum, 2: 346.

Anyphaena calcarata Emerton, 1890, Trans. Connecticut Acad. Sci., 8: 187, pl. 6, figs. 3–3d (♂, ♀). Male holotype, female allotype from West Haven, Connecticut, in MCZ, examined. Emerton, 1902, Common Spiders, p. 12, figs. 42, 43, ♂, ♀.

Gayenna calcarata, Banks, 1910, Bull. U.S. Nat. Mus., 72: 13.

Gayenna pectorosa, Comstock, 1912, Spider Book, p. 563 (in part), fig. 636, ♀ (not fig. 637).

Diagnosis. Anyphaena pectorosa is closest to *A. alachua*, but may readily be distinguished from it by the highly curved median apophysis of males (Fig. 55) and the pronounced posterolateral corners of the sclerotized epigynal plate of females (Fig. 74).

Male (Fairfax Co., Virginia). Total length 5.40 mm. Carapace 2.43 mm long, 1.98 mm wide, cephalic width 0.88 mm, clypeus height 0.11 mm, yellow with thin dark border and two dark paramedian longitudinal bands. Eyes: diameters (mm):

→

Plate 5

Figures 51–54. Left palpi, ventral view. Figures 55–58. Left palpi, retrolateral view. Figures 59–62. Male coxae, ventral view. 51, 55, 59. *Anyphaena pectorosa* L. Koch. 52, 56, 60. *Anyphaena fraterna* (Banks). 53, 57, 61. *Anyphaena alachua* new species. 54, 58, 62. *Anyphaena lacka* new species.

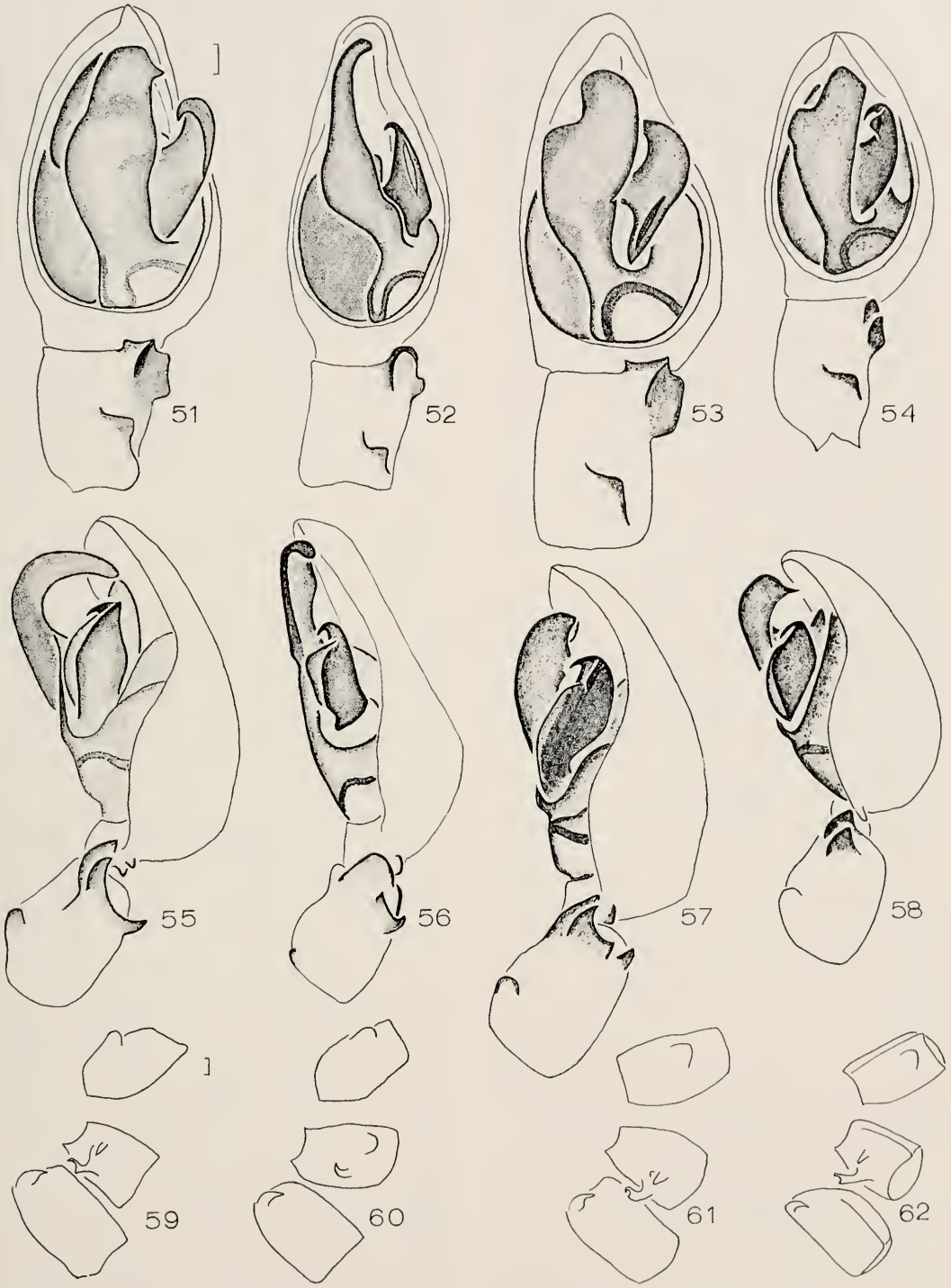
51
52
53
54
55
56
57
58
59
60
61
62

AME 0.06, ALE 0.11, PME 0.11, PLE 0.12; anterior eye row 0.48 mm long, slightly recurved; posterior eye row 0.65 mm long, procurved; MOQ length 0.28 mm, front width 0.20 mm, back width 0.35 mm; eye interdistances (mm): AME–AME 0.07, AME–ALE 0.04, PME–PME 0.14, PME–PLE 0.13, ALE–PLE 0.05.

Sternum 1.35 mm long, 1.01 mm wide, pale yellow with translucent border, darkened extensions to coxae and a low hirsute knob behind middle. Chelicerae 0.73 mm long with 4 promarginal teeth and 7 retromarginal denticles, pale yellow with boss outlined in gray. Labium and endites yellow, darkest proximally. Endites slightly invaginated at middle.

Abdomen 3.15 mm long, 1.67 mm wide, pale white with transverse rows of dark markings, venter pale. Epigastric furrow 1.01 mm from tracheal spiracle, spiracle 1.06 mm from base of spinnerets.

Legs pale yellow with distal segments darkest. Tibial lengths (mm) and indices: I 3.10, 7; II 2.52, 9; III 1.82, 16; IV 2.56, 10. Ventral spination: tibiae I 2–2–1, II–IV 2–2–2; metatarsi I, II 2–2–0, III 2–0–2, IV 2–2–2. Coxae II, III and IV modified as in Figure 59.

Palpus as in Figures 51, 55.

Female (Fairfax Co., Virginia). Coloration as in male.

Total length 5.44 mm. Carapace 2.41 mm long, 1.91 mm wide, cephalic width 0.97 mm, clypeus height 0.08 mm. Eyes: diameters (mm): AME 0.07, ALE 0.12, PME 0.11, PLE 0.12; anterior eye row 0.52 mm long, recurved; posterior eye row 0.71 mm long, procurved; MOQ length 0.33 mm, front width 0.20 mm, back width 0.37 mm; eye interdistances (mm): AME–AME 0.05, AME–ALE 0.04, PME–PME 0.15, PME–PLE 0.10, ALE–PLE 0.07.

Sternum 1.31 mm long, 1.06 mm wide, without hirsute knob. Chelicerae 0.72 mm long with 4 promarginal teeth and 8 retromarginal denticles.

Abdomen 3.10 mm long, 1.76 mm wide. Epigastric furrow 0.70 mm from tracheal spiracle, spiracle 1.22 mm from base of spinnerets.

Legs unmodified. Tibial lengths (mm) and indices: I 2.41, 11; II 2.05, 13; III 1.44, 19; IV 2.20, 12. Ventral spination: tibiae I, II 2–2–0, III, IV 1–2–1; metatarsi I, II 2–2–0, III, IV 2–2–2.

Epigynum as in Figure 74, internal genitalia as in Figure 75.

Natural history. Mature males have been taken from mid-April through early September, mature females from mid-April through mid-August. Specimens have been taken by sweeping foliage, in Malaise and pitfall trips, and under rocks. Egg cases taken with females contained 65–95 eggs.

Distribution. New England west to Michigan, south to western Florida and eastern Texas (Map 2).

Anyphaena alachua new species
Map 2; Figures 53, 57, 61, 79, 80

Types. Male holotype, female paratype from west of Gainesville, Alachua Co., Florida, 18 April 1938 (Willis J. Gertsch), deposited in AMNH. Male and female paratypes from Alachua Co., Florida, deposited in MCZ. The specific name is a noun in apposition and refers to the type locality.

Diagnosis. Anyphaena alachua is closest to *A. pectorosa* but the median apophysis is not highly curved (Fig. 57) and the epigynal plate lacks pronounced posterolateral corners (Fig. 79).

Male (Alachua Co., Florida). Coloration as in *Anyphaena pectorosa.*

Total length 4.90 mm. Carapace 2.41 mm long, 2.01 mm wide, cephalic width 0.79 mm, clypeus height 0.13 mm. Eyes: diameters (mm): AME 0.07, ALE 0.12, PME 0.12, PLE 0.13; anterior eye row 0.51 mm long, slightly recurved; posterior eye row 0.70 mm long, procurved; MOQ length 0.30 mm, front width 0.22 mm, back width 0.36 mm; eye interdistances (mm): AME–AME 0.07, AME–ALE 0.04, PME–PME 0.12, PME–PLE 0.11, ALE–PLE 0.06.

Sternum 1.26 mm long, 1.01 mm wide, with low hirsute knob behind middle. Chelicerae 0.76 mm long with 4 promarginal teeth and 9 retromarginal denticles.

Abdomen 2.48 mm long, 1.48 mm wide. Epigastric furrow 0.76 mm from tracheal spiracle, spiracle 0.83 mm from base of spinnerets.

Tibial lengths (mm) and indices: I 2.77, 10; II 2.27, 11; III 1.44, 22; IV 1.94, 14. Ventral spination: tibiae I, II 2–2–0, III 1–2–2, IV 2–2–2; metatarsi I, II 2–2–0, III 2–0–2, IV 2–2–2. Coxae II, III and IV modified as in Figure 61.

Palpus as in Figures 53, 57.

Female (Alachua Co., Florida). Coloration as in male of *A. pectorosa*.

Total length 6.17 mm. Carapace 2.45 mm long, 1.80 mm wide, cephalic width 0.94 mm, clypeus height 0.12 mm. Eyes: diameters (mm): AME 0.08, ALE 0.13, PME 0.12, PLE 0.13; anterior eye row 0.57 mm long, slightly recurved; posterior eye row 0.73 mm long, procurved; MOQ length 0.30 mm, front width 0.22 mm, back width 0.40 mm; eye interdistances (mm): AME–AME 0.07, AME–ALE 0.04, PME–PME 0.15, PME–PLE 0.11, ALE–PLE 0.07.

Sternum 1.35 mm long, 1.08 mm wide, without hirsute knob. Chelicerae 0.84 mm long with teeth as in male.

Abdomen 3.53 mm long, 2.02 mm wide. Epigastric furrow 1.10 mm from tracheal spiracle, spiracle 1.21 mm from base of spinnerets.

Legs unmodified. Tibial lengths (mm) and indices: I 2.30, 13; II 1.91, 14; III 1.31, 22; IV 2.09, 13. Ventral spination as in male save metatarsi III 2–2–2.

Epigynum as in Figure 79, internal genitalia as in Figure 80.

Natural history. Mature males have been taken in late April and early May, mature females from late March through mid-May, by sweeping.

Distribution. Known only from Florida (Map 2).

Anyphaena lacka new species
Map 2; Figures 54, 58, 62

Type. Male holotype from Lake Corpus Christi State Park, southwest of Mathis, San Patricio Co., Texas, 28 June 1962 (J. A. Beatty), deposited in MCZ. The specific name is an arbitrary combination of letters.

Diagnosis. Anyphaena lacka is most closely related to *A. alachua* but has a distinct point on the tip of the median apophysis (Fig. 58). Females of *A. lacka* are unknown.

Male (San Patricio Co., Texas). Coloration as in *Anyphaena pectorosa*.

Total length 4.61 mm. Carapace 2.05 mm long, 1.69 mm wide, cephalic width 0.79 mm, clypeus height 0.12 mm. Eyes: diameters (mm): AME 0.07, ALE 0.12, PME 0.11, PLE 0.11; anterior eye row 0.47 mm long, slightly recurved; posterior eye row 0.61 mm long, procurved; MOQ length 0.26 mm, front width 0.19 mm, back width 0.32 mm; eye interdistances (mm): AME–AME 0.05, AME–ALE 0.03, PME–PME 0.11, PME–PLE 0.08, ALE–PLE 0.04.

Sternum 1.24 mm long, 0.90 mm wide, with low hirsute knob behind middle. Chelicerae 0.64 mm long with 4 promarginal teeth and 9 retromarginal denticles.

Abdomen 2.41 mm long, 1.33 mm wide. Epigastric furrow 0.74 mm from tracheal spiracle, spiracle 0.90 mm from base of spinnerets.

Tibial lengths (mm) and indices: I 2.38, 9; II 1.91, 12; III 1.32, 30; IV 1.93, 12. Ventral spination: tibiae I, II 2–2–0, III, IV 1–2–2; metatarsi I, II 2–2–0, III 2–0–2, IV 2–2–2. Coxae II, III, and IV modified as in Figure 62.

Palpus as in Figures 54, 58.

Female. Unknown.

Natural history and distribution. Known only from the type specimen.

Anyphaena fraterna (Banks)
Map 2; Figures 52, 56, 60, 77, 78

Anyphaena conspersa Keyserling, 1887, Verh. zool. bot. Ges. Wien, 37: 453, pl. 6, fig. 23

(♀). Female holotype from Bee Spring, Kentucky, in MCZ, examined; preoccupied by *Anyphaena conspersa* Simon, 1878.

Gayenna fraterna Banks, 1896, Trans. Amer. Ent. Soc., 23: 63. Male holotype from Sea Cliff, New York, in MCZ, examined.

Anyphaena fraterna, Simon, 1897, Hist. Natur. Araign., 2: 96. Bryant, 1931, Psyche, 38: 110, pl. 6, fig. 6, pl. 8, fig. 23, ♂, ♀. Comstock, 1940, Spider Book, rev. ed., p. 577, fig. 637, ♂. Kaston, 1948, Bull. Connecticut Geol. Natur. Hist. Surv., 70: 408, figs. 1454–1456, ♂, ♀. Roewer, 1954, Katalog der Araneae, 2: 529. Bonnet, 1955, Bibliographia Araneorum, 2: 344.

Sillus conspersus, Petrunkevitch, 1911, Bull. Amer. Mus. Natur. Hist., 29: 511.

Gayenna pectorosa, Comstock, 1912, Spider Book, p. 563 (in part), fig. 637, ♂.

Diagnosis. Anyphaena fraterna is a distinctive species easily recognized by the long and narrow median apophysis of males (Fig. 52) and by the female's epigynal plate being wider anteriorly than posteriorly (Fig. 77).

Male (Hall Co., Georgia). Coloration as in *Anyphaena pectorosa.*

Total length 4.93 mm. Carapace 2.23 mm long, 1.85 mm wide, cephalic width 0.81 mm, clypeus height 0.10 mm. Eyes: diameters (mm): AME 0.06, ALE 0.12, PME 0.11, PLE 0.11; anterior eye row 0.45 mm long, slightly recurved; posterior eye row 0.64 mm long, procurved; MOQ length 0.30 mm, front width 0.18 mm, back width 0.33 mm; eye interdistances (mm): AME–AME 0.05, AME–ALE 0.04, PME–PME 0.12, PME–PLE 0.08, ALE–PLE 0.05.

Sternum 1.28 mm long, 0.99 mm wide, without hirsute knob. Chelicerae 0.59 mm long with 4 promarginal teeth and 9 retromarginal denticles.

Abdomen 2.83 mm long, 1.60 mm wide. Epigastric furrow 0.97 mm from tracheal spiracle, spiracle 0.85 mm from base of spinnerets.

Legs with scattered dark spots. Tibial lengths (mm) and indices: I 2.60, 8; II 2.16, 11; III 1.52, 16; IV 2.47, 10. Ventral spination: tibiae I, II 2–2–0, III 1–2–2, IV 2–2–2; metatarsi I, II 2–2–0, III, IV 2–2–2. Coxae II, III and IV modified as in Figure 60.

Palpus as in Figures 52, 56.

Female (Hall Co., Georgia). Coloration as in male of *A. pectorosa.*

Total length 5.00 mm. Carapace 2.32 mm long, 1.80 mm wide, cephalic width 0.94 mm, clypeus height 0.10 mm. Eyes: diameters (mm): AME 0.06, ALE 0.11, PME 0.11, PLE 0.11; anterior eye row 0.49 mm long, recurved; posterior eye row 0.69 mm long, procurved; MOQ length 0.27 mm, front width 0.18 mm, back width 0.36 mm; eye interdistances (mm): AME–AME 0.05, AME–ALE 0.04, PME–PME 0.15, PME–PLE 0.09, ALE–PLE 0.05.

Sternum 1.28 mm long, 1.04 mm wide. Chelicerae 0.75 mm long with teeth as in male.

Abdomen 2.97 mm long, 1.71 mm wide. Epigastric furrow 0.85 mm from tracheal spiracle, spiracle 0.85 mm from base of spinnerets.

Legs unmodified. Tibial lengths (mm) and indices: I 2.29, 11; II 1.89, 13; III 1.30, 19; IV 2.16, 13. Ventral spination as in male.

Epigynum as in Figure 77, internal genitalia as in Figure 78.

Natural history. Mature males have been taken from late March through early July, mature females from late March through late August. Specimens have been taken by sweeping foliage, in Malaise and pitfall traps, and under logs. I collected this species in great abundance by sweeping honeysuckle (*Lonicera* sp.) at night in southern West Virginia during June 1971.

Distribution. Southern New York west to eastern Kansas, south to western Florida and eastern Texas (Map 2).

Anyphaena pacifica Group

Diagnosis. The *pacifica* group is closely related to the *pectorosa* group and appears to displace it in the western United States. The males have similarly short retrolateral tibial apophyses (Figs. 69–71), but *pacifica* group males lack the coxal spurs characteristic of the *pectorosa* group, though

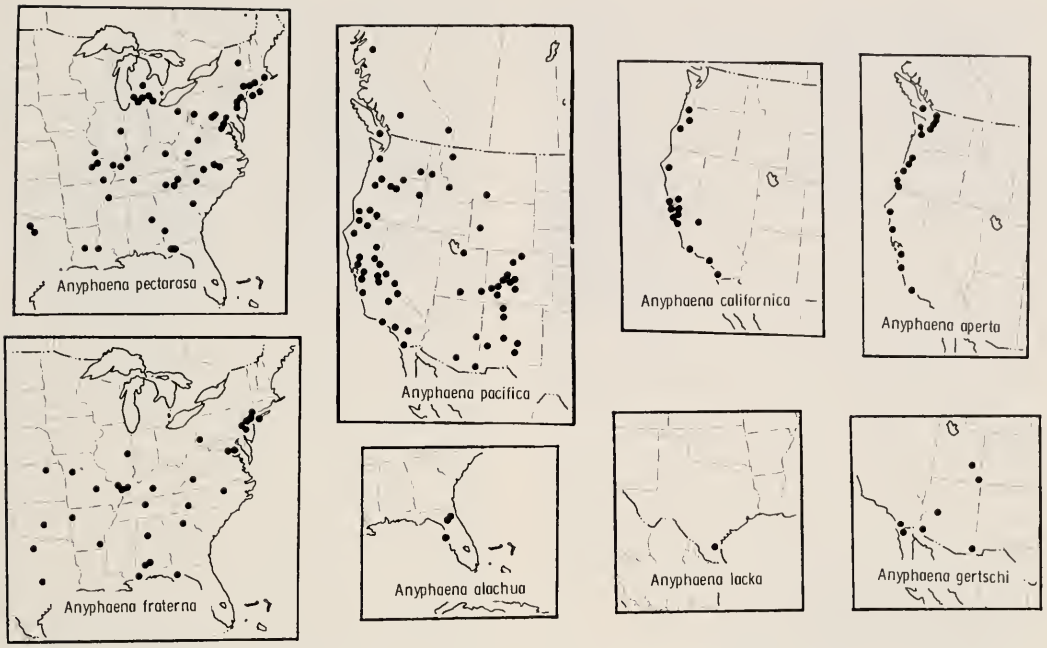

Map 2. Distributions of *Anyphaena alachua*, *A. aperta*, *A. californica*, *A. fraterna*, *A. gertschi*, *A. lacka*, *A. pacifica* and *A. pectorosa*.

males of *Anyphaena gertschi* have rounded knobs on the coxae. Females lack the sclerotized epigynal plates found in the *pectorosa* group, but have a lightly sclerotized atrium-like area posteromedially (Figs. 66, 67, 72) and long, sometimes coiling, ducts (Figs. 68, 73, 76).

Description. Total length 4–6 mm. Carapace longer than wide, narrowed in front by at least one-third of its maximum width, often by more than half. Clypeus height roughly equal to anterior median eye diameter. All eyes subequal in size. Procurved posterior eye row longer than slightly recurved anterior eye row. Median ocular quadrangle longer than wide in front, wider in back than long. Anterior median eyes separated by less than their diameter, much closer to anterior laterals than to each other. Posterior medians separated by more than their diameter, much closer to posterior laterals. Anterior laterals separated by slightly more than their radius from posterior laterals. Sternum longer than wide, without a hirsute knob. Chelicerae with 3 promarginal teeth and 6–9 retromarginal denticles. Abdomen longer than wide, tracheal spiracle midway between epigastric furrow and base of spinnerets. Leg formula 1423. Metatarsi I and II with two pairs of ventral spines. Males with legs unmodified. (*A. pacifica* and *A. californica*) or with coxae bearing round knobs and femora II and III bearing patches of short stiff setae ventrally (*A. gertschi*). Palpus with an elongated median apophysis, enlarged conductor and inconspicuous embolus. Retrolateral tibial apophysis short. Epigynum not on a sclerotized plate, without a hood, with a more or less pronounced atrium-like lightly sclerotized area posteromedially. Internal genitalia with long ducts that coil in some species.

Variation. Two species in this group, *A. pacifica* and *A. californica*, show a great deal of variation in genitalic structure. In both species the shape of the tip of the pal-

pal median apophysis and the coiling of the epigynal ducts are strikingly variable, and it was initially thought that many species were involved. Three sources of evidence, however, have indicated otherwise. First, many females are found in which the ducts on one side of the epigynum coil differently from those on the other side. Secondly, when many specimens are taken together at one locality on a single day, several variants are often found. Finally, the retrolateral tibial apophysis, which usually provides excellent diagnostic characters in anyphaenids, is stable within the species as they are defined here. Until such time as biological evidence on the breeding habits of these spiders can be obtained, it seems best to consider both *A. pacifica* and *A. californica* as widespread, variable species.

Key to Species

1a. Retrolateral tibial apophysis (RTA) without a dorsal process (Fig. 69). Median apophysis with a deep invagination below tip giving the tip a chelate appearance (Fig. 65). Epigynum with large wing-shaped paramedian flaps (Fig. 72) ..... *gertschi*

1b. Retrolateral tibial apophysis (RTA) with a dorsal process (Figs. 70, 71). Median apophysis without a deep invagination below tip (Figs. 63, 64). Epigynum without large wing-shaped paramedian flaps (Figs. 66, 67) 2

2a. Dorsal process of RTA short, located distally (Fig. 70). Median apophysis narrowing gradually towards tip (Fig. 63). Internal ducts with many coils (Fig. 68) ..... *pacifica*

2b. Dorsal process of RTA long, located proximally (Fig. 71). Median apophysis narrowing abruptly towards tip (Fig. 64). Internal ducts without many coils (Fig. 73) ..... *californica*

Anyphaena pacifica (Banks)
Map 2; Figures 63, 66, 68, 70

Gayenna pacifica Banks, 1896, Trans. Amer. Ent. Soc., 23: 63. Female holotype from Olympia, Washington, in MCZ, examined.

Anyphaena pacifica, Simon, 1897, Hist. Natur. Araign., 2: 96. Bryant, 1931, Psyche, 38: 115, pl. 8, fig. 36, ♀. Levi and Levi, 1951, Zoologica (New York), 36: 228, fig. 25, ♂. Roewer, 1954, Katalog der Araneae, 2: 529. Bonnet, 1955, Bibliographia Araneorum, 2: 346.

Anyphaena mundella Chamberlin, 1920, Pomona Coll. J. Ent. Zool., 12: 12, pl. 5, fig. 3 (♀, not ♂, = *Aysha incursa*). Female holotype from Claremont, California, in MCZ, examined. Bryant, 1931, Psyche, 38: 120 (sub *Aysha decepta* [sic]). Roewer, 1954, Katalog der Araneae 2: 534 (sub *Aysha decepta* [sic]). Bonnet, 1955, Bibliographia Araneorum, 2: 836 (sub *Aysha decepta* [sic]). NEW SYNONYMY.

Anyphaena intermontana Chamberlin, 1920, Canad. Ent., 52: 200, fig. 22–6 (♀). Female holotype from Mill Creek, Salt Lake Co., Utah, in MCZ, examined. Bryant, 1931, Psyche, 38: 114 (sub *Anyphaena californica* [sic]). Roewer, 1954, Katalog der Araneae, 2: 528 (sub *Anyphaena californica* [sic]). Bonnet, 1955, Bibliographia Araneorum, 2: 343 (sub *Anyphaena californica* [sic]). NEW SYNONYMY.

Gayenna saniuana Chamberlin and Gertsch, 1928, Proc. Biol. Soc. Wash., 41: 185. Male holotype from Verdure, San Juan Co., Utah, in AMNH, examined. Roewer, 1954, Katalog der Araneae, 2: 540. NEW SYNONYMY.

Anyphaena saniuana, Bryant, 1931, Psyche, 38: 107. Bonnet, 1955, Bibliographia Araneorum, 2: 347.

Anyphaena pomona Chamberlin and Ivie, 1941, Bull. Univ. Utah, Biol., 6: 23, pl. 2, fig. 16 (♀). Female holotype from Mill Creek, Tehama Co., California, in AMNH, examined. Roewer, 1954, Katalog der Araneae, 2: 529. NEW SYNONYMY.

Gayenna jollensis Schenkel, 1950, Verh. Naturf. Ges. Basel, 61: 77, fig. 27 (♀). Female holotype from La Jolla, California, in Naturhistorisches Museum, Basel, examined. Roewer, 1954, Katalog der Araneae, 2: 540. NEW SYNONYMY.

→

Plate 6

Figures 63–65. Left palpi, ventral view. Figures 69–71. Left palpal tibiae, retrolateral view. Figures 66, 67, 72, 74, 77, 79. Epigyna, ventral view. Figures 68, 73, 75, 76, 78, 80. Internal genitalia, dorsal view. 63, 66, 68, 70. *Anyphaena pacifica* (Banks). 64, 67, 71, 73. *Anyphaena californica* (Banks). 65, 69, 72, 76. *Anyphaena gertschi* new species. 74, 75. *Anyphaena pectorosa* L. Koch. 77, 78. *Anyphaena fraterna* (Banks). 79, 80. *Anyphaena alachua* new species.

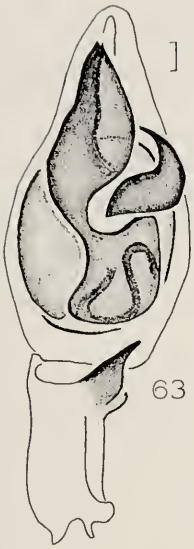
63

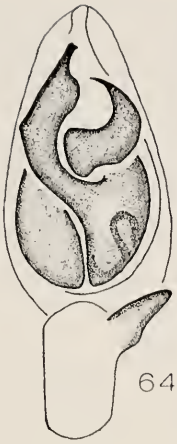
64

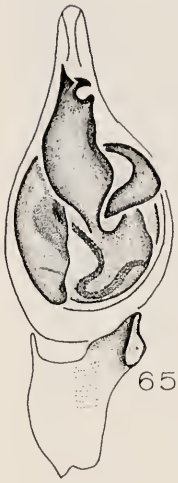
65

66

67

68

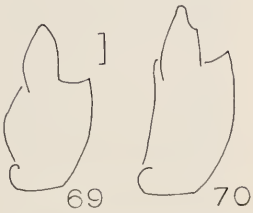
69 70 71

72

73

74

75

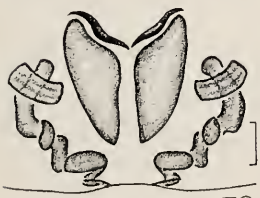
76

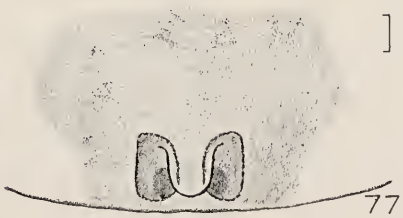
77

78

79

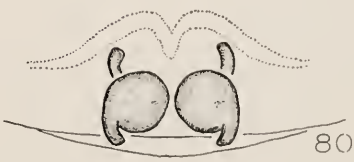
80

Diagnosis. Anyphaena pacifica is closest to *A. californica*, but males may be distinguished by the short, distal, dorsal process of the retrolateral tibial apophysis (Fig. 70) and the gradually narrowing tip of the median apophysis (Fig. 63), while females have distinctive highly coiled internal ducts (Fig. 68). Variation in this species is discussed above.

Male (El Dorado Co., California). Total length 5.18 mm. Carapace 2.34 mm long, 1.94 mm wide, cephalic width 0.86 mm, clypeus height 0.12 mm, pale orange with thin dark border and two dark paramedian longitudinal bands. Eyes: diameters (mm): AME 0.09, ALE 0.12, PME 0.10, PLE 0.11; anterior eye row 0.51 mm long, slightly procurved; posterior eye row 0.69 mm long, procurved; MOQ length 0.28 mm, front width 0.24 mm, back width 0.34 mm; eye interdistances (mm): AME–AME 0.07, AME–ALE 0.03, PME–PME 0.14, PME–PLE 0.10, ALE–PLE 0.05.

Sternum 1.49 mm long, 1.04 mm wide, pale orange with darker border. Chelicerae 0.67 mm long with 3 promarginal teeth and 8 retromarginal denticles, dark orange-brown proximally, pale orange distally, with boss outlined in gray. Labium and endites orange, darkest proximally. Endites slightly invaginated at middle.

Abdomen 2.81 mm long, 1.69 mm wide, reddish-brown throughout. Epigastric furrow 0.85 mm from tracheal spiracle, spiracle 0.92 mm from base of spinnerets.

Legs pale orange, unmodified. Tibial lengths (mm) and indices: I 2.11, 12; II 1.87, 13; III 1.44, 20; IV 2.07, 15. Ventral spination: tibiae I, II 2–2–0, III 1–2–2, IV 2–2–2; metatarsi I, II 2–2–0, III, IV 2–2–2.

Palpus as in Figures 63, 70.

Female (Mono Co., California). Coloration as in male.

Total length 5.39 mm. Carapace 2.34 mm long, 1.62 mm wide, cephalic width 0.94 mm, clypeus height 0.09 mm. Eyes: diameters (mm): AME 0.10, ALE 0.12, PME 0.11, PLE 0.11; anterior eye row 0.51 mm long, slightly recurved; posterior eye row 0.73 mm long, procurved; MOQ length 0.29 mm, front width 0.25 mm, back width 0.36 mm; eye interdistances (mm): AME–AME 0.06, AME–ALE 0.03, PME–PME 0.15, PME–PLE 0.10, ALE–PLE 0.07.

Sternum 1.44 mm long, 1.01 mm wide. Chelicerae 0.71 mm long with teeth as in male.

Abdomen 3.02 mm long, 1.69 mm wide. Epigastric furrow 0.81 mm from tracheal spiracle, spiracle 0.86 mm from base of spinerets.

Tibial lengths (mm) and indices: I 1.84, 15; II 1.71, 15; III 1.39, 19; IV 2.07, 13. Ventral spination as in male save tibiae III 1–1–2 and IV 1–2–2.

Epigynum as in Figure 66, internal genitalia as in Figure 68.

Natural history. Mature males have been taken from late February through late July, mature females year round. Specimens have been taken in montane forests, in pitfall traps, under rocks and commonly in houses.

Distribution. Western North America from British Columbia south to California, Arizona and New Mexico (Map 2).

Anyphaena californica (Banks)
Map 2; Figures 64, 67, 71, 73

Gayenna californica Banks, 1904, Proc. California Acad. Sci., 3: 338, pl. 38, fig. 2 (♀). Female holotype from Palo Alto, California, in MCZ, examined.

Anyphaena ruens Chamberlin, 1920, Pomona Coll. J. Ent. Zool., 12: 11, pl. 5, fig. 1 (♂). Male holotype from Claremont, California, in MCZ, examined. Bryant, 1931, Psyche, 38: 113. Roewer, 1954, Katalog der Araneae, 2: 529. Bonnet, 1955, Bibliographia Araneorum, 2: 347. NEW SYNONYMY.

Anyphaena californica, Bryant, 1931, Psyche, 38: 114. Roewer, 1954, Katalog der Araneae, 2: 528. Bonnet, 1955, Bibliographia Araneorum, 2: 343.

Diagnosis. Anyphaena californica is most closely related to *A. pacifica*, but males have a long, proximal, dorsal process on the retrolateral tibial apophysis (Fig. 71) and an abruptly narrowed tip of the me-

dian apophysis (Fig. 64), while the internal ducts of the female are not highly coiled (Fig. 73). Variation in this species is discussed above.

Male (San Diego Co., California). Coloration as in *Anyphaena pacifica* except that the abdomen is pale white with transverse rows of dark markings.

Total length 4.68 mm. Carapace 2.21 mm long, 1.78 mm wide, cephalic width 0.68 mm, clypeus height 0.07 mm. Eyes: diameters (mm): AME 0.07, ALE 0.09, PME 0.10, PLE 0.11; anterior eye row 0.43 mm long, recurved; posterior eye row 0.59 mm long, procurved; MOQ length 0.30 mm, front width 0.20 mm, back width 0.32 mm; eye interdistances (mm): AME–AME 0.06, AME–ALE 0.04, PME–PME 0.13, PME–PLE 0.11, ALE–PLE 0.07.

Sternum 1.31 mm long, 0.90 mm wide. Chelicerae 0.60 mm long with 3 promarginal teeth and 8 retromarginal denticles.

Abdomen 2.97 mm long, 1.34 mm wide. Epigastric furrow 0.79 mm from tracheal spiracle, spiracle 0.85 mm from base of spinnerets.

Tibial lengths (mm) and indices: I 3.28, 5; II 3.20, 7; III 2.27, 8; IV 2.93, 7. Ventral spination: tibiae I 2–2–0, II 2–2–2, III 1–1–2, IV 1–2–2; metatarsi I, II 2–2–0, III, IV 2–2–2.

Palpus as in Figures 64, 71.

Female (Humboldt Co., California). Coloration as in male.

Total length 5.98 mm. Carapace 2.56 mm long, 1.91 mm wide, cephalic width 1.03 mm, clypeus height 0.08 mm. Eyes: diameters (mm): AME 0.09, ALE 0.11, PME 0.12, PLE 0.12; anterior eye row 0.52 mm long, recurved; posterior eye row 0.69 mm long, procurved; MOQ length 0.35 mm, front width 0.25 mm, back width 0.37 mm; eye interdistances (mm): AME–AME 0.07, AME–ALE 0.04, PME–PME 0.13, PME–PLE 0.10, ALE–PLE 0.06.

Sternum 1.44 mm long, 1.08 mm wide. Chelicerae 0.86 mm long with 3 promarginal teeth and 9 retromarginal denticles.

Abdomen 3.64 mm long, 2.43 mm wide. Epigastric furrow 1.15 mm from tracheal spiracle, spiracle 1.33 mm from base of spinnerets.

Tibial lengths (mm) and indices: I 2.16, 12; II 1.87, 13; III 1.30, 19; IV 2.06, 14. Ventral spination as in male except tibiae II 1–2–0.

Epigynum as in Figure 67, internal genitalia as in Figure 73.

Natural history. Mature males have been taken from early March through mid-July, mature females from mid-March through mid-November. Specimens have been taken in redwood forests, on citrus trees and in houses.

Distribution. Oregon and California (Map 2).

Anyphaena gertschi new species
Map 2; Figures 65, 69, 72, 76

Types. Male holotype, female paratype from Bluff, San Juan Co., Utah, 11 May 1933 (Wilton Ivie), deposited in AMNH. Male and female paratypes from Emery Co., Utah, deposited in MCZ. The specific name is a patronym in honor of Willis J. Gertsch, who first recognized the species as new.

Diagnosis. Anyphaena gertschi is a distinctive species easily recognized by the chelate appearance of the tip of the median apophysis of males (Fig. 65) and the large wing-shaped paramedian flaps on the female epigynum (Fig. 72).

Male (Emery Co., Utah). Coloration as in *Anyphaena pacifica* except that carapace has paramedian bands only vaguely indicated and abdomen is pale yellow throughout.

Total length 4.00 mm. Carapace 1.85 mm long, 1.42 mm wide, cephalic width 0.92 mm, clypeus height 0.14 mm. Eyes: diameters (mm): AME 0.09, ALE 0.09, PME 0.09, PLE 0.09; anterior eye row 0.45 mm long, slightly recurved; posterior eye row 0.59 mm long, procurved; MOQ length 0.26 mm, front width 0.22 mm, back width 0.32 mm; eye interdis-

tances (mm): AME–AME 0.04, AME–ALE 0.03, PME–PME 0.14, PME–PLE 0.08, ALE–PLE 0.04.

Sternum 1.12 mm long, 0.85 mm wide. Chelicerae 0.65 mm long with 3 promarginal teeth and 6 retromarginal denticles.

Abdomen 2.11 mm long, 1.31 mm wide. Epigastric furrow 0.67 mm from tracheal spiracle, spiracle 0.76 mm from base of spinnerets.

All coxae with round knobs ventrally. Femora II and III with patches of short, thick setae ventrally. Tibial lengths (mm) and indices: I 2.00, 9; II 1.69, 13; III 1.30, 17; IV 1.87, 12. Ventral spination: tibiae I 2–2–0, II 1–2–0, III, IV 1–2–2; metatarsi I, II 2–2–0, III, IV 2–2–2.

Palpus as in Figures 65, 69.

Female (San Diego Co., California). Coloration as in male.

Total length 5.04 mm. Carapace 2.25 mm long, 1.76 mm wide, cephalic width 0.95 mm, clypeus height 0.12 mm. Eyes: diameters (mm): AME 0.10, ALE 0.13, PME 0.10, PLE 0.13; anterior eye row 0.51 mm long, straight; posterior eye row 0.68 mm long, procurved; MOQ length 0.28 mm, front width 0.26 mm, back width 0.36 mm; eye interdistances (mm): AME–AME 0.06, AME–ALE 0.03, PME–PME 0.16, PME–PLE 0.08, ALE–PLE 0.05.

Sternum 1.28 mm long, 0.90 mm wide. Chelicerae 0.70 mm long with teeth as in male.

Abdomen 3.10 mm long, 2.02 mm wide. Epigastric furrow 0.77 mm from tracheal spiracle, spiracle 1.03 mm from base of spinnerets.

Legs unmodified. Tibial lengths (mm) and indices: I 1.62, 14; II 1.49, 15; III 1.17, 21; IV 1.69, 14. Ventral spination as in male save tibiae III 1–1–0.

Epigynum as in Figure 72, internal genitalia as in Figure 76.

Natural history. Mature males have been taken from late April through late June, mature females from mid-May through late September. Nothing is known of the habits of this species.

Distribution. Southern Utah south to southern California and Arizona (Map 2).

Anyphaena accentuata Group

Diagnosis. Members of this group can be immediately differentiated from the other nearctic *Anyphaena* by the presence of only one pair of ventral spines on metatarsi I and II. Only one species occurs in America north of Mexico.

Description. Total length 4–6 mm. Carapace longer than wide, narrowed in front to less than half its maximum width in males, to slightly more than half in females. Clypeus height roughly equal to anterior median eye diameter. Median eyes smaller than laterals. Procurved posterior eye row longer than recurved anterior row. Median ocular quadrangle longer than wide in front, wider in back than long. Anterior median eyes separated by less than their diameter, closer to anterior laterals. Posterior medians separated by 1.5 times their diameter, closer to posterior laterals. Anterior laterals separated by their radius from posterior laterals. Sternum longer than wide, unmodified. Chelicerae with 3 promarginal teeth and 5–7 retrolateral denticles. Abdomen longer than wide, tracheal spiracle midway between epigastric furrow and base of spinnerets. Leg formula 1423, legs unmodified. Metatarsi I and II with one pair of ventral spines. Palpus with short median apophysis, short conductor and conspicuous embolus. Cymbial groove compressed to retrolateral side of cymbium. Epigynum with hood. Internal genitalia with anterior membranous dorsal cover.

Variation. No significant variation was detected in *Anyphaena aperta.*

Anyphaena accentuata (Walckenaer) Figure 134

Aranea accentuata Walckenaer, 1802, Faun. Paris, 2: 226. Type lost, presumed destroyed.

Anyphaena accentuata, Roewer, 1954, Katalog der Araneae, 2: 522. Bonnet, 1955, Bibliographia Araneorum, 2: 338.

A drawing of the palpus of this European spider, type species of the genus *Anyphaena*, is included for purposes of comparison to *A. aperta*. Confusion exists between *Anyphaena accentuata, A. obscura* (Sundevall) and *A. sabina* L. Koch, and the female is therefore not illustrated and no description is given. The male illustrated is from England.

Anyphaena aperta (Banks)
Map 2; Figures 135–137

Gayenna aperta Banks, 1921, Proc. California Acad. Sci., 11: 100, fig. 3 (♀). Female holotype from Olympia, Washington, in MCZ, examined.

Anyphaena aperta, Bryant, 1931, Psyche, 38: 114, pl. 8, fig. 35, ♀. Fox, 1938, Iowa State Coll. J. Sci., 12: 238, pl. 1, fig. 6, ♂. Roewer, 1954, Katalog der Araneae 2: 528. Bonnet, 1955, Bibliographia Araneorum, 2: 342.

Diagnosis. In addition to the diagnostic character of the species group, *Anyphaena aperta* can readily be distinguished from all other North American anyphaenids by the sharply pointed median apophysis of males (Fig. 135) and the membranous dorsal cover of the internal genitalia of females (Fig. 137). Although the distribution indicates that this might be an introduced species, no specimens or described species from the Palearctic or Oriental regions resemble *Anyphaena aperta*.

Male (Yamhill Co., Oregon). Total length 4.32 mm. Carapace 1.98 mm long, 1.63 mm wide; cephalic width 0.74 mm, clypeus height 0.08 mm, light orange-brown, darker towards sides, with two dark paramedian longitudinal bands. Eyes: diameters (mm): AME 0.07, ALE 0.11, PME 0.09, PLE 0.11; anterior eye row 0.44 mm long, recurved; posterior eye row 0.62 mm long, procurved; MOQ length 0.26 mm, front width 0.20 mm, back width 0.32 mm; eye interdistances (mm): AME–AME 0.05, AME–ALE 0.03, PME–PME 0.14, PME–PLE 0.10, ALE–PLE 0.06.

Sternum 1.04 mm long, 0.89 mm wide, pale orange with translucent border and darkened extensions to coxae. Chelicerae 0.55 mm long with 3 promarginal teeth and 5 retromarginal denticles, orange-brown with boss outlined in gray. Labium and endites pale orange, darkest proximally. Endites not invaginated.

Abdomen 2.52 mm long, 1.51 mm wide, pale white with transverse rows of dark markings, venter pale with a clump of thick elongate setae posteriorly. Epigastric furrow 0.86 mm from tracheal spiracle, spiracle 0.74 mm from base of spinnerets.

Legs pale yellow, unmodified. Tibial lengths (mm) and indices: I 1.87, 12; II 1.70, 13; III 1.27, 18; IV 1.73, 14. Ventral spination: tibiae I, II 2–2–2, III 1–2–2, IV 2–2–2; metatarsi I, II 2–0–0, III 2–0–2, IV 2–2–2.

Palpus as in Figure 135.

Female (Curry Co., Oregon). Coloration as in male.

Total length 5.83 mm. Carapace 2.65 mm long, 2.05 mm wide, cephalic width 1.17 mm, clypeus height 0.09 mm. Eyes: diameters (mm): AME 0.10, ALE 0.12, PME 0.12, PLE 0.13; anterior eye row 0.61 mm long, slightly recurved; posterior eye row 0.87 mm long, procurved; MOQ length 0.35 mm, front width 0.30 mm, back width 0.44 mm; eye interdistances (mm): AME–AME 0.09, AME–ALE 0.05, PME–PME 0.19, PME–PLE 0.14, ALE–PLE 0.07.

Sternum 1.46 mm long, 1.04 mm wide. Chelicerae 0.80 mm long with 3 promarginal teeth and 7 retromarginal denticles.

Abdomen 4.00 mm long, 2.60 mm wide, without thick setae ventrally. Epigastric furrow 0.81 mm from tracheal spiracle, spiracle 1.03 mm from base of spinnerets.

Tibial lengths (mm) and indices: I 1.87, 16; II 1.77, 16; III 1.31, 22; IV 1.87, 17. Ventral spination as in male except tibiae I 2–2–0 and IV 1–2–2.

Epigynum as in Figure 136, internal genitalia as in Figure 137.

Natural history. Mature males have been taken from late March through early September, mature females from late March

through early November. Specimens have been taken from redwoods and red cedars.

Distribution. Pacific coast from British Columbia south to southern California (Map 2).

Wulfila O. P.-Cambridge

Wulfila O. P.-Cambridge, 1895, Biologia Centrali Americana, Aran., 1: 158. Type species *Wulfila pallidus* O. P.-Cambridge, 1895, designated by Simon, 1897, Hist. Natur. Araign., 2: 103.

Cragus O. P.-Cambridge, 1896, Biologia Centrali Americana, Aran., 1: 215. Type species by monotypy *Cragus pallidus* O. P.-Cambridge, 1896. NEW SYNONYMY.

Anyphaenella Bryant, 1931, Psyche, 38: 115. Type species by original designation *Clubiona saltabunda* Hentz, 1847. NEW SYNONYMY.

Diagnosis. Wulfila may be easily recognized by their long, thin, pale white legs. Leg I in particular is greatly elongated, with its tibial index usually 5 or less. Palpal structure indicates that this genus is closely related to *Anyphaena*. There are probably more than fifty species in this genus; most occur in Central America and the West Indies.

Description. Total length 2.5–4.5 mm. Carapace longer than wide, narrowed in front to from one-half to two-thirds its maximum width. Clypeus height greater than anterior median eye diameter. Posterior median, posterior lateral and anterior lateral eyes subequal in size, somewhat larger than anterior medians. Procurved posterior eye row longer than straight anterior row. Median ocular quadrangle twice as wide in back as in front. Anterior median eyes separated by less than their diameter, by roughly their diameter from anterior laterals. Posterior medians separated by almost twice their diameter, by their diameter from posterior laterals. Anterior laterals separated by roughly their diameter from posterior laterals. Sternum longer than wide, unmodified. Chelicerae with 3–6 promarginal teeth, often on carina, and 5–10 retromarginal denticles. Abdomen longer than wide, tracheal spiracle midway between epigastric furrow and base of spinnerets. Leg formula 1423, legs long, thin, pale white. Leg I greatly elongated. Metatarsi I and II with two pairs of ventral spines. Coxae of males often with spurs and knobs; leg III spination often reduced. Palpus with an elongated median apophysis, enlarged conductor and conspicuous embolus. Retrolateral tibial apophysis greatly expanded except in *W. wunda*. Epigyna and internal genitalia small and diverse.

Variation. None of the species in this genus show any significant individual or geographic intraspecific variation in structure, size or coloration.

Key to Species

1a. Carapace and abdomen with dark markings ..... *saltabunda*
1b. Carapace and abdomen without dark markings 2
2a. Males 3
2b. Females 7
3a. At least one pair of coxae modified with spurs or knobs 4
3b. All coxae unmodified ..... *alba*
4a. Coxae I and/or II modified with spurs or knobs 5
4b. Coxae III and/or IV modified with spurs or knobs 6
5a. Retrolateral tibial apophysis more than half the tibial length (Fig. 93) ..... *bryantae*
5b. Retrolateral tibial apophysis less than half the tibial length (Fig. 95) ..... *wunda*
6a. Retrolateral tibial apophysis greatly expanded at tip (Fig. 86) ..... *tantilla*
6b. Retrolateral tibial apophysis not greatly expanded at tip (Fig. 88) ..... *immaculella*
7a. Epigynum with long ducts (Figs. 91, 97, 98) 8
7b. Epigynum without long ducts (Figs. 90, 96) 10
8a. Epigynum with a heart-shaped atrium (Fig. 97) ..... *wunda*
8b. Epigynum without a heart-shaped atrium 9
9a. Epigynal ducts terminating far anterior of epigynal openings (Fig. 91) ..... *tantilla*
9b. Epigynal ducts terminating near epigynal openings (Fig. 98) ..... *immaculella*
10a. Epigynum with anterolateral flaps, without a medial ridge (Fig. 90) ..... *alba*
10b. Epigynum without anterolateral flaps, with a medial ridge (Fig. 96) ..... *bryantae*

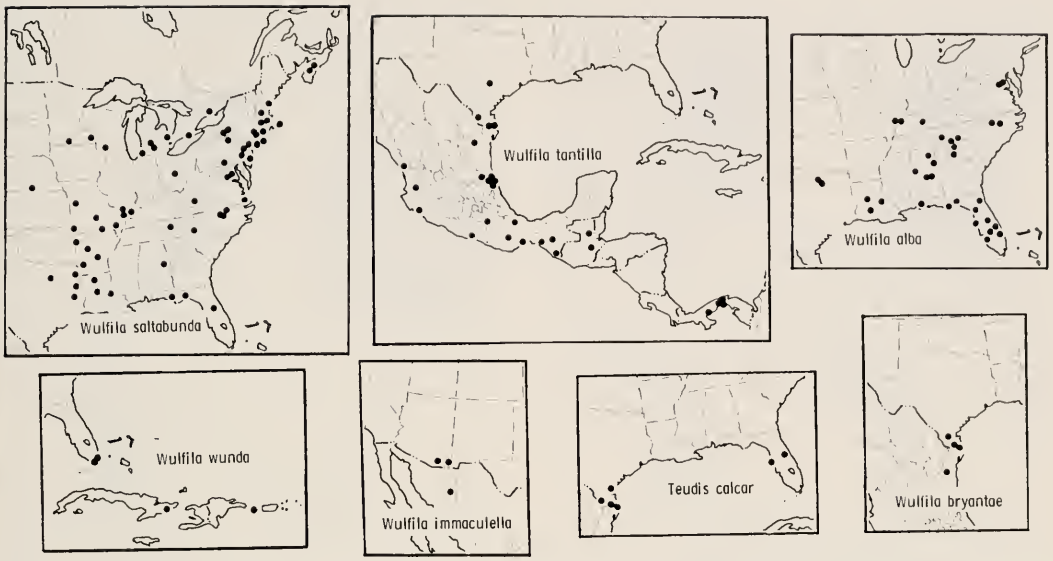

Map 3. Distributions of *Teudis calcar*, *Wulfila alba*, *W. bryantae*, *W. immaculella*, *W. saltabunda*, *W. tantilla* and *W. wunda*.

Wulfila pallidus O. P.-Cambridge
Figure 144

Wulfila pallidus O. P.-Cambridge, 1895, Biologia Centrali Americana, Aran., 1: 159, pl. 19, fig. 11 (♀). Female holotype from Teapa, Tabasco, Mexico, in BMNH, examined. Bonnet, 1959, Bibliographia Araneorum, 2: 4832.

Wulfila pallida, Simon, 1897, Hist. Natur. Araign., 2: 94. Roewer, 1954, Katalog der Araneae, 2: 554.

Vulfila pallida, Simon, 1897, Hist. Natur. Araign., 2: 103.

This Mexican species, though belonging to a distinct species group, closely resembles the North American *Wulfila* in body form, leg length and coloration. It is the type species of *Wulfila*.

Wulfila saltabunda (Hentz), new combination
Map 3; Figures 81, 82, 89, 99

Clubiona saltabunda Hentz, 1847, J. Boston Soc. Natur. Hist., 5: 453, pl. 23, fig. 23 (♀). Female holotype from Alabama in Boston Soc. Natur. Hist. (Boston Museum of Science), destroyed by beetles.

Anyphaena saltabunda, Emerton, 1890, Trans. Connecticut Acad. Sci., 8: 187, figs. 4–4d, ♂, ♀. Emerton, 1902, Common Spiders, p. 14, figs. 46, 47, ♂, ♀.

Gayenna saltabunda, Comstock, 1912, Spider Book, p. 563, figs. 638, 639, ♂, ♀.

Anyphaenella saltabunda, Bryant, 1931, Psyche, 38: 116, pl. 7, figs. 18, 22, ♂, ♀. Comstock, 1940, Spider Book, rev. ed., p. 576, figs. 638, 639, ♂, ♀. Kaston, 1948, Bull. Connecticut Geol. Natur. Hist. Surv., 70: 406, figs. 1465–1470, ♂, ♀. Roewer, 1954, Katalog der Araneae, 2: 530. Bonnet, 1955, Bibliographia Araneorum, 2: 349.

Diagnosis. *Wulfila saltabunda* is the only species in this area which has dark markings on the carapace and abdomen. In addition, the shape of the retrolateral tibial apophysis (Fig. 82) and spermathecae (Fig. 99) serve to distinguish it from *W. alba*, its closest relative.

Male (Suffolk Co., New York). Total length 3.06 mm. Carapace 1.46 mm long, 1.04 mm wide, cephalic width 0.54 mm, clypeus height 0.07 mm, pale white with thin dark border and two dark paramedian longitudinal bands. Eyes: diameters (mm): AME 0.05, ALE 0.09, PME 0.09, PLE 0.09; anterior eye row 0.39 mm long, straight; posterior eye row 0.50 mm long,

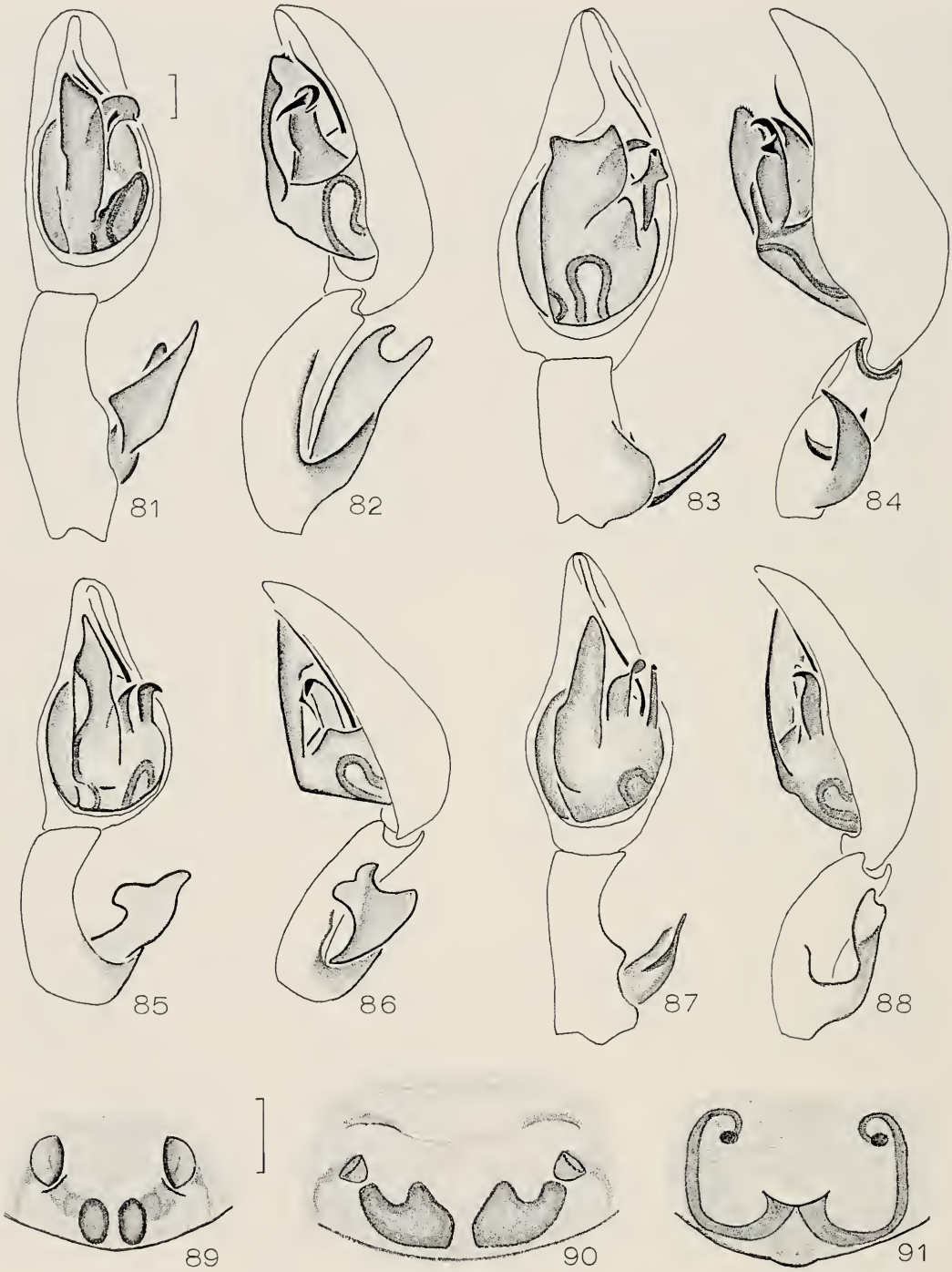

Plate 7

Figures 81, 83, 85, 87. Left palpi, ventral view. Figures 82, 84, 86, 88. Left palpi, retrolateral view. Figures 89–91. Epigyna, ventral view. 81, 82, 89. *Wulfila saltabunda* (Hentz). 83, 84, 90. *Wulfila alba* (Hentz). 85, 86, 91. *Wulfila tantilla* Chickering. 87, 88. *Wulfila immaculella* (Gertsch).

procurved; MOQ length 0.22 mm, front width 0.14 mm, back width 0.30 mm; eye interdistances (mm): AME–AME 0.04, AME–ALE 0.03, PME–PME 0.12, PME–PLE 0.06, ALE–PLE 0.03.

Sternum 0.86 mm long, 0.59 mm wide, pale white with thick translucent border with extensions to coxae and large triangular dark spots between coxae. Chelicerae 0.40 mm long with 6 promarginal teeth and 7 retromarginal denticles, pale white with boss outlined in gray and several very long setae. Labium and endites pale white, endites not invaginated at middle.

Abdomen 1.60 mm long, 0.97 mm wide, pale white with transverse rows of dark spots, venter with thin dark median line anterior of epigastric furrow and two large median dark spots between epigastric furrow and spinnerets. Epigastric furrow 0.40 mm from tracheal spiracle, spiracle 0.45 mm from base of spinnerets.

Legs pale white, unmodified, though leg III spination reduced. Tibial length (mm) and indices: I 2.70, 4; II 1.42, 9; III 1.08, 13; IV 1.55, 10. Ventral spination: tibiae I 2–2–0, II 1–1–0, III 0–1–0, IV 1–1–0; metatarsi I, II 2–2–0, III 0–0–0, IV 1–2–2.

Palpus as in Figures 81, 82.

Female (Suffolk Co., New York). Coloration as in male.

Total length 4.18 mm. Carapace 1.78 mm long, 1.28 mm wide, cephalic width 0.70 mm, clypeus height 0.09 mm. Eyes: diameters (mm): AME 0.06, ALE 0.09, PME 0.09, PLE 0.10; anterior eye row 0.43 mm long, straight; posterior eye row 0.58 mm long, procurved. MOQ length 0.28 mm, front width 0.15 mm, back width 0.32 mm; eye interdistances (mm): AME–AME 0.04, AME–ALE 0.05, PME–PME 0.14, PME–PLE 0.08, ALE–PLE 0.04.

Sternum 0.99 mm long, 0.74 mm wide. Chelicerae 0.56 mm long with 6 promarginal teeth and 10 retromarginal denticles.

Abdomen 2.47 mm long, 2.27 mm wide. Epigastric furrow 0.85 mm from tracheal spiracle, spiracle 0.85 mm from base of spinnerets.

Tibial lengths (mm) and indices: I 2.56, 5; II 1.31, 12; III 0.90, 20; IV 1.67, 12. Ventral spination as in male except tibiae II 2–2–0 and III 1–1–0 and metatarsi III 2–1–0.

Epigynum as in Figure 89, internal genitalia as in Figure 99.

Natural history. Mature males have been taken from mid-April through late August, mature females from late April through late August. Specimens have been taken by sweeping and on apple trees.

Distribution. Nova Scotia west to Minnesota and Nebraska, south to Florida and eastern Texas (Map 3).

Wulfila alba (Hentz), new combination

Map 3; Figures 83, 84, 90, 100

Clubiona albens Hentz, 1847, J. Boston Soc. Natur. Hist., 5: 454, pl. 23, fig. 24 (♂). Male holotype from Alabama in Boston Soc. Natur. Hist. (Boston Museum of Science), destroyed by beetles.

Anyphaena albens, Marx, 1883, *in* Howard, A List of the Invertebrate Fauna of South Carolina, p. 24.

Chiracanthium albens, Marx, 1890, Proc. U.S. Nat. Mus., 12: 513.

Anyphaenella alba, Bryant, 1931, Psyche, 38: 116, pl. 7, figs. 20, 21, ♂, ♀. Roewer, 1954, Katalog der Araneae, 2: 530. Bonnet, 1955, Bibliographia Araneorum 2: 349.

Diagnosis. Wulfila alba is closest to *W. saltabunda* but may be distinguished from it by its lack of dark markings, the spur-like retrolateral tibial apophysis (Fig. 84) and the shape of the spermathecae (Fig. 100).

Male (Orange Co., Florida). Coloration as in *Wulfila saltabunda* except that dark markings are entirely absent.

Total length 3.65 mm. Carapace 1.57 mm long, 1.21 mm wide, cephalic width 0.59 mm, clypeus height 0.07 mm. Eyes: diameters (mm): AME 0.04, ALE 0.07, PME 0.07, PLE 0.07; anterior eye row 0.36 mm long, straight; posterior eye row 0.49 mm long, procurved; MOQ length 0.22 mm, front width 0.12 mm, back width

0.26 mm; eye interdistances (mm): AME–AME 0.04, AME–ALE 0.05, PME–PME 0.11, PME–PLE 0.06, ALE–PLE 0.04.

Sternum 0.95 mm long, 0.70 mm wide. Chelicerae 0.45 mm long with 6 promarginal teeth and 7 retromarginal denticles.

Abdomen 2.12 mm long, 1.15 mm wide. Epigastric furrow 0.67 mm from tracheal spiracle, spiracle 0.79 mm from base of spinnerets.

Tibial lengths (mm) and indices: I 3.13, 4; II 1.85, 7; III 1.12, 13; IV 2.03, 6. Ventral spination: tibiae I 2–2–0, II 1–2–0, III 0–1–0, IV 1–1–0; metatarsi I, II, III 2–2–0, IV 1–1–2.

Palpus as in Figures 83, 84.

Female (Indian River Co., Florida). Coloration as in male.

Total length 4.00 mm. Carapace 1.62 mm long, 1.28 mm wide; cephalic width 0.58 mm, clypeus height 0.06 mm. Eyes: diameters (mm): AME 0.04, ALE 0.07, PME 0.08, PLE 0.08; anterior eye row 0.40 mm long, straight; posterior eye row 0.54 mm long, procurved; MOQ length 0.25 mm, front width 0.14 mm, back width 0.29 mm; eye interdistances (mm): AME–AME 0.05, AME–ALE 0.06, PME–PME 0.13, PME–PLE 0.10, ALE–PLE 0.06.

Sternum 0.92 mm long, 0.74 mm wide. Chelicerae 0.41 mm long with 6 promarginal teeth and 9 retromarginal denticles.

Abdomen 2.66 mm long, 1.51 mm wide. Epigastric furrow 0.68 mm from tracheal spiracle, spiracle 0.88 mm from base of spinnerets.

Tibial lengths (mm) and indices: I 3.13, 4; II 1.91, 8; III 1.05, 13; IV 2.07, 8. Ventral spination as in male except tibiae II 2–2–0 and III 1–2–0 and metatarsi IV 2–2–2.

Epigynum as in Figure 90, internal genitalia as in Figure 100.

Natural history. Mature males have been taken from late March through early August, mature females from early April through late August. Specimens have been taken by sweeping, on pines, and in Malaise and pitfall traps.

Distribution. Maryland west to southern Illinois, south to Florida and eastern Texas (Map 3).

Wulfila tantilla Chickering
Map 3; Figures 85, 86, 91, 101

Cragus pallidus O. P.-Cambridge, 1896, Biologia Centrali Americana, Aran., 1: 215, pl. 26, fig. 10 (♂). Male holotype from Santa Ana, Guatemala, in BMNH, examined. Preoccupied by *Wulfila pallidus* O. P.-Cambridge, 1895. Roewer, 1954, Katalog der Araneae, 2: 535. Bonnet, 1956, Bibliographia Araneorum, 2: 1246.

Wulfila tantilla Chickering, 1940, Trans. Amer. Microsc. Soc., 59: 119, figs. 64–66 (♂). Male holotype from El Valle, Panama, in MCZ, examined. Roewer, 1954, Katalog der Araneae, 2: 555. NEW SYNONYMY.

Wulfila tenella Chickering, 1940, Trans. Amer. Microsc. Soc., 59: 120, figs. 67, 68 (♀). Female holotype from El Valle, Panama, in MCZ, examined. Roewer, 1954, Katalog der Araneae, 2: 555. NEW SYNONYMY.

Diagnosis. Wulfila tantilla is very closely related to *W. immaculella* but may be distinguished by the greatly expanded tip of the retrolateral tibial apophysis (Fig. 86) and by the epigynal ducts terminating far anterior of the epigynal openings (Fig. 91).

Male (Webb Co., Texas): Coloration as in *Wulfila alba*, except that the posterior declivity of the carapace is darkened.

Total length 3.02 mm. Carapace 1.62 mm long, 1.12 mm wide, cephalic width 0.63 mm, clypeus height 0.09 mm. Eyes:

→

Plate 8

Figures 92, 94, 107. Left palpi, ventral view. Figures 93, 95, 105. Left palpi, retrolateral view. Figures 96–98, 106. Epigyna, ventral view. Figures 99–104, 108. Internal genitalia, dorsal view. Figure 109. Body, dorsal view. 92, 93, 96, 102. *Wulfila bryantae* new species. 94, 95, 97, 104. *Wulfila wunda* new species. 98, 103. *Wulfila immaculella* (Gertsch). 99. *Wulfila saltabunda* (Hentz). 100. *Wulfila alba* (Hentz). 101. *Wulfila tantilla* Chickering. 105–109. *Oxysoma cubana* Banks. (Figs. 105, 106, 109 by Wilton Ivie, not to scale.)

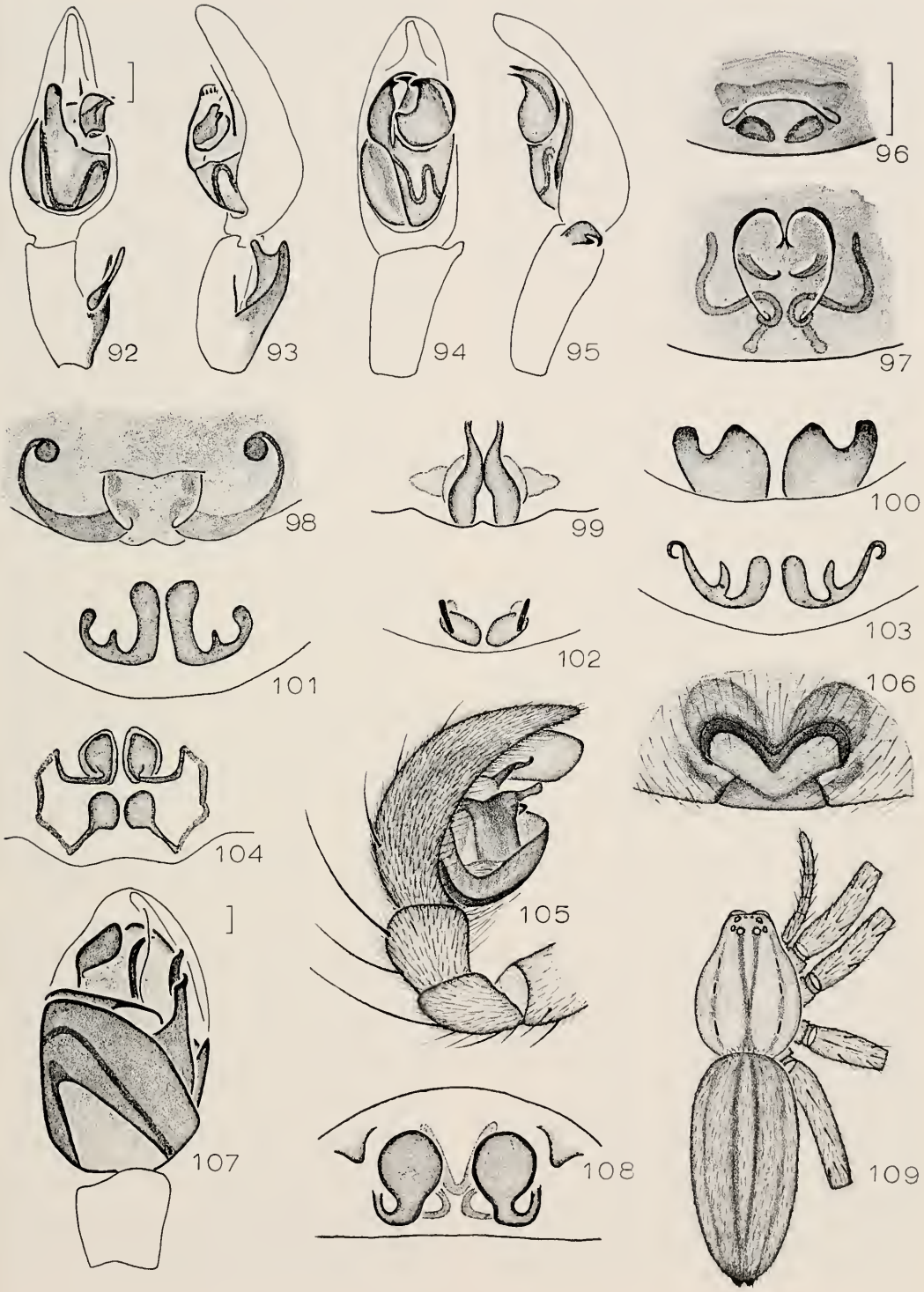
92
93
94
95
96
97
98
99
100
101
102
103
104
105
106
107
108
109

diameters (mm): AME 0.06, ALE 0.07, PME 0.09, PLE 0.09; anterior eye row 0.41 mm long, straight; posterior eye row 0.53 mm long, procurved; MOQ length 0.23 mm, front width 0.16 mm, back width 0.30 mm; eye interdistances (mm): AME–AME 0.05, AME–ALE 0.04, PME–PME 0.13, PME–PLE 0.06, ALE–PLE 0.04.

Sternum 0.74 mm long, 0.63 mm wide. Chelicerae 0.58 mm long with 5 promarginal teeth on a carina and 8 retromarginal denticles.

Abdomen 1.57 mm long, 0.97 mm wide. Epigastric furrow 0.50 mm from tracheal spiracle, spiracle 0.44 mm from base of spinnerets.

Coxae III and IV with two small knobs. Tibial lengths (mm) and indices: I 2.77, 3; II 1.51, 9; III 0.86, 15; IV 1.51, 9. Ventral spination: tibiae I, II 2–2–0, III, IV 1–2–0; metatarsi I, II 2–2–0, III, IV 2–2–2.

Palpus as in Figures 85, 86.

Female (Hidalgo Co., Texas). Coloration as in male of *Wulfila alba.*

Total length 2.92 mm. Carapace 1.34 mm long, 0.99 mm wide, cephalic width 0.67 mm, clypeus height 0.08 mm. Eyes: diameters (mm): AME 0.05, ALE 0.06, PME 0.06, PLE 0.06; anterior eye row 0.37 mm long, straight; posterior eye row 0.50 mm long, procurved; MOQ length 0.20 mm, front width 0.16 mm, back width 0.26 mm; eye interdistances (mm): AME–AME 0.05, AME–ALE 0.04, PME–PME 0.13, PME–PLE 0.06, ALE–PLE 0.05.

Sternum 0.89 mm long, 0.61 mm wide. Chelicerae 0.50 mm long with 4 promarginal teeth and 6 retromarginal denticles.

Abdomen 1.62 mm long, 1.15 mm wide. Epigastric furrow 0.59 mm from tracheal spiracle, spiracle 0.52 mm from base of spinnerets.

Legs unmodified. Tibial lengths (mm) and indices: I 2.36, 5; II 1.21, 11; III 0.77, 18; IV 1.40, 11. Ventral spination as in male save tibiae IV 1–1–0.

Epigynum as in Figure 91, internal genitalia as in Figure 101.

Natural history. Mature males have been taken from mid-April through mid-October, mature females apparently year-round. Nothing is known of the habits of this species.

Distribution. Southern Texas south to the Canal Zone (Map 3).

Wulfila immaculella (Gertsch), new combination
Map 3; Figures 87, 88, 98, 103

Anyphaenella immaculella Gertsch, 1933, Amer. Mus. Novitates, No. 637: 9, fig. 14 (♀). Female holotype from Sabino Basin, Santa Catalina Mountains, Arizona, in AMNH, examined. Roewer, 1954, Katalog der Araneae, 2: 530. Bonnet, 1955, Bibliographia Araneorum, 2: 349.

Diagnosis. Wulfila immaculella is very closely related to *W. tantilla* but may be distinguished by the unexpanded tip of the retrolateral tibial apophysis (Fig. 88) and by the epigynal ducts terminating near the epigynal openings (Fig. 98).

Male (Sonora, Mexico). Coloration as in *Wulfila alba.*

Total length 3.60 mm. Carapace 1.64 mm long, 1.12 mm wide, cephalic width 0.67 mm, clypeus height 0.08 mm. Eyes: diameters (mm): AME 0.05, ALE 0.08, PME 0.08, PLE 0.08; anterior eye row 0.40 mm long, straight; posterior eye row 0.52 mm long, procurved; MOQ length 0.22 mm, front width 0.14 mm, back width 0.31 mm; eye interdistances (mm): AME–AME 0.05, AME–ALE 0.05, PME–PME 0.14, PME–PLE 0.08, ALE–PLE 0.04.

Sternum 0.90 mm long, 0.68 mm wide. Chelicerae 0.51 mm long with 4 promarginal teeth and 5 retromarginal denticles.

Abdomen 2.07 mm long, 1.00 mm wide. Epigastric furrow 0.63 mm from tracheal spiracle, spiracle 0.74 mm from base of spinnerets.

Coxae III with one, coxae IV with two small knobs. Tibial lengths (mm) and indices: I 3.42, 3; II 2.05, 5; III 1.30, 11; IV 2.11, 8. Ventral spination: tibiae I 2–2–0, II 1–2–0, III 0–1–0, IV 1–1–0; metatarsi I, II 2–2–0, III, IV 2–1–2.

Palpus as in Figures 87, 88.

Female (Sonora, Mexico). Coloration as in male of *Wulfila alba*.

Total length 3.64 mm. Carapace 1.58 mm long, 1.08 mm wide, cephalic width 0.61 mm, clypeus height 0.10 mm. Eyes: diameters (mm): AME 0.05, ALE 0.07, PME 0.08, PLE 0.07; anterior eye row 0.40 mm long, straight; posterior eye row 0.53 mm long, procurved; MOQ length 0.22 mm, front width 0.15 mm, back width 0.30 mm; eye interdistances (mm): AME–AME 0.05, AME–ALE 0.04, PME–PME 0.12, PME–PLE 0.08, ALE–PLE 0.04.

Sternum 0.94 mm long, 0.71 mm wide. Chelicerae 0.53 mm long with teeth as in male.

Abdomen 2.05 mm long, 1.40 mm wide. Epigastric furrow 0.65 mm from tracheal spiracle, spiracle 0.74 mm from base of spinnerets.

Legs unmodified. Tibial lengths (mm) and indices: I 2.81, 4; II 1.62, 9; III 0.92, 15; IV 1.75, 8. Ventral spination as in male except tibiae II 2–2–0 and III 1–1–0.

Epigynum as in Figure 98, internal genitalia as in Figure 103.

Natural history. Mature males have been taken in July, mature females in June and July. One male was taken on *Platanus* sp.

Distribution. Southern Arizona and Sonora (Map 3).

Wulfila bryantae new species
Map 3; Figures 92, 93, 96, 102

Types. Male holotype, female paratype from 5 miles east of Edinburg, Hidalgo Co., Texas, 20 April 1937 (S. Mulaik), deposited in AMNH. Male and female paratypes from Jim Wells and Cameron Counties, Texas, deposited in MCZ. The specific name is a patronym in honor of Miss Elizabeth Bryant, in recognition of her pioneering work on North American anyphaenids.

Diagnosis. *Wulfila bryantae* is a distinctive species easily recognized by its stubby median apophysis (Fig. 92) and the medial ridge on the epigynum (Fig. 96).

Male (Hidalgo Co., Texas). Coloration as in *Wulfila alba*.

Total length 3.35 mm. Carapace 1.44 mm long, 1.08 mm wide, cephalic width 0.81 mm, clypeus height 0.10 mm. Eyes: diameters (mm): AME 0.06, ALE 0.06, PME 0.07, PLE 0.07; anterior eye row 0.49 mm long, slightly recurved; posterior eye row 0.62 mm long, procurved; MOQ length 0.26 mm, front width 0.20 mm, back width 0.30 mm; eye interdistances (mm): AME–AME 0.07, AME–ALE 0.07, PME–PME 0.15, PME–PLE 0.13, ALE–PME 0.06.

Sternum 0.97 mm long, 0.55 mm wide. Chelicerae 0.73 mm long with 3 promarginal teeth on a carina and 7 retromarginal denticles.

Abdomen 1.80 mm long, 1.12 mm wide. Epigastric furrow 0.56 mm from tracheal spiracle, spiracle 0.68 mm from base of spinnerets.

Coxae I with a small knob, coxae II with two spurs. Tibial lengths (mm) and indices: I 2.76, 4; II 1.85, 7; III 0.92, 15; IV 1.89, 7. Ventral spination: tibiae I, II 2–2–0, III 1–2–0, IV 1–1–0; metatarsi I, II 2–2–0, III, IV 2–1–2.

Palpus as in Figures 92, 93.

Female (Hidalgo Co., Texas). Coloration as in male of *Wulfila alba*.

Total length 3.78 mm. Carapace 1.44 mm long, 0.99 mm wide, cephalic width 0.74 mm, clypeus height 0.07 mm. Eyes: diameters (mm): AME 0.06, ALE 0.07, PME 0.06, PLE 0.07; anterior eye row 0.42 mm long, slightly recurved; posterior eye row 0.59 mm long, procurved; MOQ length 0.23 mm, front width 0.17 mm, back width 0.27 mm; eye interdistances (mm): AME–AME 0.06, AME–ALE 0.05, PME–PME 0.14, PME–PLE 0.13, ALE–PLE 0.06.

Sternum 0.74 mm long, 0.64 mm wide. Chelicerae 0.62 mm long with 5 promarginal teeth and 5 retromarginal denticles.

Abdomen 2.59 mm long, 2.16 mm wide. Epigastric furrow 0.90 mm from tracheal spiracle, spiracle 0.88 mm from base of spinnerets.

Legs unmodified. Tibial lengths (mm) and indices: I 2.24, 5; II 1.37, 9; III 0.72, 19; IV 1.35, 10. Ventral spination as in male except tibiae III, IV 2–2–0 and metatarsi III, IV 2–0–2.

Epigynum as in Figure 96, internal genitalia as in Figure 102.

Natural history. Mature males have been taken from late April through early June, mature females from early April through early December. Nothing is known of the habits of this species.

Distribution. Southern Texas and Tamaulipas (Map 3).

Wulfila wunda new species
Map 3; Figures 94, 95, 97, 104

Wulfila immaculata, Bryant (not Banks), 1936, Psyche, 43: 98, fig. 1, ♂. Male allotype from Brichell Hammock, Florida Keys, in MCZ, examined. Not *Wulfila immaculata* Banks, 1914, Bull. Amer. Mus. Natur. Hist., 33: 640, pl. 43, fig. 7, ♀. Female holotype from Vinales, Pinar del Rio, Cuba, in AMNH, examined.

Types. Male holotype, female paratype from Tavernier, Monroe Co., Florida, 16 February 1951 (A. M. Nadler), deposited in AMNH. Male and female paratypes from Dade Co., Florida, deposited in MCZ. The specific name is an arbitrary combination of letters.

Diagnosis. Wulfila wunda is a distinctive species the genitalia of which are quite different from those of the other *Wulfila* in America north of Mexico: the retrolateral tibial apophysis is very short (Fig. 95) and the epigynum has an atrium (Fig. 97).

Male (Dade Co., Florida). Coloration as in *Wulfila alba.*

Total length 3.42 mm. Carapace 1.55 mm long, 1.08 mm wide, cephalic width 0.68 mm, clypeus height 0.06 mm. Eyes: diameters (mm): AME 0.05, ALE 0.07, PME 0.08, PLE 0.08; anterior eye row 0.48 mm long, straight; posterior eye row 0.59 mm long, procurved; MOQ length 0.20 mm, front width 0.14 mm, back width 0.29 mm; eye interdistances (mm): AME–AME 0.05, AME–ALE 0.09, PME–PME 0.14, PME–PLE 0.12, ALE–PLE 0.04.

Sternum 1.06 mm long, 0.70 mm wide. Chelicerae 0.85 mm long with 4 promarginal teeth and 6 retromarginal denticles.

Abdomen 1.91 mm long, 1.01 mm wide. Epigastric furrow 0.70 mm from tracheal spiracle, spiracle 0.76 mm from base of spinnerets.

Coxae II with a small knob. Tibial lengths (mm) and indices: I 4.10, 3; II 1.87, 8; III 1.01, 15; IV 2.05, 7. Ventral spination: tibiae I, II 2–2–0, III 0–1–0, IV 0–2–0; metatarsi I, II 2–2–0, III 0–2–0, IV 2–1–2.

Palpus as in Figures 94, 95.

Female (Dade Co., Florida). Coloration as in male of *Wulfila alba.*

Total length 3.74 mm. Carapace 1.55 mm long, 1.15 mm wide, cephalic width 0.72 mm, clypeus height 0.07 mm. Eyes: diameters (mm): AME 0.04, ALE 0.06, PME 0.07, PLE 0.07; anterior eye row 0.49 mm long, straight; posterior eye row 0.59 mm long, procurved; MOQ length 0.20 mm, front width 0.15 mm, back width 0.30 mm; eye interdistances (mm): AME–AME 0.06, AME–ALE 0.10, PME–PME 0.16, PME–PLE 0.12, ALE–PME 0.04.

Sternum 0.90 mm long, 0.67 mm wide. Chelicerae 0.65 mm long with 5 promarginal teeth and 9 retromarginal denticles.

Abdomen 2.16 mm long, 1.15 mm wide. Epigastric furrow 0.74 mm from tracheal spiracle, spiracle 0.83 mm from base of spinnerets.

Legs unmodified. Tibial lengths (mm) and indices: I 3.13, 4; II 1.44, 10; III 0.76, 20; IV 1.58, 9. Ventral spination as in male except tibiae III 1–2–0 and IV 0–1–0 and metatarsi III 1–2–0 and IV 1–2–2.

Epigynum as in Figure 97, internal genitalia as in Figure 104.

Natural history. Mature males have been taken from mid-February through mid-May, mature females apparently year-round. Nothing is known of the habits of this species.

Distribution. Southern Florida, Cuba, and Mona Island (Map 3).

Aysha Keyserling

Aysha Keyserling, 1891, Spinn. Amer. (Brasil. Spinn.), 3: 83, 129. Type species *Aysha prospera* Keyserling, 1891, designated by Simon, 1897, Hist. Natur. Araig., 2: 104.

Diagnosis. Aysha is easily recognized by the greatly advanced placement of the tracheal spiracle, located just behind the epigastric furrow. The genitalic structure is quite different from that of *Anyphaena* and *Wulfila* and the genus undoubtedly represents a different evolutionary line. There are probably more than thirty species in this genus; they occur commonly in both North and South America.

Description. Total length 4–9 mm. Carapace longer than wide, narrowed in front to more than half its maximum width. Clypeus height roughly equal to anterior median eye diameter. All eyes subequal in size. Procurved posterior eye row longer than recurved anterior row. Median ocular quadrangle longer than wide in front, wider in back than long. Anterior median eyes separated by slightly less than their diameter, slightly closer to anterior laterals. Posterior medians separated by up to twice their diameter, closer to posterior laterals. Anterior laterals separated by their radius from posterior laterals. Sternum longer than wide, unmodified. Chelicerae with 3–4 promarginal teeth and 7–9 retromarginal denticles. Abdomen longer than wide, tracheal spiracle much closer to epigastric furrow than to base of spinnerets. Leg formula 1423, legs unmodified. Metatarsi I and II with one pair of ventral spines. Palpus with greatly enlarged base of embolus, long curving embolus and short conductor. Ventral tibial apophysis sometimes present in addition to retrolateral tibial apophysis. Epigynum with anterior median opening and two sidepieces. Internal genitalia with long, sometimes coiling, ducts.

Variation. Only *Aysha gracilis* shows significant variation, and that is in size and not structure or coloration. The size of both the whole animal and of the genitalia vary geographically. The largest specimens (males with cymbium length averaging 1.3 mm) occur in Virginia and surrounding states, with smaller individuals occurring in the north (New England and Michigan males with cymbium length averaging 1.1 mm) and in the south (Texas males with cymbium length averaging 0.9 mm).

Key to Species

1a. Males 2
1b. Females 7
2a. Palpus without a ventral tibial apophysis (VTA) (Figs. 111, 119) 3
2b. Palpus with a ventral tibial apophysis (VTA), sometimes small, transparent, easily overlooked (Figs. 113, 115, 117, 121) .. 4
3a. Embolus restricted to distal half of palpal bulb (Fig. 118) ..... *arunda*
3b. Embolus not restricted to distal half of palpal bulb (Fig. 110) ..... *velox*
4a. VTA erect, sclerotized, relatively large (Figs. 113, 115) 5
4b. VTA recumbent, transparent, relatively small (Figs. 117, 121) 6
5a. Distal retrolateral tip of tegulum with a flap covering embolus (Fig. 112) .. *decepta*
5b. Distal retrolateral tip of tegulum with a sharp point underlying embolus (Fig. 114) ..... *incursa*
6a. Base of embolus recurved, with a sharp spike (Fig. 120) ..... *cambridgei*
6b. Base of embolus not recurved, forming a smooth arc (Fig. 116) ..... *gracilis*
7a. Internal genitalia with simple uncoiled ducts (Figs. 124, 127, 141, 143) 9
7b. Internal genitalia coiled or with accessory ducts (Figs. 125, 142) 8
8a. Internal genitalia highly coiled (Fig. 125) ..... *velox*
8b. Internal genitalia not coiled but with looping accessory ducts (Fig. 142) ..... *arunda*
9a. Median epigynal opening near anterior rim (Figs. 123, 126, 138) 10
9b. Median epigynal opening near middle of epigynum (Fig. 140) ..... *gracilis*
10a. Median epigynal opening much wider than epigynal sidepieces (Fig. 138) .. *cambridgei*
10b. Median epigynal opening not wider than epigynal sidepieces (Figs. 123, 126) 11
11a. Base of epigynal sidepieces near epigastric furrow (Fig. 126); internal genitalia with angular ducts (Fig. 127) ..... *incursa*

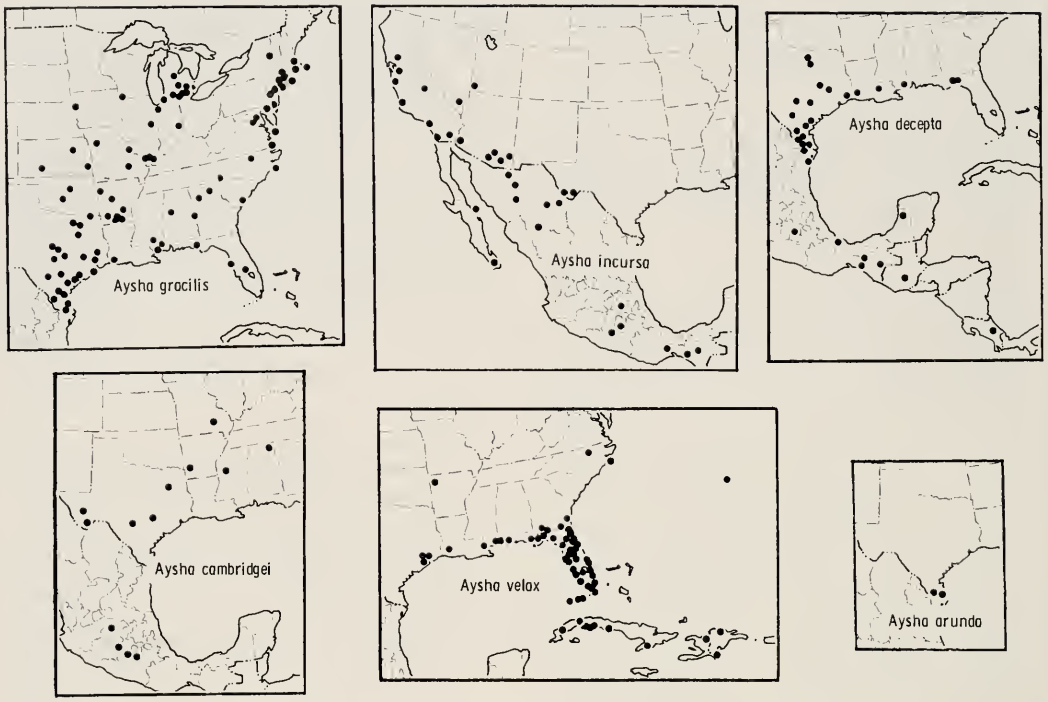

Map 4. Distributions of *Aysha arunda*, *A. cambridgei*, *A. decepta*, *A. gracilis*, *A. incursa* and *A. velox*.

11b. Base of epigynal sidepieces far from epigastric furrow (Fig. 123); internal genitalia with rounded ducts (Fig. 124) ..... *decepta*

Aysha prospera Keyserling
Figure 145

Aysha prospera Keyserling, 1891, Spinnen Amerikas (Brasil. Spinn.), 3: 129, pl. 4, fig. 88 (♀). Female holotype from Rio Grande, Brasil, in BMNH, examined. Roewer, 1954, Katalog der Araneae, 2: 533. Bonnet, 1955, Bibliographia Araneorum, 2: 838.

This South American species, type species of *Aysha*, is a member of a large, distinct species group. Somatic characters clearly ally it with the North American forms included in the genus.

Aysha gracilis (Hentz)
Map 4; Figures 116, 117, 140, 143

Clubiona gracilis Hentz, 1847, J. Boston Soc. Natur. Hist., 5: 452, pl. 23, fig. 9 (♂). Type specimens from North Carolina and Alabama in Boston Soc. Natur. Hist. (Boston Museum of Science), destroyed by beetles.

Anyphaena gracilis, L. Koch, 1866, Arach. Fam. Drassidae, p. 195, pl. 8, fig. 130, ♀. Comstock, 1912, Spider Book, p. 561, fig. 633, ♂ (not fig. 632).

Anyphaena rubra Emerton, 1890, Trans. Connecticut Acad. Sci., 8: 186, pl. 6, fig. 1 (♀). Male allotype (?) from Franklin Park, Boston, Massachusetts, in MCZ, examined. Emerton, 1909, Trans. Connecticut Acad. Sci., 14: 220, pl. 9, fig. 8–8c, ♂.

Aysha gracilis, Bryant, 1931, Psyche, 38: 119, pl. 7, fig. 13, pl. 8, fig. 26, ♂, ♀. Chickering, 1939, Pap. Michigan Acad. Sci., 24: 53, figs. 9–11, ♂, ♀. Comstock, 1940, Spider Book, rev. ed., p. 575, fig. 633, ♂ (not fig. 632). Kaston, 1948, Bull. Connecticut Geol. Natur. Hist. Surv., 70: 405, figs. 1452, 1459–1464, ♂, ♀. Roewer, 1954, Katalog der Araneae, 2: 534. Bonnet, 1955, Bibliographia Araneorum, 2: 837.

Diagnosis. *Aysha gracilis* is closest to *A. cambridgei* but lacks the sharp spike on the proximal edge of the base of embolus (Fig. 116) of that species. Females have

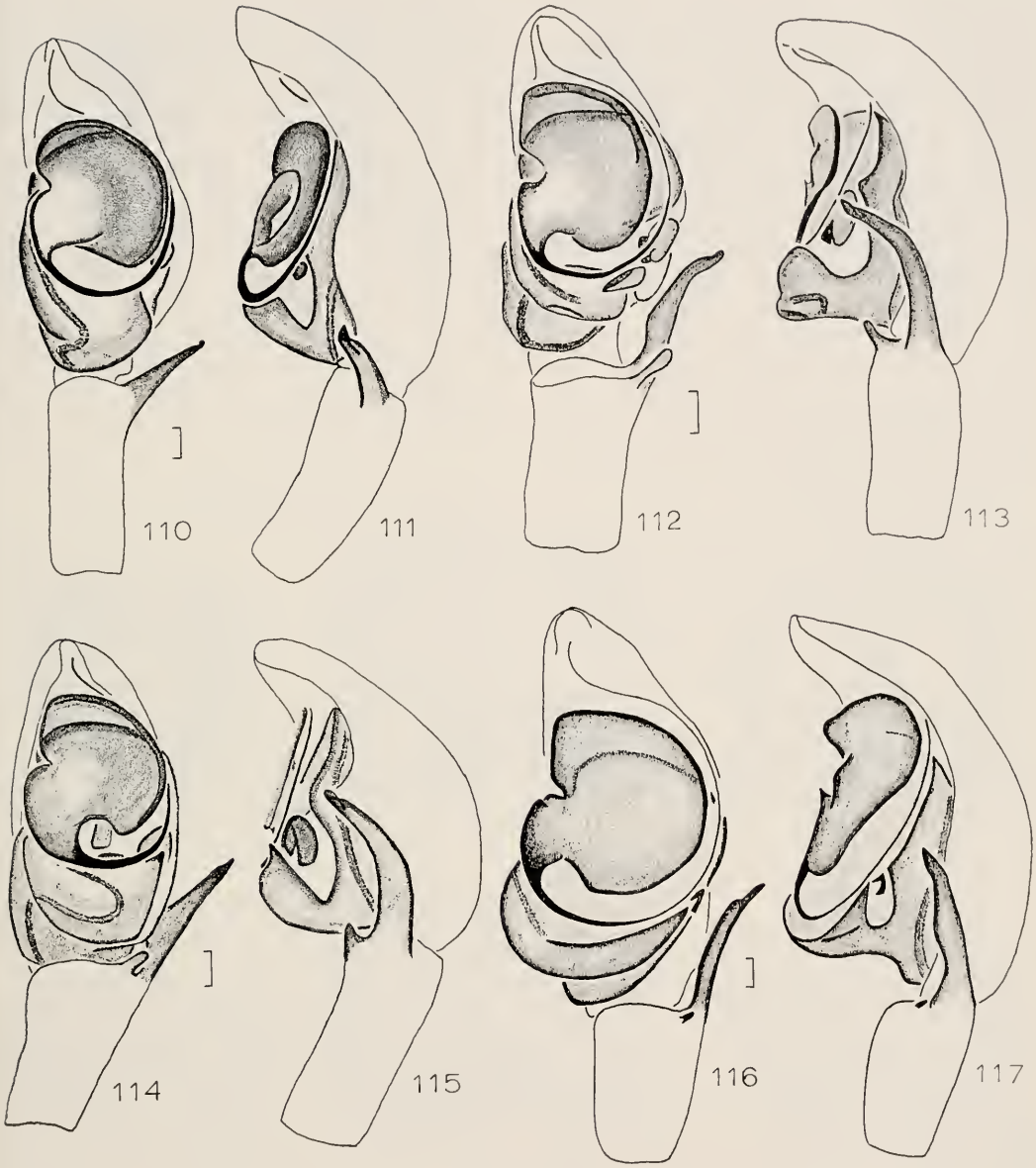

Plate 9

Figures 110, 112, 114, 116. Left palpi, ventral view. Figures 111, 113, 115, 117. Left palpi, retrolateral view. 110, 111. *Aysha velox* (Becker). 112, 113. *Aysha decepta* (Banks). 114, 115. *Aysha incursa* (Chamberlin). 116, 117. *Aysha gracilis* (Hentz).

the median epigynal opening near the middle of the epigynum (Fig. 140). Variation in this species is discussed above.

Male (Middlesex Co., Massachusetts). Total length 5.73 mm. Carapace 2.56 mm long, 2.02 mm wide, cephalic width 1.17 mm, clypeus height 0.09 mm, light orange-brown, darkest anteriorly, with thin dark border and two dark paramedian longitudinal bands. Eyes: diameters (mm): AME

0.09, ALE 0.11, PME 0.09, PLE 0.11; anterior eye row 0.60 mm long, slightly recurved; posterior eye row 0.80 mm long, procurved; MOQ length 0.32 mm, front width 0.26 mm, back width 0.38 mm; eye interdistances (mm): AME–AME 0.09, AME–ALE 0.07, PME–PME 0.19, PME–PLE 0.15, ALE–PLE 0.06.

Sternum 1.44 mm long, 1.08 mm wide, light orange-brown with translucent border and darkened extensions to coxae. Chelicerae 1.12 mm long with 4 promarginal teeth and 8 retromarginal denticles, dark orange-brown proximally, dark brown distally. Labium and endites light orange-brown, darkest proximally. Endites sharply invaginated at middle.

Abdomen 3.20 mm long, 1.73 mm wide, pale grayish-brown with transverse rows of dark markings, venter pale. Epigastric furrow 0.40 mm from tracheal spiracle, spiracle 1.73 mm from base of spinnerets.

Legs light orange-brown with distal segments darkest. Tibial lengths (mm) and indices: I 2.64, 10; II 1.87, 15; III 1.19, 26; IV 2.09, 15. Ventral spination: tibiae I, II 2–2–2, III 1–2–2; IV 2–2–2; metatarsi I, II 2–0–0, III 2–1–2, IV 2–2–2.

Palpus as in Figure 116, 117.

Female (Washington Co., Arkansas). Coloration as in male.

Total length 8.42 mm. Carapace 2.75 mm long, 2.11 mm wide, cephalic width 1.47 mm, clypeus height 0.10 mm. Eyes: diameters (mm): AME 0.14, ALE 0.14, PME 0.13, PLE 0.14; anterior eye row 0.43 mm long, recurved; posterior eye row 1.04 mm long, procurved; MOQ length 0.43 mm, front width 0.36 mm, back width 0.49 mm; eye interdistances (mm): AME–AME 0.09, AME–ALE 0.08, PME–PME 0.22, PME–PLE 0.18, ALE–PLE 0.06.

Sternum 1.84 mm long, 1.31 mm wide. Chelicerae 1.57 mm long with teeth as in male.

Abdomen 5.76 mm long, 3.53 mm wide. Epigastric furrow 0.68 mm from tracheal spiracle, spiracle 3.24 mm from base of spinnerets.

Tibial lengths (mm) and indices: I 2.56, 16; II 1.94, 20; III 1.26, 30; IV 2.30, 17. Ventral spination: tibiae I 2–2–0, II 1–2–1, III 1–1–2, IV 1–2–2; metatarsi I, II 2–0–0, III 2–0–2, IV 2–2–2.

Epigynum as in Figure 140, internal genitalia as in Figure 143.

Natural history. Mature males and females have been taken year-round. Specimens have been taken by sweeping, in pitcher plants, on loblolly pine, in fall webworm nests and frequently in houses.

Distribution. New England west to Wisconsin and Iowa, south to Florida and eastern Texas (Map 4).

Aysha cambridgei Bryant
Map 4; Figures 120, 121, 138, 141

Aysha cambridgei Bryant, 1931, Psyche, 38: 119, pl. 7, fig. 15 (♂). Male holotype from Guanajuato, Mexico, in MCZ, examined. Roewer, 1954, Katalog der Araneae, 2: 532. Bonnet, 1955, Bibliographia Araneorum, 2: 836.

Diagnosis. Aysha cambridgei is closely related to *A. gracilis* but has a distinctive spike on the proximal edge of the base of the embolus (Fig. 120) and the median epigynal opening near the anterior rim of the epigynum (Fig. 138).

Male (Jeff Davis Co., Texas). Coloration as in *Aysha gracilis* except that the abdomen is pale white with two dark paramedian longitudinal bands.

Total length 5.87 mm. Carapace 2.41 mm long, 1.91 mm wide, cephalic width 0.97 mm, clypeus height 0.11 mm. Eyes: diameters (mm): AME 0.11, ALE 0.12, PME 0.11, PLE 0.11; anterior eye row 0.57 mm long, recurved; posterior eye row 0.75 mm long, procurved; MOQ length 0.33 mm, front width 0.28 mm, back width 0.38 mm; eye interdistances (mm): AME–AME 0.06, AME–ALE 0.05, PME–PME 0.16, PME–PLE 0.11, ALE–PLE 0.05.

Sternum 1.42 mm long, 1.01 mm wide. Chelicerae 0.98 mm long with 4 promarginal teeth and 7 retromarginal denticles.

Abdomen 3.49 mm long, 1.58 mm wide. Epigastric furrow 0.68 mm from tracheal

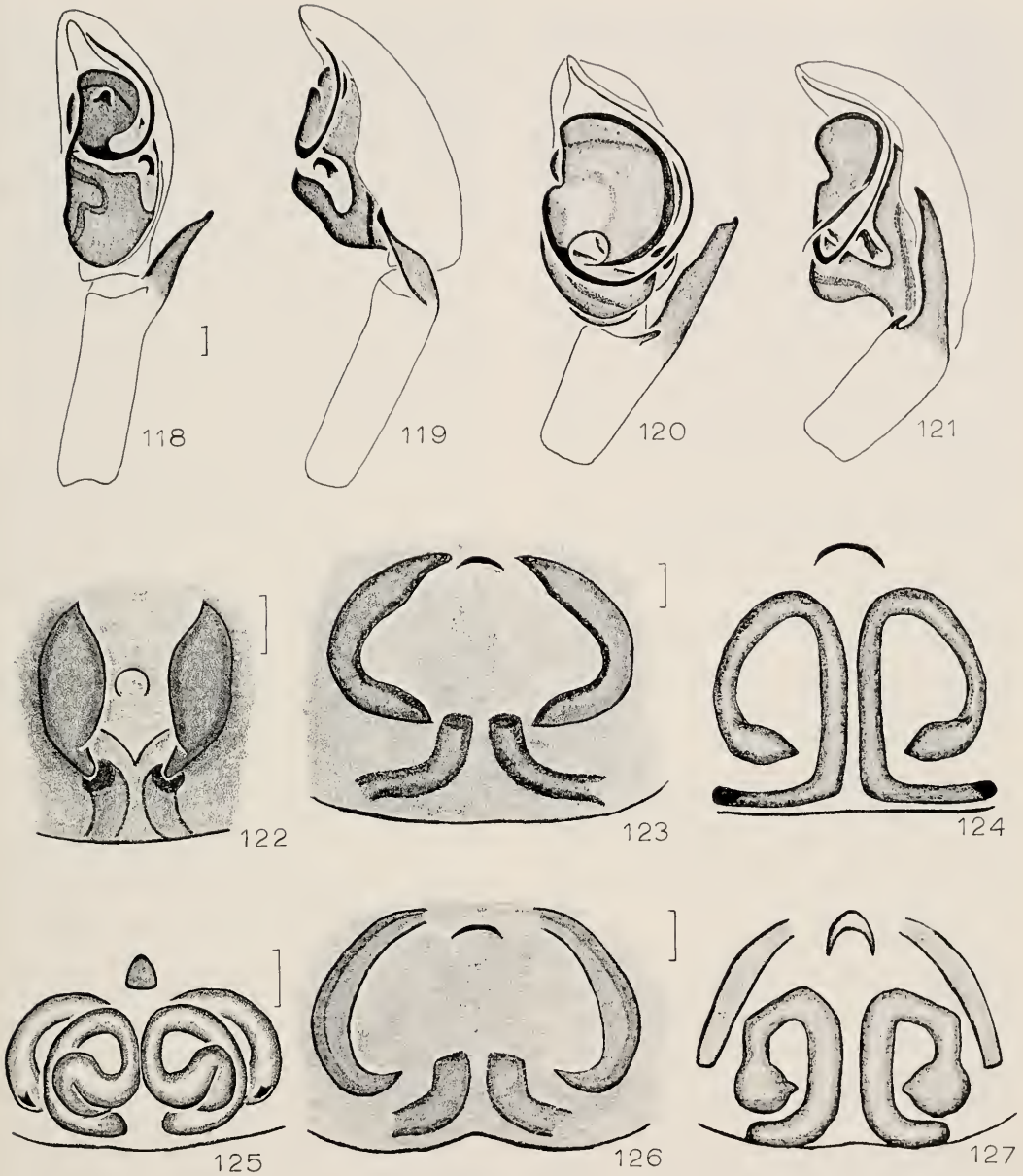

Plate 10

Figures 118, 120. Left palpi, ventral view. Figures 119, 121. Left palpi, retrolateral view. Figures 122, 123, 126. Epigyna, ventral view. Figures 124, 125, 127. Internal genitalia, dorsal view. 118, 119. *Aysha arunda* new species. 120, 121. *Aysha cambridgei* Bryant. 122, 125. *Aysha velox* (Becker). 123, 124. *Aysha decepta* (Banks). 126, 127. *Aysha incursa* (Chamberlin).

spiracle, spiracle 1.55 mm from base of spinnerets.

Tibial lengths (mm) and indices: I 3.06, 8; II 1.87, 13; III 1.28, 21; IV 2.16, 12. Ventral spination: tibiae I, II 2–2–2, III 1–2–2, IV 2–2–2; metatarsi I, II 2–0–0, III, IV 2–2–2.

Palpus as in Figures 120, 121.

Female (Henderson Co., Texas). Coloration as in male.

Total length 8.50 mm. Carapace 3.35 mm long, 2.52 mm wide, cephalic width 1.69 mm, clypeus height 0.12 mm. Eyes: diameters (mm): AME 0.14, ALE 0.16, PME 0.14, PLE 0.14; anterior eye row 0.84 mm long, recurved; posterior eye row 1.11 mm long, procurved; MOQ length 0.42 mm, front width 0.37 mm, back width 0.50 mm; eye interdistances (mm): AME–AME 0.10, AME–ALE 0.07, PME–PME 0.22, PME–PLE 0.20, ALE–PLE 0.05.

Sternum 1.91 mm long, 1.22 mm wide. Chelicerae 1.69 mm long with teeth as in male.

Abdomen 5.04 mm long, 2.88 mm wide. Epigastric furrow 0.61 mm from tracheal spiracle, spiracle 3.17 mm from base of spinnerets.

Tibial lengths (mm) and indices: I 2.88, 12; II 2.07, 17; III 1.40, 26; IV 2.57, 15. Ventral spination as in male except tibiae I, II 2–2–0 and III 2–2–2.

Epigynum as in Figure 138, internal genitalia as in Figure 141.

Natural history. Mature males have been taken from mid-June through early August, mature females from late May through early August. Specimens have been taken on trees and shrubs.

Distribution. South central states from Alabama to western Texas, south to central Mexico (Map 4).

Aysha decepta (Banks)
Map 4; Figures 112, 113, 123, 124

Anyphaena decepta Banks, 1899, Proc. Ent. Soc. Washington, 4: 190. Female holotype from Brazos Co., Texas, in MCZ, examined.

Aysha minuta F. O. P.-Cambridge, 1900, Biologia Centrali Americana, Aran., 2: 99, pl. 7, figs. 18–19 (♂, ♀). Male holotype, female allotype from Guatemala, in BMNH, examined. Bryant, 1931, Psyche, 38: 120, pl. 7, fig. 17, ♂. Roewer, 1954, Katalog der Araneae, 2: 533. Bonnet, 1955, Bibliographia Araneorum, 2: 838. NEW SYNONYMY.

Aysha decepta, Bryant, 1931, Psyche, 38: 120, pl. 7, fig. 16, pl. 8, fig. 27, ♂, ♀. Roewer, 1954, Katalog der Araneae, 2: 534. Bonnet, 1955, Bibliographia Araneorum, 2: 836.

Diagnosis. Aysha decepta is very closely related to *A. incursa* but has a characteristic flap (on the retrolateral tip of the tegulum) that covers the embolus (Fig. 112), while the base of the epigynal sidepieces is a considerable distance from the epigastric furrow (Fig. 123). Both morphological and zoogeographical data (Map 4) indicate that these two species are each other's nearest relatives.

Male (Hidalgo Co., Texas). Coloration as in *Aysha cambridgei*.

Total length 4.82 mm. Carapace 2.25 mm long, 1.76 mm wide, cephalic width 1.06 mm, clypeus height 0.10 mm. Eyes: diameters (mm): AME 0.08, ALE 0.10, PME 0.11, PLE 0.11; anterior eye row 0.58 mm long, straight; posterior eye row 0.75 mm long, procurved; MOQ length 0.23 mm, front width 0.24 mm, back width 0.39 mm; eye interdistances (mm): AME–AME 0.08, AME–ALE 0.06, PME–PME 0.18, PME–PLE 0.12, ALE–PLE 0.05.

Sternum 1.37 mm long, 0.85 mm wide. Chelicerae 0.97 mm long with 4 promarginal teeth and 7 retromarginal denticles.

Abdomen 2.74 mm long, 1.39 mm wide. Epigastric furrow 0.38 mm from tracheal spiracle, spiracle 1.28 mm from base of spinnerets.

Tibial lengths (mm) and indices: I 2.54, 9; II 1.67, 14; III 1.01, 25; IV 1.89, 16. Ventral spination: tibiae I 2–2–0, II 1–2–0, III 1–2–2, IV 2–2–2; metatarsi I, II 2–0–0, III, IV 2–2–2.

Palpus as in Figures 112, 113.

Female (E. Baton Rouge Parish, Louisiana). Coloration as in male of *Aysha cambridgei*.

Total length 5.76 mm. Carapace 2.45 mm long, 1.80 mm wide, cephalic width 1.17 mm, clypeus height 0.09 mm. Eyes: diameters (mm): AME 0.10, ALE 0.13, PME 0.12, PLE 0.12; anterior eye row 0.60 mm long, recurved; posterior eye row 0.76 mm long, procurved; MOQ length 0.30 mm, front width 0.26 mm, back width

0.38 mm; eye interdistances (mm): AME–AME 0.07, AME–ALE 0.05, PME–PME 0.15, PME–PLE 0.11, ALE–PLE 0.04.

Sternum 1.35 mm long, 0.95 mm wide. Chelicerae 0.89 mm long with 4 promarginal teeth and 8 retromarginal denticles.

Abdomen 3.51 mm long, 2.20 mm wide. Epigastric furrow 0.41 mm from tracheal spiracle, spiracle 1.78 mm from base of spinnerets.

Tibial lengths (mm) and indices: I 1.84, 14; II 1.40, 19; III 0.93, 29; IV 1.82, 17. Ventral spination as in male except tibiae III 1–1–2 and metatarsi III 2–1–2.

Epigynum as in Figure 123, internal genitalia as in Figure 124.

Natural history. Mature males and females have been taken every month except January and February. Specimens are commonly found in great quantities in wasp nests and occasionally in houses.

Distribution. Northern Florida west to eastern Texas, south to Costa Rica (Map 4).

Aysha incursa (Chamberlin)
Map 4; Figures 114, 115, 126, 127

Anyphaena incursa Chamberlin, 1919, Pomona Coll. J. Ent. Zool., 12: 12, pl. 5, fig. 2 (♀). Female holotype from Claremont, California, in MCZ, examined. Bryant, 1931, Psyche, 38: 120 (sub *Aysha decepta* [sic]). Roewer, 1954, Katalog der Araneae, 2: 534 (sub *Aysha decepta* [sic]). Bonnet, 1955, Bibliographia Araneorum, 2: 836 (sub *Aysha decepta* [sic]).

Anyphaena johnstoni Chamberlin, 1924, Proc. California Acad. Sci., 12: 662, figs. 105, 106 (♂, ♀). Female holotype, male allotype from San Pedro Nolasco Island, Gulf of California, in California Academy of Sciences. Paratype male from San Marcos Island, Gulf of California, in MCZ, examined. Bryant, 1931, Psyche, 38: 120 (sub *Aysha decepta* [sic]). Bonnet, 1955, Bibliographia Araneorum, 2: 836 (sub *Aysha decepta* [sic]).

Anyphaena nigrifrons Chamberlin and Woodbury, 1929, Proc. Biol. Soc. Washington, 42: 137, pl. 1, fig. 4 (♀). Female holotype from St. George, Utah, in AMNH, examined. NEW SYNONYMY.

Aysha nigrifrons, Bryant, 1931, Psyche, 38: 121. Roewer, 1954, Katalog der Araneae, 2: 534. Bonnet, 1955, Bibliographia Araneorum, 2: 838.

Diagnosis. Aysha incursa is very closely related to *A. decepta* but has a distinctive sharp point on the retrolateral tip of the tegulum (Fig. 114), while the base of the epigynal sidepieces is near the epigastric furrow (Fig. 126).

Male (Tulare Co., California). Coloration as in *Aysha cambridgei*.

Total length 6.08 mm. Carapace 3.02 mm long, 2.18 mm wide, cephalic width 1.22 mm, clypeus height 0.12 mm. Eyes: diameters (mm): AME 0.11, ALE 0.12, PME 0.11, PLE 0.12; anterior eye row 0.66 mm long, recurved; posterior eye row 0.84 mm long, procurved; MOQ length 0.33 mm, front width 0.31 mm, back width 0.42 mm; eye interdistances (mm): AME–AME 0.10, AME–ALE 0.07, PME–PME 0.21, PME–PLE 0.17, ALE–PLE 0.05.

Sternum 1.67 mm long, 1.08 mm wide. Chelicerae 1.22 mm long with 3 promarginal teeth and 8 retromarginal denticles.

Abdomen 3.38 mm long, 1.80 mm wide. Epigastric furrow 0.50 mm from tracheal spiracle, spiracle 1.75 mm from base of spinnerets.

Tibial lengths (mm) and indices: I 3.15, 9; II 2.16, 14; III 1.40, 26; IV 2.34, 16. Ventral spination: tibiae I 2–2–0, II, III, IV 2–2–2; metatarsi I, II 2–0–0, III, IV 2–2–2.

Palpus as in Figures 114, 115.

Female (Santa Barbara Co., California). Coloration as in male of *Aysha cambridgei*.

Total length 5.72 mm. Carapace 2.09 mm long, 1.66 mm wide; cephalic width 1.04 mm, clypeus height 0.05 mm. Eyes: diameters (mm): AME 0.08, ALE 0.09, PME 0.10, PLE 0.10; anterior eye row 0.50 mm long, recurved; posterior eye row 0.67 mm long, procurved; MOQ length 0.25 mm, front width 0.23 mm, back width 0.33 mm; eye interdistances (mm): AME–AME 0.07, AME–ALE 0.05, PME–PME 0.14, PME–PLE 0.11, ALE–PLE 0.06.

Sternum 1.30 mm long, 0.85 mm wide. Chelicerae 0.70 mm long with 3 promarginal teeth and 8 retromarginal denticles.

Abdomen 4.00 mm long, 2.38 mm wide. Epigastric furrow 0.70 mm from tracheal spiracle, spiracle 1.91 mm from base of spinnerets.

Tibial lengths (mm) and indices: I 1.57, 14; II 1.26, 17; III 0.86, 29; IV 1.64, 15. Ventral spination as in male except tibiae II, III 1–1–0 and IV 1–1–2 and metatarsi III 2–0–2.

Epigynum as in Figure 126, internal genitalia as in Figure 127.

Natural history. Mature males have been taken from late April through early September, mature females year-round. Specimens have been taken on poplars, in fields, and in houses.

Distribution. California west to Utah, south to southern Mexico (Map 4).

Aysha velox (Becker)
Map 4; Figures 110, 111, 122, 125

Anyphaena velox Becker, 1879, Ann. Ent. Soc. Belgique, 22: 83, pl. 2, figs. 5–7 (♀). Female holotype from Pascagoula, Mississippi, should be in the Institute Royal des Sciences Naturelles de Belgique but could not be located there by Mr. J. Kekenbosch in 1971; lost, presumed destroyed. Banks, 1904, Proc. Acad. Nat. Sci. Philadelphia, 56: 123, pl. 8, fig. 19, ♂.

Anyphaena floridana Banks, 1896, Trans. Amer. Ent. Soc., 23: 63. Female holotype from Lake Worth, Florida, in MCZ, examined.

Aysha orlandensis Tullgren, 1901, Bih. Svenska Akad., 27: 19, fig. 4 (♀). Female holotype from Orlando, Florida, in Uppsala Univ. Zool. Mus., examined. Bryant, 1931, Psyche, 38: 119 (sub *Aysha gracilis* [sic]). Roewer, 1954, Katalog der Araneae, 2: 534 (sub *Aysha gracilis* [sic]). Bonnet, 1955, Bibliographia Araneorum, 2: 837 (sub *Aysha gracilis* [sic]). NEW SYNONYMY.

Aysha velox, Banks, 1909, Estacion central agronomica de Cuba, Second Report, p. 158. Bryant, 1931, Psyche, 38: 119, pl. 7, fig. 14, pl. 8, fig. 34, ♂, ♀. Roewer, 1954 Katalog der Araneae 2: 534. Bonnet, 1955, Bibliographia Araneorum, 2: 839.

Chiracanthium falculum Chamberlin, 1925, Bull. Mus. Comp. Zool., 67: 220. Male holotype from Sebastian, Florida, in MCZ, examined.

Diagnosis. Aysha velox is a distinctive species easily recognized by its short retrolateral tibial apophysis and its lack of a ventral tibial apophysis (Fig. 111) and the embolus' not being restricted to the distal half of the palpal bulb (Fig. 110). The coiled internal ducts of females (Fig. 125) are diagnostic.

Male (Alachua Co., Florida). Coloration as in *Aysha gracilis* except that the abdomen lacks dark markings.

Total length 7.31 mm. Carapace 3.45 mm long, 2.52 mm wide, cephalic width 1.51 mm, clypeus height 0.13 mm. Eyes: diameters (mm): AME 0.15, ALE 0.14, PME 0.13, PLE 0.15; anterior eye row 0.80 mm long, recurved; posterior eye row 1.01 mm long, procurved; MOQ length 0.42 mm, front width 0.38 mm, back width 0.47 mm; eye interdistances (mm): AME–AME 0.09, AME–ALE 0.09, PME–PME 0.22, PME–PLE 0.18, ALE–PLE 0.05.

Sternum 1.92 mm long, 1.28 mm wide. Chelicerae 1.58 mm long with 4 promarginal teeth and 8 retromarginal denticles.

Abdomen 4.14 mm long, 1.76 mm wide. Epigastric furrow 0.31 mm from tracheal spiracle, spiracle 2.46 mm from base of spinnerets.

Tibial lengths (mm) and indices: I 3.92, 8; II 2.86, 12; III 1.69, 21; IV 2.52, 14. Ventral spination: tibiae I–IV 2–2–2; metatarsi I, II 2–0–0, III, IV 2–2–2.

Palpus as in Figure 110, 111.

Female (Alachua Co., Florida). Coloration as in male.

Total length 8.42 mm. Carapace 3.96 mm long, 2.88 mm wide; cephalic width 1.87 mm, clypeus height 0.14 mm. Eyes: diameters (mm): AME 0.15, ALE 0.14, PME 0.14, PLE 0.14; anterior eye row 1.02 mm long, recurved; posterior eye row 1.31 mm long, procurved; MOQ length 0.48 mm, front width 0.45 mm, back width 0.57 mm; eye interdistances (mm): AME–AME 0.14, AME–ALE 0.14, PME–PME 0.28, PME–PLE 0.27, ALE–PLE 0.09.

Sternum 2.16 mm long, 1.62 mm wide. Chelicerae 1.87 mm long with teeth as in male.

Abdomen 4.50 mm long, 2.41 mm wide.

Epigastric furrow 0.36 mm from tracheal spiracle, spiracle 2.48 mm from base of spinnerets.

Tibial lengths (mm) and indices: I 3.46, 11; II 2.68, 14; III 1.66, 24; IV 2.79, 14. Ventral spination as in male.

Epigynum as in Figure 122, internal genitalia as in Figure 125.

Natural history. Mature males and females have been taken year-round. Specimens have been taken on *Casuarina* sp., *Citrus* sp., *Paurotis* sp., *Calamandra* sp., *Pinus* sp., *Nelumbo* sp., and in houses.

Distribution. North Carolina west to Arkansas, south to east Texas and Florida, Cuba, Haiti, the Dominican Republic and Bermuda (Map 4).

Aysha arunda new species
Map 4; Figures 118, 119, 139, 142

Types. Male holotype, female paratype from Edinburg, Hidalgo Co., Texas, May 1934 (Mulaik), deposited in AMNH. Male and female paratypes from Hidalgo Co., Texas, deposited in MCZ. The specific name is an arbitrary combination of letters.

Diagnosis. Aysha arunda is a distinctive species easily recognized by the restriction of the embolus to the distal half of the palpal bulb (Fig. 118) and the triangular shape of the epigynum (Fig. 139).

Male (Hidalgo Co., Texas). Coloration as in *Aysha cambridgei.*

Total length 6.23 mm. Carapace 3.04 mm long, 2.02 mm wide, cephalic width 1.49 mm, clypeus height 0.10 mm. Eyes: diameters (mm): AME 0.13, ALE 0.13, PME 0.14, PLE 0.14; anterior eye row 0.74 mm long, recurved; posterior eye row 0.95 mm long, procurved; MOQ length 0.44 mm, front width 0.34 mm, back width 0.43 mm; eye interdistances (mm): AME–AME 0.07, AME–ALE 0.06, PME–PME 0.16, PME–PLE 0.19, ALE–PLE 0.07.

Sternum 1.73 mm long, 1.24 mm wide. Chelicerae 1.62 mm long with 4 promarginal teeth and 8 retromarginal denticles.

Abdomen 3.62 mm long, 1.67 mm wide. Epigastric furrow 0.31 mm from tracheal spiracle, spiracle 1.75 mm from base of spinnerets.

Tibial lengths (mm) and indices: I 4.03, 7; II 2.72, 12; III 1.53, 20; IV 2.58, 15. Ventral spination: tibiae I–IV 2–2–2; metatarsi I, II 2–0–0, III, IV 2–2–2.

Palpus as in Figures 118, 119.

Female (Hidalgo Co., Texas). Coloration as in male of *Aysha cambridgei.*

Total length 6.59 mm. Carapace 2.99 mm long, 2.23 mm wide, cephalic width 1.33 mm, clypeus height 0.09 mm. Eyes: diameters (mm): AME 0.11, ALE 0.13, PME 0.13, PLE 0.13; anterior eye row 0.70 mm long, recurved; posterior eye row 0.91 mm long, procurved; MOQ length 0.40 mm, front width 0.32 mm, back width 0.43 mm; eye interdistances (mm): AME–AME 0.10, AME–ALE 0.07, PME–PME 0.18, PME–PLE 0.17, ALE–PLE 0.06.

Sternum 1.62 mm long, 1.13 mm wide. Chelicerae 1.37 mm long with 4 promarginal teeth and 9 retromarginal denticles.

Abdomen 3.76 mm long, 2.12 mm wide. Epigastric furrow 0.40 mm from tracheal spiracle, spiracle 2.23 mm from base of spinnerets.

Tibial lengths (mm) and indices: I 2.65, 12; II 2.00, 16; III 1.22, 27; IV 2.25, 16. Ventral spination as in male.

Epigynum as in Figure 139, internal genitalia as in Figure 142.

Natural history. Mature males have been taken from early May through late September, mature females from early April through late September. Nothing is known of the habits of this species.

Distribution. Southern Texas (Map 4).

Oxysoma Nicolet

Oxysoma Nicolet, 1849, *in* Gay: Hist. Chili, 10 (3): 511. Type species *Oxysoma punctatum* Nicolet, 1849, designated by Simon, 1897, Hist. Natur. Araign., 2: 100.

Gayennina Gertsch, 1935, Amer. Mus. Novitates, No. 805: 21. Type species by monotypy *Gayennina britcheri* Gertsch, 1935.

Diagnosis. Oxysoma can be quickly distinguished from all other North Ameri-

can anyphaenids by the presence of only two teeth on the cheliceral retromargin. In addition, the coloration pattern shown in Figure 109 is typical for the genus throughout its range. Predominantly South American, only one species occurs north of Mexico. *Oxysoma* is more closely related to *Aysha* than to *Anyphaena* or *Wulfila*.

Description. Total length 5–7 mm. Carapace longer than wide, narrowed in front to about half its maximum width. Clypeus height more than twice the anterior median eye diameter. Posterior median, posterior lateral and anterior lateral eyes subequal in size, much larger than anterior medians. Procurved posterior eye row longer than recurved anterior row. Median ocular quadrangle more than twice as wide in back as in front. Anterior median eyes separated by their diameter, closer to anterior laterals than to each other. Posterior medians separated by almost three times their diameter, closer to posterior laterals. Anterior laterals separated by their diameter from posterior laterals. Sternum longer than wide, unmodified. Chelicerae with 3 promarginal and 2 retromarginal teeth. Abdomen longer than wide, tracheal spiracle roughly midway between epigastric furrow and base of spinnerets. Leg formula 1423, legs unmodified. Metatarsi I and II with one pair of ventral spines. Palpus bulbous, with elongated conductor and conspicuous embolus. Retrolateral tibial apophysis lacking. Epigynum on a sclerotized plate. Internal genitalia with two large spermathecae and accessory ducts.

Variation. The two males of *Oxysoma cubana* known from Arizona are slightly larger than the eastern specimens. One has a broken conductor, the other matches the eastern specimens in genitalic details.

Oxysoma punctatum Nicolet

Oxysoma punctatum Nicolet, 1849, *in* Gay: Hist. Chili, 10(3): 513, pl. 4, fig. 13 (♀). Female holotype from Chile, possibly in Muséum National d'Histoire Naturelle, Paris, unavailable. Roewer, 1954, Katalog der Araneae, 2: 544. Bonnet, 1958, Bibliographia Araneorum, 2: 3269.

Types of this species, type species of *Oxysoma*, were unfortunately unavailable for examination.

Oxysoma cubana Banks
Map 5; Figures 105–109

Oxysoma cubana Banks, 1909, Estacion central agronomica de Cuba, Second Report, II (2): 157, pl. 10, fig. 7 (♂). Male holotype from Havana, Habana, Cuba, in MCZ, examined. Bryant, 1940, Bull. Mus. Comp. Zool., 86: 435, pl. 16, figs. 218, 222, pl. 17, fig. 234, ♂, ♀. Kaston, 1948, Bull. Connecticut Geol. Natur. Hist. Surv., 70: 405.

Gayennina britcheri Gertsch, 1935, Amer. Mus. Novitates, No. 805: 21, figs. 35, 36 (♀). Female holotype from Woods Hole, Massachusetts, in AMNH, examined. Kaston, 1948, Bull. Connecticut Geol. Natur. Hist. Surv., 70: 405. Roewer, 1954, Katalog der Araneae, 2: 540. Bonnet, 1957, Bibliographia Araneorum, 2: 1981.

Oxysoma cubanum, Roewer, 1954, Katalog der Araneae, 2: 543. Bonnet, 1958, Bibliographia Araneorum, 2: 3268.

Diagnosis. The characters of the genus distinguish this species from all other nearctic anyphaenids. The bulbous palp (Fig. 107) and characteristic epigynum (Fig. 106), as well as the color pattern (Fig. 109), are diagnostic. Variation in this species is discussed above.

Male (Suffolk Co., New York). Total length 5.22 mm. Carapace 2.68 mm long, 2.14 mm wide, cephalic width 1.08 mm, clypeus height 0.23 mm, pale yellow with a median dark band and two submarginal longitudinal rows of dark spots. Eyes: diameters (mm): AME 0.05, ALE 0.11, PME 0.09, PLE 0.08; anterior eye row 0.49 mm long, slightly recurved; posterior eye row 0.76 mm long, procurved; MOQ length 0.26 mm, front width 0.19 mm, back width 0.44 mm; eye interdistances (mm): AME–AME 0.06, AME–ALE 0.05, PME–PME 0.26, PME–PLE 0.16, ALE–PLE 0.12.

Sternum 1.42 mm long, 0.95 mm wide, pale yellow with translucent border. Chelicerae 0.65 mm long, pale yellow with 3

Map 5. Distributions of *Oxysoma cubana* and *Teudis mordax*.

promarginal and 2 retromarginal teeth. Labium and endites pale yellow. Endites not invaginated at middle.

Abdomen 2.97 mm long, 1.39 mm wide, pale white with a median longitudinal dark band, venter pale. Epigastric furrow 0.58 mm from tracheal spiracle, spiracle 1.13 mm from base of spinnerets.

Legs pale yellow with scattered dark markings, unmodified. Tibial lengths (mm) and indices: I 2.09, 17; II 1.78, 20; III 1.35, 26; IV 2.07, 14. Ventral spination: tibiae I, II 2–2–2, III 1–2–2, IV 2–2–2; metatarsi I, II 2–0–0, III 2–0–2, IV 2–2–2.

Palpus as in Figures 105, 107.

Female (Barnstable Co., Massachusetts). Coloration as in male.

Total length 5.90 mm. Carapace 2.66 mm long, 1.91 mm wide, cephalic width 1.01 mm, clypeus height 0.14 mm. Eyes: diameters (mm): AME 0.06, ALE 0.12, PME 0.09, PLE 0.10; anterior eye row 0.46 mm long, recurved; posterior eye row 0.74 mm long, procurved; MOQ length 0.34 mm, front width 0.19 mm, back width 0.41 mm; eye interdistances (mm): AME–AME 0.05, AME–ALE 0.04, PME–PME 0.25, PME–PLE 0.13, ALE–PLE 0.11.

Sternum 1.42 mm long, 0.86 mm wide. Chelicerae 0.86 mm long with teeth as in male.

Abdomen 3.71 mm long, 1.71 mm wide. Epigastric furrow 1.19 mm from tracheal spiracle, spiracle 1.13 mm from base of spinnerets.

Tibial lengths (mm) and indices: I 1.55, 23; II 1.46, 23; III 1.10, 21; IV 1.42, 18. Ventral spination as in male except tibiae III 0–2–2 and metatarsi IV 0–0–0.

Epigynum as in Figure 106, internal genitalia as in Figure 108.

Natural history. Mature males have been taken from late May through late August, mature females from late March through late August. One specimen was taken in a pitfall trap, but the habits of this widespread but rare species are unknown.

Distribution. Southeastern Arizona to Michigan, Massachusetts, Florida, and Cuba (Map 5).

Teudis O. P.-Cambridge

Teudis O. P.-Cambridge, 1896, Biologia Centrali Americana, Aran., 1: 198. Type species *Teudis gentilis* O. P.-Cambridge, 1896 (= *Teudis geminus* Petrunkevitch, 1911), designated by F.O. P.-Cambridge, 1900, *ibid.*, 2: 100.

Diagnosis. The limits of this genus are not known with certainty. One of the

species here placed in *Teudis* was included in the genus by its original author, O. P.-Cambridge. As here construed, the genus is a large one, including a large number of neotropic species with diverse genitalia. The following somatic characters are diagnostic: the carapace is only slightly narrowed in front, is reddish brown, darkest at the sides, with a shiny, glabrous cephalic area and without dark paramedian longitudinal bands; the legs are short and thick; the chelicerae are often produced forward. The affinities of the genus are uncertain, but it is probably more closely related to *Aysha* and *Oxysoma* than to *Anyphaena* or *Wulfila.*

Description. Total length 3–5 mm. Carapace longer than wide, narrowed in front to two-thirds to four-fifths of its maximum width. Clypeus height roughly equal to anterior median eye diameter. Posterior median, posterior lateral and anterior lateral eyes subequal in size, slightly larger than anterior medians. Procurved posterior eye row longer than recurved anterior row. Median ocular quadrangle longer than wide in front, wider in back than long. Anterior median eyes separated by their diameter, closer to anterior laterals than to each other. Posterior medians separated by 1.5 times their diameter, closer to posterior laterals. Anterior laterals separated by their radius from posterior laterals. Sternum longer than wide, unmodified. Chelicerae often produced forward, with 3–4 promarginal teeth and 4–6 retromarginal denticles. Abdomen longer than wide, tracheal spiracle slightly closer to epigastric furrow than to base of spinnerets. Leg formula 1423, legs unmodified. Metatarsi I and II with one or two pairs of ventral spines. Palpus with a sharply pointed median apophysis, short conductor and conspicuous curving embolus. Retrolateral tibial apophysis spur-like, retrolateral patellar apophysis sometimes present. Epigynum with conspicuous openings; two simple spermathecae.

Variation. Teudis mordax is a polymorphic species. Two forms of males occur, one in which the chelicerae are similar to those of females, averaging 1.0 mm in length and one in which the chelicerae are greatly elongated, averaging 2.3 mm in length. This polymorphism occurs in both areas from which adequate population samples exist, the southeastern United States and Panama. The proportion of males with long chelicerae is about one in five. The genitalia are identical in both forms. The paratype male of *Gayenna absoluta* from Baja California, a synonym, has normal chelicerae; the holotype male of *Teudis mordax* from Guerrero, Mexico, has elongate chelicerae. The California population is unfortunately known only from females, which are slightly larger than those from other parts of the range. The special uses, if any, of the long chelicerae are unknown.

Key to Species

1a. Metatarsi I and II with two pairs of ventral spines. Chelicerae produced forward. Leg segments uniform in color. Palpus without a retrolateral patellar apophysis (Fig. 131). Epigynum as in Fig. 132 ..... *mordax*

1b. Metatarsi I and II with one pair of ventral spines. Chelicerae not produced forward. Femora much darker than other leg segments. Palpus with a retrolateral patellar apophysis (Fig. 128). Epigynum as in Fig. 129 .... *calcar*

Teudis gentilis O. P.-Cambridge
Figure 146

Teudis gentilis O. P.-Cambridge, 1896, Biologia Centrali Americana, Aran., 1: 199, pl. 25, fig. 6 (♂). Male holotype from Coban, Guatemala, in BMNH, examined.

Teudis geminus Petrunkevitch, 1911, Bull. Amer. Mus. Natur. Hist., 29: 516, *nom. nov.* for *T. gentilis*, possibly preoccupied by *Anyphaena gentilis* Keyserling, 1891. Roewer, 1954, Katalog der Araneae, 2: 548. Bonnet, 1959, Bibliographia Araneorum, 2: 4366.

This species, type species of *Teudis*, is genitalically close to several species from Panama described by Chickering in the genus *Sillus* and is somatically similar to the species here included in *Teudis.*

Teudis mordax (O. P.-Cambridge)
Map 5; Figures 131–133

Delozeugma mordax O. P.-Cambridge, 1896, Biologia Centrali Americana, Aran., 1: 182, pl. 22, fig. 11 (♂). Male holotype from Omiltemi, Guerrero, Mexico, in BMNH, examined.

Teudis mordax, O. P.-Cambridge, 1896, Biologia Centrali Americana, Aran., 1: 198. Roewer, 1954, Katalog der Araneae, 2: 549. Bonnet, 1959, Bibliographia Araneorum, 2: 4368.

Anyphaena fragilis Banks, 1897, Canad. Ent., 29: 194. Female holotype from Jacksonville, Florida, in MCZ, examined. Bryant, 1931, Psyche, 38: 114, pl. 8, fig. 32, ♀. Roewer, 1954, Katalog der Araneae, 2: 527. Bonnet, 1955, Bibliographia Araneorum, 2: 344. NEW SYNONYMY.

Gayenna parvula Banks, 1899, Proc. Ent. Soc. Washington, 4: 191. Female holotype from Shreveport, Louisiana, in MCZ, examined.

Gayenna absoluta Chamberlin, 1924. Proc. California Acad. Sci., 12: 661, figs. 103, 104 (♂, ♀). Female holotype, male allotype from Concepcion Bay, Baja California, in California Academy of Sciences. Male and female paratypes from same locality in MCZ, examined. Roewer, 1954, Katalog der Araneae, 2: 535. Bonnet, 1957, Bibliographia Araneorum, 2: 1976. NEW SYNONYMY.

Anyphaena laticeps Bryant, 1931, Psyche, 38: 108, pl. 6, fig. 4, pl. 8, fig. 24 (♂, ♀). Male holotype, female allotype from Thompson's Mills, Jackson Co., Georgia, in MCZ, examined. Roewer, 1954, Katalog der Araneae, 2: 529. Bonnet, 1955, Bibliographia Araneorum, 2: 345. NEW SYNONYMY.

Sillus coloratus Chickering, 1937, Pap. Michigan Acad. Sci., 22: 548, pl. 58, fig. 10, pl. 59, figs. 23, 32 (♀). Female holotype from Barro Colorado Island, Panama Canal Zone, in MCZ, examined. Roewer, 1954, Katalog der Araneae, 2: 545. Bonnet, 1958, Bibliographia Araneorum, 2: 4048. NEW SYNONYMY.

Anyphaena barrowsi Chamberlin and Ivie, 1946, Bull. Univ. Utah, 36: 9, fig. 12 (♀). Female holotype from Fort Myers, Florida, in AMNH, examined. Roewer, 1954, Katalog der Araneae, 2: 524. NEW SYNONYMY.

Teudis fragilis, Barnes, 1953, Amer. Mus. Novitates, No. 1632: 18.

Diagnosis. Teudis mordax may be distinguished from all other anyphaenids in America north of Mexico by the chelicerae, which project forward. The shape of the palpal median apophysis (Fig. 131) and the epigynum (Fig. 132) are also diagnostic. Variation in this species is discussed above.

Male (Sarasota Co., Florida). Total length (exclusive of chelicerae) 3.67 mm. Carapace 1.79 mm long, 1.31 mm wide, cephalic width 0.99 mm, clypeus height 0.05 mm, light reddish brown, darkest at sides, cephalic area shiny, glabrous. Eyes: diameters (mm): AME 0.07, ALE 0.09, PME 0.08, PLE 0.09; anterior eye row 0.50 mm long, recurved; posterior eye row 0.62 mm long, procurved; MOQ length 0.27 mm, front width 0.22 mm, back width 0.31 mm; eye interdistances (mm): AME–AME 0.07, AME–ALE 0.05, PME–PME 0.14, PME–PLE 0.13, ALE–PLE 0.04.

Sternum 1.04 mm long, 0.74 mm wide, pale yellow, darker around borders. Chelicerae 1.00 mm long with 3 promarginal teeth and 6 retromarginal denticles, dark orange-brown. Labium and endites light orange-brown. Endites slightly invaginated at middle.

Abdomen 2.00 mm long, 1.13 mm wide, pale white with transverse rows of dark spots, venter pale. Epigastric furrow 0.50 mm from tracheal spiracle, spiracle 0.65 mm from base of spinnerets.

Legs light orange-brown, unmodified. Tibial lengths (mm) and indices: I 1.60, 12; II 1.33, 14; III 0.80, 24; IV 1.26, 18. Ventral spination: tibiae I 2–2–0, II 1–2–0, III 1–2–2, IV 2–2–2; metatarsi I, II 2–2–0, III 2–1–2, IV 2–2–2.

Palpus as in Figure 131.

Female (Sarasota Co., Florida). Coloration as in male.

Total length 3.86 mm. Carapace 1.71 mm long, 1.39 mm wide, cephalic width 1.06 mm, clypeus height 0.09 mm. Eyes: diameters (mm): AME 0.08, ALE 0.09, PME 0.09, PLE 0.09; anterior eye row 0.55 mm long, straight; posterior eye row 0.70 mm long, procurved; MOQ length 0.22 mm, front width 0.23 mm, back width 0.34 mm; eye interdistances (mm): AME–AME 0.06, AME–ALE 0.07, PME–PME 0.16, PME–PLE 0.14, ALE–PLE 0.05.

Sternum 0.97 mm long, 0.76 mm wide. Chelicerae 0.82 mm long with teeth as in male.

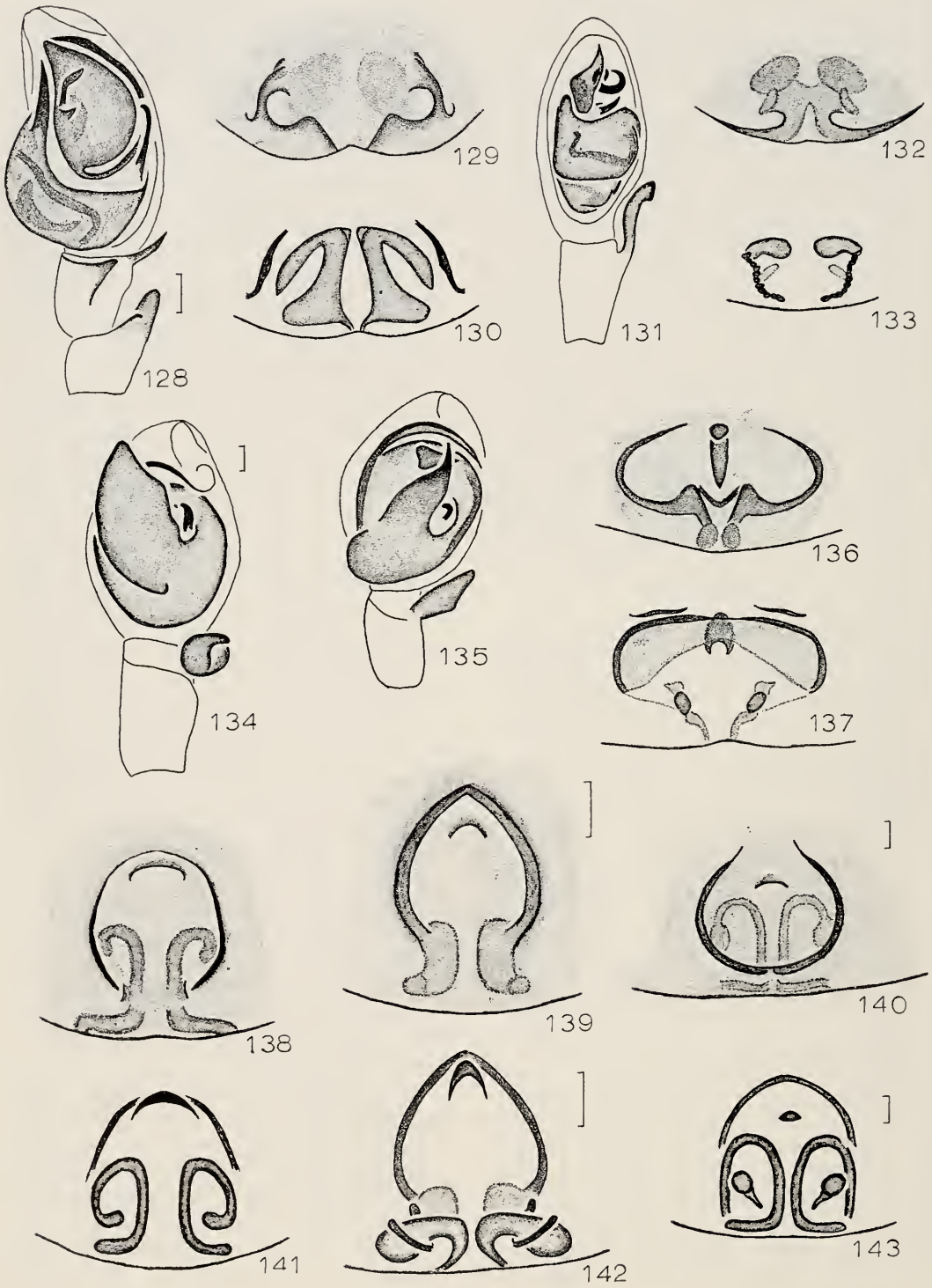
128
129
130
131
132
133
134
135
136
137
138
139
140
141
142
143

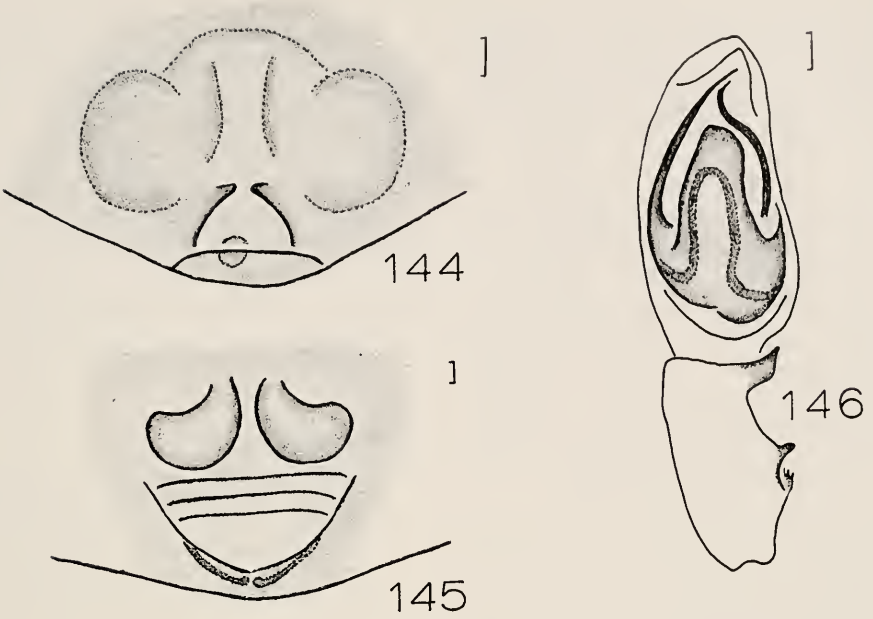

Plate 12

Figures 144–145. Epigyna, ventral view. Figure 146. Left palp, ventral view. 144. *Wulfila pallidus* O. P.-Cambridge. 145. *Aysha prospera* Keyserling. 146. *Teudis gentilis* O. P.-Cambridge.

Abdomen 2.20 mm long, 1.44 mm wide. Epigastric furrow 0.68 mm from tracheal spiracle, spiracle 0.85 mm from base of spinnerets.

Tibial lengths (mm) and indices: I 1.13, 18; II 0.97, 21; III 0.67, 30; IV 1.06, 22. Ventral spination as in male except tibiae III, IV 1–1–2 and metatarsi IV 2–1–2.

Epigynum as in Figure 132, internal genitalia as in Figure 133.

Natural history. Mature males and females have been taken year-round. Specimens have been taken on loblolly pine and fall webworm nests.

Distribution. Southern North America, from Maryland south to Florida, Mexico, and Panama, west to California and Baja California (Map 5).

Teudis calcar (Bryant), new combination
Map 3; Figures 128–130

Anyphaena calcar Bryant, 1931, Psyche, 38: 107, pl. 6, fig. 3 (♂). Male holotype from Dunedin, Florida, in MCZ, examined. Roewer, 1954, Katalog der Araneae, 2: 524. Bonnet, 1955, Bibliographia Araneorum 2: 342.

Anyphaena schwarzi Gertsch, 1933, Amer. Mus. Novitates, No. 637: 10, fig. 12 (♀). Female holotype from Brownsville, Texas, in AMNH, examined. Roewer, 1954, Katalog der Araneae, 2: 529. Bonnet, 1955, Bibliographia Araneorum, 2: 347. NEW SYNONYMY.

Diagnosis. Teudis calcar may be distinguished from all other anyphaenids in America north of Mexico by the retrolateral patellar apophysis of males (Fig. 128) and the epigynum of females (Fig. 129).

←

Plate 11

Figures 128, 131, 134, 135. Left palpi, ventral view. Figures 129, 132, 136, 138–140. Epigyna, ventral view. Figures 130, 133, 137, 141–143. Internal genitalia, dorsal view. 128–130. *Teudis calcar* (Bryant). 131–133. *Teudis mordax* (O. P.-Cambridge). 134. *Anyphaena accentuata* (Walckenaer). 135–137. *Anyphaena aperta* (Banks). 138, 141. *Aysha cambridgei* Bryant. 139, 142. *Aysha arunda* new species. 140, 143. *Aysha gracilis* (Hentz).

Male (Hidalgo Co., Texas). Coloration as in *Teudis mordax* except that the abdomen is uniformly light gray and the femora are much darker than the other leg segments.

Total length 3.78 mm. Carapace 1.76 mm long, 1.42 mm wide, cephalic width 0.95 mm, clypeus height 0.10 mm. Eyes: diameters (mm): AME 0.07, ALE 0.11, PME 0.11, PLE 0.11; anterior eye row 0.43 mm long, recurved; posterior eye row 0.64 mm long, procurved; MOQ length 0.25 mm, front width 0.22 mm, back width 0.35 mm; eye interdistances (mm): AME–AME 0.07, AME–ALE 0.03, PME–PME 0.14, PME–PLE 0.11, ALE–PLE 0.03.

Sternum 1.03 mm long, 0.83 mm wide. Chelicerae 0.75 mm long with 3 promarginal teeth and 4 retromarginal denticles.

Abdomen 2.30 mm long, 1.33 mm wide. Epigastric furrow 0.49 mm from tracheal spiracle, spiracle 0.81 mm from base of spinnerets.

Tibial lengths (mm) and indices: I 1.23, 17; II 1.01, 19; III 0.67, 30; IV 1.12, 21. Ventral spination: tibiae I, II 1–2–0, III, IV 1–1–2; metatarsi I, II 2–0–0, III, IV 2–2–2.

Palpus as in Figure 128.

Female (San Patricio Co., Texas). Coloration as in male.

Total length 4.97 mm. Carapace 1.94 mm long, 1.55 mm wide, cephalic width 1.00 mm, clypeus height 0.09 mm. Eyes: diameters (mm): AME 0.07, ALE 0.11, PME 0.11, PLE 0.11; anterior eye row 0.52 mm long, recurved; posterior eye row 0.72 mm long, procurved; MOQ length 0.27 mm, front width 0.23 mm, back width 0.38 mm; eye interdistances (mm): AME–AME 0.09, AME–ALE 0.04, PME–PME 0.17, PME–PLE 0.11, ALE–PLE 0.06.

Sternum 1.16 mm long, 0.96 mm wide. Chelicerae 0.72 mm long with 4 promarginal teeth and 4 retromarginal denticles.

Abdomen 3.13 mm long, 1.98 mm wide. Epigastric furrow 0.70 mm from tracheal spiracle, spiracle 1.16 mm from base of spinnerets.

Tibial lengths (mm) and indices: I 1.22, 20; II 1.08, 22; III 0.86, 29; IV 1.35, 21. Ventral spination as in male save metatarsi III 2–0–2.

Epigynum as in Figure 129, internal genitalia as in Figure 130.

Natural history. Mature males have been taken from early April through mid-July, mature females from late May through mid-July. Nothing is known of the habits of this species.

Distribution. Florida and Texas (Map 3).

REFERENCES

Bryant, E. B. 1931. Notes on North American Anyphaeninae in the Museum of Comparative Zoology. Psyche, **38**: 102–126.

Chickering, A. M. 1937. Anyphaenidae of Barro Colorado Island, Panama Canal Zone. Pap. Michigan Acad. Sci., Arts, Letters, **22**: 541–561.

———. 1940. New Anyphaenidae from Panama with notes on known species. Trans. Amer. Micros. Soc., **59**: 78–122.

Forster, R. R. 1970. The Spiders of New Zealand. Part III. Otago Mus. Bull., **3**: 1–184.

Hickman, V. V. 1949. Tasmanian littoral spiders with notes on their respiratory systems, habits and taxonomy. Pap. Proc. Roy. Soc. Tasmania, **1948**: 31–43.

Krombein, K. V. 1967. Trap-nesting wasps and bees: life histories, nests, and associates. Smithsonian Press, Washington, 570 pp.

Lamoral, B. H. 1968. On the ecology and habitat adaptations of two intertidal spiders. Ann. Natal. Mus., **20**: 151–193.

Lehtinen, P. T. 1967. Classification of the cribellate spiders and some allied families. Ann. Zool. Fennici, **4**: 199–468.

Levi, H. W. 1967. Adaptations of respiratory systems of spiders. Evolution, **21**: 571–583.

Marx, G. 1890. Catalog of the described Araneae of temperate North America. Proc. U. S. Nat. Mus., **12**: 497–594.

Petrunkevitch, A. 1930. The spiders of Porto Rico. Part III. Trans. Connecticut Acad. Arts Sci., **31**: 1–191.

Platnick, N. I. 1971. The evolution of courtship behaviour in spiders. Bull. British Arachn. Soc., **2**: 40–47.

Warren, L. O., W. B. Peck and M. Tadić. 1967. Spiders associated with the fall webworm, *Hyphantria cunea* (Lepidoptera: Arctiidae). J. Kansas Ent. Soc., **40**: 382–395.

US ISSN 0027-4100

Bulletin OF THE
Museum of
Comparative
Zoology

The Orb-weaver Genus *Zygiella* (Araneae: Araneidae)

HERBERT W. LEVI

HARVARD UNIVERSITY
CAMBRIDGE, MASSACHUSETTS, U.S.A

VOLUME 146, NUMBER 5
21 NOVEMBER 1974

PUBLICATIONS ISSUED
OR DISTRIBUTED BY THE
MUSEUM OF COMPARATIVE ZOOLOGY
HARVARD UNIVERSITY

Breviora 1952–
Bulletin 1863–
Memoirs 1864–1938
Johnsonia, Department of Mollusks, 1941–
Occasional Papers on Mollusks, 1945–

SPECIAL PUBLICATIONS.

1. Whittington, H. B., and E. D. I. Rolfe (eds.), 1963. Phylogeny and Evolution of Crustacea. 192 pp.
2. Turner, R. D., 1966. A Survey and Illustrated Catalogue of the Teredinidae (Mollusca: Bivalvia). 265 pp.
3. Sprinkle, J., 1973. Morphology and Evolution of Blastozoan Echinoderms. 284 pp.
4. Eaton, R. J. E., 1974. A Flora of Concord. 250 pp.

Other Publications.

Bigelow, H. B., and W. C. Schroeder, 1953. Fishes of the Gulf of Maine. Reprint.

Brues, C. T., A. L. Melander, and F. M. Carpenter, 1954. Classification of Insects.

Creighton, W. S., 1950. The Ants of North America. Reprint.

Lyman, C. P., and A. R. Dawe (eds.), 1960. Symposium on Natural Mammalian Hibernation.

Peters' Check-list of Birds of the World, vols. 2–7, 9, 10, 12–15.

Proceedings of the New England Zoological Club 1899–1948. (Complete sets only.)

Publications of the Boston Society of Natural History.

Price list and catalog of MCZ publications may be obtained from Publications Office, Museum of Comparative Zoology, Harvard University, Cambridge, Massachusetts, 02138, U.S.A.

© The President and Fellows of Harvard College 1974.

THE ORB-WEAVER GENUS *ZYGIELLA* (ARANEAE: ARANEIDAE)

HERBERT W. LEVI

Abstract. The fifteen known species of *Zygiella* are redescribed and illustrated. Eleven are Palearctic, one Holarctic, one Nearctic, one Oriental and one Asiatic. *Zygiella atrica* and Z. *x-notata* are introduced to North America from Europe; Z. *x-notata* has probably been spread by man, especially to temperate South America.

Zygiella differs from *Araneus* in having the eye region more compact and in having characteristic markings on the dorsoventrally flattened, oval abdomen. Also the epigynal scape, when present, is smooth and there is a projection or sculpturing of the male tegulum. *Zygiella* exhibits diverse modifications of the paracymbium; the paracymbium is simple and hook-shaped in *Araneus*. In addition, the web of *Zygiella* has an open sector, whereas that of *Araneus* is complete.

Despite their diverse genitalia, the species of *Zygiella* appear closely related.

A few measurements of differently sized individuals of Japanese *Zygiella sia*, presumably individuals that matured in different instars, indicate that in females growth in leg length is proportional to carapace length, and distance from lateral eyes to median eyes increases at a slightly slower rate than growth of carapace (the eye diameter presumably grows slightly, but less than the carapace). Larger males may have relatively longer legs. There were hardly any differences in size of the genitalia.

INTRODUCTION

Spiders of the families Araneidae and Linyphiidae have far more complicated genitalia than spiders of other families. The temptation is to use these excellent species-separating characters to group the species into genera. That generic grouping has been a problem is well-known. Simon, perhaps the foremost 19th century arachnologist, synonymized most araneid genera in *Araneus* (1895). I believe this was an action of despair by a specialist who minimized the importance of genitalia. On the other hand, Archer (1951a, b) more recently grouped the species into genera mainly on the basis of the shape of the median apophysis, one of numerous sclerites in the male palpus. Neither extreme is satisfactory.

The difficulty of using only genitalia in separating genera is perhaps best demonstrated in *Mangora* (Levi, in preparation). The high thorax and the feathered trichobothria, a sense organ on the third tibia, make it easy to separate *Mangora* species on first inspection from species belonging to other genera. The genitalia of the numerous species show great diversity. All indications are that the body shape and sense organs reflect close relationship of the many species and that it is a monophyletic group despite the variability in the genitalia.

But are there other araneid genera whose species, while readily recognized as belonging together, show diversity in geni-

talia? *Zygiella* species, most of which are Palearctic, have females with and without an epigynal scape; males with and without a palpal terminal apophysis. Despite this it seems that the species included in *Zygiella* are closely related. They are easily recognized by their body shape as belonging to *Zygiella*, even though it is not easy to characterize those features that make them distinct. Also the different species make a similar web with a vacant sector. And when the seemingly diverse genitalia are carefully studied, similarities are found that separate the species from those of other genera.

Modern araneologists subscribe to widely differing concepts of what is a genus, Europeans more than Americans tending to fragment genera in the interest of showing relationships, though the result is just the opposite. They forget the usefulness to themselves in having all oak trees in the genus *Quercus*, all pines in *Pinus*, and forget that araneologists who study taxonomy produce knowledge used by colleagues in fields other than spider taxonomy.

As the American species of *Zygiella* have recently been revised by Gertsch (1964), an attempt was made to revise the group world wide. Gertsch's illustrations do not show the palpal sclerites sufficiently distinctly. (This may be a subjective opinion, just because I did not illustrate them myself.) Some Asian species that have never been illustrated before add new dimensions to the interesting problem of genitalic differences in related species. I did not describe new species, partly because I do not like to describe new forms but also because I suspect that additional *Zygiella* species already described may be misplaced in wrong genera and families. Because I was not describing new species, I did not make an attempt to borrow large unsorted collections of *Zygiella* from other institutions.

Because of the difficulties in visiting European museums and in borrowing type-specimens of both previously described American species and those from other parts of the world, I have to thank many curators and colleagues for their help in making this study possible; as I know from my own experience as curator, it is very time-consuming to locate obscure specimens in the large collections. I wish to thank A. Timothea da Costa of the Museu Nacional, Rio de Janeiro; M. Grasshoff, Senckenberg Museum, Frankfurt; J. Gruber, Naturhistorisches Museum, Vienna; M. Hubert of the Muséum National d'Histoire Naturelle, Paris; C. E. O'Riordan, National Museum of Ireland, Dublin; F. H. Rindge and N. Platnick of the American Museum of Natural History; J. O. Hüsing and R. Piechocki of the Martin Luther Universität of Halle (Saale) of the German Democratic Republic; J. Prószyński and W. Staręga of the Institute of Zoology, Polska Akademia Nauk, Warszawa; G. Schmidt; E. Tortonese of the Museo Civico de Storia Naturale, Genova; G. C. Varley and H. Taylor of the Hope Department of Entomology, Oxford; F. Wanless and D. Norman of the British Museum (Natural History); and T. Yaginuma. D. McGrath and D. McGrath, Jr. were helpful in obtaining specimens. Lorna R. Levi and Ian R. Mackay edited the paper and made helpful comments. The research and publication was in part supported by National Science Foundation research grant GB–36161.

Zygiella F.O. Pickard-Cambridge

Zygia C. L. Koch, 1834, *in* Panzer, Deutschlands Insekten, Heft 123, 17–19. The type species is *Araneus calophylla* Walckenaer 1802 (? = *x-notata* Clerck) as the only included species. Name *Zygia* preoccupied by Fabricius 1775 for an insect.

Zygiella F. O. Pickard-Cambridge, 1902. Ann. Mag. Natur. Hist. (7)9: 15. New genus "to replace *Zygia* with *Z. atrica* (C. L. Koch) as the type species," as indicated by original designation. The name is of feminine gender.

Description. *Zygiella*, unlike *Araneus*, has the eye region compact, with the eyes closely spaced. The median ocular area

Plate 1. Female *Zygiella atrica* (C. L. Koch) from Nahant, Massachusetts, in the laboratory.

is as long as wide in front, always slightly narrower behind than in front (Figures 1, 12, 57, 65). The anterior eyes are about equally spaced. But in larger specimens (*Z. sia*) they are separated as much as two times their diameter from laterals. The posterior median eyes are only about one and one-half times the distance of the median eye interval from the lateral eyes (to almost 5 times in large specimens of *Z. sia*). The carapace is always considerably wider than the eye region in the eye area, at least in females (Figures 1, 12). The anterior median eyes are larger to much larger than the others. Because eye distance increases almost proportionally with length (see below), the eyes of only the smallest *Araneus* species are closely spaced.

The chelicerae have three to four teeth on the anterior margin, about as many on the posterior, and denticles in the groove between (Figure 58).

The carapace, in contrast to that of *Araneus*, is glabrous brown with very few hairs. The head region is often darker than the thorax. The abdomen, unlike that of *Araneus*, is oval, widest in the middle, dorsoventrally flattened, as in species of *Nuctenea*, but differs from these by being mainly black and white, not brownish (in living as well as in preserved animals). The dorsal folium is almost symmetrical anterior to posterior, widest in middle; the cardiac area, however, generally has a white area while the posterior end of the folium is darkest (Plate 1; Figures 1, 12, 26, 70, 84, 92, 95). There may be a median longitudinal line through the white cardiac spot (Figure 103). The pattern resembles

that of the theridiid genus *Enoplognatha*, but not of other araneids. The venter has a white longitudinal line on each side enclosing a median black or pigmentless area between genital furrow and spinnerets (Figure 27). The epigynum is variable with a posterior median depression (Figures 3, 24, 35) or a scape which is not wrinkled as is the *Araneus* epigynal scape (with few exceptions) (Figures 71, 89, 93, 97, 104, 112). The palpus can be readily distinguished from an *Araneus* palpus by the modified diverse paracymbium (Figures 7, 13, 20, 30, 42, 56, 68, 86, 101, 110, 120). But unlike most Araneidae the palpus has the tegulum often "vertical" in the palpus, the long axis parallel to the long axis of the cymbium (Figures 14, 28, 41, 85), and the tegulum bears unique projections (Figures 42, 56, 60, 68, 75, 85, 118) or sculpturing (Figure 100). A terminal apophysis may be present in some species (Figures 40, 60), but not in *Zygiella atrica*, Z. *keyserlingi*, Z. *x-notata*, and Z. *minima* (Figures 7, 30).

The male palpal femur lacks the proximal ventral tooth present in *Araneus*. The male palpal patella usually has only one seta in *Zygiella*, two in *Araneus*. However, *Zygiella sia* may have one or two. The first coxa does not have a hook and the tibiae of the first two legs of the male are not modified. The first patella-tibia of the female is about 1.2–1.5 carapace lengths, that of the male 1.5–2.0.

Zygiella differs from *Meta*, which also has a modified paracymbium, in having more complex genitalia (the sculptured tegulum and complex median apophysis). I suspect the genera are related.

Most *Zygiella* webs have a vacant sector on the upper half in the direction of the retreat, but sometimes complete webs are made.

Zygiella species have been confused with species of *Enoplognatha* and *Steatoda*, both Theridiidae. *Steatoda*'s abdomen is usually purplish brown while that of *Zygiella* is black and white. The male *Enoplognatha* palpus is of very characteristic shape, having only a minute paracymbial hook on the lateral edge of the cymbium, some distance from the tibia. *Enoplognatha* and *Zygiella* females are difficult to separate on first impression, but female *Zygiella* have three to four teeth on the posterior margin of the chelicerae and denticles between the two rows of teeth (Figure 58), while *Enoplognatha* females have only one or two teeth on the posterior cheliceral margin and lack the denticles in the groove.

Very few specimens were available for most species examined here. No attempt was made to borrow the hundreds of specimens that are usually available for studies of American species. It would have been impossible to obtain large series even if I had tried.

The vast difference in sizes of the few Japanese *Zygiella sia* available indicates a taxonomic problem easily overlooked (see under Z. *sia* below). The larger the araneid spider, the farther apart the eyes. The growth in distance between median and lateral eyes is almost proportional to growth of carapace width. A careful study of proportional or allometric growth of structures used as taxonomic features in the family may be worthwhile.

The following species described or placed in *Zygiella* do not belong to it or the types are lost.

alpina, Zilla, Giebel, 1867. Zeitschr. gesammt. Naturwissensch., 30: 434. Female holotype from La Flegère, Chamonix Valley, Switzerland [? sic] in the Zoology Dept. of the Martin Luther Universität, Halle, German Democratic Republic (examined). = *Theridion sisyphium* (Clerck). NEW SNYONYMY.

ancora, Epeira, Krynicki, 1837. Bull. Soc. Imp. Natur. Moscow, 5: 81 from Russia is *Steatoda bipunctata* according to Roewer (1955, Katalog der Araneae, 26: 1477).

aureola, Zilla, Keyserling, 1884. Verhandl. zool. bot. Ges. Wien, 33: 652, pl. 21, fig. 4, ♀ from the Amazon in the Muséum National d'Histoire Naturelle, Paris, is a species close to *Meta*. The type had been marked "*Meta aureola* Keys." by Simon.

calophylla, Aranea, Walckenaer, 1802, Faune Parisienne, 2: 200, doubtful name. Roewer (1942) considers it to be a senior synonym of Z. *atrica* (C. L. Koch), Bonnet (1959) a junior synonym of Z. *x-notata.* For purposes of nomenclatural stability the synonymy of Bonnet should be followed.

crucinotata, Zilla, Pokrovskii, 1904. Zap Imp. Roussk. Geogr. Obtch., 41: 300, fig. 25, 25a is not recognizable, but almost certainly is an *Enoplognatha.* The author compares it with another *Enoplognatha* species.

decolorata, Zilla, Keyserling, 1893. Spinnen Amerikas, 4: 306, pl. 15, fig. 226, ♀. Male holotype from Brazil (examined) is a *Mangora.*

gigans, Zilla, Franganillo, 1913. Broteria, 11: 128. Not recognizable.

guttata, Zilla, Keyserling, 1880. Verhandl. zool. bot. Ges. Wien, 30: 551, pl. 16, fig. 3, ♀. Female holotype from Peru (examined) is a *Leucauge.*

guyanensis, Zilla, Keyserling, 1880. Verhandl. zool. bot. Ges. Wien, 30: 554, pl. 16, fig. 5, ♂. Male type from Guyana (examined) is of an unknown genus, not *Zygiella.*

melanocephala, Linyphia, Taczanowski, 1874. Hor. Soc. Ent. Rossicae 10: 70. Types from Guyana (examined) are *Mangora.*

nawazi, Zilla, Dyal, 1935. Bull. Dept. Zool. Panjab Univ., 1: 186, pl. 11, fig. 6, pl. 16, fig. 124 from India is an *Araneus* judging by the illustrations.

punctata, Zilla, Keyserling, 1893. Spinnen Amerikas, 4: 305, pl. 15, fig. 225, ♀. Female type from Brazil, lost.

rogenhoferi, Zilla, Keyserling, 1877. Verhandl. zool. bot. Ges. Wien 27: 578, pl. 14, fig. 6, ♀. Female holotype from Brazil (examined) is a *Metazygia.*

Key to Males of *Zygiella* Species

(Males of Z. *calyptrata,* Z. *inconvenicus* and Z. *melanocrania* are not known.)

1 Palpal tibia much longer than cymbium (Figs. 5, 13) 2
– Palpal tibia of same length or shorter than cymbium 3

2(1) Palpal tibia with a distal bulge (Fig. 13); paracymbium pointed at tip (Fig. 13); median apophysis with two long spines (Fig. 14); Europe ..... *keyserlingi*
– Palpal tibia with sides parallel (Fig. 5); paracymbium rounded at tip (Fig. 5); median apophysis with short spines (Fig. 6); North America and Europe ..... *atrica*

3(1) Tegulum of palpus without projection (other than conductor) (Figs. 28, 29); cosmopolitan ..... *x-notata*
– Tegulum of palpus with a projection or sculpturing (other than conductor) (Figs. 42, 56, 68) 4

4(3) Tegulum in "horizontal" position in cymbium, its long axis transverse to that of cymbium (Fig. 119); projection with teeth "vertical" and surrounding conductor (Fig. 119); paracymbium a hook, barely modified (Figs. 118–120); Japan ..... *sia*
– Tegulum in more or less "vertical" position in cymbium, its long axis parallel to cymbium (Fig. 100); projection not vertical 5

5(4) Tegulum projection in ventral view in the shape of a human ear (Fig. 100); paracymbium square (Fig. 101) ..... *thorelli*
– Tegulum with simple projection; paracymbium not a square (Figs. 68, 75) 6

6(5) In lateral view tegulum projection almost as long or longer than tegulum width (Figs. 68, 110) 7
– In lateral view tegulum projection shorter than width of tegulum (Figs. 75, 86) 8

7(6) Tegulum projection pointed (Fig. 68); paracymbium with a dorsally directed point (Fig. 68); California ..... *carpenteri*
– Tegulum projection truncate (Fig. 109); paracymbium a ventrally directed lobe (Fig. 110); Europe ..... *stroemi*

8(6) Palpus with a sclerite (? terminal apophysis) more or less parallel to embolus (in ventral view) in distal part of palpus (Figs. 41, 55); paracymbium complex with a notch (Figs. 47–49, 59) 9
– Palpus with no sclerite parallel to embolus (in ventral view) (Figs. 19, 74, 85); paracymbium without notch (Figs. 20, 75, 86) 10

9(8) A sclerite (? terminal apophysis) longer than embolus in ventral view (Fig. 41); paracymbium with a distal notch (Figs. 47–49); eastern Asia, North America ..... *dispar*
– Terminal apophysis shorter than embolus in ventral view (Fig. 55); paracymbium with a ventral notch (Fig. 59); Europe ..... *montana*

10(8) Base of conductor sitting in a depression surrounded by a rim, or base of conductor surrounded by wrinkles (Figs. 75, 85); Eurasia 11
– Base of conductor not surrounded by wrinkles or a rim (Fig. 19); Canary Isl. ..... *minima*

11(10) Base of conductor in a depression surrounded by a rim (Fig. 85) ..... *kochi*

– Base of conductor surrounded only by wrinkles of the tegulum (Figs. 74, 75) ..... *caspica*

KEY TO FEMALES OF *ZYGIELLA* SPECIES

1 Posterior rim of epigynum with a semicircular lobe (Fig. 71) ..... *caspica*
– Posterior rim otherwise 2
2(1) Epigynum with a scape (Figs. 89, 93, 97, 104, 112) 3
– Epigynum without a scape (Figs. 3, 10, 16, 22, 34, 77, 82) 7
3(2) Openings ventral underneath heart-shaped scape (Fig. 112); Japan ..... *sia*
– Openings posterior 4
4(3) Scape constricted at base (Figs. 89, 93) 5
– Scape not constricted at base (Figs. 97, 104) 6
5(4) Scape heart-shaped, slightly longer than wide (Fig. 89) ..... *kochi*
– Scape more than twice as long as wide (Fig. 93); Palestine ..... *inconveniens*
6(4) Scape a broad lobe with a posterior median extension (Fig. 97) ..... *thorelli*
– Scape much longer than wide with parallel sides (Fig. 104) ..... *stroemi*
7(2) No depression, openings or sculpturing visible in ventral view of epigynum, at most a posterior rim (Figs. 16, 22); posterior view with two separate openings (Figs. 18, 24) 8
– In ventral view a depression, openings or sculpturing visible (Figs. 3, 10, 34, 77, 82); no distinct pair of openings in posterior view 9
8(7) Total length more than 4 mm; epigynum heavily sclerotized (Figs. 22, 24); probably cosmopolitan ..... *x-notata*
– Total length less than 3.5 mm; epigynum lightly sclerotized (Figs. 16, 18); Canary Isl. ..... *minima*
9(7) Semicircular openings bordered on venter of epigynum (Fig. 82); Burma ..... *melanocrania*
– Openings not so; venter of epigynum with a median depression or bulge (Figs. 3, 10, 34, 77) 10
10(9) A median, posterior, indistinctly bordered, dark depression in ventral view of epigynum (Fig. 77); fourth coxae drawn out posteriorly into a spine (Fig. 80); Malaysia ..... *calyptrata*
– Posterior depression or bulge distinctly bordered (Figs. 3, 10, 34); fourth coxae without a spine; Holarctic region 11
11(10) Median area of epigynum a depression in ventral view much wider than long (Fig. 63); California ..... *carpenteri*
– Median area at most one and one half times as wide as long (Figs. 3, 10, 34) 12
12(11) Median area of epigynum a bulging lobe framed anteriorly only by a lip (Fig. 10); Europe ..... *keyserlingi*
– Median area depressed, framed anteriorly and laterally (Figs. 3, 34, 52)..13
13(12) Median depressed area extending posteriorly in ventral view (Fig. 3); in posterior view sides of epigynum lightly sclerotized and smaller than median depression (Fig. 4); Europe, North America ..... *atrica*
– Median depressed area not projecting beyond sclerotized area of epigynum in ventral view (Figs. 34, 38, 52); in posterior view sides of epigynum heavily sclerotized and sclerotized areas larger in area than median depression (Figs. 35, 39, 54) 14
14(13) Median area with a constriction as seen in both ventral and posterior views (Figs. 34, 35, 38, 39); Eastern Asia, North America ..... *dispar*
– Median area without constriction as seen in both ventral and posterior views (Figs. 52, 54); Europe ..... *montana*

Zygiella atrica (C. L. Koch) Plate 1; Figures 1–8

Encharia atrica C. L. Koch, 1843, Die Arachniden, 12: 103, figs. 1030, 1031, ♀, ♂. Specimens came from Germany and France and are presumably in the museum of the Humboldt Universität, Berlin.

Zilla atrica, - Wiehle, 1931, Tierwelt Deutschlands, 23: 33, figs. 38–40, ♀, ♂.

Zygiella atrica, - Bonnet, 1959, Bibliographia Araneorum, 2: 4998. Gertsch, 1964, Amer. Mus. Novitates, No. 2188: 16, figs. 18–20, ♂, ♀.

Diagnosis. This species can be confused only with *Z. keyserlingi*. The male differs from other *Zygiella* by the long palpal tibia and, unlike that of *Z. keyserlingi*, the tibia has its sides parallel (Figure 5) with setae equally distributed. The epigynum has a wide median lobe extending posteriorly in ventral view; the lobe is depressed in the middle and the lateral sclerotized areas are relatively small (Figures 3, 4).

Natural history. This species is common-

Figures 1–8. *Zygiella atrica* (C. L. Koch). 1. Female. 2–4. Epigynum. 2. Posterodorsal view, cleared. 3. Ventral. 4. Posterior. 5–7. Left male palpus. 5. Lateral view. 6. Ventral. 7. Expanded. 8. Eye region and chelicerae of female.

Figures 9–14. *Z. keyserlingi* (Ausserer). 9–11. Epigynum. 9. Dorsal, cleared. 10. Ventral. 11. Posterior. 12. Female. 13–14. Male palpus. 13. Lateral. 14. Ventral.

Abbreviations. C, conductor; DH, distal hematodocha; E, embolus; M, median apophysis; P, paracymbium; R, radix; S, subtegulum; T, tegulum.

Size lines. 0.1 mm, except Figures 1, 8, 12, 1 mm.

est on ocean coasts, but is found in Europe also in other locations (Wiehle, 1931), on shrubs, junipers, etc. In America the species is certainly introduced and is found in coastal areas of the ocean and of Lake Erie. On the peninsula of Nahant, Massachusetts, it is very common under and between boulders placed to prevent the road

from being washed away by high tides. As it can be found abundantly among these boulders year after year, the species can presumably tolerate the occasional high waves and salt spray from the ocean. Adult males and females have been found in this location in October.

The web (Wiehle, 1931) has more radii (43–50) than that of *Z. x-notata* and many other orb-weavers; most radii are in the lower half of the web. The free sector is narrow and the hub has a fine mesh. There are many frame threads, many close to the spiral region. The retreat is not as well built as that of *Z. x-notata*. Emerton's picture of the web (1902, The Common Spiders of the United States) shows only a few radii.

Distribution. Europe; in America from Nova Scotia to Long Island, New York; Port Credit, Ontario, and British Columbia coast. For map see Gertsch (1964).

Zygiella keyserlingi (Ausserer) Figures 9–14

Zilla keyserlingi Ausserer, 1871, Verhandl. zool. bot. Ges. Wien, 21: 830, pl. 5, fig. 11, ♀. Female holotype from Dalmatia in the Keyserling collection of the British Museum, Natural History, not examined. Wiehle, 1931, Tierwelt Deutschlands, 23: 35, figs. 41, 42, ♀, ♂.

Zygiella keyserlingi, - Roewer, 1942, Katalog der Araneae, 1: 884. Bonnet, 1959, Bibliographia Araneorum, 2: 5002.

Description. Female from unknown locality in Europe. Carapace light brown, cephalic region not much darker. Legs not banded. Dorsum of abdomen with characteristic pattern (Figure 12) and venter with a white line on each side. Diameter of posterior median eyes 0.9 diameter of anterior medians, anterior laterals 0.8, posterior laterals 0.7 diameter of anterior median eyes. Anterior median eyes one diameter apart, one from laterals. Posterior median eyes one diameter apart, 1.5 from laterals. There are three teeth on the anterior margin of the chelicerae, three on the posterior, with denticles between the margins. Total length 8.0 mm. Carapace 2.7 mm long, 2.3 mm wide. First femur, 3.1 mm; patella and tibia, 4.0 mm; metatarsus, 3.1 mm; tarsus, 1.0 mm. Second patella and tibia, 2.9 mm; third, 1.7 mm; fourth, 2.6 mm.

Male from unknown locality. Coloration like that of female. Diameter of posterior median eyes and of anterior lateral eyes 0.7 diameter of anterior median eyes; that of posterior lateral eyes 0.6 diameter of anterior medians. Anterior median eyes slightly less than their diameter apart, and slightly less than their diameter from laterals. Posterior median eyes slightly less than one diameter apart, 1.5 diameters from laterals. Total length 6 mm. Carapace 2.9 mm long, 2.0 mm wide. First femur, 4.1 mm. Second patella and tibia, 3.6 mm; third, 2.0 mm; fourth, 2.9 mm.

Additional female and male specimens were available from Krivosije, Dalmatia.

Diagnosis. The long palpal tibia is found also in *Z. atrica*; however, *Z. keyserlingi* has the tibia distally swollen with the swollen area having more setae than the basal part (Fig. 13). The epigynum has a central bulging area bordered anteriorly only by a transverse lip (Figures 10, 11). The species is less pigmented than *Z. atrica.*

Distribution. Portugal, Italy, Hungary to Greece (Bonnet, 1959).

Zygiella minima (Schmidt) Figures 15–20

Zygiella x-notata minima Schmidt, 1968, Zool. Beitr., 14: 414, fig. 11, ♂. Female, male syntypes in poor physical condition from Esperanza Forest, Tenerife, Canary Islands, owned by the author G. Schmidt, but made available to me.

Description. Female. Coloration difficult to determine. Eyes seem about subequal in size. The anterior median eyes slightly less than their diameter apart, their radius from laterals. Posterior median eyes their radius apart, about 0.8 diameter from laterals. Total length 3 mm. Cara-

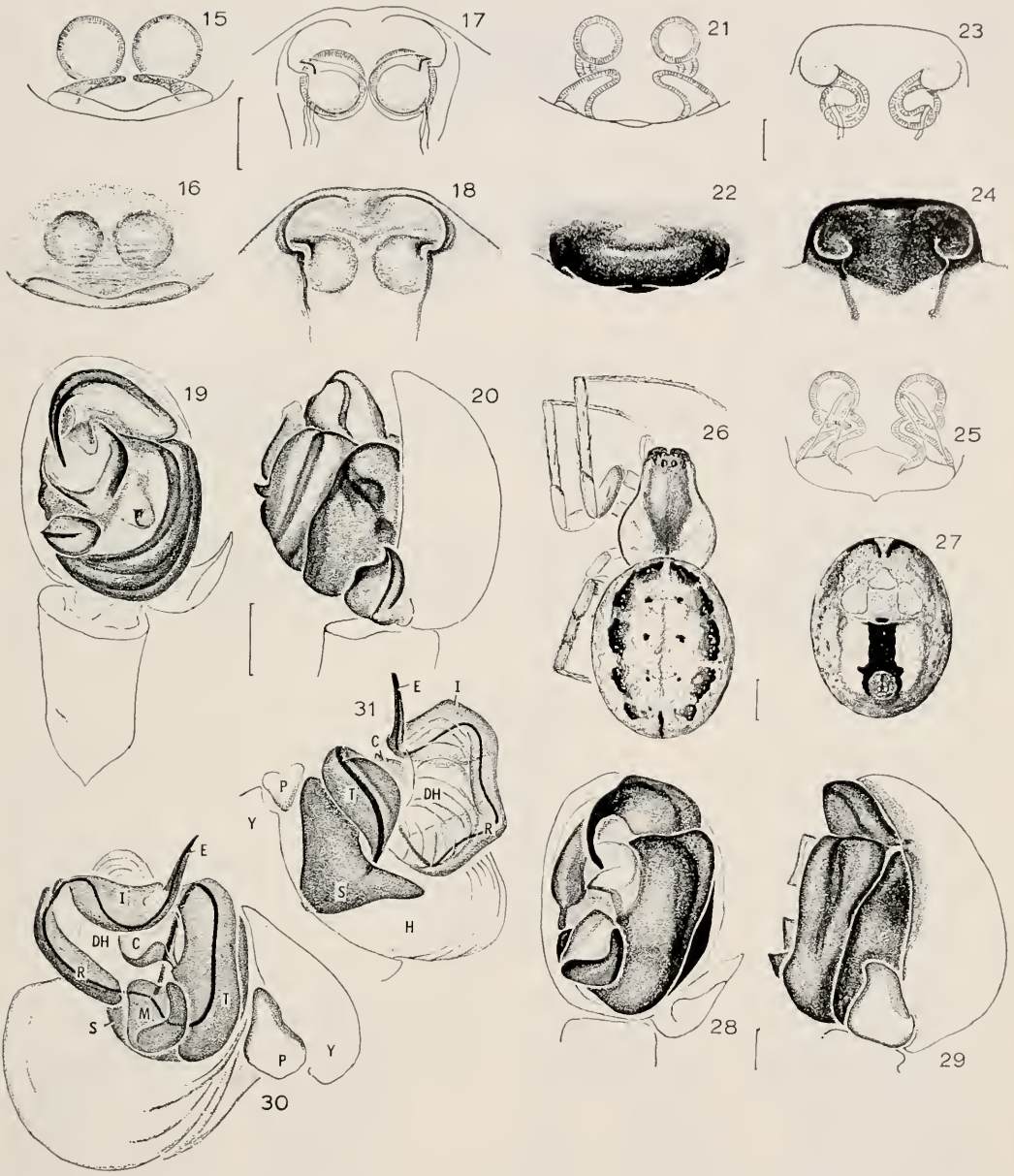

Figures 15–20. *Zygiella minima* (Schmidt). 15–18. Epigynum. 15. Ventral, cleared. 16. Ventral. 17. Posterior, cleared. 18. Posterior. 19–20. Left male palpus. 19. Ventral. 20. Lateral.

Figures 21–31. *Z. x-notata* (Clerck). 21–25. Epigynum. 21. Ventral, cleared. 22. Ventral. 23. Posterior, cleared. 24. Posterior. 25. Dorsal, cleared. 26. Female. 27. Female abdomen, ventral. 28–31. Male palpus. 28. Ventral. 29. Lateral. 30, 31. Expanded. 30. Subventral view of bulb. 31. Dorsal view of bulb.

Abbreviations. C, conductor; DH, distal hematodocha; E, embolus; I, stipes; M, median apophysis; P, paracymbium; R, radix; T, tegulum; Y, cymbium.

Size lines. 0.1 mm except Figures 26, 27, 1 mm.

pace 1.5 mm long. First femur, 2.0 mm; patella and tibia, 2.4 mm; metatarsus, 1.8 mm; tarsus, 0.7 mm. Second patella and tibia, 1.7 mm; third, 1.0 mm; fourth, 1.6 mm.

Male. In slightly better physical condition than female. Eyes subequal in size. Anterior median eyes their diameter apart, 0.8 diameter from laterals. Posterior median eyes slightly less than their diameter apart, their diameter from laterals. Total length 2.5 mm. Carapace 1.2 mm long, 0.9 mm wide. First femur, 1.6 mm; patella and tibia, 2.1 mm; metatarsus, 1.6 mm; tarsus, 0.7 mm. Second patella and tibia, 1.5 mm; third, 0.8 mm; fourth, 1.2 mm.

Diagnosis. Zygiella minima differs from *Z. x-notata* in that the female has the epigynum lightly sclerotized and with differently sized openings in posterior view (Figures 16, 18); the male has a small tooth-shaped projection on the face of the tegulum (Figures 19, 20) absent in *Z. x-notata.*

Distribution. Canary Islands.

Zygiella x-notata (Clerck) Figures 21–31, 57–58

Araneus x-notatus Clerck, 1758, Aranei Svecici, 46, pl. 2, fig. 5. A Clerck specimen bearing this name as labeled by Thorell is in the Swedish Museum of Natural History, Stockholm; not examined.

Zilla bösenbergi Keyserling, 1878, Verhandl. zool. bot. Ges. Wien, 28; 575, pl. 14, fig. 4, 5, ♀, ♂. Female and male syntypes from Uruguay in the museum of the University of Hamburg and the British Museum (Natural History), examined. NEW SYNONYMY.

Zilla californica Banks, 1896, J. New York Ent. Soc., 4: 90. Female holotype from Palo Alto, California, in the Museum of Comparative Zoology, examined. Gertsch (in letter, 1957) indicated that Stanford University Museum had specimens marked types. This spider collection has since been sent to the Los Angeles County Museum and was destroyed (C. L. Hogue, personal communication).

Larinia maulliana Mello-Leitão, 1951, Rev. Chilena Hist. Natur., 51–53: 331, figs. 5, 6, ♂. Male holotype from Maullín, Chile, in the Museu Nacional, Rio de Janeiro, examined. NEW SYNONYMY.

Zygiella x-notata, - Bonnet, 1959, Bibliographia Araneorum, 2: 5007. Gertsch, 1964, Amer. Mus. Novitates, No. 2188, 12, figs. 2, 15–17, ♀, ♂, map.

Diagnosis. The epigynum, unlike that of *Z. minima*, is heavily sclerotized. It has two diagnostic openings seen in posterior view (Figure 24). The palpus is simple with the tegulum's long axis parallel to that of the cymbium (Figures 28–30); the lack of terminal apophysis (Figures 30, 31) separates males from those of other species, the lack of a tegulum projection from males of *Z. minima.*

Natural history. Numerous references to habits and webs can be found in Bonnet (1959). The web, which has a vacant sector, has been used in ethological studies. It is illustrated in Wiehle (1931), figure 37, and J. Comstock, 1940, The Spider Book, figure 470. The species is very common in southern Chile. In the city park of Osorno, Chile, I found suspended from a web on a telephone pole a dried, shrivelled, 6-cm long lizard on which a *Z. x-notata* had apparently fed (15 March 1965).

→

Figures 32–50. *Zygiella dispar* (Kulczynski). 32–39. Epigynum. 32, 33. Posterior view, cleared. 34, 36, 38. Ventral. 35, 37, 39. Posterior. 32. (Michigan). 33–35. (Mendocino Co., California). 36, 37. British Columbia. 38, 39. (Virginia). 40–50. Left male palpus. 40. Expanded. 41. Ventral. 42. Lateral. 43–46. Embolus and apophysis. 43. (Alaska). 44. (California). 45. (Manitoba). 46. (Maine). 47–49. Paracymbium. 47. (Alaska). 48. (California). 49. (Manitoba). 50. (Maine).

Figures 51–56. *Zygiella montana* (C. L. Koch). 51–54. Epigynum. 51. Anterodorsal view, cleared. 52. Ventral. 53. Posterior, cleared. 54. Posterior. 55, 56. Male palpus. 55. Ventral. 56. Lateral.

Abbreviations. A, terminal apophysis; C, conductor; E, embolus; H, hematodocha; I, stipes; M, median apophysis; T, tegulum.

Scale lines. 0.1 mm.

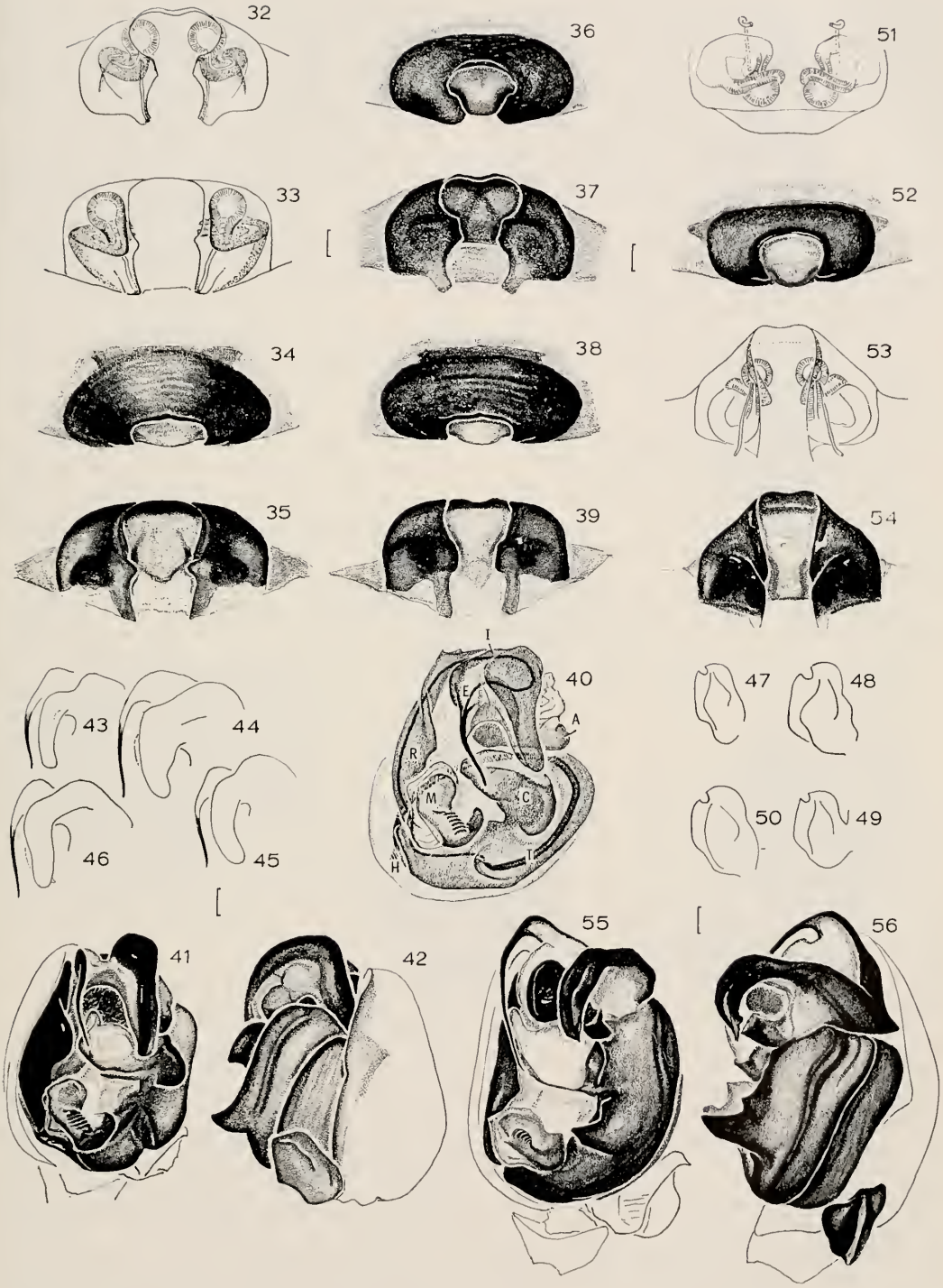
32
36
51
33
37
52
34
38
53
35
39
54
I
E
A
R
M
C
T
H
40
43
44
46
45
47
48
50
49
41
42
55
56

Adult males are found from July until September on the Pacific coast of North America.

Distribution. Europe, but probably cosmopolitan, carried around the world by man. It is introduced in America and found along the Atlantic coast from Maine to Virginia, the Pacific coast from southern British Columbia to southern California. Gertsch (1964) maps the North American distribution. It is very common in Chile and is found in Uruguay and Argentina.

Zygiella dispar (Kulczyński) Figures 32–50

Zilla dispar Kulczyński, 1885, Denkschrift. Akad. Wissenschaften Krakow, 11: 24, pl. 9, fig. 7, ♀, ♂. Male type from Kamtchatka, Siberia, in Polish Academy of Sciences, Warsaw, in poor physical condition, examined.

Zygiella montana, - numerous authors of American records only.

Zygiella dispar, - Gertsch, 1964, Amer. Mus. Novitates, No. 2188: 7, figs. 7–10, ♀, ♂.

Zygiella nearctica Gertsch, 1964, Amer. Mus. Novitates, No. 2188: 4, figs. 3–6, ♀, ♂. Male holotype from Seba, Alberta, in the American Museum of Natural History, not examined. NEW SYNONYMY.

Note. Gertsch (1964) used the name *dispar* for the population along the Pacific coast from Alaska to south-central California; other specimens he called *nearctica.* Gertsch separated *Z. nearctica* from *Z. dispar* by the following characters: the male palpus has the apical [= ? subterminal] apophysis less developed, and has "differences of the various apophysis"; the female epigynum has the "fovea" visible from below. The last character is a matter of position of the epigynum during examination. Gertsch's figure 7 (*dispar*) is much more characteristic of all specimens of the species in ventral view than is figure 4 (*nearctica*), which is the view from slightly posterior. The subterminal apophysis differs among individuals (Figures 43–46), as do the paracymbium (Figures 47–50) and, to a lesser extent, the median apophysis (not illustrated). Similarities of the internal female genitalia also indicate that we have only one species, not two. California specimens of the species are the largest; a male from Alaska was the smallest specimen examined.

Gertsch is probably correct in stating that *Z. dispar* is distinct from *Z. montana* of Europe. Perhaps intermediates will be found in the vast area between Europe and Siberia from which no collections have been examined, but I would not expect this.

Diagnosis. Females of *Z. dispar* differ from those of the related *Z. montana* in that the median depression of the epigynum has a constriction (Figures 35, 39) in posterior view. The palpus is similar to that of *Z. montana* but differs in that most sclerotized parts of the palpus have a different shape and are positioned slightly differently (Figures 41, 42).

Natural history. The species is found on trees and rocks (Emerton, 1902, The Common Spiders, p. 185). Parts of the web have been illustrated by Emerton (1884, pl. 40, fig. 2). Emerton collected the species in the Adirondack Mountains, New York State, and the White Mountains, New Hampshire.

Distribution. Kamtchatka, Siberia, and North America along the Pacific coast, across Canada, the northern states, south in the western states, and in the Appalachian mountains in the east (Gertsch, 1964, fig. 1, a map).

Zygiella montana (C. L. Koch) Figures 51–56, 59–61

Zilla montana C. L. Koch, 1839, Die Arachniden, 6: 146, pl. 536, 537, ♀, ♂. Syntypes probably from Nassfelder Alpen in Salzburg, Austria, in the Museum of the Humboldt University, Berlin, not examined. Wiehle, 1931, *in* Dahl, Tierwelt Deutschlands, 23: 38, figs. 46–48, ♀, ♂.

Zygiella montana, - Roewer, 1942, Katalog der Araneae, 1: 886. Bonnet, 1959, Bibliographia Araneorum, 2: 5003.

Description. Female from Seefeld, Tirol, Austria. Coloration as in other species.

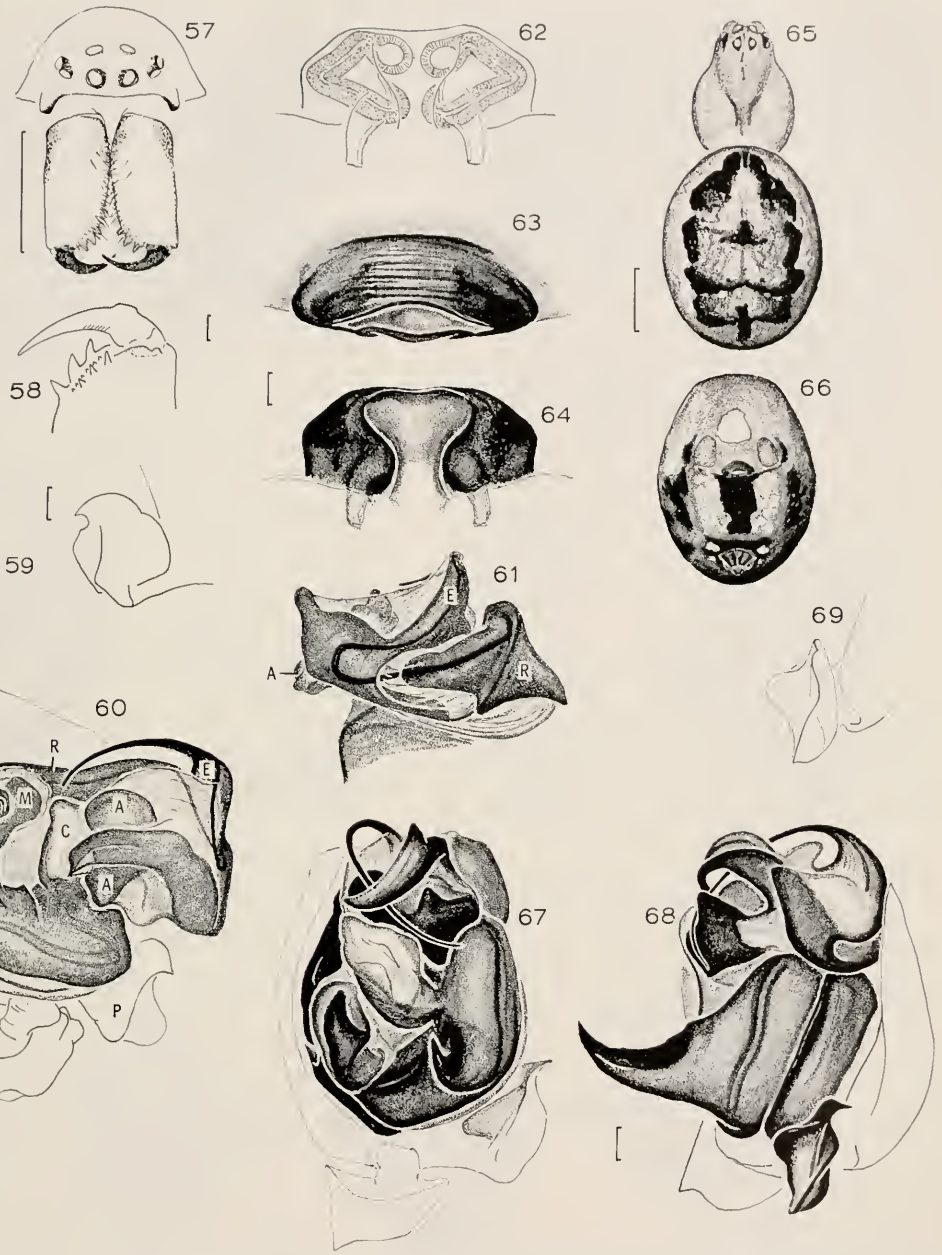

Figures 57–58. *Zygiella x-notata* (Clerck). 57. Eye region and chelicerae. 58. Left chelicera from inside.

Figures 59–61. *Z. montana* (C. L. Koch). 59. Paracymbium dorsolateral view. 60–61. Left male palpus, expanded. 60. Subventral. 61. Dorsal, cymbium removed.

Figures 62–69. *Z. carpenteri* Archer. 62–64. Epigynum. 62. Posterior, cleared. 63. Ventral. 64. Posterior. 65. Female. 66. Female abdomen, ventral 67–69. Male palpus. 67. Ventral. 68. Lateral. 69. Paracymbium.

Abbreviations. A, terminal apophysis; C, conductor; E, embolus; M, median apophysis; P, paracymbium; R, radix; T, tegulum.

Scale lines. 0.1 mm, except Figures 57, 65, 66, 1.0 mm.

Secondary eyes 0.8 diameter of anterior medians. Anterior median eyes 0.7 diameter apart, 0.6 diameter from laterals. Posterior median eyes one diameter apart, 1.2 from laterals. Total length 8.0 mm. Carapace 2.9 mm long, 2.2 mm high. First femur, 3.0 mm; patella and tibia, 3.7 mm; metatarsus, 2.9 mm; tarsus, 1.2 mm. Second patella and tibia, 3.1 mm; third, 1.9 mm; fourth, 2.6 mm.

Male from Seefeld, Tirol, Austria. Secondary eyes 0.6 diameter of anterior medians. Anterior median eyes 0.6 diameter apart, 0.5 diameter from laterals. Posterior median eyes their diameter apart, 1.6 from laterals. Total length 6.5 mm. Carapace 3.0 mm long, 2.4 mm wide. First femur, 3.2 mm; patella and tibia, 5.0 mm; metatarsus, 4.3 mm; tarsus, 1.0 mm. Second patella and tibia, 3.9 mm; third, 2.3 mm; fourth, 3.2 mm.

Diagnosis. This European species can easily be confused with Z. *dispar* but the epigynum lacks the constriction of the median depression in posterior view (Figure 54; the palpus has many sclerites, all slightly different in shape (Figures 55, 56).

Natural history. According to Wiehle (1931) this is a mountain species found in the Alps above 1000 m elevation, most commonly between 1300–1800 m. The species is found on buildings, rocks, bark and branches of trees and shrubs. The web is similar to that of Z. *x-notata* with 19–35 radii. The vacant sector is especially wide and the hub has a rough structure.

Both sexes are mature from June until September, and may take several years to mature.

Distribution. European mountains.

Zygiella carpenteri Archer
Figures 62–69

Zygiella carpenteri Archer, 1951, Amer. Mus. Novitates, No. 1487: 18, fig. 34, ♀. Female holotype from Del Monte Forest, Pacific Grove, Monterey Co., California, in the American Museum of Natural History, examined. Gertsch, 1964, Amer. Mus. Novitates, No. 2188: 9, figs. 1, 11–14, ♀, ♂, map.

Diagnosis. The wide depression of the epigynum (Figure 63), the long, pointed projection of the palpal tegulum (Figure 68) and the shape of the paracymbium (Figures 68, 69) separate the species from Z. *dispar.*

Distribution. Sierra mountains of Oregon and Washington. There are also a few records from near Spokane, Washington, and the coast of California. There is a distribution map in Gertsch (1964).

Zygiella caspica (Simon)
Figures 70–75

Zilla caspica Simon, 1889, Verh. zool. bot. Ges. Wien, 39: 382. Two female, one male syntypes from Transylvania in the Muséum National d'Histoire Naturelle, Paris, examined.

Zygiella caspica, - Roewer, 1942, Katalog der Araneae, 1: 883. Bonnet, 1959, Bibliographia Araneorum, 2: 5002.

Description. Female. Color like that of other species. Legs not banded, yellowish brown. Dorsal pattern as is characteristic in *Zygiella* (Figure 70), venter with very

→

Figures 70–75. *Zygiella caspica* (Simon). 70. Female. 71, 72. Epigynum. 71. Ventral. 72. Posterior. 73–75. Left male palpus. 73. Mesal. 74. Ventral. 75. Lateral.

Figures 76–80. *Z. calyptrata* (Workman). 76–78. Epigynum. 76. Dorsal, cleared. 77. Ventral. 78. Posterior. 79. Female. 80. Fourth coxae, ventral.

Figures 81–84. *Z. melanocrania* (Thorell). 81–83. Epigynum. 81. Ventral, cleared. 82. Ventral. 83. Posterior. 84. Female.

Figures 85–86. *Z. kochi* (Thorell), male palpus. 85. Ventral. 86. Lateral.

Scale lines. 0.1 mm except Figures 70, 79, 84, 1.0 mm.

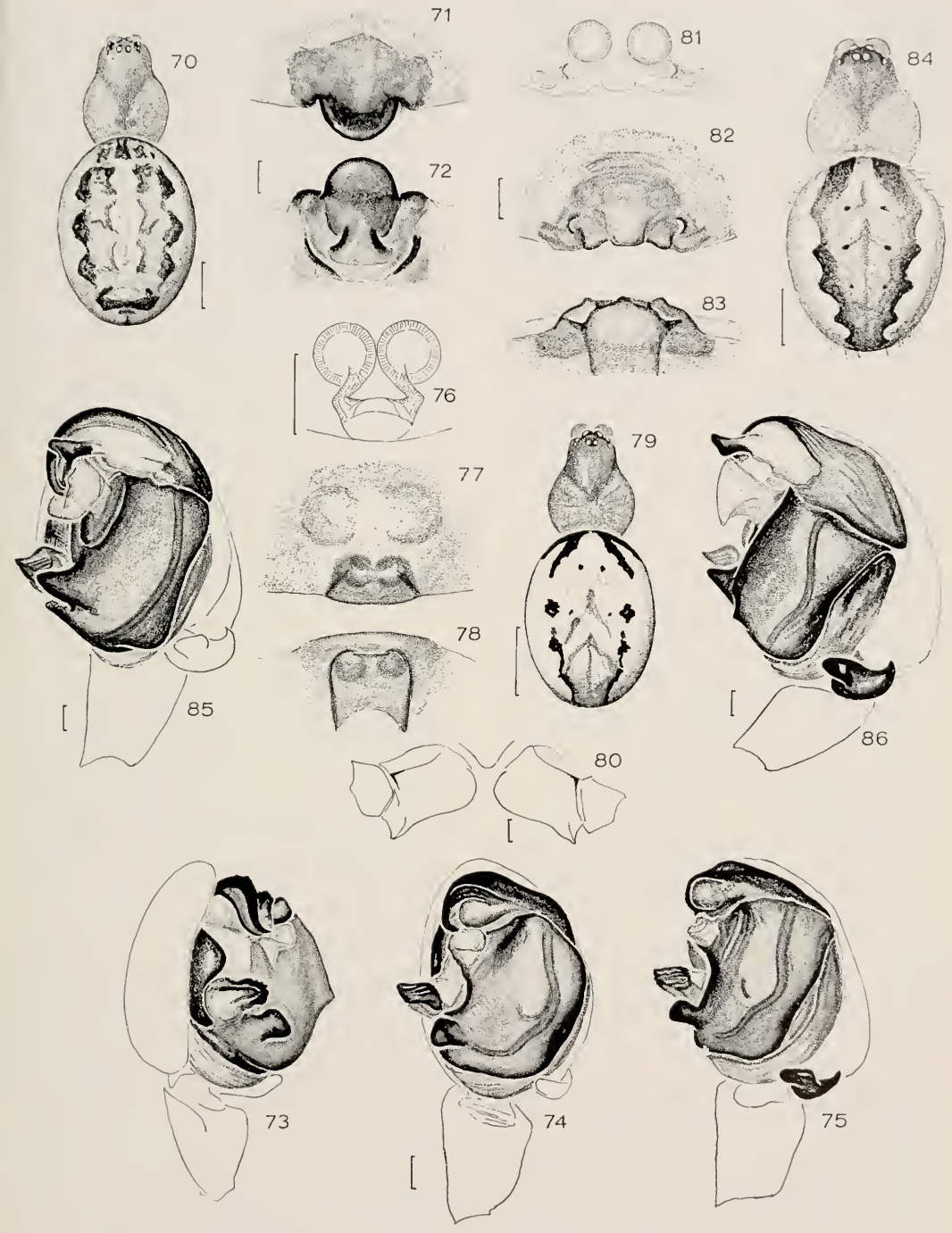
70
71
72
81
82
83
84
76
77
78
79
80
85
86
73
74
75

little black pigment. The posterior median eyes are slightly smaller than anterior medians, laterals 0.8 diameter of anterior median eyes. The anterior median eyes are their radius apart, their radius from laterals. Posterior median eyes their diameter apart, and slightly more than one diameter from laterals. Total length 6.5 mm. Carapace 2.4 mm long, 1.9 mm wide. First femur, 2.8 mm; patella and tibia, 3.6 mm; metatarsus, 2.6 mm; tarsus, 0.9 mm. Second patella and tibia, 2.8 mm; third, 1.7 mm; fourth, 2.3 mm.

Male. Coloration as in female. The eyes are slightly larger and closer together. Total length 5.0 mm. Carapace 2.3 mm long, 1.7 mm wide. First femur, 2.9 mm; patella and tibia, 4.3 mm; metatarsus, 2.9 mm; tarsus, 1.2 mm. Second patella and tibia, 2.9 mm; third, 1.7 mm; fourth, 2.3 mm.

Diagnosis. While the short semicircular scape of the epigynum (Figures 71, 72) is distinct, the palpus is similar to that of *Z. kochi*, but differs in the shape of the tegulum at the base of the conductor and the terminal apophysis (Figures 73–75).

Distribution. Trans-Carpathian region.

Zygiella calyptrata (Workman)
Figures 76–80

Epeira calyptrata Workman, 1894, Malaysian Spiders, p. 21, plate 21. One female lectotype here designated and two female paralectotypes from Singapore in the National Museum of Ireland, Dublin, examined.

Epeira (Zilla) calyptrata, - Thorell, 1895, Descr. Catalogue of the Spiders of Burma, p. 188.

Zygiella calyptrata, - Roewer, 1942, Katalog der Araneae, 1: 886.

Araneus calyptratus, - Bonnet, 1955, Bibliographia Araneorum, 2: 450.

Description. Female lectotype. Carapace brown; head region very much darker, glossy. Sternum, legs brown. Dorsum of abdomen white with black marks (Figure 79). Sides brownish black. Venter gray. Anterior median eyes much larger than others. Diameter of posterior median eyes 0.8 diameter of anterior medians; laterals 0.6 diameter of anterior median eyes. Anterior median eyes their diameter apart, slightly more than their diameter from laterals. Posterior median eyes slightly less than their radius apart, 2.5 diameters from laterals. The fourth coxa has a posterior distal spine (Figure 80). Total length 4 mm. Carapace 1.7 mm long, 1.3 mm wide. First femur, 1.5 mm; patella and tibia, 2.0 mm; metatarsus, 1.5 mm; tarsus, 0.6 mm. Second patella and tibia, 1.7 mm; third, 1.0 mm; fourth, 1.5 mm.

Diagnosis. Unlike females of *Z. melanocrania*, those of *Z. calyptrata* have the median area of the epigynum dark with an indistinct border (Figure 77). It is doubtful that this species belongs to *Zygiella* and is related to the other *Zygiella* species.

Distribution. Malaysia, Burma. (Of Thorell's specimens labeled *Epeira calyptrata* in the British Museum, Natural History, one is this species, the other specimen is a related species.)

Zygiella melanocrania (Thorell)
Figures 81–84

Epeira melanocrania Thorell, 1887, Ann. Mus. Civica Storia Natur. Genova, (2)5: 209. Female holotype from Teinzo, Burma, in the Museo Civico di Storia Naturale, Genova, examined.

Zygiella melanocrania, - Roewer, 1942, Katalog der Araneae, 1: 886.

Araneus melanocranius, - Bonnet, 1955, Bibliographia Araneorum, 2: 543.

Description. Carapace shiny brown. Head region dark brown. Chelicerae brown, darker than head region. Sternum yellow-brown. Legs brown, first two darker than last two, with faint indications of darker rings. Dorsum of abdomen with characteristic black and white *Zygiella* pattern (Figure 84). Venter with white pigment spots only. Secondary eyes 0.8 diameter from anterior median eyes. Anterior median eyes are a diameter apart, slightly more than one diameter from laterals. Posterior median eyes are their radius apart, 2.5 diameters from laterals. The laterals are separated by their radius from each

other. The height of the clypeus is about equal to the radius of the anterior median eyes. The chelicerae of one specimen have four teeth on the anterior margin of the fang furrow, but the posterior margin has four on one chelicera, three on the other; there are denticles in the furrow. The abdomen is oval and hairy. Total length 5.5 mm. Carapace 2.6 mm long, 2.0 mm wide. First femur, 2.7 mm; patella and tibia, 3.3 mm; metatarsus, 2.1 mm; tarsus, 0.9 mm. Second patella and tibia, 2.7 mm; third, 1.6 mm; fourth, 2.2 mm.

Diagnosis. The epigynum (Figures 82, 83), with two semicircular openings on the ventral side, separates this species from all other known *Zygiella.*

Distribution. This species is known only from the type specimen. The specimen illustrated by Dyal (1935, Bull. Dept. Zool., Panjab Univ. 1: 183, pl. 16, fig. 125) is probably not this species.

Zygiella kochi (Thorell) Figures 85–91

Zilla kochii Thorell, 1870, Remarks on Synonyms of European Spiders, p. 33. Syntypes from Nice and Monaco presumably in the Stockholm Natural History Museum. Bösenberg, 1901, Zoologica, 13: 43, pl. 3, fig. 32, ♀, ♂. Wiehle, 1929, Z. Morphol. Ökol. Tiere, 15: 262–308. Wiehle, 1931, *in* Dahl, Tierwelt Deutschlands, 23: 41, figs. 52, 53, ♀, ♂.

Zygiella kochi, - Simon, 1929, Arachnides de France, 6(3): 663, 754, figs. 1021, 1025, ♀, ♂. Roewer, 1942, Katalog der Araneae, 1: 884. Bonnet, 1959, Bibliographia Araneorum, 2: 5002.

Description. Female from France. Carapace brown, with darker lines going from eye region to thoracic depression (Figure 87). Sternum brown. Legs very indistinctly banded. Dorsum of abdomen with usual pattern (Figure 87). Venter with a black spot framed by white on each side. Secondary eyes 0.7 diameter of anterior medians. Anterior median eyes 0.7 diameter apart, one diameter from laterals. Posterior median eyes one diameter apart, a little less than two diameters from laterals. Total length 7.5 mm. Carapace 3.5 mm long, 2.5 mm wide. First femur, 3.2 mm; patella and tibia, 4.3 mm; metatarsus, 3.0 mm; tarsus, 1.3 mm. Second patella and tibia, 3.2 mm; third, 2.0 mm; fourth, 2.9 mm. The entrance into the seminal receptacles is through pockets and folds rather than through distinct ducts (Figures 88, 91).

Description of male from unknown locality. Posterior median eye diameter about the radius of anterior median eyes; anterior lateral eyes 0.7 diameter of anterior median eyes; posterior lateral eye diameter about the radius of anterior median eyes. Anterior median eyes their radius apart and about their radius from laterals. Posterior median eyes their diameter apart, 1.5 diameters from laterals. There are no modifications on appendages. Total length 7 mm. Carapace 3.1 mm long, 2.3 mm wide. First femur, 3.2 mm; patella and tibia, 4.7 mm; metatarsus, 3.1 mm; tarsus, 1.3 mm. Second patella and tibia, 3.6 mm; third, 2.0 mm; fourth, 2.6 mm.

Diagnosis. The heart-shaped scape of the epigynum (Figure 89) separates this species readily from others. The scape has a central depression. The rim on the tegulum surrounding the base of the conductor, and the shape of the subterminal apophysis of the palpus separate males from *Z. caspica* (Figures 85, 86).

Natural history. The species is found on trunks of trees, cork bark and chestnut in Corsica; its retreat is in cracks in bark (Wiehle, 1929, 1931). The web is similar to that of *Z. x-notata*; of fifteen webs four did not have the vacant sector but had complete orbs (Wiehle, 1929).

Distribution. Central and southern Europe, Mediterranean region and North Africa (Bonnet, 1959).

Zygiella inconveniens (O.P.-Cambridge) Figures 92–94

Epeira inconveniens (O.P.-Cambridge), 1872, Proc. Zool. Soc. London, p. 298. Female holo-

type and juvenile lectotype from Beirut, Lebanon.

Zygiella inconveniens, - Roewer, 1942, Katalog der Araneae, 1: 883.

Araneus inconveniens, - Bonnet, 1955, Bibliographia Araneorum, 2: 522.

Description. Coloration characteristic for the genus (Figure 92). The secondary eyes are about 0.8 diameter of anterior medians. Anterior median eyes are 0.7 diameter apart, their radius from laterals. The posterior median eyes are slightly less than one diameter apart, slightly more than one from laterals. Total length 5.5 mm. Carapace 2.5 mm long, 1.9 mm wide. First femur, 2.3 mm; patella and tibia, 3.2 mm; metatarsus, 2.4 mm; tarsus, 0.9 mm. Second patella and tibia, 2.5 mm; third, 1.5 mm; fourth, 2.2 mm.

Diagnosis. Females differ from *Z. kochi* in the longer, narrower scape of the epigynum (Figure 93).

Distribution. Only known from Beirut, Lebanon.

Zygiella thorelli (Ausserer)
Figures 95–101

Zilla thorelli Ausserer, 1871, Verhandl. zool. bot. Ges. Wien, 21: 830, pl. 5, fig. 10, ♀. Female from Prater (amusement park), Vienna, Austria, probably in the Naturhistorisches Museum, Wien, not examined. Wiehle, 1931, *in* Dahl, Tierwelt Deutschlands, 23: 39, figs. 49–51, ♀, ♂.

Zygiella thorelli, - Simon, 1929, Arachnides de France, 6(3): 663, 664, 755, figs. 1019, 1024, ♀ ♂. Roewer, 1942, Katalog der Araneae, 1: 884. Bonnet, 1959, Bibliographia Araneorum, 2: 5006.

Description. Female from France. Carapace brown, black lines from each posterior lateral eye to thoracic region, fusing there with a lateral branch; black line around margin of the thoracic region (Figure 95). Chelicerae dark brown. Sternum dark brown with light brown median longitudinal narrow band. Legs brown with narrow dark bands. Dorsum with characteristic pattern (Figure 95) containing black and with white pigment spots. Venter black between genital furrow and spinnerets, with a white line on each side. Posterior median eyes 0.6 diameter of anterior median eyes. Anterior lateral eyes 0.7 diameter of anterior medians, posterior lateral eyes 0.5 diameter of anterior median eyes. Anterior median eyes 0.7 diameter apart, one diameter from laterals. Posterior median eyes slightly less than their diameter apart, 1.7 from laterals. On the anterior margin of the fang furrow, the chelicerae have three large teeth; on the posterior margin, four teeth and, farthest from fang, a denticle. Total length 10 mm. Carapace 4.5 mm long, 3.2 mm wide. First femur, 4.9 mm; patella and tibia, 6.7 mm; metatarsus, 5.0 mm; tarsus, 1.7 mm. Second patella and tibia, 5.0 mm; third, 2.9 mm; fourth, 4.0 mm.

Male from Kochem on the Mosel, Germany. Coloration like that of female. Secondary eye diameter 0.6 diameter of anterior median eyes. Anterior median eyes slightly less than their radius apart, their diameter from laterals. Posterior median eyes 0.7 diameter apart, 1.5 diameters from laterals. The chelicerae have three teeth on the anterior margin; three smaller teeth on the posterior. Total length 7.5 mm. Carapace 3.9 mm long, 2.8 mm wide. First femur, 4.8 mm; patella and tibia, 7.0 mm; metatarsus, 6.5 mm; tarsus, 1.8 mm. Second patella and tibia, 5.0 mm; third, 2.8 mm; fourth, 3.5 mm.

Diagnosis. This species has a longer, narrower carapace than is seen in other species of *Zygiella*. Females are distinct in the shape of the epigynal scape, a lobe with a distal extension (Figure 97). Males are characterized by the sculptured, human-ear-shaped tegulum (Figure 100). No other known species is close to *Z. thorelli*.

Natural history. This central European species prefers warm locations such as walls of ruins and cliffs. It has also been found on wooden buildings. The sexes are mature in August and September (Wiehle, 1931). The web, a typical *Zygiella* web,

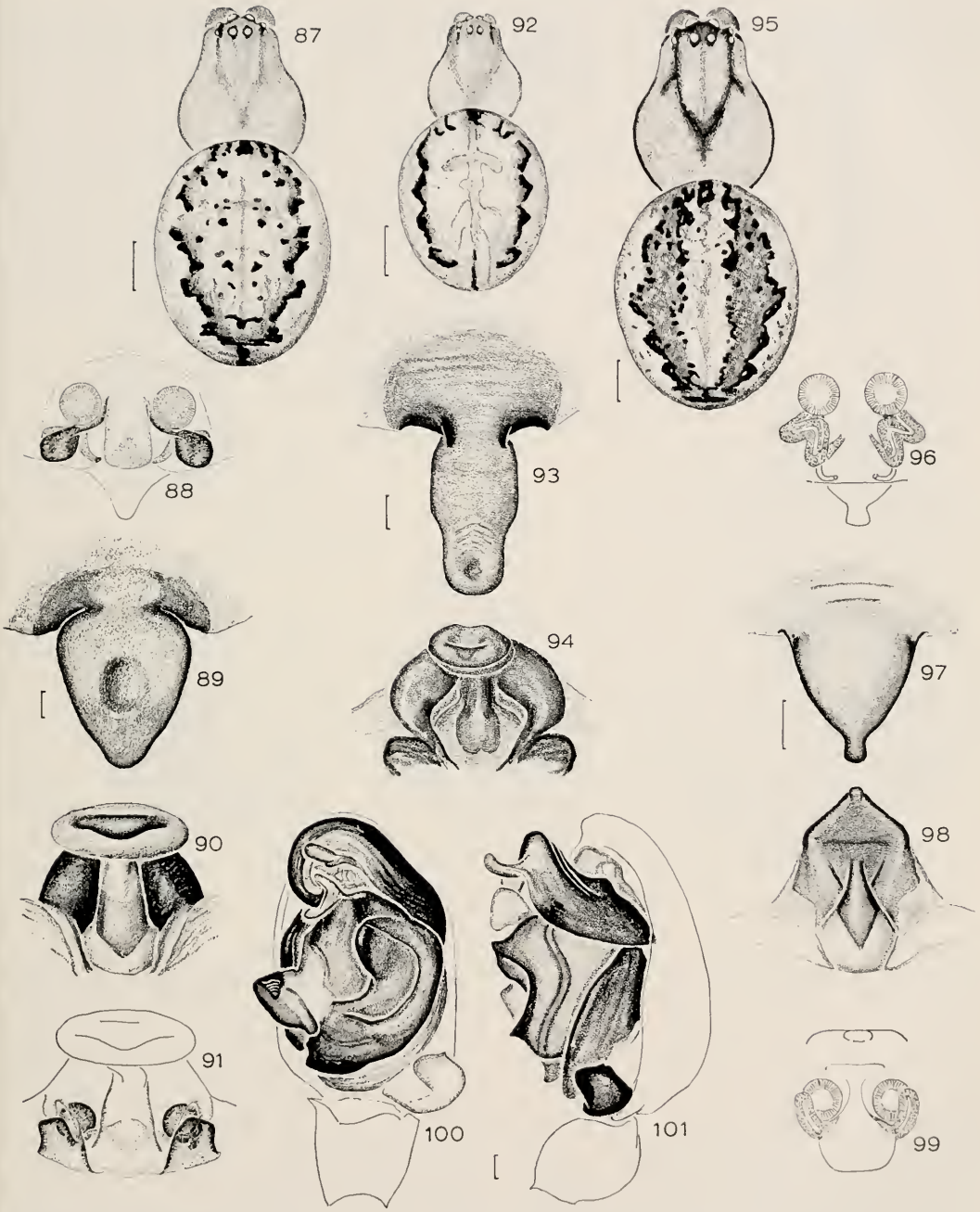

Figures 87–91. *Zygiella kochi* (Thorell). 87. Female. 88–91. Epigynum. 88. Dorsal, cleared. 89. Ventral. 90. Posterior. 91. Posterior, cleared.

Figures 92–94. *Z. inconveniens* (O. P.-Cambridge). 92. Female. 93, 94. Epigynum. 93. Ventral. 94. Posterior.

Figures 95–101. *Z. thorelli* (Ausserer). 95. Female. 96–99. Epigynum. 96. Dorsal, cleared. 97. Ventral. 98. Posterior. 99. Posterior, cleared. 100, 101. Left male palpus. 100. Ventral. 101. Lateral.

Scale lines. 0.1 mm except Figures 87, 92, 95, 1.0 mm.

is pictured in Lendl (1891, Potpüz Termész. közl., Budapest, 13: 31, figure 8).

Distribution. France, southern Germany, Czechoslovakia, Poland to Italy and Roumania (Bonnet, 1959).

Zygiella stroemi (Thorell) Figures 102–110

Zilla stroemi Thorell, 1870, Remarks on Synonyms of European Spiders, p. 235. New name for *Zilla montana*, Westring (not C. L. Koch) from Sweden. Wiehle, 1931, *in* Dahl, Tierwelt Deutschlands, 23: 36, figs. 43–45, ♀, ♂.

Zygiella x-notata, - Roewer, 1942, Katalog der Araneae, 1: 884 (not *x-notata* Clerck).

Zygiella stroemi, - Locket and Millidge, 1953, British Spiders, 2: 163, figs. 108b, 109c, ♀, ♂. Bonnet, 1959, Bibliographia Araneorum, 2: 5005.

Description. Female from Plitvice, Croatia, Jugoslavia. Coloration similar to that of other species (Figure 103). Diameter of posterior median eyes 0.8 diameter of anterior medians. Anterior lateral eyes 0.9 diameter of anterior medians and posterior lateral eyes 0.8 diameter of anterior medians. Anterior median eyes slightly less than their radius apart, the same distance from laterals. Posterior median eyes their diameter apart, slightly more than their diameter from laterals. Total length 4.5 mm. Carapace 1.9 mm long, 1.5 mm wide. First femur, 2.2 mm; patella and tibia, 2.7 mm; metatarsus, 2.0 mm; tarsus, 0.9 mm. Second patella and tibia, 1.9 mm; third, 1.3 mm; fourth, 1.9 mm.

Male from Plitvice, Croatia, Jugoslavia. Diameter of secondary eyes 0.7 diameter of anterior medians. Anterior medians 0.3 diameter apart, the same distance from laterals. Posterior median eyes slightly less than their diameter apart, slightly more than their diameter from laterals. Total length 3.4 mm. Carapace 1.7 mm long, 1.6 mm wide. First femur, 2.2 mm; patella and tibia, 3.0 mm; metatarsus, 2.6 mm; tarsus, 1.0 mm. Second patella and tibia, 2.2 mm; third, 1.1 mm; fourth, 1.5 mm.

Diagnosis. The flat, long scape with almost parallel sides (Figure 104) separates females from all other *Zygiella*. Males are distinguished by the truncate projection of the tegulum of the palpus (Figures 108–110).

Natural history. The web is on the trunks of pines (Wiehle, 1931; Locket and Millidge, 1953); the retreat is under bark. Wiehle (1931) reports that the species matures from May until June, and several specimens may be found near each other.

Distribution. Most of Europe to Siberia and Turkestan (Bonnet, 1959).

Zygiella sia (Strand) Figures 111–120

Aranea (*Zilla*) *sia* Strand, 1906, *in* Bösenberg and Strand, Abhandl. Senckenberg. Ges., 30 (1–2): 237, pl. 4, fig. 24, ♂. Adult female, male, and 5 juvenile syntypes from Japan in the Senckenberg Museum, Frankfurt, examined.

Zygiella sia, - Roewer, 1942, Katalog der Araneae, 1: 884.

Araneus sia, - Bonnet, 1955, Bibliographia Araneorum, 2: 598. Yaginuma, 1960. Spiders of Japan in Colour, Osaka, p. 54, figs. 1, 3, plate 19, fig. 115, ♀, ♂.

Zilla sia, - Saito, 1959, The Spider Book Illustrated in Colours, Tokyo, p. 109, fig. 23, pl. 17, fig. 129 a, b, pl. 18, fig. 129 d, ♀, web.

Description. Female syntype. Carapace brown, head region darker brown, darker area coming to a point posteriorly in thoracic depression. Some white hairs on sides. Sternum dark brown. Legs indistinctly to distinctly banded. Abdomen with the characteristic pattern. Venter with a white longitudinal line on each side. Posterior median eyes 0.6 diameter of anterior medians, anterior lateral eyes 0.6, posterior laterals 0.5 diameter. Anterior median eyes 0.8 diameter apart, 1.5 diameters from laterals. Posterior median eyes 0.7 diameter apart, 3.0 diameters from laterals. Lateral eyes slightly separated. There are three teeth on the anterior margin of chelicerae. Total length 7 mm. Carapace 2.7 mm long, 2.2 mm wide. First femur, 2.9 mm; patella and tibia, 4.0 mm; metatarsus, 2.7 mm; tarsus, 0.7 mm. Second patella and tibia, 3.4 mm; third, 1.9 mm; fourth, 2.7 mm.

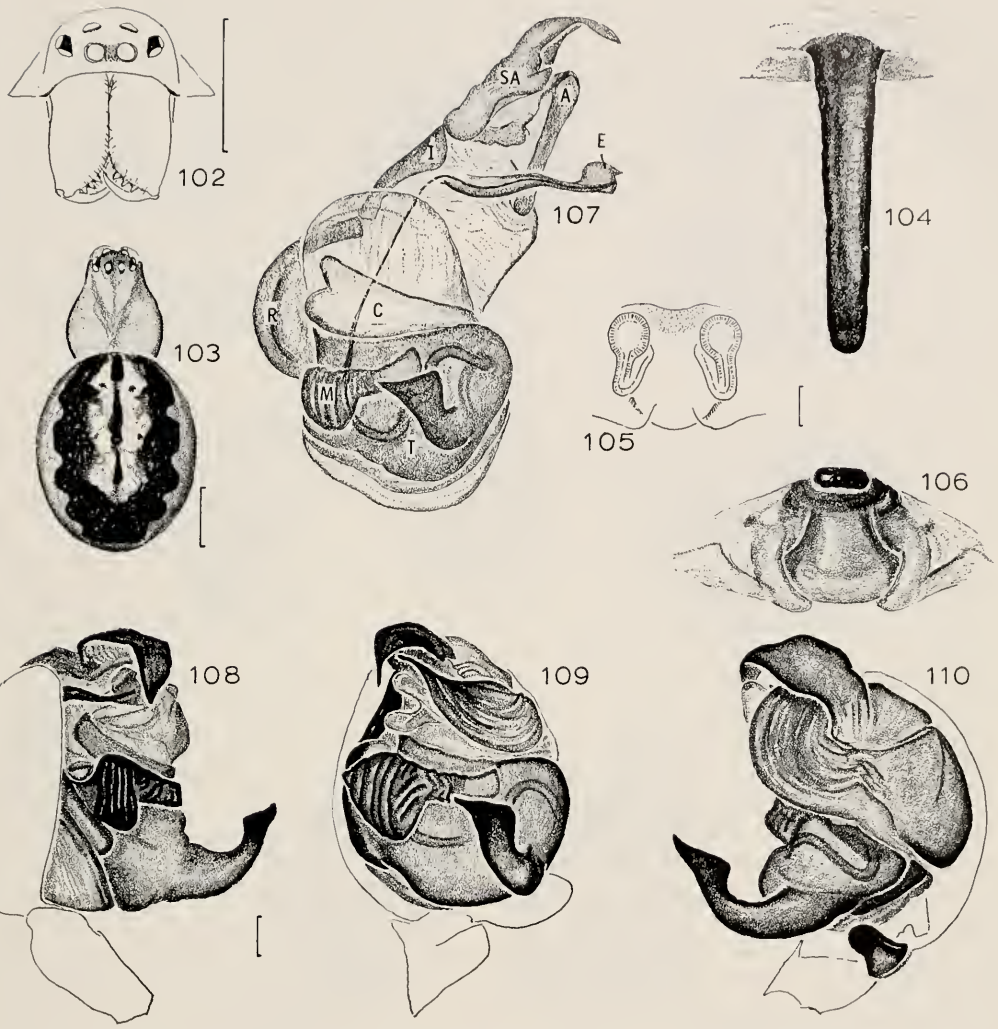

Figures 102–110. *Zygiella stroemi* (Thorell). 102. Eye region and chelicerae. 103. Female. 104–106. Epigynum. 104. Ventral. 105. Anterodorsal, cleared. 106. Posterior. 107–110. Left male palpus. 107. Expanded. 108. Mesal. 109. Ventral. 110. Lateral.

Abbreviations. A, terminal apophysis; C, conductor; E, embolus; I, stipes; M, median apophysis; R, radix; SA, subterminal apophysis; T, tegulum.

Scale lines. 0.1 mm except Figures 102, 103, 1.0 mm.

Male syntype from Japan. Coloration as in female, but abdominal pattern more distinct. Diameter of secondary eyes about equal to radius of anterior medians. Posterior lateral eyes slightly smaller than other secondary eyes. Anterior median eyes 0.7 diameter apart, one diameter from laterals. Posterior median eyes 0.6 diameter apart, three diameters from laterals. There are three teeth anteriorly on chelicheral fang margin and three posteriorly. Total length 6 mm. Carapace 2.6 mm long, 2.1 mm wide. First femur, 3.0 mm; patella and tibia, 4.1 mm; metatarsus, 2.9

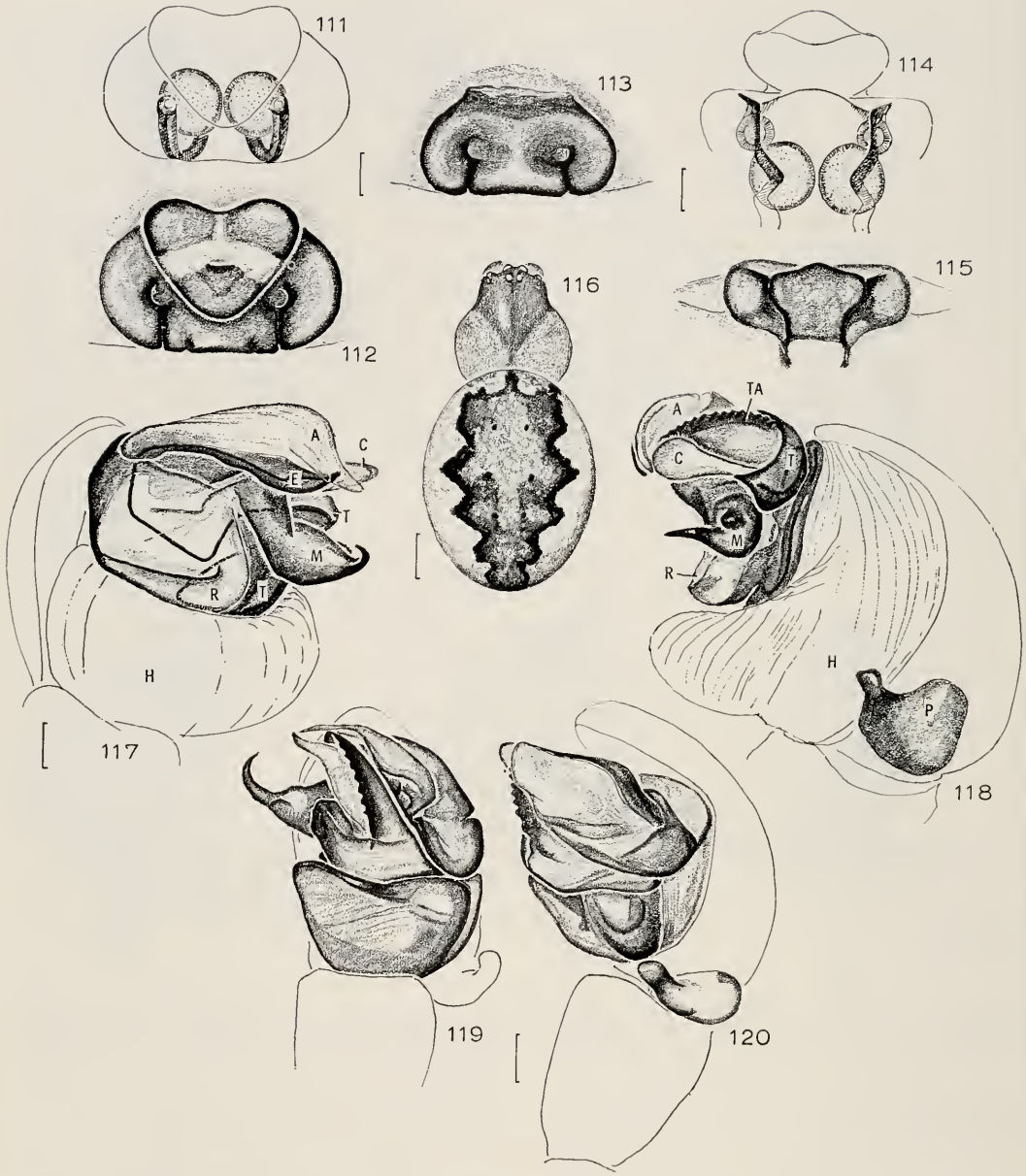

Figures 111–120. *Zygiella sia* (Strand). 111–115. Epigynum. 111. Ventral, cleared. 112. Ventral. 113. Ventral, scape torn off. 114. Posterior, cleared. 115. Posterior. 116. Female. 117–120. Left male palpus. 117, 118. Expanded. 119. Ventral. 120. Lateral.

Abbreviations. A, terminal apophysis; C, conductor; E, embolus; H, hematodocha; M, median apophysis; P, paracymbium; R, radix; T, tegulum; TA, projection of tegulum.

Scale lines. 0.1 mm except Figure 116, 1.0 mm.

mm; tarsus, 1.0 mm. Second patella and tibia, 3.3 mm; third, 1.8 mm; fourth, 2.6 mm.

Note on size. Several other specimens of this species were examined. They were much larger. And with the size increase there was a proportionate increase in the *distance* of the laterals from the median eyes. A female from Shiga Prefecture was 12.5 mm total length. The specimen had a carapace 4.7 mm long and 4.1 mm wide, about 1.7 times the size of the female syntype. The legs were of proportionate length, 1.7 times that of the syntype. The comparative eye sizes stayed the same but anterior median eyes were about twice their diameter from laterals (a *distance* increase of about 1.3 times) and the posterior medians slightly less than five times from laterals (a *distance* increase of 1.6 times almost proportionate to growth). The eyes thus grew relatively less.

Male specimens from Naga Prefecture were also larger: total length 7.5 and 10.5 mm; carapace 3.8 and 5.1 mm long, 2.7 and 3.9 mm wide. These measurements are 1.4 times and 2.0 times the corresponding measurements of the syntype; the appendage articles were, however, 1.7 times and 2.2 times the length of the carapace of the type. Growth of males' legs thus did not seem proportional. However, in the two different-sized males from Naga Prefecture, carapace and leg sizes were in proportion.

The Naga males had the diameter of the secondary eyes 0.7 diameter of the medians (the syntypes about 0.5 diameter). The syntype had the anterior median eyes one diameter from laterals, the smaller Naga specimen one and one-half, the larger one slightly less than two. The posterior median eyes were three diameters from laterals in the syntype, about four in the smaller Naga specimen (1.3 times the distance), about five times in the larger one (1.7 times the distance in the syntype). The eye distances increase less than size; there appears to be only little increase in eye sizes.

Presumably the specimens had matured in different instars. But these proportional differences seem surprising considering the similarity in proportion and size of the epigyna and male palpi.

The male specimen whose carapace was twice as long as the carapace of the syntype, also had the palpal tibia 2.5 times as long as that of the syntype (a proportional increase with leg length), but the critical palpal cymbium was only 1.4 times longer than that of the syntype. The larger specimen thus had relatively a much longer palpal tibia. No differences were noted in the position and proportion of the sclerites held within the cymbium.

Diagnosis. The heart-shaped scape covering the ventral openings of the epigynum (Figure 112) separates the female from all other *Zygiella.* The scape has a transverse light mark. The male palpus (Figures 119–120) is superficially very different from other species: it has a huge basal hematodocha, a minute tegulum bearing a toothed projection, and the median apophysis has a projecting hook (Figures 117–118). As in *Z. atrica* the palpal tibia is slightly elongated, but of a different shape.

There is some doubt in placing this species in *Zygiella,* because of the wider spacing of the eyes and the cap on the palpal embolus in the expanded palpus (Figure 117), not otherwise seen in the genus. The course of the duct into and through the tegulum remains uncertain, despite its having been illustrated in Figures 117, 118.

Distribution. Japan. Fox (1938, J. Washington Acad. Sci. 28: 367) reported specimens from Szechwan Prov. China, but the specimens of the U.S. National Museum could not be found.

REFERENCES CITED

Archer, A. 1951a. Studies in the orbweaving spiders (Argiopidae), 1. Amer. Mus. Novitates, No. 1487: 1–52.

———. 1951b. Studies in the orbweaving spi-

ders (Argiopidae), 2. Amer. Mus. Novitates, No. 1502: 1–34.

Bonnet, P. 1959. Bibliographia Araneorum, Vol. 2. Imprimerie Douladoure, Toulouse, vol. 2, 4231–5058.

Emerton, J. H. 1884. New England spiders of the family Epeiridae. Trans. Connecticut Acad. Arts Sci., **6**: 295–342.

Gertsch, W. J. 1964. The spider genus *Zygiella* in North America (Araneae, Argiopidae). Amer. Mus. Novitates, No. 2188: 1–21.

Roewer, C. F. 1942. Katalog der Araneae. Verlag Natura, Hamburg, vol. 1.

Simon, E. 1895. Histoire Naturelle des Araignèes. Roret, Paris: Libraire Encyclopédique vol. 1.

Wiehle, H. 1931. Araneidae. *In* Dahl, F. Die Tierwelt Deutschlands, G. Fischer Verlag, Jena **23**: 1–136.

INDEX

Valid names are printed in italics. Page numbers refer to main references, starred page numbers to illustrations.

alpina, Zilla 270
ancora, Epeira 270
atrica, Eucharia 272
atrica, Zilla 272
atrica, Zygiella 269*, 272, 273*
aureola, Zilla 270
bösenbergi, Zilla 276
californica, Zilla 276
calophylla, Aranea 271
calyptrata, Epeira 282
calyptrata, Zygiella 281*, 282
calyptratus, Araneus 282
carpenteri, Zygiella 279*, 280
caspica, Zilla 280
caspica, Zygiella 280, 281*
crucinotata, Zilla 271
decolorata, Zilla 271
dispar, Zilla 278
dispar, Zygiella 277*, 278
gigans, Zilla 271
guttata, Zilla 271
guyanensis, Zilla 271
inconveniens, Araneus 284
inconveniens, Epeira 283
inconvenieus, Zygiella 283, 285*
keyserlingi, Zilla 274
keyserlingi, Zygiella 273*, 274
kochii, Zilla 283
kochi, Zygiella 281*, 283, 285*
maulliana, Larinia 276
melanocephala, Linyphia 271
melanocrania, Epeira 282
melanocrania, Zygiella 281*, 282
melanocranius, Araneus 282
minima, Zygiella 274, 275*
montana, Zilla 278
montana, Zygiella 277*, 278, 279*
montana, Zygiella 278
nawazi, Zilla 271
nearctica, Zygiella 278
punctata, Zilla 271
rogenhoferi, Zilla 271
sia, Aranea 286
sia, Araneus 286
sia, Zilla 286
sia, Zygiella 286, 288*
stroemi, Zilla 286
stroemi, Zygiella 286, 287*
thorelli, Zilla 284
thorelli, Zygiella 284, 285*
x-notata, Zygiella 275*, 276, 279*
x-notata, Zygiella 286
x-notatus, Araneus 276
Zygia 268
Zygiella 268

US ISSN 0027-4100

Bulletin OF THE
Museum of
Comparative
Zoology

The Orb-weaver Genera *Araniella* and *Nuctenea* (Araneae: Araneidae)

HERBERT W. LEVI

HARVARD UNIVERSITY
CAMBRIDGE, MASSACHUSETTS, U.S.A

VOLUME 146, NUMBER 6
21 NOVEMBER 1974

PUBLICATIONS ISSUED
OR DISTRIBUTED BY THE
MUSEUM OF COMPARATIVE ZOOLOGY
HARVARD UNIVERSITY

Breviora 1952–
Bulletin 1863–
Memoirs 1864–1938
Johnsonia, Department of Mollusks, 1941–
Occasional Papers on Mollusks, 1945–

SPECIAL PUBLICATIONS.

1. Whittington, H. B., and E. D. I. Rolfe (eds.), 1963. Phylogeny and Evolution of Crustacea. 192 pp.
2. Turner, R. D., 1966. A Survey and Illustrated Catalogue of the Teredinidae (Mollusca: Bivalvia). 265 pp.
3. Sprinkle, J., 1973. Morphology and Evolution of Blastozoan Echinoderms. 284 pp.
4. Eaton, R. J. E., 1974. A Flora of Concord. 250 pp.

Other Publications.

Bigelow, H. B., and W. C. Schroeder, 1953. Fishes of the Gulf of Maine. Reprint.

Brues, C. T., A. L. Melander, and F. M. Carpenter, 1954. Classification of Insects.

Creighton, W. S., 1950. The Ants of North America. Reprint.

Lyman, C. P., and A. R. Dawe (eds.), 1960. Symposium on Natural Mammalian Hibernation.

Peters' Check-list of Birds of the World, vols. 2–7, 9, 10, 12–15.

Proceedings of the New England Zoological Club 1899–1948. (Complete sets only.)

Publications of the Boston Society of Natural History.

Price list and catalog of MCZ publications may be obtained from Publications Office, Museum of Comparative Zoology, Harvard University, Cambridge, Massachusetts, 02138, U.S.A.

© The President and Fellows of Harvard College 1974.

THE ORB-WEAVER GENERA *ARANIELLA* AND *NUCTENEA* (Araneae: Araneidae)

HERBERT W. LEVI

ABSTRACT. The species included in *Araniella* and *Nuctenea* have traditionally been included in *Araneus*, but males differ in lacking the embolus cap. The lack of embolus cap can be related to differences in mating behavior. Those orb-weavers with cap (*Araneus*) can mate only once with each palpus; *Nuctenea* males lacking a cap can mate several times.

Four species of *Araniella* are known, one of them Holarctic, the others Palearctic. Some European populations are of interest as there are indications that the species hybridize.

Of the six species known to belong to *Nuctenea*, three are Holarctic, and three Palearctic. One of the Holarctic species may be a recent introduction to North America; another may be cosmopolitan.

Other species belonging to these two genera may be hidden among the two thousand species placed in *Araneus* and mostly poorly described.

INTRODUCTION

Araniella and *Nuctenea* species have traditionally been placed in *Araneus*. They include our commonest orb-weavers. Nevertheless the species are not well known, and in looking through the collections available, I found that many specimens were misidentified.

The species of both genera are mainly Palearctic with some Holarctic species.

I would like to thank the following for providing specimens for this study: D. Bixler; W. J. Gertsch and J. A. L. Cooke of the American Museum of Natural History, Cornell and Utah University collections; J. E. Carico; M. Grasshoff of the Senckenberg Museum; C. Dondale and R. Leech, Canadian National collections, Ottawa; W. Hackman; G. H. Locket; M. Martelli of the Zoological Museum of the University of Florence; W. W. Moss of the Academy of Natural Sciences, Philadelphia; W. Peck, Exline-Peck collection; R. X. Schick of the California Academy of Sciences; J. Prószyński and W. Staręga of the Polish Academy of Sciences; B. Vogel; H. K. Wallace and H. V. Weems, Florida State Collection of Arthropods. Information was provided by T. Kronestedt of the Natural History Museum, Stockholm; M. Moritz of the Zoological Museum of the Humboldt University, Berlin; and F. Wanless and D. Newman of the British Museum, Natural History. Lorna R. Levi and Ian Mackay edited the paper. This investigation and its publication were supported in part by National Science Foundation grant number GB–36161.

One of the striking and puzzling features of these common orb-weavers is the enormous individual variation in genitalic structure (Figs. 8–15, 17, 18, 67–76), while there is little variation in the size and shape of the whole animal. This variation is found in Holarctic *Araniella displicata* and *A. cucurbitina* of Europe as well as in Holarctic *Nuctenea patagiata* and Holarctic *N. cornuta*. Not infrequently specimens of these common species are sent to the museum by collectors who believe them to

be a new species. In their unusual variation, *Araniella* and *Nuctenea* contrast with the small *Araneus* species (Levi, 1973). Even though the species are fairly widespread, the differences between small *Araneus* species are far less than is found among individuals of a single collection of *N. cornuta*. The larger-sized *Araneus* species (*A. nordmanni, A. saevus*) are intermediate in this respect (Levi, 1971). Large variation was not found in any of the widespread, common theridiids such as *Achaearanea tepidariorum*, although it does occur in the *Tidarren* species and *Enoplognatha ovata*. Variation in the genitalic structure of individuals was found in the zone of overlap between *Araneus gemma* and *Araneus gemmoides*; all evidence indicates hybridization (Levi, 1971). *Araniella* species may also hybridize in Europe. Perhaps the individual variation of *Araniella cucurbitina* of Europe is due to separation of northern and southern populations during the Pleistocene and the later hybridization occurred after the receding of the ice. In none of the species of *Araniella* or *Nuctenea* is the variation geographic. But I have not studied various populations in detail. Shortly after Petrunkevitch (1925) wrote on the remarkable variation of genitalia of *Agelena naevia*, Seyler (1940), following up a hint from Gertsch (1934), correctly found that what Petrunkevitch called one species was in fact several. But I doubt that populations of *Araniella displicata* or *Nuctenea patagiata* and *N. cornuta* consist of sibling species.

Of considerable interest is the relationship of *Araniella* species in Europe. Mr. Locket made me aware of this. While *A. inconspicua* and *A. alpica* appear distinct on the Continent, intermediates are found in Great Britain.

While in many American araneid and theridiid species specimens from the Gulf Coast and Florida are noticeably smaller than those from other parts of North America, Alaskan specimens of *N. cornuta* are smaller than those from southern Canada and the United States. To judge by the labels, *N. cornuta* is less dependent on houses in Alaska and probably competes with the native *Araneus* species. In northeastern America all three *Nuctenea* species are usually found on buildings, but this is not true throughout their ranges. *Nuctenea patagiata* may be found under bark in woods.

It is most unfortunate that at times names have to be changed as a result of revisionary studies.

Araniella Chamberlin and Ivie

Araniella Chamberlin and Ivie, 1942, Bull. Univ. Utah, biol. ser., 7(1): 76. Type species *Epeira displicata* Hentz, by original designation. The name is of feminine gender.

Note. Chamberlin and Ivie (1942) do not give reasons for separating *E. displicatus* from *Araneus* other than that the species is close to those of *Neoscona*. I agree with this opinion.

Diagnosis. There are no good superficial characters that separate female *Araniella* from the small species of *Araneus*. Females have a glabrous carapace and an oval abdomen, widest in the middle, lacking setae and lacking a folium pattern, but usually with paired black spots (Plate 1, Figs. 1, 16). The epigynum has a short, wide, wrinkled scape (Figs. 8, 25, 34, 40). The scape is not always clearly set off from the base of the epigynum. Unlike *Araneus* species, however, *Araniella* has, besides a single pair of seminal receptacles, a pair of sclerotized sacs (Figs. 7, 27, 33, 39) between the external entrance from outside to the connecting duct and the seminal receptacles. The entrance of the duct to the sclerotized sacs on each side is a slit. The ducts are hard to see in very sclerotized epigyna (*A. cucurbitina*).

Unlike other araneids I have examined, *Araniella* has three macrosetae (Figs. 31, 42) on the patella of the male palpus. Species of most genera have only two or one. However, the palpal femur has a basal ventral tooth facing a tooth on the

endite as in *Araneus*. The palpus resembles that of *Neoscona* (Berman and Levi, 1971, fig. 31) in having the sclerites nearly fused, a small flap-like terminal apophysis (A in Figs. 20–22), and in lacking a distal hematodocha (Fig. 21). This contrasts with the huge terminal apophysis and distal hematodocha in *Araneus* and *Nuctenea* (Figs. 58, 61). *Araniella* species also differ from *Neoscona* and *Araneus* in the hook-shaped, sclerotized, median apophysis (M), dorsally directed toward the cymbium (Figs. 20, 22), and in the unusually complex, large conductor (C). The embolus (E) lacks a cap. An embolus cap is always present in virgin males of *Araneus* species; the cap breaks off in mating.

Araniella males have a hook on the distal margin of the first coxa, and the second femur has a matching depression. The legs of males are longer than those of females, and bear many macrosetae.

Most *Araniella* are green or yellow to reddish in color when alive, similar to small species of *Araneus*. The color, except the black spots, washes out in alcohol. All species are about the same size and proportions (Figs. 1, 16).

Natural history. All species build a small web between leaves; the web may be horizontal. The spiders are active at daytime. The egg sac has a loose woollen appearance (Plate 1).[1]

Distribution. The known species are all Palearctic, except A. *displicata* which is Holarctic in distribution.

Misplaced species. Araniella geayi Caporiacco, 1954, Comm. Pontifica Acad. Sci., 16: 104 from Guyana has as a holotype a juvenile specimen belonging to the genus *Araneus* deposited in the Zoological Museum of the University of Florence, examined.

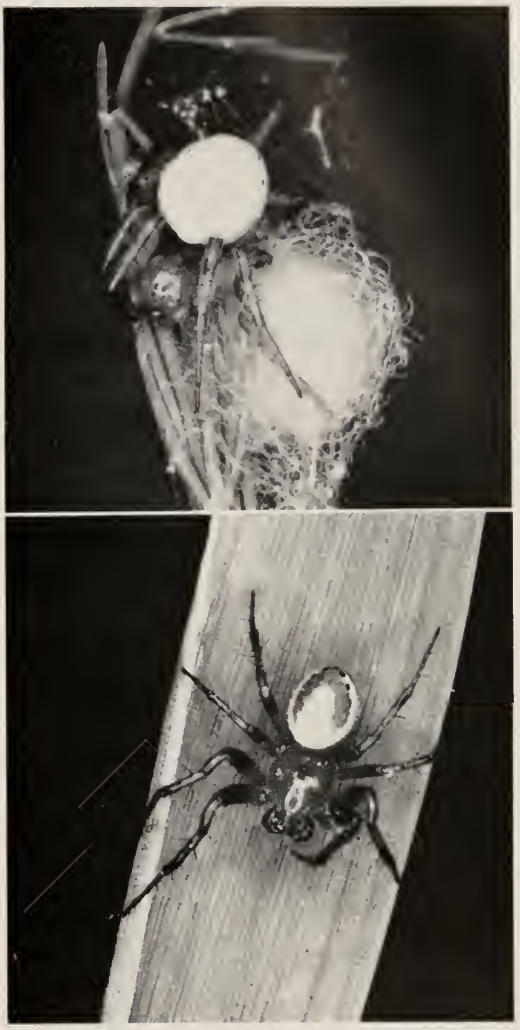

Plate 1. *Araniella displicata* (Hentz). Above, female with egg sac. Below, male. Both laboratory photographs, from Massachusetts.

[1] I had anticipated that *Araniella* males, which resemble males of *Nuctenea* species in lacking a cap on the embolus, would likewise be able to mate repeatedly. Therefore, it was with considerable interest that, after submitting my own manuscript, I received R. Blanke (1973, Neue Ergebnisse zum Sexualverhalten von *Araneus cucurbitinus*, Forma et Functio, 6: 279–290). Blanke did indeed observe differences between the behavior of A. *cucurbitinus* and that of *Araneus* species: The female approaches the male, the male taps the tarsi of females, and the male mates several times.

Key to Species of *Araniella*

1 Male, conductor of palpus with a distal lobe directed at and close to palpal patella (Figs. 37, 42); female with epigy-

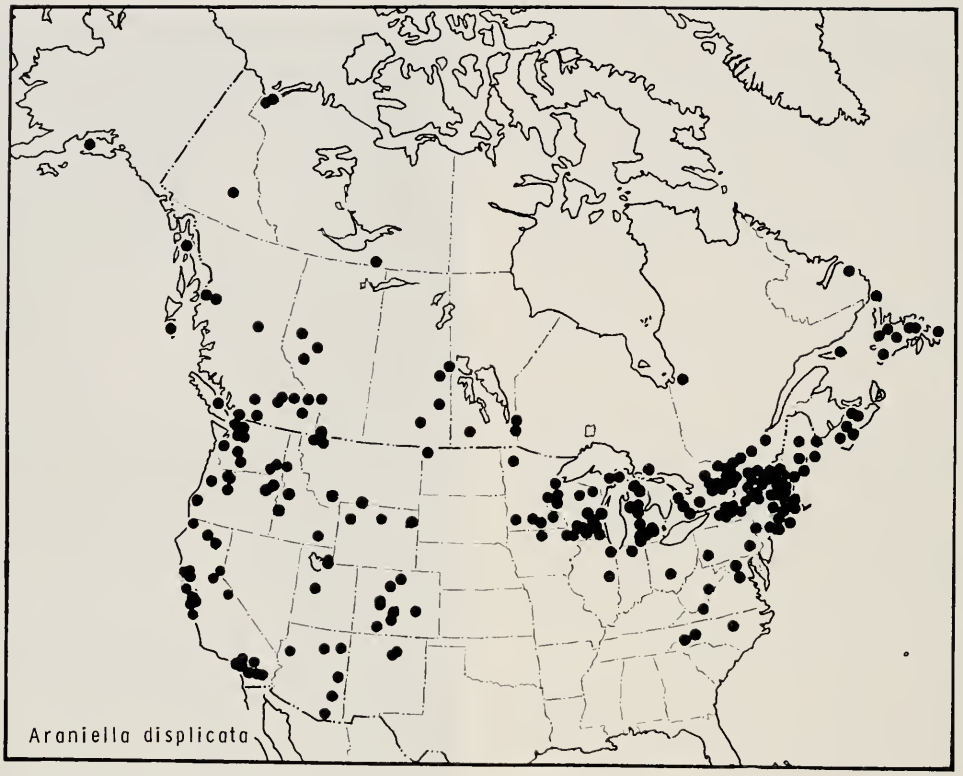

Map 1. North American distribution of *Araniella displicata* (Hentz).

num scape having proximal part widest, much wider than tip (Figs. 34, 40) 2

– Male palpal conductor without distal lobe toward patella (Figs. 18, 30); female epigynum with scape having parallel sides or proximal constriction (Figs. 10, 25) 3

2(1) Median apophysis with fin toward the embolus (Fig. 42); female with base of epigynum showing on each side of scape (Fig. 40); Europe ..... *alpica*

– Median apophysis without fin (Fig. 37); female epigynum base not showing in ventral view (Fig. 34); Eurasia ..... *inconspicua*

3(1) Conductor with a set-off piece which holds terminal apophysis and embolus (Figs. 22, 30, 31); scape of epigynum narrower or of equal width to part of base visible on each side of it (Figs. 23, 25); Eurasia, perhaps Arctic North America ..... *cucurbitina*

– Conductor without set-off piece holding terminal apophysis and embolus (Figs. 17, 18); scape of epigynum much wider than part of base showing on each side of it (Figs. 8–14); North America and Eurasia ..... *displicata*

Araniella displicata (Hentz)
Plate 1; Figures 1–21; Map 1

Epeira displicata Hentz, 1847, J. Boston Soc. Natur. Hist., 5: 476, pl. 31, fig. 17. Types from Alabama, May, Oct., destroyed. Emerton, 1884, Trans. Connecticut Acad. Sci., 6: 313, pl. 34, fig. 4, pl. 36, fig. 20, 342. Keyserling, 1893, Spinnen Amerikas, 4: 219, pl. 10, fig. 162, ♀. Emerton, 1902, Common Spiders, p. 172, fig. 405. Kaston, 1948, Bull. Connecticut Geol. Natur. Hist. Surv., 70: 258, fig. 806, ♀.

Epeira decipiens Fitch, 1856, Trans. New York Agric. Soc., 15: 451. Male specimen from New York, lost.

Epeira sexpunctata Keyserling, 1884, Verhandl. Zool. Bot. Gesell. Wien, 34: 530, pl. 13, fig. 28, ♀. Female type from North America in the Museum of Comparative Zoology, examined. Keyserling, 1892, Spinnen Amerikas, 4: 200, pl. 9, fig. 148.

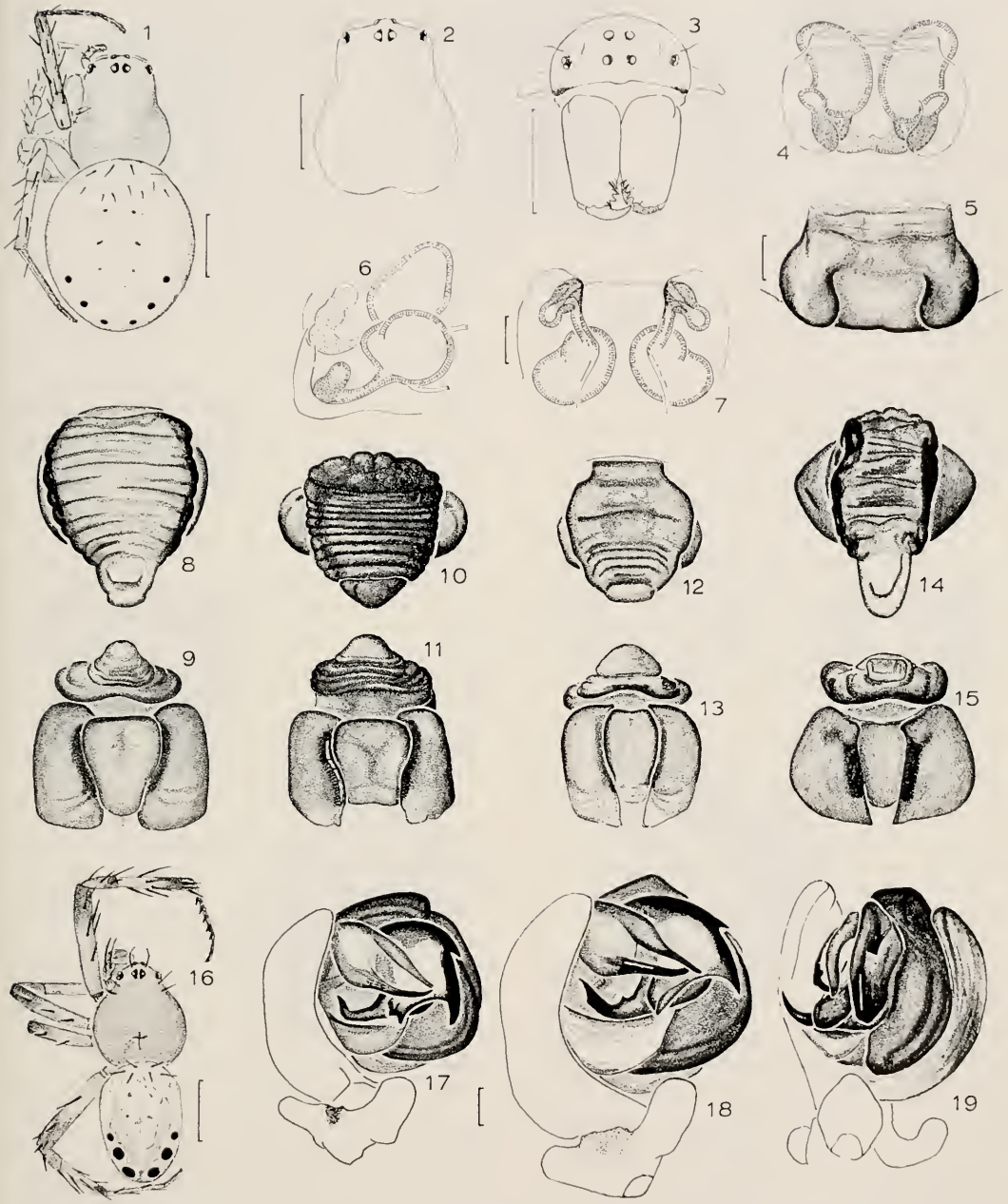

Figures 1–19. *Araniella displicata* (Hentz). 1–15. Female. 1. Dorsal view. 2. Carapace. 3. Eyes and chelicerae. 4. Internal genitalia with epigynum cleared. 5. Epigynum having scape torn off. 6–7. Internal genitalia. 6. Anterolateral. 7. Posterior. 8–15. Epigynum. 8, 10, 12, 14. Ventral view. 9, 11, 13, 15. Posterior view. 8, 9, 10, 11, 14, 15. (California.) 12, 13. (Oregon.) 16–19. Male. 16. Dorsal view. 17, 18. Left male palpus, mesal view. 19. Palpus, ventral view. 17. (Minnesota.) 18, 19. (Montana.)

Scale lines. 0.1 mm; Figs. 1–3, 16, 1 mm.

Epeira alba Keyserling, 1884, Verhandl. Zool. Bot. Gesell. Wien, 34: 530, pl. 13, fig. 20, ♀. Female type from Kentucky in the Museum of Comparative Zoology, examined.

Epeira cucurbitina, - McCook, 1893, American Spiders, 3: 150, pl. 3, figs. 1–3, pl. 4, fig. 6, ♀, ♂. Not *A. cucurbitina* (Clerck).

Araneus croaticus Kulczyński, 1905, Bull. Acad. Sci. Cracovie, 233, pl. 7, figs. 22, 30, ♀. Female holotype from Croatia in the Polish Academy of Sciences, Warsaw, examined. NEW SYNONYMY.

Aranea displicata, - Comstock, 1912, Spider Book, p. 494, figs. 524, 525, ♀, web. Wiehle, 1931 *in* Dahl, Tierwelt Deutschlands, 23: 109, figs. 167–170, ♀, ♂. Comstock, 1940, Spider Book, 2nd ed., p. 508, figs. 524, 525, ♀, web. Roewer, 1942, Katalog der Araneae, 1: 798.

Araniella displicata, - Chamberlin and Ivie, 1942, Bull. Univ. Utah, biol. ser., 32(13): 76.

Araniella displicata octopunctata Chamberlin and Ivie, 1942, Bull. Univ. Utah, biol. ser., 32(13): 76. Female holotype from Emigration Canyon, Wasatch Mts., Utah, in the American Museum of Natural History, paratype, examined.

Araneus displicatus, - Locket and Millidge, 1953, British Spiders, 2: 149, figs. 96b, 97c, 99c, 100c-e, ♀, ♂.

Araneus cucurbitinus displicatus, - Bonnet, 1955, Bibliographia Araneorum, 2: 478.

Note. It is of interest that this species described from Alabama is very rare at the present time in the Gulf states if present at all. Only a juvenile from Bankhead National Forest, Alabama, might be this species. Others collected by Archer in Alabama were *Araneus gadus* Levi that had been misidentified.

Description. Female from California. Carapace yellowish with eyes on black spots. Legs yellow. Dorsum of abdomen yellowish with three pairs of circular black spots on the posterior part (Fig. 1). Carapace smooth, almost without setae. There is no thoracic depression. Diameter of posterior median eyes 1.2 diameters of anterior medians; anterior laterals 0.8 diameters of anterior medians; posterior laterals subequal in size to anterior medians. Anterior median eyes 1.5 diameters apart, 3.2 from laterals. Posterior median eyes one diameter apart, three from laterals. The height of the clypeus is about 1.5 diameters of the anterior median eyes. The chelicerae, which are not very strong, have four teeth on the anterior margin, three on the posterior. The legs are relatively heavy, with many macrosetae. The abdomen is suboval, widest in the middle. Total length 5.3 mm. Carapace 2.5 mm long, 1.9 mm wide. First femur, 1.9 mm; patella and tibia, 2.4 mm; metatarsus, 1.4 mm; tarsus, 0.6 mm. Second patella and tibia, 2.2 mm; third, 1.3 mm; fourth, 2.2 mm.

Male from California. Coloration as in female, except legs tend to be banded or distal ends of leg articles darker. Carapace smooth with head region relatively high and a shallow thoracic depression, having two lines crossing each other at right angles (Fig. 16). Eyes are subequal in size. Anterior median eyes 1.7 diameters apart, two from laterals. Posterior median eyes their diameter apart, 2.5 from laterals. The height of the clypeus is 1.5 diameters of the anterior median eyes. Total length 4.0 mm. Carapace 1.8 mm long, 1.7 mm wide. First femur, 1.8 mm; patella and tibia, 2.3 mm; metatarsus, 1.3 mm; tarsus, 0.6 mm. Second patella and tibia, 2.0 mm; third, 1.2 mm; fourth, 1.9 mm.

Variation. Total length of females 4.8 to 7.2 mm. Carapace 2.0 to 2.7 mm long, 1.7 to 2.0 mm wide. Total length of males 4.0–5.0 mm. Carapace 2.0–2.4 mm long, 1.7–2.2 mm wide. The coloration is much more variable than the size; it is often greenish, reddish, brownish or yellowish on the abdomen. This pigment washes out, however, and in alcohol the abdomen is generally white.

Diagnosis. This is probably the only species of *Araniella* occurring in North America, although *A. cucurbitina* may occur in northern Canada and Alaska. *Araniella displicata* females can be separated by the wider and longer scape, which often hides the base of the epigynum; the widest part of the scape is generally toward its middle (Figs. 8–14). In posterior view the base is shorter, wider (Figs. 9, 11, 13, 15) than that of *A. cucurbitina.*

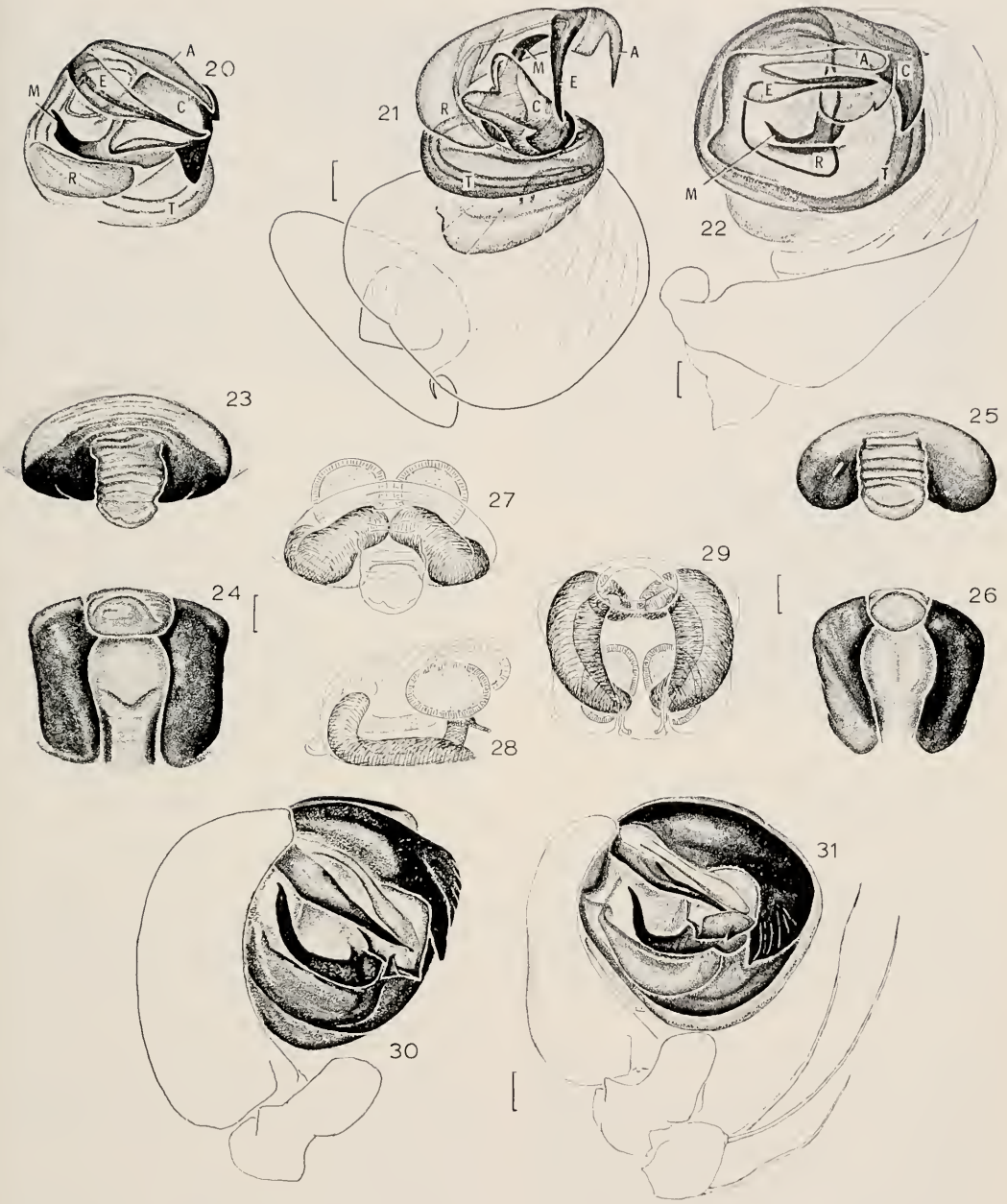

Figures 20–21. *Araniella displicata* (Hentz). 20. Left male palpus, ventral view without cymbium, cleared. 21. Palpus expanded.

Figures 22–31. *A. cucurbitina* (Clerck). 22. Male palpus, expanded. 23–26. Epigynum. 23, 25. Ventral. 24, 26. Posterior. 23, 24. (Taunus, Germany.) 25, 26. (Scotland.) 27–29. Epigynum cleared. 27. Ventral. 28. Lateral. 29. Posterior. 30, 31. Palpus, mesal. 30. (Poland.) 31. (Germany.)

Abbreviations. A, terminal apophysis; C, conductor; E, embolus; M, median apophysis; R, radix; T, tegulum.

Scale lines. 0.1 mm.

Males can readily be separated from *A. cucurbitina* and other species by the shape of the conductor, which holds the tip of the embolus and terminal apophysis (Figs. 17–21). That of *A. displicata* has several large teeth around its margin while a special lobe on the conductor of *A. cucurbitina* holds the tip of embolus and terminal apophysis (Figs. 22, 30, 31). The main sclerotized part of the conductor of *A. cucurbitina* has just one tip.

Habits. Males are mature from late spring until late summer, females until fall. The spider is found by sweeping meadows and low bushes. This species makes a relatively small orb web, often among the leaves of bushes or underneath a single large leaf.

Distribution. Europe, North America, from the Arctic to North Carolina, probably Alabama, and Arizona in the south; but apparently absent from the south-central states, southern Iowa, Nebraska to the Gulf (Map 1).

Araniella cucurbitina (Clerck) Figures 22–31

Araneus cucurbitinus Clerck, 1757, Aranei Svecici, p. 44, pl. 2, fig. 4, ♀. Clerck's specimens in the Natural History Museum of Stockholm, originally pinned and labeled by Thorell, not examined. Locket and Millidge, 1953, British Spiders, 2: 144, figs. 96a, 97b, 98a, 99a, ♀, ♂. Bonnet, 1955, Bibliographia Araneorum 2: 472 (in part).

Epeira proxima Kulczyński, 1885, Pamiet. Akad. Umiejet. Kraków, 11: 19, pl. 9, fig. 11. Male holotype from Kamchatka in the Polish Academy of Sciences, examined. NEW SYNONYMY.

Araneus cucurbitina opisthographa Kulczyński, 1905, Bull. Acad. Sci. Cracovie, p. 232, pl. 7, figs. 2, 20, 23, 26, ♀, ♂. Syntypes from numerous localities in Poland in the Polish Academy of Sciences, Warsaw, examined.

Aranea cucurbitina, - Wiehle, 1931, *in* Dahl, Tierwelt Deutschlands, 23: 106, figs. 161, 164, ♀, ♂. Roewer, 1942, Katalog der Araneae, 1: 785.

Aranea proxima, - Roewer, 1942, Katalog der Araneae, 1: 790.

Araneus proximus, - Bonnet, 1955, Bibliographia Araneorum, 2: 571.

Note. I could not find any consistent differences between specimens labeled *opisthographa* and others. Figure 30 was prepared from a syntype of *A. opisthographa.*

Diagnosis. The short, narrow scape with parallel sides which exposes most of the base of the epigynum in ventral view (Figs. 23–26) readily separates *A. cucurbitina* from other *Araniella* females. The more complex conductor with a distinct, separate lobe holding the tip of embolus and terminal apophysis (Figs. 22, 30, 31) distinguishes males (from other *Araniella* species).

Natural history. Very common in trees and bushes in Europe (see Wiehle, 1931).

Distribution. Common and widespread in Eurasia from Great Britain to Kamchatka (Wiehle, 1931; Locket and Millidge, 1953). The species is believed not to occur in North America. The single record is probably the result of comparing specimens and misplacing them, or perhaps the species may occur in poorly collected Alaska and northern Canada. The female was from Fort Smith, Northwest Territory, 20.VI. 1967 (R. Leech), in white poplar.

Araniella inconspicua (Simon) Figures 32–37

Epeira inconspicua Simon, 1874, Arachnides de France, 1: 84. Female type in the Muséum National d'Histoire Naturelle, Paris, not examined.

Aranea inconspicua, - Wiehle, 1931, *in* Dahl, Tierwelt Deutschlands, 23: 112; figs. 174–176, ♀, ♂. Roewer, 1942, Katalog der Araneae, 1: 787.

Araneus inconspicuus, - Locket and Millidge, 1953, British Spiders, 2: 146; figs. 97a, 98c, 99d, 100b, ♀, ♂. Bonnet, 1955, Bibliographia Araneorum, 2: 521.

Diagnosis. The abdomen usually lacks the black spots. The female has a triangular wrinkled scape that completely hides the base in ventral view (Fig. 34); in posterior view, the median groove is shorter (Figs. 35, 36) than that of *A. alpica.* The palpus lacks the distally directed fin of

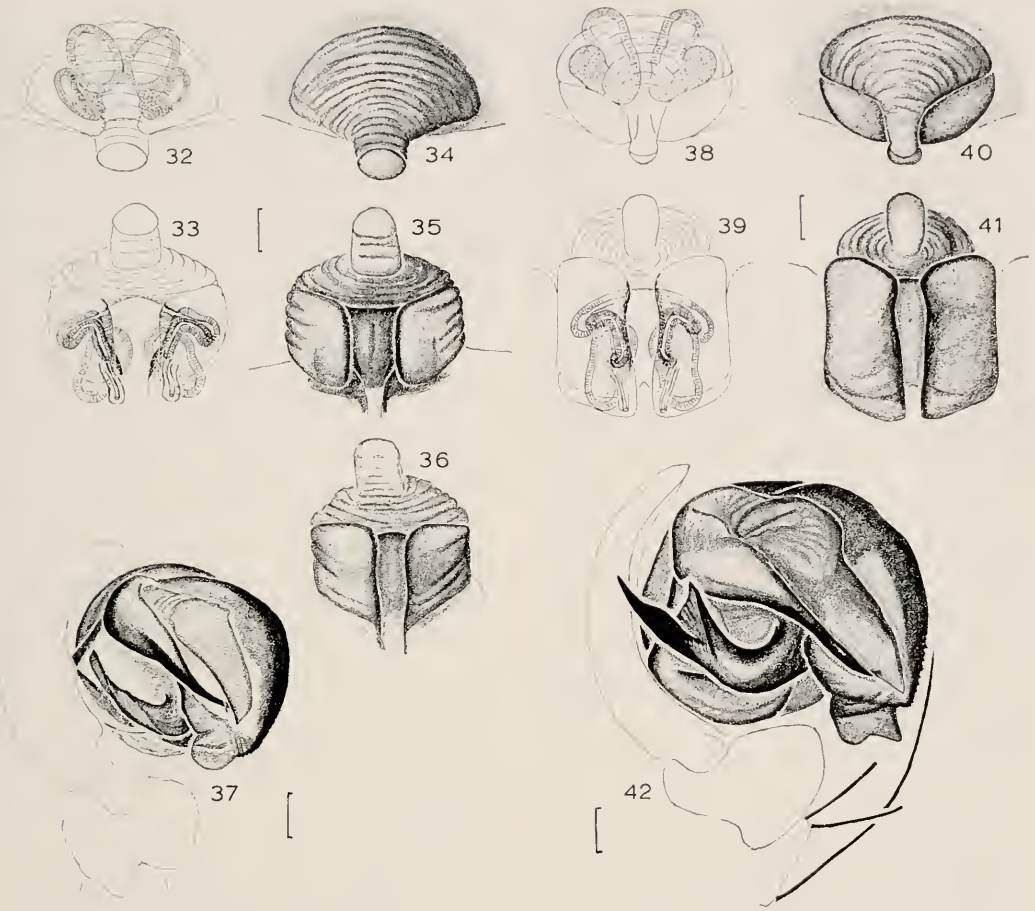

Figures 32–37. *Araniella inconspicua* (Simon). 32–36. Epigynum. 32. Ventral, cleared. 33. Posterior, cleared. 34. Ventral. 35, 36. Posterior. 32–35. (France.) 36. (England.) 37. Left male palpus, mesal.

Figures 38–42. *A. alpica* (L. Koch). 38–41. Epigynum. 38. Ventral, cleared. 39. Posterior, cleared. 40. Ventral. 41. Posterior. 42. Male palpus, mesal.

Scale lines. 0.1 mm.

the median apophysis (Fig. 37) present in *A. alpica*. While Continental specimens are readily separated from *A. alpica*, this is not true for those of the British Isles. Perhaps as a result of a recent introduction of *A. alpica* they hybridize.

Natural history. Found in trees and bushes at low elevations (Wiehle, 1931).

Distribution. Europe from Great Britain, northern Spain to Macedonia (Wiehle, 1931). There are also references to *A. inconspicua* occurring in eastern Asia (Bonnet, 1955).

Araniella alpica (L. Koch)
Figures 38–42

Epeira alpica L. Koch, 1869, Z. Ferdinandeum Tirol., (3)14: 173. Specimens from Tyrol and other localities in the Koch collection of the British Museum (Natural History); presumably types but not examined.

Aranea alpica, - Wiehle, 1931, *in* Dahl, Tierwelt Deutschlands, 23: 110, figs. 171–173, ♀, ♂. Roewer, 1942, Katalog der Araneae, 1: 781.

Araneus alpicus, - Locket and Millidge, 1953, British Spiders, 2: 149, figs. 96c, 98d, 99b, 100a, ♀, ♂. Bonnet, 1955, Bibliographia Araneorum, 2: 428.

Araniella alpica, - Archer, 1951, Natur. Hist. Misc., 84: 3, fig. 4, ♂.

Diagnosis. In ventral view the base of the epigynum shows as two bulges posterior and lateral to the scape (Fig. 40). In posterior view the central area is much longer (Fig. 41) than that of *A. inconspicua*. The median apophysis has a distally directed fin (Fig. 42) and the terminal apophysis is wider than that of other species. The abdomen has at most four black spots (see note under *A. inconspicua* diagnosis).

Natural history. This species is found in European mountains above 300 m to krummholz (1800 m in the alps) and is limited to fir and spruce. Males are mature until August (Wiehle, 1931).

Distribution. Great Britain (Locket and Millidge, 1953), Scandinavia, Central Europe (Wiehle, 1931), Balkans (Bonnet, 1955).

Nuctenea Simon

Nuctenea Simon, 1864, Histoire Naturelle des Araignées, p. 261. New subgenus of *Epeira* with the type species *Epeira umbratica* designated by Bonnet, 1950, Bibliographia Araneorum, 2: 3118. The name is of feminine gender.

Cyphepeira Archer, 1951, Natur. Hist. Misc., Chicago, 84: 4. New subgenus of *Epeira* with the type species by original designation *Epeira* (*Cyphepeira*) *silvicultrix* C. L. Koch. The name is of feminine gender.

Note. The species included here had been placed by Wiehle (1931) in groups 4 and 5 of *Aranea*, by Locket and Millidge (1953) in groups 3 and 5 of *Araneus*. Archer (1951), following F. P.-Cambridge (1903), considered the group a distinct genus, *Epeira*, with *Araneus cornutus* (Clerck) the type of the genus. But this type designation is an error as *Epeira* is an objective synonym of *Aranea* and a subjective synonym of *Araneus*, having *Epeira diadematа* as type designated by Latreille, 1810 (Levi, 1971).

In considering the group included here as distinct, I am following older authors and also Archer. In 1959 Yaginuma and Archer included the species in *Cyphepeira*, as did Prószyński and Staręga (1971). Wiehle (1927), discussing orb-web building, included *Epeira umbratica*, *E. sclopetaria*, *E. cornuta* and *E. patagiata* in a group making an *umbraticus*-type web. Gerhardt (1926) separated the group because of different mating behavior: males can mate three or four times with each palpus. *Araneus* species can mate only once with each palpus. Also, the female assumes a different mating position, approaching and hanging opposite the male, with cephalothorax lowered and abdomen raised, and pulls in the male on threads. The male will court a female that does not have an orb-web, and in mating the male's body is not as close to the female's as in *Araneus*. Males do not refill their palpi with sperm immediately after mating, as males of *Araneus* have been observed to do (observations on *N. umbratica*, *N. cornuta*, *N. sclopetaria*).

Description. All species are gray to brown, none brightly colored (Plate 2). The abdomen is dorsoventrally flattened, oval in outline, widest in the middle, with a folium on the dorsum (Figs. 97–109). The cardiac mark is usually dark. The venter of the abdomen is black with a pair of comma-shaped or bracket-shaped white marks (Figs. 98, 99, 102, 104).

The genitalia are heavily sclerotized. The opening of the epigynum is hard to find and the connecting duct difficult to make out, even in epigyna digested with 10 percent NaOH. The openings of the *N. umbratica* epigynum are anterior on the base (Figs. 45, 46), those of other species, posterior in a groove (Figs. 71, 72, 81, 82, 85, 86).

The palpus has a simple conductor (C in Figs. 58–62), unlike that of *Araniella* (Figs.

20, 22) and even simpler than that of *Araneus*. A complex terminal apophysis shields the embolus from above (A in Figs. 58–62) and is connected to the bulb by distal hematodocha. The distal hematodocha may be sclerotized, and reveals its origin by the presence of folds and grooves. Despite sclerotization, parts of it expand (Figs. 58, 61, 62). The embolus lacks a cap and is a relatively simple structure. The tiny structure visible on the opening of the embolus (Figs. 119, 122, 123, 125) is found only in mated males and is presumably dried up sperm fluid. The median apophysis is on the mesal side and may project (except in *N. umbratica*). In most species it is biforked (Figs. 61, 62, 110–117, 126–129). It is a simple projection in *N. silvicultrix* (Figs. 55, 60) and a lancet-shaped, appressed sclerite in *N. umbratica* (M in Fig. 58). Males have a hook on the distal margin of the first coxa and a corresponding depression on the second femur; also the second tibia may be swollen and bear macrosetae.

Diagnosis. In the Americas the species of *Nuctenea* can be confused only with those of *Metazygia*. However, the carapace of *Nuctenea* is setose (Figs. 105–109), that of *Metazygia* lacks setae. Unlike most species of *Araneus, Nuctenea* species have the abdomen dorsoventrally flattened, oval in outline, and widest in the middle with a dorsal folium. The venter is black between genital furrow and spinnerets, enclosing a white, comma-shaped mark on each side (Figs. 97–109). The cardiac mark on the abdomen, if present, is dark, not light as it often is in *Araneus*. The only *Araneus* species that have the abdomen oval are marked differently. More important, *Nuctenea* genitalia are much more sclerotized, and the embolus lacks a cap. Externally the epigynum base seems more complex (Figs. 43–46, 50–54, 71–76, 81–92) than in *Araneus* and *Metazygia*. The *Metazygia* epigynum lacks the scape present in *Nuctenea*; in its place there is a ventrally extended, laterally flattened lobe with the opening on each side of the base. The palpus of *Metazygia* has a terminal apophysis with a large proximal part and is very different from that of *Nuctenea*. The palpal femur lacks the basal ventral tooth present in *Araneus* and *Araniella* but has a corresponding tooth on the side of the endite.

Natural history. Nuctenea species, at least those found in North America, may be mature the year around; adult males can be found at all seasons. In contrast, in all *Araneus* species observed in the temperate region, mature males can be found only during a short period of the year. Males, as well as females, can mate numerous times; species belonging to *Araneus*, to judge by the work of U. Gerhardt (Levi, in preparation), can mate only twice, once with each palpus, perhaps three times if the mating was unsuccessful. No doubt these differences in habits are a result of the cap, which is found on the embolus of *Araneus*, and is absent in *Nuctenea*.

The species all build in the evening and are nocturnal. The webs of all the species have few radii (fewer than 20) with few viscous threads, widely separated; those of adult *N. umbratica* are separated by 10 mm or more. Thus the web, especially in wind, gives the impression of being a flimsy structure. The center is small with rough threads and few scaffolding threads. Although usually made nearly vertical, the web may be horizontal (*N. cornuta*, Plate 2). All species make a retreat or sit near the web during the day, in the web at night.

In the northeastern United States the species are commonly found on houses. Comstock (1912, 1940) refers to these spiders as the House Araneas, J. H. Emerton calls them House Epeiras. But, as Comstock points out, they are often found in suitable habitats far away from houses.

In America the species have a wide distribution, *N. cornuta* from the Arctic to the tropics. Only *N. sclopetaria* appears introduced; the other two species,

though they are commonly found on buildings and in trash (Maps 2–4), as introduced species often are, have a continuous Holarctic distribution.

Misplaced species. Epeira carolinalis Archer, 1951, Amer. Mus. Novitates, No. 1487: 40, fig. 57, ♀, may belong to the genus *Metazygia*. The male is not known.

KEY TO SPECIES OF *NUCTENEA*

1 Male with median apophysis of palpus split into two branches (Figs. 110–117); female with scape of epigynum originating at anterior of base (Figs. 71–91) 3
– Male with median apophysis of palpus not split into two branches (Figs. 47, 48, 55, 56, 58, 60); female with scape originating in center of base or lacking scape (Figs. 43, 51); Eurasia, North Africa 2
2(1) Terminal apophysis of male palpus a massive shield (Figs. 48, 49, 58); median apophysis spindle-shaped (Figs. 47, 58); epigynum with triangular scape pointing posteriorly (Fig. 43); Europe and North Africa ..... *umbratica*
– Terminal apophysis of palpus with teeth (Figs. 55, 60); median apophysis a knob (Figs. 55, 60); epigynum with cone-shaped base drawn out anteriorly (Figs. 51, 53); northern, Central Europe to Siberia ..... *silvicultrix*
3(1) Males 4
– Females 7
4(3) Terminal apophysis a prong with a narrow neck (Figs. 61, 110); embolus with tip hidden by a lamella (Figs. 61, 110, 118, 119), probably cosmopolitan ..... *cornuta*
– Terminal apophysis a sclerotized lobe without neck (Figs. 112–117); embolus cylindrical (Figs. 112, 114, 116) 5
5(4) Embolus with a distal, set-off finger (Fig. 116); Central Europe to Iran ..... *ixobola*
– Embolus cylindrical, pointed at end but without set-off finger (Figs. 112, 114, 120–125) 6
6(5) Median apophysis massive with the two prongs about of equal width in ventral view (Fig. 113); conductor leaning toward median apophysis (Fig. 113); Holarctic ..... *patagiata*
– Median apophysis more slender with "upper" prong narrower than "lower" one (Fig. 115); conductor bending away from median apophysis (Fig. 115); Holarctic ..... *sclopetaria*
7(3) Epigynal base posteriorly corrugated (Fig. 84); scape widest near tip with a narrow neck (Figs. 78–81); Holarctic ..... *patagiata*
– Epigynal base not corrugated (Figs. 74, 76, 88, 92) 8
8(7) Epigynum covered by a lamella on each side (Figs. 65–76); base with a ventral, anterolateral fold and swollen posteriorly (Figs. 63, 65, 67, 69, 73, 75); probably cosmopolitan ..... *cornuta*
– Epigynal lamellae not visible in ventral view or hidden behind base (Figs. 85–92); base without anterolateral fold and posterior swelling 9
9(8) Anterior part of scape framed by a lip of the base (Fig. 87); Holarctic ..... *sclopetaria*
– Anterior part of scape not framed by lips from base, base with anterolateral pockets (Fig. 91); Central Europe to Iran ..... *ixobola*

Nuctenea umbratica (Clerck)
Figures 43–49, 58, 59, 93, 99, 105

Araneus umbraticus Clerck, 1757, Aranei Svecici, p. 31, pl. 1, fig. 7, ♀. Clerck's specimens from Sweden in the Museum of Natural History, Stockholm, labeled by Thorell; not examined. Locket and Millidge, 1953, British Spiders, 2: 139, fig. 92, ♀, ♂. Bonnet, 1955, Bibliographia Araneorum, 2: 621.

Aranea sexpunctata Linnaeus, 1758, Systema Naturae, 10 ed., p. 622. Type specimens believed lost. Wiehle, 1931, *in* Dahl, Tierwelt Deutschlands, 23: 93, figs. 138–141, ♀, ♂. Roewer, 1942, Katalog der Araneae, 1: 791.

Epeira (*Nuctenea*) *umbratica*, - Simon, 1864, Histoire Naturelles des Araignées, p. 261.

Epeira umbratica, - Nielsen, 1932, The Biology of Spiders, Copenhagen, vol. 2, figs. 299–304, web, egg sac, retreat.

Chinestela umbratica, - Archer, 1951, Natur. Hist. Misc., Chicago, 84. Prószyński and Staręga, 1971, Katalog Fauny Polski, 16: 85.

Description. Female from England. Carapace dark brown. Legs dark brown, with light bands. Dorsum of abdomen with usual dark brown pattern. Venter black with two lateral white marks. Diameter of posterior median eyes 0.9 diameters of anterior medians, laterals 0.8 diameters of anterior medians. Anterior median eyes their diameter apart, posterior medians slightly more than their diameter apart. Height of clypeus equals about the diameter of the anterior median eyes. The abdo-

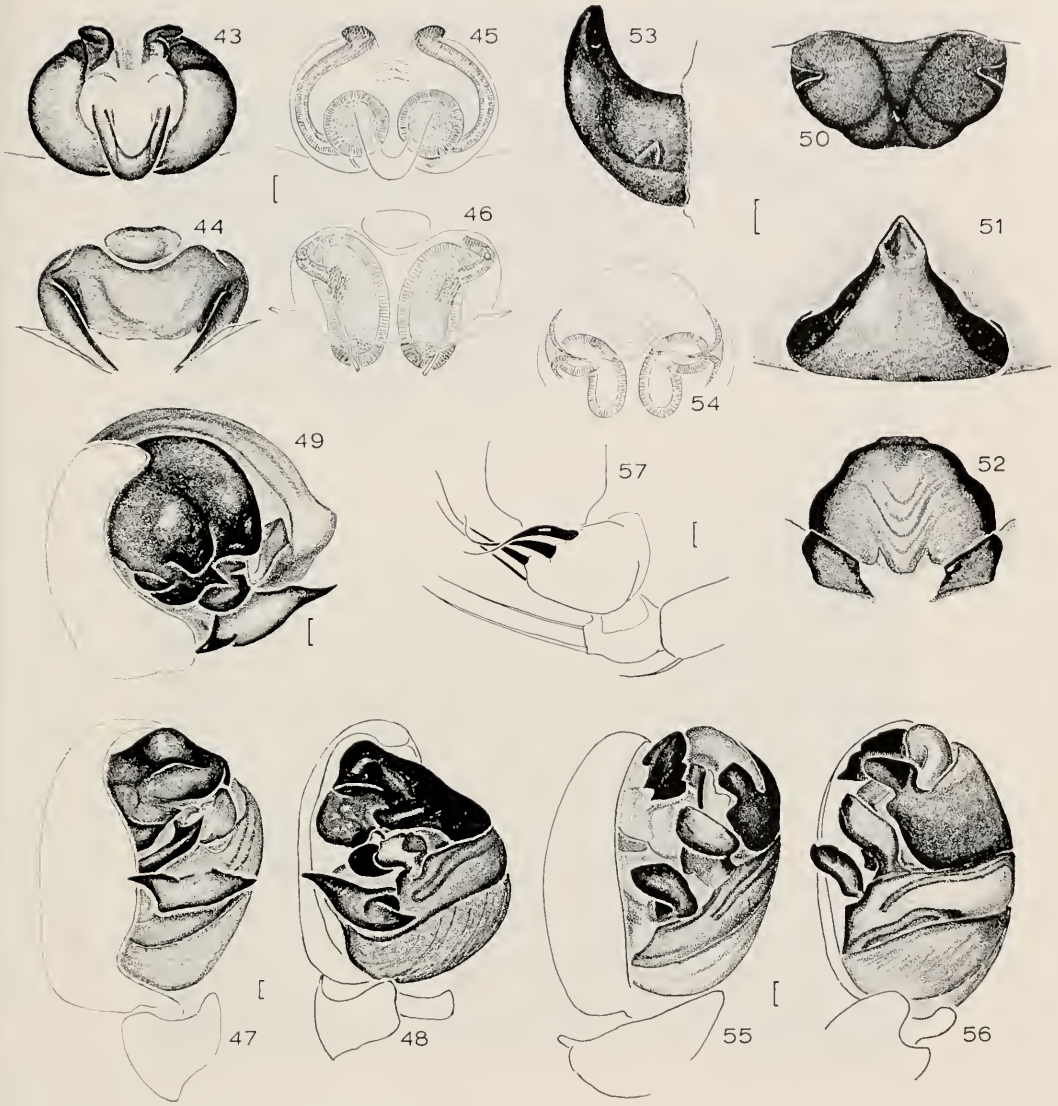

Figures 43–49. *Nuctenea umbratica* (Clerck). 43–46. Epigynum. 43. Ventral. 44. Posterior. 45. Ventral, cleared. 46. Posterior, cleared. 47–49. Left male palpus. 47. Mesal. 48. Ventral. 49. Apical.

Figures 50–57. *N. silvicultrix* (C. L. Koch). 50–54. Epigynum. 50. Anterior. 51. Ventral. 52. Posterior. 53. Lateral 54. Posterior, cleared 55–57. Male palpus. 55. Mesal. 56. Ventral. 57. Tibial macrosetae.

Scale lines. 0.1 mm.

men is much flattened. Total length 12 mm. Carapace 4.7 mm long, 4.1 mm wide. First femur, 3.9 mm; patella and tibia, 5.8 mm; metatarsus, 3.6 mm; tarsus, 1.8 mm. Second patella and tibia, 5.3 mm; third, 3.0 mm; fourth, 4.6 mm.

Male from England. Coloration as in female, with abdominal pattern more distinct. Diameter of posterior median eyes 0.8 diameters of anteriors. Laterals very slightly smaller than posterior median eyes. Anterior median eyes their diameter apart,

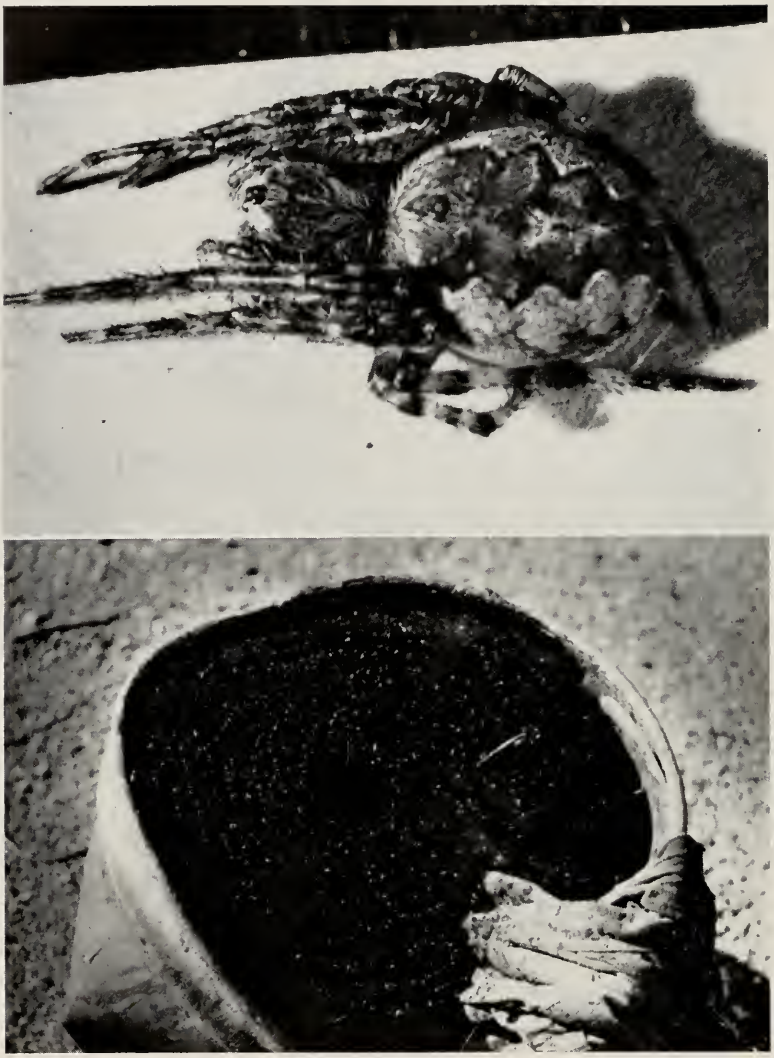

Plate 2. *Nuctenea cornuta* (Clerck). Above, female (Wisconsin). Horizontal web with flies caught (Minnesota).

posterior medians their diameter apart. The height of the clypeus is slightly less than the diameter of the anterior median eyes. Total length 8 mm. Carapace 4.0 mm long, 3.6 mm wide. First femur, 5.2 mm; patella and tibia, 7.3 mm; metatarsus, 5.3 mm; tarsus, 2.0 mm. Second patella and tibia, 5.9 mm; third, 3.0 mm; fourth, 4.7 mm.

Diagnosis. Nuctenea umbratica is readily separated from the other species of *Nuctenea* by being flatter (Figs. 93, 105), and by the distinct genitalia (Figs. 43–48). The openings of the epigynum, unlike those of other species, are anterior on the base (Figs. 45, 46) and the median apophysis is spindle-shaped (Figs. 47, 48, 58).

Natural history. Nuctenea umbratica has its retreat in crevices under bark, between

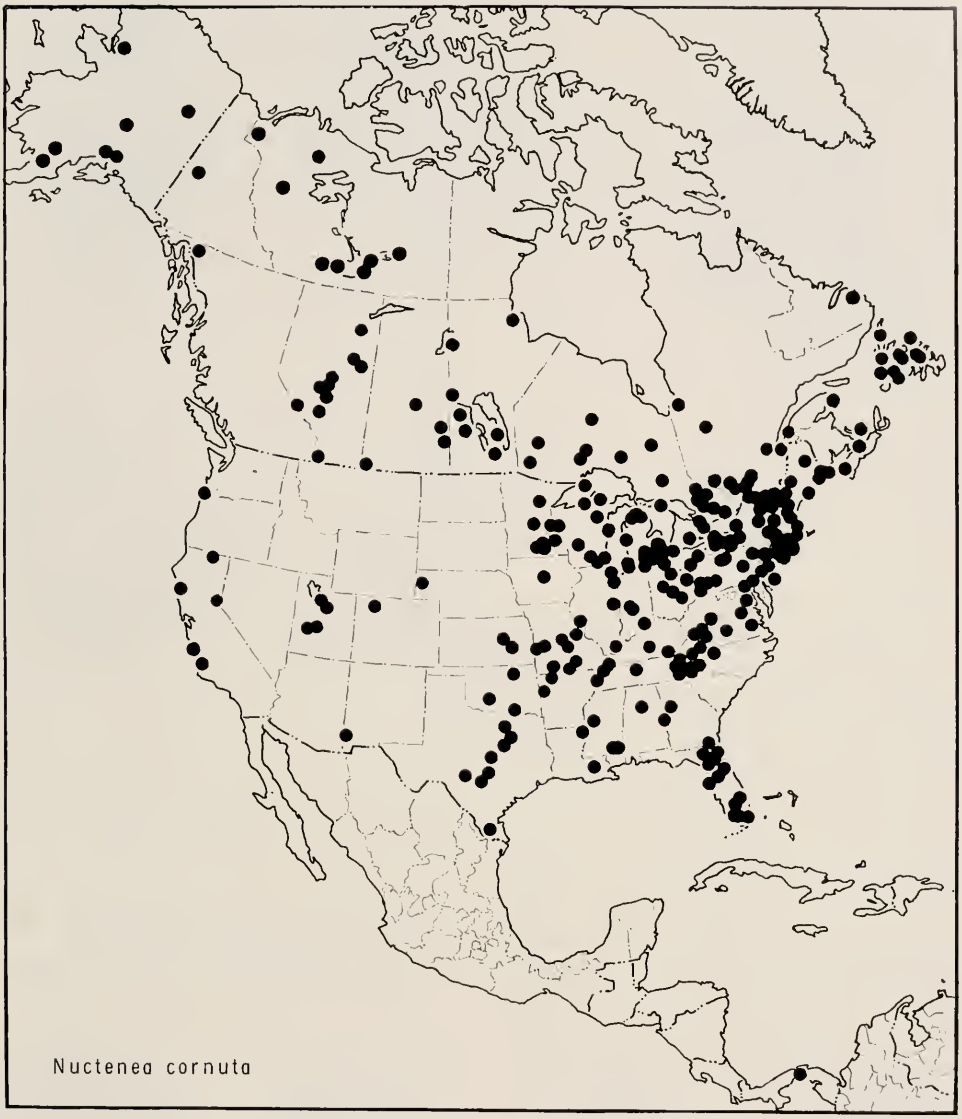

Map 2. North American distribution of *Nuctenea cornuta* (Clerck).

planks, in masonry, in barns, houses and greenhouses, up to 820 m in the Alps, but in southern Switzerland to 1200 m (Wiehle, 1931). Mature females can be found at all seasons, males from June until October. The eggs are laid in a flattened ball surrounded by loose, woolly silk.

The web is more eccentric than that of *N. patagiata*, with the center closest to the retreat. The viscous threads may span 70 cm and there are about 20 radii. There is a line to the retreat. The animal is strictly nocturnal (Wiehle, 1927, 1931). Mating has been described by Gerhardt, 1926.

Distribution. Nuctenea umbratica is only found in Europe and North Africa.

Nuctenea silvicultrix (C. L. Koch), new combination
Figures 50–57, 60, 106

Epeira silvicultrix C. L. Koch, 1845, Die Arachniden, 11: 131, pl. 932, 933, ♀, ♂. In the Berlin Museum are specimens from the L. Koch collection, presumably from Nürnberg, but no specimens that can readily be interpreted as types of C. L. Koch. The British Museum (Natural History) has specimens from Nürnberg belonging to the L. Koch collection and presumably the types. They were not examined.
Aranea silvicultrix Wiehle, 1931, *in* Dahl, Tierwelt Deutschlands, 23: 96, figs. 142–145, ♀, ♂. Roewer, 1942. Katalog der Araneae, 1: 792.
Araneus silvicultor, - Bonnet, 1955, Bibliographia Araneorum, 2: 598.
Epeira (*Cyphepeira*) *silvicultrix*, - Archer, 1951, Natur. Hist. Misc., Chicago, 84: 4.
Cyphepeira silvicultrix, - Yaginuma and Archer, 1959, Acta Arachnol., 16: 41, fig. 12, ♂. Prószyński and Staręga, 1971, Katalog Fauny Polski, 16: 85.

Description. Female from Schönhaid [near Neustadt, Bavaria]. Carapace red-brown, head lighter, with a double, median, longitudinal darker line. White setae in the head region. The legs are indistinctly banded with narrow, light bands. The dorsum of abdomen has a black folium outlined by white. The venter is black with a white mark on each side. The diameter of the posterior median eyes is 0.8 diameters of anterior medians, laterals about 0.6 diameters. The anterior median eyes are about their diameter apart; the posterior medians slightly less than one diameter. The ocular quadrangle is slightly longer than wide, much narrower behind than in front. The clypeus slants back and its height is about equal to or slightly less than the diameter of anterior median eyes. The opening of the epigynum appears to be on the side of the base and is quite difficult to see. Total length 7.0 mm. Carapace 3.1 mm long, 2.8 mm wide. First femur, 3.0 mm; patella and tibia, 3.9 mm; metatarsus, 2.7 mm; tarsus, 0.9 mm. Second patella and tibia, 3.6 mm; third, 2.1 mm; fourth, 3.3 mm.

Male from Erlangen, Bavaria. Coloration as in female. There is a shallow, round thoracic depression. Posterior and anterior median eyes subequal in size, laterals 0.8 diameters of medians. The anterior median eyes are one diameter apart; posterior medians also one diameter apart. The height of the clypeus equals slightly less than the diameter of the anterior median eyes. Total length, 5.8 mm. Carapace 3.2 mm long, 2.6 mm wide. First femur, 3.8 mm; patella and tibia, 5.0 mm; metatarsus, 3.7 mm; tarsus, 1.5 mm. Second patella and tibia, 4.0 mm; third, 2.3 mm; fourth, 3.4 mm.

Diagnosis. The epigynum is triangular, anteriorly extended (Figs. 50–54); the terminal apophysis (Figs. 55, 60) and strong setae on the palpal tibia (Fig. 57) separate this species from other *Nuctenea.*

Natural history. In northern Bavaria the species is found among lichens on stunted pines growing on infertile, moist ground; it uses crevices as retreats. Mature males are collected in April, May and again in July and August. The web is similar to that of *N. umbratica* (Wiehle, 1931).

Distribution. Norway, Finland, Germany, Switzerland to Balkans, Ural Mountains and Turkmen (Bonnet, 1955).

Nuctenea cornuta (Clerck), new combination, Furrow Spider
Plate 2; Figures 61–76, 94, 97–98, 110–111, 118–119, 126; Map 2*

Araneus cornutus Clerck, 1757, Aranei Svecici, p. 39, pl. 1, fig. 11, ♀. Female types from Sweden lost. Locket and Millidge, 1953, British Spiders, 2: 134, figs. 88a, 89b, 90c, ♀, ♂. Bonnet, 1955, Bibliographia Araneorum, 2: 463.
Aranea foliata Fourcroy, 1785, Entomologia Parisiensis, 533. Type specimen from Paris, France,

* Correction, July 1974. K. Thaler recently found that what has been called *Araneus cornutus* in Europe in fact represents two species, a northern one and a southern one (Zool. Anz., in press). The American specimens are all like the northern European *N. cornuta.* I have examined specimens sent by K. Thaler and agree with his conclusions. Figures 63–66 of this paper thus do not belong to *N. cornuta.*

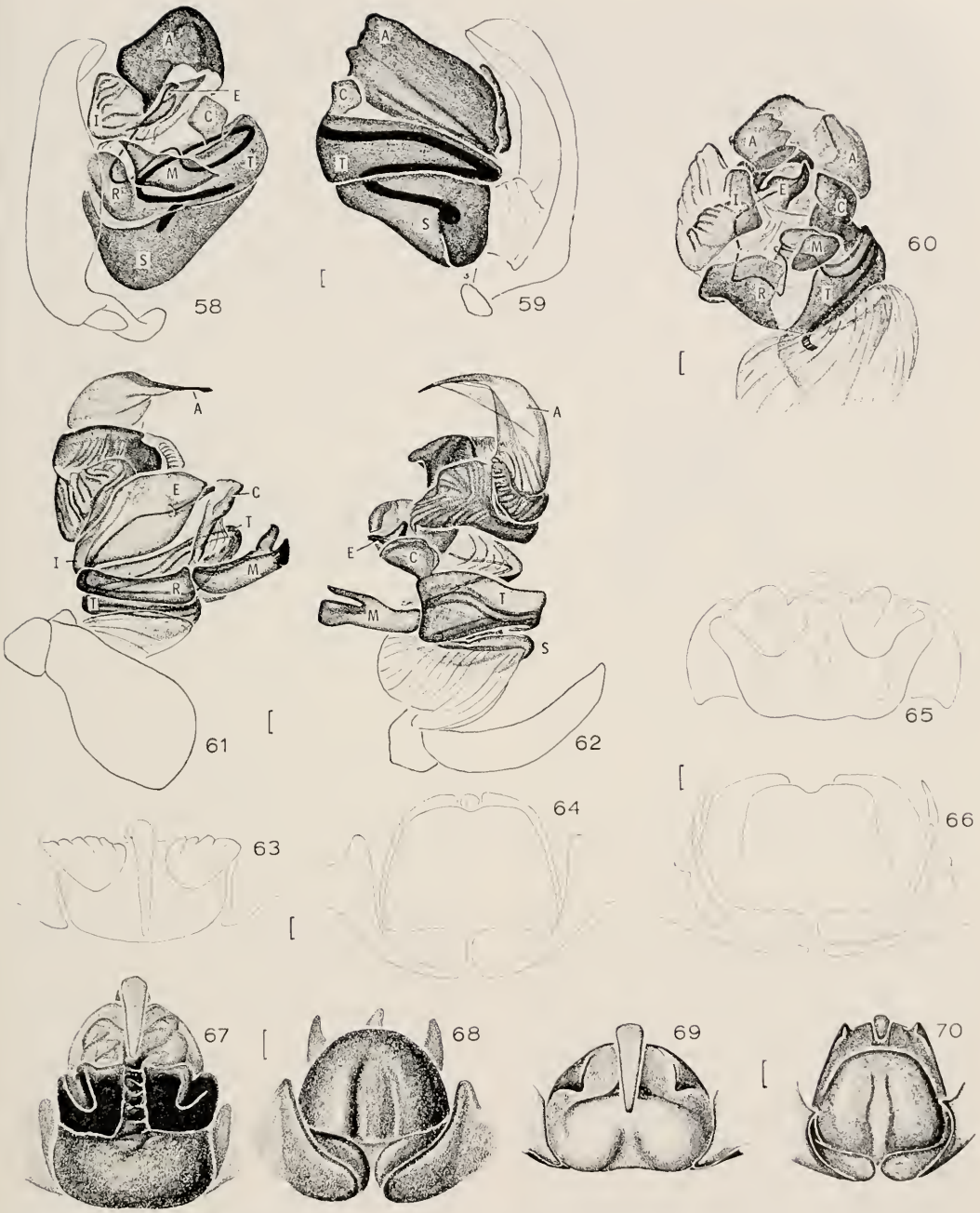

Figures 58–62. *Nuctenea* expanded left male palpus. 58, 59. *N. umbratica* (Clerck). 60. *N. silvicultrix* (C. L. Koch). 61, 62. *N. cornuta* (Clerck).

Figures 63–70. *N. cornuta* (Clerck), epigynum, variation. 63, 65, 67, 69. Ventral. 64, 66, 68, 70. Posterior. 63–66. (Burgenland, Austria.) 67, 68. (Kamtchatka.) 69, 70. (Poland.)

Abbreviations. A, terminal apophysis; C, conductor; E, embolus; I, stipes; M, median apophysis; R, radix; S, subtegulum; T, tegulum.

Scale lines. 0.1 mm.

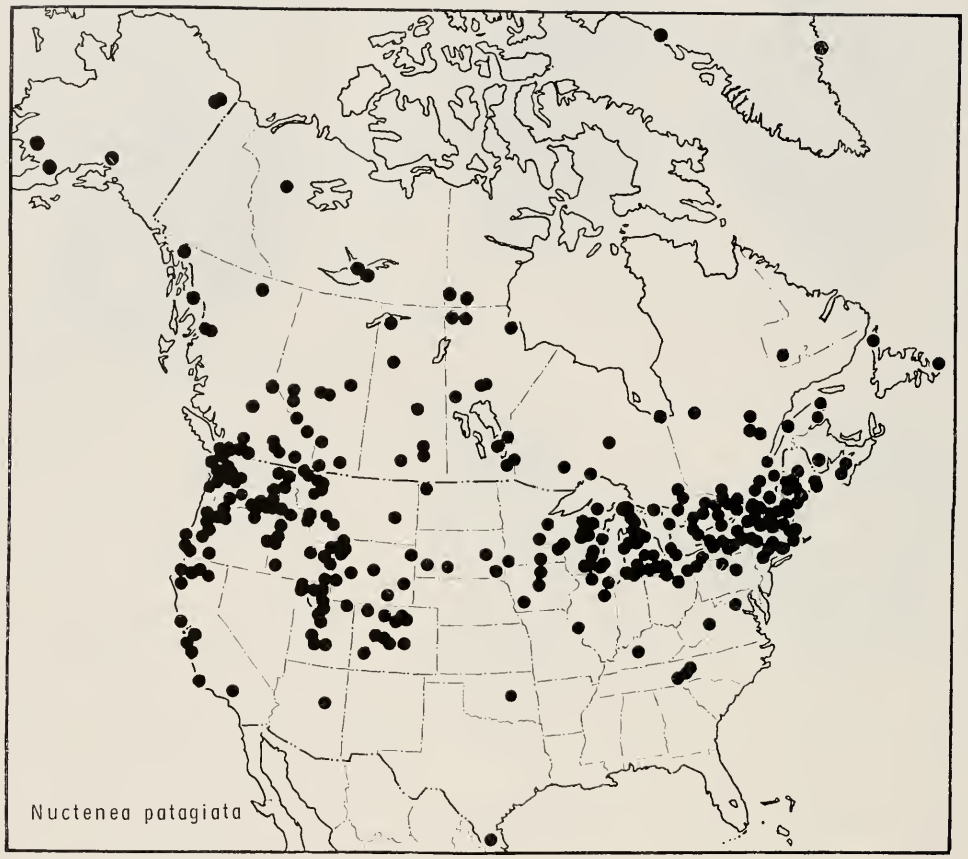

Map 3. North American distribution of *Nuctenea patagiata* (Clerck).

believed lost. Wiehle, 1931, *in* Dahl, Tierwelt Deutschlands, 23: 86, figs. 124–127, ♀, ♂. Roewer, 1942, Katalog der Araneae, 1: 800.

?*Epeira frondosa* Walckenaer, 1841, Histoire Naturelle des Insectes, Aptères 2: 65. The type is Abbot's manuscript illustration, fig. 326, from Georgia in the British Museum, Natural History, copy in the Museum of Comparative Zoology, examined.

Epeira strix Hentz, 1847, J. Boston Natur. Hist. Soc., 5: 473, pl. 31, fig. 5, ♀. Type specimens from Pennsylvania and Alabama destroyed.

Epeira vicaria Kulczyński, 1885, Pam Akad. Umiej. Kraków, 11: 5. Female holotype from Kamchatka in the Polish Academy of Sciences, examined.

Aranea frondosa, - Comstock, 1912, Spider Book, p. 487, figs. 104–106, 128, 186, 194, 509, 513–516, ♀, ♂, web; 1940, *op. cit.*, rev. ed., p. 501, figs. 104–106, 128, 186, 194, 509, 513–516, ♀, ♂, web.

Epeira cornuta, - Nielsen, 1932, The Biology of Spiders, Copenhagen, vol. 2, figs. 289, 290, retreat.

Epeira foliata, - Kaston, 1948, Connecticut Geol. Natur. Hist. Surv. Bull., 70: 254, figs. 787, 803, 812, 2043, ♀, ♂, web.

Cyphepeira cornuta, - Yaginuma and Archer, 1969, Acta Arachnol., 16: 41. Prószyński and Staręga, 1971, Katalog Fauny Polski, 16: 82.

Note. Figures 67, 68 were prepared from the holotype of *A. vicaria.*

Variation. Total length of females 6.5–14.0 mm. Carapace 2.4–5.0 mm long, 1.9–4.5 mm wide; first patella and tibia, 2.6–5.8 mm long. The total length of males 4.7–8.5 mm. Carapace 2.1–4.2 mm long, 1.8–3.5 mm wide; first patella and tibia 3.0–6.0 mm. The smallest American speci-

mens come from Alaska, the largest from the area of New England to Texas.

Diagnosis. The two anterior lateral lobes of the base of the epigynum are bent over and face posteriorly (Figs. 63, 65, 67, 69, 73, 75). (Those of *N. sclopetaria* are not bent over.) The posterior face of the epigynum is smooth (Figs. 74, 76), not grooved as in *N. patagiata.* The palpal terminal apophysis has a prong with a tip wider than its neck (Figs. 61, 110); in *N. sclopetaria* and *N. patagiata* it is wide. The embolus of *N. cornuta* has a wide lamella toward the mesal side (Figs. 61, 110, 118, 119) while in *N. sclopetaria* and *N. patagiata* it is simple and cylindrical.

Natural history. The web is found around houses, frequently in bushes (Comstock, 1912), often near water (Wiehle, 1931; Kaston, 1948); it has 15–20 spokes and is up to 60 cm in diameter (Kaston, 1948). It is illustrated by figure 516 in Comstock (1912) and by Kaston (1948). The web is made at night, when the spider leaves its retreat. The silken retreat may be in crevices of walls, on railings, or among plants. The retreat has been illustrated by Nielsen (1932). Both sexes are mature all summer, from March in the southern part of the range; males are more commonly mature in spring and late fall (Kaston, 1948). Egg sacs, according to Kaston (1948), are 7–10 mm in diameter, covered with yellowish threads, hidden in the retreat, and contain 50 to 250 eggs. A female may make as many as ten egg sacs.

Distribution. Holarctic, perhaps carried by man worldwide. In North America it occurs from the Arctic to Central America, but is most common in the eastern U.S. and Canada, Newfoundland to Florida (Map 2).

Nuctenea patagiata (Clerck), new combination
Figures 77–84, 100–102, 107, 112–113, 120–123, 127; Map 3

?*Araneus ocellatus* Clerck, 1757, Aranei Svecici, p. 36, pl. 1, fig. 9, ♀. Female holotype from Sweden, lost. Bonnet, 1955, Bibliographia Araneorum, 2: 555.

Araneus patagiatus Clerck, 1757, Aranei Svecici, p. 38, pl. 1, fig. 10, ♀. Locket and Millidge, 1953, British Spiders, 2: 136, figs. 89c, 90b, ♀, ♂.

Aranea dumetorum Fourcroy, 1785, Entomologia Parisiensis, p. 534. Type from Paris, France, believed lost. Wiehle, 1931, *in* Dahl, Tierwelt Deutschlands, 23: 88, figs. 128, 129, ♀, ♂.

Epeira ithaca McCook, 1893, American Spiders, 3: 152, pl. 4, fig. 3, ♂. Male lectotype from Ithaca, New York, in the Academy of Natural Sciences, Philadelphia, examined. NEW SYNONYMY.

Aranea ocellata, - Comstock, 1912, Spider Book, p. 489, figs. 107, 517–518; 1940, *op. cit.,* rev. ed., p. 503, figs. 107, 517–518, ♀, ♂.

Epeira patagiata, - Nielsen, 1932, The Biology of Spiders, Copenhagen, vol. 2, fig. 305, web.

Epeira dumetorum, - Kaston, 1948, Connecticut Geol. Natur. Hist. Surv. Bull., 70: 255, figs. 788, 804, 813, ♀, ♂.

Cyphepeira patagiata, - Yaginuma and Archer, 1969, Acta Arachnol., 16: 41. Prószyński and Staręga, 1971, Katalog Fauny Polski, 16: 84.

Note. According to Bonnet (1955), C. L. Koch, 1845 (Die Arachniden, 11: 115) was the first revisor, synonymizing the two names of Clerck and choosing the name *patagiata.*

Variation. Total length of females 5.5–11.0 mm. Carapace 2.5–4.0 mm long, 2.2–3.3 mm wide; first patella and tibia, 3.5–5.2 mm. Total length of males 5.8–6.5 mm. Carapace 2.9–3.8 mm long, 2.3–3.1 mm wide; first patella and tibia, 4.5–5.5 mm.

Diagnosis. Females are separated from the other species by the epigynum: its base is furrowed posteriorly and its scape has a narrow neck (Figs. 78–84). The male differs from *N. cornuta* by having the terminal apophysis a flat lobe (as in *N. sclopetaria*); it differs from both the other species in having a deep division in the heavy median apophysis (Figs. 112, 113, 127) and in having a finger-shaped embolus (Figs. 112, 120–123).

Natural history. Kaston (1948) indicates that its habits are similar to those of *N. cornuta.* According to Wiehle (1931) the web has 20–24 spokes with about 16 viscid threads above, and 23 below center;

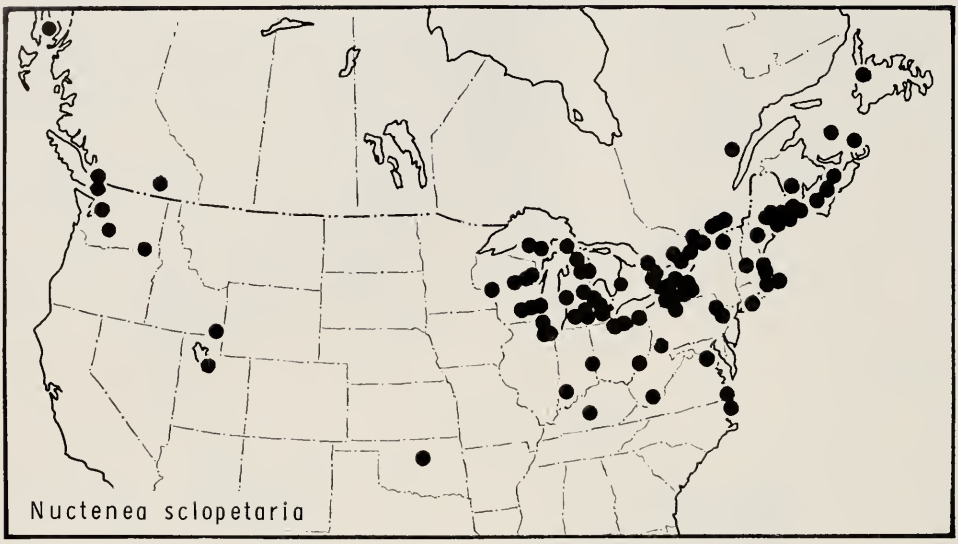

Map 4. North American distribution of *Nuctenea sclopetaria* (Clerck).

the orb is 25 cm across. The retreat is less silk lined than that of *N. cornuta*. The web has been illustrated by Nielsen (1932, fig. 305). I think the species prefers more arid, shaded areas than *N. cornuta*. I have found the retreat under bark in lodgepole pine at Jackson Hole, Wyoming, in a rather dry area. According to Wiehle (1931) and Kaston (1948) there may be a signal thread to the retreat or the spider may use a radius to return to it.

Distribution. Some American authors indicate that this is a more northern species than *N. cornuta*. This may not be quite correct; however, the species is not found in the southeastern states. It appears to be common from the Arctic to North Carolina and Arizona but is much commoner than *N. cornuta* in the west, the Rocky Mountains, and the Pacific northwest states (Map 3); also Eurasia.

Nuctenea sclopetaria (Clerck), new combination
Bridge spider, Gray-cross spider
Figures 85–88, 103–104, 108, 114–115, 124, 125, 128; Map 4

Araneus sericatus Clerck, 1757, Aranei Svecici, p. 40, pl. 2, fig. 1, ♀. Female type from Sweden lost. Bonnet, 1955, Bibliographia Araneorum, 2: 594.

Araneus sclopetarius Clerck, 1757, Aranei Svecici, p. 43, pl. 2, fig. 3, ♂. Type specimen from Sweden lost. Locket and Millidge, 1953, British Spiders, 2: 136, figs. 88b, 89a, 90a, ♀, ♂.

Aranea undata Olivier, 1789, Encycl. Méthod. Hist. Nat. Ins. Paris, 4: 206. New name for *sclopetarius* Clerck, but preoccupied by DeGeer, 1778. Wiehle, 1931, *in* Dahl, Tierwelt Deutschlands, 23: 90, figs. 130–133.

Aranea ovigera Panzer, 1804, Syst. Nomencl., *in* Schäffer, Icon. Ins. Ratisb., 1: 244, pl. 174, fig. 3.

Aranea sericata, - Comstock, 1912, Spider Book, p. 486, figs. 510–512, ♀, ♂; 1940, *op. cit.*, rev. ed., p. 500, figs. 510–512, ♀, ♂.

Aranea ovigera, - Roewer, 1942, Katalog der Araneae, 1: 801.

Epeira undata, - Kaston, 1948, Bull. Connecticut Geol. Natur. Hist. Surv., 70: 256, figs. 789, 805, 814–815, 2044–2046, ♀, ♂, web, egg sac.

Cyphepeira sclopetaria, - Yaginuma and Archer, 1959, Acta Arachnol., 16: 41.

Cyphepeira sericata, - Prószyński and Staręga, 1971, Katalog Fauny Polski, 16: 84.

Note. According to Bonnet (1955), O. P.-Cambridge (1874, Trans. Linnean Soc., 30: 330) first synonymized the two simultaneously, published names *sericatus* and *sclopetarius*, and chose *sclopetarius*. However, this seems to be an error; the names were first synonymized by Westring (1851,

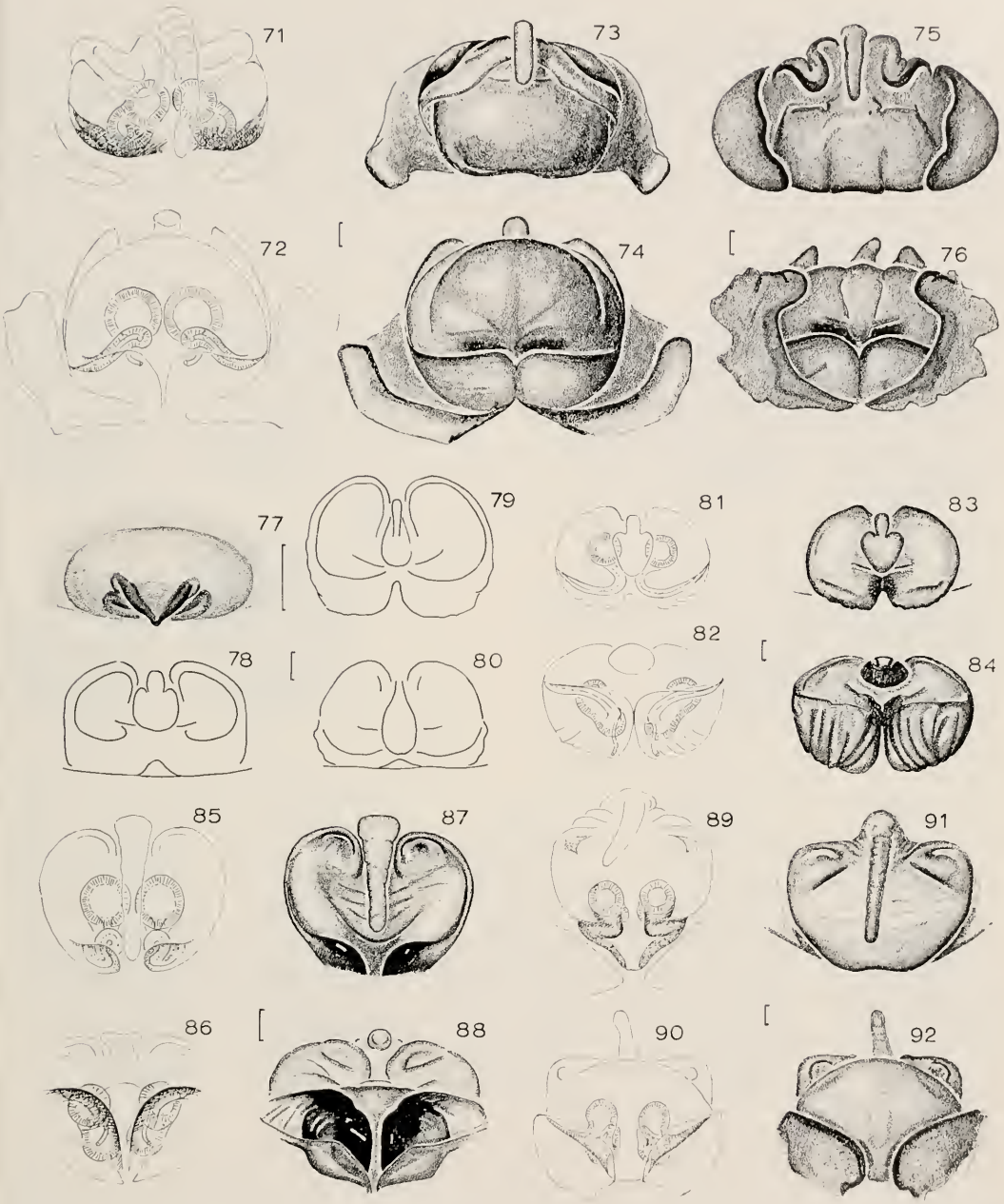

Figures 71–76. *Nuctenea cornuta* (Clerck), epigynum. 71, 73, 75. Ventral view. 72, 74, 76. Posterior view. 71–72. Cleared. 71–74. (Panama Canal Zone.) 75, 76. (Alberta.)

Figures 77–84. *N. patagiata* (Clerck), epigynum. 77–81, 83. Ventral. 82, 84. Posterior. 81, 82. Cleared. 77. Probably epigynum before last molt. (South Dakota.) 78, 79. (Alberta.) 80. (British Columbia.) 81–84. (Ontario.)

Figures 85–88. *N. sclopetaria* (Clerck), epigynum. 85, 87. Ventral. 86, 88. Posterior. 85, 86. Cleared.

Figures 89–92. *N. ixobola* (Thorell), epigynum. 89, 91. Ventral. 90, 92. Posterior. 89, 90. Cleared.

Scale lines. 0.1 mm.

Göteborg Kongl. Vet. Handl., 2: 34), who also chose *sclopetaria*. Thorell (1856, N. Acta Reg. Soc. Sci. Uppsala, p. 22) also lists the synonymy under *sclopetaria*. Bonnet shows that prior to 1938 the usage of *sclopetaria* outweighed *sericata*, although *sericata* has been uniformly used in North America and also by Bonnet (1955). I will follow European arachnologists and use *sclopetaria* as do Locket and Millidge (1953, British Spiders, 2). (See Article 24a of the International Code on Zoological Nomenclature, 1961.)

Variation. Total length of females 8–14 mm. Carapace 3.9–4.3 mm long, 3.1–4.0 mm wide. First patella and tibia 5.3–7.0 mm. Total length of males 6–7 mm. Carapace 3.7–3.2 mm long, 2.9–3.3 mm wide. First patella and tibia 6.2–7.0 mm.

Diagnosis. This species can usually be separated from *N. cornuta* and *N. patagiata* by the white hairs around the border of the carapace and by the fact that the background of the eye region is lighter brown than the area behind it and than the area of the clypeus (Fig. 108). The female's epigynum has the scape finger-shaped, as in *N. cornuta* but not as in *N. patagiata*, and the anterolateral margins of the base lobed and flat (Fig. 87), not as in *N. cornuta*. The openings of the epigynum are in dark posterior swellings of the base (Fig. 85). The palpus has a lobe-shaped terminal apophysis (Figs. 114, 115), somewhat like that of *N. patagiata*. The median apophysis is not as deeply divided as that of *N. patagiata* (Figs. 115, 128). The embolus resembles that of *N. patagiata* (Figs. 124, 125).

Natural history. This is the least common of the three *Nuctenea* species in North America and is found on houses and other buildings, often near water. One collection from West Virginia came from sweeping honeysuckle bushes (*Lonicera* sp.). Many webs may be found touching one another (Kaston, 1948). In Europe the species is also found on buildings, and especially on bridges and cliffs above water (Wiehle, 1931). The orbs have up to 20 radii, with the viscid spiral separated, and the web reaches 70 cm in diameter (Wiehle, 1931). The web is illustrated in Kaston (1948, figs. 2044, 2046). The spider rests near the end of one of the frame threads rather than in a retreat. The egg sac, according to Kaston, contains 114–337 eggs, and is illustrated in his figure 2045.

Distribution. Eurasia. In America this species is probably introduced, judging by its close association with buildings and its limited distribution, which matches that of *Araneus diadematus* Clerck. It is found from Newfoundland to southern Alaska, south to North Carolina, and is most abundant in the Great Lakes states (Map 4).

Nuctenea ixobola (Thorell) new combination
Figures 89–92, 95, 109, 116–117, 129

Epeira ixobola Thorell, 1873, Remarks on Synonyms of European Spiders, p. 545. Two male and three female syntypes from Austria in the Natural History Museum in Stockholm, not examined.

Aranea ixobola, - Wiehle, 1931, *in* Dahl, Tierwelt Deutschlands, 23: 92, figs. 134–137, ♀, ♂. Roewer, 1942, Katalog der Araneae, 1: 788.

Araneus ixobolus, - Bonnet, 1955, Bibliographia Araneorum, 2: 523.

Description. Female from Poland. Carapace very flat, no thoracic depression. Secondary eyes all about 0.7 diameter of anterior median eyes. Anterior median eyes slightly more than their diameter apart, posterior median eyes their diameter apart. Lateral eyes on tubercles and widely separated from the median eyes. The height of the clypeus equals 0.6 diameters of the anterior median eyes. Total length 13 mm. Carapace 6.5 mm long, 5.3 mm wide. First femur, 6.3 mm; patella and tibia, 8.6 mm; metatarsus, 5.7 mm; tarsus, 2.0 mm. Second patella and tibia, 8.0 mm; third, 4.4 mm; fourth, 6.3 mm.

Male from Poland. Carapace and eye arrangement as in female. Total length 12 mm. Carapace 5.4 mm long, 4.7 mm

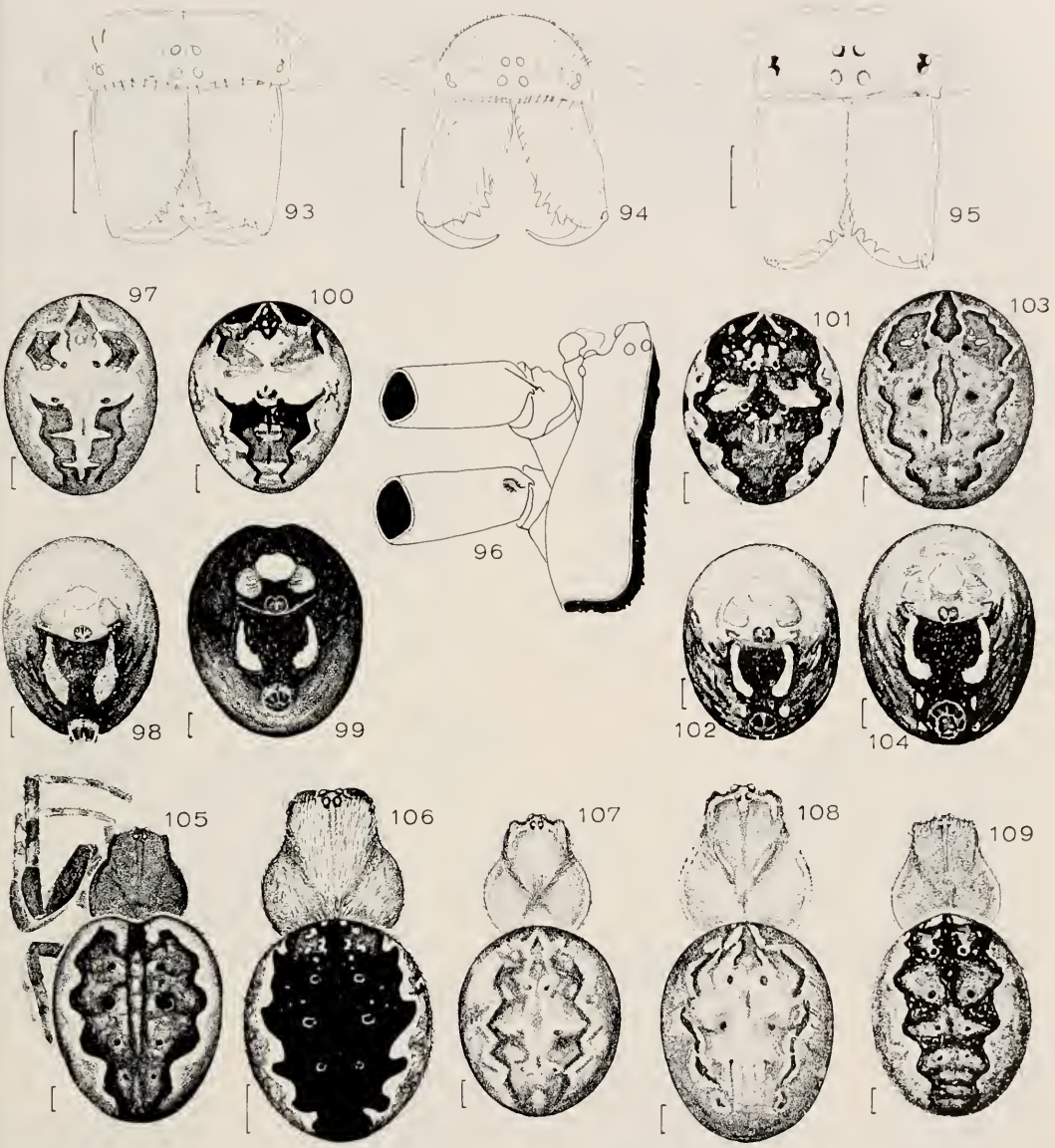

Figures 93–95. Eye region and chelicerae. 93. *Nuctenea umbratica*. 94. *N. cornuta*. 95. *N. ixobola*.

Figure 96. Left anterior femora and carapace of *N. patagiata*.

Figures 97–104. Abdomen. 97–98. *N. cornuta*. 99. *N. umbratica*. 100–102. *N. patagiata*. 103–104. *N. sclopetaria*. 97, 100, 101, 103. Dorsal. 98, 99, 102, 104. Ventral.

Figures 105–109. Carapace and abdomen, dorsal. 105. *N. umbratica*. 106. *N. silvicultrix*. 107. *N. patagiata*. 108. *N. sclopetaria*. 109. *N. ixobola*.

Scale lines. 1.0 mm.

wide. First femur, 8.3 mm; patella and tibia, 11.8 mm; metatarsus, 8.2 mm; tarsus, 3.3 mm. Second patella and tibia, 10.0 mm; third, 5.0 mm; fourth, 7.4 mm.

Diagnosis. Females have a narrow scape in the epigynum as does *Nuctenea sclopetaria*, with which it has been confused. However, the anterior lateral end of the base differs (Figs. 89, 91) and posterior lobes of the base do not extend ventrally. The male differs from that of *N. sclopetaria* in having a differently shaped embolus (Fig. 116).

Natural history. According to Wiehle (1931), this species is similar in habits to *N. sclopetaria* and replaces it in eastern Europe. It lives on buildings, fences, and bridges near water.

Distribution. From Central Europe to Iran (Roewer, 1942; Bonnet, 1955). Specimens examined came from Leopoldshall (Anhalt, German Democratic Republic), Biolowieza, Distr. Hajnowka, and Distr. Kosice, Poland.

REFERENCES CITED

Berman, J. D., and H. W. Levi. 1971. The orb-weaver genus *Neoscona* in North America (Araneae: Araneidae). Bull. Mus. Comp. Zool., **141**: 465–500.

Cambridge, F. O. Pickard-. 1903. Araneidea, *In* Biologia Centrali-Americana, 2.

Comstock, J. H. 1912. The Spider Book. Garden City, New York: Doubleday, Doran and Co.

———. 1940. The Spider Book, rev. ed. Ithaca: Comstock Publ. Co.

Gerhardt, U. 1926. Weitere Untersuchungen zur Biologie der Spinnen. Z. Morphol. Ökol. Tiere, **6**: 1–77.

Gertsch, W. J. 1934. Further notes on American spiders. Amer. Mus. Novitates, No. 726: 1–26.

Levi, H. W. 1971. The *Diadematus* group of the orb-weaver genus *Araneus* north of Mexico (Araneae: Araneidae). Bull. Mus. Comp. Zool., **141**: 131–179.

———. 1973. Small orb-weavers of the genus *Araneus* north of Mexico (Araneae: Araneidae). Bull. Mus. Comp. Zool. **145**(9): 473–552.

———. in preparation. The presence of the cap on palpal emboli and mating behavior.

Locket, G. H., and A. F. Millidge. 1953. British Spiders, **2**: 1–449.

Petrunkevitch, A. 1925. External reproductive organs of the common grass spider *Agelena naevia* Walckenaer. J. Morphol., **40**: 559–573.

Prószyński, J., and W. Staręga. 1971. Katalog Fauny Polski, **33**: 1–382.

Seyler, P. J. 1940. The generic and specific status of four spiders of the genus *Agelenopsis*. Ohio J. Sci., **41**: 51–69.

Wiehle, H. 1927. Beiträge zur Kenntnis des Radnetzbaues der Epeiriden, Tetragnathiden und Uloboriden. Z. Morphol. Ökol. Tiere, **8**: 468–537.

———. 1931. Araneidae. *In* F. Dahl, Die Tierwelt Deutschlands, **23**: 1–136.

Yaginuma, T., and A. F. Archer. 1959. Genera of the Araneine Argiopidae found in the Oriental region and generally placed under the comprehensive genus *Araneus*. Acta Arachnol., **16**: 34–41.

INDEX

Valid names are printed in italics. Page numbers refer to main references, starred page numbers to illustrations.

alba, Epeira 296
alpica, Aranea 299
alpica, Araniella 299*
alpica, Epeira 299
alpicus, Araneus 300
Araniella 292
cornuta, Cyphepeira 308
cornuta, Nuctenea 304*, 306, 307*, 311*, 313*, 315*
cornutus, Araneus 306
croaticus, Araneus 296
cucurbitina, Aranea 298
cucurbitina, Araniella 297*, 298
cucurbitina, Epeira 296
cucurbitinus, Araneus 298
Cyphepeira 300
decipiens, Epeira 294
displicata, Aranea 296
displicata, Araniella 293*, 294, 295*, 297*
displicata, Epeira 294
displicatus, Araneus 296
dumetorum, Aranea 309
dumetorum, Epeira 309

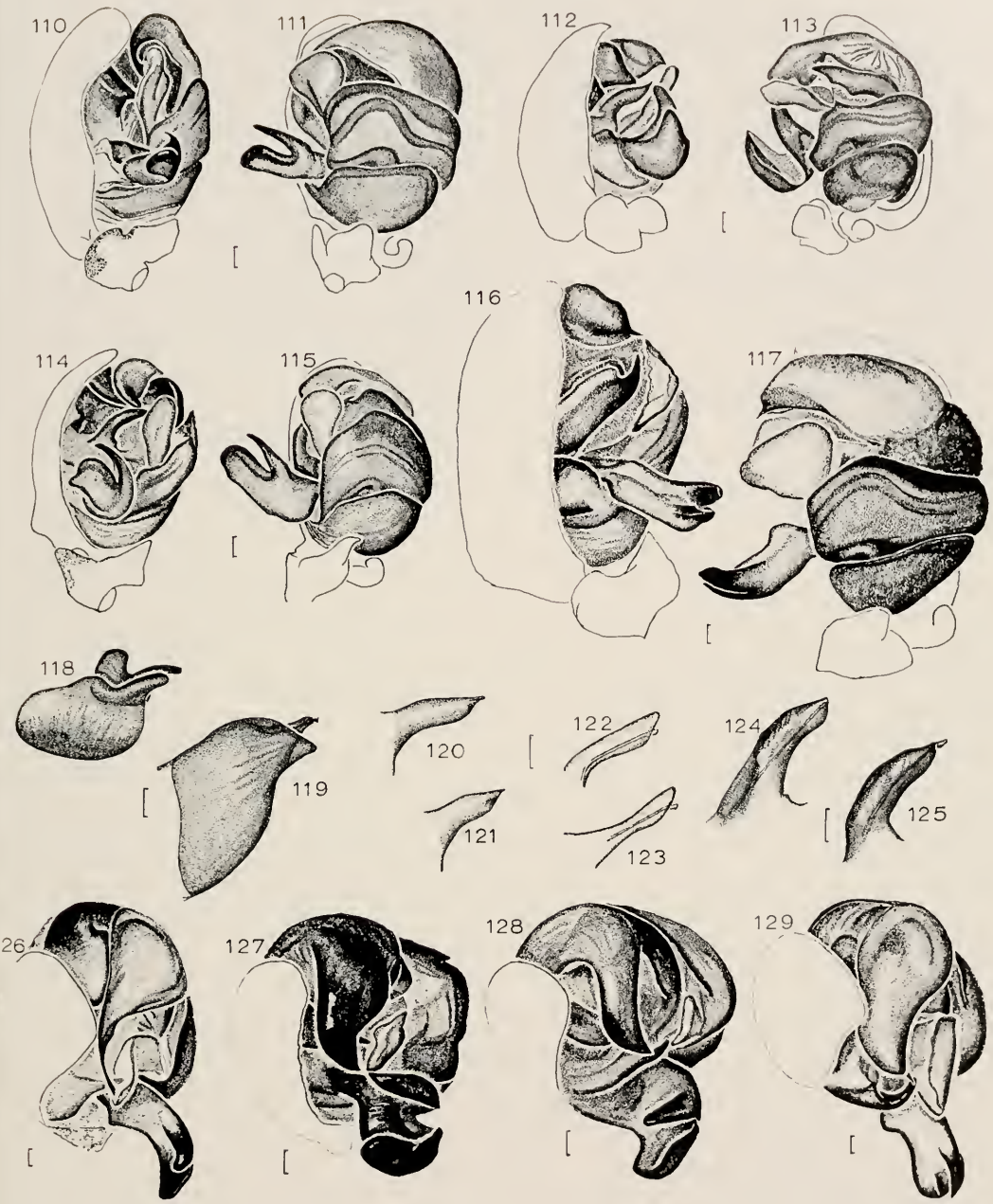

Figures 110–117. Left male palpus. 110, 111. *Nuctenea cornuta* (Clerck). 112, 113. *N. patagiata* (Clerck). 114, 115. *N. sclopetaria* (Clerck). 116, 117. *N. ixobola* (Thorell).

Figures 118–125. Embolus of male palpus. 118, 119. *N. cornuta*. 120–123. *N. patagiata*. 124, 125. *N. sclopetaria*. 118, 120, 121, 124. Probably virgin. 119, 122, 123, 125. Probably mated. 118. Mesal-apical. 119–125. Mesal.

Figures 126–129. Male palpus, apical view. 126. *N. cornuta*. 127. *N. patagiata*. 128. *N. sclopetaria*. 129. *N. ixobola*.

Scale lines. 0.1 mm.

foliata, Aranea 306
foliata, Epeira 308
frondosa, Aranea 308
frondosa, Epeira 308
inconspicua, Aranea 298
inconspicua, Araniella 298, 299*
inconspicua, Epeira 298
inconspicuus, Araneus 298
ithaca, Epeira 309
ixobola, Aranea 312
ixobola, Epeira 312
ixobola, Nuctenea 311*, 312, 313*, 315*
ixobolus, Araneus 312
Nuctenea 300
ocellata, Aranea 309
ocellatus, Araneus 309
octopunctata, Araniella displicata 296
opisthographa, Araneus cucurbitina 298
ovigera, Aranea 310
patagiata, Cyphepeira 309
patagiata, Epeira 309
patagiata, Nuctenea 309, 311*, 313*, 315*
patagiatus, Araneus 309
proxima, Aranea 298
proxima, Epeira 298
sclopetaria, Cyphepeira 310
sclopetaria, Nuctenea 310, 311*, 313*, 315*
sclopetarius, Araneus 310
sericata, Cyphepeira 310
sericatus, Araneus 310
sexpunctata, Aranea 302
sexpunctata, Epeira 294
silvicultor, Araneus 306
silvicultrix, Aranea 306
silvicultrix, Cyphepeira 306
silvicultrix, Epeira 306
silvicultrix, Nuctenea 303*, 306, 307*, 313*
strix, Epeira 308
umbratica, Chinestela 302
umbratica, Epeira 302
umbratica, Nuctenea 302, 303*, 307*, 313*
undata, Aranea 310
undata, Epeira 310
vicaria, Epeira 308

US ISSN 0027-4100

Bulletin OF THE
Museum of
Comparative
Zoology

The Anatomy of *Saurosuchus galilei* and the Relationships of the Rauisuchid Thecodonts

WILLIAM D. SILL

HARVARD UNIVERSITY
CAMBRIDGE, MASSACHUSETTS, U.S.A

VOLUME 146, NUMBER 7
21 NOVEMBER 1974

PUBLICATIONS ISSUED
OR DISTRIBUTED BY THE
MUSEUM OF COMPARATIVE ZOOLOGY
HARVARD UNIVERSITY

BREVIORA 1952–
BULLETIN 1863–
MEMOIRS 1864–1938
JOHNSONIA, Department of Mollusks, 1941–
OCCASIONAL PAPERS ON MOLLUSKS, 1945–

SPECIAL PUBLICATIONS.

1. Whittington, H. B., and E. D. I. Rolfe (eds.), 1963. Phylogeny and Evolution of Crustacea. 192 pp.
2. Turner, R. D., 1966. A Survey and Illustrated Catalogue of the Teredinidae (Mollusca: Bivalvia). 265 pp.
3. Sprinkle, J., 1973. Morphology and Evolution of Blastozoan Echinoderms. 284 pp.
4. Eaton, R. J. E., 1974. A Flora of Concord. 250 pp.

Other Publications.

Bigelow, H. B., and W. C. Schroeder, 1953. Fishes of the Gulf of Maine. Reprint.

Brues, C. T., A. L. Melander, and F. M. Carpenter, 1954. Classification of Insects.

Creighton, W. S., 1950. The Ants of North America. Reprint.

Lyman, C. P., and A. R. Dawe (eds.), 1960. Symposium on Natural Mammalian Hibernation.

Peters' Check-list of Birds of the World, vols. 2–7, 9, 10, 12–15.

Proceedings of the New England Zoological Club 1899–1948. (Complete sets only.)

Publications of the Boston Society of Natural History.

Price list and catalog of MCZ publications may be obtained from Publications Office, Museum of Comparative Zoology, Harvard University, Cambridge, Massachusetts, 02138, U.S.A.

© The President and Fellows of Harvard College 1974.

THE ANATOMY OF *SAUROSUCHUS GALILEI* AND THE RELATIONSHIPS OF THE RAUISUCHID THECODONTS

WILLIAM D. SILL[1]

Abstract. *Saurosuchus galilei* was a large quadrupedal carnivorous thecodont from the Ischigualasto Formation of western Argentina, which is of approximately Carnian age. Its skull anatomy indicates that it descended from an erythrosuchid type of primitive thecodont. *Saurosuchus*, together with *Luperosuchus, Prestosuchus, Ticinosuchus, "Mandasuchus,"* and possibly some other less well known genera, form a well-defined lineage that can be traced throughout most of the Triassic. *Rauisuchus* is considered a member of the same family, and thus the earlier name Rauisuchidae is retained for the group. Two other thecodont lineages, the Proterochampsidae and the Ornithosuchidae, are traced throughout the Triassic. The relationships of the three families strongly suggest that they are independent derivations of the three Early Triassic primitive families. Dinosaur origins remain unclear. There is no good evidence for associating the Rauisuchidae with early dinosaurs; on the contrary, there is an unexplained time overlap of large carnivorous dinosaurs and thecodonts that have nearly identical adaptations.

INTRODUCTION

Saurosuchus galilei is one of the 18 or more genera of reptiles found in the now legendary Ischigualasto Basin of western Argentina. Its significance for paleontologic studies lies in the excellent preservation of the material, particularly of the skull and tarsus, which makes possible the clarification of the anatomy of the closely related Brazilian thecodonts, and generally aids interpretation of the family Rauisuchidae on a worldwide basis. Together with *Ticinosuchus* from the Middle Triassic of Switzerland, *Saurosuchus* provides a key for tracing a thecodont lineage that was world-wide in distribution throughout most of the Triassic Period.

Most of the specimens used for this study were collected in the Ischigualasto Formation by expeditions from the Instituto Miguel Lillo of Tucumán, Argentina. The first specimen was collected in 1959, under the direction of Dr. Osvaldo Reig. Subsequent expeditions, led by José Bonaparte, recovered parts of four additional individuals. From these various parts, most of the skeleton can be reconstructed, although the forelimb is not represented in any of the specimens.

Saurosuchus was one of the largest thecodonts of its time, and no doubt competed with the emerging dinosaurs for the large carnivore role. Thecodonts, of course, lost the competition, and contemporary dinosaurs, both saurischian and ornithischian, from the Ischigualasto Formation indicate that superior locomotion was a factor related to dinosaurian dominance. At present, although *Saurosuchus* appears to be the most advanced member of the family yet described, it is less progressive anatomically than its dinosaurian contemporaries. The lineage of *Saurosuchus* provides evidence to support the premise that progressive thecodonts were competitors rather than progenitors of the dinosaurs.

Abbreviations for the institutions referred to in this report are as follows:

[1] Universidad Nacional de San Juan, Dept. Geologia, San Juan, Argentina.

PVL	Instituto Miguel Lillo, Tucumán, Argentina
DGM	Division of Mines and Geology, Brazil
T	University of Tübingen, Germany
PIMZ	Paleontological Institute, Zürich, Switzerland
MSJ	Museum of Natural Sciences, San Juan, Argentina

Acknowledgements. This study was made during a year's stay at the Instituto Miguel Lillo in Tucumán, Argentina. Special thanks are due to José Bonaparte and the directors of the Institute, whose help and generosity made the study possible. I am also greatly indebted to A. W. Crompton of Harvard University and John Ostrom of Yale for their technical help and personal assistance. Many colleagues offered suggestions and gave perspective to the research; among them were A. S. Romer, Bernard Krebs, Alan Charig, A. Keyser, and Alick Walker. Drawings were made by Alexander Gavriloff.

Funds for the Research were provided by NSF Grant GB–4435X1.

Geologic Setting

The Ischigualasto Basin (Hoyada de Ischigualasto or Valle de la Luna) forms a depression on the western limb of a large syncline whose axis runs northwest–southeast. Differential erosion of the soft claystones of the Ischigualasto Formation created a prominent depression at the base of the cliff–forming red sandstones of the Los Colorados Formations (see Fig. 1). The Triassic sediments extend approximately one hundred kilometers, and are bounded on the south by the Valle Fértil mountains and on the north by the Sierra de Mas range. Within this area of outcrop there are numerous minor flexures, principally anticlines. One such saddle-shaped anticline divides the basin into a northern and southern portion; this division coincides with the boundary between the provinces of San Juan and La Rioja. The southern, or San Juan, portion is the larger of the two and has produced most of the fossils known from the basin. East of the depression, the opposite limb of the large syncline has exposed the type area of the earlier Chañares Formation.

Interpretation of the time-stratigraphic relationships of the sedimentary units in the Ischigualasto basin has varied considerably. For many years the whole succession was considered "Rhaetic," or uppermost Triassic. With the discovery of vertebrate fossils that were more primitive than the classic Upper Triassic fauna, vertebrate paleontologists assigned the Ischigualasto Formation to the Middle Triassic. As new discoveries are being made a consensus is forming that the Ischigualasto Formation is most probably of Carnian age, possibly Late Ladinian, with the underlying Los Rastros Formation closely equivalent in time to the Santa Maria Formation of Brazil. (I have elsewhere summarized the various interpretations of the South American Triassic: Sill, 1969.)

Although the general geologic relationships between the various formations are quite straightforward, no attempt has yet been made to study sedimentary cycles within the Ischigualasto Formation, or to correlate the occurrence of specific fossils with different sedimentary regimes.

TAXONOMY AND MORPHOLOGY

Introduction

Taxonomic history of the Rauisuchidae began with Huene's work on the specimens he found in the Triassic of Brazil. In a short paper on thecodont relationships (Huene, 1936), he proposed the subfamily Rauisuchinae as a part of the family Stagonolepidae to include the genera *Rauisuchus* and *Prestosuchus* from Brazil. Later, (Huene, 1942) the group was elevated to familial rank and the genus *Rhadinosuchus*, also from the Triassic of Brazil, was included. At about the same time (Huene, 1938), he described *Stagono-*

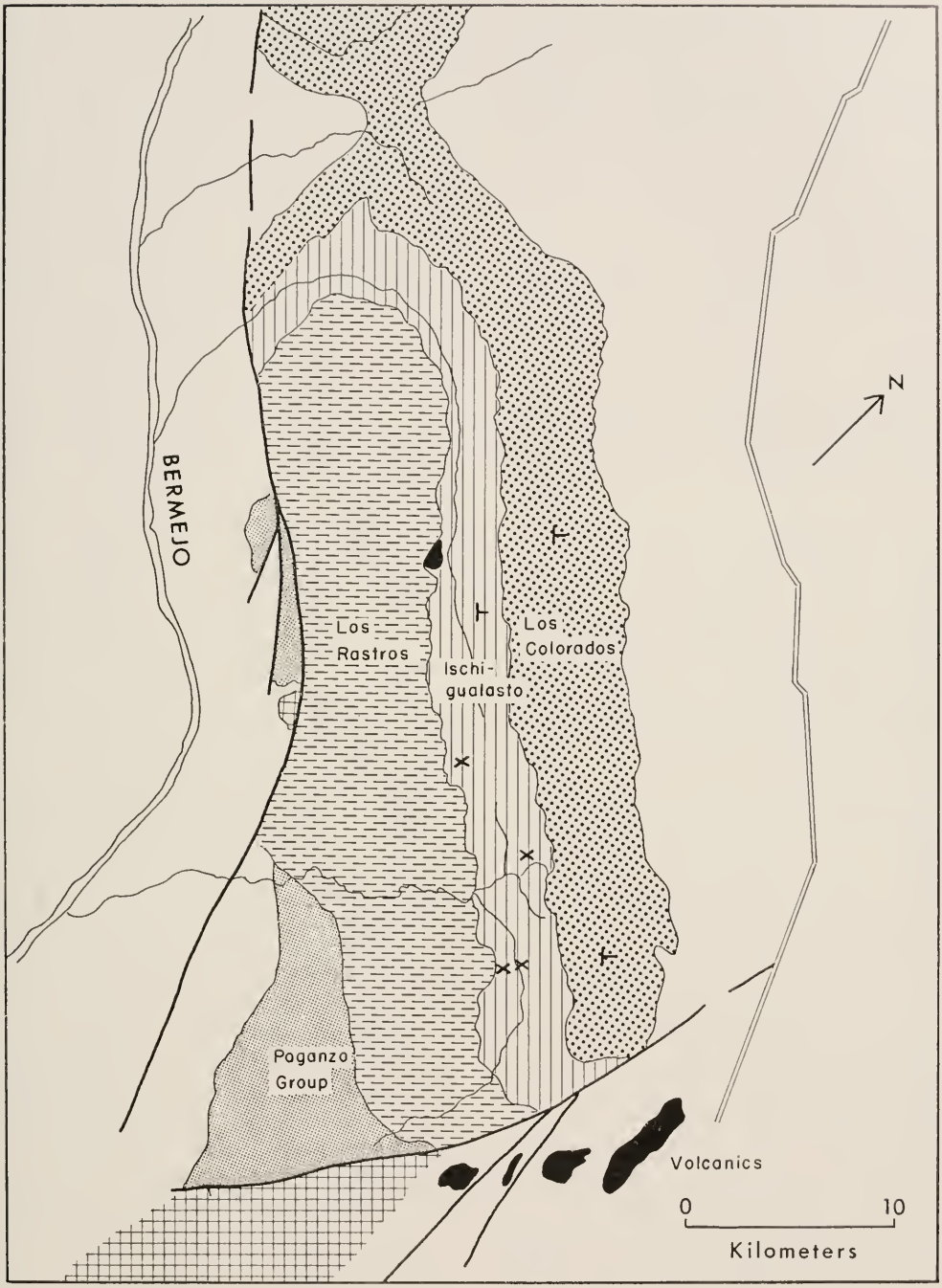

Figure 1. Generalized geologic map of the southern portion of the Ischigualasto Basin. × marks *Saurosuchus* localities.

suchus from the Manda Beds of East Africa and noted its similarity to the Brazilian forms. However, not until 1956 did Huene formally place *Stagonosuchus* in the family Rauisuchidae, at which time he also included a number of poorly known thecodonts that are no longer considered to be closely related to the family.

Since then, interpretations of the broader relationships of the Rauisuchidae have followed the general pattern of uncertainty that has been the hallmark of thecodont taxonomy. Huene (1956) continued to maintain the family in close association with the stagonolepid-aetosaurid groups and included in the family such diverse genera as *Cerritosaurus* and *Episcoposaurus*. Romer (1956) was the first to separate most of the genera of the Rauisuchidae from the armored thecodonts, and tentatively placed *Rauisuchus, Prestosuchus, Stagonosuchus, Rhadinosuchus*, and *Procerosuchus* in the Ornithosuchidae. Hoffstetter (1955) retained the family in the Stagonolepoidea, but removed *Stagonosuchus* to the Stagonolepidae. Reig (1961) presented a comprehensive review of the family and showed beyond reasonable doubt that the family Rauisuchidae should consist only of the genera *Rauisuchus, Prestosuchus, Stagonosuchus,* and the then recently discovered *Saurosuchus* from Ischigualasto. He also presented convincing evidence showing that the family is not closely related to the Stagonolepidae, and placed it in the "traditional" thecodont group which he termed Ornithosuchia (the equivalent of Pseudosuchia of most authors). Hughes (1963), on the other hand, tentatively placed *Rauisuchus* and *Saurosuchus* in the primitive thecodont group Proterosuchia as members of the Erythrosuchidae, a ranking that has not been accepted by the majority of paleontologists. *Ticinosuchus,* on the basis of a complete skeleton, was added to the family by Krebs (1965); its affinities with the other members of the family as described by Reig are evident. A further genus, *Luperosuchus,* from the Chañares Formation, was added to the family by Romer (1971a), and a closely related form has recently been found in the Los Colorados Formation (Bonaparte, personal communication). These latter discoveries are especially significant, for they permit the *Saurosuchus* lineage to be traced through the major part of the Triassic in a single basin of deposition. Romer (1966) followed Hughes in tentatively associating *Rauisuchus* and *Saurosuchus* with the Erythrosuchidae, and adopted the term Prestosuchidae from Charig's unpublished thesis for the remaining genera *Prestosuchus, Procerosuchus,* "*Mandasuchus*"[1] and, tentatively, *Stagonosuchus*. However, he later (1968) replaced *Rauisuchus* and *Saurosuchus* with the above mentioned forms, but did not suppress Prestosuchidae. Meanwhile Prestosuchidae was carried on by Charig[2] (1967), who notes that the group is essentially the same as the Rauisuchidae of Huene (1942) but with the genus *Rauisuchus* excluded.

In a more recent work on thecodont taxonomy Romer (1972a) continued to use the family name Prestosuchidae on the grounds that *Rauisuchus* was too poorly known. However, he included *Rauisuchus* within the family Prestosuchidae (see Discussion with regard to the affinities of *Rauisuchus*).

Assignment of the Rauisuchidae to a suborder is difficult given the present unstable nature of thecodont taxonomy. Romer (1972a) places the family with the primitive thecodonts in the Proterosuchia; other authors, Charig (1967) and Bonaparte (1971) place it in the usual "catch-all" suborder Pseudosuchia. Rauisuchids certainly appear to have been derived from the erythrosuchid lineage of the Proterosuchia (see discussion on thecodont phylogeny),

---

[1] *Mandasuchus* is technically a *nomen nudum*, as it has never been described in print.

[2] In Charig's paper, origin of the Prestosuchidae was ascribed to Charig 1967. This paper has not been published. In an erratum, the family name was given as Romer 1966.

but they are much more specialized and progressive than any of its known members. On the other hand, they do not have a great deal in common with the "typical" ornithosuchid pseudosuchians. As thecodont relationships become more clearly understood, a new suborder will probably have to be erected for this and perhaps other lineages descended from the erythrosuchids, but at present such a step would be premature.

Discovery of nearly complete remains of *Ticinosuchus* and *Saurosuchus*, representing what appear to be the earliest and the latest members of the lineage so far described, has provided the means for an accurate characterization of the family. Basically, the new evidence tends to confirm the definitions of the family given by Krebs (1965) and by Reig (1961); Reig's paper provides an excellent summary of the taxonomic history of the family and of the Thecodontia in general.

The family may be defined as follows: Medium- to large-sized carnivorous quadrupedal thecodonts. Skull large, deep, orbit keyhole-shaped, large elongate antorbital fenestra, small crescent-shaped accessory antorbital fenestra present in some genera, teeth flattened, recurved, serrated. Pelvis triradiate, acetabulum closed, ischium elongated and rodlike, fused at the midline along most of its length. Femur long, slightly sigmoid, without a well-defined fourth trochanter. Calcaneum and astragalus articulate by a ball and socket joint, the socket on the calcaneum, the ball on the astragalus. Five digits, fifth metatarsal short and hooked. Many of these features are generalized characteristics of the primitive thecodonts which have been carried over in the family and are retained throughout their known history.

Family distribution. Middle and Late Triassic; Argentina, Brazil, East Africa, Switzerland, possibly China. Family Rauisuchidae Huene 1936 (as a subfamily); genera *Rauisuchus* Huene 1936 Brazil, *Prestosuchus* Huene 1936 Brazil, *Stagonosuchus* Huene 1938 East Africa, *Saurosuchus* Reig 1959 Argentina, *Ticinosuchus* Krebs 1965 Switzerland, *Luperosuchus* Romer 1971 Argentina, "*Mandasuchus*" unpublished thesis Charig 1956. A number of additional genera are sometimes included in the family (see Romer, 1966 and 1972), but they are not well known. These additional genera are: *Cuyosuchus, Hoplitosaurus, Rhadinosuchus, Pallisteria, Spondylosoma, Procerosuchus, Fenhosuchus.*

Saurosuchus Reig 1959

Type species. Saurosuchus galilei.

Distribution. Late Ladinian or Carnian, Ischigualasto Basin, Western Argentina.

Diagnosis. As for the species.

Saurosuchus galilei Reig 1959

Type. PVL 2062, nearly complete skull, posteriormost portion missing.

Hypodigm. The type and: PVL 2198, partial maxilla, left ilium, both ischia, nine articulated dorsal vertebrae and fragments, part of the dermal armour, associated ribs and teeth. PVL 2557, two dorsal vertebrae, both sacrals, nine caudals, right ilium and ischium, partial pubis, parts of right femur, tibia, fibula, complete right tarsus and foot, associated ribs and chevrons. PVL 2267, poorly preserved partial ilium, partial femur, tibia, fibula, well-preserved tarsus, partial foot. PVL 2472, poorly preserved cervical vertebra, tibia, astragalus. MSJ 102, fragment of maxilla and lower jaw.

Horizon. Apparently all levels of the Ischigualasto Formation, San Juan province, Argentina. The five specimens of *Saurosuchus* were collected from four localities, all in the southern portion of the outcrop area. The type, PVL 2062, consists of a nearly complete skull and was found in the upper third of the strata. The more complete skeletons, PVL 2198 and PVL 2557, came from the middle part of the section, and the remaining two individuals, PVL 2267 and 2472, were found in the lower third of the strata, as was MSJ 102 (see map for specific localities).

Emended diagnosis. Large carnivorous thecodonts, up to six meters in length. Skull deep, elongate, finely sculptured, with keyhole-shaped orbit, large antorbital fenestra elongated anteriorly, small crescent-shaped accessory antorbital fenestra present between premaxilla and maxilla. Large elongate, nearly vertical external nares bordered only by premaxilla and nasal. Teeth robust, recurved, laterally compressed with serrate edges. Four teeth on premaxilla, ten on maxilla. Strong orbital arch formed by the frontal, small supratemporal fenestra lying in dorsal plane of the skull below the crest of the orbital arch. Vertebrae amphicoelous, spines broad and flat with prominent interspinous notch on anterior face. Cervicals apparently elongated, dorsals strongly compressed laterally, rib facets well separated and on different levels throughout column. Two sacral vertebrae. Shoulder girdle and forelimb unknown. Pelvis with closed acetabulum, pubis almost excluded. Ilium with broad brevis shelf, ischium long, rodlike, expanded at the tip and fused at the midline along most of its length. Femur slightly sigmoid, without a large greater trochanter, and with a small fourth trochanter. Fibula bears a prominent iliofibularis tubercle. Tarsus of the "crocodiloid" type, calcaneum bearing a large tuber and a prominent medial socket for articulation of the astragalar ball. Facets for articulation of the tibia and fibula close together. Fourth tarsal large, subtriangular with prominent rounded facet for articulation of fifth metatarsal. Five digits on foot, first two most robust, third is the longest, fifth is broad, flat, and oriented outward. Dermal armour present, two rows of small scutes along each side of most of the vertebral column, leaf-shaped and imbricating.

General Description

Skull

Cranium. Cranial material is represented almost exclusively by the type, in which most of the dermal elements are preserved, but the occipital region and braincase are lacking. A fragment of the right maxilla of PVL 2198 is identical to the corresponding region of the type and allows assignment of the specimen to the genus with a considerable degree of confidence. The lower jaw is known only from a fragment.

The skull is long, approximately 65 centimeters, triangular in shape, and sturdily constructed. The cranial table is high and narrow. Orbits are large, keyhole-shaped openings, of which the upper part is a well-defined circle high up the side of the skull. A large antorbital fenestra is present, subtriangular in shape and slightly smaller than the orbit. It is surrounded by a well-defined smooth border set in from the sculptured surface of the maxilla. An unexpected feature is the presence of a narrow accessory antorbital fenestra located between the maxilla and the premaxilla, extending from above the tooth-bearing surface to the posterior tip of the external nares.

Like the antorbital fenestra, the external nares are subtriangular in shape, relatively large, and situated principally in the vertical plane of the skull. Notable for their small size are the supratemporal fenestrae, which lie in the horizontal plane of the skull roof just behind and slightly below the heavy orbital arch. Only the anterior border of the infratemporal fenestra is preserved, but it indicates a triangular or subrectangular shape approximately the same size as the orbit.

The large size of the skull and its sturdy construction indicate that *Saurosuchus* was an active predator. Using the head size index of skull length to length of the presacral vertebral column, a value of either .27 or .34 is obtained, the latter calculated on the assumption that neck vertebrae were approximately the same length as the dorsals, while the smaller ratio assumes elongated cervicals. Both indices are in the range of the large predaceous dinosaurs; *Allosaurus* is .28, *Tyrannosaurus* is .41.

Premaxilla. Both premaxillae of the type are complete and well preserved. The main body of the bone is a massive rectangle from which a slender process extends upward and backward around the external naris to a long overlapping contact with a similar process of the nasal, and a second rodlike extension that forms the entire lower border of the naris and terminates wedged between the nasal and the maxilla. At its anterior border the premaxilla forms a straight vertical line from the tip of the naris to the first tooth position. Below the narial opening the bone swells to a thick, slightly undulating ridge that bears four large teeth. At the most anterior part, just above the tooth row, lie three foramina. No sculpturing is present. The rodlike process that forms the lower border of the naris is an isolated structure that separates the accessory antorbital fenestra and the external naris.

Medially, the premaxillae meet in a long sturdy symphysis. The alveolar margin is thick and slightly vaulted behind the first two teeth. Of the four teeth, the third is the largest. Two deep pits are present in the vaulted area, one beside the second tooth, the other between the third and the fourth. A large foramen is present above the third alveolus. The interalveolar septum between the third and fourth teeth is expanded on the lingual surface to form a small interdental plate.

Posteroventrally, a clearly defined suture is not present between the maxilla and the premaxilla, but above the thick tooth-bearing portion of the bone the accessory antorbital fenestra serves to separate the two elements.

Maxilla. The maxilla is a large platelike bone that slopes posteriad and upward from its suture with the premaxilla to meet the nasal and lacrimal dorsally and the jugal ventrally. It is deeply emarginated by the antorbital fenestra, around which runs a broad smooth shelf. Outside the shelf area the maxilla is heavily sculptured by an irregular network of grooves. It forms

Table 1. Measurements of the skull (in centimeters) of *Saurosuchus galilei* based on the type PVL 2062. Note, further preparation has modified some of the measurements made by Reig (1959) in his preliminary account.

Total length of the skull (estimated)	67
Length from tip of snout to anterior border of the supratemporal fenestra	54
Length from lower anterior corner of infratemporal fenestra to tip of snout	47
Diameter of the upper portion of the orbit	10
Maximum height of the orbit	17
Maximum length of the antorbital fenestra	19
Maximum height of the antorbital fenestra	8
Maximum length of the depression surrounding the antorbital fenestra	21.5
Maximum height of the depression surrounding the antorbital fenestra	10
Maximum height of the skull between top of the rim of the orbit and bottom of jugal	20.5
Length of nasals along the midline	32
Length of the premaxillary tooth row	9
Length of the maxillary tooth row	27
Length of the external naris	12
Distance from tip of snout to anterior border of the antorbital fenestra	21
Width of skull across the supratemporal fenestrae	17
Width of skull in front of the orbits	10

Length of teeth alveoli

Premaxilla	Left	Right
1.	1.5	—
2.	1.5	1.6
3.	2.0	1.8
4.	1.3	1.5
Maxilla		
1.	1.8	1.5
2.	2.4	2.3
3.	3.0	3.0
4.	2.6	2.3
5.	2.7	2.4
6.	2.2	2.3
7.	2.3	2.1
8.	1.9	—
9.	1.8	—
10.	1.8	—

Length of maxillary teeth, left side, from lateral edge of the maxilla to the tip of the teeth

Tooth No.	Anterior curvature	Posterior curvature
3.	4.6	3.5
5.	5.8	4.7
6.	3.5	2.5
7.	5.0	3.9
8.	3.9	3.1

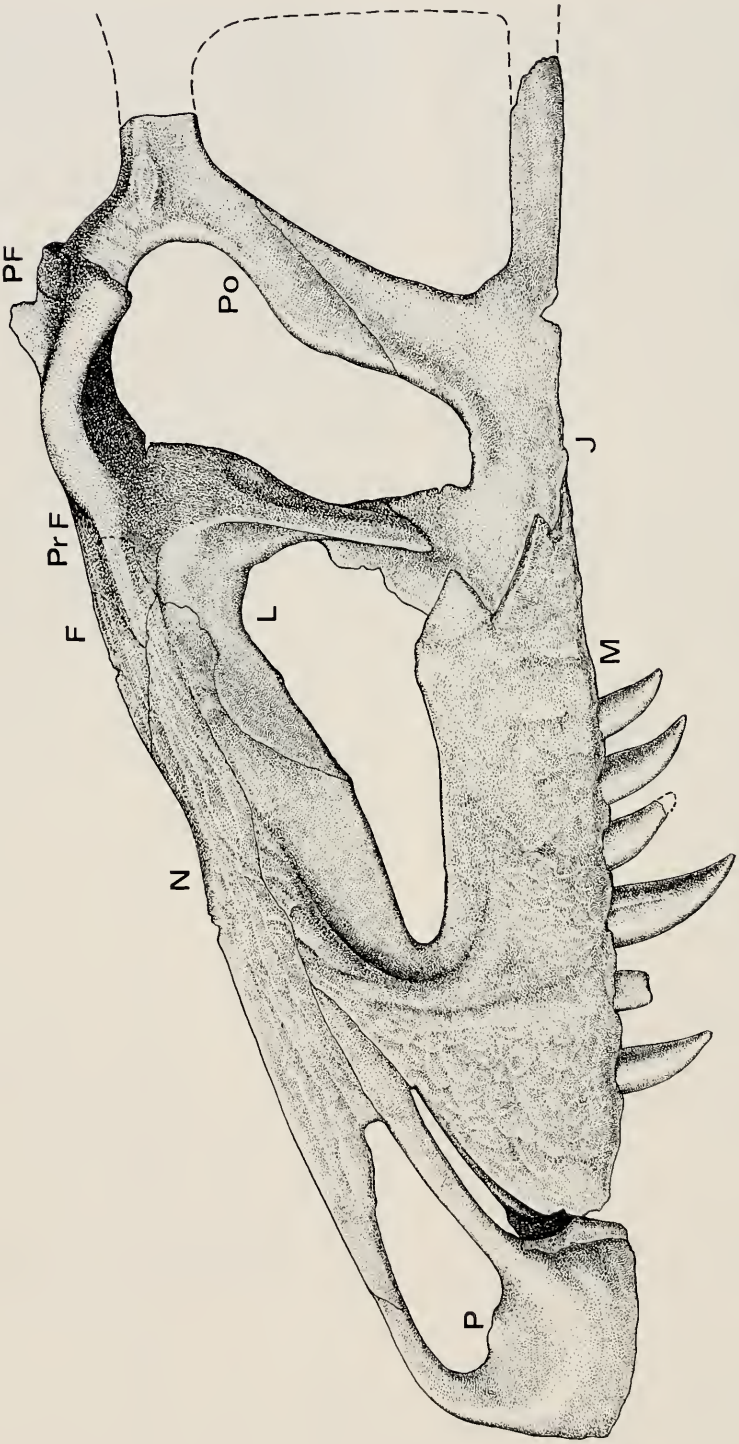

Figure 2. Lateral view of the skull of *Saurosuchus*. P—premaxilla, M—maxilla, N—nasal, J—jugal, F—frontal, L—lacrimal, PrF—prefrontal, PF—postfrontal, Po—postorbital. × ¼.

the entire ventral, and half of the dorsal borders of the antorbital fenestra, meeting the lacrimal in a broad overlapping suture on the smooth shelf portion, and the jugal in a broad zig-zag digitate union. Ten teeth were present on the maxilla, of which seven were apparently functional at any one time. Numerous foramina are present on the lateral surface just above the tooth row.

On the medial surface the most prominent feature of the maxilla is the formation of the alveoli by large interdental plates. The plates are leaf-shaped extensions of the alveolar septa and slightly overlap one another at the middle of the tooth body. Above the plates a prominent groove runs to the dental lamina, which slopes downward posteriorly to terminate on the ventral surface of the maxilla just behind the last tooth. From the groove foramina representing the replacement teeth open directly above each tooth. This morphology apparently represents a standard pattern of tooth replacement, analyzed by Edmund (1957, 1960), in which the fibrous connective bone that surrounds the tooth is partially resorbed during the replacement process to form the shield-shaped interdental plates.

Above the tooth row, in the anterior portion of the maxilla, a massive buttress projects medially to meet the vomer and form part of the vault of the premaxillary chamber. Dorsally, on the medial surface, the maxilla terminates in a straight sloping contact with the nasal and the broad overlap of the lacrimal. Posteriorly the jugal is laminated to the maxilla just above the tooth row. A large maxillary foramen is present just anterior to the jugal suture midway between the tooth row and the ventral border of the antorbital fenestra, on the medial surface.

Nasal. Anteriorly, the nasal is a thin bar above the external naris overlapping the similar element of the premaxilla. From this position it broadens to a dorsal and component thickens considerably near its lateral plate of bone. Posteriorly the dorsal union with the frontals, from .5 to 1.5 cm. The lateral component is not extensive and disappears entirely at the beginning of the antorbital fenestra. At their maximum width the joined nasals are approximately seven centimeters wide, an indication of the narrowness of the anterior portion of the skull. Sculpturing on the nasal is in the form of irregular longitudinal grooves. Union with the maxilla and lacrimal is in a straight sloping line. The suture with the frontal is an inverted V located at the level of the posterior border of the antorbital fenestra.

Prefrontal. The area corresponding to the prefrontal is badly fractured, but this element appears to be a small platelike bone lying in the horizontal plane above the lacrimal. It does not participate in the orbit, but sutures are difficult to distinguish.

Lacrimal. Most of the lacrimal lies in the depression surrounding the antorbital fenestra and is therefore completely smooth, as is that part of the maxilla that participates in the same depression. The lacrimal is an extensive thin plate, forming most of the smooth shelf around the upper part of the antorbital fenestra. Anteriorly it is overlapped by the maxilla. Posteriorly it forms a ventral prong that overlies the dorsal extension of the jugal to form the preorbital bar. The border between lacrimal and prefrontal is not discernible, but must lie in the zone behind the smooth depression of the fenestra. This area is thick and heavily sculptured, and from it arises a prominent lateral ridge that runs down the surface of the preorbital bar, terminating at the tip of the ventral prong of the bone. The lacrimal forms the upper third of the posterior border of the antorbital fenestra, and virtually all of the anterior border of the orbit. There is no definite lacrimal foramen, but a rounded depression is present on the ill-defined internal border between the lacrimal and the frontal. There is no transverse component of the lacrimal.

Jugal. The large skull openings of *Saurosuchus* have reduced the jugal to a hori-

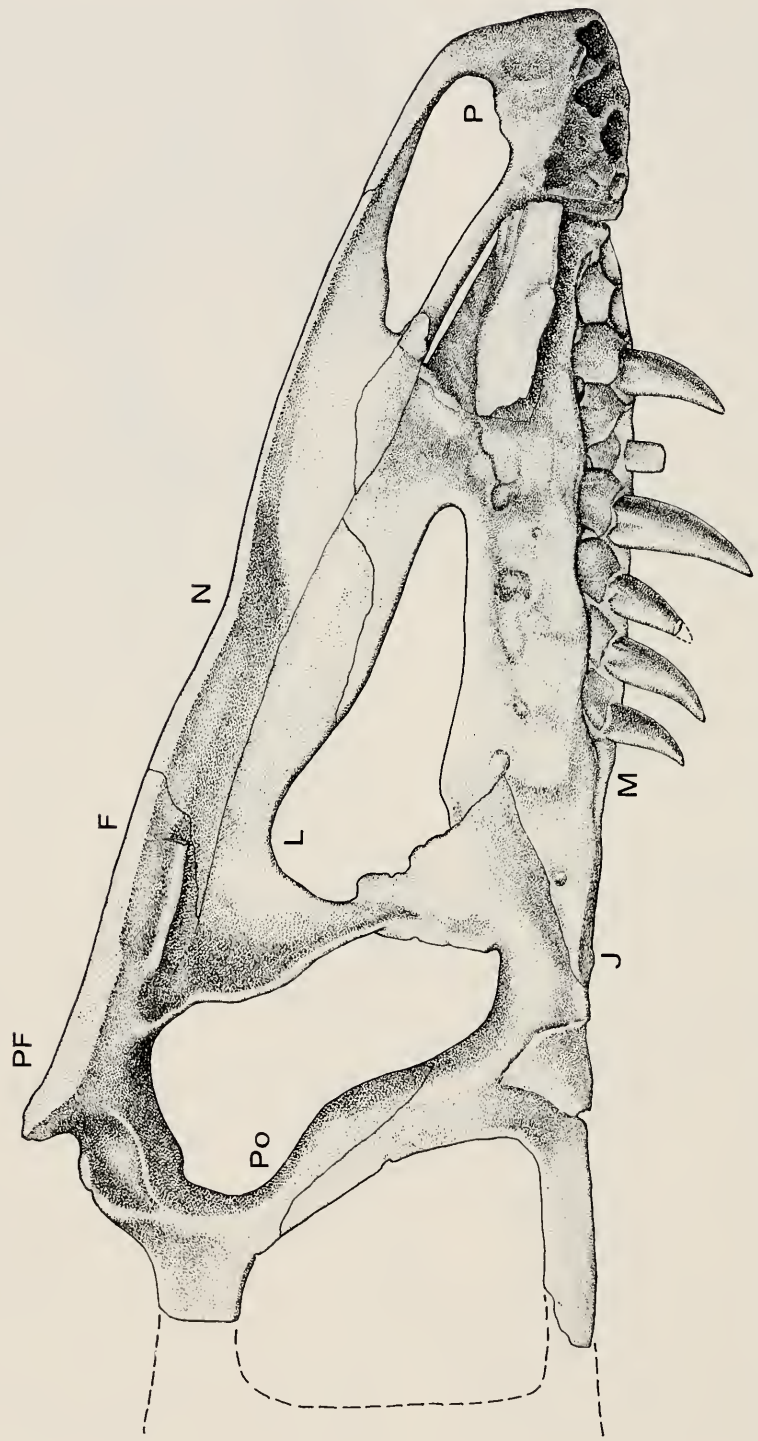

Figure 3. Medial view of the skull of *Saurosuchus*. P—premaxilla, M—maxilla, N—nasal, J—jugal, F—frontal, L—lacrimal, PF—postfrontal, Po—postorbital. × ¼.

zontal rod with two dorsal prongs projecting upwards to form parts of the pre- and postorbital bars. It is most expanded anteriorly where it is platelike and overlapped by the maxilla in a prominent zig-zag suture. Immediately behind this union, the dorsal projection of the preorbital bar reaches up medial to the narrow ridge of the lacrimal. Behind the orbit the second prong of the jugal extends upward and backward to form a strong, sloping, abutted contact with the ventral expression of the postorbital. At the ventral border of the infratemporal fenestra, the jugal is a relatively narrow uniform bone. It thins out to a fine edge on its lateral surface, showing clearly the area where it was overlapped by the quadratojugal. Sculpturing is present only in the anterior portion of the bone, where it meets the maxilla, and even that is light. Only the ventralmost part of the orbit is formed by the jugal, but it constitutes nearly all of the anterior border of the infratemporal fenestra. Directly below the postorbital bar there is an outward bulge in the jugal, forming a distinct pocket on the internal surface, possibly the contact for the ectopterygoid.

Frontal. The frontal is a thick strong bone dominated by the massive supraorbital arch. Medially it curves down from the arch to the midline where its posterior portion meets the anterior projection of the parietal. Anteriorly it joins the nasal and prefrontal in a zig-zag suture. Sculpturing is present, principally on the arch, and is of the pit and groove variety. The thickest part of the frontal is the area of the midline, which in the type is two centimeters deep. Internally there does not appear to be an interorbital septum, but the orbit is well defined by the medial continuation of the orbital arch. Anteriorly the arch forms the previously mentioned pocket at its junction with the lacrimal. Anterior to the orbit the frontal thins to slightly over one centimeter in thickness, and bears a downward-projecting ridge near the midline. This ridge, presumably the border of the olfactory tract, is eight millimeters high at its maximum and tapers off to the level of the bone at the anterior end of the frontal. Behind the orbit, at the junction of the frontal, parietal, postfrontal, and postorbital, a prominent circular pocket is present. This most probably received the anterior process of the laterosphenoid.

Postfrontal. This is a small semicircular bone lying on the dorsolateral surface of the skull between the frontal and the postorbital. It does not enter into the supratemporal fenestra. On the ventral surface of the skull it is not possible to distinguish the borders of the postfrontal.

Postorbital. The postorbital forms nearly all of the posterior border of the orbit, and the upper third of the anterior border of the infratemporal fenestra. Dorsally, just behind the orbital arch, it bears a prominent, sculptured tuberosity. Ventrally, it meets the ascending process of the jugal in a long diagonal contact. The anterior border of the postorbital bar is emarginated and beveled at the delimitation of the circular part of the "keyhole" orbit. On the cranial table the postorbital forms most of the lateral and anterior border of the small supratemporal fenestra. A well-defined, smooth margin surrounds this fenestra, otherwise the upper region of the postorbital is sculptured by linear grooves. Internally, the anteromedial portion of the postorbital forms the rear part of the socket for the laterosphenoid articulation. The posterior part of the postorbital is not preserved in the type.

Nothing remains of the cranial table behind the frontal and postorbital bones in the available material.

Palatal Complex

Palatal remains of *Saurosuchus* are not well preserved, but allow reconstruction of the major features. A primitive character of the palate is the long triangular interpterygoid vacuity. The internal nares are somewhat displaced toward the rear and close to the sides of the maxillae. No traces

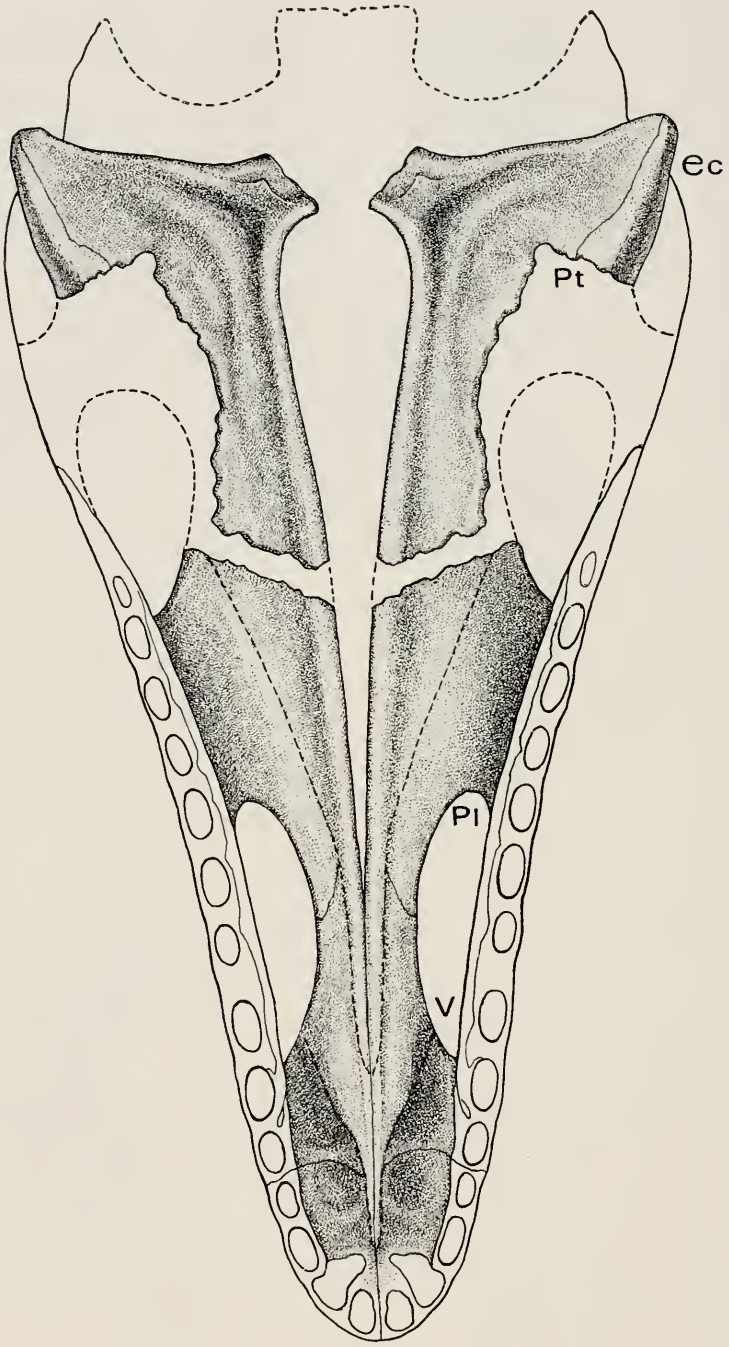

Figure 4. Palatal view of the skull of *Saurosuchus*. Ec—ectopterygoid, Pt—pterygoid, Pl—palatine, V—vomer. × ¼.

of teeth are found on the palatine or on the pterygoid. Although crushed, the palate appears to have formed a deep vault rather than a shelf. The basicranium is not known.

Pterygoid. As usual, the pterygoid is the largest of the palatal bones, and is divided into the customary three components: flange, palatal, and quadrate rami. The palatine ramus consists of a broad thin plate of bone that extends forward from the base of the flange portion and narrows anteriorly to a V-shaped ridge that meets the vomer near the midline. The medial border of the pterygoid is formed by a rounded ridge and steep shelf of bone that form the edge of the interpterygoid fenestra. Only at the anteriormost tip do the pterygoids join at the midline. On the dorsal surface of the palatal ramus a deep groove is present just lateral to the wall of the interpterygoid vacuity. This groove may continue onto the vomer. The flange portion of the pterygoid is massively constructed, and bears a thick, rounded posterior border that curves out to form the "wing." Where the wing meets the heavy ridge that borders the interpterygoid fenestra a deep pocket is formed. Posteromedial to this pocket lies a thick remnant of the basipterygoid articular bar. Anteriorly the flange thins considerably, becoming the same thickness as the palatine. At the posterior margin the flange is 15 mm thick, while anteriorly it is only 4 mm. The angle of inclination of the flange is approximately 45 degrees.

Ectopterygoid. Only the massive portion of the ectopterygoid that forms the lateral border of the pterygoid flange is preserved. This portion forms a strong buttress along the entire lateral edge of the pterygoid "wing." There is no identifiable scar on the maxillae or jugal to indicate the articulation of the ectopterygoid, although it seems probable that the bulge just below the postorbital bar was for reception of the ectopterygoid strut. The massive nature of the preserved portion of the bone indicates that the ectopterygoid served to strengthen the lateral part of the pterygoid.

Palatine. As preserved, the palatine is a thin plate, not possessed of unusual characteristics. Anteriorly it forms the posterior half of the internal naris; the suture with the vomer is well preserved. Laterally it is applied to the side of the maxilla, opening posteriorly into the pterygoid fenestra. The medial border is not well preserved, but appears to have been of the usual platelike contact with the pterygoid.

Vomer. The vomer is poorly preserved and represented only by a distorted and ill-defined mass of bone anterior to the internal nares. As near as can be determined, the vomer formed the anterior half of the internal naris, above which it expanded considerably in the form of a laminar sheet of bone applied to the medial side of the massive maxillary buttress. Possibly, a portion of the vomer behind the maxilla formed a secondary buttress behind the laminar part.

Dentition. Most of the 14 sturdy teeth in the upper jaw are of equal or nearly equal size. In the premaxilla the teeth are not preserved, but to judge from the size of the alveoli, the first and fourth teeth are slightly smaller than the second and third. In the maxilla, the last three teeth show a slight reduction in size compared with the anterior ones. All of the maxillary alveoli show the presence of functional teeth, with the possible exception of the first two, although at least two and possibly three growth stages are represented. The third, fifth, and seventh teeth are the largest, with the fifth slightly larger than the others. The fourth, sixth, and eighth are approximately the same size. The ninth and tenth teeth are broken off at the alveolar border, but were similar to the eighth in size. All of the teeth are of similar shape, heavily constructed, laterally compressed, sharply pointed, and recurved. The last three or four of the maxillary series seem to be more strongly recurved than the anterior members, but this may be due to deformation.

Roots of the teeth are approximately twice as long as the crown. Near the alveolar margin, the teeth are much more compressed and elongate than in the main body of the crown, and on the fully erupted teeth a slight depression is present on the lingual face of the tooth near the margin formed by the alveolar septum (see Plate 1). The teeth are essentially symmetrical, but the plane of symmetry, taken between the anterior and posterior serrations, is slightly rotated anteromedially-posterolaterally. Enamel on the crown is thin and not striated.

Serrations are present on the distal three-quarters of the anterior edge and along all of the posterior margin. However, this condition can be fully appreciated only on the fully erupted teeth; in those teeth that have not reached maturity the serrations continue to the alveolus. Form of the serrations is the same on both edges; they consist of simple crosscuts perpendicular to the long axis of the tooth. Density of the serrations is 12–14 per 5 mm, and is the same on both the anterior and posterior edges. There are no wear facets on the teeth, although the larger ones have a somewhat more rounded apex.

Axial Skeleton

The exact number of presacral vertebrae is not known. Two vertebral series are preserved, PVL 2198 and PVL 2557. The former consists of nine dorsals, all of which bore ribs; the latter series is from the sacral and caudal region and does not duplicate any of the vertebrae of the PVL 2198 series. In PVL 2557 the first two presacrals are preserved and show that ribs were not present on these. As the anterior members of the PVL 2198 series do not show characteristics of cervical vertebrae, it seems reasonable to assume that not more than two vertebrae represent the gap between the presacrals of the two series. Assuming the usual presence of seven or eight cervicals, the vertebral count would fall into the 23 to 25 characteristic of archosaurs. In general, structure of the vertebral column parallels the development found in some prosauropods, and seems to be related to size.

Cervical vertebrae. Only one cervical is known, PVL 2472. It is poorly preserved and of questionable reference to *Saurosuchus*. It was found in association with a tibia and astragalus, also poorly preserved, that appear to be identical to those of PVL 2267. However, the unusual features of the vertebrae warrant its inclusion in this study even though its association with *Saurosuchus* is not completely reliable. Only the centrum is preserved; it is an elongated, flattened structure generally constricted in the middle. The anterior (?) face is strongly concave and bears a protruding lower margin that would seem to indicate a cervical flexure. The rear (?) surface is only slightly concave. There is no keel. In the middle portion, the body of the centrum is not only constricted laterally, but is also greatly flattened, which transforms the whole into a very lightly built structure. Prominent pleurocoels are present just behind the flared articulating surfaces. Thus the lateral border of the centrum is almost a horizontal plate that curves inward to the narrow waist (see Fig. 5). The characteristics of the vertebrae represent an early development of a strong, lightweight support for the cervical region. As such it is compatible with the dorsal vertebrae of PVL 2198, but the flatness and presence of pleurocoels are not found on any of the known dorsal vertebrae. This condition creates an element of doubt about the affinity of this strange cervical. Measurements are as follows: length, 18 cm; width of the anterior surface, 11 cm; width of the constricted waist, 4 cm; and approximate height at waist, 2 cm.

Dorsal vertebrae. Vertebrae of the dorsal series are represented by the first two presacrals of PVL 2557 and by nine articulated members of PVL 2198. The anterior members of the PVL 2198 series are poorly preserved. The most striking feature of the *Saurosuchus* vertebrae is the reduction of

A

B

C

Plate 1. A. Type of Skull of *Saurosuchus*, PVL 2062. × ⅛. B. Lingual view of left maxilla, note interdental plates. × 1. C. Enlarged view of a recently erupted tooth, showing serrations on the posterior edge. × 8.

TABLE 2. MEASUREMENTS OF THE VERTEBRAL COLUMN OF *SAUROSUCHUS GALILEI* (IN CENTIMETERS).

PVL 2472 cervical (?)	
Maximum length	20.0
Transverse width of posterior face	10.5
Transverse width of anterior face	9.0
Minimum width of constricted waist measured on ventral surface	4.0
Height of anterior face	5.3
Height of centrum body at waist	2.0

Dorsal vertebrae PVL 2198	Anterior	Posterior
Maximum length of centrum	7.5	8.5
Height of anterior rim	—	8.7
Width of anterior rim	—	7.2
Width of posterior rim	6.0	—
Total height of vertebrae	20.0	22.0
Minimum width of constricted waist	1.2	1.3
Lateral extension of transverse process from the midline	5.5	4.8
Width of neural spine table	3.0	2.4
Diameter of parapophysis	2.5	2.5
Diameter of diapophysis	2.7	2.7
Height of neural arch above centrum	12.6	13.0

Lumbar and sacral vertebrae PVL 2557	Presacral 1	Sacral 1	Sacral 2
Length of centrum	9.0	10.5	10.0
Height posterior rim	12.0	9.5	10.0
Width posterior rim	10.5	10.0	8.5
Height anterior rim	—	11.0	9.5
Width anterior rim	—	12.0	10.0
Minimum width of constricted waist	4.0	3.7	3.1
Width of neural spine table	4.5	3.6	—
Height of neural arch above centrum	17.6	19.5	—
Total height of vertebrae	28.0	29.5	—

Caudal vertebrae PVL 2557	Caudal 3	Caudal 9
Length of centrum	8.0	7.5
Height posterior rim	9.5	7.0
Height anterior rim	9.0	7.0
Width anterior rim	9.0	6.0
Width posterior rim	9.0	6.0
Minimum width of constricted waist	3.9	2.3
Width of transverse process from midline	11.5	7.0

Chevrons PVL 2557	No. 1	No. 2	No. 3	No. 4	No. 5
Length	18.0	21.0	21.5	21.2	18.5
Width between articulations	7.5	7.5	6.7	6.2	6.0
Width of articular facets	4.0	4.0	4.0	3.0	2.5
Length from facet to fusion with opposite side	4.5	3.8	4.0	3.5	3.2

the centrum to a thin vertical plate between the flared rims. This condition is not as well developed in other thecodonts and seems to be a unique weight-reduction specialization of the genus. Another notable feature of the dorsals is the complete separation between the diapophysis and the parapophysis along the entire known series;

the latter is always found on the neural arch, never on the centrum. Transverse processes are larger in the anterior region than in the posterior, but all are rather short and stubby. The neural arches sit high on the centra and bear flat rectangular spines that are not inclined posteriorly. Size and shape of the vertebrae appear to be uniform throughout the series. All centra are uniformly amphycoelus and do not bear keels. Morphologic changes along the series are not prominent and consist principally of the reduction of the transverse processes in the lumbar region.

In end view the centra are oval-shaped with the long axis in the vertical plane. The rims are flared and rounded, not beveled. Reduction of the body of the centrum took place by expansion towards the rims of the common "hour-glass" constriction. The results are a steeper angle of the constriction behind the rims and the formation of a narrow plate between them (see Fig. 6). No ridges, rugosities or excavations are present on the body of the centrum. Length of the centrum is 7 to 8 cm, width 6 to 7 cm, height is around 9 cm. The body of the centrum expands slightly to receive the neural arch and form the floor of the neural canal.

The neural arch is a large structure that sits high up on the centrum. Contact with the centrum is a simple butt union, without the formation of pedicels. Prezygapophyses are not well preserved, but form short processes that sweep forward on either side of the prominent interspinous notch of the neural spine, just above the articular facet for the capitulum. Apparently the prezygapophyses did not overhang the border of the centrum. The postzygapophyses lie on the same level as the transverse process and are formed from lateral expansions that diverge from the base of the neural spine, creating a wedge-shaped cleft behind it. The zygapophyseal facets are relatively small smooth areas facing downward with a slight inclination toward the midline.

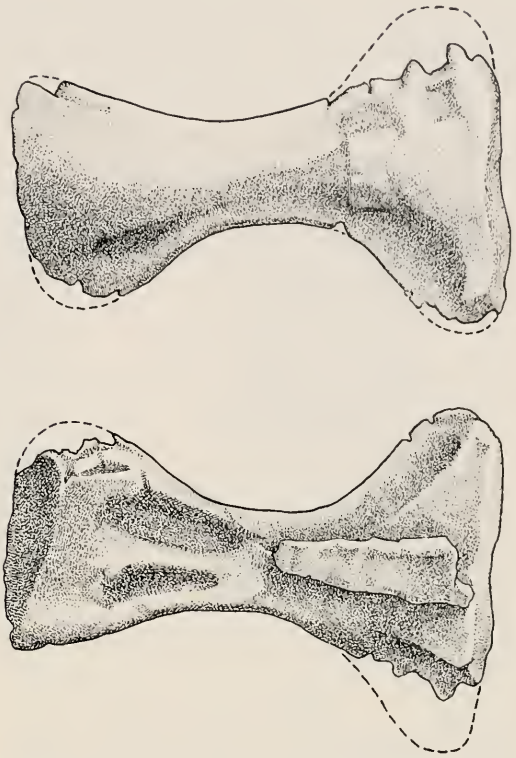

Figure 5. Supposed cervical vertebra of *Saurosuchus*. Top, ventral, Bottom, dorsal. × ¼.

Rib articulations are restricted entirely to the neural arch. The parapophysis is a round facet on the anterior vertebrae of the dorsal series, but becomes laterally expanded into a peduncle on the posterior vertebrae. On all of the dorsals the parapophysis lies below and in front of the transverse process. These processes are short and robust; those of the shoulder region are larger than those of the lumbar series and project posteriorly approximately 30 to 45 degrees. The diapophysis forms as an expanded foot at the tip of the transverse process. On the anterior dorsals this expansion is considerably larger than the parapophyseal facet, while in the lumbar region it is of the same size. A notable feature of the transverse process is the presence of strutlike ridges on the under-

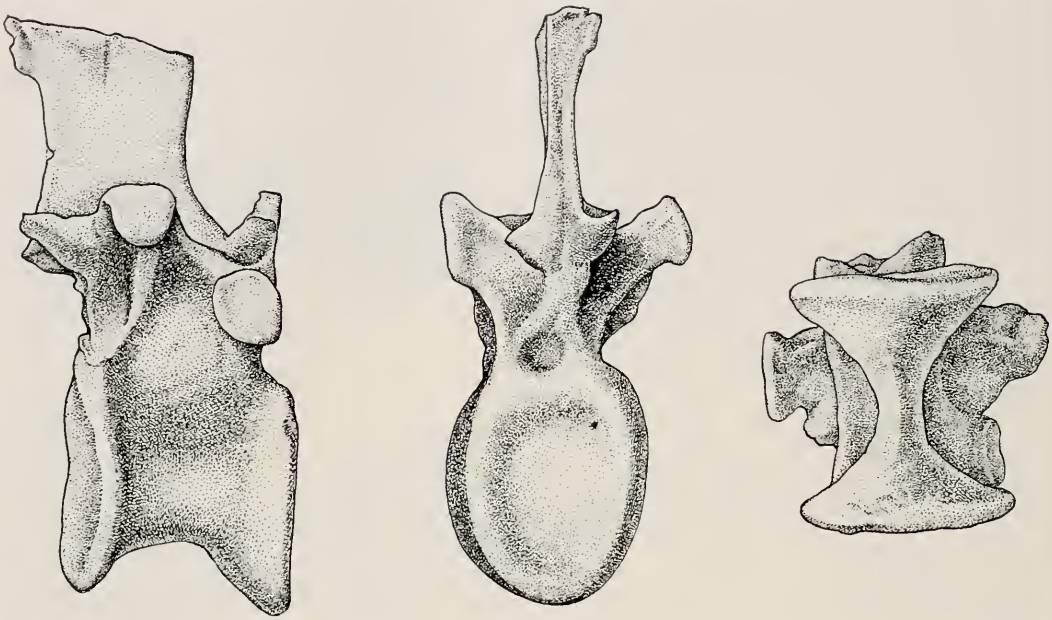

Figure 6. Three views of a dorsal vertebra of *Saurosuchus*. Left, right lateral; middle, posterior; right, ventral. × ¼.

side and edges. In the shoulder region, where the transverse process is largest, four struts are present. One extends to the prezygapophysis, another to the postzygapophysis, a third down to the parapophysis, and a fourth down and back to the rim of the centrum. All of the ridges extend the entire length of the transverse process, and form a strong supporting structure. In the posterior dorsals the strut structure is modified by a reduction to three struts. The parapophysis has moved slightly dorsal, almost to the level of the prezygapophysis and the transverse process is smaller. Only one ridge is present in the anterior portion, extending from the transverse process to the parapophysis. The shorter transverse process and the lateral expanded parapophysis change the aspect of the supporting strut from that of a ridge to a sheet of bone (see Fig. 6).

The neural spine on all of the dorsal vertebrae is a robust rectangular blade, slightly higher than the centrum. As well as can be determined, the blade is not inclined posteriorly on any of the vertebrae. On its dorsal surface the spine is expanded into a spine table, presumably for the attachment of dermal armour. At the anterior and posterior borders the spine does not attenuate, but bears prominent grooves for the interspinalis musculature. On the leading edge the groove occupies the lower half of the length and is deeper at the base. The groove on the posterior margin is shallower but extends the entire length of the blade.

A distinct lumbar region was present in *Saurosuchus*, but it is not possible to determine the number of vertebrae involved. Specimen PVL 2557 has preserved the two vertebrae immediately anterior to the sacrum, and these vary from the other dorsals principally in their lack of normal ribs. It is not possible to determine whether the short downcurved processes are ribs or transverse processes. They appear to be transverse processes, arising from the same

position on the neural arches as those of the anterior dorsals. The processes are oval in cross section and heavily constructed. Their origin on the arch is considerably broader than that of the dorsals of PVL 2198. From the arch they curve slightly forward, then strongly downward.

Sacral vertebrae. The sacral vertebrae are known exclusively from the well-preserved representatives of PVL 2557. Two sacrals are present in *Saurosuchus.* The centra are slightly more elongate than the other dorsals, but otherwise are not different. The sacrals are not fused, but there is a considerable reduction of the rims where the two meet, with the posterior rim of the first sacral flared out at the sides and a corresponding reduction and slight forward extension of the anterior rim of the second sacral. This imparts a slightly V-shaped configuration to the union between the two vertebrae. This condition is repeated in the junction between the last sacral and the first caudal. Such a union must have essentially immobilized the three vertebrae involved, providing a partial substitute for the fusion of the sacrals. The transverse processes of the first caudal vertebrae are not preserved, so it is not possible to determine if it participated in supporting the pelvis. Position and shape of the transverse processes of the sacrals are essentially of the type found in primitive archosaurs; the first is large, oval-shaped, and positioned near the anterior border of the centrum, while the second is more crescent-shaped and arises from the center of the centrum. Both are impressive structures, greatly enlarged and heavily constructed.

Neural spines and arches of the sacral vertebrae are not significantly different from those of the presacrals that form the lumbar region. The spines are heavily constructed and expanded, but form a well-matched series with those of the lumbars. The same is true for the neural arches.

It should be pointed out that the vertebrae of specimen PVL 2557 do not have the centra constricted nearly as much as those of specimen PVL 2198. Whether this difference is due to the difference in size between the two animals (PVL 2557 is considerably larger than PVL 2198) or to their different positions in the vertebral column cannot be ascertained.

Caudal vertebrae. In general the caudals of *Saurosuchus* are of shorter length than the other vertebrae, and have large rounded rims. The first three caudals do not bear chevrons. Diameter of the centra of the first five caudals is essentially equal to that of the sacrals. Beginning with the sixth caudal, there is a gradual reduction in size. Rims of all of the caudal vertebrae are broad and rounded compared to the somewhat thinner rims of the other vertebrae. The area between the rims is not reduced as in the dorsals; the centra are more "typical" in their squat rounded shape. Beginning with the seventh caudal, a slight groove appears on the ventral surface of the centrum. At the eighth or ninth the shape of the centrum changes to the more elongate and spool-like shape characteristic of tail vertebrae in general. Large lateral processes are present on the nine articulated caudals preserved in specimen PVL 2557. The processes of the first four or five caudals are large bladelike structures that extend outward and backward from the level of the dorsal surface of the centra. In caudals numbers six and seven, the outward extensions of the processes are greatly reduced, but they retain the blade shape. In caudals eight and nine, the lateral process loses the bladelike expansion and becomes a simple short lateral process.

Neural spines of the first four caudals are large, cover the entire length of the centrum, and in general are like those of the dorsals. Beginning with the fifth caudal there is a relatively sharp reduction in the anteroposterior length, and in the height of the spine. The spine becomes more inclined caudad and develops a more prominent interligamentum cleft in the anterior border near the base. The sides of the cleft

Table 3. Measurements of the pelvis of *Saurosuchus galilei* (in centimeters).

	PVL 2198	PVL 2557
Ilium		
Length along dorsal border	36.0	41.0
Length of anterior spine from the ventral curvature	4.2	6.5
Length of posterior spine from the ventral curvature	17.0	23.5
Height of dorsal border above acetabulum	6.5	10.5
Maximum height of ilium	23.5	29.0
Width of dorsal border	1.8	2.1
Ischium		
Total length along curvature	42.5	50.0
Width of shaft	3.7	4.1
Height of shaft	3.9	4.6
Height of terminal expansion	5.3	9.3
Width of terminal expansion	5.9	6.1

develop progressively into prominent ridges that sweep forward to form the prezygapophyses. Position of the zygapophyses undergoes a slight progressive shift towards the front; the prezygapophysis begins to overhang the centrum and is accompanied by a corresponding anterior displacement in the postzygapophysis.

Chevrons. Chevron bones first appear on the fourth caudal. The first four chevrons are Y-shaped and bear large disclike pedicels for articulation with the vertebrae. The arms of the "Y" become progressively closer together until they join at the fifth chevron (eighth caudal), leaving a small opening of which only a vestige remains in the sixth chevron (ninth caudal). Construction of the chevrons is simple and not unusual; the expanded pedicel is followed by a long sturdy shaft fused with its opposite just below the centrum. A slight ridge is present on the posterior surface of the shaft. The six preserved chevrons are all approximately the same length (equal to the total height of the vertebrae) and are strongly inclined caudad.

Ribs. Few ribs are preserved. Those available are fragmentary and are covered with a thick iron-rich matrix. They appear to be heavily constructed, thick-bodied, and with a prominent ridge on the upper third of the anterior edge. The posterior surface (at least in the proximal section) is flat with a slight depression down the middle. Rib articulations appear to be well ossified. As may be expected, the largest ribs were the anterior members (size inferred from the relative size of the articular surfaces on the vertebrae).

Appendicular Skeleton

Pelvic girdle. The pelvis of *Saurosuchus* is well represented except for the distal portion of the pubis. Elements available are: left ilium and paired ischia of PVL 2198; right ilium, complete right and partial left ischia of PVL 2557; and a poorly preserved fragmented ilium of PVL 2267. The proximal portion of the right pubis of PVL 2557 is articulated with the ilium of that specimen.

The usual elements of the pelvis were present, in typical triradiate forms. There is no indication of perforation of the acetabulum. A notable feature of the pelvis, apparently common to the Rauisuchidae, is the high position of the pubic articulation and the limited participation of this element in the acetabulum.

Ilium. Two major structural divisions are present on the ilium; the acetabulum and the iliac blade. Most of the ilium is

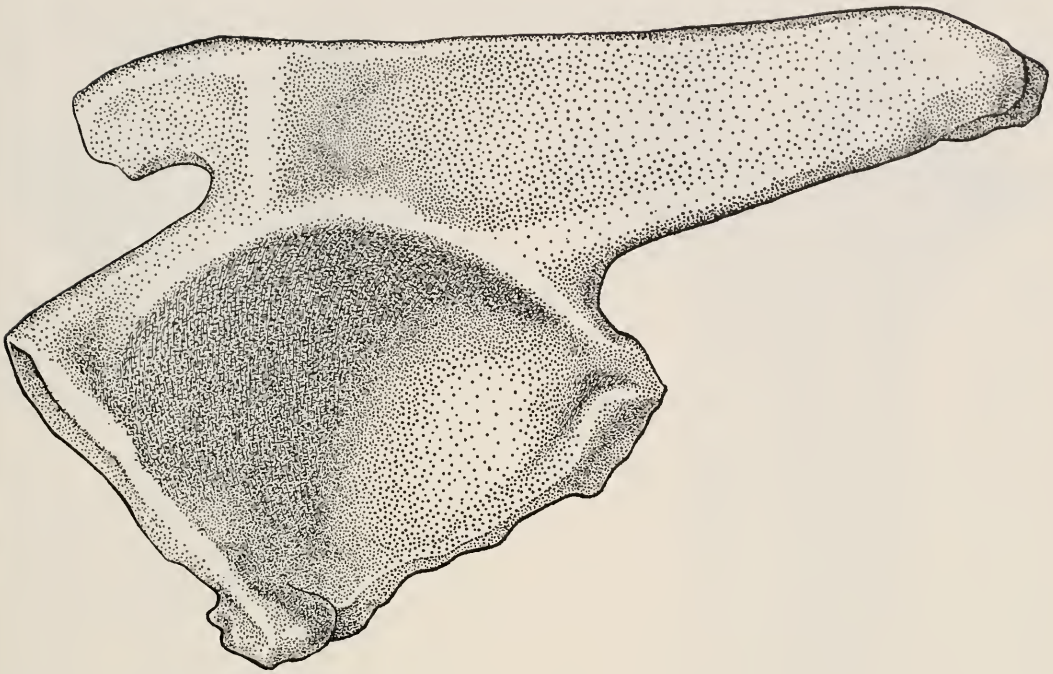

Figure 7. Ilium of *Saurosuchus*. × ¼.

incorporated into the acetabulum, which is a large deep depression that faces slightly downwards. The dorsal margin of the acetabulum is formed by a thick lateral flange positioned just below the anterior emargination of the iliac blade. Ventrally the acetabulum wall thins considerably at its borders with the ischium and pubis. Anteriorly it expands transversely where it meets the dorsal border of the pubis, below which the bone thins, presenting a teardrop shape in cross section. A notable feature of the ilium is its articulation with the pubis and ischium; the suture of the pubis occupies nearly all of the anterior border, starting from a level almost at the dorsal border of the acetabulum, whereas the ischium meets the ilium more in the ventral plane. The ilium is not constricted above the acetabulum. Rather, the anterior origin of the iliac blade arises from an emargination immediately above the thick dorsal margin of the acetabulum, while the posterior portion of the blade sweeps upward and backwards from a level slightly above the midline of the acetabulum. The anterior tip of the blade is short and thick; it does not reach the anterior border of the acetabulum. The posterior portion of the blade consists of three prominent elements: 1) a rounded dorsal ridge, 2) a horizontal shelf on the medial side, midway between the dorsal and ventral borders, and 3) the very thick rounded ventral border of the blade. The internal shelf corresponds to the structure termed "brevis shelf" by Romer (1927) and originates just behind the acetabulum, becoming considerably heavier and thicker at the terminal end of the blade. At its posterior tip the iliac blade is heavily constructed with the brevis shelf lying perpendicular to the blade. Rugosities present in the tip region indicate that it was probably continued in cartilage. Facets for the sacral ribs lie just above the level of the acetabulum. Total

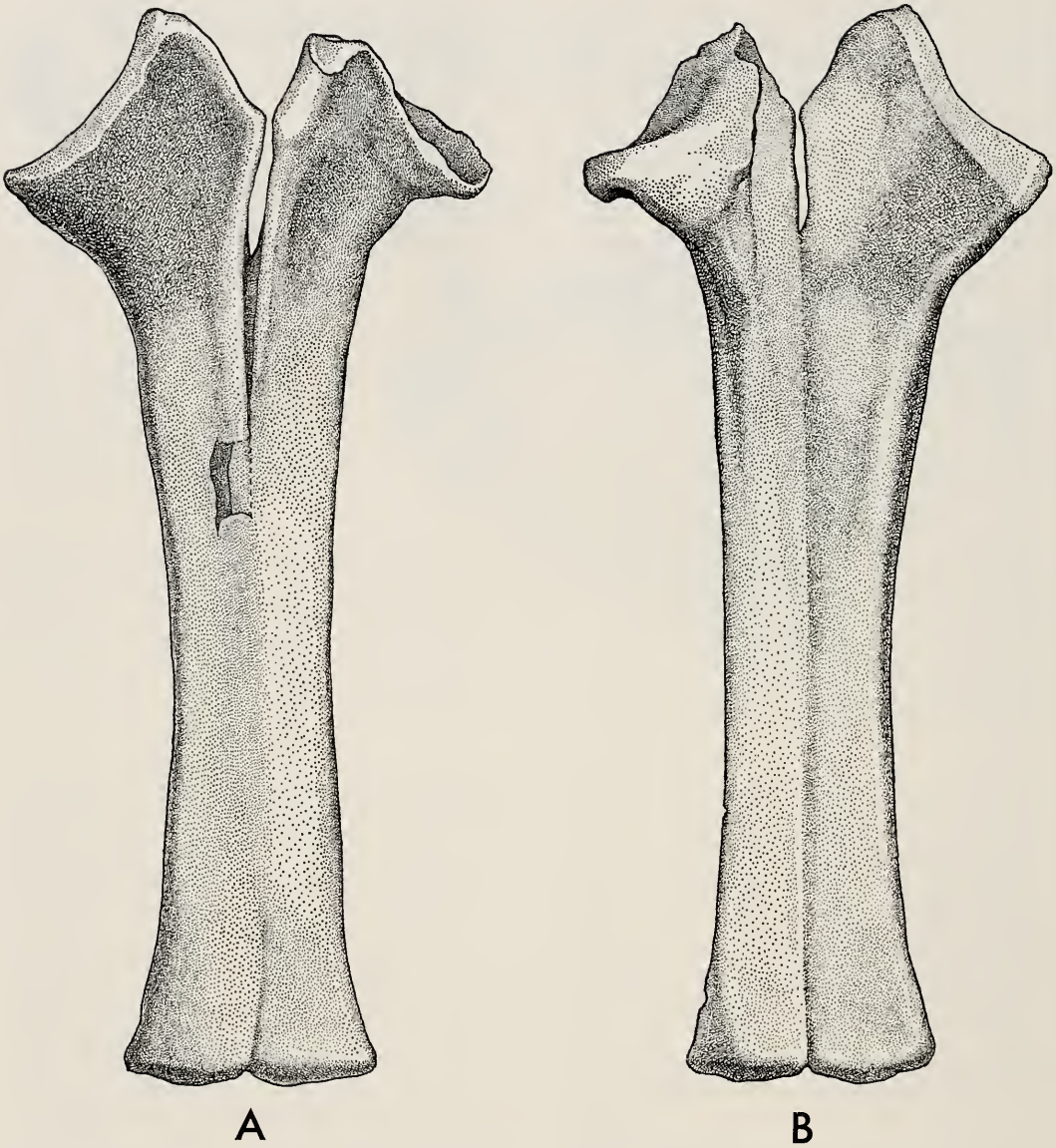

Figure 8. Two views of the paired ischia of *Saurosuchus*. A, ventral; B, dorsal. × ¼.

length along the dorsal border of PVL 2198 is 36 cm of which 16.5 lie below the acetabular rim. Thus the blade above the acetabulum is only 6 cm high.

Ischium. The ischium of *Saurosuchus* consists of a broad flange followed by a relatively long shaft that bears a mild terminal expansion. In general it resembles somewhat that of the dinosaurs in that it is rodlike rather than platelike. Proximally the ischium bears a large expanded head with a prominent lateral lip. As usual, the anterior portion of the head is considerably thinner than the posterior. Anteriorly, below the lip is a deep concavity, where the bone becomes a thin plate that angles to-

Table 4. Measurements of the hind limb of *Saurosuchus galilei* (in centimeters).

	PVL 2267	PVL 2557
Femur		
Approximate total length	65.0	—
Maximum width of proximal articulation	—	7.0
Distance of 4th trochanter from head	17.0	26.0
Thickness of shaft at midpoint	5.0	—
Approximate width of distal articulation	9.0	—

Tibia	PVL 2472	PVL 2267	PVL 2557
Length	46.5	45.0	—
Minimum shaft width	4.0	3.5	—
Width distal articulation	6.5	5.5	6.8
Width proximal articulation	12.0	—	—

Fibula	PVL 2267	PVL 2557
Length approximate	43.0	—
Minimum shaft width	2.7	3.0
Anteroposterior width of distal articulation	8.5	8.2
Transverse width of distal articulation	4.0	5.3
Distance between distal articulation and ilio-fibularis trochanter	21.0	22.0

Astragalus	PVL 2472	PVL 2557
Maximum width across anterior face	10.5	10.6
Maximum anteroposterior length	8.5	9.6
Height on anterior face	3.8	5.0

Calcanium	PVL 2267	PVL 2557
Maximum anteroposterior length	12.5	16.0
Maximum height of tuber	7.5	11.0
Maximum height of anterior face	3.8	5.5
Maximum transverse width	8.0	8.5

wards the midline, terminating in a smooth rounded border that does not touch its opposite member. Posterodorsally, the ischium is a heavy rounded strut arising from the thick buttress that forms the posteroventral rim of the acetabulum. Distal to the expanded head region the two ischia are solidly fused. The symphysis forms a slight ridge down the ventral (anterior) surface of the paired bones. At the distal termination the ischium flares out to a moderately expanded foot, similar to that of *Ticinosuchus,* but more rodlike. In cross section the rod portion is tear-drop shaped, the thin portion being fused to its opposite. This fusion created a channel along the dorsal midline and a corresponding ridge along the ventral surface. The ischium makes an approximately 45-degree angle with the iliac blade, and the strut portion is slightly concave upwards.

Pubis. Only the proximal portion of PVL 2557 is known. It shows that the dorsal portion of the articulation with the ilium was a very thick continuation of the anterior border of the ilium beneath the blade. Below this thick rounded border, the pubis thins rapidly, matching the thickness of the ilium. As noted previously, only the edge of the pubis actually participates in the acetabular depression. From the cross section of the broken portion of the

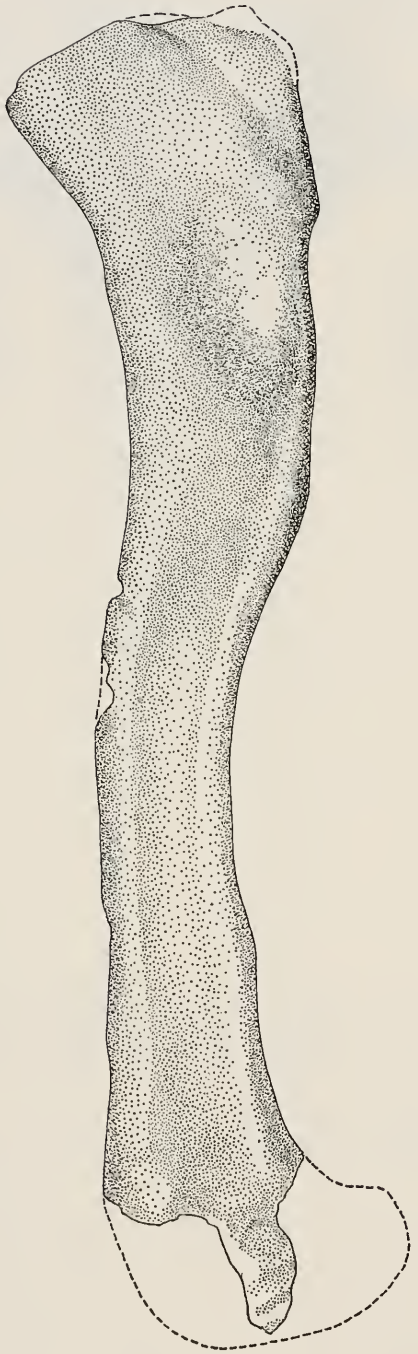

Figure 9. Femur of *Saurosuchus*, composite drawing. × ⅓.

pubis, it would appear that the bone thinned considerably in its anterior portion below the rounded dorsal margin.

Femur. The femur is known from two nearly complete specimens. The complete proximal half of the femur is well preserved in specimen PVL 2557, and was found articulated with the corresponding pelvis. It is well-preserved material but appears to be slightly compressed. PVL 2267, the other femur, consists of a complete shaft but lacks the extreme articular surfaces at both ends. This specimen was figured by Reig (1961) and shows a slight intertrochanteric depression. The depression is a deformation of the particular specimen and not a true anatomical feature.

In its overall aspect, the femur of *Saurosuchus* is of the crocodile type rather than like that of the dinosaurs. The proximal portion is a flange with a wedge-shaped articular head. The shaft is gently sigmoid and oval-shaped in cross section. Distally the termination flares out to what must have been large articular condyles. Owing to the deformation of PVL 2267, it is not possible to determine the degree of rotation of the two extremes, but it appears to have been slightly greater than that of crocodiles. The proximal articulation consists of a rugose tear-drop-shaped surface, the broad portion of which forms a continuation of the thick anterior border of the femur. Behind this section the bone thins rapidly to the posterior edge. In PVL 2557 the broad portion is 5.5 cm thick, the tapered posterior edge is 2 cm. Curvature of the head in toward the acetabulum takes the form of an arc along the anterior border and reaches a maximum of 4 cm of inward displacement from the shaft. There is no formation of structures that can be defined as greater or lesser trochanters. The anterior border of the femur is uniformly thick below the articular head, but in the upper portion it thins rapidly, forming a slight depression on the posterior flange area. Ventrally the bone is smooth, decreasing in thickness from the expansion

of these; there is no intertrochanteric fossa. The posterior edge of the flange area thickens rapidly, becoming part of the shaft at the level of the fourth trochanter. Midway between the articular head and the fourth trochanter a slight expansion is present on the posterior edge. The fourth trochanter is a relatively small rugose bulge arising in the center of the ventral surface, approximately one third of the way down from the proximal articulation, very much like that of crocodiles. Below the fourth trochanter, at approximately half the total length, the proximal flattened expansion disappears into the oval-shaped shaft.

Distally the shaft expands evenly into the distal condyles. These are not preserved, but a remnant of the intercondylar fossa on the dorsal surface indicates that the posterior condyle was the larger of the two.

Tibia. This bone is known from the complete but poorly-preserved specimens PVL 2472, PVL 2267, and the well-preserved distal half of PVL 2557. The tibia is a robust bone approximately twenty percent shorter than the femur. Proximally, the head expands to a triangular shape, the narrow point of which projects anteriorly and medially to form the cnemial crest. This crest extends down one third of the length before merging with the shaft. Posteriorly, the proximal surface is separated by a prominent depression into the condyles for articulation with the femur. This area of PVL 2472 is shattered, but from the area surrounding the depression it would appear that the two condyles were of nearly the same size. The medial surface of the proximal expansion formed the shortest leg of the triangle and bears a slight depression, probably indicating the contact for the fibula. Anterolaterally a broad flat area was present, separating the cnemial crest from the lateral condyle. The shaft is long, subround in cross section and slightly flattened on the anterolateral surface. Distally, the tibia flares out to a transverse expansion equal in size to the articulating surface for the femur. However, it should be noted that in actual articulation with the astragalus the tibia was rotated approximately thirty degrees, orienting the cnemial crest directly forward. Thus the lateral side of the distal termination rested on the anterolateral portion of the astragalus and the medial portion on the posteromedial. The lateral expansion is broad and oval-shaped, the medial is narrow and tapering. Separating the two areas of expansion is a narrow groovelike depression on the posterior face that extends up the shaft to the midpoint (see Plate 2). The major surface of articulation is concave on the underside. All articulations are well ossified and have a shiny surface.

Fibula. The fibula is known from the right distal half of specimen PVL 2557. The shaft is oval in cross section, the long axis oriented anteroposteriorly, and is flat on the medial surface facing the tibia. The most prominent feature of the shaft is the large tubercle on the anterolateral face, just above the midpoint. Presumably, this was for the insertion of the iliofibularis muscle. Above the tubercle the shaft curves slightly outward; below, it is characteristically concave toward the tibia. Distally the tibia has a flared surface for articulation with the calcaneum and astragalus. The articulating surface is lower on the lateral side than on the medial, and bears two grooves corresponding to the two tarsal elements. Articulation with the calcaneum occurs on the large lateral groove behind an anterolateral expansion of the bone. The astragalar articulation occupied a smaller diagonal groove on the anteromedial side of the distal termination.

Tarsus. The tarsus of *Saurosuchus* was of the "crocodilian" type, in which the calcaneum was functionally a part of the foot and the astragalus rotated with the crus. Four elements were present: proximally the large triangular astragalus and the equally large tuberous calcaneum, distally a large lateral tarsal and a much smaller medial one. Elements preserved are: left and right

Plate 2. A. Ilium and Ischium of *Saurosuchus*, PVL 2198. × ⅛. B. Dorsal view of the paired Ischia. × ¼. C. Distal portions of the tibia and fibula of *Saurosuchus* specimen, PVL 2557. × ¼.

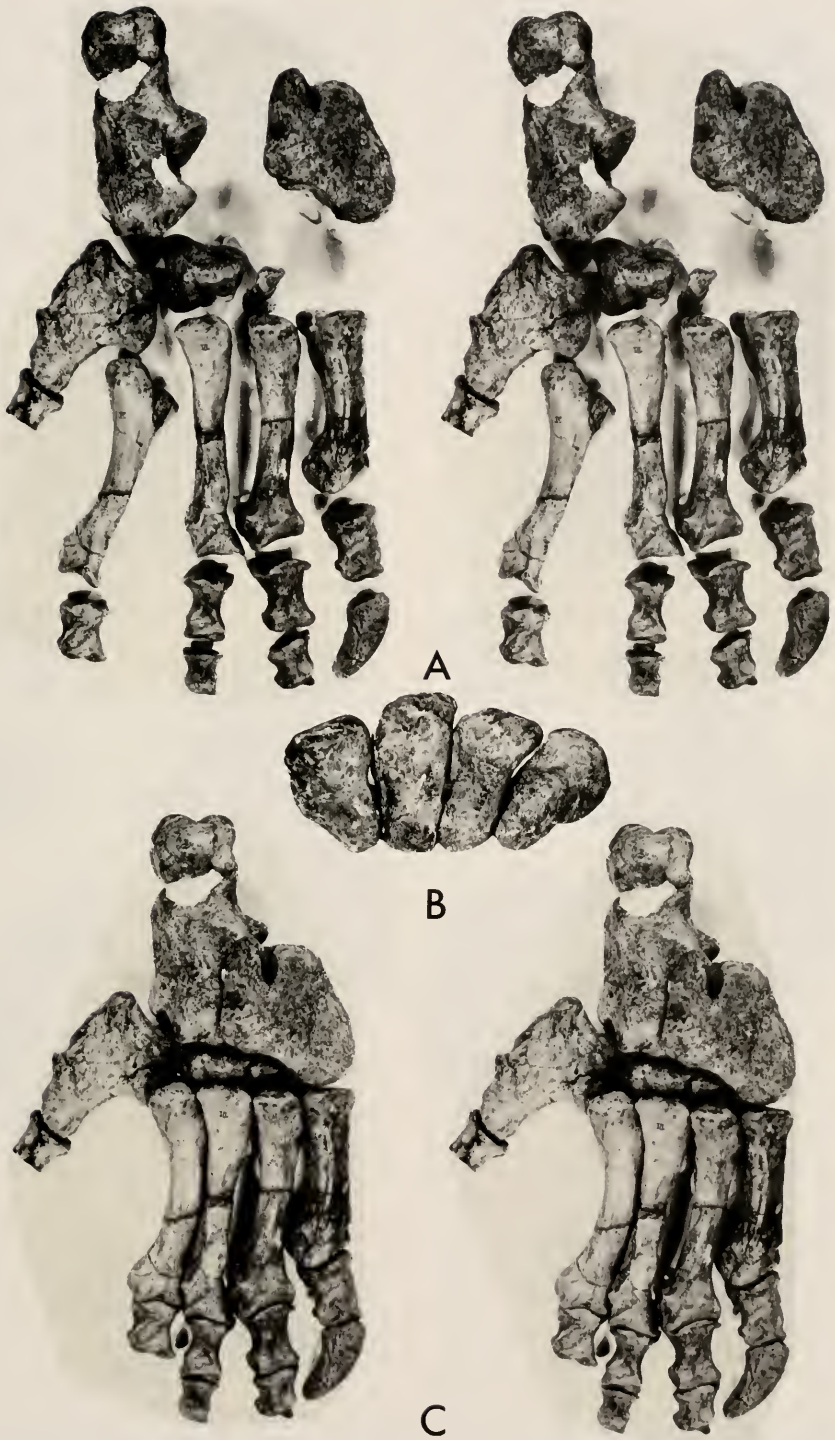

Plate 3. A. Exploded and stereo view of the foot and tarsus, PVL 2557. B. Proximal view of the articulated metatarsals. C. Articulated foot.

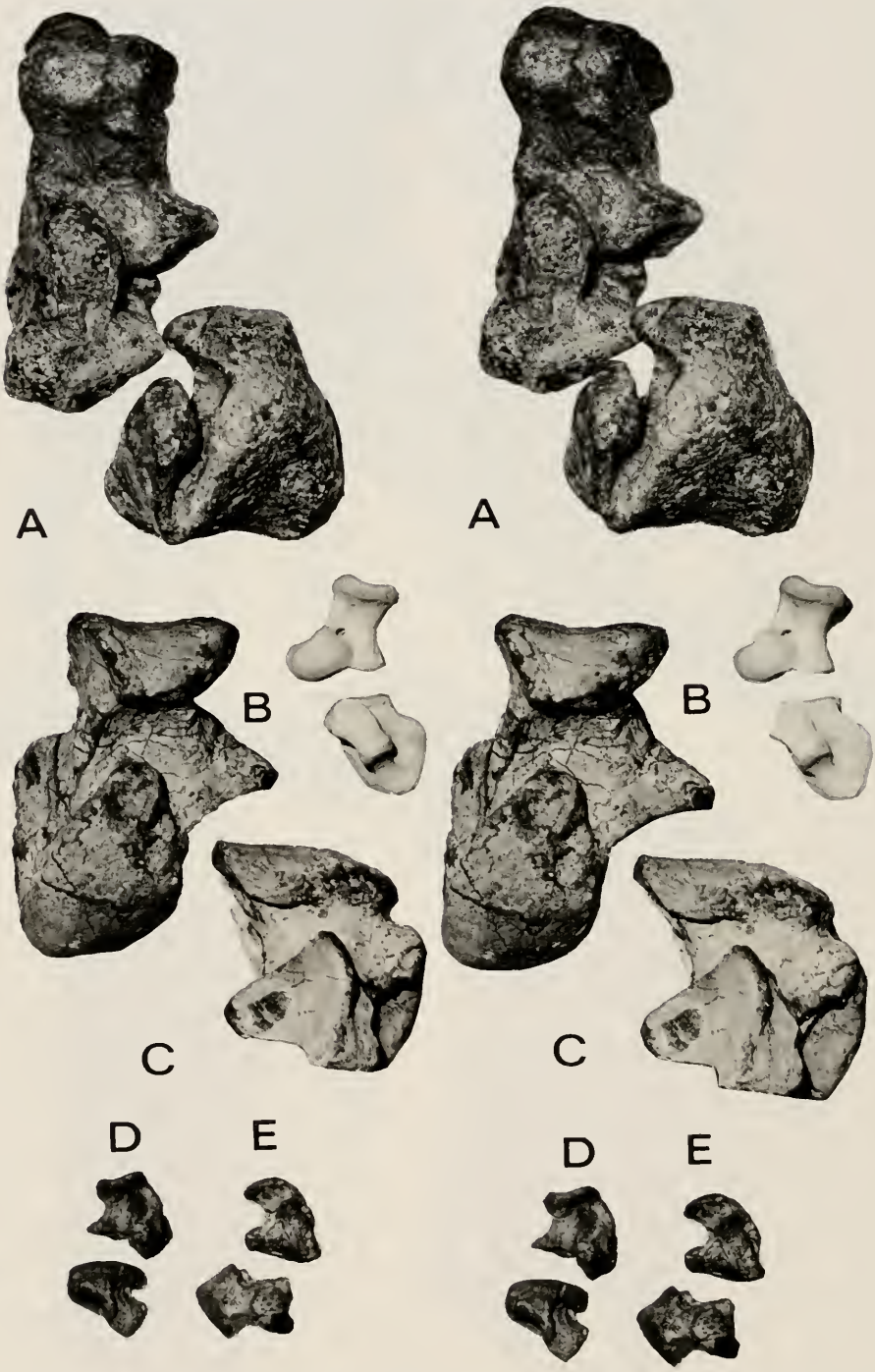

Plate 4. Stereo views of Tarsal elements of: A. *Saurosuchus*, B. *Crocodylus*, C. Undescribed rauisuchid from Los Colorados Fm. (courtesy of Jose Bonaparte), D. *Neoaetosauroides*, E. *Riojasuchus*. (All to same scale.)

calcaneum of PVL 2262, left astragalus of PVL 2472, all poorly preserved but easily identifiable, and the extremely well-preserved complete tarsus and foot of PVL 2557. Adequate description of these complex irregular bones is difficult, and the reader is referred to the stereo-photographs (Plates 3 and 4). The tarsus of *Saurosuchus* appears to be virtually identical to that of *Ticinosuchus*, as described by Krebs (1965), except for minor details. However, *Saurosuchus* was a much larger animal and the tarsal elements are naturally much larger and more heavily constructed. All tarsal elements were well ossified.

Astragalus. The astragalus is an irregular triangular block of bone. On its dorsomedial surface it bears a large, triangular, saddle-shaped area for articulation with the tibia. On the lateral side and separated from this area by a small, steep, forward-inclined ridge, lies the much smaller facet for articulation with the fibula. This surface is much more steeply inclined than that of the tibial articulation, and lies at approximately seventy degrees to it. Anteriorly, the surface of the bone bears a deep excavation, common to most reptiles that have a crocodiloid tarsus, medial to which is the bulbous convexity for articulation with the first metatarsal. A notable feature of the astragalus is its shallow depth. Thus the anteriormost border of the tibial facet is practically on the same level as the first metatarsal articulation. Posterolaterally the face of the astragalus is inclined downward from the peak of the ridge separating the epipodial articulations to the rounded ball that articulates with the calcaneum. Just behind the ridge peak a deep groove is present, which opens up posteroventrally to a curved depression in front of the ball joint. This depression fits over the anteromedial rounded border of the calcaneum. When thus articulated the fibular facets of both astragalus and calcaneum are brought together and a more or less double ball and socket joint is formed. The posteromedial border of the astragalus forms a rather featureless thick rounded border.

Calcaneum. Basically, the calcaneum is a rectangular block of bone that bears a posterior upturned tuber and a medial process that forms the rear border of an anteromedially directed hemispherical socket. Four polished articular surfaces are present on the bone. The anteriormost border is formed by the rounded, slightly ginglymoid articular surface for the fibula. This area is clearly marked and by its terminal position indicates that the calcaneum must have been strongly rotated through its transverse axis, elevating the anterior end and depressing the tuber portion. Medial to the fibular facet is the rounded convexity that faces anteromedially at a forty-five degree angle from the face of the fibular surface, which articulated with the previously described concavity of the astragalus. Again, the area of movement is well marked by the polished surface. Immediately behind this area is the small excavation that forms the anterior expression of the hemispherical socket that constitutes the major articulation between the two proximal tarsal elements. This excavation is continued medially onto the anterior face of the medially projecting process mentioned above, the whole forming a well-developed spherical depression directed inward at an angle of approximately forty-five degrees from the anterior face. The fourth articular surface is a small rounded depression ventral to the fibular facet. This was for the reception of the large fourth tarsal bone. On the dorsal surface of the calcaneum, behind the fibular facet and lateral to the socket, lies a raised molding of bone that did not function as an articular surface and is not marked by muscle or tendon scars. It appears to have been an artifact of ossification. Continuing dorsally, the large tuber calcaneum projects upward and rearward. The dorsal and posterior surface of the tuber is rugose, indicating ligament attachment. The lateral surface is a flat wall, slightly depressed in

Table 5. Measurement of the pes of *Saurosuchus galilei* (in centimeters).

Lateral tarsal								
Transverse width of anterior face	7.0							
Length of lateral articulation with fifth metatarsal	5.5							
Maximum height	4.0							
Medial tarsal								
Height	3.3							
Width	2.2							
Metatarsals PVL 2557	I	II	III	IV	V			
Length	13.7	17.2	17.7	16.5	12.0			
Minimum shaft width	2.5	2.6	2.2	2.2	—			
Width proximal end	4.0	3.5	3.9	3.9	8.0			
Height proximal end	6.3	7.6	7.2	7.0	—			
Width distal end	3.5	4.5	3.8	4.0	4.0			
Height distal end	4.7	4.6	3.8	3.5	—			
Phalanges								
PVL 2557	I_1	I_2	II_1	II_2	III_1	III_2	IV_1	V_1
Length	5.6	8.5	5.8	4.0	5.8	3.4	4.3	3.7
Height proximal	4.3	3.4	4.1	2.7	3.9	2.9	3.0	3.0
Height distal	2.8	1.2	2.7	2.2	2.5	2.0	2.1	2.2

the center portion. Ventrally the surface is also flat, but a small pitlike depression is present at the base of the tuber.

Distal tarsals. Two distal tarsals were present in the foot of *Saurosuchus*, apparently corresponding to numbers III and IV of the primitive reptilian tarsus. The lateral one is the largest of the two and is tetrahedral in shape; the ventral surface is flat, the other three sides form a rounded pyramid dorsally. The dorsal surface is slightly divided into a concavity for reception of an expansion on the astragalus, and a convexity that fits into a shallow pit on the calcaneum ventral to the fibular articulation. Laterally the fourth tarsal bears a large, saddle-shaped, convex, articular surface for the fifth metatarsal. Anteromedially are two convex surfaces, separated by a prominent groove, for articulation of the third and fourth metatarsals. At the extreme medial tip, beside the convexity for the third metatarsal, lies a small concave facet for reception of the third tarsal bone (see Plate 3). This element is a small rounded bone wedged between the lateral side of the second metatarsal and the astragalus.

Pes. The pes of *Saurosuchus* had five sturdily constructed digits in the usual reptilian fashion. Metatarsal V was widely separated from the others, hooked, and bore a broad medial expansion. The remaining four metatarsals were directed straight out from the foot, with a prominent transverse arch in the "instep" region. It is perhaps notable that the expansion of the proximal articulation surfaces of the metacarpals lies in the vertical rather than the horizontal plane (see Plate 3B). Virtually all of the information available comes from the well-preserved right foot of PVL 2557, which is complete except for some of the distal phalanges. Additional elements of the foot are represented by poorly preserved portions of left and right members of PVL 2267. Apparently the phalangeal formula was 2, 3, 4, 5, 3 in the usual primitive fashion. However, the fifth toe may have been reduced to but one or two phalanges. Metatarsal No. 1 is shorter than 2, 3, or 4, is thick bodied, and bears a pulley-shaped distal articulation behind which a prominent diagonal groove traversed the dorsal surface. Proximally, a concave facet is present on the medial side of the articulating surface, the remainder of the surface being smooth. The lateral margin of the proximal tip is vertical, its shape matching the medial border of the second metatarsal, with which it makes a very close fit. The first phalanx is relatively large, almost half the length of the metatarsal, and bears a proximal concavity with a ventrally projecting "heel" for articulation with the rolling surface of the metatarsal. Distally, the joint with the ungual is a shallow ginglymus, narrow at the tip and expanded ventrally. The ungual is a thick-bodied pointed claw, narrow at the top, wider on the bottom, and is half the length of the metatarsal. Largest of the metatarsals

is the second, although numbers 3 and 4 are of similar length. It bears a large narrow proximal articulation, expanded almost exclusively in the vertical plane. On the medial side of the expansion are two facets for the first metatarsal. Laterally, the proximal articulation forms a straight vertical surface with no overlapping contact for the third metatarsal. Midway down the side is a prominent pit, corresponding to a similarly sized notch on the medial side of the adjacent metatarsal. Presumably this formed a channel for nerve and blood supply. The shaft is thickly built, similar to the construction of the first metatarsal, and is concave on the lateral margin but straight on the medial side. Distally the articulation is a large rolling surface with a prominent groove on the ventral border. Just behind the articular surface, on the lateral side, an indentation is present between the flange of the articulation and the body of the shaft. Shape and articulation of metatarsals show that the axis of the transverse "instep" arch ran between the second and third metatarsals. Two phalanges of the second metatarsal are preserved. As might be expected, they are the largest and most heavily constructed of the digits. The first bears a large concave flange proximally, a short shaft, and a distal articulation similar to that of the metatarsal. However, the groove is considerably larger than that of the metatarsal. The second phalanx is subrectangular in shape, and has a smooth concavity proximally and a pulley-shaped articulation distally. Although the ungual is missing, the size and shape of the distal articulation indicates that the claw was approximately the same size as that of the first ungual. Metatarsal number 3 is appreciably more slender than the others and is slightly longer than the second or the fourth. Its proximal expansion is of similar size and shape to that of metatarsal number 2, but whereas that of the second is a straight vertical surface, the third has a diagonal proximal surface with the dorsal portion extended more posteriorly than the ventral. The medial margin is expanded at the top to form a bulge, with the aforementioned groove lying just below it. Laterally the proximal articulation bears a concavity on the dorsal portion and a small convexity ventrally, corresponding to opposite features on the close-fitting fourth metatarsal. Distally the articular surface of metatarsal number 3 is similar to that of number 2 but smaller. The rounded flange is more expanded on the medial side than on the lateral, and a groove is present behind the flange on the medial side. Only the first two phalanges are preserved; they are virtually identical to those of the second digit, but somewhat more slender. The fourth metatarsal is slightly shorter and more heavily constructed than the third. Its proximal articulation is diagonal in the vertical plane like that of the third, but on the surface itself a prominent excavation is present below the side dorsal border for the reception of the bulge of the fourth tarsal. A major feature of the fourth metatarsal is its bowed shape; it is concave on the lateral side, with the convex medial side fitting closely against the side of metatarsal number 3. This curvature also serves to rotate the plane of the promixal articulation approximately twenty degrees from the vertical, toward the lateral side, from the plane of the distal articulation. On the lateral surface of the shaft in the proximal region anterior to the articular surface is a prominent triangular depression, apparently for muscles and flesh related to the lateral plantar pad of the foot. Distally, the articular surface consists of a pulley-shaped convexity somewhat different from that of the other metatarsals. The groove runs diagonally across the articulation from ventrolateral to dorsomedial. Ventrally, medial to the groove a prominent heel projects downward. Laterally, just behind the articular surface lies an expanded process that continued onto the shaft, making a pronounced curvature of the lateral border of the shaft, and giving the distal articulation the aspect of being offset towards

Figure 10. Two views of a posterior scute of *Sauro-suchus*. Left, dorsal; right, ventral. × ½.

the medial side (see Plate 3). Only one phalanx of the fourth digit is present; it is rectangular, heavily constructed, and in general similar to that of the second digit, although somewhat smaller and flatter. The proximal surface is more clearly divided into lateral and medial concavities than in the other digits. Distally the articular surface is considerably flatter, and lacks the downward extension of the rolling surface found on the first phalanges of the other digits. These are indications that the fourth toe was probably long and relatively slender. Specimen PVL 2267 has three isolated articulated phalanges that probably belonged to the fourth digit. These show a rectangular shape that rapidly diminishes in length distally with the last of the series, probably the pre-ungual, little more than a transverse rectangular chip of bone. However, the association of these three phalanges (PVL 2267) is not certain. In *Ticinosuchus* all of the phalanges are longitudinally rectangular, as are all of the proximal ones preserved in PVL 2557. Metatarsal number five is a massive hook-shaped element that bears a large hemicylindrical articular surface on its medial side for the matching concavity of the fourth tarsal bone. On the anterodorsal face of the surface is a small facet for the lateral edge of the fourth metatarsal. Behind the large ball surface, the posterior border curves laterally and posteriorly to terminate in a rounded point at the rear lateral edge. From this point the lateral margin curves out and forward to the distal tip. A small expanded process is present on the lateral edge one third of the way back from the distal articulation. The medial surface of the "shaft" curves smoothly from the anterior tip of the major proximal articulation to terminate in the blunt surface of the distal articulation. This articular surface bears neither flanges nor grooves, but is a simple, slightly convex surface. The first phalanx is rectangular in shape, broader at the proximal end, and bears an expanded concave articular surface that partially envelopes the convexity of the metatarsal. Distally, the phalanx terminates in a simple flat vertical surface devoid of rounded features. No other phalanges are known for the fifth digit. The fifth toe was widely separated from the other digits.

Dermal Armour

Scutes have been found associated only with PVL 2198. These were found partially articulated with the vertebral column, and like most of the vertebrae, are poorly preserved. Three articulated scutes, much smaller than the others, were found in association with the other bones of the specimen, but not in a definable position. As they are very well preserved, and in general the degree of preservation becomes better caudally in PVL 2198, it is assumed that these scutes were from the posterior dorsal region. Two paramedian rows of scutes were present on the dorsal region of *Sauro-suchus*, the total width being 10 cm on specimen PVL 2198. As preserved, the two rows do not appear to have been joined by a strong sutural contact. The dorsal scutes are slightly asymmetrical and leaf-shaped in outline, drawn to a point in front and truncated at the rear. They are imbricated, the wide rear margin overlapping the point of the scute just caudal to it. Although the two rows join at the midline, the medial border is only slightly thicker than the

lateral. The anterior point is slightly asymmetrical; it is off center toward the medial border. Dorsally the scutes are gently arched in cross section, slightly more so on the lateral side than on the medial. A keel as such is not present, but there is a slight longitudinal ridge. Possibly a small indentation was present on the posterior border. Ventrally there appears to be but a slight indentation in the posterior portion to receive the point of the following scute. A significant change in size takes place along the length of the series; the posterior scutes are smaller than the anterior ones, changing from approximately 5 cm in width to 4.

The three isolated scutes differ considerably from the others, but are of the same pattern and certainly belong to the same specimen. They are, however, perfectly symmetrical, with each edge tapered to a very thin border (see Fig. 10). Anteriorly the point is longer and more tapered than in the other scutes, and fits into a wedge-shaped groove in the preceding scute. The dorsal surface is prominently ridged in the center, leading to the point anteriorly and to an indentation posteriorly. These characteristics suggest that these were members of a single row of scutes, rather than paired. A similar condition is reported for *Ticinosuchus* by Krebs (1965), and is to be expected given the other similarities of the two genera. The greatest difference between the dorsal and the lumbar scutes is size; the former are 5 cm wide and approximately 7 cm long while the latter are 3 cm wide and approximately 4 cm long. This condition differs from that of *Ticinosuchus* in which the scutes of the unpaired row are larger than the paired. However, the overall aspect of the armour of *Saurosuchus* is that it is more reduced relative to the size of the animal than is that of *Ticinosuchus*.

DISCUSSION

Origin of the Rauisuchidae

The anatomical characteristics of the known members of the family strongly

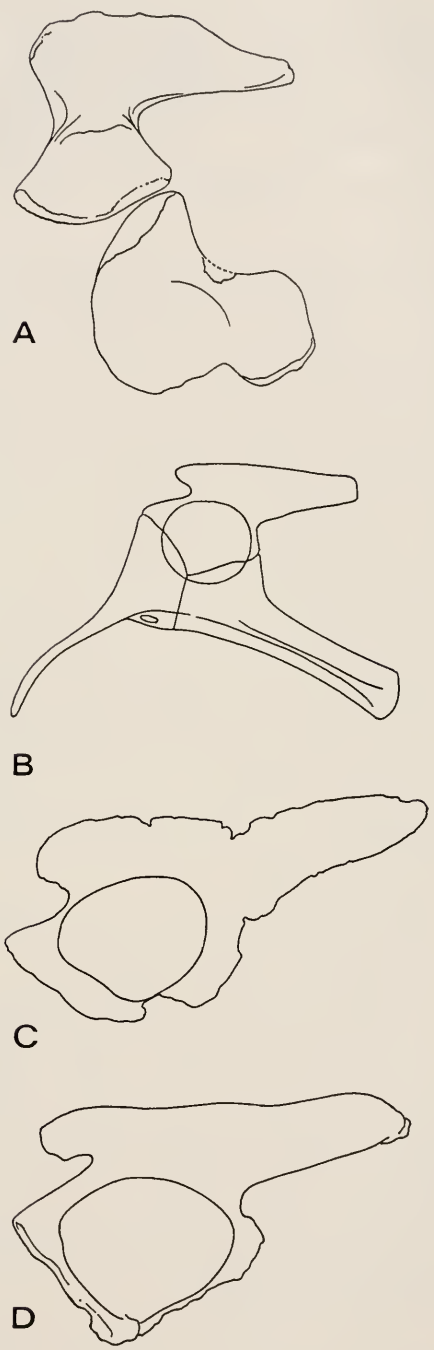

Figure 11. Pelvis of: A, *Shansisuchus* (after Young); B, *Ticinosuchus* (after Krebs); C, *Rauisuchus* (from a photograph *in* Huene, 1942); D, *Saurosuchus*.

Figure 12. Left, calcaneum; right, astragalus of *Shansisuchus* (after Young).

suggest direct derivation from the erythrosuchids, rather than from ornithosuchids or from a common erythrosuchid-ornithosuchid ancestry. Cranial anatomy is but little modified from the erythrosuchid condition (see Fig. 13). Within the Erythrosuchidae, the most advanced member (both anatomically and stratigraphically) appears to be *Shansisuchus* from the Ehrmaying Series of China (see Young, 1964; Reig, 1970; and Charig and Reig, 1970). This genus provides a rather good intermediate between the two families, and indeed was tentatively included in the "Prestosuchidae" by Romer (1972a). However, it still retains the primitive pelvic girdle and simple tarsal structure common to the Erythrosuchidae. As locomotory abilities seem to have been a principal evolutionary factor within the Rauisuchidae, it would seem appropriate to consider the less advanced *Shansisuchus* as an erythrosuchid.

Major characteristics of the rauisuchids that can be traced with a reasonable degree of confidence through the lineage are:

1) Skull configuration: a keyhole-shaped orbit, large antorbital fenestra surrounded by a smooth depression, small supratemporal fenestra, high narrow cranial table, and a posterior prong on the premaxilla. Some of the genera have an accessory antorbital fenestra between the premaxilla and the maxilla.

2) Vertebrae: high neural arch, straight rectangular spine with distal expansion, deep interspinous clefts.

3) Pelvis: prominent posterior spine, presence of a brevis shelf, styliform ischium with an expanded tip, greatly reduced pubic plate, pubis with slight participation in the acetabulum.

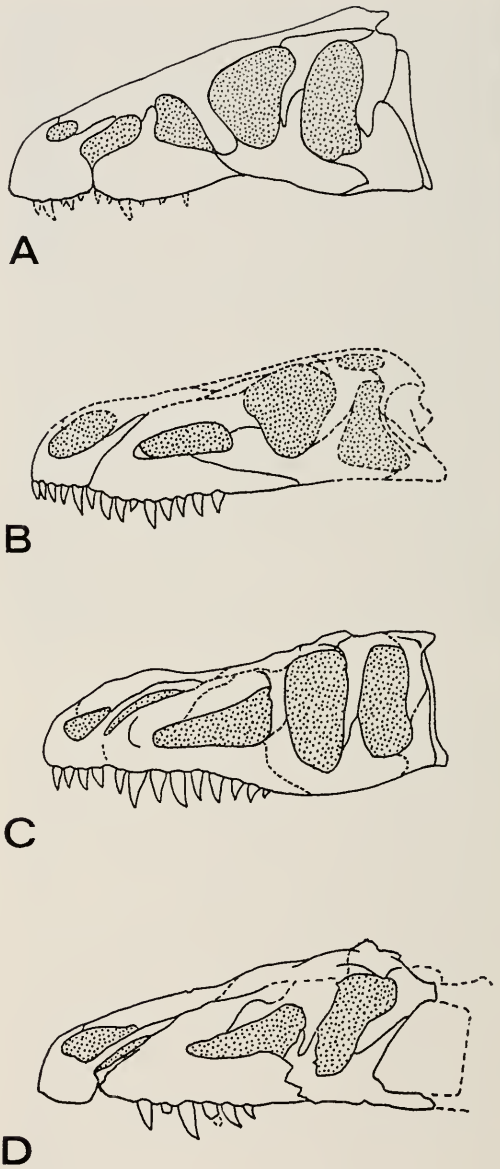

Figure 13. Comparison of cranial morphology in A, *Shansisuchus* (after Young); B, *Ticinosuchus* (modified from Krebs); C, *Luperosuchus* (from Romer); D, *Sauro-suchus*. Not to same scale.

4) Femur: crocodilelike, without rounded medial expansion.

5) Tarsus: ball and socket crocodiloid type, fifth metatarsal hooked.

The several genera that make up the

Rauisuchidae can be separated into three morphologic groupings that reflect both their stratigraphic position and their probable phylogeny: 1) an early group, represented by *Ticinosuchus* from the earliest Middle Triassic; 2) an extensive intermediate group represented by *Luperosuchus, Stagonosuchus, "Mandasuchus", Prestosuchus,* and *Rauisuchus* from the later Middle Triassic; and 3) *Saurosuchus* and the undescribed form from the Los Colorados, of earlier and later Late Triassic respectively. *Ticinosuchus,* the earliest member of the family, and the only one known from a complete skeleton, has a skull that has been highly fractured and compressed to a largely two-dimensional state. As reconstructed by Krebs, the skull is similar, but not strikingly so, to *Saurosuchus* and *Luperosuchus.* However, using the more complete knowledge afforded by the Argentine specimens, it is possible to reinterpret to some degree the skull of *Ticinosuchus* on the basis of the published photographs. Two modifications of Krebs' reconstruction appear feasible: the antorbital fenestra was probably smaller than shown and was surrounded by a smooth shelf, and the anterior border of the maxilla was inflected just above the tooth row, possibly indicating a small accessory opening similar to that of *Saurosuchus.*

Cervical vertebrae represent the only anatomical character that shows a considerable degree of variation among the several genera of the family. In *Ticinosuchus* the cervicals are elongated, but otherwise unspecialized. A similar condition appears to be present in *"Mandasuchus"* but not in *Stagonosuchus, Prestosuchus,* or *Rauisuchus.* Only one cervical vertebrae is known from *Saurosuchus;* it is a highly specialized elongate structure so different from other known forms that it is assigned to the genus with reservation.

In the other comparable features characteristic of the family, there is a remarkable similarity among the genera definitely assigned. More subtle differences distinguish *Saurosuchus* as the most progressive of the described rauisuchids[1]; centra of the vertebrae are constricted, the ischium is longer and more rodlike, and the femur is more gracile than the corresponding features of the other genera.

Within the Ischigualasto Basin three rauisuchids are found in the sequential continental sediments. The earliest of these is *Luperosuchus* from the Chanares Formation (Romer, 1971a). It has already attained the large size characteristic of most of the family, but is known only from an incomplete skull. Changes in the skull from *Luperosuchus* to *Saurosuchus* to the Los Colorados form were slight; the orbit became more circular in the upper portion and the smooth shelf around the antorbital fenestra is larger in the later genera. It seems reasonable to assume that these three forms were continuous members of a single regional lineage. Very possibly *Prestosuchus* from Brazil should be included in the lineage. *Prestosuchus* is very comparable to *Saurosuchus;* apparently the only significant difference is that the femur of the former appears to be more heavily constructed and less gracile than that of the latter. Relationship of the Ischigualasto Basin forms to other members of the family is not as close. The vertebrae of *Stagonosuchus* are somewhat constricted like those of *Saurosuchus,* but the pelvis is more primitive. *"Mandasuchus"* is quite similar to *Saurosuchus,* and the two may be congeneric or they may be closely related forms similar to *Prestosuchus* and *Rauisuchus. Rauisuchus* itself is less like the other members of the family and its association with the group has been questioned (Charig 1967, Romer, 1972a, Walker, personal communication). Walker (personal communication) has suggested that *Rauisuchus* may be an ornithosuchid. His suggestion is based principally on some aspects

[1] The undescribed rauisuchid from the Los Colorados Formation is larger than *Saurosuchus;* it had a considerably more advanced tarsus, but a very similar skull (Bonaparte, personal communication).

of the skull fragments and on the dermal armour. However, the premaxilla bears the posterior projecting prong that separates the external naris from the maxilla, and its overall shape is similar to that of *Saurosuchus* and *Luperosuchus*. The ilium figured by Huene (1942, plate 27) is remarkably like that of *Prestosuchus* and *Saurosuchus* (see Fig. 7). Other elements are not as closely comparable, giving rise to the doubts about the affinities of the genus. However, the morphology of the vertebrae and dermal armour are not inconsistent with that of the other members assigned to the family, and their resemblance to ornithosuchids may be superficial, as are a number of the resemblances between the two groups (see discussion of vertebrae and tarsus). For the present, I would leave *Rauisuchus* in the family association that is termed "Prestosuchidae" by some authors, but recognize that it is less comparable to the larger genera *Prestosuchus, Saurosuchus,* and *"Mandasuchus"* than these are to each other.

It would seem likely then that the Brazilian and Argentine genera were part of a South American radiation, perhaps from a *Luperosuchus*-like stock. The African forms, *Mandasuchus* and *Stagonosuchus,* may represent a separate but closely related line.

A summary of the evolutionary history of the Rauisuchidae would then be: origin in the early Middle Triassic from a progressive group of erythrosuchids, the first members of the family probably near the *Ticinosuchus* level; adaptive radiation in the Ladinian and Carnian; survival of specialized members that could compete with dinosaurs in the uppermost Triassic, and extinction of the group by the Early Jurassic (see Fig. 14).

Habits of the Rauisuchidae

On the basis of the known remains, the rauisuchids can be described as large quadrupedal animals ranging in total length from three to six meters. The sharp serrated dentition leaves no doubt that they they were carnivores, and the deep narrow skull would suggest predaceous habits. During the Middle and Late Triassic they were probably among the largest of the terrestrial carnivores. Regarding locomotion, the hind limbs were of the crocodiloid grade of evolution, and as such the rauisuchids were reasonably good runners, although no doubt less agile that the later dinosaurs and probably less agile than the contemporary Ornithosuchidae.[1] Rise of the rauisuchids may have been parallel to the rise of the rhynchosaurs and the gomphodont cynodonts during the Ladinian and Carnian in a predator-prey relationship. It is usually assumed that the large thecodont predators disappeared during the Late Triassic owing to the competition from dinosaurs. However, the presence of a very large, advanced rauisuchid in sediments considered to be Late Norian in age (see Bonaparte, 1972a and Sill, 1969 for details on the stratigraphic relationships of the Argentine Triassic), would indicate that these thecodonts had become adapted to prey on the early saurischians, many of which were herbivores. The last known rauisuchid was a very large animal and had an advanced digitigrade foot. Nevertheless, the femur remained at the crocodiloid stage of development, namely, without the formation of a medial condyle or a shift to the parasagittal plane of the body. Assuming that the vertical position of the limbs was an important adaptation, the rauisuchids would have been at a disadvantage with regard to the emerging carnivorous dinosaurs. Such a relationship presumably would explain the extinction of the group as the dinosaurs became dominant.

Thecodont Taxonomy and Phylogeny

Although thecodonts have long been recognized as the key group in the rise of

[1] However, Bakker (1972, and in press) has shown by experimental data that the physiologic cost of locomotion is dependent only on speed and body weight, entirely independently of limb posture.

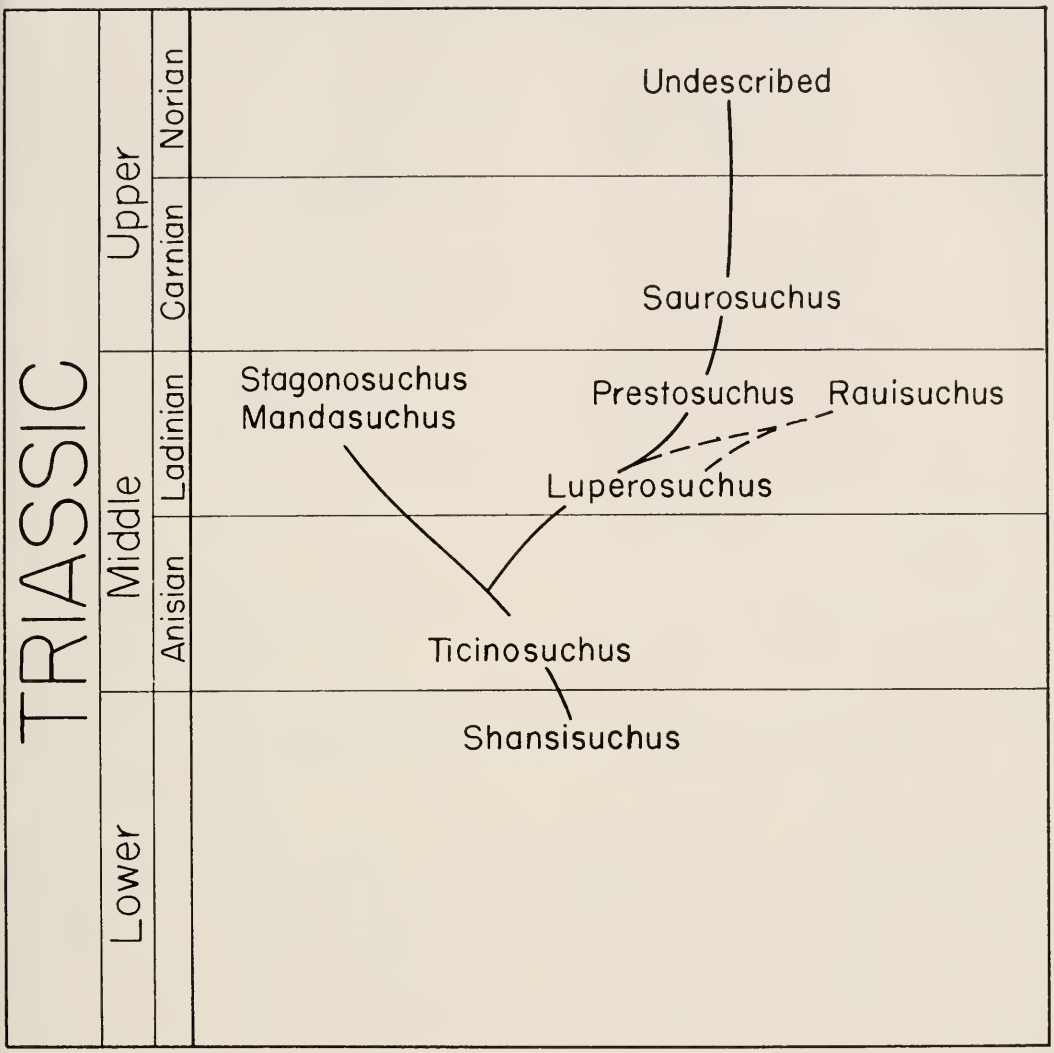

Figure 14. Suggested phylogeny of the Rauisuchidae.

the archosaur faunas that dominated the later Mesozoic, they have been a poorly known and confusing group. As new discoveries have been made in the last few years there has been a renewed interest in the order, and at last the prospect emerges of unraveling the many and varied thecodont lineages. Traditionally, thecodonts have been divided into three groups: 1) the very primitive forms from the Early Triassic, 2) the highly specialized taxa of the Late Triassic, phytosaurs and aetosaurs, and 3) the main stream, Pseudosuchia, somewhat of an "everything else" suborder. The new discoveries have permitted the clarification of some relationships, and have added a new lineage, Proterochampsidae, to the order. But the major relationships are still far from settled, and there is a considerable number of genera that do

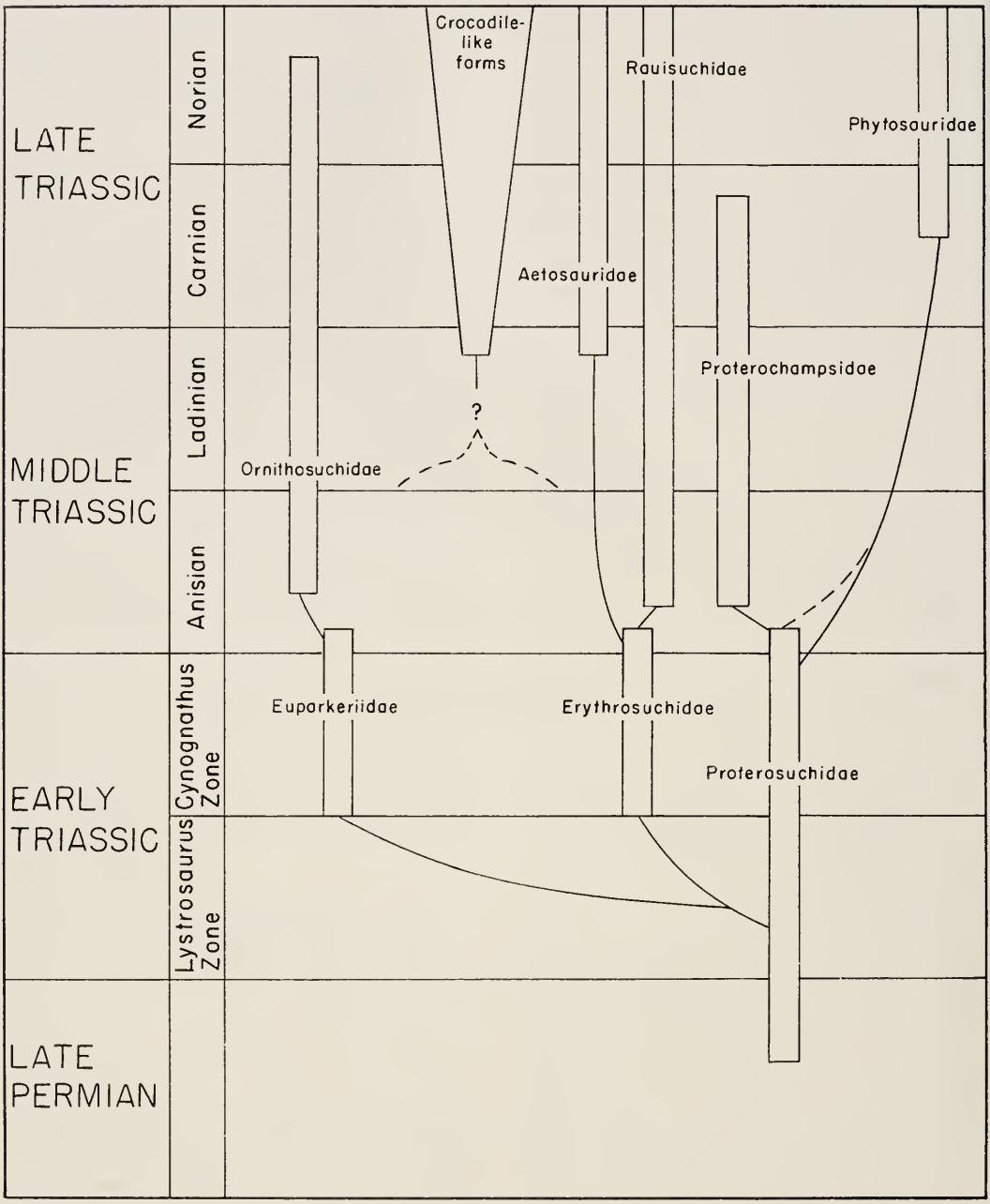

Figure 15. Suggested phylogeny of some thecodont lineages.

not fit into known families or even suborders.

Current thinking on thecodont taxonomy is perhaps best reflected in recent papers by Romer (1972a) and by Bonaparte (1971), as follows (the sequential order followed by these authors has been changed to facilitate comparison):

Romer	Bonaparte
Order Thecodontia	Order Thecodontia
Suborder Proterosuchia	Suborder Proterosuchia
Family Proterosuchidae	Family Proterosuchidae
Family Erythrosuchidae	Family Erythrosuchidae
Family Prestosuchidae (=Rauisuchidae)	
Family Proterochampsidae	
Suborder Pseudosuchia[1]	Suborder Pseudosuchia
	Infraorder Ornithosuchia
Family Ornithosuchidae	Family Ornithosuchidae
	Family Rauisuchidae
	Family Pallisteridae
	Family Teleocrateridae(?)
Family Scleromochlidae	Family Scleromochlidae
	Infraorder Sphenosuchia
	Family Sphenosuchidae
	Family Triassolestidae
	Infraorder Proterochampsia[2]
	Family Cerritosauridae
	Family Proterochampsidae
Suborder Aetosauria	Suborder Aetosauria
Family Aetosauridae (=Stagonolepidae)	Family Stagonolepidae (=Aetosauridae)
Suborder Parasuchia (Phytosauria)	Suborder Parasuchia
Family Phytosauridae	Family Phytosauridae

[1] The family Sphenosuchidae was placed by Romer in the suborder Protosuchia of the Crocodilia. *Teleocrater* and *Triassolestes*, together with other poorly known genera, are not assigned to families.
[2] The suborder Archeosuchia was previously erected for the Proterochampsidae (Sill, 1967).

Both of these authors retain the usual categories mentioned previously, but it is interesting to note the different interpretations given to the newly defined lineages Rauisuchidae and Proterochampsidae. Romer considers them to be continuations of the primitive radiation, while Bonaparte would suggest they are offshoots of the pseudosuchian stock.

It is perhaps still premature to restructure thecodont taxonomy, but the new discoveries do make it possible for the first time to trace some of the lineages throughout the Triassic.

Primitive thecodonts consist of three families; the ancestral stem Proterosuchidae (see Cruickshank, 1972), the large terrestrial Erythrosuchidae, derived from the Proterosuchidae, and the progressive Euparkeriidae, usually considered the first of the Pseudosuchia (see Ewer, 1965 and Charig and Reig, 1970). The proterosuchids were probably aquatic or semi-aquatic carnivores that somewhat resembled crocodiles. Erythrosuchids show many characters that relate them to the stem group, but were fairly large terrestrial carnivores. *Euparkeria* was apparently derived from an early lineage that separated from the Erythrosuchidae and evolved rapidly towards a more agile locomotory system. It has usually been assumed that it was the euparkeriid stock that produced the later thecodont radiation (Romer, 1966, and other textbooks). The new discoveries of fossil thecodonts, in particular those from South America, make it possible to connect some evolutionary lines of all three primitive groups from the Early to the Late Triassic.

As has been noted previously, the origin of the Rauisuchidae almost certainly lies in the Erythrosuchidae. Rauisuchids can be

traced through much of the Triassic with closely related forms present in every stage of the period from the Anisian to the Norian (see Fig. 14). The Proterochampsidae represents a newly defined lineage at present known only from South America. Earliest members of the family are from the Chañares Formation, *Chanaresuchus* and *Gualosuchus,* probably of Early Ladinian or Late Anisian age (Romer 1971b). Later forms occur in the Santa Maria Formation of Brazil, *Cerritosaurus* (Price, 1946; Bonaparte, 1971), and in the Ischigualasto Formation of Argentina, *Proterochampsa* (Reig, 1959; Sill, 1967). Most members of the family show semiaquatic tendencies, the Brazilian form *Cerritosaurus* less so, and *Proterochampsa* itself more so. The apparently more aquatic habitus of *Proterochampsa* was used by Bonaparte to separate the other genera from it as the family Cerritosauridae, but the genera are no doubt closely related and probably should be placed in the same family. Placing the Proterochampsidae as an infraorder of the Pseudosuchia implies a common origin after the acquisition of the pseudosuchian adaptive characteristics. It appears more likely that the Proterochampsidae were independent derivatives of the primitive stem proterosuchians, as suggested by Romer's classification, but they had advanced beyond the level common to the proterosuchids and erythrosuchids. On the basis of the skull, I previously (Sill, 1967) believed them to be primitive crocodiles, but the posteranial material of the earlier forms described by Romer renders this interpretation unlikely.

The third lineage to be well documented is not new at all, but is the "mainline" family Ornithosuchidae. As redefined by Bonaparte (1972a) this family would be restricted to the following well-defined genera: *Venaticosuchus* from the Ischigualasto Formation (Bonaparte, 1972b), *Riojasuchus* from the Los Colorados Formation (Bonaparte, 1969, 1972a), and *Ornithosuchus* itself from the Elgin Sandstones (Newton, 1894; Walker, 1964). To these Romer (1972b) recently added *Gracilisuchus* from the Chañares Formation. These genera in turn show reasonably close affinities to *Euparkeria,* and appear to represent a descendant lineage from the euparkeriid type of early thecodont.

In tracing these families from their origins in the early history of the Thecodontia, mention has been made only of those genera that are well enough known to show definite relationships; there are, of course, still many thecodonts whose systematic associations are not clear at present and who are usually assigned to families on a rather uncritical basis.

There remains the two well-known specialized suborders, the Aetosauria and the phytosaurs. In general these groups are limited to the Late Triassic, although an isolated phytosaur has long been noted, and disputed, from the Early Triassic of Europe (Jaekel, 1910; Gregory, 1962). Phytosaurs are well known morphologically, except for the tarsus, but no sure indication exists regarding their relationship to the primitive groups. In general it has been assumed that they were pre-crocodile derivatives of the Pseudosuchia, driven into extinction by the appearance of the true crocodiles (see Gregory, 1962). However, phytosaurs were basically primitive animals, retaining additional skull elements that were lost early in the development of the other thecodonts. Also, the pelvic girdle consisted of large platelike bones similar to the pattern of the primitive groups (see Camp, 1930; Gregory, 1962, 1969). On the basis of the recently described proterochampsids, it seems possible that phytosaurs may have been derived from an earlier continuation of the aquatic forms of the Proterosuchia.

Aetosaurs are the other closely-knit group of specialized thecodonts. Like phytosaurs they are known principally from the Upper Triassic, the earliest ones coming from the Ischigualasto Formation of Argentina (Car-

nian).[1] Those from Ischigualasto are fully specialized members of the family, bearing little indication of primitiveness. Aetosaurs were probably an early specialization for a rooting, pig-like habit (see Walker, 1961). Aside from their obvious specializations, aetosaurs retain many primitive characteristics common to the Erythrosuchidae and Euparkeriidae. As noted by Ewer (1965), *Euparkeria* was already more advanced in its locomotory apparatus than the aetosaurs. Therefore, the origins of the Aetosauria must have been from a progressive line of erythrosuchids or an early member of the Euparkeriidae. If it is true that the *Euparkeria* lineage represents an early departure from the Erythrosuchidae, based largely on limb specialization, then it would be more likely that the aetosaurs were an independent derivation from the erythrosuchid stem, perhaps from the same group that produced the rauisuchids.

Indirect anatomical evidence supporting the affinity of Aetosauria with erythrosuchids is found in the tarsus. It has long been noted that the astragalus and calcaneum of aetosaurs is of the "crocodile-type" in common with a number of other thecodonts. The closest comparison of these elements seems to be with the Rauisuchidae (see Plate 4).

Another group of thecodonts, which has long been particularly difficult to interpret consists of those that share a number of characteristics of the crocodiles, but are not true crocodiles. These have been an enigma since they were first discovered around the turn of the century. They have been considered alternately as stages in the evolution of crocodiles (Huene, 1925), independent lineages (Haughton, 1924) and aberrant or primitive members of the Crocodylia (Sill, 1967; Romer, 1972a). Walker (1970) has recently separated out the crocodilelike thecodonts and placed them as a suborder, Paracrocodylia, of equal rank with the Crocodylia in a new order Crocodylomorpha. Walker's work, based largely on re-examination of *Sphenosuchus* and *Hallopus*, indicates the presence of a possibly unified lineage that shared many anatomical characteristics of crocodiles, but were not ancestral to them. Whether or not a new order should be erected to place this group in juxtaposition with the Crocodylia will be decided by future discoveries. At the moment it does not seem to be justified. The Crocodylia are a well-defined group. Walker's Paracrocodylia is based on the Triassic family Pedeticosauridae (or Sphenosuchidae), the genus *Hallopus*—an apparent Jurassic derivative of the earlier family—and the Baurusuchidae, which he removes from the crocodilian suborder Sebecosuchia. Such a classification does not reflect the same degree of natural grouping that is found in the present category Crocodylia. It would seem more reasonable at present to consider the Pedeticosauridae as either a derivation of the thecodont line that gave rise to the true crocodiles, or as aberrant crocodiles from the early radiation of the Crocodylia.

An alternative possibility is that crocodiles arose from an early branch of the Ornithosuchidae, possibly a derivative of the *Euparkeria* line, or from a continuation of the Erythrosuchidae, perhaps from the same stock that produced the Rauisuchidae (and possibly aetosaurs). Evidence suggesting the possibility of such a relationship is found in the similarity of the crocodilian tarsus to that of thecodonts in the above-mentioned categories. The so-called crocodilian tarsal joint, in which the calcaneum bears a prominent tuber and is functionally part of the foot while the astragalus is fixed to the crus, appears to have been better developed in these lines than in either *Proterosuchus* or the Proterochampsidae. In addition, there appears to be a funda-

[1] It is possible that an aetosaur was present in the earlier Ehrmaying Series of China. A calcaneum figured by Young (1964:81) is very much like that of the Ischigualasto aetosaur, and quite unlike that of ornithosuchians.

mental difference between the construction of the tarsus in ornithosuchids and the groups presumably derived from erythrosuchids. In the Ornithosuchidae the major joint between the proximal tarsal elements is formed by a ball on the anteromedial surface of the calcaneum and a corresponding socket on the astragalus. On the other hand, in rauisuchids, aetosaurs, and crocodiles, the main socket is on the calcaneum and the ball is on the astragalus. Both forms appear to be functionally the same, but possibly represent parallel evolutionary paths. Recognition of this condition, first noticed by Bonaparte (1971), tends to diminish the difficulty noted by Krebs (1963) and Reig (1970) of explaining apparently unrelated thecodonts that possess very similar complicated tarsal joints. The "true" crocodile tarsus then becomes an impressive argument against derivation of this group from the Ornithosuchidae-Euparkeriidae type of pseudosuchian, and would tend to suggest a closer affinity with the erythrosuchid lineage, and the presumed derivatives of that line. Nevertheless, not enough is known about the tarsal joint of the Proterosuchidae, Proterochampsia, or Phytosauridae, to exclude them from a common ancestry with the Crocodylia. Tarsal joints of various members of the Thecodontia are currently under study by a number of paleontologists, some of whom feel that the structure may represent a key to both thecodont and dinosaur phylogeny.

There remains a considerable number of thecodonts that are not members of any of the groups mentioned in this paper. Some of these are almost certainly cladogenetic derivatives of these groups (see the generic list in Romer, 1966, 1972a). The various phylogenetic possibilities of these forms have been discussed recently by Reig (1970) and little more can be said until additional fossil material is available. In addition there are a number of "ghost thecodonts," forms that have been named and placed in the ordinal hierarchy, but have never been duly described.[1] These forms, largely from critical Middle Triassic strata, should provide additional insights into the thecodont radiation.

Dinosaur origins remain unclear. Both saurischian and ornithischian representatives are present and clearly recognizable in the Ischigualasto Formation of Argentina (Late Ladinian-Early Carnian); saurischians occur in the earlier Santa Maria Formation of Brazil. There is no solid evidence for linking saurischians with either ornithosuchid or rauisuchid thecodonts. However, Charig (1967) suggested the possibility of prosauropods arising from the latter group (Prestosuchidae in his usage). Reig (1970) considered it more likely that saurischians had descended directly from an erythrosuchid lineage than from a *Euparkeria* type of thecodont. No clues at all exist regarding the origin of the ornithischian dinosaurs; the earliest representative (*Pisanosaurus* from the Ischigualasto Formation) is a fully developed member of the group. It seems to be an inescapable conclusion that dinosaurs separated from thecodonts earlier than has usually been assumed, and that most thecodonts were competitors of dinosaurs rather than their progenitors.

Thecodont-Dinosaur Transition

It is perhaps paradoxical that the more we learn about thecodont evolution the less we know about dinosaur origins. Theco-

[1] *Mandasuchus* and *Teleocrater* were described by Charig in his doctoral thesis of 1956 and the names then published in an abstract in 1957. The names were incorporated into the literature by Huene (1956) and Romer (1966), but no formal descriptions have ever been published. In a later paper Charig, Attridge, and Crompton (1965) referred to the genera, but added a footnote to the effect that they were *nomina nuda*. Charig (1967) mentions both genera, an additional one from the same area, *Pallisteria*, and also two families, Pallisteriidae and Teleocrateridae. As author of all three genera and both families, he cites Charig (1967), a paper which has not yet been published. All of these names, except *Pallisteria* and its family, are listed in Romer (1966), but all appear to be without proper foundation.

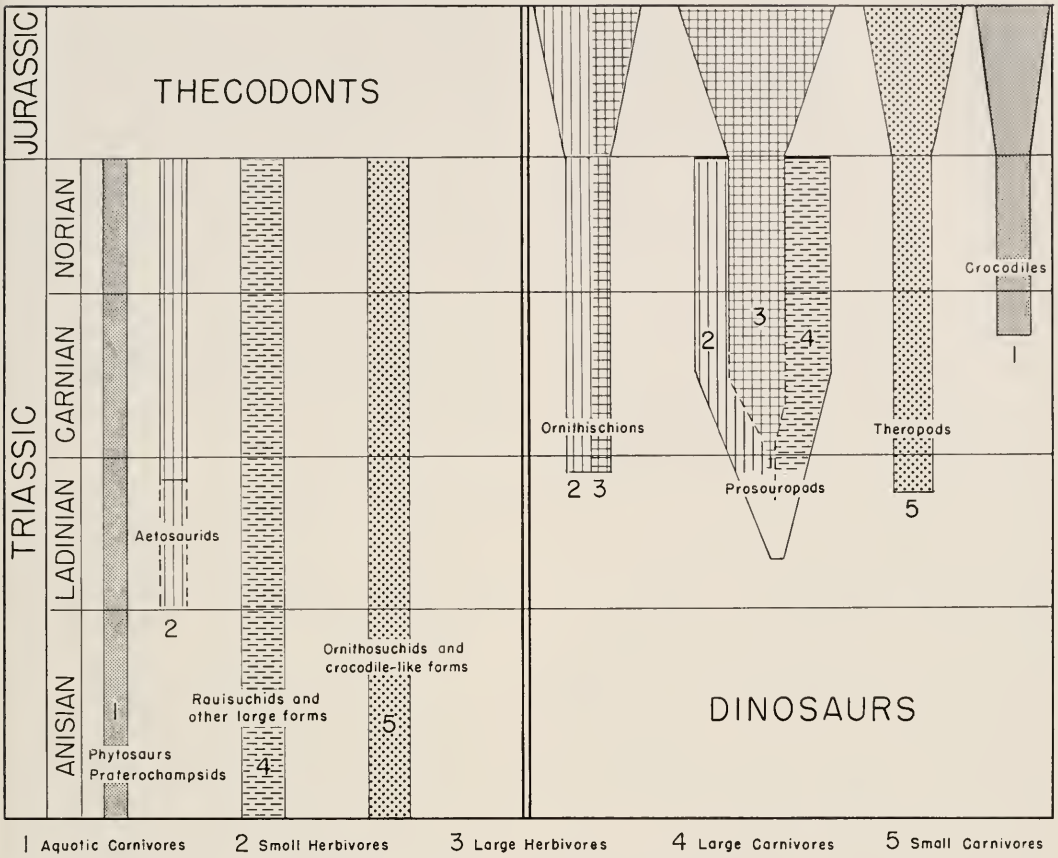

Figure 16. Time-habitat relationships of thecodonts and dinosaurs (see text).

donts evidently were successful, widespread, and diversified during the major part of Triassic time. Yet dinosaurs, usually considered as more or less the end result of thecodont evolution, had their origins well into the Middle Triassic (see Fig. 16). Thecodonts and dinosaurs apparently lived side by side during at least the last half of the Triassic. This situation naturally raises some questions about the selective forces involved and the nature of the competition that presumably existed between the two groups.

The superiority of dinosaurs relative to thecodonts is usually ascribed to a shift from a semi-erect to a fully erect body stance (Bakker, 1971; Charig, 1972). In this case the more agile dinosaur locomotion supposedly would have driven the thecodonts into extinction (but see footnote, p. 352). However, an early or transitional stage of dinosaurian limb posture is not found in any of the known thecodonts, and in particular there is no evidence of the shift to the simple hinge type of foot characteristic of dinosaurs. Charig (1972) postulated an as yet unknown thecodont ancestor in which the calcaneum was reduced and rotated with the crus rather than with the pes. Reig (1970), on the other hand, would have the dinosaurs originate directly from a primitive thecodont of an erythrosuchid level in the Early Triassic, and evolve essentially independently of the

major thecodont radiation of the Middle and early Late Triassic. However, if this were the case it would be expected that dinosaurs rather than thecodonts would have dominated the Middle Triassic.

The earliest dinosaur remains currently known come from the Manda and Santa Maria Formations of approximately Anisian or Ladinian age (Charig, 1967; Colbert, 1970). These genera, "*Nyasasaurus*" (undescribed) and *Staurikosaurus* are contemporaries of rauisuchid thecodonts, found in the same sediments ("*Mandasuchus*" and *Prestosuchus*). *Staurikosaurus* was moreover a predator of approximately the same size as *Prestosuchus.* A similar situation obtains in the Ischigualasto Formation, where the carnivorous dinosaur *Herrerasaurus* is found with the same size carnivorous thecodont *Saurosuchus.* The earliest ornithischian, *Pisanosaurus,* is found in the Ischigualasto Formation and, although poorly preserved, shows that the basic features of the group had been acquired by that time (Casamiquela, 1967). The first theropods occur at approximately the same time (Charig, 1967), apparently occupying an ecologic role parallel to that of the ornithosuchid thecodonts.

Nevertheless, the thecodonts were considerably more abundant and varied in the sediments of the Middle and lower Late Triassic. They apparently took over the carnivore niche previously occupied by the carnivorous cynodonts, but did not extend into the herbivore field (with the exception of the aetosaurs). Dinosaurs produced both carnivores and herbivores early in their history. The origins of both categories are still virtually unknown.

Actual data from the fossil record allow three well-supported concepts to be stated: 1) dinosaurs were in existence at least during the last half of the Triassic; 2) thecodonts were abundant and diverse during the Middle and first half of the Late Triassic, becoming less so during the latter part of the Late Triassic; 3) although dinosaurs existed earlier, their major expansion did not begin until the last half of the Late Triassic. The reasons for the difference in expansion phases between the two groups are not clearly understood, nor can the apparent ecologic overlap between the large carnivores be explained on the basis of current data. However, it seems an inescapable conclusion that the more agile mechanical condition of the dinosaur limbs was a factor in their eventual replacement of the thecodonts. It is also possible that the dinosaurs were undergoing more extensive physiologic changes, perhaps related to the changes in locomotion (see Bakker, 1972).

LITERATURE CITED

Bakker, R. T. 1971. Dinosaur physiology and the origin of mammals. Evolution, **25**: 636–658.

———. 1972. Locomotor energetics of lizards and mammals compared. The Physiologist, **15**(3): 278.

———. In press. Lizard locomotor energetics and the Reptile-Mammal transition.

Bonaparte, J. F. 1969. Dos nuevas "faunas" de réptiles Triásicos de Argentina. Gondwana Stratigraphy, IUGS Sumposium, Buenos Aires, 1–15 October 1967, UNESCO, pp. 283–284.

———. 1971. *Cerritosaurus binsfeldi* Price, tipo de una nueva familia de Tecodontes (Pseudosuchia Proterochampsia). An. Acad. Brasil. Cienc. (1971), **43**: 417–421.

———. 1972a. Los tetrápodos del sector superior de la Formación Los Colorados, La Rioja, Argentina. Opera Lilloana, **22**: 1–183.

———. 1972b. Annotated list of the South American Triassic tetrapods. Proc. II Gondwana Symposium, South Africa, 1970, Pretoria, pp. 665–682.

Camp, C. L. 1930. A study of the phytosaurs, with description of new material from North America. Mem. Univ. Calif., **10**: 1–174.

Casamiquela, R. M. 1967. Un nuevo dinosaurio ornitisquio Triásico (*Pisanosaurus mertii:* Ornithopoda) de la Formación Ischigualasto, Argentina. Ameghiniana, **4**(2): 47–64.

Charig, A. J. 1957. New Triassic archosaurs from Tanganyika including *Mandasuchus* and *Teleocrater.* Abstr. Diss. Univ. Cambridge, 1955–56: 28–29.

———. 1967. Archosauria. The Fossil Record. Geological Soc. London, pp. 695–731.

———. 1972. The evolution of the archosaur pelvis and hindlimb: an explanation in functional terms. *In* Joysey, K. A. and T. S. Kemp

(Eds.), Studies in Vertebrate Evolution. Edinburgh: Oliver and Boyd, pp. 121–155.

———, J. Attridge, and A. W. Crompton 1965. On the origin of the sauropods and the classification of the Saurischia. Proc. Linn. Soc. London, **176**: 197–221.

———, and O. Reig. 1970. The classification of the Proterosuchia. Bio. Jour. Lin. Soc., **2**: 125–171.

Colbert, E. H. 1970. A saurischian dinosaur from the Triassic of Brazil. Am. Mus. Novitates, No. 2405: 1–39.

Cruickshank, A. R. I. 1972. The proterosuchian thecodonts. *In* Joysey, K. A. and T. S. Kemp (eds.), Studies in Vertebrate Evolution. Edinburgh: Oliver and Boyd, pp. 89–119.

Edmund, A. G. 1957. On the special foramina in the jaws of many ornithischian dinosaurs. Cont. Roy. Ontario Mus. Zool. and Palaeo., No. 48: 1–14.

———. 1960. Tooth replacement phenomena in the lower vertebrates. Roy. Ontario Mus., Life Sci. Div., **52**: 1–64.

Ewer, R. R. 1965. The anatomy of the thecodont reptile *Euparkeria capensis* Broom. Phil. Trans. Roy. Soc. London, B, **248**: 379–435.

Gregory, J. T. 1962. The genera of phytosaurs. Amer. Jour. Sci., **260**: 652–690.

———, and F. Westphal. 1969. Remarks on the phytosaur genera of the European Trias. Jour. Paleont., **43**: 1296–1298.

Haughton, S. H. 1924. The fauna and stratigraphy of the Stormberg Series. Ann. So. Africa Mus., **12**: 323–497.

Hoffstetter, R. 1955. Thecodontia. *In* Traité de Paleontologie, **5**: 665–694.

Huene, F. V. 1925. Die Bedeutung der *Sphenosuchus* Gruppe für Ursprung der Krokodile. Z. Indukt. Abstamm.-Vererbungsl., **38**: 307–320.

———. 1936. The constitution of the Thecodontia. Amer. Jour. Sci., Ser. 5, **32**: 207–217.

———. 1938. Ein grosser Stagonolepide aus der jüngeren Trias Ostafrikas. Neues Jahrb. Min. Geol. Pal., Beilage-Bd., **80**: 264–278.

———. 1942. Die fossilen Reptilien des Südamerikanishen Gondwanalandes. Ergebnisse der Sauriergrabungen in Südbrasilien, 1928/1929. München: C. H. Beck'she. 332 pp.

———. 1956. Paläontologie und Phylogenie der niederen Tetrapoden. Jena: G. Fischer. 716 pp.

Hughes, B. 1963. The earliest archosaurian reptiles. S. Afr. Jour. Sci., **59**: 221–241.

Jaekel, O. 1910. Ueber einen neuen Belodonten aus dem Buntsandstein von Bernburg. Sitzungsber. Ges. naturf. Freunde, Berlin, **1910**: 197–229.

Krebs, B. 1963. Bau und Funktion des Tarsus eines Pseudosuchiers aus der Trias des Monte San Giorgio (Kanton Tessin, Schweiz). Paleont. A., **37**: 88–95.

———. 1965. *Ticinosuchus ferox* nov. gen. nov. sp. Ein neuer Pseudosuchier aus der Trias des Monte San Giorgio. Schweiz. Palaont. Abh., **81**: 1–140.

Newton, E. T. 1894. Reptiles from the Elgin sandstone. Description of two new genera. Phil. Trans. Roy. Soc. London, B, **185**: 573–607.

Price, L. I. 1946. Sobre um novo pseudosuquio deo Triassico superior do Rio Grande do Sul. Bol. Ser. Geol. Min. Brasil, **120**: 7–38.

Reig, O. A. 1959. Primeros datos descriptivos sobre nuevos reptiles arcosaurios del Triásico de Ischigualasto (San Juan, Argentina). Rev. Asoc. Geol. Argentina, **13**: 257–270.

———. 1961. Acerca de la posición sistemática de la familia Rauisuchidae y del genero *Saurosuchus* (Reptilia, Thecodontia). Publ. Mus. Munic. Cien. Nat. Trad. Mar de la Plata, **1**: 73–114.

———. 1970. The Proterosuchia and the early evolution of the archosaurs; an essay about the origin of a major taxon. Bull. Mus. Comp. Zool., **139**: 229–292.

Romer, A. S. 1927. The pelvic musculature of ornithischian dinosaurs. Acta Zoologica, **8**: 225–275.

———. 1956. Osteology of the Reptiles. Chicago: Univ. Chicago Press. 772 pp.

———. 1966. Vertebrate Paleontology. Chicago: Univ. Chicago Press. 468 pp.

———. 1968. Notes and comments on vertebrate paleontology. Chicago: Univ. Chicago Press. 304 pp.

———. 1971a. The Chañares (Argentina) Triassic reptile fauna. VIII. A fragmentary skull of a large thecodont, *Luperosuchus fractus*. Breviora, Mus. Comp. Zool., No. 373: 1–8.

———. 1971b. The Chañares (Argentina) Triassic reptile fauna. IX. Two new long-snouted thecodonts, *Chanaresuchus* and *Gualosuchus*. Breviora, Mus. Comp. Zool., No. 379: 1–22.

———. 1972a. The Chañares (Argentina) Triassic reptile fauna. XVI. Thecodont classification. Breviora, Mus. Comp. Zool. No. 395: 1–24.

———. 1972b. The Chañares (Argentina) Triassic reptile fauna. XIII. An early ornithosuchid pseudosuchian, *Gracilisuchus stipanicicorum*, gen. et sp. nov. Breviora, Mus. Comp. Zool., No. 389: 1–24.

Sill, W. D. 1967. *Proterochampsa barrionuevoi* and the early evolution of the Crocodilia. Bull. Mus. Comp. Zool., **135**: 415–446.

———. 1969. The tetrapod-bearing continental

Triassic sediments of South America. Am. Jour. Sci, **267**: 805–821

Walker, A. D. 1961. Triassic reptiles from the Elgin area: *Stagonolepis*, *Dasygnathus* and their allies. Phil. Trans. Roy. Soc. London, B, **244**: 103–204

———. 1964. Triassic reptiles from the Elgin area: *Ornithosuchus* and the origin of carnosaurs. Phil Trans. Roy. Soc. London, B, **248**: 53–134.

———. 1970. A revision of the Jurassic reptile *Hallopus victor* (Marsh) with remarks on the classification of crocodiles. Phil. Trans. Roy. Soc. London, B, **257**: 323–372.

Young, C. C. 1964. The pseudosuchians in China. Palaeont. Sinica, New Ser. C, **19**: 106–205.

US ISSN 0027-4100

Bulletin OF THE
Museum of
Comparative
Zoology

The Cranial Foramina of Protrogomorphous Rodents; An Anatomical and Phylogenetic Study

JOHN H. WAHLERT

HARVARD UNIVERSITY
CAMBRIDGE, MASSACHUSETTS, U.S.A.

VOLUME 146, NUMBER 8
18 DECEMBER 1974

PUBLICATIONS ISSUED
OR DISTRIBUTED BY THE
MUSEUM OF COMPARATIVE ZOOLOGY
HARVARD UNIVERSITY

Breviora 1952–
Bulletin 1863–
Memoirs 1864–1938
Johnsonia, Department of Mollusks, 1941–
Occasional Papers on Mollusks, 1945–

SPECIAL PUBLICATIONS.

1. Whittington, H. B., and E. D. I. Rolfe (eds.), 1963. Phylogeny and Evolution of Crustacea. 192 pp.
2. Turner, R. D., 1966. A Survey and Illustrated Catalogue of the Teredinidae (Mollusca: Bivalvia). 265 pp.
3. Sprinkle, J., 1973. Morphology and Evolution of Blastozoan Echinoderms. 284 pp.
4. Eaton, R. J. E., 1974. A Flora of Concord. 250 pp.

Other Publications.

Bigelow, H. B., and W. C. Schroeder, 1953. Fishes of the Gulf of Maine. Reprint.

Brues, C. T., A. L. Melander, and F. M. Carpenter, 1954. Classification of Insects.

Creighton, W. S., 1950. The Ants of North America. Reprint.

Lyman, C. P., and A. R. Dawe (eds.), 1960. Symposium on Natural Mammalian Hibernation.

Peters' Check-list of Birds of the World, vols. 2–7, 9, 10, 12–15.

Proceedings of the New England Zoological Club 1899–1948. (Complete sets only.)

Publications of the Boston Society of Natural History.

Price list and catalog of MCZ publications may be obtained from Publications Office, Museum of Comparative Zoology, Harvard University, Cambridge, Massachusetts, 02138, U.S.A.

© The President and Fellows of Harvard College 1974.

THE CRANIAL FORAMINA OF PROTROGOMORPHOUS RODENTS; AN ANATOMICAL AND PHYLOGENETIC STUDY

JOHN H. WAHLERT[1]

Dedicated to
Katherine
Alexander and James
Carol and Daniel

CONTENTS

LIST OF FIGURES 363
ABSTRACT 363
INTRODUCTION 364
CRANIAL FORAMINA OF RODENTS WITH SPECIAL REFERENCE TO *MARMOTA* 366
Systems:
Cranial nerves 367
Arteries 368
Veins 369
Foramina of the rodent skull 369
PARAMYIDAE
Paramys 374
Leptotomus 379
Reithroparamys 380
Ischyrotomus 381
Pseudotomus 383
Manitsha 384
SCIURAVIDAE 385
ISCHYROMYIDAE 388
CYLINDRODONTIDAE 393
PROSCIURIDAE 397
APLODONTOIDEA 400
CONCLUSIONS 405
REFERENCES 408

LIST OF FIGURES

1. *Marmota monax* 370
2. *Paramys copei* 375
3. *Paramys delicatus* 376
4. Auditory and pterygoid regions of *Paramys copei* 377
5. *Reithroparamys delicatissimus* 380
6. Auditory and pterygoid regions of *Ischyrotomus oweni* 382
7. *Sciuravus nitidus* 385
8. Auditory region of *Sciuravus nitidus* 387
9. *Ischyromys typus* 389
10. *Ardynomys occidentalis* 394
11a. *Prosciurus* sp. 398
11b. *Prosciurus* aff. *saskatchewaensis* 398
12. *Allomys nitens* 400
13. *Mylagaulus laevis* 401

[1] American Museum of Natural History, Vertebrate Paleontology Department, Central Park West at 79th Street, New York, N. Y. 10024.

ABSTRACT. The cranial foramina and the blood vessels and nerves passing through them are described in detail for the sciurid genus *Marmota;* this data serves as the basis for understanding structures seen in the fossils. The cranial foramina are described and compared in North American specimens of the protrogomorphous rodent families Paramyidae, Sciuravidae, Ischyromyidae, Cylindrodontidae, Prosciuridae, Aplodontidae, and Mylagaulidae. The least variable foramina are those that transmit nerves; the most variable, veins. Presence or absence, relative position, number, and relative size of foramina are useful characters in determining relationships. Within the Paramyidae differences indicate an early radiation of lineages. Paramyids and sciuravids have many primitive features in common, but differ in several details; of especial interest in these families are the pathways of the internal carotid artery and its branches. Peculiarities common to the foramina of ischyromyids and cylindrodontids suggest that the two groups can be made subfamilies of the family Ischyromyidae. The Prosciuridae are included likewise with the Aplodontidae and Mylagaulidae in the Aplodontoidea.

INTRODUCTION

The origin of the Rodentia and their successful radiation can be attributed to a unique design for gnawing and chewing. Perfection of the design has involved modification of the jaw and skull for more efficient muscle configuration, and specialization of the incisors and cheek teeth in response to the multitude of specific niches into which rodents have diversified. The masticatory system has been subjected to great selection pressure and has been modified from the original design in ways that were limited by genetic potential and by the efficiency of certain modifications relative to others. These are the principal reasons for the parallelism so typical of rodent phylogeny.

To date, the classification of rodents has been based primarily on the structure of the masticatory muscles, the infraorbital foramen, the lower jaw, and the cheek teeth. These characters are all part of the masticatory system, and, when traced through time, their observed modifications reveal a complex phylogeny. Gaps in the sequence, however, cannot always be filled. Whole families of rodents stand in uncertain relationships to proposed phylogenies. This situation is not surprising; in a phase of rapid evolution a gap of a few million years is enough to permit a discrete group to appear full-blown in the fossil record. The ancestry of such a group is often unclear because of parallelism among the earlier lineages from which it could have descended.

The cranial foramina, unlike the components of the masticatory apparatus, are not part of a single functional system. There is no reason to suppose that selection acts on them as a unit or that selection pressure from the external environment acts on them directly. In the main, foramina serve a passive function; they permit nerves and blood vessels to pass through the bones of the skull. It is reasonable to suppose that foramina may vary in position and soft-part content so long as they satisfy the requirements of the circulatory and nervous systems. Within these limits selection is unimportant, and changes fixed in a small population by random genetic processes will characterize a new lineage arising from it. Fusion and division of foramina are possible examples.

The position or the existence of foramina may be changed as they are impinged upon by other structures. Foramina in the orbit are modified to lead around the roots of high-crowned cheek teeth. In the temporal region they may be closed off by enlarged bullae, and some other combination of foramina then acquires their function.

A foramen may be taken over by a different functional system. The infraorbital foramen has been seized upon in the hystricomorphous and myomorphous rodents for transmission of a part of the medial masseter muscle. From the moment of seizure it ceased to behave solely as the foramen it was and came under the influence of the selective forces acting upon the masticatory system. The tough connective tissue around a foramen may change to accommodate a new structure. In those sciurids which lack an infraorbital canal, a tough membrane shielding the transmitted nerves and vessels from the lateral division of the masseter takes its place.

Hill (1935 and 1937), Guthrie (1963 and 1969), and Bugge (1970, 1971a, b, and c) have been the principal contributors to knowledge of cranial foramina and the cephalic nervous and vascular systems in living rodents. They describe differences that appear to have a systematic basis. But the very nature of their work, limited primarily to modern examples, precludes discernment of the primitive and derived conditions for each aperture. The pattern of evolution can be seen with certainty only when the time-dimension of paleontology is added. Detailed consideration of the fossils indicates which features in a group are primitive and eliminates the need to

rely on a so-called, but not in fact, primitive living genus such as *Aplodontia*.

This paper on the protrogomorphous North American rodents is the first half of my Ph.D. dissertation (Wahlert, 1972), which included the sciuromorphs also. Description of the cranial foramina in the latter families will be presented elsewhere, and I hope to extend the work to myomorphous and hystricomorphous forms. The Protrogomorpha as defined by Wood (1937 and 1955) contain the families Paramyidae and Sciuravidae, which are parts of the initial rodent radiation, and the derived families Cylindrodontidae, Ischyromyidae, Prosciuridae[1], Mylagaulidae, Aplodontidae, and Protoptychidae. *Protoptychus* was found to be both hystricomorphous and hystricognathus; a separate paper deals with its cranial and dental morphology (Wahlert, 1973).

This approach to the study of rodent evolution brings with it a special set of problems. The number of fossil skulls adequately preserved is very small in comparison with the number of forms known from teeth. The forms whose skulls can be examined include representatives of every family, but they may be from specialized side branches and not from the main lines of evolution. Most specimens are incomplete. The task of assembling data may be compared with that of a man in the dark who attempts to describe an exquisite topiary arabesque with only the aid of an unreliable flashlight.

The text is divided into sections, each dealing with a single taxon; for extinct lineages this is the family, and for surviving lineages, the superfamily. Sections are subdivided according to the importance of the included material and the completeness of the specimens.

Paramyid genera are considered separately because many rodent lineages may have originated from within the family. Differences between genera may be critical in determining relationships to later forms, and it is important to recognize that information about cranial foramina in the fossils is quite uneven.

The genera within several families and even within a superfamily are enough alike that a single section describing each group is sufficient. The ischyromyids, cylindrodontids, prosciurids, and aplodontoids are treated in this manner.

Discussions at the end of each section compare features within the groups described and compare the most interesting features of the entire assemblage with those considered in preceding sections.

The bearing of the evidence provided by cranial foramina on the phylogeny and relationships of North American protrogomorphous rodents is discussed in the conclusion.

A list of the specimens examined is presented at the beginning of each section or subsection. Definitions of the stratigraphic names can be found in Wood (H. E. Wood *et al.*, 1941) and Keroher (Keroher *et al.*, 1966; Keroher, 1970).

Abbreviations are as follows:

AMNH	American Museum of Natural History
CM	Carnegie Museum of Natural History
F:AM	Frick Collections, American Museum of Natural History
FMNH	Field Museum of Natural History
KU	University of Kansas Museum of Natural History
LACM (CIT)	Los Angeles County Museum (California Institute of Technology Collection)
MCZ	Museum of Comparative Zoology, Harvard University
USNM	National Museum of Natural History

[1] I have followed Wilson (1949c) and assigned the prosciurids to a taxon of rank equal to the paramyid group. Wood places them in the Paramyidae as a subfamily.

SDSM	South Dakota School of Mines and Technology
UCMP	University of California Museum of Paleontology
UNSM	University of Nebraska State Museum
UOMNH	University of Oregon Museum of Natural History
YPM	Peabody Museum of Natural History, Yale University

A letter code, which follows each number, indicates the completeness of the fossil specimens:

s – whole skull	o – orbit
n – snout	t – pterygoid region
p – palate	c – cranium

A code such as npo indicates that the snout, palate, and orbit of the particular specimen are preserved and provided information for this study; the pterygoid region and cranium are either gone or are damaged and the detail destroyed.

Measurements of length were taken with a dial caliper calibrated to 1/20 mm. The diastemal length is a straight line measurement from the back of the incisor alveolus to the anteriormost edge of the alveolus of the first cheek tooth. The sizes of foramina smaller than 1.0 mm were estimated with a Dunlap spark-plug gauge.

Most of the figures were drawn with the aid of proportional dividers; enlargements of detail and outlines of small specimens were traced with a camera lucida microscope. I have made no attempt to show crenulations in the sutures but have taken care to illustrate the relationship of sutures to foramina. I have omitted detail from the teeth because excellent figures of the dentitions of all species studied are available in the literature. Solid lines indicate structures and sutures that I have seen in at least one specimen of the genus illustrated. Dashed lines indicate details that are less certain but probable in view of similar features in closely related forms. Dotted lines represent guesses. To some degree all the figures are restorations. I have attempted to eliminate distortions and to reconstruct all broken elements; the figures are not copies of the specimens. The key to abbreviations in the illustrations is given in the caption of Figure 1.

Acknowledgements. I would like to thank Bryan Patterson for his assistance and criticism throughout the course of this study, and Albert Wood for his suggestion of the topic and his assistance in the initial stages of the work. I am indebted to the staff members of the institutions, listed above, for making such a wealth of material available, and to many of these same people for their kind hospitality when I toured museums. I appreciate greatly the comments of Craig C. Black, Mary R. Dawson, Robert J. Emry, and T. Mylan Stout, all of whom read parts of the manuscript, and of Farish A. Jenkins, Jr., who read the entire thesis and had many excellent suggestions for improvement of this manuscript. Barbara Lawrence and Charles Mack of the Mammal Department, Museum of Comparative Zoology, provided me with skulls for sectioning and specimens for dissection.

Travel was financed by the Departments of Geological Sciences and of Biology at Harvard University. Other expenses were generously sustained by Katherine H. Wahlert.

Special thanks are due to Carol C. Jones for incisive criticism of my grammar and for advice on the figures, to Daniel C. Fisher and James M. Labaugh, III, for help in preparing the final manuscript, and to Katherine H. Wahlert for devoted typing.

CRANIAL FORAMINA OF RODENTS WITH SPECIAL REFERENCE TO *MARMOTA*

Hill (1935) was the first to attempt a complete listing of the foramina in rodent skulls. From dissections and prepared skulls he described the position and contents of each foramen and stated how they differ

among several genera, but he gave no account of the circulatory and nervous systems themselves. Unless these systems are understood it is not possible to interpret and name several of the foramina. Tandler (1899, 1901, and 1902), Guthrie (1963 and 1969), and Bugge (1970, 1971a, b, and c) have examined the cephalic arterial circulation of various rodents, but, apart from Guthrie, these authors pay little attention to the foramina involved.

As an introduction to what follows, I present an account of the foramina and the circulatory system and cranial nerves in *Marmota monax* (Fig. 1). I follow Hyman (1942) and Greene (1935) for terminology of the soft parts. *Marmota* has several advantages for this purpose. Although fully sciuromorphous, it retains most of the cranial foramina met with in the earliest rodents, and the bones of the skull do not fuse in the adult.

Systems

Cranial Nerves

The hypoglossal (XII) emerges from one or more hypoglossal foramina and runs anteromedially into the base of the tongue. The foramina are situated just anterior to the occipital condyle on the ventral side of the skull.

The vagus (X), accessory (XI), and glossopharyngeal (IX) emerge from the jugular foramen. It is between the bulla and the basioccipital and is lenticular in shape.

The facial (VII) emerges from the stylomastoid foramen deep between the mastoid process and the bulla. The main part of the nerve runs anteriorly and diversifies over the masseter muscle. The chorda tympani branch of the facial emerges from a tiny slot, the canal of Huguier, in the front surface of the bulla. It runs anteromedially to join the lingual branch of the trigeminal (V) nerve.

The mandibular division (3rd) of the trigeminal nerve (V) emerges from the large foramen ovale in the pterygoid region. Initially it runs anterolaterally through a notch in the lateral pterygoid flange. A strut of bone may cross the notch to form a foramen which I am calling the foramen ovale accessorius. The strut separates the mandibular nerve and its internal pterygoid branch. The auriculotemporal branch diverges just outside the foramen ovale. The mandibular nerve continues around the outside of the external pterygoid muscle and splits into three parts. The inferior alveolar branch enters the mandibular canal of the lower jaw. The mylohyoid and lingual, which is joined by the chorda tympani, run around the muscle and turn medially into the soft tissue.

Two portions of the mandibular division, the masseteric and buccinator nerves, run dorsolaterally from the foramen ovale through a canal in the alisphenoid bone; the canal shares its posterior opening with the alisphenoid canal, but runs through the bone above it. These nerves emerge on the side of the head. Both nerves may pass through one foramen or each through its own (masticatory and buccinator foramina); the two cases can occur together on opposite sides of a single skull. The buccinator nerve runs anteriorly, but a small branch turns back on leaving the foramen. The masseteric nerve also has two branches; the smaller runs dorsally to the temporal muscle. The main part remains against the alisphenoid region in a shallow vertical channel. When this branch reaches the front of the posterior root of the zygoma, it turns laterally, passes through the mandibular notch of the jaw, and descends to the masseter muscle.

The maxillary division (2nd) of the trigeminal nerve enters the orbit through the sphenoidal fissure. On cutting away the lateral surface of the alisphenoid region, the alisphenoid canal is exposed. Two large branches of the maxillary enter the canal dorsally through two large foramina; the small zygomatic branch emerges in some cases from a separate small foramen be-

tween them. The posterior foramen (or two foramina) seems comparable to the foramen rotundum in other mammals. The two branches of the maxillary division unite to form the infraorbital nerve. The vidian nerve could not be separated or distinguished from these. The main trunk of the infraorbital nerve enters the infraorbital canal; inside the canal a twig, the anterior superior alveolar nerve, descends into the maxillary bone. The trunk continues out onto the side of the snout. A small medial branch, the sphenopalatine, comes off the infraorbital nerve where it enters the orbit; it re-enters the skull through the sphenopalatine foramen. As it crosses the orbital floor it gives off a descending palatine branch, which enters the dorsal palatine foramen, runs through the palatine canal, and emerges on the palate through the posterior palatine foramen.

In company with the anterior portion of the maxillary division, the ophthalmic division (1st) of the trigeminal, and the abducens (VI), trochlear (IV), and oculomotor (III) nerves enter the alisphenoid canal. The foramen through which they pass is comparable to the orbital fissure in other mammals. The nasociliary branch of the ophthalmic re-enters the skull through the more anterior of the two ethmoid foramina. The frontal branch of the ophthalmic ascends the medial wall of the orbit and exits onto the top of the skull through the supraorbital notch.

The optic nerve (II) enters the orbit through the large, oval optic foramen. It is situated entirely within the orbitosphenoid.

Arteries

The common carotid artery gives off three branches when it reaches the back of the larynx. The superior thyroid artery diverges medially; the stapedial and occipital arteries branch off on the lateral side. The main trunk continues as the external carotid. The occipital artery turns posteriorly and crosses ventral to the stapedial. It runs through a channel between the condyle and the paroccipital process to the back of the head and neck.

The stapedial artery in company with the vagus, accessory, and glossopharyngeal nerves passes through the jugular foramen, and it enters the stapedial foramen in the bulla. It exits from the middle ear and enters the cranial cavity via the stapedial artery canal in the periotic. A dorsal branch from it continues out the temporal foramen to the temporal muscle. The main portion runs anteriorly and exits via the sphenofrontal foramen into the orbit; this is the ophthalmic artery, which supplies the eye and eye muscles with blood. One branch, the ethmoidal artery, enters the posterodorsal ethmoid foramen. Another, the superior ophthalmic artery, ascends the medial wall of the orbit with the frontal branch of the ophthalmic nerve and goes through the supraorbital notch onto the top of the head.

The external carotid artery bends laterally and gives rise to auricular, internal maxillary, and other branches which supply the lower jaw, jaw muscles, and ear region with blood. At the bend, the external maxillary artery diverges and runs anteriorly between the masseter and digastric muscles. It gives off a lingual artery and a glandular branch. In this region a third branch proceeds dorsally, gives off a tiny meningeal twig to the foramen ovale, enters the alisphenoid canal, and passes as the internal maxillary into the orbit where it divides into three branches.

The outermost branch of the internal maxillary artery, the posterior superior alveolar, runs anterolaterally to the cheek region. The middle branch, the infraorbital, gives off minute branches that enter the nutritive foramina. It passes through the infraorbital foramen where a miniscule orbital twig pierces the bone dorsally, emerges from the malar foramen, and goes into the tissue anterior to the eye; a ventral branch, the anterior superior alveolar, in company with the nerve of the same name, enters a foramen below. The main trunk

continues out onto the snout. The innermost branch of the internal maxillary artery gives rise to the descending palatine artery and continues on into the sphenopalatine foramen. The descending palatine artery enters the dorsal palatine foramen, runs through the palatine bone, and emerges from the posterior palatine foramen; it diversifies in the tissue of the palate and disappears again into the incisive foramen.

Veins

Three distinct trunks carry blood from various parts of the head. These are the anterior and posterior facial veins, which unite in the neck to form the external jugular vein, and the internal jugular vein.

The posterior facial receives blood from the temporal and orbital-palatine regions. The infraorbital vein begins on the snout and passes through the infraorbital canal where it picks up a small twig from the anterior alveolar foramen. In the orbit, as the internal maxillary vein, it collects twigs from the nutritive foramina and small branches from veins passing through the sphenopalatine foramen and palatine canal. The descending palatine vein ascends through the posterior maxillary notch and joins it at the back of the maxilla. There are two ethmoid foramina, and the ethmoid vein exits through the posterodorsal one. It joins the ophthalmic, which then unites with the internal maxillary just before it enters the sphenoidal fissure. The internal maxillary occupies most of the space within the alisphenoid canal, the internal maxillary artery filling only a small dorsal portion of the canal. The vein communicates through the transverse canal in the basisphenoid with the same vein on the opposite side. It empties into the pterygoid plexus.

The superficial temporal vein gathers the posterior deep temporal, transverse facial, masseteric, and auricular branches. It is joined by a large vein from the temporal foramen and condylar area. This broad vessel also continues into the pterygoid plexus. The inferior alveolar vein enters the plexus from the mandibular foramen in the jaw. The plexus anastomoses dorsally with the internal maxillary vein and ventrally with the submental vein. A meningeal branch enters it through a small foramen between the bulla and the basisphenoid bone; this aperture may be a remnant of the middle lacerate foramen. The pterygoid plexus changes from a sack-like structure into a large vein that proceeds posteriorly and is called the posterior facial vein.

The anterior facial vein begins on the snout. It gathers tributaries from the masseteric and submental regions. It passes back into the neck where it unites with the posterior facial vein to form the external jugular.

The internal jugular vein is quite small. It collects a branch from the inferior petrosal sinus in the carotid canal, leaves the cranium through the jugular foramen in company with the nerves and the stapedial artery, turns posteriorly with them, and passes into the neck.

Foramina of the Rodent Skull

I have followed, as far as possible, the terminology used by Hill (1935) and have attempted to find names commonly used in the literature for foramina he did not describe. My main points of departure from Hill are in the temporal and pterygoid regions. I have retained the term postglenoid foramen but have abandoned the names subsquamosal, postsquamosal, suprasquamosal, and squamosal in favor of the general term temporal foramina. In the Rodentia the temporal foramina are quite variable and cannot be categorized. The new terms post-alar fissure, squamosomastoid foramen, and foramen ovale accessorius are used for apertures that are different from anything in Hill's list. The fossils demonstrate that Hill's distinction between alisphenoid and sphenopterygoid canals is not universal in the order; only one canal, the alisphenoid, is present in the earliest rodents, and the sphenopterygoid

appears to be unique to geomyoids among the groups examined.

The following topographic list of foramina and their contents is based mainly on the woodchuck (*Marmota monax*) unless otherwise stated. I have indicated also those foramina present but not figured, because they are hidden by another structure. Foramina lacking in *Marmota* are described from the rodents in which they occur. No rodent possesses all of the foramina listed.

1. The unpaired interpremaxillary foramen does not occur in the woodchuck. When present it is situated just behind the incisors on the median premaxillary suture, and it transmits a branch of the palatine

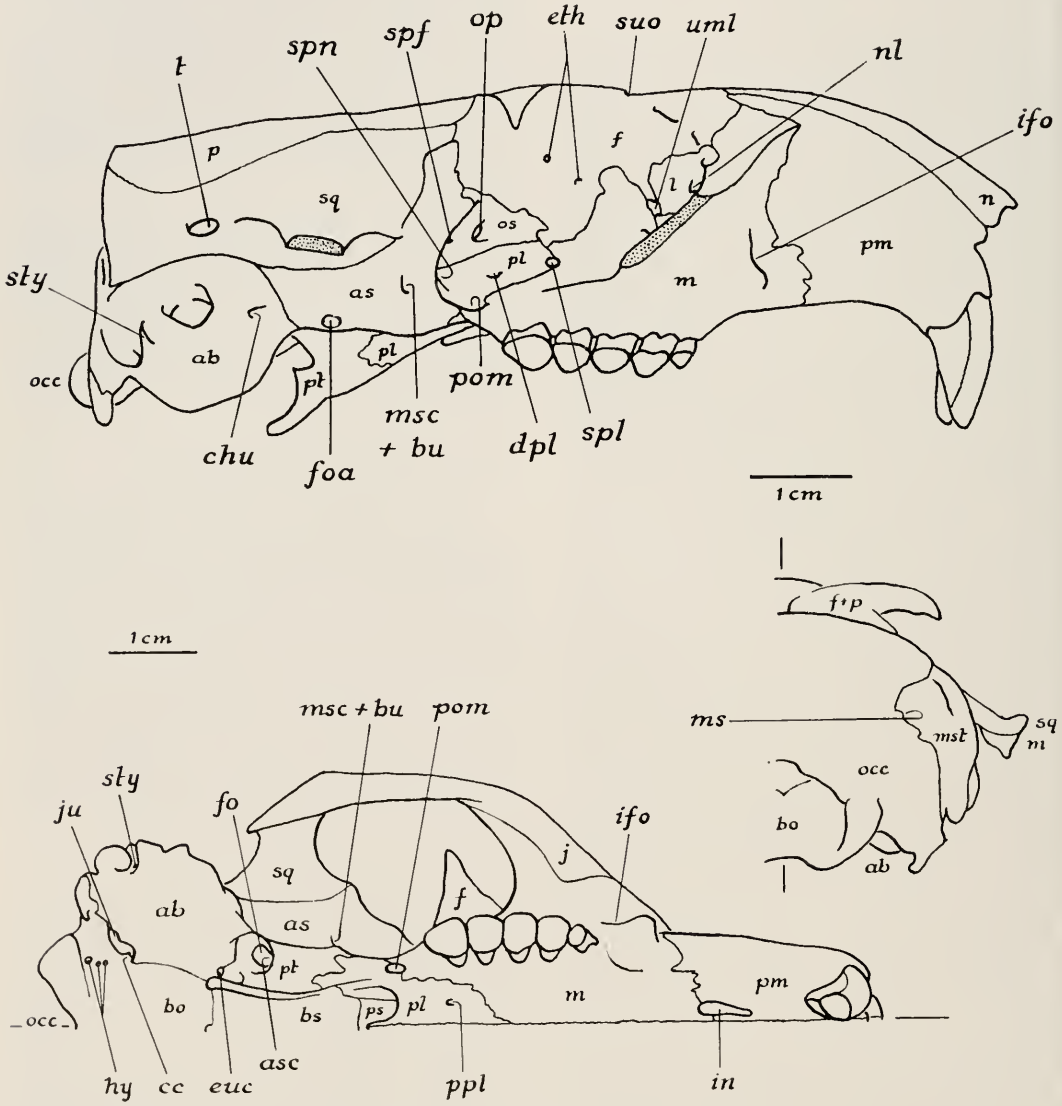

Figure 1. *Marmota monax* (MCZ B9911).

artery. As Hill (1935:122) states, it is relatively large in *Aplodontia*.

2. The incisive foramina flank the midline of the diastema. The lateral margin of each is intersected posteriorly by the premaxillary-maxillary suture. Each transmits a duct from the nasal passage, a branch of the palatine artery, and a branch from the palatine vein.

3. The major posterior palatine foramen is usually situated in the maxillary-palatine suture. It transmits the descending palatine arteries and nerves and a small vein. In many rodents a posterior pair is present in the palatine.

4. The posterior maxillary notch is situated between the end of the maxilla and the pterygoid extension of the palatine; it transmits the descending palatine vein. In many forms the notch is enclosed as a foramen.

5. The infraorbital foramen opens on the side of the snout in the maxilla. It is the anterior opening of the infraorbital canal and transmits the infraorbital nerve, artery, and vein. Protrogomorphous rodents lack the canal.

6. The anterior alveolar foramen (not figured) occurs in the floor of the infraorbital canal and transmits the anterior superior alveolar nerve plus a small artery and vein.

←

Key to figures: Foramina and related structures (numbers correspond to those in text):

aa — anterior alveolar (6)
asc — alisphenoid canal (21)
bu — buccinator (24)
bup — posterior aperture, buccinator nerve canal (24p)
cc — carotid canal (30)
cca — anterior end, carotid canal (30a)
chu — canal of Huguier (40)
dpl — dorsal palatine (16)
euc — Eustacian canal (29)
eth — ethmoid (12)
fac — facial canal (43)
fco — fenestra cochleae (41)
fo — foramen ovale (26)
foa — foramen ovale accessorius (27)
fro — foramen rotundum (20)
fv — fenestra vestibuli (42)
hy — hypoglossal (33)
ifo — infraorbital (5)
in — incisive (2)
iom — depression, origin of inferior oblique eye muscle
ipm — interpremaxillary (1)
ito — interorbital (13)
ju — jugular (32)
ma — malar (7)
mlf — middle lacerate (28)
mn — meningeal
ms — mastoid (38)
msc — masticatory (23)
msp — posterior aperture, masseteric nerve canal (23p)
nl — nasolachrymal (8)
nu — nutritive (17)
of — orbital fissure (19)
op — optic (14)
paf — post-alar fissure (35)
pgl — postglenoid (34)
pom — posterior maxillary notch or foramen (4)
ppl — posterior palatine (3)
spf — sphenofrontal (15)
spl — sphenopalatine (11)
spn — sphenoidal fissure (18)
spt — sphenopterygoid canal (22)
sqm — squamoso-mastoid (39)
st — stapedial (31)
stc — stapedial artery canal (44)
sty — stylomastoid (37)
suo — supraorbital notch (10)
t — temporal (36)
trc — transverse canal (25)
uml — unossified area in maxillary-lachrymal suture (9)

Bones:

ab — auditory bulla
as — alisphenoid
bo — basioccipital
bs — basisphenoid
f — frontal
j — jugal
l — lachrymal
m — maxillary
mst — mastoid
n — nasal
occ — occipital
os — orbitosphenoid
p — parietal
pet — petrosal
pl — palatine
pm — premaxillary
ps — presphenoid
pt — pterygoid
sq — squamosal

stippled areas: cut through bone
solid line: seen in specimen
dashed line: probable position
dotted line: hypothetical position

7. The malar foramen (not figured) is situated in the orbit where the orbital and zygomatic portions of the maxilla meet above the infraorbital foramen. It transmits the malar artery from the infraorbital canal to the tissue in front of the eye. It is rarely present; presumably the artery is usually external to the bone.

8. The nasolachrymal foramen is situated in the lachrymal bone and is bounded anteriorly by the zygomatic portion of the maxilla. It transmits the lachrymal duct.

9. An unossified area between the lachrymal bone and the orbital and zygomatic portions of the maxilla is not a foramen, but the area of origin of the inferior oblique eye muscle. It has occasionally been confused with the nasolachrymal foramen.

10. The supraorbital notch is an indentation in the supra-orbital flange of the frontal bone. It permits passage of the frontal branch of the ophthalmic nerve and the superior ophthalmic artery to the top of the head. No superior ophthalmic vein was found accompanying them; it may have been too small to see. The notch occurs in the Sciuridae, only.

11. The sphenopalatine foramen is situated at the front end of the orbital process of the palatine bone above the junction of the second and third molars. The maxilla forms the rest of its margin. It transmits the sphenopalatine nerve, artery, and vein. The bones participating in the margin of the foramen differ among rodent groups.

12. The two ethmoid foramina are entirely within the orbital lamina of the frontal bone. The anterior one faces ventrally into a shallow channel and transmits the nasociliary branch of the ophthalmic nerve. The posterior is larger and more dorsal; it transmits the ethmoid artery and vein. A single ethmoid foramen, which carries the nerve, artery, and vein, is present in the orbitosphenoid-frontal suture in most rodents.

13. A single or multiple interorbital foramen pierces the orbitosphenoid in many rodents; it is absent in *Marmota* but present in some other sciurids. In geomyids it transmits a sinusoid vein between the orbits (Hill 1935:124).

14. The optic foramen is large and is entirely within the orbitosphenoid. It transmits the optic nerve.

15. The sphenofrontal foramen is situated between the orbitosphenoid and alisphenoid. It is not quite separate from the orbital fissure in some specimens. It transmits the ophthalmic artery. The foramen is absent in many groups.

16. The dorsal palatine foramen leads into the palatine canal, which runs from the orbit downward through the palatine bone and out the posterior palatine foramen. It transmits the descending palatine artery and nerve and a small vein.

17. Many nutritive foramina (not figured) occur in the orbital surface of the maxilla above the cheek tooth roots. They transmit minute branches of nerves and arteries, and are present in all the specimens examined.

18. The sphenoidal fissure has as its outer wall the alisphenoid bone. The nerves and vessels transmitted by the orbital fissure (no. 19), the foramen rotundum (no. 20), and the alisphenoid canal (no. 21) exit from it.

19. The orbital fissure (not figured) is bounded anteriorly by the orbitosphenoid, and posterolaterally by the alisphenoid. It transmits the oculomotor, trochlear, and abducens nerves, and the ophthalmic division and part of the maxillary division of the trigeminal nerve. In most rodents the fissure is united with the foramen rotundum.

20. The foramen rotundum (not figured) is completely concealed within the alisphenoid canal. It pierces the inner wall formed by the alisphenoid and transmits the remainder of the maxillary nerve; the

zygomatic branch may have a separate foramen. The foramen rotundum and orbital fissure are united in most rodents.

21. The alisphenoid canal passes lengthwise through the alisphenoid bone. It transmits the internal maxillary artery and vein.

22. The sphenopterygoid canal is absent in *Marmota.* I have found it only in geomyoids; it leads from the pterygoid fossa to the sphenoidal fissure. It transmits the internal maxillary artery, and its walls are the area of origin of the internal pterygoid muscle.

23. The masticatory foramen is situated in the alisphenoid and is often confluent with the buccinator (no. 24). It transmits the masseteric branch of the maxillary nerve.

23p. The posterior aperture of the masseteric nerve canal (not figured) can be seen just anterior to the foramen ovale in some rodents.

24. The buccinator foramen is anteroventral to the masticatory or confluent with it. It transmits the buccinator division of the maxillary nerve.

24p. The posterior aperture of the buccinator nerve canal (not figured) can be seen in a specimen of *Paramys;* usually this canal and the masseteric share a common aperture, as in *Marmota.*

25. The single transverse canal (not figured) runs between the alisphenoid canals through the basisphenoid. It transmits a vein connecting the two internal maxillary veins.

26. The foramen ovale is situated posterolaterally in the pterygoid region. It transmits the mandibular branch of the trigeminal nerve and a minute meningeal artery.

27. I define as new the foramen ovale accessorius that is lateral to the foramen ovale and transmits the mandibular branch of the trigeminal nerve to the side of the head. It is present in forms having a substantial lateral pterygoid flange that reaches the auditory region.

28. The middle lacerate foramen is between the pterygoid region and the anterior end of the tympanic bulla or periotic as the case may be. The foramen is absent in *Marmota;* a minute aperture in the region (not figured) transmits a meningeal vein.[1]

29. The Eustachian canal emerges dorsal to the anteromedial portion of the tympanic bulla. It transmits the Eustachian tube.

30. The carotid canal begins at or in front of the anterior end of the jugular foramen and runs anteriorly between the basioccipital and the periotic and tympanic. In many rodents having a canal it transmits the internal carotid artery. In *Marmota,* however, it transmits a vein, the inferior petrosal sinus, which joins the internal jugular vein.

30a. In some fossil rodents there is a foramen leading into the cranium anteromedial to the periotic. It seems to be the anterior end of the carotid canal.

31. The stapedial foramen (not figured) is dorsolateral to the jugular foramen and shares a common aperture with it. It enters the middle ear probably in the fused suture between the tympanic and periotic, and transmits the stapedial artery.

32. The lenticular jugular foramen is between the basioccipital and the posteromedial part of the bulla. It transmits the vagus, accessory, and glossopharyngeal nerves, the stapedial artery, and the internal jugular vein.

---

[1] The function of the foramen is uncertain; no description exists of its contents in any of the Recent forms I have examined. In muroids it transmits the portion of the stapedial artery which emerges from the anterior part of the middle ear (Guthrie, 1963). In the dog the internal carotid artery passes through the foramen into the cranium (Gregory, 1910:430).

33. The hypoglossal foramen in the basioccipital is anterior to the condyle and may be subdivided into two or more parts. It transmits the hypoglossal nerve.

34. The postglenoid foramen pierces the squamosal bone ventral to the zygomatic root and posteromedial to the glenoid fossa. It is absent in many *Marmota* skulls. When present, it transmits a large vein that drains most of the cranial cavity.

35. The post-alar fissure is absent in *Marmota*. I introduce this term for an opening between the alisphenoid wing and the tympanic bulla; it probably serves a function similar to that of the postglenoid foramen. In some forms it separates a part of the squamosal from the tympanic.

36. The temporal foramen is absent in *Marmota*. When present it is within the squamosal bone or in the squamoso-parietal suture, usually posterodorsal to the root of the zygomatic arch. It serves the same function as the postglenoid foramen and can take over the entire function of that opening. In some forms there are two or more temporal foramina.

37. The stylomastoid foramen is between the external auditory meatus and the mastoid process. It transmits the facial nerve, and is constant in all rodents that possess a bulla.

38. The mastoid foramen is on the occipital surface between the occipital bone and the medial portion of the mastoid bone. It transmits a small vessel which, according to Hill (1935:128), is a vein from the neck muscles to the transverse sinus.

39. The squamoso-mastoid foramen is absent in *Marmota*. I introduce the term for the foramen, which is present in many rodents, on the occipital surface between the squamosal and the mastoid. It transmits a vein.

40. The canal of Huguier is a minute slit in the anterior surface of the bulla. It transmits the chorda tympani division of the facial nerve.

The following, which are not, strictly speaking, cranial foramina, have been shown in figures of several early rodents. They are useful as points of reference, and the canals are, of course, associated with soft parts intimately related to cranial foramina.

41. The fenestra cochleae (rotundum) is a round, membrane-covered aperture leading into the scala tympani of the cochlea.

42. The fenestra vestibuli (ovale) is an oval, membrane-covered aperture leading into the scala vestibuli of the cochlea. The footplate of the stapes rests on this membrane.

43. The facial canal is in the periotic dorsolateral to the promontorium and is the canal in which the facial nerve traverses the middle ear.

44. The stapedial artery canal is also situated in the periotic dorsolateral to the promontorium, and is the canal by which the stapedial artery exits from the middle ear. In many of the fossils it appears to be united, in part, with the facial canal.

PARAMYIDAE

Paramys

Specimens examined:

Paramys copei (Figs. 2 and 4): Lysite Member, Wind River Formation: PU 16564 p. Lost Cabin Member, Wind River Formation: AMNH 4755 (type) npot, 4756 potc.

P. delicatior: Twin Buttes Member equivalent, Bridger Formation: AMNH 55675 po.

P. delicatus (Fig. 3): Blacks Fork Member, Bridger Formation: AMNH 12506 s, 13090 s; USNM 23556 s; YPM 13381 npo.

P. sp.: Willwood Formation: PU 17421 np.

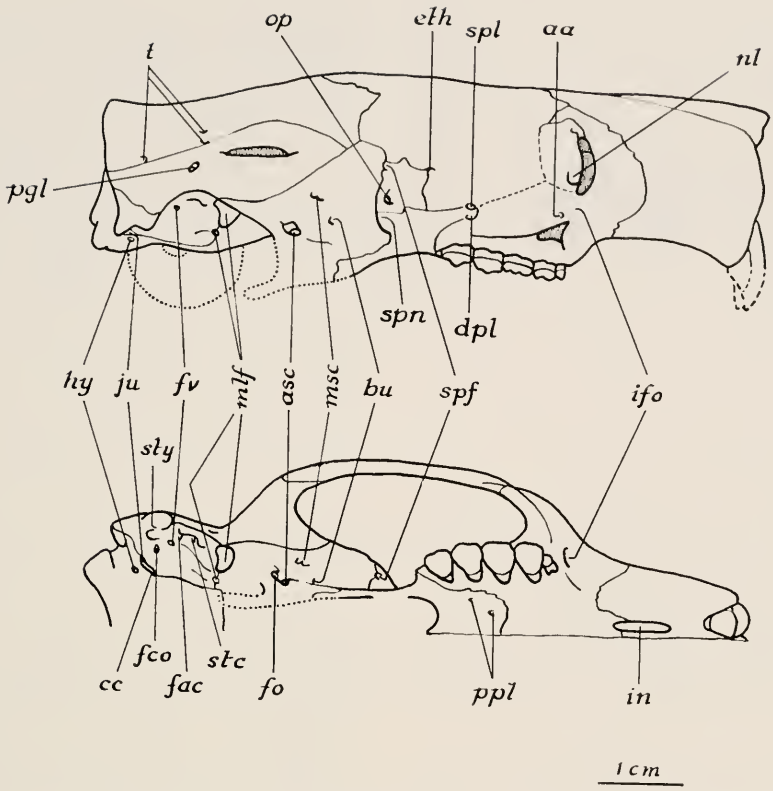

Figure 2. *Paramys copei* (composite of AMNH 4755 and 4756). See Fig. 1 for key to foramina.

Foramina

The ratio of length of the incisive foramina to diastemal length ranges from .42 to .45. The lateral margins of the foramina are interseeted behind the middle by the premaxillary-maxillary suture, which runs posterolaterally away from them.

The posterior palatine foramina are wholly within the palatine bones. The larger anterior pair is close behind the maxillary-palatine suture and medial to the posterior halves of the first molars. The smaller posterior pair is more laterally situated than the anterior and is medial to the posterior halves of the second molars. The maxilla ends behind the cheek teeth in a blunt point. There is a slight posterior maxillary notch between it and the pterygoid extension of the palatine.

In front view the infraorbital foramen is elliptical; the major axis is inclined so that the top of the foramen is farther lateral than the bottom. The axis in *P. copei* measures 3.0 mm; in *P. delicatus,* 4.0 mm. In lateral view the foramen is approximately vertical. The anterior alveolar foramen, which is in the curve formed by the orbital wall and floor, is just posterior to the infraorbital, and is directed anteromedially. In front of the infraorbital there is a small foramen, probably for the nasal branches of the infraorbital artery and nerve. This foramen is more pronounced and more ventral in *P. delicatus* than in *P. copei.*

The lachrymal region is preserved only in the type specimen of *P. copei,* AMNH 4755. The nasolachrymal foramen is dorsal

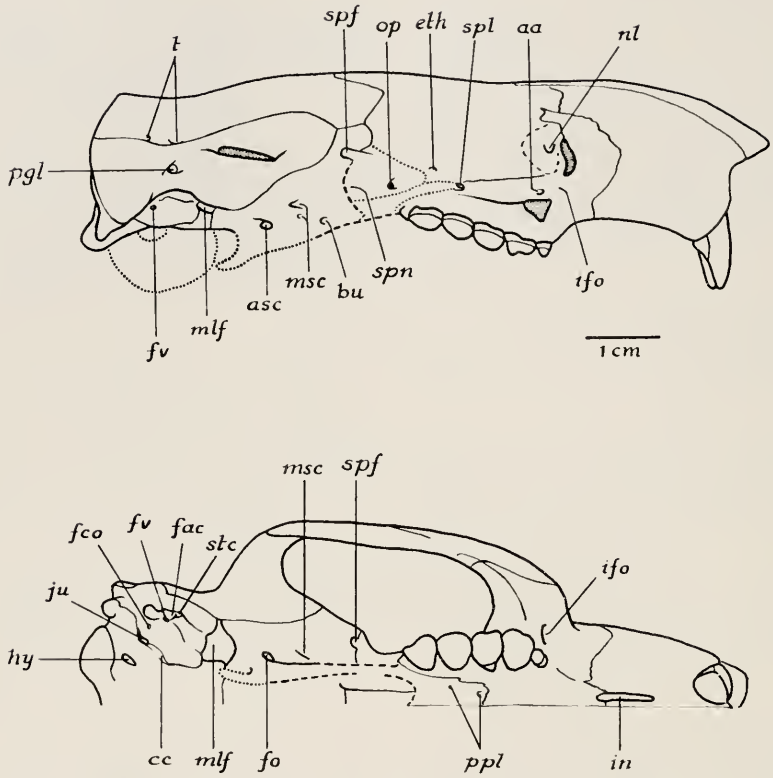

Figure 3. *Paramys delicatus* (USNM 23556). See Fig. 1 for key to foramina.

to and not far above the infraorbital, and it is below the lachrymal flange of the zygoma. A channel for the lachrymal duct descends the face of the lachrymal bone to the foramen. Sutures around the foramen are not visible.

The sphenopalatine foramen is dorsal to the junction of the second and third molars. The maxilla and orbital process of the palatine make up its borders; the frontal may reach it dorsally, but this is not clear. The orbitosphenoid is excluded from the margin. Wood (1962:15, fig. 3A) figures the sutures incorrectly and shows the foramen surrounded by the maxilla. The ethmoid foramen is dorsal and posterior to the third molar. It is within the frontal bone and is overhung by a lip from it. In the type specimen of *P. copei*, the frontal-orbitosphenoid suture reaches it posteriorly; in *P. delicatus*, AMNH 12506, the suture does not. The optic foramen, which is within the orbitosphenoid, is nearly 1.0 mm in diameter. It is dorsal and considerably posterior to the third molar. In *P. copei* it is closer to the sphenoidal fissure than in *P. delicatus*.

The dorsal palatine foramen, which is in the maxillary-palatine suture, is immediately ventral to the sphenopalatine, and both are within a single depression. Three specimens, AMNH 4755, 12506, and 55675, show this condition clearly. The same occurs in *Thisbemys corrugatus*, AMNH 94008 (for which there is no locality data; this is the only detail known of the foramina of *Thisbemys*, so I include it here). Minute nutritive foramina are present, as in all rodents, in the floor of the orbit above the roots of the cheek teeth.

The sphenoidal fissure at its opening is separated from the cranial cavity by a wall of bone; it is situated well behind the cheek teeth. In *P. delicatus* a slight ridge sets off the dorsal portion as a distinct channel. The alisphenoid canal joins the sphenoidal fissure laterally.

The prominent sphenofrontal foramen is in the orbitosphenoid-alisphenoid suture near its junction with the frontal. In *P. delicatus,* USNM 23556, a conspicuous channel leads gradually downward and forward from the foramen. Wood (1962: 15, fig. 3A) has labeled a puncture in the bone as the sphenofrontal foramen; actually, it is indicated in his figure by a dark area 2 mm behind and 3 mm above the point he has labeled.

The masticatory and buccinator foramina are separate, the distance between them ranging from 1.0 to 3.0 mm. They face anterodorsally and anteriorly, respectively, and are a minimum of 3 mm from the foramen ovale. A minute foramen occurs between them in *P. delicatus* but not in *P. copei;* this was possibly for a branch that split off the masseteric nerve before it emerged from the masticatory foramen. The buccinator foramen is farther anterior with respect to the masticatory in *P. delicatus.* Wood (1962:15, fig. 3) has interpreted these foramina differently and, I believe, incorrectly.

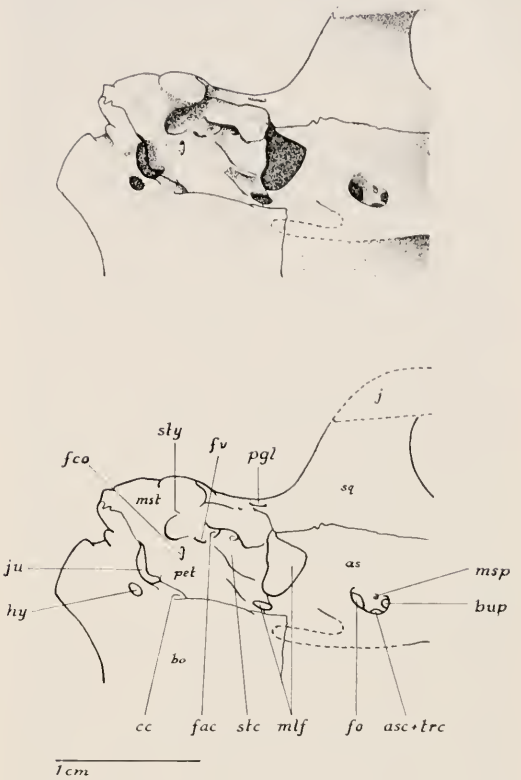

Figure 4. Auditory and pterygoid regions of *Paramys copei* (AMNH 4756). Labeled outline drawing (hamular process hypothetical), and shaded drawing of the same. See Fig. 1 for key to foramina.

The pterygoid region of *P. copei* is bounded medially by a flange and laterally by a faint ridge that is sufficient to enclose a foramen ovale accessorius. Medial to the foramen there is an oval depression. Within it are four foramina (Fig. 4). The posterior one leads from the braincase and is clearly the foramen ovale. The medial foramen leads into two canals; one, anteriorly directed, is the alisphenoid; the other, medially directed, is the transverse canal. The anterior and lateral foramina lead to the buccinator and masseteric nerve canals respectively. I am in agreement with Black (1968a:291, fig. 18) as regards their interpretation. In *P. delicatus* the lateral pterygoid ridge is somewhat weaker. A single large foramen, the foramen ovale, is visible in ventral view; in one specimen, AMNH 12506, a small foramen, probably the transverse canal, opens in its anteromedial wall.

The tympanic bones are absent in all specimens of *Paramys,* and the middle lacerate foramen is completely exposed. In *P. delicatus* it seems to be a single, irregular opening. In *P. copei* a strut of bone transforms the medial portion into a separate, oval-shaped foramen. Wood (1962:42) interprets this latter as the entire middle lacerate foramen and states that the larger lateral part is apparently the foramen ovale. Since the specimen has a readily identifi-

able foramen ovale in the usual position, Wood's designation cannot be correct. Black (1968a:291, fig. 18) has identified the foramina as I do; the smaller medial one he identifies as a part of the carotid canal.

The carotid canal begins at the anterior end of the jugular foramen, it was probably open ventrally, and presumably transmitted a branch of the internal carotid artery. The canal may emerge from between the basioccipital and the petrous portion of the periotic and enter the cranium through the medial portion of the middle lacerate foramen, but this cannot be determined with certainty. The jugular foramen, as in all rodents, is lenticular in shape and is situated between the periotic and basioccipital. The hypoglossal foramen is single in *P. copei* and *P. delicatus*. The posterior of two hypoglossal foramina shown by Wood (1962:15, fig. 3E) is a break in the bone.

The postglenoid foramen, which is behind the glenoid fossa below the zygomatic root, is in the squamosal bone. Its major axis is smaller in *P. copei* than in *P. delicatus*, about 1.5 and 2.5 to 3.5 mm respectively. Temporal foramina are concentrated in the squamoso-parietal suture. Anterodorsal to the postglenoid is a single foramen in the suture. In some specimens it is accompanied by a second opening either above in the parietal (AMNH 4756, right side; AMNH 12506, left side) or below in the squamosal (USNM 23556, left side). A smaller foramen, also situated in the suture, is about halfway between these foramina and the back of the parietal.

A mastoid foramen is present in the mastoid-occipital suture. It is well above the level of the top of the foramen magnum. The foramina within the auditory region are exposed because the tympanic was not attached and has been lost. The least distorted periotic is preserved in a specimen of *P. copei*, AMNH 4756. The major features of the auditory region are shown in Figure 4. Wood (1962:43, fig. 14A) and Black (1968a:291, fig. 18) figure the same portion of this specimen. The most complete description of a paramyid periotic is given for *P. delicatus* by Wood (1962:15, fig. 3B and C; page 18).

A lateral shelf of the periotic begins at the middle lacerate foramen and continues posteriorly for two-thirds of the length of the petrous portion. Behind it the mastoid portion broadens, curves medially to the posterior end of the jugular foramen, and ascends the occipital surface; most of this region is exposed outside the middle ear. Lateral to the fossa for the stapedius muscle there is a protuberance of the mastoid that is not situated so far posteriorly as the mastoid process in later rodents.

Medial to the lateral shelf a broad channel, which narrows posteriorly, runs from the middle lacerate foramen to the fossa for the stapedius muscle. In the absence of a tympanic the stylomastoid foramen is simply a groove lateral to the fossa on the medial surface of the mastoid protuberance and not a foramen as indicated in Wood's figure. The anterior part of the channel is presumably the area of origin of the tensor tympani muscle. In the middle portion are two posteriorly facing foramina, which are just internal to the shelf. The anterior one appears to be the foramen through which the stapedial artery left the middle ear; the posterior one, the foramen through which the facial nerve entered the middle ear.

The medial portion of the auditory region is occupied by the promontorium. A faint channel, which marks the course of the stapedial artery, runs from the fenestra vestibuli to the anterior end of the jugular foramen. This portion of the channel corresponds in position to the indentation for the stapedial foramen in the bulla of *Reithroparamys* (Fig. 5). The fenestra cochleae is in the posterior surface of the promontorium.

I do not see, as Wood did (1962:18), evidence for the position of the auditory bulla. He states that the ridge paralleling

the median margin of the petrosal and overhanging the petrosal-basioccipital suture (in AMNH 12506) seems to have served for bracing the median wall of the bulla. But the particular specimen he described is distorted; the petrosal has been tipped and the basioccipital crushed so that this ridge, which originally abutted against the basioccipital, now stands away from it. The ridge in its proper position could not have braced the bulla.

Wood also states that the depression between the mastoid region and the lateral shelf of the periotic " . . . seems to have held the meatal tube of the bulla" (p. 18). It is more likely, however, that the meatus was lower down, as in *Reithroparamys* (Fig. 5) and *Sciuravus* (Fig. 7) and that the depression contained the dorsal portion of the tympanic.

Leptotomus

Specimens examined:

Leptotomus bridgerensis: Twin Buttes Member, Bridger Formation: AMNH 12507 t.

L. costilloi: Huerfano Formation: AMNH 55110 s, 55111 (type) s.

L. parvus: Twin Buttes Member, Bridger Formation: AMNH 12519 (type) p, 93030 p.

Foramina

Although two of these specimens are complete skulls, they are so fractured and crushed that very little information can be gotten from them.

The two partial palates of *L. parvus* show that the posterior palatine foramina are wholly within the palatine bones, close behind the maxillary-palatine suture. The large pair is medial to the anterior part of the second molars. These are connected, each by a canal through the bone, to their respective dorsal palatine foramen. The latter is situated in the maxillary-palatine suture immediately ventral to the sphenopalatine foramen and above the anteriormost part of the third molar.

In lateral view the infraorbital foramen is vertical; its exact shape and disposition cannot be determined.

The sphenoidal fissure at its opening is separated from the cranial cavity by a wall of bone. It is well behind the last molar. Details of the region are visible in the fragmentary specimen of *L. bridgerensis*. A slight ridge sets off the dorsal portion as a distinct channel. The alisphenoid joins the fissure laterally. A foramen in the medial wall of the alisphenoid canal is probably the entrance to the transverse canal; it would be completely hidden in an unbroken specimen. The exposed channel through the bone to the sphenofrontal foramen is large and runs anteroventrally to a position that was probably very close to the top of the sphenoidal fissure.

The pterygoid region is partially preserved in AMNH 55110. The foramen ovale is large, and the lateral pterygoid flange bridges it ventrally to form a foramen ovale accessorius.

The carotid canal appears to be like that of *Paramys;* it was probably open ventrally with the lateral lip of the basioccipital shielding the artery. Whether it carried the artery, or just the inferior petrosal sinus, however, cannot be determined.

The postglenoid foramen is in the squamosal under the root of the zygoma. Its major axis measures about 1.8 mm.

The auditory region is poorly preserved, but important details can be seen in the type of *L. costilloi*. The channel for the stapedial artery crosses the promontorium laterally to the fenestra vestibuli as in *Paramys*. At a point about a third of the way along its course another channel about half as wide diverges anterolaterally. Within a short distance this channel subdivides. The diverging branch runs anteromedially across the promontorium. This bifurcating channel, I believe, marks the course of the promontory artery.

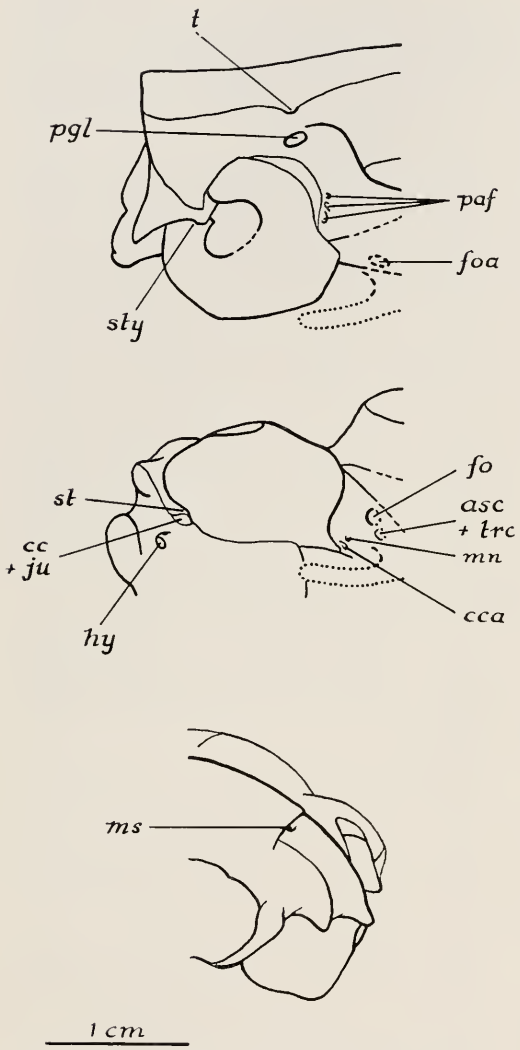

Figure 5. *Reithroparamys delicatissimus* (AMNH 12561). See Fig. 1 for key to foramina.

Reithroparamys

Specimens examined:

Reithroparamys delicatissimus (Fig. 5): Blacks Fork Member, Bridger Formation: AMNH 12561 (type) npc.

Foramina

The ratio of length of the incisive foramina to diastemal length is .48. The lateral margins of the foramina are intersected very near the back by the premaxillary-maxillary suture, which runs posterolaterally away from them.

A single pair of posterior palatine foramina is present within the palatine bones. It is situated far laterally, almost on the maxillary-palatine suture, and is medial to the anterior ends of the second molars. The maxilla ends behind the cheek teeth in a blunt point. There is a slight posterior maxillary notch between it and the pterygoid extension of the palatine.

In front view, the infraorbital foramen is elliptical. The major axis, which measures 3.5 mm, is inclined so that the top of the foramen is farther lateral than the bottom. In side view the foramen is approximately vertical. The anterior alveolar foramen, which is in the curve made by the orbital floor and wall, is just behind the infraorbital foramen.

The wall of the orbit and the alisphenoid bone are missing. Enough of the nasolachrymal canal is present to show that the nasolachrymal foramen was dorsal and close to the infraorbital.

The pterygoid region (Fig. 5) is mostly missing. Several details can be made out, however. The external pterygoid flange, homologous to the lateral ridge in *Paramys*, is substantial and seems to enclose a foramen ovale accessorius. Medial to the flange, the back of the foramen ovale is preserved; a channel, which is most likely the entrance to the alisphenoid and transverse canals, leads anteromedially from the foramen ovale. The middle lacerate foramen is completely covered by the auditory bulla. Just anterior to the bulla and lateral to the styloid process are two elongate foramina. A channel extends posteriorly under the bulla from the medial one. This suggests that the foramen may have been an aperture for a branch of the internal carotid artery, possibly the promontorial. The Eustachian canal passes over it. The lateral foramen may have transmitted a meningeal vessel.

The carotid canal appears to begin at the

anterior end of the jugular foramen and does not have a distinct entrance. A shelf of the periotic is exposed anterolateral to the jugular foramen at the point where the bulla is indented. The stapedial foramen is in this indentation and between the tympanic and periotic. The hypoglossal foramen is double on both sides. The larger foramen opens ventrally and faces anterolaterally; its rim continues out toward the jugular foramen. The second foramen is under the rim of the larger and opens and faces anteromedially.

The postglenoid foramen is within the squamosal bone. Its major axis is 2.1 mm long. On the left side of the skull are three foramina in front of the periotic, which is sandwiched between the bulla and squamosal. These foramina may be homologous with the post-alar fissure of some later sciuromorphous forms. A large temporal foramen is present in the squamoso-parietal suture above the postglenoid. There seems to be a much smaller one, behind it, also in the suture.

The stylomastoid foramen is bounded by the bulla and mastoid element. There is a short protuberance of the mastoid lateral to it. The mastoid foramen is above the level of the top of the foramen magnum and is in the mastoid-occipital suture.

Ischyrotomus

Specimens examined:

Ischyrotomus oweni: Blacks Fork Member, Bridger Formation: USNM 17161 s; 17160 (type) s (specimen not available to me; information taken from Wood, 1962).

I. horribilis: Blacks Fork Member, Bridger Formation: USNM 17159 (type) s.

I. petersoni: Myton Member, Uinta Formation: AMNH 2018 (type) s.

Foramina

The ratio of length of the incisive foramina to diastemal length ranges from .18 to .21. The lateral margins of the foramina are intersected near the back by the premaxillary-maxillary suture, which runs posterolaterally away from them.

The pair of larger posterior palatine foramina is in the maxillary-palatine suture and is medial to the middle region of the first molars. The smaller posterior pair, entirely within the palatine, is in line with the larger pair and medial to the anterior halves of the second molars. In *I. oweni*, USNM 17161, there are two minute foramina situated more laterally in the palatine. The maxilla ends behind the cheek teeth in a distinct point that is best seen in *I. horribilis*. There is a posterior maxillary notch between it and the pterygoid extension of the palatine.

In front view, the infraorbital foramen is elliptical, and the major axis is inclined so that the top of the foramen is farther lateral than the bottom. The axis in *I. horribilis* is 3.3 mm long; in *I. oweni*, 4.4 mm; in *I. petersoni*, 4.5 mm. In side view the foramen is approximately vertical. The lachrymal region in these specimens is either missing or damaged. Wood (1962: 189) reports that the nasolachrymal foramen is between the lachrymal and maxillary bones in the medial wall of the orbit.

Wood (1962:189–190) states, "The sphenopalatine foramen sometimes lies on the frontal-maxillary suture and sometimes in the maxilla as in *Paramys*. It is a little farther to the rear, just behind M^3 instead of just in front of it." His interpretation of its position in *Paramys* is incorrect, as noted above, and his placement of it in *Ischyrotomus* also seems erroneous. Wood (1962: 207, fig. 71), in his figure of USNM 17160, shows the foramen within the maxilla and dorsal to the back of the second molar. Its position cannot be determined in the other specimens. The ethmoid foramen is above and between the sphenopalatine and optic foramina. A slight lip of bone overhangs it. Sutures in this region are indeterminate. The optic foramen, which is about 1.0 mm in diameter, is dorsal and considerably

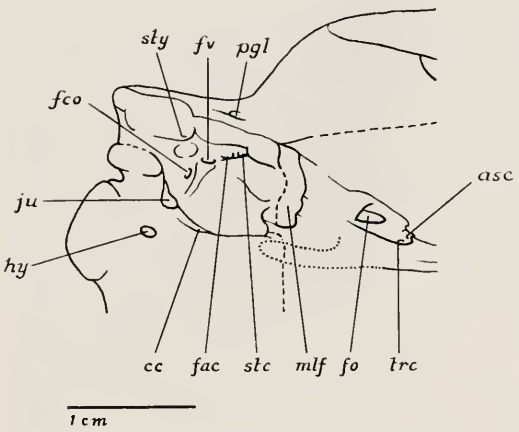

Figure 6. Auditory and pterygoid regions of *Ischyrotomus oweni* (USNM 17161). See Fig. 1 for key to foramina.

posterior to the third molar, and it is near the sphenoidal fissure.

The dorsal palatine foramen was not seen; the region in which it would occur is fractured in every specimen. The sphenoidal fissure at its opening is separated from the cranial cavity by a wall of bone. A low ridge sets off its dorsal portion as a distinct channel. The alisphenoid canal unites with the fissure. The sphenofrontal foramen is dorsal to the sphenoidal fissure and posterodorsal to the optic foramen; a conspicuous channel leads downward and forward from it. Sutures in this area are indistinct in all specimens. Available specimens are too crushed in the alisphenoid region to reveal whether the masticatory and buccinator foramina were separate or united.

The pterygoid region of *Ischyrotomus* (Fig. 6) is bounded medially by a flange and laterally by a ridge; it is not developed into a fossa and is occupied almost entirely by a depression in which there are two openings. Posterolaterally the foramen ovale opens from the cranium; the lateral ridge is interrupted alongside it, and the beginning of a foramen ovale accessorius is suggested by the hook-like termination of the ridge. Anterior and medial to the foramen ovale is the second opening; it is deep within the angle formed where the lateral ridge and internal pterygoid flange meet. The alisphenoid canal runs anteriorly from it, the transverse canal medially. The dorsal portion of the alisphenoid canal is slightly damaged, but one small foramen, which probably transmitted the buccinator nerve, is clearly visible in its wall. The middle lacerate foramen is distorted by crushing in all specimens.

The carotid canal begins at the anterior end of the jugular foramen. The hypoglossal foramen is either single or double; when double, the apertures open into a single pit.

The postglenoid foramen is wholly within the squamosal bone. The major axis measures 1.5 mm in *I. horribilis* and 2.7 mm in *I. oweni*. Temporal foramina are in the vicinity of the squamoso-parietal suture. The largest foramen is dorsal to the postglenoid and above the zygomatic root; in some specimens it is entirely within the squamosal; in others on the suture. There is a small foramen anterior to it and another posterior in the parietal. The occipital surface is damaged, and sutures near the mastoid foramen cannot be distinguished.

The major features of the auditory region (Fig. 6) are essentially as in *Paramys*, but there are differences in detail. The mastoid portion of the periotic has a descending process lateral and posterior to the fossa for the stapedius muscle. This mastoid process is essentially modern in aspect. The foramina in the petrosal for the stapedial artery and for the facial nerve bear the same relationship to each other as in *Paramys*. In ventral view, however, they are hidden under a single shelf which runs anterolaterally from a point on a level with the front of the fenestra vestibuli to a point overhung by the lateral shelf of the periotic. There is a distinct channel for the stapedial artery which crosses the promontorium. It is broadest at the fenestra vestibuli and narrows somewhat near the anterior end of the jugular foramen. This portion corresponds in position to the in-

dentation for the stapedial foramen in the bulla of *Reithroparamys* (Fig. 5) and *Sciuravus* (Fig. 7).

Pseudotomus

Specimens examined:

Pseudotomus hians: ?Blacks Fork Member, Bridger Formation: AMNH 5025 (type) nptc.

Foramina

A portion of the external margin of the right incisive foramen is present. Its curvature suggests that the foramen was relatively short, as in *Ischyrotomus*.

At the back of the maxilla, near the middle of the palate, a slight channel leads posterodorsally into what was probably the larger of the posterior palatine foramina. It was evidently medial to the middle of the first molar and in the maxillary-palatine suture.

The infraorbital foramen is broad and elliptical. The major axis, which measures 3.5 mm, is inclined so that in front view the top of the foramen is farther lateral than the bottom, and in side view the top is slightly farther anterior than the bottom. The anterior alveolar foramen, which is in the curve made by the orbital floor and wall, is just behind the infraorbital. The nasolachrymal foramen is dorsal to and not far above the infraorbital and is below the posterior protuberance of the lachrymal bone. A wide channel descends the surface of the lachrymal and bends anteriorly into the foramen. The maxilla appears to form the ventral margin of the foramen.

Both orbits are considerably damaged and the fragments of bone displaced; sphenopalatine and dorsal palatine foramina cannot be seen. The anterior part of the ethmoid foramen is preserved on the right side; a lip from the frontal overhangs it. The optic foramen, about 1.0 mm in diameter, seems to have been dorsal and considerably posterior to the last molar.

The sphenoidal fissure at its opening seems to be separated from the cranial cavity by a wall of bone. The sphenofrontal foramen is visible on the right side of this specimen just dorsal to the sphenoidal fissure. I do not see a channel leading from it.

The masticatory and buccinator foramina are separate and over 4.0 mm anterior to the foramen ovale. A broad channel leads dorsally from the masticatory foramen. The buccinator foramen opens anteriorly; it is directly under the middle of the masticatory and less than 1.0 mm away from it.

The pterygoid portion of *Pseudotomus* is similar to that of *Ischyrotomus*. The foramen ovale has only a hint of a lateral pterygoid ridge alongside it; there is no suggestion of a foramen ovale accessorius. The anterior portion of the pterygoid depression leads into the alisphenoid and transverse canals. A posterior projection from the anterior margin of the middle lacerate foramen indicates that the foramen was partially differentiated into medial and lateral portions. The posterior margin is not preserved.

The bullae are missing. The left periotic and the anterior end of the right are gone, and the portion of the basioccipital that normally abuts the periotic is exposed. The ventral surface of the basioccipital extends laterally as a flange that would have overlapped the anterior extremity of the periotic. Dorsal to the flange on the lateral surface of the basioccipital, there is a channel that turns up toward the cranium just behind the middle lacerate foramen; possibly this is the carotid canal, or the course of the inferior petrosal sinus. The area of the basioccipital contained within the curve of the channel is sculptured and was most likely the place where the periotic attached. The posterior part of the basioccipital is missing.

The postglenoid foramen is within the squamosal bone. Temporal foramina are present in or near the squamoso-parietal suture, but their number and exact positions are indeterminate. The mastoid foramen is above the level of the top of the

foramen magnum in the mastoid-occipital suture.

Manitsha

Specimens examined:

Manitsha tanka: Chadron Formation[1]: AMNH 39081 (type) np.

Foramina

The ratio of length of the incisive foramina to diastemal length is .23. The lateral margins of the foramina are not intersected by the premaxillary-maxillary suture, and it crosses the diastema behind them. The maxilla ends behind the cheek teeth in a point appressed to the palatine; there is no posterior maxillary notch.

The infraorbital foramen seems small relative to the skull size. In side view it is approximately vertical. A single hypoglossal foramen is preserved on the left side.

Discussion of the Paramyidae

The paramyid rodents form a unified group with respect to cranial foramina. There are some differences between genera and species, among which changes in the pterygoid region and various patterns of arterial channels in the auditory region are the most striking.

The ratio of length of the incisive foramina to diastemal length is high in *Paramys* and *Reithroparamys*, .42 to .48, and low in *Ischyrotomus, Pseudotomus,* and *Manitsha,* .18 to .23. The lateral margins of the foramina are intersected behind the midpoint, but not at the very back, by the premaxillary-maxillary suture. In *Manitsha* the suture crosses the diastema behind the foramina and does not run into their margins.

The posterior palatine foramina are wholly within the palatine bone in *Paramys, Leptotomus,* and *Reithroparamys.* In *Ischyrotomus* they are in the maxillary-palatine suture. A posterior maxillary notch is present in all except *Manitsha.*

In *Paramys, Thisbemys,* and *Leptotomus* the dorsal palatine foramen is associated with, but separate from, the sphenopalatine foramen; its position is uncertain in the other genera owing to crushing in the orbital region. The sphenofrontal foramen is present in *Paramys, Leptotomus, Ischyrotomus,* and *Pseudotomus.* Other skulls were too damaged for it to be found. The presence of this foramen indicates that the ophthalmic artery was a branch of either the stapedial or the internal carotid artery.

Masticatory and buccinator foramina are separate from each other and not especially close to the foramen ovale. I do not expect that *Ischyrotomus* will prove to be an exception when adequate material is found.

Foramina in the vicinity of the foramen ovale differ among genera and even among species. The pattern found in *Paramys copei* could be that from which later arrangements were derived. In this species the foramen ovale, masseteric nerve canal, buccinator nerve canal, and alisphenoid and transverse canals open into a single depression. In *Ischyrotomus* and *Pseudotomus* entrances to the masseteric and buccinator nerve canals are hidden, and the depression is differentiated into two parts, one for the foramen ovale and another for the alisphenoid and transverse canals. The transverse canal was hidden in *Leptotomus* and a foramen ovale accessorius may have been present. The only available specimen of *Reithroparamys* appears to have been similar to *Ischyrotomus.* In *Paramys delicatus* the alisphenoid canal is hidden, and the foramen ovale is the only conspicuous opening in the region; the transverse canal is small but visible in one specimen and hidden in the other.

The middle lacerate foramen, when present and undistorted, appears to be

[1] The American Museum catalogue incorrectly gives the horizon and locality for this specimen as Lower Brule, North Point of Slim Buttes, and this misinformation has been perpetuated in the literature. The correct data, supplied by M. F. Skinner (personal communication), are as follows: Chadron Formation, west side of Reva Pass, Harding County, South Dakota.

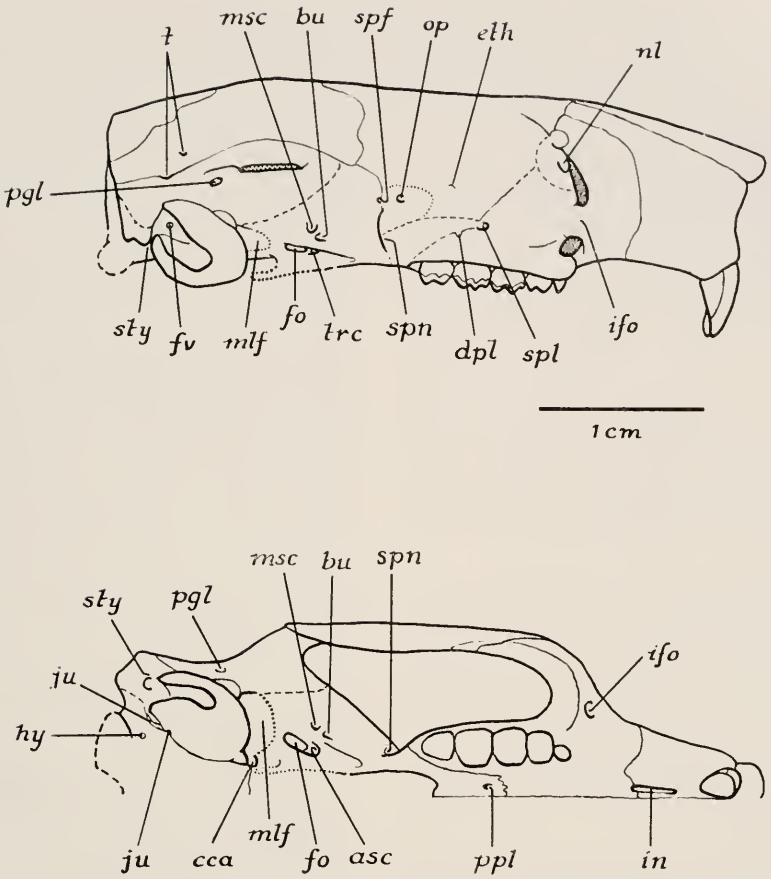

Figure 7. *Sciuravus nitidus* (reconstructed from USNM 17683, 18100, and 22477). See Fig. 1 for key to foramina.

divided into two parts, the small medial one possibly for passage of the internal carotid artery. In *Reithroparamys,* only this small aperture is visible; the tympanic bulla covers the middle lacerate foramen if it is present.

In the auditory region of *Paramys* and *Ischyrotomus* there is a channel for the stapedial artery which crosses the promontorium, and a stapedial foramen is present in *Reithroparamys.* In *Paramys* and *Ischyrotomus* there is no channel indicating the presence of the promontorial artery, whereas in *Leptotomus* this channel is clearly marked. The hypoglossal foramen is single in *Paramys,* single or double in *Ischyrotomus,* and double in *Reithroparamys.* A rudimentary post-alar fissure is present in *Reithroparamys* and absent in the other genera.

SCIURAVIDAE

Specimens examined:

Sciuravus nitidus (Fig. 7): Blacks Fork Member, Bridger Formation: AMNH 12531 n, 12551 npte, 13101 npoc; USNM 17683 c, 17697 np, 17700 np, 18023 np, 18100 s, 22477 s; CM 9683 np; YPM 13458 p.

Foramina

Accurate measurement of the incisive foramina is possible in three specimens. The ratios of their lengths to diastemal

lengths are .41, .45, and .47. The lateral margins of the foramina are intersected near the back by the premaxillary-maxillary suture, which runs posterolaterally away from them.

The posterior palatine foramina are within the palatine bones. The large anterior pair is close behind the maxillary-palatine suture and medial to the junction of the first and second molars in some specimens, medial to the second molars in others. The smaller posterior pair is somewhat more lateral in position than the anterior and is medial to the junction of the second and third molars. The maxilla ends behind the cheek teeth in a blunt point. There is a slight posterior maxillary notch between it and the pterygoid extension of the palatine.

In front view, the infraorbital foramen is elliptical. The major axis is inclined so that the top of the foramen is farther lateral than the bottom. The axis ranges in five specimens from 1.7 to 2.6 mm. In side view the foramen is approximately vertical. The anterior alveolar foramen is just behind the infraorbital foramen in the curve made by the orbital wall and floor, and plunges anteromedially.

The structure of the lachrymal region, although not entirely preserved in any one specimen, can be determined for the most part. The nasolachrymal foramen is well above and slightly posterior to the infraorbital. It is directly below the posterior protuberance of the lachrymal bone and may be surrounded by that bone, but sutures are not clear. A short channel leads into the nasolachrymal foramen and continues anteroventrally as a canal. The canal, exposed in AMNH 12531, passes internal to the infraorbital foramen and turns medially a short distance in front of it.

The sphenopalatine foramen is dorsal to the anterior half of the second molar. It seems to be bounded posteriorly by a long orbital process of the palatine, and on the other sides by the maxilla. The frontal may be barely excluded from its margin; the orbitosphenoid is completely excluded. The minute ethmoid foramen is in the frontal above and about halfway between the sphenopalatine and optic foramina. The orbitosphenoid does not seem to reach it. It is overhung by a slight lip from the frontal. The optic foramen is not preserved clearly in any specimen, but seems, at least in USNM 18100, to have been within the orbitosphenoid. It is posterodorsal to the third molar and near the sphenoidal fissure.

The small dorsal palatine foramen is in the floor of the orbit posterior and slightly lateral to the sphenopalatine. The suture between the palatine and maxilla dips into it. The entire course of the canal descending from it can be traced in two specimens, USNM 18100 and YPM 13458 (better seen in the latter). For a short distance the canal runs between maxilla and palatine; then it emerges and continues anteroventrally on the internal surface of the palatine as a channel open into the choanae; finally it turns anteriorly through the posterior palatine foramen.

The available specimens are too damaged to show whether the sphenoidal fissure at its opening is separated from the cranium. It is situated well behind the cheek teeth. The sphenofrontal foramen, seen in one specimen, USNM 18100, is in the orbitosphenoid-alisphenoid suture just below the point at which the suture meets the frontal. A short channel leads anteroventrally from it.

The masticatory and buccinator foramina are clearly preserved in only one specimen, USNM 18100. They are close together near the foramen ovale; channels from them lead upward and forward respectively.

The pterygoid region is a relatively flat triangular surface bounded medially by a flange and laterally by a ridge; it is not developed into a fossa. There is an elongated depression medial and parallel to the posterior half of the lateral ridge. The foramen ovale opens from the cranial cavity into the posterior part of this depression. The alisphenoid canal runs forward from

the depression, and a lateral canal branches off from it to lead toward the masticatory and buccinator foramina. Medial to the alisphenoid canal is the opening into the transverse canal. Details of this region are clear in two specimens, USNM 18100 and 22477. Dawson (1961:10, plate II) figured a distorted specimen and did not restore structures to their original positions; her sphenopalatine canal is my alisphenoid canal.

In specimens lacking the auditory bulla, the middle lacerate foramen is exposed. Its exact shape cannot be determined from the material available, but the medial portion is partially separated from the large lateral part. The medial portion is in the basisphenoid-basioccipital suture and pierces the side of the cranial floor. A channel leads posteriorly from the aperture across the anterior shelf of the periotic onto the promontorium. At the anterior end of the jugular foramen there is no space between the periotic and basioccipital for a carotid canal, and there is no separate entrance to a carotid canal elsewhere. The hypoglossal foramen is single.

The postglenoid foramen is within the squamosal bone. Temporal foramina can be seen clearly in USNM 18100. The largest is in the squamoso-parietal suture about halfway between the back of the zygomatic root and the posterior margin of the skull. A second small foramen is immediately behind it in the suture, and there is a small foramen in the parietal anterodorsal to these.

In most specimens the auditory bullae are missing; the periotic (Fig. 8) is clearly displayed in three specimens, USNM 18100 and 22477, and AMNH 13101. The major features are similar to those described for *Paramys*, but there are differences in relative proportions. The fenestra vestibuli, the fenestra cochleae, and the fossa for the stapedius muscle, indicated by a depression, are as in *Paramys*. A channel leads anteriorly from the stylomastoid foramen to a single foramen that is slightly anterior

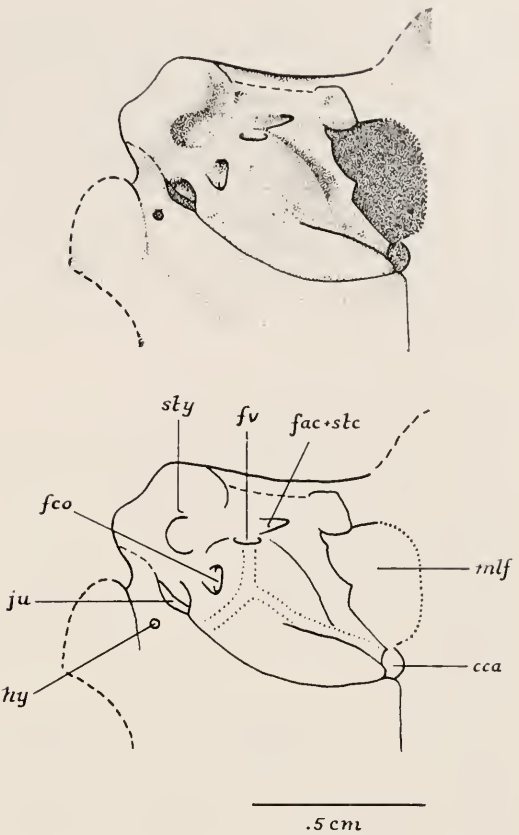

Figure 8. Auditory region of *Sciuravus nitidus* (restored from USNM 17683). See Fig. 1 for key to foramina.

to the fenestra vestibuli; the facial nerve and the stapedial artery evidently shared this one opening. Channels showing the courses of blood vessels are present on the surface of the promontorium. The main channel for the internal cartoid artery, possibly the promontory branch, begins just anterior to the jugular foramen; midway across the promontorium it turns anterodorsally and runs to the medial portion of the middle lacerate foramen. A channel for the stapedial artery curves posterodorsally from the point where the internal carotid turns anteriorly, and it leads to the fenestra vestibuli.

The bulla is preserved on one specimen,

USNM 22477. It has been moved out of place, and no markings on the periotic indicate precisely where it was situated. I did not notice a stapedial foramen, but one must have been present in the margin of the bulla, as indicated in Figure 7, to permit passage of the internal carotid artery. It is not possible to see in the specimen whether the bulla completely covered the middle lacerate foramen; measurements suggest that it did not, and I have so shown it in the figure.

Discussion of the Sciuravidae

The ratio of length of the incisive foramina to diastemal length is high, as in *Paramys* and *Reithroparamys,* and is much higher than those of *Ischyrotomus* and *Manitsha.* The posterior palatine foramina are within the palatine bone, again as in *Paramys* and *Reithroparamys.* A posterior maxillary notch is present, as in most paramyids.

The orbital process of the palatine reaches the back of the sphenopalatine foramen, whereas the orbitosphenoid does not. This arrangement occurs in *Paramys.* The sphenopalatine and optic foramina are farther forward relative to the cheek teeth than those of paramyids.

In *Sciuravus* the dorsal palatine foramen clearly is separated from the sphenopalatine, a condition perhaps foreshadowed in paramyids. The sphenofrontal foramen is in the orbitosphenoid-alisphenoid suture, as in paramyids. Masticatory and buccinator foramina are present and considerably closer to the foramen ovale than they are in paramyids. The arrangement of foramina in the pterygoid region is similar only to that of *Ischyrotomus* and *Pseudotomus.*

Separation of the medial part of the middle lacerate foramen to receive a branch of the internal carotid artery occurs in paramyids. *Sciuravus,* however, does not have a carotid canal between the periotic and basioccipital. Instead, the internal carotid artery entered the middle ear and crossed the promontorium in a shallow channel before entering the cranial cavity. The carotid circulation in *Leptotomus* may be the same, though the carotid canal is also present. There is only a single aperture in the petrosal for the stapedial artery and the facial nerve to exit from the middle ear, whereas in paramyids a pair of openings is visible. The postglenoid and temporal foramina are of about equal size, as in paramyids.

ISCHYROMYIDAE

Specimens examined:

I have seen and measured so many specimens (approximately 65) that a complete list would be excessive. The specimens recorded below are only those that are nearly complete or are cited in the text.

Ischyromys douglassi: Chadron Formation equivalent: CM 1123 pot; 10966 potc.

I. typus (Fig. 9): Orella Member, Brule Formation: AMNH 694 s; FMNH, P 12747 poc; MCZ 18979 potc; YPM 12521 s; PU 11383 s. Brule Formation: USNM 15929 npc; 15933 s.

I. sp: Chadron Formation equivalent: CM 24129 c. Orella Member, Brule Formation: AMNH 38865 s; CM 9463 npoc. Brule Formation: USNM 16953 s; 175352 tc; 175354 npo; CM 9755 pt.

Titanotheriomys veterior: Chadron Formation equivalent: CM 9809 p; 10660 npot. ?Orella Member, Brule Formation: MCZ 17202 s.

T. wyomingensis: Chadron Formation equivalent: AMNH 14579 (type) npt.

T. sp.: Chadron Formation equivalent: CM 8924 npt.

Foramina

The ratio of length of the incisive foramina to diastemal length, measured in seventeen ischyromyids, ranges from .21 to .30 with a cluster of nine around .24 and a cluster of eight around .28. The three specimens of *Titanotheriomys* in which this region is preserved fall at the low end of the range. The lateral margins of the

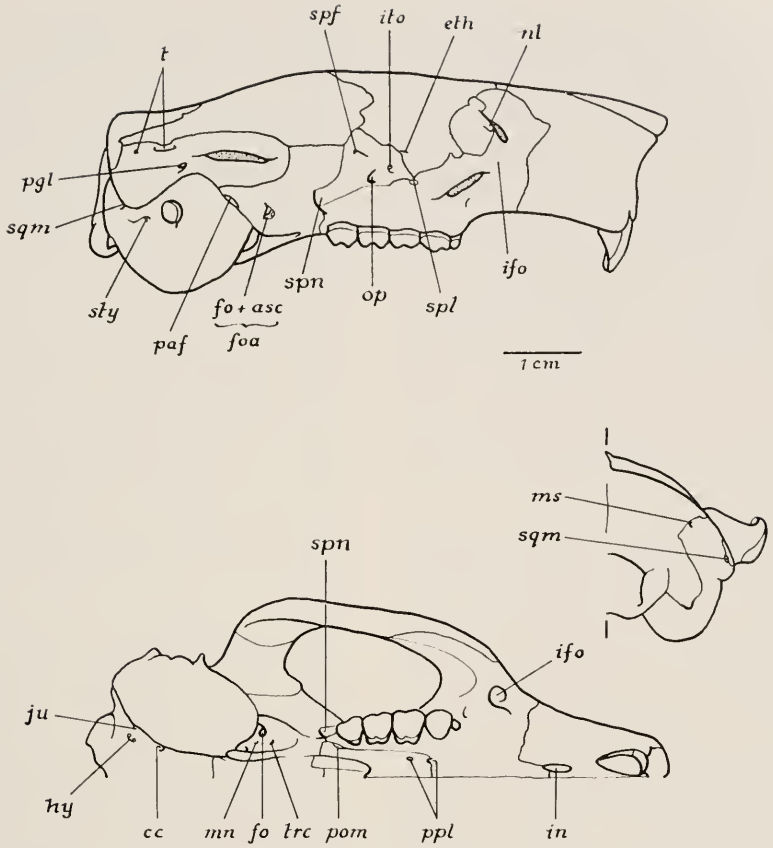

Figure 9. *Ischyromys typus* (AMNH 694). See Fig. 1 for key to foramina.

foramina are intersected at the very back by the premaxillary-maxillary suture, which runs posteriorly away from them.

The pair of larger posterior palatine foramina lies in the maxillary-palatine suture medial to an area extending from the middle of the last premolar to the middle of the first molar. The suture crosses the palate between the foramina (in one specimen, CM 9809, behind them, and a process from the palatine runs forward into the back of each foramen). There is usually a second pair of small foramina within the palatine medial to the first or second molars, and in some specimens a third pair of minute openings is present behind these. The maxilla ends behind the cheek teeth in a long point that is appressed to the pterygoid extension of the palatine; there is a lenticular aperture between them.

In front view, the infraorbital foramen forms a pinched ellipse with the acute end ventral. The major axis has an average length of 3.6 mm and ranges from 3.0 to 4.6 mm; it is inclined so that in front view the top of the foramen is farther lateral than the bottom, and in side view the top is farther anterior than the bottom. The anterior alveolar foramen is a short distance behind the infraorbital foramen in the curve made by the orbital floor and wall, and is directed anteromedially.

The nasolachrymal foramen is dorsal to the infraorbital foramen and below the posterior protuberance of the lachrymal bone. The maxilla appears to participate

in its anterior margin. The internal course of the nasolachrymal canal can be seen clearly in one specimen of *Ischyromys,* CM 1123. A short channel descends the face of the lachrymal bone, its slight anterior inclination continuing inside the bone. It turns sharply forward near the base of the snout and proceeds anteriorly a short distance before it bends medially under the arch of the incisor. In some specimens, between the lachrymal and the orbital portion of the maxilla, there seems to be a small unossified area that is roughly horizontal and in line with the middle of the infraorbital foramen. This may mark the site of origin of the inferior oblique eye muscle, as in *Marmota.*

The sphenopalatine foramen is dorsal to the first molar. The fused maxilla and palatine surround it almost entirely, and only a very small arm of the orbitosphenoid reaches it posteriorly. The ethmoid foramen is posterodorsal to the sphenopalatine. The frontal surrounds it on three sides and a lip from the frontal overhangs it; the orbitosphenoid meets it posteriorly. In one specimen, USNM 15933, the ethmoid foramen is double. The anterior opening has the usual slit-like appearance, and a slender process from the orbitosphenoid touches it. The posterior opening is nearly round; a channel in the orbitosphenoid leads to it from behind. In this one specimen the nerve and blood vessels probably entered the bone through separate foramina, as in *Marmota.* The optic foramen, usually 1.0 mm in diameter but slightly larger in a few specimens, is within the orbitosphenoid. In most specimens it is above the posterior part of the second molar or the anterior part of the third molar; in one, CM 10966, it is above the posterior portion of the third molar.

Within the triangle formed by the optic, ethmoid, and sphenopalatine foramina is a depression in front of and closest to the optic foramen. Its deepest and most clearly defined portion is posterior. A counterpart of this depression occurs in *Marmota* in which it is the place of origin of the rectus muscles of the eye. Usually there is a small foramen in the deep part of the depression. In one fragmentary specimen, USNM 175354, the pit is deepened to a pocket, and the foramen within was large enough to clean out. The foramina on the two sides of the skull proved to communicate across the midline. There is no exit from this passage either dorsally or posteriorly through the orbitosphenoid. In another specimen, USNM 16953, there is only a minute foramen within the depression, and a larger and apparently similar foramen occurs just anterior and medial to the optic foramen. The facts that the passage between the orbits has no other exit and that the position of the foramen is variable suggest that this was part of the venous system and that the aperture is a true interorbital foramen.

The dorsal palatine foramen is hidden. One broken specimen, CM 9809, shows it clearly just inside and ventral to the sphenopalatine foramen. This means that the descending palatine artery and nerve entered the sphenopalatine foramen before passing through the dorsal palatine foramen. The sphenoidal fissure at its opening is separated from the cranial cavity by a wall of bone. The alisphenoid canal enters the sphenoidal fissure laterally. A very slight ridge sets off the dorsal part of the fissure as a separate channel. A small sphenofrontal foramen is present in all undistorted specimens of *Ischyromys;* skulls identified as *Titanotheriomys* are not well enough preserved for me to determine whether the foramen occurs in them also. The sphenofrontal foramen is a short distance posterodorsal to the optic foramen. In some skulls it is entirely within the orbitosphenoid and close to the orbitosphenoid-alisphenoid suture, whereas in others it is in the suture. In all a channel leads gradually downward and forward from it.

The masticatory and buccinator foramina are separate from each other and are at a

substantial distance from the foramen ovale accessorius in specimens of *I. douglassi* from McCarty's Mountain; in CM 1123 the distance is 2.0 mm (see also Black, 1968a: 291, fig. 20 for CM 1122). In one specimen of *Ischyromys* from the middle Oligocene, PU 11383, only a slight bar of bone separates these foramina from the foramen ovale accessorius. In the remaining Orellan specimens of *Ischyromys* and *Titanotheriomys* the masticatory and buccinator foramina are united with the foramen ovale accessorius from which a broad channel runs anterodorsally across the alisphenoid, revealing the course of the masseteric nerve. The foramen ovale accessorius is bounded ventrally by a substantial lateral pterygoid flange, homologous to the lateral ridge in paramyids. The pterygoid fossa is deep in ischyromyids. The foramen ovale is dorsomedial to the foramen ovale accessorius and, in ventral view, is mostly obscured by the lateral pterygoid flange that bridges it. In some specimens there is a small foramen, which probably transmitted a meningeal vessel, medial to the foramen ovale. The entrance to the alisphenoid canal is at the anterior end of the foramen ovale and cannot be seen in ventral view. The middle lacerate foramen, if present, is hidden by the large auditory bulla. An aperture in the middle part of the pterygoid fossa leads to the transverse canal. In most specimens it is directed anteriorly; in one, CM 10966, it heads medially. The transverse canal has other entrances, too, inside the cranium. The largest of these is just behind the basisphenoid-presphenoid suture in the side of the raised cranial floor. A few foramina open into the canal from the surface of the raised portion. These details were seen in one specimen, CM 1123, in which the bone is translucent; upon shining a light through the bone, the matrix-filled canals became apparent.

The posterior opening of the carotid canal is clearly delimited by the basioccipital and the bulla. It is at the anterior end of the same slot that contains the jugular foramen. The bulla has a faint channel running dorsally into the carotid canal. The course of the canal can be seen in one specimen, CM 1123, in which it runs between the basioccipital and the bulla and arches up and over the medially swollen anterior portion of the bulla. It appears to enter the cranial cavity at the level where the medial side of the bulla curves outward. The jugular foramen is directed dorsally at the back of the slot between the basioccipital and the bulla. Black (1968:290, fig. 19) interprets this as the stapedial foramen. However, there must be a jugular foramen to transmit the vagus, accessory, and glossopharyngeal nerves, and the internal jugular vein; this opening is the only possibility. There is no stapedial foramen. The hypoglossal foramen is double except in one specimen of *I. typus,* USNM 15933, in which it is single. The two foramina, of nearly equal size, open into a pit that deepens medially; the anterior foramen faces posterolaterally, the posterior, anterolaterally.

The postglenoid foramen is reduced to a slit-like opening with a major axis measuring 1.5 mm. It is enclosed within the squamosal. A channel can be traced from this foramen through the bone to the single temporal foramen (USNM 175352). In several specimens there seems to be a postalar fissure between the alisphenoid bone and the front of the bulla (AMNH 694 and MCZ 17202 show it clearly). The temporal foramen, single in most specimens, is primarily in the squamosal bone; the squamoso-parietal suture descends into it on the medial side. Its anterior end is above the posterior part of the postglenoid foramen, and its major axis ranges from 2.5 to 3.0 mm. In one specimen, AMNH 694, a second minute foramen is present behind it in the squamosal bone. The squamosomastoid foramen is present on the occipital surface; one broken specimen, USNM 175352, has a matrix-filled channel running from it to the temporal foramen; another,

CM 24129, preserves the channel without infilling.

The minute mastoid foramen is in the occipital-mastoid suture well above the level of the top of the foramen magnum. The stylomastoid foramen is well defined and very deep because the bulla is large and the mastoid element inflated.

Discussion of the Ischyromyidae

There is ample skull material of *Ischyromys* to permit thorough description of its morphology. With respect to the cranial foramina, ischyromyids and paramyids are so different from each other that I must agree with those (*e.g.*, Wood, 1965; Wilson, 1949c; Schaub, 1958) who consider them to be separate groups of equivalent rank. I did not find any differences in cranial foramina which would distinguish *Ischyromys* from *Titanotheriomys*.

The ratio of length of the incisive foramina to diastemal length has a range that overlaps that of *Ischyrotomus* and *Manitsha* but does not overlap those of *Paramys*, *Reithroparamys*, and *Sciuravus*. The lateral margins of the incisive foramina are intersected farther posteriorly by the premaxillary-maxillary suture in ischyromyids. The pair of major posterior palatine foramina are on the maxillary-palatine suture and are usually farther forward relative to the cheek teeth than in paramyids and *Sciuravus*. In ischyromyids the posterior extremity of the maxilla is appressed to the pterygoid extension of the palatine. There is a slit between them which may be homologus to the posterior maxillary notch in paramyids and *Sciuravus*.

In side view the ischyromyid infraorbital foramen is inclined, not vertical as in paramyids and *Sciuravus*. The absolute lengths of the major axes are about the same as in paramyids although the skull size is smaller in ischyromyids; if only the vertical dimension is considered, the length in ischyromyids is shorter than that in paramyids.

Relative to the cheek teeth, the major foramina of the orbit—the optic, ethmoid, and sphenopalatine—are considerably farther forward than in paramyids and *Sciuravus*. The sphenopalatine is bordered by a fused maxilla and palatine and is met posteriorly by the orbitosphenoid; these features differ in paramyids and *Sciuravus*. The dorsal palatine foramen is internal to the sphenopalatine, whereas in paramyids the two foramina are within a single depression, and in *Sciuravus* they are separated. In ischyromyids the posterior palatine foramen, through which the descending palatine artery and nerve emerge, is anterior to its position in paramyids and *Sciuravus*. The depression in the orbitosphenoid in front of the optic foramen for the rectus muscles of the eye and the interorbital foramen accompanying it do not occur in paramyids or *Sciuravus*. The sphenofrontal foramen is small and, in some specimens, entirely within the orbitosphenoid. Where seen in paramyids and *Sciuravus*, it is relatively larger and always in the orbitosphenoid-alisphenoid suture.

Masticatory and buccinator foramina are united with the foramen ovale accessorius in most specimens. When both foramina are present, the channels leading to them through the alisphenoid bone are very short in comparison to those of paramyids but similar to those of *Sciuravus*. The foramen ovale accessorius is present in ischyromyids and in some paramyids, but lacking in *Sciuravus*. In ischyromyids the external pterygoid flange is very well developed and reaches the bulla. The mandibular division of the trigeminal nerve emerged from the foramen ovale, bent laterally, and passed through the foramen ovale accessorius in the extended flange.

The entrance to the transverse canal is separated from the alisphenoid canal. It is possible to picture the transition from a condition like that found in *Ischyrotomus* and *Sciuravus* to this arrangement. As the external pterygoid flange extended and the pterygoid fossa developed for muscle at-

tachment, the entrance to the alisphenoid canal moved as far back as the foramen ovale. The foramen ovale, through which the mandibular division of the trigeminal nerve passes, acted as a barrier to further extension.

The absence of a stapedial foramen indicates that ischyromyids lacked the stapedial artery, and the ophthalmic artery must have arisen, therefore, from the internal carotid. In paramyids and *Sciuravus* a channel for the artery crosses the promontorium. A double hypoglossal foramen occurs in ischyromyids, *Reithroparamys,* and *Ischyrotomus.*

Although the postglenoid foramen is similar in length to those measured in paramyids, it is reduced in width; this suggests that the major course of the venous system that drains the cranial cavity has shifted away from it. There is one large temporal foramen rather than a few small ones as in paramyids. The post-alar fissure and the squamoso-mastoid foramen do not occur in paramyids or *Sciuravus.*

CYLINDRODONTIDAE

Specimens examined:

Ardynomys occidentalis (Fig. 10): Chadron Formation equivalent: CM 1055 npo, 9991 npte, 9992 c, 16995 npot, 21701 npot.

Cylindrodon fontis: Chadron Formation equivalent: CM 17180 np, 17181 np, 17204 pc. White River Series equivalent: AMNH 14584 pc, 14585 np.

C. sp.: Chadron Formation equivalents: F:AM 79100 s, 79102 np, 79104 np, 79105 np, 79109 s; CM 6546 np, 6643 np, 8904 np.

Pseudocylindrodon medius: Chadron Formation equivalent: CM 1135 np, 10000 np, 10001 s.

P. neglectus: Chadron Formation equivalent: CM 10100 np.

P. sp.: Chadron Formation equivalent: CM 1126 n, 6545 np.

Foramina

The ratio of length of the incisive foramina to diastemal length is quite variable in cylindrodontids. Two specimens of *Pseudocylindrodon,* CM 10100 and 6545, have ratios of .37 and .40; the rest range from .50 to .55. The ratio in *Ardynomys* ranges from .28 to .44; in *Cylindrodon,* from .28 to .38. The lateral margins of the foramina are intersected near the back in some specimens, and at the back in others, by the premaxillary-maxillary suture. The suture runs laterally and somewhat posteriorly away from them.

The pair of posterior palatine foramina is in the maxillary-palatine suture medial to the middle part of the first molars. In a few specimens of *Cylindrodon* it is slightly farther posterior, medial to the junction of the first and second molars. The maxilla ends in a point behind the cheek teeth, and in most specimens it is so closely appressed to the pterygoid extension of the palatine that there is neither a posterior maxillary notch nor a foramen. In one specimen of *Pseudocylindrodon,* CM 10001, a posterior maxillary foramen is visible.

In front view the infraorbital foramen is approximately circular with some flattening on the dorsomedial side so that the major axis appears to slant outward. The axis has a wide size range; in *Pseudocylindrodon* from 1.2 to 1.6 mm; in *Ardynomys,* a sample of only two, around 2.0 mm; in *Cylindrodon* from 0.9 to 1.7 mm. In side view the foramen is approximately vertical. In one specimen of *Cylindrodon,* F:AM 79104, the foramen is double on both sides. The anterior alveolar foramen is in the curve made by the orbital wall and floor. It is within the infraorbital foramen and is directed anteromedially in *Pseudocylindrodon* and *Cylindrodon;* in one specimen of *Cylindrodon,* CM 17180, it is almost in front of the infraorbital foramen and heads medially. In *Ardynomys* the foramen is farther posterior and is directed even more medially.

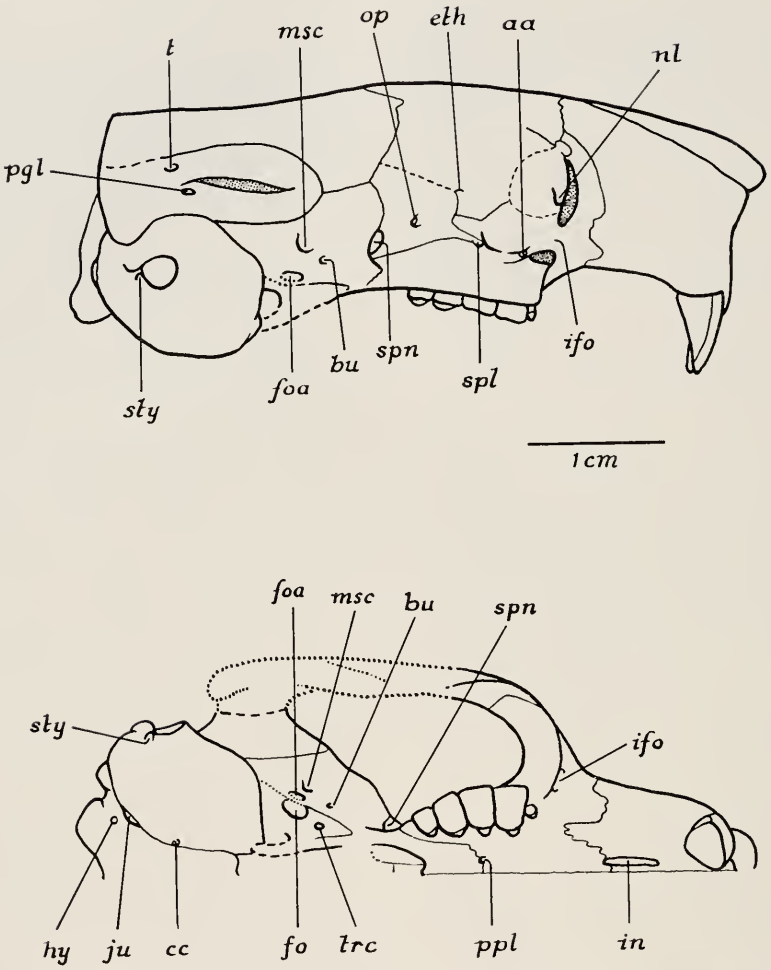

Figure 10. *Ardynomys occidentalis* (composite of all specimens examined; CM 9991 used as base). See Fig. 1 for key to foramina.

The nasolachrymal foramen is dorsal to the infraorbital. The maxilla may participate in its anterior margin, but I cannot determine this for certain. Some specimens have a slight channel leading down into the foramen; others have none. The canal inside the bone runs anteroventrally past the infraorbital foramen; then it plunges medially under the arch of the incisor. For the first part of its course it is external to the incisor alveolus, which reaches back into the orbit in *Ardynomys* and *Cylindrodon*. In the orbital wall of *Pseudocylindrodon* and in some specimens of *Ardynomys* (Wood, 1970: fig. 4), there is a slight saddle posteroventral to the nasolachrymal foramen; the saddle most likely marks the area of origin of the inferior oblique eye muscle, as in *Marmota*.

The sphenopalatine foramen is dorsal to the posterior part of the first molar in *Pseudocylindrodon* and is directed anteromedially. The maxilla forms its ventral and anterior margins; sutures are not distinct enough for other bones reaching it to be distinguished. The position of the foramen

in *Ardynomys* is somewhat variable. In three specimens, CM 1055, 16995, and 21701, it is above the junction of the first and second molars, while Wood (1970: fig. 4 of CM 12010) shows it as being dorsal to the anterior part of the second molar. It plunges anteroventrally behind the incisor root capsule. The fused maxilla and palatine forms the border on three sides, and a process from the orbitosphenoid reaches the foramen posteriorly. Specimens of *Cylindrodon* are fragmentary and difficult to interpret; the position of the sphenopalatine foramen seems to differ from individual to individual.

The ethmoid foramen is dorsal to the back of the sphenopalatine in *Pseudocylindrodon,* CM 10001, and *Cylindrodon,* CM 17180, and above and about equidistant between the sphenopalatine and optic in *Ardynomys.* It is overhung by a lip from the frontal bone. The orbitosphenoid reaches it posteriorly.

The optic foramen measures 0.5 mm in diameter in *Pseudocylindrodon,* CM 10001; it is dorsal to the junction of the second and third molars and very close to the orbitosphenoid-maxillary suture. In *Ardynomys* its diameter ranges from 0.7 to 0.9 mm, and its position is dorsal to an area ranging from the front part of the third molar to a point slightly posterior to that tooth. Wood (1970: fig. 4) shows the alisphenoid as forming the back of the optic foramen; this is not the case in the specimens I have examined. In one specimen of *Cylindrodon* in which the optic foramen is preserved, CM 17180, it is above the back of the second molar and about 0.5 mm in diameter. In this same specimen there is a depression in front of the optic foramen that is more pronounced on the right side than on the left. Presumably this marks the place of origin of the rectus muscles of the eye.

The dorsal palatine foramen is hidden in all three genera. There is evidence in one specimen of *Ardynomys,* CM 1055, that it and the sphenopalatine are contained in a single depression, as in *Paramys.* The sphenoidal fissure at its entrance is open medially into the cranial cavity; the opening extends a short distance in front of the margin of the fissure. This condition probably occurs in *Cylindrodon* also. Burke (1936:139) indicated two openings in this region in *Ardynomys,* CM 1055, not recognizing that the partition between them was a mineral-filled fracture; the specimen has a normal, single sphenoidal fissure.

In *Pseudocylindrodon* the minute sphenofrontal foramen is level with but quite far behind the top of the optic foramen, and it may be on the alisphenoid-orbitosphenoid suture although this is indistinct in all specimens. A channel leads anteroventrally from it. I have found the foramen in one specimen of *Ardynomys,* CM 21701, at the point of intersection of the orbitosphenoid, parietal, and alisphenoid bones; it is very small. The foramen seems to be absent in other specimens of *Ardynomys* and in *Cylindrodon.*

The masticatory and buccinator foramina are separate, and relatively close to the foramen ovale, about 1.0 mm from it. A broad channel runs anterodorsally from the masticatory foramen; a short one proceeds forward from the buccinator. Burke (1936: 139; and 1938:260) identified the buccinator as the masticatory and did not detect the masticatory foramen. The existence of a foramen ovale accessorius is uncertain. The lateral pterygoid ridge is expanded into a flange, and what remains of it defines the anterior end of a foramen or at least a notch. The flange may have reached the bulla, in which case there would have been a foramen.

The transverse canal, as such, has been lost, being reduced to a foramen that opens directly into the cranial cavity from the middle of the moderately deep pterygoid fossa. This is seen clearly in a specimen of *Ardynomys,* CM 21701, in which the inside of the cranium is partially cleaned out. Burke (1936:139; and 1938:259) incorrectly identified this foramen in the pterygoid

fossa as the sphenopterygoid. The alisphenoid canal is small and begins just anteroventral to the foramen ovale. It is clearly defined in *Pseudocylindrodon* and *Cylindrodon*. In *Ardynomys* the wall separating it from the cranial cavity is almost gone; in CM 1055 little more than a strut of bone internal to the buccinator foramen is left. The middle lacerate foramen, if present, is covered by the tympanic bulla. In *Ardynomys* and *Cylindrodon* a foramen of uncertain function pierces the side of the basisphenoid just anterior to the bulla; it is hidden by the hamular process in Figure 10.

The posterior opening of the carotid canal is very small and is separate from the jugular foramen. In *Pseudocylindrodon* the aperture seems to be between the bulla and the basioccipital. In *Ardynomys* and *Cylindrodon* a short channel leads anterodorsally across the medial side of the bulla to the canal. The canal enters and runs anteriorly through the periotic in *Ardynomys;* its course can be seen in one broken specimen, CM 9991. It also enters the periotic in at least one specimen of *Cylindrodon,* CM 17204. There is no stapedial foramen. The hypoglossal foramen is minute in *Pseudocylindrodon* and seems to be situated on the margin of the jugular foramen. The region is somewhat damaged, and this interpretation could be incorrect. In the other two genera it is more medial; in one specimen of *Ardynomys,* CM 9991, it is single on the left side and double on the right; the two foramina face anteriorly into a single depression.

The postglenoid foramen is within the squamosal bone. In *Pseudocylindrodon,* CM 10001, the major axis measures 0.6 mm; in two specimens of *Ardynomys,* 1.1 mm, The temporal foramen is about 1.0 mm long in one specimen of *Pseudocylindrodon* and 0.8 and 1.3 mm in two specimens of *Ardynomys.* In all specimens the region is too crushed for the possible presence of other, smaller temporal foramina to be detected. In *Ardynomys,* at least, the parietal-squamosal suture does not dip down far enough to reach the foramen. Burke (1938:258) stated that in *Pseudocylindrodon* the foramen apparently "marks the suture between the parietal and squamosal." The suture is not visible, however, and his surmise is doubtful. He (1936: 136) calls the foramen a subsquamosal in *Ardynomys.* The squamoso-mastoid foramen is conspicuous in all three genera. In one specimen of *Cylindrodon,* CM 17204, the squamosal is broken away, and the channel from this foramen to the temporal foramen can clearly be seen in the surface of the underlying bone.

The mastoid foramen is probably present but too minute to be found. The stylomastoid foramen is anteroventral to the low mastoid process just behind the external auditory opening.

Discussion of the Cylindrodontidae

The three genera of cylindrodontid rodents examined are very similar to one another in their cranial foramina. They are quite different from paramyids and *Sciuravus* and in some features resemble the ischyromyids.

The ratio of incisive foramen length to diastemal length has a great range. It includes the ranges of *Paramys, Reithroparamys,* and *Sciuravus,* has a slight overlap at the low end with that of ischyromyids, and does not overlap the range of the other paramyids measured. The margins of the foramina are intersected very far back by the premaxillary-maxillary suture, as in ischyromyids. The posterior palatine foramina are on the maxillary-palatine suture, as they are in *Ischyrotomus, Pseudotomus,* and ischyromyids. Relative to the cheek teeth they are situated as in paramyids and are slightly anterior to the position in *Sciuravus.* The posterior maxillary foramen is present in *Pseudocylindrodon.* In *Ardynomys* and *Cylindrodon* the end of the maxilla is appressed to the pterygoid extension of the palatine as in ischyromyids, but there is no aperture between them.

The infraorbital foramen is nearly vertical, as in paramyids and *Sciuravus*. The orbital foramina, as in ischyromyids, are considerably farther forward relative to the cheek teeth than in paramyids and *Sciuravus*. The sphenopalatine foramen is bounded by a fused maxilla and palatine, and is met posteriorly by the orbitosphenoid; both characters occur in ischyromyids and not in paramyids and *Sciuravus*. The sphenofrontal foramen is minute in *Pseudocylindrodon* as in ischyromyids, and it is absent in the other cylindrodontids.

The reduction of bone internal to the sphenoidal fissure and to the alisphenoid bone does not occur either in paramyids or in ischyromyids. The masticatory and buccinator foramina are separate as in paramyids, but they are close to the foramen ovale as are those seen in *Sciuravus* and the earliest skulls of ischyromyids. The development of a pterygoid fossa with a foramen, presumably leading to the transverse canal, in the middle of it, the possible presence of a foramen ovale accessorius, and the position and relative size of the entrance to the alisphenoid canal are as in ischyromyids. The foramen in the basisphenoid just anterior to the front of the bulla may be homologous to the medial division of the middle lacerate foramen in paramyids.

The separation of the entrance to the carotid canal from that to the jugular foramen, and the passage of the canal through the periotic, which occur in *Ardynomys* and *Cylindrodon*, are different from the conditions in paramyids, *Sciuravus*, and ischyromyids. Both cylindrodontids and ischyromyids lack the stapedial foramen. The hypoglossal foramen is usually single, as in *Sciuravus* and some paramyids, whereas in ischyromyids the foramen is always double.

The shift in emphasis of the venous system away from the postglenoid foramen, the presence of a single temporal foramen below the parietal-squamosal suture, and the opening-up of a squamoso-mastoid foramen are all changes from the paramyid condition that occur in ischyromyids.

PROSCIURIDAE

Specimens examined:

Prosciurus relictus: Cedar Creek Member, White River Formation: KU 8333 npo, 8345 npo.

P. aff. *saskatchewaensis* (Fig. 11b): Orella Member, Brule Formation: AMNH 1429 c.

P. cf. *vetustus*: Orella Member, Brule Formation: FMNH, PM 14674 np.

P. sp. (Fig. 11a): Orella Member, Brule Formation: SDSM 62365 npo.

?*Cedromus* sp.: Cedar Creek Member, White River Formation: KU 8342 pte.

Foramina

The ratio of length of the incisive foramina to diastemal length ranges from .39 to .48. The lateral margins of the foramina are intersected near the back by the premaxillary-maxillary suture, which runs laterally and somewhat posteriorly away from them.

The pair of major posterior palatine foramina is in the palatine medial to an area ranging from the posterior portions of the second molars to the anterior portions of the third molars. A second, smaller pair is medial to the third molars. The maxilla ends in a blunt point, and a posterior maxillary notch is formed between it and the pterygoid extension of the palatine.

In front view, the infraorbital foramen is nearly circular. The major axis measures 1.3 mm, and it is inclined so that the top of the foramen is farther lateral than the bottom. In side view the foramen slopes forward slightly. The anterior alveolar foramen, which is in the curve made by the orbital floor and wall, lies either within or a short distance behind the infraorbital foramen and is directed anteromedially.

The nasolachrymal foramen is dorsal to the infraorbital. A channel descends the face of the lachrymal bone into the fora-

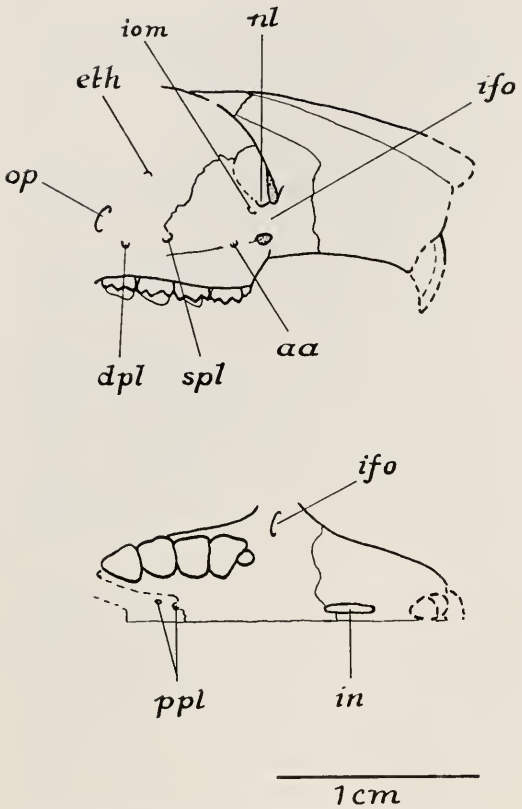

Figure 11a. *Prosciurus* sp. (SDSM 62365). See Fig. 1 for key to foramina.

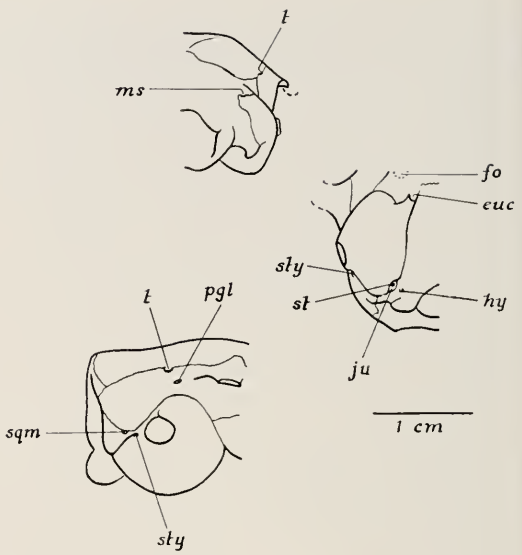

Figure 11b. *Prosciurus* aff. *saskatchewaensis* (AMNH 1429; modified from Wood, 1937: plate 13; lateral view additional). See Fig. 1 for key to foramina.

men. Immediately posterior and slightly ventral to the nasolachrymal foramen is a depression in the bone, whether in the maxilla or lachrymal cannot be determined. This was apparently the area of origin of the inferior oblique eye muscle.

The sphenopalatine foramen is above the middle or the posterior part of the second molar. The maxillary-frontal suture intersects it dorsally; the orbital portion of the palatine reaches it posteriorly, and the orbitosphenoid is wholly excluded from its margin. The ethmoid foramen is dorsal to the posterior part of the second molar. It is within the frontal bone and overhung by a lip of that bone. The orbitosphenoid does not reach it posteriorly. Only the anterior part of the optic foramen is preserved in one specimen, SDSM 62365; it is dorsal to the posterior part of the third molar. Although damaged, the foramen was about 1.5 mm long. In two specimens, KU 8333 and 8345, a depression is present immediately anterior to the optic foramen. It contains a minute interorbital foramen and was probably the area of origin for the rectus muscles of the eye.

The dorsal palatine foramen in the orbital floor is above the posterior part of the third molar and lies within the palatine near the maxillary suture in KU 8342, and in the suture in KU 8333. The sphenoidal fissure is dorsal and wholly posterior to the last molar. The region in which the sphenofrontal foramen would be situated is not preserved in any of the specimens.

My interpretation of the orbital region is at variance with Galbreath's identification of certain foramina in *Prosciurus relictus*, KU 8333 (Galbreath, 1953:53, fig. 16). The foramen he labeled the optic is the interorbital, and the sphenoidal fissure is the optic foramen. The posterior of two foramina shown in the orbital floor is the

dorsal palatine; the maxillary-palatine suture is not very clear in the specimen, but it seems to pass through this foramen. The anterior aperture is an exposed root of the second molar.

The alisphenoid region is preserved only in KU 8342. Galbreath (1953:60, fig. 19) identified the most conspicuous foramen as the masticatory. It is situated rather far ventrally in comparison with the masticatory in other rodent skulls examined, and it faces anteriorly; both the position and orientation would indicate that it is the buccinator foramen. However, a second aperture leading from the alisphenoid canal is present anterior to it near the edge of the alisphenoid; this opening is either the buccinator foramen or a foramen that does not occur in any of the other rodent skulls I have examined. The problem of identifying these foramina with certainty cannot be solved because the region in which the mastoid foramen would normally occur is damaged. The area labeled by Galbreath as the buccinator foramen is a damaged foramen ovale accessorius.

The shallow pterygoid fossa is partially preserved in this same specimen. The foramen ovale is situated posterolaterally within the fossa. The alisphenoid canal begins ventral to the anterior end of the foramen ovale, the transverse canal medial to it. The middle lacerate foramen is absent or covered by the tympanic bulla.

The carotid canal, if present, shares an opening with the jugular foramen and is very narrow. The jugular foramen appears to be broader than in other protrogomorphs, but this is due to the presence of the stapedial foramen lateral and slightly dorsal to it in a common depression. The hypoglossal foramen is single and medial to the jugular.

The postglenoid foramen, which is hardly more than a slit in the squamosal, is in line with the zygomatic root; its major axis measures 0.8 mm. There is one temporal foramen in the squamoso-parietal suture dorsal and slightly posterior to the postglenoid foramen. The squamosal is broken off on the left side of the specimen, and a conspicuous channel connecting the two foramina can be seen on the surface of the underlying bone. A channel also runs posteroventrally from the postglenoid foramen to the region where the rounded tip of the squamosal meets the mastoid element. This indicates the presence of a squamoso-mastoid foramen.

The mastoid foramen is very dorsally situated in the mastoid-occipital suture. The stylomastoid foramen is in its usual position between the external auditory meatus and the mastoid.

Discussion of the Prosciuridae

The ratio of length of the incisive foramen to diastemal length has a range that includes those of *Paramys*, *Reithroparamys*, and *Sciuravus*. It overlaps the upper end of the ranges in cylindrodontids and it is above those in other protrogomorphs. The major pair of posterior palatine foramina is situated farther posterior relative to the cheek teeth than that of any other protrogomorphous form. The posterior maxillary notch is as in paramyids.

The infraorbital foramen is not vertical as in paramyids and *Sciuravus*. It slopes anteriorly though not as much as that in ischyromyids. The depression for attachment of the inferior oblique eye muscle does not occur in other protrogomorphous rodents, although the site is indicated in *Ischyromys*, *Pseudocylindrodon*, and *Ardynomys*. The sphenopalatine foramen is surrounded by the frontal, maxillary, and palatine bones, as in paramyids and *Sciuravus*, in which the frontal is barely excluded from the dorsal margin; the orbitosphenoid does not reach the foramen in any of these forms. The ethmoid foramen is within the frontal, as in *Sciuravus* and some specimens of *Paramys*. The size of the optic foramen is relatively large for a protrogomorphous rodent. The depression for attachment of the rectus muscles of the eye and the interorbital fora-

men within it are also present in ischyromyids, but not in other protrogomorphs. The dorsal palatine foramen is separate from and posterior to the sphenopalatine, as in *Sciuravus*.

The pterygoid fossa is shallow and the foramina within it are situated as in *Ischyrotomus* and *Sciuravus*. The stapedial foramen indicates the presence of a stapedial artery, which was also present in paramyids and *Sciuravus;* ischyromyids and cylindrodontids lacked it.

The postglenoid foramen is greatly reduced, but a temporal foramen and the squamoso-mastoid foramen are present. This arrangement is unlike that of paramyids and sciuravids and similar to that of ischyromyids and cylindrodontids.

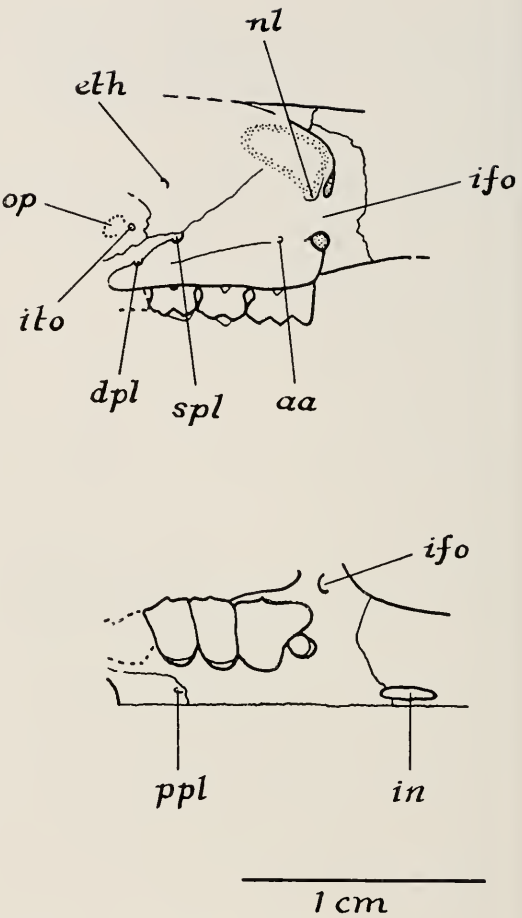

Figure 12. *Allomys nitens* (UCMP 1100). See Fig. 1 for key to foramina.

APLODONTOIDEA

Specimens examined:

Aplodontidae:

Allomys nitens (Fig. 12): John Day Formation: UCMP 1100 np.

Liodontia furlongi: Barstovian deposits, Nevada: UCMP 61716 s, 75666 np.

Aplodontia rufa: Recent: UNSM, Z.M. 275: MCZ 799, 1893, 5645, 6369, 6822, 13183, 17810, 18352.

Mylagaulidae:

The taxonomy of mylagaulids is at present so uncertain that I prefer to list the specimens examined in stratigraphic order.

Rosebud Formation:

Promylagaulus riggsi (see McGrew, 1941:6 for figure): FMNH, P 26256 npo.

Marsland Formation and equivalents:

Mesogaulus laevis: UNSM 04953 npot, 04954 p; F:AM 65004 npo.

Sheep Creek Formation:

Promylagaulus novellus[1]: F:AM 65001 np.

Mesogaulus sp.: F:AM 65002 potc, 65003 s, 65005 np, 65006 s, 65007 np, 65011 nptc.

Mylagaulus vetus: AMNH 18903 pot, 18904 np, 20507 npt.

Mylagaulus laevis (Fig. 13): AMNH 17576 s.

Ceratogaulus rhinocerus: AMNH 18899 p.

large mylagaulid: F:AM 65016 s, 65017 nptc.

Pawnee Creek Formation:

Ceratogaulus rhinocerus: AMNH 9456 (type) npt.

Mylagaulus laevis: AMNH 9043 (type) np.

[1] This species has heretofore been placed in the genus *Mylagaulus,* but Stout (personal communication) now places it in the genus *Promylagaulus.*

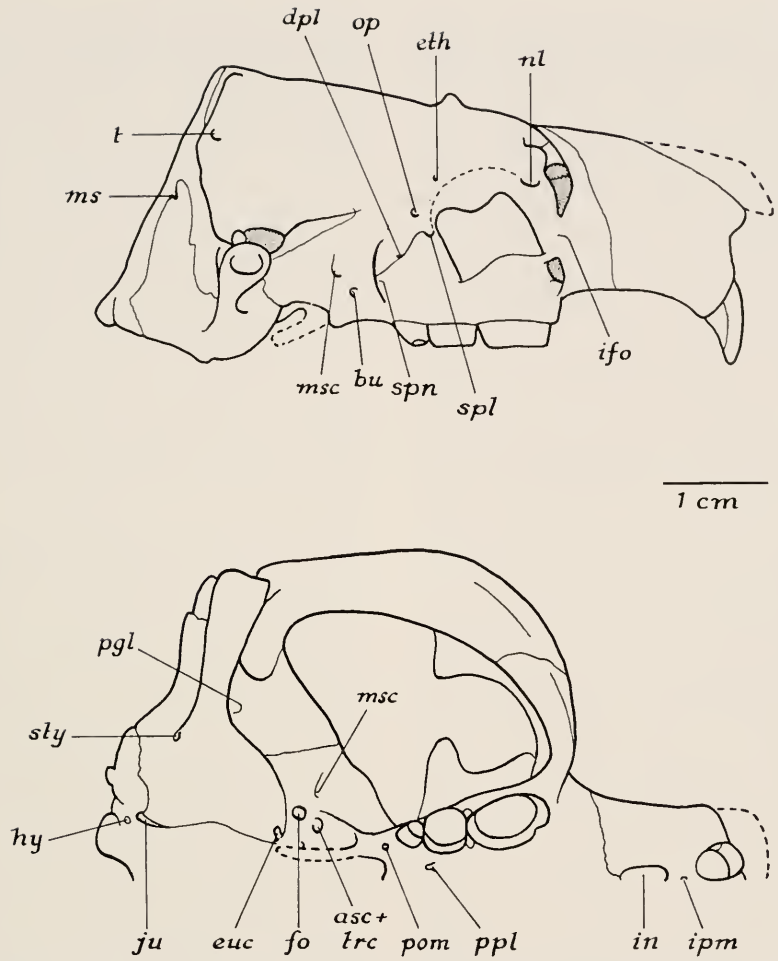

Figure 13. *Mylagaulus laevis* (mostly based on AMNH 17576; basicranium restored from various specimens). See Fig. 1 for key to foramina.

Barstovian deposits, Montana:
Mylagaulus douglassi: UCMP 44694 npo.
Mylagaulus sp.: PU 18186 s.
Deep River beds:
Mylagaulus sp.: AMNH 21307 s.
Valentine Formation:
Mylagaulus sp.: UNSM 04957 n.
Burge Member, Valentine Formation:
Mylagaulus sp.: UNSM 04956 np; F:AM 65009 potc, 65010 potc, 65012 s, 65013 tc.
Clarendonian deposits, South Dakota:
Mylagaulus sp.: UCMP 32323 potc.
Ash Hollow Formation:
Mylagaulus sp.: UNSM 04955 n.
Kimball Formation:
Mylagaulus sp.: UNSM 04958 npo.
Pliocene deposits, Nebraska:
Mylagaulus sp.: F:AM 65008 np., 65014 npo, 65015 np.

Foramina

The interpremaxillary foramen is a conspicuous feature in *Aplodontia*. It is quite variable in the fossils. *Liodontia* seems to have a small one; the region is not pre-

served in *Allomys*. In mylagaulids a pit and sometimes a minute foramen are present in its position. *Promylagaulus* lacks the foramen.

The ratio of length of the incisive foramina to diastemal length in aplodontoids ranges from .28 to .43, and values are quite evenly distributed. The ratio does not vary with the geologic age of the specimens. No ratio can be obtained for *Allomys*; *Promylagaulus* falls at .33. In *Allomys*, as in all aplodontids, the lateral margins of the foramina are intersected at the back by the premaxillary-maxillary suture, which runs laterally and somewhat posteriorly away from them. In most mylagaulids the ends of the foramina are intersected by the suture, which runs posteriorly from them; in some specimens the maxilla does not appear to reach the foramina, which may be entirely within the premaxillary bones.

The major pair of posterior palatine foramina is medial to an area ranging from the middle of the second molars to the anterior part of the third molars in all aplodontoids. In *Allomys* and in juvenile specimens of *Aplodontia* the pair is very close to the maxillary-palatine suture, but within the palatine; the suture is not visible in adult aplodontoids. In one specimen of *Liodontia* a second, smaller pair is in line with the first pair and medial to the back of the second molars. *Aplodontia* commonly has one or two pairs of small foramina in line with and posterior to the major pair. The maxilla ends behind the cheek teeth in a point, which is fused to the lateral side of the pterygoid region in all but juvenile specimens. The posterior maxillary foramen, enclosed between the two parts, opens above in the floor of the sphenoidal fissure and may have transmitted a palatine vein. The region is not preserved in *Allomys* and is unclear in *Promylagaulus*.

In front view, the infraorbital foramen is of variable shape; it may be elliptical with the major axis running diagonally or horizontally, or it may be nearly round. In *Allomys* the major axis measures 1.8 mm; in other aplodontids, from 2.5 to 4.0 mm, the low values being from juveniles; in *Promylagaulus*, 1.2 mm; and in other mylagaulids, from 1.9 to 4.8 mm. In side view the foramen is nearly vertical. The anterior alveolar foramen in *Allomys* is above the fourth premolar in the curve formed by the orbital wall and floor. The position of the foramen is extremely variable in *Aplodontia;* it is seen most commonly in the medial wall of the infraorbital foramen. The foramen was not seen in most mylagaulid specimens; it is probably obscured by the great alveolus of the fourth premolar. In one specimen, UCMP 32323, it lies in the medial wall of the infraorbital foramen.

The lachrymal region is very well preserved in most specimens. In *Allomys* the lower margin of the nasolachrymal foramen is medial to the upper part of the infraorbital. Sutures in the area are unclear, and it is not possible to determine which bones surround the foramen. In *Promylagaulus* the nasolachrymal is considerably farther dorsal. In other aplodontids and mylagaulids it is a short distance above and slightly posterior to the infraorbital, and a channel leads ventromedially down the face of the bone to it. In one juvenile specimen of *Aplodontia*, MCZ 5645, sutures can be seen; the maxilla forms the anteroventral edge of the foramen. In one mylagaulid, PU 18186, the first part of the canal is exposed. It slopes to a point just anteroventral to the infraorbital foramen where it turns anteromedially. In many large specimens of *Aplodontia* a rounded notch is present in the posterior projection of the lachrymal; clearly it transmitted a vessel or nerve to the top of the head.

In order to render the positions of the orbital foramina intelligible it is necessary to digress and to explain the mode of cheek tooth replacement in mylagaulids. The cheek teeth of mylagaulids are very hypsodont, but the fourth premolar greatly surpasses the molars in this respect. This tooth is shaped like a long wedge, and, as

it erupts, the first molar and then possibly the second are eliminated by interdental wear. A cheek tooth dentition may contain P^4, M^1, M^2, M^3, or P^4, M^2, M^3, or just P^4, M^3. The apparent differences in position of the orbital foramina relative to the cheek teeth are determined by the degree of encroachment of the fourth premolar on the molars. In contrast, the cheek teeth of *Liodontia* and *Aplodontia* are all hypselodont; the orbital foramina are high and above the alveoli, and major differences in position do not occur.

The sphenopalatine foramen is above the second molar in *Allomys;* the orbital process of the palatine reaches it posteriorly, and the orbitosphenoid is excluded from its margin. In *Aplodontia* the foramen is dorsal to the posterior part of the premolar; the cheek tooth alveoli obscure all sutures in the region. In *Promylagaulus* the foramen is dorsal to the junction of the first and second molars, whereas in other mylagaulids the foramen is above the second molar, posterior to the great alveolus of the last premolar. In UCMP 32323, in which the premolar is almost fully erupted and the second molar worn away, the foramen is above the posterior part of the premolar. Orbital sutures are fused in all specimens.

The ethmoid foramen is dorsal to the posterior part of the second molar in *Allomys;* sutures in its vicinity cannot be determined. The foramen is overhung by a slight lip of bone. In *Aplodontia* the foramen is posterodorsal to the sphenopalatine and above the junction of the first and second molars. There are commonly two or three minute foramina close together; the number may differ on the two sides of a skull, and the orientation of individual apertures in such a group may differ substantially. In juvenile specimens the ethmoid foramen is within the frontal bone. I could not identify the ethmoid foramen in *Promylagaulus.* In other mylagaulids it is dorsal and slightly anterior to the sphenopalatine foramen; it opens upward. Only the anteroventral margin of the optic foramen is preserved in *Allomys* and *Promylagaulus;* it is dorsal to the posterior part of the third molar. The curvature of both margins suggests that the optic foramina were about 1.0 mm in diameter. In *Aplodontia* the optic foramen is dorsal to an area ranging from the middle of the second molar to the front part of the third molar, and it is nearly reached by the alveolus of the second molar. The diameter of the foramen ranges from 1.0 to 1.5 mm. Juvenile specimens demonstrate that it is wholly within the orbitosphenoid. In mylagaulids, other than *Promylagaulus,* the optic foramen is close behind the sphenopalatine and dorsal to the same area as in *Aplodontia;* it ranges in size from 0.6 to 0.9 mm.

An interorbital foramen is present in *Allomys* immediately in front of the optic. McGrew (1941:7, fig. 2) identifies it as the optic foramen, but it has no connection with the cranial cavity; I believe that his sphenoidal fissure is the optic foramen and that the sphenoidal fissure itself is missing from the specimen he examined. In mature specimens of *Aplodontia* a short process of bone and a pit anterior to it are present in front of the optic foramen; this is probably the site of origin of the rectus muscles of the eye.

The dorsal palatine foramen is on the palatine-maxillary suture dorsal to the anterior part of the third molar in *Allomys.* It is hidden in *Aplodontia* but can be located by pushing a hair through the posterior palatine foramen. The hair comes out above the third molar in the crevice between the molar alveolus and the orbitosphenoid. The foramen cannot be seen in most mylagaulids; when visible, it is dorsal to the third molar. The specimens of *Allomys* and *Promylagaulus* are broken off at this point. The sphenoidal fissure at its entrance is open medially into the cranial cavity in mylagaulids and *Aplodontia.* There is no sphenofrontal foramen.

The masticatory foramen is separated from the buccinator by a distance of over

2.0 mm in some specimens of mylagaulids and of *Aplodontia*. The buccinator foramen is much smaller than the masticatory in the latter. Although the pterygoid fossa is deep, the lateral flange is short, and a foramen ovale accessorius is lacking.

In mylagaulids and *Aplodontia* the alisphenoid canal is very large and situated anterolaterally in the fossa. The aperture of the transverse canal is just inside the medial border of the alisphenoid canal. In mylagaulids the canal is very broad; one broken specimen, PU 18186, reveals a pair of channels running posterodorsally from the canal into the cranium. This same specimen demonstrates that, as in *Aplodontia*, the masseteric and buccinator portion of the mandibular nerve splits off before that nerve emerges from the foramen ovale. The foramen ovale is situated posterolaterally in the pterygoid fossa. There is a slight gap between the roof of the fossa and the bulla. In one mylagaulid specimen, UCMP 32323, the foramen ovale is confluent with this gap, and in *Aplodontia* the foramen may be separate, or confluent, on one or both sides of the skull.

Aplodontia lacks both carotid and stapedial arteries (Guthrie, 1969; Bugge, 1971b); however, in many specimens a minute foramen can be seen in the medial wall of the periotic at the anterior end of the jugular foramen. This foramen was noted in one mylagaulid specimen, AMNH 17576; in some others a separate, minute opening is present between the bulla and the basioccipital. It is possible that these foramina are remnants of embryonic arterial passageways. The hypoglossal foramen is usually double, but occasionally single.

The postglenoid foramen is between the squamosal and the tympanic. Although it resembles a post-alar fissure, it is too far dorsal to be that aperture. Temporal foramina are present near the occipital crest. A single foramen is the most common condition, but two foramina either in an anteroposterior line or side by side are not unusual. In one specimen of *Aplodontia*, MCZ 5645, a channel connecting the temporal and postglenoid foramina can be seen inside the cranium.

The mastoid foramen is in the occipitalmastoid suture slightly above the level of the top of the foramen magnum. The stylomastoid foramen is in its usual position, although the external auditory meatus is greatly extended beyond it.

Discussion of the Aplodontoidea

A conspicuous interpremaxillary foramen, or a distinct depression in this position, which is present in many aplodontoids does not occur in other protrogomorphous rodents. The ratio of length of the incisive foramina to diastemal length has a range that nearly matches those of *Ardynomys* and *Cylindrodon*. It is below the ranges in *Paramys, Reithroparamys, Sciuravus, Pseudocylindrodon,* and prosciurids, and above that in *Ischyrotomus;* it overlaps the high end of the range in ischyromyids. The posterior palatine foramina are farther posterior than in other protrogomorphs except prosciurids. The posterior maxillary foramen is similar only to that of *Pseudocylindrodon* within this group.

The infraorbital foramen is vertical, and of a size range similar to that in most protrogomorphs. The ethmoid foramen may be entirely within the frontal throughout the aplodontoids, although its position relative to the orbitosphenoid suture can be determined only in juvenile specimens of *Aplodontia*. The foramen is also within the frontal in prosciurids, *Sciuravus*, and some individuals of *Paramys*. The sphenopalatine and optic foramina are considerably farther forward relative to the cheek teeth than in paramyids, but are in positions similar to those in *Sciuravus*, *Ardynomys*, and prosciurids. The size of the optic foramen is approximately as in other protrogomorphs. The interorbital foramen resembles that of ischyromyids and prosciurids. Complete separation of the dorsal palatine

foramen from the sphenopalatine is a resemblance to *Sciuravus* and prosciurids. The sphenofrontal foramen is absent, as in *Ardynomys* and *Cylindrodon* among protrogomorphs. Reduction of bone internal to the sphenoidal fissure is a feature that is also encountered within the suborder. The presence of separate masticatory and buccinator foramina and the absence of the foramen ovale accessorius are characters shared with paramyids and *Sciuravus*.

The arrangement of foramina in the pterygoid fossa is very similar to that occurring in *Ischyrotomus*, *Sciuravus*, and prosciurids. It is very different from that of ischyromyids and cylindrodontids. The positions of the postglenoid foramen and the temporal foramina differ from those seen in other protrogomorphous rodents.

CONCLUSIONS

Cranial foramina vary within definite limits. Those that transmit nerves are always present although their number may increase if a nerve divides inside rather than outside the bone, or decrease if two foramina fuse. Foramina transmitting arteries vary by fusion and by loss when an artery is eliminated; once a new pattern of arterial circulation is fixed, it is perpetuated in the lineage concerned. Foramina transmitting veins are the most plastic in number and presence or absence, within certain bounds imposed by the requirements of circulation. With these principles in mind the characters of the cranial foramina may be used to test ideas on rodent phylogeny and taxonomy. To this end, I present, first, those features that set families and superfamilies apart, one from another, and those that indicate relationships between groups. Next, I briefly discuss each family and superfamily in an endeavor to integrate these data with those presented by various workers on the basis of other structures. Following this, I propose a classification of the groups studied that seems plausible in light of the available evidence.

The Paramyidae, first appearing in the late Paleocene, are the earliest known rodents. Sciuravids, though recovered first from slightly younger strata, are so similar, that I shall consider the families together. The paramyid skulls I have examined represent three of the four subfamilies designated by Wood (1962:11)[1]. They date from the middle early Eocene (Lysite), and later, and therefore may differ in some features from the earliest members of the family. The skulls of *Sciuravus* are of early middle Eocene (Bridger) age and may differ likewise from older members of the Sciuravidae.

The dorsal palatine foramen and sphenopalatine open into a common depression in the three paramyid genera in which the region remains intact. I believe this arrangement to be primitive within the Rodentia. In *Sciuravus* and in all rodent families derived from paramyids (except ischyromyids and cylindrodontids), the dorsal palatine foramen is in the floor of the orbit posterior to the sphenopalatine foramen.

Three patterns of foramina in the pterygoid region occur in paramyids. The inclusion of the foramina within a small depression in *Paramys copei* could well be structurally ancestral to the condition seen in *Ischyrotomus* and *Pseudotomus* and in *Paramys delicatus*. The pterygoid region of *Sciuravus* is like that in *Ischyrotomus* and *Pseudotomus;* from this arrangement of foramina can be derived those in all later rodents.

In *Paramys, Leptotomus, Ischyrotomus,* and *Pseudotomus* a canal is present that begins at the anterior end of the jugular foramen and runs between the basioccipital and periotic. I have called it the carotid canal, since it is so termed in living rodents. However, the mere presence of this canal is no sure evidence that there was

[1] Wood's fifth subfamily, the Prosciurinae, I exclude from the Paramyidae for reasons given below.

a medial branch of the internal carotid artery running through it; the canal also transmits the inferior petrosal sinus and would be present if either or both of these vessels existed. The fact that some later rodents of apparent paramyid descent have an internal carotid artery in the canal, *e.g.*, ischyromids (almost certainly) and castorids, is evidence that some or all members of the family had the artery.

The auditory region is preserved in the genera above, except *Pseudotomus*. A channel marking the course of the stapedial artery runs across the promontorium from the region of the jugular foramen to the fenestra vestibuli. If the medial branch of the internal carotid artery ran through the carotid canal, then the stapedial branch diverged from it outside, *i.e.*, medial to, the middle ear, as it does in later rodent groups.

Leptotomus has not only a carotid canal and stapedial artery channel, but also a groove marking the course of the promontorial artery. Did this genus have a three-branched internal carotid as has been attributed to early mammals (*cf.*, *e.g.*, Szalay, 1972:71) and to primitive insectivores (McKenna, 1966)? If this is the case, then rodents had a very early origin within the Mammalia or they are derived from an insectivore retaining the medial branch of the internal carotid; the promontorial artery in *Leptotomus* is, then, a primitive relict. Perhaps the genus did not have a third, medial branch of the internal carotid, and the carotid canal transmitted only the inferior petrosal sinus. If this is the case, then the carotid circulation was like that in *Sciuravus*, in which stapedial and promontorial branches are present, but a carotid canal is lacking. This arrangement is like those in living and most fossil insectivores (Tandler, 1899:749; van Kampen, 1905: 422ff.; McDowell, 1958:205), and it is described as primitive for primates (Gregory, 1920; Hill, 1953, 1955; McKenna, 1966:7). If division of the internal carotid within the middle ear is primitive for rodents, too, and if the third, medial branch was lost prior to their origin, then rodents may be related in some way to these orders. The artery in the carotid canal in paramyids and later rodents is, then, the branch that crosses the promontorium in *Leptotomus* and *Sciuravus*. Examination of the canal transmitting the carotid artery in the array of living rodents reveals a variety of structural detail (Hill, 1935; Wahlert, 1972) which suggests that the carotid canal arose separately in different groups. This is to be expected if the artery did not run in a canal in the earliest rodents.

The ischyromyids and cylindrodontids retain the close association of sphenopalatine and dorsal palatine foramina encountered in paramyids. In both families the orbital foramina are farther anterior relative to the cheek teeth than they are in any other protrogomorphous group. The orbitosphenoid reaches the sphenopalatine in these and in no other groups. The sphenofrontal foramen is reduced or absent; the arrangement of foramina in the pterygoid region is unique to these two families. The association of palatine and sphenopalatine foramina is a primitive feature also encountered in *Paramys*. The presence of a carotid canal in ischyromyids is evidence supporting derivation from the paramyids. The canal is reduced in cylindrodontids, and has a peculiar course in two of the genera.

The prosciurids and aplodontoids form a natural assemblage as regards their foramina, and they have two peculiar features in common. The ethmoid foramen is well within the frontal bone rather than in or near the orbitosphenoid-frontal suture, and the posterior palatine foramina are, in general, farther posterior than in other rodents.

None of the early aplodontids are known from skulls. The fragment of *Allomys* has an interorbital foramen anteroventral to the optic foramen, as do some of the specimens of *Prosciurus*. The fragment of *Promylagaulus* indicates only that the genus is a

side branch of the Mylagaulidae. The arrangement of foramina in mylagaulids is so much like that of *Aplodontia* that, on this basis, the two groups could be placed in one family.

The cranial foramina of prosciurids do not provide any clear evidence as to whether their ancestors were sciuravids or paramyids. Separation of dorsal palatine and sphenopalatine foramina occurs in *Sciuravus*, but this condition in prosciurids could be derived easily from that in paramyids. The position of the ethmoid foramen just within the frontal seems to occur in some paramyids and in *Sciuravus*. The positions of the orbital foramina, relative to the cheek teeth, are different from those of either group. Differences in the pterygoid region indicate that Wood's (1962: 243) suggested derivation of prosciurids from *Paramys delicatus* is unlikely, but this by no means excludes the possibility of descent from some other paramyid.

This is the evidence, based on cranial foramina, that suggests the unity of certain assemblages and their affinities to others. What bearing does it have on the various hypotheses concerning the relationships of the groups discussed that have been proposed on other grounds?[1]

Sciuravids date from the early Eocene Lysite Member of the Wind River Formation. At that time sciuravids and paramyids were so closely related that "... a contemporary taxonomist would never have considered them distinct families" (Wood, 1965:133). The cranial foramina in the two groups are nearly alike even at the beginning of the middle Eocene, when the two are easily separated on the basis of the dentition. The distinctive characteristics of paramyids and *Sciuravus* may well stem from differential retention of primitive features in these genera and may not be consistent throughout their respective families. Wood believed the Sciuravidae arose from, or near to, the Microparamyinae, a group for which no skulls are known. There is no available evidence that would cast doubt on this conclusion.

Leptotomus with its primitive carotid circulation occupies a special place within the Paramyidae; this is in keeping with Woods' phylogeny (1962:243), which shows it as part of a distinct lineage since early in the family's history. Whether or not the genus should be retained in the Paramyinae cannot be decided without a better sample of paramyid skulls. The primitiveness of the genus makes it an unlikely candidate for the ancestor of *Ischyromys* as proposed by Wood (1962:248).

Ancestry of the ischyromyids has long been in doubt because of dental resemblances to both paramyids and sciuravids. Wood (1962:248) has, after earlier hesitation, advocated a paramyid ancestry. Black (1968a) compared early Oligocene species of *Ischyromys* with paramyids and sciuravids and found so great a similarity to the former that he included the genera of both groups in a single family, the Ischyromyidae. The evidence from cranial foramina, although not conclusive, supports a paramyid ancestry for the family, but striking differences in the arrangement of foramina from that in the known paramyids indicate that the two groups are distinct at the familial level.

The cylindrodontids have been derived from sciuravids by Wood (1955 and 1959). The unique features of the cranial foramina common to cylindrodontids and ischyromyids suggest that the two groups had a common ancestry, which, on the evidence of *Ischyromys*, I suspect to have lain within the Paramyidae.

Wilson (1949b) and Wood (1962) believed that the Prosciuridae (Prosciurinae in their usage) were derived from paramyids. The cranial foramina, as stated above, neither oppose nor support this

[1] Wilson (1949c) presents an excellent review tracing the history of opinion regarding relationships of all of the groups discussed here. I have not thought it necessary, therefore, to repeat such information, but limit myself to contributions subsequent to his paper.

view; they do suggest, however, that the group is entitled to familial rank, and this is supported by other features. All the following characters differ from those of paramyids: stapedial foramen situated dorsolaterally within jugular foramen; dorsal palatine foramen above third molar; optic foramen, in part, dorsal to third molar; lateral pterygoid ridge prominent, possibly enclosing foramen ovale accessorius (in *Reithroparamys* and *Leptotomus* among paramyids); ethmoid foramen situated well within frontal; cranium distinctly domed in profile; flattened lyrate area on skull roof; postorbital process present and strong; auditory bullae inflated; incisor enamel uniserial; masseteric fossa extending ventral to first molar (only in *Manitsha* among paramyids). I agree, therefore, with Wilson (1949c) and with Schaub (1958) that familial rank is warranted.

The Aplodontidae appear in the latest Eocene. Resemblances to the prosciurids were demonstrated in detail by Wilson (1949a and c). Wood (1962:243, 247) suggested derivation of the group from a prosciurine, probably *Mytonomys,* in the middle late Eocene. Although Black (1968b), on the basis of new material, demonstrated that *Mytonomys* is not a prosciurid, the cranial foramina provide strong support for the descent of aplodontids from prosciurids. Mylagaulids and aplodontids are so similar that I am in complete agreement with those who derive the former from aplodontids in the late Oligocene. The three groups are very closely related, and can be considered as members of a single superfamily.

There remains for consideration the bearing on formal taxonomy of the evidence reviewed. Certain changes within the suborder Protrogomorpha would seem to be required, and the following arrangement of the groups studied emerges:

Protrogomorpha
  Ischyromyoidea
    Paramyidae
    Ischyromyidae
      Ischyromyinae
      Cylindrodontinae
    Sciuravidae
    Protoptychidae (*inc. sed.*)
  Aplodontoidea
    Prosciuridae
    Aplodontidae
      Aplodontinae
      Mylagaulinae

Subdivision of the Protrogomorpha into two superfamilies separates the ancestral and primitive, derived families from the relatively more advanced aplodontoids. Until more forms of protoptychids are known, I prefer to retain the family within the Protrogomorpha (Wahlert, 1973) and have placed it tentatively in the superfamily Ischyromyoidea. In view of the similarities between ischyromyids and cylindrodontids, I propose that the rank of each group be reduced to subfamily and that they be combined under the older family name, Ischyromyidae Alston, 1876. This association, based on the foramina, merits further study from other evidence.

The cranial foramina of aplodontids and mylagaulids are so alike that I have likewise reduced the rank of each group to subfamily and united them under the older family name, Aplodontidae Trouessart, 1897 (= Haploodontini Brandt, 1855). The prosciurids have been included in a superfamily with them to express the many characters unique to the two families.

The cranial foramina and relationships of sciuromorphous, myomorphous, and hystricomorphous rodents to these protrogomorphous groups will be the subject of future publications; work on the first of these groups is completed (Wahlert, 1972).

REFERENCES

Black, C. C. 1968a. The Oligocene rodent *Ischyromys* and discussion of the family Ischyromyidae. Ann. Carnegie Mus., **39**: 273–305.

———. 1968b. The Uintan rodent *Mytonomys.* Jour. Paleontol., **42**: 853–856.

Bugge, J. 1970. The contribution of the stapedial artery to the cephalic arterial supply in muroid rodents. Acta anat., **76**: 313–336.

———. 1971a. The cephalic arterial system in mole-rats (Spalacidae), bamboo rats (Rhizomyidae), jumping mice and jerboas (Dipodoidea) and dormice (Gliroidea) with special reference to the systematic classification of rodents. Acta anat., **79**: 165–180.

———. 1971b. The cephalic arterial system in sciuromorphs with special reference to the systematic classification of rodents. Acta anat., **80**: 336–361.

———. 1971c. The cephalic arterial system in New and Old World hystricomorphs, and in bathyergoids, with special reference to the systematic classification of rodents. Acta anat., **80**: 516–536.

Burke, J. J. 1936. *Ardynomys* and *Desmatolagus* in the North American Oligocene. Ann. Carnegie Mus., **25**: 135–154.

———. 1938. A new cylindrodont rodent from the Oligocene of Montana. Ann. Carnegie Mus., **27**: 255–274.

Dawson, M. R. 1961. The skull of *Sciuravus nitidus*, a middle Eocene rodent. Postilla, No. 53: 1–13.

Galbreath, E. C. 1953. A contribution to the Tertiary geology and paleontology of northeastern Colorado. Univ. Kansas Paleontol. Contrib., Art. 4:1–120.

Greene, E. C. 1935. Anatomy of the rat. Trans. Amer. Phil. Soc. n.s., **27**: 1–370.

Gregory, W. K. 1910. The orders of mammals. Part II. Genetic relations of the mammalian orders. Bull. Amer. Mus. Nat. Hist., **27**: 105–524.

———. 1920. On the structure and relations of *Notharctus*, an American Eocene primate. Mem. Amer. Mus. Nat. Hist. n.s., **3**(pt. 2): 49–243, plates 23–59.

Guthrie, D. A. 1963. The carotid circulation in the Rodentia. Bull. Mus. Comp. Zool., **128**: 455–481.

———. 1969. The carotid circulation in *Aplodontia*. Jour. Mammal., **50**: 1–7.

Hill, J. E. 1935. The cranial foramina in rodents. Jour. Mammal., **16**: 121–129.

———. 1937. Morphology of the pocket gopher mammalian genus *Thomomys*. Univ. California Publ. Zool., **42**: 81–172.

Hill, W. C. O. 1953. Primates. V. I. Strepsirhini. Edinburgh: University Press. 798pp.

———. 1955. Primates. V. II. Haplorhini. Edinburgh: University Press. 347pp.

Hyman, L. H. 1942. Comparative Vertebrate Anatomy. Chicago: Chicago University Press. 544pp.

Kampen, P. N. van. 1905. Die Tympanalgegend des Säugetierschädels. Morphol. Jahrb., **34**: 321–722.

Keroher, G. C. 1970. Lexicon of geologic names of the United States for 1961–1967. U. S. Geol. Surv. Bull., **1350**: 1–848.

——— et al. 1966. Lexicon of geologic names of the United States for 1936–1960. U. S. Geol. Surv. Bull., **1200**: 1–4341.

McDowell, S. B. 1958. The Greater Antillean insectivores. Bull. Amer. Mus. Nat. Hist., **115**: 113–214.

McGrew, P. O. 1941. The Aplodontoidea. Geol. Ser., Field Mus. Nat. Hist., **9**: 1–30.

McKenna, M. C. 1966. Paleontology and the origin of the Primates. Folia primat., **4**: 1–25.

Schaub, S. 1958. Simplicidentata, p. 659–818. *In* J. Piveteau (ed.), Traité de Paléontologie, 6(2). Paris: Masson et C^{ie}.

Szalay, F. S. 1972. Cranial morphology of the early Tertiary *Phenacolemur* and its bearing on primate phylogeny. Amer. Jour. Phys. Anthrop, **36**: 56–76.

Tandler, J. 1899. Zur vergleichenden Anatomie der Kopfarterien bei den Mammalia. Denkschr. Akad. Wiss. Math.- Nat. Cl., Wien, **67**: 677–784.

———. 1901. Zur vergleichenden Anatomie der Kopfarterien bei den Mammalia. Anat. Hefte, **59**: 327–368.

———. 1902. Zur Entwicklungsgeschichte der Kopfarterien bei den Mammalia. Morphol. Jahrb., **30**: 275–373.

Wahlert, J. H. 1972. The cranial foramina of protrogomorphous and sciuromorphous rodents; an anatomical and phylogenetic study. Ph.D. Thesis. Harvard Univ. 230pp.

———. 1973. *Protoptychus*, a hystricomorphous rodent from the late Eocene of North America. Breviora, No. 419: 1–14.

Wilson, R. W. 1949a. Additional Eocene rodent material from Southern California. Carnegie Inst. Washington Publ., **584**: 1–25.

———. 1949b. On some White River fossil rodents. Carnegie Inst. Washington Publ., **584**: 27–50.

———. 1949c. Early Tertiary rodents of North America. Carnegie Inst. Washington Publ., **584**: 67–164.

Wood, A. E. 1937. Rodentia, p. 155–269. *In* W. B. Scott and G. L. Jepsen, The mammalian fauna of the White River Oligocene. Trans. Amer. Phil. Soc. n.s., **28**(pt. 2).

———. 1955. A revised classification of the rodents. Jour. Mammal., **36**: 165–187.

———. 1959. Eocene radiation and phylogeny of the rodents. Evolution, **13**: 354–361.

———. 1962. The early Tertiary rodents of the family Paramyidae. Trans. Amer. Phil. Soc. n.s., **52**(pt. 1): 1–261.

———. 1965. Small rodents from the early Eocene Lysite Member, Wind River Formation of Wyoming. Jour. Paleontol., **39**: 124–134.

———. 1970. The early Oligocene rodent *Ardynomys* (family Cylindrodontidae) from Mongolia and Montana. Amer. Mus. Novitates, No. 2418: 1–18.

Wood, H. E. et al. 1941. Nomenclature and correlation of the North American continental Tertiary. Bull. Geol. Soc. Amer., **52**: 1–48.

US ISSN 0027-4100

Bulletin OF THE
Museum of
Comparative
Zoology

Osteology and Classification of the Neotropical Characoid Fishes of the Families Hemiodontidae (Including Anodontinae) and Parodontidae

TYSON R. ROBERTS

HARVARD UNIVERSITY
CAMBRIDGE, MASSACHUSETTS, U.S.A.

VOLUME 146, NUMBER 9
18 DECEMBER 1974

PUBLICATIONS ISSUED
OR DISTRIBUTED BY THE
MUSEUM OF COMPARATIVE ZOOLOGY
HARVARD UNIVERSITY

Breviora 1952–
Bulletin 1863–
Memoirs 1864–1938
Johnsonia, Department of Mollusks, 1941–
Occasional Papers on Mollusks, 1945–

SPECIAL PUBLICATIONS.

1. Whittington, H. B., and E. D. I. Rolfe (eds.), 1963. Phylogeny and Evolution of Crustacea. 192 pp.
2. Turner, R. D., 1966. A Survey and Illustrated Catalogue of the Teredinidae (Mollusca: Bivalvia). 265 pp.
3. Sprinkle, J., 1973. Morphology and Evolution of Blastozoan Echinoderms. 284 pp.
4. Eaton, R. J. E., 1974. A Flora of Concord. 250 pp.

Other Publications.

Bigelow, H. B., and W. C. Schroeder, 1953. Fishes of the Gulf of Maine. Reprint.

Brues, C. T., A. L. Melander, and F. M. Carpenter, 1954. Classification of Insects.

Creighton, W. S., 1950. The Ants of North America. Reprint.

Lyman, C. P., and A. R. Dawe (eds.), 1960. Symposium on Natural Mammalian Hibernation.

Peters' Check-list of Birds of the World, vols. 2–7, 9, 10, 12–15.

Proceedings of the New England Zoological Club 1899–1948. (Complete sets only.)

Publications of the Boston Society of Natural History.

Price list and catalog of MCZ publications may be obtained from Publications Office, Museum of Comparative Zoology, Harvard University, Cambridge, Massachusetts, 02138, U.S.A.

© The President and Fellows of Harvard College 1974.

Plate I. The species of Anodontinae. Upper: *Anodus* cf. *elongatus* from the Orinoco (after Steindachner, 1888; type specimen of *Elopomorphus orinocensis*). Middle: *Anodus elongatus* from Iquitos (Academy of Natural Sciences, Philadelphia 122595, 129.3 mm). Lower: *Anodus melanopogon* from Iquitos (ANSP 122596, 131.0 mm).

OSTEOLOGY AND CLASSIFICATION OF THE NEOTROPICAL CHARACOID FISHES OF THE FAMILIES HEMIODONTIDAE (INCLUDING ANODONTINAE) AND PARODONTIDAE

TYSON R. ROBERTS[1]

CONTENTS

Introduction 412
Osteological observations 415
  Terminology 415
  Material examined 415
  Hemiodontidae 416
    Hemiodontinae 416
      Cranium 416
      Otoliths 416
      Facial bones 417
      Jaws and jaw teeth 417
      Suspensorium 417
      Hyoid and branchial arches 417
      Weberian apparatus 418
      Pectoral girdle 418
      Pelvic girdle 418
      Vertebral counts 418
      Caudal skeleton 418
    Bivibranchiinae 418
      Cranium 418
      Otoliths 418
      Facial bones 418
      Jaws 419
      Jaw teeth 419
      Suspensorium 419
      Hyoid arch 420
      Gill arches 420
      Gill rakers 420
      Pharyngeal teeth 421
      Weberian apparatus 421
      Pectoral girdle 421
      Pelvic girdle 422
      Vertebral counts 422
      Caudal skeleton 422
    Anodontinae 422
      Cranium 422
      Otoliths 422
      Facial bones 422
      Jaws 423
      Suspensorium 423
      Hyoid and branchial arches 423
      Gill rakers 423
      Weberian apparatus 424
      Pectoral girdle 424
      Pelvic girdle 424
      Vertebral counts 424
      Caudal skeleton 424
  Parodontidae 424
      Cranium 424
      Otoliths 425
      Facial bones 425
      Jaws and jaw teeth 425
      Suspensorium 426
      Hyoid and branchial arches 426
      Weberian apparatus 427
      Pectoral girdle 427
      Pelvic girdle 427
      Vertebral counts 427
      Caudal skeleton 427
Discussion 427
  Relationship between Hemiodontidae and Parodontidae 427
  Transfer of Anodontinae from Curimatidae to Hemiodontidae 429
  Remarks on lower taxa 432
    Genera of Hemiodontinae 432
    Genera of Bivibranchiinae 432
    Genera and species of Anodontinae 433
    Genera of Parodontidae 433
Conclusion 434
Literature cited 434
Figures 437

ABSTRACT. The family Parodontidae is highly specialized and readily distinguished from Hemiodontidae and all other characoid families. The three genera it contains differ relatively little from each other and clearly cannot be separated at a

[1] Museum of Comparative Zoology, Cambridge, Massachusetts, U. S. A. 02138.

level higher than that of genus. In contrast, the seven genera of Hemiodontidae fall into four subfamilies, each characterized by specialized trophic structures unlike those of any other characoids. The osteology of Parodontidae and of three hemiodontid subfamilies is described and figured, based on study of all genera except *Atomaster* and *Pterohemiodus*. Although similarities in the jaws and suspensoria are suggestive of shared specializations, the evidence that the two families are closely related is inconclusive. The genera and species of Hemiodontinae are still poorly defined and need systematic study. The trophic structures of *Bivibranchia*, considered as a whole, are more specialized than those of any other characoid. Although *Argonectes* is much more primitive than *Bivibranchia*, its specializations clearly indicate that it belongs in Bivibranchiinae. Bivibranchiinae are the only characoids with protrusible jaws, and the mechanism of protrusion is unique. The subfamily Anodontinae, which is transferred into Hemiodontidae from Curimatidae, consists of a single genus with probably only two valid species, *Anodus elongatus* and *A. melanopogon*.

The genera and subfamilies of the two families can be classified as follows

Parodontidae
  Parodon, Apareiodon, Saccodon (*Parodontops* a synonym of *Saccodon*)
Hemiodontidae
  Hemiodontinae
    Hemiodus (*Hemiodopsis* a synonym), *Pterohemiodus* (of doubtful validity)
  Bivibranchiinae
    Argonectes, Bivibranchia, Atomaster (probably a synonym of *Bivibranchia*)
  Micromischodontinae
    Micromischodus
  Anodontinae
    Anodus (*Eigenmannina* a synonym)

INTRODUCTION

The poorly known characoid families Hemiodontidae and Parodontidae include some of the most interesting fishes in the fresh waters of South America. Hemiodontidae range throughout the lowlands of the Guianas and the basins of the Orinoco and Amazon, and southwards to include the Plata basin. Mostly six inches to a foot long when adult, they form small schools in lakes and large rivers. All are swift swimmers with streamlined bodies. Seven genera and about 27 species are currently recognized, belonging to four subfamilies: Hemiodontinae, Bivibranchiinae, Anodontinae, and Micromischodontinae. The best known genera are *Hemiodus* Müller 1842, *Bivibranchia* Eigenmann 1912, and *Anodus* Spix 1829 (*in* Agassiz and Spix, 1829). *Bivibranchia* and its poorly known relatives *Argonectes* Böhlke and Myers 1956 and *Atomaster* Eigenmann and Myers 1927 are the only characoids with truly protrusible upper jaws. The greatly reduced premaxillaries are freed from the cranium, and the maxillaries and anterior end of the suspensorium are very loosely bound to it. When the lower jaw is depressed, the entire upper jaw and the palatine-ectopterygoid portion of the suspensorium move slightly forward and strongly downward and away from the cranium. The mouth is apparently able to close when the upper jaw is protruded. The highly specialized mechanism of protrusion is probably unlike that in any other teleosts. *Anodus*, hitherto assigned to Curimatidae, is one of the few Amazonian fishes with pharyngeal structures apparently specialized for filter feeding on plankton (Roberts, 1972: 138–40). It has edentulous jaws and far more gill rakers than any other characoid. The gill arches are exceptionally elongate, and the number of gillrakers undergoes a considerable increase with growth of individuals.

Parodontidae occur in the eastern half of Panamá, on the Pacific and Caribbean coasts of Colombia and the Pacific coast of Ecuador, in the Orinoco and Amazon basins, in the Guianas, and southwards to include the Plata basin. There are about 25 species, mostly four to six inches long when adult. All are mountain stream fishes, typically found in swift streams at altitudes from 100 to over 1000 meters. Several species occur in headwaters on the periphery of the Amazon basin, but no specimens have been reported from the Middle or Lower Amazon. Their expanded and flattened pectoral fins are presumably adapted to help maintain position in swift current. Nuptial tubercles occur in several species (Wiley and Collette, 1970). The

pedicellate teeth and the apparently very mobile (but nonprotrusible) premaxillaries are highly specialized for browsing on algae. Three genera are currently recognized: *Parodon* Valenciennes 1849 (*in* Cuvier and Valenciennes, 1849), *Saccodon* Kner and Steindachner 1863, and *Apareiodon* Eigenmann 1916. *Saccodon,* restricted to coastal basins in Panamá, Colombia, and Ecuador, is of exceptional interest to evolutionary biologists because populations of the two principal species exhibit extraordinary polymorphism with respect to trophic structures (Roberts, 1974). Greater diversity of premaxillary tooth morphology occurs in a single population of *Saccodon dariensis* than in all species of *Parodon* and *Apareiodon* combined.

The pedicellate, multicuspid dentition in the nonprotrusible upper jaw of *Hemiodus* is very similar to that in many Parodontidae, and parodontids with relatively terminal mouths such as *Saccodon terminalis* (cf. Roberts, 1974) and some species of *Apareiodon* bear a striking resemblance to *Hemiodus.* Most students of characoids, including Regan (1911), Eigenmann (1912), Fowler (1950), Géry (1959), and Greenwood et al. (1966), either stated that Hemiodontidae and Parodontidae are closely related or else at least provisionally accepted this hypothesis by placing them either in the same family or subfamily or next to each other in a classification.

The scant literature on the osteology of Hemiodontidae and Parodontidae can be rapidly reviewed. Regan (1911) gave an extremely brief account of the jaws and suspensorium of Hemiodontidae and Parodontidae. Travassos (1951; 1952) gave extensively illustrated accounts of the opercular series, jaws and dentition of Parodontidae. The highly specialized replacement tooth trenches characteristic of the family can be seen in many of his figures. Géry (1959) briefly compared the superficial skull bones of Parodontidae and Hemiodontidae. Géry (1963a) described the jaws and suspensorium of *Bivibranchia;* unfortunately, there are several errors in this account. Lastly there is my account of the osteology of *Micromischodus* (Roberts, 1971), a new genus from the rio Negro and Middle Amazon. These six references constitute all that has been published on the osteology of the two families.

The present account deals with the osteology of Parodontidae and of the hemiodontid subfamilies Hemiodontinae, Bivibranchiinae and Anodontinae. The osteology of the one remaining hemiodontid subfamily, the monotypic Micromischodontinae, has already been treated (Roberts, 1971), but may be reviewed briefly here. *Micromischodus* is the only hemiodontid in which the lower jaws bear teeth throughout life. In all others the lower jaw is either toothless throughout life or becomes toothless early in life. The specialized unicuspid pedicellate dentition on the jaws and pharyngeal toothplates of *Micromischodus* is unique. My original account should have mentioned that *Micromischodus,* like other hemiodontids, has three openings into each posttemporal fossa. Excepting the teeth and elongated slender pharyngeal toothplates, the osteology of *Micromischodus* is very similar to that of *Hemiodus.*

Following the general osteological accounts, diagnoses are presented for all of the higher taxa: Hemiodontidae, Hemiodontinae, Bivibranchiinae, Anodontinae, and Parodontidae. The possible relationship of Hemiodontidae and Parodontidae to each other is reviewed in the Discussion section. The question of relationships of Parodontidae and Hemiodontidae to other characoids is left in abeyance, pending osteological and morphological investigations of other groups including Chilodontidae and Anostomidae. I have already pointed out that the relationship of the "semifunctional" preformed replacement teeth to the functional unicuspid pedicellate teeth on the pharyngeal toothplates of *Micromischodus* may parallel an evolutionary stage on the way to the multicuspid

pharyngeal teeth characteristic of Chilodontidae and Anostomidae (Roberts, 1971). The most important conclusion about classification of characoids reached in this paper is that Anodontinae belong to Hemiodontidae rather than to Curimatidae.

The biology of Hemiodontidae and Parodontidae is largely unknown. Knöppel (1972) gave an account of the stomach contents of several species of Parodontidae and Hemiodontidae (Hemiodontinae and Bivibranchiinae). His findings may be summarized as follows: Parodontidae and Hemiodontinae ingested mainly sand, detritus, algae (diatoms mentioned for *Parodon*, filamentous algae for *Hemiodus*), and higher plants. Of the ten species of Hemiodontinae examined, only *Hemiodus immaculatus* had fed on chironomid larvae. The stomach contents of this species also included ephemeropteran larvae but no plant material of any kind. In three species of *Bivibranchia* Knöppel found sand, detritus, and chironomid larvae. One of the species also contained algae (kind not specified) and a copepod (Harpacticidae?). Stomach contents of *Micromischodus* (Roberts, 1971: 8) include an assortment of bottom material or detritus, some of which may be droppings of other fishes, and many small insects, especially larval Diptera and a corixid. There is no published information on the food items of *Argonectes* and *Anodus*. The behavior and reproductive biology of Parodontidae and Hemiodontidae have not been studied.

This paper provides further documentation for the hypothesis that diversification of feeding structures has played a major role in the evolution of higher taxa in the suborder Characoidei (Roberts, 1967; 1971; 1973). An attempt to compare the amount of trophic specialization among various characoids seems worthwhile. Regardless of whether the conical tooth morphology and the arrangement of the teeth in *Salminus* are correctly interpreted as primitive (Roberts, 1969), the feeding structures of this genus are clearly generalized for characoids. Using *Salminus* as a guideline, I have judged the character states of ten structures involved in the mechanics of feeding as they occur in a variety of characoid taxa. The structures are scored either "0" (generalized condition), "1" (some specialization), or "2" (high specialization). The individual scores for the ten structures are then totalled to give the amount of trophic specialization in each taxon. Subjectivity is probably inevitable in any methods that could be devised to determine the amount of specialization between organisms as unalike as the proverbial apples and oranges, and it has not been eliminated here. The method has been arbitrarily designed, and evaluation of the character states is still relatively subjective. On the other hand, the steps have been broken down, so that they can be followed by other workers, subjected to reevaluation and further analysis, extended to additional taxa, and perhaps improved upon. The data for a number of taxa is presented in Table 1. Note that the range of theoretically possible total scores is from 0 to 20. *Salminus*, generalized in all respects, would automatically score 0. Of

Table 1. Amount of trophic specialization among various characoid taxa.

	Brycon	Curimatidae	*Hemiodus*	*Anodus*	Serrasalminae	*Micromischodus*	Parodontidae	Cynodontidae	*Argonectes*	Prochilodontidae	*Bivibranchia*
Jaws	1	1	1	1	1	1	2	2	2	2	2
Jaw teeth	1	1	2	1	2	2	2	2	2	2	2
Replacement teeth	1	0	1	0	1	1	2	1	1	2	1
Lips	0	0	0	0	0	0	0	0	0	2	0
Palate	0	0	0	0	2	0	0	0	0	0	2
Suspensorium	0	0	0	0	0	0	1	1	2	1	2
Pharyngeal arches	0	0	0	2	0	1	0	1	1	0	2
Gill rakers	0	1	1	2	0	0	1	1	1	1	1
Pharyngeal teeth	0	0	0	0	0	2	0	0	0	1	2
Pharyngeal epithelium	0	1–2	0	0	0	0	0	0	0	2	2
Total	3	4–5	5	6	6	7	8	8	9	13	16

the groups tabulated, *Bivibranchia* is most specialized, with a score of 16. I do not know of any other characoid group that would score this high. The group with the next most specialized feeding structures is probably the Prochilodontidae, which scores 13 (see Roberts, 1973, for an account of the feeding structures of this iliophytophagous family). *Argonectes,* which shares several trophic specializations with *Bivibranchia,* scores only 9. The piscivorous family Cynodontidae also scores 9. Most piscivorous groups, including the Serrasalminae (piranhas), score low, mainly because they tend to have generalized pharyngeal trophic structures. The iliophagous Curimatidae are generalized in most features and score very low. Of groups not tabulated, Anostomidae and Chilodontidae have perhaps the most specialized feeding structures and would probably score around 8 or 10.

Acknowledgments. It is a pleasure to express my thanks for specimens received for this study from the following individuals and their respective institutions: Loren P. Woods of the Field Museum of Natural History; James E. Böhlke of the Philadelphia Academy of Natural Sciences; William Fink and Stanley H. Weitzman of the Smithsonian Institution; Jacques Géry; Warren C. Freihofer of the California Academy of Sciences; and Heraldo A. Britski of the Museu de Zoologia of the Universidade de São Paulo. I also thank Stanley Weitzman for helpful comments on the manuscript.

OSTEOLOGICAL OBSERVATIONS

Terminology

The osteological terminology used in this account is based primarily on that in Weitzman (1962), with three main exceptions, namely that for gill arches, precaudal and caudal vertebrae, and caudal skeleton. The gill arch terminology followed is that recommended by Nelson (1969). It is essential to define gill arch elements precisely and to standardize their terminology if the information they represent is to be useful in phyletic analysis. Nelson emphasized the distinction between endoskeletal elements and dermal toothplates, an important clarification. An adequate nomenclature for the bony elements collectively known as basihyals and basibranchials has yet to be developed. In characoids these apparently include dermal as well as endoskeletal elements, and yet the dermal elements in most cases are not toothplates. In many characoids the basihyal is a compound element, consisting of an anterior (dermal?) portion and a posterior endoskeletal portion. Concerning the vertebrae, caudal vertebrae are herein defined as the first vertebra bearing a complete hemal canal and all of the vertebrae succeeding it, counting the compound ural centrum as one. The precaudal count includes the four vertebrae bearing the Weberian apparatus. The terminology for the caudal skeleton is that proposed by Monod (1969).

Material Examined

This account is based on alizarin preparations of the following specimens of Hemiodontidae and Parodontidae (MCZ = Museum of Comparative Zoology, Harvard; MZUSP = Museu de Zoologia da Universidade de São Paulo; CAS = California Academy of Sciences; USNM = Smithsonian Institution; FMNH = Field Museum of Natural History, Chicago):

Anodus elongatus, MCZ 20671. One specimen, 180 mm. Lago Alexo, Amazonas, Brazil. Thayer expedition.

Anodus melanopogon, MZUSP 5959. Three specimens, 54.0 to 55.0 mm. Mouth of the rio Purus, Amazonas, Brazil. Expedição Permanente da Amazônia, 1–5 April 1967.

Apareiodon affinis, FMNH 71228. Three specimens, 26.5 to 46.8 mm. Río Uruguay at Soriana, south of Dolores. C. C. Sanborn, 25–31 January 1927.

Apareiodon itapicuruensis, FMNH 56991. Two specimens, 19.8 and 21.0 mm. Rio Itapicuru at Queimadas, Bahia, Brazil. J. D. Haseman, 2 March 1908.

Argonectes longiceps, MCZ 20635. One specimen, 198 mm. Rio Xingu, Amazonas, Brazil. Thayer Expedition.

Bivibranchia protractila, CAS(SU) 48847. One specimen, 39.9 mm. Río Cassiquiare at mouth of Río Curamoni, Venezuela. C. Ternetz, 7 March 1925; CAS(SU) 48608. One specimen, 115.2 mm. Rio Negro at Camanaos rapids, Brazil. C. Ternetz, 23 January 1925.

Hemiodus quadrimaculatus, MCZ 29926. One specimen, 35.0 mm. Lower Potaro River at Tumatumari, Guyana. C. H. Eigenmann, 1908.

Hemiodus semitaeniatus, MCZ 49072. Two specimens, 54.4 and 55.8 mm. Jauré ranch, North Savannah, Rupununi, Guyana. C. Hopkins, 18 May 1971.

Parodon caliensis, MCZ 47682. One specimen, 63.5 mm. Probable locality data: small streams of Sierra Azul, easternmost range of Andes [Peru?]. O. Barton, December 1945.

Parodon guyanensis, MCZ 48969. One paratype, 38.5 mm. Upper Mana River at Saut-Fini, French Guiana. Lelong, 25 November 1957.

Saccodon dariensis (Meek and Hildebrand), USNM 208503. Two specimens of dental morph I, 83.4 and 89.4 mm, and two specimens of dental morph IV, 97.2 and 100.7 mm. Río Sabalo, Bayano basin, one mile above Naragandi, Panamá. Battelle Memorial Institute NW Lab., 21 March 1967.

Saccodon wagneri Kner and Steindachner, MCZ 48745. Four specimens of dental morph I, 45.5 to 57.2 mm; and MCZ 48746. Five specimens of dental morph IV, 52.0 to 103.3 mm. Arroyo Bambine (tributary of Río Cristal), Guayas basin, at Montalvo. T. R. Roberts, R. Gilbert, F. Silva M., 6 November 1971.

The only genera not represented in this list are the hemiodontids *Pterohemiodus* Fowler 1940 (closely related to, and perhaps indistinguishable from, *Hemiodus*), and *Atomaster* (a close relative and possible congener of *Bivibranchia*). Alizarin preparations of the following Curimatidae have been examined: *Acuticurimata macrops, Cruxentina nasa, Curimata cyprinoides, Curimatorbis ocellatus, Gasterotomus latior, Potamorhina pristigaster, Semitapicis planirostris,* and *Suprasinelichthys laticeps.*

Hemiodontidae

Hemiodontinae

Cranium (*Figures 1–5*). Frontoparietal fontanel complete; frontal portion narrow anteriorly, widening in front of epiphyseal bar; parietal portion uniformly wide. Ethmoid narrow, its head with a dorsomedian projection and lateral projections (one on either side) articulating with premaxillaries. Supraoccipital crest flattened dorsally; tip of supraoccipital spine rounded in dorsal view, extending to end of cranium. Posttemporal fossae well developed, with three openings. Lateral opening, largest in size, bordered entirely by epiotic and pterotic; dorsomedial opening, bordered by epiotic, parietal and supraoccipital; ventroposterior opening, lying in posteromedian portion of epiotic. Lateral and dorsomedial openings separated from each other only by a narrow bony bridge formed by epiotic. Dilator groove well developed, frontal participating in its formation.

Vomer with a concave lamellar component ventrally and two separately formed lamellar components dorsolaterally. Lateral ethmoid large, with anterior processes articulating with vomer. Rhinosphenoid present. Interorbital septum large, rhinosphenoid and orbitosphenoid widely separated from parasphenoid. Posterior portion of parasphenoid cleft for most of its length. Subtemporal fossa well developed.

Otoliths. Otoliths of generalized characoid morphology, similar in size and shape

to those in *Brycon* (cf. fig. 7 in Weitzman, 1962).

Facial bones (*Figure 6*). Facial bones present no unusual features. Circumorbital series complete, with a supraorbital, antorbital, and six moderately large infraorbital bones bearing infraorbital canal of cephalic laterosensory system. Infraorbital canal with posteriorly directed branches on infraorbital bones 3 and 4. Infraorbital bones flat, ventral portions of infraorbitals 1–4 not strongly curving beneath head. Infraorbital 1 not greatly enlarged. Size and shape of infraorbitals as in *Micromischodus:* infraorbital 3 largest, infraorbital 2 relatively slender. Infraorbital six contacting or closely approaching supraorbital.

Opercular bones of generalized characoid morphology, apparently without conditions of phyletic significance at familial or generic levels. Lateral surface of opercle smooth. Dorsoanterior corner of opercle strongly notched.

Jaws and jaw teeth (*Figures 6–10*). Premaxillary, with a short ascending process, loosely joined to maxillary; maxillary larger than premaxillary, its proximal end with a median knoblike projection. In *H. semitaeniatus* descending limb of premaxillary lies medial to anterior edge of maxillary; in *H. quadrimaculatus* descending limb of premaxillary much shorter, scarcely or not at all extending medially to maxillary. Upper jaw with a single row of 10–15 or more loosely articulated (movably attached) multicuspid teeth. Tooth crown rounded, cusps in a straight row, number of cusps increasing with age. In *H. semitaeniatus* a maximum of two replacement teeth for each functional tooth; in *H. quadrimaculatus* up to four replacement teeth per functional tooth. Inner surface of premaxillaries without bony partitions separating rows of replacement teeth. In *H. semitaeniatus* about eight teeth articulated with premaxillary and seven with maxillary; in *H. quadrimaculatus* about four or five teeth with premaxillary and five with maxillary. In *H. quadrimaculatus* premaxillary curving around replacement tooth rows more strongly than in *H. semitaeniatus.*

Lower jaw toothless, elongate. Portion of dentaries meeting at symphysis slender; middle portion of dentary moderately elevated. A single fenestra near anterior edge of dentary. Coronomeckelian bone low set, lying well below dorsal margin of articular bone.

Suspensorium (*Figures 6–8, 11*). Palatine straight, immovably attached to ectopterygoid, its anterior end moderately expanded. Ectopterygoid loosely (movably) attached to quadrate. Mesopterygoid loosely attached to quadrate and metapterygoid; metapterygoid loosely attached to hyomandibular. Anterior margin of metapterygoid separated by a gap from dorsoposterior margin of quadrate. Metapterygoid-quadrate fenestra relatively small. Anteroventral limb of metapterygoid (entering border of metapterygoid-quadrate fenestra) developed more strongly and anterior margin of hyomandibular more oblique in *H. quadrimaculatus* than in *H. semitaeniatus* (compare Figs. 7 and 8).

Hyoid and branchial arches (*Figures 12–14*). Hyoid arch without unusual features, of generalized characoid morphology. Four or five branchiostegal rays (four in *H. semitaeniatus,* five in *H. quadrimaculatus*). Proximal portion of next to last branchiostegal ray not enlarged (cf. *Argonectes* and *Micromischodus*). Basihyal slender, consisting of two ossifications, an anterior (dermal) bone and a posterior (endoskeletal) bone. Urohyal fairly long, its lateral wings moderately depressed and its dorsomedian lamina moderately high and extending slightly posterior to lateral wings.

Branchial arches including ceratobranchial 5 of relatively generalized characoid morphology, endoskeletal elements excepting infrapharyngobranchials and basibranchials similar in size and shape to those in *Brycon.* Three basibranchials; basibranchial 1 minute, basibranchials 2

and 3 very long. Three infrapharyngobranchials infrapharyngobranchials 2 and 3 greatly enlarged.

Gill rakers variable in form, often with large ctenii (not true teeth) (Fig. 14), and relatively numerous: 45 gill rakers on first gill arch of a 35.0-mm *H. quadrimaculatus*, 58 in a 55.8-mm *H. semitaeniatus* (Fig. 13), 70 in a 235-mm *H. microlepis* and 75 in a 113.5-mm *H. notatus*.

Pharyngeal dentition consisting of numerous small conical teeth, either nonpedicellate or with very short pedicels, confined to three or four pairs of upper pharyngeal toothplates and a single pair of lower pharyngeal toothplates. Upper pharyngeal toothplates on ventral surface of infrapharyngobranchials 2 and 3 and loosely associated with median ends of epibranchials 3 and 4.

Weberian apparatus (*Figure 15*). Weberian apparatus, very similar to that of *Micromischodus* and *Brycon meeki*, apparently without features of phyletic significance at generic or familial levels.

Pectoral girdle (*Figure 16*). Pectoral girdle of generalized characoid morphology, apparently lacking in features of phyletic significance at generic or even family levels. Three postcleithra, postcleithrum 3 slender for most of its length but with a lamellar portion near its proximal end (as in *Micromischodus*, *Brycon dentex* and many other characoids).

Pelvic girdle (*Figure 17*). Pelvic bone simple anteriorly; ischiac process relatively large. Four radials associated with each pelvic bone; innermost radial comma-shaped. Pelvic fin with 11 rays. Pelvic girdle evidently without features useful for phyletic analysis at generic or family levels.

Vertebral counts. Total vertebral and precaudal plus caudal vertebral counts in two specimens of *H. semitaeniatus* 40 (26 + 14) and 41 (26 + 15).

Caudal skeleton (*Figure 18*). Caudal skeleton with two or three epurals and two uroneurals. Hypurals 3–6 separate. Hypural 2 fused to hypural 1 and not to complex ural centrum. No bony projections comparable to parhypurapophyses or hypurapophyses. Principal caudal rays 10 + 9.

Bivibranchiinae

Cranium (*Figures 19–24*). Cranium of *Argonectes* similar in most respects to that in Hemiodontinae and Micromischodontinae. Anterior end of ethmoid of distinctive shape: narrow, slightly up-turned, with a dorsomedian groove terminating as a notch in tip of ethmoid (Fig. 19). Shapes of frontoparietal fontanel and of three openings into each posttemporal fossa as in *Hemiodus* and *Micromischodus*. Pterotic spine pronounced, epiotic spine moderate. Dilator fossa well developed. Rhinosphenoid moderately large and relatively simple in shape (Fig. 20). Posterior portion of parasphenoid cleft for virtually its entire length. Subtemporal fossa well developed. Hyomandibular fossa formed by contiguous surfaces of sphenotic and pterotic (Fig. 21).

Cranium of *Bivibranchia* broadly similar to that of *Argonectes* but with some notable departures: anterior end of ethmoid depressed, without a dorsomedian groove but with anterolateral projections; vomer relatively broad; rhinosphenoid greatly enlarged and of distinctive shape (Fig. 23); pterotic and epiotic spines enlarged; anterior portion of parasphenoid immediately in front of attachment of gill arches with a strong, ventrally projecting keel (absent in *Argonectes*). Dilator fossa less prominent than in *Argonectes*. Condition of frontoparietal fontanel, openings into posttemporal fossae, and hyomandibular fossa similar to *Argonectes*. In *Argonectes* and *Bivibranchia* ventromedian opening into posttemporal fossa partially closed by thin irregular bridges of bone from epiotic.

Otoliths. Otoliths of Bivibranchiinae not examined.

Facial bones (*Figures 25–29*). In *Argonectes* facial bones departing only in minor details of size and shape from those of *Hemiodus*: infraorbitals 1 and 4 relatively small. Infraorbital 6 contacting supraorbital.

In *Bivibranchia* facial bones differ in size and shape from those in *Argonectes* and *Hemiodus*: infraorbital 2 enlarged; infraorbital 1 relatively elongate; infraorbital 6 widely separated from supraorbital. Dorsal margin of opercle straight, without indentation characteristic of other hemiodontids.

Jaws (*Figures 25, 27–29*). Lower jaw similar in shape to that of Hemiodontinae; *Argonectes* and *Bivibranchia* differ from *Hemiodus* in having a posteriorly directed knob on symphyseal process of dentary and coronomeckelian bone elevated in position. In *Bivibranchia* coronomeckelian more elevated than in *Argonectes,* forming part of dorsal margin of lower jaw (Fig. 28); articular bone more elongate in *Bivibranchia,* its anterior end loosely fitted into dentary (not directly applied to internal surface of dentary), its posterior end with a knoblike projection that fits into a recess in median surface of quadrate when lower jaw is depressed.

Upper jaw highly specialized. Premaxillary minute. Maxillary slender and highly curved, more so in *Bivibranchia* than in *Argonectes.*

Jaw teeth (*Figures 27–29*). Jaw teeth highly specialized, diagnostic of subfamily. A single row of eight or nine minute, tricuspid, pedicellate teeth loosely attached to premaxillary and concave proximal portion of maxillary. Three or four preformed replacement teeth for each functional tooth in *Argonectes,* one or two in *Bivibranchia.* Lower jaw edentulous.

Suspensorium (*Figures 27–28*). In *Argonectes,* palatine, mesopterygoid and hyomandibular relatively generalized in morphology, not greatly different from these bones in other characoids. Mesopterygoid contacting and movably articulated with ectopterygoid and metapterygoid, not contacting palatine or quadrate. Ectopterygoid, quadrate and metapterygoid highly specialized: proximal end of ectopterygoid with a slender rounded head loosely fitting into a deep recess or socket in anterior margin of quadrate just above quadratomandibular joint. Metapterygoid movably articulated with mesopterygoid and hyomandibular, as in *Hemiodus.* Metapterygoid-quadrate joint more extensive (and less movable?) than in *Hemiodus,* metapterygoid quadrate foramen relatively small. Ventroposterior edge of metapterygoid contacting dorsal margin of symplectic distal end.

In *Bivibranchia* every bone in suspensorium highly specialized in shape and in relationships to other bones. Palatine bone S-shaped, its anterior end slender, forming a concavity into which elongated distal end of maxillary rides. Proximal end of ectopterygoid slender, forming the finger of a highly specialized, loose-fitting "finger and ring" joint with quadrate bone. Anterior margin of quadrate dorsal to quadratomandibular joint with a completely open ring of bone inside of which rides proximal end of ectopterygoid. Median surface of quadrate ventral to quadrato-mandibular joint with a well-developed concavity into which free-ending posterior projection from articular bone slides when lower jaw is depressed. Ectopterygoid of a highly modified and characteristic shape, much more specialized than in *Argonectes.* Ectopterygoid terminating anteriorly in a slender process to which ectopterygoid-vomerine ligament attaches. Ectopterygoid with an extensive movable articulation with quadrate, contact with metapterygoid reduced compared to *Argonectes,* no direct contact with ectopterygoid. Metapterygoid-quadrate articulation even more extensive than in *Argonectes,* rectilinear. Metapterygoid-quadrate foramen reduced in size, as in *Argonectes,* but metapterygoid and distal end of symplectic separated by a distinct gap. Metapterygoid-hyomandibular articulation specialized; hyomandibular with a strutlike process immovably joined to dorsoposterior margin of metapterygoid. Metapterygoid strengthened by a well-developed longitudinal keel on its median

surface extending anterior to and immediately below strut from hyomandibular.

Hyoid arch (*Figures 30, 34–36*). In *Argonectes* basihyal slender and moderately elongate, composed of separate anterior and posterior ossifications firmly sutured together; anterior ossification about twice as long as posterior one. Dorsal and ventral hypohyals closely joined. Hyoid bar perhaps slightly shorter than in *Hemiodus* but otherwise not strongly modified. Five branchiostegal rays, four on ceratohyal and one on epihyal. Proximal portion of branchiostegal ray 4 expanded so that it reaches dorsal edge of ceratohyal, as in *Micromischodus*. Urohyal moderately long, its lateral wings relatively narrow and only slightly depressed (ventral surface of urohyal moderately concave). Dorsomedian lamina moderately high, extending to posterior end of urohyal. Head of urohyal (attaching to ventral surface of ventral hypohyals) moderately wide, "neck" immediately behind head narrowed.

In *Bivibranchia* basihyal slender and moderately elongate, composed of separate anterior and posterior ossifications; anterior ossification about one-third as long as posterior one, and firmly attached to anterior end of posterior ossification, but not sutured to it as in *Argonectes*. Dorsal and ventral hypohyals closely joined. Hyoid bar slightly shorter than in *Hemiodus*, expanded dorsally and ventrally at junction of ceratohyal and epihyal; edge of dorsal expansion sharp; middle of hyoid bar thickened. Five branchiostegal rays, four on ceratohyal and one on epihyal. Branchiostegal ray 4 with its proximal portion only slightly enlarged. Urohyal specialized, its lateral wings wider and more depressed than in *Argonectes*, dorsomedian lamina forming a strong low-lying ridge behind head of urohyal but increasingly weak on posterior half of urohyal until it is almost absent. Head and neck of urohyal wider than in *Argonectes*.

Note. In *Argonectes* branchiostegal membranes relatively free from isthmus, gill openings extending forward almost to point of attachment of branchiostegal rays to hyoid bar. In *Bivibranchia* branchiostegal membranes broadly joined to isthmus below middle of eye, gill openings extending forward only to posterior ends of branchiostegal rays 1 and 2.

Gill arches (*Figures 31–37*). In *Argonectes* gill arches relatively generalized for characoids, similar to those in *Hemiodus*, without any obvious specializations. Apparently three basibranchials; basibranchial 1 minute. Small accessory ossifications (dermal bones?) between basibranchials 1 and 2 and basibranchials 2 and 3. Three hypobranchials. Four infrapharyngobranchials (a separate ossification dorsal to posteriormost upper pharyngeal toothplates interpreted as infrapharyngobranchial 4). Epibranchials 1–3 and ceratobranchials 1–4 morphologically generalized, their adpharyngeal surfaces simply rounded (as in *Hemiodus*). Epibranchial 4 with a moderately large abpharyngeal laminar extension (a widespread feature in characoids).

In *Bivibranchia* gill arches highly specialized. Three basibranchials; basibranchial 1 much larger than in *Argonectes* and most other hemiodontids, almost as long as basibranchials 2 and 3. Three hypobranchials. Hypobranchial 1 specialized: elongate and enlarged, peculiarly bowed inwards, its anterior end distinctly expanded. Hypobranchial 2 less modified than hypobranchial 1, but also relatively elongate. Three epibranchials. Epibranchials 1–3 and ceratobranchials 1–4 highly specialized, their adpharyngeal surfaces with a greatly expanded, thin bony lamina. These laminae completely separate gill rakers on leading edge of each gill arch from those on trailing edge, and are covered by highly specialized epithelium.

Gill rakers (*Figures 34, 36*). In *Argonectes* gill rakers present on leading and trailing edges of gill arches 1–4 and on leading edge of gill arch 5 (ceratobranchial 5). A 177-mm specimen has 14 + 1 + 8 rakers on arch 1, 8 + 1 + 9 on arch 2, 8 + 1 + 9 on

arch 3, 7 + 1 + 6 on arch 4, and 8 on arch 5.

In *Bivibranchia* gill rakers present on leading and trailing edges of most of gill arches 1–4 and on leading edge of arch 5. Gill rakers absent on basibranchials, infrapharyngobranchials, hypobranchials 1 and 2, and anterior half of ceratobranchial 1. Gill rakers slender and moderately elongate, only tripodlike basal portion and sometimes a small part of shaft absorbing alizarin. A 39.9-mm specimen has 12 + 1 + 11 rakers on arch 1, 12 + 1 + 15 on arch 2, 13 + 1 + 17 on arch 3, 10 + 1 + 17 on arch 4, and 23 on arch 5. A 115.2-mm specimen has 12 + 1 + 10 on arch 1, 14 + 1 + 17 on arch 2, 10 + 1 + 19 on arch 3, 12 + 20 on arch 4, and 23 on arch 5. (Note: in smallest rakers basal portion ossifies in two places; cf. rakers on epibranchials 3 and 4 in Fig. 36).

Remarks. In *Bivibranchia* the adpharyngeal epithelium is thrown into a uniform series of prominent, finely papillose ridges. One such ridge extends from the base of each gill raker on the leading edge of the gill arches to the base of the gill raker at the same position on the trailing edge. Thus the number of ridges corresponds to that of rakers. The ridges of successive arches interdigitate when the branchial apparatus is contracted. Eigenmann (1912: 258) referred to these epithelial structures as "broad laminae with papillated ridges." The ridges are well shown in the photographs of the gill arches accompanying Eigenmann's original description (op. cit., pl. 33, figs. 2–4). In these figures the gill rakers themselves are poorly or not at all discernible except on the lower portion of the first gill arch (fig. 2a).

The functional anatomy of the hyoid and branchial arches should be examined in live *Bivibranchia*. To judge from alizarin preparations, the hyoid arch may move independently of the branchial arches, using basibranchial 1 as a pivot. When the hyoid arch is forward, basibranchial 1 lies horizontally. When the hyoid arch is pushed backward, basibranchial 1 assumes a vertical orientation with its posterior end directed ventrally (Figs. 34, 35). This presumably would effect the pharyngeal pumping mechanism.

Pharyngeal teeth (*Figures 31–34, 36–37*). In *Argonectes* pharyngeal toothplates and pharyngeal dentition generalized. Upper pharyngeal dentition occurs on four pairs of separate toothplates that are intimately associated with ventral surface of infrapharyngobranchials 2, 3 and 4 and epibranchial 4. Lower pharyngeal dentition restricted to a pair of toothplates of fifth ceratobranchials. Dentition on all toothplates consisting of dense patches of moderate-sized simple conical teeth.

In *Bivibranchia* pharyngeal dentition highly specialized. Upper pharyngeal dentition restricted to a single pair of toothplates loosely associated with medially directed processes of infrapharyngobranchial 3 and epibranchials 3 and 4 (infrapharyngobranchial 4 absent). Upper toothplate of each side bearing two nearly coextensive, close-set rows of eight to ten tricuspid, pedicellate teeth (rows more regular in 115.2-mm specimen than in 39.9-mm specimen). Lower pharyngeal dentition restricted to a single pair of toothplates intimately associated with dorsal surface of ceratobranchial 5. Lower pharyngeal dentition consisting of three or four irregular rows of pedicellate teeth. In 39.9-mm specimen only anteriormost tooth row consisting of tricuspid teeth, remaining teeth unicuspid. In 115.2-mm specimen first two or three tooth rows almost entirely tricuspid, last row unicuspid. Tricuspid pharyngeal teeth morphologically similar to jaw teeth. Teeth on upper pharyngeal toothplates of equal size throughout tooth rows; teeth on lower toothplates substantially larger towards middle of pharynx.

Weberian apparatus. Weberian apparatus similar to that in *Hemiodus*, apparently without modifications useful for phyletic analysis within Hemiodontidae.

Pectoral girdle. Pectoral girdle of

generalized characoid morphology, similar to that of *Hemiodus*, except for postcleithra of *Bivibranchia*. In *Argonectes* three postcleithra, similar in shape and size to those of *Hemiodus*. In *Bivibranchia* only two postcleithra, corresponding to postcleithra 2 and 3 in other characoids. Shape of postcleithrum 3 as in *Hemiodus*, strutlike distally, with a proximal lamina. Shape of postcleithrum 2 specialized, with a strutlike extension dorsally.

Pelvic girdle. Shape of pelvic girdle similar to that in *Hemiodus*. Base of ischiac process directed medially, perpendicular to pelvic bone. *Argonectes* with 12 pelvic rays, *Bivibranchia* with ten.

Vertebral counts. Total vertebral and precaudal plus caudal vertebral counts: *Argonectes*, 43 (24 + 19); *Bivibranchia*, 40(22 + 18) (in two specimens).

Caudal skeleton (*Figures 38–39*). Caudal skeleton of typical hemiodontid morphology.

Anodontinae

Cranium (*Figures 40–42*). Cranium relatively narrow and shallow. Frontoparietal fontanel complete; frontal portion about half as wide as parietal portion and uniform in width for most of its length, widening slightly immediately in front of epiphyseal bar. Frontal portion prolonged anteriorly by opening between diverging posterior limbs of ethmoid bone (Fig. 40). Ethmoid moderately wide, more so than in Hemiodontinae but much less than in Curimatidae, its anterior end with processes articulating with premaxillaries and maxillaries (as in *Hemiodus*). Supraoccipital crest flattened dorsally but narrower than in *Hemiodus* and failing to reach end of cranium. Exoccipitals and basioccipital extend considerably further posteriorly than supraoccipital crest. Posttemporal fossae with three openings as in Hemiodontidae, Curimatidae and many other characoids. Dilator groove well developed, opening broadly onto dorsal surface of cranial roof. Posterior margin of epiotic strongly angulated but without posteriorly directed spine. Pterotic with very elongate, slender, posteriorly directed process.

Vomer with a relatively flat ventral surface (no ventrally directed median ridge), and a pair of relatively small, separately formed lamellae on its dorsal surface, these dorsolateral elements considerably smaller than comparable elements present in Hemiodontinae (comparable elements absent in Curimatidae?) Ventral portion of vomer with strongly demarcated anterior and posterior portions; anterior portion circular in ventral view, posterior portion circular anteriorly but drawn out to a point posteriorly. Parasphenoid relatively straight, gently sloping upwards anteriorly, with a poorly developed, ventrally directed median lamella. Posterior portion of parasphenoid cleft for about one-eighth of its length only (cleft for all or almost all of its length in other Hemiodontidae). Lateral ethmoids similar in shape to those in Hemiodontinae, although somewhat smaller, and with anterior processes articulating with vomer more elongate. Rhinosphenoid present. Interorbital septum smaller than in Hemiodontinae. Subtemporal fossa shallow but distinct. Intercalar bone large, with a short, posteriorly directed process bearing ligament of attachment with lower limb of posttemporal bone. Auditory fenestra large. Lagenar capsules moderate in size (not greatly enlarged as in Curimatidae).

Otoliths (*Figure 43*). All three otoliths in Anodontinae relatively elongate compared to those in *Hemiodus* and *Brycon*. Lapillus enlarged, even larger than asteriscus.

Facial bones (*Figures 44–45*). Circumorbital series complete. Infraorbital 4 with a posteriorly directed canal from infraorbital branch of cephalic laterosensory system. Infraorbitals flat and relatively small, especially infraorbital 6, leaving much of cheek (nearly all of preopercle) exposed. Nasal bone an elongate open canal or trough, without a lamellar portion. Antorbital small, contacting supraorbital

but separated by a gap from infraorbital 1. Opercle and interopercle relatively large; gill cover prolonged posteriorly by subopercle (similarly developed opercular bones occur in curimatids such as *Gasterotomus* and *Suprasinelichthys*). Dorsal border of opercle notched, as in Hemiodontinae (in Curimatidae dorsal margin of opercle invariably rounded). Lateral surface of opercle without a flange external to hyomandibulo-opercular joint but with an oblique flange just behind and parallel to its anterior margin (Fig. 44).

Jaws (*Figures 44–45*). Jaws toothless in adults and in smallest specimens known thus far (down to 46.4 mm). Gape large, extent of mouth-opening greater than in any other Hemiodontidae or in any Curimatidae. Premaxillary small, maxillary and dentary enlarged. A large oval fenestra near anterior margin of dentary. Articular bone moderately elongate. A small, horizontally oriented slit where dorsal margin of articular passes internally to dentary. Coronomeckelian bone small, its position relatively ventral (not elevated as in Bivibranchiinae and Parodontidae).

Suspensorium (*Figure 45*). Palatine small, immovably attached to ectopterygoid. Ectopterygoid slender, failing to contact quadrate posteriorly. Mesopterygoid greatly expanded, immovably (?) attached to ectopterygoid and metapterygoid but movably attached to quadrate. Symplectic and posterior limb of quadrate elongate. Metapterygoid-quadrate fenestra large. Metapterygoid without anteroventral limb forming posteroventral border of metapterygoid-quadrate fenestra. Main body of hyomandibular vertically oriented, its anteroventral border greatly indented or concave; posterior end of metapterygoid lying in this indentation but failing to contact hyomandibular.

Hyoid and branchial arches (*Figures 48–50*). Basihyal slender and elongate, seemingly a single ossification. Hyoid bar, especially ceratohyal, relatively elongate. Interhyal small. Dorsal and ventral hypohyals separated from each other slightly, not so closely fitted together as in other hemiodontids. Ceratohyal with dorsal and ventral processes extending from its anterior end and applied to lateral surface of dorsal and ventral hypohyals, respectively (Fig. 48). Five branchiostegal rays; four on ceratohyal and one on epihyal. Proximal end of branchiostegal ray 4 not greatly expanded. Branchiostegal rays elongate and moderately slender. Urohyal extremely elongate. Lateral wings of urohyal narrow and strongly depressed (ventral surface of urohyal deeply indented). Dorsomedian lamina of urohyal well developed, its crest extending posteriorly beyond lateral wings (Fig. 48).

Branchial arches with three basibranchials and three hypobranchials, basibranchials 1–3 and hypobranchials 1–3 successively more elongate. Basibranchial 1 very small, basibranchial 2 moderately elongate, and basibranchial 3 extremely elongate (twice as long as basibranchial 2). Hypobranchials 1 and 2 flat or nearly so; hypobranchial relatively elongate, its dorsal surface moderately excavated (much less so than in *Hemiodus*). Ceratobranchials 1–4 successively shorter; ceratobranchial 1 very elongate; ceratobranchial 4 distinctly shorter and ceratobranchial 5 narrower than ceratobranchials 1–3. Four epibranchials and three infrapharyngobranchials (a very thin, slivery and elongate ossification where infrapharyngobranchial 4 would be located is interpreted as an upper pharyngeal toothplate; it bears minute teeth and is similar to lower pharyngeal toothplate in appearance). Epibranchials 1–3 and infrapharyngobranchials 1–3 with well-developed apophyses. Infrapharyngobranchials 1–3 successively larger, infrapharyngobranchial 3 twice as long as infrapharyngobranchial 2. Pharyngeal dentition consisting of minute conical teeth rather widely spaced on elongate and extremely narrow toothplates.

Gill rakers (*Figures 48–51*). Numerous gill rakers on both leading and trailing

edges of first four gill arches and on leading edge of fifth gill arch (ceratobranchial 5). Gill rakers of arch 5 interdigitating with those on trailing edge of arch 4 and extending distally into a sort of pocket or epibranchial organ, although arrangement of distal gill rakers basically similar to that in other Hemiodontidae and in Parodontidae (cf. Fig. 13 of *Hemiodus* and Fig. 74 of *Saccodon*). Rakers very elongate and slender, directed foreward at an acute angle; long axis of rakers on leading and trailing edges of first three gill arches closely parallel. One margin of each raker smooth, with a narrow membranous flap for its entire length; opposite margin armed with a double row of minute ctenii. Rakers on leading edges of arches with ctenii directed medially, opposing laterally-directed ctenii on rakers of trailing edges. Ctenii increasing in number with age. In a 55.0-mm *A. melanopogon* most rakers about 3 mm long, with a double row of 40 + 40 ctenii. A 212-mm individual has most rakers about 11 mm long, with just over 130 + 130 ctenii. A 200-mm *A. elongatus* has most rakers about 10 or 11 mm long, with about 130 + 130 or more ctenii. In large specimens ctenii approximately 0.2–0.3 mm long and 0.1 mm or less apart (Fig. 51). Rakers of successive arches not diminished in size, and with ctenii equally numerous. Rakers on trailing edge of arches as long as those on leading edge.

Number of rakers increasing with age, first arch with 90–100 rakers in specimens of 50–55 mm and almost 200 in large specimens. A 55.0-mm *A. melanopogon* has 35 + 1 + 62 rakers on its first arch, a 212-mm specimen 73 + 1 + 115; a 200-mm *A. elongatus* has 80 + 1 + 110. Number of rakers on upper limb of arch greater in arches 2–4 than in arch 1. *A. melanopogon* of 55.0-mm with 35 + 1 + 62 rakers on arch 1 has 48 + 1 + 65 on arch 2, 58 + 1 + 51 on arch 3, and 51 + 1 + 63 on arch 4. Rakers at extremes of arches may extend beyond bones of arches, most notably on lower limb of arch 4, where a long series of rakers extends anteriorly from anteromedial end of ceratobranchial (Fig. 50) (no comparable series of rakers in *Hemiodus*).

Weberian apparatus (*Figure 52*). Weberian apparatus differing from that of *Hemiodus* only in details of shape and proportion of some parts, most notably neural complex, which is very elongate and low-lying.

Pectoral girdle (*Figure 53*). Pectoral girdle complete, each half with extrascapular, posttemporal, supracleithrum, cleithrum, three postcleithra, mesocoracoid, coracoid, scapular, four proximal radials, and an irregular series of small distal radials (not figured). Postcleithra relatively small but shaped as in *Hemiodus*. Coracoid small, failing to contact anterior end of lower limb of cleithrum. Posttemporal, supracleithrum and upper limb of cleithrum unusually slender and elongate, as in curimatids such as *Gasterotomus* and *Suprasinelichthys*, which have greatly expanded gill covers and gill openings superficially similar to those of *Anodus*.

Pelvic girdle (*Figure 54*). Pelvic girdle similar to that in *Hemiodus*. Pelvic bone slightly narrower and ischiac process more elongate than in *Hemiodus*. Pelvic fin with 11 rays.

Vertebral counts. Anodontinae exhibit total vertebral and precaudal plus caudal vertebral counts as follows: *A. elongatus*, 45 (32 + 13); *A. melanopogon*, 44 (29 + 15) and 45 (29 + 16).

Caudal skeleton (*Figure 55*). Caudal skeleton of generalized hemiodontid morphology. Three slender epurals. Hypurals 1 and 2 fused to each other and both separate from ural centrum. Principal caudal rays 10 + 9.

Parodontidae

Cranium (*Figures 56–59*). Cranial roof including supraorbital portion of frontal bone convex and smooth. Frontal and parietal bones of opposite sides broadly overlapping at midline of cranium for their entire length (frontoparietal fontanel ab-

sent). Dilator fossa roofed by frontal bone, not extending onto dorsal surface of cranium. Ventroposterior extension of supraorbital process of frontal bone with a large foramen open into dilator fossa. Ventral rim of foramen formed by a thin semicircle of bone. Supraoccipital crest absent; posterior margin of supraoccipital either with a bifid dorsal process (*P. guyanensis, A. affinis*), bilateral, horizontal flanges (*P. caliensis*), or evenly rounded (*Saccodon*). Posttemporal fossa with three openings (as in Hemiodontidae, Curimatidae, etc.). Head of ethmoid with a thin ventromedian lamella and lateral projections for articulation of movable premaxillaries. Posterior portion of ethmoid with a strong ventromedian process broadly joined to vomer. Ethmoid and vomer rigidly joined to each other; posterior laminae of ethmoid loosely attached to ventroanterior surface of frontals, apparently moving freely beneath them. Articulation of vomer with parasphenoid and lateral ethmoids apparently movable (permitting head of ethmoid to move in a vertical plane?). Rhinosphenoid absent. Orbitosphenoid enlarged, ventroanterior process of orbitosphenoid sutured to posteromedially directed processes from lateral ethmoids, orbitosphenoid failing to contact parasphenoid. Anterior portion of parasphenoid straight, not curving upwards as in Hemiodontidae and many other characoids. Hyomandibular fossa developed on lateral margin of prootic bone and anterior portion of pterotic (in most characins, including Hemiodontidae, the main articular surfaces of the hyomandibular fossa are on the sphenotic and pterotic). Subtemporal fossa well developed, lying entirely on pterotic bone. In *Saccodon* exoccipitals with a narrow but deep bony ridge extending laterally from lagenar capsules to intercalar bone. Lagenar capsules reduced in size. Intercalars relatively large. Epiotic with moderately elongate posterior process. Posterior process of pterotic short and rounded.

Otoliths (*Figure 60*). Otoliths of relatively generalized characoid morphology, not greatly different in size and shape from those in *Brycon*.

Facial bones (*Figures 61–65, 70*). Nasal bone slender and moderately elongate, almost entirely tubular. Circumorbital series complete, with a supraorbital, antorbital and six relatively large infraorbitals. Antorbital a small, triangular element, its apex separated by a slight gap from supraorbital, its base resting on dorsal margin of infraorbital 1. Infraorbital 1 covering posterior portion of premaxillary. Infraorbital 2 covering most of dentary. Infraorbitals 2–4 almost entirely hiding preopercle from view. Ventral portion of infraorbitals 2 and 3 curving strongly underneath head.

Opercular series complete, with a preopercle, interopercle, subopercle and opercle. No supraopercle or suprapreopercle. Lateral surface of opercle smooth, dorsal margin of opercle broadly rounded. Posterior portion of interopercle greatly deepened. Subopercle relatively shallow for its entire length, with a well-developed ascending process internal to "junction" of preopercle, opercle and interopercle. Anterior end of preopercle immovably joined to quadrate; anterolateral surface of preopercle completely covered by bony extension of quadrate. Opercle and subopercle oriented parallel to main axis of head. Anterior ends of preopercle and interopercle inclined inwards towards quadrato-mandibular junction.

Jaws and jaw teeth (*Figures 63–71*). Premaxillaries greatly expanded, with from $2+2$ to $5+5$ functional teeth in a single row. Replacement tooth trenches for each functional tooth position separated from each other by bony ridges on inner face of premaxillaries with from four to 30 preformed replacement teeth. Replacement teeth largely enclosed by lateral and median walls of premaxillary and in varying degrees by a ventrally directed extension arising from dorsoposterior margin of premaxillary. In *Apareiodon affinis* this extension is short and replacement teeth lie

relatively exposed posteriorly. It extends further ventrally in *Parodon caliensis.* In dental morph I of *S. wagneri,* entire dorsoposterior margin of premaxillary extends ventrally to cover almost half of extent of replacement tooth rows. In dental morph IV of *S. wagneri* dorsoposterior margin of premaxillary extends ventrally to cover two-thirds of extent of replacement tooth rows. Flattened median walls of premaxillaries of opposite sides firmly united to each other by tough connective tissue. Premaxillaries with dorsomedian process articulating to ethmoid. Dorsomedian processes greatly expanded in *A. affinis* and *P. caliensis,* moderately expanded in *P. guyanensis,* and relatively small in *S. wagneri.* A longitudinal depression or groove in dorsal surface of premaxillary, lateral to dorsomedian process, into which fit lateral projections from head of ethmoid.

Maxillary relatively small and slender, strongly curved, edentulous or with one to three small teeth. One preformed replacement tooth for each functional tooth lies in a pocket in maxillary. Ascending process of maxillary loosely attached to premaxillary. Some specimens of *S. wagneri* with a small supramaxillary at tip of ascending premaxillary process.

Lower jaw extremely similar in form to that in Hemiodontidae, albeit of relatively stouter construction. Dentaries with an oval fontanel near anterior margin, slender symphysial processes joined to each other by tough connective tissue, and elevated lateral walls just inside rictus of jaws. Dentary either toothless (*Apareiodon, Saccodon,* young *Parodon*) or with one to three large stout teeth planted on inner surface of lateral expansion just inside rictus of jaws. Articular bone and posterior portion of dentary slender. Coronomeckelian bone large, its position near dorsal edge of articular much higher than in most other characoids.

Suspensorium (*Figures 63–65, 70, 72*). Palatine large, its anterior end expanded, its posterior end immovably attached to ectopterygoid and lying in a long trough or groove in dorsoanterior surface of ectopterygoid. Ectopterygoid moderately expanded anteriorly, slender posteriorly, its posterior end forming a narrow, movable joint with dorsal edge of quadrate. Mesopterygoid movably articulated with median surfaces of ectopterygoid and metapterygoid. Posterior portion of metapterygoid loosely bound to hyomandibular. Metapterygoid-quadrate foramen moderately large. Anterior end of hyomandibular inclined inwards towards quadrato-mandibular joint. Quadrate firmly united to preopercle, a bony extension from quadrate overlying lateral surface of anterior end of preopercle. Quadrato-mandibular condyle very large. Lateral surface of quadrate posterior to condyle greatly thickened.

Hyoid and branchial arches (*Figures 73, 74*). Basihyal moderately elongate, narrow posteriorly and slightly expanded anteriorly. Hyoid bar of generalized characoid morphology. Dorsal and ventral hypohyals separate (not fused together). Interhyal relatively small. *Apareiodon* with three branchiostegal rays, *Saccodon* and *Parodon* with four. In *Saccodon* branchiostegal rays 1 and 2 ending basally in slender flanges articulating on inner surface of ceratohyal. Branchiostegal rays 3 and 4 with relatively stout basal flanges articulating with external surface of ceratohyal and epihyal, respectively. Urohyal short and stout, its horizontal laminar portions relatively broad, its dorsal median lamina terminating in a high crest.

Three basibranchials. Basibranchial 1 short, basibranchials 2 and 3 elongate. Three hypobranchials. Hypobranchial 1 flat, hypobranchials 2 and 3 with strongly concave dorsal surfaces. Epibranchials and ceratobranchials relatively shorter than in Hemiodontidae. Epibranchials oriented almost at a right angle to main axis of body when viewed from above; ceratobranchials at an angle of about 45 degrees. Three infrapharyngobranchials;

infrapharyngobranchials 2 and 3 moderately enlarged.

Gill rakers moderately elongate or short and platelike, without ctenii. Number of gill rakers moderate, increasing slightly with age. *Saccodon wagneri* of 50 to 55 mm have 32–35 gill rakers on first gill arch. A 103.3-mm specimen of dental morph IV with gill rakers on leading and trailing edges of gill arches as follows: arch 1, 20 + 1 + 22 on leading edge and 30 + 27 on trailing edge; arch 2, 15 + 1 + 39 and 23 + 1 + 36; arch 3, 32 + 1 + 42 and 23 + 43; arch 4, 23 + 46 + (?) and 0 + 35; and arch 5, 0 + 28 (on leading edge only of ceratobranchial 5). A 63.5-mm *Parodon caliensis* has 16 + 1 + 23 rakers on leading edge of arch 1, a 46.8-mm *Apareiodon affinis,* 12 + 1 + 22. In *A. affinis* gill rakers on leading edge of arches 2 and 3 enlarged, much larger than those on arch 1; in other parodontids examined, largest rakers occur on leading edge of arch 1 (Fig. 74). Row of gill rakers on leading edge of ceratobranchial 5 terminating distally in a semicircle of rakers of diminutive size, joining a complementary semicircle of similar rakers from trailing edge of ceratobranchial 4 (Fig. 74). A comparable condition occurs in Hemiodontidae (Hemiodontinae and Anodontinae) and perhaps in other characoids.

Pharyngeal dentition consisting of numerous, small conical teeth, apparently non-pedicellate, well developed only on last pair of upper pharyngeal toothplates (those loosely associated with medial ends of epibranchials 3 and 4) and on lower pharyngeal toothplates associated with dorsal surface of ceratobranchial 5. Toothplates on ventral surface of infrapharyngobranchials 2 and 3 either absent or small and with few teeth.

Weberian apparatus (*Figure 75*). Weberian apparatus similar to that in numerous characoids, apparently without useful features for phyletic studies.

Pectoral girdle (*Figure 76*). In *A. affinis* pectoral girdle, including postcleithra 1–3, relatively similar to morphologically generalized pectoral girdle of *Hemiodus* (no close relationships implied). In *Saccodon* and *Parodon* cleithrum enlarged, its anterior and posterior limbs curving strongly inwards; medially directed lamina from anterior and ascending limbs of cleithrum very strong; postcleithrum 2 greatly expanded, postcleithrum 3 strutlike, narrow for its entire length. In *Saccodon,* first two pectoral fin rays simple; in *Parodon* and *Apareiodon* only first pectoral ray simple.

Pelvic girdle (*Figure 77*). Anterior portion of pelvic bone simple (not bifid or trifid), broader in *Saccodon* than in *Apareiodon* or *Parodon.* Ischiac process relatively short and simple in *Saccodon.* In *P. caliensis* and *A. affinis* ischiac process elongate and thin posteriorly, especially in *P. caliensis,* and bearing a short, lateral projection near its base. Eight or nine pelvic fin rays.

Vertebral counts. Parodontidae exhibit total vertebral counts and precaudal plus caudal vertebral counts as follows: *P. caliensis* 35 (14 + 21); *A. affinis* 41 (20 + 21, 21 + 20); dental morph 1 of *S. wagneri* 38 or 39 (18 + 20, 20 + 18, 19 + 20); and dental morph IV of *S. wagneri* 38 (18 + 20 in two specimens, 19 + 19, 20 + 18).

Caudal skeleton (*Figure 78*). Caudal skeleton morphologically generalized for characoids, similar to caudal skeleton of most Characidae, Curimatidae, etc. Epurals two. Uroneurals two. Hypurals six; hypural 2 slender, separate from hypural 1, fused to complex ural centrum (as in most characoids). Principal caudal rays 10 + 9.

DISCUSSION

Relationship Between Hemiodontidae and Parodontidae

The superficially similar appearance of Hemiodontidae and Parodontidae together with the unique disposition of the jaw teeth common to many species in both families, has led most students of characoid classification to regard them as closely related

Table 2. Distinguishing characteristics of Parodontidae and Hemiodontidae

	Parodontidae	Hemiodontidae
Premaxillary	Highly mobile.	Immobile or only slightly mobile.
	Greatly enlarged.	Minute to considerably enlarged but never as much as in Parodontidae.
	From four to over 30 preformed replacement teeth for each functional tooth lying in trenches with bony partitions.	A maximum of four to six preformed replacement teeth for each functional tooth; no trenches or bony partitions separating them.
Maxillary	Lies entirely lateral to premaxillary, without contacting ethmoid.	Tends to articulate directly with ethmoid.
Frontoparietal fontanel	Absent.	Present.
Rhinosphenoid	Absent.	Present.
Adipose eyelid	Absent.	Present.
Branchiostegal rays	Three or four.	Four or five.
Hypural 2	Fused to ural centrum and separate from hypural 1.	Separate from ural centrum and fused to hypural 1.
Vertebrae	35 to 41.	40 to 45.

(Regan, 1911; Eigenmann, 1912; Fowler, 1950; Géry, 1959; Greenwood et al., 1966). Only Regan (1911) and Géry (1959) presented osteological evidence bearing on this problem, and their evidence is brief and not very informative. Regan pointed out some similarities in the suspensorium (similarities shared with the unrelated forms *Nannostomus* and *Characidium*), stated that the hyomandibular is single-headed (I find it bicipital in both families), and incorrectly indicated that the maxillaries in both Hemiodontidae and Parodontidae articulate with the ethmoid (in some Hemiodontidae the maxillaries articulate with the ethmoid, but in Parodontidae they lie entirely lateral to the expanded premaxillaries). Géry (1959) compared the superficial cranial features of *Parodon guyanensis* with those of *Hemiodus quadrimaculatus* and found them similar in a number of respects but the similarities involved do not include any specialized features.

The similarity of the jaws (especially the lower jaws) and dentition of many Parodontidae and Hemiodontidae is undeniably striking. The shape of the upper jawbones in *H. quadrimaculatus,* together with the decrease in number of functional teeth and increase in replacement teeth in this species (Fig. 10), does suggest a step towards the highly specialized premaxillaries and maxillaries of Parodontidae. On the other hand, the premaxillaries of *H. quadrimaculatus* show no indication of bony septae separating the replacement teeth for each functional tooth position (such septae are diagnostic of Parodontidae). The similarity in shape of the lower jaws in the two families can be seen by comparing Figures 7 and 8 with 65 and 70. The specialized suspensorium is also very similar. The slightly overlapping condition of the quadrate with the anterior end of the preopercle in Hemiodontinae suggests a step towards the highly specialized condition in Parodontidae (compare Figs. 11 and 72). It seems, however, that phyletically suggestive osteological similarities do not extend beyond the jaws and suspensoria. The cranium of Parodontidae is highly specialized and differs in many respects. The hyoid and branchial arches, Weberian ap-

paratus, pectoral and pelvic girdles and vertebral columns in both families are of relatively generalized characoid morphology and do not seem to offer useful characters in the present context. The caudal skeleton of Parodontidae is more generalized than that of Hemiodontidae in having hypurals 1 and 2 separate and hypural 2 fused to the ural centrum. Whether Hemiodontidae and Parodontidae are indeed close relatives will have to be resolved by further study. In any event, there are considerable differences between the two families (Table 2).

Transfer of Anodontinae from Curimatidae to Hemiodontidae

Anodontinae has been placed in Curimatidae by most students of characoid classification (Eigenmann and Eigenmann, 1889; Regan, 1911; Fernandez-Yepez, 1948; Greenwood et al., 1966) because its members lack jaw teeth and superficially resemble curimatids such as *Gasterotomus*. Evidence that Anodontinae should be transferred from Curimatidae to Hemiodontidae can be marshalled as follows:

1. Curimatidae are characterized by a strong flange on the lateral surface of the opercle, just above the hyomandibulo-opercular joint (Fig. 46). This feature is readily observable, without dissection, in alcoholic specimens, and is present in all species of Curimatidae seen by me. I do not know of any other characoids with a comparable opercular flange. The flange is absent in *Anodus*.

2. In the lower jaw of Curimatidae the articular is relatively short; both the dentary and articular are elevated; where the dentary and articular join there is a large vertical gap or fenestra, and there is no oval fenestra in the dentary (Figs. 46–47). In Hemiodontidae the articular is relatively elongate; the dentary is elevated in varying degrees, but the articular is never elevated; where the dentary and articular join there are either no gaps or only horizontally oriented gaps (cf. *Bivibranchia*), and there is an oval fenestra in the dentary. In all of these features the lower jaw of *Anodus* agrees with that of Hemiodontidae. *Anodus* has an exceptionally large oval fenestra in the dentary.

3. In Curimatidae the gill rakers are absent or poorly developed: with little or no ossification, short and "fleshy" and relatively few in number. In most hemiodontids the gill rakers are well developed: well ossified, elongate, often bearing ctenii, and relatively numerous. The gill rakers of *Anodus* are exceptionally well developed: well ossified, very elongate, provided with minute ctenii, and more numerous than in any other characoids (increasing in number with age).

4. Curimatidae usually (always?) have four branchiostegal rays. Hemiodontidae often have five branchiostegal rays (four or five in *Hemiodus*, five in *Micromischodus*, *Argonectes*, *Bivibranchia*). *Anodus* has five branchiostegal rays. In Curimatidae the branchial membranes are united to the isthmus. In Anodontinae and in other Hemiodontidae excepting *Bivibranchia* the branchial membranes are free from the isthmus and the gill openings extend relatively far forward ventrally.

5. Curimatidae are characterized by a joint between the palatine and lateral ethmoid which is absent in Hemiodontidae and Anodontinae. In Curimatidae the dorsal surface of the posterior end of the palatine is expanded into a facet (Fig. 47) which either attaches directly to a facet on the ventral surface of the lateral ethmoid just internal to its lateral wing or else is joined to such a facet by dense connective tissue (sometimes cartilaginous). There is no indication of these facets on the palatine and lateral ethmoid in Hemiodontidae or Anodontinae.

6. Curimatidae are characterized by a greatly enlarged lagenar capsule. In Ano-

dontinae, as in Hemiodontidae, the lagenar capsule is relatively small.

7. In Curimatidae body shape is extremely variable, but rarely, if ever, is it truly subcylindrical and fusiform as in all Hemiodontidae and in Anodontinae. Many curimatids are deep bodied or laterally compressed. The ventral abdominal surface is frequently squared off, keeled, or carinate. The body contour is frequently modified in front of or along the base of the dorsal and anal fins.

8. Of more than 100 species, only one curimatid—*Curimatorbis ocellatus* Eigenmann and Eigenmann 1889—has an oval spot on the middle of the body just behind the dorsal fin. Such a spot is more characteristic of Hemiodontidae, being present in several species of *Hemiodus,* in *Argonectes,* and in two undescribed species of *Bivibranchia* from Surinam (Géry, personal communication). A comparable spot is always present in *A. elongatus* and sometimes present (although faint) in *A. melanopogon* (Plate I).

9. Excepting very small species and young stages, Curimatidae have an intestine with numerous coils. In Hemiodontidae and in *Anodus* the intestine is moderately coiled.

10. Curimatidae have low vertebral counts, from 30 to 36, about evenly divided between precaudal and caudal vertebrae. Anodontinae have 44 or 45 vertebrae, precaudal vertebrae twice as numerous as caudal. Hemiodontidae other than Anodontinae have 40 to 43 vertebrae, and precaudals about twice as many as caudals.

11. In Curimatidae hypural 2 is fused to the complex ural centrum and entirely separate from hypural 1. In *Anodus,* as in Hemiodontidae, hypural 2 is fused to hypural 1 and has lost its connection with the ural centrum.

In comparing the skull of *Anodus* with those of other characoids, one is struck by how much space is occupied by the gill arches and expanded gill covers and how little by the elongate, narrow and relatively depressed cranium. In curimatids such as *Gasterotomus* and *Suprasinelichthys* in which the gill covers are also enlarged and the external appearance of the head strongly resembles that of *Anodus,* the cranium is relatively heavy, broad and deep. The general appearance of the cranium of *Anodus* is more like that of *Hemiodus* than of any curimatids I have examined.

Anodus agrees with both Hemiodontidae and Curimatidae in having three openings into each posttemporal fossa and a rhinosphenoid bone. These characters are of minor phyletic significance, since three openings into the posttemporal fossa occur in many noncharacid characoids, African as well as South American, and the rhinosphenoid is present in many South American groups. The only character shared exclusively by Curimatidae and Anodontinae is absence of jaw teeth, a loss character, and therefore of dubious significance.

The characteristics of Anodontinae are approached in some ways by *Hemiodus microlepis.* The superficial resemblance between this species and *A. elongatus* is as striking as that between *A. elongatus* and curimatids such as *Curimatorbis ocellatus* or *Gasterotomus latior. H. microlepis* has about 105–115 scales in a lateral series and an oval spot on the body just posterior to the dorsal fin. The gill rakers, although not elongate as in *A. elongatus,* are relatively numerous (probably increasing in number with growth) and denticulate. A 235-mm specimen has 30 + 40 gill rakers on the first gill arch. Each comblike raker bears about 10 large ctenii (Fig. 14). Fowler (1906: 319) reported 22? + 38? ciliate rakers in a specimen nine inches long. Gill rakers of the last arch are relatively large and interdigitate with trailing gill rakers of the fourth arch, as in other species of *Hemiodus* and in *Anodus.* The teeth, although typical in shape for *Hemiodus,* are relatively small and numerous (about 20–22 on each side

Table 3. Distinguishing Characteristics of the subfamilies of Hemiodontidae

	Hemiodontinae	Bivibranchiinae	Anodontinae	Micromischodontinae
Jaw teeth	Upper jaw only. A single row of 16–44 on premaxillary and maxillary. Fan-shaped, pedicellate, ca. 10–20 cusps. Several sets preformed replacement teeth.	Upper jaw only. A single row of 16 on premaxillary and maxillary. Tricuspid, short pedicel. One to four sets preformed replacement teeth.	Absent.	Both jaws. Premaxillary with single row of 28; maxillary toothless; dentaries with two nearly coextensive rows of 100–120. Unicuspid, with minute, recurved cusps, elongate, swollen pedicels. Single set preformed replacement teeth.
Jaws	Nonprotrusible. Premaxillary large, immobile or only slightly movable.	Highly protrusible. Premaxillary minute, firmly attached to anterior end of maxillary, entirely freed from cranium	Nonprotrusible. Premaxillary moderate-sized, immobile or only slightly movable.	Nonprotrusible. Premaxillary moderate-sized, immobile or only slightly movable.
Suspensorium	Generalized. Anterior end immovable, joined to cranium, or capable only of slight movement. Ectopterygoid-quadrate joint generalized.	Highly specialized. Anterior end freely movable downwards and away from cranium. Ectopterygoid-quadrate joint extremely mobile and specialized.	Generalized. Conditions comparable to those in Hemiodontinae.	Generalized. Conditions comparable to those in Hemiodontinae.
Gill rakers	Variable in form and number, usually moderately numerous. Often bearing large, moderately numerous ctenii.	Reduced in size, relatively few in number. Ctenii absent.	Extremely elongate and numerous. Ctenii minute, extremely numerous, disposed in a double row.	Moderately elongate and numerous. Ctenii absent.
Branchiostegal rays	Four or five.	Four.	Five.	Five.

of the upper jaw). The tapered posterior chamber of the swimbladder extends to or slightly beyond the base of last anal fin ray. I have examined two specimens (MCZ 20652; 229 and 235 mm; Tefé, Amazonas, Brazil. Thayer Expedition). The osteology of this species has not been investigated.

The distinguishing characteristics of the Anodontinae and of the other three subfamilies of Hemiodontidae are presented in Table 3.

Remarks on Lower Taxa

Genera of Hemiodontinae. Three genera of Hemiodontinae are currently recognized: *Hemiodus* Müller 1842, *Hemiodopsis* Fowler 1906, and *Pterohemiodus* Fowler 1940. *Anisitsia* Eigenmann and Kennedy 1903 is a synonym of *Hemiodus; Hemiodus* includes only those species in which the scales below the lateral line are larger than those above it (Géry, 1961; 1963b; 1964). The three genera are split very finely. There is a complete gradation between species in which scales above and below the lateral line are the same size and species in which scales below the lateral line are larger. Larger scales below the lateral line occur also in *Micromischodus* (Roberts, 1971: 7, fig. 1) and in many species of Curimatidae. The scales below the lateral line are slightly larger than those above it, even in some species of *Hemiodus* in which they are stated to be of equal size, e.g., *H. microlepis.* In itself this character is insufficient grounds for recognition of a separate genus, and no other distinction between *Hemiodus* and *Hemiodopsis* (cf. Géry, 1964) has been offered. Employment of single characters leads to proliferation of taxa, many of which will be polyphyletic. If a genus is based on such a simple character as scale size there is no way of determining whether it is monophyletic or polyphyletic. For these reasons I do not recognize *Hemiodopsis.* Similar grounds can be given for rejecting *Pterohemiodus,* erected for a species with a filamentous extension of the dorsal fin. Géry (1961: 338) gave a more detailed diagnosis of *Pterohemiodus,* and there is perhaps more reason for retaining this genus than for *Hemiodopsis.* The vertical disposition of the teeth, indicated by Géry as diagnostic of *Pterohemiodus,* is a characteristic feature of *Hemiodus quadrimaculatus* as well as most Parodontidae. Systematic revision of the species of *Hemiodus* is sorely needed. Systematists should note that in this genus the numbers of jaw teeth, of cusps on the jaw teeth, and of gill rakers tend to increase with age.

Genera of Bivibranchiinae. Three genera are currently recognized in Bivibranchiinae: *Bivibranchia* Eigenmann 1912, *Atomaster* Eigenmann and Myers 1927, and *Argonectes* Böhlke and Myers 1956. I have not examined *Atomaster.* Eigenmann and Myers distinguished it from *Bivibranchia* because of its small ctenoid scales. Myers (personal communication) is inclined to think that *Atomaster* is too much like *Bivibranchia* to be recognized as a separate genus.

Böhlke and Myers (1956) regarded *Argonectes* as a closely allied, specialized derivative of *Hemiodus,* having some of the same specializations in the jaws and dentition as *Bivibranchia.* I find that the two genera share several unique specializations in the jaws, jaw teeth and suspensoria, and thus they constitute a well-defined subfamily (see definition above). Their protractile jaws and suspensoria are highly specialized in much the same way, and yet in many respects, even in the structure of the jaws, *Argonectes* is clearly more primitive than *Bivibranchia.* The posterior portion of the maxillary is much more elongate and curved in *Bivibranchia,* perhaps an indication of greater protractility. *Argonectes* lacks the specialized valves found in the roof of the mouth in *Bivibranchia* (and in *Atomaster*) (Eigenmann, 1912; Géry, 1963a; Eigenmann and Myers, 1927). The shapes of the palatine and mesopterygoid, highly specialized in *Bivibranchia,* are relatively generalized or only slightly

modified in *Argonectes*. The ectopterygoid-quadrate joint, highly specialized in *Argonectes*, is even more specialized in *Bivibranchia* (compare Figs. 27 and 28). The gill arches, pharyngeal epithelium and pharyngeal dentition, strikingly specialized in *Bivibranchia*, are generalized in *Argonectes*, although *Argonectes* has even fewer gill rakers than *Bivibranchia*. The infraorbital bones and postcleithra, generalized in *Argonectes*, are moderately specialized in *Bivibranchia*. *Argonectes* has a complete adipose eyelid, *Bivibranchia* the more usual condition in which there is an opening in the adipose eyelid over the pupil. *Argonectes* apparently grows larger than *Bivibranchia*. I have not seen any specimens of *Bivibranchia* larger than 115 mm (the largest reported by Eigenmann, 1912), whereas *Argonectes* attains 198 mm (MCZ 20635), and I have seen specimens from several localities larger than 115 mm.

Genera and species of Anodontinae (*Plate I: Frontispiece*). Two genera of Anodontinae are currently recognized: *Anodus* Spix 1829 and *Eigenmannina* Fowler 1906. (*Elopomorphus* Gill 1878 is a synonym of *Anodus;* Eigenmann and Eigenmann, 1889.) The generic type of *Anodus* is *A. elongatus* Spix 1829, by monotypy, a well known and widely distributed Amazonian species. *Elopomorphus jordanii* Gill 1878 and *Anodus steatops* Cope 1878 have been placed (correctly, I think) in the synonymy of *A. elongatus* (Eigenmann and Eigenmann, 1889; Fowler, 1906; Fernandez-Yepez, 1948; Fowler, 1950). "*Elopomorphus*" *orinocensis* Steindachner 1888 (pp. 66–67, pl. 2), from the Orinoco (no other locality given) is probably another synonym of *A. elongatus*. This is the only non-Amazonian record of Anodontinae, and has been overlooked by subsequent authors (Fernandez-Yepez, 1948; Mago Leccia, 1970). ("*Anodus*" *latior,* recorded from Venezuela by Mago Leccia [1970], is the generic type of *Gasterotomus* Eigenmann 1910 and should be known as *G. latior*. It is a curimatid.)

Only one other species of *Anodus* has been described, *A. melanopogon* Cope 1878, and it is clearly distinct. Widely distributed in the Amazon, it has been taken together with *A. elongatus* in the Río Marañon at Iquitos and in the rio Negro near lago Alexo. It differs from *A. elongatus* in having a more slender build and smaller scales (ca. 125–130 scales in a lateral series vs. 100–105) (Plate I). Specimens of the two species of comparable length seem to have about the same number of gill rakers, but this should be studied in more extensive series than are presently available. *Eigenmannina* Fowler 1906 takes *A. melanopogon* as its generic type, but *A. melanopogon* is so similar to *A. elongatus* that generic separation is unwarranted. I have compared Cope's type specimens of *A. melanopogon* with a series of freshly preserved young specimens of the same size (MZUSP 5959). Although the types are in very poor condition, my examination indicated that they are the same species as the fresh material. The "strongly concave upper profile of the head," used as a generically diagnostic character by Fowler (1906: 306–307, fig. 10), is clearly an artifact of preservation. Both lots have the extensive black coloration on the underside of the jaws, high scale counts and narrow caudal peduncle, and protruding lower jaw that are characteristic of the species. In half-grown and adult specimens of *A. melanopogon* the lower jaw projects only slightly or not at all, as in larger specimens of *A. elongatus*. The largest specimens of *A. melanopogon* examined, 209 and 212 mm, are very similar to *A. elongatus* of the same size.

Genera of Parodontidae. Three genera of Parodontidae are currently recognized: *Parodon* Valenciennes 1849 (*in* Cuvier and Valenciennes, 1849), *Saccodon* Kner and Steindachner 1863, and *Apareiodon* Eigenmann 1916. *Parodontops* Schultz and Miles 1943 has been placed in the synonymy of *Saccodon* as a result of my studies on trophic polymorphism in that genus (Rob-

erts, 1974). *Parodon, Saccodon* and *Apareiodon* are so poorly defined in the literature (cf. Schultz and Miles, 1943; Géry, 1959) that their distinctness may be questioned. *Parodon* differs from the other two genera in having teeth in the lower jaw; according to Géry (1959), the cusps on the premaxillary teeth are more deeply incised. Schultz and Miles stated that the lower jaw is sometimes toothless in young specimens of *Parodon* and questioned the validity of *Apareiodon. Saccodon* differs from the other two genera in having two unbranched rays in each pectoral fin instead of only one (Roberts, 1974). Since my observations have been extended to only two species of *Parodon* and two of *Apareiodon* (see Material Examined), I lack sufficient information to provide meaningful definitions of Parodontidae at the generic level.

CONCLUSION

Modification of trophic structures obviously has played a major role in the adaptive radiation of Hemiodontidae and Parodontidae. The four subfamilies of Hemiodontidae are definable primarily in terms of trophic adaptations. Diversification of jaw teeth, complete loss of jaw teeth, radical innovations in functional anatomy of the jaws, and modification of oral and pharyngeal epithelia, of gill rakers, of pharyngeal teeth, and even of endoskeletal elements in the gill arches have occurred. Within Hemiodontidae, Hemiodontinae and Micromischodontinae, although specialized in certain respects, are relatively generalized. In Bivibranchiinae *Argonectes* is clearly more primitive than *Bivibranchia* in many important respects. I see no reason to doubt that *Bivibranchia* had ancestors extremely similar to the living *Argonectes.* Bivibranchiinae differ radically from all other characoids in their highly modified suspensoria and protrusible upper jaws. If *Argonectes* or a form very similar to it gave rise to *Bivibranchia,* then the development of protrusibility set the stage for further modification of the suspensorium and for structural innovations in the oral and pharyngeal epithelia, endoskeletal gill arch elements and pharyngeal dentition found in *Bivibranchia.* In no other characoids are the trophic structures more highly modified than in *Bivibranchia.* Hemiodontinae are generalized enough relative to Bivibranchiinae to have been near the ancestral line to *Argonectes.* Apart from lacking jaw teeth, Anodontinae have little in common with Curimatidae. Unlike Curimatidae (which feed on the bottom and ingest quantities of mud) and other Hemiodontidae (which also feed mainly on the bottom but more selectively than Curimatidae), Anodontinae presumably strain small organisms from midwater. Examination of the guts of preserved *Anodus* reveals only that they do not ingest any mud. Determination of their food items will probably require microscopic examination of fresh stomach contents. Hemiodontidae and Parodontidae offer excellent opportunities for multidisciplinary investigations of the role of feeding habits and trophic adaptations in the evolution of higher taxonomic categories.

LITERATURE CITED

Agassiz, L., and J. B. de Spix. 1829. Selecta genera et species piscium brasiliensium. i-xv + I-II + 138 pp, 100 pls. (irregularly numbered).

Böhlke, J. E., and G. S. Myers. 1956. Studies on fishes of the family Characidae.—No. 11. A new genus and species of hemiodontins from the Rio Orinoco in Venezuela. Acad. Nat. Sci. Philadelphia, Notulae Naturae, No. 286: 1–6.

Cope, E. D. 1878. Synopsis of the fishes of the Peruvian Amazon obtained by Professor Orton during his Expeditions of 1873 and 1877. Proc. Amer. Phil. Soc., **17**: 673–701.

Cuvier, G., and A. Valenciennes. 1849. Histoire Naturelle des Poissons. Paris. Vol. 22, xx + 532 pp.

Eigenmann, C. H. 1910. Catalogue of the freshwater fishes of tropical and south temperate America. Reports Princeton Expeds. to Patagonia 1896–1899, zool., **3**(2): 375–511.

———. 1912. The fresh-water fishes of British

Guiana. Mem. Carnegie Mus., **5**, xxii + 578 pp.

———. 1916. On *Aparciodon*, a new genus of characid fishes. Ann. Carnegie Mus., **10**: 71–76, pls. 11–12.

———, and R. S. Eigenmann. 1889. A revision of the edentulous genera of Curimatinae. Ann. New York Acad. Sci., **4**: 409–440.

———, and C. H. Kennedy. 1903. On a collection of fishes from Paraguay, with a synopsis of the American genera of cichlids. Proc. Acad. Nat. Sci. Philadelphia, **59**: 497–537.

———, and G. S. Myers. 1927. A new genus of Brazilian characin fishes allied to *Bivibranchia*. Proc. Nat'l. Acad. Sci. (Washington), **13**(8): 565–566.

Fernandez-Yepez, A. 1948. Los curimatidos (peces fluviales de Sur America). Catalogo descriptivo con nuevas adiciones genericas y especificas. Ministerio de Agricultura y Cria (Caracas). 79 pp. + index.

Fowler, H. W. 1906. Further knowledge of some heterognathous fishes. Part 1. Proc. Acad. Nat. Sci. Philadelphia, **58**(2): 293–351.

———. 1940. A collection of fishes obtained by Mr. William C. Morrow in the Ucayali river basin, Peru. Proc. Acad. Nat. Sci. Philadelphia, **91**: 219–289.

———. 1950. Os peixes de áqua doce do Brasil (part 2). Arq. Zool. Est. São Paulo, **6**: 205–404.

Géry, J. 1959. Contributions a l'étude des poissons characoïdes. *Parodon guyanensis* n. sp. de Guyane Francaise, avec quelques considérations sur le groupe (Hemiodontinae). Bull. Mus. natl. Hist. nat., ser. 2, **31**(6): 481–490.

———. 1961. *Pterohemiodus luelingi* sp. nov., un curieux poisson characoïde à nageoire dorsale filamenteuse, avec une clé des genres d'Hemiodontinae (Ostariophysi-Erythrinidae). Bonner zoologische Beiträge, **314**(12): 332–342.

———. 1963a. L'appareil protracteur buccal de *Bivibranchia* (Characoidei) avec une note sur *Phractolaemus* (Chanoidei) (Pisces). Vie et Milieu, **13**(4): 729–740.

———. 1963b. Sur la nomenclature et la systematique du genre *Hemiodus* Müller (Pisces, Characoidei). Bull. Mus. nat'l. Hist. nat., ser. 2, **35**(6): 598–605.

———. 1964. New species of hemiodin characoid fishes forming the *Hemiodopsis quadrimaculatus* group. Tropical Fish Hobbyist, November 1964: 11–15, 69–74.

Gill, T. 1878. On a remarkable generic type of characins. Ann. Mag. Nat. Hist., ser. 5, **2**: 112.

Greenwood, P. H., D. E. Rosen, S. H. Weitzman, and G. S. Myers. 1966. Phyletic studies of teleostean fishes, with a provisional classification of living forms. Bull. Amer. Mus. nat. Hist., **131**(4): 339–456, pls. 21–23.

Kner, R., and F. Steindachner. 1863. Eine Uebersicht der ichthyologischen Ausbeute des Herrn Professors Dr. Mor. Wagner in Central-Amerika. Sitzungsber. Akad. Wiss. München, 1863, vol. 2, pp. 220–30 (attributed in text to Kner and Steindachner).

Knöppel, H. A. 1972. Zur Nahrung tropischer Süsswasserfische aus Südamerika- Einige ausgewählte Arten der Anostomidae, Curimatidae, Hemiodidae und Characidae (Pisces, Characoidei). Amazoniana (Kiel), **3**(2): 231–246.

Mago Leccia, F. 1970. Lista de los peces de Venezuela, incluyendo un estudio preliminar sobre la ictio-geografía del país. Ministerio de Argricultura y Cria (Caracas). 283 pp.

Monod, T. 1969. Le complexe urophore des téléostéens. Mém. Inst. Fond. Afrique Noire (Dakar), No. 81: 1–705.

Müller, J. 1842. Beobachtungen über die Schwimmblase der Fische, mit Bezug auf einige neue Fischgattungen. Ber. Akad. Wiss. Berlin, **1842**: 177–186, 202–210.

Nelson, G. J. 1969. Gill arches and the phylogeny of fishes, with notes on the classification of vertebrates. Bull. Amer. Mus. nat. Hist., **131**(4): 475–552, pls. 79–92.

Regan, C. T. 1911. The classification of the teleostean fishes of the order Ostariophysi. — I. Cyprinoidea. Ann. Mag. Nat. Hist., ser. 8, **8**: 13–32, pl. 2.

Roberts, T. R. 1967. Tooth formation and replacement in characoid fishes. Stanford Ichth. Bull., **8**(4): 231–47.

———. 1969. Osteology and relationships of characoid fishes, particularly the genera *Hepsetus, Salminus, Hoplias, Ctenolucius,* and *Acestrorhynchus*. Proc. California Acad. Sci., **35**(15): 391–500.

———. 1971. *Micromischodus sugillatus*, a new hemiodontid characin fish from Brazil, and its relationship to the Chilodontidae. Breviora, No. 367: 1–25.

———. 1972. Ecology of fishes in the Amazon and Congo basins. Bull. Mus. Comp. Zool., **143**(2): 117–47.

———. 1973. Osteology and relationships of the Prochilodontidae, a South American family of characoid fishes. Bull. Mus. Comp. Zool., **145**(4): 213–35.

———. 1974. Dental polymorphism and systematics in *Saccodon*, a neotropical genus of freshwater fishes (Parodontidae, Characoidei). J. Zool. (London), **173**(3): 303–321.

Schultz, L. P., and C. Miles. 1943. Descriptions of a new genus and a new species of Parodontinae, characinid fishes from South America. J. Washington Acad. Sci., **33**(8): 251–255.

Steindachner, F. 1888. Ichthyologische Beiträge (XIV). Sitzungsber. math.–nat. Cl. Akad. Wiss. (Wien), **96**(2): 56–68, pls. 1–4.

Travassos, H. 1951. Contribuição ao estudo da subordem Characoidei Berg, 1940 – VII. Estudo da região opercular de três espécies de Parodontinae Eigenmann, 1910 (Actinopterygii – Cypriniformes). Bol. Mus. Nac. (Rio de Janeiro), zool., No. 103: 1–17, 7 pls.

———. 1952. Contribuição ao estudo da subordem Characoidei Berg, 1940–VIII. Estudo de alguns ossos da região oromandibular de três espécies de Parodontinae Eigenmann, 1910. (Actinopterygii – Cypriniformes). Bol. Mus. Nac. (Rio de Janeiro), zool., No. 108: 1–17.

Weitzman, S. H. 1962. The osteology of *Brycon meeki*, a generalized characid fish, with an osteological definition of the family. Stanford Ichthyological Bulletin, **8**(1): 1–77.

Wiley, M. L., and B. B. Collette. 1970. Breeding tubercles and contact organs in fishes: their occurrence, structure, and significance. Bull. Amer. Mus. nat. Hist., **143**: 143–216.

FIGURES

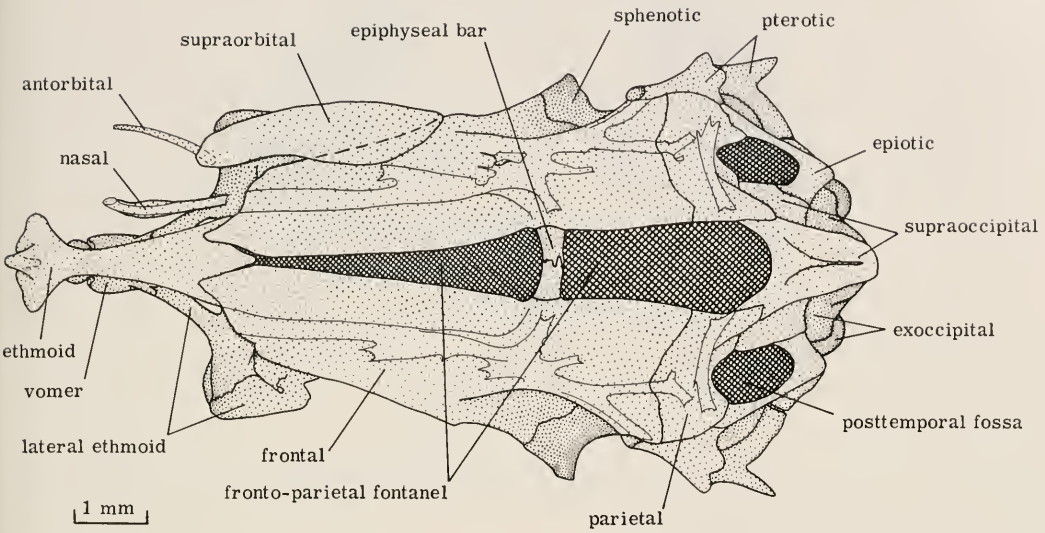

Figure 1. *Hemiodus semitaeniatus*, 55.8 mm. Cranium with nasal bone, antorbital and supraorbital of the right side in place (dorsal view).

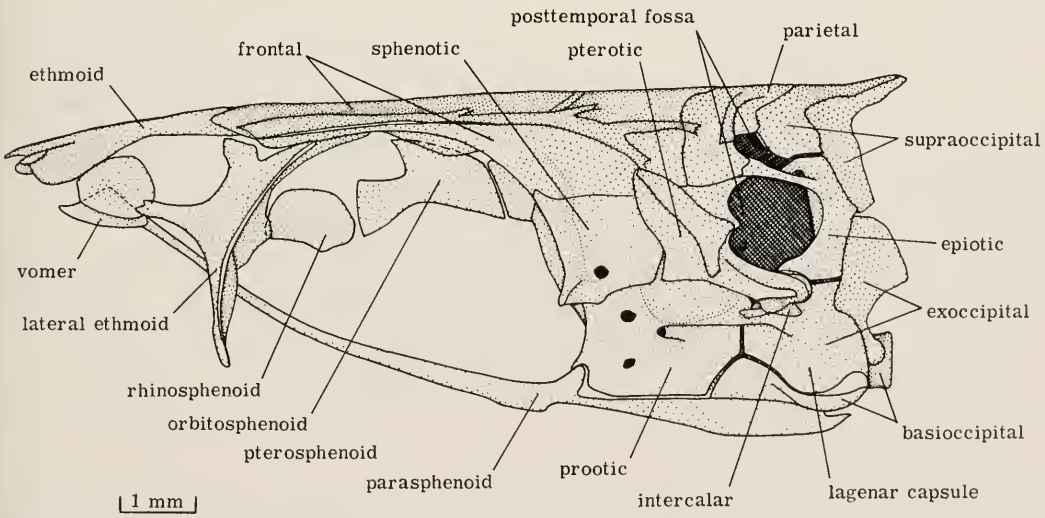

Figure 2. *Hemiodus semitaeniatus*, 55.8 mm. Cranium (lateral view).

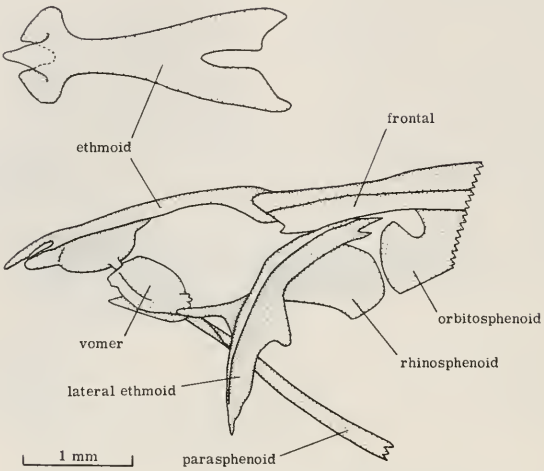

Figure 3. *Hemiodus quadrimaculatus*, 35.0 mm. Anterior portion of cranium (lateral view); inset, ethmoid bone (dorsal view).

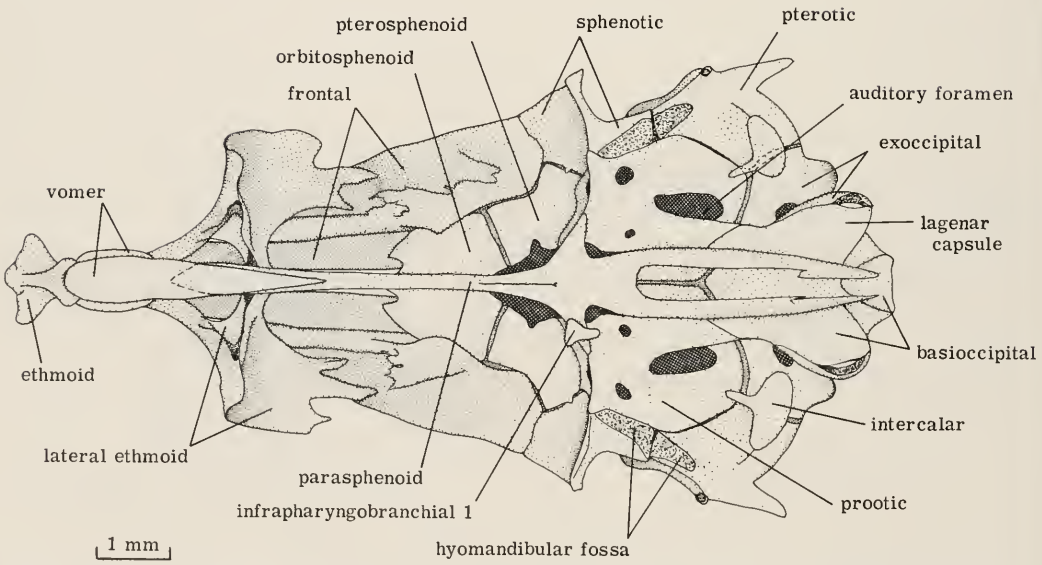

Figure 4. *Hemiodus semitaeniatus*, 55.8 mm. Cranium with infrapharyngobranchial 1 of the right side in place (ventral view).

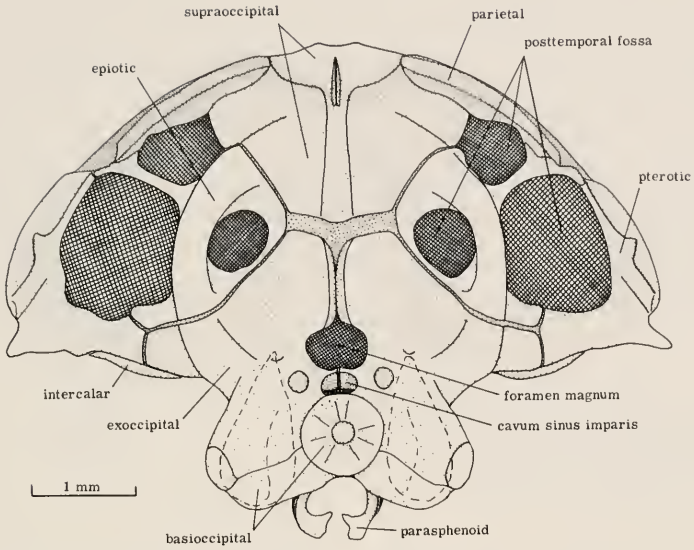

Figure 5. *Hemiodus semitaeniatus*, 55.8 mm. Cranium (occipital view).

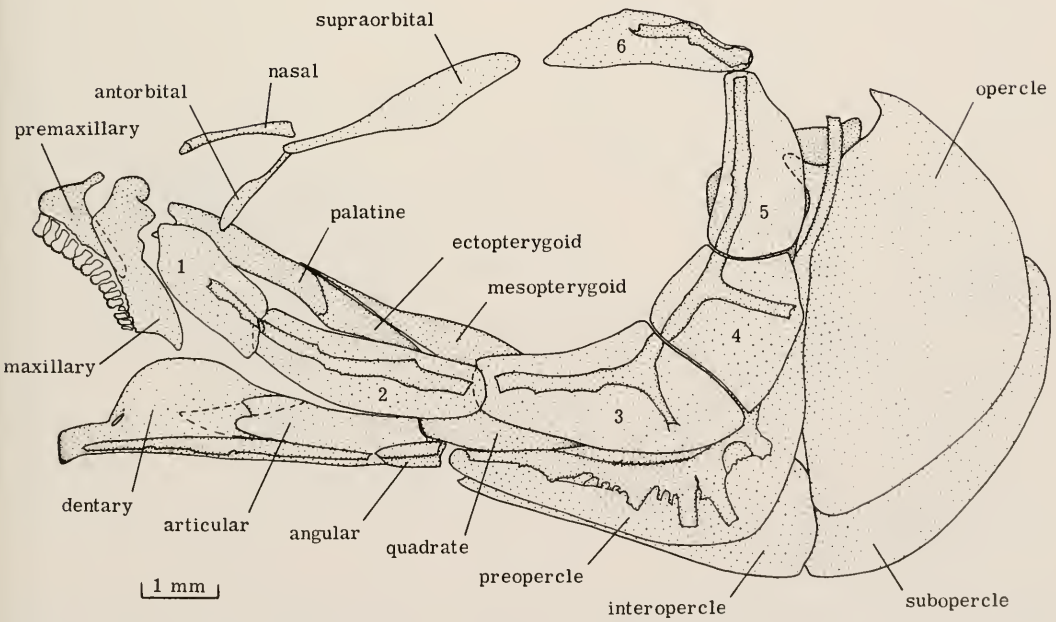

Figure 6. *Hemiodus semitaeniatus*, 55.8 mm. Jaws, facial bones, and suspensorium (lateral view).

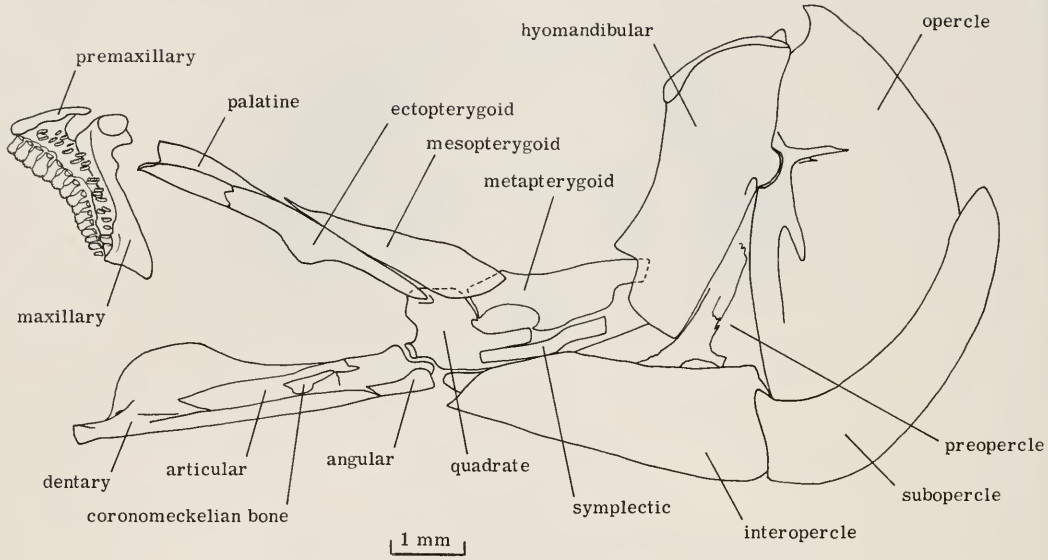

Figure 7. *Hemiodus semitaeniatus*, 55.8 mm. Jaws, suspensorium and opercular bones (medial view).

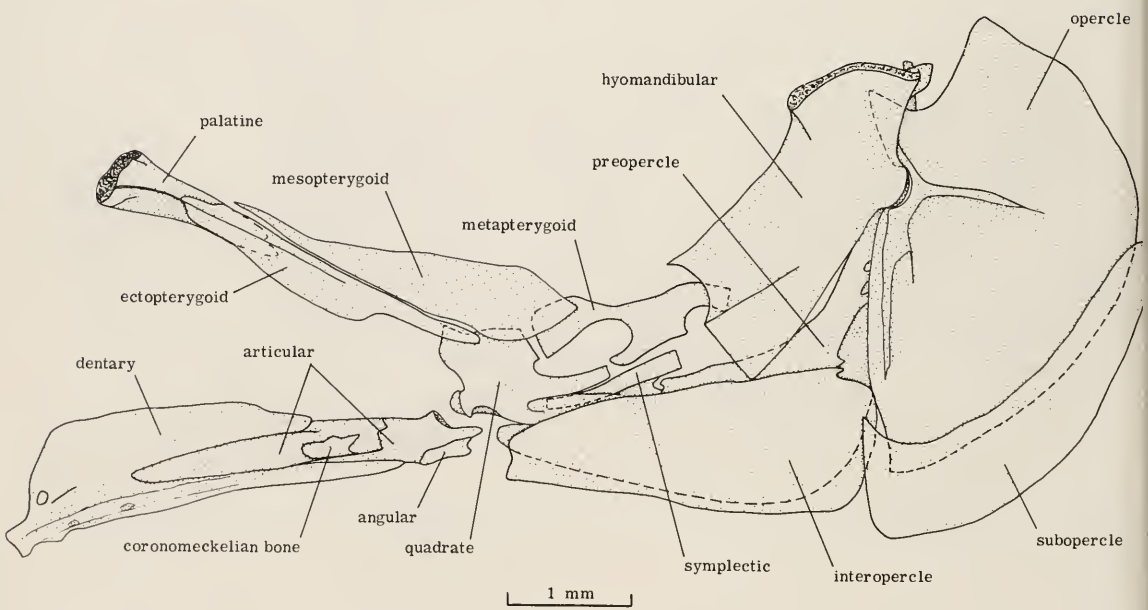

Figure 8. *Hemiodus quadrimaculatus*, 35.0 mm. Lower jaw, suspensorium and opercular bones (medial view).

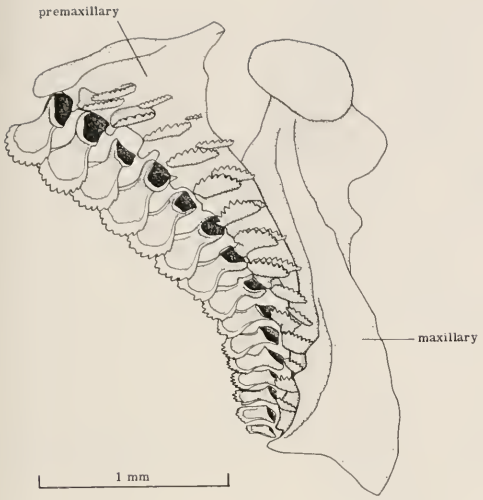

Figure 9. *Hemiodus semitaeniatus*, 55.8 mm. Upper jaw showing functional and replacement teeth (medial view).

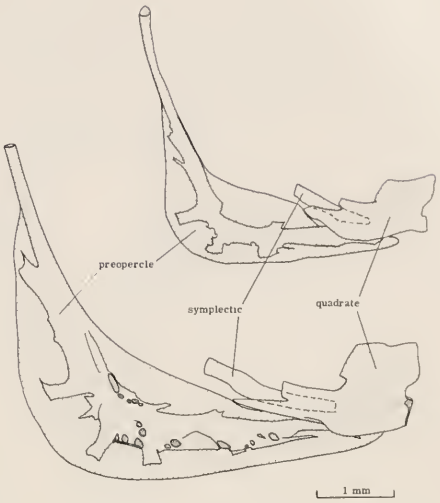

Figure 11. *Hemiodus*. Relationship of quadrate to preopercle (lateral view of bones from the right side). Upper: *H. quadrimaculatus*, 35.0 mm. Lower: *H. semitaeniatus*, 55.8 mm.

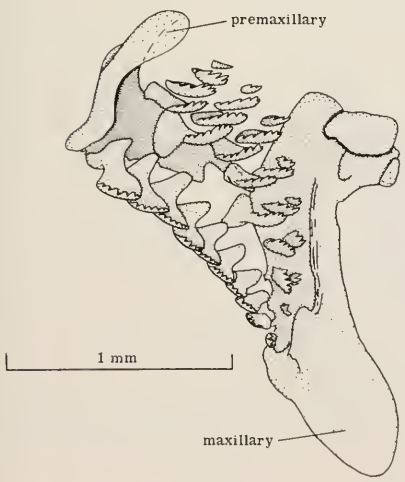

Figure 10. *Hemiodus quadrimaculatus*, 35.0 mm. Upper jaw showing functional and replacement teeth (medial view).

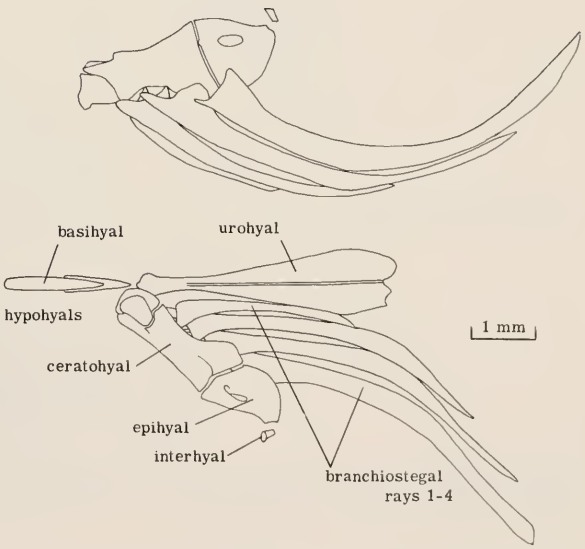

Figure 12. *Hemiodus semitaeniatus*, 55.8 mm. Upper: hyoid bar and branchiostegal rays (lateral view). Lower: hyoid arch and urohyal (dorsal view).

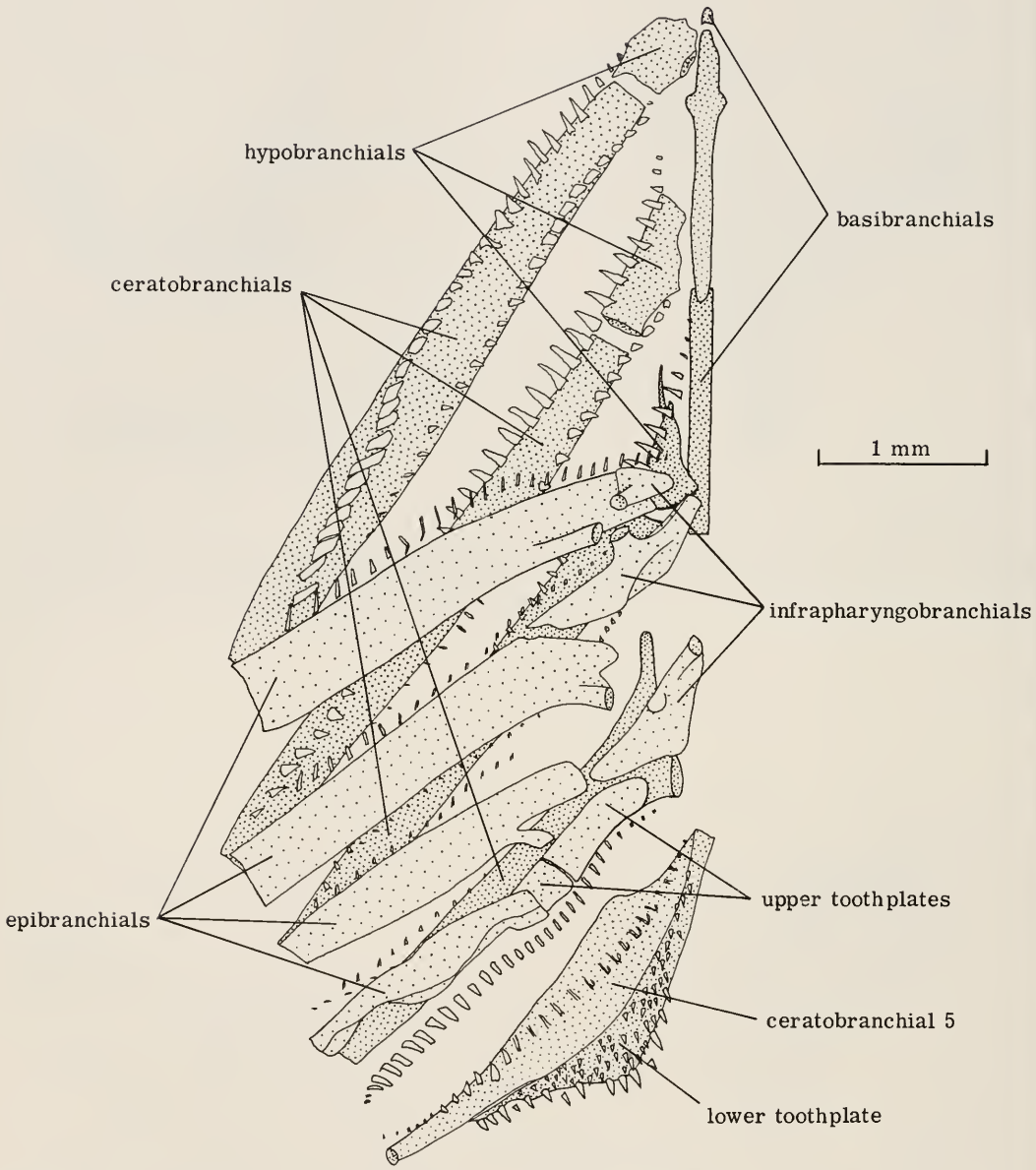

Figure 13. *Hemiodus semitaeniatus*, 55.8 mm. Branchial arches (dorsal view, with lateral elements of the right side removed).

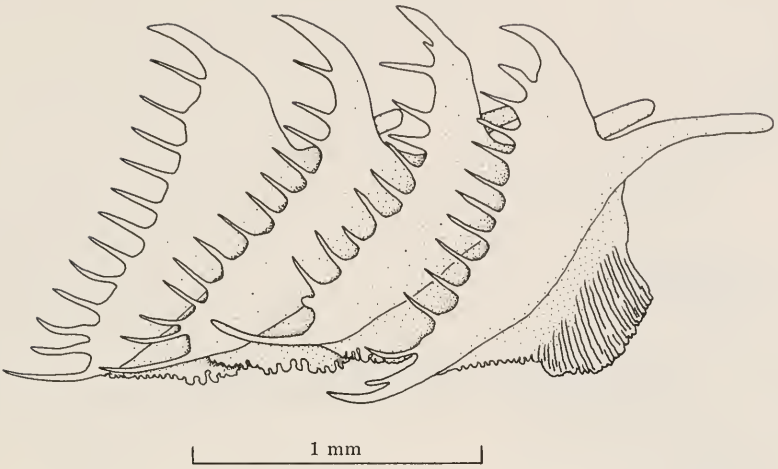

Figure 14. *Hemiodus microlepis*, 235 mm. Series of gill rakers from leading edge of ceratobranchial 1; rakers of trailing edge are nearly identical mirror images (dorsal view).

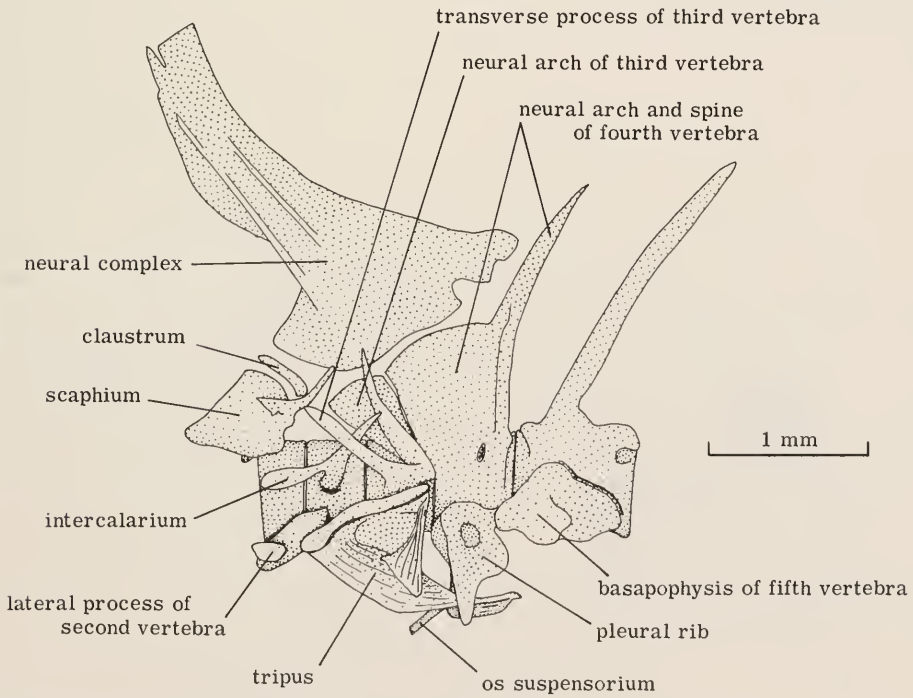

Figure 15. *Hemiodus semitaeniatus*, 55.8 mm. Weberian apparatus (lateral view).

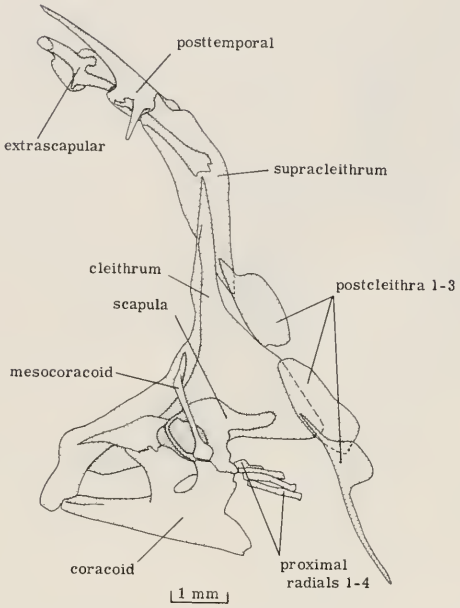

Figure 16. *Hemiodus semitaeniatus*, 55.8 mm. Right half of pectoral girdle (medial view).

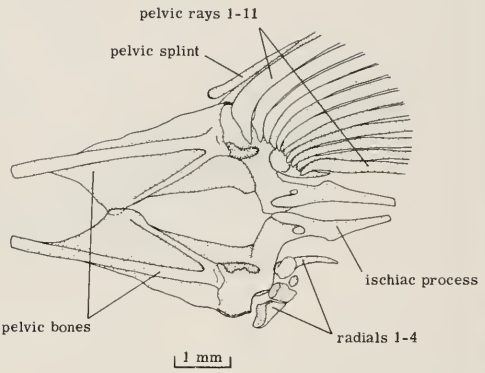

Figure 17. *Hemiodus semitaeniatus*, 55.8 mm. Pelvic girdle (ventral view).

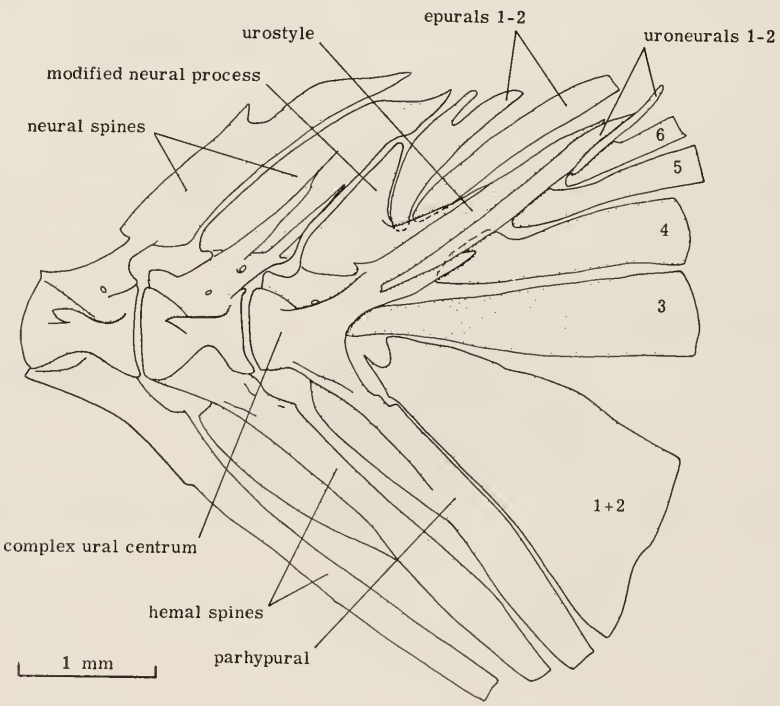

Figure 18. *Hemiodus semitaeniatus*, 54.4 mm. Caudal skeleton (lateral view).

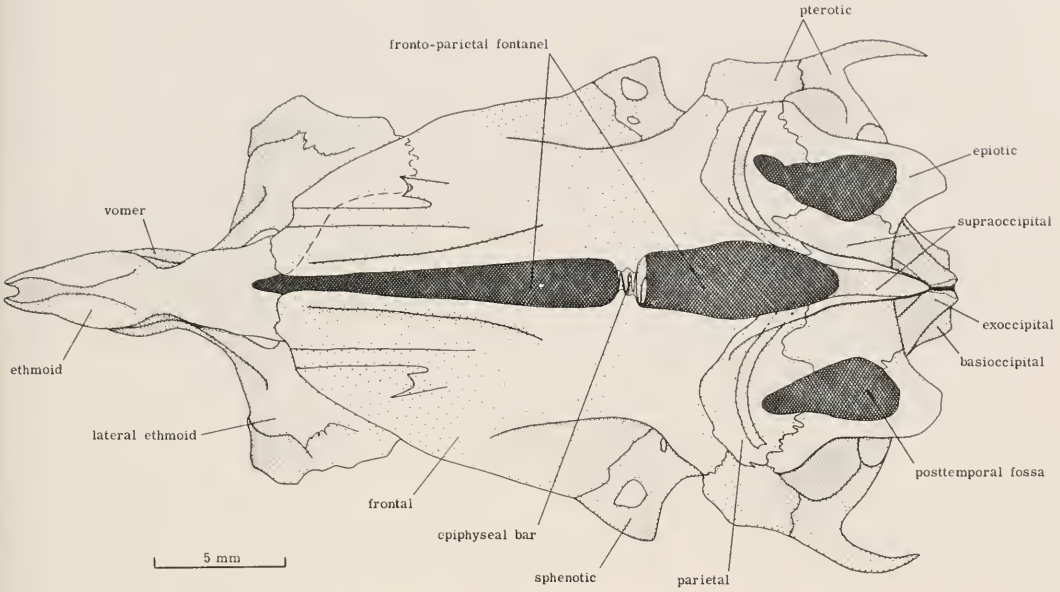

Figure 19. *Argonectes longiceps*, 198 mm. Cranium (dorsal view).

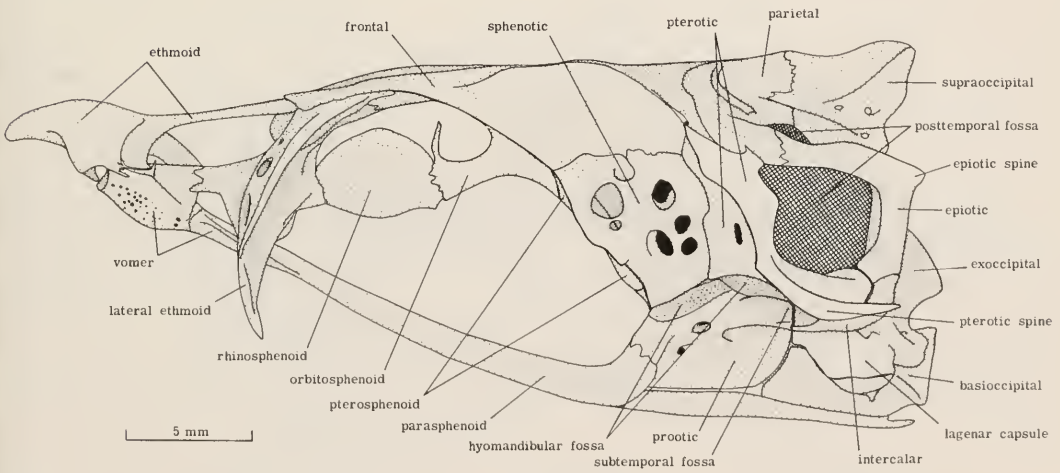

Figure 20. *Argonectes longiceps*, 198 mm. Cranium (lateral view).

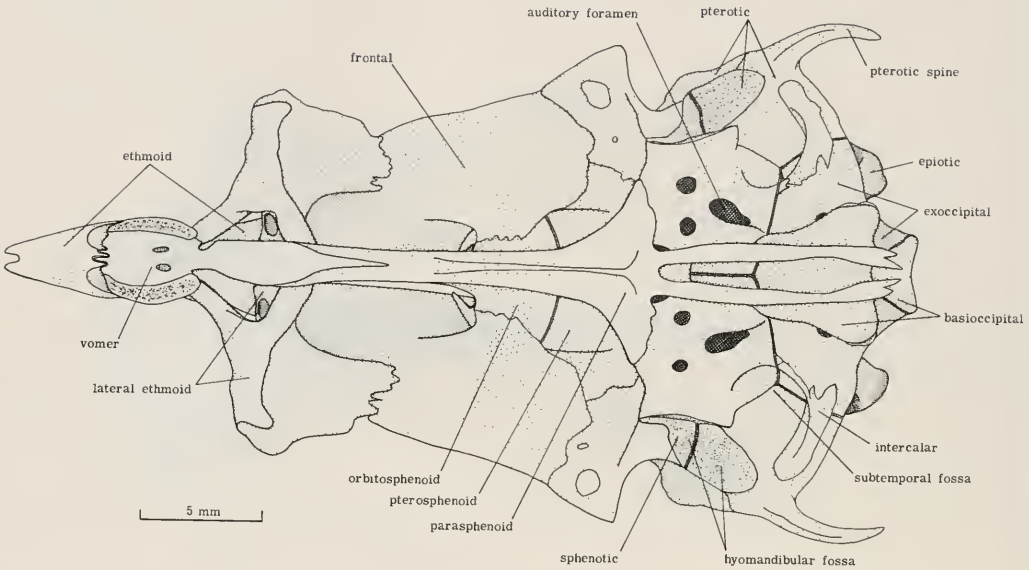

Figure 21. *Argonectes longiceps*, 198 mm. Cranium (ventral view).

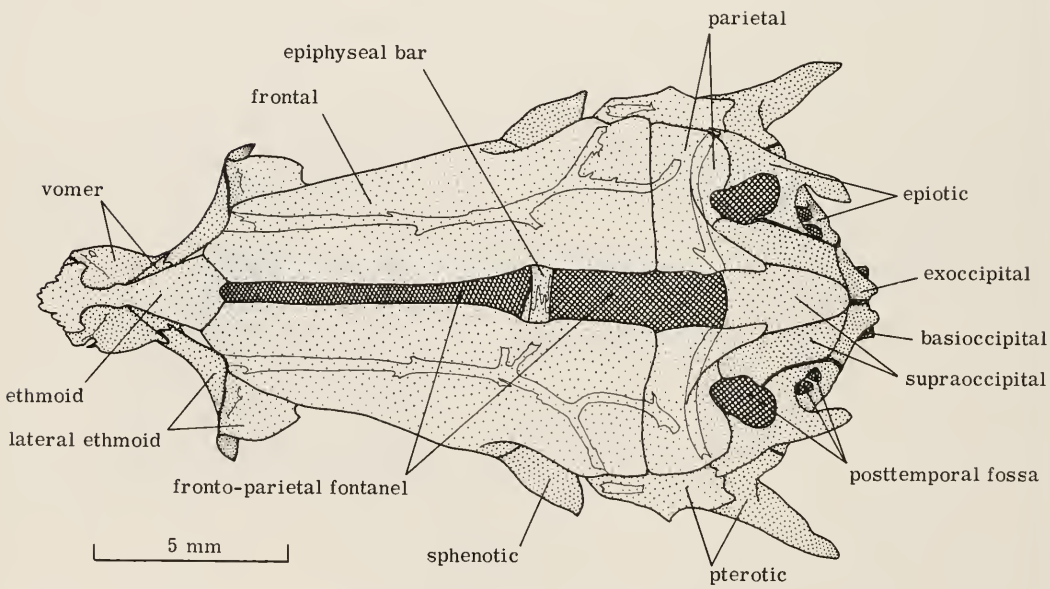

Figure 22. *Bivibranchia protractila*, 115.2 mm. Cranium (dorsal view).

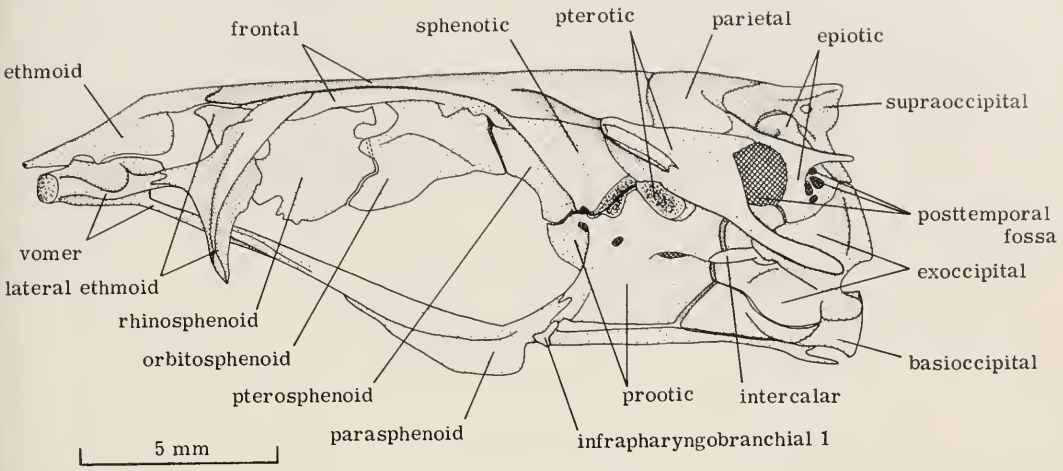

Figure 23. *Bivibranchia protractila*, 115.2 mm. Cranium (lateral view).

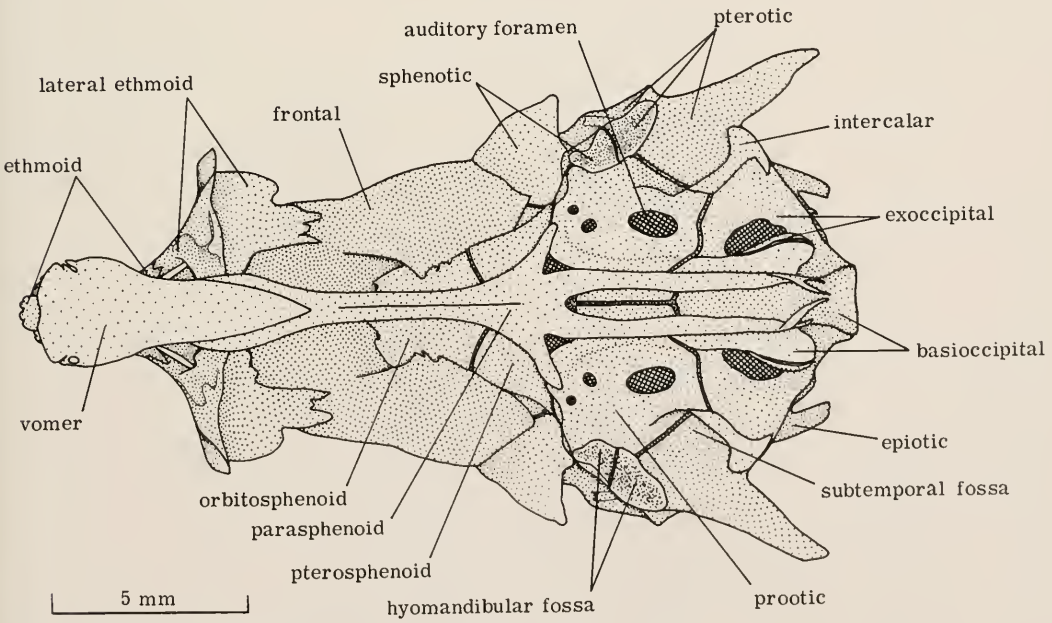

Figure 24. *Bivibranchia protractila*, 115.2 mm. Cranium (ventral view).

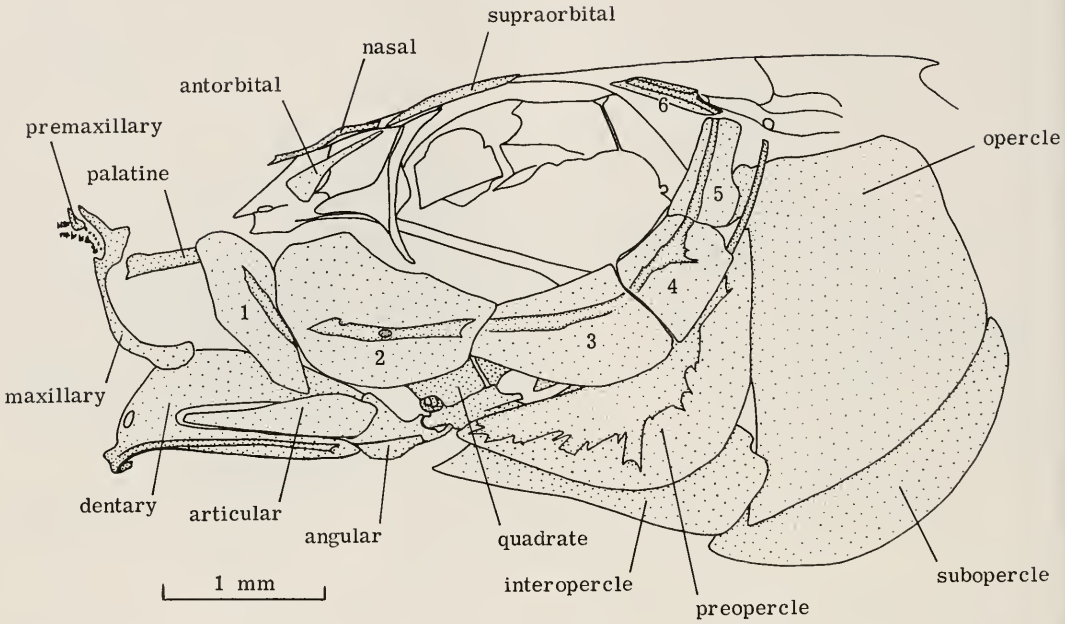

Figure 25. *Bivibranchia protractila*, 39.9 mm. Lateral bones of skull (lateral view) (upper jaw of specimen slightly damaged).

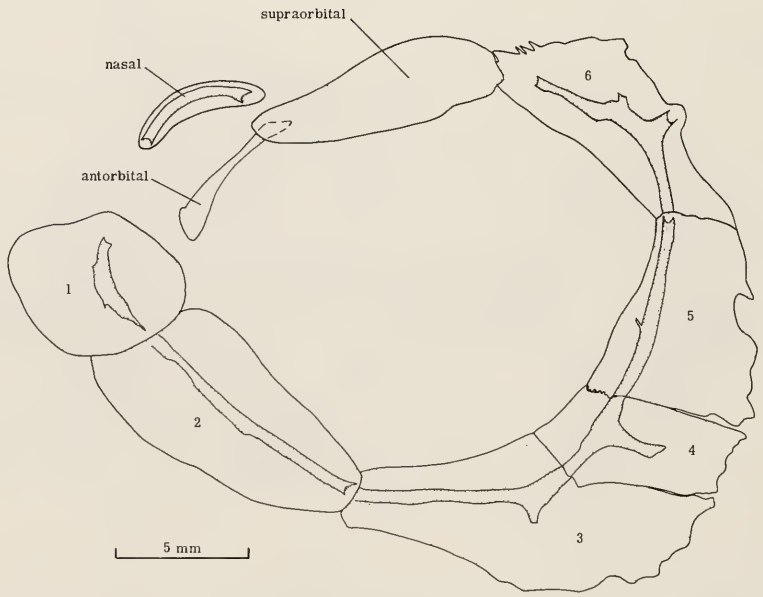

Figure 26. *Argonectes longiceps*, 198 mm. Nasal, antorbital and circumorbital bones (lateral view).

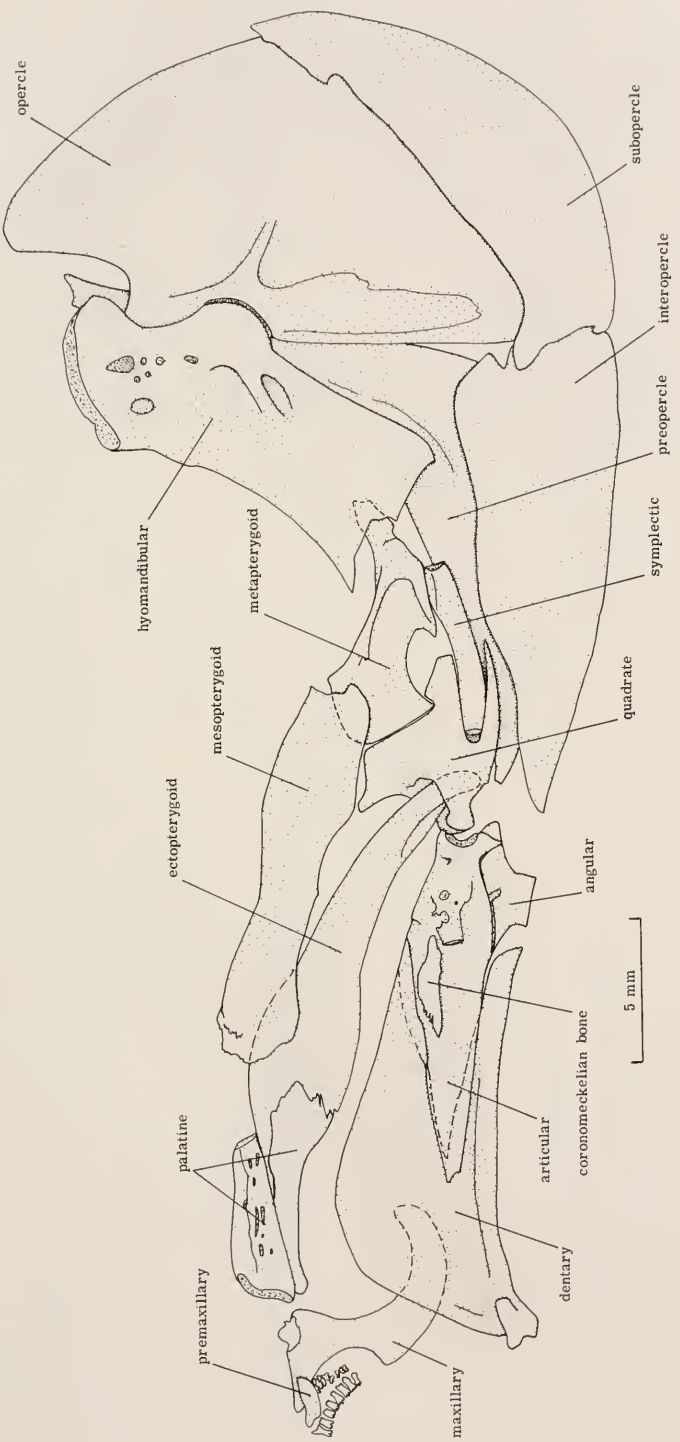

Figure 27. *Argonectes longiceps*, 198 mm. Jaws, suspensorium and opercular bones (medial view).

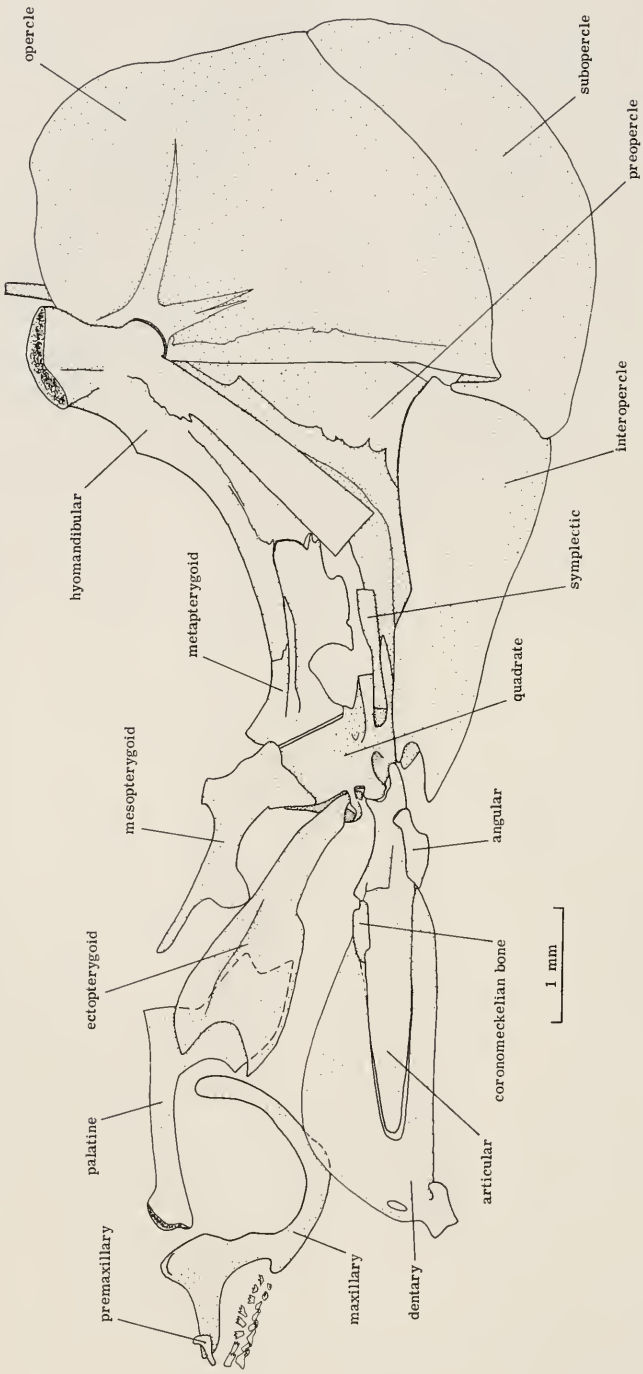

Figure 28. *Bivibranchia protractila*, 39.9 mm. Jaws, suspensorium and opercular bones (medial view) (upper jaw based on 115.2-mm specimen).

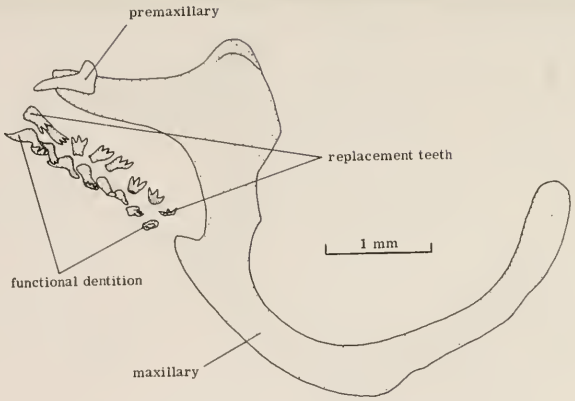

Figure 29. *Bivibranchia protractila*, 115.2 mm. Upper jaw showing functional and replacement teeth (medial view).

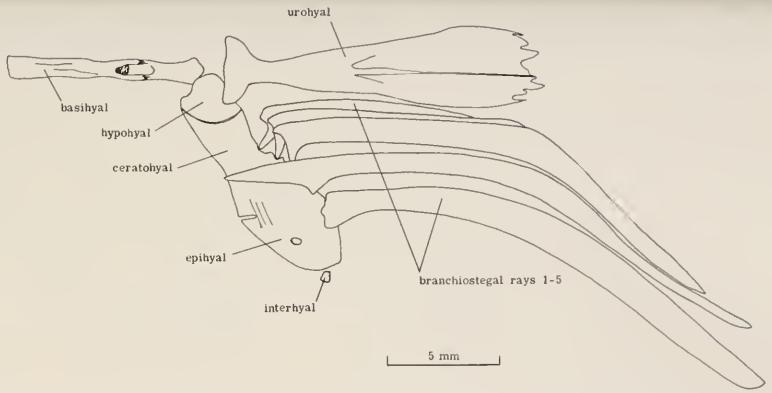

Figure 30. *Argonectes longiceps*, 198 mm. Hyoid arch and urohyal bone (ventral view).

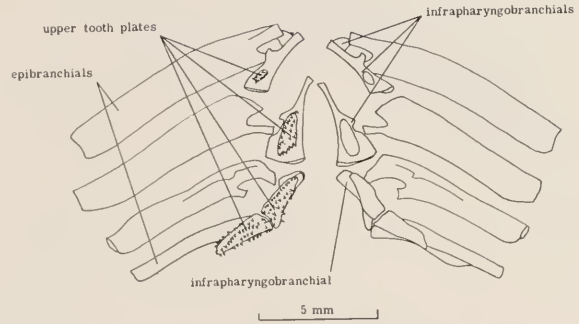

Figure 31. *Argonectes longiceps*, 198 mm. Upper half of branchial arches (ventral view) (gill rakers removed).

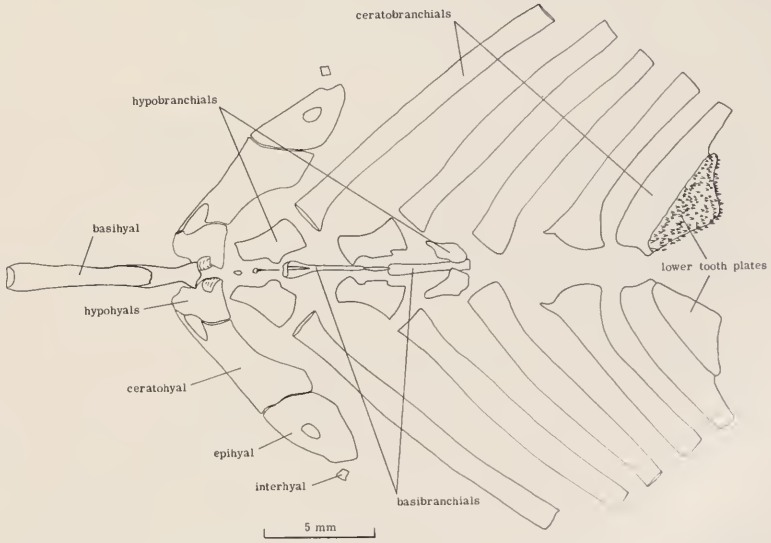

Figure 32. *Argonectes longiceps*, 198 mm. Lower half of branchial arches (dorsal view) (gill rakers removed).

Figure 33. *Argonectes longiceps*, 198 mm. Fifth ceratobranchial and lower pharyngeal toothplate of left side (dorsal view).

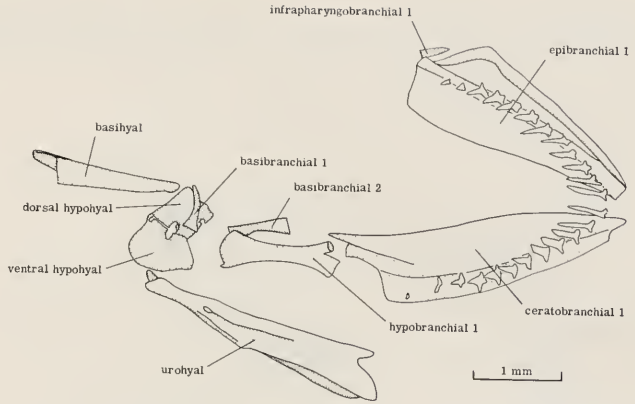

Figure 34. *Bivibranchia protractila*, 39.9 mm. Portions of hyoid arch and first two branchial arches (lateral view) (hypohyals of left side removed).

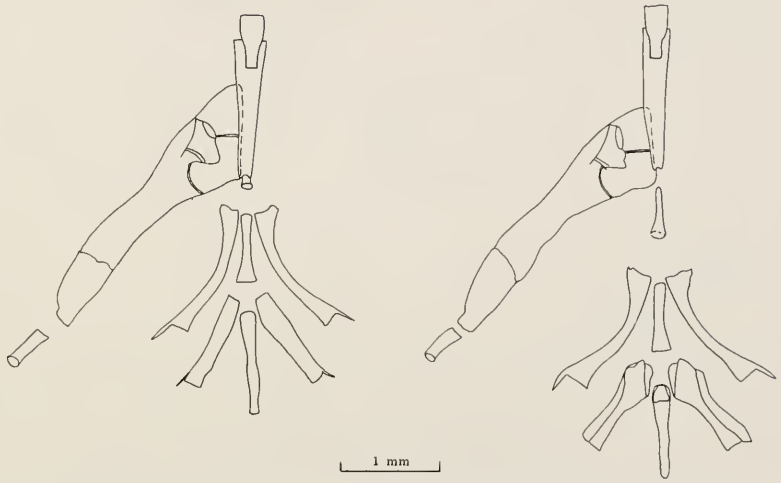

Figure 35. *Bivibranchia protractila*, 39.9 mm. Portion of hyoid arch and first two branchial arches to show possible pivotal movement of basibranchial 1. Left, contraction. Right, expansion (dorsal view).

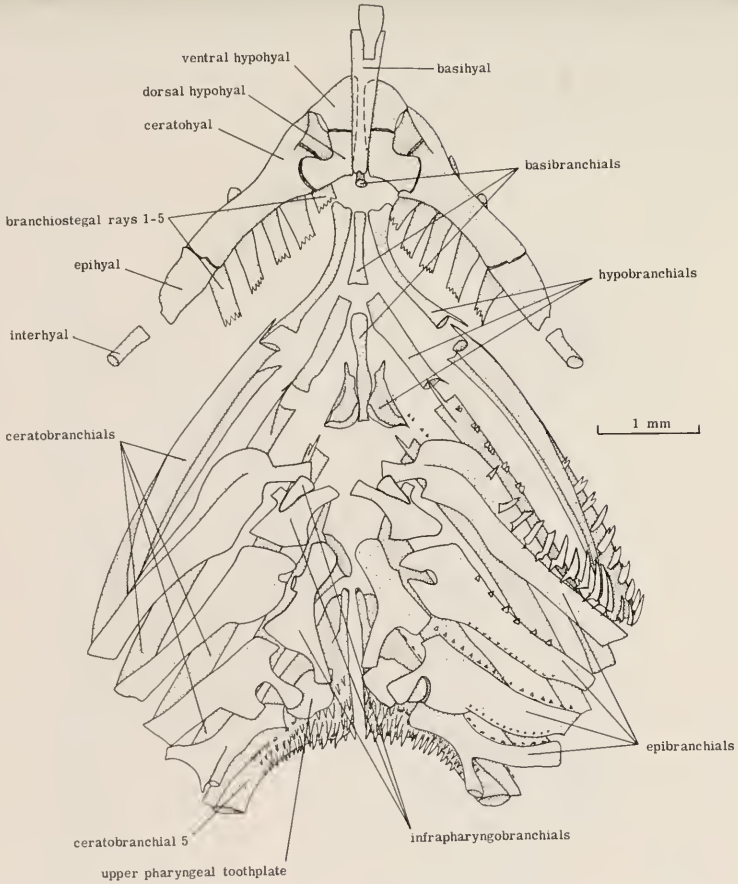

Figure 36. *Bivibranchia protractila*, 39.9 mm. Hyoid and branchial arches (dorsal view).

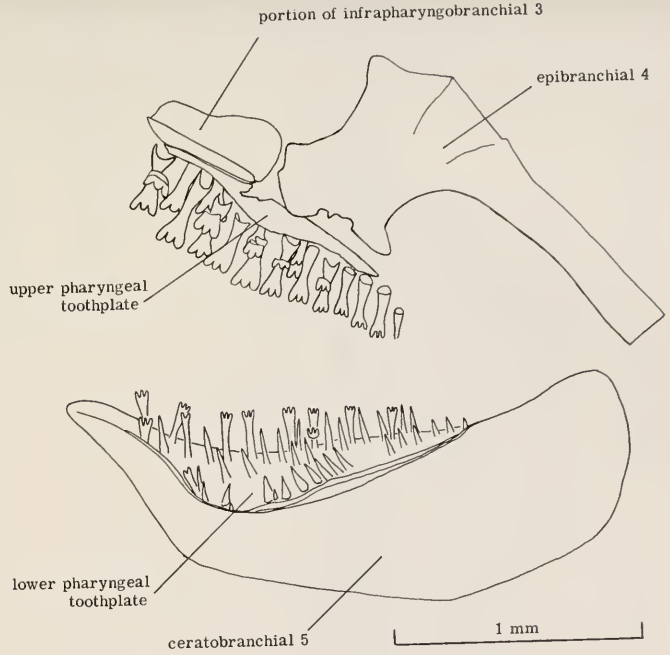

Figure 37. *Bivibranchia protractila*, 39.9 mm. Ceratobranchial 5, epibranchial 4, portion of infrapharyngobranchial 3 and associated upper and lower pharyngeal toothplates of the right side (slightly oblique posterior view).

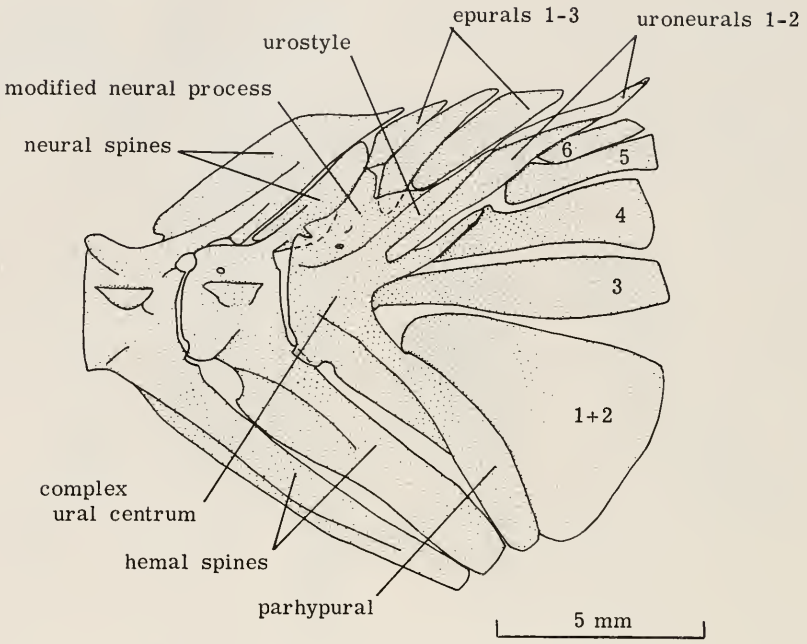

Figure 38. *Argonectes longiceps*, 198 mm. Caudal skeleton (lateral view).

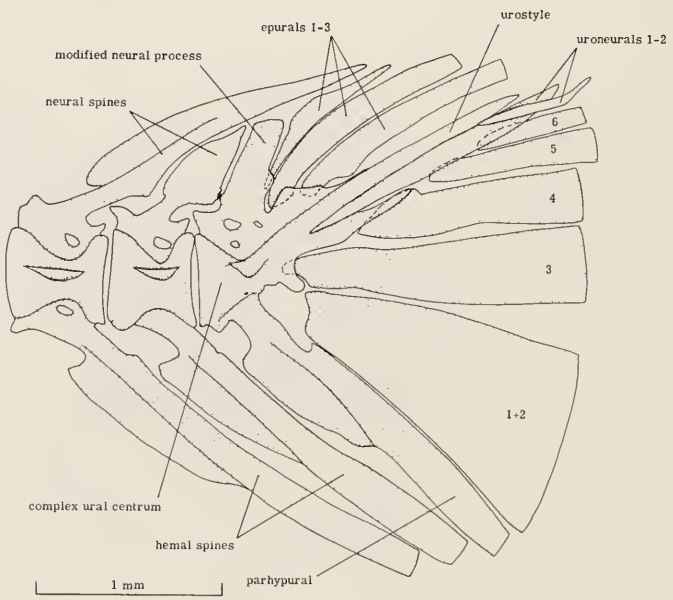

Figure 39. *Bivibranchia protractila*, 39.9 mm. Caudal skeleton (lateral view).

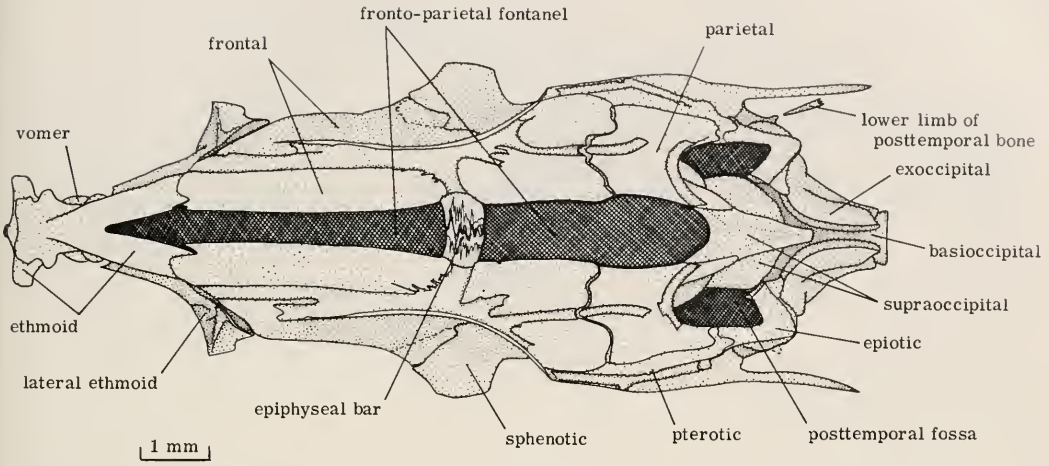

Figure 40. *Anodus melanopogon*, 55.0 mm. Cranium (dorsal view).

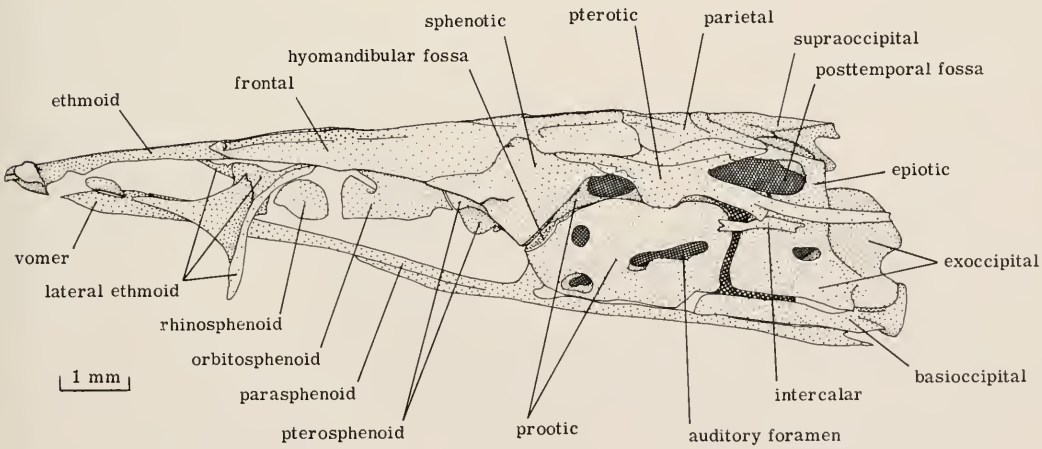

Figure 41. *Anodus melanopogon*, 55.0 mm. Cranium (lateral view).

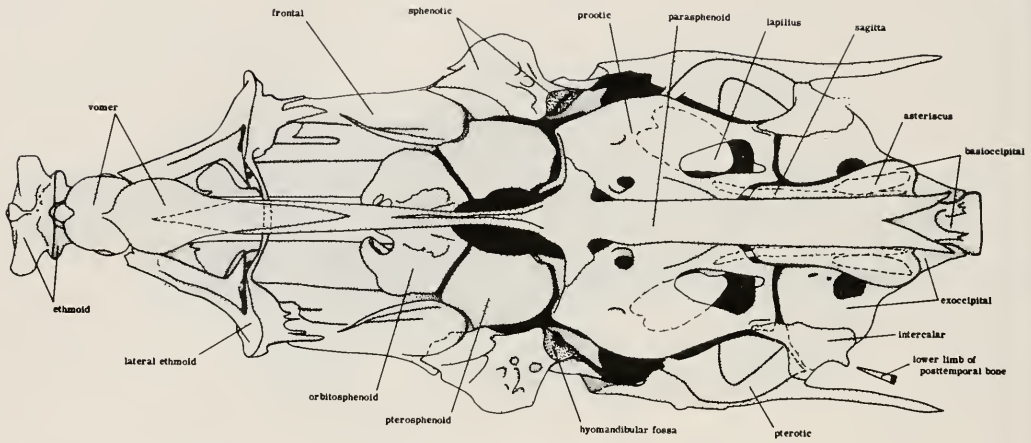

Figure 42. *Anodus melanopogon*, 55.0 mm. Cranium (ventral view).

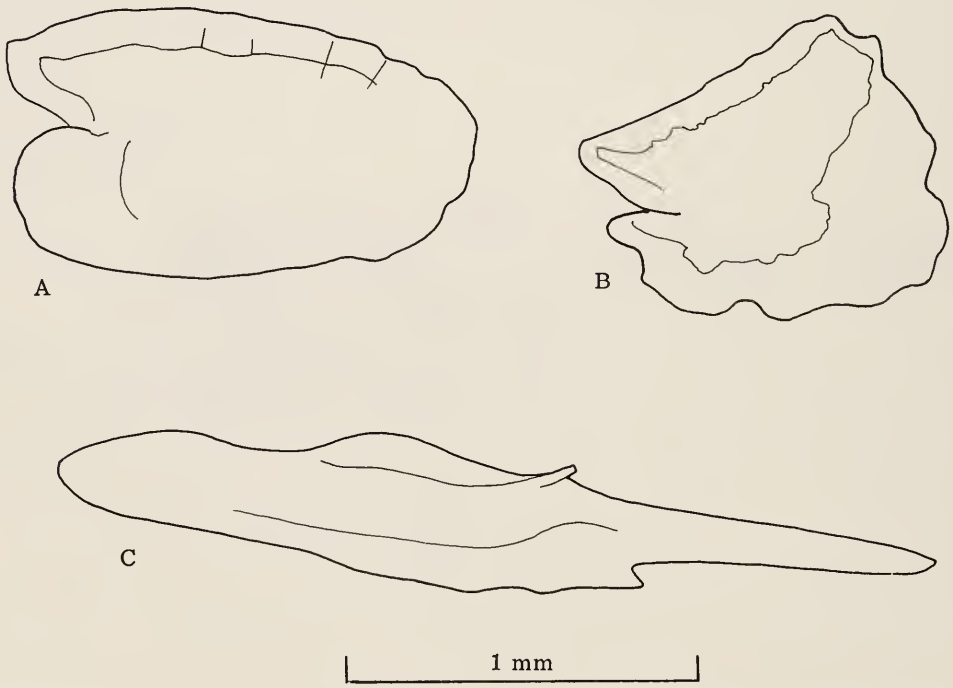

Figure 43. *Anodus melanopogon*, 55.5 mm. Otoliths of left side. A. Lapillus (ventral view). B. Asteriscus (lateral view). C. Sagitta (lateral view).

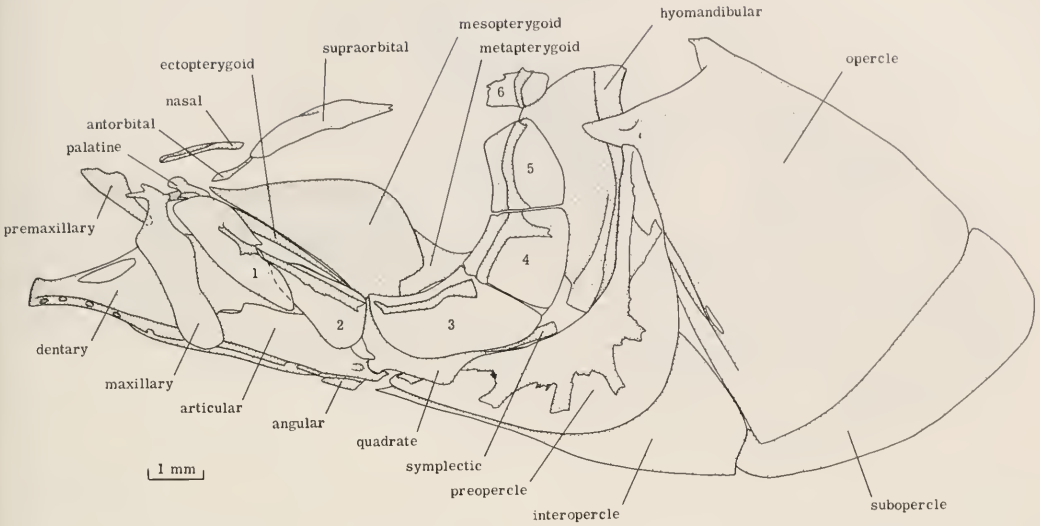

Figure 44. *Anodus melanopogon*, 55.0 mm. Lateral bones of skull (lateral view).

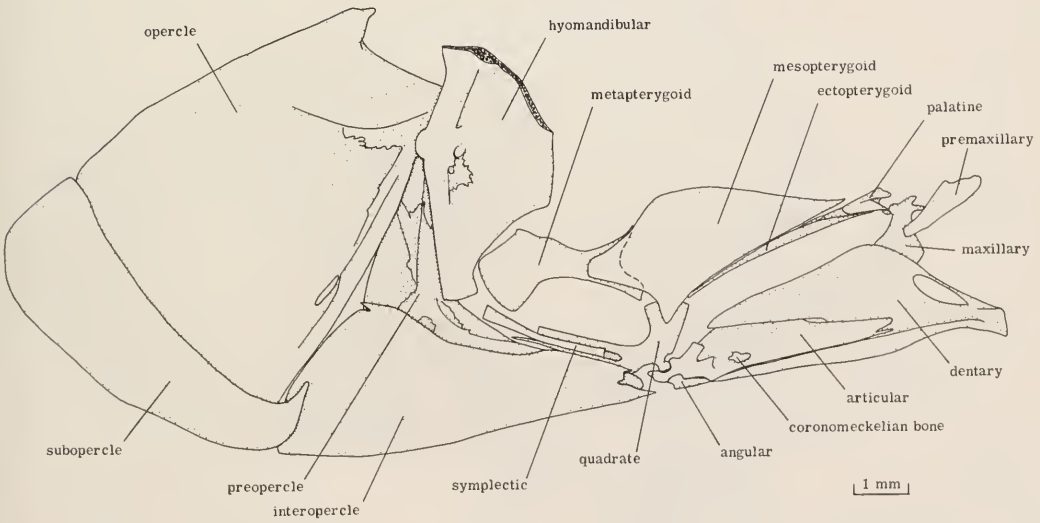

Figure 45. *Anodus melanopogon*, 55.0 mm. Jaws, suspensorium and opercular bones (medial view).

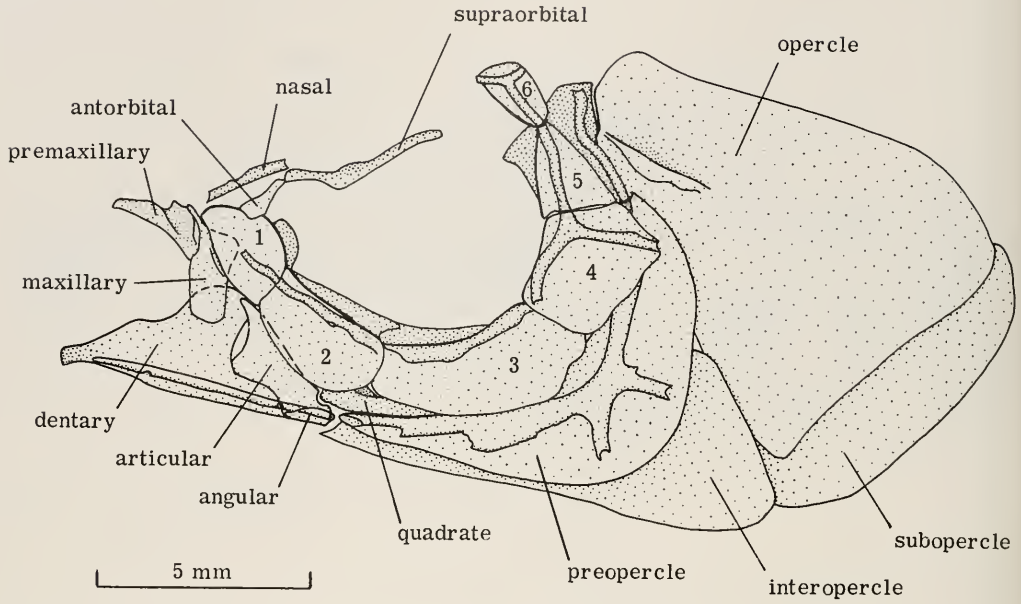

Figure 46. *Gasterotomus latior*, 76.7 mm. Lateral bones of skull (lateral view).

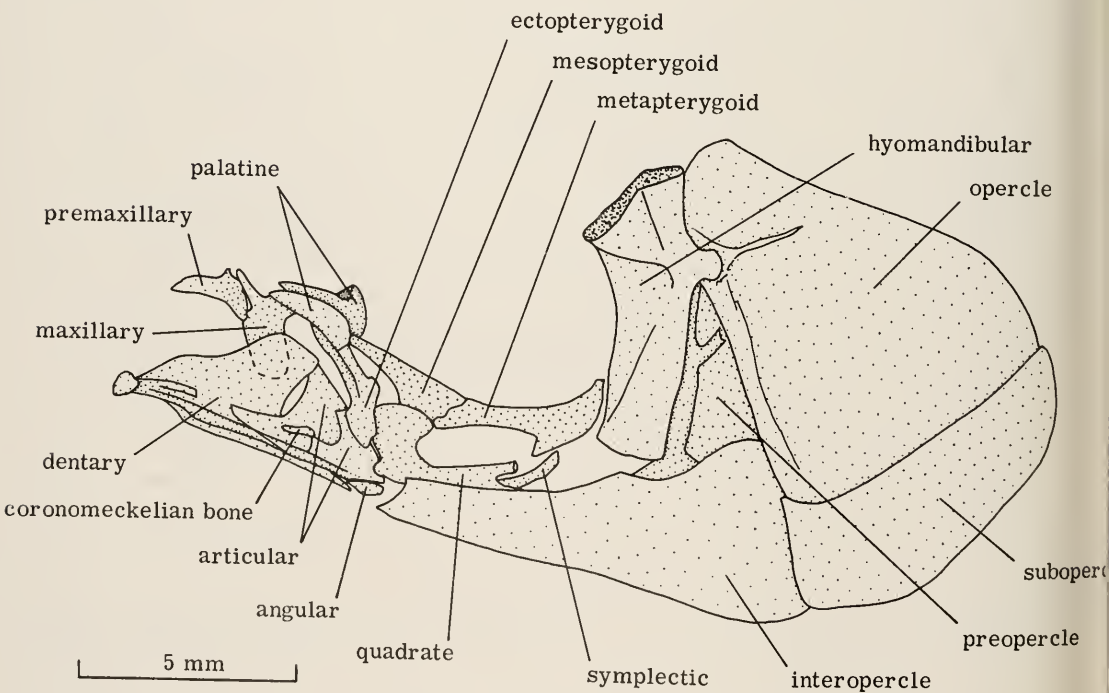

Figure 47. *Gasterotomus latior*, 76.7 mm. Jaws, suspensorium and opercular bones (medial view).

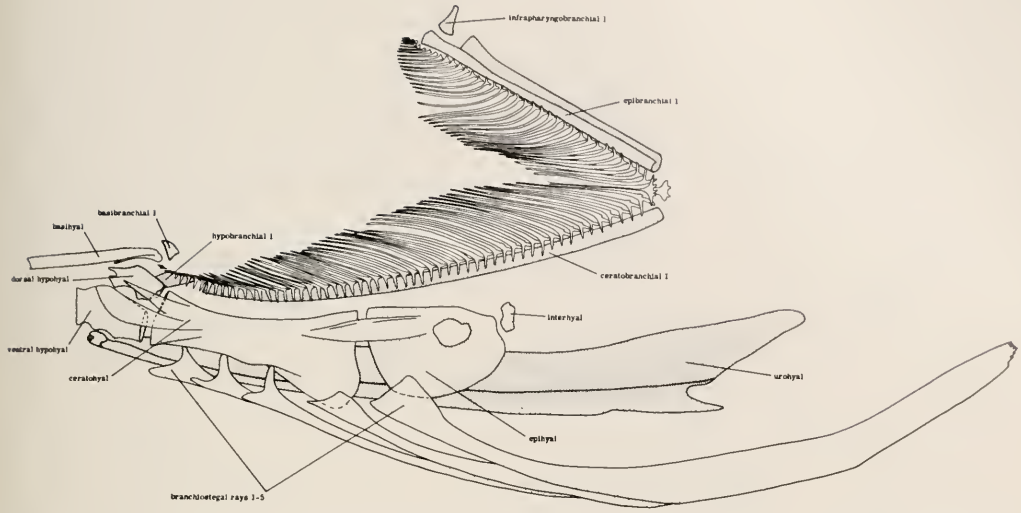

Figure 48. *Anodus melanopogon*, 55.0 mm. Hyoid arch, urohyal bone and first branchial arch (lateral view).

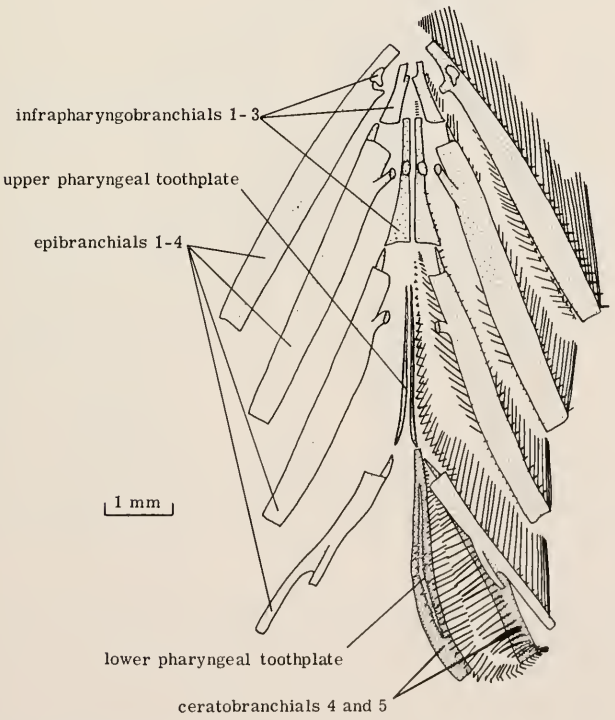

Figure 49. *Anodus melanopogon*, 55.0 mm. Upper half of branchial arches (dorsal view).

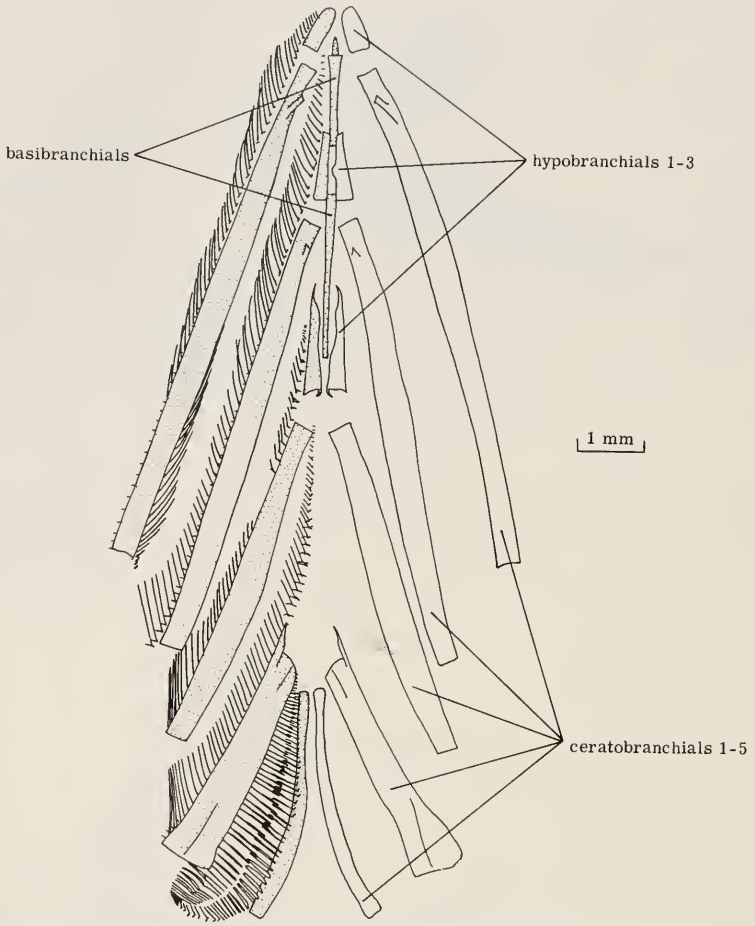

Figure 50. *Anodus melanopogon*, 55.0 mm. Lower half of branchial arches (dorsal view).

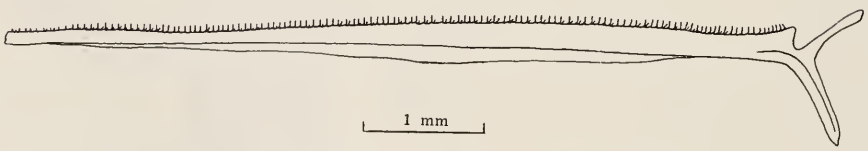

Figure 51. *Anodus elongatus*, 180 mm. Gill raker from leading edge of ceratobranchial 1 showing ctenii.

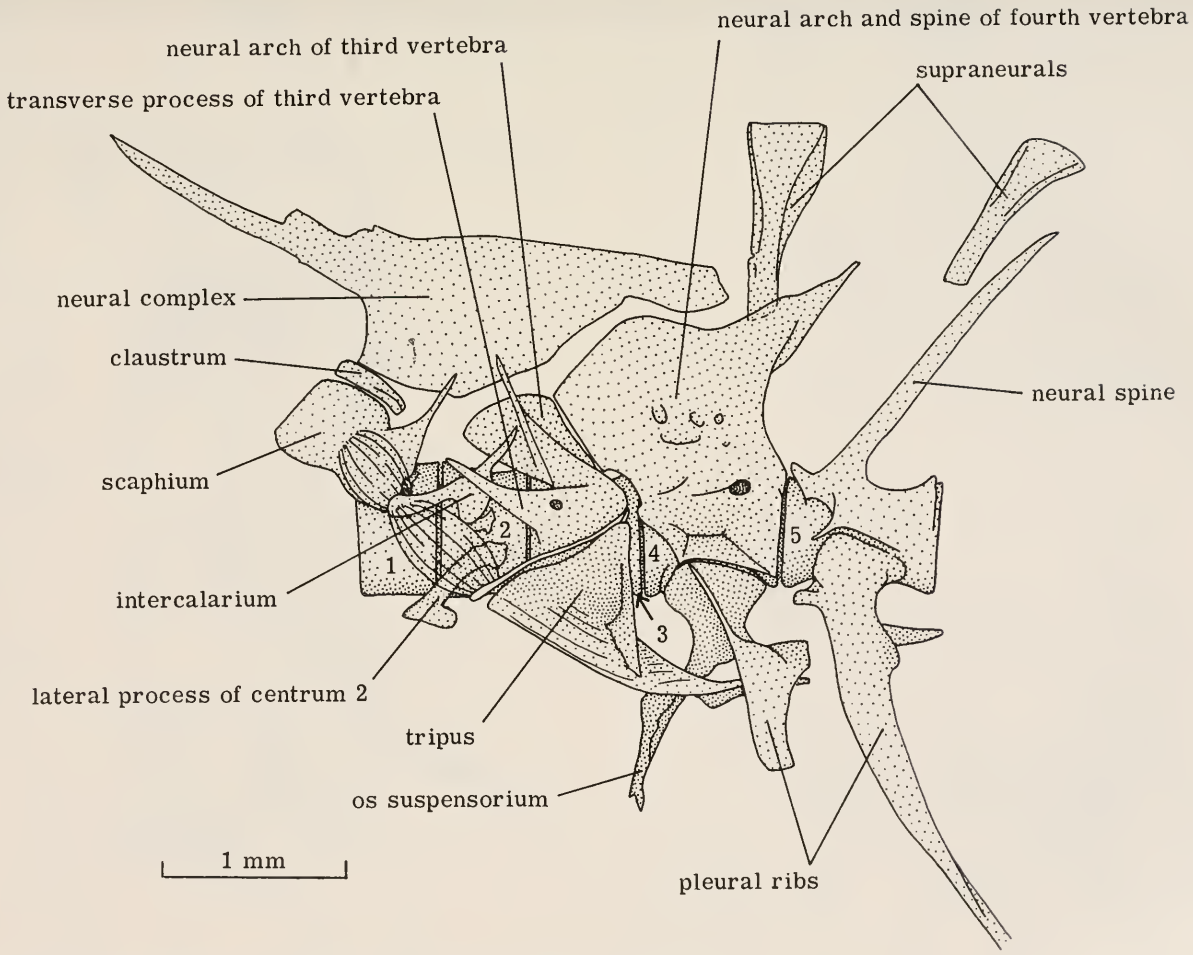

Figure 52. *Anodus melanopogon*, 55.0 mm. Weberian apparatus (lateral view).

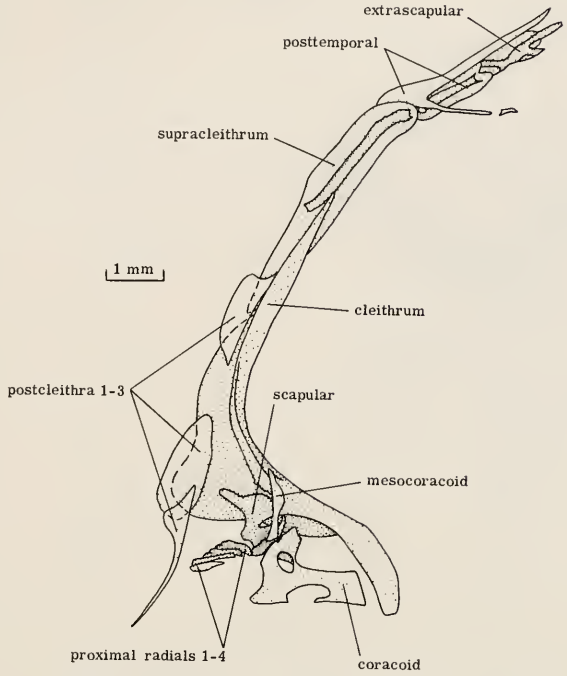

Figure 53. *Anodus melanopogon*, 55.0 mm. Left half of pectoral girdle (medial view).

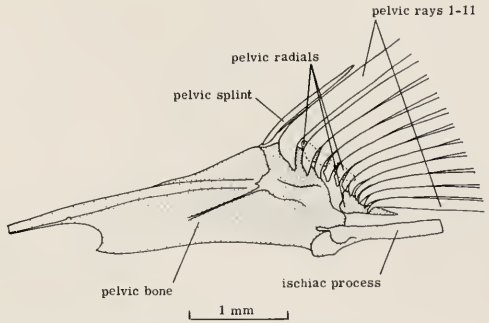

Figure 54. *Anodus melanopogon*, 55.0 mm. Left half of pelvic girdle (ventral view).

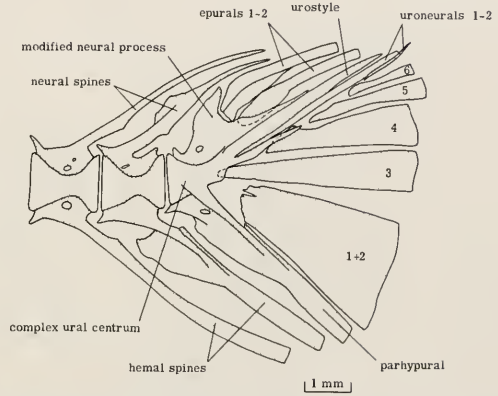

Figure 55. *Anodus melanopogon*, 55.0 mm. Caudal skeleton (lateral view).

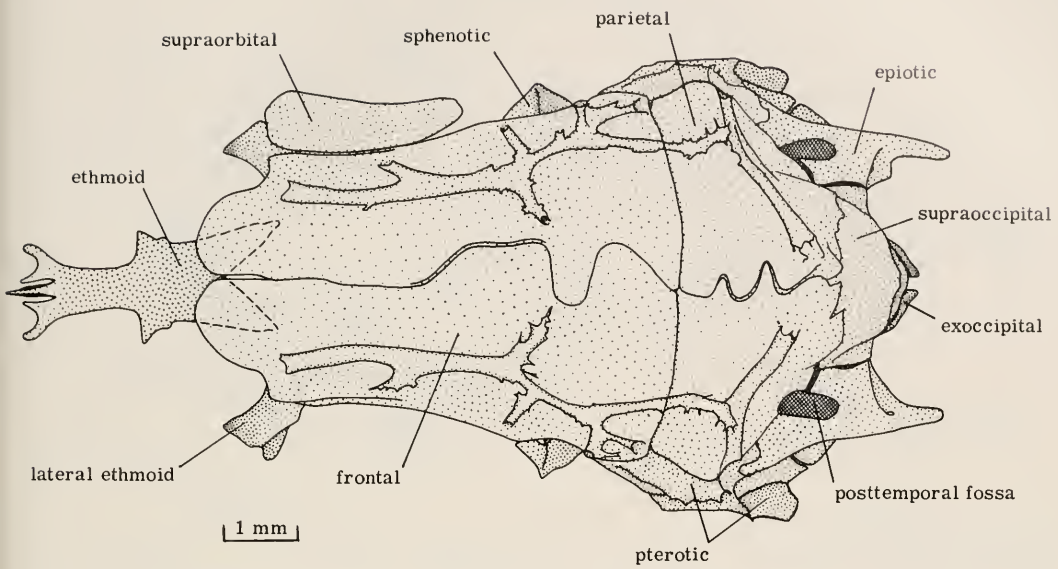

Figure 56. *Saccodon wagneri* (dental morph IV), 55.4 mm. Cranium with right supraorbital in place (dorsal view).

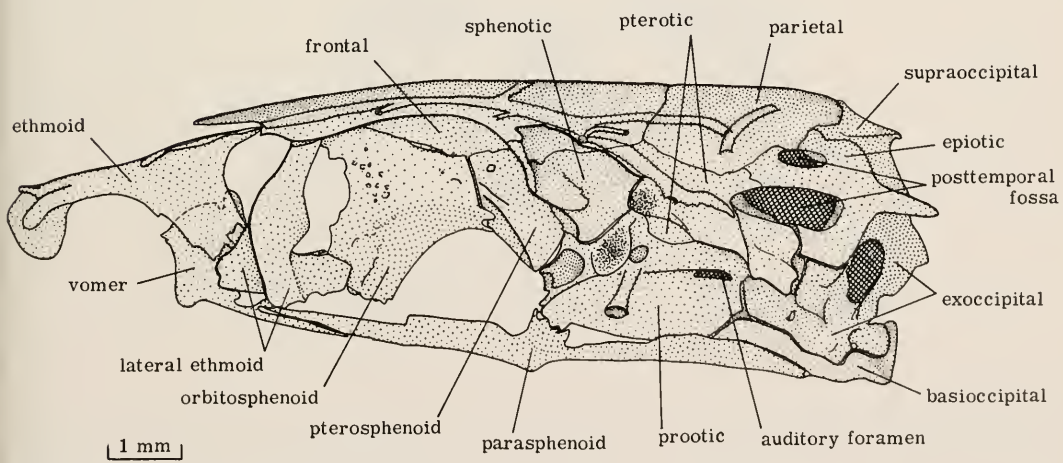

Figure 57. *Saccodon wagneri* (dental morph IV), 55.4 mm. Cranium (lateral view).

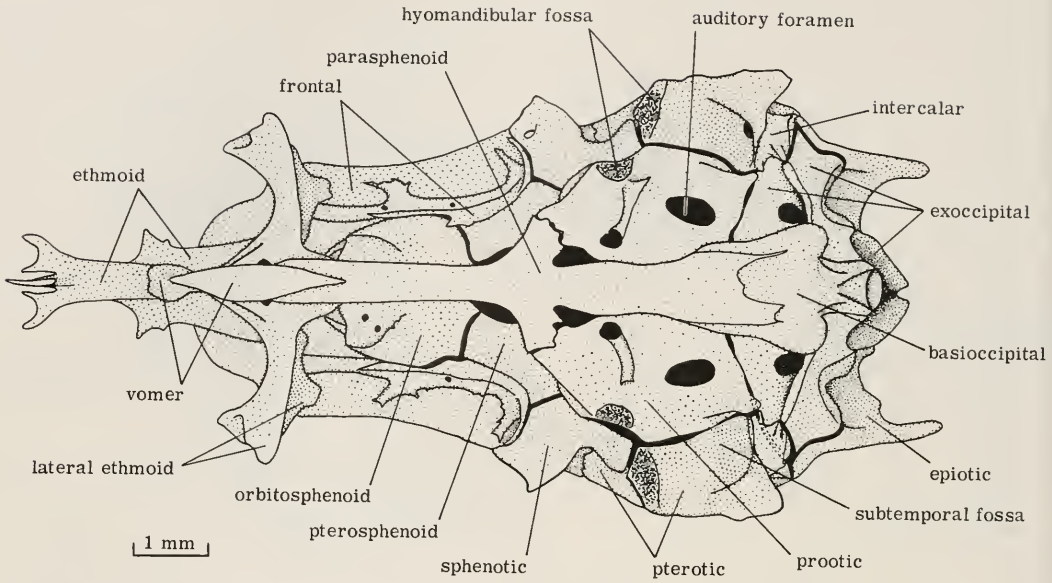

Figure 58. *Saccodon wagneri* (dental morph IV), 55.4 mm. Cranium (ventral view).

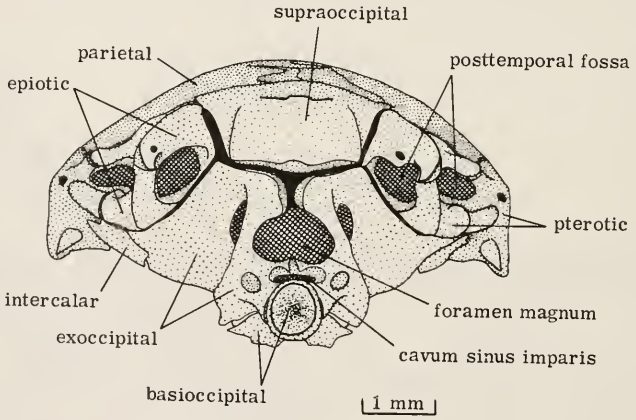

Figure 59. *Saccodon wagneri* (dental morph IV), 55.4 mm. Cranium (occipital view).

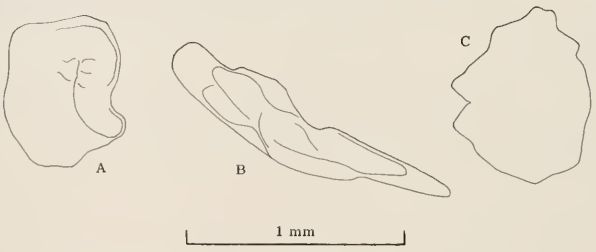

Figure 60. *Saccodon wagneri* (dental morph I), 52.0 mm. Otoliths. A. Lapillus (ventral view). B. Sagitta (lateral view). C. Asteriscus (lateral view).

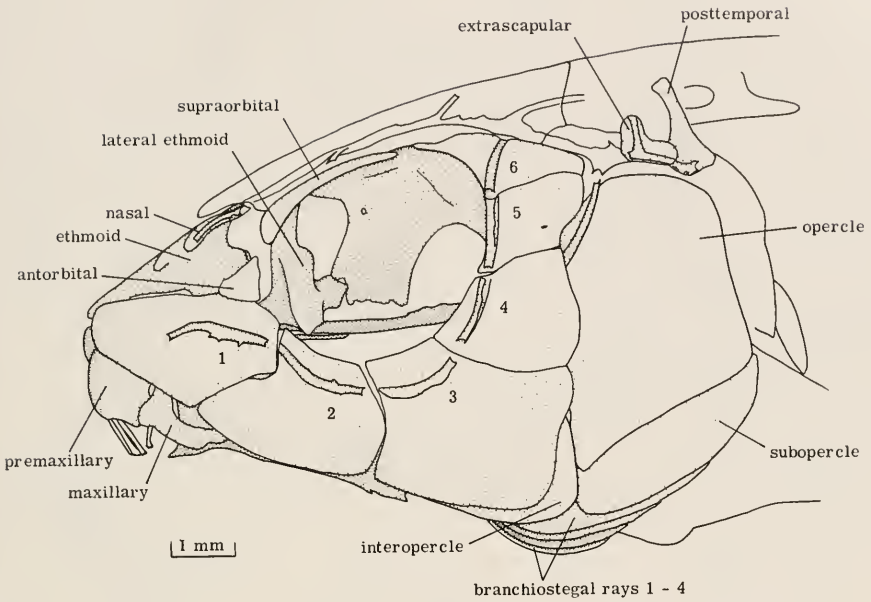

Figure 61. *Saccodon wagneri* (dental morph I), 57.2 mm. Lateral bones of skull (lateral view).

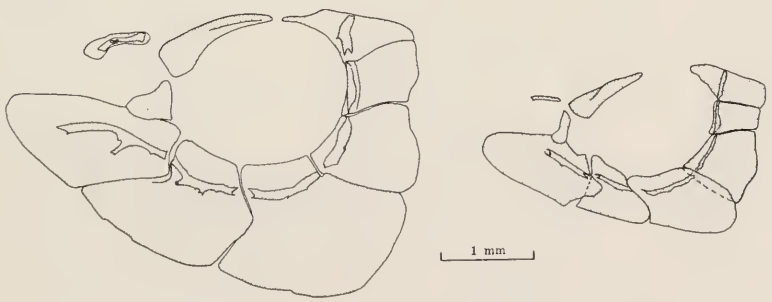

Figure 62. Parodontidae. Nasal, antorbital and circumorbital bones. Left, *Saccodon wagneri* (dental morph I), 57.2 mm. Right, *Parodon guyanensis*, 38.5 mm.

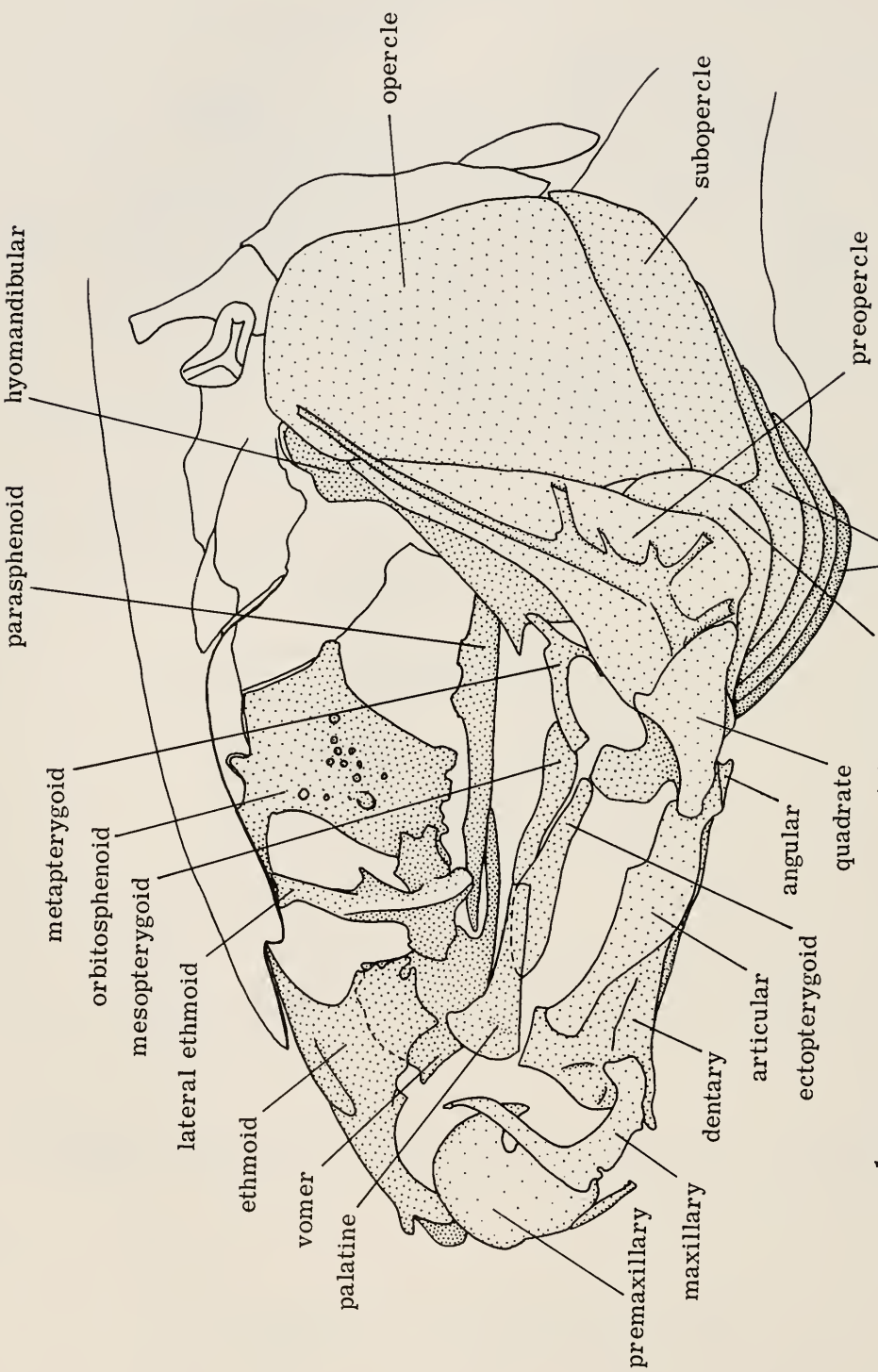

Figure 63. *Saccodon wagneri* (dental morph I), 57.2 mm. Lateral view of skull with nasal, antorbital and circumorbital bones removed.

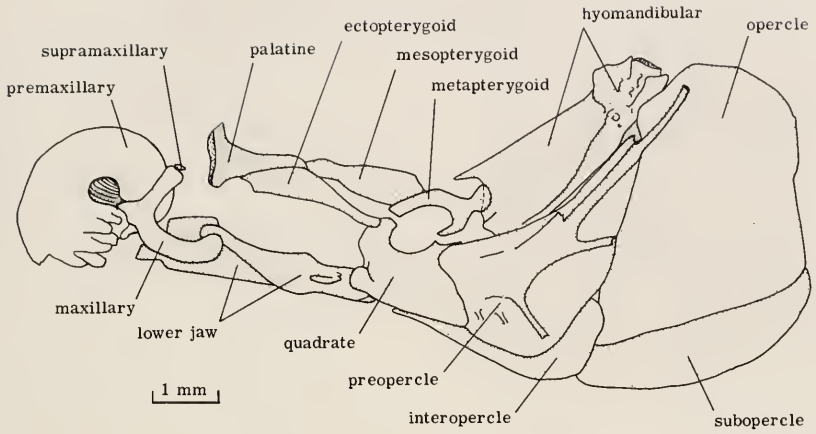

Figure 64. *Saccodon wagneri* (dental morph IV), 55.4 mm. Jaws, suspensorium and opercular bones (lateral view) (teeth removed).

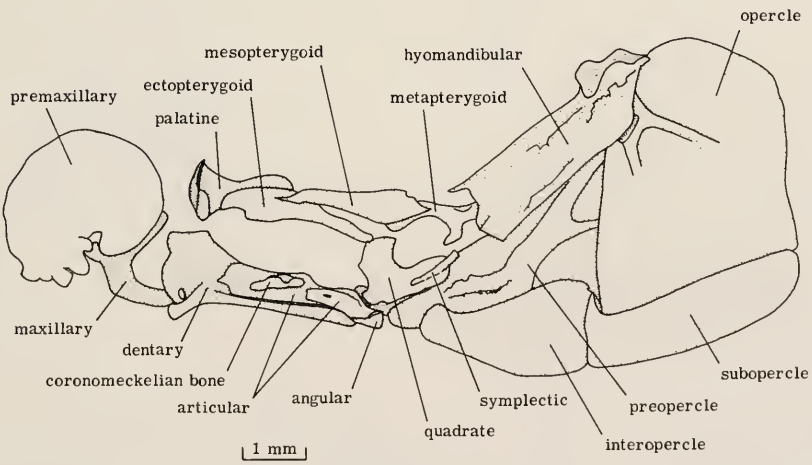

Figure 65. *Saccodon wagneri* (dental morph IV), 55.4 mm. Jaws, suspensorium and opercular bones (medial view) (teeth removed).

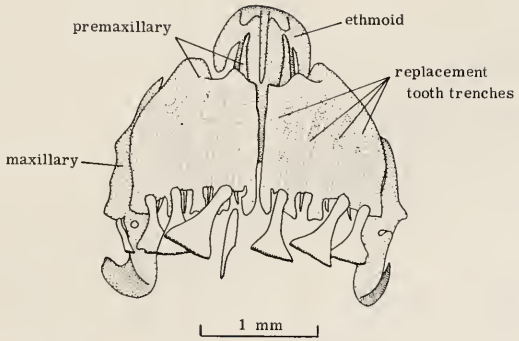

Figure 66. *Saccodon wagneri* (dental morph I), 45.5 mm. Upper jaws showing tooth replacement in progress (frontal view).

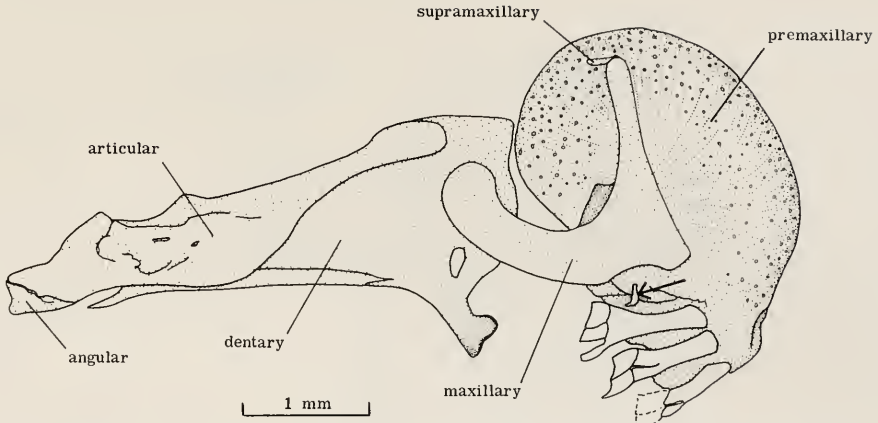

Figure 67. *Saccodon wagneri* (dental morph IV), 55.4 mm. Jaws and jaw teeth (lateral view). Note. This specimen unusual in having a minute, unicuspid, pedicellate tooth lateral to main series of functional teeth (indicated by an arrow).

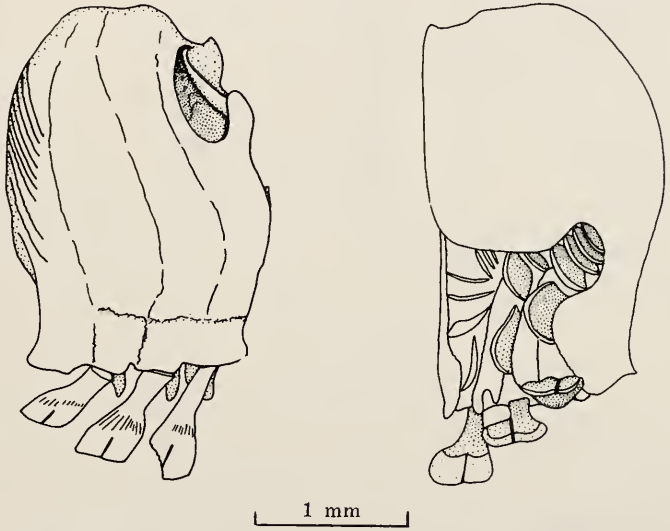

Figure 68. *Saccodon wagneri* (dental morph IV), 52.0 mm. Premaxillary bone. Left, frontal view. Right, ventral view.

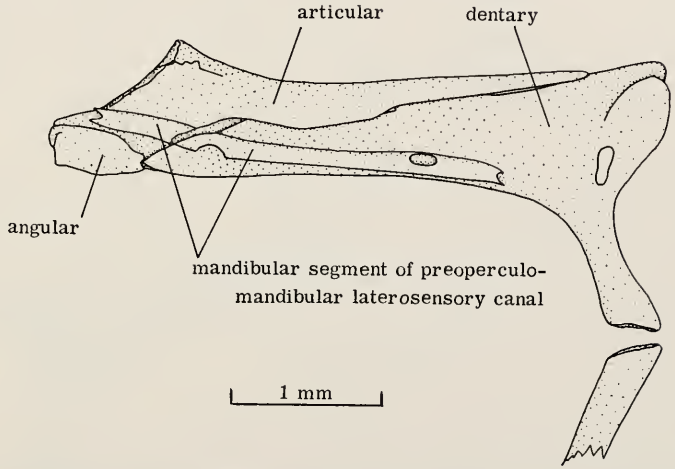

Figure 69. *Saccodon wagneri* (dental morph IV), 55.4 mm. Lower jaw (ventral view).

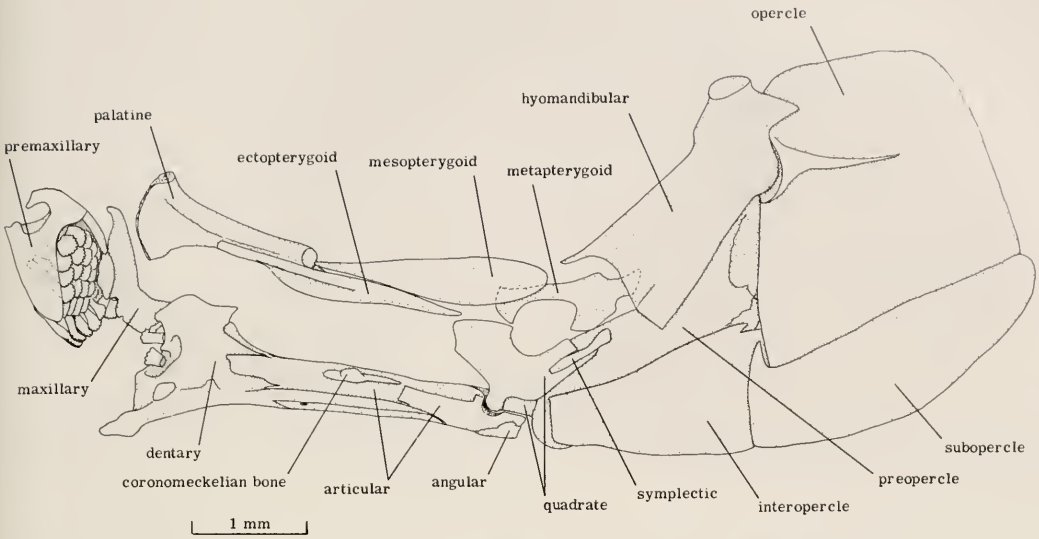

Figure 70. *Parodon guyanensis*, 38.5 mm. Jaws, suspensorium and opercular bones (medial view).

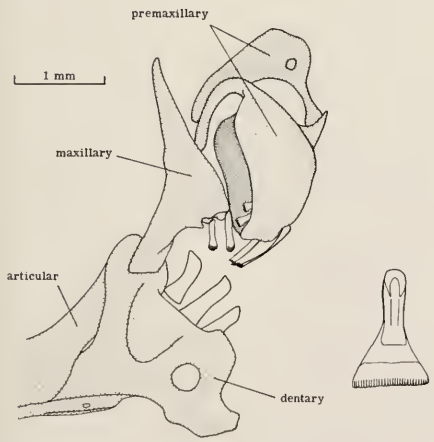

Figure 71. *Parodon caliensis*, 63.5 mm. Upper jaw and portion of lower jaw showing dentition (lateral view). Inset on right, functional tooth from premaxillary (medial view).

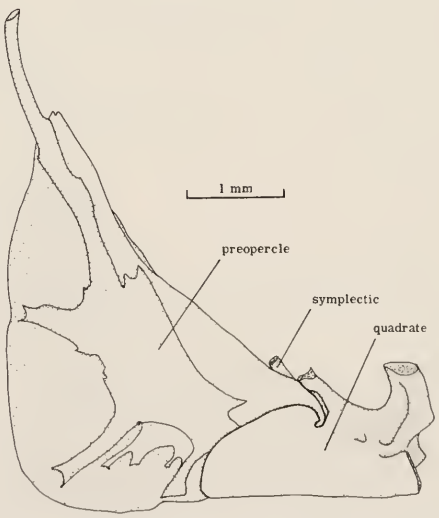

Figure 72. *Saccodon wagneri* (dental morph IV), 55.4 mm. Relation of quadrate to preopercle (lateral view).

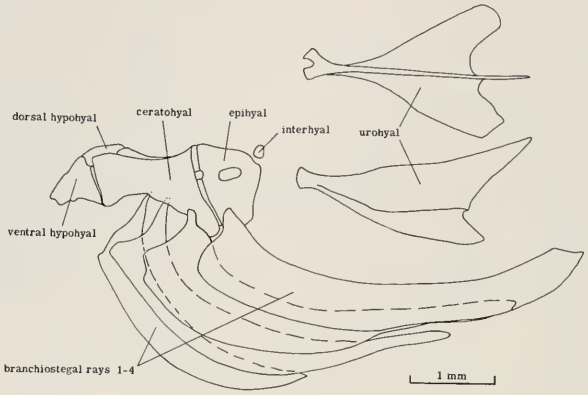

Figure 73. *Saccodon wagneri* (dental morph IV), 52.0 mm. Hyoid arch with basihyal removed (lateral view) and urohyal bone (lateral and dorsal views).

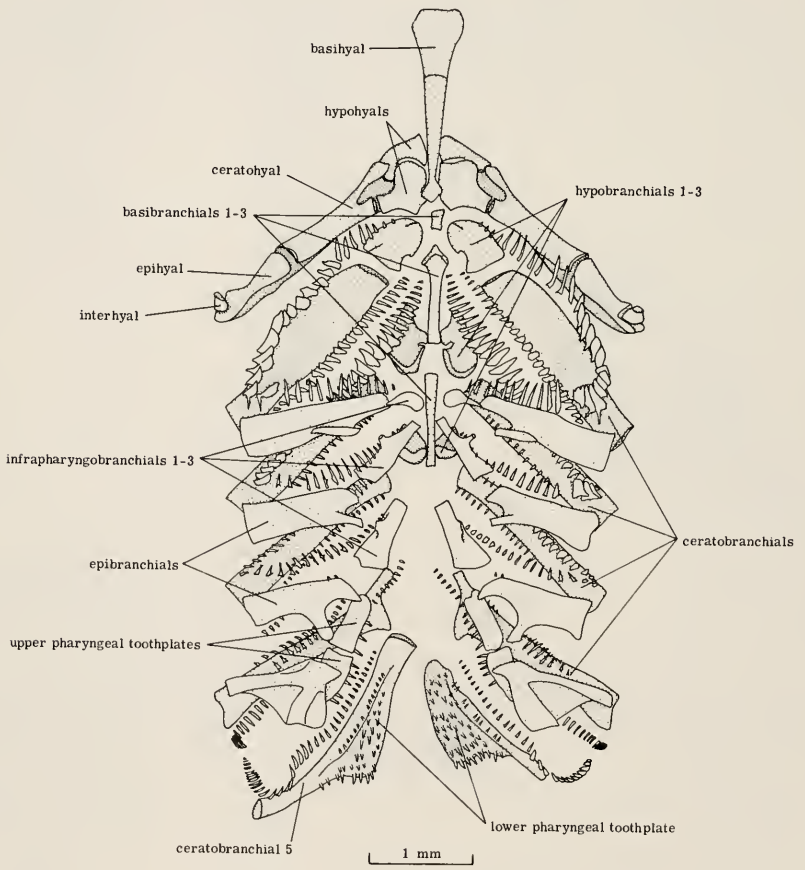

Figure 74. *Saccodon wagneri* (dental morph IV), 55.4 mm. Hyoid and branchial arches (dorsal view).

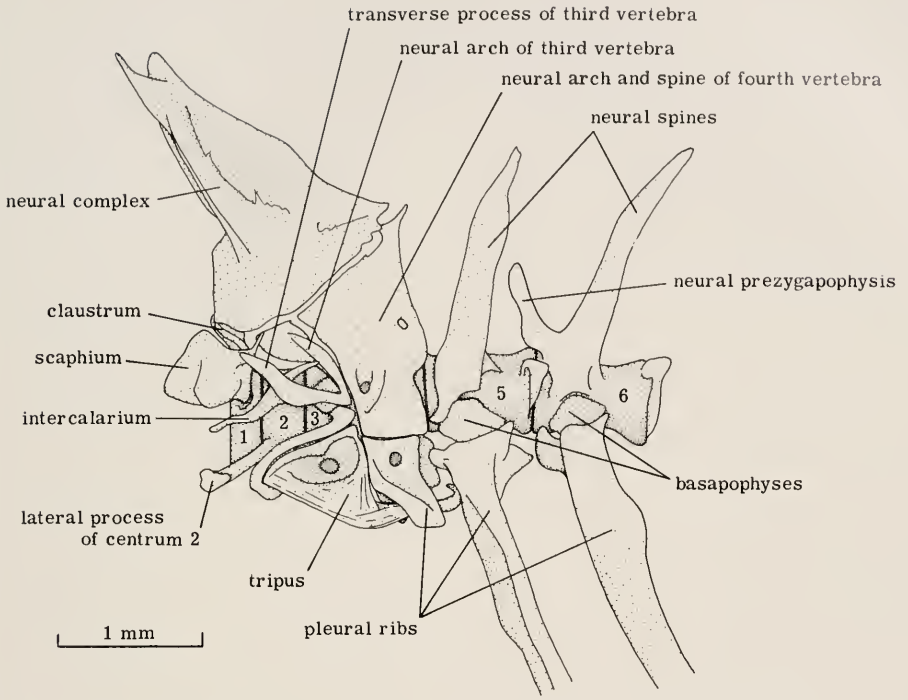

Figure 75. *Saccodon wagneri* (dental morph IV), 55.4 mm. Weberian apparatus (lateral view).

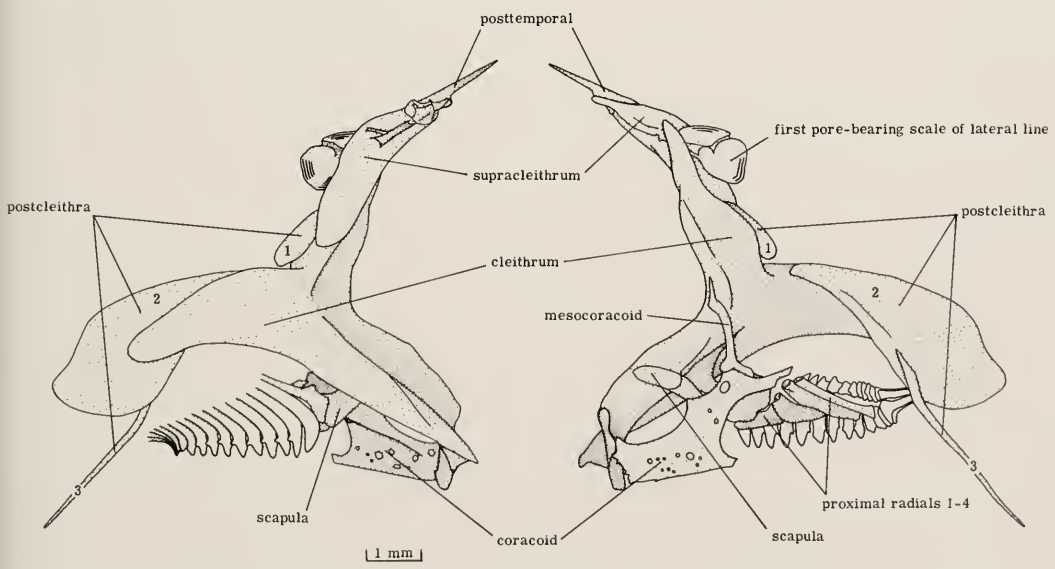

Figure 76. *Saccodon wagneri* (dental morph IV), 55.4 mm. Right half of pectoral girdle (lateral and medial views).

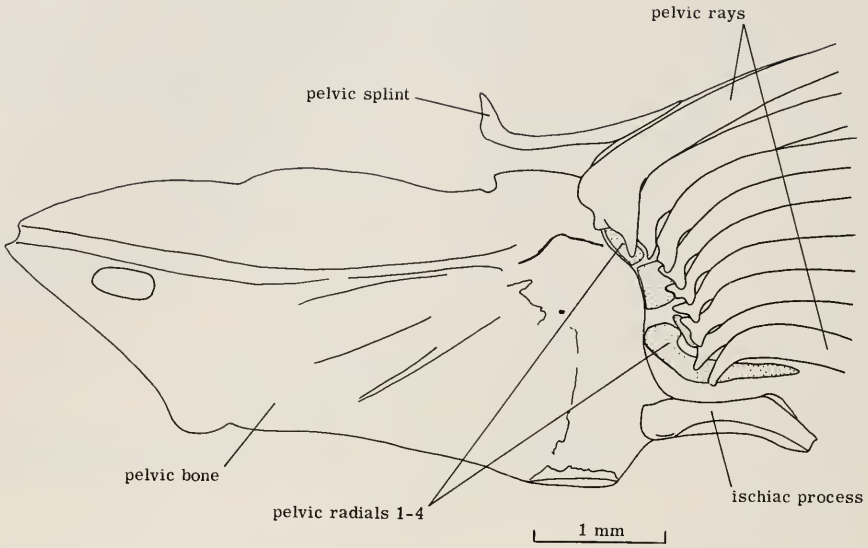

Figure 77. *Saccodon wagneri* (dental morph IV), 55.4 mm. Left half of pelvic girdle (ventral view).

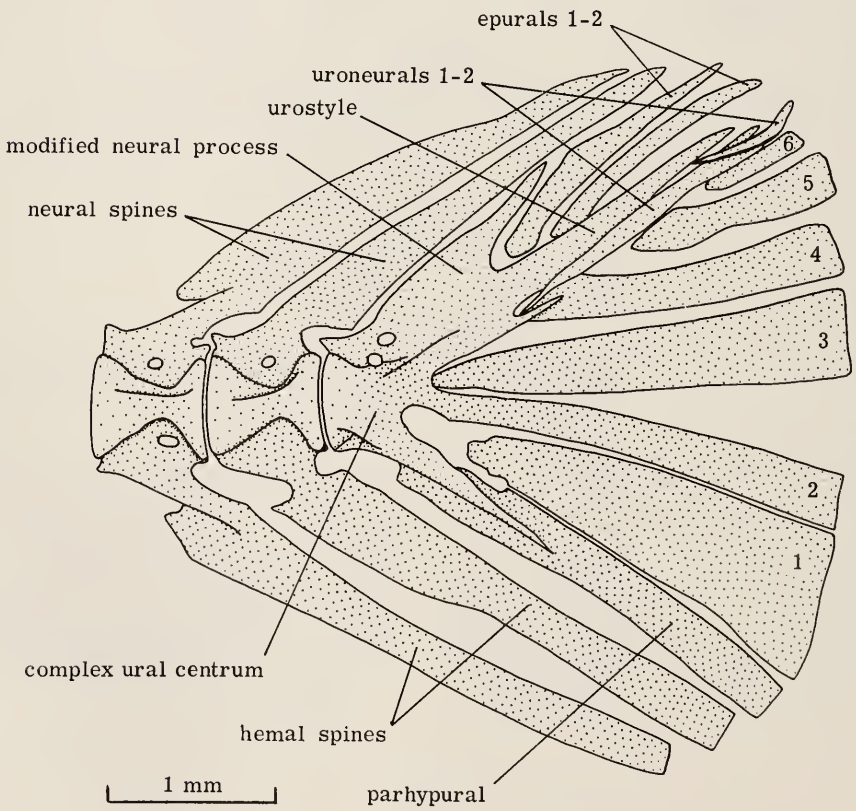

Figure 78. *Saccodon wagneri* (dental morph IV), 55.4 mm. Caudal skeleton (lateral view).

US ISSN 0027-4100

Bulletin OF THE
Museum of
Comparative
Zoology

The Taphonomy and Paleoecology of Plio-Pleistocene Vertebrate Assemblages East of Lake Rudolf, Kenya

ANNA K. BEHRENSMEYER

HARVARD UNIVERSITY
CAMBRIDGE, MASSACHUSETTS, U.S.A.

VOLUME 146, NUMBER 10
21 FEBRUARY 1975

END OF VOLUME

PUBLICATIONS ISSUED
OR DISTRIBUTED BY THE
MUSEUM OF COMPARATIVE ZOOLOGY
HARVARD UNIVERSITY

Breviora 1952–
Bulletin 1863–
Memoirs 1864–1938
Johnsonia, Department of Mollusks, 1941–
Occasional Papers on Mollusks, 1945–

SPECIAL PUBLICATIONS.

1. Whittington, H. B., and E. D. I. Rolfe (eds.), 1963. Phylogeny and Evolution of Crustacea. 192 pp.
2. Turner, R. D., 1966. A Survey and Illustrated Catalogue of the Teredinidae (Mollusca: Bivalvia). 265 pp.
3. Sprinkle, J., 1973. Morphology and Evolution of Blastozoan Echinoderms. 284 pp.
4. Eaton, R. J. E., 1974. A Flora of Concord. 236 pp.

Other Publications.

Bigelow, H. B., and W. C. Schroeder, 1953. Fishes of the Gulf of Maine. Reprint.

Brues, C. T., A. L. Melander, and F. M. Carpenter, 1954. Classification of Insects.

Creighton, W. S., 1950. The Ants of North America. Reprint.

Lyman, C. P., and A. R. Dawe (eds.), 1960. Symposium on Natural Mammalian Hibernation.

Peters' Check-list of Birds of the World, vols. 2–7, 9, 10, 12–15.

Proceedings of the New England Zoological Club 1899–1948. (Complete sets only.)

Publications of the Boston Society of Natural History.

Price list and catalog of MCZ publications may be obtained from Publications Office, Museum of Comparative Zoology, Harvard University, Cambridge, Massachusetts, 02138, U.S.A.

© The President and Fellows of Harvard College 1975.

THE TAPHONOMY AND PALEOECOLOGY OF PLIO-PLEISTOCENE VERTEBRATE ASSEMBLAGES EAST OF LAKE RUDOLF, KENYA

ANNA K. BEHRENSMEYER[1]

CONTENTS

Abstract 474
Introduction 474
The Taphonomy of Macro-Vertebrate Assemblages 476
Factors Relating to Mode of Death 476
Factors Relating to Weathering and Decomposition 479
Transport and Burial 480
Diagenetic Factors 482
Conclusions 482
Characteristics of Recent Bones as Sedimentary Particles 483
Properties of Bones as Sedimentary Particles 485
Measurements of Bone Size and Density 485
Relative Dispersal Potential of Bones 488
The Hydraulic Equivalence of Bones and Quartz Grains 490
Experiments in Bone-settling Velocities 492
The Hydraulic Equivalents of Fossil Bones 493
Current Velocities and Bone Transport 495
Additional Factors Affecting Bone Transport in Natural Situations 497
Bottom Morphology and Current Profile 498
Fluid Density 498
Burial Potential 498
Conclusions: Bones as Sedimentary Particles 499
Sedimentary Environments of the Koobi Fora Formation, East Rudolf 500
Geologic Setting 500
Regional Stratigraphy 503
Recent Limnology 505
Stratigraphy of the Koobi Fora Formation 507
Sedimentary Environments of the Fossil Vertebrate Localities 509
Designation of Sampling Localities .. 509
Method of Geologic Analysis 509
Sedimentary Environments of the Sample Localities 514
Discussion and Conclusions 525
Sorting in Bone Assemblages of the Koobi Fora Formation 526
Sampling of Bone Assemblages 526
Choosing the Sample Areas 527
Sample Size 528
Method of Representing Fossil Abundance 528
Characteristics of the Bone Assemblages 529
Identification of Bones 530
Significance of the Frequency Data 531
Comparisons of Overall Bone Concentrations 531
Relative Abundance of Skeletal Parts 532
Correlations Based on Bone Abundance 532
Factor Analysis of the Bone Assemblages 534
Comparisons with Voorhies Groups 536
Single Skeleton Comparisons 536
Discussion of Evidence for Transport Sorting 537
Additional Aspects of the Bone Assemblages 538
The Reptilian Assemblages 540
Conclusions Concerning the Bone Assemblages 540
Faunal Assemblages of the Koobi Fora Formation 541
Method of Identification 541
Abundance of Vertebrate Classes 542
Reptiles 543
Mammals 545
Discussion of the Most Abundant Mammalian Groups 547
Abundances of Selected Mammalian Groups 549
Suids 549
Equids 551
Bovids 551
Hippos 552
Conclusions Regarding the Faunal Assemblages 553

[1] Department of Paleontology, University of California, Berkeley, California 94720

Paleoecology of the Vertebrate Assemblages of the Koobi Fora Formation 554
Ecological Comparisons of the Samples ... 557
Aquatic and Terrestrial Faunas 557
Open and Closed Habitat Mammalian Faunas 557
Comparisons of Koobi Fora Formation Faunas and Recent Terrestrial Faunas 558
Hominid Paleoecology 561
East Rudolf in Relation to Other Studies in Vertebrate Paleoecology 562
Summary 564
General Conclusions 564
Taphonomy 564
Paleoecology 565
Conclusions for the Vertebrate Assemblages of the Koobi Fora Formation, East Rudolf 565
Acknowledgments 566
References 567
Appendix 1. Bone Measurements: Density, Volume and Weight 570
Appendix 2. Calculation of Hydraulic Equivalence 573
Plates 574

Abstract. The object of this study is to show that paleoecologic information can be derived from fossil vertebrate assemblages fragmented prior to burial if a taphonomic history can be established for these assemblages. Such paleoecologic information can lead to knowledge of the character and evolution of vertebrate communities through time. Within the Koobi Fora Formation of East Rudolf, Kenya, vertebrate bones are preserved in fluvial and lacustrine depositional environments through a time span between about 3.0 and 1.2 million years Before Present. A total of seven bone assemblages were collected from lake margin, channel and floodplain deposits. Detailed geological studies were done in the seven laterally extensive sedimentary environments sampled for bones. The bone samples were taken from surface lag concentrations utilizing widely spaced 10×10 meter squares. The seven assemblages were analyzed for numbers of different skeletal parts and vertebrate taxa. Theoretical and experimental evidence for the characteristics of bones as sedimentary particles formed the background for the analysis of the East Rudolf assemblages. The flume experiments of M. Voorhies (1969), plus measurements of whole-bone densities and settling velocities, supported the hypothesis that bones form distinctive dispersal groups when sorted by various taphonomic processes, especially fluvial transport. Therefore, the dispersal groups represented in fossil assemblages can indicate the taphonomic histories of these assemblages. Mammalian skeletal parts from the seven sample assemblages were analyzed for the percentages of different dispersal groups. The numbers of different parts were also compared with the ratios of parts in a single, average skeleton. The fossil assemblages from fluvial deposits showed distinctive alteration from the ratios of parts in undisturbed skeletons. This resulted from the absence of the lighter bones which form the most easily transported dispersal group. The delta margin assemblages showed little alteration of bone percentages from those in an undisturbed skeleton, indicating little selective sorting prior to burial in this environment. The bones, hence the faunas, did not appear to be substantially mixed or transported from the general ecological province inhabited by the living animals. This information allows paleoecological inferences to be drawn from faunal distributions in the different environments. Faunal assemblages were analyzed for the patterns of occurrence of reptilian and mammalian groups. Aquatic and nonaquatic vertebrates (excluding fish) are preserved in approximately equal abundance in the delta margin deposits. Nonaquatic forms are significantly more abundant in the fluvial deposits. Several members of the mammalian faunas, particularly hippos, suids and bovids, show differential abundances in the two environments. Certain members of the Bovidae and Suidae have patterns of occurrence indicating preferences for delta margin or fluvial habitats. The paleoecologic information from the more abundant vertebrate groups helps to establish an ecological framework for the hominid fossils from the Koobi Fora Formation.

INTRODUCTION

The primary object of this study is to determine the paleoecology of vertebrate faunas that occur in the East Rudolf deposits of northern Kenya. Taphonomic analysis will provide the background for the paleoecologic interpretations. The crucial link between a fossil assemblage and the original ecosystem from which it was derived lies in the taphonomy of the assemblage, the history of its passage from the biosphere into the lithosphere. When bones of different animals are found together in a particular sedimentary deposit it is essential to know whether these bones were buried together because they were transported together (perhaps from different points of origin), or whether their close association indicates that the animals lived and died in the same habitat. The taphonomic history of a bone assemblage can provide this information.

Methods for establishing the taphonomic histories of fossil vertebrate assemblages in East Rudolf are explored and developed in this study in order to permit the fossil faunas to be related to former living vertebrate communities. These methods apply specifically to the East Rudolf bone assemblages, which represent thanatocoenoses (death assemblages) of large vertebrates that were disarticulated, fragmented and transported prior to burial. However, many of the conclusions concerning the interaction of these bones with processes of transport and weathering will have broad implications for paleoecologic interpretations of vertebrate assemblages from other regions and time periods.

This study consists of two major parts, the first providing theoretical and experimental models for the second, which analyzes particular bone assemblages from the East Rudolf deposits. The first part discusses factors contributing to bone dispersal and destruction in recent East African habitats and then examines in detail the properties of bones as sedimentary particles, including their dispersal potentials when subjected to fluid stress and their hydraulic equivalence to quartz particles. The second part describes the geologic context of East Rudolf bone assemblages sampled from seven different localities, analyzes their taphonomic histories, and then interprets the paleoecology of the faunas represented in each of the seven samples.

Many aspects of the East Rudolf region proved extremely advantageous as a background for the study of the taphonomy and paleoecology of a series of fossil vertebrate assemblages. The East Rudolf Research Expedition, led by R. E. Leakey of the National Museums of Kenya, has been active in the area since 1967 and has brought together a large team of scientists representing a wide range of disciplines. The collection of fossil vertebrates from the region as a whole has established the composition of the local Plio-Pleistocene faunas and has provided evidence for faunal succession between about 4.5 and 1.3 my. B.P. The regional geology has been worked out through the combined efforts of several teams of geologists, and the overall stratigraphy and dating are reasonably well established. Archaeological investigations are providing evidence relating the cultural artifacts of primitive man to the broader context of the Plio-Pleistocene faunas and environments. In addition, the Recent faunas and environments of East Rudolf are comparable in many ways to those of the Plio-Pleistocene and serve as readily available analogues for the interpretation of the taphonomy and of the paleoecology of former time periods. A study of the recent taphonomy of lake margin areas is in progress (A. Hill, Bedford College, London) and this should give further valuable evidence for comparison with the fossil assemblages. On a broader scale, geological and paleontologic information currently available for sedimentary deposits throughout East Africa, plus the wealth of data on the recent ecosystems, have greatly enhanced and broadened the scope of this study.

As an added attraction to all of the other advantages that characterize East Rudolf, the area is one of the richest known localities for fossil man. At present, over 120 specimens have been recovered, and these represent at least two taxa of contemporaneous, Plio-Pleistocene hominids. This study provides a background for the paleoecologic context of fossil man at East Rudolf in terms of faunal associations, environments, and possible habitat separation between the two forms.

The initial decision to undertake a study of the East Rudolf bone assemblages was in part inspired by previous, intriguing research in vertebrate paleoecology. The outstanding works that have helped to shape many of the viewpoints to be presented later include: Olson (1952, 1958), Shotwell (1955, 1963), Clark, Beerbower and Kietzke (1967), Voorhies (1969), and Dodson (1971, 1974). Information has been

drawn from various other studies relevant to the interpretation of assemblages consisting of bones of the larger vertebrates. These include the investigations of recent carcass decay and dispersal by Weigelt (1927) and Schäfer (1972). The overall theoretical background for taphonomy is derived primarily from Efremov (1940, 1953), the founding father of this line of scientific investigation.

Research on the East Rudolf bone assemblages and their relationships to different sedimentary environments was begun in the summer of 1971. Prior to this, I had spent two field seasons working on the stratigraphy and sedimentary environments of East Rudolf, as well as five weeks at Lothagam Hill on the southwest side of Lake Rudolf. Field work on the East Rudolf assemblages encompassed two field seasons of three months each in 1971 and 1972. Surface bones associated with different lithofacies were collected according to a consistent procedure that permitted later statistical comparisons between assemblages. All collecting and bone identifications were done by me or under my close supervision.

THE TAPHONOMY OF MACROVERTEBRATE ASSEMBLAGES

Many processes can influence the progression of bones from the living animal to the final place of burial and fossilization. All of these must be considered in order to derive paleoecological information from a fossil assemblage. Efremov (1940:85) applied the term *taphonomy* to this special area of geological and biological problems, and specified it as "the study of the transition (in all its details) of animal remains from the biosphere into the lithosphere." Processes included in taphonomy have been discussed in the general context of vertebrate assemblages by various authors (e.g., Efremov, 1940; 1953; Clark *et al.*, 1967; Müller, 1957). As an introduction to the study of the East Rudolf fossil assemblages, it will be useful to consider these processes in some detail where they are relevant to the East African situation.

Factors Relating to Mode of Death

Causes of death initially determine which bones and which animals will have a potential for fossilization. Causes of death may include predation, disease, physical accident, poison, starvation and intraspecific strife (Clark *et al.*, 1967: 115). Predators have the greatest initial influence on the widespread dispersal of bones. Animals that die of other causes are likely to be similarly dispersed by scavengers, at least in East Africa, unless the carcass is somehow protected.

Lion, leopard, cheetah, hyaena, jackal, man and crocodile are the most important predator/scavenger members of the communities of large vertebrates in East Africa today. All of these both hunt and scavenge (Kruuk, 1972; Van Lawick-Goodall, 1971; Schaller, 1972). Vultures also are important contributors to bone dispersal. The effects of these predators and scavengers on a carcass are referred to as "carnivore activity" in the following discussion. Disassociation of a skeleton can be amazingly rapid and thorough. Kruuk (1972:126) reports that a young wildebeest killed by hyaenas had its parts completely dispersed from the site in 13 minutes. Both hyaenas and lions will kill in shallow water and may have their meal there rather than dragging the carcass onto land. However, lions often will drag whole carcasses or parts away from the site of death. Hyaenas may carry favorite parts long distances (away from other hyaenas). Kruuk (1972:119) observed hyaenas caching parts of carcasses in 30–50 cm of standing water, with variable success in retrieving the cache later on. When a shallow pool dried up, many bones were exposed, apparently as a result of this behavior.

The preferences of carnivores for consuming particular parts of a carcass have an important bearing on what would remain to be fossilized and which bones would be

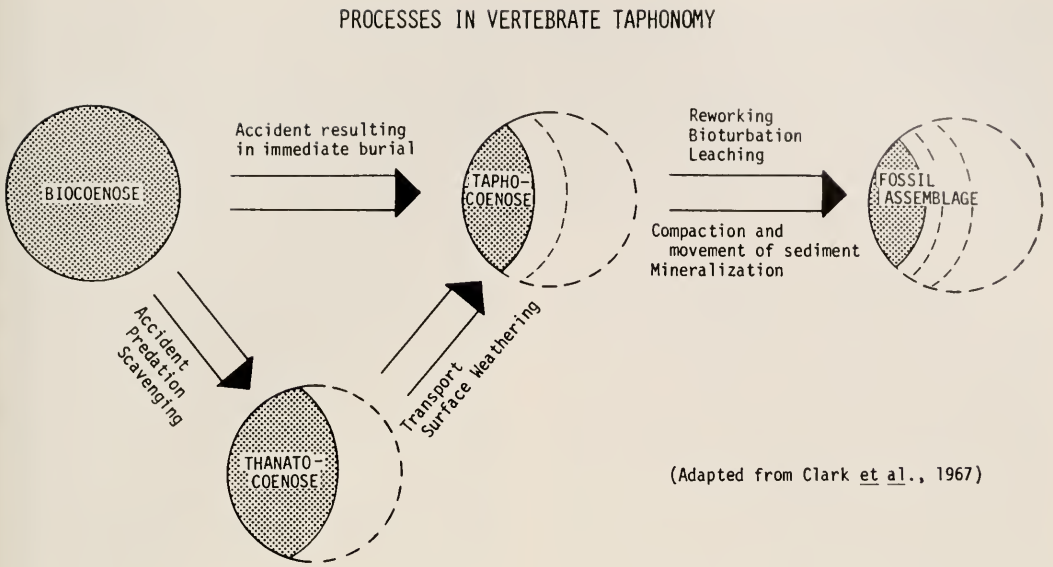

Figure 1.

likely to remain near the site of death. Kruuk (1972:126) reports: "If any part of a corpse is left by hyaenas in both Ngorongoro and Serengeti, the skull is most likely to remain uneaten, followed by the vertebrae, ribs, pelvis and ends of long leg bones." Lions will also consume everything but "horns, teeth and a few bone splinters and scraps," of small prey such as gazelle (Schaller, 1972:269). Carnivore activity by man would probably result in less total destruction of bones, but limb shafts might be split for marrow and skulls broken open for the brain (White, 1955, Brain, 1967b).

It is obvious that a crucial factor in the number of bones which survive to become a thanatocoenose (death assemblage) will be the proportion of carnivores to the number of food animals at any one time. In Kruuk's study areas, the number of predators was high, and the number of carcasses left intact was low. Observations of carcasses in the East Rudolf region reveal a fairly large number of intact or partial skeletons, reflecting a relatively low number of carnivores. The reciprocal relationship between numbers of carnivores and numbers of complete bones or carcasses has been generally noted in East Africa (e.g., Estes, 1967:39).

Not only numbers, but relative sizes of carnivores as well as their degree of adaptation for bone mastication will have important effects on a thanatocoenose. The strength of bones with nutritional value must exceed the crushing force of the jaws of hyaenas and lions in order to remain intact, unless there is a surplus of food (e.g., mass deaths), which would make bones less attractive food items.

Crocodile predation or scavenging will tend to bring bones into close association with depositional environments but may totally destroy bones that are consumed. The proportion of large animals in a crocodile's diet increases with its size, and prey can range up to the size of an adult black rhino (Selous, 1908:201). Crocodiles generally kill by dragging animals into the water and drowning them. They are also active scavengers, ranging as much as half a mile from water, and may even compete with lions for a kill (Cott, 1961:302–303). Carcasses are torn apart or may be cached (underwater) until decomposition makes dismembering easier (Guggisberg, 1972:

94). Bones and teeth are demineralized during digestion, and remaining organic material (mainly collagen) disintegrates rapidly after defecation (D. Fisher, personal communication). Thus, only bones that are too large or cumbersome to ingest (e.g., skulls), or that are neglected by the crocodile, would survive. However, these would have optimal chances for burial.

Drowning, disease, starvation and other causes leading to mass deaths can have different effects on a thanatocoenose. Any mass death situation is likely to create a surfeit of food for the local carnivores, and many skeletons may be left more or less intact. Schaller (1972:215) notes that lions do not seem to scavenge from such deaths. It takes only a short time for carcasses to mummify in dry conditions and become unattractive to most scavengers. Once mummified, a carcass could probably survive a certain degree of transport without becoming disarticulated.

Mass death by drowning seems to be fairly common among the East African ungulate species. The social behavior of herd-oriented species (e.g., zebra, wildebeest) can result in mass panics in which the fright of a single animal may cause a group stampede. Such events often occur at waterholes, and many animals may be trampled and drowned (R. Estes, personal communication). Schaller (1972:215) reports the death of 62 wildebeest in a waterhole at one time, and 83 in the same place a few years later. Apparently many herd-oriented animals also drown during river crossings. Abel (1912:12) mentions panic as one of the causes of massed vertebrate remains, but the idea has not generally been used in the interpretation of massed fossil assemblages.

In a discussion of the causes of mass deaths leading to fossilization, Kurtén (1953:72) favors seasonally occurring floods or, in a more general sense, linked causes of death and deposition. Voorhies (1969: 52) supports a catastrophic event of this kind in the case of the Pliocene Verdigre Quarry in Nebraska, and suggests large-scale drought or winter storm followed by flash-flooding as the cause of the deposit. Drought may concentrate animals that are not normally herd oriented. However, in some cases it would be worth considering social catastrophes as well as climatic events in interpreting massed assemblages of fossil vertebrates.

The drowning of single animals, as in river crossings, initially provides good conditions for the burial of a whole skeleton or articulated parts. Scavenging by crocodiles, and possibly also by fish and turtles, can destroy such carcasses, and if they float long enough to decay, various parts may gradually drop off and be widely dispersed. However, drowning can lead to the preservation of whole or partial skeletons. As a consequence, wildebeest, and other non-aquatic animals, might be among the best preserved fossils in channel and point-bar deposits.

The above observations are relevant to paleoecological interpretations based on the preservation of vertebrates in channel and point-bar deposits. Dodson (1971:69) has suggested that the excellent, complete preservation of hadrosaur skeletons in the channel deposits of the Oldman Formation (western Canada, Cretaceous) indicates that a good portion of the hadrosaurs' time was spent living in the channels. By analogy, it might be possible to conclude that wildebeest occupy aquatic habitats, based on where the most complete skeletons would be preserved. The fact is that wildebeest are terrestrial in their habits, but occasionally die in channels. In many cases, the exception (e.g., drowning) may produce the fossil, while "normal" habits will leave little or no record. The hadrosaurs may have been partly aquatic, but their place and state of preservation in the channel deposits should be used only in support of other evidence for aquatic habits.

In general, it appears that two major kinds of thanatocoenoses can be derived from modern large-vertebrate communities;

an incomplete, broken and dispersed one resulting from carnivore activity, and a relatively complete one (in terms of whole bones and associated skeletons) resulting from mass deaths. The first can form fossil assemblages which sample faunas over periods of months or years, while the second may lead to assemblages which sample the standing crop of vertebrates at specific points in time. Intermediate kinds of thanatocoenoses will depend on the numbers of carnivores and the effects of scavenging on the available carcasses.

In East Africa today, many thanatocoenoses are composed of broken and incomplete skeletons, owing to the large numbers of carnivores. The parts that are left to continue toward fossilization chiefly include skulls, horn cores, vertebrae, ribs, ends of limb bones and teeth, *of the larger animals* (primarily ungulates). These are subjected to weathering and transport and are treated as sedimentary particles by the various geologic processes. More complete carcasses occur in situations where they are not subject to scavenging. From the recent evidence, it appears that a thanatocoenose composed of fragmented skeletons is likely to occur in an area broadly representative of the habitats of the living animals, although later the bones may be dispersed from the area by fluvial processes. A thanatocoenose composed of massed, complete skeletons is more likely to represent localized conditions of death and/or transport. Thus, a fossil assemblage composed of bones from a fragmented thanatocoenose *that has not been transported* should preserve the best evidence for the paleoecology of the fauna.

The foregoing discussion applies to the larger vertebrates, and it is assumed that the bones of animals of sheep size and smaller will be much less likely to survive carnivore activity. However, small vertebrates such as turtles and fish probably form thanatocoenoses comparable to those of the large mammals and reptiles, reflecting both carnivore activity and occasional mass deaths. Processes leading to thanatocoenoses composed of small mammals are not well understood and are worthy of further investigation. However, since the East Rudolf deposits have so far yielded a negligible number of small mammals, such an investigation will not be undertaken in this study.

Factors Relating to Weathering and Decomposition

The biological and chemical properties of the place where an animal dies will have an important effect on bone destruction. Humid surface environments will facilitate the decay of organic material and will cause dissolution of bone minerals. Dry environments dehydrate the organic component of fresh bones, resulting in cracking and splitting. For the most part, since teeth have less residual organic matter, they will survive surface weathering better than other parts, although large teeth tend to split when dehydrated.

The rate of decay of muscles and ligaments is of interest in determining how long parts will remain articulated. In the absence of vertebrate carnivores, insect activity is an important process in defleshing a skeleton and is enhanced by warm, humid, subaerial conditions. In such conditions (summer in South Carolina, U.S.A.), Payne (1965:597) has observed complete removal of flesh from the carcass of a baby pig in eight days when insects were present, but flesh remained after 100 days when insects were absent. Voorhies observed sheep carcasses in the drier conditions of Nebraska and reports complete disarticulation after 90 days of normal insect activity. Carcasses of mammals that are submerged in water may disarticulate in 1 to 3 months (Dodson, 1974:79; Schäfer, 1972:21). The evidence suggests that the most rapid rates of disarticulation owing to insects and the activity of micro-organisms may be achieved on land. However, under certain conditions, bones can remain articu-

lated for weeks or months in either subaerial or aquatic environments.

Very little is known about the textural characteristics of bones weathered under different conditions. However, there is some data on the length of time bones can survive surface weathering. Voorhies (1969: 31) reports that bones left for a year in the Nebraska climate were soft and cracked, showing noticeable signs of disintegration. Bone-weathering experiments in East Africa show nearly complete destruction in 7 to 8 years (Isaac, 1967:40). Observations on bones in various East African game parks indicate they can last several years, but are usually in good condition for only a few months (A. Hill, personal communication). In the semi-arid climate of Lake Rudolf (annual rainfall ~ 250 mm [10 inches]), bones acquire distinctive characters indicative of surface weathering, including flaking, splitting and splintering (Plate 1) during the first few months of exposure. Bone is evidently a very short-lived material in surface environments, and must be left in actively aggrading depositional situations in order to survive intact. If bones are to maintain a fresh and unweathered appearance, they must be buried soon after the death of an animal.

The characteristic appearance of naturally weathered bone surfaces is often distinguishable after they have been fossilized. This can provide invaluable evidence for the taphonomic history of a bone or bone assemblage. Typical surface textures are shown in Plate 1. Certain types of fractures also appear to result only from breakage in fresh bones. These include spiral, fibrous and sawtooth fractures as shown in Plate 2. Some work has been done on the characteristic weathering and fracture patterns of bones (e.g., Sadek-Kooros, 1966; Brain, 1967a; Reif, 1971). Preliminary experiments using tumbling mills show that bones can be abraded and rounded during transport without extensive fragmentation. Projections on the bones are usually broken off and surfaces become smooth and rounded (G. Jepsen, personal communication). More experimental work is needed in order to establish the causes of the observed fracture patterns and surface textures of recent bones.

The major factor determining bone appearance and survival potential under surface conditions appears to be the content of organic matter. Crystals of hydroxyapatite which form bone are supported in an extensive system of organic material. Bones that have this organic material removed artificially can be reduced to powder with very little force (a vertebra can be crushed in one's hand). Bones that have been demineralized, leaving only the organic material (principally collagen), maintain their form and can be bent and twisted like rubber (F. A. Jenkins, Jr., personal communication). Weathered bones that have obviously lost much of their organic content can be easily crushed and broken and are particularly friable when wet, with relative strength proportional to the compactness of the bone structure. These bones would be easily abraded and destroyed in transport situations, while bones with greater residual organic content would survive longer under similar conditions.

Bone can be regarded as a very labile kind of sedimentary particle that is characteristically altered by the geologic processes to which it is subjected. Therefore, bones may reveal a great deal about the influence of weathering and transport on their pre-burial history.

Transport and Burial

Bones can be transported from the place of death either within a floating carcass or as isolated objects that behave as discrete sedimentary particles. Flotation could lead to considerable transport of bones away from the habitat of the living animal with little damage to bone surfaces. There are no experimental data as yet to show how far isolated bones can be transported. However, a certain amount of information can be derived from a theoretical consideration

of the properties of bones as sedimentary particles. These will be given detailed examination in the following chapter, since an understanding of bone transport is crucial for paleoecological interpretations from assemblages of isolated bones such as those found in the deposits of East Rudolf.

Whole or nearly whole carcasses can be floated intact to places of deposition as long as gases remain trapped inside (Schäfer, 1972). In East Africa today, transport of floating carcasses for long distances is probably rare owing to the prevalence of crocodiles. However, in at least one case, long-distance carcass transport has been observed. A skeleton of a topi (*Damaliscus*) was found on the shores of North Island in the center of Lake Rudolf, 24 km. (15 miles) from land across waters in which crocodiles are abundant (I. Findlater, personal communication).

Transport of articulated parts that do not float will also occur. Ligament softens when immersed in water but may still hold bones together, particularly body parts such as feet and limb joints (Dodson, 1974:79). The principal factors limiting long-distance transport of articulated parts would be the rate of ligament decay and the combined size and shape of the object.

The place where an animal dies will have a great effect on the dispersal potential of its bones. For example, a skeleton lying in dense bush on a floodplain or levee has a lower chance for dispersal than one on open flats, simply because of the obstruction caused by vegetation. The trapping effect of vegetation, particularly along levees, would greatly reduce the probability of transporting bones from floodplains to channels or vice-versa. Levees might effectively trap bones during flood stages when the potential for burial is high, and thus would preserve a mixed or allochthonous fauna. Bones of animals that actually died on the levees would be preserved there only if they were buried before being destroyed by surface weathering. On the deltas, recent examples show a trapping and binding effect of grasses on bones which would prevent their movement unless the vegetation was destroyed (Plate 3).

Transport of parts of carcasses and isolated bones by predators and scavengers is also a factor in bone dispersal. This may be significant for individual carcasses, but it is probably not effective in moving an entire thanatocoenose away from the general area of the biocoenose, at least for large animals with fairly broad habitats. Specific cases may be important taphonomically, such as the dispersal of fish and crocodile remains away from aquatic environments by carnivore activity.

Re-excavation of buried bone is potentially important in floodplain situations with laterally eroding and aggrading channels and in lacustrine transgressions involving erosion of former shoreline deposits. Experimental evidence[1] shows that bones continue to lose organic matter (presumably used by soil bacteria) after burial and become very soft and friable after a few years of burial in wet sediment. Re-excavation would rapidly destroy all but the most durable parts, leaving teeth and compact bone fragments. Beaches or channels that erode into previous deposits would tend to concentrate teeth and the most durable bone fragments and redeposit them. In some cases, bones might become well enough mineralized during burial to survive re-excavation intact, particularly if they were protected by carbonate concentrations formed in floodplain or levee soils.

[1] Experiments are in progress on the shore of Lake Rudolf, where controlled samples of recent bone have been buried below the water table. These were examined in 1970 and 1972 for changes in color, weight, and surface texture. All ligaments joining originally articulated parts disappeared after one year of burial. After two years of burial, bones had lost 10–20% of their dry weight (loss of organic material) and had acquired a characteristic brown patina on their external surfaces. Otherwise there was minimal change in appearance, but all bones were soft and friable.

Diagenetic Factors

Bones can be destroyed after burial by a variety of processes. Bioturbation, in which sediment is mixed by the action of roots and burrowers, is probably an important factor in some cases of bone destruction. Once bone is softened underground by the loss of organic matter and by ground water, it could easily be penetrated and disrupted by the agents of bioturbation. This may account for the observed low frequency of bones in paleosol horizons in the East Rudolf deposits. In floodplain deposits, bones would be best preserved when the increments of sediment added during a flood were thicker than the average depth (e.g., 10–50 cm) of the root and burrow penetration that would affect the new land surface. Accumulations of this magnitude have been observed after a single major flood of a small river in central Colorado (McKee *et al.*, 1967:835). Rapidly aggrading floodplains lacking extensive plant cover would provide an ideal depositional situation for preserving floodplain thanatocoenoses with minimal subsurface destruction.

Compaction of sediment can crush and distort buried bones, particularly if they are wet and friable because of subsurface conditions. Distortion could occur if the bones are somehow decalcified and rubbery or if organic material has been lost, leaving a fragile structure of hydroxyapatite crystallites. The effects of compaction will be greater in clay-rich sediments that lose a significant volume of water when compacted. Clay units also may undergo a considerable degree of expansion and contraction, creating minor slickensides and joint systems. As noted by Dodson (1971: 55) this can cause breakage of enclosed bones, although the broken pieces may themselves be well preserved (B. Patterson, personal communication). Sandy units are less subject to compaction and fracturing, and enclosed bones will be less disturbed. Thus, for purely physical reasons relating to sediment type, bones buried in clays and silty clays will have much less chance of undisturbed preservation than bones buried in coarser sediments.

An abundance of $CaCO_3$ in a deposit, or the seasonal movements of ground water charged with a Ca^{++} and CO_2, may either help to preserve a buried bone or to destroy it. Bones can serve as centers of $CaCO_3$ nodule formation and are often permineralized with $CaCO_3$. In some cases, however, bones can be "exploded" by the outward growth of a carbonate nodule. East Rudolf fossils provide examples of this as well as bones which have breaks that are "healed" by $CaCO_3$ deposits. The processes of carbonate deposition in association with bones are poorly known. In some cases the original apatite is not altered by fossilization, as shown by unaltered carbon contents of recently fossilized bone apatite (Haynes, 1968). There is some evidence that the amount of organic matter in a buried bone will influence its fossilization, with fresher bones tending to encourage nodule formation (Konizeski, 1957:141). Environments with locally high concentrations of calcium, such as those associated with high-calcium vulcanism in the East African Rift System (Bishop, 1968:38), seem to promote thorough permineralization of bones and later resistance to surface destruction of the fossils.

Carbonate concentrations imply fairly alkaline soil conditions (Millar *et al.*, 1966: 143), which will be more likely to preserve bone than acid conditions. Rates for the dissolution of bones in association with acid soils are not known, but over time, even slight acidity (undersaturation of Ca^{++}) would contribute to their destruction.

Conclusions

The points of taphonomic interest for the interpretation of East Rudolf (and other) fossil assemblages include the following:

1) Mode of death will be of primary importance in determining which skeletal parts will be available for

fossilization. When carnivores exert their maximum effect on carcasses of relatively large animals (> 150 kg), skulls will be the most common residue, followed by vertebrae, ribs, pelves, and ends of long bones. Smaller animals may be destroyed entirely except for teeth and parts such as horn cores. Burial of articulated skeletons will occur rarely, and then only when scavenging is held to a minimum. The proportion of complete bones that survive scavenging will be a function of the density of carnivores in relation to prey at any particular place and time; the greater the carnivore density, the fewer the complete bones.

2) Terrestrial animals may have the best chances for complete preservation in environments that are not their normal habitat (e.g., drowned wildebeest buried in channel deposits). The parts of a thanatocoenose that are *not* subject to immediate transport will be the most useful in reconstructing a biocoenose. Once bones are disarticulated and exposed to weathering, their chances for dispersal away from the immediate area, without significant alteration of the thanatocoenose, are greatly reduced. Dispersal potentials are then dependent on the size, density and weight of each bone and its rate of destruction *in situ* or in transport.
3) Bones quickly show the effects of surface weathering after initial exposure (usually a matter of weeks or months), and they will not last more than 3 to 10 years under most surface conditions in any sort of intact state. Fossil bones with intact fresh-appearing surfaces were probably buried relatively soon after the death of the animal.
4) Teeth should outlast bones in most taphonomic situations, and small teeth will probably have a higher survival potential than large. Compact bone weathers and abrades more slowly than porous. Bones that have lost a good proportion of their residual organic content (collagen) will be more quickly abraded and destroyed during transport than fresh bones.
5) Well-preserved fossil bones record the fact that the deposit they are in has not been extensively reworked. Reworking should result in the fragmentation or total destruction of bones unless they are thoroughly mineralized. However, teeth may survive and be concentrated from older deposits.
6) Buried bones can be disrupted or destroyed by bioturbation, acid ground water, carbonate nodule formation, and movement of enclosing sediment with a high clay content. Alkaline conditions with available $CaCO_3$ are an optimal chemical environment for bone preservation.

CHARACTERISTICS OF RECENT BONES AS SEDIMENTARY PARTICLES

Vertebrate remains can be transported along with other material moving from place to place on the earth's surface. Bones from different sources can be mixed, and some can be carried long distances while others lag behind. In order to determine the ecological provenance of the bones, it is first necessary to understand their behavior in transport situations.

A few experiments have been done on bone transport under controlled conditions in laboratory flumes. Voorhies' (1969) study on the transport of disarticulated sheep and coyote skeletons provides data on bones of moderately large vertebrates. Dodson (1974) conducted flume experiments on the dispersal of mouse bones. His data show that mouse bones can be easily transported by relatively low velocity currents (6–35 cm/sec.), and he concludes that dispersal will be so great as to render the bones essentially useless for paleoecologic

Table 1. Voorhies dispersal groups: bones of sheep and coyote which are transported together in a flume with current velocities up to 152 cm/sec.

GROUP I	GROUP II	GROUP III
Immediately transported by flotation or by saltation.	Transported later than Group I, usually by traction.	Resisted transport, lagging far behind other groups.
RIBS	FEMUR	SKULL
VERTEBRA	TIBIA	MANDIBLE
SACRUM	HUMERUS	(ramus)
STERNUM	METAPODIAL	
(scapula)	PELVIS	
(phalanx)	RADIUS	
(ulna)	(scapula)	
	(ramus)	
	(phalanx)	
	(ulna)	

Parentheses indicate occurrence in more than one group.

(From Voorhies, 1969)

interpretations (Dodson, 1973:82). However, Voorhies' data show that most sheep and coyote bones require greater current velocities to move, and that distinct groups of bones with different dispersal potentials form at velocities comparable to those found in natural streams (~ 20–150 cm/sec. (Leopold *et al.*, 1964:166)).

The dispersal groups of bones (referred to as "Voorhies Groups"), are shown in Table 1. These are formed of skeletal parts that tend to be transported together as the current velocity in a flume is increased to a maximum of 152 cm/sec. Fifteen separate trials were run and the results averaged to give the three dispersal groups (Voorhies, 1969:66).

Voorhies' work shows that different bones require different minimum fluid shear stresses for transport. This provides a valuable basis for interpreting fossil assemblages of bones of sheep and coyote size. An assemblage composed primarily of either Group I, Group II or Group III would indicate that sorting processes related to transport had been operating on the original thanatocoenose. An assemblage composed of Group III would retain more paleoecologic information than one consisting of Group I or II, since this group requires the greatest stress for transport.

The flume data are restricted to sheep and coyote bones and provide little direct information on how bones of other animals, of other sizes, will sort under current action. However, Voorhies' data can be used to indicate the relative importance of basic characters of bones in forming the dispersal groups. These characters are size, density and shape, the important parameters of any sedimentary particle. In order to show how these parameters affect bone transport, it

is necessary to understand how they affect the transport of sedimentary particles in general. The principles and formulae that describe fluid-particle interactions are reviewed in a number of recent texts, and references used for this study include J. Allen (1970), Pettijohn *et al.* (1972), and Shapiro (1961).

Properties of Bones as Sedimentary Particles

Data on the sizes, densities and shapes of bones are necessary for a theoretical consideration of bones as sedimentary particles. Since there is little or no information of this kind available, it was necessary to carry out a series of measurements to determine the general range of densities and sizes (volumes and weights) of bones. These provide the basis for subsequent discussion of bone transport potentials.

Measurements of Bone Size and Density

In order to relate the characters of measured bones to the East Rudolf fossil assemblages, bones of recent representatives of fossil taxa were used. These included museum skeletons of hippopotamus, zebra, a large and a small antelope (*Redunca, Damaliscus*), and a pig (*Hylochoerus*), as well as parts of two crocodiles and various fish species. In addition, the skeleton of a sheep was used for comparison of size and density characters with Voorhies' flume data. The bones included variable amounts of residual organic material, but in general were thoroughly degreased.

Volumes and weights were measured for each bone. Volumes were measured by a simple water-displacement method. Bones were soaked for 5 minutes, or until bubbling stopped, and then measured for volume which included the absorbed water. Wet-weight, also including this water, was measured, in order to derive a wet density for each bone. Wet density is the parameter of interest if bones are transported while wet and take up water quickly upon immersion. Rates of water uptake will be discussed further below.

Densities, weights and volumes of most of the skeletal parts of the animals listed above are given in Appendix 1. In general, densities range from less than 1.0 to about 2.3, volumes from 1.0 to 3000 cc, and weights from 1.5 to 4900 grams (g). Bone densities are comparable for all mammals except hippos, which are generally slightly higher. Crocodile and fish bones have generally higher densities than mammal bones. Within each skeleton, the range of densities is very broad, from foot bones and vertebrae that float to teeth, which are the heaviest parts for their size.

How representative are these measurements of bones that are actually parts of natural thanatocoenoses? Several possible sources of error can be examined and their overall importance analyzed:

1) *Differential uptake of water.* It was apparent during the measurements of volumes that bones varied in their rates of immediate water absorption. Some floated for several hours with essentially no water gain, while others were immediately permeated. In nearly all cases the major weight gain from water uptake occurred in the first 1–5 minutes of immersion. Figure 2 shows the rates of water absorption for various bones. It is significant that the naturally weathered bovid femur gained all of its water in the first moments of immersion, while the museum femur continued to gain weight after 70 hours of soaking. This indicates air pockets in the unweathered bones which are probably blocked by organic matter. All pores are open in the weathered bone and water quickly permeates it.

   Naturally occurring, unweathered bones also will have trapped air pockets that can lower their densities during initial transport. However, the rates of surface weathering are rapid enough so that most exposed bone

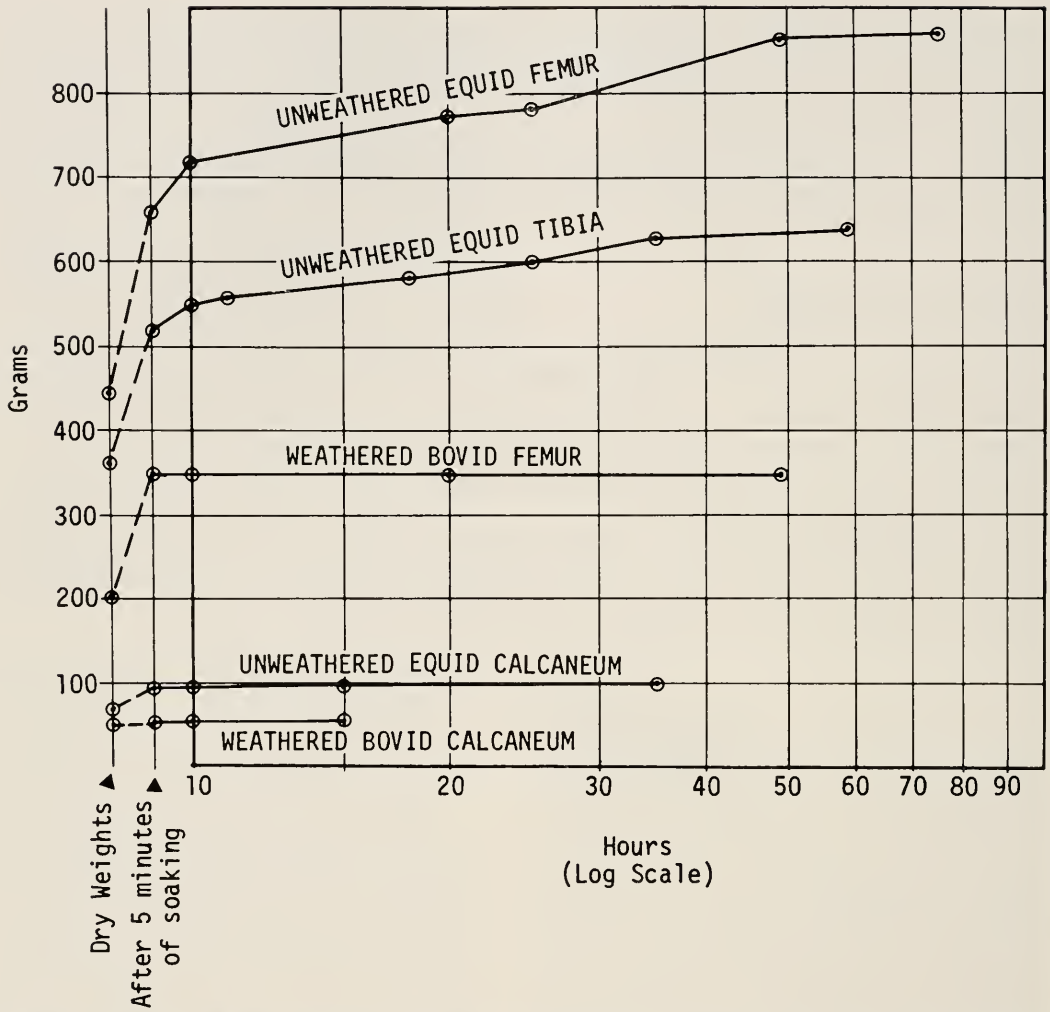

Figure 2. Water uptake rates of different mammal bones. Weathered bones and small or compact bones gain essentially all of their water content within five minutes of soaking. Large, unweathered bones with residual organic matter gain weight more slowly as pockets of trapped air are gradually displaced.

would become permeable in a matter of a few months. Therefore, the museum assemblage differs from natural ones in its greater number of blocked pore spaces, which will tend to lower the measured densities. For the larger and more porous parts, the wet weights and densities recorded in Appendix 1 are thus *minimum* estimates of these measures for naturally weathered bones.

2) *The original organic content of the bones.* Aside from contributing to air entrapment in a bone, residual organic matter probably does little to affect its overall weight and density. The density of cartilage is 1.1 and tendon 1.3 (Currey, 1970:30). Other tissues have densities close to 1.0 since they are composed primarily of water. A bone filled with water should have about the same weight as a bone filled with tissue, and after initial submergence, the two would have

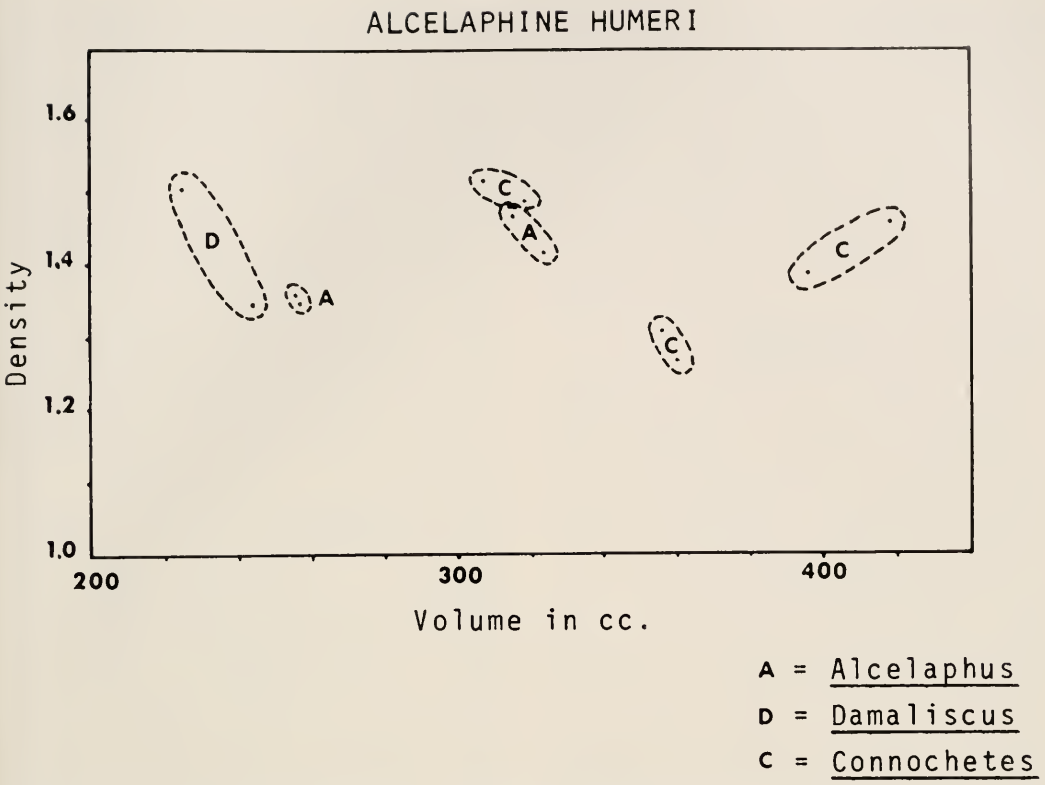

Figure 3. Graphs showing density variation in a sample of 12 alcelaphine humeri. Dotted lines encircle the left and right bones from the same animal. Density differences between right and left of a pair are due to variation in the amount of air initially trapped in the bones. Density differences between pairs may be due in part to original variations in the amount of bone per cubic centimeter in the individual animals.

approximately the same density, other factors being equal.

3) *Variations in bones from different individuals.* The same skeletal part may vary in density in individuals of the same group of animals because of body size, age, diet, etc. How great is this variation? A series of humeri from a single bovid group were measured in order to answer this question. Figure 3 shows that the humeri vary from 1.27 to 1.52 in density. Density variations owing to differential water uptake are indicated by the differences between right and left sides. Compared with the range in volume, there is relatively little variation in the densities of humeri from the different genera. It appears that differential uptake of water is more important in affecting the densities of fresh bones than variations between individuals of different sizes or genera. Experimental work on the density variations of weathered bones should be done, but it seems probable that individual variation in similar skeletal parts is not an important factor affecting bone dispersal potentials.

4) *Experimental error.* Repeated trials showed this to be much less than other causes of density and weight variation. The error was generally less than 5 percent for wet weight and volume.

The differential uptake of water in fresh

bones appears to be the major factor that may cause the measurements given in Appendix 1 to be different (i.e., lower) than the actual properties of naturally occurring, waterlogged bones. Measurements of weights and densities of weathered bones and thoroughly waterlogged fresh bones (Fig. 2) indicate that the densities given in Appendix 1 are within about 15 percent of the true densities for large, porous bones and are much closer for smaller, more compact ones.

Published data on bone density indicates a range similar to that given in Appendix 1. Samples of porous (cancellous) and compact (cortex) human bone have densities of 1.78 and 1.88, respectively (Johnson, 1965:550). Currey (1970:30) lists the specific gravity of "bone" as 2.0, "ear bone" (= petrous part of temporal) as 2.4 and tooth enamel as 2.6. The density of the bone mineral, hydroxyapatite, is 3.1 to 3.2 (Berry and Mason, 1959:454). (Published determinations of bone density usually relate to a cubic centimeter of average boney material, not the bulk density of whole bones, which is less owing to the number of naturally occurring open spaces and the presence of trapped air pockets.)

From the above discussion, it can be concluded that measurements of bone size and density as given in Appendix 1 are generally representative of the variation that would be present in a natural bone assemblage, and they can be used to predict hydraulic behavior if the limitations of the data are kept in mind. For the following discussion of the relative dispersal potentials of bones, absolute measures of bone density, etc., are less important than consistent differences in the *relative* properties of different skeletal parts.

Relative Dispersal Potential of Bones

How does the dispersal potential (probability of transport) of bones relate to characters of size, density and shape? This can be shown by plotting density versus wet weight for all the skeletal parts of the sheep, as given in Appendix 1, and comparing the distribution of bones with the Voorhies Groups. Figure 4 shows that Group I consists of the smallest, lowest density bones. Groups II and III are composed of bones that are denser than those of Group I but not necessarily larger. Density appears to be more important than size in determining whether bones will disperse with Group I.

The scapula and mandibular ramus (with teeth) fall within Group II on Figure 4 although they do not always belong there according to the flume experiments (Table 1). The scapula can belong to Group 1, yet its size and density do not show this. The shape factor must be operating to increase the dispersal potential of the scapula, and this is reasonable considering its high surface area to volume ratio. Its form, with the spine projecting at right angles to the scapular blade, also would contribute to bottom instability. The ramus, on the other hand, is more of a lag element (Group III) than its size and density indicate. Its surface area to volume ratio is fairly high, and this should operate to make it more transportable. However, as noted by Voorhies (1969:67), rami have a convex-up (buccal side up) stable bottom position and are relatively flat. Once they attain a stable bottom position, the size and density combine with a relatively small cross-sectional area (as seen by the current) to decrease transport potential.

It is clear that density and size characters of bones can explain their dispersal potential as shown by Voorhies Groups, with shape becoming an important factor only for particular bones. Although natural transport conditions will vary greatly from those of the flume, the sorting of groups of bones with different transport potentials would seem an inevitable consequence of their differences in size, density and shape. Dispersal groups of bones of sheep size and above should form at current velocities found in natural flow conditions, unless these flows are competent enough to carry

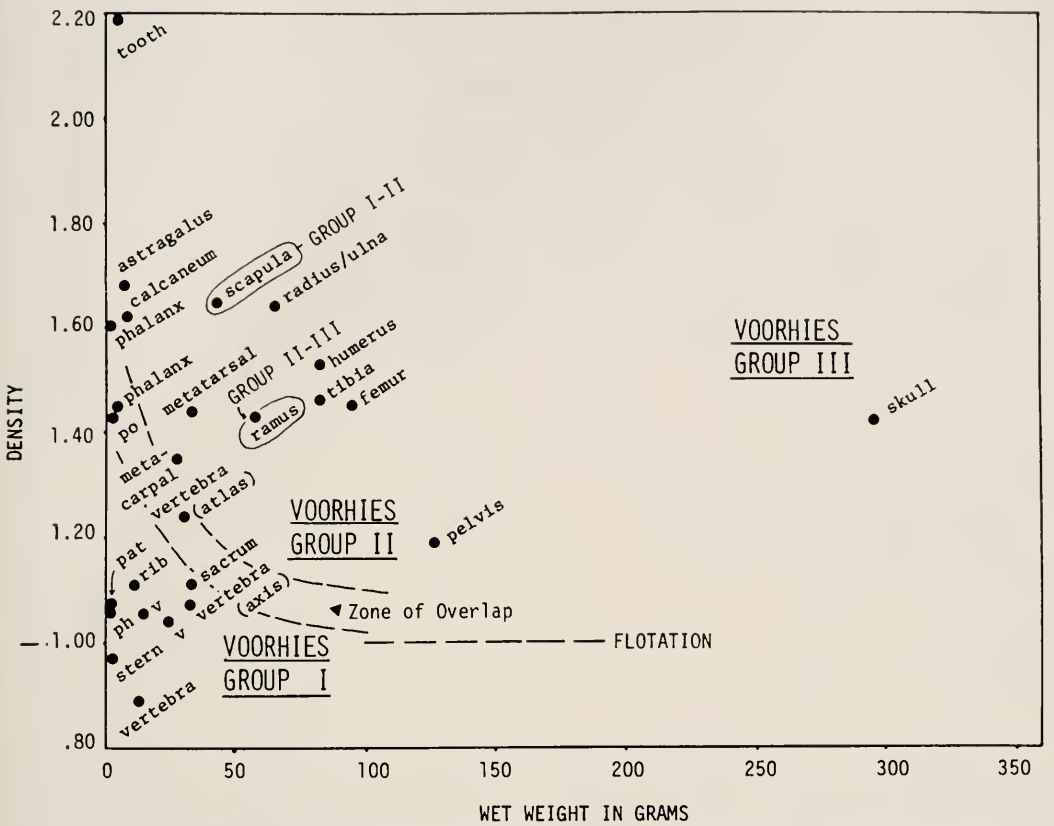

Figure 4. Plot of density versus wet weight for sheep bones showing that these two variables can be related to the Voorhies Dispersal Groups. Group I is the most easily transported according to Voorhies' flume experiments, and Group I elements have low densities and/or weights. The scapula and ramus, which do not plot within their dispersal group, indicate that shape has an important effect in their potential for transport under fluid stress. Abbreviations: po = podial, pat = patella, v = vertebra, ph = phalanx, stern = sternum.

all bones together (e.g., high density mudflows).

Using density and weight data for the other animals given in Appendix 1, it is possible to predict, in general, which bones of these animals would sort out with Voorhies Groups I, II and III, under the same experimental conditions. Those elements which fall in the Group I zone and in the mixed Groups I/II zone are listed for each animal in Table 2. If these were placed in the flume with the sheep bones, their size and density should cause them to sort out with the easily dispersed group, and they would be transported away from the other skeletal parts. For the different animals, the same skeletal parts are consistently present in Group I, but the number of Group I elements decreases with increased animal size.

Since Voorhies Group I is the most easily affected by transport, its presence or absence in fossil assemblages can provide specific information on the sedimentary history of these assemblages. For example, if one of the East Rudolf assemblages were composed only of bovid vertebrae and ribs, equid vertebrae, terminal phalanges of hippos, etc., then this would almost surely represent a transported, allochthonous bone concentration. Various models of this kind can be constructed for later comparison

Table 2. Bones of different sized recent animals which should disperse as Voorhies Group I or Group I/II under fluid stress. The dispersal potential of most of these bones is determined by their low weight and/or density. All other bones should lag behind. Bones in Group I/II are shown in lower case.

OVIS	REDUNCINE	SUID	ALCELAPHINE	EQUUS	HIPPO	CROCODYLUS	FISH
Phalanges	Ulna	Podial	Phalanges(t)	Calcaneum	Phalanges(t)	Scutes	Pectoral
Sacrum	Podial	Phalanges	Rib	Podials	Sesamoids	--	Spine (Bagrus)
Sternum	Sacrum	Patella	Ulna-P	Phalanges	--	scutes	Skull (Lates)
Vertebrae	Vertebrae	Sesamoids	Vert. Cent.	Vertebrae	phalanges(t)	small teeth	--
Axis	Atlas	--	Sesamoids	Cervical	phalanges		pectoral
Cervical	Axis	rib	--	Lumbar	sesamoids		pectoral + spine
Thoracic	Cervical	astragalus	podial	Patella			skull parts (Clarius)
Lumbar	Thoracic	podial	phalanges	Vert. Cent.			
Patella	Patella	phalanges	vertebrae	Sesamoids			
Humerus-P	Ulna-P		cervical	--			
Metacarp-D	Vert. Cent.		lumbar	vert.-thor.			
Vert. Cent.	Sesamoids		patella	rib			
Rib	Phalanges		rib	calcaneum			
Sesamoids	--			astragalus			
--	calcaneum						
astragalus	phalanges						
podial	vert.-lumb.						
vert.-atlas	rib						
metatars-P							
metacarp-P							
phalanges							

Vert. = Vertebra
(t) = Terminal
P = Proximal
D = Distal

with the fossil assemblages. These are summarized in Figure 5. Three basic kinds of assemblages can occur, with transitional phases: "undisturbed" (Groups I, II, III), "winnowed" and "lag" (Groups II, III), or "transported" (Group I), in decreasing order of paleoecological importance.

The proportions of different Voorhies Groups in fossil assemblages should provide evidence for the proximity of fossils to the original thanatocoenose and the habitats of the living animals. This is a different approach from that of Shotwell (1955, 1963), who attempted to distinguish proximal and distal (more transported) paleocommunities on the basis of numbers of different skeletal parts representing each fossil taxon. The basis for Shotwell's method was the idea that the proximity of an animal's habitat to the site of deposition would increase the number of different skeletal parts that were likely to be preserved together. As Voorhies (1969:53) has pointed out, the number of different parts is less important than their characteristics of sorting. Figure 5 shows that a single large or dense Group III bone, such as a skull, could have more paleoecologic significance than a large number of Group I bones, such as vertebrae, ribs, podials, etc. For both small animals and large, bones vary enough in relative dispersal potential so that the proportions of different dispersal groups, rather than the absolute numbers of different bones, will provide the most useful taphonomic information.

The Hydraulic Equivalence of Bones and Quartz Grains

The size of a quartz grain that is hydraulically equivalent to any given bone can be calculated by using either direct measurements of the bone's settling velocity or calculations based on the properties of size, density and shape of the bone. The

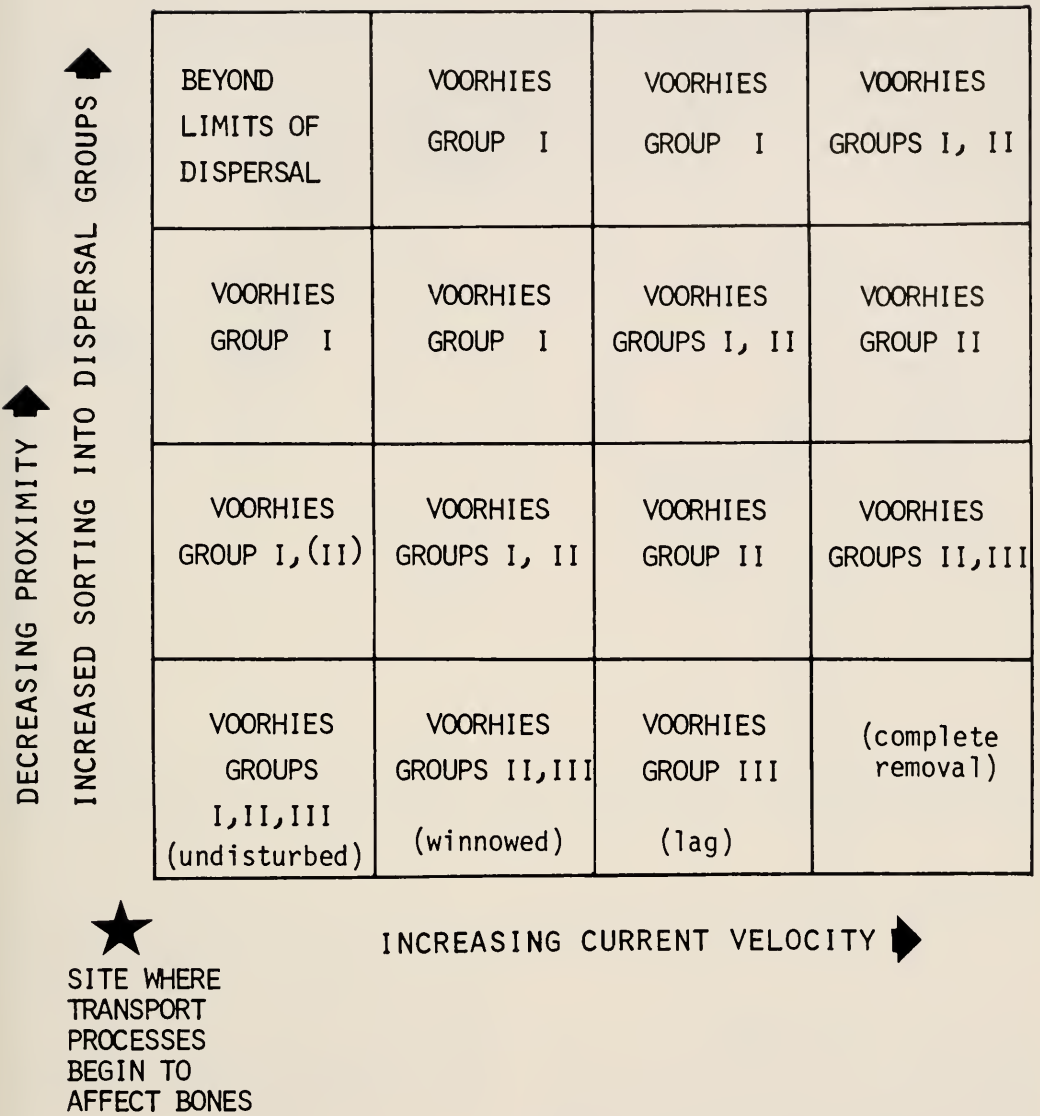

Figure 5. The formation of hypothetical dispersal groups of bones according to current velocity and proximity to the place where bones begin transport (usually the site of death). The bones included in each Voorhies Group are given in Table 2. For bones that have been disarticulated prior to transport, the three groupings on the bottom part of the chart represent the skeletal associations most "proximal" to the place of disarticulation. For fossil vertebrates, such associations can provide the most paleoecologic information on the habitats of the living animals, when examined in the context of the sedimentary environment where the bones were preserved.

equations for calculating hydraulic equivalence are given in Appendix 2. Since the shape factor is very difficult to quantify, calculations of quartz equivalence are of limited value without actual experimental data on bone-settling velocities. A series of such experiments was conducted which provides information on the relative importance of the shape factor in affecting settling velocities.

Table 3. Experimental data on bone settling velocities and hydraulic equivalents. Measured settling velocities shown below are averaged from 10 separate trials.

	Bone Volume cc.	Bone Density gm/cc	Measured Settling Velocity (v_s) cm/sec	Diameter of Quartz Equivalent (d_q) mm	Predicted Settling Velocity (for a sphere) (v_p) cm/sec	(v_p)-(v_s)
Vertebral Centrum #1	25.2	1.10	16.7	2.6	15.4	-1.3
Vertebral Centrum #2	29.0	1.14	21.9	4.4	18.7	-3.2
Phalanx (Suid)	13.4	1.14	20.0	3.7	16.4	-3.6
Patella (Ovis)	4.3	1.33	17.9	3.0	20.9	3.0
Calcaneum (Bovid)	13.2	1.39	22.7	4.8	27.3	4.6
Scapula (Ovis)	39.0	1.41	33.6	10.5	33.6	0.0
Axis (Bovid)	88.0	1.42	34.5	10.1	38.9	4.4
Metatarsal (Bovid)	48.0	1.51	29.8	8.2	30.0	0.2
Tibia-Dist. (Bovid)	10.3	1.56	27.1	6.8	31.4	4.3
Astragalus (Bovid)	7.0	1.76	31.8	9.4	34.3	2.5
Premolar (Hippo)	16.7	2.03	38.5	13.8	46.2	7.7
Molar (Equus)	40.0	2.12	53.8	26.9	55.7	1.9
Molar (Ovis)	2.6	2.12	30.5	8.6	35.4	4.9
Rib (Bovid)	25.0	1.43	18.3	3.1	31.9	13.6
Rib Part (Ovis)	14.2	1.46	20.8	4.0	30.2	9.4
Scute (Croc.)	4.5	1.69	18.4	3.1	24.5	6.1

Experiments in Bone-Settling Velocities

The settling velocities of 16 vertebrate bones of varying size, density, and shape were measured by using a stop watch and a large plexiglass tank (30 cm × 60 cm × 60 cm). The length of fall was 50 cm, and each bone was dropped ten times from the same initial orientation just below the surface of the water. All bones were thoroughly soaked before the settling experiments. The average settling velocities for each bone are given in Table 3.

The diameters of quartz spheres (d_q) that would settle at the same rates as the bones can be calculated by using the equation:

$$d_q = \frac{2 \cdot (v_s)^2}{4/3 \cdot g \cdot (\rho_q - 1)}$$

$$d_q = .000928 \cdot v_s^2$$

d_q = quartz diameter
v_s = bone settling velocity
g = 980 cm/sec^2
ρ_q = quartz density, = 2.65

The quartz equivalents given in Table 3 show that the bones are comparable to coarse sand- to pebble-grain sizes. The

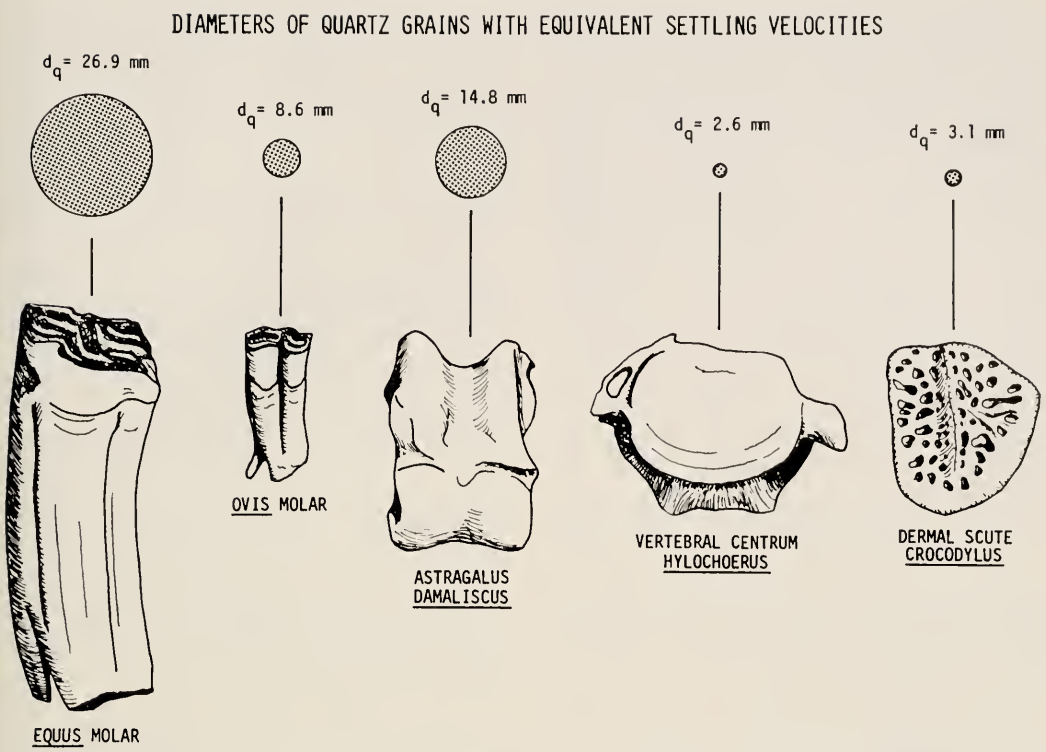

Figure 6. The hydraulic equivalents of different recent bones, as determined by settling velocity experiments. The equivalent quartz grain sizes were calculated using the method shown on Page 492 and the data given in Table 3. Density variation in the bones is the primary factor causing the variability of the hydraulically equivalent grain sizes. (Bones and grains are drawn to correct relative sizes.)

variation in bone-quartz equivalence is shown graphically in Figure 6. It is obvious that the lighter bones, such as the vertebral centrum, and bones with high surface area to volume ratios, such as the crocodile scute, will be more easily transported than the heavier and more spherical bones. The quartz equivalents agree well with the evidence for differential dispersal potentials of these bones from Voorhies' (1969) flume study. Combined evidence from the settling velocity and flume experiments provide the general background necessary for predicting the behavior of bones in transport situations. More work is needed, however, since in specific cases, the hydraulic equivalence and flume data do not agree. The sheep scapula, for instance, has a relatively large quartz equivalent (10.5 mm), which is inconsistent with its high potential for dispersal in Voorhies Groups I/II.

The Hydraulic Equivalents of Fossil Bones

It would be useful to be able to predict, in general, the original quartz equivalent of any given fossil bone. Such data could then be compared with matrix grain sizes associated with the fossils. The quartz equivalent of any object can be calculated if its density and volume are known, and if shape can be disregarded or corrected for. The basic equation is:

$$d_q = (\rho_b - 1) \cdot d_b / 1.65$$

d_b = Nominal diameter of the bone = $\sqrt[3]{1.91 \times \text{Volume}}$

ρ_b = Bone density

For bones, the crucial question is, "How important is shape in affecting the size of the quartz equivalent?" This can be clarified by comparing the actual settling velocities of bones with predicted rates based only on volume and density. Table 3 shows that most predicted settling velocities are faster than the measured rates, by an average of about 12 percent. For the lightest bones, the predictions indicate slower rates than are actually observed, with an average error of about 14 percent. The ribs and crocodile scute show a much greater difference, with predicted settling velocities exceeding the observed velocities by 33 to 74 percent.

For most bones, it will be possible to estimate quartz equivalents by using volume and density, and to estimate a possible range of error owing to the shape factor. For bones that have predicted settling velocities within ± 15 percent of the actual settling velocities, the quartz equivalents can be estimated within about ± 25 percent. Most bone shapes will fall within this range. Although the range of possible equivalent quartz sizes is broad, it should be possible to equate bones with general grain-size groups such as coarse sand, pebbles, etc. Bones with high surface area to volume ratios, such as ribs and crocodile scutes, will have a much broader range of possible quartz equivalents, and cannot be satisfactorily approximated using the method described above.

Table 4. Average densities of porous and compact bones and teeth.

	Porous	Compact	Teeth
No. in sample	14	18	10
Mean	1.11	1.65	1.96
Range	1.01–1.29	1.36–2.00	1.70–2.24

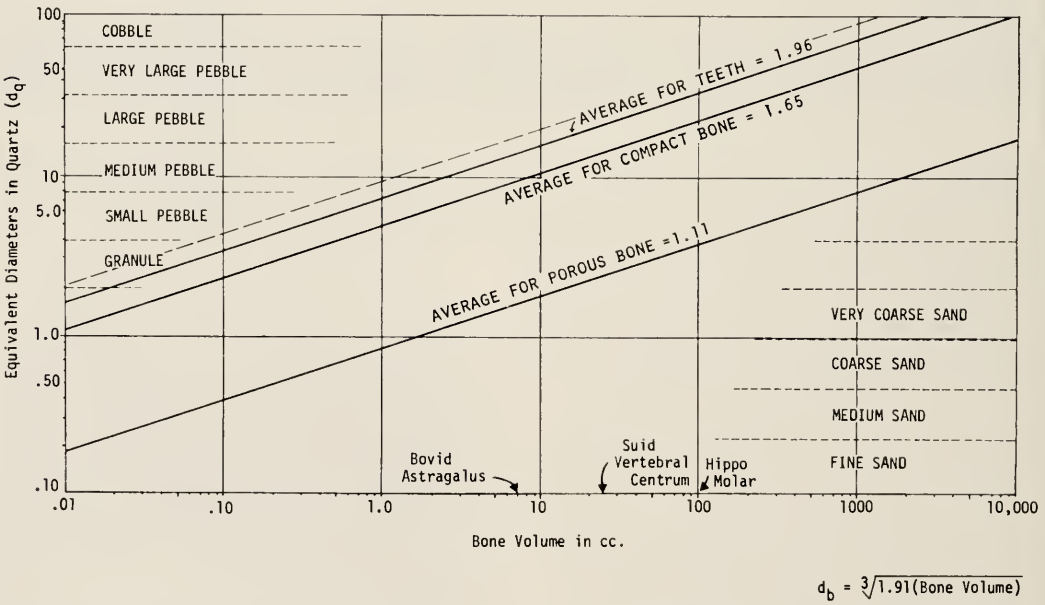

Figure 7. A log-log graph relating bone volumes to hydraulically equivalent spherical quartz grains for three average bone densities: 1.11, 1.65 and 1.96. Given the volume of any recent (or fossil) bone and a measure (or estimate) of its density, a range of hydraulic equivalents can be read off the ordinate. This estimate should be within ±25% of the actual quartz equivalent (d_q) for most bones, with the exception of high surface area to volume bones such as ribs. See Appendix 2 for method of calculating hydraulic equivalence (d_b = nominal diameter of bone).

Quartz equivalence gives the size of quartz grains that would settle at the same rate as a given bone. This is not necessarily the size of quartz grains that would be transported with the bone. However, settling velocities are related to transport potential, as shown by the Drag and Critical Stress formulas (Pettijohn *et al.*, 1972:335), and hydraulic equivalence provides a general idea of how bone and sediment sizes should be related if both are transported by similar processes.

For fossil bones, an important factor in calculating hydraulic equivalence lies in correctly estimating the original density. Mammalian skeletal parts are composed of three basic structural components of differing densities; porous bone, compact bone and enamel/dentine. Most whole bones include both porous and compact parts, and overall densities range between the two. It may not be possible to tell the original proportions of porous and compact bone in a fossil, but the original density should lie between the average values for each structural type. This will put upper and lower limits on predicted values for quartz equivalents.

In order to obtain representative average densities, the data given in Appendix 2 were averaged for teeth and a selection of the most porous and the most compact bones. The porous bones include patellae, vertebral centra and terminal phalanges, while the compact bones include metatarsals, distal tibiae, scapulae and ribs. These provide generalized but realistic average densities for porous and compact bones (Table 4). Using the average densities, it is possible to construct a graph relating bone volume to equivalent quartz grain sizes (Fig. 7).

Figure 7 can be used to relate fossil bones to hydraulically equivalent quartz grains in a general way. A rather low level of resolution is all that can be expected considering both the wide range of quartz diameters that are possible owing to the shape factor ($\pm 25\%$) and the problems encountered in estimating the densities of fossil bones. However, this is enough to provide useful information. Thus, a 100 cc tooth (e.g., a large hippo molar), is theoretically equivalent to a quartz pebble between about 34 and 56 mm (nominal diameter). The tooth is within the large to very large pebble size range. A bovid astragalus of 7.0 cc, considered as a compact bone, has an estimated range of quartz equivalents between 7.3 and 12.3 mm (9.8 mm $\pm$ 25%). The actual quartz equivalent of an astragalus of this size was measured at 9.4 mm (Table 3). Thus, Figure 7 can be used to estimate ranges of quartz equivalents possible for fossil bones (excluding ribs, scapulae, etc.), and in most cases the actual quartz equivalents will probably be close to the median of this range.

Current Velocities and Bone Transport

Since bones of different sizes and densities can be related in a general way to hydraulically equivalent quartz grains, it is theoretically possible to predict what current velocities are needed to move bone particles. This can be done by using the graph of J. Allen (1965: 109) which relates current velocities to quartz grain sizes in terms of transport and deposition (Fig. 8). The scale for quartz grain size is simply converted to scales for bone grain size at each of the three average density values. Thus, it should take a flow velocity of about 80 cm/sec. to move a bovid metapodial of 100 cc (nominal diameter = 5.7 cm). To move large mammal bones (1000 cc, nominal diameter = 12.4 cm) should require flows of over 150 cm/sec.

From a theoretical standpoint, bones of the size range for most East African mammals should be transportable in flow velocities of between 10 and 150 cm/sec. Bones > 1000 cc of animals such as hippo, rhino and elephant will disperse much less readily, and only at flow velocities of > 150 cm/sec. Predictions for the transport velocities of any bone or bone assemblage

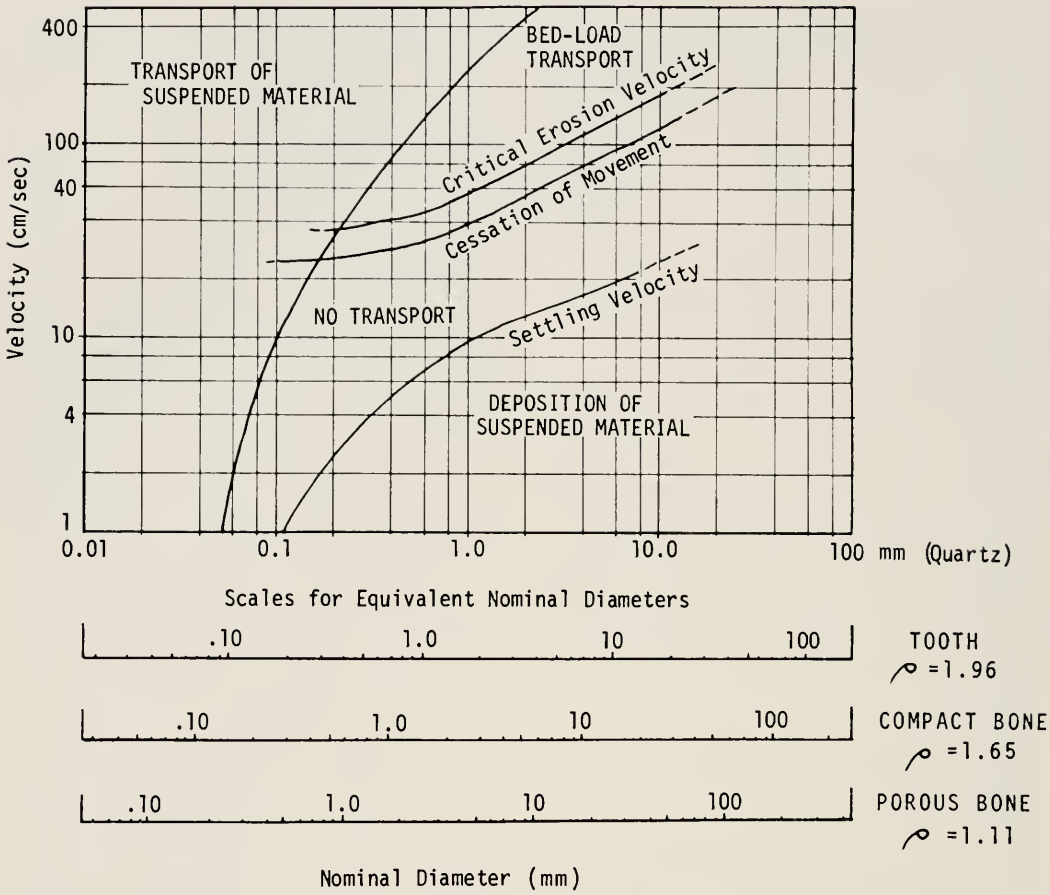

Figure 8. Theoretical transport velocities for bones, using the graph of J. Allen (1965: 109), which plots quartz grain sizes against current velocities. The three lower scales show nominal diameters of bones of three average densities. These scales give the calculated hydraulic equivalents of the quartz grain sizes shown directly above them on the abscissa of the graph. Bones and quartz grains are considered as ideal spheres. The actual shapes of bones will cause their quartz equivalents to range between about ±25% of the quartz equivalent for a sphere (with a broader range for ribs and other high surface area to volume bones).

are possible if volumes are known. The theoretical framework for bone transport should be tested experimentally to determine how closely predictions fit facts.[2] However, until such experimentation can be carried out, the theory provides a general framework for understanding bones as sedimentary particles.

[2] Allen's (1965) graph refers to the current velocity necessary to move a particular grain *on a bed of similar-sized grains*. Therefore, the analogy to bones must be restricted to those bones which are associated with a bed of clasts of similar nominal diameter (or, more precisely, on a bed of bones of similar shape and size). Preliminary flume experiments conducted in 1974 (subsequent to the completion of the above manuscript) indicate that bones on a bed of smaller grain size will move at lower current velocities than those predicted from Figure 8. Experiments in a natural stream show that large bones (e.g., a cow tibia) on a sand and gravel bottom may not move even at mean flow velocities of 150 cm/sec. However, in both flume and stream experiments, the Voorhies Groups for bone sorting remain valid.

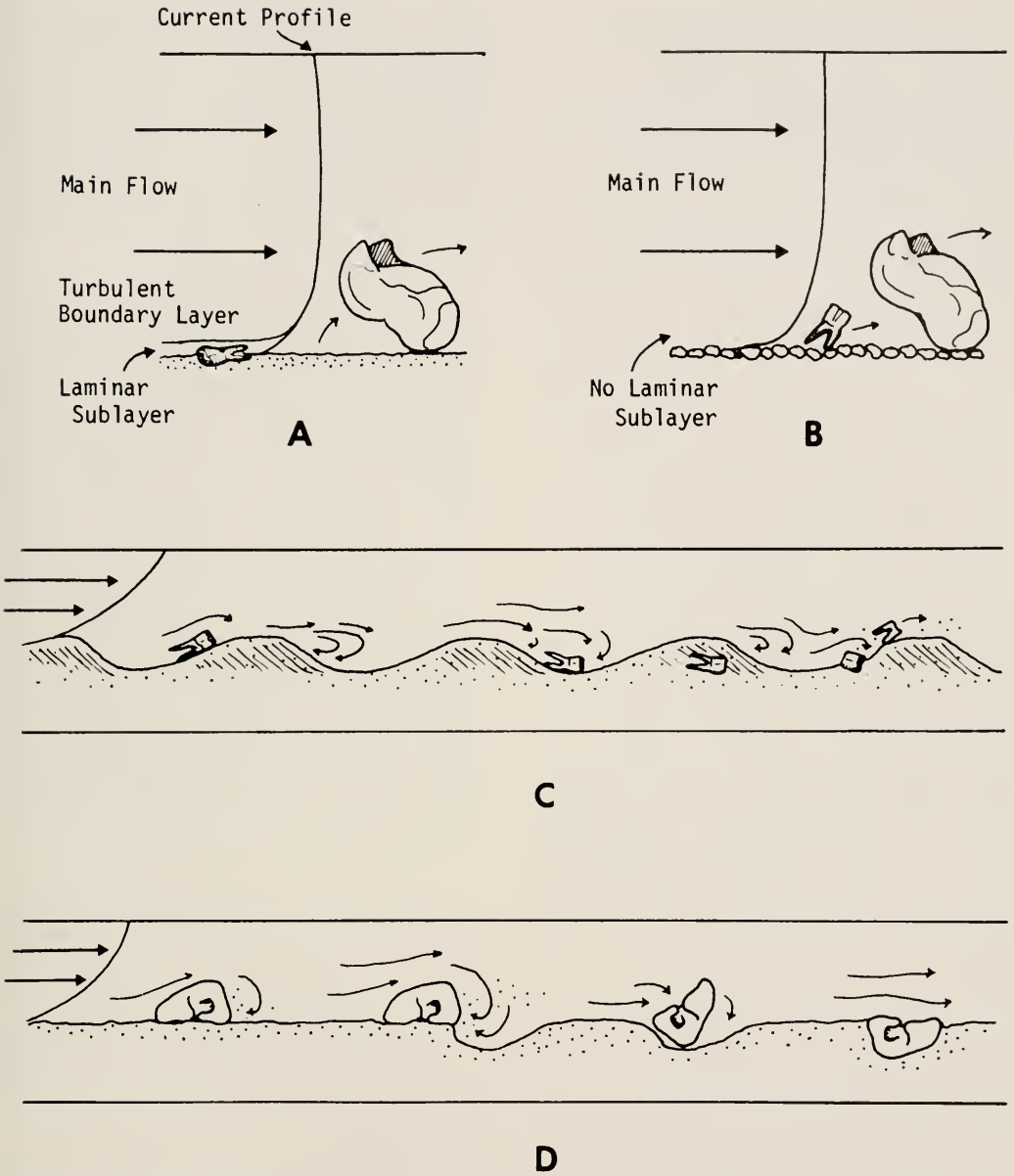

Figure 9. The effects of current profile and bottom morphology on bone transport: A, a small tooth remains at rest in the low-velocity laminar sublayer while an astragalus is moved by the turbulent boundary layer; B, on a coarser bottom with no laminar sublayer, both tooth and astragalus are transported together; C, a tooth is dropped on the downstream side of migrating ripples, buried, and re-excavated, losing its roots during the erosional period; D, a metapodial (seen end-on) creates turbulence and a scour pit, rolls into the scour pit and is buried.

Additional Factors Affecting Bone Transport in Natural Situations

Many factors can affect bone transport besides the basic parameters of size, density and shape. These primarily concern the character of the environment where transport occurs (e.g., channels) and the nature of the fluid flow.

Bottom Morphology and Current Profile

Stream velocities in natural situations are on the order of 20–150 cm/sec., with flood velocities reaching over 400 cm/sec. (Leopold *et al.*, 1964:167). However, these are *mean* velocities for the flow, measured at about 40 percent of the total depth above the bottom of the channel (for a channel 10 m deep, mean velocity is at about 4 m above the channel bottom). Velocities at the bottom of a channel are usually much less, and vary widely according to bottom morphology. The rate of decrease of current velocity near the base of a flow is plotted as a "current profile" (Fig. 9).

If the channel bottom is smooth, a thin, low velocity sublayer will separate turbulent flow in the main part of the channel from the sediment interface (Pettijohn *et al.*, 1972:333). Particles that are smaller than the depth of the sublayer may be left behind as lag while larger particles that penetrate into the main flow are transported. In this way, very small or flat bones and teeth could be sorted from larger bones, creating lag and transport groups that might not fit predictions based on relative settling velocities. It is possible that this had some effect on the lag behavior of jaws in Voorhies' (1969:66) experiments, since his flume had a fine-grained, smooth-surfaced bed.

If a channel bottom is rough, the turbulent boundary layer extends to the surface of the bed, and the velocity of the flow increases upward less abruptly than for smooth beds (Pettijohn *et al.*, 1972:334). Ripples and dunes or coarse sediment can cause this effect. A relatively large bone transported as part of the bed load over a smooth bottom would tend to be retarded if it encountered a rough bottom by the decrease in the velocity gradient. In areas of active dunes or ripples, the bone should have a good chance of being buried by the advancing bed forms (Fig. 9). Bones would also tend to be retarded or trapped in areas of coarser sediment such as gravel bars. Not only does the bottom velocity decrease over gravel, but the critical boundary stress for a bone among large particles greatly increases. This is related to the "kinematic wave" effect of Langbein and Leopold (1968), in which large particles tend to concentrate other large particles during sediment transport.

Fluid Density

Fluid density is generally considered to be close to 1.0. However, if it is increased by a large suspended load, then bones will be transported more easily. A high density boundary layer or a sediment-charged flow resulting from a flood can significantly increase the ability of a flow to transport bones. Sorting of bones that are less than or equal to the density of the flow would not occur since all would "float," regardless of size. This is one of the only ways to produce a completely unsorted but transported bone assemblage, where current velocity and fluid density are large enough that bones of all sizes and densities become part of the suspended load. This would be a very unusual natural transport situation.

Burial Potential

The more easily a bone can be buried, the less likely it is to be transported any significant distance. Bottom conditions will have an important effect. Loosely packed sand or soft mud can effectively anchor a bone, particularly if it has projecting parts. A scapula would be unstable if oriented spine-down on a hard bottom, but would be quite stable if the spine were buried in bottom sediment. This would instantly convert a Voorhies Group I/II bone to Group III "lag."

The potential for deep burial of large particles in active channels is low, even under heavy flow conditions (Leopold *et al.*, 1966:213). Low density elements such as bones would have little potential for deep burial during sediment movement un-

less covered by advancing dune or ripple fronts. Flow separation and turbulence on the leeward side of a ripple or dune is likely to trap larger particles at the base of the slip face where they can be buried (Fig. 9). As the ripple moves on, the bone may be re-excavated and carried further. Thus, progression of a bone down a channel with active bed forms would be a series of stops and starts, with a good deal of abrasion occurring during each re-excavation.

Larger bones that are beyond the carrying capacity of the flow may also move slowly along the bottom due to localized effects on the flow. A large particle on a sandy bottom creates turbulence and eddies on its leeward side which will tend to remove the sand, creating a scour pit (Leopold *et al.*, 1966). The bone could be tipped into its scour pit and buried, or a new scour pit could form, thus moving it slowly downstream (Fig. 9). A good deal of abrasion would occur during this process.

The most likely places for final burial are in the actively aggrading parts of a channel such as point bars and sand or gravel bars, or in the fill phase of scour-and-fill. Bones will move along a channel, suffering progressive abrasion, until they encounter such a situation.

Conclusions: Bones as Sedimentary Particles

A number of points can be made which are relevant to the interpretation of fossil assemblages. These are as follows:

1) Densities of bones soaked in water for five minutes vary from less than 1.0 to about 2.00, and teeth range from about 1.7 to 2.24. Variation in the densities of bones available for transport is high owing to differences in densities of different skeletal parts and to the presence of trapped air pockets in bones with remaining organic matter.
2) For mammal bones of sheep size and above, current velocities typical of sedimentary systems can form distinct dispersal groupings of elements (Voorhies Groups). The theoretical dispersal potential of bones appears to depend primarily on density and size, with shape becoming more important for those with high surface area to volume ratios (e.g., ribs).
3) Close proximity of a bone assemblage to the original habitats of the living animals can be indicated by the presence of all dispersal groups in association (but disarticulated), or in some cases by the presence of lag elements. The total number of different skeletal parts in a disarticulated assemblage is not a valid measure of proximity unless these represent the full range of dispersal potentials (e.g., patellae to skulls).
4) Settling velocity experiments indicate that shape factors will increase or decrease bone settling rates by about 15 percent from rates predicted on the basis of density and size alone. The nominal diameters of quartz grains that are hydraulically equivalent to fossil bones can be approximated within a range of ± 25 percent (owing to the shape factor), using estimated original densities. Such approximations cannot be used for bones with high surface area to volume ratios (ribs, scapulae, etc.). Most bones of mammals smaller than hippopotamus are equivalent in settling velocity to quartz particles of sand to pebble size. An association of fine-grained sediment and relatively large bones suggests (but does not prove) that different processes may have led to their deposition (e.g., bones dropped into fine sediment by a floating carcass rather than transported along with the sediment).
5) Considering bone-quartz equivalent grain sizes and the standard current velocities required to transport quartz particles, it can be shown that bones

under 1000 cc should be transported by currents of from 10 to 150 cm/sec. However, in order to achieve the higher velocities in this range, mean velocities would normally have to exceed 200 cm/sec. (flood conditions). Voorhies Group I would move at normal flow velocities, but Groups II and III in general would require flood conditions for significant transport.

6) Bottom conditions can have significant effects on bone dispersal, with irregular, coarse-grained or loosely compacted beds tending to retard bones and decrease their transport potential. This may alter the composition of the dispersal groups.

The overall conclusion relevant to the following analysis of the East Rudolf fossil assemblages is that bones, as sedimentary particles, are particularly sensitive to *sorting* according to density and size factors. In the following pages, it should be kept in mind that the interpretations of the East Rudolf material depend on the assumption that Voorhies Groups will tend to form in natural systems because of the hydraulic effects of bone size, density and shape. Various factors discussed above may alter the compositions of the bone dispersal groups in natural systems, and the interpretations of the East Rudolf assemblages should be accepted with some caution until this assumption can be tested with experiments in natural systems.

SEDIMENTARY ENVIRONMENTS OF THE KOOBI FORA FORMATION, EAST RUDOLF

The objective of this part of the study is to characterize particular East Rudolf sedimentary environments in terms of their geology and fossil assemblages. The resulting geologic, taphonomic and biologic data will then be analyzed for paleoecologic information. This section presents a geologic background for the East Rudolf deposits followed by detailed discussions of seven sedimentary units that were sampled for fossil content. The following two sections characterize the fossil assemblages in terms of the sorting of skeletal parts and in terms of kinds of animals represented in each of the seven units.

Geologic Setting

The East Rudolf region lies on the northeastern side of the Lake Rudolf Basin in the northern part of the East African Rift System (Fig. 10). This part of the Rift has been tectonically and volcanically active since at least 25 million years (my.) Before Present (B.P.), when general downwarping began (Walsh and Dodson, 1969; Baker and Wohlenberg, 1971). There are no well-defined boundary faults forming a single "rift valley" in this region. Instead, Lake Rudolf lies along the axis of a broad depression containing numerous horst and graben structures of various ages. The majority of the faults are north-south and are steeply dipping to vertical. The main segment of the Rift System passes through the southern end of Lake Rudolf and east of the major part of the basin, through Lake Stephanie and north to the Red Sea.

Several cycles of faulting and vulcanism have affected the Lake Rudolf Basin during the last 3 my., and the region remains tectonically active today. The structural instability has given rise to numerous local sediment traps that have been subsequently uplifted and exposed at the surface. This activity is superimposed on the broader downwarping of the basin as a whole, which has acted as a large-scale sediment trap since the Miocene. The lake itself is shallow ($\sim$ 100 m) and the depth of sediment along the basin axis is unknown. Given the large drainage area (now a closed drainage system of 146,000 km^2 [Butzer, 1971a:1]), the amount of sediment accumulated since the Miocene is probably considerable.

The overall sedimentary situation, which provides for relatively rapid deposition, is ideal for fossil preservation. Throughout

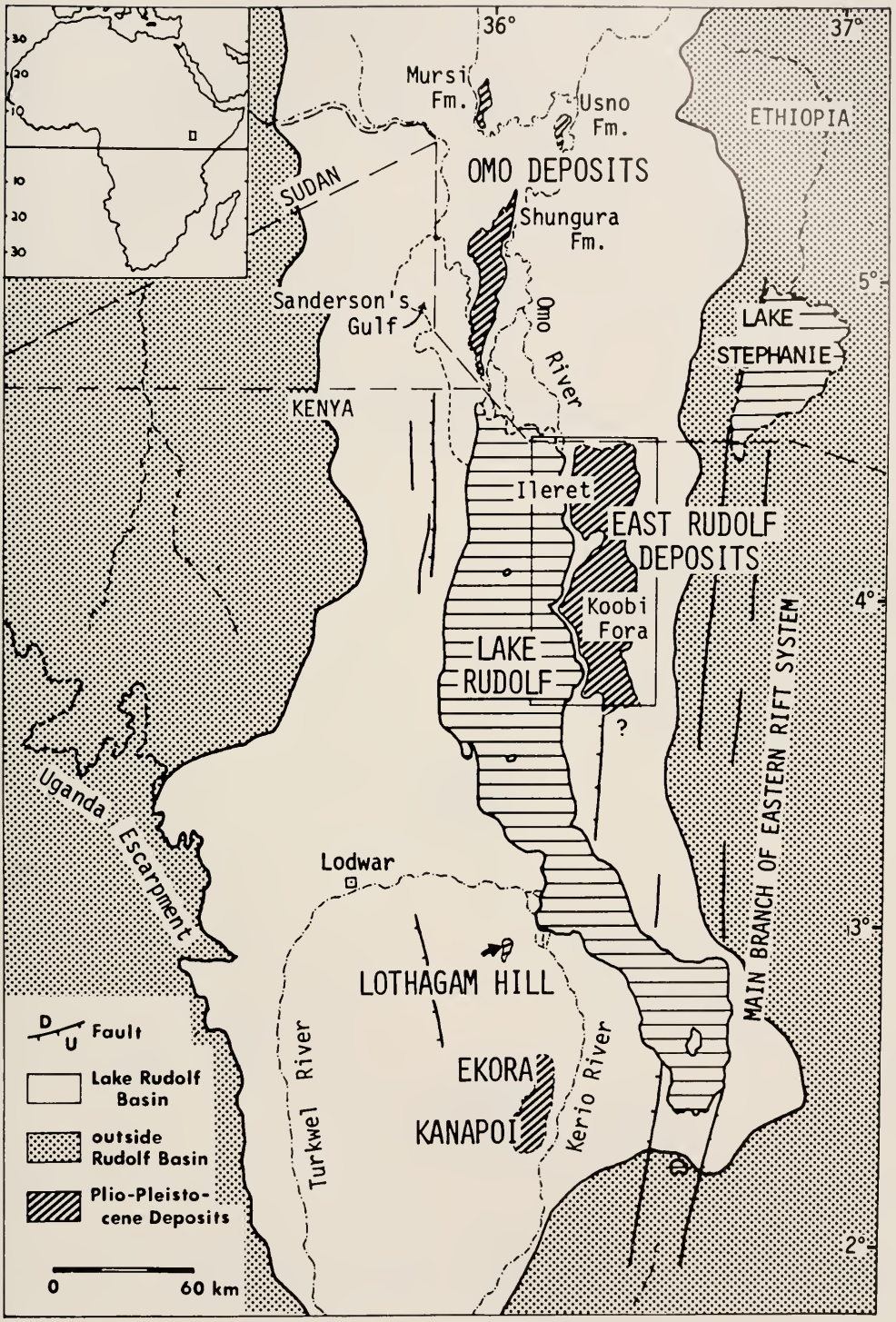

Figure 10. Map of the Lake Rudolf Basin. The area presently draining into the lake is shown in white.

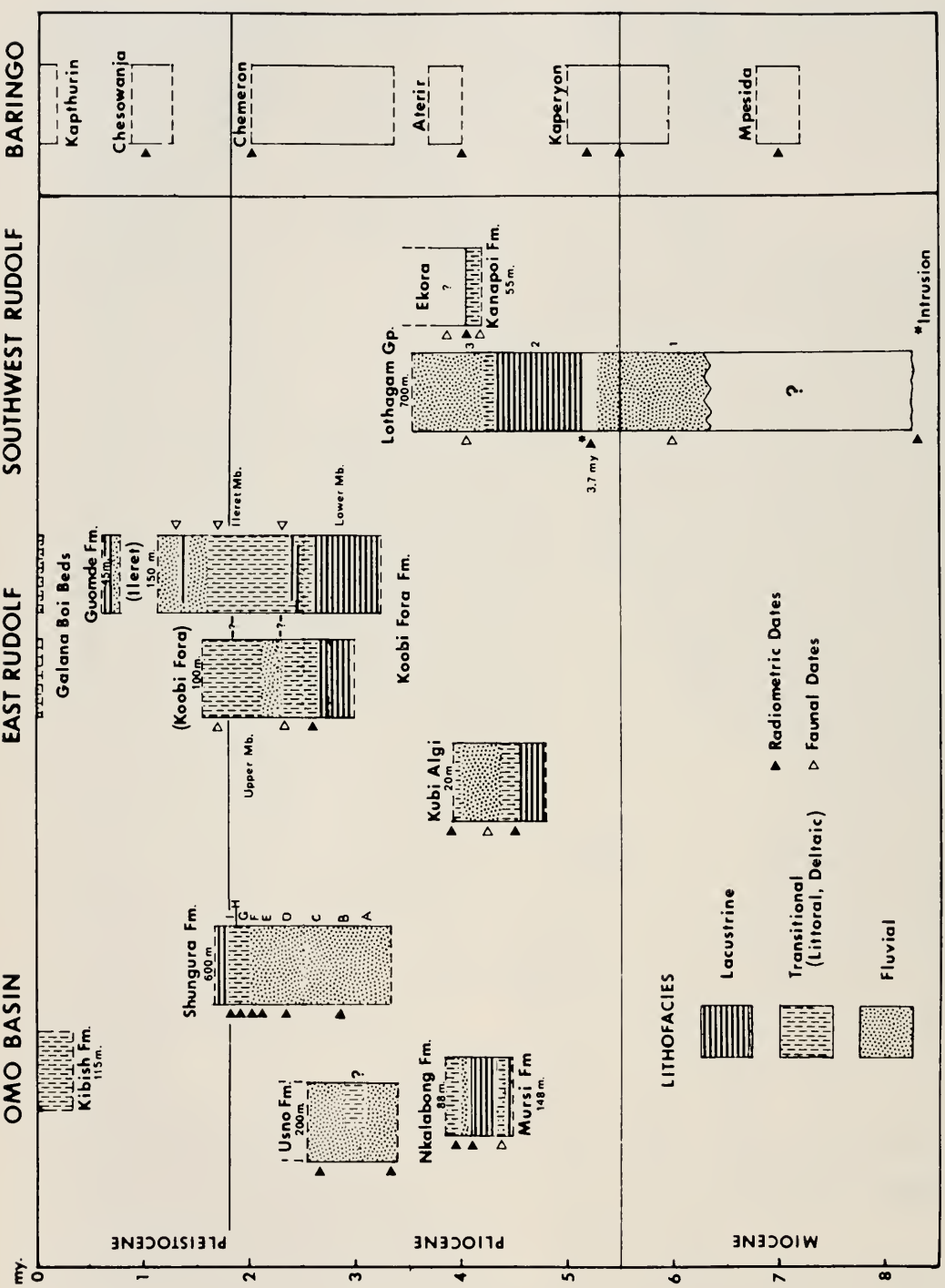

Figure 11. Correlation chart showing time-stratigraphic sequences of the Lake Rudolf Basin. Generalized lithofacies are given for each section, and their vertical range indicates the *time span* covered by fluvial, lacustrine or transitional deposition. The Baringo sequence, which lies to the south of the Rudolf Basin, includes several sedimentary formations of comparable age. Epoch boundary lines are drawn according to Berggren and Van Couvering, 1973, who have based their conclusions on new calibration of the type sections.

the Rift System, vertebrate fossils have been collected from various time horizons, and eventually should provide a continuous picture of faunal succession in this part of East Africa from Miocene to Recent times.

Regional Stratigraphy

Three major sedimentary deposits in the Lake Rudolf Basin are known in detail: the Omo sequence, Lothagam Hill, and East Rudolf. Extensive deposits south of Lothagam, including Kanapoi and Ekora, have provided important faunal collections and are currently under geologic investigation. These areas record periods of sedimentation for the last 5 to 8 my. in the southwestern, northern and northeastern parts of the basin (Fig. 10). Correlations between areas are based on evolutionary stages of the faunas and Potassium-Argon (K/Ar) dating, with paleomagnetic reversal chronology currently showing promise as a third method. The stratigraphic relationships of the three areas are given in Figure 11. Generalized lithofacies shown in Figure 11 also demonstrate the variability of sedimentary conditions from region to region on any given time plane. For the most part, the deposits represent local conditions relating to fluctuations in base level which may or may not have been basin-wide in scale. Average rates of sediment accumulation, calculated for continuous sequences between two dated horizons, vary from 50 cm/1000 years for the Shungura Formation (Omo) to 10 cm/1000 years for parts of the Koobi Fora Formation (East Rudolf) (Behrensmeyer, 1974).

The Omo Basin includes several sedimentary formations of varying ages and lithologies. Of these, the Shungura Formation (Fm.) represents the thickest continuous sequence, on the basis of radiometric age control. K/Ar dating on a succession of volcanic tuffs has provided a time scale for over 500 m of section. The Shungura Fm. has also produced a large assemblage of vertebrate fossils which can be accurately placed in the stratigraphic sequence. These factors combined have made it a standard reference for faunal and time correlations between 1.7 and 3.8 my. B.P. in the Lake Rudolf Basin. The sediments represent fluvial deposition in a large-scale river system (the ancestral Omo), with a change to littoral and lacustrine deposition above "Tuff G," at about 1.9 my. B.P. (Butzer, 1971b; de Heinzelin *et al.*, 1971).

The Lothagam Group includes a thick sequence of volcanics and sediments exposed in a tilted fault block on the southwest side of Lake Rudolf. The area of exposure is only a few square kilometers, much less than for the Omo or East Rudolf sequences. Dates from a basalt flow and an intrusive sill, plus evolutionary stages of the fossil faunas, put the Lothagam sediments between about 8 and 3.5 my. B.P. Deposits of Lothagam-1 and -3 bear lithologic similarities to the Shungura Fm. and are fluvio-deltaic in origin whereas Lothagam-2 is clearly lacustrine (Patterson *et al.*, 1971).

East Rudolf covers some 5500 square kilometers (900 square miles) and its sediments represent an overall accumulation of over 300 m (Fig. 12). The oldest unit, the Kubi Algi Fm., occurs primarily in the southern part of the region. It is sparsely fossiliferous and has not been studied in detail, thus it is not discussed in this study. The Koobi Fora Fm., which forms the bulk of the fossiliferous deposits, is spread over a wide area and is extremely variable in composition, so that correlation is difficult even along continuous exposures. A K/Ar date of 2.6±.26 my. B.P. (Fitch and Miller, 1970) and paleomagnetic chronology (Brock and Isaac, 1974) indicate a time span of 3.0 to 1.4 my. for this unit.

The East Rudolf deposits are bounded on the east by Miocene volcanics, which they lap onto unconformably. The Kokoi Ridge, which divides the Ileret and Koobi Fora areas, is formed of recently uplifted Pliocene basalts with interbedded lacustrine sediments (Bowen and Vondra, 1973:391).

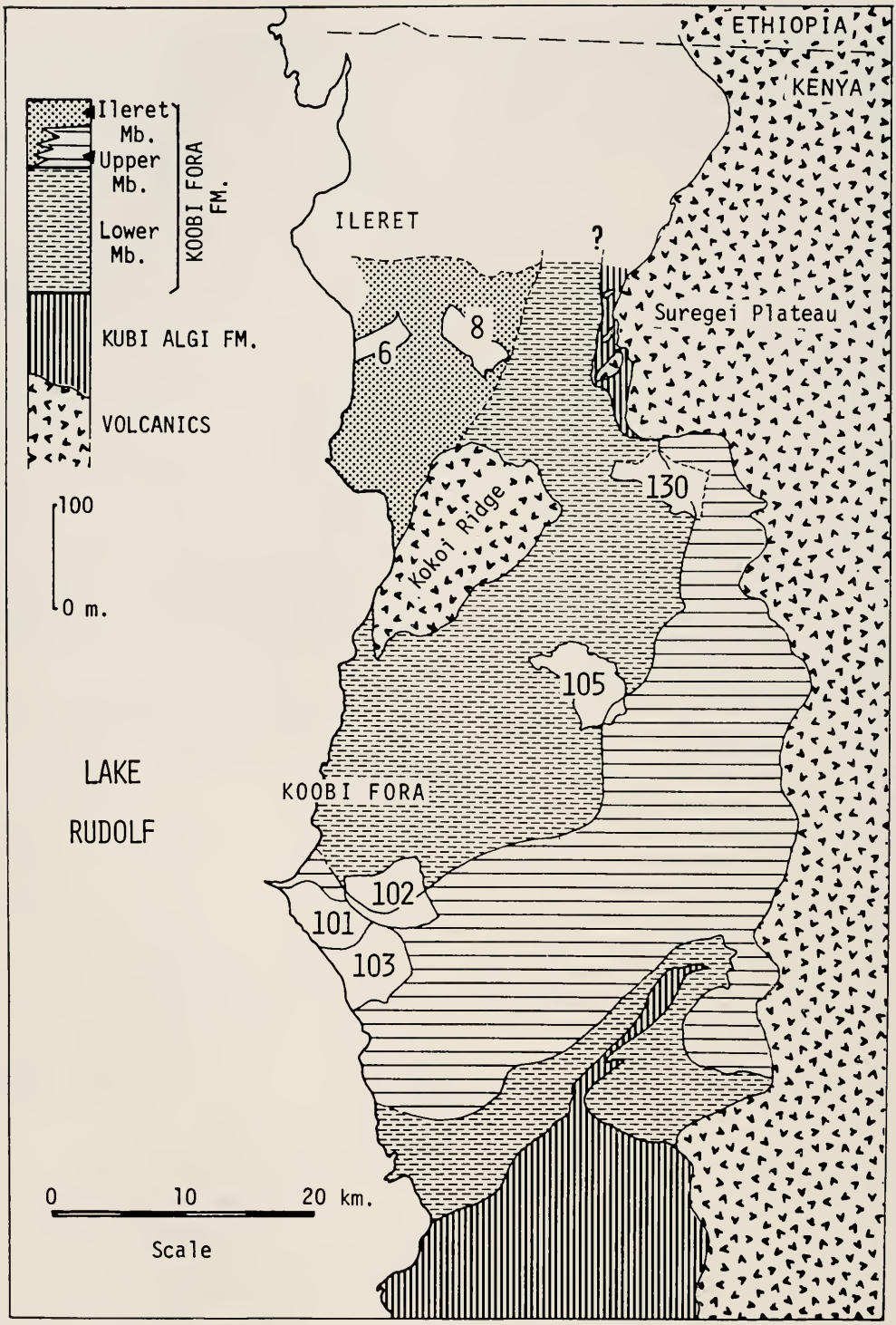

Figure 12. Generalized geologic map and stratigraphic section of East Rudolf, based on Bowen and Vondra (1973) plus unpublished work by Bowen. Numbered areas were used for controlled sampling of the vertebrate fossils which provided the material for this study.

The paleoslope, as indicated by numerous determinations of paleocurrents, inclined toward the southwest, as it does today. The Stephanie Basin probably drained across this area periodically during the Plio-Pleistocene (B. E. Bowen and C. F. Vondra, personal communication), but it is doubtful that a major river system such as the Omo River existed in the East Rudolf region. Rather, the geomorphic and sedimentary situation can be reconstructed as set of coalescing piedmont fans and deltas derived from moderate relief (about 600 m or 2000′) volcanic and basement terrain toward the east. The distance from the major part of the Plio-Pleistocene lake margin deposits to the areas of highest relief (if similar to today) was on the order of 40–50 km, and the regional gradient would thus have been 600 m/50 km or about 12 m/km.

The geologic evidence indicates that this part of the Rudolf Basin contained a lake which acted as base level during the period of Plio-Pleistocene deposition. At present, it is not known whether this lake was connected to the Nile drainage during the deposition of the Koobi Fora Fm. The fossil and modern aquatic faunas (vertebrates and invertebrates) show close Nilotic affinities, and it is fairly certain that at least periodic connections have existed (Butzer *et al.*, 1972). The abundant and diverse molluscan fauna of the Koobi Fora Fm. indicates fresh water conditions. It seems likely that both closed and open drainage situations, and saline and freshwater conditions, existed periodically during the Plio-Pleistocene in the Lake Rudolf Basin.

Recent Limnology

A summary of the recent characteristics of Lake Rudolf is useful for comparison with Plio-Pleistocene conditions. Today Lake Rudolf has a surface area of 7500 km^2 and a catchment area of 146,000 km^2 (Butzer, 1971a:1). Most of the influx of water comes from the Ethiopian Plateau via the Omo River during its seasonal floods in July (Butzer, 1971a:37). The lake basin itself is semiarid, with about 380 mm (15″) of rainfall annually (1936–1970), as measured along its shores (Butzer, 1971a). Maximum daily temperatures range from 34.0–36.0 C, and this plus the strong southeast trade winds encourages evaporation from the lake surface. The seasonal fluctuation in water level is over one meter. Longer-range fluctuations have caused the lake to drop 20 m between 1896 and 1940, and to rise 5 m in the last ten years. During the period between 9500–7500 B.P., Lake Rudolf was approximately 80 m above its present level (Butzer, 1971a: 15).

The present alkalinity of the lake is .0194–0.210, and the *p*H about 9.5 (Beadle, 1932: 187). Ca is low in the lake water owing to the high *p*H, and Beadle (1932: 186) noted evidence for active precipitation of $CaCO_3$. Alkalinity is due to high K and Na content. The overall conditions of the lake are presently outside the tolerance of most of the molluscan forms that are typical of the Plio-Pleistocene and Holocene deposits, and only three living species have been recovered (T. Hopson, personal communication). Fish and plankton are abundant, however. Recent, apparently living stromatolite formations have been dredged up by a fisheries research vessel near South Island (T. Hopson, personal communication).

It is evident simply on faunal grounds that the lake has changed greatly since the Plio-Pleistocene, and also in the past 10,000 years. The water level has fluctuated widely, and along with it, alkalinity and *p*H have altered. All evidence indicates that the lake has been fresher, and the regional climate probably wetter (at least periodically), than at present.

The recent sedimentary environments associated with the Omo Delta have been examined by Butzer (1971a). These include "flood basin" (alluvial flats associated with the Omo river channel), "delta fringe" (distributary and inter-distributary flats) and the "prodeltaic zone" (subaquatic

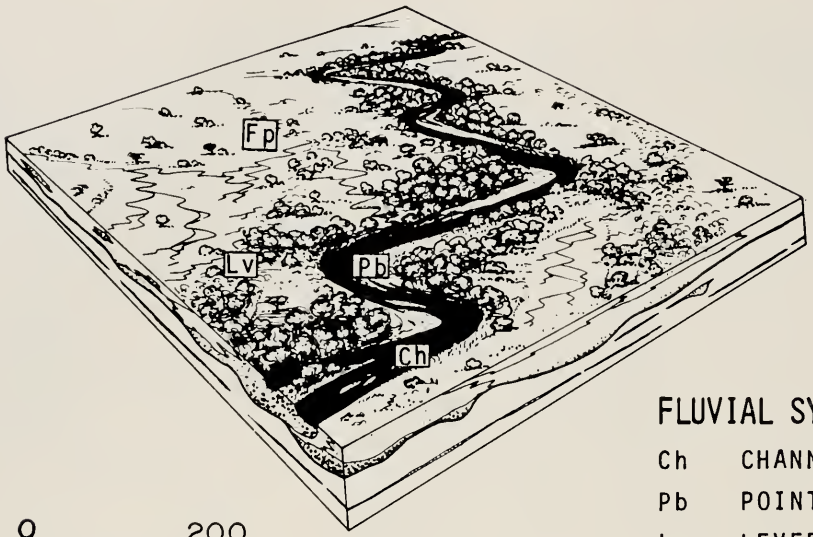

FLUVIAL SYSTEM

Ch	CHANNEL
Pb	POINT BAR
Lv	LEVEE
Fp	FLOODPLAIN

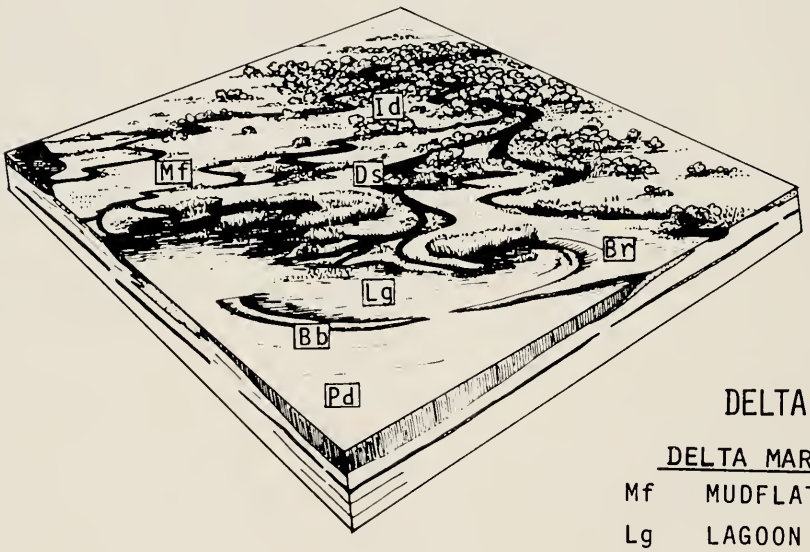

DELTA

DELTA MARGIN

Mf	MUDFLATS
Lg	LAGOON
Br	BEACH RIDGE
Bb	BARRIER BAR
Ds	DISTRIBUTARY
Pd	PRODELTA

DELTAIC PLAIN

Id	INTERDISTRIBUTARY
Ds	DISTRIBUTARY

Figure 13. Diagrammatic representation of the fluvial and deltaic sedimentary environments that are recorded in the Plio-Pleistocene deposits. The diagrams are based on characters of recent fluvial and deltaic environments near the shores of Lake Rudolf.

sedimentary extension of the delta). Characteristics of these environments, including information on sediment type, vegetation, and sedimentary structures, are invaluable in interpreting the Plio-Pleistocene sediments around the Lake Rudolf Basin. Observations (by the author) of recent environments along the eastern shore of the lake, outside the Omo delta system, have also proved useful in the interpretation of the older sedimentary environments.

In order to discuss the paleoenvironments of the East Rudolf sediments, it is necessary to provide a terminology that describes the environments present in the combined lake-margin and fluvial system of the Lake Rudolf Basin. Figure 13 and Plate 4 give a verbal and pictorial description of the recent environments to be used for interpretation of the Plio-Pleistocene deposits.

Stratigraphy of the Koobi Fora Formation

The Koobi Fora Fm. as a whole has been interpreted as a "prograding deltaic complex," with general upward coarsening indicating outward growth and thickening of the deltaic deposits through time (Bowen and Vondra, 1973:392). The paleogeography of the deltaic complex at particular time horizons has yet to be understood, but a primary lobe probably originated from the Lake Stephanie region. Sedimentary sequences in the Ileret and Koobi Fora areas are different during similar periods of time, and the Kokoi volcanics may have divided the two regions into separate depositional basins during early phases of uplift.

Stratigraphic nomenclature and sedimentary relationships have been established by Bowen and Vondra (1973). Although direct stratigraphic correlation between the discontinuous outcrops typical of East Rudolf is difficult, there are several marker horizons of reworked volcanic ash which are recognizable over much of the area covered by the Koobi Fora Fm. Three of these tuffs, the "KBS," the "Tulu Bor" and the "Suregei," are indicated in the stratigraphic sections given in Figure 14. They lie within about 150 m of predominantly lacustrine and prodeltaic deposits. The Ileret Member (Mb.), above the KBS Tuff, includes deltaic and prodeltaic sediments that pass upward into subaerial deposits indicating floodplain or deltaic plain conditions. These are followed by an erosional unconformity overlain by the Guomde Fm., a primarily lacustrine unit of undetermined age. In the Koobi Fora region, the deltaic and lacustrine deposits which include the KBS Tuff are followed by an erosional unconformity that may be of regional significance. Fluvial deposits follow in the northeastern part of Koobi Fora, and these pass laterally into deltaic deposits toward the southwest, which is down the regional paleoslope. The Guomde Fm. is absent in the Koobi Fora region. The Holocene Galana Boi beds cap the sedimentary sections both at Ileret and Koobi Fora.

Deposits north and south of the Kokoi Ridge show increased structural deformation near the present lake shore. In the Koobi Fora region, extensive faulting occurs west of a north-south hinge-line approximately 5 km from the Koobi Fora peninsula. The Upper Member (Mb.) of the Koobi Fora Fm. also thickens toward the west at this point. There is evidence that minor tectonic events occurred in this area during the time of sedimentation of the Upper Mb. These events are represented by truncated normal faults, and at least three episodes have been recognized (G. D. Johnson, personal communication). It is likely that faulting and increased subsidence in this region have affected rates of sedimentation and, along with this, bone preservation.

With the general stratigraphic and tectonic framework of East Rudolf as a background, the following sections will deal specifically with the characteristics of the sedimentary units sampled for vertebrate fossils.

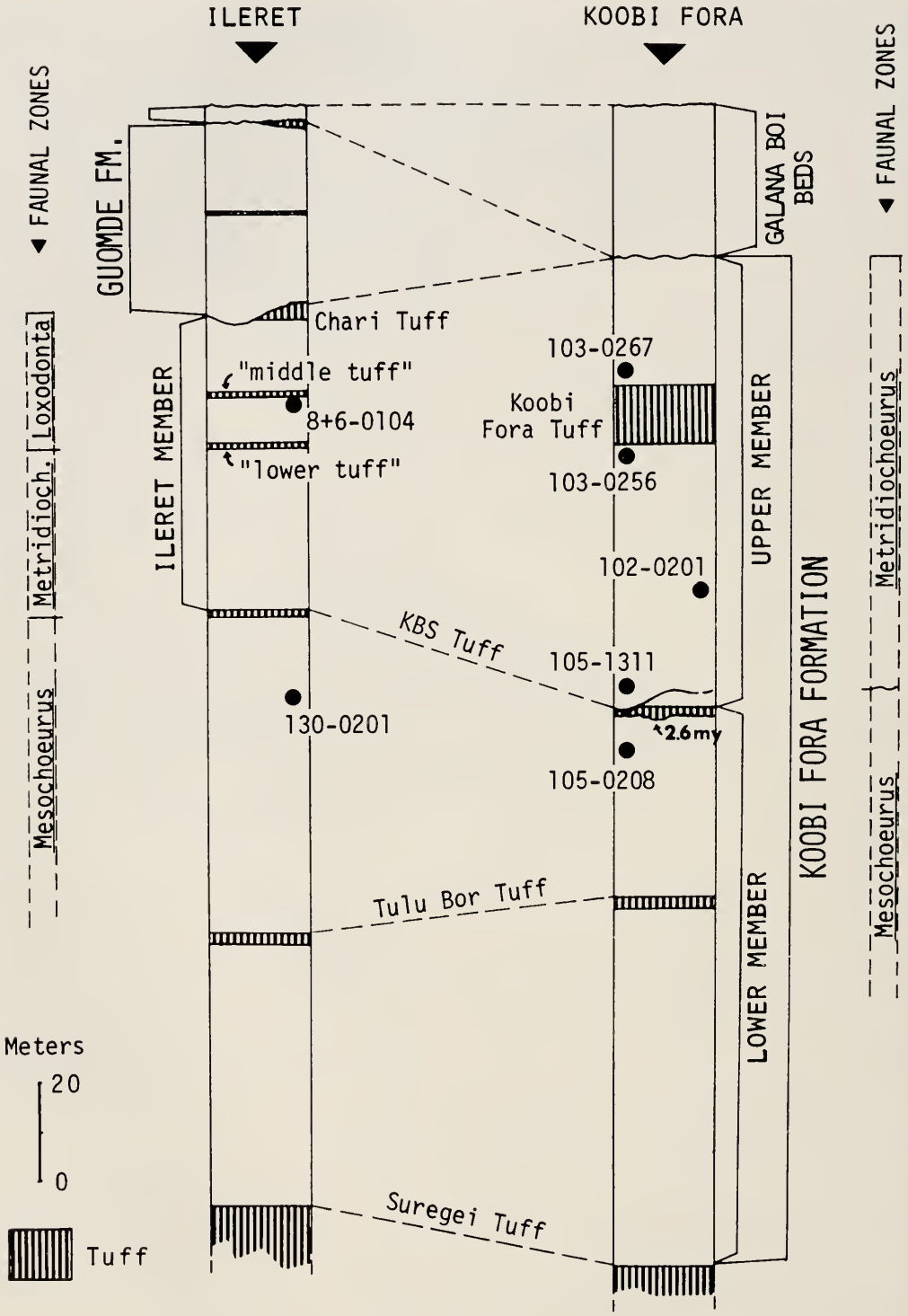
ILERET
KOOBI FORA
FAUNAL ZONES
Metridioch.
Loxodonta
Mesochoeurus
GUOMDE FM.
ILERET MEMBER
Chari Tuff
"middle tuff"
8+6-0104
"lower tuff"
130-0201
KBS Tuff
Tulu Bor Tuff
Suregei Tuff
103-0267
Koobi
Fora Tuff
103-0256
102-0201
105-1311
2.6my
105-0208
GALANA BOI
BEDS
UPPER MEMBER
LOWER MEMBER
KOOBI FORA FORMATION
Meters
20
0
Tuff

Sedimentary Environments of the Fossil Vertebrate Localities

Designation of Sampling Localities

Vertebrate fossils are particularly abundant in the upper part of the Koobi Fora Fm. from just below the KBS Tuff to the top of the unit. Extensive areas of surface fossil concentrations closely associated with particular sedimentary environments provided ideal situations for bone sampling. Seven sampling localities were chosen to provide data on bone-sediment associations.

The discontinuous nature of East Rudolf exposures has led to a numerical system of outcrop "area" designation. This has been used informally by the various East Rudolf research groups. In the interest of consistency, the fossil sampling localities used for paleoecologic analysis will be coded according to this system. Each locality is thus designated by a two-part number, as follows: 103–0256; "103" indicating that the locality is in Area 103 and "0256" indicating a stratigraphic section ("02") and a bed or horizon in the section ("56").

For the purposes of this study, a locality is defined as an area of outcrop where there is a clear association between a particular lithofacies and an assemblage of vertebrate fossils. The location of each general area where sampling took place is indicated in Figure 12. Stratigraphic positions of the seven sampling localities are shown in Figures 15 and 16. Choice of sampling localities depended primarily on the nature of the fossil assemblage, and the criteria used will be explained in the chapter dealing with the fossils. An effort was made, however, to choose localities where bone was associated with a variety of lithofacies, so that assemblages from different sedimentary environments, such as channel, lake margin and floodplain, could be compared.

Method of Geologic Analysis

Most of the information used for the interpretation of the fossiliferous sedimentary environments was obtained in the field. Each of the sample localities was documented by using closely spaced stratigraphic sections. Lithologic samples were collected from each section and examined later in the laboratory for specific information on sediment size and texture. In addition, lateral facies changes and overall stratigraphic context were examined and mapped in each locality.

The important criteria for distinguishing lithofacies in the Koobi Fora Fm. have been worked out over the course of several field seasons. The sample localities were specifically examined in terms of these characters, which are as follows:

1) Grain size and sorting

2) Thickness and lateral continuity of consistent lithologies

3) Presence and nature of clay clasts and/or reworked $CaCo_3$ nodules

4) Limonitic nodules and mottling

5) Primary $CaCO_3$ nodules and/or beds

6) Presence or absence of root casts

7) Evidence of bioturbation, particularly burrows

8) Cross-stratification (large- and small-scale)

9) Lateral persistence of well-defined,

←

Figure 14. The stratigraphy of East Rudolf, after Bowen and Vondra (1973). Faunal Zones as determined by Maglio (1972) are given for the Koobi Fora Fm. The Ileret Mb. is only in part the time equivalent of the Upper Mb. (see Fig. 12). The Kubi Algi Fm. continues downward from the top of the Suregei Tuff but is not included in this figure. The two-part numbers (e.g., 130–0201) designate the fossil sampling localities used for this study and show their relative stratigraphic positions.

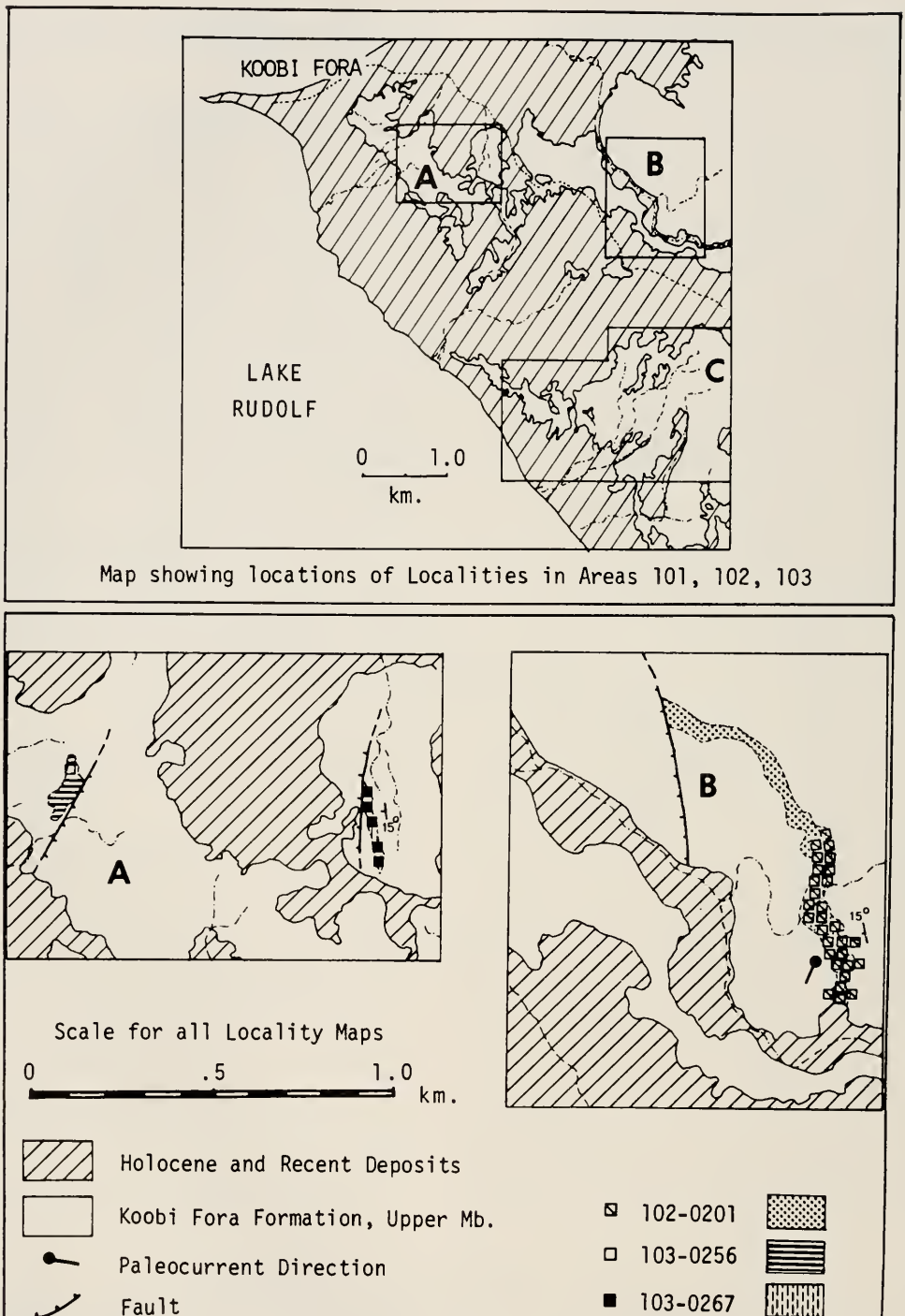

Figure 15. Maps showing the distribution of bone sampling squares (10 × 10 m) in the area near the Koobi Fora Peninsula. An index map shows the relative positions of the three more detailed maps. All maps showing square distribution are drawn to the same scale. The squares themselves are shown slightly larger than true scale.

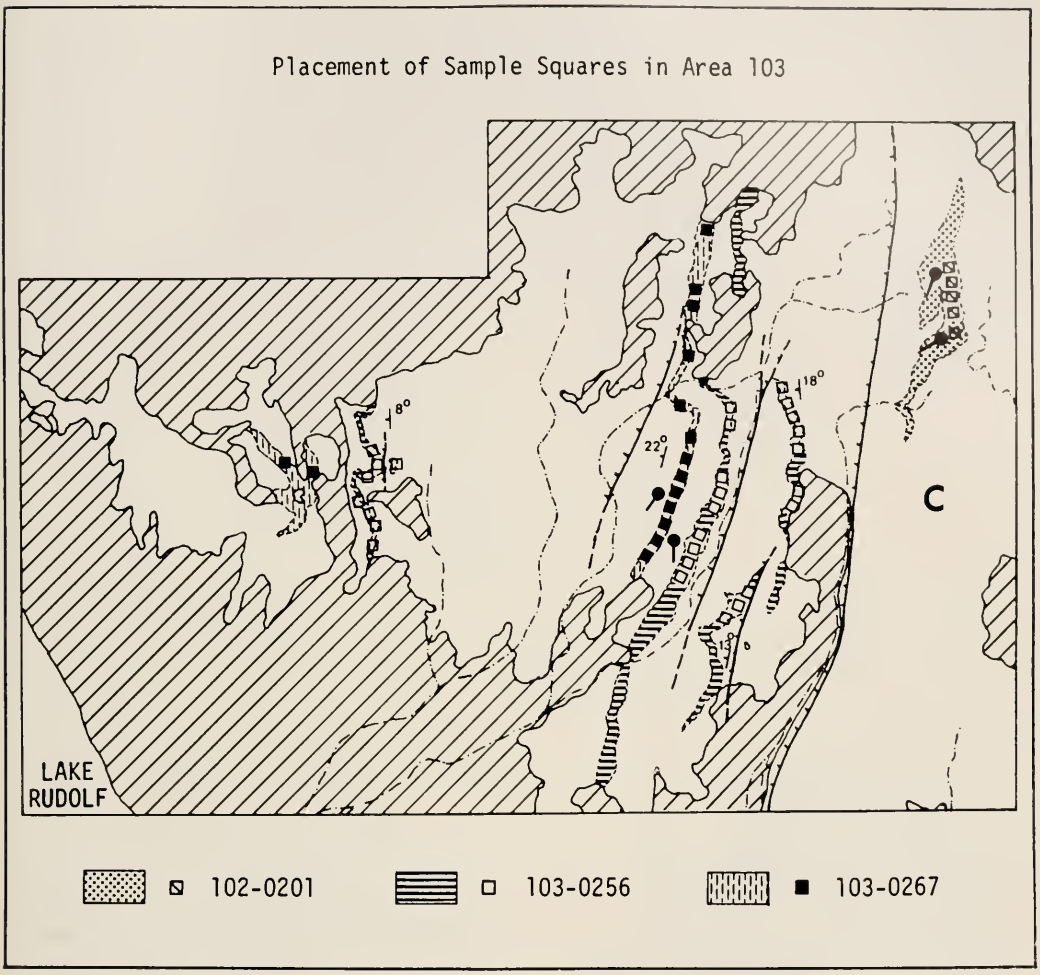

Figure 15 Continued.

even horizontal bedding and small-scale laminations

10) Desiccation structures (mudcracks)

11) Slickensides, prismatic cracking, evidence for paleosol development

12) Invertebrate fossil content

Generalized stratigraphic sections for each of the sample localities are given in Figure 17. Each locality is described in Table 5 according to the sedimentary characters outlined above, and the following interpretations of sedimentary environments are based on this evidence. Vertebrate evidence is not included for the specific purpose of keeping this separate from other characters used in interpreting the environments of deposition. This permits the sedimentary evidence to be related to the vertebrate assemblages without danger of circular reasoning. Surface textures, hydraulic equivalents and other aspects of the bone assemblages are discussed below, after conclusions are drawn concerning each environment of deposition.

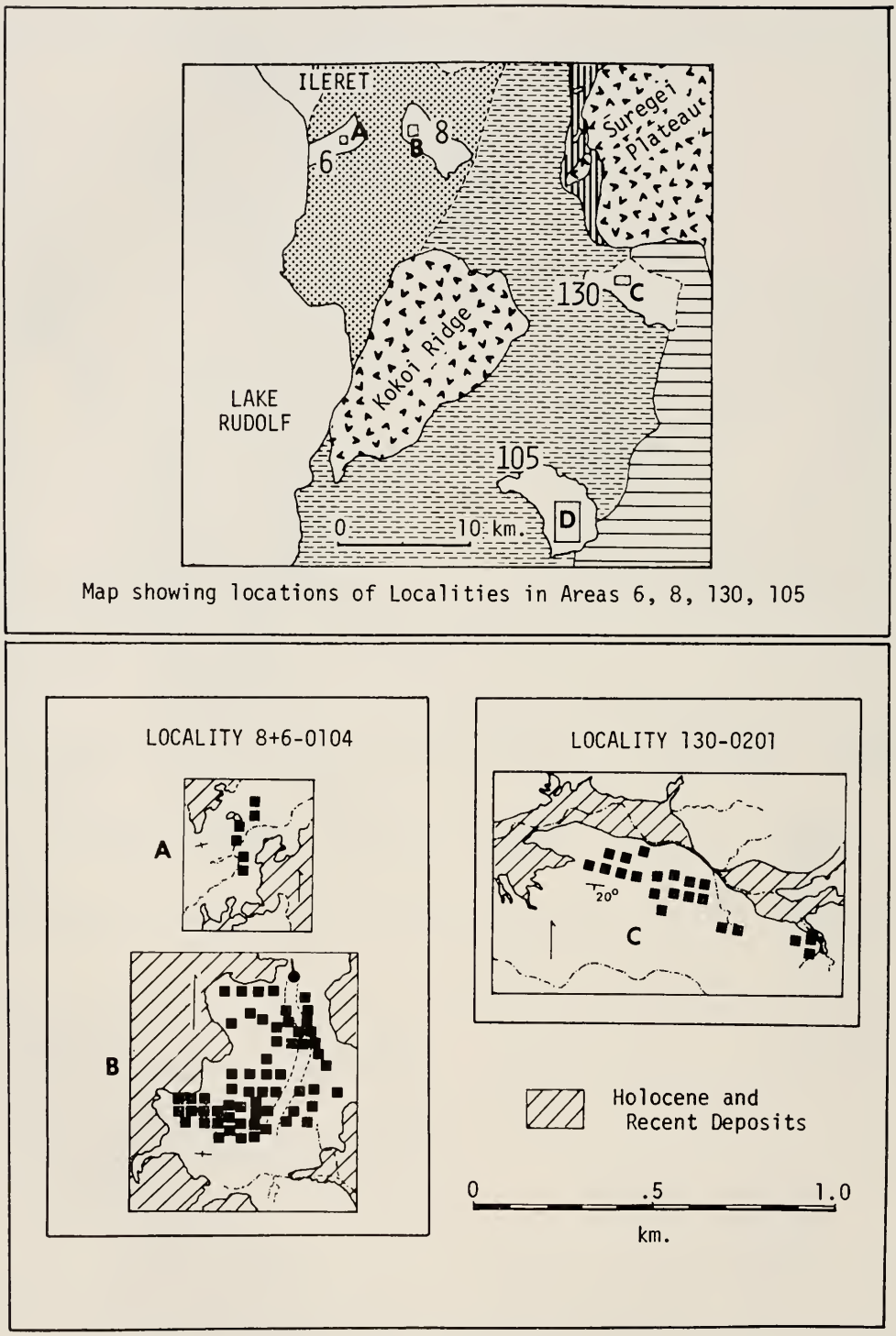

Figure 16. Maps showing the distribution of bone sampling squares (10 × 10 m) in the Ileret region and east of the Kokoi Ridge. An index map shows the relative positions of the four more detailed maps. Locality maps are drawn to the same scale as those in Figure 15, and squares are slightly larger than true scale.

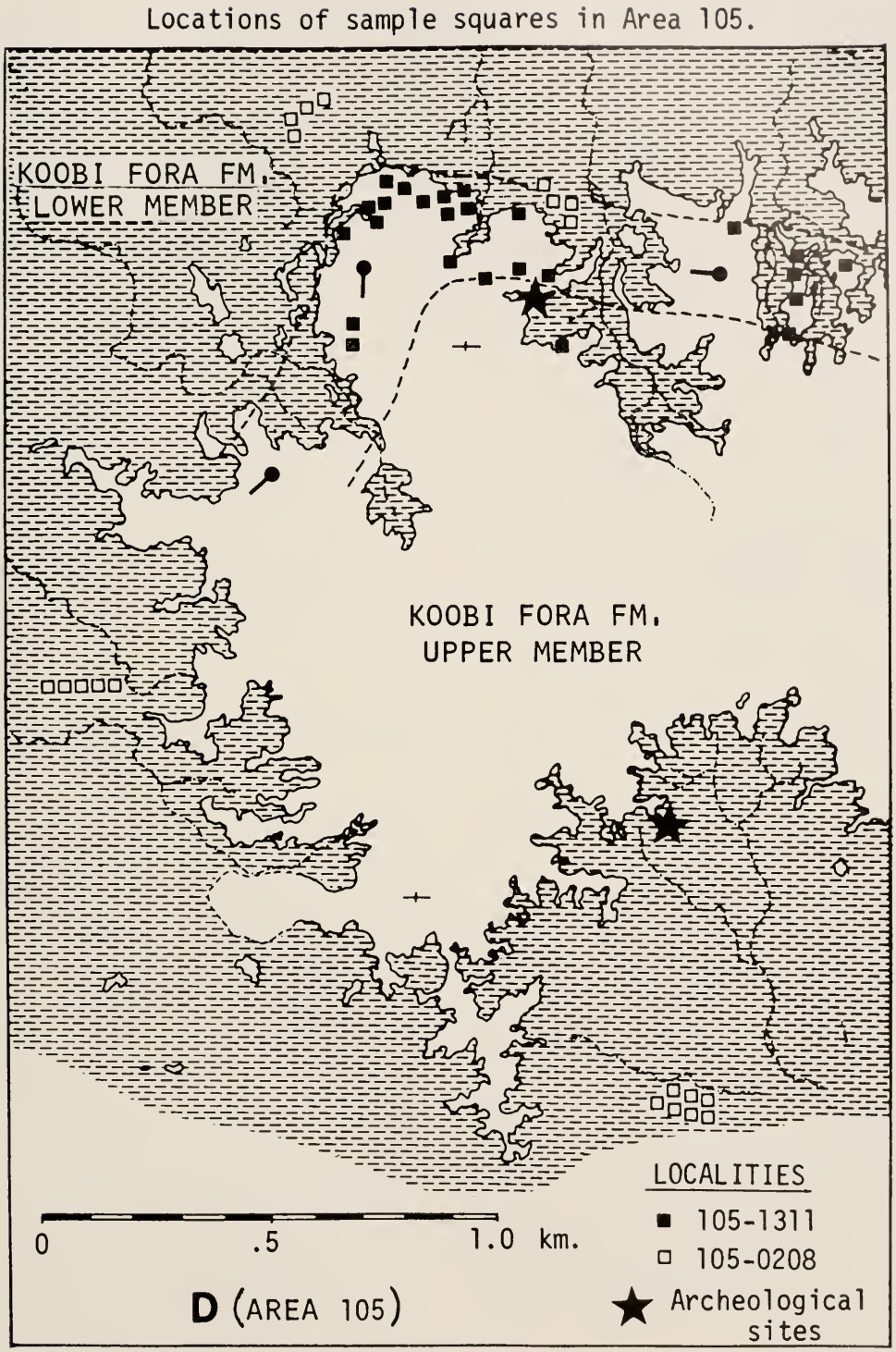

Figure 16 Continued.

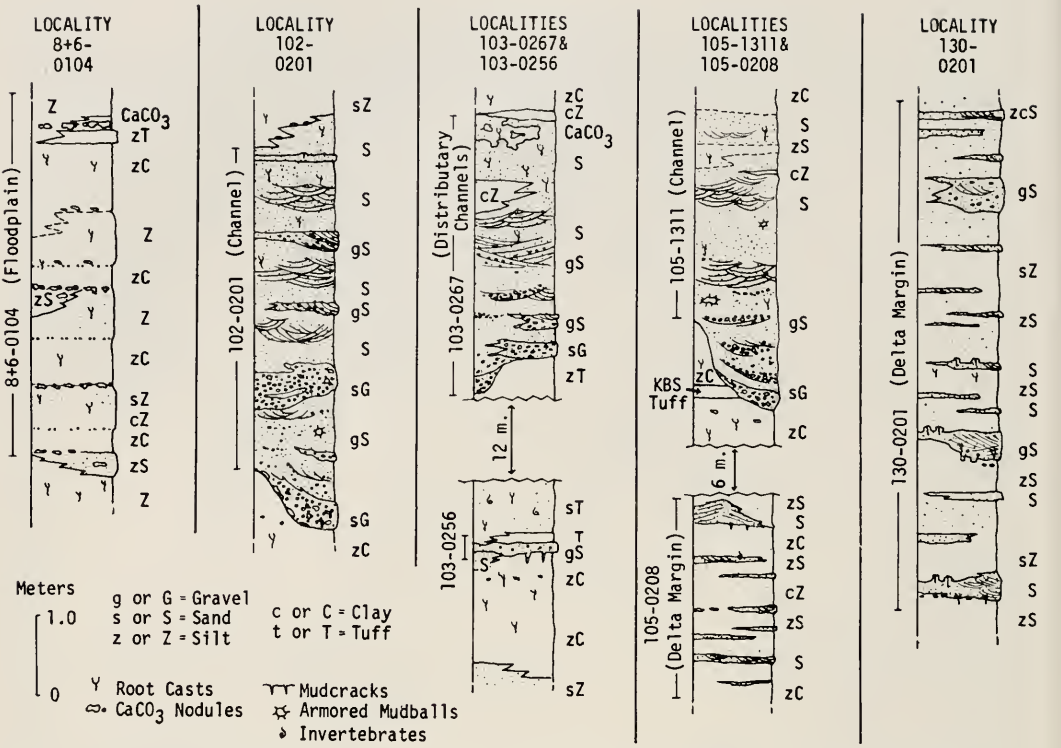

Figure 17. Detailed stratigraphic sections for each of the fossil sampling localities. The sections represent the total stratigraphic interval sampled for fossil bones, and combine the sedimentary data from many sections measured in each locality.

Sedimentary Environments of the Sample Localities

Locality 103–0256: Deltaic Flats.

Most of the fossil material is derived from a thin and very extensive sand which overlies mudcracked silty clays. In the few places where the sand was not deposited, the horizon can be recognized by the mudcracked surface. There are no obvious lateral changes in the grain size of the sand unit, which is dominantly coarse to fine over the entire area. This sand is overlain by the tuffaceous silts and sands that form the base of the Koobi Fora Tuff, a 12–15 m thick unit that also covers some 2–3 km^2. The tuff is extensively cross-stratified in its lower part but generally is horizontally bedded with persistent horizons of mollusk shell fragments.

The sediments underlying the mudcracked surface are much less uniform laterally and have interbedded silty clays, sandy silts and occasional lenses of coarse, clean sands. There is a general tendency toward fining from northeast to southwest, roughly following the regional paleoslope. Root casts and $CaCO_3$ nodules <3 cm in diameter are typical of the silty clay beds. The mudcracks on the upper surface of the unit are up to 15 cm in depth and are firm evidence for subaerial exposure. They are filled with the overlaying fine to coarse grained sand.

The evidence indicates a deltaic mudflats environment of deposition for the silty clays and silts underlying the mudcracked surface. The interbedded sand lenses represent distributary channels. Bioturbation, partly due to root growth, has obscured evidence

Table 5. Summary of lithofacies characteristic of the seven localities sampled for fossil vertebrates.

FOSSIL SAMPLING LOCALITIES →	130-0201	105-0208	103-0267	103-0256	102-0201	105-1311	8+6-0104
MAJOR LITHOLOGY	silty sand	silty sand	gravelly sand	sand	gravelly sand	gravelly sand	silt
GRAIN SIZE	1-6.0 mm	.1-2 mm	.1-30 mm	.1-1.0 mm	.1-25 mm	1.0-60 mm	.1-1.0 mm
SORTING	good-poor	good-poor	good-poor	good-mod.	good-poor	poor	poor
THICKNESS	7.0 m	2.5 m	3.0 m	.75 m	5 m	3.0 m	4.5 m
EXTENT OF MAJOR LITHOLOGY	.5 km^2	2 km^2	4 km^2	2 km^2	3 km, N-S	.8 km^2	3-4 km^2
MUD CLASTS	+	+	+	+	mud balls and clasts	armored mud balls	-
REWORKED $CaCO_3$	-	+	+	+	+	+	trace
LIMONITE	+	+	-	-	grain coatings	grain coatings	-
PRIMARY $CaCO_3$	trace in zC	trace in zC	+	-	-	?	+
ROOT CASTS	trace	+	+	trace	+	+	+
BIOTURBATION	trace	+	+	trace	+	+	+
CROSS-STRATIFICATION	small-scale troughs in S and gS	planar foresets, small-scale troughs	small-large scale troughs	poorly developed small-scale troughs	small-large scale troughs, planar foresets	small-large scale troughs	troughs in sand lenses
HORIZONTAL BEDDING	+	+	rare	+	rare	rare	+
MUDCRACKS	-	+	-	+, on surface below sand	-	-	trace
EVIDENCE FOR PALEOSOL DEVELOPMENT	-	-	+?	+, in beds below sand	-	-	+
INVERTEBRATES	-	4+ species of gastropods, some bivalves	-	gastropods, bivalves in growth position	-	-	-
ENVIRONMENT OF DEPOSITION	Delta Margin	Delta Margin and Lagoon	Distributary Channel and Beach	Deltaic Mudflats	Channel	Channel	Floodplain

+ = observed
- = none observed

for successive land surfaces, although in some areas paleosols appear to be present (G. D. Johnson, personal communication). A laterally continuous beach sand transgressed over the deltaic flats, but apparently nowhere formed preserved beach bars or ridges. Predominantly lacustrine conditions followed, with influxes of tuffaceous material from distributary mouths and spreads of shell debris over level subaqueous surfaces.

The lack of extensive erosion on the mudflats with the coming of lacustrine conditions indicates the character of the transgression. Although the mudclasts and $CaCO_3$ nodules incorporated in the sand are no doubt derived from the mudflat (as are the fossil bones), the mudcracks on the surface have not been eroded away. This can only mean a very low gradient shoreline, low wave energy, and probably a relatively rapid transgression. Otherwise, it is difficult to explain why the increased energy level which carried the sand would not have formed beach ridges and eroded beach fronts, destroying the upper surface of the mudflats.

The Cretaceous Wealden Lake environment in the Anglo-Paris Basin provides some close analogues for the transgressive deposits of the Koobi Fora Fm., and particularly those of 103–0256. P. Allen (1959) reports graded sheets of pebbly sand that were spread extensively over deltaic deposits as the Wealden Lake rose. One of these, the "Top Ashdown Pebble Bed," is a graded unit with pebbly sands fining upward to sands and silts. It is only 10–20 cm thick, and truncates all underlying structures and sediments. The base is erosional, and the components of the bed are derived from underlying deposits (P. Allen, 1959:292). This is directly comparable in most characteristics to the 103–0256 transgressive sand, but differs in that 103–0256 does not appear to be derived from the underlying beds, except for the mudclasts and carbonate nodules. The base is less erosional than in the Wealden transgressive sheets. The sand in 103–0256 was evidently redistributed from former beach and distributary mouth deposits and carried shoreward by the advancing lake.

The fossil bones derived from the transgressive sand and the mudflats deposits are concentrated on the slope below a strike ridge created by the westward tilted, resistant sand. They are highly mineralized, although the pore spaces of many of the fossils are not filled with cement of any kind, a unique characteristic of this assemblage. There is evidence for mixing of bones with varying degrees of predepositorial weathering. Some retain fresh, uncracked and unflaked surfaces while others are weathered and have cracked or worn surfaces preserved under their sandstone matrix cover.

The quartz equivalents for the fossils, estimated according to their densities when fresh (Table 4) range from 1.0–>20 mm. This is a very different size range than that of the quartz sand which forms the matrix of the fossils (<.1–1.0 mm). The distributary sands associated with the mudflats contain grains up to 5 mm in diameter, yet this size range is absent from the transgressive sand and apparently was not present on the deltaic flats. If the bones were derived from the distributaries, it is reasonable to expect them to be associated with sand larger than 1.0 mm. It is possible to conclude that most of the bones were probably not brought into the area by fluvial processes, but were derived from a death assemblage that lay upon the deltaic flats. The presence of many fresh, unabraded bone surfaces further supports a locally derived fossil deposit. The bones were probably redistributed by the transgression, but final burial was evidently rapid and abrasion minimal.

Locality 130–0201: Delta Margin

Vertebrate fossils were sampled from a relatively large stratigraphic thickness (7.0 m) of tilted and faulted sediments. A variety of lithologies occur, and overall

grain sizes range from <.1–6.0 mm. The dominant lithologies are evenly stratified sandy silts, silty clays and medium-grained flagstone sands. The sands are generally clean and rich in biotite. Coarser, more poorly sorted sediment occurs in laterally restricted lenses.

This locality lies within the marginal deltaic facies of the Lower Mb. of the Koobi Fora Fm. The units sampled for fossil vertebrates appear to be on an actively aggrading margin of the deltaic complex. The sedimentary characteristics listed in Table 5 agree in many respects with Butzer's (1971a:79) description of the modern Omo interdistributary basins (lagoonal mudflats and marsh), including the presence of limonitic mottling in the silts and clays. The more evenly bedded and extensive silts and sands may belong to the prodeltaic zone as well. The lack of evidence for surface exposure and root-bioturbation suggests generally subaqueous conditions, with water depths greater than the maximum tolerated by aquatic vegetation (about 1–2 m).

The poorly sorted gravelly sands are restricted to lenses that represent channels. Pebbles up to 6 mm in diameter occur in these lenses as floating grains in a coarse sand matrix. Mudclasts are also present. The combined evidence suggests at least periodic currents over 100 cm/sec., and possibly flood deposition of the kind leading to the very poor sorting and large floating grains (Pettijohn, 1957:254–255). (Vertebrate bone fragments and teeth are often extremely abundant in these gravelly sands, and include a high proportion of nonaquatic forms, in contrast to the aquatic assemblages derived from laterally associated lithologies.)

Cross-stratification is often well-developed in the medium- to fine-grained sandstones. These include small-scale structures comparable to "Kappa" and "Nu" cross-stratification that indicate linguoid ripples (Fig. 18). The well-sorted medium to coarse sands show planar foresets, and in some cases the cross-stratification suggests beach or barrier bar deposition comparable to that reported for recent barrier environments (Davies *et al.*, 1971). Current directions for the various forms of cross-stratification are highly variable. The bed forms and grain sizes indicate water movement in the lower flow regime.

The deltaic margin interpretation of 130–0201 agrees well with the lacustrine and deltaic models of Visher (1965) for sediment types and bedding characteristics. The transgressive sand-pebble sheets of the Wealden Lake and 103–0256 are absent or poorly developed. Instead, the delta of 130–0201 appears to have been continuously aggrading into a subsiding basin, with occasional periods when sediment accumulation overtook subsidence and shallow water features (root casts, sand and gravel lenses) developed.

Hydraulic equivalents for the bones range up to 50 mm, which is much larger than the maximum size of other associated particles. However, when large aquatic animals are eliminated (e.g., hippopotamus and crocodile), the mammalian remains have an estimated maximum hydraulic equivalence of 20 mm and most are less than 10 mm. This is closer to the matrix grain size in the channel lenses. The bones that are close to being hydraulically equivalent to their matrix grains also show more evidence of abrasion and weathering. These may have been carried to the delta margin during periods of high discharge (i.e., floods), and therefore may be derived from a variety of upstream source areas.

Locality 105–0208: Delta Margin and Lagoon.

The sediments are predominantly silty sands, poorly sorted and ripple-laminated with abundant mica. These form a recognizable 2–3 m thick unit over much of 105, bounded above and below by finer units of silty clays. Abundant vertebrate bone occurs in association with the silty sands but is rare in the silty clays. The silty sands

Cross-stratification typical of the sediments sampled for vertebrate fossils. (Localities in parentheses)

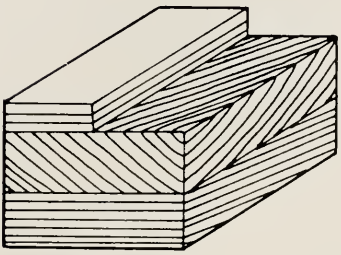

Beta-cross-stratification
(102-0201, 103-0267)

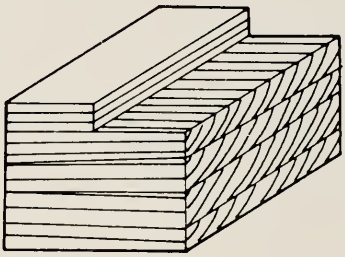

Mu-cross-stratification
(102-0201)

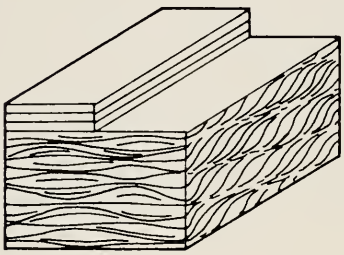

Kappa-Cross-stratification
(130-0201, 105-0208)

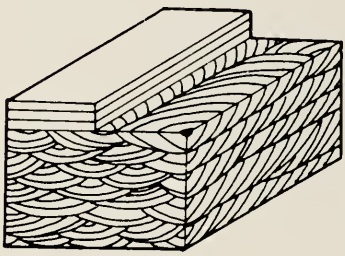

Nu-cross-stratification
(130-0201, 105-0208, 103-0267)

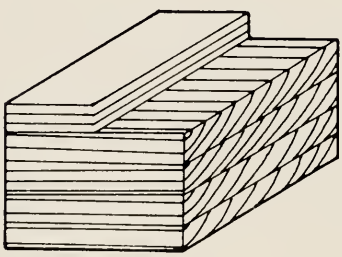

Omikron-cross-stratification
(102-0201)

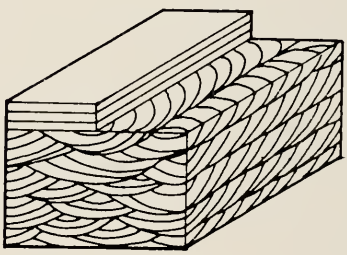

Pi-cross-stratification
(102-0201)

(From J. Allen, 1963)

Figure 18.

are characterized by horizontal, evenly bedded cosets of small-scale "Kappa" and "Nu" cross-stratification (Fig. 18). The individual beds are between 2 and 5 cm in thickness. Contorted bedding and uneven lenses of silt are present, but the bedding shows little evidence of disturbance from bioturbation. Bedding structures indicate aggradation from the advance of successive ripple fronts, such as might be expected in a prodeltaic, lagoonal environment.

Coarser sands are interbedded in discontinuous sheets and lenses. In one lens, the overall characteristics suggest a barrier or beach bar. This sand overlies the mudcracked surface of a thin lens of silty clay, and incorporates clay clasts in its lower 10 cm. The sand body is elongate and extends for over 100 m before pinching out. Large tubular structures resembling root casts are abundant. Upward the bed becomes better sorted and has well-developed low angle planar cross-bedding that closely resembles the cross-stratification reported for barrier and beach environments (e.g., Davies *et al.*, 1971).

The more tabular, thinner sand bodies interbedded in the silty sands are commonly cross-stratified, with single sets of planar and concave-upward laminae. Shallow troughs are also common. Ripple formation at variable current velocities and depths is indicated, as in 130–0201. The sands pinch out into discontinuous nodular layers. Root casts are common, in association with the sheet sands, but mudcracks at the lower bedding contact are rare. The sands occasionally preserve a variety of fresh-water mollusks that are unbroken and locally autochthonous, including *Bellamya, Cleopatra, Melanoides, Pila* and *Pseudobovaria.* The invertebrate fauna indicates "prodeltaic or even marshy" conditions (D. Van Damme, personal communication).

There are no poorly sorted, coarse-grained channel lenses within this part of the Area 105 section, in contrast to 130–0201. The overall sedimentary characteristics suggest a lagoonal environment, with sand and silt provided from nearby distributary mouths. This compares well with delta margin conditions in actively aggrading sectors of the Omo Delta (Butzer, 1971a:75). Beach ridges and barrier bars formed at the lakeward side of the lagoonal complex and occasionally transgressed shoreward over lagoonal sediments. The water in the lagoon probably varied in depth with shallower phases represented by coarser sand lenses with root casts indicating the spread of shoreline vegetation. The area may have been periodically (perhaps seasonally) subaerial, although most characteristics indicate overall shallow subaqueous conditions.

Localities 105–0208 and 130–0201 are closely comparable in stratigraphic position within the Koobi Fora Fm. Both lie near the top of the Lower Member; 105–0208 is about 8 m below the KBS Tuff, and 130–0201 between 10 and 15 m below the tuff. 130–0201 is probably the older of the two. The localities are about 15 km apart, and represent related depositional situations on the margins of the prograding delta system.

Bones of aquatic and nonaquatic animals are abundant and well preserved, and often consist of associated skeletal parts. Bone surfaces are generally fresh, with only occasional evidence of predepositional weathering and abrasion. Most of the bones of nonaquatic animals are fragmented, with spiral and saw-tooth fractures indicating predepositional breakage.

The largest bones are of hippo, and these reach hydraulic equivalents of 15–30 mm, well outside the sediment range for the coarser sands. Most of the other bone fragments and teeth are between 1.0 and 20 mm in quartz equivalent sizes. This overlaps the size range for other sediment in 105–0208, but most of the bones, and particularly the teeth, exceed 2 mm in equivalent size. Larger sediment grains occur in laterally associated facies to the east and northeast, but are absent in 105–0208. The combined evidence points to a local source of bones from the lagoon and shoreline environ-

ments, with perhaps a small component from the distributaries, including some floating carcasses. Bones were probably redistributed and buried during the migration of beach sands, a process similar in some respects to that proposed for 103–0256.

Locality 105–1311: Channel Complex.

The fossil-bearing unit is up to 4.5 m thick and overlies an erosional surface with up to 12 m of relief. Coarse gravels, including $CaCO_3$ nodules reworked from the underlying beds, are concentrated primarily near the base of the unit. The lithology is consistently a coarse sand with lenses of gravel. As shown in Figure 16, the main body of the sand is linear, with current directions indicating a west to southwest bend. To the south, the sands and gravels intertongue with silts and silty clays representing levee and floodplain deposition lateral to the channel.

Well-developed large scale cross-stratification is present throughout the sand unit. Troughs are the most common form and are between 20–50 cm in diameter. Gravel lenses are present at the bases of many of them. These compare well in morphology and size with "Pi" cross-stratification (Fig. 18) and with the cross-strata occurring in ephemeral streams in Central Australia (Williams, 1971). Such stratification is formed by downstream-migrating ripples of varying size in the lower flow regime (Allen, 1968:110; Williams, 1971:37).

All the above characteristics indicate that the 105–1311 sand body is a fluvial channel. The upward fining of the sands is typical of point bar formations (J. Allen, 1965:140), and it is likely that much of the sand was deposited in the point bar formed by the lateral migration of the channel bend. Root casts are abundant in the sands and laterally related silty clays, but are less common in the coarse gravels near the base of the unit. This indicates vegetation lateral to the active channels, and it is likely that a gallery forest existed along the channel. The geologic evidence does not reveal the extent of this forest, or whether the water flow was permanent or ephemeral.

The fossil bones in 105–1311 form distinct groups according to surface texture. In one group, bones are highly rounded and polished and are less than 5 cm in diameter. They can accurately be described as "bone pebbles." These compare well with the second-cycle bones of Rief (1971), which were mineralized prior to final transport and burial. Although it is possible for bones to be thoroughly mineralized in relatively short periods of time (e.g., 5000 years for bones from Lake Rudolf Holocene deposits), the degree of rounding of the bone pebbles in 105–1311 indicates long-term abrasion. It is more likely that they were derived from earlier fossiliferous sediments associated with Miocene volcanics to the east than from floodplain deposits associated with the 105–1311 channel. The second group includes a wide range of sizes of relatively well-preserved teeth and bones. These are generally fragmental, and show signs of abrasion in their rounded edges, broken processes and exposed trabeculae. A third group consists of only a few specimens, including whole skulls collected outside the sampling areas, which show little or no weathering or abrasion. The latter two assemblages are composed of bones that had not been mineralized prior to transport, and that had undergone variable degrees of surface weathering and abrasion prior to burial. These can be referred to as "first cycle" bones.

The largest bone fragments are hydraulically equivalent to quartz particles up to 40 mm, and most of the teeth fall in the 5–25 mm range. This is well within the particle size range of the associated gravels, which range up to 60 mm in maximum diameter. A very different taphonomic situation exists in 105–1311 compared with the three localities discussed previously, which have bones that exceed the associated quartz particles in hydraulically equivalent grain sizes. It is clear that the bone as-

semblage in 105–1311 is much more likely to reflect the processes that have affected the associated sediment, i.e., abrasion and sorting through hydraulic transport. The same forces that moved sediment through the channel could also have moved the bones. A large proportion of these are probably derived from upstream sources, with a more local component derived from the undercutting and reworking of previous floodplain deposits by the laterally migrating channel. Both of these assemblages should consist of isolated teeth and the more durable parts such as ends of limb bones, all showing some degree of abrasion. The third component, consisting of the best-preserved material, would come from bones left in the immediate vicinity of the channel and rapidly buried. The bone assemblage of 105–1311 is thus a mixture of autochthonous and allochthonous material, and most of the bones show the effects of being in a fluvial system. Since the general environment of deposition is fluvial, the bones should belong to animals found in the floodplain or channel habitats, as opposed to the deltaic or lacustrine habitats.

Locality 102–0201: Channel.

The sequence is tilted some 15–20° west both in Area 102 and its continuation in Area 103. Current directions indicated in the sand are dominantly NNE to SSW, so that the strike of the beds is roughly parallel to the current. The deposits of 102–0201 overlie a scoured surface on silty clays with paleosol development, and they are followed by widespread sheet sands with stromatolites and shell debris. The stromatolites indicate shallow-water lacustrine conditions (S. Awramik, personal communication). 102–0201 represents a brief period of channel cutting between two longer lacustrine and deltaic depositional phases.

The dominant lithology is a coarse sand with gravel near the base, fining upward to medium and fine-grained sand and finally to silt. There is no obvious trend toward downstream fining in the 3 km segment examined. Large-scale lenses of gravel up to 1.5 m thick are common in the lower 3 m of the unit. The upper 2 m have only occasional small gravel lenses and dispersed pebbles. Mudclasts and carbonate nodule clasts, which are abundant near the base of the unit, appear to be derived from the underlying silty clays. Otherwise the gravel is composed of mixed quartz, feldspar, volcanic material such as welded tuff and pieces of silicified wood, all well-rounded. There are a few polished bone pebbles and occasional large polished bone fragments indicating a source of previously mineralized material.

Cross-stratification includes planar foresets 10–25 cm in height, and a variety of trough cosets. Many cosets of the planar cross-beds are comparable to "Beta"-type stratification (Fig. 18). In some cases the cross-strata are more upwardly concave than planar, comparing well with "Mu" and "Omikron" stratification (Fig. 18). Allen (1963:110) attributes the formation of the latter types of cross-strata to migrating asymmetrical ripples. "Beta" cross-strata result from the downstream migration of single, straight edged ripple trains over a planar eroded surface (J. Allen, 1963: 102). It seems that both of these conditions of ripple bedding, plus intermediates, took part in the formation of 102–0201. The troughs are generally large-scale (10–50 cm across) and compare with Allen's "Pi" or "Nu" types of cross-stratification (Fig. 18). These are attributed to the migration of large-scale asymmetrical ripples with curved crests and projecting lobes or tongues (J. Allen, 1963:110). All of the above structures can be formed by flowing water in the lower flow regime.

The evidence is conclusively in favor of a channel origin for the 102–0201 sand. The gravel concentrations near the base represent channel bars and channel lag deposits. In one case, where the coarse material includes an unusual amount of bone, bedding

structures and local upward fining suggest point bar formation. Root casts are more common in the finer sands of the upper part of the unit than in the gravels. Vertebrate fossils show a sharp upward decrease in abundance and were clearly concentrated along with coarse sediment near the base of the channel.

The stratigraphic context of 102–0201 indicates much closer proximity to the lake than for 105–1311. In fact, 102–0201 can be regarded as a channel or complex of channels incised into a temporarily inactive delta. Evidently, base level was lowered due to either tectonic or climatic processes. The period of cut and fill separating two deltaic-lacustrine units may reflect one of the local tectonic events which affected this part of the Koobi Fora Fm. during its deposition (G. D. Johnson, personal communication).

The channel-cutting and gravels of 102–0201 may be the downstream counterpart of 105–1311. Both lie near the base of the Upper Member of the Koobi Fora Formation, and are in the *Metridiochoerus* faunal zone (Fig. 14). The composition of the gravels is similar, and some evidence for an extensive erosion surface analogous to that in Area 105 has been found in the vicinity of Area 103. If 102–0201 is the deltaic-distributary counterpart of 105–1311, then it is probably slightly earlier in time. After an erosional phase, the areas closer to base level (i.e., 102) would begin to aggrade earlier than more upland areas such as 105.

The fossil vertebrate material is variable in surface texture and overall preservation. Bones of aquatic and semiaquatic forms show minimal abrasion and are often complete. Other vertebrates are represented by teeth, limb parts, etc., usually broken and weathered. This indicates probable transport and a subaerial source (i.e., channel banks) for the bones of nonaquatic animals. A few relatively complete parts, such as a complete rhinoceros jaw, indicate closer sources and less transport.

The bone fragments are occasionally over 50 mm (e.g., the rhinoceros jaw) in hydraulically equivalent quartz sizes. However, most are equivalent to grains less than 20 mm, and thus are similar to the size range of the gravels. As in 105–1311, most of the bone in 102–0201 has probably been subjected to winnowing and abrasion during transport. The close association between bones and gravels in 102–0201 implies similar concentrating processes. This may be an example of Langbein and Leopold's "kinematic wave" effect (1968), where large particles tend to concentrate other large particles and form gravel bars.

The sediment particles, including bones, are a mixture of allochthonous and autochthonous material. The more complete skeletal parts, the mudclasts and the armored mudballs, are examples of locally derived material from the channel banks or channel bed. The gravels, including the polished bone fragments, have been transported from upstream sources. The largest proportion of bones and teeth may have either local or distant sources, and probably represent animals which inhabited channel and floodplain environments as well as the temporarily dry and emergent deltaic plain.

Locality 103–0267: Distributary complex.

The fossil-bearing horizon is exposed in widely separated areas covering over four square kilometers. The dominant lithology is a poorly sorted gravelly sand. The sands are of variable thickness and occasionally cut several meters into the underlying beds. Coarse sediment fines upward and intertongues with silts and silty clays near the top of the unit.

The 103–0267 sands and gravels overlie the Koobi Fora Tuff, which is predominantly lacustrine in origin and is capped by a widespread, oolitic carbonate sand with stromatolites. The deposits of 103–0267 are followed by lacustrine silts and shell beds. Thus, the channeling and sand deposition represent a brief period of subaerial exposure and erosion similar to that of 102–

0201. About 50 m of continuous section separates the two units. G. D. Johnson (personal communication) has suggested that a tectonic event may be responsible for 103–0267 as well as 102–0201.

The upper part of 103–0267 is occasionally characterized by a discontinuous horizon of $CaCO_3$ concentration with abundant root casts. The root casts are truncated by the overlying sediment. $CaCO_3$ layers are formed of linked, irregular nodules which become more massive upward. This layer appears to bear a primary relationship to the associated sediments; i.e., it formed at the time when the top of 103–0267 was a land surface. The carbonate layer is thus tentatively identified as a caliche. It is comparable in structure and form to caliches of the American Southwest (Reeves, 1970; Aristarain, 1962; Bretz and Horberg, 1949). Although the processes leading to caliche formation are not well known, seasonal upward and downward percolation of ground water is usually indicated by such carbonate concentrations in soil horizons (Reeves, 1970: 353).

Cross-stratification is more widely variable in scale than in the 105–1311 or 102–0201 channels. The largest sets are up to 20 m across and are broadly concave upward. They compare with "Pi" cross-stratification (Fig. 18) and "festoon" bedding of the mega-ripple zone (Visher, 1965:47). A variety of smaller scale cross-stratifications are also present, including "Beta" and "Nu" types (Fig. 18). Troughs are well developed in sandy gravels near the base of the unit, while the festoon bedding occurs near the middle in coarse sands with gravel lenses.

Characteristics of 103–0267 suggest a distributary complex, with some redistribution of sediment by shoreline processes. Current directions are highly variable, from NW to S. The deposits represent laterally extensive channel cut and fill with subsequent aggradation over emergent deltaic flats. The large-scale cross-strata indicate distributary channels with flow depths of several meters. This contrasts with the channels in 105–1311 and 102–0201, which lack cross-stratification of comparable scale and probably carried shallower flows.

The bones of 103–0267 are concentrated in the lower 3 m, and are usually associated with pebbles of about 1 cm in diameter. Large-scale gravel and bone concentrations such as in 102–0201 are absent and bones are more or less evenly dispersed over the area covered by the deposit. There is a mixture of bone surface textures indicating various kinds of weathering and abrasion before burial. Parts of aquatic animals are generally the best preserved. Second cycle "bone pebbles" are present, as in the channel deposits of 102–0201 and 105–1311.

Grain size equivalents for the bones range up to 30 mm in diameter, but most fall between 5–15 mm. Since grain sizes in the gravels are up to 30 mm, the bones are within the overall sediment size range. Many have been transported, and the assemblage includes both autochthonous and allochthonous bones, as in the 102–0201 and 105–1311 channels.

Locality 8+6–0104: Floodplain.

This unit is composed of lithofacies unique to the upper part of the Koobi Fora Fm., occurring only in the Ileret Mb. and in the Upper Mb. in Areas 130 and 131 (Fig. 12). The dominant lithology is a light-colored tuffaceous silt. The environment of deposition evidently extended over a wide area, and the silts are exposed in Areas 6 and 8, which are some 2.5 km apart. The unit is stratigraphically marked by the "middle tuff complex," which includes locally discontinuous lenses of reworked volcanic ash and pumice.

The silts are remarkably consistent in texture and appearance. They are interbedded at regular intervals with zones of silty clays. These show vertical prismatic structure and clay concentrations suggesting paleosol development. Zones of $CaCO_3$ nodules occur within the silts and at contacts of silty clays on silts or sandy silts. The nodule horizons are often laterally continu-

ous and formed of elongate or flattened, irregular carbonate concentrations. Internally these are composed of fine sand floating in structureless micrite. They vary in size from 2–15 cm maximum diameter. Smaller nodules of $CaCO_3$ are dispersed throughout the clays and silts. The sediments themselves have very little dispersed carbonate, and do not react to the HCL test. Fragments of nodules are incorporated in sand lenses representing small channels interbedded in the silts. In some cases the nodule horizons are truncated by later beds. The combined evidence leads to the conclusion that the carbonate concentrations formed during the deposition of 8+6–0104.

The nodule horizons can best be explained as incipient caliches or carbonate concentrations formed in the "B" soil zones of successive subaerial deposits. Lobova (1967:290–299) describes the formation of similar carbonate concentrations in desert soils of the USSR. He suggests they are formed by biogenic carbonate concentrated in water percolating downward from the surface which later evaporates, leaving $CaCO_3$ precipitates. These nodule horizons commonly form at depths of 20–60 cm below the surface. The presence of such horizons in primary association with the sediments of 8+6–0104 indicates seasonal fluctuations of water content in soils with a local (biogenic?) source of $CO_3^=$ and a source of Ca^{++} (clays?). The absence of extensive, thicker caliches is perhaps due to the steady aggradation of the floodplain, with continued burial of former land surfaces.

Root casts are abundant throughout the unit. They are usually less than 1 cm in diameter and are formed of $CaCO_3$ similar to that found in the nodule horizons. $CaCO_3$-filled root casts are also found in the desert soils of the USSR, and are used as evidence of biogenic formation of carbonate concentrations (Lobova, 1967: 290). Some of the root casts are truncated by the channel scour-and-fill structures. The silts are riddled with tubes which may be burrows rather than root holes. These are usually 1.5 mm in diameter and have distinctive clay rims.

One well-developed channel can be traced NNW across the exposures in Area 8. It is approximately 40 m across and is filled with medium- to coarse-grained sand plus pumice cobbles up to 10 cm in diameter. Some of the silt beds (and perhaps the Area 8 lens of "middle tuff") represent levee and overbank deposits from this channel. Other channels occur within the silts and clays. Most are small scale, with variable current directions. The channel sands are often well sorted and cemented with $CaCO_3$, and in some cases the cemented sands weather out as rounded, resistant blocks and nodules.

It would be difficult to assign 8+6–0104 to any environment other than a floodplain. In general, the characteristics fit Allen's (1965) concept of vertically accreting floodbasin deposits. The whole complex of small channels and silt deposits may represent a zone intermediate between deltaic fan and floodplain, similar to that 1 to 2 km east of the margin of the present-day Tulu Bor Delta at Ileret. In Area 6, the "middle tuff" forms a widespread, mudcracked surface indicating deposition in a pond or lagoon, with later desiccation. It is possible that more deltaic conditions existed farther to the west of Area 8 in Area 6.

The bones of 8+6–0104 are generally very well preserved and often covered with a $CaCO_3$ crust. Some show surface weathering and cracking, and there are abundant isolated teeth. Associated skeletal parts of terrestrial mammals are also fairly common. This evidence suggests variable degrees of surface weathering and rates of burial.

The bones in 8+6–0104 are associated with much smaller grain sizes than in the channels. Hydraulic equivalents of most of the bones fall well above the 1 mm maximum grain size of the silts and sandy silts in which they occur. If individual bones had been carried in the channels and spread over the floodplain during floods, then they

should be found in association with grains closer to their hydraulic equivalents, i.e., coarser sand and gravel. Sediment of this size is available in channels lateral to the silt deposits. Since it is not found with the bones, and since these show a general lack of abrasion, most of the bones are probably autochthonous to the floodplain environment. The presence of associated skeletal parts may indicate carcasses buried *in situ* or floated in during the floods. Most of the bones probably were buried by the periodic influxes of floodstage silts. The trapping effect of floodplain vegetation may have been influential in anchoring the bones until they could be buried. Some of the lighter elements may have been dispersed by these floods, but most of the thanatocoenose remained in place as a lag deposit to be covered, or destroyed by later weathering.

Discussion and Conclusions

The seven localities can be grouped into three broad categories on the basis of similarities in lithofacies:

1) Delta: 103–0256, 130–0201, 105–0208, (103–2067)
2) Channel: 102–0201, 105–1311, (103–0267)
3) Floodplain: 8+6–0104

These groupings are similar in lithology, bedding structures, and lateral facies relationships. The deltaic localities are more diverse in these characteristics than the channels, with 103–0256 representing a transgressive beach, 130–0201 distributaries and a delta margin, and 105–0208 a beach and lagoon complex. 103–0267 can also be regarded as deltaic, since it represents a distributary complex rather than a single, well-defined channel. However, its lithology and sedimentary structures are more like those of the channels. Hence, it is intermediate between the deltaic and channel groupings, and is included parenthetically in both.

If the composition of the bone assemblages is linked to sedimentary processes, then the channel assemblages should be more like other channel assemblages than like floodplain or deltaic assemblages. The characteristics that should be similar within similar deposits include the degree of bone-sorting and the degree of weathering and abrasion. In the extreme case, the depositional processes could sort and partially destroy a given thanatocoenose so as to obscure all of the original ecological information in the assemblage.

Thus, the first step in recovering ecological information from East Rudolf assemblages is to isolate those cases where the effects of depositional processes are minimal. The evidence presented so far against extensive alteration of a thanatocoenose by sedimentary processes includes:

1) Bones with fresh, unabraded surfaces
2) Complete bones, skulls with teeth and delicate structures intact
3) Associated skeletal parts (indicating lack of reworking)

On these criteria, the assemblages of Localities 103–0256, 105–0208 and 8+6–0104 have been least affected by depositional processes, and retain a maximum amount of paleoecologic information. The other localities have assemblages with mixed histories, and ecological information may be more difficult to isolate.

Fossil assemblages from the channel environments (including 103–0267) are similar in that they all bear evidence for bone abrasion and include mixed autochthonous and allochthonous material. The lacustrine-deltaic environments are less similar among themselves, with Locality 130–0201 combining the characteristics of transported and nontransported assemblages, while the others appear primarily untransported. In general, however, it appears that some aspects of the bone assemblages are similar in similar lithologies, and thus reflect the processes operating in the different sedimentary environments.

SORTING IN BONE ASSEMBLAGES OF THE KOOBI FORA FORMATION

The primary object of this section is to establish the relative numbers of different skeletal parts in the seven bone assemblages and to discuss their taphonomic implications. Different skeletal parts have very different potentials for dispersal, as discussed in the section on bones as sedimentary particles. Depositional processes operating on bones should affect the ratios of skeletal parts, particularly those that have widely different densities, such as teeth and vertebrae or phalanges. Assemblages that have a concentration of elements with similar dispersal potential indicate sorting of the original components of the thanatocoenose. Assemblages with a mixture of heavy and light, large and small bones indicate either less alteration of the thanatocoenose before burial, or a mixture of bones with different taphonomic histories.

Most skeletons are incomplete when their parts become sedimentary particles, due primarily to destruction by carnivores. The initial assemblage, after carnivore activity (such as in East Africa today), consists of teeth, skulls, horn cores, vertebrae and limb ends, with more parts surviving for large animals than small. This results in an assemblage of bones with a wide range of sizes and densities, which will be subject to sorting in transport situations. The bones and teeth also have different survival potentials in most situations, with the former being more readily destroyed by taphonomic processes than the latter.

Sampling of Bone Assemblages

Most of the fossil vertebrates of the East Rudolf deposits occur in surface lag concentrations due to the removal of surrounding sediment. In general, movement of fossils away from their source rocks is minimal, and they remain in clear association with particular sediments. Conditions of preservation and recent erosion are such that even delicate fossils usually remain reasonably intact, once exposed, and compact objects such as teeth may last for long periods of time (100+ years?) on the surface. This provides a large amount of accessible material for collection.

Bones from the seven localities described in the previous section were collected using the following procedure: Grid squares of 10×10 m were laid out over the chosen area of outcrop. The first square in each locality was positioned using an arbitrary spot on an aerial photograph or simply by selecting a local landmark (e.g., a tree or conspicuous outcrop), without specific reference to the degree of surface bone concentration. Subsequent squares were measured off from the first, with a minimum of 20 m between squares. On horizontal strata, the squares were laid out on an orthogonal 30×30 m grid. On dipping strata, the squares were positioned along the strike of the units being sampled. The grid system was adjusted, where necessary, to avoid patches of recent sediment and vegetation. The selection of squares was *not* adjusted to sample particularly attractive patches of bone fragments, in order to prevent subjective biasing of the bone samples. Collecting was done by systematically traversing a square first east-west, then north-south (for a square oriented NSEW). All the surface bone larger than 5 cm (mamixum length) was collected in addition to those smaller bones that could be identified to class (Fish, Mammal, Reptile, Bird). During the first field season all samples were removed for identification and study. During the second season, after workers were familiarized with the vertebrate taxa and skeletal parts, it was possible to do most identification in the field. This greatly simplified the logistics of the sampling, and enabled workers to leave the field with a card for each square recording taxa and skeletal elements plus geological data. This was a welcome alternative to carrying out 50–60 lbs. of fossil bone fragments after each day of collecting.

Table 6. Stratigraphic data and sample size of the seven fossil sampling localities. Sample squares are 10 × 10 meters, representing 100 m^2 each.

SAMPLING LOCALITY	# OF SAMPLE SQUARES	STRATIGRAPHIC INTERVAL SAMPLED (IN METERS)	BASIC LITHOLOGY	GENERAL DEPOSITIONAL ENVIRONMENT	KOOBI FORA FM. FAUNAL UNIT	STRATIGRAPHIC UNIT
130-0201	21	7.0	Sand, silt, and clay	Delta margin	Mesochoerus	Lower Mb., Koobi Fora Fm.
105-0208	20	2.5	Sand, silt, and clay	Delta margin and lagoon	Mesochoerus	Lower Mb., Koobi Fora Fm.
103-0267	20	3.0	Sand and gravel	Distributary-beach complex	Metridiochoerus	Upper Mb., Koobi Fora Fm.
103-0256	27	.75	Sand	Transgression over deltaic mudflats	Metridiochoerus	Upper Mb., Koobi Fora Fm.
102-0201	34	5.0	Sand and gravel	Channel	Metridiochoerus	Upper Mb., Koobi Fora Fm.
105-1311	25	3.0	Sand and gravel	Channel	Metridiochoerus	Upper Mb., Koobi Fora Fm.
8+6-0104	66	4.5	Silt	Floodplain	Loxodonta	Ileret Mb., Koobi Fora Fm.

Maps of each locality showing the positioning of the sample squares are given in Figures 15 and 16, and the number of squares collected in each locality is given in Table 6. The major problems encountered in the sampling were: 1) choosing localities that showed a clear relationship between the surface bones and the sedimentary units, 2) obtaining comparable samples from each locality that adequately represented the bone assemblages.

Choosing the Sample Areas

The primary goal was to collect an assemblage of bones that represented the material buried in a well-defined sedimentary deposit. In selecting the sampling localities, the following guidelines were established:

1) A locality was chosen on beds, or a series of beds, representing deposition in one of three broad environmental categories: channel, floodplain or delta.
2) The topographic situation was such that contamination of the fossil concentrations with material from other horizons was minimal. Efforts were made, for example, to sample beds on drainage divides rather than in valleys.
3) Vegetation and recent sediment in the area were minimal.
4) Previous collecting in the area was minimal, or collection sites were marked and the removed fossils recorded.
5) The locality was extensive enough so that a representative sample of the fossil assemblage could be collected.

Fortunately, the East Rudolf region provided many areas that satisfactorily met all these requirements. Since stratigraphic *series* of environmentally related beds rather than single beds were used, the chances of contamination from different series of beds representing different depositional environments was greatly reduced. In the course of sampling, the actual bone-producing beds were often indicated by matrix adhering to fossils, and some of the samples could be assigned to particular horizons. Such evidence further supported the association of bones with the environmental units of interest.

The advantage of sampling different lithologies that are genetically related (e.g., sands, silts, and clays, all deposited in deltaic conditions) is that this will give a more general picture of the faunal and skeletal elements preserved in a rather broadly defined environment. This con-

trasts with sampling a particular bed (as in some quarry deposits), which is more likely to be the result of very local or special conditions. The sampling method described above allows coverage of extensive areas (square kilometers) of outcrops representing single, broadly defined sedimentary environments. This permits sampling on a scale more comparable to the habitat sizes of many East African vertebrates (on the order of square kilometers to thousands of square kilometers). Sampling by widely spaced squares should establish faunal and bone abundances that represent broad-scale differences between sedimentary environments and the habitats associated with them. Moreover, sampling through several meters of sedimentary strata representing extended periods of time should reveal more general pictures of bone and sediment associations than assemblages representing single events.

Sample Size

Surface bones are so abundant in the sampling localities that even a few 10×10 meter squares provided large numbers of fragments, and over 9,000 were collected in the total sample from 213 squares. More than 7,000 (78%) of these were identifiable as to skeletal part or vertebrate group or both. Very few of the sample squares lacked fossil material, even though they were laid out without regard to fossil distribution.

The abundance of fossil material was sufficient to provide an average of 34 identifiable pieces per square and to give a good representation of the most common parts and animals. Field collecting was aimed at obtaining the largest possible comparative samples from all the localities. Since the surface concentration of bone varied from locality to locality, the number of squares collected in each varied as well. Thus, it was necessary to collect over 60 squares for 8+6-0104, which had a low surface concentration, but only 20 for 105–0201. At least 20 squares ($= 2000$ m^2) were collected in each locality.

Method of Representing Fossil Abundance

It is possible to represent the relative abundance of different bones in more than one way. For instance, within each locality the total number of fragments identifiable as vertebrae can be compared with the total number of tooth fragments. Percentage representations of these totals can be compared between localities. Alternatively, the total number of *squares* with vertebrae can be compared with the total number of squares with teeth, etc. For reasons described below, the second method of representing relative abundance is used in all the following analyses of the fossil assemblages.

Difficulties in using total numbers of parts for comparative purposes include the following:

1) One tooth, for instance, can weather on the surface into dozens of fragments which are still identifiable as teeth, but a vertebra may only produce a few fragments that can definitely be identified as vertebrae. In both cases the numbers of broken fragments, if totaled, would count for more than the whole elements, and give erroneous data on the relative numbers of these elements. This problem is particularly pertinent to a fragmented surface sample, and is almost impossible to correct for by attempting to calculate the "minimum numbers" of fragments per bone in the manner of Shotwell (1955).
2) A single skeleton, if disassociated prior to burial or during recent erosion, may be counted as several individuals of the same animal group, while the whole skeleton would be counted as one individual. This can lead to errors in representing the actual abundance of different animals. Shotwell's method of using mini-

mum numbers of individuals[3] helped to resolve this problem for his quarry samples (1955). In the East Rudolf surface assemblages, with many vertebrate groups represented by a wide range of identifiable bone fragments, the minimum numbers method was not feasible.

The more satisfactory method of representing bone abundance for the East Rudolf localities is to use the number of squares with a particular skeletal part. This is done as follows: if one vertebra, or several, or dozens of pieces of the same one, occur in a sample square, this is counted as 1 occurrence. If one tooth of the same taxon occurs in each of 5 squares, this is counted as 5 occurrences. The number of occurrences of each bone can be converted into a "square frequency" by dividing by the total number of squares in each locality. Thus, 5 occurrences out of a sample of 20 squares gives a frequency of .25 or 25%.

This method has a number of advantages which make it a valid measure of bone abundance in the broadly defined sedimentary units of interest for this study:

1) It gives a measure of the *dispersed* abundance of the different bones in space and time, which should be a result of the *overall* conditions of each sedimentary environment.
2) The problems encountered in using fragment totals are essentially eliminated, since using occurrences in squares will greatly reduce the effects of differential identifiability and fragmentation of the surface bones. Also, since the squares are widely spaced, the probability of sampling parts of the same bone or even of the same animal more than once is very low.

A comparison of the two measures of abundance, by fragment number and by squares, illustrates the advantages of the latter method. In Figure 19, the frequency of vertebrae in each locality is given according to total numbers of fragments identifiable as vertebra, and by the frequency in terms of squares with vertebrae. Numbers of vertebral fragments that are high relative to the square frequencies, as in 8+6–0104, imply localized concentrations. In fact, for 8+6–0104 the large number of vertebrae results from two associated partial skeletons of bovids. In contrast, a high square frequency and a low fragment number shows a widely dispersed sample of isolated vertebrae, as in 103–0256 and 103–0267, where only one or two vertebrae occur per square. The representation of the dispersed abundance is more useful in comparing bone assemblages that result from interrelated processes in channel, floodplain or deltaic environments. The "square frequency" of bones (= the number of squares with a particular bone or taxon divided by the total number of squares per locality) will thus be used in the following sections.

Characteristics of the Bone Assemblages

During the collecting of the bone sample, and prior to numerical analysis, it was apparent that some parts, such as teeth, were more abundant in some localities than others. However, most of the differences in bone proportions among the localities became apparent only after relative abundances were tabulated in the laboratory.

The bone sample contains abundant skeletal fragments from mammals, reptiles and fish, and a few from birds. Analysis of bone frequencies is restricted mainly to the mammals, which form the largest and most diverse component of the sample. Frequencies of the skeletal parts are given in Table 7. Discussion of the method of identification, which can influence the apparent abundance of parts, will precede analysis of the data.

[3] The relative abundance of different taxa is represented by the number of the most common similar skeletal part (e.g., left femora) of each taxon (Shotwell, 1955:331).

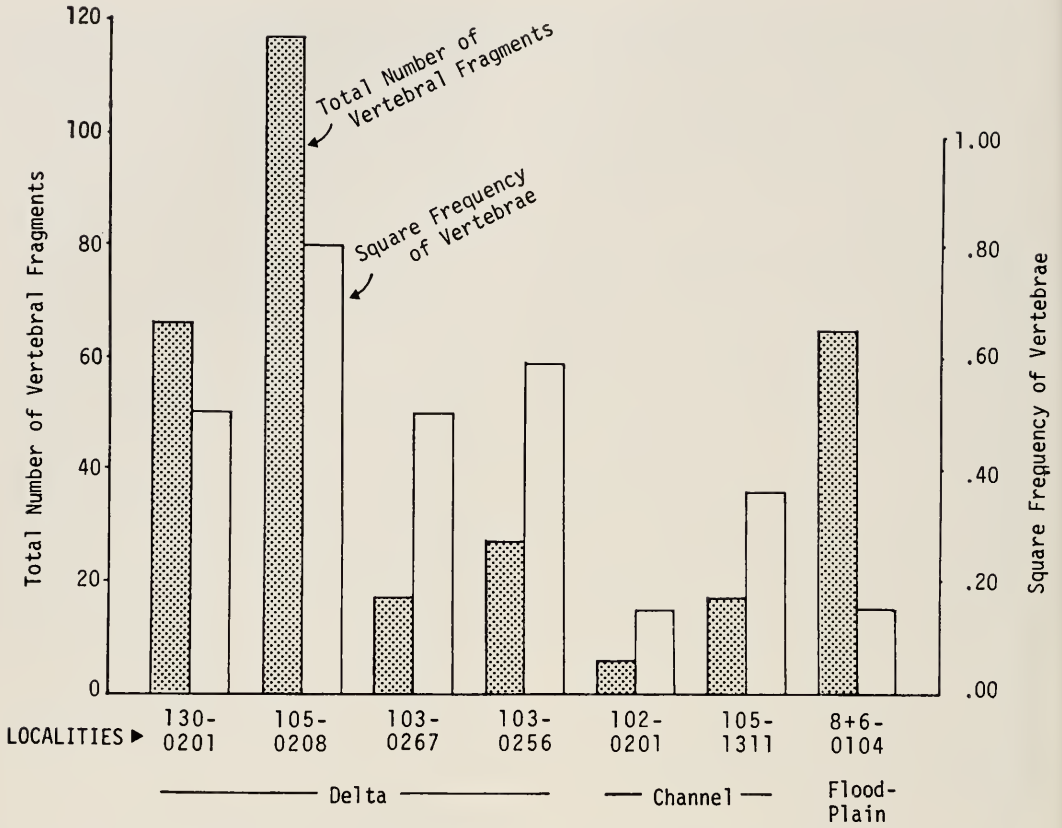

Figure 19. A comparison of two ways to represent the abundance of vertebrae in the fossil samples. The shaded bars on the histogram represent the total number of vertebrae and vertebral fragments from each locality. The white bars represent the square frequency of vertebrae, the proportion of squares in each locality which contained at least one vertebral part. Localities with a large number of fragments in proportion to the square frequency generally have associated vertebral columns (e.g., 105–0208, 8+6–0104). Localities with high square frequencies but low numbers of fragments indicate wide dispersal of vertebrae.

Identification of Bones

A large proportion of the collection was identifiable as to skeletal part. For reptiles and mammals, 24 categories include all the identifiable bones. Mammals have 19 categories which can be assigned to a specific class with certainty (Table 7). Rib and diaphysis fragments, plus some phalangeal, vertebral and pelvic fragments, cannot always be assigned to class. These are not included in the frequencies for either mammals or reptiles.

The number of identifiable fragments of different bones is variable and can lead to a bias for greater apparent abundance of the bones with more identifiable parts. However, since all the bone fragments were identified in a consistent manner by one person (A.K.B.), there should be little or no effect on the locality to locality comparisons. There will be some effect on the absolute abundance of certain elements within each locality. Teeth, for example, are always more identifiable than other parts and thus will appear to have higher frequencies than is actually the case. The use of "square frequency" helps to minimize this effect, since only squares with at least one partial tooth (excluding fragments of

dentine or enamel) were counted. Differences in the numbers of identifiable fragments of other bones, particularly for mammals, probably have an insignificant effect on their relative "square frequencies" in this study. Most bones were represented in each square by at least one relatively complete part (e.g., ends of limb bones, vertebral centra, whole phalanges, etc.).

Significance of the Frequency Data

The data given in Table 7 show that most of the skeletal parts are represented in each locality. Some have consistently high frequencies, such as teeth; some low, such as patellae, and some are variable. The lower frequencies indicate occurrence in only a few squares out of the total for each locality. Both high and low frequencies are of interest in comparing the samples.

To assess the statistical significance of the frequencies, one must ask, "How representative of the actual bone assemblage in each locality are the 'square frequencies'?" In some respects the problem is comparable to establishing binomial sampling limits for accurately detecting character frequencies in any given population (Simpson *et al.*, 1960:199). In such cases, tables are available for relating actual frequencies to observed frequencies using various sample sizes. For example, a character with 40% frequency in the actual population could vary from 12–35 occurrences in a sample of 60, with a probability of only .001 that fewer than 12 or greater than 35 occurrences would be observed.

The binomial sampling limits for square frequencies can be calculated using the Harvard Tables (1955). For a sample of 34 squares, a frequency of .32 (11 squares) could represent a possible range of actual frequencies between .17 and .48, with a probability of only $p = .05$ that the actual frequencies in the bone assemblage would fall outside of this range. The sampling error indicated by simple binomial probability is potentially rather large. However, it can be assumed that the square frequencies are more closely representative of the true bone frequencies because: 1), each sample square consists of a 10×10 m area, which greatly increases the probability of finding a particular bone if it is present in the assemblage and 2), many squares include more than one bone of a particular kind, and the actual frequency is higher in these cases than representation by square frequency would indicate. Therefore, the square frequencies will be treated as representative frequencies for the following data analysis. The bone abundances, as represented by these frequencies, should be comparable from locality to locality. The statistical significance of specific differences or similarities between localities was tested using Chi-Square analysis.

Comparisons of Overall Bone Concentrations

The relative concentration of identifiable bones varies greatly in the sample squares of the seven localities. Overall bone abundance can be conveniently expressed by dividing the cumulative total of bone occurrences in squares by the number of squares in each locality. These figures are given for identifiable mammal and reptile parts in Table 7. Locality 8+6–0104 has the lowest concentration and 105–0208 the highest. The three channel assemblages are no more concentrated than the lacustrine-deltaic ones for mammals, but are slightly less prolific in terms of reptiles. There does not appear to be any consistent correlation between sediment grain sizes and identifiable bone abundance in the deposits sampled.

The localities with more bones per square do not appear to have more of any particular elements. Rather, they show an increase in the frequencies of all skeletal parts. This implies better conditions for preserving bones of all kinds, regardless of size and density, and argues against accumulation due to selective processes of sorting (which would tend to concentrate bones of similar sizes or densities or both).

TABLE 7. THE SQUARE FREQUENCIES OF REPTILE AND MAMMAL SKELETAL PARTS IN THE SEVEN SAMPLE LOCALITIES. FREQUENCIES ARE CALCULATED AS THE NUMBER OF SQUARES WITH A PARTICULAR ELEMENT DIVIDED BY THE TOTAL NUMBER OF SQUARES IN EACH LOCALITY. THE FREQUENCIES OF ASSOCIATED PARTIAL SKELETONS AND JUVENILE BONES ARE CALCULATED IN THE SAME MANNER. MAMMAL AND REPTILE BONES ARE COMBINED IN THE SECOND LISTING TO INCLUDE THOSE WHICH COULD NOT BE DEFINITELY ASSIGNED TO ONE OR THE OTHER CLASS. THIS SHOWS THE RELATIVELY HIGH PROPORTION OF RIB AND DIAPHYSIS FRAGMENTS IN THE TOTAL BONE SAMPLE.

	DELTA				CHANNEL		FLOOD-PLAIN
REPTILE	130-0201	105-0208	103-0267	103-0256	102-0201	105-1311	8+6-0104
Tooth	.86	.85	.50	.33	.26	.68	.12
Skull/jaw	.10	.05	.30	.07	.15	.08	.00
Vertebra	.19	.05	.15	.19	.18	.00	.02
Limb	.14	.05	.05	.15	.09	.00	.00
Scute	.24	.40	.50	.30	.24	.40	.02
Phalanx	.10	.15	.00	.04	.00	.04	.00
Carapace/plastron	.24	1.00	.70	.81	.24	.32	.12
# occurrences per square (average)	1.9	2.5	2.2	1.9	1.1	1.1	.3
MAMMAL AND REPTILE							
Tooth	.95	1.00	.80	.59	.76	1.00	.67
Rib	.76	.90	.85	.63	.53	.64	.32
Pelvis	.14	.25	.25	.04	.06	.16	.05
Diaphysis	.57	1.00	.95	.89	.71	.92	.55
Phalanx	.52	.55	.35	.30	.15	.32	.12
Vertebra	.57	.85	.55	.59	.29	.48	.15

RELATIVE ABUNDANCE OF SKELETAL PARTS

The frequency data in Table 7 can be analyzed: 1), in terms of the most common bones in each locality and 2), in terms of the correlations between localities caused by similar proportions of different mammalian bones. Teeth are the most common mammalian element in all localities except 103–0256. Otherwise, the patterns of frequency are variable, with some indication that vertebrae and phalanges concentrate in the deltaic environments. In order to clarify possible correlations between localities, two numerical analyses were used: a multiple regression analysis, which gives correlation coefficients for locality to locality comparisons, and a Q-Mode Factor Analysis, which shows groupings of the localities in terms of skeletal parts.

CORRELATIONS BASED ON BONE ABUNDANCE

Figure 20 shows a correlation matrix resulting from multiple regression treatment of skeletal part frequencies in the squares. The correlation is "Pearson's product moment correlation" which assumes con-

Table 7 (cont.)

MAMMAL	DELTA				CHANNEL		FLOOD-PLAIN
	130-0201	105-0208	103-0267	103-0256	102-0201	105-1311	8+6-0104
Tooth	.67	.85	.70	.56	.62	1.00	.52
Jaw part	.24	.10	.10	.04	.21	.08	.09
Maxilla	.05	.00	.00	.00	.00	.00	.02
Cranial part	.05	.25	.15	.07	.12	.08	.08
Horn core	.19	.25	.35	.15	.18	.36	.03
Vertebra	.48	.75	.50	.59	.15	.36	.15
Sacrum	.00	.00	.05	.04	.00	.00	.00
Scapula	.14	.45	.15	.15	.12	.20	.09
Pelvis	.10	.20	.20	.04	.03	.12	.05
Humerus	.19	.50	.30	.11	.06	.20	.14
Radius/ulna	.14	.40	.20	.11	.15	.20	.15
Femur	.14	.40	.05	.07	.18	.16	.08
Tibia	.10	.30	.25	.07	.06	.28	.14
Patella	.05	.05	.00	.00	.00	.04	.00
Metapodial	.10	.40	.40	.22	.18	.32	.14
Astragalus	.10	.20	.25	.11	.03	.08	.14
Calcaneum	.10	.15	.15	.15	.00	.12	.08
Podial	.10	.45	.10	.19	.24	.20	.18
Phalanx	.48	.65	.35	.26	.15	.28	.12
Total # squares	21	20	20	27	34	25	66
# occurrences per square (average)	3.4	6.4	4.2	2.9	2.4	4.1	2.2
Associated parts	.04	.20	.05	.04	.00	.00	.06
Juveniles	.14	.30	.05	.04	.06	.12	.00
% hippo bones	18%	16%	21%	6%	12%	7%	2%

Total # squares for all localities: 213

Average occurrences per square: 690/213 = 3.2

tinuous data and normal bivariate distributions. Both conditions are satisfactorily met by the squares data. Correlations are based on the five most common elements: teeth, vertebrae, phalanges, scapulae and radii/ulnae.

An obvious feature of all the correlations is that they are high ($> .5$). This shows a basic similarity in the ratios of the five skeletal elements in all the sample assemblages, although these elements vary greatly in size and density. Therefore, the differences in the sedimentary environments were not enough to alter the basic similarity of the thanatocoenoses sampled in each deposit. This similarity is probably produced by those bones most likely to survive carnivore activity and become sedimentary particles.

Many of the correlations shown in Figure 20 are significantly different, in spite of the overall similarity. The highest and lowest coefficients differ significantly, with a probability of $<.05$ according to the "z test"

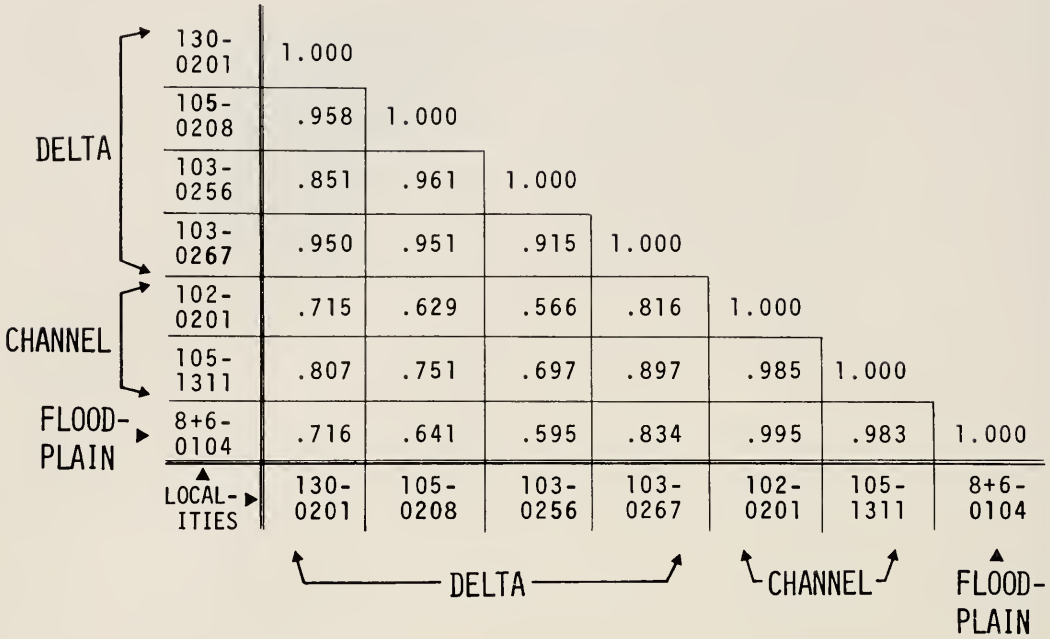

Figure 20. Correlation coefficients (Pearson's product moment correlation) between sampling localities according to the proportions of the five most common skeletal parts: teeth, vertebrae, phalanges, radii/ulnae and scapulae. Highest correlations show strong similarities between channel and floodplain environments in terms of the proportions of different skeletal parts.

for significance (Simpson *et al.*, 1960:246). Other coefficients are indicative of trends even when their differences are not within the acceptable limits of significance ($p \leq .05$).

The coefficients show that the channel assemblages, 105–1311 and 102–0201, are closely correlated with each other and with the floodplain, 8+6–0104. The deltaic assemblages have relatively low correlations with the floodplain, variable degrees of correlation with the channels, and high correlations among themselves. Thus the proportions of the five different bones are similar in similar sedimentary environments, showing the effects of processes operating within these environments. Some of the close interenvironmental correlations, such as between the floodplain and channel assemblages, and between 130–0201 and 103–0267, suggest processes that are common to more than one sedimentary situation. These can be further clarified by examining which bones are influential in causing the interlocality correlations.

Factor Analysis of the Bone Assemblages

Factor analysis was used to indicate which skeletal parts cause similarities or differences among the seven bone assemblages. The Q-Mode Factor Analysis, "CABFAC," was run on the frequency data from all of the mammalian skeletal parts. A solution of three varimax factors (axes placed within the data array) explains 97% of the total variance in the assemblages. The projection of the data for each locality on these axes is plotted on the triangle diagram shown in Figure 21. The diagram shows graphically how the three factors group (cluster) the bone assemblages.

The three factors consist of 1) vertebrae

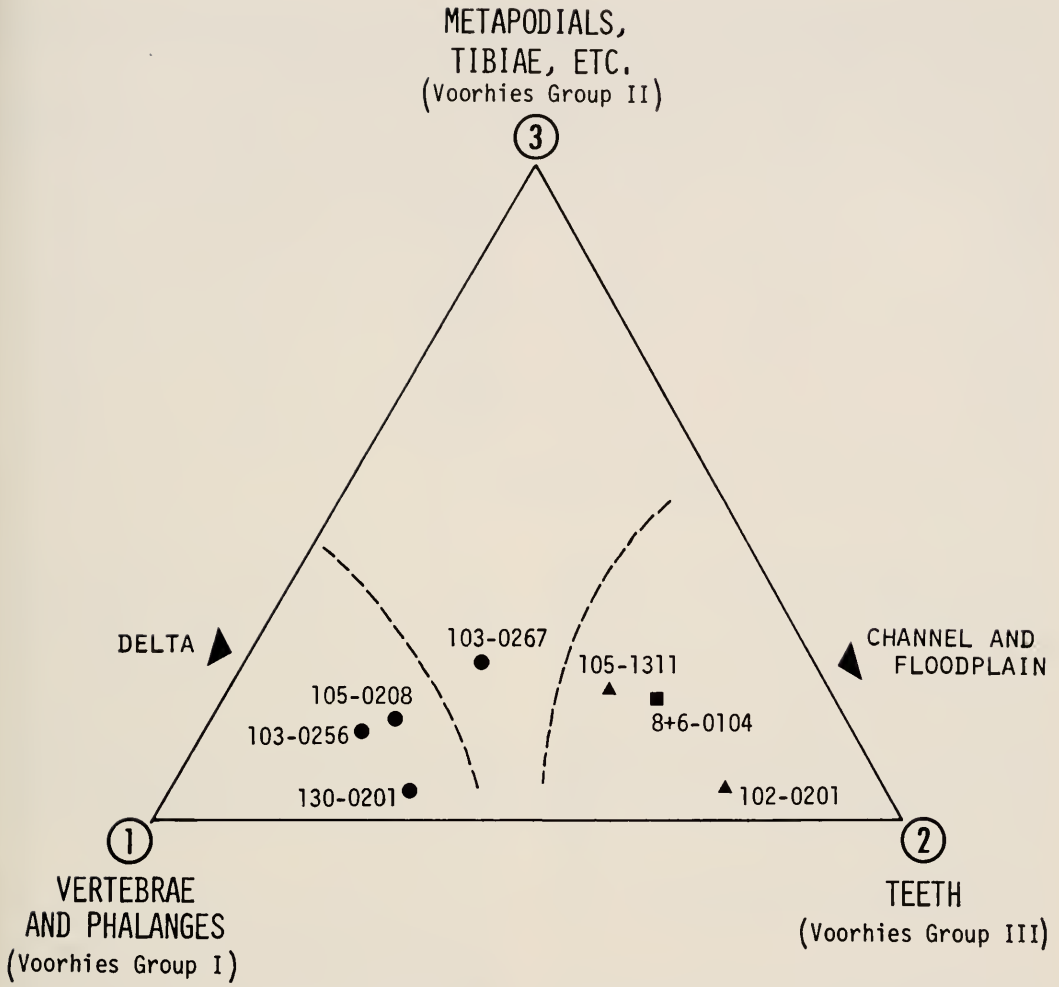

Figure 21. Triangle diagram showing the results of a three-factor analysis of the frequency data for all mammalian bones. The factors correlate with Voorhies' dispersal groups, showing a relatively high proportion of Group I (most easily dispersed) in the deltaic assemblages and Group III (lag) in the channel and floodplain assemblages.

and phalanges, 2) teeth, 3) limb parts such as tibiae, metapodials, and astragali. The triangle diagram shows a clear separation of assemblages on the basis of Factors 1 and 2. The three deltaic localities have a high proportion of vertebrae and phalanges, while the channels and the floodplain have high proportions of teeth. 103–0267 falls between the two groupings, and is somewhat anomalous in its lack of similarity to the channel assemblages. Localities 103–0267 and 8+6–0104 both show that there is no strict correlation between tooth concentrations and coarse-grained sediment. 103–0267 is a coarse-grained deposit lacking a high proportion of teeth; 8+6–0104 is fine-grained, but is characterized by a high tooth concentration.

It is clear that the high correlation coefficients between assemblages from similar sedimentary environments are due to the proportions of teeth, vertebrae and

Table 8. The relative frequencies of skeletal parts in a single skeleton, the average of bovid, suid, equid and hippo skeletal proportions. Underlined parts are those which are most common or most consistently present in the fossil assemblages.

	No. in average skeleton	No. of each part/total no. of parts in average skeleton (156)		No. in average skeleton	No. of each part/total no. of parts in average skeleton (156)
Teeth	38	.26	Radii/Ulnae	2	.01
Jaw	1	.01	Femora	2	.01
Maxilla	1	.01	Tibiae	2	.01
Cranium	1	.01	Patellae	2	.01
Horn Cores	2	.01	Metapodia	4	.03
Vertebrae	28	.18	Astragali	2	.01
Sacrum	1	.01	Calcanea	2	.01
Scapulae	2	.01	Podials	22	.14
Pelvis	1	.01	Phalanges*	42	.27
Humeri	2	.01			
			TOTAL	156	

* Including metapodials of suid and hippopotamus.

phalanges. These two groups of skeletal parts have very different properties of density and destructibility. The deltaic environments preserve more of the easily transported and destructible elements, the vertebrae and phalanges. The channel and floodplain environments preserve more of the denser and durable parts, primarily teeth. The experimental data on bone transport discussed in the section on bones as sedimentary particles can be used to interpret these differences in the fossil assemblages.

Comparisons with Voorhies Groups

The Voorhies Groups consist of bones with very different dispersal potentials. For animals from suid- to equid-size, phalanges and vertebrae are included in Group I, limb parts in Group II to III and teeth in Group II–III. Group I is most easily transported, Group III least easily transported and Group II intermediate, in currents up to 150 cm/sec, given Voorhies' (1969) experimental conditions.

The three factors shown in Figure 21 are closely comparable to the three Voorhies Groups. Group I is more typical of the deltaic assemblages and Group II of the channel and floodplain assemblages. This provides evidence that transport sorting may be an important process in creating differences between the bone assemblages, i.e., the lag group is left behind in the channels while the transportable group is carried out to the deltaic and lacustrine deposits. The loss of Group I in the floodplain may result from winnowing of the lighter elements during floods, if the current velocities on the floodplain exceed 10–20(?) cm/sec.

Single Skeleton Comparisons

Comparisons of the bone frequency data with the percentages of different bones in a single, whole skeleton show how the assemblages have been altered from their original states. If all bones had been preserved together, then the correlations between the proportions of different parts in the sample assemblages and a single skeleton should be high.

Average proportions of parts in a single skeleton were calculated, combining the most common mammal groups in the fossil assemblages. These consist of bovids, hippos, suids and equids. Frequencies of the different parts are given in Table 8. Figure 22 shows the comparison of fossil and single skeleton bone frequencies for

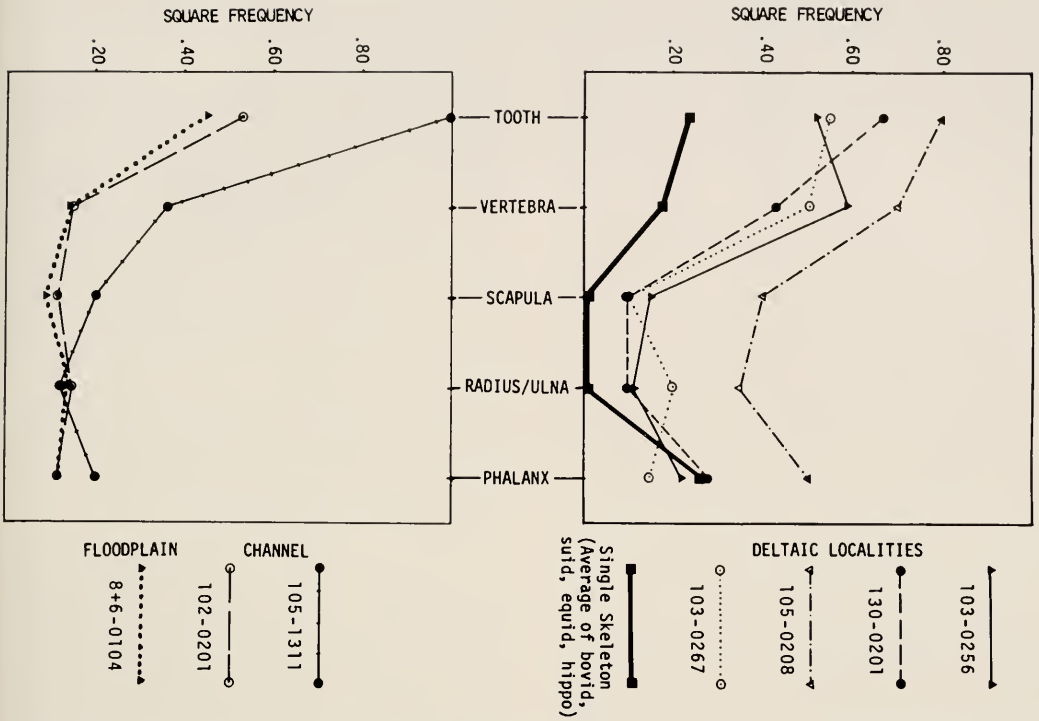

Figure 22. The square frequencies of the five most common mammalian skeletal elements in each locality compared with the proportions of the same elements in a single, average skeleton. The localities separated by factor analysis (Fig. 21) are distinct in their degree of alteration from single skeleton proportions.

the 5 most common or most consistently occurring parts. The assemblages fall into two obvious groups: 103–0256, 130–0201, 105–0208 and 103–0267 are closely correlated with the single skeleton, and 105–1311, 102–0201 and 8+6–0104 are not.

It appears that the lacustrine-deltaic environments, plus the 103–0267 channel-beach complex, preserve skeletal parts with a minimum of change from the original proportions. This implies the absence of processes that would sort the bones according to size, density or destructibility. In contrast, the channels, 102–0201 and 105–1311, and the floodplain, 8+6–0104, preserve altered assemblages with a high proportion of the heavier and more durable parts and a much lower proportion of the lighter and more destructible elements.

Discussion of Evidence for Transport Sorting

The combination of evidence from the comparisons of bone assemblages with Voorhies Groups and single skeletons leads to important conclusions regarding the histories of the bones in each locality. In the deltaic deposits, bones from all Voorhies Groups are present in proportions similar to those of an average single skeleton. Therefore, the major component of Group I in these deposits is probably not transported from elsewhere (i.e., the channels). If it were, then it has combined with lag assemblages to closely approximate the proportions in one skeleton. A better interpretation for the deltaic assemblages is that they have not been sorted. The relatively

fresh, unabraded surface textures of many of the bones, plus their lack of hydraulic equivalence with matrix grain sizes, further supports this interpretation. The high proportion of Voorhies Group I in the deltaic assemblages is a product of nonselective taphonomic processes rather than selective ones.

In the 105–1311 and 102–0201 channels, the concentration of teeth is the result of sorting by fluvial processes. This sorting combines the lag concentration of teeth because of their greater density *and* because of their greater durability in transport situations. In addition, teeth are probably concentrated from floodplain deposits as the channel migrates laterally, eroding its banks. Other parts derived from re-excavated skeletons would not be likely to survive erosion unless already mineralized.

The 103–0267 distributary-beach complex combines the sedimentary characteristics of the other channels with a bone assemblage similar to the deltaic ones. The assemblage shows lack of selective sorting, and apparently a large lag component of teeth was not a product of the fluvial processes operating in 103–0267. Why this should be so is as yet unexplained.

The floodplain assemblage shows selective preservation of teeth in a fine-grained sedimentary context. As mentioned on p. 536, this indicates the removal of lighter elements from an untransported thanatocoenose. Such removal could result from winnowing out of the light parts *or* from surface weathering and preferential destruction of vertebrae and phalanges relative to teeth. The relative importance of these two processes can be determined by future experimental work on the critical entrainment velocities of vertebrae and phalanges, and by observation of thanatocoenoses on modern floodplains. The low frequency of horn cores in 8+6–0104 may provide a clue indicating selective destruction by weathering, since in modern situations horn cores are often destroyed by worms that feed on their organic constituents (H. B. S. Cooke, personal communication) (Plate 3).

The extent to which sedimentary processes have altered the bone assemblages is clear from the examination of bone frequencies. The deltaic assemblages are least altered, and probably represent autochthonous accumulations in sedimentary environments where the potential for rapid burial, without re-excavation, is high. The floodplain assemblage is also autochthonous but has been altered by taphonomical processes so that it resembles the channel assemblages. These show the most extensive alteration of bone ratios due to sedimentary processes. 103–0267 is intermediate in the degree to which taphonomic processes have affected the bone assemblage.

The most useful localities for paleoecologic information are thus established as the deltaic and floodplain environments. The channels will also prove useful, since the factors contributing to their bone assemblages are known. They will include a mixture of animals from the vicinity of a fluvial system, in contrast to deltaic deposits, which preserve animals that frequented lake margin habitats.

Additional Aspects of the Bone Assemblages

More information regarding taphonomic history can be drawn from bone characteristics unrelated to relative abundance. These include the occurrences of associated skeletal parts and the ratios of proximal and distal ends of limb bones.

Associated parts of skeletons are rare in the East Rudolf deposits in general. The frequencies of these in the sample localities are included in Table 7. The channels 105–1311 and 102–0201 have none, while the floodplain and deltaic localities, including 103–0267, have at least one. Most of these consist of associated vertebrae, with more complete partial skeletons occurring in 105–0208 and 8+6–0104.

The associated skeletal parts may result

Table 9. Totals of proximal (P) and distal (D) limb ends in the fossil assemblages from each sample locality.

		DELTA				CHANNEL		FLOOD-PLAIN	
		130-0201	105-0208	103-0267	103-0256	102-0201	105-1311	8+6-0104	TOTAL
Humerus	P	2	2	2	0	3	2	2	13
	D	3	8	1	3	2	2	7	26
Radius/ulna	P	1	11	3	1	2	1	10	29
	D	1	1	2	1	1	1	4	11
Femur	P	1	4	1	0	2	1	3	12
	D	4	5	1	2	5	3	2	22
Tibia	P	1	4	1	1	1	5	5	18
	D	2	1	2	3	4	3	6	21
Metapodial	P	4	1	4	5	0	3	6	23
	D	1	6	6	2	1	2	8	26
Total	P	9	22	11	7	8	12	26	95
	D	11	21	12	11	13	11	27	106

from carcasses buried at the site of death or from carcasses transported by flotation. There are very few criteria that could be used to distinguish between these two possible taphonomic histories. However, the associated parts do indicate a minimum of reworking of the bone assemblages after initial burial. This agrees well with other evidence for lack of reworking of the delta margin and floodplain assemblages. The absence of associated parts in the channels is consistent with the abraded surface textures of the bones as an indication for extensive reworking of sedimentary particles in the channel environments.

Most of the limb bones in the samples are represented by one end or the other. It is of interest to determine whether some ends are more common than others, as an indication of preferential sorting or destruction prior to burial.

The numbers of proximal and distal ends of the major limb bones are listed in Table 9. For all localities and all limbs combined, the totals of 95 proximal and 106 distal are very close to a 1:1 ratio. This might be interpreted as indicating that no more proximal than distal ends are preserved, or vice versa. When the totals for each limb in all localities are examined, however, the relative frequencies of proximal and distal ends prove to be quite variable. There are nearly twice as many distal as proximal ends of humeri and femora, and many more proximal ends of radii/ulnae than distal. From the density measures of proximal and distal recent bones given in Appendix 2, it is apparent that the denser end is more commonly preserved in humeri and radii/ulnae, while the lighter end is more common in femora. A model for differential preservation because of transport sorting or more rapid weathering of low density ends does not fit this evidence.

The differences in frequency of the proximal and distal ends can best be explained by carnivore activity. In animals killed by carnivores or scavenged after death, the limbs are usually pulled off the carcass at the proximal articulation (humerus/scapula and femur/pelvis joints) (Müller, 1957:256–258). Proximal ends of the humerus and femur would be subjected to stress and later exposed for gnawing. In contrast, the elbow and knee joints are more likely to remain held together by

ligaments and survive the bone-crushing activity directed at more nourishing parts such as marrow-filled diaphyses. This explains the relatively high proportion of distal humeri and femora. The disproportionate number of proximal "radii/ulnae" actually consist primarily of olecranon processes from the ulnae. These are ligament-covered, lack a marrow cavity, and thus would survive better than the distal ends of radii.

The pattern of proximal and distal limb element frequencies can be regarded as good evidence for carnivore activity in fossil assemblages in general. Such evidence has also been used by Voorhies (1969:20) to indicate carnivore activity prior to the final burial of the Pliocene Verdigre Quarry bone assemblage. For the East Rudolf localities, the evidence for carnivore activity can be detected in spite of differences in the taphonomic histories of the bone assemblages in the different depositional environments.

The Reptilian Assemblages

Reptilian parts form less consistent frequency patterns than those of mammals. The most common elements, as shown in Table 7 are crocodilian teeth and chelonian shell parts. The relative numbers of crocodilian parts are very similar from locality to locality. There is no indication of any increase in similarity between assemblages from similar sedimentary environments. This is probably a result of the universal availability of crocodile bones in the aquatic (generally depositional) environments where crocodiles live. The low frequency of crocodiles in the floodplain environment, which crocodiles do not usually frequent, emphasizes this point. The chelonian shell parts are variable in occurrence, and are slightly more abundant in the deltaic deposits including 103–0267. This suggests some correlation between the more aquatic sedimentary environments and the chelonian occurrences.

Conclusions Concerning the Bone Assemblages

The evidence given in the preceding two major sections of this study brings out a number of taphonomically important factors that can be combined to support a definite history for any given vertebrate fossil assemblage comparable to those occurring in the Koobi Fora Fm.:

1) The correlation of bone assemblages with dispersal groups from Voorhies' flume study
2) The correlation of bone assemblages with the proportions of a single skeleton
3) The comparison of hydraulic equivalents of bones with grain sizes in the associated sediments
4) The completeness of bones, and surface characteristics that indicate presence or absence of weathering or abrasion prior to burial
5) Presence or absence of articulated or associated skeletal parts
6) Ratios of proximal and distal ends of limb bones that deviate from 1:1

All of these factors provide a basis for interpreting the East Rudolf data. The bone frequencies for each locality thus can be used to determine the taphonomic histories of the vertebrate assemblages. The following points can be made:

1) The different sedimentary environments of East Rudolf show a general similarity in the compositions of their mammalian bone assemblages. The same bones are present in all environments, and none of the assemblages consist exclusively of one of the three Voorhies Dispersal Groups.
2) Evidence for a certain degree of sorting and redistribution of bones is present in the different sedimentary environments. Significant differences in relative numbers of different bones are shown by the concentrations of teeth in the channels (105–1311 and

102–0201) plus the floodplain (8+6–0104), and by the concentrations of vertebrae and phalanges in the deltaic localities (130–0201, 105–0208, 103–0256, 103–0267). These can be correlated with the sorting effects of taphonomic processes in the channels and on the floodplain, and the absence of sorting on the delta/margins.

3) Consideration of the bone frequencies in the light of Voorhies Groups, hydraulic equivalence and single-skeleton comparisons shows that autochthonous and allochthonous assemblages of fragmental vertebrate bones can be distinguished. The deltaic and floodplain localities consist of basically autochthonous vertebrate fossils, while the channels contain a mixture of allochthonous and autochthonous assemblages.

FAUNAL ASSEMBLAGES OF THE KOOBI FORA FORMATION

Taphonomic analysis has shown that all of the sample fossil assemblages can be considered autochthonous in the broadly defined deltaic and fluvial environments. It is now possible to examine the faunal compositions of the seven bone assemblages and to relate these to the different sedimentary environments. Comparisons can be made from environment to environment which should indicate true paleoecologic differences or similarities in the faunas. In the following discussion, several aspects of the paleoecology of the Koobi Fora Fm. and its vertebrates will be given particular attention. These include the differences in numbers of aquatic and nonaquatic vertebrates, the relative frequency of different terrestrial mammals in the different environments, and the patterns of occurrence of mammalian groups that have close counterparts in modern ecosystems.

The fauna from the square sample as a whole includes 14 out of the 20 major vertebrate groups listed by Maglio (1972: 380–381) for the Koobi Fora Fm. The sample assemblages also include most of the genera of bovids, suids, equids and hippos. The carnivores listed by Maglio (1972:380–381) are the most poorly represented groups in the samples used for this study.

Method of Identification

The fossil collections consist of material that can be identified at a number of different taxonomic levels. Major groupings of vertebrates used for faunal comparisons among the sample localities were designated so that each member of a group has approximately equal numbers of identifiable parts. In practice, for example, this amounted to teeth, skull parts, limb ends and foot parts for mammals. The mammals listed below could be identified equally well using any of these parts. Consideration of this factor was necessary to prevent undue biasing of the square frequency for a form with substantially more or less identifiable parts. The fossil assemblages can be divided into faunal groups, corresponding roughly to several taxonomic Categories, as follows:

1) Class: Mammal, Reptile, Bird, Fish. Identifications were based primarily on the morphology of the bone fragments. Bone micro-structure was useful as a distinguishing character for very small fragments. In some cases parts of pelves, scapulae, ribs and diaphyses could not be certainly assigned either to mammal or reptile, and such parts are not included in any of the totals.

2) Groups of Reptiles and Mammals.

Mammals		*Reptiles*
Elephant	Suid	*Crocodylus*
Deinothere	Equid	*Euthecodon*
Hippopotamus	Primate	Trionychid
Rhinoceros	Carnivore	Pelomedusid
Giraffe	Rodent	*Geochelone*
Bovid		Varanid

The common denominator in these groups is that they are approximately equally identifiable, within each list. For

example, using the figures for relative numbers it will be possible to determine whether there are more hippos than elephants in the sample assemblages, but not whether there are more hippos than trionychids. Some of the reptiles produce many more abundant and readily identifiable bones than do the mammals (e.g., crocodile scutes), and may *appear* relatively more abundant in the samples. Thus, relative frequencies are only comparable *within* the mammals and reptiles, and some caution should be observed in comparing the different reptilian groups as well. *Crocodylus* and *Euthecodon* are comparable since they were identified only on the basis of teeth, and the three chelonian groups should be comparable since only shell parts were used. Problems in separating small *Geochelone* from Pelomedusids may lower the abundances of these two groups relative to the Trionychids.

3) Groups of Suids, Equids, Bovids and Hippos.

Suids	Equids
Mesochoerus	*Equus*
Notochoerus	*Hipparion*
Metridiochoerus	(= "Stylohipparion")
Bovids*	**Hippos**
Alcelaphinae	*Hippopotamus* sp. (large)
Large = *Megalotragus*	*H.* sp. nov. (small) (S. C. Savage, personal communication)
Small = *Damaliscus*-like	
Reduncinae	
Tragelaphini	
Bovini (*Pelovis*)	

*Nomenclature after Ansell (1971).

These groups occur in significant abundance in the sample assemblages and can be compared between localities. Other groups are represented by only one or two occurrences and cannot be used for comparative purposes. These include the bovid groups Antilopini, Hippotraginae, Cephalophinae and Neotragi, and a suid that is probably *Potomachoerus*.

Identification of the suids was done only on the basis of teeth. The equids were distinguished using teeth and metapodials, and the hippos using relative size of the skeletal parts identifiable as hippo. Bovids were identified primarily on the basis of teeth, but also from horn cores, ends of limb bones, podials and phalanges. The bone samples were equally identifiable within each of these groups. However, when the groups are compared, the suid and equid genera will have lower apparent abundances than the bovid tribes and subfamilies since they are represented by many fewer identifiable parts.

Although various other groups of vertebrates are identifiable to genera and species, they are not discussed in this study. These include primarily the fish and chelonians. Future work may reveal interesting patterns of abundance for members of these groups in the different sedimentary environments.

The relative numbers of all vertebrate groups will be expressed as "square frequencies," the percentage of squares in a locality that contain a given animal. This is the same measure as that used for skeletal parts (p. 529), and represents the "dispersed" or overall abundance of an animal in a sample locality.

Abundance of Vertebrate Classes

The class frequencies (Table 10) show that mammals, reptiles and fish are well represented in all seven localities. Birds occur in low frequency in two deltaic localities and in the floodplain. Mammals are at least as abundant as reptiles and fish in nearly all localities. Since most of the mammals are terrestrial, while the fish and most of the reptiles are aquatic, the relative numbers of vertebrate classes in the channels and deltas is not directly related to which animals were actually living within the depositional environments. Otherwise, fish and reptiles should be more common

Table 10. Class abundance in terms of square frequency.

	Delta				Channel		Floodplain
	130–0201	105–0208	103–0267	103–0256	102–0201	105–1311	8+6–0104
Mammal	.90	1.00	1.00	1.00	.82	.82	.83
Reptile	.90	1.00	.95	.89	.62	.62	.18
Bird	.00	.15	.00	.07	.00	.00	.03
Fish	1.00	1.00	.95	1.00	.79	.79	.30

than mammals. The large proportion of mammalian fossils probably means that there was a greater large vertebrate biomass in the terrestrial habitats close to the depositional environments. In the floodplain (8+6–0104), the relative numbers of the classes are more closely correlated with nonaquatic habitat preferences, and fish and reptiles are much less abundant than the predominantly terrestrial mammals.

Overall, the deltaic environments have a larger proportion of fish and reptiles than the channels. This is consistent with the more permanent and extensive lacustrine-deltaic aquatic environments, particularly if the nondeltaic channels were seasonally dry.

Calculated correlation coefficients based on the class frequencies are high among all localities (.97–.99) except for 8+6–0104. Here, the larger number of terrestrial animals over aquatic reflects a basic paleoecologic distinction consistent with the geologic interpretation of the floodplain environment for 8+6–0104. In this case, and probably for many similar fossil-bearing environments throughout the geologic record, the fauna which is preserved is primarily terrestrial. The deltaic and channel environments, in contrast, consistently preserve mixtures of aquatic and nonaquatic animals.

Abundance of Vertebrate Groups

Much paleoecologic information is available from the relative frequencies of the groups of mammals and reptiles listed on p. 541. The East Rudolf samples are best suited for such analysis since they provide abundant, easily identified fossil material representing these groups. The relative frequencies of mammals and reptiles are given in Table 11 and discussed below.

Reptiles

Three groups of reptiles are represented: crocodilians, chelonians and squamata. The last is rare, and the sample consists of a few vertebrae comparable in size to those of *Varanus* (Monitor Lizard). Crocodilians and chelonians occur in all areas, with chelonians more variable in relative abundance.

The crocodilians can be separated into two groups (Genera): *Crocodylus* (represented by at least two species) and the long-snouted *Euthecodon* (represented by at least one species). The two groups occur in similar frequencies except in 130–0201 and 102–0201, where *Crocodylus* is more abundant, and 103–0256, where *Euthecodon* is more common. It is unlikely that sorting during transport had any significant effect on the frequencies, since the hydraulic properties of the teeth are similar. Therefore, it is valid to conclude that, in general, the two crocodilians occupied overlapping ranges, i.e., both were present in the deltaic and channel environments. The living, long-snouted relatives of *Euthecodon* (*Tomistoma*) are found in quiet, open water (A. Greer, personal communication). Specific habitat preferences of *Euthecodon* are not clear from its patterns of abundance in the sample localities at East Rudolf. However, the conditions in 103–0256 after the transgression of the lake seem to have

Table 11. The square frequencies of the mammal and reptile families, calculated as the number of squares with identifiable parts of each family divided by the total number of squares for each area.

	DELTA				CHANNEL		FLOOD-PLAIN
MAMMALS	130-0201	105-0208	103-0267	103-0256	102-0201	105-1311	8+6-0104
Elephant	.05	.25	.10	.04	.09	.36	.05
Dinothere	.00	.00	.00	.00	.12	.08	.00
Hippopotamus	.62	.85	.70	.37	.41	.92	.21
Rhinoceros	.00	.00	.10	.00	.06	.12	.02
Giraffe	.00	.15	.05	.00	.03	.28	.06
Bovid	.62	.75	.70	.63	.50	.96	.58
Suid	.29	.60	.20	.19	.32	.60	.27
Equid	.14	.30	.15	.11	.12	.56	.12
Primate	.05	.20	.00	.04	.06	.12	.03
Carnivore	.00	.05	.00	.00	.00	.04	.03
Rodent	.05	.00	.00	.00	.00	.04	.00
REPTILES							
Crocodilus	.86	.60	.45	.04	.21	.52	.09
Euthecodon	.48	.65	.55	.33	.12	.52	.03
Trionychid	.19	.70	.45	.30	.18	.25	.03
Pelomedusid	.05	.75	.20	.48	.00	.60	.08
Geochelone	.00	.05	.25	.33	.03	.04	.00
Varanid	.00	.05	.00	.04	.00	.04	.02

been exceptionally favorable to *Euthecodon* and not so to *Crocodylus*. Many articulated parts, including complete skulls, have been found in 103–0256 in addition to the samples from the squares.

The chelonian sample consists of three family groups: Trionychids, (soft-shelled aquatic turtles), Pelomedusids, (semi-aquatic to aquatic turtles), and *Geochelone*, (land tortoise) (Loveridge, 1941; Loveridge and Williams, 1957). Both aquatic forms are common in all localities except 130–0201, 102–0201 and 8+6–0104. Trionychids are most consistently abundant. The occurrences of *Geochelone* and the Pelomedusids do not conform to any consistent pattern that can be related to habitat preferences of their recent counterparts. The shell fragments have fairly low hydraulic equivalents (< 3 mm except for large *Geochelone*) and are readily transportable. This may affect the proportions of large and small turtles preserved in an assemblage, and would tend to concentrate large *Geochelone* in lag deposits. Sorting should not affect the relative frequencies of the other forms, if they are of comparable size ranges.

The pattern of chelonian occurrences in the fossil samples is not readily explained either by sorting or by inferred habitat preferences. Other factors are involved, and one of these probably concerns ecological preferences of the fossil turtles that cannot be adequately inferred from the modern ones without identification of the fossil material to species. This is further complicated by the probability that factors

influencing turtle abundance (e.g., water turbidity, vegetation) may not be evident from the sedimentary record.

The low frequencies of chelonians in the floodplain assemblage are consistent with all other evidence for its predominantly nonaquatic environment of deposition. In other localities, at least some crocodilians and chelonians inhabited the environments of deposition. This is indicated by the variety of skeletal parts of crocodilians present in all deltaic and channel assemblages (parts with a wide range of hydraulic equivalents). It is also indicated by the presence of associated, unreworked parts of both crocodilians and chelonians in many of the localities.

Mammals

The numbers of different mammalian groups represented varies among the localities (Table 11). The 105–1311 channel assemblage is most diverse, with 11 groups represented. 105–0208, which has the largest number of identifiable bones (2389), has a relatively low faunal diversity (8 groups). In general, the deltaic environments have lower numbers of different terrestrial mammals. The short time span postulated for the deposition of 103–0256 (the transgressive sand) may help to account for its low faunal diversity. As would be expected, the more terrestrial depositional environments preserve more kinds of terrestrial animals. As many mammal bones are preserved in the more aquatic environments as in the nonaquatic ones, but they represent fewer terrestrial groups. The relative diversity of the fossil mammal assemblages apparently gives a true representation of the greater diversity of forms in the more terrestrial habitats.

The most common groups in all localities are bovids, hippos, suids and equids. Bovids are the dominant forms in all assemblages except 130–0201, 105–0208, and 103–0267, where hippos are slightly more numerous. The frequencies given in graphic form in Figure 23, show similar patterns for most of the assemblages. For the autochthonous assemblages of the deltaic and floodplain environments, these probably reflect the actual frequencies of animals in the death assemblages over the time periods sampled. The channel assemblages also should be broadly representative of the original relative abundance of the mammalian groups in the habitats sampled by fluvial processes. However, there is a definite bias against the smaller animals due primarily to their greater destructibility and transportability in all environments.

Rodents are rare throughout the East Rudolf vertebrate-bearing deposits. Since they are abundant in recent terrestrial habitats in the area, there can be little doubt that they are under-represented because of taphonomic processes that did not lead to preservation with the larger vertebrates. These probably involve carnivore destruction, rapid surface weathering of bones (due to high surface area to volume ratios) and high dispersal potentials (Dodson, 1974). The difficulties in collecting very small bones from the sample squares is another potentially important factor, although care was taken to minimize this during the sample collection.

Carnivores and primates have low frequencies in the samples, and this is partly a result of the same size factors affecting the rodent sample. However, some of the primates and carnivores reach sizes comparable to those of the smaller bovids and suids, and factors relating to size do not entirely explain the low frequencies. For carnivores, a low abundance compared with herbivores is consistent with their low relative biomass in the Eltonian Pyramid, in which a few carnivores are ecologically balanced with large numbers of herbivores. The scarcity of carnivore fossils probably reflects this ecological character. Primates are comparable in abundance to giraffes and rhinos in most localities. The samples consist primarily of baboons (*Simopithecus*), plus two occurrences of hominids (cf. *Australopithecus*, in the 105–1311 channel).

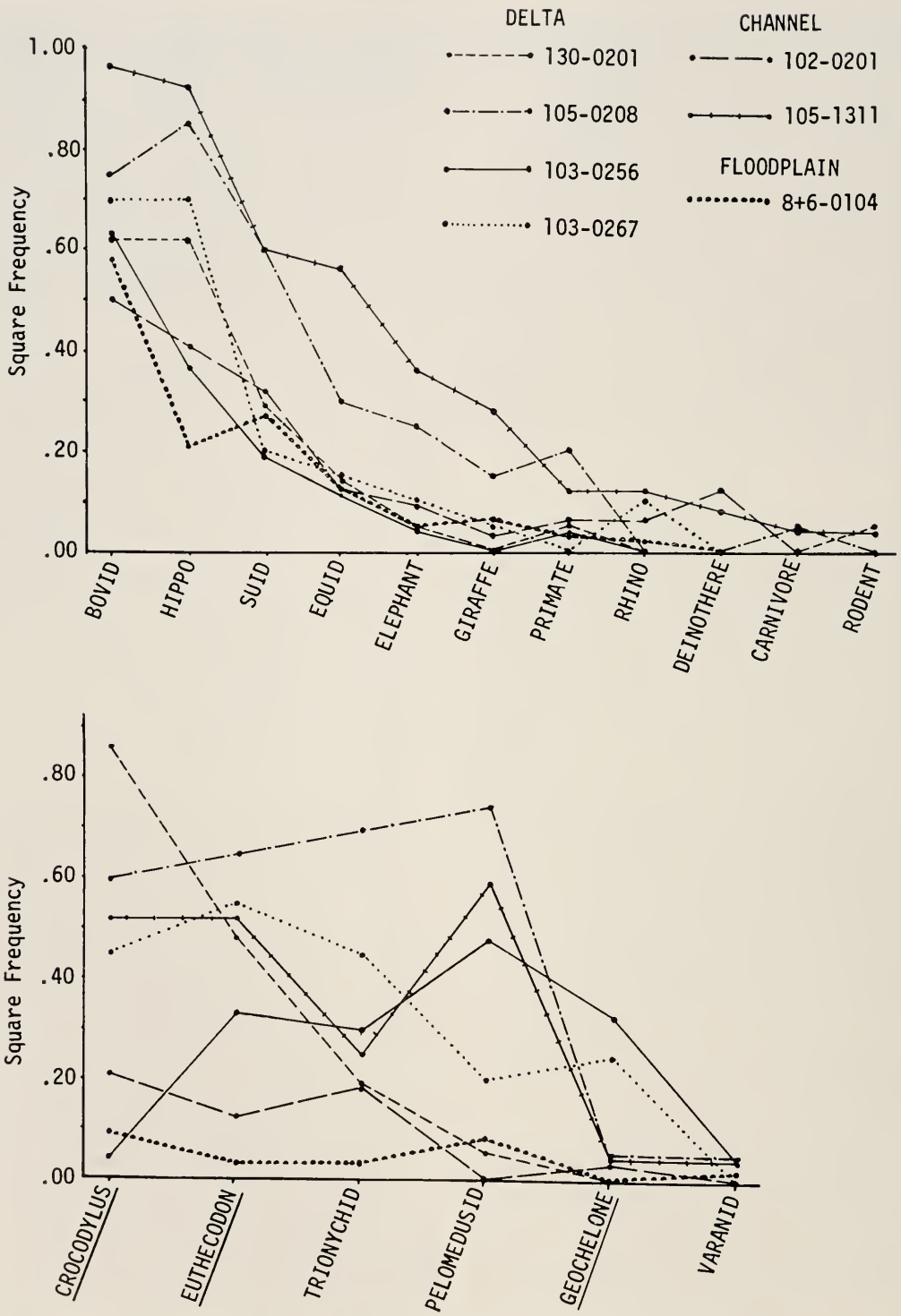

Figure 23. Comparisons of the square frequencies of mammal and reptile groups in the seven sample localities.

The relatively low frequency of primates is probably due to a combination of destructibility, high dispersal potential and lower original abundance or more localized groups than the better represented ungulate families.

The extinct Deinotheres are represented only in the 105–1311 and 102–0201 channels, together with rhinos. Rhinos also occur in the floodplain assemblage, in the *Loxodonta* Faunal Zone (Fig. 14), which may represent a time (~ 1.3 my.?) when deinotheres had become locally extinct. Neither is found in the deltaic environments sampled. Elephants, whose parts have similar low dispersal potentials, are found in all localities. The patterns of occurrence are best explained by habitat preferences, with the deinotheres and rhinos preferring dry, upland savanna and bush habitats while the elephants were more ubiquitous.

Discussion of the Most Abundant Mammalian Groups

The relative frequencies of the four most common groups, hippos, bovids, suids and equids, can be combined with data on the skeletal representation of each family for more detailed analysis of taphonomic and paleoecologic factors.

Comparisons of the frequencies given in Table 11 show that there is a close similarity between localities in the proportions of the four families, except in the cases of 103–0256 and 8+6–0104. The mammals of these localities include high frequencies of bovids and low frequencies of hippos. For the floodplain environment, this correlates nicely with the low representation of other aquatic forms. However, for the transgressive deposit in 103–0256, with its abundant aquatic fauna, the low proportion of hippos is anomalous.

All four common groups are represented by teeth and other skeletal elements of different sizes and densities. These would have different dispersal potential, according to the Voorhies Groups (Table 2) and size-density considerations. If any of the mammal groups were transported into the fossil assemblages as disarticulated skeletal parts, then they should be represented by a higher proportion of phalanges, podials, etc. Autochthonous animals should have mixed representation with teeth, limb parts, phalanges, etc.

For bovids and hippos, elements of widely variable original size and density occur together in all localities. These include teeth, phalanges and ends of limb bones, which fall into all three of Voorhies' dispersal groups. It is evident that these assemblages do not reflect extensive sorting by taphonomic processes. These processes may have been operating, particularly in the channels, but the bone input was enough to maintain an unsorted character in the assemblages. The best explanation for the skeletal representation is that the bone input was generally local, and the bovids and hippos are autochthonous with respect to the deltaic and fluvial environments.

Suids and equids are less abundant as fossils and are also represented by a lower diversity of skeletal parts. Both teeth and phalanges are present in the suid samples from all areas except 105–1311. Equids are represented by teeth, with only a few examples of other parts. The suid samples are more likely to be autochthonous since they combine elements of widely differing transport potential. The equid sample consists mainly of lag elements, many of which show evidence of transport abrasion. These are probably allochthonous in the channels, but are at least partly autochthonous in the floodplain and deltaic assemblages. For both suids and equids, the relatively low frequencies and poor skeletal representation imply lower original abundance than bovids in the floodplain and deltaic habitats.

The comparison of tooth frequency with the frequencies of all other elements is a

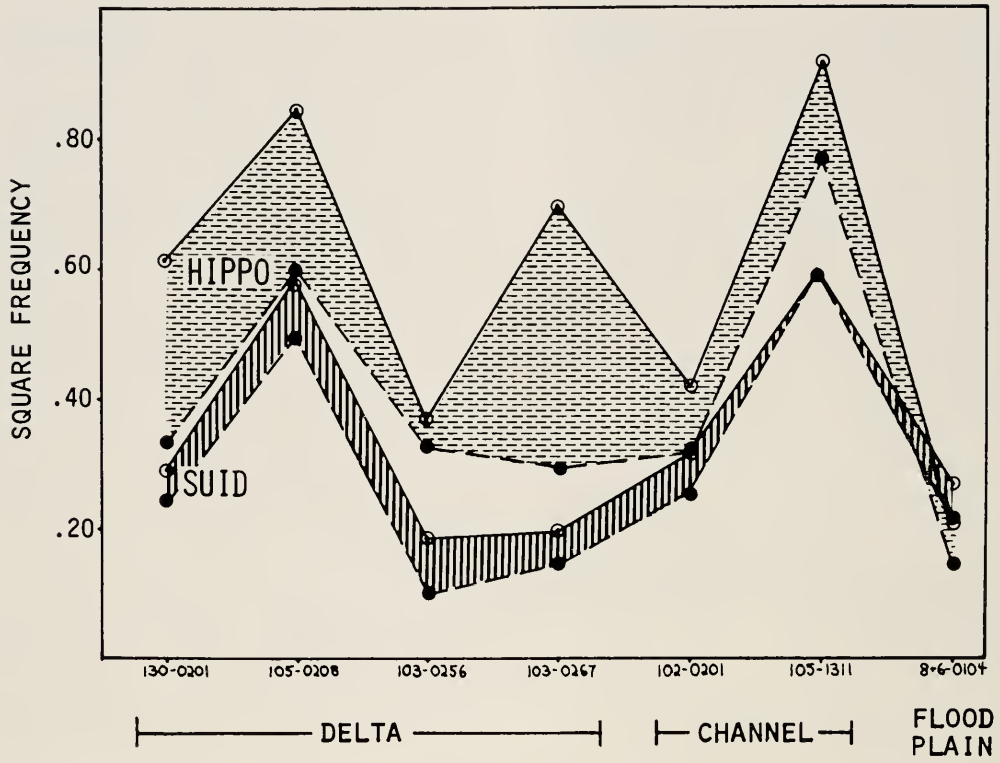
SQUARE FREQUENCY
.80
.60
.40
.20
HIPPO
SUID
130-0201
105-0208
103-0256
103-0267
102-0201
105-1311
8+6-0104
DELTA
CHANNEL
FLOOD PLAIN

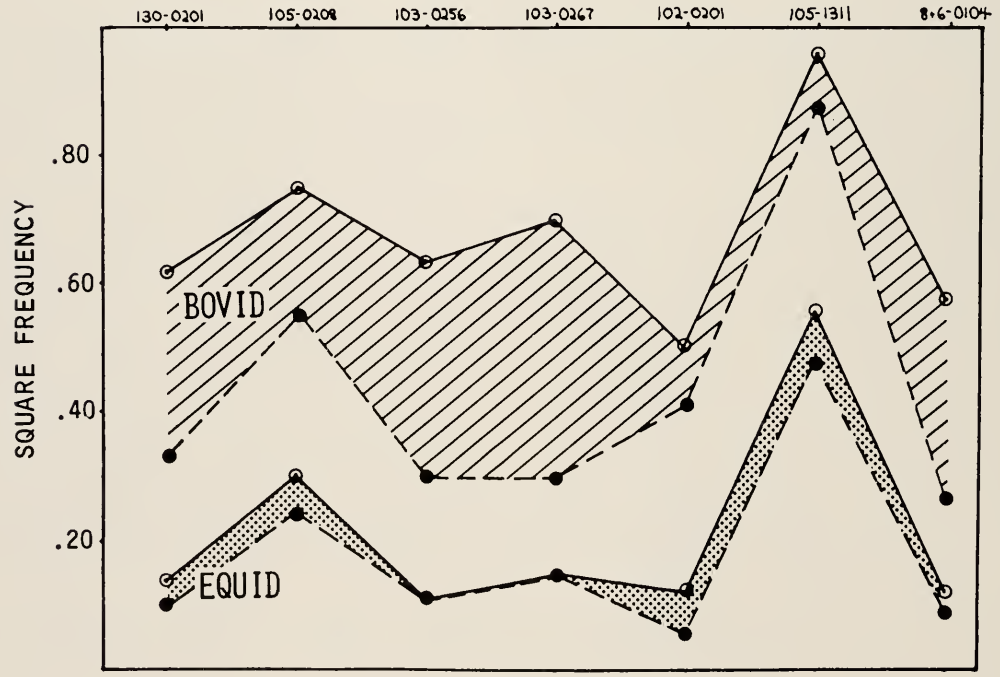
130-0201
105-0208
103-0256
103-0267
102-0201
105-1311
8+6-0104
SQUARE FREQUENCY
.80
.60
.40
.20
BOVID
EQUID

useful measure of the effects of taphonomic processes (weathering and transport) on the fossil assemblages. Figure 24 shows the frequencies of the four families in terms of all identifiable elements and in terms of teeth only. Where the lines diverge, a large proportion of the sample consists of parts other than teeth. Representation of hippos and bovids is similar in all localities except 103–0256 and 8+6–0104. The low frequency of hippos in these two assemblages is due to a lack of elements other than teeth. Since the bones from both localities are basically autochthonous, this emphasizes that there must have been relatively few hippos leaving bones in the original environments. The plots for suids and equids demonstrate the relatively greater numbers of teeth in these samples. The autochthonous or allochthonous context of these animals in the bone assemblages cannot be inferred from their skeletal representation, but *is* indicated by their *association* with autochthonous or allochthonous assemblages, as determined by the taphonomic histories of each assemblage as a whole.

The assemblage of 103–0267, which combines characteristics of channel and deltaic environments, includes a high proportion of different hippo and bovid skeletal parts, in contrast to the other channel assemblages. This indicates a closer similarity to the taphonomic histories of assemblages in 130–0201 and 105–0208, than to those of the other localities. Considering all evidence for 103–0267, it appears to have been much more permanently aquatic than the other channels. This would fit an interpretation of distributary channels close to the lake in association with beach environments.

It is of interest that the known aquatic or nonaquatic habits of bovids and hippos cannot be inferred from their overall frequencies or skeletal representation in the deltaic or channel assemblages. Without knowledge of recent ecology, it would only be valid to say that both hippos and bovids are autochthonous in the deltaic and fluvial environments. Beyond this, anatomical studies would be necessary for interpreting ecological differences. The lesson in this is important for fossil assemblages with no modern counterparts: hippos and bovids are an example of two distinct groups with comparable fossil representation that *does not* necessarily reflect their ecological differences, even though one is more closely tied to aquatic habitats than the other.

Abundances of Selected Mammalian Groups

Suids

Three genera of suids are common in the fossil assemblages and occur in variable frequencies from locality to locality. Table 12 gives the frequency data for these genera, based only on teeth. *Notochoerus* and *Metridiochoerus* are combined since molar fragments of the two are difficult to distinguish. They are similar in having high-crowned, elongate third molars adapted to eating the relatively abrasive grasses, and both are thought to belong to the same group as *Phacochoerus*, the modern warthog (Cooke and Maglio, 1972: 312), which is generally an open-habitat form (Dorst and Dandelot, 1970:174). *Mesochoerus* is easily distinguished from the other suids by its low-crowned third molar. Its dentition is adapted to softer vegetation than in *Metridiochoerus* and *Notochoerus*. *Mesochoerus* is believed to be close to the ancestral stock of the recent

←

Figure 24. Comparisons of skeletal representation of the four most common mammal groups in each sample locality. Solid circles and dashed (lower) lines indicate the frequencies of all squares with teeth. Open circles and solid (upper) lines indicate the total square frequency, counting all teeth and bones. The space between the lines is large if a group is represented by parts other than teeth. Bovids and hippos show comparable skeletal representation except for the delta flats (103–0256) and the floodplain (8+6–0104).

Table 12. Square frequencies of Suid genera.

	Delta				Channel		Floodplain
	130–0201	105–0208	103–0267	103–0256	102–0201	105–1311	8+6–01014
Notochoerus/ Metridiochoerus	.00	.20	.05	.04	.24	.24	.01
Mesochoerus	.14	.30	.00	.04	.03	.04	.08

Hylochoerus (Giant Forest Hog), a dense bush or forest animal (Cooke and Maglio, 1972:311).

Figure 25 shows that the *Notochoerus* group (= *Notochoerus* + *Metridiochoerus*) is far more common in the channel assemblages, and *Mesochoerus* is more typical of the deltaic assemblages. Chi-square tests (Simpson *et al.*, 1960) show that this difference is significant with $p \leq .05$. Paleoecologic separation of the two groups is strongly indicated, and in a way that is con-

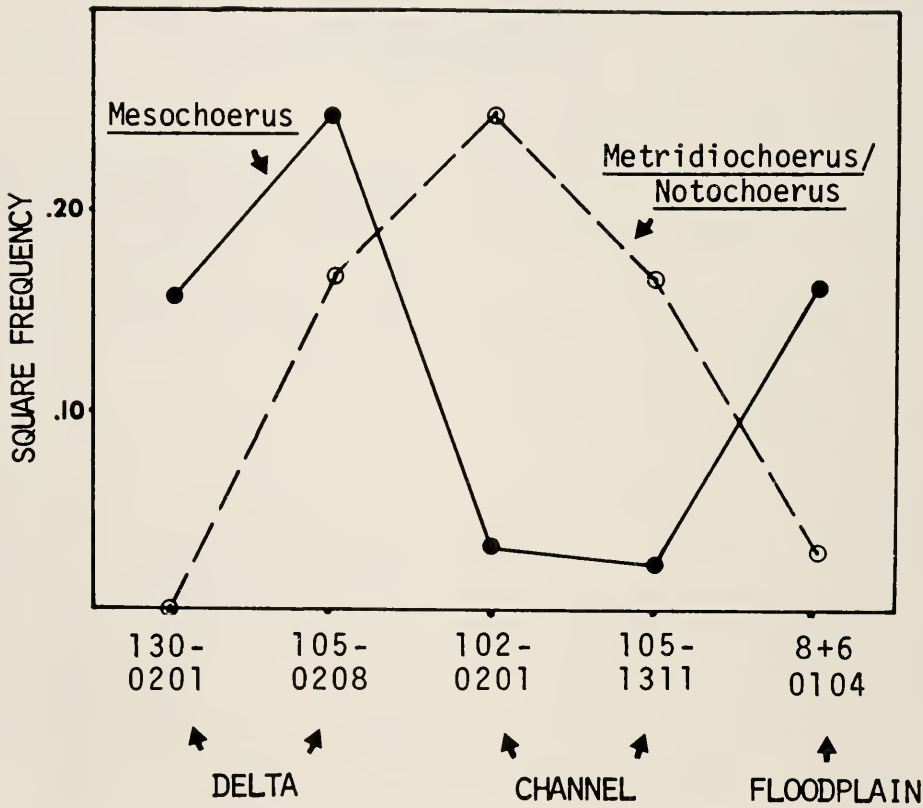

Figure 25. A comparison of the square frequencies of the two suid groups, *Mesochoerus* and *Notochoerus/ Metridiochoerus*. *Mesochoerus* is considered here to be a more closed habitat (bush) form due to its relationship to the modern *Hylochoerus* (Giant Forest Hog), and to its low-crowned molars, which appear to be adapted for relatively soft vegetation. *Notochoerus/Metridiochoerus* suids are more closely related to the modern *Phacochoerus* (Warthog) and have high-crowned molars adapted for abrasive vegetation. These suids may have been more open habitat (grassland) forms. Localities 103–0256 and 103–0267 are omitted due to the low frequencies of suids identifiable to genus (Table 12).

Table 13. Generalized ecological characteristics of Recent bovid groups that are common in the East Rudolf fossil assemblages. (Modified from R. Estes, ms. in press.)

	Habitat	Water proximity		Food habits	Social habits
		Near	Far		
Tragelaphini	Dense Bush	×	(×)	Browsers	small groups
Reduncinae	Woodlands, Floodplains	×		Grazers	small groups
Alcelaphinae	Open grasslands	(×)	×	Grazers	large herds

sistent with predictions based on tooth morphology and recent analogues. The channel assemblages might be expected to sample the more open-country habitats, particularly if the gallery forests fringing the channels are not very extensive. Deltaic environments, if comparable to the most vegetated areas of the recent Omo Delta, would have more forested habitats. The paleoecologic evidence associates *Mesochoerus* with deltaic, potentially more densely vegetated environments and *Notochoerus/Metridiochoerus* with fluvial, mixed- to open-habitat environments.

The third molars of the two suid groups are different in size, and there is a possibility that the smaller *Mesochoerus* teeth have been sorted out of the channel deposits. *Mesochoerus* third molars are between about 40 and 60 mm long and 20 mm in height, while *Notochoerus/Metridiochoerus* third molars are from about 50 to 75 mm in length and 40 to 60 mm in height. However, the hydraulic equivalents of the teeth in both channels fall within the 10–25 mm range, which is near the median for the total range of other teeth in the deposits as well as the associated sediment. One cannot logically assume that sorting would separate the pig teeth but nothing else with similar size differences. Therefore, sorting can be eliminated, and ecological factors provide the best explanation for the separation of the two suids in the fossil assemblages.

Equids

Although the equid sample is poor and consists mainly of teeth (Figure 24) there is some suggestion of habitat separation of *Equus* and *Hipparion* in the samples. *Equus* is most abundant in 105–1311 and 102–0201, and *Hipparion* in 130–0201 and 105–0208. There is a time separation between these two groups of samples, but *Equus* is known to occur elsewhere in East Rudolf at the same level as *Hipparion*. The correlation of *Equus* with the channel environments and *Hipparion* with lake margins is comparable to the pattern of occurrences of *Notochoerus/Metridiochoerus* and *Mesochoerus*. *Hipparion* is preserved in association with the environment most likely to have been densely vegetated, and *Equus* is found in the deposits more likely to have sampled open country, savanna forms.

Bovids

Three bovid groups are abundant enough in the sample assemblages for detailed analysis. These include the Alcelaphinae (hartebeest, etc.), Tragelaphini (kudus, elands, etc.) and Reduncinae (bush buck, waterbuck, etc.). Recent members of these groups are well known in terms of habitat preference (Bigalke, 1972; Estes, in press; Dorst and Dandelot, 1970). Ecological characters are listed in Table 13. Frequencies of bovid tribes in the fossil assemblages are given in Table 14.

All localities combined, alcelaphines and reduncines are nearly equal in abundance, while Tragelaphines are less common. The high frequencies of the smaller alcelaphines in 103–0256 and of both large and small in 105–1311 are significantly larger than the frequencies of the other groups in these localities, with $p \leq .05$ (Chi-square tests).

Table 14. Frequencies of fossil bovids and the small hippopotamus in the East Rudolf assemblages.

	Delta				Channel		Floodplain
	130–0201	105–0208	103–0267	103–0256	102–0201	105–1311	8+6–0104
Tragelaphini	.24	.10	.20	.00	.12	.16	.02
Reduncinae	.24	.25	.15	.11	.15	.12	.15
Alcelaphinae (*Damaliscus*-size)	.14	.15	.05	.33	.06	.40	.12
Alcelaphinae (*Megalotragus*)	.00	.00	.15	.04	.00	.48	.03
Hippopotamus sp. nov.	.05	.20	.10	.26	.09	.00	.06

Reduncines and tragelaphines are of similar frequency except in 103–0256 and 8+6–0104, which have a high proportion of reduncines and few tragelaphines. These differences are probably related to ecological factors since it is difficult to imagine any other processes which could preferentially sort the tribes. (They are of approximately equal body size.) All are represented by multiple skeletal parts where they are abundant. The patterns of occurrence are not as well defined as for the suids, but bush forms (reduncines) are generally more common in the deltaic environments while alcelaphines are associated with the potentially more open environments sampled in the 105–1311 channel and in the 103–0256 mudflats.

The alcelaphine *Megalotragus* is a large, extinct form known only from teeth in the sample assemblages. It has an unusually high frequency in the 105–1311 channel. This is significantly different from its occurrences in the other localities and cannot be explained except by ecological factors. *Megalotragus* is associated with the grassland suids and equid, and may well have been an open-country form itself. Its absence in 102–0201 is somewhat puzzling, if it is typically preserved in fluvial deposits. However, another large bovid (probably *Pelorovis*) is represented in 102–0201 with a frequency of .18. The data may indicate a rather finely resolved habitat separation between the two forms which can only be clarified by additional sampling.

Hippos

The habitat of the extinct small hippo, *H.* sp. nov., can be generally inferred from its frequency in the bone assemblages (Table 15). It occurs in all localities except 105–1311 and is most abundant in 103–0256. Nearly all the hippo remains in 103–0256 belong to this form, and a variety of skeletal parts exist in the sample squares together with teeth. It is generally more abundant in the deltaic environments, including 103–0267, and is associated with both bush and open country animals. It is definitely autochthonous in the deltaic mudflats environment of 103–0256. From this evidence, it can be concluded that *H.* sp. nov. was probably a lake margin form, preferring deltaic flats with mixed bush and grassland environments. It may have been less aquatic than the larger hippos, but this can only be validly inferred from morphological data, not from the taphonomic evidence now available.

A large extinct hippo, peculiar to the East Rudolf Plio-Pleistocene, cannot be definitely identified in the fossil assemblages from the squares. Ecological data on this hippo would be interesting since somehow three or more forms of *Hippopotamus* managed to coexist at East Rudolf.

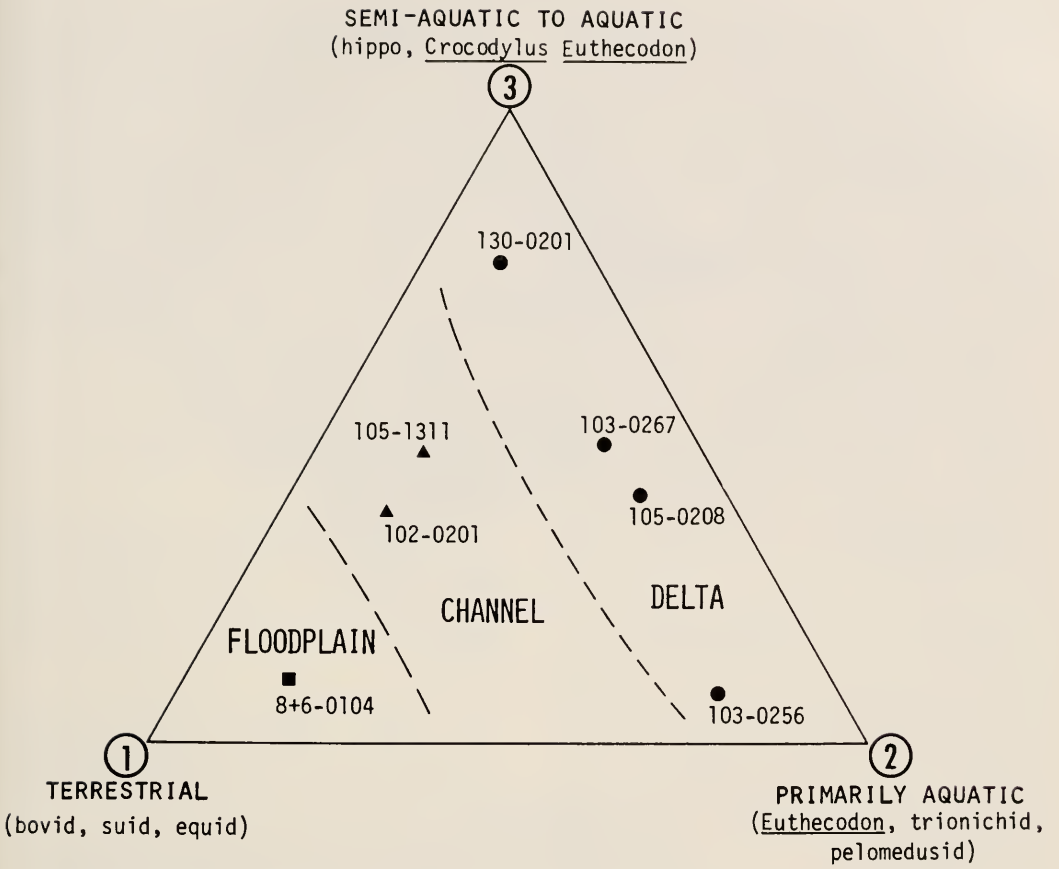

Figure 26. Triangle diagram showing the results of a three factor analysis of the frequency data from all groups of mammals and reptiles. The deltaic localities are spread between two "aquatic" factors, and the channel and floodplain localities are distributed closer to the "terrestrial" factor.

At least one of these is not present in the entire Omo sequence, suggesting significant ecological differences between the two regions, at least as far as the hippos were concerned. We might assume that these differences were expressed in the utilization of broadly different environments. If so, further careful sampling of the sedimentary evidence should reveal more about the ecology of the different hippos.

Conclusions Regarding the Faunal Assemblages

Much of the information provided by the faunal frequencies is summarized in the triangular diagram in Figure 26. This shows the results of a CABFAC Q-Mode Factor analysis for three varimax axes (which explains 97% of the variance). The data consist of the square frequencies for all the animal groups given in Table 11. The three factors can be directly related to the aquatic or nonaquatic affinities of the various animals. Factor 1 includes the terrestrial forms and the other two factors include aquatic and semiaquatic forms with affinities for channel or deltaic-lacustrine habitats. These separate the sample localities into three groups depending on their components of aquatic animals.

Thus, the evidence at various taxonomic

levels indicates faunal differences between the localities which agree with environmental interpretations based on geological data. These are real and meaningful *ecological* differences between environments; differences expressed in the square frequencies of the faunas and supported by the geologic and taphonomic characters of the sediments and their bone components. The important points brought out by the faunal data include:

1) The relative numbers of the different vertebrate classes in the fossil assemblages is more dependent on their original numbers and proximity of habitat to a sedimentary environment, than on their aquatic or nonaquatic habits.

2) Relative numbers of animals can indicate whether they were aquatic or nonaquatic in *nonaquatic* sedimentary environments, but not in aquatic ones.

3) The more terrestrial sedimentary environments preserve a greater *diversity* of terrestrial animals. However, the more aquatic environments may preserve an equivalent or greater number of *bones* from terrestrial animals, representing fewer groups.

4) For terrestrial families larger than a baboon or a small antelope, the frequencies expressed in the sample assemblages should be roughly proportional to their original numbers.

5) The more abundant mammals (bovids and hippos) are generally represented by more kinds of skeletal parts of different sorting potential, indicating autochthonous accumulations of bones. This is consistent with the generally autochthonous nature of the assemblages on the deltaic and floodplain environments.

6) The different sedimentary environments clearly preserve different ratios of some animals with different habitat preferences. Terrestrial animals which prefer grassland habitats are found in greater abundance in fluvial deposits, while bush or forest mammals occur in greater abundance in the deltaic deposits. This indicates deltas with denser vegetation than the gallery forests which fringed the channels while the sample bones were accumulating.

PALEOECOLOGY OF THE VERTEBRATE ASSEMBLAGES OF THE KOOBI FORA FORMATION

Much independent but cross-supporting evidence provides a basis for interpreting the paleoecology of the East Rudolf fossil assemblages. These lines of evidence include:

1) *Geologic evidence.* Characteristics of the overall sedimentary environments and the processes operating within them (Fig. 27).

2) *Taphonomic evidence.* a) The extent and type of sorting in the bone assemblages, interpreted with the aid of theoretical considerations from experimental evidence for bone disposal. b) Relationships of the hydraulic equivalences of the bones and of the associated matrix sediment. c) Characteristics of the bone fragments, interpreted according to observations on weathering, fracturing and abrasion of modern bones.

3) *Faunal evidence.* Interpretations based on the faunal composition of the fossil assemblages, using the ecology of modern analogues to Plio-Pleistocene animals.

→

Figure 27. Block diagrams showing reconstructions of East Rudolf sedimentary environments. Circles show the interpretation of the general sedimentary environment of each fossil sampling locality, indicated by locality numbers. The representation is schematic; the localities do *not* occur on the same time planes or closely adjacent to each other as might be construed from the diagrams. 102–0201 is more closely associated with an emergent delta than can be shown on the diagram. 103–0267 includes a more extensive complex of distributary mouth and beach environments than is indicated by the encircled area.

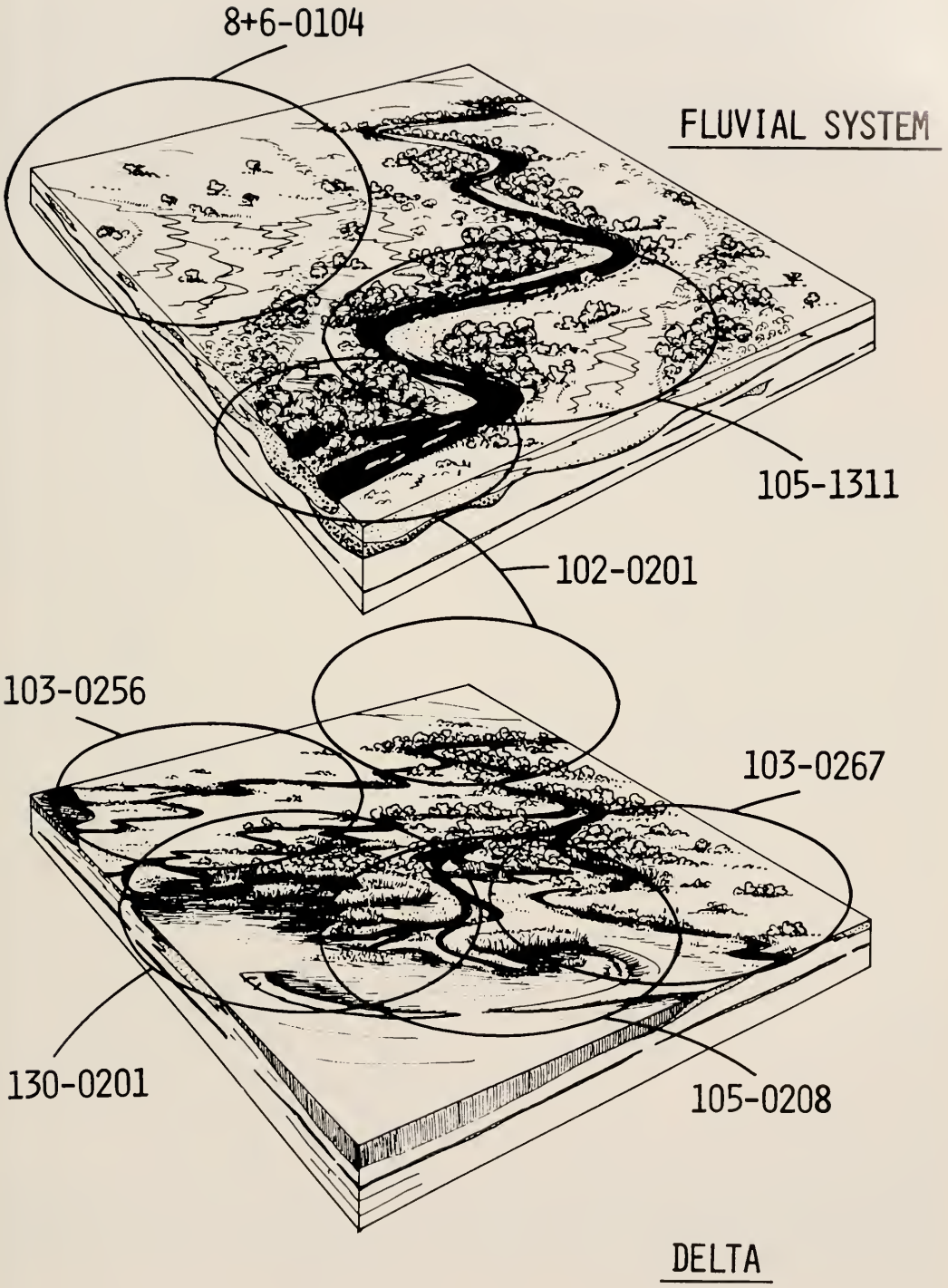
8+6-0104
FLUVIAL SYSTEM
105-1311
102-0201
103-0256
103-0267
130-0201
105-0208
DELTA

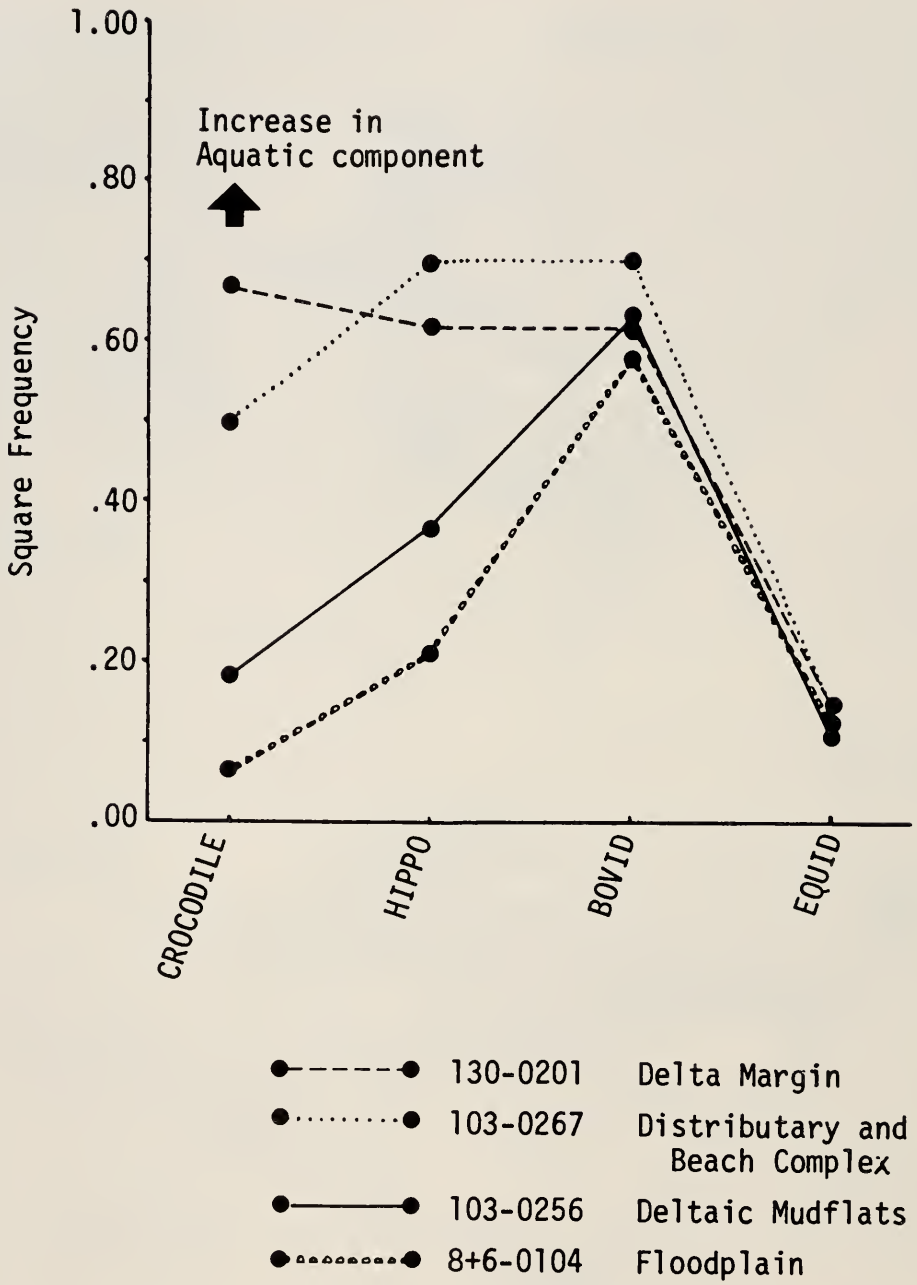

Figure 28. A comparison of the square frequencies of four vertebrate groups with aquatic, semiaquatic and terrestrial habits in four different depositional environments. These environments range from primarily aquatic to primarily terrestrial in terms of their *geologic* characteristics. The frequencies of the aquatic and semiaquatic animals increase as the depositional environments become more aquatic (floodplain to delta margin). However, the frequencies of terrestrial forms remain essentially constant in all environments.

Other lines of evidence can be important in paleoecologic interpretations but are not at present available for the East Rudolf assemblages. These include botanical and geochemical data, which can reveal important factors about vegetation, climate, and salinity of the lake. Continuing research should eventually provide such data.

Ecological Comparisons of the Samples

The overall similarities and differences among localities show that sedimentary environments can be characterized according to distinct taphocoenoses and biocoenoses. At East Rudolf, three broadly defined sedimentary environments are represented: delta, channel and floodplain. The faunas are all basically autochthonous in each of these environments and reveal meaningful ecological differences among them.

Aquatic and Terrestrial Faunas

The more aquatic sedimentary environments as determined from geologic evidence have an increased representation of aquatic animals but show *no* decrease in the absolute number of terrestrial animals. This is demonstrated in Figure 28 by the increase in the frequencies of crocodilians and hippos relative to bovids and equids. The absolute frequency of bovids and equids does not change significantly from environment to environment, even though these range from floodplain to delta margin.

The pattern of aquatic and terrestrial occurrences can be represented for faunas from each locality as shown in Figure 29. The ratio of terrestrial animals increases as environments become more terrestrial, at the expense of the aquatic forms. The ratio of the semiaquatic hippo, which spends approximately half its time in and half out of the water (Dorst and Dandelot, 1970: 172), changes little from aquatic to nonaquatic environments. These patterns are the result of geologic and taphonomic processes which should have similar effects on fossil assemblages other than these East Rudolf examples. The crucial variables appear to be: 1) the total volume of bones available from aquatic and nonaquatic animals and 2) the proximity of an animal's habitat to an actively aggrading sedimentary environment. The habits of a fossil vertebrate cannot be inferred from its abundance in an aquatic sedimentary environment unless this can be compared with more terrestrial environments from about the same time.

Open and Closed Habitat Mammalian Faunas

The mammalian assemblages provide evidence for two terrestrial faunas with preferences for open (grassland) or closed (bush) habitats. In order to establish these ecological differences, the habitats of the fossil mammals must be inferred from morphologic evidence plus analogy to related living forms. For the paleoecologic interpretation of the East Rudolf fossil assemblages, *Mesochoerus*, reduncines and tragelaphines are used to represent the closed habitat fauna, and *Damaliscus*-size alcelaphines, *Notochoerus/Metridiochoerus* suids and *Equus* represent the open habitat fauna. The evidence for relating these mammals to the different ecologic situations has been discussed previously. The ecological separation of such groups according to habitat preference for grassland or bush environments is a common feature of recent East African ecosystems (Lamprey, 1963; Harris, 1970; Estes, 1973).

The relative percentages of closed and open habitat forms in the seven fossil localities are shown in Figure 30. All localities include both, but the deltaic environments in general include more closed habitat forms and the channels more open habitat forms. The deltaic mudflats (103–0256) have an open habitat fauna, in agreement with geologic evidence for an extensive, unforested delta margin environment. The patterns of faunal occurrence indicate that the deltaic, channel and flood-

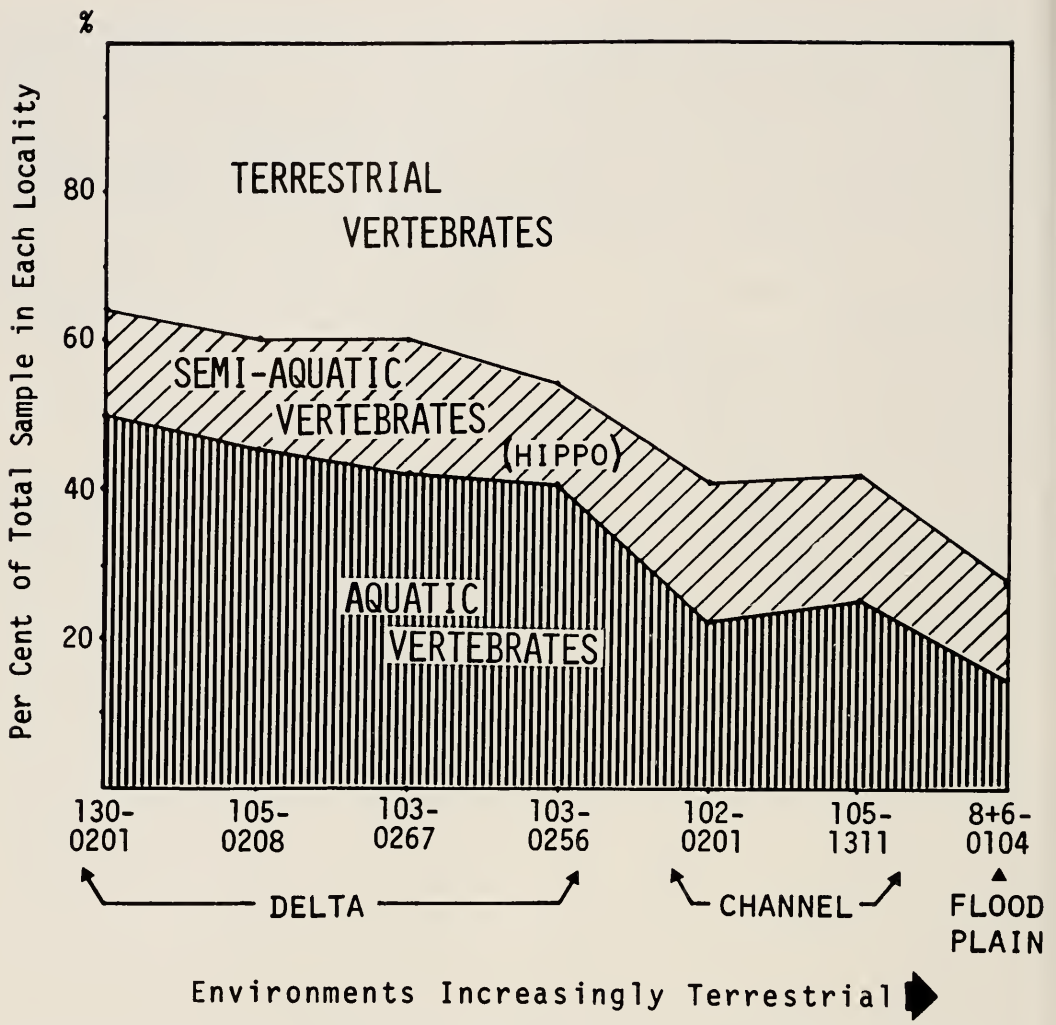

Figure 29. The ratios of aquatic, semiaquatic and terrestrial vertebrate groups represented in the East Rudolf fossil assemblages. The sample localities are arranged from the more aquatic to least aquatic depositional environments on the basis of geologic interpretations. Aquatic animals include crocodilians and chelonians except *Geochelone*; semiaquatic includes only hippopotamus, and all other groups are considered to be terrestrial. Abundance is calculated as the % of the cumulative square frequencies for each locality.

plain sedimentary environments sample both closed and open habitats, but that closed habitats were more abundant on the deltas. A comparison between 130–0201, representing a deltaic fauna, and 105–1311, representing a nondeltaic fauna, shows the most distinct ecological difference among any of the localities (Fig. 31).

Comparisons of Koobi Fora Formation Faunas and Recent Terrestrial Faunas

Bovids, suids and equids are the most abundant large mammals in the fossil assemblages and also in most of the recent undisturbed East African ecosystems (e.g., Foster, 1967; Sheppe and Osborn, 1971). The ratios of these mammals in the fossil

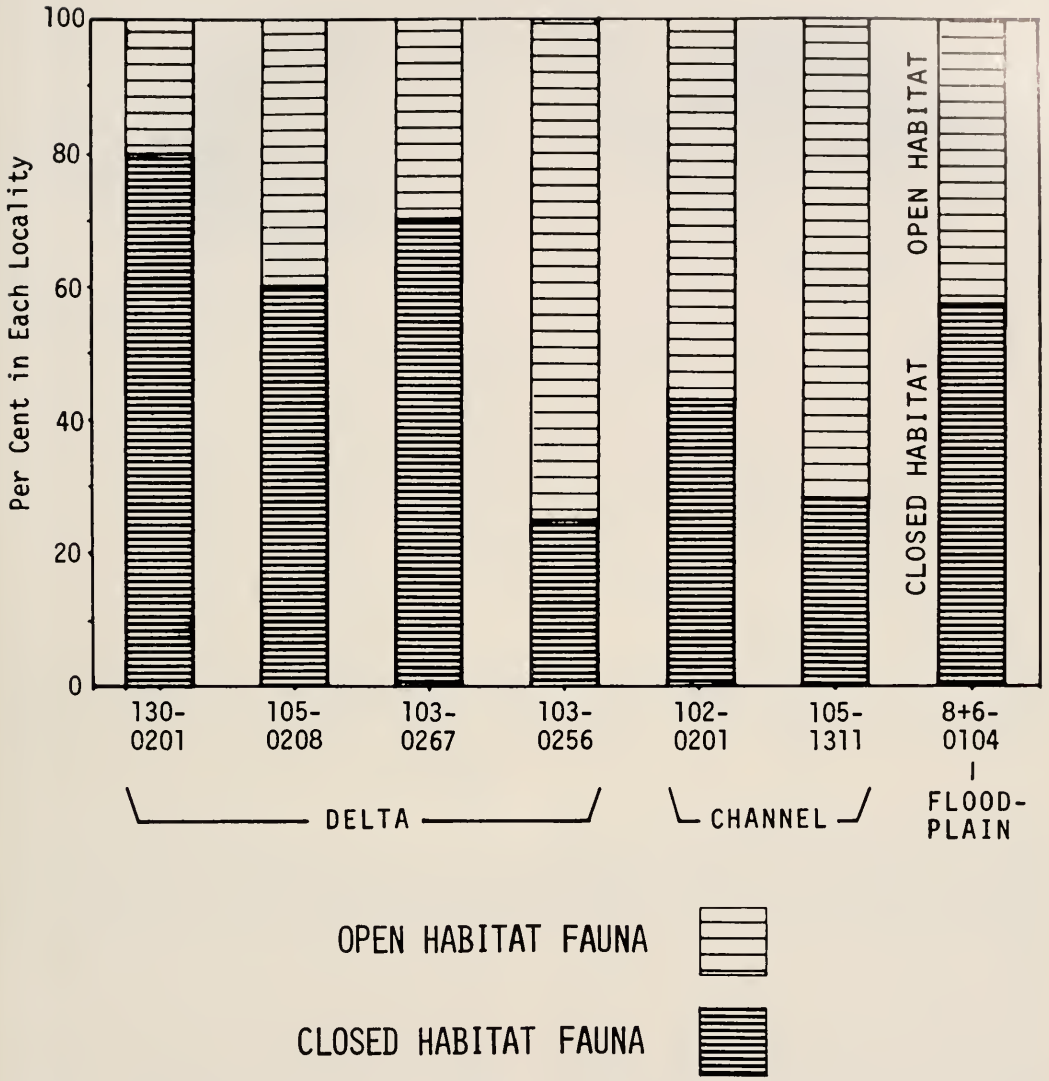

Figure 30. Histogram showing the relative percentages of closed and open habitat mammals in each of the sample localities. Closed habitat forms include *Mesochoerus*, reduncines and tragelaphines; open habitat forms include *Damaliscus*-size alcelaphines, *Notochoerus/Metridiochoerus* and *Equus*. Percentages were calculated on the basis of the total square frequencies for the closed and open habitat groups.

faunas is compared with their relative numbers in recent faunas in Figure 32. Bovids are most common in both cases. However, equids are less common than suids in all seven of the fossil sampling localities, and the faunal proportions are most similar to the recent Kafue Park fauna in Zambia. Taphonomic causes do not adequately explain the greater frequency of suids in the fossil assemblages. Therefore, equids may have lower representation than suids because they were more ecologically separated from the sedimentary environments, or because they were generally less abundant in the East Rudolf region during the time period represented by the

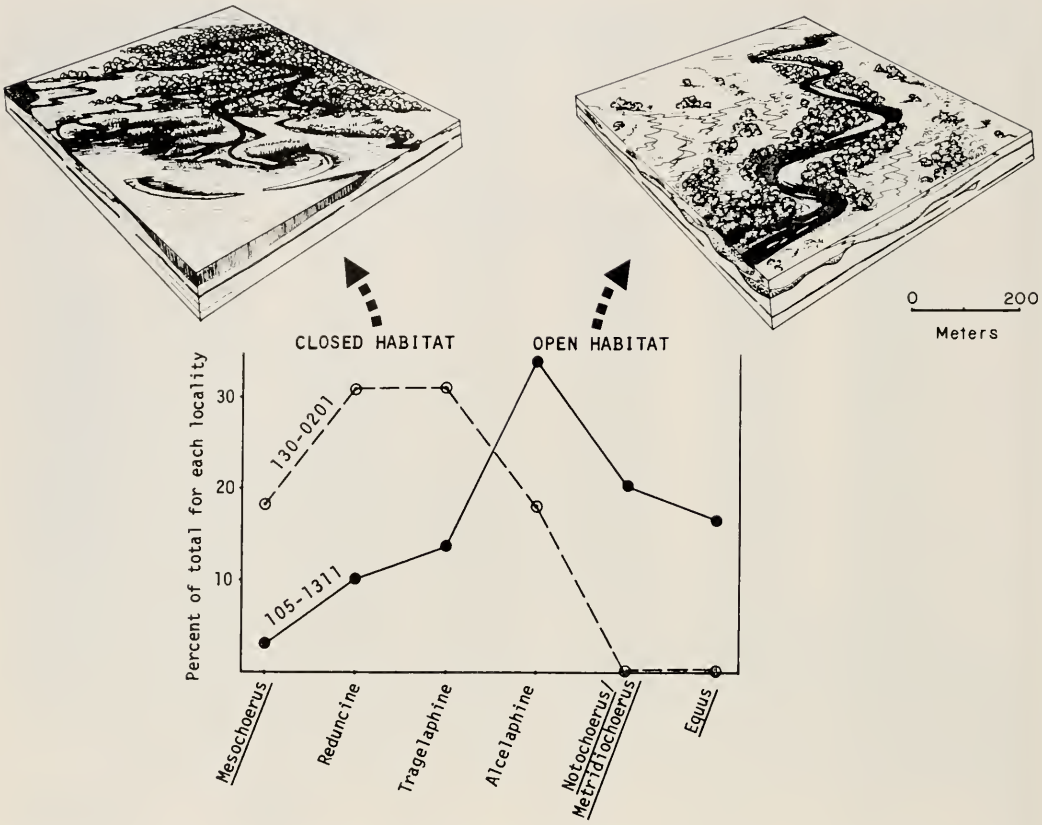

Figures 31. A comparison of the relative abundances of the six mammal groups chosen to represent open and closed habitat faunas in the two localities that show the clearest separation of these two faunas, 105–1311 and 130–0201. Percentages were calculated on the basis of the cumulative totals of square frequencies of the six animals in each locality. The reconstructions represent the *general* sedimentary contexts of each fossil assemblage.

fossil deposits. A greater number of fossil suids agrees well with the greater diversity of this group in the Plio-Pleistocene, with at least 5 species (Maglio, 1972) present in the East Rudolf area.

At present East Rudolf supports a mammalian fauna of at least six bovid species, two species of zebra and a single species of suid, the warthog. Giraffe, hippo, baboon, man and a variety of carnivores and rodents are also present. Rhinoceros has only recently become extinct in the area, and elephants were recorded there near the end of the last century (R. E. Leakey, personal communication). Most of the fossil mammalian groups are represented in the recent ecosystem, with the exception of the deinotheres, now extinct. However, in terms of species and genera, East Rudolf today is much less diverse than in the Plio-Pleistocene. The fossil faunas are more similar in terms of numbers of species represented (Maglio, 1972) to the recent faunas of wetter areas such as Nairobi National Park or the Kafue Floodplain in Zambia. Environmental change in the East Rodolf region during at least the past 1.5 my. has been great, and apparently is continuing to affect the vertebrate community.

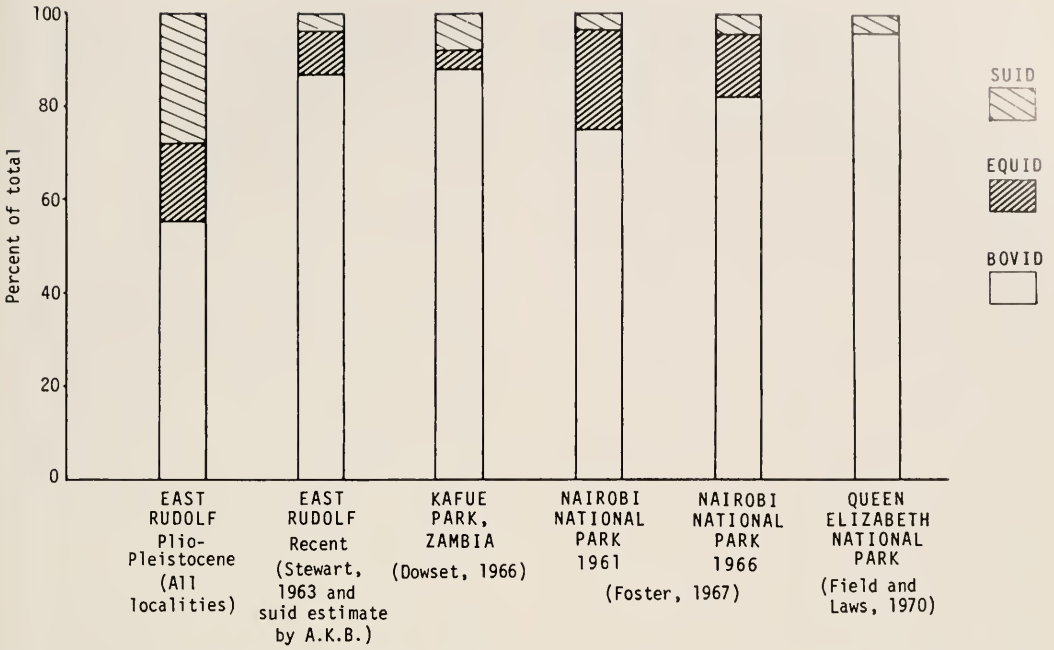

Figure 32. Comparisons of the relative percentages of bovids, suids and equids in the seven Plio-Pleistocene localities used for this study, and in Recent ecosystems. All relative numbers for the recent examples are based on numbers of individuals (game counts). The abundances shown for East Rudolf (Plio-Pleistocene) were averaged from the square frequencies for bovids, suids and equids in all of the seven localities, but are consistent with relative abundances in each separate locality.

Hominid Paleoecology

The hominid fossils that occur in the Koobi Fora Fm. should reflect the same taphonomic processes as the remains of other vertebrates. Therefore, they can be examined in the context of the rest of the fauna for possible paleoecological factors. The abundance of hominids in the East Rudolf collections is due to the intensive program of hominid collecting and does not reflect their relative abundance in the total fauna. In reality, they are fairly rare, as indicated by an occurrence in only 2 out of 213 sample squares in the seven localities used for this study. This is comparable to the relative abundance of rodent fossils in the squares. It would be necessary to sample hundreds or thousands of squares to provide enough hominid material for valid quantitative comparisons of frequencies in different sedimentary environments. This is not feasible, but it will be possible to relate the hominid fossils to the different sedimentary environments and to the closed or open habitat faunas using the sedimentary and faunal context of each specimen. Based on the patterns of occurrence of other mammals, it seems possible that the two lineages of hominids recognized from East Rudolf (Leakey, 1973) were associated with the two different habitats.

The East Rudolf hominid collection as of April, 1973, consisted of 50 specimens assigned to *Australopithecus*, 34 assigned to *Homo*, and 10 unassigned (M. Leakey, personal communication). Both taxa are represented by a wide variety of skeletal parts. The greater number of *Australopithecus* specimens is due primarily to a larger number of partial mandibles of this form. This may reflect taphonomic processes (e.g., carnivore activity, surface

weathering) that operated to selectively destroy the less robust *Homo* mandibles. There is no clear pattern as yet indicating occurrences of the two forms in different sedimentary environments.[4] Both occur in deltaic and floodplain deposits. *Australopithecus* is possibly the only hominid occurring in the 105–1311 channel, where it is relatively common (at least 7 separate specimens). This is interesting in that it correlates with other faunal peculiarities of 105–1311, which has a high proportion of open habitat mammals plus forms (deinotheres, rhinos) that are not present in the deltaic assemblages. However, since a variety of habitats were sampled in 105–1311, it would be premature to draw any conclusions on the habitat preferences of *Australopithecus*.

The sample assemblage from 105–0208 occurs in delta margin deposits several meters below the KBS Tuff (Fig. 17), which is the horizon bearing the oldest known hominid "campsites" (Isaac *et al.*, 1972). The relative abundance of the different vertebrate groups (Fig. 23) is probably broadly representative of the fauna that was extant on the delta margin at the time of the hominid habitation sites. At this time, however, the delta margin had changed in position, probably receding farther to the southwest. The deposits directly associated with the KBS Tuff (which is primarily a channel fill) are fine-grained silty clays, which indicate extensive interdistributary marshes and mudflats that were probably seasonally dry. Such environments do not seem to be conducive to fossil preservation on the recent Omo Delta (Butzer, 1971:103), and fossils are indeed rare in the silty clays associated with the habitation sites. Thus, evidence for the faunal context of the tool-manufacturing hominids must come indirectly from the older 105–0208 fauna. This provides at least regional, if not local, evidence for the vertebrate fauna most closely associated with the hominids.

[4] Additional research conducted in 1973 indicates that the *Homo* lineage sample is much more restricted to lake margin deposits that the *Australopithecus* sample, which is abundant in both lake margin and fluvial deposits (Behrensmeyer, In press).

East Rudolf in Relation to Other Studies in Vertebrate Paleoecology

Although vertebrate paleoecology has long been an area of recognized research value, there are relatively few comprehensive studies in print. Those that are available provide useful comparisons for paleoecologic interpretations of the Koobi Fora Fm. and show how this study relates to broader research on the evolution of vertebrate communities and ecosystems through time.

The major studies that have defined terrestrial paleo-communities include Olson (1952, 1958), Shotwell (1955, 1963) and Clark *et al.* (1967). Olson's interpretation of the Permian Vale and Choza Fauna of Texas shows a correlation between environmental change (increasing aridity), as determined from geologic evidence, and significant changes in the vertebrate fauna. A study of the Oligocene Chadron fauna of South Dakota by Clark *et al.* (1967:69–73) reveals two distinct ecological assemblages of mammals, referred to as "savanna" and "aquatic-wet forest" faunas. Environmental changes to cooler, more arid conditions led to restriction and finally to the elimination of the wet-forest fauna during the time span represented by the Chadron Fm. Shotwell's studies of Pliocene faunas of the Juntura Basin of eastern Oregon included pioneer work in quantitative methods for reconstructing ecological associations of animals from quarry samples. Using these methods, the fossil mammals of the Drewsey Fm. are assigned to four paleo-communities: woodland, savanna, open grassland and pond-bank. Change through time shows reduction in the woodland and savanna faunas with the development of the open

grasslands fauna (Shotwell, 1963:19). All of these studies rely on geologic and faunal evidence plus a variety of taphonomic assumptions. The paleoecologic interpretations, particularly those of Shotwell, could be further supported or perhaps altered by more detailed taphonomic analysis.

Olson (1952) developed the concept of a "chronofauna" to describe the nature of the vertebrate fauna of the Texas Permian. A chronofauna is defined as "a geographically restricted, natural assemblage of interacting animal populations that has maintained its basic structure over a geologically significant period of time" (1952:181). According to Olson, the members of a chronofauna may change by such processes as expansion into unoccupied niches or the substitution of one species for another in any given niche, but the vertebrate community is in adaptive equilibrium with the environment and will maintain its structure until environmental change occurs. Clark *et al.* (1967) refer to their aquatic-wet forest and savanna faunas as chronofaunas, and Shotwell's communities might also be considered as chronofaunas. The resolution of evidence for the Cenozoic faunas leads to more refined ecological interpretations and to the consideration of shorter time spans than is possible for the Permian.

In these three studies of vertebrate paleo-communities, the chronofaunas show change due to increasingly arid conditions. This leads to the expansion of grassland mammals in the Cenozoic faunas and a decrease in the diversity of the Permian reptile and amphibian fauna. The absence of evidence for significant morphological change in the vertebrate species during the time span represented by the chronofaunas has been noted by Olson (1952:193) and Clark *et al.* (1967:73). During periods of environmental change, extinction, migration and niche modification apparently were more common patterns of faunal response than rapid morphologic modification.

The fauna of the Koobi Fora Fm records interaction between vertebrate communities and environmental conditions between about 3.0 and 1.5 my. B.P. A comparison between the Plio-Pleistocene fauna and the Recent one shows a restriction of species diversity which is more comparable to the terminal stages of the Permian chronofauna than to the shifts in the Cenozoic paleo-communities of South Dakota or Oregon. The general significance of the faunal change at East Rudolf may reflect either the short- or long-term effects of increasing aridity, but it is clearly an example of how environmental change may affect vertebrate communities.

The evidence now available suggests at least one significant difference between the evolution of East African faunas and the evolution of the Texas Permian, the Juntura Basin Mio-Pliocene and the Chadron Oligocene faunas. Some of the East African species, particularly the elephants and suids, show rapid evolutionary change during their Plio-Pleistocene histories (Cooke and Maglio, 1972). Such change has not been recognized in the other faunas, and it is unlikely that this contrast is an artifact of taxonomy or of inadequate sampling. Documentation and comparison of the histories of vertebrate faunas at different time levels and in different regions should do much more to clarify the patterns of evolutionary response to environmental change.

Further reconstruction of vertebrate communities in the Lake Rudolf Basin will provide a more detailed history of faunal change over the past 5–6 my. The open (grassland) and closed (bush) habitat faunas of East Rudolf probably represent distinct ecological communities that can be documented elsewhere in East Africa and followed through time. The Omo sequence offers an ideal opportunity for comparing vertebrate faunas of a major river-floodplain complex with the lake margin faunas of East Rudolf. Using the combination of geologic, taphonomic and faunal evidence,

it will be possible to compare fossil vertebrate communities throughout East Africa and to reconstruct changes in chronofaunas through much of the latter part of the Cenozoic.

SUMMARY

This study has developed methods for deriving paleoecologic information from fossil assemblages of fragmented vertebrate bones subjected to various geologic processes before burial. These methods have been applied to paleoecologic interpretation of the Plio-Pleistocene bone deposits of East Rudolf, Kenya. The conclusions relate to vertebrate assemblages in general as well as to the assemblages of East Rudolf and the Lake Rudolf Basin in particular.

General Conclusions

Taphonomy

1) The amount of fragmented bone buried in any given sedimentary environment will depend on the rate of sedimentation and the amount of bone originally put into that environment. The important factors which control bone input are: a) vertebrate abundance, b) carnivore activity, c) the proximity of bones to depositional environments, d) the rates of surface weathering of bones, and e) the dispersal potential of bones. The composition of the resulting fossil assemblage will also in part depend on diagenetic factors.

2) Carnivore activity will have a major effect on the composition of a thanatocoenose. Intense mammalian carnivore activity results in fewer bones of small animals and increased fragmentation of bones of large animals. The evolution of bone-crushing dentitions in mammals has changed the character of Cenozoic thanatocoenoses compared with those of the Mesozoic, when reptilian carnivores lacked the capacity for bone mastication.

3) Bones are disarticulated and acquire characters of surface weathering in months to years if exposed on a land surface. Hydrodynamic transport will tend to leave features of rounding and abrasion on bones. Therefore, well-preserved bones with fragile parts intact and surfaces unflaked or uncracked record conditions of rapid burial without subsequent re-excavation.

4) Bones vary greatly in density, size and shape and are sensitive to hydrodynamic sorting. Disarticulated thanatocoenoses include bones with a wide range of dispersal potentials. This will result in the formation of *dispersal groups* if the bones are subjected to normal or flood-stage current velocities (10–150+ cm/sec.). The dispersal groups will move at different rates from the point of origin. If bones with a wide range of dispersal potentials are found in sedimentary association, this indicates that the assemblage is not a product of *selective transport sorting* of the original thanatocoenose.

5) Mammal bones immersed in water for 5 minutes have densities from < 1.0 to 2.0, and teeth have densities between 1.7 and 2.3. Reptile and fish bones are between 1.3 to 2.3 density. Bones are generally hydraulically equivalent to quartz particles of smaller nominal diameter. Currents should transport bones together with quartz particles that are roughly equivalent hydraulically. Therefore, sedimentary associations of quartz grains and bones of a much larger hydraulic equivalence (e.g., a hippopotamus skull in a siltstone) may indicate other modes of origin for the bone-sediment association. These include *in situ* death, flotation of carcasses, or predator/scavenger transport of bone.

6) Theoretical considerations indicate that velocities of 80 to 200+ cm/sec. must be achieved near the bottom of a flow in order to move bones of moderate density (~ 1.5) and size (100+ cc). Therefore, most disarticulated, water-logged parts of large vertebrates are unlikely to move far from their point of origin except in special transport situations such as floods in channels.

Paleoecology

1) Ecological characteristics of fossil vertebrates can be defined using a combination of geologic and taphonomic evidence, independent of ecological interpretations based on vertebrate morphology or the adaptation of living analogues. Such evidence can link habitat preferences with preservation in particular sedimentary environments. This correlation can be inferred solely from the geologic context and the taphonomy of a given bone assemblage. Such evidence can then be combined with morphological and recent-counterpart data to support paleoecologic interpretations.

2) Fragmented bone assemblages can be used with confidence for paleoecologic interpretations if they: a) consist of bones with a wide range of dispersal potentials, b) are not hydraulically equivalent to associated sediment and c) retain fresh, unweathered or unabraded surfaces. Assemblages with these attributes can be interpreted as generally autochthonous to their environment of deposition. Most of the animals represented in such an assemblage were preserved in the general context of their original habitats.

3) Aquatic environments of deposition can preserve variable amounts of bone from aquatic and terrestrial vertebrates, depending on the relative bone input from each ecological group. Bone assemblages of terrestrial and aquatic animals in aquatic deposits (e.g., channel, delta margin) may differ only in the better preservation of the latter, not in their greater abundance.

4) Terrestrial environments of deposition (e.g., floodplains) preserve a high proportion of terrestrial vertebrates along with a few aquatic ones. Semiaquatic vertebrates tend to occur in both terrestrial and aquatic deposits, with better representation in aquatic environments.

5) The bone input from groups of large terrestrial vertebrates into fragmented, autochthonous taphocoenoses should generally reflect their relative numbers in the original ecosystem. The fossil abundances can be used to approximate relative numbers of different vertebrate groups in a given environment. This provides a basis for reconstructing paleo-communities and comparing them through time.

6) Vertebrate communities at different time horizons or in different regions may differ in their response to broad-scale environmental change in ways that can be detected in paleoecologic studies. These responses include rapid morphological evolution, shifts in the relative numbers of animals suited to particular habitats, and a general decline in species diversity accompanied by the extinction of forms in all the available habitats.

Conclusions for the Vertebrate Assemblages of the Koobi Fora Formation, East Rudolf

1) Fossil-bearing deposits reveal sedimentation and bone preservation in at least three major depositional environments: delta margin, channel and floodplain.

2) The three depositional environments show a basic similarity in their representation of different skeletal parts, with teeth the most abundant component. However, the relative numbers of certain skeletal elements differ in ways that reflect the different processes operating in the three environments. Teeth are relatively more abundant in the channel deposits and in the floodplain, while vertebrae and phalanges are more abundant in the delta margin deposits. This can be related to the concentration of heavy, durable parts in the channels through sorting and reworking of bones, and to the absence of such processes in the delta margin environments. The taphonomic characters of the floodplain assemblage indicate preferential removal of the lighter elements without transport or reworking of the associated heavier bones.

3) The sum of taphonomic and geologic evidence shows that the delta margin and floodplain bone assemblages are autochthonous with respect to the overall sedi-

mentary environment. Channels contain a mixture of allochthonous and autochthonous bones and show the most evidence for taphonomic alteration of the original thanatocoenose.

4) The East Rudolf faunas include aquatic, semiaquatic and terrestrial vertebrates that vary in abundance according to sedimentary environment. Analogies with recent East African ecosystems indicate that the relative fossil abundance of terrestrial mammalian families probably reflects their abundance in the original ecosystem. Bovids, suids and equids are the most common groups in the fossil assemblages and in most recent undisturbed East African faunas.

5) Two terrestrial faunas can be defined for the East Rudolf assemblages, based on ecological analogies between recent and fossil mammals. The open habitat fauna includes alcelaphines, *Metridiochoerus/Notochoerus* suids and *Equus*. The closed habitat fauna is characterized by *Mesochoerus*, reduncines and tragelaphines. There is overlap of these faunas in all of the sample assemblages. However, delta margin deposits generally preserve a greater proportion of closed habitat forms, and the channels preserve more open habitat forms.

7) The paleoecologic results for East Rudolf show that it is possible to define ecological groups of terrestrial vertebrates from surface samples of fragmental bone assemblages. Similar sampling of fossil assemblages at different time horizons can provide a basis for establishing East African chronofaunas and for reconstructing their interaction with environmental changes through time.

ACKNOWLEDGMENTS

The interdisciplinary nature of this work led to a great deal of productive and enjoyable interaction with researchers in a broad range of disciplines, including Geology, Paleontology, Zoology, Anthropology, and Ecology. An interdisciplinary approach inevitably generates a large number of well-deserved acknowledgments. I attempt here to express my gratitude to those people who have made particular contributions to this study, but I wish to preface this with a simple and very sincere note of thanks to all who provided help and encouragement during the course of the project.

I would like to give special thanks to Bryan Patterson, Richard E. Leakey, Glynn L. Isaac and Vincent J. Maglio. Without their unfailing encouragement, help and ideas, this work would not have been possible. Gratitude is due to Farish A. Jenkins, Jr., Raymond Siever, Robert T. Bakker, Daniel C. Fisher, Peter Dodson and H. B. S. Cooke for many useful comments and suggestions during the preparation of the manuscript. Discussions with Andrew Hill, Richard D. Estes, Stephen J. Gould, Jack Sepkoski, F. B. Van Houten, G. Jepsen, John Fleagle, Allen Greer, T. Hopson and Stanley Awramik resulted in many additional ideas and references. Dirk van Damme (Geologish Institute, Ghent, Belgium) also deserves thanks for identification of the invertebrate fossils. I have greatly appreciated the exchange of geological information with co-workers on the East Rudolf Expedition, including Bruce Bowen and Carl Vondra of Iowa State University, Gary Johnson of Dartmouth College and Ian Findlater of Birkbeck College, University of London. Field work (consisting of long hours of sample collecting in 10 × 10 meter squares) was accomplished through the assistance and stoicism of Susan Abell, Penny Bowen, John Barthelme, John W. Harris, John M. Harris, John Onyango-Abuje, Jonathan Karoma, John Kimingitch, Fred Lucas, Dinah Crader, Diane Gifford, Dan Stiles, Paul Abell, Kelly Stewart and Andrew Hill. John Barthelme and John Harris deserve special thanks for their help in laboratory analysis and identification of the fossil material. Barbara Lawrence and Charles Mack of the Department of Mammalogy, Museum of Comparative Zoology (Harvard) were very

helpful in providing recent skeletal material used for this study. Photographic reproduction of the figures and plates was done by John Lupo (Biological Laboratories, Harvard) and additional assistance was provided by Al Coleman (MCZ Laboratories, Harvard). Typing was the joint effort of Karen Mason, Maureen Sepkoski and Agnes Martin. Their work is gratefully acknowledged with special thanks to Agnes Martin for typing the final draft. Finally, among the many friends who have provided miscellaneous assistance in time of need, I would particularly like to thank Vickie Rowntree, Catherine Badgley, A. Gordon Brown and Elizabeth Whitehouse.

This study was done as a Ph.D. Dissertation in the Department of Geological Sciences, Harvard University, and was completed in June of 1973. The work received financial support through grants by the National Science Foundation (Grant No. 28607a) and the National Geographic Society to the East Rudolf Research Project.

REFERENCES

Abel, O. 1912. Grundzüge der Palaeobiologie der Wirbeltiere. Stuttgart· E. Schweizerbart'sche Verlagsbuchhandlung Nägele und Dr. Sproesser. 470 pp.

Allen, J. R. L. 1963. The classification of cross-stratified units, with notes on their origin. Sedimentol., **2**: 93–114.

———. 1965. A review of the origin and characteristics of recent alluvial sediments. Sedimentol., **5**: 89–191.

———. 1970. Physical Processes of Sedimentation. London: George Allen and Unwin, Ltd. 248 pp.

Allen, P. 1959. The Wealden environment: Anglo-Paris Basin. Roy. Soc. London, Phil Trans. (B), **242**(692): 283–346.

Ansell, W. H. F. 1971. Part 15: Order Artiodactyla. *In*: Meester, J. and H. W. Setzer, (eds.). The Mammals of Africa. An Identification Manual. Washington, D.C: Smithsonian Institution Press.

Aristarain, L. F. 1962. Caliche deposits of New Mexico. Ph.D. Dissertation. Harvard University, Department of Geological Sciences.

Baker, B. H., and J. Wohlenberg. 1971. Structure and evolution of the Kenya Rift Valley. Nature, **229**: 538–542.

Beadle, L. C. 1932. The waters of some East African lakes in relation to their fauna and flora. J. Linn. Soc. (Zool.), **38**: 135–156.

Behrensmeyer, A. K. 1974. Late Cenozoic sedimentation in the Lake Rudolf Basin, Kenya. Annals Geol. Soc. Egypt, IV: 287–306.

———. In press. The habitat of Plio-Pleistocene hominids in East Africa; taphonomic and microstratigraphic evidence. *In* C. Joly (ed.), African Hominidae of the Plio-Pleistocene: Evidence, Problems and Strategies. New York: Duckworth, Inc.

Berggren, W. A., and J. Van Couvering. 1973. Late Neogene chronostratigraphy, biostratigraphy, biochronology and paleoclimatology. Woods Hole Oceonogr. Inst. Tech. Rep., WHOI–73–40. 334 pp.

Berry, L. G., and B. Mason. 1959. Mineralogy. San Francisco: W. H. Freeman and Co. 630 pp.

Bigalke, F. C. 1972. The contemporary mammalian fauna of Africa. *In* Keast, A., B. Glass, F. C. Erk, (eds.). Evolution, Mammals and Southern Continents. Albany, New York: State University of New York Press. 141–194.

Bishop, W. W. 1968. The evolution of fossil environments in East Africa. Trans. Leicester Lit. and Phil Soc., **62**: 22–44.

Bowen, B. E., and C. F. Vondra. 1973. Stratigraphical relationships of the Plio-Pleistocene deposits, East Rudolf, Kenya. Nature, **242**: 391–393.

Brain, C. K. 1967a. Bone weathering and the problem of bone pseudo-tools. S. Afr. J. Sci., **63**(3): 97–99.

———. 1967b. Hottentot food remains and their bearing on the interpretation of fossil bone assemblages. Sci. Pap. Namib Des. Res. Sta., No. 32.

Bretz, J. H., and L. Horberg. 1949. Caliche in southeastern New Mexico., J. Geol. **57**: 491–511.

Briggs, L. I., D. S. McCulloch, and F. Moser. 1962. The hydraulic shape of sand particles. J. Sediment. Pet., **32**(4): 645–656.

Brock, A., and G. Isaac. 1974. Paleomagnetic stratigraphy and chronology of hominid bearing sediments east of Lake Rudolf, Kenya. Nature, **247**: 344–348.

Butzer, K. W. 1971a. Recent History of an Ethiopian Delta. Res. Pap. No. 136, Dept. Geogr. Chicago: The University of Chicago Press. 184 pp.

———. 1971b. The Lower Omo Basin· geology, fauna and hominids of Plio-Pleistocene formations. Naturwiss., **58**: 7–16.

Butzer, K. W., G. L. Isaac, J. L. Richardson,

and C. Washbourn-Kamau. 1972. Radiocarbon dating of East African lake levels. Science, **175**(4027): 1069–1076.

Clark, J., J. R. Beerbower, and K. K. Kietzke. 1967. Oligocene sedimentation, stratigraphy and paleoecology and paleoclimatology in the Big Badlands of South Dakota. Fieldiana, Geol., **5**. 158 pp.

Cooke, H. B. S., and V. J. Maglio, 1972. Plio-Pleistocene stratigraphy in East Africa in relation to proboscidean and suid evolution. *In* Bishop, W., and J. Miller, (eds.). Calibration of Hominoid Evolution. New York: Scottish Academic Press. 303–329.

Cott, H. B. 1961. Scientific results of an inquiry into the ecology and economic status of the Nile Crocodile (*Crocodylus niloticus*) in Uganda and Northern Rhodesia. Trans. Zool. Soc. Lond., **29**(4): 211–356.

Currey, J. 1970. Animal Skeletons. London: Edward Arnold, Publishers.

Davies, D. K., F. G. Ethridge, and R. R. Berg. 1971. Recognition of barrier environments. Bull. Am. Assoc. Pet. Geol., **55**(4): 550–565.

Dodson, P. 1971. Sedimentology and taphonomy of the Oldman Formation (Campanian), Dinosaur Provincial Park, Alberta (Canada). Paleogeogr., Paleoclimatol., Paleoecol. **10**: 21–74.

———. 1974. The significance of small bones in paleoecological interpretation. Contrib. to Geol., Univ. of Wyoming. Spec. Pap. No. 2 Laramie, Wyoming: Univ. Wyoming Press.

Dorst, J., and P. Dandelot. 1970. Larger Mammals of Africa. London: Collins Press. 287 pp.

Dowsett, R. J. 1966. Wet season game populations and biomass in the Ngoma area of the Kafue National Park. The Puku (Occas. Pap. Dept. Game and Fish, Zambia), No. 4: 135–145.

Efremov, J. A. 1940. Taphonomy: A new branch of Paleontology. Panam. Geol., **74**: 81–93.

———. 1953. Taphonomie et annales géologiques. Ann. du Cent. d'Etud. et de Doc. Paléontol., No. 4. 164 pp.

Estes, R. D. 1967. Predators and scavengers. Nat. Hist., **75**(2, 3): 20–29, 38–47.

———. (1973), in press. Social organization of the African Bovidae. I.U.C.N., Symposium on Ungulate Behavior and Management.

Field, C. R., and R. M. Laws. 1970. The distribution of the larger herbivores in the Queen Elizabith National Park, Uganda. J. Appl. Ecol., **7**(2): 273–294.

Fitch, F. J., and J. A. Miller. 1970. Radioisotopic age determinations of Lake Rudolf artefact site. Nature, **226**(5242): 226–228.

Foster, J. B. 1967. Nairobi National Park Game Census, 1966. East Afr. Wildl. J., **5**: 112–120.

Guggisberg, C. A. W. 1972. Crocodiles. Newton Abbot, England: David & Charles, Publishers. 195 pp.

Harris, L. D. 1970. Some structural and functional attributes of a semi-arid East African ecosystem. Ph.D. Dissertation, Michigan State University.

Harvard Tables of the Cumulative Binomial Probability Distribution. 1955. Cambridge, Massachusetts: Harvard University Press. 503 pp.

Haynes, V. 1968. Radiocarbon: analysis of inorganic carbon of fossil bone and enamel. Science, **161**: 687–688.

de Heinzelin, J., F. H. Brown and F. C. Howell. 1971. Pliocene/Pleistocene formations in the Lower Omo Basin, southern Ethiopia. Quaternaria, **13**: 247–268.

Isaac, G. L. 1967. Towards the interpretation of occupation debris: some experiments and observations. The Kroeber Anthropol. Soc. Pap. **37**: 31–57.

Isaac, G. L., R. E. F. Leakey and A. K. Behrensmeyer. 1971. Archeological traces of early hominid activities, east of Lake Rudolf, Kenya, Science, **173**: 1129–1134.

Johnson, L. C. 1965. Morphological analysis in Pathology. *In* Frost, H. M. (ed.). Bone Biodynamics. (Henry Ford Hospital Int. Symp.). Boston: Little, Brown and Co. 543–654.

Konizeski, R. L. 1957. Paleoecology of the middle Pliocene Deer Lodge Local Fauna, western Montana. Bull. Geol. Soc. Am. **68**: 131–150.

Kruuk, Hans. 1972. The Spotted Hyaena. Chicago: The University of Chicago Press. 335 pp.

Kurten, B. 1953. On the variation and population dynamics of fossil and recent mammal populations. Acta Zool. Fenn., **76**: 5–118.

Lamprey, H. F. 1963. Ecological separation of the large mammal species in the Tarangire Game Reserve, Tanganiyika. East Afr. Wildl. J., **1**: 63–92.

Langbein, W. B., and L. B. Leopold, 1968. River channel bars and dunes — theory of kinematic waves. U. S. Geol. Surv. Prof. Pap. No. 422–L: 1–20.

Leakey, R. E. F. 1973. Further evidence of Lower Pleistocene hominids from East Rudolf, North Kenya, 1972. Nature, **242**: 170–173.

Leopold, L. B., M. G. Wolman and J. P. Miller. 1964. Fluvial Processes in Geomorphology. San Francisco: W. H. Freeman and Co. 522 pp.

Leopold, L. B., W. W. Emmett and R. M. Myrick. 1966. Channel and hillslope processes in a semiarid area, New Mexico. U. S. Geol. Surv. Prof. Pap. No. 352–G: 193–253.

Lobova, E. V. 1967. Soils of the Desert Zone of the USSR Jerusalem: Israel Program for Scientific Translations. 405 pp.

Loveridge, A. 1941. Revision of the African terrapin of the family Pelomedusidae. Bull. Mus. Comp. Zool., **88**(6): 462–524.

Loveridge, A., and E. E. Williams. 1957. Revision of the African tortoises and turtles of the suborder Cryptodira. Bull. Mus. Comp. Zool., **115**(6): 163–557.

Maglio, V. J. 1972. Vertebrate faunas and chronology of hominid-bearing sediments east of Lake Rudolf, Kenya. Nature, **239**: 379–385.

McKee, E. D., E. J. Crosby and H. L. Berryhill, Jr. 1967. Flood deposits, Bijou Creek, Colorado, June, 1965. J. Sediment. Pet., **37**(3): 829–851.

Millar, C. E., L. M. Turk and H. D. Foth. 1966. Fundamentals of Soil Science. New York: John Wiley & Sons. 491 pp.

Muller, A. H. 1957. Lehrbuch der Palaozoologie. Vol. 1: Allgemeine Grundlagen. Jena: Gustav Fischer Verlag. 322 pp.

Olson, E. C. 1952. The evolution of a Permian vertebrate chrono-fauna. Evolution, **6**(2): 181–196.

———. 1958. Fauna of the Vale and Chosa: 14. Fieldiana, Geol., **10**(32): 397–448.

Patterson, B., A. K. Behrensmeyer, and W. D. Sill. 1970. Geology and fauna of a new Pliocene locality in north-western Kenya. Nature, **212**(5062): 918–921.

Payne, J. E. 1965. Summer carrion study of the baby pig, *Sus scrofa*. Ecology, **46**(5): 592–602.

Pettijohn, F. J. 1957. Sedimentary Rocks. New York: Harper & Row, Publishers. 718 pp.

Pettijohn, F. J., P. E. Potter and R. Siever. 1972. Sand and Sandstone. New York: Springer-Verlag. 618 pp.

Reeves, C. C. 1970. Origin, classification and geologic history of caliche on the southern high plains, Texas and eastern New Mexico. J. Geol., **78**: 352–362.

Reif, Wolf-Ernst. 1971. Zur Genese des Muschelkalk-Keuper-Grenzbonebeds in Südwestdeutschland. Neues Jahrb. Geol. Palaontol. Abh., **139**(3): 369–404.

Rittenhouse, G. 1943. Transportation and deposition of heavy minerals. Bull. Geol. Soc. Am., **54**(12): 1725–1780.

Sadek-Kooros, H. 1966. Jaguar Cave: an early man site in the Beaverhead Mountains of Idaho. Ph.D. Dissertation. Harvard University, Department of Anthropology.

Sanders, H. L. 1968. Marine benthic diversity: a comparative study. Am. Nat., **102**(925): 243–282.

Schäfer, W. 1972. Ecology and Palaeoecology of Marine Environments. Craig, G. (ed.), I. Oertel (transl.). Chicago: The University of Chicago Press. 568 pp.

Schaller, G. B. 1972. The Serengeti Lion. Chicago: The University of Chicago Press. 480 pp.

Selous, F. C. 1908. African Nature Notes and Reminiscences. London: MacMillan and Co. 356 pp.

Shapiro, A. H. 1961. Shape and Flow: The Fluid Dynamics of Drag. New York: Doubleday & Co., Inc., Anchor Books. 186 pp.

Sheppe, W., and T. Osborne. 1971. Patterns of use of a floodplain by Zambian mammals. Ecol. Monogr., **41**(3): 181–205.

Shotwell, J. A. 1955. An approach to the paleoecology of mammals. Ecology, **36**(2): 327–337.

———. 1963. The Juntura Basin: studies in earth history and paleoecology. Trans. Am. Phil. Soc., (N. S.), **53**(1): 3–77.

Simpson, G. G., A. Roe, and R. C. Lewontin. 1960. Quantitative Zoology. New York: Harcourt, Brace & World, Inc. 440 pp.

Stewart, D. R. M. 1963. Wildlife census, Lake Rudolf. East Afr. Wildl. J., **1**: 121.

Van Lawick-Goodall, H. and J. 1971. Innocent Killers. Boston: Houghton Mifflin Co. 222 pp.

Visher, G. S. 1965. Use of vertical profile in environmental reconstruction. Bull. Am. Assoc. Pet. Geol., **49**(1): 41–61.

Voorhies, M. 1969. Taphonomy and population dynamics of an early Pliocene vertebrate fauna, Knox County, Nebraska. Contrib. to Geol. Univ. of Wyoming. Spec. Pap. No. 2. Laramie, Wyoming: Univ. Wyoming Press. 69 pp.

Walsh, J. and R. G. Dodson. 1969. Geology of Northern Turkana. Rep. No. 82, Geol. Surv. Kenya. 42 pp.

Weigelt, J. 1927. Rezente Wirbeltierleichen und ihre paläobiologische Bedeutung. Leipzig: Verlag von Max Weg. 208 pp.

White, T. 1955. Observations on the butchering techniques of some aboriginal peoples, numbers 7, 8, and 9. Am. Antiq., **21**(2): 170–178.

Williams, G. E. 1971. Flood deposits of the sand-bed ephemeral streams of Central Australia. Sedimentology, **17**: 1–40.

APPENDIX 1

MEASUREMENTS OF DENSITIES, VOLUMES AND WET WEIGHTS OF MODERN BONES. DENSITIES ARE CALCULATED FOR THE BONES AFTER THEIR PORE SPACES WERE FILLED WITH WATER.

DENSITIES

Skeletal part	*Ovis* (sheep) MCZ 1939	*Redunca* (reedbuck) MCZ 14917	*Hylochoerus* (forest hog) MCZ 27851	*Damaliscus* (topi) MCZ 15724	*Equus* (zebra) MCZ 5003	*Hippopotamus* MCZ 5020
HUMERUS	1.53	1.40	1.55	1.51	1.77	1.74
RADIUS }	1.64	1.58	1.66	1.72	1.45	1.69
ULNA }		1.16		1.41		
FEMUR	1.45	1.36	1.41	1.37	1.36	1.79
TIBIA	1.46	1.23	1.54	1.71	1.45	1.55
METATARSAL	1.44	1.33	1.07	1.62	1.68	1.50
METACARPAL	1.35	1.45	1.15	1.51	1.52	1.34
ASTRAGALUS	1.68	1.81	1.28	1.66	1.16	1.46
CALCANEUM	1.62	1.37	1.22	1.50	1.00	1.52
PODIAL #1	1.43	1.13	1.30	1.46	1.23	1.31
#2	–	1.25	1.20	1.48	1.01	1.46
PHALANX #1	1.45	1.34	–	1.40	1.00	1.37
#2	1.60	–	1.36(t)	1.34	1.02	1.29(t)
#3	1.06	–	1.02(t)	1.01(t)	1.05(t)	1.07(t)
TEETH M	2.19	–	–	2.23	2.08	2.00
PM	–	–	–	2.24	1.97	1.97
C	–	–	1.53	–	–	1.83
I	–	–	1.53	1.88	–	1.74
RIB #1	1.11	1.54	1.41	1.36	1.22	1.63
#2	–	1.43	1.20	1.08	1.84	–
VERTEBRA ATLAS	1.24	.78	1.56	1.43	1.28	1.64
AXIS	1.07	.94	1.41	1.33	1.24	1.87
CERVICAL	1.04	1.13	–	1.11	.98	1.82
THORACIC	1.06	1.05	1.21	1.30	1.11	1.26
LUMBAR	.89	1.23	1.23	1.13	.99	1.36
SACRUM	1.11	.92	1.18	1.07	–	–
PATELLA	1.07	1.07	1.01	1.30	.64	1.24
PELVIS	1.19	1.17	–	–	–	–
STERNUM	.97	–	–	–	–	–
SKULL	1.42	1.39	–	–	–	–
JAW (½)	1.43	1.74	–	1.58	–	–
SCAPULA	1.65	1.88	–	1.53	–	–
VERT. CENT. #1	.98	.75	1.60	1.00	1.06	1.29
#2	1.09	–	1.40	–	1.00	–
ULNA, PROX.	–	.90	–	1.21	–	–
SESAMOID #1	–	–	–	–	–	1.46
#2	–	–	–	–	–	1.18
HUM. PROX.	1.26	1.34	1.42	1.32	1.63	1.55
DIST.	1.75	1.96	1.69	1.81	1.83	1.96
R/U. PROX.	1.64	1.47(R)	1.65	1.96(R)	1.29	1.74
DIST.	1.59	1.72(R)	1.67	1.52(R)	1.50	1.63
FEM. PROX.	1.47	1.44	1.50	1.58	1.33	1.83
DIST.	1.42	1.30	1.29	1.21	1.45	1.64
TIB. PROX.	1.32	1.20	1.27	1.43	1.27	1.30
DIST.	1.64	1.28	1.96	2.30	1.77	1.91
MT. PROX.	1.31	–	–	1.48	1.49	–
DIST.	1.56	–	–	1.55	1.36	–
MC. PROX.	1.38	–	–	1.33	1.40	–
DIST.	1.25	–	–	1.37	1.40	–
SCAPULA (GLENOID)	1.30	1.48	1.58	1.29	1.32	–

R = Radius only.
t = Terminal Phalanx

VOLUMES (Cubic Centimeters)

Skeletal part	*Ovis* (sheep) MCZ 1939	*Redunca* (reedbuck) MCZ 14917	*Hylochoerus* (forest hog) MCZ 27851	*Damaliscus* (topi) MCZ 15724	*Equus* (zebra) MCZ 5003	*Hippopotamus* MCZ 5020
HUMERUS	53.5	67.0	404	225	310	2542
RADIUS	39.6	39.0	232	148	303	1700
ULNA		11.0		39.0		
FEMUR	65.0	116	383	296	635	3000
TIBIA	56.0	128	186	246	411	1852
METATARSAL	21.0	46.0	23.0	117	140	144
METACARPAL	20.5	40.0	25.5	116	176	174
ASTRAGALUS	4.1	7.2	27.5	20.4	63	296
CALCANEUM	5.5	14.1	44.5	36.0	87	352
PODIAL #1	2.8	6.4	12.2	16.2	10.4	150
#2	–	2.0	8.8	5.6	14.8	94
PHALANX #1	2.9	4.5	12.0	17.9	48	78
#2	1.0	4.8	7.4(t)	8.1	–	17.8(t)
#3	1.7	–	8.5(t)	7.9(t)	20.0(t)	10.7(t)
TEETH M	1.7	–	–	3.6	25.4	73.0
PM	–	–	–	–	–	17.6
C	–	–	42.2	–	–	290
I	–	–	–	0.8	–	130
RIB #1	10.0	5.2	55.0	14.0	26.5	229
#2	–	7.7	31.8	33.0	25.0	–
VERTEBRA ATLAS	25.0	24.4	75.0	63.0	139	866
AXIS	30.5	19.8	56.0	67.0	155	500
CERVICAL	24.0	18.4	–	62.0	170	450
THORACIC	14.0	8.4	57.0	22.8	64.0	480
LUMBAR	15.6	16.6	45.0	40.0	49.0	480
SACRUM	30.0	33.0	165	125	–	–
PATELLA	2.9	5.2	28.0	20.0	45.0	244
PELVIS	107	64.0	–	–	–	–
STERNUM	3.2	–	–	–	–	–
SKULL	209	124	–	–	–	–
JAW (½)	39.5	23.0	–	119	–	–
SCAPULA	26.0	20.5	–	110	–	–
VERT. CENT. #1	5.1	6.0	25.0	20.0	31.0	233
#2	4.7	–	25.0	30.0	28.0	–
ULNA, PROX.	–	7.8	–	20.0	–	–
SESAMOID #1	–	–	–	–	–	7.0
#2	–	–	–	–	–	10.6
HUM. PROX.	32.5	35.0	220	129	168	1420
DIST.	23.4	24.0	184	94.0	150	1122
R/U. PROX.	19.5	21.0(R)	117	65.0(R)	170	822
DIST.	20.1	18.0(R)	115	84.0(R)	147	878
FEM. PROX.	32.0	55.0	179	128	325	1466
DIST.	33.0	61.0	204	168	299	1634
TIB. PROX.	31.0	66.0	113	154	235	1100
DIST.	25.0	62.0	73.0	96.0	168	750
MT. PROX.	11.5	–	–	61.0	68.0	–
DIST.	9.7	–	–	58.0	68.0	–
MC. PROX.	10.0	–	–	60.0	82.0	–
DIST.	12.0	–	–	58.0	90.0	–
SCAPULA (GLENOID)	16.6	13.0	97.0	65.0	100	–

WET WEIGHTS (Grams)

Skeletal part	*Ovis* (sheep) MCZ 1939	*Redunca* (reedbuck) MCZ 14917	*Hylochoerus* (forest hog) MCZ 27851	*Damaliscus* (topi) MCZ 15724	*Equus* (zebra) MCZ 5003	*Hippopotamus* MCZ 5020
HUMERUS	82.1	93.5	626	340	550	4413
RADIUS }	64.9	61.6	385	255	440	2869
ULNA }		12.8		55		
FEMUR	94.5	158	539	407	866	5364
TIBIA	82.1	158	286	420	597	2873
METATARSAL	30.3	70.8	24.7	190	244	216
METACARPAL	27.7	62.3	29.3	171	176	234
ASTRAGALUS	6.9	13.2	35.1	33.9	71	432
CALCANEUM	8.9	19.9	54.3	54.0	88	536
PODIAL #1	4.0	7.2	15.8	23.7	12.8	196
#2	–	2.5	10.6	8.3	15.0	137
PHALANX #1	4.2	6.3	–	21.9	49	107
#2	1.6	7.1	12.2(t)	11.4	47	23(t)
#3	1.8	–	10.2(t)	7.5(t)	21(t)	11.5(t)
TEETH M	4.4	–	–	6.7	68.7	146
PM	–	–	–	11.4	M35.0*	35
C	–	–	64.5	–	–	530
I	–	–	–	1.5	–	226
RIB #1	11.1	8.0	77.8	18.7	34.2	374
#2	–	11.0	38.2	35.8	46.0	–
VERTEBRA ATLAS	30.9	19.0	117	90.0	178	1418
AXIS	32.6	18.7	78.7	89.0	193	934
CERVICAL	24.9	20.7	–	69.0	166	818
THORACIC	14.8	8.8	69.2	29.7	71.3	606
LUMBAR	13.9	20.4	55.3	45.0	48.9	652
SACRUM	33.4	30.5	195	134	–	–
PATELLA	3.1	5.9	28.4	25.9	29.0	276
PELVIS	127	75.0	–	–	–	–
STERNUM	3.1	–	–	–	–	–
SKULL	296	171	–	–	–	–
JAW (½)	56.5	40.0	–	–	–	–
SCAPULA	43.0	38.6	–	168	–	–
VERT. CENT. #1	5.0	4.5	40	25.0	33.0	300
#2	5.1	–	35	–	28.0	–
ULNA, PROX.	–	6.4	–	30.0	–	–
SESAMOID #1	–	–	–	–	–	10.2
#2	–	–	–	–	–	12.5
HUM. PROX.	41.0	47.0	313	170	275	2206
DIST.	41.0	47.0	313	170	275	2206
R/U. PROX.	32.0	31.0(R)	192	127(R)	220	1434
DIST.	32.0	31.0(R)	192	127(R)	220	1434
FEM. PROX.	47.0	79.0	269	203	433	2682
DIST.	47.0	79.0	269	203	433	2682
TIB. PROX.	41.0	79.0	143	220	298	1436
DIST.	41.0	79.0	143	220	298	1436
MT. PROX.	15.1	–	–	90.0	88.0	–
DIST.	15.1	–	–	90.0	88.0	–
MC. PROX.	13.8	–	–	85.0	122.0	–
DIST.	13.8	–	–	85.0	122.0	–
SCAPULA (GLENOID)	21.5	19.3	153	84.0	132.0	–

* M = Molar.

APPENDIX 2

Calculation of Hydraulic Equivalence

Processes of sediment transport are generally explained in terms of quartz grains with a standard density of 2.65. Some work has been done on the hydraulic equivalence ("equivalent settling velocity") of quartz and particles with greater densities to show how small, dense grains sort out with larger, lighter ones (Rittenhouse, 1943; Briggs, 1962). However, there is a lack of information on the hydraulic equivalence of quartz with particles of lower density such as bones.

Hydraulic equivalence can be considered in terms of any two particles that have the same settling velocity. Given a particular bone, it is possible to determine what size of quartz grain will settle at the same rate as the bone. For spheres, hydraulic equivalence to quartz can be easily calculated using the Impact law. If the settling velocity for quartz (v_q) is to equal the settling velocity of a bone (v_b), then:

$$1307 \cdot (\rho_q - 1) \cdot r_q = 1307 \cdot (\rho_b - 1) \cdot r_b$$
$$(\rho_q - 1) \cdot r_q = (\rho_b -) \cdot r_b$$
$$1.65 \cdot r_q = (\rho_b - 1) \cdot r_b$$
$$r_q = \frac{(\rho_b - 1) \cdot r_b}{1.65}$$

$\rho_q = 2.65$
$\rho_b =$ bone density
$r_q =$ radius of quartz grain
$r_b =$ ½ the nominal diameter of a given bone.

If $\rho_b = 1.5$ and $r_b = 1.0$ cm, then $r_q = .30$ cm.

The value of r_q represents an idealized quartz equivalent for the bone which disregards the effects of shape.

It is difficult to predict the effects of shape on bone-quartz equivalents. In some cases bone shape may decrease settling velocity by increasing the frictional drag on the bone, and this will reduce the size of the equivalent quartz grain. On the other hand, a bone shape (e.g., a streamlined one) that reduces drag may increase the size of the quartz equivalent. The orientation of a bone may have great effects on settling velocity and quartz equivalence. Thus, a metapodial dropped parallel to its long axis may fall faster than a sphere of equivalent volume, but the same bone dropped with its long axis horizontal could settle at a rate slower than that of a sphere. The same bone can alter from equivalence to small or large quartz grains by slight changes in orientation. In actual transport situations, some bones tend to orient with long axes parallel to current direction (Voorhies, 1969:66–67), and these will have maximum hydraulic equivalents for their volume. Bones also tend to orient perpendicular to the current, and these will have smaller effective quartz equivalents. The bones that orient transverse to the current should be more mobile in transport situations.

There is a great need for experimental work which will show the relationship between bone settling velocities and quartz equivalents and the actual current velocities necessary for bone entrainment and transport.

Plate 1. Surface textures of weathered and unweathered bones.
A: a) Unweathered recent bovid radius, showing a smooth, "fresh" surface texture; b) Naturally weathered bovid femur from the recent East Rudolf thanatocoenose, showing slight roughening and cracking of the bone surface; c) Distal end of an equid femur from the recent East Rudolf thanatocoenose, showing extreme flaking and roughening of the bone surface. (Scale in 1 cm and 2 cm intervals)
B: a) Fossil astragalus from the 102–0201 channel sand, showing pre-burial abrasion; b) Fossil astragalus from the 103–0267 distributary channel and beach complex, showing considerable pre-burial abrasion; c) Recently weathered astragalus from the modern East Rudolf thanatocoenose, showing the typical cracked weathering pattern on its articular surface (Note: pattern lacking in a) and b)); d) Recent, unweathered astragalus; e) Unweathered and unabraded fossil astragalus from Locality 8+6–0104 (floodplain). (Scale in 1 cm and 2 cm intervals)
C: a) Distal end of a fossil humerus that was probably weathered prior to burial, showing the typical cracking pattern on its articular surface; b) Distal end of a recently weathered humerus, showing a similar cracking pattern; c) Recent, unweathered humerus; d) Fossil humerus from Area 8, East Rudolf, showing no sign of pre-burial weathering or abrasion. (Scale in 1 cm and 2 cm intervals)

Plate 2. Fracture patterns in recent and fossil bones.
A: a) "Sawtooth" fracture (right side of bovid pelvis); b) "Step" fracture (bovid metapodial); c) "Splintered" fracture (sheep rib); d) "Spiral" fracture (distal end of bovid humerus; e) Weathered bovid humerus (distal end) with a spiral fracture incurred prior to weathering. (Scale in 1 cm intervals)
B: Spiral fracture on the metatarsal of a recently killed giraffe, presumably caused by a hyaena. (Scale in 10 cm intervals)
C: a) and b) Typical fracture patterns of bones after mineralization; c) Recent humerus (distal) showing spiral fracture; d) Fossil fragment of a diaphysis, showing a spiral fracture probably incurred prior to burial and mineralization. (Scale in 1 cm and 2 cm intervals)

Plate 3. The trapping effect of surface vegetation on bones in the recent thanatocoenose on the delta of Laga Tulu Bor, Ileret, East Rudolf.
A: Bovid femur bound by shoreline grass and partially buried. (Scale in 10 cm intervals)
B: Bovid skull and vertebrae, showing loose entrapment by grass. The horn cores are bound firmly to to the ground by warm tubes (just to right of camera lens cover).

Plate 4. Recent sedimentary environments south of Ileret, East Rudolf.
A: A beach bar on the shore of the delta of Laga Tulu Bor, with the open lake to the right and a closed lagoon or back beach pond to the left. Pebbles and bone debris litter the beach. Beach bars such as this move shoreward seasonally with the annual rise in lake level (about 1 m fluctuation per year). Depositional environments such as this were probably active in the formation of Plio-Pleistocene deposits such as those of Localities 130–0201, 105–0208, 103–0267 and 103–0256.
B: Laga Tulu Bor after a brief but heavy rainstorm, with a flow depth of about 1.5 m. The channel is normally dry for most of the year. A break in the gallery forest that fringes the channel is visible in the upper right of the photograph. This opens onto the grass-covered floodplain. Some characteristics of this depositional environment are probably comparable to Localities 102–0201 and 105–1311.
C: The upper part of the deltaic plain of Laga Tulu Bor, showing flooding of a low area (atrophied channel) after a heavy rain. This area lies in the transition zone between floodplain and deltaic plain. The sediment is primarily silt. This depositional environment is probably comparable to that of Locality 8+6–0104 (floodplain).

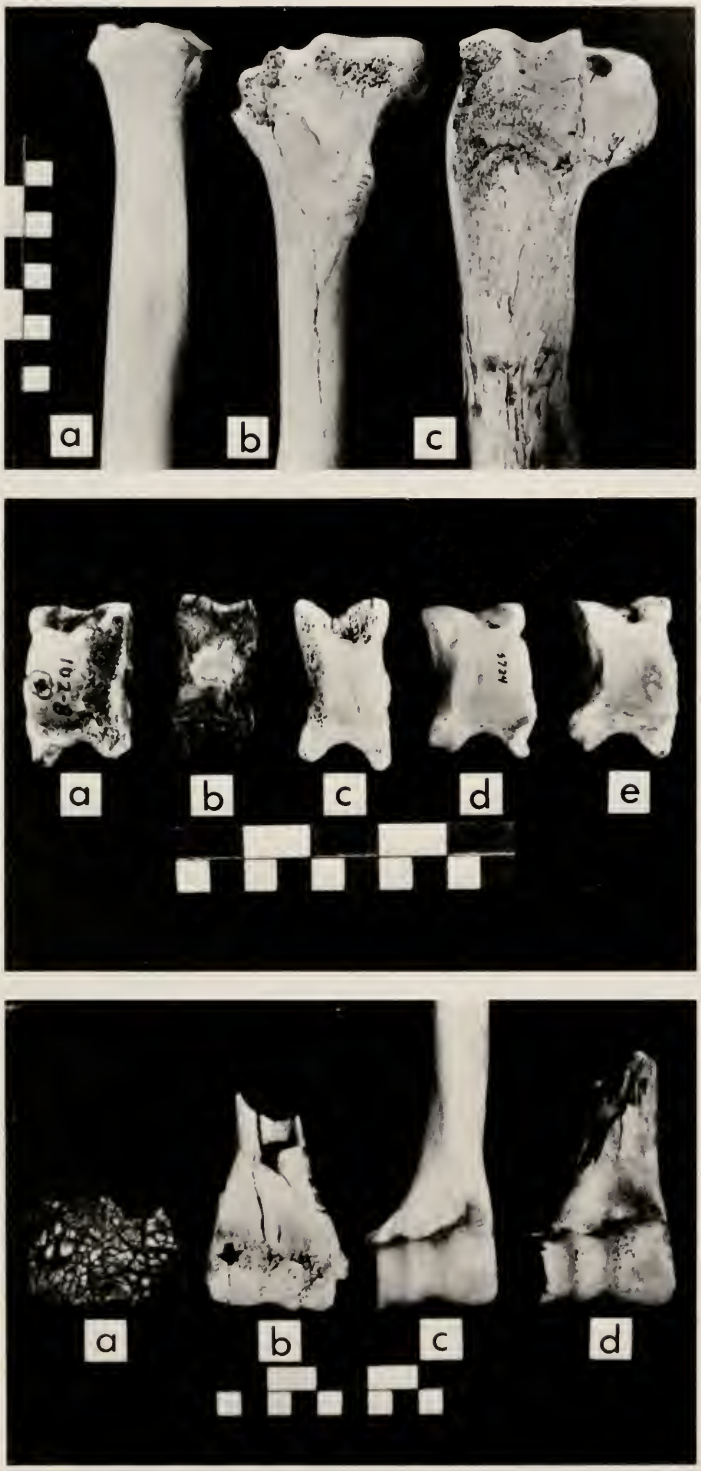

Plate 1

Plate 2

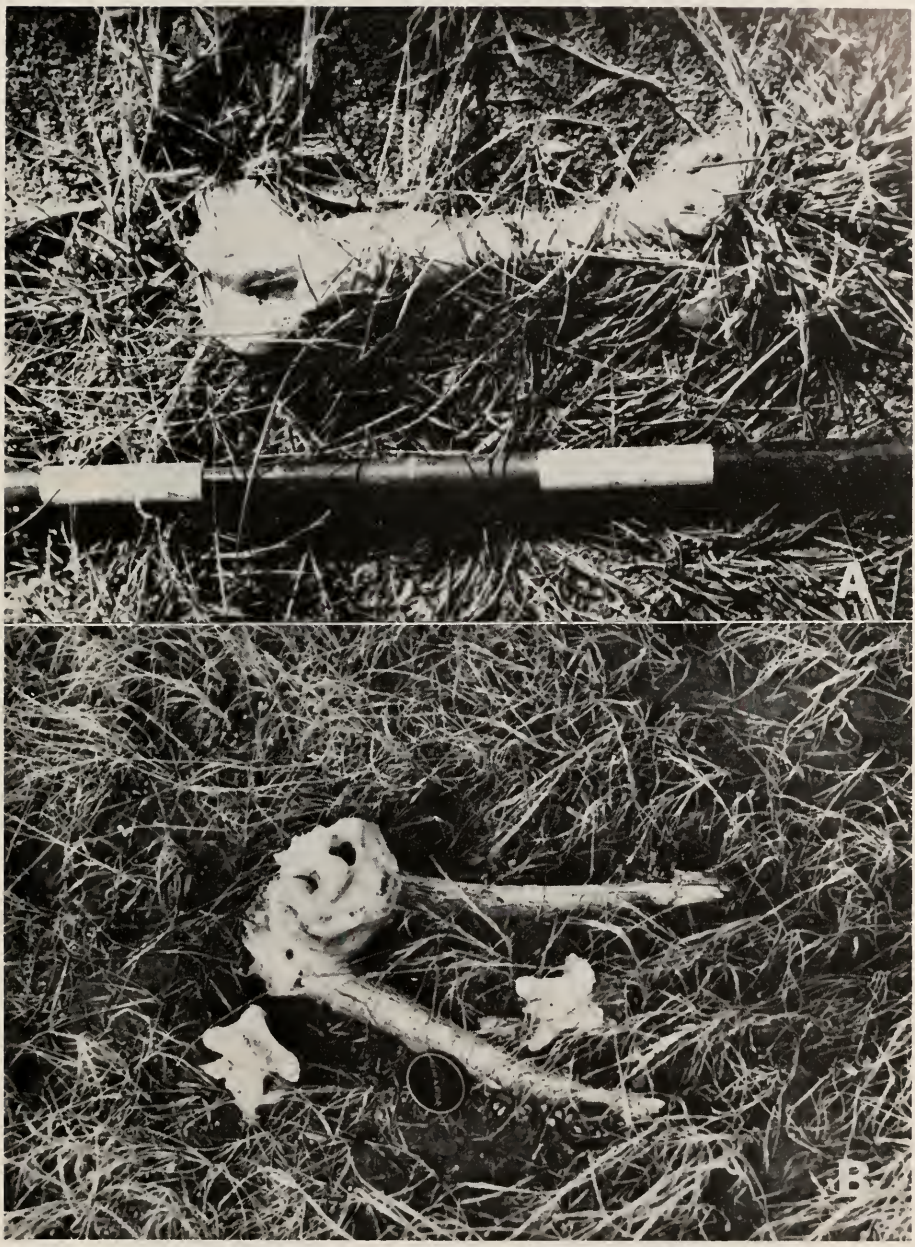

Plate 3

Plate 4

8278 070

Harvard MCZ Library
3 2044 066 304 205